British Journal of Pharmacology

June 1993

Volume 109 Number 2 pages 285–600

Br. J. Pharmacol. (1993), **109**, 287–288

SPECIAL REPORT

© Macmillan Press Ltd, 1993

Characterization of the binding of [^{3}H]-L-N^G-nitro-arginine in rat brain

[1]Anton D. Michel, Ravinder K. Phul, Tracy L. Stewart & Patrick P.A. Humphrey

Glaxo Institute of Applied Pharmacology, Department of Pharmacology, University of Cambridge, Tennis Court Road, Cambridge, CB2 1QJ

In the present study tritiated L-N^G-nitro-arginine (L-NOARG) has been shown to label specific binding sites in rat brain cytosol. We conclude that this ligand is directly labelling nitric oxide synthase (NOS). This conclusion is based on our observations (i) that binding was stereoselectively inhibited by L-arginine, in preference to D-arginine, and (ii) that a number of different NOS inhibitors were able to displace [^{3}H]-L-NOARG binding at similar concentrations to those required to inhibit the activity of rat brain cytosol NOS in functional studies.

Keywords: Nitric oxide synthase; [^{3}H]-L-N^G-nitro-arginine; radioligand binding; nitric oxide synthase inhibitors

Introduction Nitric oxide synthase (NOS) is the enzyme involved in the synthesis of nitric oxide from L-arginine and has been shown to exist in at least three isoforms (Bredt *et al.*, 1991; Lyons *et al.*, 1992; Lamas *et al.*, 1992). As part of a study to provide further information on these enzymes, we have investigated whether tritiated L-N^G-nitro-arginine (L-NOARG) can be used to label the isoform of NOS present in rat brain. This compound was selected for study since it is the most potent inhibitor of the enzyme NOS yet described (Moore *et al.*, 1990) and, despite its rather low affinity for use as a radioligand (K_i = 0.1 μM), the compound displays slow inhibition kinetics in both *in vitro* and *in vivo* studies (Dwyer *et al.*, 1991), suggesting that it might be suitable as a radioligand for directly labelling NOS.

Methods A crude preparation of NOS was obtained from the brains of 200–300 g male Sprague-Dawley rats. The whole brain (including cerebellum) was homogenized in 5 vol (w/v) of 50 mM Tris buffer (pH 7.0 at 4°C), centrifuged at 48,000 *g* for 20 min, the pellet discarded and the supernatant passed through a 5 ml column of Dowex AG50WX-8 resin (Na^+ form), in order to remove >99% of endogenous arginine. The supernatant was collected, the pH adjusted to 7.0 at 22°C and this cytosolic preparation was used immediately or frozen and stored at −85°C until required. In the binding assays [^{3}H]-L-NOARG (specific activity 55 Ci mmol^{-1}, Amersham), was incubated with the brain cytosol in a final volume of 0.15 ml of 50 mM Tris, 10 μM $CaCl_2$ buffer at pH 7.0. Incubations were performed at 22°C and were terminated by vacuum filtration over 0.3% polyetheyleneimine pretreated GF/B glass fibre filters which were subsequently washed with 10 ml of 4°C distilled water. Non specific binding was defined by use of 100 μM L-NOARG. In functional studies the rate of conversion of a trace concentration of [^{3}H]-arginine (30–40 nM) to [^{3}H]-citrulline was used to measure NOS activity in the brain cytosol by the methods of Dwyer *et al.* (1991). In the functional studies a 50 mM Tris (pH 7.4) buffer containing 3 mM $CaCl_2$ and 1 mM NADPH was used. The NOS inhibitors used in this study were obtained from Sigma with the exception of 7-nitroindazole which was obtained from Lancaster Chemicals (MTM). All competition curves were analysed by iterative curve fitting techniques (Michel & Whiting, 1984) to obtain Hill slopes and pIC_{50} values (− logarithm of the concentration of competing compound causing 50% inhibition of either receptor binding or NOS enzyme activity).

Results In initial studies, using a 30 min incubation, the binding of [^{3}H]-L-NOARG was shown to be calcium-dependent in that binding of the ligand (10 nM) was decreased by EGTA (1 mM: 67% of control), while addition of calcium ions increased binding by up to about 250% (EC_{50} = 192 ± 98 nM; mean ± s.e.mean of 4 determinations) in EGTA-treated enzyme solutions. Optimal binding of the radioligand was obtained in the presence of 10 μM calcium chloride which was therefore included in all subsequent binding assays. Binding of the ligand was also sensitive to pH with maximal binding occurring at pH levels below 6.8 and a progressive decrease in binding observed when pH was increased from 6.8 to 9.0. A pH of 7.0 was used for all subsequent studies.

In kinetic studies performed at 22°C, with a 10 nM radioligand concentration, steady state levels of binding were achieved after 2 h and remained stable for up to 5 h. Dissociation of the radioligand was slow (10–20% dissociation of ligand over 2 h). In saturation studies performed over a 2 h period, the ligand bound to an apparently homogeneous population of sites (K_D = 22.3 ± 2.0 nM; B_{max} = 903.4 ± 96.1 fmol mg^{-1} protein; mean ± s.e.mean of 4 determinations).

Table 1 presents a comparison of the characteristics of the [^{3}H]-L-NOARG binding sites with the functional properties of NOS in the rat brain. The values shown represent pIC_{50} values for a series of arginine analogues, as well as 7-nitroindazole, as inhibitors of either the binding of the radioligand or the conversion of [^{3}H]-arginine to [^{3}H]-citrulline (both measured over a 15 min incubation period). Binding of the radioligand was stereoselectively inhibited by L-arginine, in preference to D-arginine, and a number of NOS inhibitors were able to inhibit completely specific binding of the radioligand. The pIC_{50} values in the binding and functional studies were highly correlated (r = 0.962) although for several of the NOS inhibitors the value obtained in the binding assay was somewhat greater than that obtained in the functional assay.

Discussion In the present study, [^{3}H]-L-NOARG bound with high affinity to a single population of sites in rat brain cytosol which displayed the characteristics expected of NOS. First, binding was stereoselectively inhibited by L- rather than D-arginine with the pIC_{50} value for L-arginine being similar to that determined in the functional studies. Secondly, radioligand binding was inhibited by all of the NOS inhibitors studied, including 7-nitroindazole recently reported to inhibit rat brain NOS (Moore *et al.*, 1993). Overall the corresponding pIC_{50} values were highly correlated with their

[1] Author for correspondence.

Table 1 Comparison of binding and functional potencies of a series of compounds in rat brain cytosol

Compound	*Binding studies*		*Functional studies*	
	pIC_{50}	nH	pIC_{50}	nH
L-NOARG	7.10 ± 0.20	1.07 ± 0.04	6.75 ± 0.02	1.09 ± 0.01
L-NMMA	6.99 ± 0.05	0.92 ± 0.09	6.19 ± 0.14	1.12 ± 0.17
7-NI	6.86 ± 0.08	0.81 ± 0.06	6.23 ± 0.02	0.97 ± 0.05
L-NAME	6.50 ± 0.08	1.00 ± 0.14	5.46 ± 0.04	0.95 ± 0.08
L-Arginine	5.99 ± 0.15	0.94 ± 0.06	6.00 ± 0.30	1.00 ± 0.04
D-Arginine	3.10 ± 0.10	1.11 ± 0.20	3.30 ± 0.17	0.79 ± 0.20

All incubations were for 15 min. Data shown are the pIC_{50} value and Hill slope (nH) (mean ± s.e.mean from 3–6 experiments). L-NMMA is L-N^G-monomethyl-arginine, 7-NI is 7-nitroindazole and L-NAME is L-N^G-nitro-arginine methyl ester. In the binding assays the radioligand concentration was 10 nM and total and non-specific binding (NSB) represented 1000–2000 d.p.m. and 80–160 d.p.m. respectively. In the functional studies 30–40 nM [^{3}H]-arginine was used and basal values represented 6000–7000 d.p.m. and stimulated values represented 30,000–40,000 d.p.m.

respective potency estimates obtained in functional studies.

However, despite the high level of correlation between the functional and binding studies it should be noted that several of the NOS inhibitors were more potent in absolute terms in the binding assay than in the functional assay. This may be a reflection of their slow inhibition kinetics. Thus, in the functional assay, where the kinetics of the arginine to citrulline conversion are rapid, it is possible that appreciable conversion of arginine to citrulline may have occurred before equilibrium of the inhibitors had been achieved. Indeed previous studies of Dwyer *et al.* (1991) have shown that the potency of L-NOARG increases when the compound is pre-incubated with the enzyme before addition of arginine substrate. In contrast, in the binding assay, where the compounds were competing for the slowly equilibrating radioligand [^{3}H]-L-NOARG, problems of equilibration may not be as pronounced. To address this issue it would be necessary to use a longer incubation period in both the binding and the functional studies. While this can be achieved in the binding assay, to date it has not been possible to measure enzyme activity with incubation periods in excess of 15 min due to problems with the functional stability of the enzyme following these longer periods of incubation.

It was noteworthy that the binding of the radioligand was very sensitive to calcium. It is known that NOS is a calcium-dependent enzyme (Bredt *et al.*, 1991) and the present binding data therefore demonstrate that not only is calcium necessary for enzyme activity but that it also facilitates the binding of NOS inhibitors.

In conclusion, these results suggest that [^{3}H]-L-NOARG is able to label NOS in rat brain cytosol and, as such, represents a useful tool for the further characterization of NOS. Preliminary unpublished observations in our laboratory suggest that this ligand may also be used to label NOS in tissue slices and so the ligand could be used for the autoradiographic study of enzyme distribution.

References

BREDT, D.S., HWANG, P.M., GLATT, C.E., LOWENSTEIN, C., REED, R.R. & SNYDER, S.H. (1991). Cloned and expressed nitric oxide synthase structurally resembles cytochrome P-450 reductase. *Nature*, **351**, 714–718.

DWYER, M.A., BREDT, D.S. & SNYDER, S.H. (1991). Nitric oxide synthase: irreversible inhibition by L-N^G-nitroarginine in brain in vitro and in vivo. *Biochem. Biophys. Res. Commun.*, **176**, 1136–1141.

LAMAS, S., MARSDEN, P.A., LI, G.K., TEMPST, P. & MICHEL, T. (1992). Endothelial nitric oxide synthase: molecular cloning and characaterisation of a constitutive enzyme isoform. *Proc. Natl. Acad. Sci. U.S.A.*, **89**, 6348–6352.

LYONS, C.R., OROLOFF, G.J. & CUNNINGHAM, J.M. (1992). Molecular cloning and functional expression of an inducible nitric oxide synthase from a murine macrophage cell line. *J. Biol. Chem.*, **267**, 6370–6374.

MICHEL, A.D. & WHITING, R.L. (1984). Analysis of ligand binding data using a microcomputer. *Br. J. Pharmacol.*, **83**, 460P.

MOORE, P.K., AL-SWAYEH, O.A., CHONG, N.W., EVANS, R.A. & GIBSON, A. (1990). L-N^G-nitro-arginine (L-NOARG), a novel, L-arginine-reversible inhibitor of endothelium-dependent vasodilatation *in vitro*. *Br. J. Pharmacol.*, **99**, 408–412.

MOORE, P.K., BABBEDGE, R.C., WALLACE, P., GAFFEN, Z.A. & HART, S.L. (1993). 7-Nitroindazole, an inhibitor of nitric oxide synthase, exhibits anti-nociceptive activity in the mouse without increasing blood pressure. *Br. J. Pharmacol.*, **108**, 296–297.

(Received February 12, 1993
Accepted February 23, 1993)

Br. J. Pharmacol. (1993), **109**, 289–290

SPECIAL REPORT

© Macmillan Press Ltd, 1993

Peripheral endotoxin induces hypothalamic immunoreactive interleukin-1β in the rat

[1]E.W. Hillhouse & *K. Mosley

Department of Clinical Biochemistry, The School of Biomedical and Biomolecular Sciences, The University of Newcastle, Newcastle upon Tyne NE2 4HH and *The Multiple Sclerosis Society Laboratory, The Institute of Neurology, 1 Wakefield Street, London WC1N 1PJ

Interleukin-1 (IL-1) is a polypeptide produced by a variety of cells and contributes to the general host response to inflammation. It displays a wide spectrum of inflammatory, metabolic, physiological, haematopoietic and immunological activities. Brain cells, including neurones, microglia, endothelial cells and astrocytes can all produce IL-1β in response to various physiological and pathological stimuli. In this report we show that peripherally administered endotoxin stimulates the appearance of immunoreactive IL-1β (IL-1β) in the rat hypothalamus as measured by an ultrasensitive, highly specific enzyme amplified immunometric assay for rat IL-1β.

Keywords: Endotoxin; interleukin-1β; hypothalamus

Introduction The mechanism whereby exogenous pyrogens activate thermoregulatory mechanisms remains uncertain, although a number of molecular signals are thought to be involved including the cytokines and prostaglandins (Kluger, 1991). In patients with infectious disease in which endotoxin plays a role it is likely that several cytokines, including interleukin-1 (IL-1), contribute to the clinical picture. Many of the central nervous system responses to endotoxin such as fever, sleep and anorexia can be reproduced by either peripheral or central administration of IL-1β (Rothwell, 1991). These observations strengthen the hypothesis that peripherally generated cytokines mediate both the central and peripheral metabolic responses to endotoxin.

Central to this hypothesis, is the integrity of the blood brain barrier. This appears to be impermeable to IL-1 (Dinarello *et al.*, 1978), although the barrier may alter during sepsis or other pathological states. Alternatively, IL-1 may penetrate the brain at areas outside the barrier, such as the organum vasculosum lamina terminalis (Katsuura *et al.*, 1990). Another possibility is that IL-1 might be generated centrally and would not therefore need to cross the blood brain barrier. Such a central IL-1 network has been identified within the hypothalamus (Koenig, 1991). Furthermore, IL-1 has been shown to activate neuroendocrine cells via a direct action at the hypothalamus (Scarborough *et al.*, 1989). In an effort to characterize further the effect of endotoxin on neuroendocrine mechanisms we sought to investigate whether peripherally administered endotoxin might stimulate the production of hypothalamic IL-1β.

Methods *Animals* Male Wistar-derived rats, weighing 250–300 g, were injected intraperitoneally with either endotoxin (1st International Reference Preparation 57/7, NIBSC) or vehicle (sterile, endotoxin-free 0.9% saline) at 09 h 00 min. The animals were killed by decapitation at various time intervals following the injection and each hypothalamus was rapidly removed and immediately homogenized in 1 ml of RPMI tissue culture medium (ICN Flow). The homogenates were stored at − 70°C before assay.

IL-1β immunoassay IrIL-1β was measured with an ultrasensitive highly specific, enzyme amplified, immunometric assay for rat IL-1β using a sheep polyclonal antiserum (Bristow *et al.*, 1989). The capture antibody was DEAE-purified and the detection antibody immunoaffinity-purified on a rat IL-1β affigel 10 column. The detection antibody was then conjugated to alkaline phosphate with a kit (Pierce) and purified by h.p.l.c. to obtain a conjugate with high sensitivity and low non-specific binding characteristics. Nunc immunoplates were coated with the capture antibody (1 μg/well) in carbonate buffer at 4°C overnight. Following blocking of unbound sites with 5% lactose and 0.2% casein, recombinant rat IL-1β standards (Dr S. Poole, NIBSC, Potters Bar, Herts) in RPMI, or tissue extracts were diluted in assay buffer (50 mM Tris + 0.1% bovine serum albumin) and added to the plates (10 μl/well). Following overnight incubation at 4°C the conjugated detection antibody (1:1000) was added and incubated at room temperature for 2 h. After washing AMPAK (Novo Biolabs) substrate (100 μl/well) was added followed, after 15 min, by AMPAK amplifier (100 μl/well). The absorbance of each well at 492 nm was measured with a Titertek Multiskan MCC plate reader.

Results *IL-1β immunoassay* The immunoassay for rat IL-1β had a sensitivity of 3 pg ml^{-1} and showed cross-reactivity with both murine IL-1β (17.5%) and human IL-1β (13%). No cross-reactivity was observed with human IL-1α, human IL-6, human/rat corticotrophin-releasing factor-41 (CRF-41), arginine vasopressin and α-melanocyte stimulating hormone. The recovery of rat IL-1β added to the hypothalamic homogenate was 67%. IL-1β extracted from endotoxin stimulated

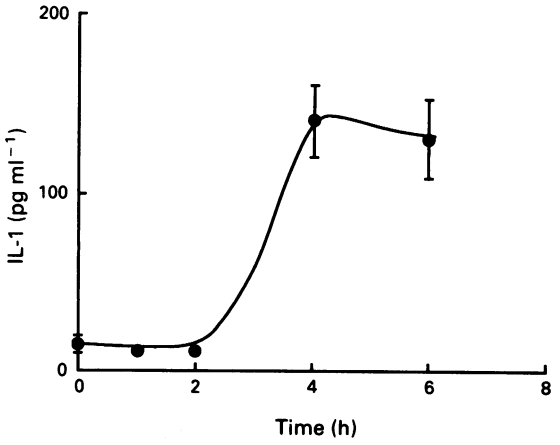

Figure 1 Time course of the effect of intraperitoneal endotoxin (250 μg/animal) on the immunoreactive interleukin-1β (IL-1) content of the rat hypothalamus. Each point represents the mean ± s.e.mean of at least four observations.

[1] Author for correspondence.

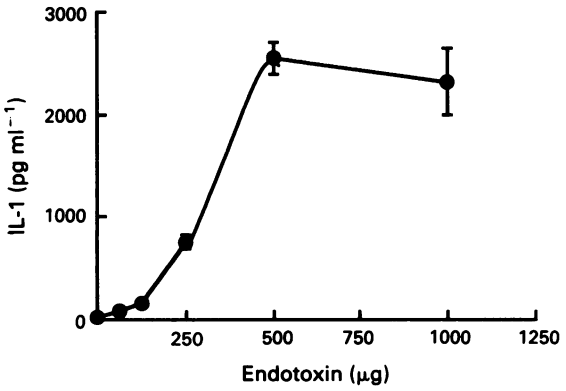

Figure 2 The effect of various doses of intraperitoneal endotoxin on the immunoreactive interleukin-1β (IL-1) content of the rat hypothalamus. Each point represents the mean ± s.e.mean of at least four observations.

rat hypothalami diluted in parallel with the standard curve (data not shown).

Time course When animals were treated with endotoxin (250 μg/animal) there was a delay of 2 h before any increase in the hypothalamic immunoreactive IL-1β content (Figure 1). This effect was maximal between 4–6 h. Control animals showed no response to vehicle control (data not shown).

Dose-dependancy The effect of endotoxin on hypothalamic IL-1β immunoreactivity was dose-dependent over the range of 125–500 μg (Figure 2). Control animals showed no response to vehicle control (data not shown).

Discussion This study presents some new insights into the mechanisms whereby endotoxin might activate central neuroendocrine systems. The cellular sources of brain IL-1β remain controversial. It appears to be present within neurones paricularly in areas involved in the regulation of anterior pituitary function (Koenig, 1991). Furthermore, microglia, brain endothelial cells and astrocytes have all been shown to produce IL-1β in response to various physiological and pathological stimuli (Benveniste, 1992). The IL-1β produced under these circumstances has been implicated in both tissue damage and repair. Our study indicates that endotoxin induces the synthesis of IL-1β in the brain either directly or via some secondary neural or humoral mediator. Of these possibilities the latter seems the most likely and it is possible that peripheral IL-1β itself might be one of these mediators. Previous reports have shown endotoxin-induced synthesis of IL-1β by use of immunocytochemistry and *in situ* hybridization (Van Dam *et al.*, 1992; Ban *et al.*, 1992) but this is the first report showing time- and concentration-dependance. In this short study we cannot completely exclude the possibility that the IL-1β found in the hypothalamus is transported from the peripheral circulation. This seems unlikely, however, in view of the fact that circulating concentrations of IL-1β are low and transport into the brain is less than 1% of circulating protein. In conclusion, endotoxin induces hypothalamic IL-1β and this may participate in the integration of the neuroendocrine responses to sepsis.

References

BAN, E., HAOUR, F. & LENSTRA, R. (1992). Brain interleukin 1 gene expression induced by peripheral lipopolysaccharide administration. *Cytokine*, **4**, 48–54.

BENVENISTE, E., (1992). Inflammatory cytokines within the central nervous system: sources, functions and mechanisms of action. *Am. J. Physiol.*, **263**, C1-C16.

BRISTOW, A.S., MOSLEY, K. & POOLE, S. (1991). Interleukin-1β production *in vivo* and *in vitro* in rats and mice measured using specific immunoradiometric assays. *J. Mol. Endocrinol.*, **7**, 1–7.

DINARELLO, C., WEINER, P. & WOLFF, S.M. (1978). Radiolabelling and deposition in rabbits of purified human leukocytic pyrogen. *Clin. Res.*, **26**, 522A.

KATSUURA, H., ARIMURA, A., KOVES, K. & GOTTSCHALL, P.E. (1990). Involvement of organum vasculosum of lamina terminalis and preoptic area in interleukin 1-induced ACTH release. *Am. J. Phsiol.*, **122**, E163–E171.

KLUGER, M.J. (1991). Fever: role of pyrogens and cryogens. *Physiol. Rev.*, **71**, 93–127.

KOENIG, J.I. (1991). Presence of cytokines in the hypothalamic-pituitary axis. *Prog. Neuro. Endocrin. Immunol.*, **4**, 143–153.

ROTHWELL, N. (1991). Functions and mechanisms of Interleukin-1 in brain. *Trends Pharmacol. Sci.*, **12**, 430–436.

SCARBOROUGH, D.E., LEE, S.L., DINARELLO, C.A. & REICHLIN, S. (1989). Interleukin-1 beta stimulates somatostatin biosynthesis in primary cultures of fetal rat brain. *Endocrinology*, **124**, 549–551.

VAN DAM, A., BROUNS, M., LOUISSE, S. & BERKENBOSCH, F. (1992). Appearance of interleukin-1 in macrophages and in ramified microglia in the brain of endotoxin-treated rats: a pathway for the induction of non-specific symptoms of sickness. *Brain Res.*, **588**, 291–296.

(Received January 11, 1993
Accepted February 23, 1993)

Br. J. Pharmacol. (1993), **109**, 291–292

SPECIAL REPORT

© Macmillan Press Ltd., 1993

Mg^{2+} and caffeine-induced intracellular Ca^{2+} release in human vascular endothelial cells

Aimin Zhang, *Toni P.-O. Cheng, Bella T. Altura & [1]Burton M. Altura

Department of Physiology and *Department of Anatomy and Cell Biology, State University of New York, Health Science Center at Brooklyn, NY, U.S.A.

Interaction of ionized magnesium ($[Mg^{2+}]_o$) and caffeine in regulation of intracellular free calcium concentration ($[Ca^{2+}]_i$) in human aortic endothelial cells was studied using fura-2 and digital imaging microscopy. In 1.2 mM $[Mg^{2+}]_o$, basal $[Ca^{2+}]_i$ was 73.7 ± 22.4 nM, with a heterogeneous distribution within the cells. No significant changes of basal $[Ca^{2+}]_i$ were found either when cells were treated with 10 mM caffeine or when $[Mg^{2+}]_o$ was lowered from 1.2 mM to 0.3 mM. However, a combined superfusion of the cells with 0.3 mM $[Mg^{2+}]_o$ and 10 mM caffeine resulted in a significant elevation of $[Ca^{2+}]_i$ to 382.8 ± 57.1 nM, probably by release of Ca^{2+} from internal stores, which was attenuated by $NiCl_2$ (1 mM). These results suggest that a Ca^{2+}-induced Ca^{2+} release mechanism is involved in regulation of $[Ca^{2+}]_i$ in endothelial cells, which may be either regulated or modulated by Mg^{2+}.

Keywords: Magnesium; calcium; caffeine; endothelial cells; fura-2

Introduction A rise of intracellular free Ca^{2+} concentration ($[Ca^{2+}]_i$) is known to be closely coupled to important functional properties of the vascular endothelial cells, such as synthesis/release of prostacyclin (PGI_2) or endothelial-derived relaxing factors (EDRFs) and cell contraction, in response to a number of agonists or physical stimuli (Furchgott & Vanhoutte, 1989; Moncada *et al.*, 1991). The elevated $[Ca^{2+}]_i$ in endothelial cells is due to an influx of extracellular Ca^{2+} and release of intracellular Ca^{2+} (Schilling & Elliott, 1992). It has been well-established that intracellular Ca^{2+} release can be mediated by activation of plasma membrane receptors coupled to phospholipase C and generation of inositol 1,4,5-trisphosphate(IP_3) (Schilling & Elliot, 1992). However, the contribution of Ca^{2+} release via non-IP_3-dependent or Ca^{2+}-induced Ca^{2+} release mechanism(s) in endothelial cells remains controversial. For example, opposite effects of caffeine, a marker for Ca^{2+}-induced Ca^{2+} release, on $[Ca^{2+}]_i$ have been found (Buchan & Martin, 1991; Schilling & Elliott, 1992).

Magnesium ions (Mg^{2+}) play an inhibitory role in caffeine-mediated Ca^{2+} release (Karaki & Weiss, 1988) and on $[Ca^{2+}]_i$ regulation in vascular smooth muscle cells (Zhang *et al.*, 1992), but little is known regarding the effects of Mg^{2+} in endothelial cells. Recent reports indicate that Mg^{2+} may be involved in regulation of Ca^{2+} homeostasis in endothelium since changes of extracellular Mg^{2+} ($[Mg^{2+}]_o$) affect release of EDRFs from endothelium in isolated blood vessels (Altura & Altura, 1987). It would thus be of importance to define the interaction of Mg^{2+} and caffeine in the regulation of $[Ca^{2+}]_i$ in endothelium and thus elucidate the mechanism(s) of intracellular Ca^{2+} release in endothelial cells.

Methods Experiments were carried out on a human aortic endothelial cell line (No. AG09799A, 20 passages) obtained from the NIA Aging Cell Repository (Camden, NJ, U.S.A.). Endothelial cells were cultured in 199 media (Sigma Chem. Co., St Louis, MO, U.S.A.) with 15% FSA at 37°C in a humidified atmosphere composed of 95% air:5% CO_2. To avoid synchronized activities of endothelial cells (Sage *et al.*, 1989), coverslips containing cells in near confluent density were used. The cells were loaded with fura-2 (Molecular Probes, Eugene, OR, U.S.A.) by incubating them with 2 μM fura-2/AM in the culture media for 60 min under 95% air:5% CO_2. Then, the coverslips were placed in a chamber on a thermostat-regulated stage of a Nikon fluorescence microscope and superfused with 2.2 mM Ca^{2+}-HEPES buffer solutions (pH 7.4, 37°C) containing 0.3 mM or 1.2 mM Mg^{2+}, respectively, followed by treatment with 10 mM caffeine. In other experiments, effects of a calcium channel influx blocker, $NiCl_2$ (1 mM), on $[Ca^{2+}]_i$ was tested in 0.3 mM Mg^{2+} solution. The ionic activities of Mg^{2+} and Ca^{2+} in HEPES buffer solutions were monitored by ion selective electrodes (NOVA Biomedical Corp, Waltham, MA, U.S.A.) and adjusted with $MgSO_4$ or $CaCl_2$ (Altura *et al.*, 1992). The HEPES buffer solutions also contained (mM): NaCl 118, KCl 4.7, KH_2PO_4 1.2, HEPES 5, and glucose 10. $[Ca^{2+}]_i$ was measured with a TN8500 FluorPlex III Image Analyzer (Tracor Northern, Madison, WN, U.S.A.). Images of fura-2 fluorescence at 510 nm emission were obtained with 340 and 380 nm excitation wavelengths with a silicon intensified target (SIT) camera. The time interval of switching between these two wavelengths was 5 s. Background fluorescence for both excitation wavelengths were acquired from blanks for each experiment and subtracted from each pair of images separately before ratioing. Fluorescence ratios ($R_{340/380}$) were obtained by dividing the 340 nm image by the 380 nm image. No image misalignments occurred when these two ratiometric images were superimposed.

An *in vitro* calibration method was used to calculate $[Ca^{2+}]_i$ of single endothelial cells. Fura-2 pentapotassium salt (5 μM) was dissolved in small volumes of EGTA-buffered standard solutions (pH 7.1, 37°C) containing either 2.51 mM (max) or 0 mM-Ca^{2+} (min), to generate the maximum (R_{max}) and minimum (R_{min}) fluorescence ratios at the 340 nm and 380 nm wavelength, *i.e.* 5.0550 and 0.3512, respectively. $[Ca^{2+}]_i$ was calculated according to the following equation:

$$[Ca^{2+}]_i = K_d \times B \times (R-R_{min})/(R_{max}-R)$$

A K_d of 224 nM was used for the fura-2/Ca^{2+} complex (Zhang *et al.*, 1992). B is the ratio of fluorescence intensity of fura-2 to the Ca:fura-2 complex excited at 380 nm.

Results Table 1 shows effects of caffeine on $[Ca^{2+}]_i$ in human cultured vascular endothelial cells at 1.2 mM and 0.3 mM extracellular Mg^{2+} concentrations ($[Mg^{2+}]_o$). With 1.2 mM $[Mg^{2+}]_o$, the basal level of $[Ca^{2+}]_i$ in cultured endothelial cells, estimated from the ratio (F340/F380), was 74 ± 22 nM. The values are comparable with basal values found by others (Sage *et al.*, 1989; Buchan & Martin, 1991). The distribution of $[Ca^{2+}]_i$ appeared heterogeneous within the

[1] Author for correspondence at Box 31, Suny-Health Science Center at Brooklyn, 450 Clarkson Avenue, Brooklyn, New York 11203, U.S.A.

Table 1 Effects of extracellular magnesium and caffeine on intracellular free calcium ion in human aortic endothelial cells

$[Mg^{2+}]_o$ (mM)	n	$[Ca^{2+}]_i$ (nM) Basal	$[Ca^{2+}]_i$ (nM) Caffeine (10 mM) treatment
1.2	5	73.7 ± 22.4	76.8 ± 11.9
0.3	7	56.2 ± 14.1	382.8 ± 57.1*
0.3 + $NiCl_2$ 1 mM	12	79.9 ± 10.7	114.1 ± 9.3*

n = the number of cells; Values (means ± s.e.mean) represent $[Ca^{2+}]_i$ in the same group of endothelial cells before and 10 min after caffeine.
*Significantly different from all other values by Student's t test ($P<0.05$).

cells, *i.e.* there were areas of higher intracellular free calcium concentrations, referred to as brightness spots which were scattered among the cells, and around these brightness spots were areas with very low $[Ca^{2+}]_i$ concentration. The brightness spots most probably represent Ca^{2+} release from the extensive Ca^{2+} binding and uptake elements of internal storage sites which strongly limit Ca^{2+}diffusion. Subsequent treatment (10 min, which should permit a steady state to develop; Buchan & Martin, 1991) of 10 mM caffeine, exhibited little effects on $[Ca^{2+}]_i$ (76 ± 14 nM) and its subcellular distribution in all cells tested.

Lowering $[Mg^{2+}]_o$ to 0.3 mM Mg^{2+} caused insignificant changes in $[Ca^{2+}]_i$ (57 ± 14 nM, $P>0.05$) in the endothelial cells. However, treatment (10 min) with 10 mM caffeine (in 0.3 mM Mg^{2+}) resulted in significant elevation of $[Ca^{2+}]_i$, *i.e.* to 383 ± 57 nM, or about a 6.8 fold increment. Concomitant with the $[Ca^{2+}]_i$ elevation, the number and intensity of brightness spots were increased within endothelial cells, indicating that more Ca^{2+} ions were released from the internal stores. With 1 mM $NiCl_2$ in 0.3 mM $[Mg^{2+}]_o$ solution, caffeine still induced an increase of $[Ca^{2+}]_i$, but to a lesser degree compared to that without Ni^{2+} (Table 1).

Discussion In contrast to bovine aortic endothelial cells in which caffeine consistently elevated $[Ca^{2+}]_i$ with 1 mM $[Mg^{2+}]_o$ present in the medium (Buchan & Martin, 1991), human aortic endothelial cells responded to caffeine only when placed in low (0.3 mM) $[Mg^{2+}]_o$. These findings suggest that the elevated $[Ca^{2+}]_i$ resulted from a release of Ca^{2+} from internal stores, since caffeine is known to increase the sensitivity for Ca^{2+} release, at least in muscular tissues (Karaki & Weiss, 1988). Ni^{2+} ions, calcium channel blockers, partially inhibited such caffeine-induced $[Ca^{2+}]_i$ rises, supporting this tenet. Such a large elevation of $[Ca^{2+}]_i$ (about a 6.8 fold increment) also suggests that the caffeine-sensitive Ca^{2+} pool is large compared to the intracellular Ca^{2+} content in endothelial cells.

Our results with different $[Mg^{2+}]_o$ suggest that Mg^{2+} may regulate caffeine-mediated Ca^{2+} release in human aortic endothelial cells. Since lowering of $[Mg^{2+}]_o$ (0.3 mM) alone failed to affect basal $[Ca^{2+}]_i$ in endothelial cells (Table 1), it is unlikely that potentiation of Ca^{2+} release was brought about by an increase in the Ca^{2+} concentration in the vicinity of the internal Ca stores when $[Mg^{2+}]$ was lowered. The synergistic effects of caffeine and low $[Mg^{2+}]_o$ may be due to a release of inhibition by Mg^{2+}, as proposed for muscle cells (Karaki & Weiss, 1988). Since Ca^{2+} released by caffeine might activate phospholipase C to generate IP_3, or a decrease in hydrolysis of IP_3 by inhibition of inositol trisphosphate phosphomonoesterase might occur as a result of removing the enzyme cofactor Mg^{2+} (Downes *et al.*, 1982), an activation of an IP_3-induced Ca^{2+} release mechanism may co-exist.

Pretreatment with a calcium channel blocker, Ni^{2+}, partially inhibited caffeine-induced Ca^{2+} release in endothelial cells exposed to 0.3 mM $[Mg^{2+}]_o$, suggesting that filling or emptying of caffeine-sensitive intracellular Ca pools may be associated with $[Ca^{2+}]_o$ entry (Schilling & Elliott, 1992). Such Ca^{2+} movements across the plasma membrane in endothelial cells may be regulated by $[Mg^{2+}]_o$. However, irrespective of the precise pathway(s) of the signal transduction, the elevated $[Ca^{2+}]_i$ clearly suggests that a caffeine-mediated (or Ca^{2+}-induced) Ca^{2+} release participates in regulation of $[Ca^{2+}]_i$ in endothelial cells, which appears to be modulated by Mg^{2+}. It is thus possible that changes in $[Mg^{2+}]_o$, which have been noted in human subjects (Altura *et al.*, 1992), could induce substantial potentiation or inhibition of endothelial functions by the mechanisms described here.

This work was supported in part by NIAAA Research Grant AA-08674.

References

ALTURA, B.T. & ALTURA, B.M. (1987). Endothelium-dependent relaxation in coronary arteries requires magnesium ions. *Br. J. Pharmacol.*, **91**, 449–451.

ALTURA, B.T., SHIREY, T., YOUNG, C.C., HITI, J., DELL'ORFANO, K., HANDWERKER, S.M. & ALTURA, B.M. (1992). A new method for the rapid determination of ionized Mg^{2+} in whole blood, serum and plasma. *Methods Findings Exp. Clin. Pharmacol.*, **14**, 297–304.

BUCHAN, K.W. & MARTIN, W. (1991). Bradykinin induces elevations of cytosolic calcium through mobilization of intracellular and extracellular pools in bovine aortic endothelial cells. *Br. J. Pharmacol.*, **102**, 35–40.

DOWNES, C.P., MUSSAT, M.C. & MICHELL, R.H. (1982). The inositol trisphosphate phosphomonoesterase of the human erythrocyte membrane. *Biochem. J.*, **203**, 169–177.

FURCHGOTT, R.F. & VANHOUTTE, P.M. (1989). Endothelium-derived relaxing and contracting factors. *FASEB J.*, **3**, 2007–2018.

KARAKI, H. & WEISS, G.B. (1988). Calcium release in smooth muscle. *Life Science*, **42**, 111–122.

MONCADA, S., PALMER, R.M. & HIGGS, E.A. (1991). Nitric oxide: physiology, pathophysiology, and pharmacology. *Pharmacol. Rev.*, **43**, 109–142.

SAGE, S.O., ADAMS, D.J. & BREEMEN, C.V. (1989). Synchronized oscillations in cytoplasmic free calcium concentration in confluent bradykinin-stimulated bovine pulmonary artery endothelial cell monolayers. *J. Biol. Chem.*, **264**, 6–9.

SCHILLING, W.P. & ELLIOTT, S.J. (1992). Ca^{2+} signalling mechanisms of vascular endothelial cells and their role in oxidant-induced endothelial cell dysfunction. *Am. J. Physiol.*, **262**, H1617–H1630.

ZHANG, A., CHENG, T.P.-O. & ALTURA, B.M. (1992). Magnesium regulates intracellular free ionized calcium concentration and cell geometry in vascular smooth muscle cells. *Biochem. Biophys. Acta, Mol. Cell Res.*, **1134**, 25–29.

(Received February 22, 1993
Accepted March 16, 1993)

Br. J. Pharmacol. (1993), **109**, 293–298 © Macmillan Press Ltd, 1993

Differential effects of cocaine and cocaethylene on intracellular Ca^{2+} and myocardial contraction in cardiac myocytes

Zhihua Qiu & [1]James P. Morgan

Harvard-Thorndike Laboratory and Department of Medicine (Cardiovascular Division), Beth Israel Hospital, Harvard Medical School, 330 Brookline Avenue, Boston, MA, U.S.A.

1 Isolated cardiac myocytes of the ferret were used to investigate the influence of cocaine and cocaethylene on the intracellular Ca^{2+} transient indicated by the indo-1 405/480 nm ratio signal, and peak cell shortening.

2 Both cocaine and cocaethylene produced significant decreases in peak intracellular Ca^{2+} and peak cell shortening in a dose-dependent manner. Of interest, (1) the minimally effective dose of cocaethylene was ten fold lower (10^{-8} M versus 10^{-7} M) than that of cocaine; (2) the log EC_{50} of cocaethylene was -5.99 ± 0.13 (1.0×10^{-6} M), which was about ten fold lower than that of cocaine (-5.02 ± 0.11, 9.6×10^{-6} M); and (3) 1×10^{-4} M cocaethylene decreased the contraction amplitude by $71 \pm 7\%$, while the same concentration of cocaine decreased the amplitude only by $55 \pm 5\%$, indicating that cocaethylene is more potent than cocaine.

3 The negative inotropic effects of either cocaine or cocaethylene could be overcome by noradrenaline ($\sim 5\,\mu$M) or calcium.

4 In contrast to cocaine, cocaethylene shifted the peak $[Ca^{2+}]_i$-peak shortening relationship downward, indicating that cocaethylene decreased myofilament Ca^{2+}-responsiveness.

5 These data indicate that both cocaine and cocaethylene act directly on cardiac myocytes to produce a negative inotropic effect that is due to decreased Ca^{2+} availability. In contrast to cocaine, cocaethylene produces more potent inhibition by an additional action to decrease myofilament Ca^{2+}-responsiveness.

Keywords: Cocaine, cocaethylene; myocyte; indo-1; intracellular Ca^{2+}; myofilament Ca^{2+}-responsiveness

Introduction

The acute toxic effects of cocaine on the cardiovascular system are widely recognized, and an increased incidence of cardiovascular morbidity and sudden cardiac death has been associated with cocaine abuse (Cregler & Herbert, 1986; Isner *et al.*, 1986; Tazelaar *et al.*, 1987; Karch & Billingham, 1988). Concurrent use of alcohol is common among cocaine abusers, as indicated by recent prevalence studies (Weiss *et al.*, 1988). It has been reported that more than 50% of cocaine abusers provide a history of lifetime alcohol abuse or dependence (Weiss *et al.*, 1988), and about 30% of cocaine users drink ethanol on almost every occasion of cocaine use (Jones, 1987). Co-abuse of these two drugs may be explained by the observation that ethanol can potentiate the stimulant effects of cocaine in some patients (Masur *et al.*, 1989). However, co-abuse of ethanol and cocaine increases the cardiovascular manifestation of cocaine, as suggested by a three to five fold increase in heart rate over that observed after administration of either drug alone (Foltin & Fischman, 1989). Moreover, an epidemiological study reported that concurrent use of ethanol produces an eighteen fold increase in the risk of cocaine-related sudden death (Rose *et al.*, 1990).

Cocaine is rapidly hydrolyzed by plasma and liver esterases to its metabolites (Stewart *et al.*, 1979; Wilkinson *et al.*, 1980; Barnett *et al.*, 1981). Some cocaine metabolites have pharmacological activity in animals. Cocaethylene, the ethyl homologue of cocaine, is a pharmacologically-active cocaine metabolite found in cocaine users who simultaneously consume cocaine and ethanol (Elsworth *et al.*, 1990; Rose *et al.*, 1990; Hearn *et al.*, 1991a). The transesterification of cocaine and ethanol to cocaethylene takes place in the liver and represents a novel metabolic reaction. Cocaethylene has been detected in postmortem blood, liver, and neurological tissues, in concentrations equal to and sometimes exceeding those of cocaine (Rafla *et al.*, 1979; Smith, 1984; Rose *et al.*, 1990; Hearn *et al.*, 1991a). Comparison of the LD_{50} in Swiss-Webster mice suggests that cocaethylene is more potent in mediating lethality than cocaine (Hearn *et al.*, 1991b). However, the direct effects of cocaethylene on mammalian cardiac myocytes have not yet been described.

The purpose of the present study was to compare the effects of cocaine and cocaethylene on excitation-contraction coupling in single myocytes loaded with the Ca^{2+}-indicator, indo-1.

Methods

Myocyte isolation

Single cardiac myocytes were isolated from the left ventricle of ferret hearts (Copelas *et al.*, 1987). Briefly, the left ventricle, which was separated from the atria and right ventricle, was sliced into 4×4 mm pieces, washed three times with calcium-free solution, and then digested by stirring in a beaker under an oxygen tension of 100 mmHg at 35°C. The composition of the dispersion solution was (mM): NaCl 75, KCl 2.4, $MgCl_2$ 1.0, HEPES 10, sucrose 58, dextrose 10, $NaHCO_3$ 5, L-glutamic acid 2.5, pH 6.96 with 160 u ml^{-1} collagenase II (Worthington Biochemical, Malvern, Pennsylvania, U.S.A.) and 0.6 mg ml^{-1} bovine serum albumin (Sigma Chemical Company, St. Louis, Missouri, U.S.A.). The solution was decanted and replaced four times at 20 min intervals. Myocytes were harvested by filtration through 230 μm nylon mesh, followed by low speed centrifugation, and were then re-suspended in Medium 199. The yield of rod-shaped myocytes (80%) in the cell suspension with clear cross-striations that excluded trypan blue was routinely $>90\%$.

[1] Author for correspondence at: Cardiovascular Division, Beth Israel Hospital, 330 Brookline Avenue, Boston, MA 02215, U.S.A.

Intracellular Ca^{2+} measurement

For measurement of intracellular Ca^{2+}, myocytes were loaded with indo-1 by incubation with the acetoxymethyl ester of indo-1 (indo-1/AM) at room temperature. Briefly, 2 ml of cell suspension (approximately 10^6 myocytes ml^{-1}) were incubated with 0.1 ml of a 10 μM indo-1/AM stock solution consisting of 1.0 ml of 1 mM indo-1/AM in dimethylsulphoxide (Sigma Chemical Company) with 0.2 ml 25% (w.t/w.t) Pluronic F-127 (BASF, Wyandotte, Michigan, U.S.A.) in dimethylsulphoxide, and 8.8 ml foetal bovine serum (Hyclone Laboratories, Logan, Utah, U.S.A.) (Spurgeon *et al.*, 1990). The stock solution of indo-1/AM was 100 μM. The final concentration of indo-1/AM in the cell suspension was approximately 5 μM. The measurement of intracellular Ca^{2+} was performed with the fluorescent Ca^{2+} probe indo-1. A 75 watt continuous output xenon arc (Nikon) was used as a source of illumination for epi-fluorescence. An interferences filter was used to select a wavelength of 360 ± 5 nm (Nikon) to excite indo-1 and a 380 long-pass dichroic mirror (Omega) to direct the excitation light to a × 40, 1.3 NA u.v. objective (Nikon). After excitation at 360 nm, a 455 nm dichroic mirror split the fluorescence emission beam, and the emissions at 405 nm (the emission peak of the Ca^{2+}-bound form of the dye) and 480 nm (the emission peak of the Ca^{2+}-free form of the dye) was directed to two photomultiplier tubes (Nikon). Flourescent light was collected from the microscopic field, which contained a single myocyte. Photomultiplier outputs were passed as current to an analogue divider for instantaneous computation of the 405/580 nm ratio (Photoscan; Nikon). Fluorescence signals at 405 nm emission and 480 nm emission were stored in a personal computer (NEC, Tokyo, Japan) for data processing and analysis throughout each run, so that the time course of alteration in the Ca^{2+} transient could be followed. However, for optimal kinetic analysis, postprocessing of data was carried out. The fluorescent data collection rate for all experiments was 100 Hz. This was sufficient to resolve the rising and falling phases of the Ca^{2+} transient. The cytosolic Ca^{2+} transient was represented by the 405/480 nm ratio of the fluorescent signal.

Contractility measurement

The cell was illuminated with red (645 nm) light through the normal bright-field illumination optics of the microscope to simultaneously measure cell shortening and intracellular Ca^{2+}. Cardiac myocytes were superfused at 1 ml min^{-1} with medium containing (mM): NaCl 120, KCl 5.9, $MgCl_2$ 1.2, NaH_2PO_4 1.2, $NaHCO_3$ 25, dextrose 11.5, and $CaCl_2$ 2.5 at pH 7.4. The myocytes were maximally stimulated electrically with platinum field electrodes at 0.5 Hz pulses of 5 ms duration. All the experiments were performed at room temperature (23°C) in order to minimize compartmentalization of the Ca^{2+} probe indo-1/AM into intracellular organelles. However, it is important to note that similar results were obtained with 10^{-4} M cocaine at room temperature and at 37°C in the presence of 0.5 mM probenecid (Sigma). Changes in the contractile state of individual myocytes were assessed by the use of a phase-contrast microscope video motion detector system through measuring the amplitude of cell shortening. The cell contractility was expressed as a percentage of the baseline values.

Drugs

A stock solution of cocaine, 10^{-1} M (purchased from Mallinckrodt, St. Louis, Missouri, U.S.A.), was obtained from the Beth Israel Hospital pharmacy dissolved in a diluent containing 0.5% chlorobutanol. In the volumes added to the bath in these experiments, the diluent had no effect on the amplitude or time course of the intracellular Ca^{2+} transient or cell contraction. The metabolite of cocaine and ethanol, (−)-cocaethylene fumarate, was obtained from the National Institute of Drug Abuse, Research Technology Branch of the Division of Preclinical Research, dissolved in physiological salt solution. Solutions were freshly made just before the experiment.

Statistics

Data are expressed as means ± s.e.mean. Results were analyzed by paired Student's t test for data from the same myocytes, and unpaired t test for data from different myocytes. Statistical significance was set at $P<0.05$.

Results

Effects of cocaine on the amplitude of intracellular Ca^{2+} and contraction

Figure 1 shows representative tracings of the intracellular Ca^{2+} transient and cell shortening under the influence of different concentrations of cocaine. Cocaine decreased the amplitude of contraction (peak cell shortening), as well as peak intracellular Ca^{2+}, in a dose-dependent manner. Maximal rates of cell shortening and relaxation were also significantly reduced by cocaine in a dose-dependent manner (Table 1). These results suggest that cocaine inhibits myocardial contractility, presumably by reducing the amplitude of the intracellular Ca^{2+} transient. To test this hypothesis, myocytes were exposed to the Ca^{2+}-dependent inotropic drug noradrenaline (5 μM) during exposure to cocaine. Noradrenaline overcame the inhibitory effects of 1×10^{-4} M cocaine by increasing the peak intracellular Ca^{2+}, thereby enhancing the amplitude of contraction (Figure 2, right-hand panel), and indirectly supporting the hypothesis above.

Comparison of the effects of cocaine with those of cocaethylene

Like cocaine, cocaethylene produced a marked decrease in peak shortening that was associated with a similar decrease in peak intracellular Ca^{2+} (Figure 3a). The inhibitory action on cardiac myocytes of both cocaine and cocaethylene (data not shown) could be overcome by the use of either noradrenaline or calcium. Of interest, (1) the minimally effective dose of cocaethylene was ten fold less (10^{-8} M versus 10^{-7} M) than that of cocaine; (2) the log EC_{50} (Carpenter, 1986) of cocaethylene was -5.99 ± 0.13 (1.0×10^{-6} M), which was about ten fold lower than that of cocaine (-5.02 ± 0.11, 9.6×10^{-6} M) ($P<0.001$, Figure 3c), and (3) at the same concentration (1×10^{-4} M), cocaethylene produced more pronounced negative inotropic effects than cocaine (Figure 3b, and Table 1). Typical continuous recordings of cell shortening under the influence of cocaine and/or cocaethylene from the same myocyte (Figure 3b) clearly show that cocaethylene produces a much more pronounced negative inotropic effect than cocaine at equimolar concentrations, suggesting that cocaethylene is more potent than cocaine as a myocardial depressant. In Figure 3c, the slopes of the concentration-response curves are unusually shallow, and the explanations for this remain unknown.

Effects of cocaine and cocaethylene on myofilament Ca^{2+} responsiveness

Besides the amplitude of intracellular Ca^{2+}, the myofilament Ca^{2+}-responsiveness also contributes to myocardial contractility. Any agent that decreases the myofilament Ca^{2+}-responsiveness would reduce the amplitude of contraction. Therefore, the more pronounced negative inotropic effects of cocaethylene (Figure 3) may possibly be caused by cocaethylene-induced decrease of the myofilament Ca^{2+}-responsiveness. To test this hypothesis, peak $[Ca^{2+}]_i$-peak

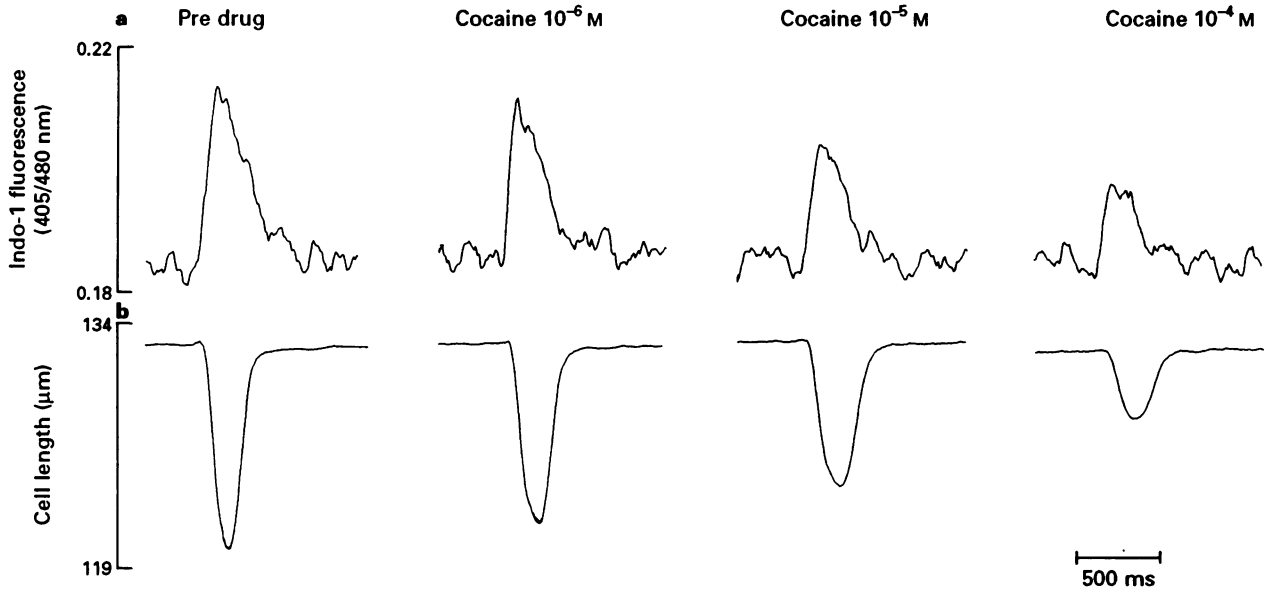

Figure 1 Tracings showing the effects of different concentrations of cocaine on the intracellular Ca^{2+} transient (a) and peak cell shortening (b). The concentrations were increased in a manner of accumulation. Tracings were from the same myocyte, and are representative of 12 similar experiments. Cell was stimulated at 0.5 Hz and at room temperature.

Table 1 Cocaine (Coc)- and cocaethylene (CEt)-induced changes in the intracellular Ca^{2+} transient and contraction (% of control) in single cardiac myocytes from the ferret

	T_{50}	S_{50}	*ROR*	*ROS*
Coc 10^{-6} M ($n = 17$)	90 ± 3	104 ± 3	78 ± 7	84 ± 8
CEt 10^{-6} M ($n = 7$)	93 ± 9	96 ± 3	72 ± 25	71 ± 4*
Coc 10^{-5} M ($n = 13$)	93 ± 4	106 ± 4	62 ± 9	72 ± 13
CEt 10^{-5} M ($n = 7$)	98 ± 8	99 ± 3	55 ± 4	54 ± 2*
Coc 10^{-4} M ($n = 13$)	101 ± 7	105 ± 4	39 ± 5	41 ± 6
CEt 10^{-4} M ($n = 7$)	106 ± 10	106 ± 6	30 ± 4*	27 ± 3*

Values are means ± s.e.mean. T_{50}, time from the beginning of the stimulation to 50% decline from peak intracellular Ca^{2+}; S_{50}, time from the beginning of the stimulation to 50% decline from peak shortening; ROR, maximum rate of relaxation of cell shortening; ROS, maximum rate of shortening of cell shortening.
*$P < 0.05$ compared to the corresponding effects of cocaine.

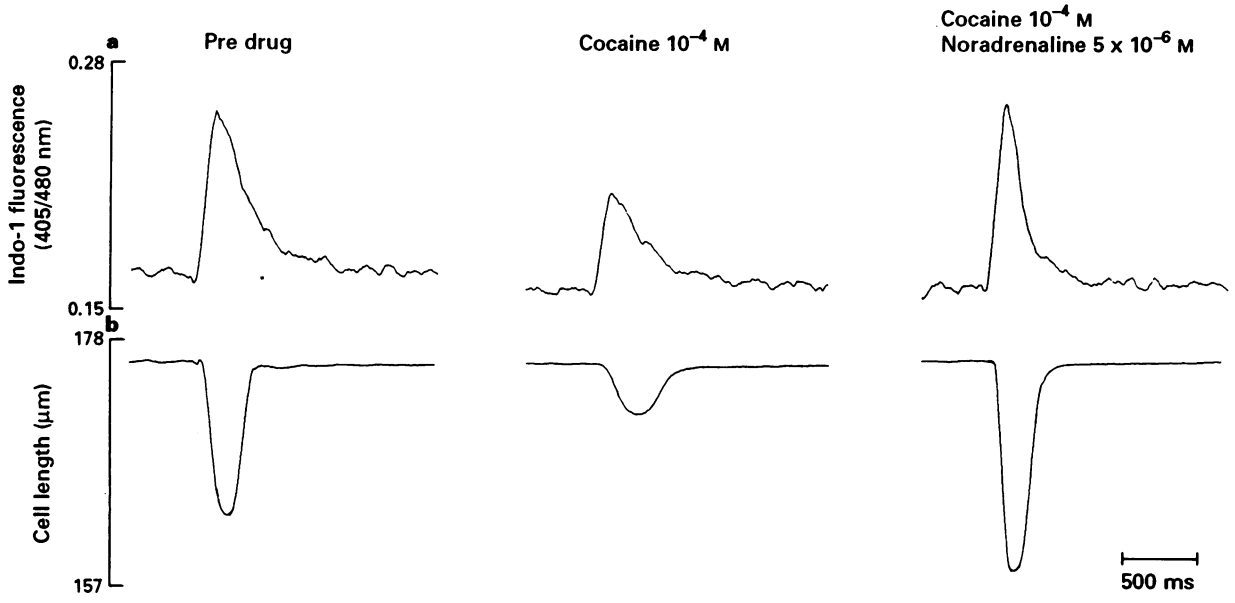

Figure 2 Tracings showing effect of noradrenaline on the intracellular Ca^{2+} transient (a) and cell peak shortening (b) in the presence of cocaine. Left panel, control; middle panel, in the presence of 1×10^{-4} M cocaine; right panel, in the presence of 1×10^{-4} M cocaine plus 5×10^{-6} M noradrenaline. Tracings are representative of five similar experiments. Cell was stimulated at 0.5 Hz and at room temperature.

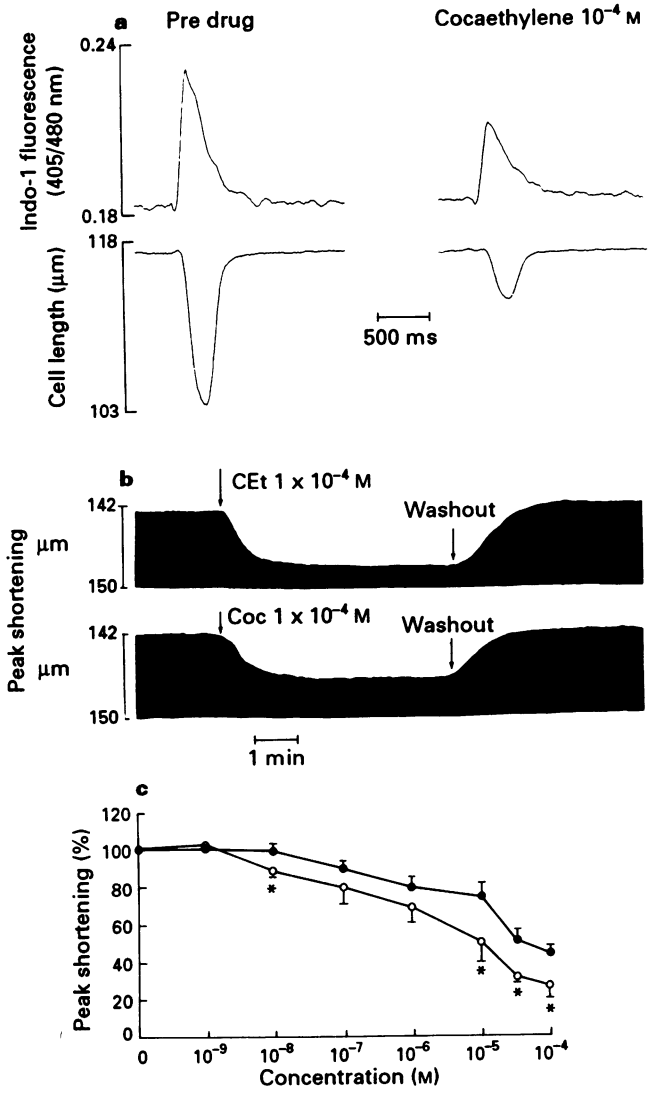

Figure 3 Effect of cocaethylene on the intracellular Ca^{2+} transient and cell contraction. (a) Effects on the intracellular Ca^{2+} transient and peak cell shortening (fron nine similar experiments); (b) comparisons of the effects of the same concentration of cocaine versus cocaethylene on peak cell shortening (data were from the same myocyte); (c) comparisons of the concentration-response curves of cocaine (●) versus cocaethylene (○) on the effect of peak cell shortening ($n = 6$).

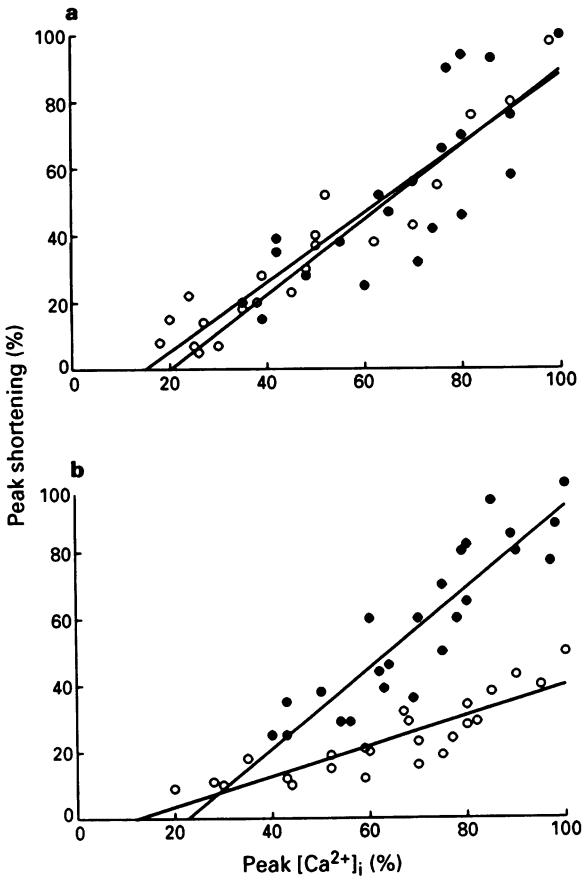

Figure 4 Comparisons of the effects of cocaine or cocaethylene on the peak $[Ca^{2+}]_i$-peak shortening relationship. (a) Effects of 1×10^{-4} M cocaine ($n = 7$); (b) effects of 1×10^{-4} M cocaethylene ($n = 8$). The maximal responses were considered as 100, and all other values were referred to 100. The changes of peak $[Ca^{2+}]_i$ were induced by increasing the $[Ca^{2+}]_o$. (●) Control values; (○) values in the presence of cocaine or cocaethylene.

shortening curves were determined first in the absence, then in the presence, of cocaine or cocaethylene. Peak $[Ca^{2+}]_i$ was increased by raising $[Ca^{2+}]_o$ from 2 to 5 and then to 8–10 mM. Cocaine did not shift the peak $[Ca^{2+}]_i$-peak shortening relationship (Figure 4a), whereas cocaethylene substantially shifted the peak $[Ca^{2+}]_i$-peak shortening relationship downwards (Figure 4b). These results suggest that, in contrast to cocaine, cocaethylene produced Ca^{2+}-desensitizing effects, which may, at least partially explain its more pronounced negative inotropic action.

Discussion

This is the first study comparing the cardiac effects of cocaine to those of its active metabolite, cocaethylene, at the cellular level. Our results indicate that the negative inotropic effect of cocaethylene is due to (1) a decrease of peak intracellular Ca^{2+} availability (Figure 3a), and (2) a decrease in myofilament Ca^{2+}-responsiveness (Figure 4b). In contrast, the negative inotropic effect of cocaine appears to be due to decreased intracellular $[Ca^{2+}]_i$ alone, with no obvious effect on myofilament Ca^{2+}-responsiveness.

The cellular mechanism of cocaethylene appears to reflect the myocardial effects of both cocaine and ethanol. Cocaine has two primary pharmacological actions on the cardiovascular system. First, it blocks the re-uptake of catecholamines at the presynaptic level in the central and peripheral nervous systems (Ritchie & Greene, 1985; Billman, 1990; Isner & Chokshi, 1991). Second, it reduces the inward Na^+ current by inhibiting the sodium channel in the sarcolemma, producing a local anaesthetic effect (Hale *et al.*, 1989; Przywara & Dambach, 1989; Billman, 1990). Reduction of the inward Na^+ current (Matthews & Collins, 1983; Reith *et al.*, 1986; Reiter, 1988) would reduce the subsequent inward Ca^{2+} current (Reiter, 1988; Stewart *et al.*, 1991). The negative inotropic effect of cocaine on cardiac muscle from a variety of different mammalian species appears to be predominantly produced by the local anaesthetic action. In addition, it is likely that cocaine may also directly inhibit the sarcolemmal voltage-sensitive Ca^{2+} channels (Stewart *et al.*, 1991). These actions would lead to the decreases of (1) trans-sarcolemmal Ca^{2+} entry, (2) Ca^{2+} loading of the sarcoplasmic reticulum, and (3) $[Ca^{2+}]_i$ available for activation of the contractile apparatus (Stewart *et al.*, 1991). These mechanisms would explain the results of the present study, since the dose-dependent decrease in contractile function produced by cocaine correlated with a progressive decrease in the amplitude of the $[Ca^{2+}]_i$ transients.

It has been established that ethanol depresses myocardial contractility in man and experimental animals, both *in situ* and in isolated heart muscle. Recent studies indicate that (1) the effects of ethanol in amounts routinely ingested by man, i.e., those leading to clinically relevant ethanol plasma concentrations (0.1–0.15%, vol/vol), produce a negative inotropic effect that is predominantly due to decreased myofilament Ca^{2+}-responsiveness (Schulman *et al.*, 1989; Danziger *et al.*, 1991). Higher concentrations (1–5%, vol/vol) depress both the amplitude of the Ca^{2+}-transient as well as alter myofilament Ca^{2+}-responsiveness (Katz, 1982; Polimeni *et al.*, 1983; Taraschi & Rubin 1985). Our results suggest that the negative inotropic effect of cocaethylene was due to both actions, in contrast to cocaine, which may explain its greater potency as a negative inotropic agent.

In addition to effects on intracellular Ca^{2+} availability and on myofilament Ca^{2+} responsiveness, drugs may produce negative inotropic effects through a direct action on sarcoplasmic reticular Ca^{2+} handling. Such an effect did not appear to be important with regard to the actions of either cocaine or cocaethylene in our experiments. All drugs studied to date that affect Ca^{2+} handling by the sarcoplasmic reticulum have been shown to alter the duration of the Ca^{2+} transient. As shown in Figures 1 and 3, and Table 1, neither drug affected the time course of the $[Ca^{2+}]_i$ transient; therefore, it does not appear likely that cocaine or cocaethylene directly affect sarcoplasmic reticular Ca^{2+} handling. However, both drugs may decrease Ca^{2+} loading of this organelle if the inward calcium current is inhibited.

Most of the previous studies of the effects of cocaine on cardiac function have been carried out *in vivo* (Hardman *et al.*, 1965; Levy & Blattberg, 1978) or with multicellular cardiac muscle (Chang & Lee, 1973; McCulloch *et al.*, 1974; Masuda & Levy, 1985) or Purkinje fibre preparations (Weidmann, 1955). The direct cardiovascular effects of cocaine are difficult to evaluate in these studies because the drug acts in part through its effects on catecholamine re-uptake and metabolism. The present study represents the first direct evidence that cocaine and cocaethylene can alter the Ca^{2+}-dependent steps of excitation-contraction coupling in adult mammalian cardiomyocytes. We previously reported that cocaine produced positive inotropic effects at concentrations of 10^{-6} to 10^{-5} M, and negative inotropic effects only at concentrations $\geq 1 \times 10^{-4}$ M in ferret papillary muscles with intact nerve endings (Perreault *et al.*, 1990). In the present study, we found negative inotropic actions on single myocytes over the entire effective dose-range, indicating that the direct action of cocaine on myocardial cells is to decrease contractility. The result that noradrenaline can reverse the negative inotropic effects of cocaine (Figure 2) and cocaethylene (data not shown) suggests that, in multicellular preparations, the negative inotropic effects of cocaine may be overcome by cocaine-induced release of catecholamines. Therefore, the local concentrations of cocaine and catecholamine determine whether the net inotropic effect is negative or positive. In the case of cocaethylene, a higher incidence of clinical cardiac toxicity might be expected due to its greater potency as a negative inotropic agent.

Partial support was provided by NIH grant DA-06306. The authors express their appreciation to Dr William Grossman for his support and many useful suggestions, and to Ms Susan Byers for her assistance in the preparation of this manuscript.

References

BARNETT, G., HAWKS, R. & RESNICK, R. (1981). Cocaine pharmacokinetics in humans. *J. Ethnopharmacol.*, **3**, 353–366.

BILLMAN, G.E. (1990). Mechanisms responsible for the cardiotoxic effects of cocaine. *FASEB J.*, **4**, 2469–2475.

CARPENTER, J.R. (1986). A method for presenting and comparing dose-response curves. *J. Pharmacol. Methods*, **15**, 283–303.

CHANG, C.C. & LEE, M.C. (1973). Studies of the effect of phenoxybenzamine on the uptake of noradrenaline and response to the sympathetic stimulation of rat heart. *Arch. Int. Pharmacodyn. Ther.*, **201**, 400–414.

COPELAS, L., BRIGGS, M., GROSSMAN, W. & MORGAN, J.P. (1987). A method for recording isometric tension development by isolated cardiac myocytes: transducer attachment with fibrin glue. *Eur. J. Physiol.*, **408**, 315–317.

CREGLER, P.H. & HERBERT, M. (1986). Medical complications of cocaine abuse. *N. Engl. J. Med.*, **315**, 1495–1500.

DANZIGER, R.S., SAKAI, M., CAPOGROSSI, M.C., SPURGEON, H.A., HANSFORD, R.G. & LAKATTA, E.G. (1991). Ethanol acutely and reversibly suppresses excitation-contraction coupling in cardiac myocytes. *Circ. Res.*, **68**, 1660–1668.

ELSWORTH, J.D., BRADBERRY, C.W., TAYLOR, J.R., WALKER, J.R., HEARN, W.L., JATLOW, P. & ROTH, R.H. (1990). Cocaethylene is a pharmacologically active metabolite of cocaine formed after combined intake of cocaine and ethanol. *Neurosci. Abstr.*, **16**, 310.11.

FOLTIN, R.W. & FISCHMAN, M.W. (1989). Ethanol and cocaine interactions in humans: cardiovascular consequences. *Pharmacol. Biochem. Behav.*, **31**, 877–883.

HALE, S.L., LEHMANN, M.H. & KLONER, R.A. (1989). Electrocardiographic abnormalities after acute administration of cocaine in the rat. *Am. J. Cardiol.*, **63**, 1529–1530.

HARDMAN, J.G., MAYER, S.E. & CLARK, B. (1965). Cocaine potentiation: the cardiac inotropic and phosphorylase response to catecholamines as related to the uptake of ^{3}H-catecholamines. *J. Pharmacol. Exp. Ther.*, **150**, 341–348.

HEARN, W.L., FLYNN, D.D., HIME, G.W., ROSE, S., CONFINO, J.C., MANTERO-ANTIENZA, E., WETLI, C.W. & MASH, D.C. (1991a). Cocaethylene: a unique cocaine metabolite displays high affinity for the dopamine transporter. *J. Neurochem.*, **56**, 698–701.

HEARN, W.L., ROSE, S., WAGNER, J., CIARLEGLIO, A. & MASH, D.C. (1991b). Cocaethylene is more potent than cocaine in mediating lethality. *Pharmacol. Biochem. Behav.*, **39**, 531–533.

ISNER, J.M. & CHOKSHI, S.K. (1991). Cardiovascular complications of cocaine. *Curr. Probl. Cardiol.*, **64**, 94–123.

ISNER, J.M., ESTES, N.A.M. III, THOMPSON, P.D., COSTANZONORDIN, M.R., SUBRAMANIAN, R., MILLER, G., KATSAS, G., SWEENEY, K. & STURNER, W.Q. (1986). Acute cardiac events temporally related for cocaine abuse. *N. Engl. J. Med.*, **315**, 1438–1443.

JONES, R.T. (1987). Psychopharmacology of cocaine. In *Cocaine: A Clinician's Handbook*. ed. Washington, A.M. & Gold, M.S. pp. 55–72. New York: Guilford.

KARCH, S.B. & BILLINGHAM, M. (1988). The pathology and etiology of cocaine-induced heart disease. *Arch. Pathol. Lab. Med.*, **112**, 225–230.

KATZ, A.M. (1982). Effects of ethanol on ion transporting muscle membranes. *Fed. Proc.*, **41**, 2456–2458.

LEVY, M.N. & BLATTBERG, B. (1978). The influence of cocaine and desipramine on the cardiac responses to exogenous and endogenous norepinephrine. *Eur. J. Pharmacol.*, **48**, 37–49.

MASUDA, Y. & LEVY, M.N. (1985). Responses of the atrial myocardium to cardiac sympathetic nerve stimulation. *Am. J. Physiol.*, **249** (Heart Circ. Physiol., 18), H207–H211.

MASUR, J., SOUZA-FORMIGONI, M.L.O. & PIRES, M.L.N. (1989). Increased stimulatory effects by the combined administration of cocaine and alcohol in mice. *Alcohol*, **6**, 181–182.

MATTHEWS, J.C. & COLLINS, A. (1983). Interactions of cocaine and cocaine congeners with sodium channels. *Biochem. Pharmacol.*, **32**, 455–460.

MCCULLOCH, M.W., RAND, M.J. & STORY, D.F. (1974). Resting and stimulation-induced efflux of tritium from guinea-pig atria incubated with ^{3}H-noradrenaline. *Clin. Exp. Pharmacol. Physiol.*, **1**, 275–289.

PERREAULT, C.L., HAGUE, N.L., RANSIL, B.J. & MORGAN, J.P. (1990). The effects of cocaine on intracellular Ca^{2+} handling and myofilament Ca^{2+} responsiveness of ferret ventricular myocardium. *Br. J. Pharmacol.*, **101**, 679–685.

POLIMENI, P.I., OTTEN, M.D. & HOESCHEN, L.E. (1983). In vivo effects of ethanol on the rat myocardium: evidence for a reversible, non-specific increase of sarcolemmal permeability. *J. Mol. Cell. Cardiol.*, **15**, 113–122.

PRZYWARA, D.A. & DAMBACH, G.E. (1989). Direct actions of cocaine on cardiac cellular electrical activity. *Circ. Res.*, **65**, 185–192.

RAFLA, F.K. & EPSTEIN, R.L. (1979). Identification of cocaine and its metabolites in human urine in the presence of ethyl alcohol. *J. Anal. Toxicol.*, **3**, 56–63.

REITER, C.A. (1988). Calcium mobilization and cardiac inotropic mechanisms. *Pharmacol. Rev.*, **40**, 189–218.

REITH, M.E.A., KIM, S.S. & LAJTHA, A. (1986). Structure requirements for cocaine congeners to interact with [^{3}H] batrachotoxinin A 20-α-benzoate binding sites on sodium channels in mouse brain synaptosomes. *J. Biol. Chem.*, **261**, 7300–7305.

RITCHIE, J.M. & GREENE, N.M. (1985). Local anesthetics. In *Pharmacological Basis of Therapeutics*. ed. Goodman, L.S. & Gilman, A. p. 309. New York: Macmillan.

ROSE, S., HEARN, W.L., HIME, G.W., WETLI, C.V., RUTTENBER, A.J. & MASH, D.C. (1990). Cocaine and cocaethylene concentrations in human post mortem cerebral cortex. *Neurosci. Abstr.*, **16**, 11.6.

SCHULMAN, S.P., GERSTEMBLITH, G. & LAKATTA, E.G. (1989). Functional and arrhythmogenic effects of ethanol withdraw in the isolated rat heart. *Clin. Res.*, **37**, 522A (Abstract).

SMITH, R.M. (1984). Ethyl esters of arylhydroxy- and arylhydroxymethoxycocaines in the urines of simultaneous cocaine and ethanol users. *J. Anal. Toxicol.*, **8**, 38–42.

SPUREGON, H.A., STERN, M.D., BAARTZ, G., RAFFAELI, S., HANSFORD, R.G., TALO, E., LAKATTA, E.G. & CAPOGROSSI, M.C. (1990). Simultaneous measurements of Ca^{2+} contraction and potential in cardiac myocytes. *Am. J. Physiol.*, **256**, (Heart Circ. Physiol., 27), H574–H586.

STEWART, D.J., INABA, T., LUCASSEN, M. & KALOW, W. (1979). Cocaine metabolism: cocaine and norcocaine hydrolysis by liver and serum esterases. *Clin. Pharmacol Ther.*, **25**, 464–468.

STEWART, G., RUBIN, E. & THOMAS, A.P. (1991). Inhibition by cocaine of excitation-contraction coupling in isolated cardiomyocytes. *Am. J. Physiol*, **260**, (Heart Circ. Physiol., 29), H50–H57.

TARASCHI, T.F. & RUBIN, E. (1985). Biology of disease: effects of ethanol on the chemical and structure properties of biological membranes. *Clin. Invest.*, **52**, 120–131.

TAZELAAR, H.D., KARCH, S.B., STEPHENS, B.G. & BILLINGHAM, M.E. (1987). Cocaine and the heart. *Hum. Pathol.*, **18**, 195–199.

WEIDMANN, S. (1955). Effects of calcium ions and local anesthetics on electrical properties of Purkinje fibers. *J. Physiol.*, **129**, 568–582.

WEISS, R.D., MIRIN, S.M., GRIFFIN, M.L. & MICHAEL, J.L. (1988). Psychopathology in cocaine abusers: changing trends. *J. Nerv. Ment. Dis.*, **176**, 719–725.

WILKINSON, P., VAN DYKE, C., JATLOW, P., BARASH, P. & BYCK, H. (1980). Intranasal and oral cocaine kinetics. *Clin. Pharmacol. Ther.*, **27**, 386–394.

(Received September 15, 1992
Revised November 17, 1992
Accepted November 18, 1992)

Br. J. Pharmacol. (1993), **109**, 299–307 © Macmillan Press Ltd, 1993

High-affinity uptake of noradrenaline in postsynaptic neurones

[1]S. Al-Damluji, L.Z. Krsmanovic & K.J. Catt

Endocrinology and Reproduction Research Branch, NICHD, National Institutes of Health, Bethesda, MD 20892, U.S.A.

1 Neurotransmitters released from nerve endings are inactivated by re-uptake into the presynaptic nerve terminals and possibly into neighbouring glial cells. While analysing the functional properties of α_1-adrenoceptors in the hypothalamus, we observed a high-affinity uptake process for noradrenaline in postsynaptic peptidergic neurones.

2 In primary hypothalamic cell cultures and in a hypothalamic neuronal cell line, [^{3}H]-prazosin bound with high affinity and was displaced by unlabelled prazosin in concentrations of 10^{-10} to 10^{-7} M. However, at concentrations of unlabelled prazosin above 10^{-7} M, there was a paradoxical increase in apparent [^{3}H]-prazosin binding.

3 Methoxamine, an α_1-adrenoceptor ligand that is not subject to significant neuronal uptake, displaced [^{3}H]-prazosin but did not cause the paradoxical increase in the apparent binding of [^{3}H]-prazosin. Cooling the cells to 4°C reduced the total amount of prazosin associated with the cells; under these conditions, methoxamine almost completely inhibited [^{3}H]-prazosin binding to the cells.

4 In the presence of desipramine (DMI), unlabelled prazosin displaced [^{3}H]-prazosin as before, but no paradoxical increase in apparent binding was seen above 10^{-7} M.

5 The paradoxical increase of [^{3}H]-prazosin binding was not observed in membrane preparations of hypothalamic neurones. These findings indicated that the paradoxical increase in apparent [^{3}H]-prazosin binding was due to a cellular uptake process that becomes evident at high concentrations of the ligand.

6 DMI (10^{-5} M) had no effect on the specific binding of [^{3}H]-prazosin. The presence of α_1-adrenoceptors was confirmed by binding of [^{125}I]-HEAT, but [^{3}H]-idazoxan (an α_2- ligand) did not bind to the cells.

7 The uptake of prazosin obeyed the Michaelis-Menten model, with similar K_m and V_{max} values in both types of cultures.

8 Noradrenaline was taken up with high affinity by both types of cultures. (±)-[^{3}H]-noradrenaline uptake was reduced by DMI and by excluding sodium from the medium, indicating that this process has some of the properties of uptake$_1$. (±)-[^{3}H]-noradrenaline uptake in the cell line was unaffected by testosterone.

9 The measured uptake of (−)-noradrenaline in the cell line was considerably increased by blockade of catechol-*O*-methyl-transferase and monoamine oxidase, suggesting that (−)-noradrenaline is metabolized to lipophilic products that escape across the plasma membrane.

10 Studies in rats, in which the noradrenaline isomer 6-hydroxydopamine was used, suggested that the postsynaptic uptake process is operative in hypothalamic CRH and vasopressin neurones *in vivo*.

11 The K_m for (−)-noradrenaline was within the range for the high affinity uptake$_1$ process in noradrenergic neurones. Uptake takes place in concentrations at which noradrenaline activates α_1-adrenoceptors. Removal of noradrenaline from the vicinity of the receptors may prevent desensitization, thus maintaining the responsiveness of postsynaptic neurones to the actions of the neurotransmitter.

Keywords: Catecholamines; noradrenaline; uptake; amine transport; postsynaptic neurones

Introduction

The hypothalamus contains high concentrations of adrenaline and noradrenaline (Vogt, 1954). The cell bodies of the noradrenergic neurones that innervate the hypothalamus are located in the brain stem (Sawchenko & Swanson, 1982; Cunningham & Sawchenko, 1988). Axons ascend in the ventral noradrenergic bundle and the nerve terminals form contacts with the postsynaptic peptidergic neurones in the hypothalamus (Hoffman *et al.*, 1982; Silverman *et al.*, 1985; Liposits *et al.*, 1986). Previous *in vivo* studies have demonstrated that α_1-adrenoceptors are abundant in the hypothalamus and participate in the physiological control of several neuroendocrine and reproductive functions (Leibowitz *et al.*, 1982; Barraclough & Wise, 1982; Muller, 1987; Cummings & Seybold, 1988; Al-Damluji, 1988; 1993). While studying the cellular and biochemical mechanisms of some of these physiological actions, we analysed the properties of α_1-adrenoceptors in cultured neonatal hypothalamic cells and in immortalised gonadotrophin-releasing hormone (GnRH) neurones. The latter cells possess many of the characteristics of differentiated hypothalamic neurones; they extend neurites, secrete the neurotransmitter GnRH in a characteristic pulsatile manner and possess fast sodium channels, synaptic membrane proteins and other neuronal (but not glial cell) markers (Mellon *et al.*, 1990; Krsmanovic *et al.*, 1991; Wetsel *et al.*, 1992). As expected, α_1-adrenoceptors were present in both the cultured neonatal cells and the GnRH cell line. However, we also detected a novel high-affinity uptake process for noradrenaline in these postsynaptic peptidergic cells. Preliminary studies suggest that the uptake process also operates *in vivo*. The postsynaptic uptake process shares some of the functional characteristics of the uptake$_1$ noradrenaline transporter that is located presynaptically in noradrenergic neurones (Axelrod, 1971; Graefe & Bonisch, 1989; Pacholczyk *et al.*, 1991).

[1] Author for correspondence at Clinical Neuroscience Branch, Building 10, Room 5N214, National Institutes of Health, Bethesda, MD 20892, U.S.A..

Methods

Hypothalamic cell cultures

Pregnant (15 days) Sprague-Dawley rats (Taconic Farms, New York, U.S.A.) were caged individually and given food and water *ad libitum*. The culture method used was a modification of previously described procedures (Wilkinson *et al.*, 1974; Loudes *et al.*, 1983; Shoemaker *et al.*, 1983; Clarke *et al.*, 1987). Within 24 h of birth, the neonatal rats were decapitated and the hypothalami were dissected under a microscope at the following borders: junction of anterior cerebral arteries anteriorly; caudal border of the mamillary bodies posteriorly and lateral sulci and perforating vessels dorsolaterally. The hypothalami were placed in ice-cold dissociation buffer consisting of (mM): NaCl 137, KCl 5, Na_2HPO_4 0.7, HEPES 25, gentamicin 0.1 g l^{-1}, pH 7.4. The hypothalami were then washed three times with 10 ml of the dissociation buffer, cut in half and incubated for 60 min at 37°C in dispersion solution consisting of 0.2% collagenase II (activity 149 u mg^{-1}), 0.4% BSA, 0.2% glucose and 0.05% DNAse I (activity 510 Kunitz units mg^{-1}) in dissociation buffer. The fragments were then dispersed by aspiration about 20 times into a sterile plastic Pasteur pipette and incubated for a further 30 min at 37°C. The tissues were again dispersed and the cells transferred to a sterile 50 ml tube via a sterile mesh with 200 μm pores. The cells were washed with dissociation buffer followed by culture medium, and were finally dispersed in fresh culture medium. The cell suspension was diluted to 1×10^6 cells ml^{-1} with culture medium and incubated in Costar 12-well plates at a density of 10^6 cells ml^{-1}, 2×10^6 cells/well, in a humidified atmosphere containing 5% CO_2 in air. Culture medium consisted of DMEM and F-12 (ratio 1:1) containing 10% heat-inactivated foetal calf serum, sodium bicarbonate 3.7 g l^{-1} and gentamicin 100 mg l^{-1}. Culture media were changed at 48 h intervals and the experiments were carried out four to eight days following culture.

Immortalised GnRH neuronal cells (GT1-1 cells; Mellon *et al.*, 1990), generously provided by Dr R.I. Weiner, were grown in the above culture medium in Corning 75 cm^2 flasks. When the cells reached confluence, they were dispersed by incubation for 5 min at 37°C with phosphate-buffered saline (PBS) containing 0.05% trypsin, 0.05% EDTA, 0.05% $NaHCO_3$, 0.02% DNAse I, 0.1% glucose and 0.01% gentamicin. The cell suspension was centrifuged for 10 min at 400 *g* and the supernatant discarded. The cells were washed once in culture medium and were then re-suspended in fresh medium at a density of 10^6 cells ml^{-1} and incubated in Costar 12-well plates (2×10^6 cells/well). Culture media were changed at 48 h intervals and the experiments were carried out four to eight days following culture.

[^{3}H]-prazosin binding and uptake

Binding studies were performed at 25°C (unless otherwise indicated) on the intact cells, using the α_1-adrenoceptor ligand, [^{3}H]-prazosin. Drugs were dissolved in 'binding medium' consisting of DMEM with 25 mM HEPES and 0.5×10^{-3} M sodium ascorbate, pH 7.4. The cells were washed twice with 1 ml binding medium and then incubated for 60 min in medium containing [^{3}H]-prazosin, alone or in combination with unlabelled drugs. At the end of the incubation period the cells were placed on ice and washed twice with 1 ml volumes of ice-cold binding medium. The cells were then solubilized with a warm solution of 0.1% sodium dodecyl sulphate and 0.1 M NaOH. Ten ml of scintillation liquid was added, mixed and then left to settle for 48 h before analysis in a β-spectrometer with an efficiency of 50%. Non-specific binding (NSB) was defined as binding in the presence of 10^{-6} M unlabelled prazosin, and represented 40–50% of the total bound radioactivity, which is similar to NSB in previous studies of α_1-adrenoceptors in cultured cells (Wikberg *et al.*, 1983; Cotecchia *et al.*, 1985). Specific binding was defined as total c.p.m. – NSB c.p.m.

An identical procedure to the above was used to study the binding of [^{125}I]-HEAT and [^{3}H]-idazoxan.

The experiments shown in Figure 3 were carried out as described above but the binding medium was Krebs-Ringer solution buffered either with 25 mM HEPES or 25 mM Tris, and did not contain DMEM or ascorbate.

[^{3}H]-prazosin binding to hypothalamic cell membranes

GT1-1 cells were grown in Corning 75 cm^2 flasks as described above. When confluence was reached, the cells were dispersed in 'binding buffer' consisting of PBS (pH 7.4) containing the following protease inhibitors: EDTA (1.3 mM); aprotinin (100 μg ml^{-1}); antipain (10 μg ml^{-1}); pepstatin (1 μg ml^{-1}). The cells were kept on ice and sonicated for 90 s with a model W185 Heat Systems sonicator (Plainview, N.Y.) fitted with an 1/8 inch diameter probe at power setting 2. The broken cells were centrifuged at 4°C (600 *g*) for 10 min to sediment the nuclei and any intact cells. The supernatant was removed and centrifuged at 4°C (150,000 *g*) for 120 min to sediment the membrane fraction. The pellet was dispersed in 2 ml of binding buffer. The binding reactions consisted of 50 μl of homogenate, 25 μl of buffer (for B_o) or unlabelled prazosin dilutions and [^{3}H]-prazosin (final concentration 3×10^{-9} M) to a total volume of 250 μl. Following a 60 min incubation, the membranes were recovered by centrifugation in a Microfuge for 1 min and the supernatant was discarded. The pellets were transferred to scintillation vials and radioactivity was analysed as described above.

[^{3}H]-noradrenaline uptake

The cells were washed once with 1 ml Krebs-Ringer HEPES buffer (KRH; Bonisch, 1984) at 37°C and then incubated in 1 ml KRH at 37°C for 15 min. KRH was then removed and replaced with 1 ml of KRH containing [^{3}H]-noradrenaline at the indicated concentrations. The cells were then incubated for 1, 5, 10 or 15 min at 37°C, washed twice with 1 ml ice cold KRH and solubilized in a warm solution of 0.1% sodium dodecyl sulphate and 0.1 M NaOH. Aliquots were removed for protein assay and radioactivity was measured in the cell extract as described above. Protein content was measured by the bicinchoninic acid modification of the biuret reaction (Smith *et al.*, 1985) using albumin standards and reagents supplied by Pierce (Rockford, Illinois, U.S.A.). At the time of culture, blank wells (containing no cells) were prepared and treated in an identical manner to the above. The radioactivity in the blank wells was subtracted from the experimental wells. When the effect of an inhibitor (e.g., desipramine) was examined, the inhibitor was present in all solutions (pre-incubation, incubation and wash). For experiments in the absence of sodium, NaCl was replaced with Tris.HCl.

Effects of 6-hydroxydopamine in vivo

Male Wistar rats weighing 250–300 g were anaesthetized with halothane and the left lateral cerebral ventricle was cannulated as previously described (Al-Damluji *et al.*, 1990a). An intracerebroventricular (i.c.v.) infusion of 6-hydroxydopamine hydrobromide (250 μg dissolved in artificial CSF containing 1 mg ml^{-1} ascorbate) or the vehicle alone was given in a volume of 20 μl over 10 min. In some of the animals, a second infusion of the same dose of 6-hydroxydopamine was given under halothane anaesthesia 72 h after the first dose. One week after the first i.c.v. infusion, the plasma adrenocorticotrophic hormone (ACTH) response to activation of brain α_1-adrenoceptors was assessed. The right external jugular vein was cannulated under halothane anaesthesia as previously described (Al-Damluji *et al.*, 1990a). The animals recovered rapidly and were placed in individual

cages, to be studied 6 h after full recovery from the anaesthetic. Artificial CSF or methoxamine 100 μg (α_1-agonist) were given i.c.v. at a rate of 1 μl min^{-1} over 10 min. Blood sampling (600 μl, replaced with 0.15 M saline) and drug infusions were carried out without disturbing the animals. Plasma ACTH concentrations were measured by a two-site immunoradiometric assay (White *et al.*, 1987). Immediately after obtaining the final blood sample, the animals were killed and the position of the i.c.v. cannula was checked with an injection of blue dye. The hypothalamus was dissected and placed in liquid nitrogen for subsequent assay of catecholamines by high performance liquid chromatography (h.p.l.c.) followed by electrochemical detection (Bouloux *et al.*, 1985).

Drugs

[^{3}H]-prazosin was obtained from Amersham (TRK.843, specific activity 77–84 Ci $mmol^{-1}$, batch numbers 17–20, 23 and 24). [^{125}I]-HEAT ((±)-β-([^{125}I]-iodo-4-hydroxyphenyl)-ethyl aminomethyl-tetralone) was from New England Nuclear (NEX-182; lot no. CQ22210; specific activity 2200 Ci $mmol^{-1}$). [^{3}H]-idazoxan was from Amersham (TRK.799; batch no. 30; specific activity 48 Ci $mmol^{-1}$). (±)-[7-^{3}H]-noradrenaline was from Amersham (TRK.174, specific activity 17–18 Ci $mmol^{-1}$, batch no. 105–107), except in the experiments shown in Figure 5c and d (New England Nuclear NET-048; lot no. 2423–298; specific activity 15 Ci $mmol^{-1}$). (−)-[2,5,6-^{3}H]-noradrenaline was from New England Nuclear (NET-678; lot no. 2727–192; specific activity 43.7 Ci $mmol^{-1}$). Unlabelled prazosin, methoxamine, desipramine, clonidine, (−)-noradrenaline, testosterone, corticosterone, pargyline, clorgyline, protease inhibitors and 6-hydroxydopamine were from Sigma. The catechol-*O*-methyl transferase (COMT) inhibitor E-N,N-diethyl-2-cyano-3-(3,4-dihydroxy-5-nitrophenyl)acrylamide (OR-611) was a gift from Orion Pharmaceutica, Finland. Collagenase was from Worthington, gentamicin and foetal calf serum from Gibco and trypsin, DNAse I, HEPES, Tris (Trizma base) and culture media (DMEM and F-12) were from Sigma. Scintillation liquid was Hydrofluor (National Diagnostics, Manville, N.J., U.S.A.).

Statistics

The data from the experiments in the cell cultures are means ± s.e.mean of three or four replicates, and the results are representative of two or three such experiments. The data from the experiments *in vivo* are the means ± s.e.mean of four rats for each drug group. Statistical assessment of the integrated data (whole time course) was by the Wilcoxon (non-parametric) test and individual time points were compared with Student's *t* test. Kinetic analysis of Lineweaver-Burk plots of the uptake of prazosin and noradrenaline was done graphically and by linear regression analysis on a MacIntosh computer. Similar results were obtained by both methods.

Results

[^{3}H]-prazosin binding and uptake

[^{3}H]-prazosin (3 to 18 × 10^{-10} M) bound to both the cultured neonatal cells and the GnRH cell line. Time course studies (not shown) indicated that apparent equilibrium was reached by 60 min at 25°C. Displacement studies at equilibrium (Figure 1) showed that [^{3}H]-prazosin was displaced by unlabelled prazosin in concentrations of 10^{-10} to 10^{-7} M, indicating the presence of α_1-adrenoceptor binding sites on both the neonatal cells and the GnRH cell line. However, at concentrations of unlabelled prazosin above 10^{-7} M there was a paradoxical increase in apparent [^{3}H]-prazosin binding (Figures 1, a and b).

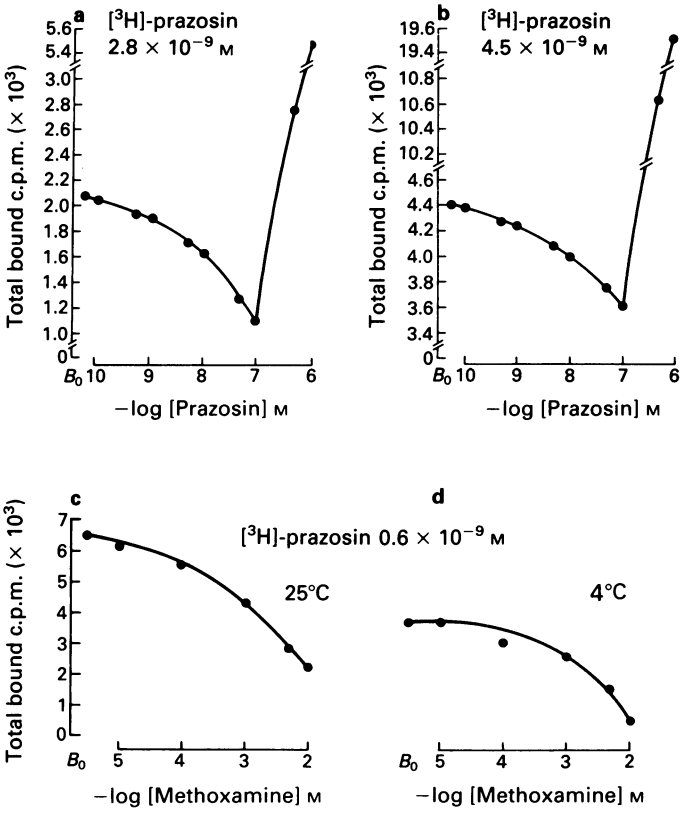

Figure 1 (a and b) Inhibition of [^{3}H]-prazosin binding by unlabelled prazosin in cultured neonatal hypothalamic cells (a) and a GnRH neuronal cell line (GT 1-1 cells; b). Displacement of the radioligand at equilibrium (60 min) was observed at prazosin concentrations of 10^{-10} to 10^{-7} M, indicating the presence of α_1-adrenoceptors in both cell types. At concentrations of unlabelled prazosin above 10^{-7} M, there was a paradoxical increase in apparent binding of [^{3}H]-prazosin. The data represent total bound c.p.m. (c and d) Inhibition of [^{3}H]-prazosin binding by unlabelled methoxamine (an α_1-agonist that is not subject to significant neuronal uptake) at 25°C (c) and at 4°C (d) in the GnRH neuronal cell line. No paradoxical increase in apparent [^{3}H]-prazosin binding was evident even at the highest concentrations of methoxamine. The data represent total bound c.p.m.

Further experiments examined the hypothesis that this paradoxical increase in apparent [^{3}H]-prazosin binding could be due to an uptake process that becomes apparent at high concentrations of the ligand. Methoxamine is a selective, low affinity α_1-adrenoceptor ligand (Drew, 1976; Williams & Lefkowitz, 1978; Schwinn *et al.*, 1990) that is not subject to significant neuronal uptake (Burgen & Iversen, 1965; Trendelenburg *et al.*, 1970). Methoxamine displaced [^{3}H]-prazosin from both neonatal and GnRH cells at 25°C, confirming the presence of α_1-adrenoceptors (Figure 1c). However, even at the highest concentrations used, methoxamine did not cause the paradoxical increase in apparent binding of [^{3}H]-prazosin to the cells. These data were compatible with the hypothesis that the paradoxical increase in cell-associated radioactivity at high prazosin concentrations (Figure 1a and b) was due to cellular uptake of the radioligand. At the highest concentration, methoxamine displaced 66% of the [^{3}H]-prazosin from the cells, suggesting that at the concentration of [^{3}H]-prazosin used (0.6×10^{-9} M), approximately half is bound to α_1-adrenoceptors and the remainder is subject to neuronal uptake. In the experiment shown in Figure 1d, the cells were cooled to 4°C in order to minimize any active uptake process; under these conditions, the total amount of prazosin associated with the cells (B_o) was reduced by 48%, and methoxamine (10^{-2} M) displaced almost all the [^{3}H]-prazosin from the cells. These data provided further evidence that [^{3}H]-prazosin both binds to α_1-adrenoceptors and is subject to active cellular uptake.

Desipramine is a tricyclic antidepressant that inhibits neuronal uptake of catecholamines (Axelrod, 1971; Graefe & Bonisch, 1989; Pacholczyk *et al.*, 1991). Desipramine (10^{-5} M) reduced the total amount of [^{3}H]-prazosin associated with the cells (B_o) by 40% (Figure 2a), which is similar to the reduction of B_o caused by cooling (Figure 1d). In the presence of 10^{-5} M desipramine, unlabelled prazosin displaced [^{3}H]-prazosin as before but no increase in binding was seen above 10^{-7} M (Figure 2a). This confirmed that the paradoxical increase in apparent binding of prazosin above 10^{-7} M was due to cellular uptake.

Although desipramine (10^{-5} M) reduced the total amount of [^{3}H]-prazosin associated with the cells, it had no effect on the specific binding of [^{3}H]-prazosin (Figure 2b), indicating that at this concentration (10^{-5} M) desipramine did not interfere with the binding of [^{3}H]-prazosin to the α_1-adrenoceptors.

Figure 2c demonstrates radioligand binding curves for [^{3}H]-prazosin and its displacement by unlabelled prazosin, in the presence of desipramine 10^{-5} M. The density (B_{max}) of the binding sites was 150 fmol mg^{-1} in the neonatal cells and 126 fmol mg^{-1} in the GnRH cell line. The affinity (K_d) of prazosin was 4.4×10^{-9} M in the neonatal cells and 11×10^{-9} M in the GnRH cell line.

Because prazosin may bind with lower affinity to α_{2B}-adrenoceptors (Regan *et al.*, 1988), we further investigated the identity of the adrenoceptors in the cell cultures. The

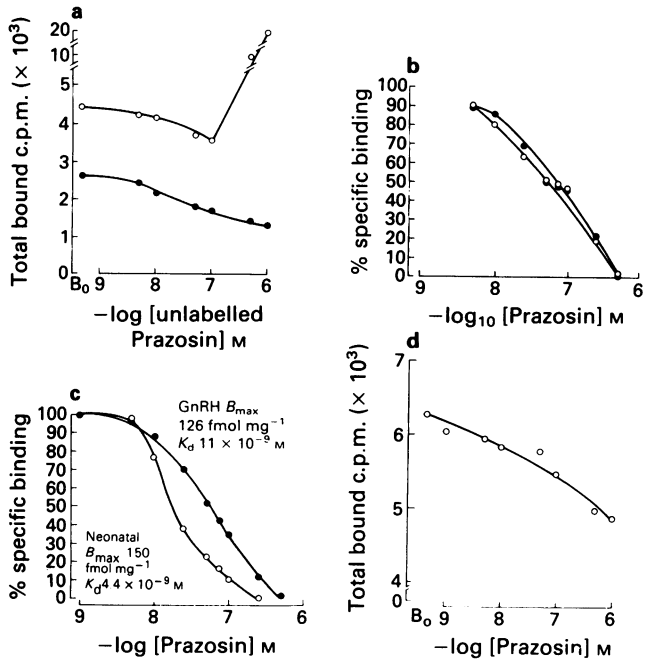

Figure 2 (a) Effects of desipramine (10^{-5} M) on [^{3}H]-prazosin (1.8×10^{-9} M) binding and its displacement by unlabelled prazosin in intact GT1-1 GnRH cells. Incubation was for 60 min at 25°C. The data represent total bound c.p.m. (○) control; (●) total c.p.m. in the presence of desipramine, with and without (B_o) increasing concentrations of unlabelled prazosin. Non-specific binding is the c.p.m. at unlabelled prazosin 10^{-6} M. Specific binding (b) was obtained by subtracting the non-specific c.p.m. from the total c.p.m. and expressed as a percentage of B_o. The data in (c) were calculated similarly. (b) Lack of effect of desipramine (●, 10^{-5} M) on specific binding of [^{3}H]-prazosin (1.6×10^{-9} M) to cultured hypothalamic cells from neonatal rats; (○) control, IC_{50} = 51 nM; (●) desipramine 10^{-5} M, IC_{50} = 56 nM. (c) Binding of [^{3}H]-prazosin and its displacement by unlabelled prazosin in intact neonatal hypothalamic cells (○) and GT1-1 GnRH cells (●). Incubation was for 60 min at 25°C in the presence of desipramine (10^{-5} M). (d) Binding of [^{3}H]-prazosin and its displacement by unlabelled prazosin in membrane preparations from broken GT1-1 GnRH cells. There was no paradoxical increase in [^{3}H]-prazosin binding at concentrations of unlabelled prazosin above 10^{-7} M. The data represent total bound c.p.m.

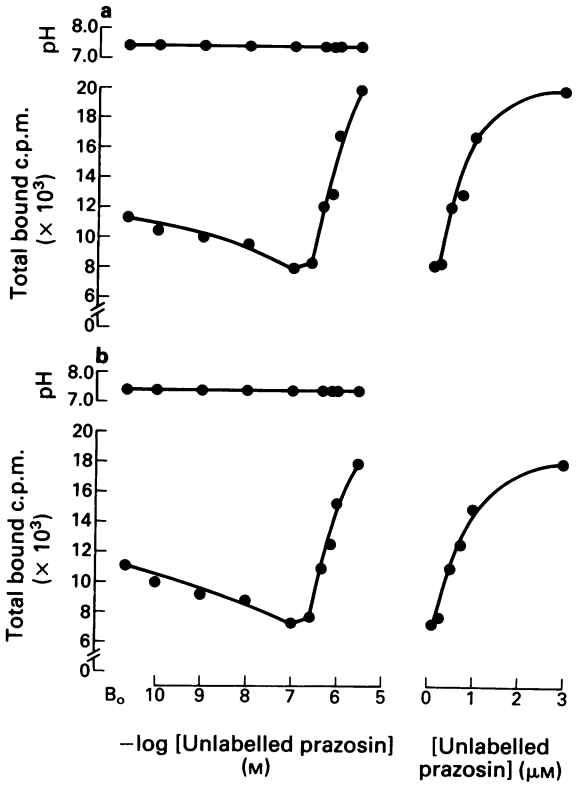

Figure 3 Inhibition of [^{3}H]-prazosin binding by unlabelled prazosin in the GnRH neuronal cell line (GT1-1 cells) and the effect of prazosin on pH of solutions. The experiments were carried out in Krebs-Ringer buffered with 25 mM HEPES (a) or 25 mM Tris (b), in the absence of DMEM and ascorbate. The data represent total bound c.p.m. In the left panels, the data are presented as log-linear plots, in order to include the full range of concentrations of prazosin that were used. In the right panels, linear-linear scales were used to represent the data from unlabelled prazosin concentrations of 10^{-7} M to 3×10^{-6} M.

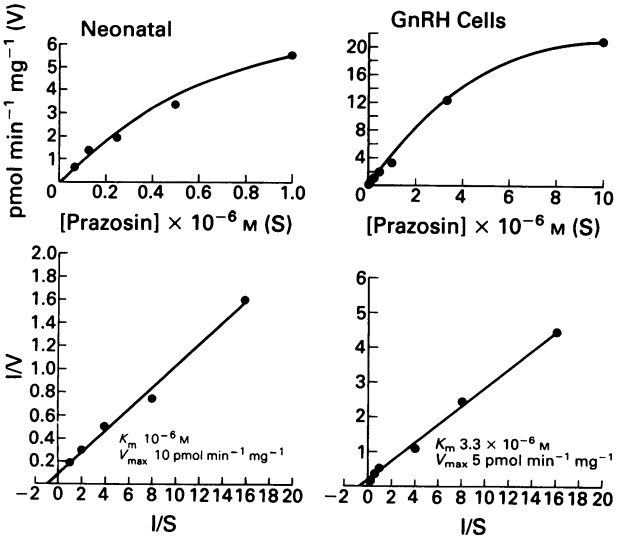

Figure 4 Kinetic analysis of the uptake of prazosin in neonatal hypothalamic cells (left) and GT1-1 GnRH cells (right) in the presence of methoxamine (10^{-3} M), which was used to minimize binding to α_1-adrenoceptors. Incubation was for 5 min at 25°C. The data are presented as plots of concentration vs initial velocity in the upper panels, and as Lineweaver-Burk plots in the lower panels.

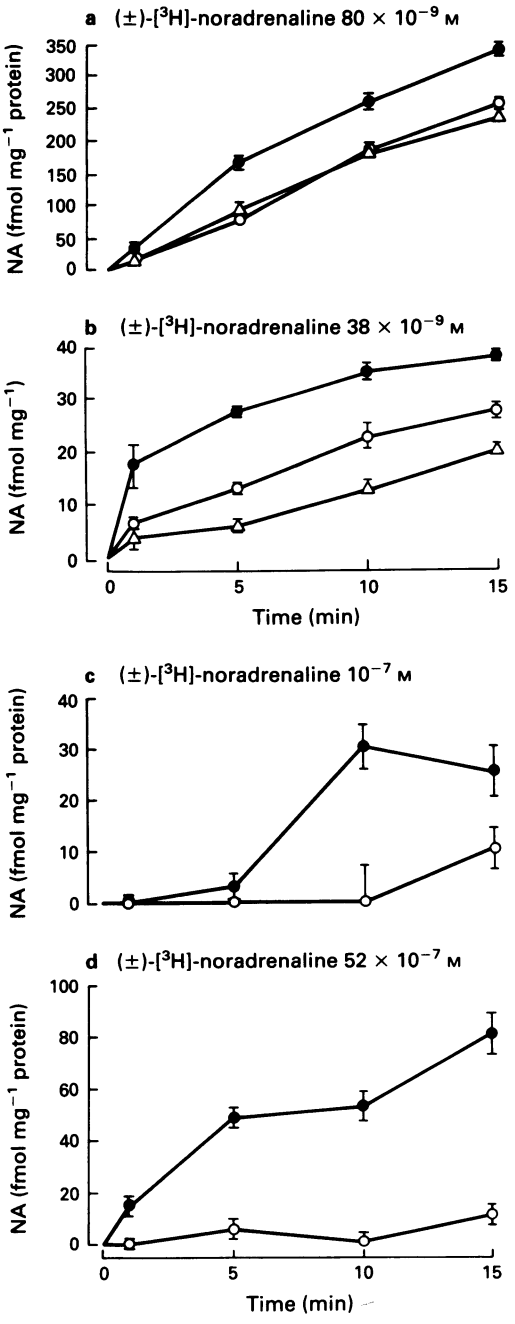

Figure 5 (a and b) Uptake of (±)-[^{3}H]-noradrenaline (NA) by GT1-1 GnRH cells (a) and neonatal hypothalamic cells (b): effects of desipramine (10^{-5} M) and omission of sodium from the incubation medium; (●) control; (○) desipramine 10^{-5} M; (△) sodium absent. (c and d) Effects of the combination of desipramine (10^{-5} M) and methoxamine (10^{-3} M) on the uptake and binding of (±)-[^{3}H]-noradrenaline in GT1-1 GnRH cells (c) and neonatal hypothalamic cells (d): (●) control; (○) desipramine 10^{-5} M + methoxamine 10^{-3} M.

selective α_1-adrenoceptor ligand, [^{125}I]-HEAT bound to the cells with high affinity (at a concentration of 3×10^{-11} M, maximum binding [B_o] was 26% of total counts and NSB was 1.9%). The α_1-adrenoceptor agonist, methoxamine (10^{-2} M), displaced 63% of the bound [^{125}I]-HEAT (data not shown), which is almost identical to the result obtained with [^{3}H]-prazosin (Figure 1c). We also examined the cells for the presence of α_2-adrenoceptors using [^{3}H]-idazoxan. In two separate experiments in the neonatal cells, [^{3}H]-idazoxan (1.8×10^{-9} M) binding did not exceed 1% of the total counts, and this was not displaced with the α_2-agonist, clonidine 10^{-6} M. Similarly, in the GnRH cells, binding of [^{3}H]-idazoxan (at concentrations up to 10^{-7} M) did not exceed 1% of the total counts and was not displaced by 10^{-6} M clonidine.

In broken cell (membrane) preparations, [^{3}H]-prazosin was displaced by unlabelled prazosin in the concentration range 10^{-9} to 10^{-6} M, and no paradoxical increase in apparent binding of [^{3}H]-prazosin was evident above 10^{-7} M (Figure 2d).

Further experiments examined the possible contribution of ionic changes to the paradoxical increase in [^{3}H]-prazosin binding above 10^{-7} M. Increasing concentrations of unlabelled prazosin had no effect on the pH of Krebs-Ringer solutions buffered with either 25 mM HEPES or 25 mM Tris (Figure 3). An identical pattern of displacement of [^{3}H]-prazosin by unlabelled prazosin (10^{-10} M to 10^{-7} M) was observed in the two buffers. At higher concentrations of unlabelled prazosin, there was an increase in the apparent binding of [^{3}H]-prazosin which was linear from 10^{-7} to

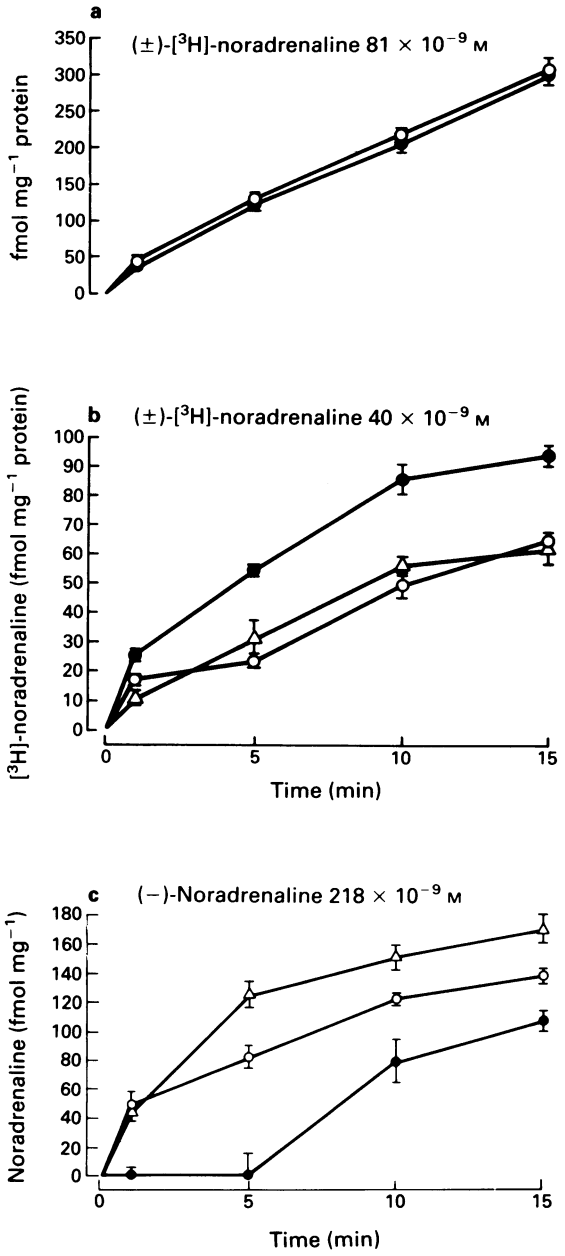

Figure 6 Effects of steroids on the uptake of (±)-[^{3}H]-noradrenaline by GT1-1 GnRH cells (a) and neonatal hypothalamic cells (b): (●) control; (○) testosterone 6×10^{-6} M; (△) corticosterone 6×10^{-6} M (c) Effect of inhibition of catechol-*O*-methyl transferase and monoamine oxidase A and B with OR-611, clorgyline and pargyline, respectively, on the measurable uptake of (−)-noradrenaline in GT1-1 GnRH cells: (●) control; (○) OR-611, 10^{-6} M; (△) OR-611, 10^{-6} M + clorgyline 10^{-4} M + pargyline 10^{-4} M.

10^{-6} M; saturation was evident above this concentration in both buffers.

The kinetics of prazosin uptake were studied in the presence of methoxamine 10^{-3} M, in order to minimize binding of prazosin to the α_1-adrenoceptors. Time course studies (not shown) demonstrated that in the presence of methoxamine, [^{3}H]-prazosin uptake was linear up to 5 min at 25°C. This time point was therefore used for kinetic studies of prazosin uptake. Figure 4 shows that in the presence of methoxamine, the uptake of prazosin conforms to the Michaelis-Menten model, which describes the interaction of substrates with carrier proteins or enzymes (Wong, 1975). Similar values for affinity (K_m) and capacity (V_{max}) were obtained in the neonatal cells and in the GnRH cell line, suggesting that prazosin is transported by the same or similar processes in the two types of cell cultures. The affinity of prazosin for the uptake process (K_m 1–3.3 × 10^{-6} M; Figure 4) was much less than its affinity for the α_1-adrenoceptors (K_d 4–11 × 10^{-9} M; Figure 2c).

Noradrenaline uptake

(±)-[^{3}H]-noradrenaline in nanomolar concentrations was taken up in a time-dependent manner by the neonatal hypothalamic cells (38 × 10^{-9} M) and by the GnRH cells (80 × 10^{-9} M; Figure 5a and b). In both cell types, (±)-[^{3}H]-noradrenaline uptake was reduced by desipramine (10^{-5} M) and by the exclusion of sodium from the medium (Figures 5a and b), indicating that this process shares some of the properties of uptake$_1$. At 5 min, desipramine reduced the measured noradrenaline uptake by 51% in the neonatal cells and by 53% in the GnRH cell line, which is similar to the 55% reduction of noradrenaline uptake by desipramine that was previously reported in noradrenergic nerve terminals (Coyle & Axelrod, 1971). The remainder of the noradrenaline associated with the cells appears to be bound to α_1-adrenoceptors, as the combination of desipramine (which blocks uptake) and methoxamine (which blocks binding to α_1-adrenoceptors) almost abolished the association of (±)-[^{3}H]-noradrenaline with the cells (Figure 5c and d).

The uptake of (±)-[^{3}H]-noradrenaline by the GnRH cells was unaffected by testosterone (6 × 10^{-6} M; Figure 6a). However, in the neonatal cultures, both testosterone and corticosterone reduced (±)-[^{3}H]-noradrenaline uptake (Figure 6b).

The measured uptake of (−)-[^{3}H]-noradrenaline in the GnRH cell line was relatively low. As previous investigators had found different rates of metabolism of (+) and (−)-noradrenaline in various tissues (for review, see Graefe & Bonisch, 1989), further experiments examined the effects of enzyme inhibitors on the apparent uptake of (−)-[^{3}H]-noradrenaline in the GnRH cell line. The COMT inhibitor OR-611 (10^{-6} M) markedly increased the apparent uptake of (−)-noradrenaline in the GnRH cell line (Figure 6c). In contrast, the combination of clorgyline (10^{-4} M) and pargyline (10^{-4} M), which inhibit monoamine oxidase A and B, respectively, had no effect on apparent (−)-noradrenaline uptake (data not shown). However, these two drugs caused a further increase in the apparent uptake of (−)-noradrenaline in the GnRH cell line when combined with OR-611 (Figure 6c).

The kinetics of (−)-noradrenaline uptake were studied in the GnRH cell line in the presence of OR-611 and in the neonatal cells in the absence of any enzyme inhibitor. In both cases, the data fitted the Michaelis-Menten model (Figure 7). In the neonatal cells, the K_m for (−)-noradrenaline was 3.3 × 10^{-7} M and the V_{max} was 143 fmol min^{-1} mg^{-1}. In the

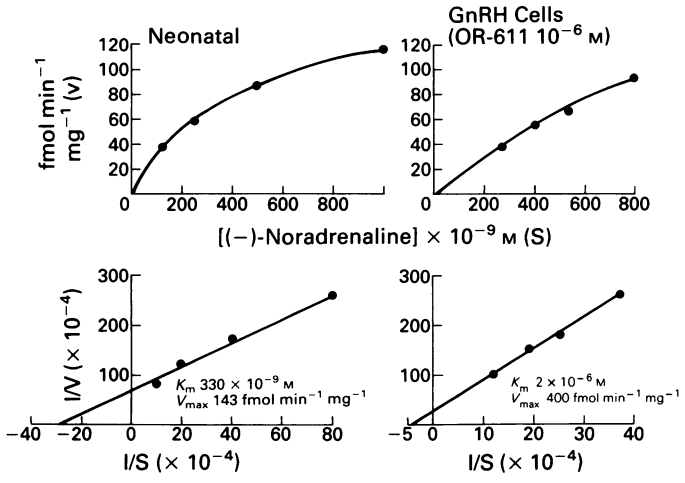

Figure 7 Kinetic analysis of the uptake of (−)-noradrenaline in neonatal hypothalamic cells (left) and GT1-1 GnRH cells (right). The GT1-1 cells were studied in the presence of OR-611 10^{-6} M to inhibit catechol-*O*-methyltransferase. Incubation was for 5 min at 37°C. The data are presented as plots of concentration vs initial velocity in the upper panels, and as Lineweaver-Burk plots in the lower panels.

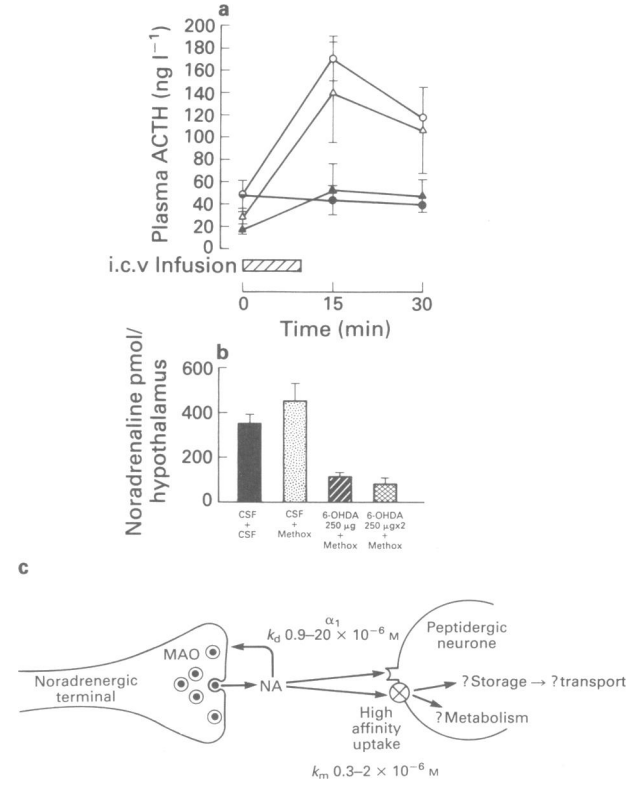

Figure 8 (a and b) Effect of intracerebroventricular (i.c.v.) 6-hydroxydopamine (6-OHDA) given as a single dose of 250 µg or as two 250 µg doses three days apart, on hypothalamic noradrenaline content (b) and the plasma ACTH response (a) to i.c.v. methoxamine in conscious, cannulated rats. Methoxamine or artificial cerebrospinal fluid (CSF) were administered seven days after the first dose of 6-OHDA. Each group consisted of four rats. (a) (●) CSF + CSF; (○) CSF + methoxamine 100 µg i.c.v.; (△) 6-OHDA 250 µg i.c.v. + methoxamine; (▲) 6-OHDA 250 µg × 2 doses + methoxamine. (c) Proposed model of the action of the postsynaptic uptake process. The affinities of (−)-noradrenaline (NA) for the postsynaptic uptake process (K_m 0.3–2 × 10^{-6} M; Figure 7) and for the postsynaptic α_1-adrenoceptors (K_d 0.9–20 × 10^{-6} M; Schwinn *et al.*, 1990; Wikberg *et al.*, 1983; Cotecchia *et al.*, 1988) suggest that the uptake process operates at concentrations of noradrenaline that activate the postsynaptic receptors. The postsynaptic uptake process may remove noradrenaline from the vicinity of the receptors, thus preventing desensitization and maintaining the responsiveness of the receptors to repeated bursts of neurotransmitter released from the noradrenergic terminals. Following uptake into the postsynaptic neurones, noradrenaline could be enzymatically degraded, or stored in the neurosecretory vesicles and subsequently transported and released at a distant site.

GnRH cell line, the K_m and the V_{max} were 2×10^{-6} M and 400 fmol $min^{-1}mg^{-1}$, respectively.

Effect of 6-hydroxydopamine on postsynaptic neurones in vivo

The neurotoxin 6-hydroxydopamine is an isomer of noradrenaline that is taken up by the uptake$_1$ process. In rats that were pretreated with i.c.v. CSF, i.c.v. administration of methoxamine (Methox) stimulated the secretion of ACTH (Figure 8a; Wilcoxon: $P<0.02$, CSF + Methox vs CSF + CSF), as previously described (Al-Damluji *et al.*, 1990a). A single dose of 6-hydroxydopamine (6-OHDA, 250 μg) reduced the hypothalamic content of noradrenaline (Figure 8b, *t* test: $P<0.01$, 6-OHDA 250 μg + Methox vs CSF + CSF) but had no significant effect on the ACTH response to methoxamine. Rats that received two doses of 6-hydroxydopamine showed a similar reduction in hypothalamic noradrenaline content (Figure 8b; *t* test: $P<0.01$, 6-OHDA 250 μg × 2 doses + Methox vs CSF + CSF), but in addition, the ACTH response to methoxamine was significantly reduced (Wilcoxon: $P<0.02$, CSF + Methox vs 6-OHDA 250 μg × 2 doses + Methox).

Discussion

In hypothalamic neurones and GT1-1 transformed neurones, binding studies with [^{3}H]-prazosin in intact cells demonstrated the presence of α_1-adrenoceptors. In addition, cellular uptake of the radioligand was observed at higher concentrations of prazosin. The physiological neurotransmitter, noradrenaline, was also found to be a substrate for the uptake process. These studies indicate that a high affinity uptake process for noradrenaline is present in postsynaptic peptidergic neurones.

The presence of α_1-adrenoceptors in the neonatal cells and the GnRH cell line was demonstrated by binding of [^{3}H]-prazosin and its displacement by methoxamine and unlabelled prazosin. In the presence of desipramine, the affinity (K_d) for prazosin was similar to previously reported data for α_1-adrenoceptors in cultured cells (K_d $2.5-5.3 \times 10^{-9}$ M; Wikberg *et al.*, 1983; Cotecchia *et al.*, 1988; Schwinn *et al.*, 1990). [^{125}I]-HEAT also bound to the cells and was displaced by methoxamine, confirming the presence of α_1-adrenoceptors. Although prazosin may bind to α_{2B}-adrenoceptors (Regan *et al.*, 1988), we did not detect α_2-binding sites in either type of cell culture using [^{3}H]-idazoxan, which binds with high affinity to both α_{2A} and α_{2B}-adrenoceptors (Regan *et al.*, 1988). These experiments confirmed the identity of the [^{3}H]-prazosin binding sites as α_1-adrenoceptors.

In binding-inhibition (displacement) studies, there was a paradoxical increase in the apparent binding of [^{3}H]-prazosin when the concentration of unlabelled prazosin was increased above 10^{-7} M. This effect was not due to non-specific ionic changes caused by increasing concentrations of unlabelled prazosin. The paradoxical increase in [^{3}H]-prazosin binding was not reproduced by methoxamine, which also binds to α_1-adrenoceptors (Drew, 1976; Williams & Lefkowitz, 1979; Schwinn *et al.*, 1990) but is not subject to significant neuronal uptake (Burgen & Iversen, 1965; Trendelenburg *et al.*, 1970). When the cells were cooled (with the aim of minimizing any active uptake process), methoxamine displaced almost all the [^{3}H]-prazosin from the cells. Desipramine, which inhibits neuronal uptake (Axelrod, 1971; Graefe & Bonisch, 1989; Pacholczyk *et al.*, 1991), abolished the increase in [^{3}H]-prazosin binding above 10^{-7} M. The experiments with both methoxamine and desipramine suggested that the paradoxical increase in apparent binding of [^{3}H]-prazosin to the cells was due to cellular uptake. Desipramine (10^{-5} M) did not inhibit [^{3}H]-prazosin binding to α_1-adrenoceptors (Figure 2b). However, at higher concentrations (10^{-4} M) desipramine reduced the specific binding of prazosin (data not shown), which is consistent with the suggestion that high concentrations of tricyclic antidepressants bind to α-adrenoceptors (U'Prichard *et al.*, 1978). Further evidence for cellular uptake and retention of prazosin at high concentrations was provided by the finding that in broken cell (membrane) preparations, there was no paradoxical increase in apparent binding of [^{3}H]-prazosin above 10^{-7} M, indicating that demonstration of this effect requires the presence of intact cells or storage organelles.

The affinity of prazosin for the uptake process (K_m $1-3.3 \times 10^{-6}$ M; Figure 4) was considerably lower than its affinity for the α_1-adrenoceptors (K_d $4-11 \times 10^{-9}$ M; Figure 2c). This explains the data shown in Figure 1, in which displacement of [^{3}H]-prazosin from the receptors was observed at low concentrations of unlabelled prazosin, whereas uptake was only evident at prazosin concentrations above 10^{-7} M. The uptake of prazosin is a linear process (Figure 4) that is demonstrable at low concentrations; cooling and desipramine both reduced the association of nanomolar concentrations of [^{3}H]-prazosin with the cells (B_o in Figures 1d and 2a). Prazosin therefore both binds to α_1-adrenoceptors and is subject to cellular uptake. The proportion of prazosin that is bound to α_1-adrenoceptors (specific binding) would be expected to be dependent on the concentration of prazosin in the assay; at low concentrations, a greater proportion of prazosin will presumably be bound to receptors than at high concentrations, when uptake becomes more prominent due to its lower affinity for prazosin.

Since hypothalamic peptidergic neurones, including GnRH neurones, are densely innervated by noradrenergic nerve terminals (Hoffman & Wray, 1982; Silverman *et al.*, 1985; Liposits *et al.*, 1986), we also determined whether the uptake process transports the physiological neurotransmitter, noradrenaline. There are two uptake processes for noradrenaline: uptake$_1$ occurs in noradrenergic nerve terminals at nanomolar concentrations of noradrenaline and is blocked by desipramine (Glowinski & Axelrod, 1964; Graefe & Bonisch, 1989; Pacholczyk *et al.*, 1991) and by the absence of sodium (Iversen & Kravitz, 1966; Bogdanski & Brodie, 1966; Graefe & Bonisch, 1989; Pacholczyk *et al.*, 1991); uptake$_2$ occurs in non-neuronal cells at much higher concentrations of noradrenaline and is insensitive to desipramine and the absence of sodium, but is blocked by high concentrations of certain steroid hormones (Iversen & Salt, 1970; Salt, 1972). The uptake of noradrenaline in our cultured hypothalamic cells shares some of the functional characteristics of the uptake$_1$ process. Thus, uptake was demonstrable at nanomolar concentrations of noradrenaline and had affinity constants within the range that has been described for uptake$_1$ (see below). Further, the postsynaptic uptake process, like uptake$_1$, was blocked by desipramine and by exclusion of sodium from the extracellular space, and was unaffected by steroids in the GnRH cells. Similar results were obtained in the GnRH cell line and in the neonatal cells, although the uptake of (±)-[^{3}H]-noradrenaline was reduced by steroids in the primary cultures. This may reflect the heterogeneous nature of the primary cell cultures, and possibly the presence of more than one uptake process in the hypothalamus.

Several previous studies have shown that both (−) and (+)-noradrenaline are transported by uptake$_1$, but that the (−)-isomer is preferentially metabolized (for review, see Graefe & Bonisch, 1989). We found that the apparent uptake of (−)-noradrenaline in the GnRH cell line was considerably increased by an inhibitor of COMT. Further enhancement of the measurable uptake of (−)-noradrenaline was observed when inhibitors of COMT and MAO were combined, although the MAO inhibitors alone had no effect. These findings suggest that following uptake into the GnRH cells, (−)-noradrenaline is rapidly metabolized, predominantly by COMT, to lipophilic compounds that can cross the plasma membrane into the larger volume of distribution of the incubation and wash buffers. A likely metabolic path would involve COMT to produce normetanephrine, followed by

MAO and aldehyde reductase to produce 3-methoxy-4-hydroxy-phenylethylene-glycol (MHPG), a lipophilic compound that has a high efflux rate from cells (Graefe & Henseling, 1983). It is possible that noradrenaline may enter the neurosecretory vesicles in other cell types, and may thus be stored and even transported with the native neurotransmitter to be released at a distant site (Figure 8c).

The measured K_ms for (−)-noradrenaline uptake in both types of cultures were within the reported range ($0.2-3.3 \times 10^{-6}$ M) for the high affinity uptake$_1$ process in a variety of tissues, including the recently cloned human uptake$_1$ presynaptic noradrenaline transporter (Iversen, 1963; Coyle & Axelrod, 1971; Ross & Gosztonyi, 1975; Graefe *et al.*, 1978; Sammet & Graefe, 1979; Henseling, 1983; Pacholczyk *et al.*, 1991). In contrast, the K_m of (−)-noradrenaline for uptake$_2$ is 250×10^{-6} M (Burgen & Iversen, 1965). The uptake of (−)-noradrenaline in the GnRH cell line had a higher apparent K_m than in the neonatal cells (2×10^{-6} M vs 0.33×10^{-6} M), but it is possible that the true affinity of (−)-noradrenaline for the uptake process in GnRH cells was underestimated due to incomplete blockade of the COMT enzyme by OR-611.

Our experiments in cultured cells, using known concentrations of noradrenaline, are difficult to replicate *in vivo*. However, the noradrenaline isomer, 6-hydroxydopamine, is a neurotoxin that is taken up into noradrenergic nerve terminals by the presynaptic uptake$_1$ process (Iversen, 1970; Jonsson & Sachs, 1970). It is then oxidized to neurotoxic products, resulting in destruction of the noradrenergic nerve terminals (Kostrzewa & Jacobowitz, 1974). The uptake of 6-hydroxydopamine and its neurotoxic effects can be blocked by desipramine (Stone *et al.*, 1964; Jonsson & Sachs, 1970). Administration of methoxamine to rats activates α_1-adrenoceptors that are located postsynaptically on vasopressin and CRH-41 neurones, whose secretory products in turn stimulate the secretion of pituitary ACTH (Al-Damluji *et al.*, 1990a,b). 6-Hydroxydopamine (250 μg i.c.v.) was found to reduce hypothalamic noradrenaline content (Figure 8b), indicating uptake into and destruction of the hypothalamic noradrenergic nerve terminals. This dose of 6-hydroxydopamine had no effect on the ACTH response to methoxamine (Figure 8a). This indicated sparing of the postsynaptic hypothalamic neurones that mediate the effects of methoxamine on ACTH secretion. Rats that received two doses of 6-hydroxydopamine (250 μg i.c.v. three days apart) had a similar reduction of hypothalamic noradrenaline content (Figure 8b), but in addition the ACTH response to methoxamine was significantly reduced (Figure 8a). This suggested destruction of the hypothalamic vasopressin and CRH-41 neurones that mediate the effects of i.c.v. methoxamine. It seems likely that 6-hydroxydopamine has a greater affinity for the presynaptic uptake$_1$ process than for the postsynaptic uptake process. This would explain why a single dose of this drug spared the postsynaptic neurones; only when the noradrenergic nerve terminals have been destroyed can a second dose of 6-hydroxydopamine exert its full effect on the postsynaptic neurones. These preliminary findings suggest that hypothalamic vasopressin and CRH-41 neurones possess an amine uptake process, and provide an experimental model that should be useful for further studies in this field.

Dispersed primary hypothalamic cell cultures contain no noradrenergic neurones (Puymirat *et al.*, 1983) but may include dopaminergic neurones which constitute approximately 0.1% of the total number of neurones in the culture (Puymirat *et al.*, 1983). However, the high affinity of (−)-noradrenaline for the primary cultures (K_m 0.33×10^{-6} M) makes it unlikely that the observed uptake was into dopaminergic neurones, which have lower affinity for (−)-noradrenaline (K_m 2×10^{-6} M; Snyder & Coyle, 1969; Iversen, 1970). The affinities of (−)-noradrenaline for the postsynaptic uptake process (apparent K_m 0.33×10^{-6} M in the neonatal cells, 2×10^{-6} M in the GnRH cells; Figure 7) and for the postsynaptic α_1-adrenoceptors (K_d $0.9-20 \times 10^{-6}$ M; Wikberg *et al.*, 1983; Cotecchia *et al.*, 1988; Schwinn *et al.*, 1990) make it likely that at concentrations that activate the postsynaptic receptors, noradrenaline will be taken up by the postsynaptic transporter. Exposure of α_1-adrenoceptors to noradrenaline leads to desensitization of the receptors (Wikberg *et al.*, 1983; Bobik *et al.*, 1984). A postsynaptically located high-affinity uptake process may serve the important function of removing noradrenaline from the vicinity of the receptors, thus maintaining the responsiveness of the postsynaptic receptors to repeated bursts of neurotransmitter released from the noradrenergic nerve terminals (Figure 8c). In contrast, the presynaptic uptake$_1$ process would presumably be less effective in removing noradrenaline from the postsynaptic receptors, as it would rely on the slow diffusion of molecules of noradrenaline across the synapse. It is possible that the presynaptic uptake$_1$ process may serve this proposed function in relation to presynaptic receptors, such as α_2-adrenoceptors.

We thank Dr I.J. Kopin for support and helpful comments and Dr R.I. Weiner for providing the GnRH cell line. We also thank Dr Anne White for the ACTH assay and Miss Elizabeth Newbold for the noradrenaline assay.

References

AL-DAMLUJI, S. (1988). Review: adrenergic mechanisms in the control of corticotrophin secretion. *J. Endocrinol.*, **119**, 5–14.

AL-DAMLUJI, S. (1993). Adrenergic control of secretion of the anterior pituitary hormones. In *Catecholamines*. ed. Bouloux, P. London: Bailliere's Clinical Endocrinology & Metabolism (in press).

AL-DAMLUJI, S., THOMAS, R., WHITE, A. & BESSER, G.M. (1990a). Vasopressin mediates alpha-1 adrenergic stimulation of adrenocorticotrophin secretion. *Endocrinology*, **126**, 1989–1995.

AL-DAMLUJI, S., WHITE, A. & BESSER, G.M. (1990b). Brattleboro rats have deficient adrenocorticotrophin responses to activation of central alpha-1 adrenoceptors. *Endocrinology*, **127**, 2849–2853.

AXELROD, J. (1971). Noradrenaline: fate and control of its biosynthesis. *Science*, **173**, 598–606.

BARRACLOUGH, C.A. & WISE, P.M. (1982). The role of catecholamines in the regulation of pituitary luteinizing hormone and follicle-stimulating hormone secretion. *Endocr. Rev.* **3**, 91–119.

BOBIK, A., CAMPBELL, J.H. & LITTLE, P.J. (1984). Desensitization of the alpha-1 adrenoceptor system in vascular smooth muscle cells. *Biochem. Pharmacol.*, **33**, 1143–1145.

BOGDANSKI, D.F. & BRODIE, B.B. (1966). Role of sodium and potassium ions in storage of norepinephrine by sympathetic nerve endings. *Life. Sci.*, **5**, 1563–1569.

BONISCH, H. (1984). The transport of (+)-amphetamine by the neuronal noradrenaline carrier. *Naunyn-Schmied. Arch. Pharmacol.*, **327**, 267–272.

BOULOUX, P., PERRETT, D. & BESSER, G.M. (1985). Methodological considerations in the determination of plasma catecholamines by high performance liquid chromatography with electrochemical detection. *Ann. Clin. Biochem.*, **22**, 194–203.

BURGEN, A.S.V. & IVERSEN, L.L. (1965). The inhibition of noradrenaline uptake by sympathomimetic amines in the rat isolated heart. *Br. J. Pharmacol.*, **25**, 34–49.

CLARKE, M.J.O., LOWRY, P. & GILLIES, G. (1987). Assessment of corticotropin-releasing factor, vasopressin and somatostatin secretion by fetal hypothalamic neurons in culture. *Neuroendocrinology*, **46**, 147–154.

COTECCHIA, S., LEEB-LUNDBERG, L.M.F., HAGEN, P.O., LEFKOWITZ, R.J. & CARON, M.G. (1985). Phorbol ester effects on alpha-1 adrenoceptor binding and phosphatidylinositol metabolism in cultured vascular smooth muscle cells. *Life Sci.*, **37**, 2389–2398.

COTECCHIA, S., SCHWINN, D.A., RANDALL, R.R., LEFKOWITZ, R.J., CARON, M.G. & KOBILKA, B.K. (1988). Molecular cloning and expression of the cDNA for the hamster alpha-1 adrenergic receptor. *Proc. Natl. Acad. Sci. U.S.A.*, **85**, 7159–7163.

COYLE, J.T. & AXELROD, J. (1971). Development of the uptake and storage of L-[^{3}H]norepinephrine in the rat brain. *J. Neurochem.*, **18**, 2061–2075.

CUMMINGS, S. & SEYBOLD, V. (1988). Relationship of alpha-1 and alpha-2 adrenergic binding sites to regions of the paraventricular nucleus of the hypothalamus containing corticotropin-releasing factor and vasopressin neurons. *Neuroendocrinology*, **47**, 523–532.

CUNNINGHAM, E.T. & SAWCHENKO, P.E. (1988). Anatomical specificity of noradrenergic inputs to the paraventricular and supraoptic nulcei of the rat hypothalamus. *J. Comp. Neurol.*, **274**, 60–76.

DREW, G.M. (1976). Effects of alpha adrenoceptor agonists and antagonists on pre- and post-synaptically located alpha-adrenoceptors. *Eur. J. Pharmacol.*, **36**, 313–320.

GLOWINSKI, J. & AXELROD, J. (1964). Inhibition of uptake of tritiated-noradrenaline in the intact rat brain by imipramine and structurally related compounds. *Nature*, **204**, 1318–1319.

GRAEFE, K.H. & BONISCH, H. (1989). The transport of amines across axonal membranes of noradrenergic and dopaminergic neurones. In *Handb. Exp. Pharmacol.*, ed. Trendelenburg, U. & Weiner, N. Vol. 90 (Part 1), pp. 193–245. Berlin: Springer-Verlag.

GRAEFE, K.H., BONISCH, H. & KELLER, B. (1978). Saturation kinetics of the adrenergic neurone uptake system in the perfused rabbit heart. A new method for determination of initial rates of amine uptake. *Naunyn-Schmiedebergs Arch. Pharmacol.*, **302**, 263–273.

GRAEFE, K.H. & HENSLING, M. (1983). Neuronal and extraneuronal uptake and metabolism of catecholamines. *Gen. Pharmacol.*, **14**, 27–33.

HENSELING, M. (1983). Kinetic constants for uptake and metabolism of ^{3}H-(−)noradrenaline in rabbit aorta. *Naunyn-Schmied. Arch. Pharmacol.*, **323**, 12–23.

HOFFMAN, G.E., WRAY, S. & GOLDSTEIN, M. (1982). Relationship of catecholamines and LHRH: light microscopic study. *Brain Res. Bull.*, **9**, 417–430.

IVERSEN, L.L. (1963). The uptake of noradrenaline by the isolated perfused rat heart. *Br. J. Pharmacol.*, **21**, 523–537.

IVERSEN, L.L. (1970). Inhibition of catecholamine uptake by 6-hydroxydopamine in rat brain. *Eur. J. Pharmacol.*, **10**, 408–410.

IVERSEN, L.L. & KRAVITZ, E.A. (1966). Sodium dependence of transmitter uptake at adrenergic nerve terminals. *Mol. Pharmacol.*, **2**, 360–362.

IVERSEN, L.L. & SALT, P.J. (1970). Inhibition of catecholamine uptake$_2$ by steroids in the isolated rat heart. *Br. J. Pharmacol.*, **40**, 528–530.

JONSSON, G. & SACHS, C. (1970). Effects of 6-hydroxydopamine on the uptake and storage of noradrenaline in sympathetic adrenergic neurons. *Eur. J. Pharmacol.*, **9**, 141–155.

KOSTRZEWZ, R.M. & JACOBOWITZ, D.M. (1974). Pharmacological actions of 6-hydroxydopamine. *Pharmacol. Rev.*, **26**, 199–288.

KRSMANOVIC, L.Z., STOJILKOVIC, S.S., BALLA, T., AL-DAMLUJI, S., WEINER, R.I. & CATT, K.J. (1991). Receptors and neurosecretory actions of endothelin in hypothalamic neurons. *Proc. Natl. Acad. Sci. U.S.A.*, **88**, 11124–11128.

LEIBOWITZ, S.F., JHANWAR-UNIYAL, M., DVORKIN, B. & MAKMAN, M.H. (1982). Distribution of alpha-adrenergic, beta-adrenergic and dopaminergic receptors in discrete hypothalamic areas of rat. *Brain Res.*, **233**, 97–114.

LIPOSITS, Z., SHERMAN, D., PHELIX, C. & PAULL, W.K. (1986). A combined light and electron microscopic immunocytochemical method for the simultaneous localization of multiple tissue antigens. *Histochem.*, **85**, 95–106.

LOUDES, C., FAIVRE-BAUMAN, A. & TIXIER-VIDAL, A. (1983). Techniques for culture of hypothalamic neurons. *Methods in Enzymology*, **103**, 313–334.

MELLON, P.L., WINDLE, J.J., GOLDSMITH, P.C., PADULA, C.A., ROBERTS, J.L. & WEINER, R.I. (1990). Immortalization of hypothalamic GnRH neurons by genetically targeted tumorigenesis. *Neuron*, **5**, 1–10.

MULLER, E.E. (1987). Neural control of somatotropic function. *Physiol. Rev.*, **67**, 962–1053.

PACHOLCZYK, T., BLAKELY, R.D. & AMARA, S.G. (1991). Expression-cloning of a cocaine- and antidepressant-sensitive human noradrenaline transporter. *Nature*, **350**, 350–354.

PUYMIRAT, J., BARRET, A., PICART, R., VIGNY, A., LOUDES, C., FAIVRE-BAUMAN, A. & TIXIER-VIDAL, A. (1983). Triiodothyronine enhances the morphological maturation of dopaminergic neurones from fetal mouse hypothalamus cultured in serum-free medium. *Neuroscience*, **10**, 801–810.

REGAN, J.W., KOBILKA, T.S., YANG-FENG, T.L., CARON, M.G., LEFKOWITZ, R.J. & KOBILKA, B.K. (1988). Cloning and expression of a human kidney cDNA for an alpha-2 adrenergic receptor subtype. *Proc. Natl. Acad. Sci. U.S.A.*, **85**, 6301–6305.

ROSS, S.B. & GOSZTONYI, T. (1975). On the mechanism of accumulation of ^{3}H-bretylium in peripheral sympathetic nerves. *Naunyn-Schmied. Arch. Pharmacol.*, **288**, 283–293.

SALT, P.J. (1972). Inhibition of noradrenaline uptake$_2$ in the isolated rat heart by steroids, clonidine and methoxylated phenylethylamines. *Eur. J. Pharmacol.*, **20**, 329–340.

SAMMET, S. & GRAEFE, K.H. (1979). Kinetic analysis of the interaction between noradrenaline and Na^+ in neuronal uptake: kinetic evidence for co-transport. *Naunyn-Schmied. Arch. Pharmacol.*, **309**, 99–107.

SAWCHENKO, P.E. & SWANSON, L.W. (1982). The organization of noradrenergic pathways from the brainstem to the paraventricular and supraoptic nuclei in the rat. *Brain Res. Rev.*, **4**, 275–325.

SCHWINN, D.A., LOMASNEY, J.W., LORENZ, W., SZKLUT, P.J., FREMEAU, R.T., YANG-FENG, T.L., CARON, M.G., LEFKOWITZ, R.J. & COTECCHIA, S. (1990). Molecular cloning and expression of the cDNA for a novel alpha-1 adrenergic receptor subtype. *J. Biol. Chem.*, **265**, 8183–8189.

SHOEMAKER, W.J., PETERFREUND, R.A. & VALE, W. (1983). Methodological considerations in culturing peptidergic neurons. *Methods Enzymol.*, **103**, 347–362.

SILVERMAN, A.J., OLDFIELD, B., HOU-YU, A. & ZIMMERMAN, E.A. (1985). The noradrenergic innervation of vasopressin neurons in the paraventricular nucleus of the hypothalamus: an ultrastructural study using radioautography and immunocytochemistry. *Brain. Res.*, **325**, 215–229.

SMITH, P.K., KROHN, R.I., HERMANSON, G.T., MALLIA, A.K., GARTNER, F.H., PROVENZANO, M.D., FUJIMOTO, E.K., GOEKE, N.M., OLSON, B.J. & KLENK, D.C. (1985). Measurement of protein using bicinchoninic acid. *Anal. Biochem.*, **150**, 76–85.

SYNDER, S.H. & COYLE, J.T. (1969). Regional differences in H^3-norepinephrine and H^3-dopamine uptake into rat brain homogenates. *J. Pharmacol. Exp. Ther.*, **165**, 78–86.

STONE, C.A., PORTER, C.C., STAVORSKI, J.M., LUDDEN, C.T. & TOTARO, J.A. (1964). Antagonism of certain effects of catecholamine-depleting agents by antidepressant and related drugs. *J. Pharmacol. Exp. Ther.*, **144**, 196–204.

TRENDELENBURG, U., MAXWELL, R.A. & PLUCHINO, S. (1970). Methoxamine as a tool to assess the importance of intraneuronal uptake of l-norepinephrine in the cat's nictitating membrane. *J. Pharmacol. Exp. Ther.*, **172**, 91–99.

U'PRICHARD, D.C., GREENBERG, D.A., SHEEHAN, P.P. & SYNDER, S.H. (1978). Tricyclic antidepressants: therapeutic properties and affinity for alpha noradrenergic receptor binding sites in the brain. *Science*, **199**, 197–198.

VOGT, M. (1954). The concentration of sympathin in different parts of the central nervous system under normal conditions and after the administration of drugs. *J. Physiol.*, **123**, 451–481.

WETSEL, W.C., VALENCA, M.M., MERCHENTHALER, I., LIPOSITS, Z., LOPEZ, F.J., WEINER, R.I., MELLON, P.L. & NEGRO-VILLAR, A. (1992). Intrinsic pulsatile secretory activity of immortalized luteinizing hormone-releasing hormone-secreting neurons. *Proc. Natl. Acad. Sci. U.S.A.*, **89**, 4149–4153.

WHITE, A., SMITH, H., HOADLEY, M., DOBSON, S.H. & RATCLIFFE, J.G. (1987). Clinical evaluation of a two-site immunoradiometric assay for adrenocorticotrophin in unextracted human plasma using monoclonal antibodies. *Clin. Endocrinol.*, **26**, 41–52.

WIKBERG, J.E.S., AKERS, M., CARON, M.G. & HAGEN, P.O. (1983). Norepinephrine-induced down regulation of alpha-1 adrenergic receptors in cultured rabbit aorta smooth muscle cells. *Life. Sci.*, **33**, 1409–1417.

WILKINSON, M., GIBSON, C.J., BRESSLER, B.H. & INMAN, D.R. (1974). Hypothalamic neurons in dissociated cell culture. *Brain Res.*, **82**, 129–138.

WILLIAMS, L.T. & LEFKOWITZ, R.J. (1978). *Receptor Binding Studies in Adrenergic Pharmacology*. New York: Raven Press.

WONG, J.T.F. (1975). *Kinetics of Enzyme Mechanisms*. London: Academic Press.

(Received January 4, 1993
Accepted January 19, 1993)

Br. J. Pharmacol. (1993), **109**, 308–315 © Macmillan Press Ltd, 1993

Effects of potassium channel openers and their antagonists on rat locus coeruleus neurones

E.P. Finta, L. Harms, J. Sevcik, *H.-D. Fischer & [1]P. Illes

Department of Pharmacology, University of Freiburg, Hermann-Herder-Strasse 5, W-7800 Freiburg and *Department of Pharmacology, Medical Academy, Karl-Marx-Strasse 3, 0-8080 Dresden, Germany

1 Intracellular recordings were obtained from a pontine slice preparation of the rat brain containing the locus coeruleus (LC). Two openers of ATP-sensitive potassium (K_{ATP}) channels, RO 31-6930 (10 μM) and cromakalim (100 μM) decreased the spontaneous discharge of action potentials without altering their amplitude or duration. Neither compound changed the resting membrane potential.

2 Of two K_{ATP} channel blockers, tolbutamide (300 μM) increased the firing rate, while glibenclamide (3 μM) only tended to do so. In addition, both compounds antagonized the effect of RO 31-6930 (10 μM). Neither glibenclamide (3 μM) nor tolbutamide (300 μM) altered the resting membrane potential.

3 Tetrodotoxin (0.5 μM) depressed the firing, but did not influence the inhibitory action of RO 31-6930 (10 μM). The excitatory amino acid antagonist, kynurenic acid (500 μM), did not change the spontaneous discharge of action potentials.

4 Small shifts (2–4 mV) of the membrane potential by hyper- or depolarizing current injections markedly decreased and increased the firing rate, respectively.

5 Noradrenaline (100 μM) hyperpolarized the cells and decreased their input resistance. This effect was not antagonized by glibenclamide (3 μM) or tolbutamide (300 μM). Ba^{2+} (2 mM), a blocker of both ATP-sensitive and inwardly rectifying potassium channels, abolished the effects of RO 31-6930 (10 μM) and noradrenaline (100 μM).

6 These data suggest that K_{ATP} channels are present on the noradrenergic LC neurones, but are not coupled to α_2-adrenoceptors.

Keywords: ATP-sensitive potassium channel; cromakalim; RO 31-6930; locus coeruleus; glibenclamide; tolbutamide

Introduction

Recently a novel type of K^+ channel has been described, which is blocked by intracellular ATP (Noma, 1983; Ashcroft, 1988; Dunne & Petersen, 1991). This ATP-sensitive K^+ conductance ($I_{K(ATP)}$) is present not only in pancreatic β-cells, heart, skeletal and smooth muscle, but also in various neurones (Ashcroft & Ashcroft, 1990; de Weille & Lazdunski, 1990). A certain class of drugs, the potassium channel openers (e.g. cromakalim and RO 31-6930), activate $I_{K(ATP)}$, while sulphonylurea antidiabetics (e.g. glibenclamide and tolbutamide) inhibit it, thereby antagonizing the effects of the channel openers (Cook, 1988).

[^{3}H]-glibenclamide has been shown to bind with high selectivity to K_{ATP} channels of central neurones (Bernardi *et al.*, 1988). Although these binding sites are widely distributed throughout the brain (Mourre *et al.*, 1989; Gehlert *et al.*, 1991), the highest densities have been observed in the substantia nigra (SN) (Mourre *et al.*, 1989; Treherne & Ashford, 1991). Most neurones of the SN zona compacta fire spontaneous action potentials at a constant rate followed by prominent afterhyperpolarizations (Kita *et al.*, 1986; Silva & Bunney, 1988; Lacey *et al.*, 1988). SN cells possess dopamine D_2-autoreceptors, which are coupled via a guanosine 5'-triphosphate- (GTP) binding protein to inwardly rectifying potassium channels (Lacey *et al.*, 1988). Dopamine or synthetic D_2-agonists such as quinpirole cause hyperpolarization, and inhibition of the spontaneous firing (Lacey *et al.*, 1988). In acutely dissociated cells, the quinpirole-induced conductance is reversed by tolbutamide suggesting the involvement of $I_{K(ATP)}$ (Roeper *et al.*, 1990). A decrease in intracellular ATP or the extracellular application of cromakalim also hyperpolarizes SN neurones confirming the presence of K_{ATP} channels (Häusser *et al.*, 1991). By contrast, in brain slices containing the SN, glibenclamide does not antagonize the effect of dopamine, and cromakalim is without effect (Hicks & Henderson, 1992).

Noradrenergic neurones of the nucleus locus coeruleus (LC) exhibit electrophysiological characteristics similar to dopaminergic SN cells. LC neurones discharge spontaneous action potentials with a pacemaker-like regularity; the stimulation of somatic α_2-adrenoceptors inhibits the firing (Cedarbaum & Aghajanian, 1977; Henderson *et al.*, 1982). These receptors hyperpolarize the membrane by increasing an inwardly rectifying potassium conductance (Aghajanian & VanderMaelen, 1982; Williams *et al.*, 1985; 1988).

Because of the similarities between SN and LC neurones, we searched for the presence of an ATP-sensitive potassium conductance in the LC. Moreover, we investigated whether the α_2-autoreceptors of LC cells are coupled to K_{ATP} channels.

Methods

Brain slice preparation

Midpontine slices of the rat brain were prepared and maintained as previously described (Illes & Nörenberg, 1990; Regenold & Illes, 1990). In brief, male Wistar rats (150–200 g) were anaesthetized with ether and decapitated. Coronal slices of about 400 μm thickness, containing the caudal part of the LC were prepared in oxygenated medium at 1–4°C with a Lancer vibratome. A single slice was placed in a recording chamber and was superfused at a rate of 2 ml min^{-1} with medium saturated with 95% O_2 plus 5% CO_2 and maintained at 35–36°C. The medium had the following composition (in mM): NaCl 126, KCl 2.5, NaH_2PO_4 1.2, $MgCl_2$ 1.3, $CaCl_2$ 2.4, $NaHCO_3$ 25 and glucose 11. Ascorbic acid (0.3 mM and EDTA (0.03 mM) were also present in order to prevent oxidation of noradrenaline. When

[1] Author for correspondence.

$MgCl_2$ was added, NaCl was reduced to maintain a similar osmolarity. No osmotic compensation was made for $BaCl_2$.

Identification of LC neurones and intracellular recording

LC neurones were identified under a binocular microscope at the ventrolateral border of the fourth ventricle. LC cells were distinguished from neighbouring mesencephalic trigeminal neurones by their electrophysiological properties including spontaneous firing at a frequency of 0.2–5 Hz and a hyperpolarizing response to noradrenaline (Henderson *et al.*, 1982; Williams *et al.*, 1985).

Recording of the membrane potential and current injection was carried out with glass micro-electrodes filled with KCl (2 M) (tip resistance, 70–120 MΩ) using a high impedance pre-amplifier and a bridge-circuit (Axoclamp 2A). In some experiments hyper- or depolarizing currents were passed through the micro-electrode in order to induce small (2–4 mV) shifts of the membrane potential. Current injection was for 2 min at 5–8 min intervals. The changes in membrane potential were evoked sequentially (−2, −4, 2 and 4 mV) in order to determine the corresponding alterations of the firing rate. Another group of LC cells was constantly hyperpolarized by about 20 mV. In addition, hyperpolarizing current pulses of constant amplitude and 250 ms duration were delivered at a frequency of 0.5 Hz. The apparent input resistance was calculated from the peak potential change produced. The membrane potential was determined on withdrawal of the micro-electrode from the cell at the end of each experiment. Changes in the membrane potential were displayed on a Gould RS 3200 pen-recorder and in addition stored on tape (Racal Store 4). The action potentials were plotted by means of a Gould 1425 digital oscilloscope on a Gould Colorwriter 6120.

Application of drugs

Drugs were applied by changing the superfusion medium by means of three-way taps. At the constant flow rate of 2 ml min^{-1} about 30 s were required until the drugs reached the bath. In some experiments we used only K_{ATP} channel openers (cromakalim, RO 31-6930) or blockers (glibenclamide, tolbutamide); in this case the superfusion times were 15 and 25 min, respectively. When the interaction of these compounds was studied, we added the blockers for 10 min at first, and then added the openers for another 15 min in the continuous presence of the blockers. A similar time-schedule was adopted when the influence of tetrodotoxin or Ba^{2+} was tested on the effect of RO 31-6930. Kynurenic acid was superfused for 10 min.

Before starting an experiment, the LC neurones were identified by their hyperpolarizing response to noradrenaline. When noradrenaline was applied both before and 25 min after the addition of glibenclamide or tolbutamide, the α-adrenoceptor agonist was present in the superfusion medium for 2 min each time. In some cases the effect of noradrenaline was determined on the input resistance both before and 10 min after the addition of glibenclamide.

Materials

The following drugs were used: RO 31-6930 (2-(6-cyano-2,2-dimethyl-2H-1-benzopyran-4-yl)pyridine-1-oxide) (M. Eltze, Byk Gulden, Konstanz, Germany); glibenclamide, tolbutamide (H. Englert; Hoechst, Frankfurt am Main, Germany); kynurenic acid (RBI, Natick, MA, U.S.A.); (−)-noradrenaline hydrochloride, tetrodotoxin (Sigma, Deisenhofen, Germany); cromakalim (S. Pathak; Smith, Kline & Beecham, Betchworth, Surrey).

Stock solutions (1–100 mM) of all compounds were prepared in the following solvents: distilled water (noradrenaline, tetrodotoxin), 70% ethanol (RO 31-6930), 0.2 N NaOH (glibenclamide, tolbutamide) or medium (cromakalim, kynurenic acid). Further dilutions were made with medium. Equivalent quantities of the solvents had no effect.

Statistics

Means ± s.e.mean are given throughout. The Kruskal-Wallis analysis followed by the Mann-Whitney-test was used for the comparison of the means and the comparison of the means with zero. A probability level of 0.05 or less was considered to be statistically significant. In the case of multiple comparisons, the significance level was adjusted according to the method of Bonferroni (Wallenstein *et al.*, 1980).

Table 1 Effects of K_{ATP} channel openers and blockers on the frequency of spontaneous action potentials in rat locus coeruleus neurones and the interaction of these compounds with each other

Treatment	μM	n	*Change in frequency (%)* 0–10 min	0–15 min	10–25 min
None		9	11.6 ± 10.2	15.0 ± 16.0	−0.2 ± 10.2
RO 31-6930	10	12		−72.1 ± 8.5[a]	
Cromakalim	100	6		−71.2 ± 12.3[a]	
Glibenclamide	3	5	70.2 ± 32.1		8.6 ± 11.2
Glibenclamide	3	11	90.4 ± 40.3		
+ RO 31-6930	10	11			1.7 ± 11.2[b]
Tolbutamide	300	5	137.8 ± 48.5[a]		−1.8 ± 6.4
Tolbutamide	300	6	161.7 ± 74.4[a]		
+ RO 31-6930	10	6			12.8 ± 9.3[b]
Tetrodotoxin	0.5	5	−52.1 ± 16.2[a]		
+ RO 31-6930	10				−59.6 ± 13.3[a]
Ba^{2+}	2000	6	−18.8 ± 8.0		
+ RO 31-6930	10	6			7.4 ± 13.8[b]

No effect of tetrodotoxin on the RO 31-6930-induced decrease in firing rate was observed.
In some experiments only K_{ATP} channel openers (cromakalim, RO 31-6930) or blockers (glibenclamide, tolbutamide) were used; in this case the superfusion times were 15 and 25 min, respectively. When the interaction of these compounds was studied, at first the blockers were added for 10 min, and then the openers for another 15 min in the continuous presence of the blockers. A similar time-schedule was adopted when the influence of tetrodotoxin or Ba^{2+} was tested on the effect of RO 31-6930. The percentage changes in frequency were calculated with respect to 0 or 10 min, as indicated. Means ± s.e.mean of *n* experiments are shown.
[a] $P < 0.05$–0.01: significant differences from corresponding changes in the absence of drugs; [b] $P < 0.01$: significant differences from the effect of RO 31-6930 alone.

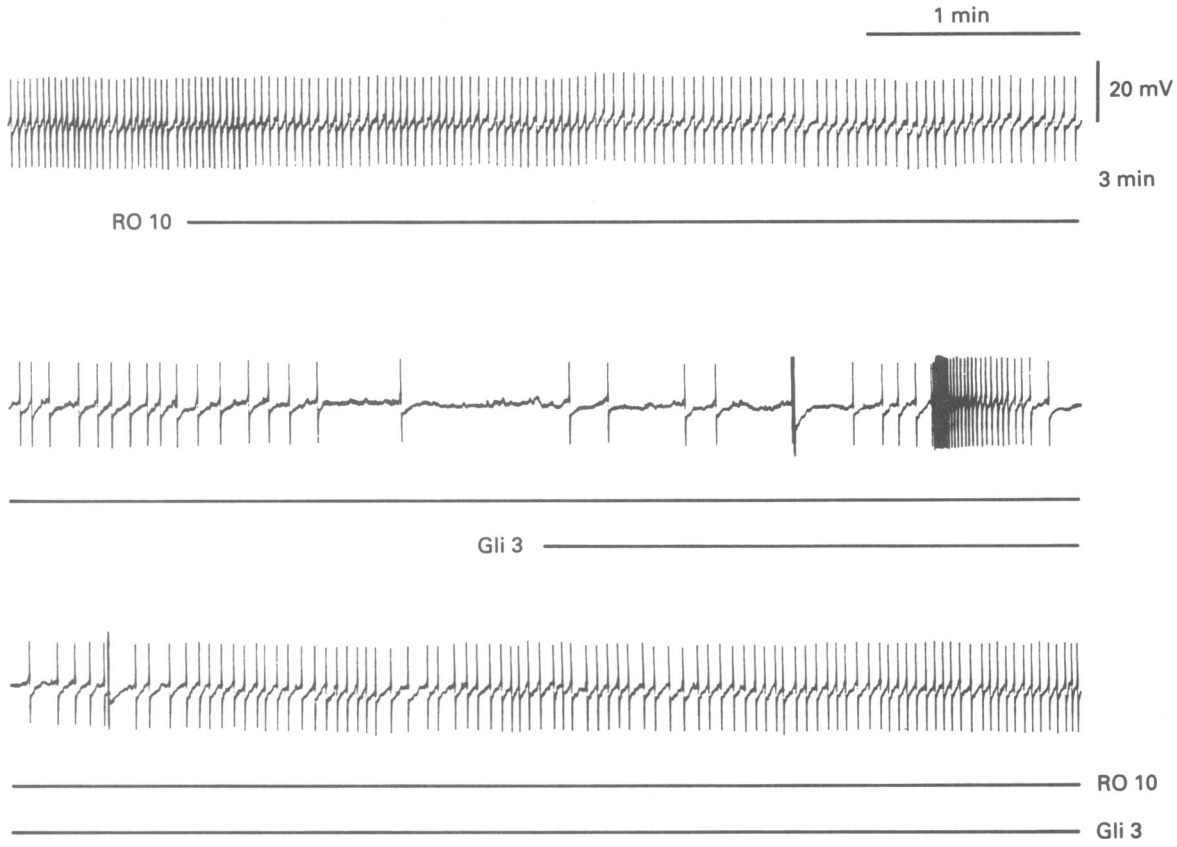

Figure 1 Effect of RO 31-6930 on the membrane potential and firing rate of rat locus coeruleus neurones and interaction with glibenclamide. The full height of action potentials was not reproduced by the pen recorder. The inhibitory effect of RO 31-6930 (RO; 10 μM) on the spontaneous firing was reversed by glibenclamide (Gli; 3 μM). The superfusion times of both compounds are indicated by the horizontal bars. The intervals between the traces are shown.

Results

A total of 84 LC cells included in this study had a resting membrane potential of -56.2 ± 0.6 mV and a spontaneous firing rate of 1.5 ± 0.1 Hz. In 9 experiments, measurements were carried out for 25 min in the absence of any drug; under these conditions both the membrane potential (2.1 ± 0.9 mV depolarization; $P > 0.05$) and the discharge of action potentials (Table 1) were stable.

Effects of K_{ATP} channel openers

In a first series of experiments, RO 31-6930 (10 μM) depressed the firing rate 15 min after its application by about 70% (Figure 1, Table 1). By contrast, the membrane potential of the LC cells was not altered by RO 31-6930 (10 μM) (0.2 ± 1.2 mV hyperpolarization; $n = 12$; $P > 0.05$) when compared with the corresponding change measured under drug-free conditions (1.0 ± 0.4 mV depolarization; $n = 9$). Moreover, the amplitude and duration of action potentials, as well as the afterhyperpolarization following a spike were stable in spite of the presence of RO 31-6930 (10 μM) (Figure 2; $n = 10$). Cromakalim (100 μM) decreased the firing rate to a similar extent as RO 31-6930 (10 μM) (Table 1), and failed to alter the membrane potential (0.5 ± 2.0 mV depolarization; $n = 6$; $P > 0.05$). Neither the amplitude and duration of action potentials, nor the afterhyperpolarization were changed by cromakalim (100 μM) ($n = 4$).

Effects of K_{ATP} channel blockers and their interaction with K_{ATP} channel openers

Glibenclamide (3 μM) did not change the frequency of action potentials in some cells (Figure 3), but increased it in others. In a total of 16 neurones, glibenclamide (3 μM) tended to increase the firing rate, although this effect did not reach statistical significance ($84.1 \pm 29.0\%$; $n = 16$; $P > 0.05$) when compared with drug-free controls ($11.6 \pm 10.2\%$; $n = 9$; see also Table 1). We noticed already in a few ($n = 3$) preliminary experiments that the inhibitory effect of RO 31-6930 (10 μM) could be counteracted by subsequently applied glibenclamide (3 μM) (Figure 1). The period of very fast spiking soon after the addition of glibenclamide (3 μM) was probably an instability of neuronal activity, since it was observed only in one cell. In most cases we used the reversed protocol; a 10 min contact with glibenclamide (3 μM) was followed by a 15 min co-application of RO 31-6930 (10 μM) and glibenclamide (3 μM). Under these conditions the K_{ATP} channel opener failed to produce any inhibition (Figure 3, Table 1).

In contrast to glibenclamide (3 μM), tolbutamide (300 μM) markedly facilitated the discharge of action potentials (Figure 4, Table 1). Moreover, the inhibitory effect of RO 31-6930 (10 μM) was abolished in the concomitant presence of tolbutamide (300 μM) (Figure 4, Table 1).

Neither glibenclamide (3 μM) (0.1 ± 0.2 mV depolarization; $n = 16$; $P > 0.05$) nor tolbutamide (300 μM) (0.6 ± 0.5 mV hyperpolarization; $n = 11$; $P > 0.05$) influenced the membrane potential of LC cells on their own; the corresponding depolarization measured under drug-free conditions was 0.5 ± 0.3 mV ($n = 9$).

Effect of current injection

The firing rate of 5 LC neurones was 2.2 ± 0.7 Hz at the resting membrane potential of -54.3 ± 2.0 mV. Already slight (2 and 4 mV) hyperpolarizations markedly decreased the firing rate by $48.4 \pm 7.7\%$ and $83.1 \pm 8.5\%$, respectively.

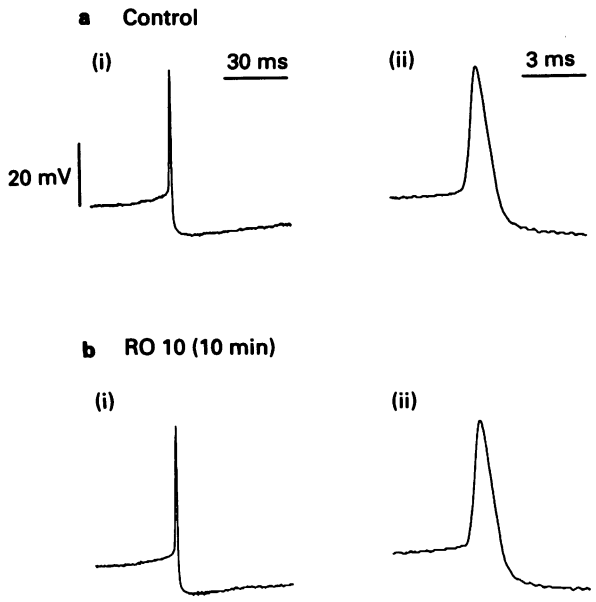

Figure 2 Effect of RO 31-6930 on spontaneous action potentials of locus coeruleus neurones. Each tracing shows the average of four spikes before (a) and 10 min after (b) the application of RO 31-6930 (RO; 10 μM). Note that the time-scale of (i) is different from that of (ii).

In contrast, similar depolarizations (2 and 4 mV) increased the firing rate by 67.5 ± 5.7% and 120.5 ± 21.3%, respectively. All changes were statistically significant ($P<0.05$).

Effects of tetrodotoxin, and a low Ca^{2+}, high Mg^{2+} medium, as well as kynurenic acid

Tetrodotoxin (TTX; 0.5 μM) decreased the amplitude and prolonged the duration of the action potentials ($n = 5$). It also markedly depressed the firing rate (Table 1). However, the inhibitory potency of RO 31-6930 (10 μM) was unaffected in the presence of TTX (0.5 μM). In order to block all synaptic inputs to LC neurones, several types of low Ca^{2+} (0.3 mM), high Mg^{2+} (5–20 mM) media were used. Unfortunately all treatments depolarized the cells, and after a transient increase produced a complete blockade of the spontaneous action potential discharge. Thus, under these conditions it was not possible to investigate the effects of K_{ATP} channel openers on the firing rate.

Kynurenic acid (500 μM) did not change the frequency of spontaneous action potentials (4.8 ± 13.7% increase; $n = 5$; $P>0.05$) when compared with measurements in the absence of drugs (11.6 ± 10.2% increase; $n = 9$).

Effect of noradrenaline in the presence of K_{ATP} channel blockers or Ba^{2+}

Noradrenaline (100 μM) hyperpolarized LC neurones to the same extent both before (13.5 ± 3.7 mV) and 25 min after superfusion with glibenclamide (3 μM) (12.4 ± 2.7 mV; $n = 5$; $P>0.05$). Tolbutamide (300 μM) also did not alter the effect

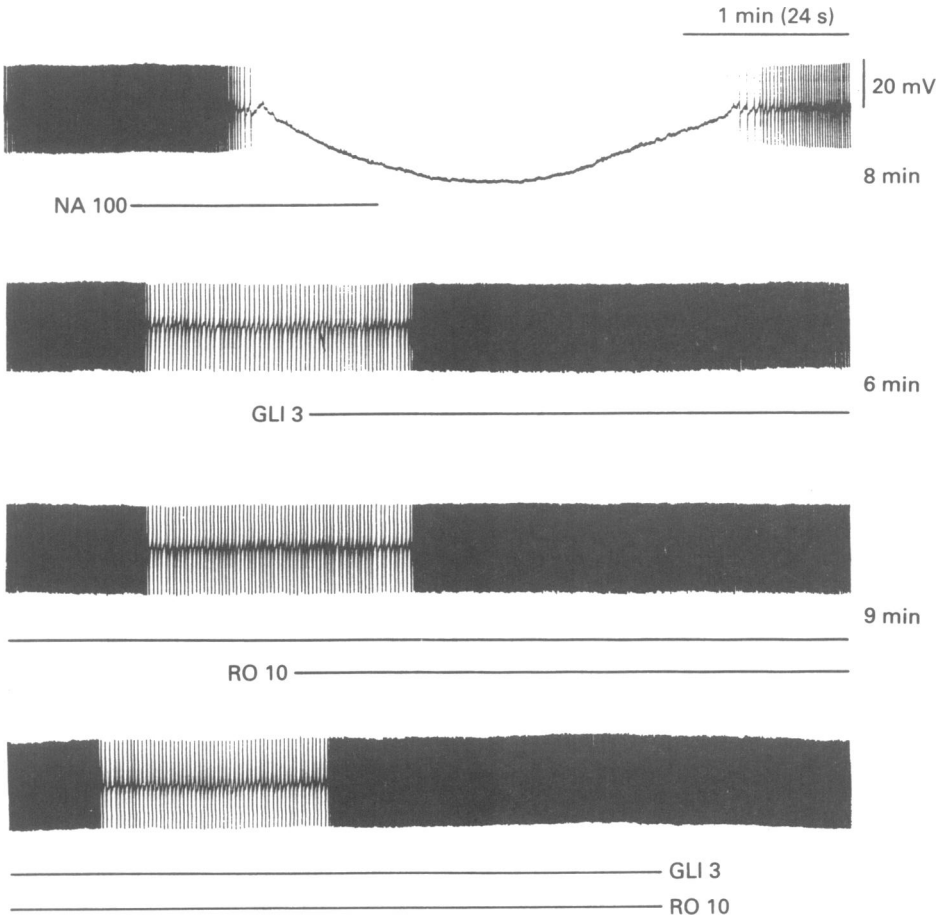

Figure 3 Effect of glibenclamide on the membrane potential and firing rate of locus coeruleus (LC) neurones and interaction with RO 31-6930. Glibenclamide (Gli; 3 μM) slightly increased the spontaneous firing and antagonized the inhibitory effect of RO 31-6930 (RO; 10 μM). The LC cell was identified by its sensitivity to noradrenaline (NA; 100 μM). The superfusion times of all compounds are indicated by the horizontal bars. The intervals between the traces are shown. Note that recording has two different time-scales.

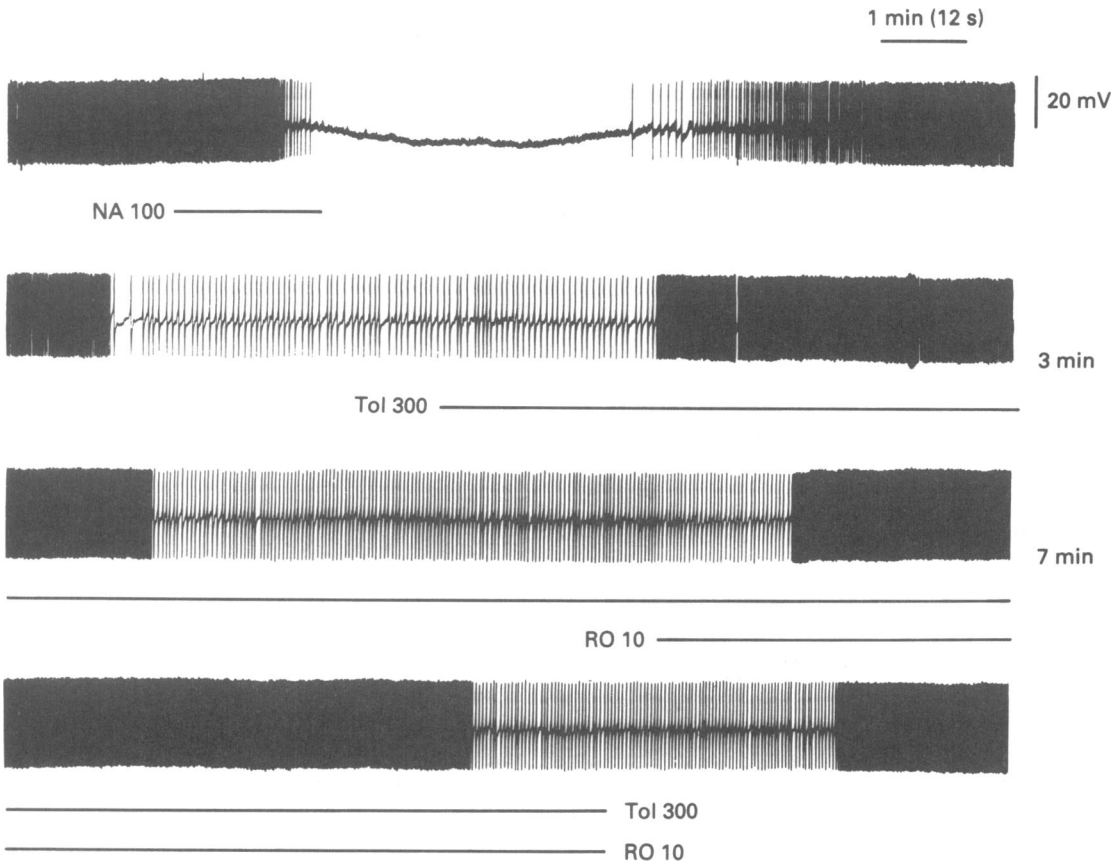

Figure 4 Effect of tolbutamide on the membrane potential and firing rate of locus coeruleus (LC) neurones and interaction with RO 31-6930. Tolbutamide (Tol; 300 μM) increased the spontaneous firing and antagonized the inhibitory effect of RO 31-6930 (RO; 10 μM). The LC cell was identified by its sensitivity to noradrenaline (NA; 100 μM). The superfusion times of all compounds are indicated by the horizontal bars. The intervals between the traces are shown. Note that recording has two different time-scales.

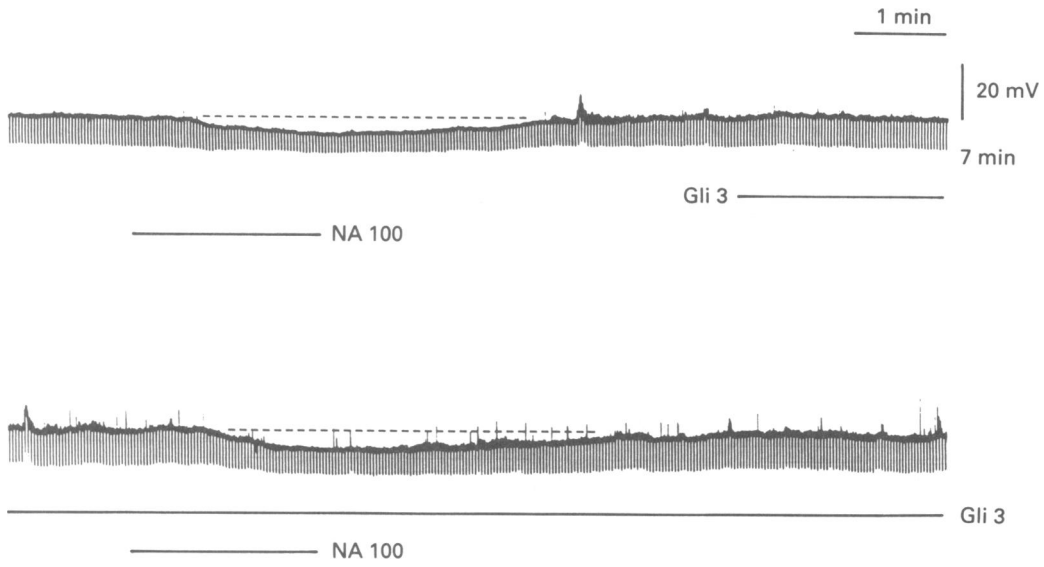

Figure 5 Effect of noradrenaline on the membrane potential and apparent input resistance of locus coeruleus neurones and interaction with glibenclamide. Constant current was passed through the electrode to hyperpolarize the neurones by about 20 mV. Downward deflections represent electrotonic potentials caused by hyperpolarizing current pulses of constant amplitude. Noradrenaline (NA; 100 μM) produced a similar hyperpolarization and decrease of input resistance, both before and 10 min after the addition of glibenclamide (Gli; 3 μM). The superfusion times of all compounds are indicated by the horizontal bars. The intervals between the traces are shown. The pre-noradrenaline membrane potential is indicated by broken lines.

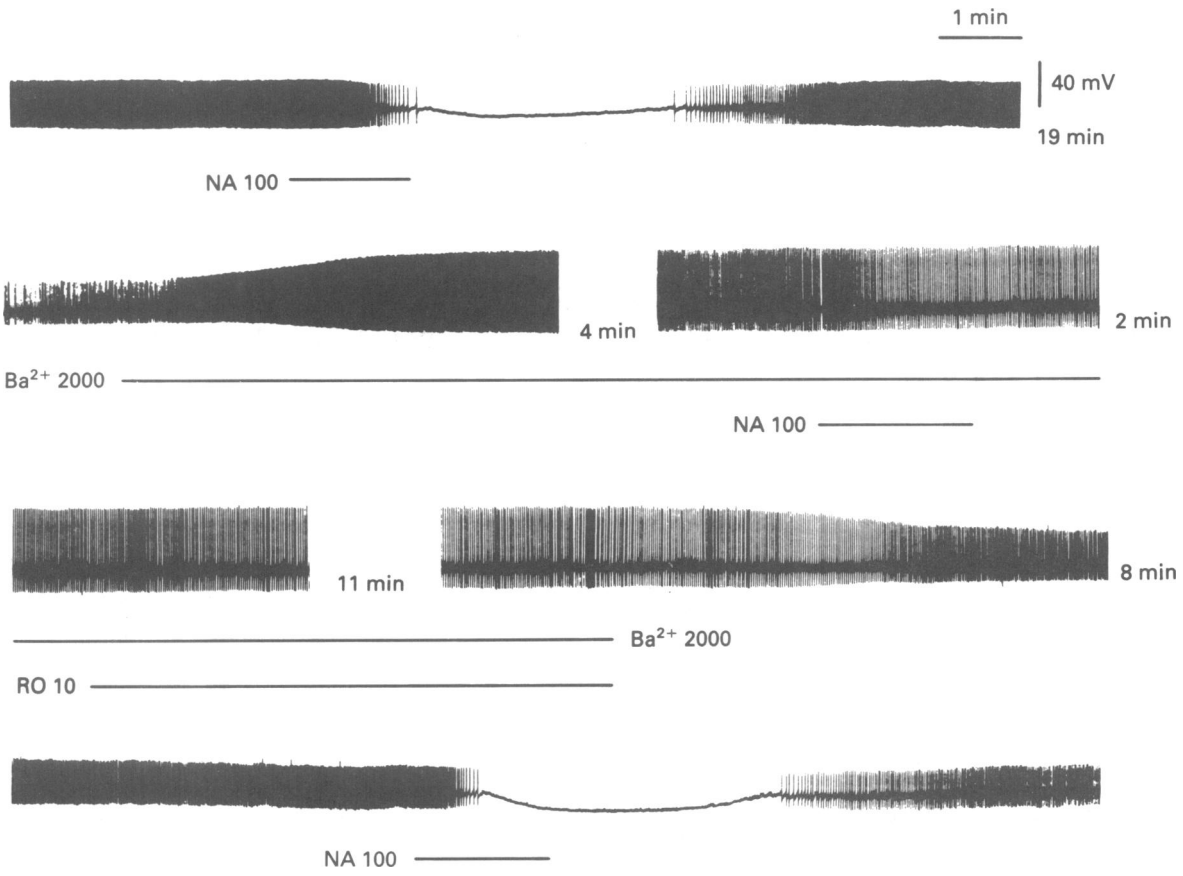

Figure 6 Effect of Ba^{2+} on the membrane potential and firing rate of locus coeruleus neurones, and interaction with noradrenaline and RO 31-6930. Ba^{2+} (2 mM) increased the duration of the action potentials. This improved the reproduction of the spike amplitude by the pen-recorder. Ba^{2+} (2 mM) antagonized the effects of noradrenaline (NA; 100 μM) and RO 31-6930 (RO; 10 μM). There is a full recovery of the noradrenaline- (100 μM) induced hyperpolarization after the washout of Ba^{2+}. The intervals between the traces are shown. The superfusion times for all compounds are indicated by the horizontal bars.

of noradrenaline on the membrane potential ($n = 5$).

In 4 further experiments, LC cells were prevented from spontaneously firing by continuous hyperpolarizing current injection through the micro-electrode (Figure 5). In addition, hyperpolarizing current pulses of constant amplitude were delivered at regular intervals in order to measure the input resistance. Noradrenaline (100 μM) caused a hyperpolarization of 8.6 ± 1.5 mV and decreased the input resistance (127.3 ± 19.7 MΩ) by $27.3 \pm 2.8\%$. After a 10 min presence of glibenclamide (3 μM) both the noradrenaline- (100 μM) induced hyperpolarization (8.8 ± 1.4 mV; $P > 0.05$) and the fall in input resistance ($29.9 \pm 1.7\%$; $P > 0.05$) were the same as in the absence of the K_{ATP} channel blocker. Furthermore, in these experiments, glibenclamide (3 μM) did not alter either the membrane potential (0.6 ± 0.6 mV depolarization; $P > 0.05$) or the input resistance ($11.0 \pm 4.3\%$ increase from 124.5 ± 22.4 MΩ; $P > 0.05$).

Ba^{2+} (2 mM) prolonged the duration, but failed to influence the amplitude of action potentials; this improved the reproduction of spike amplitudes by the pen-recorder (Figure 6). Immediately after the application of Ba^{2+} the firing rate transiently increased, but returned to its original value afterwards. However, the effects of both RO 31-6930 (10 μM) and noradrenaline (100 μM) were abolished in the presence of Ba^{2+} (2 mM) (Figure 6, Table 1).

Discussion

K_{ATP} channels provide a link between the metabolic status and electrophysiological properties of neurones in the central nervous system (Ashcroft & Ashcroft, 1990). This fact has a number of physiological and pathophysiological implications. Brain neurones are known to be extremely sensitive to hypoxia and reduced supply of glucose, conditions which lead to decreased intracellular ATP concentrations and, in consequence, to opening of K_{ATP} channels (de Weille & Lazdunski, 1990). The resulting hyperpolarization of the cell somata decreases the excitability and conserves energy. Similarly, a possible hyperpolarization of the nerve terminals inhibits transmitter release (Amoroso *et al.*, 1990; Schmid-Antomarchi *et al.*, 1990), and thereby retards metabolic exhaustion. Since hypoxia produces an excessive release of glutamate, activation of $I_{K(ATP)}$ may protect neurones innervated by excitatory amino acid pathways (Ben-Ari, 1989). Finally, in certain areas of the brain (e.g. in hypothalamic nuclei regulating food intake), neurones which possess K_{ATP} channels and respond to hyperglycemia with increased excitability have been described (Ashford *et al.*, 1990).

Various experimental approaches unequivocally document the presence of K_{ATP} channels in the brain. The methods utilized include the measurement of $^{86}Rb^+$ efflux, which is an indicator of transmembrane K^+ movements (Amoroso *et al.*, 1990; Schmid-Antomarchi *et al.*, 1990), the determination of transmitter release (Amoroso *et al.*, 1990; Schmid-Antomarchi *et al.*, 1990) and electrophysiological recordings. The application of ATP to inside-out patches from cerebral cortical (Ashford *et al.*, 1988) and hypothalamic (Ashford *et al.*, 1990) neurones directly demonstrated the subsequent closure of a K^+ channel. The evidence for the existence of K_{ATP} channels in hippocampal pyramidal cells is less convincing. Apparently, in CA3 cells cromakalim activates an inwardly rectifying K^+ conductance, which is sensitive to Ba^{2+} but not to tetraethylammonium. It was suggested that

this conductance was different from $I_{K(ATP)}$ (Alzheimer *et al.*, 1989). However, $I_{K(ATP)}$ was reported to be involved in the hyperpolarization of the same neurones by hypoxic episodes (Ben-Ari, 1989), but not by glucose deprivation (Knöpfel *et al.*, 1990). Moreover, the hypoxic depolarization following the hyperpolarization was caused by the release of glutamate from mossy fibres and could be prevented by K_{ATP} channel openers acting at these glutamatergic terminals (Ben-Ari & Lazdunski, 1989; Ben-Ari *et al.*, 1990; Mourre *et al.*, 1991).

We have found in LC cells that two openers of ATP-sensitive K^+ channels depressed the spontaneous discharge of action potentials. The compounds used were cromakalim, a racemic benzopyran derivative, and RO 31-6930, which has a related non-chiral structure of much higher biological potency (Cook, 1988; Edwards & Weston, 1990). In contrast to results in the heart (Sanguinetti *et al.*, 1988; Bott *et al.*, 1992), the duration of action potentials was not decreased in the LC. Moreover, in agreement with findings in cardiac (Sanguinetti *et al.*, 1988; Bott *et al.*, 1992), but not in smooth muscle (Hamilton *et al.*, 1986) or pancreatic β-cells (Henquin & Meissner, 1982; Cook, 1988), the resting membrane potential of LC neurones was not increased by the K_{ATP} channel openers.

Glibenclamide is a sulphonylurea blocker of $I_{K(ATP)}$; tolbutamide is structurally similar, but has a considerably lower biological activity (Schmid-Antomarchi *et al.*, 1987; de Weille & Lazdunski, 1990). In our experiments, tolbutamide given alone markedly increased the firing rate, while glibenclamide only tended to facilitate it. However, both compounds blocked the inhibitory effect of RO 31-6930 on the spontaneous discharge of action potentials. Neither glibenclamide nor tolbutamide depolarized LC cells. These results are analogous with those seen in the heart (Nakaya *et al.*, 1991; Bott *et al.*, 1992) but disagree with findings in pancreatic β-cells (Henquin & Meissner, 1982; Cook, 1988).

We used concentrations of K_{ATP} channel openers and blockers which were previously shown to be effective in cardiac muscle (Ashcroft & Ashcroft, 1990). These compounds altered the firing rate of LC neurones, although they did not change appreciably the membrane potential or the apparent input resistance. The most likely explanation is that the channel openers slightly hyperpolarized the cells whereas the blockers produced a minute depolarization. The small changes of the membrane potential developed over a considerable time, and could not be detected with the high resistance micro-electrodes used by us. In fact, we found that small shifts of the membrane potential by current injection caused immediate alterations of the firing rate, which were similar in their extent to those produced by the potassium channel openers and blockers (see also Williams *et al.*, 1985; Harms *et al.*, 1992).

In LC neurones, TTX markedly depressed the spontaneous discharge of action potentials decreasing the amplitude of the spikes and prolonging their duration. Apparently, after the blockade of sodium conductance by TTX, the cells continued to fire slower calcium action potentials (Illes & Regenold, 1989). The effect of RO 31-6930 persisted after the inhibition of action potential-dependent synaptic inputs by TTX. Thus it may be concluded that the RO 31-6930-induced depression of the firing rate arises directly at the somata of LC neurones and not indirectly via neighbouring non-LC cells. Unfortunately, we did not succeed in synaptically isolating LC cells by various low Ca^{2+}, high Mg^{2+} media. In these superfusion media, the spontaneous discharge of spikes temporarily increased and subsequently stopped impeding the measurement of RO 31-6930 effects. However, under the conditions of the present study, K_{ATP} channel openers are unlikely to diminish a tonic facilitatory input controlling LC neurones. Such an input derives mostly from the nucleus paragigantocellularis and is mediated by excitatory amino acids (EAA) (Aston-Jones *et al.*, 1991). In brain slices, focal electrical stimulation in the area of LC evokes excitatory postsynaptic potentials which are depressed by the EAA-antagonist kynurenic acid (500 μM) (Cherubini *et al.*, 1988; Williams *et al.*, 1991). Nonetheless, in the absence of electrical stimulation the spontaneous firing rate was not changed by 500 μM kynurenic acid (present study). Hence, a tonic EAA control of the neuronal activity is probably not operative under *in vitro* conditions.

In the substantia nigra, dopamine D_2-autoreceptors were suggested to be coupled to K_{ATP} channels since the D_2-receptor agonist quinpirole caused a tolbutamide-reversible hyperpolarization (Roeper *et al.*, 1990; for the opposite view see Hicks & Henderson, 1992). In LC neurones, noradrenaline stimulates α_2-adrenoceptors, and thereby enhances a potassium permeability with a resulting decrease in firing rate (Egan *et al.*, 1983; Williams *et al.*, 1985). We did not find any antagonism between glibenclamide or tolbutamide on the one hand and noradrenaline on the other, although either blocker of $I_{K(ATP)}$ abolished the effect of RO 31-6930. By contrast Ba^{2+}, which inhibits both the inwardly rectifying K^+ conductance (Constanti & Galvan, 1983; Osmanovic & Shefner, 1987) and the K_{ATP} channels (Quayle *et al.*, 1988, Adams & Nonner, 1990), prevented the inhibitory actions of both noradrenaline and RO 31-6930. These results as a whole indicate that α_2-autoreceptors of LC cells activate an inwardly rectifying K^+ current (Williams *et al.*, 1988) rather than $I_{K(ATP)}$.

In conclusion, K_{ATP} channels appear to be present on the somata of LC neurones although a presynaptic location on excitatory nerve terminals innervating the LC cannot be definitely excluded. The density of these channels is probably quite low since even relatively high concentrations of cromakalim and RO 31-6930 produce only moderate decreases in the firing rate. Similarly, rather high concentrations of glibenclamide and tolbutamide are needed to increase the spontaneous firing. However, it is possible that $I_{K(ATP)}$ is activated during hypoxia or hypoglycemia. Under these conditions K_{ATP} channels may open and protect LC neurones against further metabolic exhaustion.

J.S is recipient of a research fellowship from the Alexander von Humboldt-Stiftung. This work was supported by the Deutsche Forschungsgemeinschaft (SFB 325). The generous gift of drugs by Byk Gulden, Hoechst and Smith, Kline & Beecham is gratefully acknowledged.

References

ADAMS, D.J. & NONNER, W. (1990). Voltage dependent potassium channels: gating, ion permeation and block. In *Potassium Channels: Structure, Classification, Function and Therapeutic Potential.* ed. Cook, N.S. pp. 40–69. Chichester: Ellis Horwood.

AGHAJANIAN, G.K. & VANDERMAELEN, C.P. (1982). α_2-Adrenoceptor-mediated hyperpolarization of locus coeruleus neurones: intracellular studies *in vivo*. *Science*, **215**, 1394–1396.

ALZHEIMER, C., SUTOR, B. & TEN BRUGGENCATE, G. (1989). Cromakalim (BRL 34915) acts on an inwardly rectifying neuronal K^+ conductance, which is similar to that activated by adenosine. *Pflügers Arch.*, **414** (Suppl. 1), S121–122.

AMOROSO, S., SCHMID-ANTOMARCHI, H., FOSSET, M. & LAZDUNSKI, M. (1990). Glucose, sulfonylureas, and neurotransmitter release: role of ATP-sensitive K^+ channels. *Science*, **247**, 852–854.

ASHCROFT, F.M. (1988). Adenosine 5'-triphosphate-sensitive potassium channels. *Annu. Rev. Neurosci.*, **11**, 97–118.

ASHCROFT, S.J.H. & ASHCROFT, F.M. (1990). Properties and functions of ATP-sensitive K-channels. *Cell. Sign.*, **2**, 197–214.

ASHFORD, M.L.J., STURGESS, N.C., TROUT, N.J., GARDNER, N.J. & HALES, C.N. (1988). Adenosine-5'-triphosphate-sensitive ion channels in neonatal rat cultured central neurones. *Pflügers Arch.*, **412**, 297–304.

ASHFORD, M.L.J., BODEN, P.R. & TREHERNE, J.M. (1990). Glucose-induced excitation of hypothalamic neurones is mediated by ATP-sensitive K^+ channels. *Pflügers Arch.*, **415**, 479–483.

ASTON-JONES, G., SHIPLEY, M.T., CHOUVET, G., ENNIS, M., VAN BOCKSTAELE, E., PIERIBONE, V., SHIEKHATTAR, R., AKAOKA, H., DROLET, G., ASTIER, B., CHARLETY, P., VALENTINO, R.J. & WILLIAMS, J.T. (1991). Afferent regulation of locus coeruleus neurons: anatomy, physiology and pharmacology. *Progr. Brain Res.*, **88**, 47–75.

BEN-ARI, Y. (1989). Effect of glibenclamide, a selective blocker of an ATP-K^+ channel, on the anoxic response of hippocampal neurones. *Pflügers Arch.*, **414**, (Suppl. 1), S111–S114.

BEN-ARI, Y. & LAZDUNSKI, M. (1989). Galanin protects hippocampal neurons from the functional effects of anoxia. *Eur. J. Pharmacol.*, **165**, 331–332.

BEN-ARI, Y., KRNJEVIC, K. & CREPEL, V. (1990). Activators of ATP-sensitive K^+ channels reduce anoxic depolarization in CA3 hippocampal neurons. *Neuroscience*, **37**, 55–60.

BERNARDI, H., FOSSET, M. & LAZDUNSKI, M. (1988). Characterization, purification and affinity labelling of the brain [^{3}H]glibenclamide binding protein, a putative neuronal ATP-regulated K^+ channel. *Proc. Natl. Acad. Sci. U.S.A.*, **85**, 9816–9820.

BOTT, A., ELTZE, M. & ILLES, P. (1992). External ATP antagonizes the effect of potassium channel openers in guinea-pig ventricular papillary muscle. *Eur. J. Pharmacol.*, **213**, 141–144.

CEDARBAUM, J.M. & AGHAJANIAN, G.K. (1977). Catecholamine receptors of locus coeruleus neurones: pharmacological characterization. *Eur. J. Pharmacol.*, **44**, 375–385.

CHERUBINI, E., NORTH, R.A. & WILLIAMS, J.T. (1988). Synaptic potentials in rat locus coeruleus neurones. *J. Physiol.*, **406**, 431–442.

CONSTANTI, A. & GALVAN, M. (1983). Fast inward-rectifying current accounts for anomalous rectification in olfactory cortex neurones. *J. Physiol.*, **385**, 153–178.

COOK, N.S. (1988). The pharmacology of potassium channels and their therapeutic potential. *Trends Pharmacol. Sci.*, **9**, 21–28.

DE WEILLE, J.R. & LAZDUNSKI, M. (1990). Regulation of the ATP-sensitive potassium channel. In *Ion Channels*. ed. Narahashi, T. pp. 205–222. New York; Plenum.

DUNNE, M.J. & PETERSEN, O.H. (1991). Potassium selective ion channels in insulin-secreting cells: physiology, pharmacology and their role in stimulus-secretion coupling. *Biochim. Biophys. Acta*, **1071**, 67–82.

EDWARDS, G. & WESTON, A.H. (1990). Structure-activity relationships of K^+ channel openers. *Trends Pharmacol. Sci.*, **11**, 417–422.

EGAN, T.M., HENDERSON, G., NORTH, R.A. & WILLIAMS, J.T. (1983). Noradrenaline-mediated synaptic inhibition in rat locus coeruleus neurones. *J. Physiol.*, **345**, 477–488.

GEHLERT, D.R., GACKENHEIMER, S.L., MAIS, D.E. & ROBERTSON, D.W. (1991). Quantitative autoradiography of the binding sites for [^{125}I]iodoglyburide, a novel high-affinity ligand for ATP-sensitive potassium channels in rat brain. *J. Pharmacol. Exp. Ther.*, **257**, 901–907.

HAMILTON, T.C., WEIR, S.W. & WESTON, A.H. (1986). Comparison of the effects of BRL 34915 and verapamil on electrical and mechanical activity in rat portal vein. *Br. J. Pharmacol.*, **88**, 103–111.

HARMS, L., FINTA, E.P., TSCHÖPL, M. & ILLES, P. (1992). Depolarization of rat locus coeruleus neurons by adenosine 5'-triphosphate. *Neuroscience*, **48**, 941–952.

HÄUSSER, M.A., DE WEILLE, J.R. & LAZDUNSKI, M. (1991). Activation by cromakalim of pre- and post-synaptic ATP-sensitive K^+ channels in substantia nigra. *Biochem. Biophys. Res. Commun.*, **174**, 909–914.

HENDERSON, G., PEPPER, C.M. & SHEFNER, S.A. (1982). Electrophysiological properties of neurones contained in the locus coeruleus and mesencephalic nucleus of the trigeminal nerve in vitro. *Exp. Brain Res.*, **45**, 29–37.

HENQUIN, J.-C. & MEISSNER, H.P. (1982). Opposite effects of tolbutamide and diazoxide on $^{86}Rb^+$ fluxes and membrane potential in pancreatic B cells. *Biochem. Pharmacol.*, **31**, 1407–1415.

HICKS, G.A. & HENDERSON, G. (1992). Lack of evidence for coupling of the dopamine D_2 receptor to an adenosine triphosphate-sensitive (ATP-K^+) channel in dopaminergic neurones of the rat substantia nigra. *Neurosci. Letts.*, **141**, 213–217.

ILLES, P. & NÖRENBERG, W. (1990). Blockade of α_2-adrenoceptors increases opioid μ-receptor-mediated inhibition of the firing rate of rat locus coeruleus neurones. *Naunyn-Schmiedebergs Arch. Pharmacol.*, **342**, 490–496.

ILLES, P. & REGENOLD, J.T. (1989). ω-Conotoxin GVIA and nifedipine inhibit Ca^{2+} action potentials in rat locus coeruleus neurons. *Acta Physiol. Scand.*, **137**, 459–460.

KITA, T., KITA, H., KITAI, S.T. (1986). Electrical membrane properties of rat substantia nigra compacta neurons in an *in vitro* slice preparation. *Brain Res.*, **372**, 21–30.

KNÖPFEL, T., SPULER, A., GRAFE, P. & GÄHWILER, B.H. (1990). Cytosolic calcium during glucose deprivation in hippocampal pyramidal cells of rats. *Neurosci. Letts.*, **117**, 295–299.

LACEY, M.G., MERCURI, N.B. & NORTH, R.A. (1988). On the potassium conductance increase activated by $GABA_A$ and dopamine D_2 receptors in rat substantia nigra neurones. *J. Physiol.*, **401**, 437–453.

MOURRE, C., BEN-ARI, Y., BERNARDI, H., FOSSET, M. & LAZDUNSKI, M. (1989). Antidiabetic sulfonylureas: localization of binding sites in the brain and effects on the hyperpolarization induced by anoxia in hippocampal slices. *Brain Res.*, **486**, 159–164.

MOURRE, C., WIDMANN, C. & LAZDUNSKI, M. (1991). Specific hippocampal lesions indicate the presence of sulfonylurea binding sites associated to ATP-sensitive K^+ channels both postsynaptically and on mossy fibers. *Brain Res.*, **540**, 340–344.

NAKAYA, H., TAKEDA, Y., TOHSE, N. & KANNO, M. (1991). Effects of ATP-sensitive K^+ channel blockers on the action potential shortening in hypoxic and ischaemic myocardium. *Br. J. Pharmacol.*, **103**, 1019–1026.

NOMA, A. (1983). ATP-regulated K^+ channels in cardiac muscle. *Nature*, **305**, 147–148.

OSMANOVIC, S.S. & SHEFNER, S.A. (1987). Anomalous rectification in rat locus coeruleus neurons. *Brain Res.*, **417**, 161–166.

QUAYLE, J.M., STANDEN, N.B. & STANFIELD, P.R. (1988). The voltage-dependent block of ATP-sensitive potassium channels of frog skeletal muscle by caesium and barium ions. *J. Physiol.*, **405**, 677–697.

REGENOLD, J.T. & ILLES, P. (1990). Inhibitory adenosine A_1-receptors on rat locus coeruleus neurones. An intracellular electrophysiological study. *Naunyn-Schmiedebergs Arch. Pharmacol.*, **341**, 225–231.

ROEPER, J., HAINSWORTH, A.H. & ASHCROFT, F.M. (1990). Tolbutamide reverses membrane hyperpolarisation induced by activation of D_2 receptors and $GABA_B$ receptors in substantia nigra neurones. *Pflügers Arch.*, **416**, 473–475.

SANGUINETTI, M.C., SCOTT, A.L., ZINGARO, G.J. & SIEGL, P.K.S. (1988). BRL 34915 (cromakalim) activates ATP-sensitive K^+ current in cardiac muscle. *Proc. Natl. Acad. Sci. U.S.A.*, **85**, 8360–8364.

SCHMID-ANTOMARCHI, H., DE WEILLE, J.P., FOSSET, M. & LAZDUNSKI, M. (1987). The receptor for antidiabetic sulfonylureas controls the activity of the ATP-modulated K^+ channel in insulin-secreting cells. *J. Biol. Chem.*, **262**, 15840–15844.

SCHMID-ANTOMARCHI, H., AMOROSO, S., FOSSET, M. & LAZDUNSKI, M. (1990). K^+ channel openers activate brain sulfonylurea-sensitive K^+ channels and block neurosecretion. *Proc. Natl. Acad. Sci. U.S.A.*, **87**, 3489–3492.

SILVA, N.L. & BUNNEY, B.S. (1988). Intracellular studies of dopamine neurons *in vitro*: pacemaker modulated by dopamine. *Eur. J. Pharmacol.*, **149**, 307–315.

TREHERNE, J.M. & ASHFORD, M.L. (1991). The regional distribution of sulphonylurea binding sites in rat brain. *Neuroscience*, **40**, 523–531.

WALLENSTEIN, S., ZUCKER, C.L. & FLEISS, J.L. (1980). Some statistical methods useful in circulation research. *Circ. Res.*, **47**, 1–9.

WILLIAMS, J.T., BOBKER, D.H. & HARRIS, G.C. (1991). Synaptic potentials in locus coeruleus neurons in brain slices. *Progr. Brain Res.*, **88**, 167–172.

WILLIAMS, J.T., HENDERSON, G. & NORTH, R.A. (1985). Characterization of α_2-adrenoceptors which increase potassium conductance in rat locus coeruleus neurones. *Neuroscience*, **14**, 95–101.

WILLIAMS, J.T., NORTH, R.A. & TOKIMASA, T. (1988). Inward rectification of resting and opiate-activated potassium currents in rat locus coeruleus neurons. *J. Neurosci.*, **8**, 4299–4306.

(Received June 22, 1992
Revised January 15, 1993
Accepted January 19, 1993)

Br. J. Pharmacol. (1993), **109**, 316–321 © Macmillan Press Ltd, 1993

Inhibition by the adenosine analogue, (R-)-N^6-phenylisopropyladenosine, of kainic acid neurotoxicity in rat hippocampus after systemic administration

D.G. MacGregor & [1]T.W. Stone

Neuropharmacology Group, Department of Pharmacology, University of Glasgow, Glasgow, G12 8QQ

1 Binding of the peripheral benzodiazepine receptor ligand, [^{3}H]-PK 11195, to rat hippocampal membranes has been used to quantify the reactive gliosis resulting from neuronal death induced by intraperitoneally administered kainic acid.

2 Intraperitoneal administration of kainic acid (10 mg kg^{-1}) caused a 350–500% increase in [^{3}H]-PK 11195 binding measured in rat hippocampal P_2 membranes 7 days later. Co-treatment with the adenosine derivative **R**-phenylisopropyladenosine (**R**-PIA) (100, 25 or 10 μg kg^{-1}, i.p.) abolished this elevation. The protective action of **R**-PIA could itself be abolished by co-treatment with 8-phenyltheophylline (1 mg kg^{-1}).

3 Body temperatures were recorded in the antagonist experiments and no significant changes were recorded, suggesting that the protective action of **R**-PIA was not mediated by hypothermia.

4 Since systemic kainic acid-induced neurotoxicity has been claimed as a good model of neuronal death in temporal lobe epilepsy, the results suggest that the systemic administration of purines in low doses may provide protection against certain neurodegenerative insults.

Keywords: **R**-N^6-phenylisopropyladenosine (**R**-PIA); binding; PK 11195; peripheral benzodiazepine receptors; rat hippocampus; 8-phenyltheophylline (8-PT); neuroprotection; systemic kainate; kainate receptors; temporal lobe epilepsy

Introduction

Following a neurotoxic insult to the brain, by either physical or chemical means, there is a period of neuronal death and reactive gliosis. During gliosis there is a rapid invasion of the area of damage by phagocytes, followed by a delayed proliferation of astroglial cells and hence an increase in biochemical markers for glial cells (Andersson *et al.*, 1990). Benavides *et al.* (1987) have indicated that the increase in peripheral benzodiazepine receptors (PBR), which are associated mainly with glial cells in the CNS, is a more sensitive indirect index for neuronal death than the loss of neuronal markers. PBRs are associated with mitochondrial fractions although their function is still unclear (see Moreno-Sanchez *et al.*, 1991; Gavish *et al.*, 1992). There are now numerous reports of studies using ligands for the PBR binding site (PK 11195 and Ro5-4864), which have confirmed a significant increase in PBR binding associated with neurodegeneration, (Schoemaker *et al.*, 1982; Benavides *et al.*, 1987; Altar & Baudry, 1990; Bourdiol *et al.*, 1991).

The endogenous excitatory amino acids, glutamate and aspartate, have been implicated in the neuronal damage resulting from cerebral ischaemia (Benveniste *et al.*, 1984; Butcher *et al.*, 1987; 1990; Globus *et al.*, 1988; Mitani & Kataoka, 1991), and may also be involved in neurodegenerative disorders of different origin (see reviews by Choi, 1988; Choi & Rothman, 1989). Several compounds, structurally related to glutamate and/or aspartate, are also neurotoxic. One of the most potent of these is kainic acid, a dicarboxyl containing pyrrolidine derivative (Shinozaki & Konishi, 1970; Coyle, 1987; Winn *et al.*, 1991). The areas sensitive to kainic acid-induced damage differ from those affected by other neurotoxins, in that the limbic system is very sensitive to kainic acid but other regions are relatively insensitive. The kainic acid-sensitive areas are similar to those affected by Huntington's disease and temporal lobe epilepsy, but differ to some extent from those sensitive to ischaemic insults (Heggli *et al.*, 1981; Kish *et al.*, 1983; and Coyle, 1987 for review). Kainic acid also differs from other neurotoxins in that central damage can result from systemic injections, as well as from direct intracerebral administration (Shinozaki & Konishi, 1970; Olney *et al.*, 1974).

Recently there have been several reports indicating that pretreatment of animals with an adenosine agonist may provide varying degress of protection against both chemically and physically induced neuronal damage (Fredholm & Dunwiddie, 1988; Arvin *et al.*, 1989; Connick & Stone, 1989; von Lubitz *et al.*, 1989; Finn *et al.*, 1991). In most cases, however, the purines were delivered intracerebrally, whereas any development of purines therapeutically would need to be centred on peripheral administration. The present study was therefore designed to determine whether systemically injected **R**-phenylisopropyladenosine (**R**-PIA) would protect against kainate neurotoxicity.

Methods

In all the experiments 8 week old male Wistar rats, 190–220 g, were used. All animals were bred in house and kept under the same conditions, 12 h light/dark regime, with food and water available *ad libitum*.

Animals were injected intraperitoneally with drugs in a volume not exceeding 1 ml kg^{-1}. Kainic acid was dissolved in saline, **R**-PIA in methanol and 8-phenyltheophylline (8-PT) in ethanol/NaOH diluted with saline to give final concentrations of 17.5% ethanol (v/v) and 19.3 mM NaOH. In all cases vehicles were used as control injections. In the 8-PT experiments the rectal temperatures were recorded prior to kainate injection, and every hour, for 5 h, after the kainic acid injection. All the animals were killed for tissue preparation on the seventh day.

Tissue preparation

The method used was that of Eshleman & Murray (1989) for the preparation of P_2 membranes, with slight modifications. The animals were killed by stunning followed by cervical dislocation and decapitation. The brain was removed and

[1] Author for correspondence.

placed in 30 ml ice-cold 0.27 M sucrose pH 7.4, buffered with NaOH. The hippocampi were then removed, homogenized in 5 ml ice-cold sucrose with a Braun Homogeniser (10 strokes × 500 r.p.m.) brought to 100 volumes with sucrose solution and then stored at − 20°C for 2–4 h. The samples were defrosted and centrifuged for 10 min at 4°C, 1000 *g* (IEC DPR 6000 centrifuge), the pellet discarded and the supernatant centrifuged for 20 min at 4°C, 16000 *g* (Sorval RC 5B Refrigerated Superspeed Centrifuge, SS 34 Rotor). The pellet was resuspended in ice-cold 50 mM Tris HCl buffer pH 7.8, 100 volumes and then centrifuged for 20 min at 4°C, 30000 *g* (Sorval RC 5B). The new pellet was resuspended in Tris HCl buffer at 100 volumes and stored at − 20°C overnight.

The samples were defrosted and centrifuged for 20 min at 4°C 30000 *g*. The pellet was then homogenized in 5 ml Tris HCl buffer, 7 strokes × 1500 r.p.m, and the homogenate brought to 100 volumes, this being the P_2 mitochondrial membrane fraction.

[^{3}H]-PK 11195 assay

All assays were performed at 4°C (on ice) and samples were incubated for 60 min. For the saturation experiments the assay was performed in triplicate using 250 µl P_2 membranes, whilst in the test experiments they were performed in duplicate with 500 µl P_2 membranes. The volume of the assay chamber was 2 ml, and contained 5 µl [^{3}H]-PK 11195, 5 µl cold ligand, and P_2 membranes and the volume brought to 2 ml with Tris HCl buffer. Final assay conditions were 1.75 nM [^{3}H]-PK 11195 in ethanol (0.25% final), 0.25% dimethylsulphoxide (DMSO) ± 10 µM PK 11195 and 100–150 µg protein. The assay samples were vortexed at the start of their incubation and approximately every 20 min before filtration. The incubation was terminated by vacuum filtration, with all of the sample being filtered through prewetted Whatman GF/C glass filters using a Millipore 12 well 1225 Sampling Manifold. Filters were washed twice with 12 ml ice-cold Tris HCl buffer and vacuum dried, before being placed in scintillation vials with 5 ml Ecoscint scintillation fluid, and then counted in a Packard 2000 Scintillation Counter. Nonspecific binding was 40–50% of the total binding in vehicle-treated animals and about 10% in kainate-treated animals.

Protein concentrations were measured by the method of Lowry *et al.* (1951), following solubilization with 0.25 M NaOH and with bovine serum albumin as the standard.

Data analysis

Specific binding was calculated by subtracting the nonspecific binding from the total binding. Specific binding was also calculated as a percentage of the same day control to minimize day to day variations. Scatchard data were calculated by least-squares regression (GraphPAD Version 2.0), and no other transformations were performed. All values are mean ± s.e.mean. Statistical significance was assessed by an unpaired Student's *t* test (unequal variance), at $P<0.05$.

Materials

[^{3}H]-PK 11195 [1-(2-chlorophenyl)-*N*-methyl-*N*-(1-methylpropyl)-3-isoquinolinecarboxamide], (specific activity = 80–86 Ci mmol^{-1}) was purchased from DuPont/NEN (Stevenage, Herts). Kainic acid, R-PIA and 8-PT were from Sigma Chemical Co. (Poole, Dorset). Unlabelled PK 11195 was a gift from Pharmuka Labs.

Results

Saturation experiments

These experiments were performed in triplicate over the concentration range 0.1 nM–50 nM [^{3}H]-PK 11195, with 10 µM PK 11195 as displacing agent, to define non-specific binding. Both vehicle-treated and kainate-treated animals were examined. Binding parameters were calculated by Scatchard analysis. The values obtained showed that there was no change in K_d (10.38 ± 3.03 and 13.44 ± 3.34 nM vehicle ($n = 4$ animals) and kainate ($n = 3$ animals) respectively), but there was a significant increase ($P = 0.008$) in B_{max} in the kainate-treated animals (693.2 ± 139.2 and 2917.0 ± 319.2 fmol mg^{-1} for vehicle and treated animals respectively), (Figure 1). All subsequent assays were performed using 1.75 nM [^{3}H]-PK 11195.

[^{3}H]-PK 11195 binding

Initial experiments Initial experiments were performed on three groups of animals treated with vehicle, 5 mg kg^{-1} and 10 mg kg^{-1} i.p. kainic acid. While the vehicle (control) and 10 mg kg^{-1} kainic acid groups gave binding figures with low variance, i.e. 111.2 ± 21.1 fmol mg^{-1} protein ($n = 12$) and 356.8 ± 49.6 fmol mg^{-1} protein ($n = 19$) respectively, the animals injected with 5 mg kg^{-1} kainic acid showed greater variability and no significant increase in binding was detected (Figure 2). The 10 mg kg^{-1} dose was therefore used for all other experiments as it provided the most consistent elevation of binding and the increase in binding was highly significant, ($P<0.001$).

R-PIA injections The adenosine analogue was injected at doses of 1 mg kg^{-1}, 100, 25, 10 or 2.5 µg kg^{-1}, although the combination of the 1 mg kg^{-1} dose with kainic acid caused the death of all the animals within 3 h of injection. Following the 25 or 10 µg kg^{-1} of R-PIA together with saline 1 ml kg^{-1}, binding was not significantly different from control levels (Figure 3a). The combination of 100, 25 or 10 µg kg^{-1} R-PIA together with 10 mg kg^{-1} kainate significantly reduced the

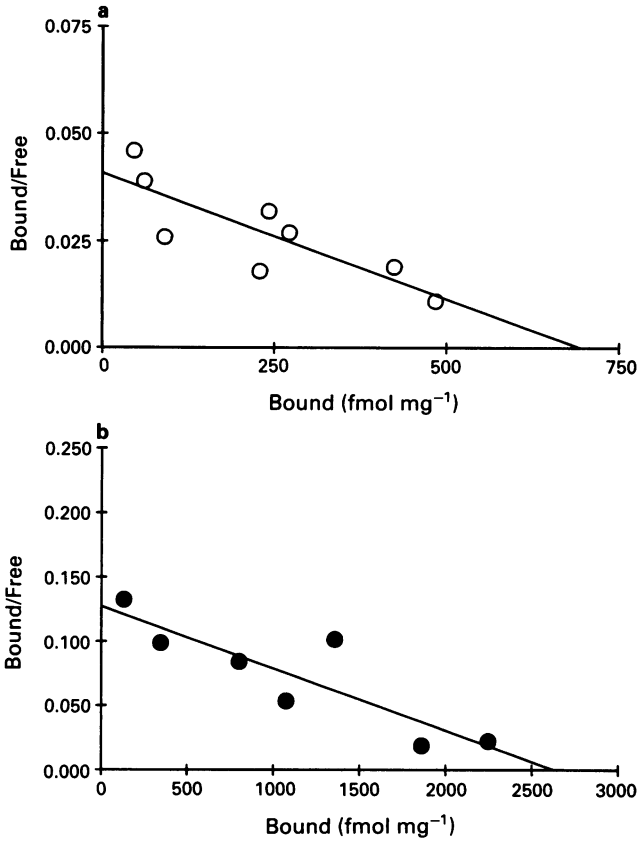

Figure 1 Scatchard analysis of [^{3}H]-PK11195 binding to rat hippocampal P_2 membranes. The data represent a single experiment carried out as described in the Methods: (a) saline-treated rat; (b) kainate (10 mg kg^{-1})-treated rat.

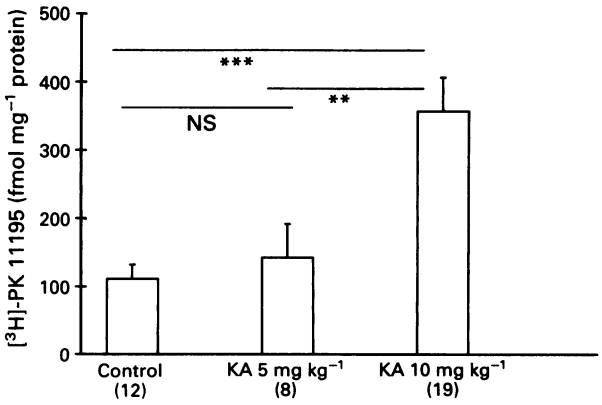

Figure 2 Increase in [^{3}H]-PK11195 binding in hippocampal P_2 membranes of kainate-treated rats. Columns indicate mean ± s.e.mean. KA = kainic acid. Control = saline. $^{**}P<0.01$; $^{***}P<0.001$; NS, not significant.

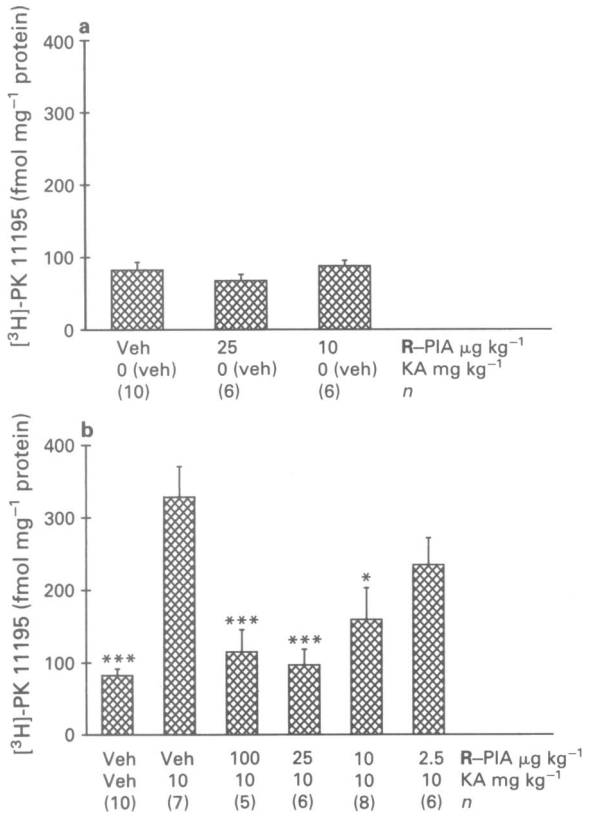

Figure 3 The effect of **R-PIA** on the kainate-evoked increase in [^{3}H]-PK11195 binding to hippocampal P_2 membranes. (a) The binding of [^{3}H]-PK11195 to P_2 membranes of control (vehicle-treated) or **R-PIA**-treated rats. (b) Dose-dependent action of **R-PIA** on the kainate-induced increase in [^{3}H]-PK11195 binding. Columns indicate mean ± s.e.mean. Vehicle = methanol and saline, KA = kainate. $^{*}P<0.05$; $^{***}P<0.001$ significance versus 10 mg kg^{-1} kainic acid.

binding relative to kainate alone, such that [^{3}H]-PK 11195 binding was not significantly different from the controls (Figure 3b). The lower dose of 2.5 μg kg^{-1} **R-PIA** failed to give significant protection against kainate treatment.

8-PT injections The 8-PT vehicle, (ethanol and NaOH) did not alter significantly the level of control binding, but did appear to reduce slightly the protective action of 25 μg kg^{-1} **R-PIA** such that the latter now only reduced the kainic acid-induced binding to 116 ± 6% of control (Figure 4). The protective action of **R-PIA** was fully reversed by treatment with 8-PT (Figure 4). Indeed there was a suggestion that 8-PT might be increasing neuronal damage, since the kainic

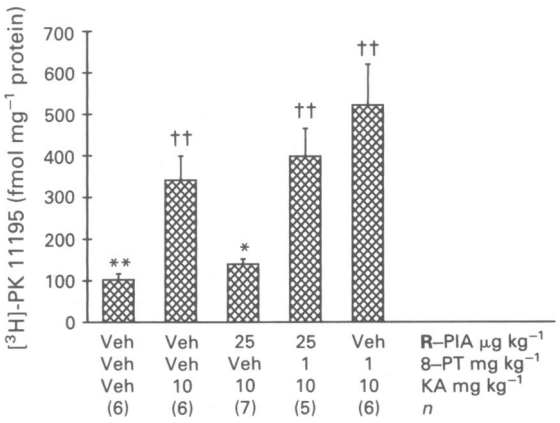

Figure 4 Comparison of the binding of [^{3}H]-PK11195 to hippocampal P_2 membranes of kainate (KA)/8-phenyltheophylline (8PT)-treated rats and controls. Columns indicate mean ± s.e.mean. Control = KA, **R-PIA** and 8-PT vehicles; KA = kainate. $^{*}P<0.05$; $^{**}P<0.01$, versus 10 mg kg^{-1} kainate; $\dagger\dagger P<0.01$ versus control.

acid/8-PT group of rats yielded greater mean levels of binding than that of the kainic acid/vehicles group. The differences in the amount of binding, however, were not statistically significant (Figure 4).

Temperature

Rectal temperatures were recorded in the 8-PT experiments. Most treatment schedules induced a transient decrease of core temperature which was not statistically significant and which returned to control levels within 2 h. Plotting changes in temperature against the binding (fmol) [^{3}H]-PK 11195 for individual animals produced no correlation (data not shown).

Behavioural observations

All the animals treated with kainate, at either 5 or 10 mg kg^{-1} displayed behavioural changes. One hour after the kainate injection the animals started to display wet dog shake activity. This activity continued over the next 5–6 h, during which the animals also underwent seizure like activity, excessive salivation, fore paw abduction, and in some cases Straub tail and loss of balance. These observations agree with those of Heggli *et al.* (1980). It was during this initial 6–7 h period that all the fatalities occurred. The **R-PIA**/kainate-treated animals were indistinguishable from the kainate control animals (as assessed by blind observations) during this period, although there was an indication that the seizure activity was less. However, on the day they were killed the kainate alone animals were hyper-responsive to handling, whilst the **R-PIA**/kainate-treated animals were similar in handling behaviour to the control animals.

Discussion

The key finding reported here is that **R-PIA**, at low doses, can protect against kainic acid-induced neuronal damage, as assessed by [^{3}H]-PK 11195 binding in the rat hippocampus and that this protection can be reversed by the adenosine A_1 antagonist, 8-PT.

Previous studies have employed histological or neurochemical analyses to demonstrate that systemic injections of kainic acid into mature rats can induce hippocampal damage (Schwob *et al.*, 1980; Fuller & Olney, 1981; Lothman & Collins, 1981; Fariello *et al.*, 1989). The present results indicate that the damage induced by kainate is also reflected in an elevation of [^{3}H]-PK 11195 binding to hippocampal P_2 membranes. Gliosis always accompanies the degeneration of

neurones induced by excitotoxins or ischaemia (Andersson *et al.*, 1991) and the demonstration that binding sites for the peripheral benzodiazepine ligands occur in central glial cells has been proposed as a sensitive, if indirect, indicator of neuronal damage (Benavides *et al.*, 1987; Dubois *et al.*, 1988; Altar & Baudry, 1990; Price *et al.*, 1990). Comparative analyses have shown an excellent correlation between the distribution of PK 11195 binding studied by autoradiography, and conventional histology (Dubois *et al.*, 1988). Binding techniques, however are more sensitive, and can reveal changes following concentrations of excitotoxins that are insufficient to cause significant alterations of enzyme markers such as glutamate decarboxylase or choline acetyltransferase (Benavides *et al.*, 1987).

There are several advantages of using a systemic route for injecting kainate. Firstly, no surgery is required as it is for direct intrahippocampal injections, and the variability inherent in the stereotaxic procedure is avoided. Secondly, the neurotoxin is likely to be more evenly distributed throughout the hippocampus than following localized injections. Thirdly, the concentration of kainate achieved is likely to be lower after intraperitoneal injection. The dose of 10 mg kg^{-1} would yield a tissue concentration of approximately 50 μM if it were evenly distributed around the body, and probably much less than this in the brain due to the limitations of the blood brain barrier. The doses of kainate used in the present work are comparable with those used by others (e.g. Fariello *et al.*, 1989) but less than the 12 mg kg^{-1} or 16 mg kg^{-1} doses which have been shown to induce severe seizure activity (Altar & Baudry, 1990; Fuller & Olney, 1981).

Adenosine or its more stable analogues have been shown to reduce neurotoxicity when co-administered into the hippocampus or striatum (Arvin *et al.*, 1989; Connick & Stone, 1989; Finn *et al.*, 1991). When **R-PIA** was administered peripherally by Connick & Stone (1989) there was a potentiation of the neuronal toxicity induced by centrally administered quinolinic acid which was attributed to decreased peripheral sympathetic activity as it could be reproduced by the ganglionic blocker, trimetaphan. The dose of **R-PIA** used in that study however, was 1 mg kg^{-1} (which was fatal in the present study with 10 mg kg^{-1} kainate), whereas the present work was based on substantially lower doses. The ability of **R-PIA** to protect against quinolinic acid toxicity when co-injected into the hippocampus (Connick & Stone, 1989) supported the view that purines were neuroprotective when used appropriately. There are, in addition, several reports that peripherally administered cyclohexyladenosine or the adenosine precursor, 5-aminoimidazole-4-carboxamide riboside (AICAR), can reduce the degree of neuronal damage following periods of cerebral ischaemia (von Lubitz *et al.*, 1989; Clough-Helfman & Phillis, 1990). Together, these various findings prompted the present study to investigate the effects of a systemically administered purine upon excitotoxin-induced neuronal damage. The results reveal that intraperitoneal **R-PIA** was able to protect substantially against the kainate-induce hippocampal damage at a range of doses down to 10 μg kg^{-1}.

The mechanism of protection by **R-PIA** is not clear from this study. Assuming the even distribution of **R-PIA** around the body, the lowest effective dose of 10 μg kg^{-1} would yield a mean tissue concentration of approximately 24 nM. This is close to the low K_m values for the A_1 receptor (Gustafsson *et al.*, 1990; Baumgold *et al.*, 1992) and would be entirely consistent with an action of **R-PIA** which involved the selective activation of these sites. A large proportion of A_1 receptors are believed to be located on the terminals of excitatory neurones, including those releasing acetylcholine and glutamate (Goodman & Snyder, 1982; Spignoli *et al.*, 1984; Fastbom & Fredholm, 1985; Dolphin & Prestwich, 1985). Kainate causes the release of radiolabelled and endogenous excitatory acids from intact neurones or synaptosomes (Ferkany *et al.*, 1982; Notman *et al.*, 1984; Connick & Stone, 1986), an effect which may contribute substantially to its excitotoxic properties (McGeer *et al.*, 1978).

A number of groups have claimed that changes in body temperature can have a profound effect upon the extent of neuronal damage following ischaemia (Welsh *et al.*, 1990; Buchan & Pulsinelli, 1990; Freund *et al.*, 1992). Mitani & Kataoka (1991) have reported that hypothermia can also significantly reduce the neuronal release of glutamate and aspartate. The temperature changes required, however, seem to be substantial (4–6°C), and the relevance of temperature has been disputed by others (Gill & Woodruff, 1990; Welsh & Harris, 1991). In addition, systemically administered purines can induce significant changes in body temperature to the extent that these may contribute, for example, to the anticonvulsant properties of purines (Bowker & Chapman, 1986). However, no significant changes of temperature were observed at doses of **R-PIA** which provided substantial protection, making it unlikely that temperature was a major factor in the results presented.

It is of interest to compare the potency of **R-PIA** in affording neuroprotection, with other agents used recently for this purpose. Compared with the lower dose used here (10 μg kg^{-1} or 5 nmol kg^{-1}) the dose of dizocilpine (MK-801) required for protection against NMDA toxicity is around 600 nmol kg^{-1} (McDonald *et al.*, 1990), while almost 1 mmol kg^{-1} of kynurenic acid only afforded 50% protection against the same insult (Germano *et al.*, 1987). Lipid-soluble purines such as **R-PIA** given at low dosage may therefore offer promising therapeutic potential.

The protective effect of **R-PIA** appears to be mediated by a conventional xanthine-sensitive P_1 purinoceptor (Burnstock, 1978; Stone & Simmonds, 1991) since protection was fully prevented by co-administration of 8-phenyltheophylline. Indeed there was an apparent tendency towards an increase in damage in the presence of this xanthine, though the effect was not large and was not statistically significant. This tendency might nevertheless indicate some blockade of an endogenous adenosine-mediated neuroprotective tone, and would be consistent with the finding that theophylline itself increases the amount of neuronal damage following cerebral ischaemia (Rudolphi *et al.*, 1987).

D.G.M. is supported by a Glasgow University Scholarship. The authors are grateful to Dr K. Hamilton, Miss K. Paisley and Mr J. Younger for technical advice and assistance.

References

ALTAR, C.A. & BAUDRY, M. (1990). Systemic injection of kainic acid: gliosis in olfactory and limbic brain regions quantified with [^{3}H] PK11195 binding autoradiography. *Exp. Neurol.*, **109**, 333–341.

ANDERSSON, P.-B., PERRY, V.H. & GORDON, S. (1990). The kinetics and morphological characteristics of the macrophage-microglial response to kainic acid-induced neuronal degeneration. *Neurosci.*, **42**, 201–214.

ARVIN, B., NEVILLE, L.F., PAN, J. & ROBERTS, P.J. (1989). 2-Chloroadenosine attenuates kainic acid-induced toxicity within the rat striatum: relationship to release of glutamate and Ca^{2+} influx. *Br. J. Pharmacol.*, **98**, 225–235.

BAUMGOLD, J., NIKODIJEVIC, O. & JACOBSON, K.A. (1992). Penetration of adenosine antagonists into mouse brain as determined by *ex vivo* binding. *Biochem. Pharmacol.*, **43**, 889–894.

BENAVIDES, J., FAGE, D., CARTER, C. & SCATTON, B. (1987). Peripheral type benzodiazepine binding sites are a sensitive indirect index of neuronal damage. *Brain Res.*, **421**, 167–172.

BENVENISTE, H., DREJER, J., SCHOUSBE, A. & DEIMER, N.H. (1984). Elevation of extracellular concentrations of glutamate and aspartate in rat hippocampus during transient cerebral ischaemia monitored by intracerebral microdialysis. *J. Neurochem.*, **43**, 1369–1374.

BOURDIOL, F., TOULMOND, S., SERRANO, A., BENAVIDES, J. & SCATTON, B. (1991). Increase in w_3 (peripheral type benzodiazepine) binding sites in the rat cortex and striatum after local injection of interleukin-1, tumour necrosis factor-α and lipopolysaccharide. *Brain Res.*, **543**, 194–200.

BOWKER, H.M. & CHAPMAN, A.G. (1986). Adenosine analogues: the temperature-dependence of the anticonvulsant effect and inhibition of [^{3}H] D-aspartate release. *Biochem. Pharmacol.*, **35**, 2949–2954.

BUCHAN, A. & PULSINELLI, W.A. (1990). Hypothermia, but not the NMDA antagonist MK-801 attenuates neuronal damage in gerbils subject to transient global ischaemia. *J. Neurosci.*, **10**, 311–316.

BURNSTOCK, G. (1978). A basis for distinguishing two types of purinergic receptors. In *Cell Membrane Receptors for Drugs and Hormones: A Multidisciplinary Approach*. ed. Bolis, L. & Straub, R.N. pp. 107–118. New York: Raven Press.

BUTCHER, S.P., LARAEWICZ, J. & HAMBERGER, A. (1987). *In vivo* microdialysis studies on the effects of decortication and excititoxic lesions on kainic acid induced Ca2+ fluxes, and endogenous amino acid release in the rat striatum. *J. Neurochem.*, **49**, 1355–1360.

BUTCHER, S.P., BULLOCK, R., GRAHAM, D.I. & MCCULLOCH, J. (1990). Correlation between amino acid release and neuropathologic outcome in rat brain following middle cerebral artery occlusion. *Stroke*, **21**, 1727–1733.

CHOI, D.W. (1988). Calcium mediated neurotoxicity relationship to specific channel types and role in ischemic damage. *Trends Neurosci.*, **11**, 465–469.

CHOI, D.W. & ROTHMAN, S.M. (1990). The role of glutamate neurotoxicity in hypoxic-ischemic neuronal death. *Annu. Rev. Neurosci.*, **13**, 171–182.

CLOUGH-HELFMAN, C. & PHILLIS, J.W. (1990). 5-aminoimidazole-4-carboxamide riboside (AICAr) administration reduces cerebral ischemic damage in the mongolian gerbil. *Brain Res. Bull.*, **25**, 203–206.

CONNICK, J.H. & STONE, T.W. (1986). Effects of quinolinic and kainate acids on release of endogenous glutamate from rat brain. *Biochem. Pharmacol.*, **35**, 3631–3635.

CONNICK, J.H. & STONE, T.W. (1989). Quinolinic acid neurotoxicity, protection by intracerebral PIA and potentiation by hypotension. *Neurosci. Lett.*, **101**, 191–196.

COYLE, J.T. (1987). Kainic acid: insights into excitatory mechanisms causing selective neuronal degradation. In *Selective Neuronal Death*. (Ciba Foundation Symposium 126) pp. 186–203. Chichester: Wiley.

DOLPHIN, A.C. & PRESTWICH, S.A. (1985). Pertussis toxin reverses adenosine inhibition of neuronal glutamate release. *Nature*, **316**, 146–148.

DUBOIS, A., BENAVIDES, J., PENY, B., DUVERGER, D., FAGE, D., GOTTI, B., MACKENZIE, E.T. & SCATTON, B. (1988). Imaging of primary and remote ischaemic and excitotoxic brain lesions. An autoradiographic study of peripheral type benzodiazepine binding sites in the rat and cat. *Brain Res.*, **445**, 77–90.

ESHLEMAN, A.J. & MURRAY, T.F. (1989). Differential binding properties of the peripheral-type benzodiazepine ligands [^{3}H]PK 11195 and [^{3}H]Ro 5-4864 in trout and mouse brain membranes. *J. Neurosci.*, **53**, 494–502.

FARIELLO, R.G., GOLDEN, G.T., SMITH, G.G. & REYES, P.F. (1989). Potentiation of kainic acid epileptogenicity and sparing from neuronal damage by an NMDA receptor antagonist. *Epilepsy Res.*, **3**, 206–213.

FASTBOM, J. & FREDHOLM, B.B. (1985). Inhibition of [^{3}H] glutamate from rat hippocampal slices by L-PIA. *Acta Physiol. Scand.*, **125**, 121–123.

FERKANY, J.W., ZACZEK, R. & COYLE, J.T. (1982). Kainic acid stimulates excitatory amino acid neurotransmitters release at presynaptic receptors. *Nature*, **298**, 757–759.

FINN, S.F., SWARTZ, K.J. & BEAL, M.F. (1991). A comparison of excitotoxic lesions of the basal forebrain by kainate, quinolinate, ibotenate, N-methyl-D-aspartate or quisqualate, and the effects on toxicity of 2-amino-5-phosphonovaleric acid and kynurenic acid in the rat. *Neurosci. Lett.*, **126**, 191–194.

FREEDHOLM, B.B. & DUNWIDDIE, T.V. (1988). How does adenosine inhibit transmitter release? *Trends Pharmacol. Sci.*, **9**, 130–134.

FREUND, T.F., YLINEN, A., MIETTINEN, R., PITKANEN, A., LAHTINEN, H., BAIMBRIDGE, K.G. & RIEKKINEN, P.J. (1992). Pattern of neuronal death in the rat hippocampus after status epilepticus – relationship to calcium binding protein and ischaemic vulnerability. *Brain Res. Bull.*, **28**, 27–38.

FULLER, T. & OLNEY, J.W. (1981). Only certain anticonvulsants protect against kainate neurotoxicity. *Neurobehav. Toxicol. Teratol.*, **3**, 355–361.

GAVISH, M., KATZ, Y., BAR-AMI, S. & WEIZMAN, R. (1992). Biochemical, physiological, and pathological aspects of the peripheral benzodiazepine receptor. *J. Neurochem.*, **58**, 1589–1601.

GERMANO, I.M., PITTS, L.H., MELDRUM, B.S., BARTKOWSKI, H.M. & SIMON, R.P. (1987). Kynurenate inhibition of cell excitation decreased stroke size and deficits. *Ann. Neurol.*, **22**, 730–734.

GILL, R. & WOODRUFF, G.N. (1990). The neuroprotective actions of kynurenic acid and MK-801 are synergistic and not related to hypothermia. *Eur. J. Pharmacol.*, **176**, 143–149.

GLOBUS, M.Y.-T., BUSTO, R., DIETRICH, W.D., MARTINEZ, E., VALDES, I. & GINSBERG, M.D. (1988). Effect of ischaemia on the *in vivo* release of striatal dopamine, glutamate and GABA studied by intracerebral microdialysis. *J. Neurochem.*, **51**, 1455–1464.

GOODMAN, R.R. & SNYDER, S.H. (1982). Autoradiographic localisation of adenosine receptors using [^{3}H] cyclohexyladenosine. *J. Neurosci.*, **2**, 1230–1241.

GUSTAFSSON, L.E., WIKLUND, C.U., WIKLUND, N.P. & STELIUS, L. (1990). Identification of subclasses of adenosine A_1 receptors, suggestion of A_{1a} and A_{1b} subclasses and evidence from antagonist data. In *Purines in Cellular Signalling: Targets for New Drugs*. ed. Jacobson, K.A., Daly, J.W. & Manganiello, V. pp. 200–205. New York: Springer-Verlag.

HEGGLI, D.A., AAMODT, A. & MALTHE-SORENSSEN, D. (1980). Kainic acid neurotoxicity: effect of systemic injection on neurotransmitter markers in different brain regions. *Brain Res.*, **230**, 253–262.

KISH, S.J., SPERK, G. & HORNYKIEWICZ, O. (1983). Alterations in benzodiazepine and GABA receptor binding in rat brain following systemic injections of kainic acid. *Neuropharmacol.*, **22**, 1303–1309.

LOTHMAN, E.W. & COLLINS, R.C. (1981). Kainic acid induced limbic seizures; metabolic, behavioural, electroencephalographic and neuropathological correlates. *Brain Res.*, **218**, 299–318.

LOWRY, O.H., ROSEBROUGH, N.J., FARR, A.L. & RANDALL, R.A. (1951). Protein measurements with the folin phenol reagent. *J. Biol. Chem.*, **193**, 265–275.

MCDONALD, J.W., SILVERSTEIN, F.S. & JOHNSTON, M.V. (1990). MK801 pretreatment enhances N-methyl-D-aspartate-mediated brain injury and increases brain N-methyl-D-aspartate recognition site binding in rats. *Neurosci.*, **38**, 103–113.

MCGEER, E.G., MCGEER, P.L. & SINGH, K. (1978). Kainate induced degeneration of neostriatal neurones: dependency upon Ca^{2+}. *Brain Res.*, **139**, 381–383.

MITANI, A. & KATAOKA, K. (1991). Critical levels of extracellular glutamate mediating gerbil hippocampal delayed neuronal death during hypothermia. Brain microdialysis study. *Neurosci.*, **42**, 661–670.

MORENO-SANCHEZ, R., BRAVO, C., GUTTIERREZ, J., NEWMAN, A.H. & CHIANG, P.K. (1991). Release of Ca^{2+} from heart and kidney mitochondria by peripheral-type benzodiazepine ligands. *Int. J. Biochem.*, **23**, 207–213.

NOTMAN, H., WHITNEY, R. & JHAMANDAS, K. (1984). Kainic acid evoked release of D-[^{3}H] aspartate from rat striatum *in vitro*: characterization and pharmacological modulation. *Can. J. Physiol. Pharmacol.*, **62**, 1070–1077.

OLNEY, J.W., RHEE, V. & HO, O.L. (1974). Kainic acid: a powerful neurotoxic analogue of glutamate. *Exp. Brain Res.*, **77**, 507–512.

PRICE, G.W., AHIER, R.G., HUME, S.P., MYERS, R., MANJIL, L., CREAMER, J.E., LUTHRA, S.K., PASCALI, C., PIKE, V. & FRACKOWIAK, R.S.J. (1990). *In vivo* binding to peripheral benzidaizepine binding sites in lesioned rat brain: comparison between [^{3}H] PK11195 and [^{18}F] PK14105 as markers for neuronal damage. *J. Neurochem.*, **55**, 175–185.

RUDOLPHI, K.A., KEIL, M. & HINZE, H.J. (1987). Effect of theophylline on ischaemically induced hippocampal damage in Mongolian gerbils: a behavioural and histopathological study. *J. Cereb. Blood Flow Metab.*, **7**, 74–81.

SCHOEMAKER, H., MORELLI, M., DESHMUKH, P. & YAMAMURA, H.I. (1982). [^{3}H]Ro5-4864 benzodiazepine binding in the kainate lesioned striatum and Huntingdon's diseased basal ganglia. *Brain Res.*, **248**, 396–401.

SCHWOB, J.E., FULLER, T., PRICE, J.L. & OLNEY, J.W. (1980). Widespread patterns of neuronal damage following systemic or intracerebral injections of kainic acid: a histological study. *Neurosci.*, **5**, 991–1014.

SHINOZAKI, H. & KONISHI, S. (1970). Actions of several anthelmintics and insecticides on rat cortical neurones. *Brain Res.*, **24**, 368–374.

SPIGNOLI, G., PEDATA, F. & PEPEU, G. (1984). A_1 and A_2 adenosine receptors modulate ACh release from brain slices. *Eur. J. Pharmacol.*, **97**, 341–342.

STONE, T.W. & SIMMONDS, H.A. (1991). *Purines: Basic and Clinical Aspects*. London: Kluwer Academic Press.

VON LUBOWITZ, D.K.E.J., DAMBROSIA, J.M. & REDMOND, D.J. (1989). Protective effect of cyclohexyl adenosine in treatment of cerebril ischaemia in gerbils. *Neurosci.*, **30**, 451–462.

WELSH, F.A. & HARRIS, V.A. (1991). Postischemic hypothermia fails to reduce ischemic injury in gerbil hippocampus. *J. Cereb. Blood Flow Metab.*, **11**, 617–620.

WELSH, F.A., SIMS, R.E. & HARRIS, V.A. (1990). Mild hypothermia prevents ischemic injury in gerbil hippocampus. *J. Cereb. Blood Flow Metab.*, **10**, 557–563.

WINN, P., STONE, T.W., LATIMER, M., HASTINGS, M.H. & CLARK, A.J.M. (1991). A comparison of excitotoxic lesions of the basal forebrain by kainate, quinolinate, ibotenate, N-methyl-D-aspartate or quisqualate, and the effects on toxicity of 2-amino-5-phosphonovaleric acid and kynurenic acid in the rat. *Br. J. Pharmacol.*, **102**, 904–908.

(Received October 19, 1992
Revised January 20, 1993
Accepted January 25, 1993)

Br. J. Pharmacol. (1993), **109**, 322–329 © Macmillan Press Ltd, 1993

Mechanisms of vasodilatation in pregnancy: studies of the role of prostaglandins and nitric-oxide in changes of vascular reactivity in the *in situ* blood perfused mesentery of pregnant rats

Z.M. Chu & [1]L.J. Beilin

University of Western Australia, Department of Medicine, Medical Research Foundation Building, Rear 50 Murray Street, Perth 6000, Western Australia

1 To examine the possible mechanisms of the vasodilatation and blunted pressor responses in late pregnancy, we have studied vascular reactivity of the *in situ* blood perfused mesenteric resistance vessels of 18–20 day pregnant Wistar-Kyoto rats (WKY).

2 Intra-arterial mean blood pressure (MBP) was lower in pregnant rats than in nonpregnant controls. There was no significant difference in basal mesenteric perfusion pressure (BPP) between groups.

3 Vascular reactivity to electrical stimulation (ES) or intra-arterial noradrenaline (NA), angiotensin II (AII) and arginine vasopressin (AVP) was decreased in the preparations from pregnant rats compared to that from nonpregnant controls. Noradrenaline spillover into mesenteric venous blood following ES was similar in pregnant and nonpregnant animals.

4 Indomethacin (5 mg kg^{-1}, i.v.), an inhibitor of cyclo-oxygenase, induced significant increases in reactivity to ES in both pregnant and nonpregnant groups while potentiating the responses to NA and AII in nonpregnant animals only and having no effect on AVP-induced contractions in the preparations from either pregnant or nonpregnant animals.

5 N^G-nitro-L-arginine (L-NOARG) (5 mg kg^{-1}, i.v.), an inhibitor of nitric-oxide synthase, increased MBP and BPP in both pregnant and nonpregnant animals, but the difference in MBP between groups was still evident.

6 L-NOARG enhanced mesenteric vascular responses to ES, NA and AII in both pregnant and nonpregnant groups. Only the difference in NA responses between groups was abolished after pretreatment with L-NOARG.

7 These data show that vasoconstrictor responses to a variety of agonists are decreased in the *in situ* blood-perfused mesenteric resistance vessels of pregnant rats. Increase in endothelial-dependent nitric-oxide generation could contribute to the vasodilatation seen in pregnancy but other mechanisms might also be involved. Cyclo-oxygenase products are not responsible for any decreased contractile responses in this preparation.

Keywords: Vascular reactivity; prostaglandins; nitric-oxide; blood perfused mesentery; pregnant rats

Introduction

Normal pregnancy is associated with decreased pressor responses to pressor stimuli. In women, decreased pressor responses to angiotensin II (AII) have been observed from the second trimester of pregnancy (Chesley *et al.*, 1965). Pregnant rats showed blunted systemic arterial pressor responses to AII, noradrenaline (NA) and arginine vasopressin (AVP) at 15 days of pregnancy (Paller, 1984). These changes in pressor responses may be related to alterations in vascular reactivity. However, using *in vitro* preparations in pregnant rats, vascular responses to NA in some studies have been reported to be decreased in perfused caudal arteries (Dogterom *et al.*, 1974), rings of superior mesenteric artery (Parent *et al.*, 1990) and perfused mesenteric vascular beds (Massicotte *et al.*, 1987), while in other studies reactivity has been unchanged in rings of caudal artery, mesenteric artery (Hart *et al.*, 1986) and perfused mesenteric vascular beds (Yin *et al.*, 1991), or even increased in aortic rings (Jansakul *et al.*, 1990; Yin *et al.*, 1991).

It has been suggested that vascular prostaglandins may play a role in the mediation of control of vascular reactivity during pregnancy (Gant *et al.*, 1987), based on the observation that inhibition of cyclo-oxygenase could attenuate blunted pressor responses to AII in pregnant women (Everett *et al.*, 1978), and increase pressor responses to NA, AII and AVP in conscious pregnant rats (Paller, 1984) and to AII in pseudopregnant rats (Paller *et al.*, 1989). In addition, urinary prostaglandin E (PGE) excretion in both pregnant and pseudopregnant rats rose to levels approximately twice that of nonpregnant controls. However, it has also been reported that pressor responsiveness to NA and AII remained lower in conscious pregnant rats even after prostaglandin synthesis inhibition by either indomethacin or meclofenamate (Conrad & Colpoys, 1986). The reduced systemic vascular resistance was also not restored by meclofenamate in awake pregnant guinea-pigs (Harrison *et al.*, 1989). Thus the possible role of prostaglandins still requires elucidation.

Endothelium-derived relaxing factor (EDRF), a potent vasodilator, could be another candidate modulating pressor responses during pregnancy. EDRF has been characterized pharmacologically as nitric-oxide (NO) or a nitrogen oxide related compound (Palmer *et al.*, 1987; Myers *et al.*, 1989). Recently, elevated tissue production of guanosine 3′:5′-cyclic monophosphate (cyclic GMP) during pregnancy and pseudopregnancy of rats has been reported (Conrad & Vernier, 1989). EDRF was suggested to be the first messenger which stimulates the synthesis of cyclic GMP and hence causes vascular relaxation or suppresses vasocontractile responses. It is thus possible that the diminished pressor responsiveness in pregnant women and animals could be caused by increased production of or sensitivity to EDRF.

[1] Author for correspondence.

In view of the paradoxical changes in vascular reactivity *in vitro*, and to try to understand the mechanisms underlying the changes in vascular reactivity and vasodilatation in pregnancy, we have studied the responses to electrical stimulation of sympathetic nerves (ES), and intra-arterial NA, AII and AVP in the *in situ* blood perfused mesenteric beds of rats. The possible roles of prostaglandins and EDRF have also been studied with the use of indomethacin and N^G-nitro-L-arginine (L-NOARG). Some of this work has been presented previously in abstract form (Chu & Beilin, 1992).

Methods

Pregnant animal models

WKY rats, 18–20 days pregnant and age matched (14 weeks old) nonpregnant female WKY rats weighing 200–220 g before mating were used in this study. Pregnancy was produced by mating oestrous phase female rats with normal male rats. The day on which plug was found was labelled day 1 of pregnancy. The gestation was further confirmed by examination of the pups in utero during the experiment. Systolic blood pressure (SBP) was measured by tail cuff sphygmomanometry on rats warmed to 39°C for 20 min in the morning of the day when the experiment was carried out.

In situ *blood perfused mesenteric preparations*

An *in situ* blood perfused mesenteric preparation which has been described previously (Jackson & Campbell, 1980) was modified and used in this study. Rats were anaesthetized with α-chloralose (150 mg kg^{-1}) administered subcutaneously. The left femoral artery and vein were cannulated for mean blood pressure (MBP) measurement and 0.9% NaCl supplementation (0.1 ml min^{-1}), respectively. Then a midline incision was made and the superior mesenteric artery was isolated. The carotid artery was also isolated. After complete haemostasis by electrical cautery, heparin (1500 units kg^{-1}) was administered into the femoral vein. After cannulation of the carotid artery, the perfusion line was filled with blood. Once the superior mesenteric artery had been cannulated, the perfusion was begun from the carotid to the mesenteric artery by a roller pump at a constant flow rate of 2 ml min^{-1}. Surgery was undertaken carefully so that no branch of the mesenteric artery was tied or blocked. In order to abolish central nervous system control of the mesenteric preparation, the mesenteric artery proximal to the cannulation point and the surrounding tissue were severed. Mesenteric lymphatic vessels were also severed and the peripheral ends opened to the abdomen. Bipolar platinum electrodes were placed perivascularly approximately 2 mm distal to the cannulation point. The ischaemic time of the mesentery was of the order of 1–2 min. The abdomen was covered with moistened gauze and the body temperature was maintained at 37°C. Femoral artery MBP and mesenteric perfusion pressure were monitored and recorded with a Grass Model 7B Polygraph. Changes in perfusion pressure were indicative of alterations in vascular resistance in this constant flow system. The preparation was allowed to equilibrate for 30 min before the examination of vascular reactivity. In this preparation, MBP and mesenteric BPP were stable, and contractile responses to NA, ES, AII and AVP were reproducible up to 3 h (at least 2.5 h). The systemic effects of ES, AII (10–300 ng) and AVP (0.3–10 munits) were very small and the systemic effects of NA (100–560 ng) were delayed compared to local vascular responses and transient (Figure 1).

Vascular reactivity

Vasoconstrictor responses to exogenous agents were obtained by bolus injections. The volume of each bolus was 0.05 ml. ES, square wave pulses of 1 ms duration with a frequency of 3–9 Hz at 15 V, from an electronic stimulator (Grass model S88) were applied until maximal responses were obtained.

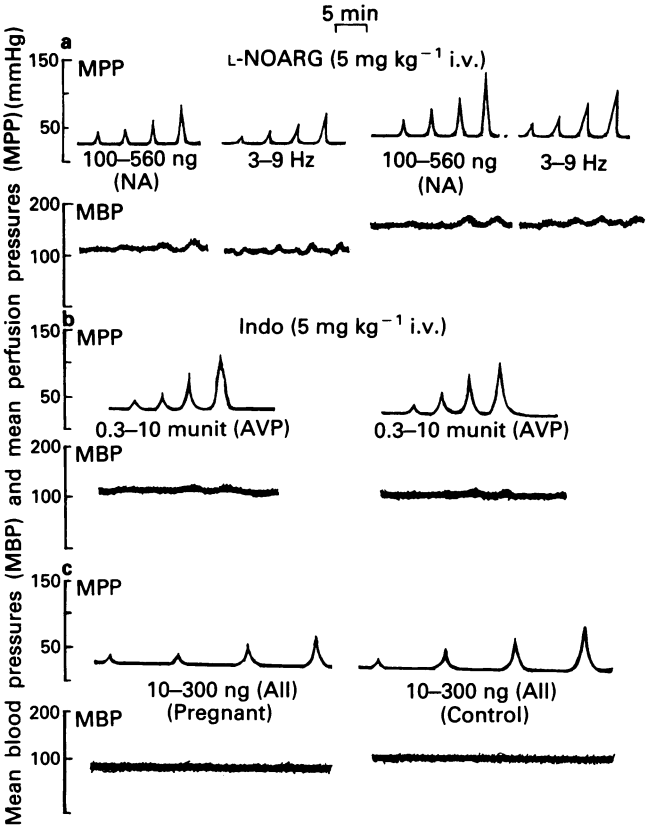

Figure 1 Changes in perfusion pressure and mean intra-arterial blood pressure after application of various stimuli in the *in situ* blood-perfused mesenteric beds of rats. (a) Shows a typical recording of the dose-dependent responses to intra-arterial noradrenaline (NA) and frequency-dependent reactivity to electrical stimulation of sympathetic nerves in a preparation from a nonpregnant rat before and after treatment with N^G-nitro-L-arginine (L-NOARG) (5 mg kg^{-1}, i.v.). (b) Indicates a typical original recording in responses to arginine vasopressin (AVP) in a preparation from a nonpregnant rat before and after treatment with indomethacin (5 mg kg^{-1}, i.v.). (c) Demonstrates a typical recording of the responses to angiotensin II (AII) in preparations from a pregnant (left) and a nonpregnant rat (right).

Reactivity to NA and ES Fifteen pregnant and 15 age-matched nonpregnant rats were used. Dose-effect curves to NA (100–560 ng) and frequency-effect curves to ES (3–9 Hz) were constructed at 3 min intervals. The interval between different stimuli was 20 min. The curves were repeated 30 min after pretreatment with indomethacin (5 mg kg^{-1}, i.v.).

Responses to AII and AVP Reactivity to AVP (15 pregnant and 12 nonpregnant) and AII (12 pregnant and 13 nonpregnant) were investigated in different groups of animals. Dose-effect curves to AVP (0.3–10 munits) were conducted at 3 min intervals, while dose-dependent reactivity to AII (10–300 ng) was tested at 10 min intervals. The responses were examined again 30 min after pretreatment with indomethacin (5 mg kg^{-1}, i.v.).

To examine the possible effects of endothelial-dependent nitric oxide generation on vascular reactivity in pregnant rats, in another series of experiments the mesenteric vascular responses to ES, NA and AII were tested following a similar protocol as above except that the curves were reconstructed 30 min after pretreatment with L-NOARG (5 mg kg^{-1}, i.v.) rather than indomethacin. This dose of L-NOARG induced maximal pressor response in our preparation. The maximal pressor effect was achieved after pretreating the animal with

a single dose of L-NOARG (5 mg kg^{-1}, i.v.) for 30–45 min and then maintained throughout our protocol (at least 2 h).

Noradrenaline spillover from mesenteric vascular beds by electrical stimulation

This experiment was carried out in a separate group of animals (8 pregnant and 8 nonpregnant). Based on the *in situ* blood-perfused mesenteric preparation, a second order branch of the mesenteric vein was cannulated with a stainless steel cannula and the cannula was inserted forward into the main trunk of the mesenteric vein for venous blood sampling. In this preparation, the blood circulation was not affected significantly by the venous cannula. Mesenteric arterial blood samples were taken from the mesenteric perfusion line prior to the roller pump so that the perfusion flow rate was not changed during blood sampling. The preparation was allowed to equilibrate for 30 min. After electrical stimulation (15 V, 1 ms, 9 Hz) had been applied for 1 min and the plateau of the contractile response was obtained, 0.5 ml blood samples were taken from the mesenteric perfusion line and mesenteric vein simultaneously within 1 min. During the blood sampling period, the speed of femoral venous fluid supplementation was set at 1 ml min^{-1} so that the blood volume was maintained and the plateau of the contractile response was stable.

The blood samples were collected in rat catecholamine assay tubes and centrifuged for 10 min at 4°C; 200 µl of plasma was placed in a plastic tube and frozen at − 80°C for radioenzymatic assay of catecholamine (Ziegler *et al.*, 1984).

Plasma thromboxane B_2 production, plasma electrolytes and haematocrit

Ten pregnant and 10 age-matched nonpregnant rats were divided into four groups: pregnant + vehicle ($n = 5$), pregnant + indomethacin ($n = 5$), nonpregnant + vehicle ($n = 5$), and nonpregnant + indomethacin ($n = 5$). Animals were anaesthetized with α-chloralose (150 mg kg^{-1}, s.c.) as described before. The left femoral vein was cannulated for drug administration. Then a midline incision was made, the abdominal aorta and superior mesenteric artery were isolated and the inferior vena cava was also exposed. After 30 min of pretreatment with either heparin (1500 units kg^{-1}) plus indomethacin (5 mg kg^{-1}) or heparin (1500 units kg^{-1}) plus vehicle, 2 ml blood was withdrawn from the inferior vena cava below the left renal vein by use of a 21 G 3/4″ scalp vein set attached to a 5 ml syringe.

One ml blood was dispensed into a 10 ml polypropylene tube and incubated at 37°C for 30 min. The samples were then centrifuged for 15 min at 2500 r.p.m.; 200 µl of plasma was taken for thromboxane B_2 analysis by radioimmunoassay (Mahoney *et al.*, 1983). The remaining 1 ml blood was sent to the Biochemistry Department at Royal Perth Hospital for plasma electrolytes and haematocrit analysis.

Abdominal aortic and superior mesenteric arterial thromboxane B_2 and 6-keto-$PGF_{1\alpha}$

After the above blood samples were collected, 1 cm of aortic tissue was removed from the abdominal aorta below the renal artery approximately 1 cm above the bifurcation to the common iliac arteries; 0.5 cm of superior mesenteric artery was also taken. The tissues were cleared of adhering connective tissues and quickly placed in a polypropylene tube containing 1 ml of Krebs buffer prebubbled with 95% O_2 and 5% CO_2. The tissue was then incubated in a water bath for 30 min at a constant temperature of 37°C. At the end of the incubation period, the tissue was removed from the tube, blotted dry and weighed. The incubate was stored at − 20°C pending analysis of prostaglandin synthesis by radioimmunoassay (Mahoney *et al.*, 1983).

Drugs and solutions

Noradrenaline bitartrate, AII, indomethacin and N^G-nitro-L-arginine (L-NOARG) were all obtained from Sigma chemicals. AVP was purchased from Parke-Davis, NSW, Australia. Heparin sodium was from Delta West, Western Australia.

The composition of Krebs solution for incubation of arterial tissues was (mM): NaCl 118, KCl 4.7, $CaCl_2$ 2.5, KH_2PO_4 1.2, $MgSO_4$ 1.2, $NaHCO_3$ 25 and glucose 11.1. Indomethacin was dissolved in 0.05 M Na_2CO_3 heated to 40°C. Then 1.0 M HCl was added to achieve a final pH of 8.0. A solution of 0.05 M Na_2CO_3 titrated to pH 8.0 served as vehicle. All other drugs were dissolved in 0.9% NaCl and all solutions were made up freshly.

Statistical analysis

All results are expressed as mean ± s.e.mean with n = number of rats. Differences in mean blood pressures and basal perfusion pressures between groups were analysed by Student's unpaired two tailed t test, while in the same group before and after pretreatment with L-NOARG or indomethacin were compared by Student's paired two tailed t test. P values < 0.05 were regarded as significant.

To test statistical differences between dose-effect curves or frequency-effect curves, the area under an individual curve (area) was first calculated mathematically by methods outlined by Matthews *et al.* (1990). The distances between given doses of the agents or frequencies of ES on the horizontal axes were set at 1 when the areas under individual curves were calculated. Means of the areas from different groups were then tested by Student's unpaired two tailed t test. Means of the areas from the same group before and after treatment with L-NOARG or indomethacin were, however, compared by Student's paired two tailed t test.

Differences in biochemical assays were first analysed by one way analysis of variance (ANOVA). When the significant group effects were found, the differences between groups were further tested by Student's unpaired two tailed t test.

Results

Blood pressure

Systolic blood pressure was decreased in pregnant rats (124 ± 2 mmHg, $n = 14$) compared to nonpregnant controls (132 ± 2 mmHg, $n = 15$, $P < 0.05$). Mean blood pressure was also lower in pregnant groups (96 ± 3 mmHg, $n = 14$) than that in controls (108 ± 4 mmHg, $n = 15$, $P < 0.05$). Indomethacin had no effect on mean blood pressure. Mean blood pressures were increased in both pregnant (138 ± 4 mmHg, $P < 0.01$) and nonpregnant (150 ± 3 mmHg, $P < 0.01$) groups after pretreatment with L-NOARG. However the difference in mean blood pressure between groups could be seen after L-NOARG treatment ($P < 0.05$).

Vascular reactivity

There was no difference in basal perfusion pressures between pregnant (29 ± 1 mmHg, $n = 14$) and control animals (31 ± 1 mmHg, $n = 15$) although a trend to lower levels could be seen in the pregnant group. Indomethacin had no effect on basal perfusion pressures. L-NOARG increased basal perfusion pressures in both pregnant (34 ± 1 mmHg, $n = 14$, $P < 0.01$) and nonpregnant (37 ± 2 mmHg, $n = 15$, $P < 0.01$) groups (Figure 1).

The contractile responses to NA were reduced in the mesenteric preparations of pregnant rats (area = 114.4 ± 8.0, $n = 15$) compared with that of nonpregnant animals (area = 142.9 ± 9.2, $n = 15$, $P < 0.05$) (Figure 2a). Reactivity to ES was also diminished in pregnant (area = 31.5 ± 4.2, $n = 15$)

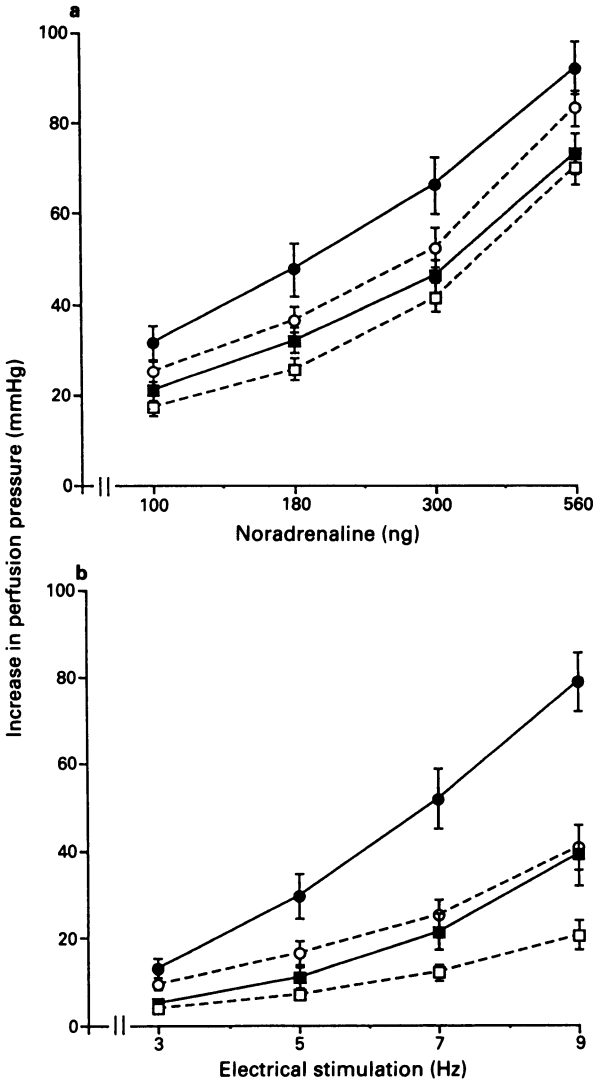

Figure 2 Mesenteric vascular contractile responses to (a) noradrenaline and (b) electrical stimulation of sympathetic nerves in the *in situ* blood-perfused mesenteric beds from pregnant (□, $n = 15$) and nonpregnant (○, $n = 15$). The responses were repeated commencing 30 min after pretreatment with indomethacin (5 mg kg^{-1}, i.v.) in preparations from pregnant (■, $n = 15$) and nonpregnant (●, $n = 15$) controls. Values are mean ± s.e.mean of n rats.

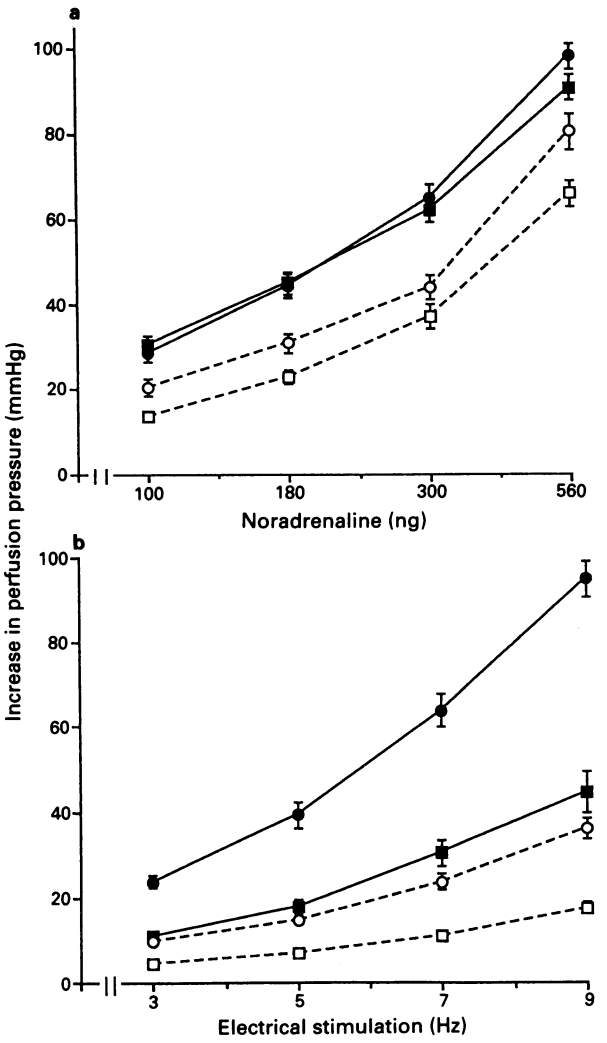

Figure 3 Mesenteric vascular contractile responses to intra-arterial noradrenaline and electrical stimulation of sympathetic nerves in the *in situ* blood-perfused mesenteric beds from pregnant rats (□, $n = 15$) and nonpregnant animals (○, $n = 14$). N^G-nitro-L-arginine (L-NOARG) (5 mg kg^{-1}, i.v.) was administered to pregnant (■, $n = 14$) and nonpregnant (●, $n = 15$) rats, 30 min before the construction of a 2nd series of curves in response to noradrenaline and electrical stimulation.

compared with nonpregnant (area = 66.72 ± 9.6, $n = 15$, $P < 0.01$) group (Figure 2b). In the vessel beds pretreated with indomethacin, reactivity to NA was increased in the nonpregnant group (area = 175.3 ± 16.2, $n = 15$, $P < 0.05$) only and responses to ES were augmented in both pregnant (area = 54.5 ± 10.0, $n = 15$, $P < 0.01$) and nonpregnant (area = 125.9 ± 16, $n = 15$, $P < 0.01$) groups, but the differences between groups were still evident ($P < 0.01$). After pretreatment with L-NOARG, responses to NA were enhanced in both pregnant (area = 100.0 ± 5.5 before L-NOARG, area = 167.5 ± 7.4 after L-NOARG, $n = 15$, $P < 0.01$) and nonpregnant (area = 124.9 ± 7.8 before L-NOARG, area = 172.3 ± 8.2 after L-NOARG, $n = 14$, $P < 0.01$) groups; the difference in NA-induced responses between pregnant and nonpregnant rats was abolished while the difference in ES responses was amplified ($P < 0.01$) (Figure 3).

Vasoconstrictor responses to AII (10–300 ng) were decreased in the preparation from pregnant rats (area = 94.6 ± 7.9, $n = 15$) compared with that from controls (area = 133.5 ± 9.4, $n = 15$, $P < 0.01$) (Figure 4a). Reactivity to AVP (0.3–10 munits) was also blunted in pregnant (area = 114.8 ± 6.5, $n = 13$) compared with nonpregnant animals (area = 157.6 ± 9.2, $n = 12$, $P < 0.01$) (Figure 4b). Pretreatment with indomethacin enhanced AII-induced contraction in nonpregnant animals (area = 150.9 ± 6.9, $n = 12$, $P < 0.01$) only (Figure 4a). Indomethacin had no effect on responses to AVP in both pregnant and nonpregnant groups (Figure 4b). The preparations pretreated with L-NOARG showed increases in reactivity to AII in both pregnant (area = 97.7 ± 5.5 before L-NOARG, area = 124.1 ± 6.7 after L-NOARG, $n = 11$, $P < 0.01$) and nonpregnant groups (area = 135.7 ± 9.2 before L-NOARG, area = 173.5 ± 12.5 after L-NOARG, $P < 0.01$) (Figure 5). The response to AII was still lower ($P < 0.01$) in the pregnant group than in nonpregnant controls.

In order to examine whether different effects of L-NOARG according to the pressor agents used are due to the dose of L-NOARG employed, we compared the vascular reactivity to ES and the effect of different doses of L-NOARG in 5 pregnant and 5 aged-matched nonpregnant rats. Contractile reactivity to ES was repeated after the animals had been given a continuous infusion of L-NOARG intravenously for 30 min at a dose of 50 mg kg^{-1}, 60 min at a dose of 100 mg kg^{-1}, 90 min at a dose of 150 mg kg^{-1} and 120 min at a dose of 200 mg kg^{-1}, respectively. A similar procedure was employed for responses to AII. At this stage the maximal

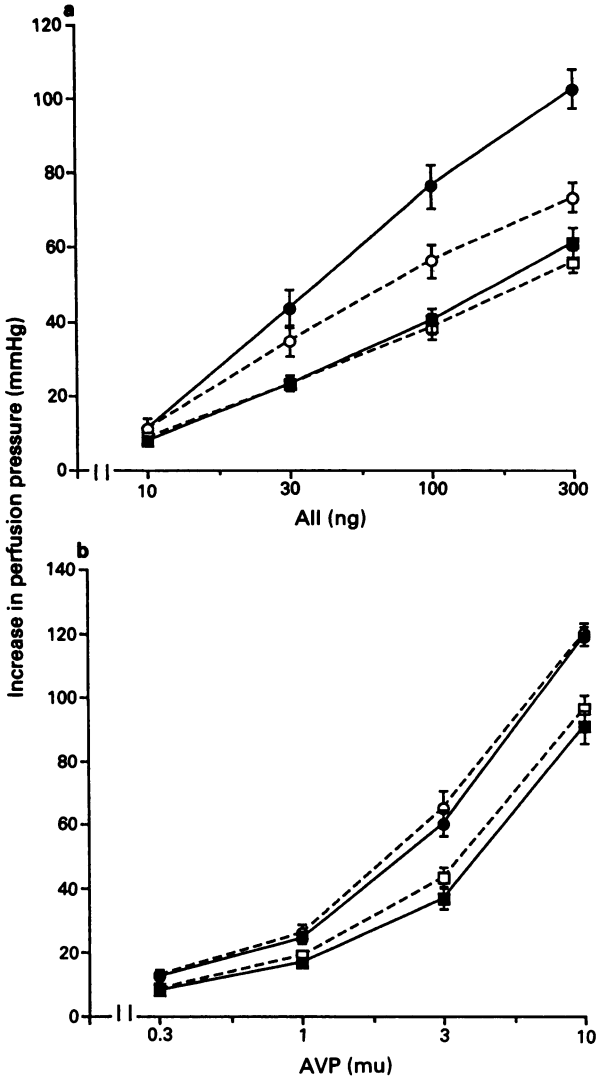

Figure 4 (a) Dose-effect curves to intra-arterial angiotensin II (AII) in the *in situ* blood-perfused mesenteric preparations from pregnant (□, $n = 15$) and nonpregnant (○, $n = 12$) rats. The responses were repeated 30 min after pretreatment with indomethacin (5 mg kg^{-1}, i.v.) in the vessel beds from both pregnant (■, $n = 15$) and nonpregnant (●, $n = 12$) rats. (b) Dose-effect curves to intra-arterial arginine vasopressin (AVP) in preparations from pregnant and nonpregnant rats before (pregnant: □, $n = 13$; nonpregnant: ○, $n = 12$) and after (pregnant: ■, $n = 13$; nonpregnant: ●, $n = 12$) 30 min pretreatment with indomethacin (5 mg kg^{-1}, i.v.). Each point is mean ± s.e.mean of n values.

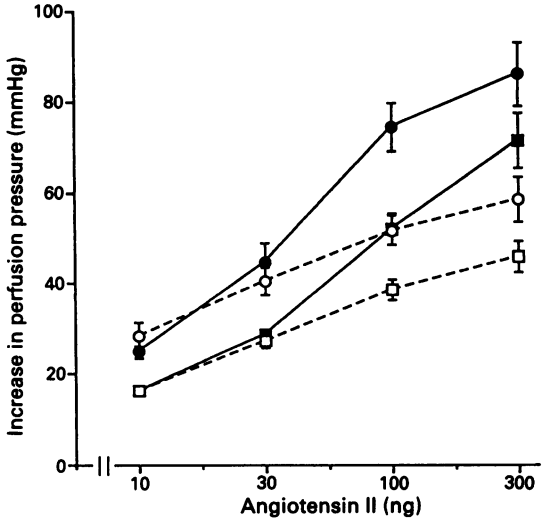

Figure 5 Dose-effect curves to intra-arterial angiotensin II in the *in situ* blood-perfused mesenteric beds from pregnant and nonpregnant rats before (pregnant: □, $n = 11$; nonpregnant: ○, $n = 12$) and after (pregnant: ■, $n = 11$; nonpregnant: ●, $n = 12$) 30 min pretreatment with N^G-nitro-L-arginine (5 mg kg^{-1}, i.v.).

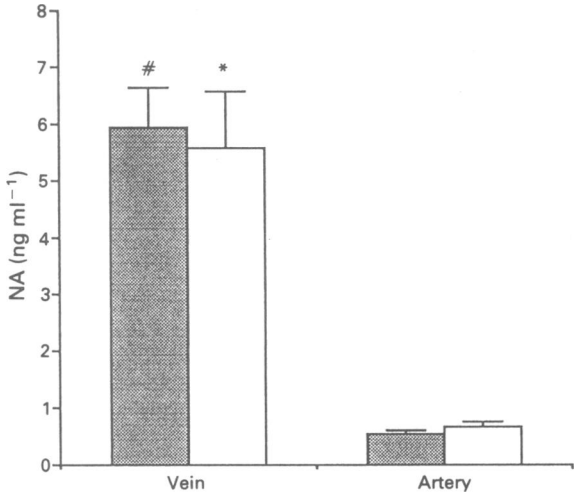

Figure 6 Plasma concentrations of noradrenaline during electrical stimulation of sympathetic nerves (15 V, 1 ms, 9 Hz) in the *in situ* blood-perfused mesenteric beds from pregnant (stippled columns, $n = 8$) and nonpregnant (open columns, $n = 8$) rats. Values are mean ± s.e.mean. Noradrenaline (NA) concentrations of mesenteric venous plasma were significantly increased compared to those of arterial plasma in both pregnant and nonpregnant groups ($P < 0.01$). There was no difference in either mesenteric arterial or venous plasma noradrenaline concentrations between pregnant and nonpregnant groups.

potential effect of L-NOARG on the vascular reactivity to ES and AII was obtained. The blunted responses to either ES or AII in pregnant rats were not restored by any given dose of L-NOARG (data not shown).

Noradrenaline spillover from mesenteric beds by electrical stimulation

NA concentrations were significantly higher in mesenteric venous plasma than in arterial plasma during electrical stimulation in both pregnant and nonpregnant groups ($P < 0.01$). The increase in NA content in venous plasma indicated the release of NA from vascular beds and its spillover into the circulation during electrical stimulation. There was no difference in either mesenteric arterial or venous plasma NA concentration between groups (Figure 6).

Eicosanoid production

Plasma thromboxane B_2, aortic and mesenteric arterial 6-keto-$PGF_{1\alpha}$ were significantly decreased in animals pretreated with indomethacin in both pregnant and nonpregnant groups indicating significant inhibition of eicosanoid production by indomethacin (Table 1).

Plasma electrolytes and haematocrit

There were no differences in plasma sodium, potassium, bicarbonate, urea and creatinine between pregnant and nonpregnant groups. The haematocrit was lower in pregnant rats (35.25 ± 0.48%, $n = 10$) than in nonpregnant animals (41.5 ± 0.95%, $n = 10$, $P < 0.01$).

Table 1 Effects of indomethacin (Indo) on the production of plasma thromboxane B_2 (P-TxB_2), aortic (Aor) 6-keto-$PGF_{1\alpha}$, aortic (Aor) TxB_2, superior mesenteric arterial (Art) 6-keto-$PGF_{1\alpha}$ and TxB_2 in pregnant and nonpregnant rats

	Pregnant ($n = 5$)	*Pregnant + Indo* ($n = 5$)	*Nonpregnant* ($n = 5$)	*Nonpreg + Indo* ($n = 5$)
P-TxB_2 (ng ml^{-1})	$3.13 \pm 0.98^{*a}$	0.14 ± 0.09^{a}	$0.48 \pm 0.30^{*}$	(—)
Aor 6-keto-$PGF_{1\alpha}$ (ng mg^{-1})	$4.04 \pm 1.09^{*}$	0.54 ± 0.05	$5.84 \pm 1.42^{*}$	1.90 ± 0.35
Aor TxB_2 (ng mg^{-1})	$0.23 \pm 0.05^{*}$	0.05 ± 0.01	$0.23 \pm 0.03^{*}$	0.12 ± 0.03
Art 6-keto-$PGF_{1\alpha}$ (ng mg^{-1} 0	$8.98 \pm 1.74^{*}$	3.70 ± 1.02	$5.38 \pm 0.97^{*}$	2.95 ± 0.48
Art TxB_2 (ng mg^{-1})	$0.47 \pm 0.11^{*}$	0.14 ± 0.02	$0.38 \pm 0.06^{*}$	0.18 ± 0.07

(—) undetectable.
$^{*}P < 0.05$ when comparison made between Indo-treated and untreated animals in pregnant or nonpregnant groups.
$^{a}P < 0.05$ when comparison made between pregnant and non-pregnant groups in Indo-treated or untreated animals.

Discussion

The present studies demonstrate that blood pressures are lower and vasoconstrictor reactivity to ES, NA, AII and AVP is decreased in the *in situ* blood-perfused mesenteric beds of 18–20 day pregnant rats as compared with non-pregnant rats. The blunted responses cannot be restored by the cyclo-oxygenase inhibitor, indomethacin. The nitric oxide synthase inhibitor L-NOARG augmented responses to all agonists in both pregnant and nonpregnant animals but only equalized the responses to NA between pregnant and non-pregnant rats. These data suggest that cyclo-oxygenase products are not responsible for any decreased contractile responses in the *in situ* blood perfused mesenteric beds of pregnant rats. On the other hand, an increase in endogenous endothelial-dependent nitric oxide generation could, in part, contribute to the vasodilatation seen in pregnancy by modulating vasomotor tone in responses to circulating catecholamines.

Although it has been well documented that blood pressures were lower and systemic arterial pressor responses were decreased in animals, as well as in women during late pregnancy, the mechanisms involved in these changes are still unclear. Especially, conflicting findings with *in vitro* and *in vivo* preparations have been reported with regard to the alterations in vascular reactivity in pregnancy.

The possible role of endogenous prostaglandins has been extensively studied in pregnant women and in pregnant animals. Pregnancy results in profoundly increased prostaglandin production in women (Bay & Ferris, 1979; Goodman *et al.*, 1982). Plasma prostaglandin levels and urinary prostaglandins excretion were elevated in pregnant and pseudopregnant rats (Paller *et al.*, 1989). It has been suggested that vascular vasodilator prostaglandins may oppose the vasoconstrictor actions of NA, AII and AVP and hence produce the apparent decrease in the action of these vasoconstrictor substances (Gant *et al.*, 1987). Although the decreased systemic arterial pressor responses to NA, AII and AVP were restored by a cyclo-oxygenase inhibitor, meclofenamate, in conscious pregnant rats (Paller, 1984), this finding has not been consistently reported (Conrad *et al.*, 1986; Harrison *et al.*, 1989). In the present studies pretreating the animals with a cyclo-oxygenase inhibitor, indomethacin, increased local mesenteric vascular responses to ES in both pregnant and nonpregnant groups, but enhanced the responses to NA and AII only in nonpregnant groups. The differences in responses between pregnant and nonpregnant animals were still evident. These results suggested that endogenous vasodilator prostaglandins, if anything, play a predominant role in non-pregnant rather than in pregnant rats, and that increases in vasodilator prostaglandins are insufficient to explain the decreased pressor responses and vasodilatation seen in pregnant rats.

Endothelium derived nitric oxide (NO) has been reported to be a potent endogenous vasodilator and to suppress vasoconstrictor reactivity to various vasoactive substances (Palmer *et al.*, 1987; Myers *et al.*, 1989) and hence may play a role in the modulation of vascular reactivity in pregnancy. A recent finding favouring this hypothesis is that the plasma level and urinary excretion of cyclic GMP were significantly elevated in pregnant rats. In studies with conscious pregnant rats, systemic administration of L-NOARG, a potent NO synthase inhibitor, has been shown to restore the lower MBP and blunted pressor responses to various vasoconstrictor agonists (Molnar & Hertelendy, 1992). However, it is still uncertain whether NO entirely accounts for pregnancy-induced vasodilatation as inconsistent results have also been reported – pregnancy did not alter the pressor effect of N-methylarginine, another NO synthase specific inhibitor in conscious rats (Umans *et al.*, 1990). The results of the present study demonstrated that intra-venous administration of L-NOARG significantly increased blood pressure and potentiated vasocontractile reactivity to ES, NA and AII in blood perfused mesenteric vessels in both pregnant and nonpregnant animals. These findings indicated that basal release of NO contributes to the physiological vasodilatation and endogenous NO opposes vasoconstrictor effects of various vasoactive agents in both pregnant and nonpregnant rats. Comparing the effects of L-NOARG on blood-perfused mesenteric vessels of pregnant and nonpregnant rats, only the difference in responses to NA was abolished while the differences in blood pressure and responses to ES and AII were still evident. These results indicated that enhanced NO generation or increased sensitivity to NO does not completely account for the lower blood pressures and decreased pressor responses seen in pregnancy, but may contribute to the vasodilatation by modulating the effects of circulating catecholamines.

The results of the present studies showing decreases in vasoconstrictor responses to ES and NA are consistent with previous reports that sympathetic vasoconstrictor influences on resistance vessels were decreased during pregnancy (Assali *et al.*, 1981; Humphreys & Joels, 1982a,b). In the preparations used in the present studies, we have confirmed that the release of endogenous noradrenaline from sympathetic nerve endings is responsible for ES-induced contraction (Jackson & Campbell, 1980), as the contraction could be abolished by pretreating the preparation with an α-receptor blocker, phentolamine (data not shown). In order to examine further whether the attenuated ES-induced contractions are due to the degeneration of sympathetic nerves, as was seen in the pregnant uterus of the guinea-pig (Marshall, 1981) and hence decreased NA release from the sympathetic nerve endings, we have studied the NA spillover from the mesenteric vessels during ES. Significant increases in NA concentrations in mesenteric venous plasma compared to arterial plasma were

found in both pregnant and nonpregnant rats during ES, indicating the release of NA and its spillover to the circulation. However, there were no significant differences in either mesenteric arterial or venous plasma NA concentration between pregnant and nonpregnant groups during ES. This makes it most unlikely that degeneration of sympathetic nerves or depletion of catecholamine store has occurred in the mesenteric vascular beds during pregnancy. This result is quite consistent with the report of Hart *et al.* (1986). In their study, no difference was found in NA content and [^{3}H]-NA accumulation by caudal arteries from pregnant (19–21 day) and nonpregnant rats. It has also been suggested that pregnancy-induced changes in the autonomic control of blood vessels may involve modification at higher levels of the autonomic nervous system other than the peripheral neuroeffector site. However, this hypothesis was not supported by the studies which showed that pregnant and nonpregnant rats had similar decreases in mean blood pressures in response to a ganglionic blocker, pentolinium or an α-adrenoceptor blocker, phentolamine (Pan *et al.*, 1990).

In the present study the relatively decreased responses to ES in pregnant as compared with nonpregnant animals persisted after L-NOARG even though the NA responses were rendered equivalent. This phenomenon raises the possibility that neurotransmitters other than NA may contribute to the decreased contractile responses to ES in pregnant rat mesentery. Recently, it has been reported that nonadrenergic and noncholinergic fibres (NANC), especially capsaicin-sensitive fibres, mediated ES-induced relaxation in isolated perfused mesenteric resistance vessels (Kawasaki *et al.*, 1988). The contractile reactivity to ES was enhanced in the preparation pretreated with capsaicin (Kawasaki *et al.*, 1990). Thus the possible involvement of NANC fibres in the decreased ES-induced contractions in mesenteric vessels during pregnancy would be worth studying, as well as the possible role of vasodilators such as calcitonin gene-related peptide (CGRP) and vasoactive intestinal polypeptide (VIP).

As the lower blood pressures in pregnant rats cannot be restored by either indomethacin or L-NOARG, and decreased vascular reactivity cannot be equalized by indomethacin, neither endogenous prostaglandins nor NO appear to account completely for the lower blood pressures and reduced vascular reactivity seen in pregnant rats. Moreover, as the abnormalities in mechanisms which account for the physiological vasodilatation and decreased pressor responses seen in pregnancy may be relevant to pregnancy-induced hypertension, this phenomenon requires further study.

In summary, the present study using a blood perfused mesenteric preparation *in vivo* demonstrates marked suppression of vascular reactivity to a variety of agonists in pregnancy. Studies with indomethacin suggested that the prostaglandins are unlikely to be responsible for these effects. The effects of L-NOARG indicate that endogenous NO synthesis or sensitivity to NO influence vascular tone and blood pressure in pregnant and nonpregnant animals and, hence, may account for the decreased vascular reactivity to circulating catecholamines. The decreased responses to AII may be due at least in part to down-regulation of vascular AII receptors in response to elevated circulating AII levels in normal pregnancy (Beilin *et al.*, 1983). However, other as yet unidentified mechanisms appear to account for the decreased responses to AVP and sympathetic nerve stimulation.

This study was supported by the Research Foundation of Royal Perth Hospital, the National Heart Foundation of Australia and the Australian National Health & Medical Research Council. We wish to thank Mrs Anne Bell for the assay of catecholamines, Ms Natasha Rossi and Dr Anne Barden for the assay of eicosanoid. We would also like to thank Dr Valerie Burke for her help with the statistics.

References

ASSALI, N.S., NUWAYHID, B., BRINKMAN III, C.R., TABSH, L., ERKKOLA, R. & USHIODA, E. (1981). Autonomic control of the circulation: in vivo and in vitro studies in pregnant and nonpregnant sheep. *Am. J. Obstet. Gynecol.*, **141**, 873–884.

BAY, W.H. & FERRIS, T.F. (1979). Factors controlling plasma renin and aldosterone during pregnancy. *Hypertension*, **1**, 410.

BEILIN, L.J., DEACON, J., MICHAEL, C.A., VANDONGEN, R., LALOR, C.M., BARDEN, A.E., DAVIDSON, L. & ROUSE, I. (1983). Diurnal rhythms of blood pressure, plasma renin activity, angiotensin II and catecholamines in normotensive and hypertensive pregnancies. *Clin. Exp. Hypertension (B)*, **2**, 271–293.

CHESLEY, L.C., TALLEDO, E., BOHLER, C.S. & ZUSPAN, F.P. (1965). Vascular reactivity to angiotensin II and norepinephrine in pregnant and nonpregnant women. *Am. J. Obstet. Gynecol.*, **91**, 837–847.

CHU, Z.M. & BEILIN, L.J. (1992). Effects of N-nitro-L-arginine and indomethacin on noradrenergic responses in the blood perfused mesenteric circulation of pregnant rats. *14th Scientific Meeting of the International Society of Hypertension*, Madrid, Spain 1992.

CONRAD, K.P. & COLPOYS, M.C. (1986). Evidence against the hypothesis that prostaglandins are the vasodepressor agents of pregnancy. Serial studies in chronically instrumented, conscious rats. *J. Clin. Invest.*, **77**, 236–245.

CONRAD, K.P. & VERNIER, K.A. (1989). Plasma level, urinary excretion, and metabolic production of cGMP during gestation in rats. *Am. J. Physiol.*, **257**, R847–R853.

DOGTEROM, J. & DE JONG, W. (1974). Diminished pressor responses to noradrenaline of the perfused tail arteries of pregnant rats. *Eur. J. Pharmacol.*, **25**, 267–269.

EVERETT, R.B., WORLEY, R.J. & MACDONALD, P.C. (1978). Effect of prostaglandin synthetase inhibitors on pressor response to angiotensin II in human pregnancy. *J. Clin. Endocrinol. Metab.*, **46**, 1007–1010.

GANT, N.F., WHALLEY, P.J., EVERETT, R.B., WORLEY, R.J. & MACDONALD, P.C. (1987). Control of vascular reactivity in pregnancy. *Am. J. Kidney Dis.*, **9**, 303–307.

GOODMAN, R.P., KILLAM, A.P., BRASH, A.R. & BRANCH, R.A. (1982). Prostacyclin production during pregnancy: comparison of production during normal pregnancy and pregnancy complicated by hypertension. *Am. J. Obstet. Gynecol.*, **142**, 817–822.

HARRISON, G.L. & MOORE, L.G. (1989). Blunted vascular reactivity in pregnant guinea pigs is not restored by meclofenamate. *Am. J. Obstet. Gynecol.*, **160**, 258–264.

HART, J.L., FREAS, W. & MULDOON, S.M. (1986). Neurovascular function in rat during pregnancy. *Am. J. Physiol.*, **251**, H1000–H1008.

HUMPHREYS, P.W. & JOELS, N. (1982a). Reflex responses of the rabbit hind-limb muscle vascular bed to baroreceptor stimulation and its modification by pregnancy. *J. Physiol.*, **330**, 461–473.

HUMPHREYS, P.W. & JOELS, N. (1982b). The responses of the hind-limb vascular bed of rabbit to sympathetic stimulation and modification by pregnancy. *J. Physiol.*, **330**, 475–488.

JACKSON, E.K. & CAMPBELL, W.B. (1980). The in situ blood perfused rat mesentery; a model for assessing modulation of adrenergic neurotransmission. *Eur. J. Pharmacol.*, **66**, 217–224.

JANSAKUL, C., KING, R.G. & BOURA, L.A. (1990). Effects of endothelium cell removal on α-adrenoceptor-mediated responses of aortae of pregnant rats. *Clin. Exp. Pharmacol. Physiol.*, **17**, 147–156.

KAWASAKI, H., TAKASAKI, K., SAITO, A. & GOTO, K. (1988). Calcitonin gene-related peptide acts as a novel vasodilator neurotransmitter in mesenteric vessels of the rats. *Nature*, **335**, 164–167.

KAWASAKI, H., NUKI, C., SAITO, A. & TAWASAKI, K. (1990). Role of calcitonin gene-related peptide-containing nerves in the vascular adrenergic neurotransmission. *J. Pharmacol. Exp. Ther.*, **252**, 403–409.

MAHONEY, D.P., BARDEN, A., BEILIN, L.J. & VANDONGEN, R. (1983). Radioimmunoassay of prostaglandins and thromboxane B2 in extracted and unextracted urine and serum using an iodinated ligand. *Prostaglandins Leukot. Med.*, **12**, 11–14.

MARSHALL, J.M. (1981). Effects of ovarian steroids and pregnancy on adrenergic nerves of uterus and oviduct. *Am. J. Physiol.*, **240,** C165–C174.

MASSICOTTE, G., ST-LOUIS, J. & SCHIFFRIN, E.L. (1987). Decreased in vitro responses to vasoconstrictor during gestation in normotensive and spontaneously hypertensive rats. *Can. J. Physiol. Pharmacol.*, **65,** 2466–2471.

MATTHEWS, J.N.S., ALTMAN, D.G., CAMBELL, M.J. & ROYSTON, P. (1990). Analysis of serial measurement in medical research. *Br. Med. J.*, **300,** 230–235.

MOLNAR, M. & HERTELENDY, F. (1992). Nω-nitro-L-arginine, an inhibitor of nitric oxide synthesis, increases blood pressure in rats and reverses the pregnancy-induced refractoriness to vasopressor agents. *Am. J. Obstet. Gynecol.*, **166,** 1560–1567.

MYERS, P.R., GUERRA, R.J. & HARRISON, D.G. (1989). Release of NO and EDRF from cultured bovine aortic endothelial cells. *Am. J. Physiol.*, **256,** H1030–1037.

PALLER, M.S. (1984). Mechanism of decreased pressor responsiveness to AGNII, NE and AVP in pregnant rats. *Am. J. Physiol.*, **247,** H100–108.

PALLER, M.S., GREGORINI, G. & THOMAS, F.F. (1989). Pressor responsiveness in pseudopregnant and pregnant rats: role of maternal factors. *Am. J. Physiol.*, **26,** R866–R871.

PALMER, R.M., FERRIGE, A.G. & MONCADA, S. (1987). Nitric oxide release accounts for the biological activity of endothelium-derived relaxing factor. *Nature*, **327,** 524–526.

PAN, Z.-R., LINDHEIMER, M.D., BAILIN, J. & BARRON, W.M. (1990). Regulation of blood pressure in pregnancy: pressor system blockade and stimulation. *Am. J. Physiol.*, **258,** H1559–1572.

PARENT, A., SCHIFFRIN, E.L. & ST-LOUIS, J. (1990). Role of the endothelium in adrenergic responses of mesenteric artery rings of pregnant rats. *Am. J. Obstet. Gynecol.*, **163,** 229–234.

UMANS, J.G., LINDHEIMER, M.D. & BARRON, W.M. (1990). Pressor effect of endothelium-derived relaxing factor inhibition in conscious virgin and gravid rats. *Am. J. Physiol.*, **259,** F293–F296.

YIN, K., CHU, Z.M. & BEILIN, L.J. (1991). Surprising changes in vascular reactivity in pregnant rats. In *Genetic Hypertension.* ed. Sassard, J., Vol. 218, pp. 55–57. Colloque INSERM/John Libbey Eurotext Ltd.

ZIEGLER, M.G. & LAKE, C.R. (1984). *Noradrenaline.* pp. 27–37. Baltimore: Williams & Wilkins.

(Received July 31, 1992
Revised January 11, 1993
Accepted January 25, 1993)

Br. J. Pharmacol. (1993), **109**, 330–335 © Macmillan Press Ltd, 1993

Novel regulation of muscarinic receptors and their coupling with G proteins in smooth muscle: transient resensitization during desensitizing process

[1]Shigeru Hishinuma, Yukio Matsumoto, *Masaatsu K. Uchida & [2]Masanori Kurokawa

Department of Pharmacology, Meiji College of Pharmacy at Tanashi, 1-22-1 Yato, Tanashi, Tokyo 188, Japan and *Department of Molecular Pharmacology, Meiji College of Pharmacy at Setagaya, 1-35-23 Nozawa, Setagaya, Tokyo 154, Japan

1 Muscarinic stimulation of the smooth muscle of guinea-pig taenia caeci was produced with 10^{-4} M carbachol for 15 s, 30 s, 1 min, 2 min and 30 min, and the time course of developing desensitization was studied by measuring the muscle contractility and the binding characteristics of muscarinic receptors.

2 The contractile response to carbachol was analyzed using dose-response curves. The response to 10^{-7} M carbachol was reduced by treatment for 15 s with 10^{-4} M carbachol (fast desensitization), but recovered partially after 30 s treatment and completely after 1 min treatment (resensitization). Contractility was reduced again after 2 min and 30 min treatment (re-desensitization).

3 The affinity of carbachol for muscarinic receptors was changed by the carbachol treatment in a manner similar to the contractility. Thus, the affinity was reduced at 15 s, restored slightly at 30 s and completely at 1 and 2 min, and was reduced again at 30 min.

4 5'-Guanylylimidodiphosphate (GppNHp), a non-hydrolysable analogue of guanosine triphosphate (GTP) reduced the affinity of muscarinic receptors for carbachol via guanine nucleotide-binding regulatory proteins (G proteins). A similar effect was observed in tissues desensitized by 15 s carbachol treatment. This effect disappeared after 30 s, recovered completely after 1 and 2 min, and disappeared again after 30 min carbachol treatment.

5 Neither the dissociation constant (K_d value) nor the maximal binding (B_{max}) of [^{3}H]-quinuclidinyl benzilate ([^{3}H]-QNB) to muscarinic receptors were changed by the carbachol treatment.

6 These results indicate that the whole process of desensitization, resensitization and re-desensitization are related to changes in the binding ability of muscarinic receptors, in their coupling with G proteins and in the post-receptor steps of the signal transduction. We emphasize that the desensitizing process involves an early transient phase of resensitization that could be caused by restoration of both the affinity of carbachol for muscarinic receptors and their coupling with G proteins. This novel resensitization mechanism may have some physiological significance for cellular homoeostasis by modulating cellular responsiveness transiently or even in an oscillatory manner during the process of desensitization.

Keywords: Desensitization; transient resensitization; muscarinic receptors; G protein; signal transduction systems; smooth muscle

Introduction

We have investigated the regulatory mechanisms of the muscarinic receptor-mediated signal transduction system in smooth muscle of guinea-pig taenia caeci. The subject of our recent analysis has been desensitization, the phenomenon of diminished cellular responses after prolonged stimulation with an agonist, which is thought to play an important role in protecting cells or tissues from abnormal stimuli. The extent of desensitization is believed to develop uniformly depending on the time period of the desensitizing stimulation. Resensitization, on the other hand, is also a crucial process for cells or tissues to function normally when they are relieved from severe stimulation. This is also believed to occur gradually depending on the time period after cessation of the desensitizing stimulation.

We have, however, found that desensitization of muscle contractility occurs in a complex time-dependent manner after desensitizing treatment with carbachol in guinea-pig taenia caeci. Contractility to carbachol was transiently restored during the early stage of the development of desensitization. The resensitization is a novel phenomenon in that some resensitizing mechanisms are operating even in the presence of the desensitizing agonist. Such transient modulation of cellular responsiveness against desensitization may have some physiological significance for cellular homoeostasis. Possible mechanisms underlying this transient resensitization were thus investigated by examining changes in the binding properties of the muscarinic receptors and in their regulation by guanine nucleotides via guanine nucleotide-binding regulatory proteins (G proteins).

Preliminary accounts have been given of part of the present study (Matsumoto *et al.*, 1992; Hishinuma *et al.*, 1992).

Methods

Measurement of contraction

Guinea-pigs of either sex, weighing 250–400 g, were killed by a blow on the neck and were exsanguinated. Strips of taenia caeci were suspended in 10 ml organ baths bubbled with air at 30°C. The bathing solution was normal Locke-Ringer solution (normal solution) with the following composition (mM): NaCl 154, KCl 5.63, $CaCl_2$ 2.16, $MgCl_2$ 2.10, $NaHCO_3$ 5.95 and glucose 5.55. Cumulative contractions induced by carbachol (10^{-9} M to 10^{-4} M) were recorded isotonically on a smoked drum with a lever having a load of about 0.5 g. For the construction of a set of the cumulative dose-response curves the muscle was exposed to each dose of carbachol for

[1] Author for correspondence.
[2] Present address: The Tokyo Institute of Psychiatry, Kamikitazawa 2-1-8, Setagaya, Tokyo 156, Japan.

1–2 min. It took about 7 min to obtain the data for a full dose-response curve. Precisely 30 min after the control curve was completed, treatment with 10^{-4} M carbachol (desensitizing treatment) was initiated. The duration of treatment was either 15 s, 30 s, 1 min, 2 min or 30 min. After the treatment the muscle was washed with the normal solution; exactly 10 min after finishing the desensitizing treatment, the cumulative contractile responses to carbachol were recorded for about 7 min to obtain a dose-response curve that served for comparison with the control.

Contractions without the desensitizing treatment with carbachol (termed none) were also measured after the control responses were recorded, because it was possible that the muscles were already desensitized before the desensitizing treatment by 10^{-4} M carbachol applied to measure the maximal contraction of the control. The base line in the resting state and the maximal contraction to 10^{-4} M carbachol in examining the control responses were taken as 0% and 100% contraction, respectively. In the dose-response relationship, the contractions over the base line were expressed as positive percentage values of the maximal contraction of the control. The prepared muscles sometimes relaxed below the base line of the control after the control responses had been measured. Contractions to carbachol subsequently applied remained below the base line. Contractions to carbachol were calculated in this case as the distance from the base line of the control, and expressed as negative percentage values of the maximal contraction of the control (Figure 1).

Preparation of membrane fraction

Isolated strips of taenia caeci were treated with or without 10^{-4} M carbachol for 15 s to 30 min in normal solution. The muscles were then minced with a pestle made of stainless steel in liquid N_2 and homogenized in 20 volumes of 20 mM MOPS buffer (pH 7.4 at 30°C) containing NaCl 154 mM, KCl 5.6 mM, $CaCl_2$ 2.16 mM, $MgCl_2$ 2.10 mM and sucrose 0.25 M (MOPS buffer A) with Polytron PT-10 operated 3 times at a power setting of 6. The homogenate was centrifuged at 11,000 *g* for 20 min, and the supernatant was recentrifuged at 100,000 *g* for 60 min. All procedures were performed at 0–4°C. The precipitate obtained by the second centrifugation was suspended in 10 volumes of 20 mM MOPS buffer (pH 7.4 at 30°C) containing NaCl 154 mM, KCl 5.6 mM, $CaCl_2$ 2.16 mM and $MgCl_2$ 2.10 mM (MOPS buffer B) as the membrane preparation (protein concentration = about 0.3 mg ml^{-1}; muscarinic receptor concentration = about 600 fmol of binding sites of [^{3}H]-quinuclidinyl benzilate ml^{-1}). The membrane preparations were stored at −85°C and used within 1 week during which the muscarinic receptors maintained normal binding characteristics.

Measurement of binding characteristics of muscarinic receptors

The membrane preparations (final concentrations in the reaction mixture; protein = about 0.03 mg ml^{-1}, muscarinic receptors = about 60 fmol ml^{-1}) were incubated with 0.1 nM to 0.8 nM [^{3}H]-quinuclidinyl benzilate (QNB) in MOPS buffer B for 20 min at 30°C for measurement of the maximal binding (B_{max}) and the equilibrium dissociation constant (K_d value) of [^{3}H]-QNB. For measuring the binding characteristics of carbachol to muscarinic receptors and their regulation by guanine nucleotide, the membrane preparations were incubated with 0.6 nM [^{3}H]-QNB containing carbachol (10^{-7} M to 10^{-1} M) in the presence and absence of 0.05 mM 5′-guanylylimidodiphosphate (GppNHp), a non-hydrolysable analogue of GTP. The reaction was stopped by filtration of 1 ml of reaction mixture through Whatman GF/C glass microfibre filters under vacuum, and radioactivity trapped on the filter was counted by liquid scintillation spectrophotometry. Non-specific binding was determined as [^{3}H]-QNB binding in the presence of 10^{-5} M atropine. Protein concentration was determined by the method of Lowry *et al.* (1951) with bovine serum albumin as an internal standard. All experiments were performed in duplicate or triplicate.

Data analysis

The extent of desensitization of contractility was evaluated by three parameters obtained from the dose-response curves for carbachol: (1) reduction in contractility to 10^{-7} M carbachol, (2) the increase in EC_{50} values and (3) reduction in the area under the dose-response curve (AUC). The AUC is calculated as follows: straight lines are drawn to connect neighbouring points of paired concentration-contraction values as illustrated in Figure 1 (dose-response curve), and the area under these lines and above the abscissa line at 0% of contraction is calculated as a sum of adequately divided triangles and squares in a range of concentrations from the value at the intersection of the dose-response and abscissa lines up to 10^{-4} M. We thought it necessary to adopt the different parameters cited above because of the relatively small and irregular changes induced by desensitization and also because the rightward shift of the dose-response curves was not exactly in parallel with the control, although there was no reduction in the maximal contraction (Figure 1). These analyses, however, yielded almost the same quantification of desensitization (see Results). Reduction in the base line by the carbachol treatment is involved in the measurement of AUC as the area under the curve in the positive range (over 0% contraction). The B_{max} and K_d values of [^{3}H]-QNB binding to muscarinic receptors were calculated by Scatchard analysis (1952) by linear regression of least squares. Reduction in the affinity of carbachol for muscarinic receptors by desensitization and/or GppNHp were evaluated by two parameters, i.e., the increase in IC_{50} values and in AUC obtained from displacement curves of [^{3}H]-QNB binding by carbachol (Figure 3). Statistical significance was evaluated by Student's *t* test, and $P = 0.05$ was taken as the upper limit of significance.

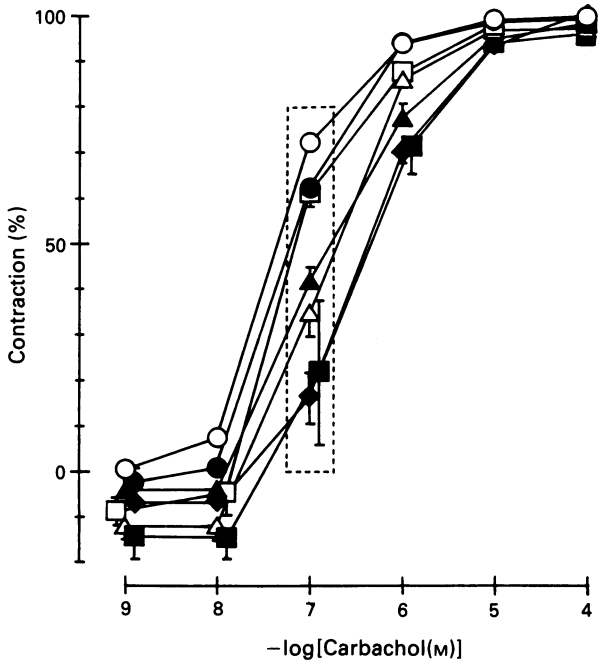

Figure 1 Concentration-contraction curves for carbachol after desensitizing carbachol treatment for various time periods. After the control response (○) to carbachol was recorded, desensitizing treatment with 10^{-4} M carbachol was carried out for 0 s (none; ●), 15 s (△), 30 s (▲), 1 min (□), 2 min (■) or 30 min (◆). Carbachol was then washed out and contractile responses to carbachol were recorded 10 min after finishing the desensitizing treatment with carbachol. Each value is a percentage of the response of the control to 10^{-4} M carbachol, expressed as mean ± s.e. of 4–9 experiments.

Drugs used

Carbachol, 3-(N-morpholino)propanesulphonic acid (MOPS) and 5'-guanylylimidodiphosphate (GppNHp) were obtained from Wako Pure Chemical Industries, Ltd. [^{3}H]-quinuclidinyl benzilate ([^{3}H]-QNB) (32.9 and 45.4 Ci mmol^{-1}) was from New England Nuclear.

Results

Contractility in the developmental process of desensitization

Figure 1 shows the concentration-contraction curves before (control) and after the desensitizing treatment with 10^{-4} M carbachol for 15 s to 30 min. Contractions without the desensitizing treatment with carbachol (none) were also measured after the control responses were recorded. As mentioned in the Methods, some muscles remained relaxed 10 min after the end of desensitizing treatment and no responses were produced to 10^{-9} M or 10^{-8} M carbachol subsequently applied. Some points in these cases remained in the negative range in Figure 1 (less than 0% contraction).

The concentration-contraction curves in Figure 1 are shifted by the desensitizing treatment with carbachol to the right along the abscissa without reduction in the maximal contraction, although not in parallel with the control. Contractility to 10^{-7} M carbachol was markedly reduced by the carbachol treatment, as indicated by the points surrounded by dotted lines. The extent of desensitization was first evaluated as the reduction in contractility to 10^{-7} M carbachol (Figure 2, Δ). As other measures we also calculated the EC_{50} values (Figure 2, ●) and the AUC (Figure 2, ○). As plotted in Figure 2, these three parameters, are similarly changed during development of desensitization. It should be noted that even the contraction without desensitizing treatment with carbachol (represented as 'none' in Figure 1 or plotted at 0 s in Figure 2) is slightly reduced when compared with the control values. Desensitization thus occurs rapidly during the first 15 s exposure to the desensitizing agent (fast desensitization), but prolonging the exposure to 30 s or 1 min causes transient resensitization (resensitization) and exposure for more than 2 min leads to further desensitization (re-desensitization).

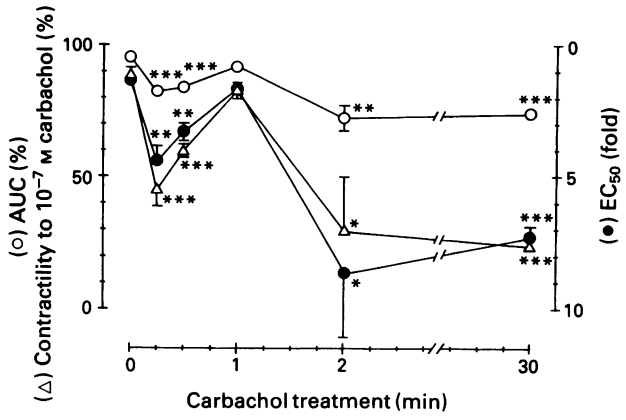

Figure 2 Contractility in the process of desensitization. Changes in contractility to 10^{-7} M carbachol (Δ), EC_{50} values (●) and the area under the curve (AUC ○) induced by desensitizing treatment with 10^{-4} M carbachol are plotted as a function of the time of exposure. Contractility to 10^{-7} M carbachol or AUC after carbachol treatment was calculated as a percentage of the control before carbachol treatment. The EC_{50} value was calculated as the ratio of the treated: control value. Each value is expressed as a mean ± s.e. of 4–9 experiments. *$P<0.05$; **$P<0.01$; ***$P<0.001$; compared with the value at 0 s (obtained from responses without carbachol treatment after measuring control responses, corresponding to 'none' in Figure 1).

Table 1 The maximal binding (B_{max}) and the dissociation constant (K_d value) of [^{3}H]-quinuclidinyl benzilate for muscarinic receptors in the process of desensitization

Carbachol treatment	K_d (nM)	B_{max} (pmol mg^{-1} protein)	n
None	0.24 ± 0.03	1.88 ± 0.11	14
15 s	0.26 ± 0.02	1.70 ± 0.30	5
30 s	0.23 ± 0.02	2.02 ± 0.19	5
1 min	0.23 ± 0.02	1.63 ± 0.35	4
2 min	0.23 ± 0.02	1.55 ± 0.15	4
30 min	0.31 ± 0.15	1.80 ± 0.22	4

The B_{max} and K_d values were obtained by Scatchard analysis with membranes prepared from control muscles not treated with carbachol (none) and from membranes treated with 10^{-4} M carbachol for 15 s to 30 min. Each value is expressed as a mean ± s.e. n = number of experiments.

Binding characteristics of [^{3}H]-quinuclidinyl benzilate to muscarinic receptors in the process of desensitization

The desensitization of contractility with the transient resensitization in its process could be caused by some functional changes at the muscarinic receptor level. We examined the maximal binding (B_{max}) and the equilibrium dissociation constant (K_d value) of [^{3}H]-QNB to muscarinic receptors in the membranes prepared from carbachol-untreated (control) and carbachol-treated muscles. These values, as listed in Table 1, exhibited no significant changes as a result of carbachol treatment at any of the durations examined ($P>0.1$).

Affinity of carbachol for muscarinic receptors in the process of desensitization

We next investigated the affinity of carbachol for muscarinic receptors. Since the binding characteristics of [^{3}H]-QNB were not changed by the carbachol treatment, changes in the affinity of carbachol could be evaluated by changes in the displacement curves by carbachol of [^{3}H]-QNB binding to muscarinic receptors in the membranes prepared from carbachol-untreated (control) and carbachol-treated muscles. As shown in Figure 3, the desensitizing treatment induced a shift

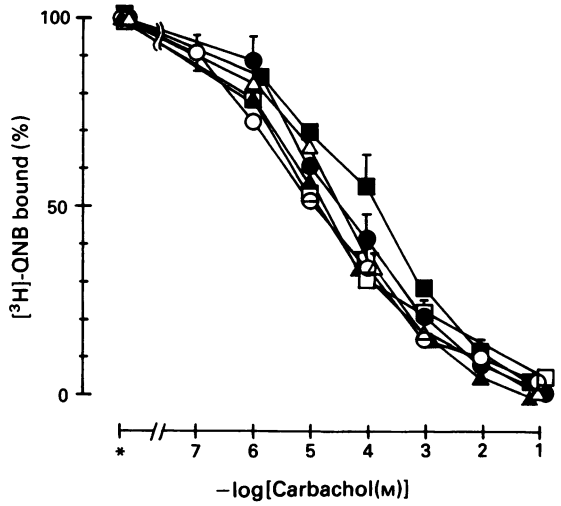

Figure 3 Changes induced by carbachol treatment in displacement curves by carbachol of [^{3}H]-quinuclidinyl benzilate ([^{3}H]-QNB) binding to muscarinic receptors. Displacement curves by carbachol of [^{3}H]-QNB binding were obtained from membranes prepared from control muscles (no carbachol) (○) and from the muscles treated with 10^{-4} M carbachol for 15 s (●), 30 s (△), 1 min (▲), 2 min (□) and 30 min (■) in normal Locke-Ringer solution bubbled with air at 30°C. Each value is expressed as a mean ± s.e. of 4–8 experiments. *; in the absence of carbachol (taken as 100%).

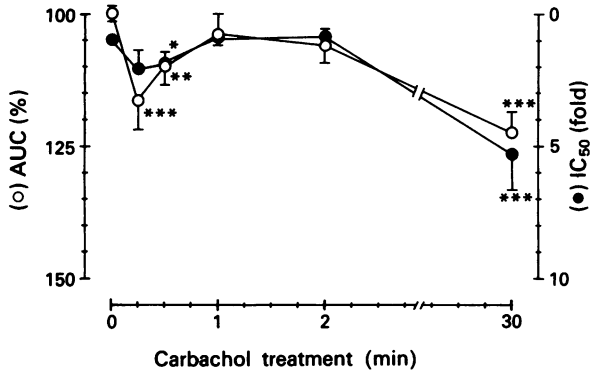

Figure 4 Affinity of carbachol for muscarinic receptors in the process of desensitization. Changes in IC_{50} values (●) and AUC (○) induced by the desensitizing carbachol are plotted against the time of exposure. AUC after the carbachol treatment was calculated as a percentage of the control before treatment. The IC_{50} value was calculated as a ratio of the treated: the control value. Each value is expressed as a mean ± s.e. of 4–8 experiments. $*P<0.05$; $**P<0.01$; $***P<0.001$; compared with the value at 0 s (obtained from control muscles not treated with carbachol).

to the right of the displacement curves, although not in parallel with the control, to varying degrees depending on the duration of treatment. This shift indicates that the affinity of carbachol for muscarinic receptors is reduced by the carbachol treatment. We evaluated reduction in the affinity by the increase of IC_{50} values (Figure 4, ●) or of the area under the displacement curves (AUC, Figure 4, ○). These parameters showed similar time courses in the desensitizing process (Figure 4): the affinity of carbachol for muscarinic receptors was rapidly reduced at 15 s, restored slightly at 30 s and completely at 1 or 2 min, and was reduced again at 30 min. Thus, the restoration of affinity was transient. These results were generally in good agreement with the desensitizing process of contractility except for the 2 min treatment that redesensitized contractility almost maximally (Figure 2).

Coupling between muscarinic receptors and G proteins in the process of desensitization

The affinity of an agonist for G protein-coupled receptors such as muscarinic receptors is known to be regulated by guanine nucleotides via G proteins: the affinity of the agonist is reduced by GTP or its non-hydrolysable analogues such as 5'-guanylylimidodiphosphate (GppNHp) when the coupling between receptors and G proteins is in the normal state. In contrast, this regulatory effect of GTP on the affinity of an agonist is thought to disappear when the receptors become uncoupled from G proteins. We examined the effects of GppNHp on the affinity of carbachol to discover whether the

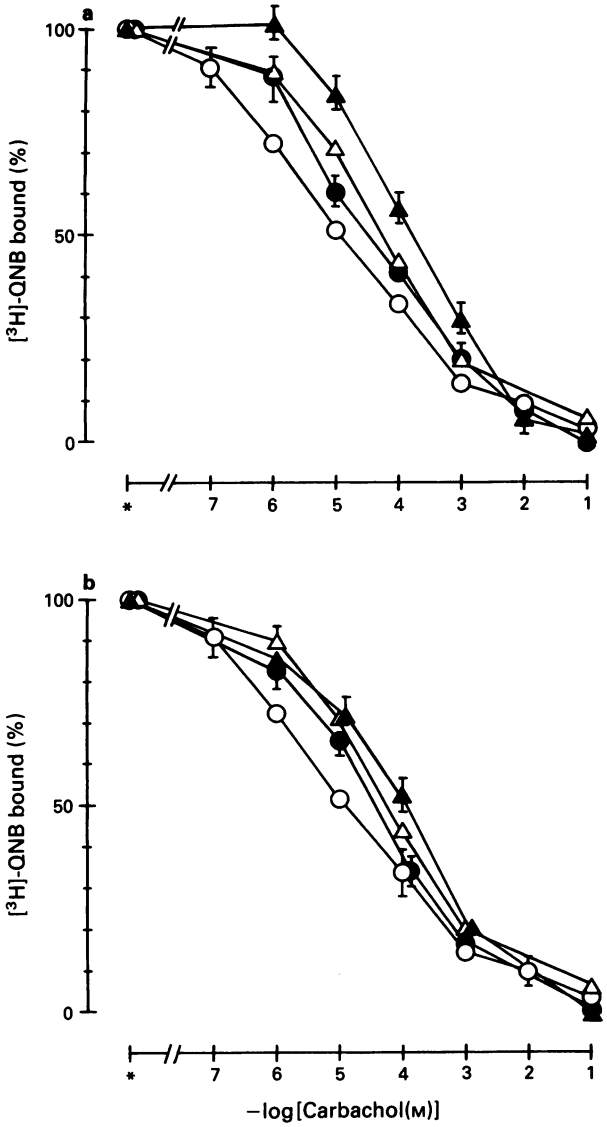

Figure 5 Effect of guanine nucleotide on binding of carbachol to muscarinic receptors in the desensitized state. The displacement curve by carbachol of [^{3}H]-quinuclidinyl benzilate binding to muscarinic receptors in carbachol-untreated control membranes (a and b; ○) was shifted rightward by 0.05 mM 5'-guanylylimidodiphosphate (GppNHp) (a and b, △). The curve obtained with membranes prepared from muscles treated with 10^{-4} M carbachol for 15 s (a, ●) was further shifted rightward by GppNHp (a, ▲). The curve obtained with membranes prepared from muscles treated with carbachol for 30 s (b, ●) was not changed by GppNHp (b, ▲). Each value is expressed as a mean ± s.e. of 4–8 experiments. *; in the absence of carbachol (taken as 100%).

Table 2 Effects of guanine nucleotide on the affinity of carbachol for muscarinic receptors in the process of desensitization

Carbachol treatment	*AUC (%)*				*−log [IC_{50} (M)]*			
	GppNHp (−)	n	*GppNHp (+)*	n	*GppNHp (−)*	n	*GppNHp (+)*	n
None	100.0 ± 1.5	22	121.4 ± 3.6***	6	4.74 ± 0.11	27	4.02 ± 0.09**	7
15 s	116.6 ± 5.5	8	135.9 ± 4.1*	7	4.31 ± 0.14	8	3.71 ± 0.12**	8
30 s	110.0 ± 3.5	8	117.7 ± 6.8	8	4.28 ± 0.11	8	3.97 ± 0.10	8
1 min	103.8 ± 4.0	7	120.6 ± 4.0*	4	4.75 ± 0.16	8	3.87 ± 0.13**	4
2 min	105.8 ± 3.5	8	121.9 ± 4.7**	10	4.71 ± 0.15	8	3.91 ± 0.09***	10
30 min	122.4 ± 4.0	8	126.4 ± 3.5	8	3.83 ± 0.11	8	3.59 ± 0.05	8

Changes in AUC and $-\log[IC_{50}$ (M)] induced by the carbachol treatment were obtained from changes in displacement curves by carbachol of [^{3}H]-quinuclidinyl benzilate binding in the presence (GppNHp(+)) and absence (GppNHp(−)) of 0.05 mM GppNHp with membranes prepared from control muscles not treated with carbachol (none) and from muscles treated with 10^{-4} M carbachol for 15 s to 30 min. AUC is calculated as a percentage of control (i.e. none). Each value is expressed as a mean ± s.e. n = number of experiments.

$*P<0.05$; $**P<0.01$; $***P<0.001$; compared with GppNHp (−).

coupling between muscarinic receptors and G proteins was impaired during the desensitizing process. As illustrated in Figure 5, the displacement curves of [^{3}H]-QNB binding by carbachol in the membranes prepared from carbachol-untreated control muscles (Figure 5; control ○ in a and b) were shifted to the right by GppNHp (Figure 5, △ in a and b). This was due to reduction in the affinity of carbachol for muscarinic receptors induced by GppNHp, and implied that the coupling of muscarinic receptors to G proteins had occurred in the normal state. In the case of 15 s carbachol treatment, the displacement curve by carbachol (Figure 5a, ●) which was shifted to the right of the control by desensitization, was further shifted to the right by GppNHp (Figure 5a, ▲). This indicates that muscarinic receptors treated for 15 s may have coupled normally with G proteins. In contrast, the displacement curve by carbachol in the case of a 30 s carbachol treatment (Figure 5b, ●), which was also shifted to the right by desensitization, was changed far less by GppNHp (Figure 5b, ▲). This indicates that the muscarinic receptors became uncoupled from G proteins in this stage of desensitization. The shift to the right of the displacement curves by GppNHp was also evaluated by the increases in IC_{50} values and in AUC. These results are summarized in Table 2. A significant difference in the values obtained in the presence and absence of GppNHp indicates normal regulation by GppNHp via G proteins, i.e., normal coupling between muscarinic receptors and G proteins. This regulatory effect of GppNHp was observed in the case of carbachol treatment for 15 s, 1 min and 2 min, but not for 30 s and 30 min. In conclusion, (1) the desensitizing process involved the coupling mechanisms between the muscarinic receptors and G proteins; (2) these coupling mechanisms also underwent transient resensitization; and (3) some discrepancies were noted in that the regulatory effect of GppNHp was still observed in the case of a 15 s carbachol treatment in which the affinity of carbachol for muscarinic receptors was markedly reduced, and in that a 30 s treatment induced uncoupling of muscarinic receptors from G proteins despite the fact that the affinity of carbachol was slightly restored (Figure 4).

Discussion

We investigated the time course of desensitization induced by muscarinic stimulation for 15 s to 30 min with 10^{-4} M carbachol in the smooth muscle of guinea-pig taenia caeci, and found a peculiar process of desensitization of contractility to carbachol with the intervention of transient resensitization. On the basis of the present analysis, the desensitizing process could be divided into five successive steps: (1) fast reduction in the affinity of carbachol for muscarinic receptors within 15 s with no change in their coupling with G proteins; (2) a slight restoration of the affinity of carbachol for muscarinic receptors at 30 s despite the uncoupling between muscarinic receptors and G proteins; (3) complete restoration of both the affinity of carbachol and the coupling between muscarinic receptors and G proteins at 1 min; (4) re-desensitization at 2 min with complete restoration of the affinity of carbachol for muscarinic receptors and of their coupling with G proteins; and (5) re-desensitization of contractility at 30 min with reduced affinity of carbachol and the uncoupling between muscarinic receptors and G proteins. In these complex regulatory mechanisms the transient resensitization that occurs even in the presence of a desensitizing agonist seems to be a novel phenomenon, as far as we know, among many receptor-mediated signal transduction systems.

Desensitization has been classified into two types: homologous, i.e., specific for a given agonist, and heterologous, i.e. not specific for the agonist. It is postulated that homologous desensitization is induced by changes at the receptor level and that heterologous desensitization is caused by changes at the post-receptor steps in the signal transduction process. In guinea-pig taenia caeci, desensitization induced by carbachol is heterologous. It is accompanied by reduction in contractility to histamine via the H_1-receptors, to high K via the voltage-dependent Ca channels in the plasma membrane, or to caffeine via the Ca-induced Ca release channels (ryanodine receptors) in the intracellular Ca storage sites (Hishinuma & Uchida, 1988; 1989; 1991; Hishinuma *et al.*, 1990), or to AHR-602, a muscarinic partial agonist, that induces contraction depending on influx of extracellular Ca but not on release of intracellularly stored Ca (Hishinuma *et al.*, 1990) without stimulation of phosphatidylinositol turnover (Gardner *et al.*, 1988). These studies suggested that carbachol desensitization as well as transient resensitization described first in this paper is of multiple origin.

Receptor phosphorylation could be involved in the regulation of receptor function and receptor distribution (Sibley *et al.*, 1987) and in both the homologous and heterologous desensitization (Sibley & Lefkowitz, 1985). Receptor kinases such as the β-adrenoceptor kinase (BARK) which modify the agonist-occupied form of receptors may be involved in the homologous desensitization (Benovic *et al.*, 1986; Lefkowitz *et al.*, 1990). On the other hand, the second messenger-activated protein kinases such as adenosine 3′:5′-cyclic monophosphate (cyclic AMP)-dependent protein kinase (protein kinase A) or protein kinase C may be involved in heterologous desensitization (Bouvier *et al.*, 1987). Heterologous desensitization could, therefore, be accompanied by changes in the receptor itself as well as those in the post-receptor steps.

The maximal binding (B_{max}) and the dissociation constant (K_d value) of [^{3}H]-QNB for muscarinic receptors were not changed by desensitization in our experimental conditions (Table 1), although desensitization is often said to coincide with reduction in the number of receptors. These results indicate that muscarinic receptors remained on the cell surface and maintained a normal affinity for the antagonist even in the desensitized state. The fact that the affinity of carbachol for muscarinic receptors was reduced by carbachol treatment in some of our experiments, suggests that the treatment is affecting the agonist-induced conformational change due to some modification of the receptor molecule. M_1 or M_2 muscarinic receptor subtypes are phosphorylated in various tissues *in vitro* by protein kinase A (Ho *et al.*, 1987; 1990; Rosenbaum *et al.*, 1987), protein kinase C (Haga *et al.*, 1990), BARK (Kwatra *et al.*, 1989a) or a BARK-like kinase (Haga & Haga, 1989). The muscarinic stimulation induces phosphorylation of muscarinic receptors *in vivo* (Kwatra & Hosey, 1986; Kwatra *et al.*, 1987; 1989b). These previous studies have suggested that the muscarinic receptor function in our preparation may also be regulated by phosphorylation during desensitization. Yet the muscarinic receptors involved in smooth muscle contraction have been classified as the M_3 subtype.

Changes in G proteins could be involved in the heterologous desensitization, as was shown in the adenylate cyclase system (Briggs *et al.*, 1983; Garrity *et al.*, 1983). G proteins are known to be phosphorylated by protein kinase C (Katada *et al.*, 1985; Haga *et al.*, 1990). It is possible that a G protein itself may be changed and uncoupled from receptors by phosphorylation in our smooth muscle preparation, since regulation by GppNHp of the affinity of carbachol for muscarinic receptors via G proteins was lost during desensitization. There is, however, another possibility that the coupling site(s) of a muscarinic receptor molecule with G proteins may be conformationally changed and functionally desensitized by some modification of the receptor itself. G proteins may also contribute to desensitization by an increase in receptor phosphorylation, since the βγ subunit of G proteins has been reported to enhance phosphorylation of muscarinic receptors purified from the porcine atrium by the BARK-like kinase (Haga & Haga, 1990).

If phosphorylation of muscarinic receptors and/or G proteins brings about desensitization via reduction in the affinity of carbachol for muscarinic receptors and uncoupling

between muscarinic receptors and G proteins in our muscle preparation, the transient resensitization might be induced by de-phosphorylation of phosphorylated muscarinic receptors by means of protein phosphatases. Phosphorylated muscarinic receptors are dephosphorylated in various tissues *in vitro* by calcineurin (Ho *et al.*, 1987; 1990; Rosenbaum *et al.*, 1987) or acid phosphatase (Haga & Haga, 1990), but not by alkaline phosphatase (Rosenbaum *et al.*, 1987). Because of shortage of muscarinic receptors in our membrane preparation such phosphorylation/dephosphorylation has not been elucidated in relation to desensitization/resensitization.

Since there were no changes in the binding properties of muscarinic receptors or in their coupling with G proteins by the 2 min carbachol treatment, re-desensitization of contractility at 2 min must have been caused by changes in the post-receptor steps of the signal transduction process, probably at a stage from activation of G proteins to the opening of Ca channels in the cell membrane. It is not, however, known that G proteins facilitate the opening of Ca channels in this preparation. Desensitization by the 30 min carbachol treatment may be caused by re-modification of muscarinic receptors and/or G proteins, as expressed by reduction in the affinity of carbachol for muscarinic receptors and uncoupling between muscarinic receptors and G proteins.

Finally, we would emphasize that the transient resensitization is a newly found phenomenon that is regulated by the affinity of agonists for the receptors and their coupling with G proteins. The resensitization may play a role of feedback control in a transient or even an oscillatory manner, depending on the state of cellular homoeostasis.

The authors wish to thank Professor Tomokazu Oshima, Department of Pharmacology, Meiji College of Pharmacy at Tanashi, for constant encouragement and discussion with valuable comments on this manuscript.

References

BENOVIC, J.L., STRASSER, R.H., CARON, M.G. & LEFKOWITZ, R.J. (1986). β-adrenergic receptor kinase: identification of a novel protein kinase that phosphorylates the agonist-occupied form of the receptor. *Proc. Natl. Acad. Sci. U.S.A.*, **83**, 2797–2801.

BOUVIER, M., LEEB-LUNDBERG, L.M.F., BENOVIC, J.L., CARON, M.G. & LEFKOWITZ, R.J. (1987). Regulation of adrenergic receptor function by phosphorylation. II. Effects of agonist occupancy on phosphorylation of α_a- and β_2-adrenergic receptors by protein kinase C and the cyclic AMP-dependent protein kinase. *J. Biol. Chem.*, **262**, 3106–3113.

BRIGGS, M.M., STADEL, J.M., IYENGER, R. & LEFKOWITZ, R.J. (1983). Functional modification of the guanine nucleotide regulatory protein after desensitization of turkey erythrocytes by catecholamines. *Arch. Biochem. Biophys.*, **224**, 142–151.

GARDNER, A.L., CHOO, L.K. & MITCHELSON, F. (1988). Comparison of the effects of some muscarinic agonists on smooth muscle function and phosphatidylinositol turnover in the guinea-pig taenia caeci. *Br. J. Pharmacol.*, **94**, 199–211.

GARRITY, M.J., ANDREASEN, T.J., STORM, D.R. & ROBERTSON, R.P. (1983). Prostaglandin E-induced heterologous desensitization of hepatic adenylate cylase: consequences on the guanyl nucleotide regulatory complex. *J. Biol. Chem.*, **258**, 8692–8697.

HAGA, K. & HAGA, T. (1989). Agonist-dependent phosphorylation of cerebral and atrial muscarinic receptors: blockade of the phosphorylation by GTP-binding regulatory proteins and its reversal by guanine nucleotdies. *Biomed. Res.*, **10**, 293–299.

HAGA, K. & HAGA, T. (1990). Dual regulation by G proteins of agonist-dependent phosphorylation of muscarinic acetylcholine receptors. *FEBS Lett.*, **268**, 43–47.

HAGA, K., HAGA, T. & ICHIYAMA, A. (1990). Phosphorylation by protein kinase C of the muscarinic acetylcholine receptor. *J. Neurochem.*, **54**, 1639–1644.

HISHINUMA, S., AOKI, Y., HIRATA, S., UCHIDA, M.K. & KUROKAWA, M. (1990). Carbachol desensitizes smooth muscle contractions elicited by release of intracellularly stored Ca and by influx of extracellular Ca. *Eur. J. Pharmacol.*, **183**, 2416–2417.

HISHINUMA, S., NARITA, F., MATSUMOTO, Y., UCHIDA, M.K. & KUROKAWA, M. (1992). Mechanisms of self- and cross-desensitization in smooth muscle. *Jpn. J. Pharmacol.*, **58**, Suppl. II, 361P.

HISHINUMA, S. & UCHIDA, M.K. (1988). Short-term desensitization of guinea-pig taenia caecum induced by carbachol occurs at intracellular Ca stores and that by histamine at H_1-receptors. *Br. J. Pharmacol.*, **94**, 882–889.

HISHINUMA, S. & UCHIDA, M.K. (1989). Short-term desensitization of phosphatidylinositol turnover via muscarinic acetylcholine receptors and histamine H_1-receptors in smooth muscle. *Biochem. Biophys. Res. Commun.*, **162**, 733–739.

HISHINUMA, S. & UCHIDA, M.K. (1991). Blockade by the local anaesthetic, tetracaine, of desensitization of Ca-induced Ca release after muscarinic stimulation in smooth muscle. *Br. J. Pharmacol.*, **103**, 1393–1398.

HO, A.K.S., LING, Q.-L., DUFFIELD, R., LAM, P.H. & WANG, J.H. (1987). Phosphorylation of brain muscarinic receptor: evidence of receptor regulation. *Biochem. Biophys. Res. Commun.*, **142**, 911–918.

HO, A.K.S., LING, Q.-L., DUFFIELD, R. & ZHENG, G.-M. (1990). Phosphorylation-dephosphorylation of muscarinic acetylcholine receptors: evidence for the *in vivo* and *in vitro* release of receptors from rat brain plasma membrane. *Cell. Signal.*, **2**, 451–460.

KATADA, T., GILMAN, A.G., WATANABE, Y., BAUER, S. & JACOBS, K.H. (1985). Protein kinase C phosphorylates the inhibitory guanine-nucleotide-binding regulatory component and apparently suppresses its function in hormonal inhibition of adenylate cyclase. *Eur. J. Pharmacol.*, **151**, 431–437.

KWATRA, M.M., BENOVIC, J.L., CARON, M.G., LEFKOWITZ, R.J. & HOSEY, M.M. (1989a). Phosphorylation of chick heart muscarinic cholinergic receptors by the β-adrenergic receptor kinase. *Biochemistry*, **28**, 4543–4547.

KWATRA, M.M. & HOSEY, M.M. (1986). Phosphorylation of the cardiac muscarinic receptor in intact chick heart and its regulation by a muscarinic agonist. *J. Biol. Chem.*, **261**, 12429–12432.

KWATRA, M.M., LEUNG, E., MAAN, A.C., MCMAHON, K.K., PTASIENSKI, J., GREEN, R.D. & HOSEY, M.M. (1987). Correlation of agonist-induced phosphorylation of chick heart muscarinic receptors with receptor desensitization. *J. Biol. Chem.*, **262**, 16314–16321.

KWATRA, M.M., PTASIENSKI, J. & HOSEY, M.M. (1989b). The porcine heart M2 muscarinic receptor: agonist-induced phosphorylation and comparison of properties with the chick heart receptor. *Mol. Pharmacol.*, **35**, 553–558.

LEFKOWITZ, R.J., HAUSDORFF, W.P. & CARON, M.G. (1990). Role of phosphorylation in desensitization of the β-adrenoceptor. *Trends Pharmacol. Sci.*, **11**, 190–194.

LOWRY, O.H., ROSEBROUGH, N.J., FARR, A.L. & RANDALL, R.J. (1951). Protein measurement with the Folin phenol reagent. *J. Biol. Chem.*, **193**, 265–275.

MATSUMOTO, Y., HISHINUMA, S., UCHIDA, M.K. & KUROKAWA, M. (1992). Transient resensitization of muscarinic receptors during desensitizing processes of smooth muscle contraction. *Jpn. J. Pharmacol.*, **58**, Suppl. I, 72P.

ROSENBAUM, L.C., MALENCIK, D.A., ANDERSON, S.R., TOTA, M.R. & SCHIMERLIK, M.I. (1987). Phosphorylation of the porcine atrial muscarinic acetylcholine receptor by cyclic AMP dependent protein kinase. *Biochemistry*, **26**, 8183–8188.

SCATCHARD, G. (1952). Some physical chemical aspects of plasma extenders. *Ann. N.Y. Acad. Sci.*, **55**, 455–464.

SIBLEY, D.R., BENOVIC, J.L., CARON, M.G. & LEFKOWITZ, R.J. (1987). Regulation of transmembrane signalling by receptor phosphorylation. *Cell*, **48**, 913–922.

SIBLEY, D.R. & LEFKOWITZ, R.J. (1985). Molecular mechanisms of receptor desensitization using the β-adrenergic receptor-coupled adenylate cyclase system as a model. *Nature*, **317**, 124–129.

(Received October 29, 1992
Revised January 25, 1993
Accepted January 26, 1993)

Br. J. Pharmacol. (1993), **109**, 336–343 © Macmillan Press Ltd, 1993

The superficial buffer barrier in venous smooth muscle: sarcoplasmic reticulum refilling and unloading

Qian Chen & [1]Cornelis van Breemen

University of Miami School of Medicine, Department of Molecular and Cellular Pharmacology (R-189), P.O. Box 016189, Miami, FL 33101, U.S.A.

1 The interaction of Ca^{2+} transport in the plasmalemma and the sarcoplasmic reticulum (SR) was investigated in smooth muscle of the rabbit inferior vena cava. We tested the possibility of direct refilling of the SR with extracellular Ca^{2+} and of the existence of a vectorial Ca^{2+} extrusion pathway from the SR lumen to the extracellular space suggested by earlier results.

2 After depletion with caffeine the SR was loaded with Ca^{2+} to increasing levels by incubation in a high potassium 1.5 mM Ca^{2+} solution and a 10 mM Ca^{2+} zero Na^+ solution, respectively. Thapsigargin, 2 μM, (a specific SR Ca^{2+}-ATPase blocker) completely blocked refilling of the SR in either of the above solutions, indicating that the SR Ca^{2+}-ATPase is essential for this process.

3 Three different agents, caffeine, ryanodine and thapsigargin, which inhibit Ca^{2+} accumulation by the SR, increased the steady state intracellular Ca^{2+} concentration in the rabbit inferior vena cava.

4 Measurements of Mn^{2+} induced quenching of the intracellular fura-2 signal during pharmacological manipulation of the SR content showed that these three agents did not stimulate divalent cation entry.

5 On the other hand, stimulation with noradrenaline caused a marked increase in Mn^{2+} influx, which was blocked by 2 mM Ni^{2+}. Mn^{2+} entry stimulated by high K^+ solution was blocked by 1 μM diltiazem.

6 We conclude that the SR refilling has to be mediated by the SR Ca^{2+}-ATPase. Inhibition of Ca^{2+} accumulation by the SR causes an increase in the steady state intracellular Ca^{2+} concentration. This observation cannot be explained by an increase in Ca^{2+} influx into the smooth muscle cells of the rabbit inferior vena cava. Alternatively these results suggest the existence of a continuous vectorial release of Ca^{2+} from the SR lumen to the extracellular space.

Keywords: Smooth muscle: plasmalemma; sarcoplasmic reticulum (SR); intracellular Ca^{2+} concentration ($[Ca^{2+}]_i$; fura-2; Mn^{2+} quenching; superficial buffer barrier (SBB)

Introduction

The sarcoplasmic reticulum (SR) of vascular smooth muscle functions both as a source and a sink of activator Ca^{2+}. The 100 kD Ca^{2+}-ATPase (Eggermont *et al.*, 1988) pumps Ca^{2+} from the cytoplasm into the SR lumen to promote relaxation and to load it for subsequent release during activation. Ca^{2+} release is mediated by inositol (1,4,5) trisphosphate (Ins-(1,4,5)P_3-sensitive Ca^{2+} channels and others sensitive to both Ca^{2+} and ATP (Saida, 1982; Saida & van Breemen, 1984; Suematsu *et al.*, 1984; Meissner *et al.*, 1986). In addition to these well established roles, the peripherally located SR may also function as a 'buffer barrier' to Ca^{2+} entry into the deeper myoplasm.

In essence the SR 'buffer barrier' hypothesis states that: (1) Ca^{2+} which enters the cell across the plasmalemma is in part pumped into the SR before it can activate contraction; (2) the Ca^{2+}-ATPase of the SR contributes to Ca^{2+} extrusion from the cells due to vectorial release of SR Ca^{2+} towards the inner surface of the plasmalemma, from where it is extruded by the Na^+/Ca^{2+} exchanger and the plasmalemmal Ca^{2+}-ATPase; and (3) a Ca^{2+} gradient in the peripheral cytoplasm is created by these processes (Figure 8). Experimental support for the 'buffer barrier' hypothesis is derived from a number of studies made over the last 15 years. The initial finding that the magnitude of contraction was more closely related to the rate than the magnitude of net Ca^{2+} entry into aortic smooth muscle suggested that the superficial SR sequestered Ca^{2+} before it could reach the myofilaments to activate them (van Breemen, 1977). In a more recent paper (Chen *et al.*, 1992a), we reported that depletion of the SR induced a delay between the rise in the intracellular Ca^{2+} concentration ($[Ca^{2+}]_i$) due to stimulation of Ca^{2+} influx and the simultaneously measured force development. This result could be explained if it was assumed that the depletion of the SR enhances its effectiveness in removing Ca^{2+} which enters the cells. This explanation was supported by the observation that caffeine, which prevents the SR buffering action by maintaining the Ca^{2+} channels on the SR in an open state, abolished the above delay. Thus it appears that the unloaded SR can effectively buffer Ca^{2+} which enters the cells. Maintenance of such a buffer barrier function would require the transfer of Ca^{2+} from the SR lumen to the extracellular space (ECS). Recent evidence derived from electrophysiological studies and $[Ca^{2+}]_i$ measurements lends support to the concept of vectorial unloading of the SR (Stehno-Bittel & Sturek, 1992; Chen *et al.*, 1992a). This aspect of Ca^{2+} homeostasis will be explored further in the present paper.

Functional connections between the plasmalemma and the SR have been proposed before; however, mostly in order to explain SR refilling from the ECS (Brading *et al.*, 1980; Casteels & Droogmans, 1981; Putney, 1986; Chen *et al.*, 1992b). In fact Casteels & Droogmans (1981) and the groups of Putney (Putney, 1986) and Daniel (Bourreau *et al.*, 1992) have postulated a direct pathway between the ECS and SR or ER lumen which can bypass the SR Ca^{2+}-ATPase. Alternatively the SR may be refilled by virtue of the SR Ca^{2+} pump removing Ca^{2+} from a restricted cytoplasmic space adjacent to the plasmalemma consistent with the buffer barrier hypothesis. In this study, we have employed the SR Ca^{2+}-ATPase inhibitor, thapsigargin, to distinguish between these two possible mechanisms in smooth muscle of the rabbit inferior vena cava.

A preliminary account of these results was presented at the International Symposium on Smooth Muscle, held January 29–February 1, 1992 in Fukuoka, Japan.

[1] Author for correspondence.

Methods

Tissue preparation

Male New Zealand white rabbits weighing 1.5–2.5 kg were killed by CO_2 asphyxiation followed by exsanguination from the carotid arteries. The inferior vena cava was rapidly excised and placed in warmed (37°C), oxygenated (100%) physiological saline solution (PSS) (pH 7.4). The vena cava was then cleaned of connective tissue and fat and opened longitudinally. The endothelium was removed by gently rubbing the intimal surface with a piece of wet filter paper. Acetylcholine failed to relax the inferior vena cava in which tension development had been stimulated with noradrenaline (NA) (data not shown). The inferior vena cava was subsequently cut into a rectangular strip approximately 7 mm in width and 15 mm in length and tied to a stainless steel tissue holder.

$[Ca^{2+}]_i$ measurement

$[Ca^{2+}]_i$ in the inferior vena cava was measured as described by Nishimura *et al.* (1989). Briefly, the mounted preparation was placed in a 3.5 ml polystyrene cuvette containing PSS, and positioned in the temperature-controlled (37°C) chamber of the spectrofluorimeter (Spex Fluorolog, Spex Industries, New Jersey, U.S.A.) to measure the autofluorescence. The luminal side of the tissue was illuminated with alternating wavelengths of 340 and 380 nm controlled by an electronic chopper, and 505 nm emitted light from the strip was collected in the front face mode via a photomultiplier. Excitation at either 340 or 380 nm was synchronized with emission by software designed by Spex Industries. The mounted muscle strip was then loaded with fura-2 by incubation in the dark in a solution containing 5 μM fura-2/AM, 0.5% cremophor, and 3 mg l^{-1} bovine serum albumin for 2–3 h at room temperature (<25°C). The tissue was then returned to the chamber and washed repeatedly for 30 min with PSS (37°C) to remove excess external fura-2/AM.

After the autofluorescences at 340 and 380 nm were subtracted, the ratio of fluorescence due to excitation at 340 nm (F340) to that at 380 nm (F380) was calculated.

When we use the equation of Grynkiewicz *et al.* (1985) to calculate $[Ca^{2+}]_i$, the resting $[Ca^{2+}]_i$ of the rabbit inferior vena cava smooth muscle cells in normal PSS was about 80 nM which is compatible with the values measured by others.

Grynkiewicz's equation:

$$[Ca^{2+}]_i = (K_d)(b)[R-R_{min}]/[R_{max}-R]$$

In the equation, K_d is the dissocation constant of Ca^{2+}-fura-2 complex; R is the above-mentioned ratio of fluorescence due to excitation at 340 nm to that at 380 nm; R_{min} and R_{max} are the ratios measured by the addition of 10 μM of the Ca^{2+} ionophore ionomycin to Ca^{2+}-free (10 mM EGTA) solution and Ca^{2+}-replete (2 mM $CaCl_2$) solution respectively; b is the ratio of the 380 nm signals in Ca^{2+}-free and Ca^{2+}-replete solution. There are several reasons for use of the ratio F340/F380 as a relative measurement of $[Ca^{2+}]_i$ instead of calculating $[Ca^{2+}]_i$ with the above equation: (1) It is very difficult to determine the K_d value in the cytoplasm. Simply applying the K_d measured in the salt solution to the above equation will not reflect the real $[Ca^{2+}]_i$. (2) The intensity of fura-2 fluorescence in the cell-free solution might be different from that in the cytoplasm. (3) Employment of ionomycin does not seem to permeabilize completely the smooth muscle cells to Ca^{2+} in our preparation and therefore cannot give satisfactory R_{max} and R_{min}.

At 360 nm wavelength, the fluorescence signal was not influenced by Ca^{2+} concentration changes. Mn^{2+} quenching of fura-2 fluorescence at this wavelength was therefore used to measure the rate of Mn^{2+} influx by measuring the slope of Mn^{2+} quenching trace.

Solutions and chemicals

Normal PSS (N-PSS) contains (in mM): NaCl 140, KCl 5, $CaCl_2$ 1.5, $MgCl_2$ 1, glucose 10, HEPES 5, pH 7.4. 0 Ca^{2+} PSS was almost the same as normal PSS except that no $CaCl_2$ was added to the solution. In Ca^{2+}-free PSS, 0.1 mM EGTA replaced 1.5 mM $CaCl_2$. For 80 K^+-PSS, 75 mM NaCl was replaced with equimolar KCl to make the final KCl concentration equal to 80 mM. In 0 Ca^{2+}/80 K^+-PSS, EGTA was added to and $CaCl_2$ was omitted from the 80 K^+ PSS. The 0 Na^+/10 Ca^{2+} PSS was prepared by substituting LiCl for NaCl and raising the calcium concentration to 10 mM.

Drugs were obtained from the following sources: caffeine (Sigma), thapsigargin (LC Service Corporation), monensin (Calbiochem), ouabain (Sigma), ryanodine (a gift from Dr M.T. Nelson) and noradrenaline (NA) (Sigma).

Results

Thapsigargin prevents the SR refilling with Ca^{2+}

Application of caffeine or physiological agonists, e.g. NA and histamine, in the absence of Ca^{2+} has proved to be an effective tool to deplete SR and to estimate SR Ca^{2+} content in smooth muscle cells (van Breemen, 1976). In the experiments displayed in Figure 1a and 1b, the SR was first depleted by 25 mM caffeine in 0 Ca^{2+}-PSS. The tissue was then exposed to either high K^+ solution or a high Ca^{2+}, Na^+-free medium. Large Ca^{2+} influxes were induced under these conditions through voltage-gated Ca^{2+} channels (VGC) and the Na^+/Ca^{2+} exchanger. In the absence of thapsigargin, the SR was refilled with Ca^{2+} in both cases as indicated by the second caffeine-induced Ca^{2+} signals, which were larger than the controls (upper panels of Figure 1a and b). Thapsigargin, a specific SR Ca^{2+}-ATPase blocker, prevented the SR refilling through both pathways, as indicated by the failure of caffeine to induce a second $[Ca^{2+}]_i$ peak regardless of whether Ca^{2+} influx was mediated by VGC or Na^+/Ca^{2+} exchanger (lower panels of Figure 1a and b).

These results indicate that in the rabbit inferior vena cava, the SR has to be refilled via the SR Ca^{2+}-ATPase and do not support the existence of a direct connection between the SR lumen and the ECS.

Selective inhibition of Ca^{2+} accumulation by the SR increases steady state $[Ca^{2+}]_i$

Three different agents, caffeine, ryanodine and thapsigargin, all enhanced the steady state $[Ca^{2+}]_i$ (Figure 2a,b,c). These three agents have in common that they inhibit Ca^{2+} accumulation by the SR. Caffeine and ryanodine open Ca^{2+} channels in the SR (Rousseau & Meissner, 1987; 1989) and cause fast and slow release of Ca^{2+} from the SR, respectively (van Breemen, 1976; Hwang & van Breemen, 1987). Thapsigargin disrupts the balance between Ca^{2+} leak and Ca^{2+} uptake through the SR membrane at rest, by blocking the 100 kD Ca^{2+}-ATPase and thus also empties the SR. The three agents were used in separate experiments to avoid possible misleading conclusions based on side effects of any particular agent. The results thus lead to the conclusion that selective inhibition of Ca^{2+} accumulation by the SR causes an increase in the steady state $[Ca^{2+}]_i$. Each experiment described above was repeated four or five times and the means of the relative steady state Ca^{2+} concentrations are depicted in Figure 2d.

The elevation in steady state $[Ca^{2+}]_i$ is caused either by an increase in Ca^{2+} influx or a decrease in Ca^{2+} efflux. Putney (1990) proposed that SR depletion causes an increase in plasmalemmal Ca^{2+} permeability by an as yet unspecified mechanism. Since this hypothesis enjoys broad support, its possible application to venous smooth muscle was investigated by measurement of divalent cation influx.

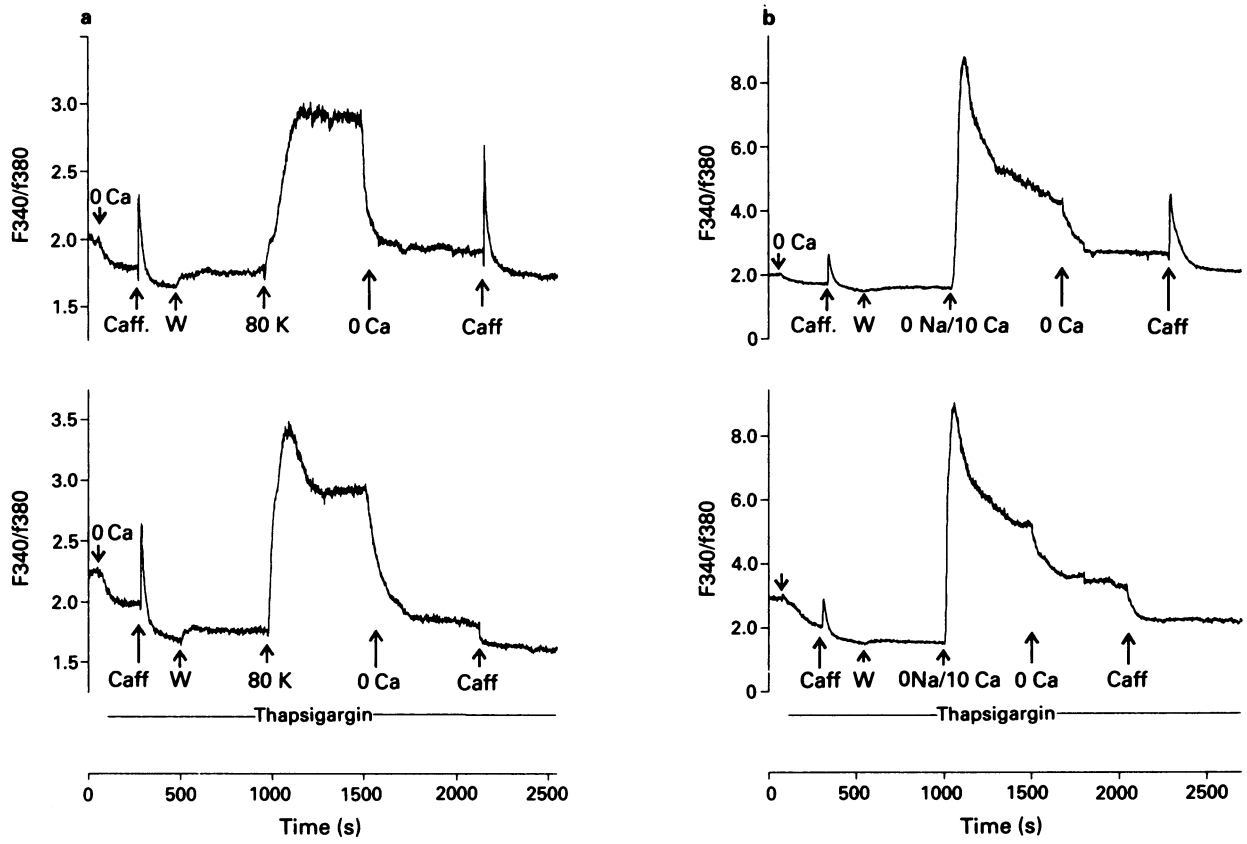

Figure 1 (a) Thapsigargin blocks sarcoplasmic reticulum (SR) refilling by Ca^{2+} influx through VGC (upper panel). Caffeine (Caff, 25 mM) was added for 3 min in the absence of Ca^{2+} in order to deplete the SR. A $[Ca^{2+}]_i$ peak was induced during this process. After 80 K^+ solution was applied, the $[Ca^{2+}]_i$ signal increased to an elevated steady state level. 80 K^+ solution was then replaced by 0 Ca^{2+}-PSS causing a decline in F340/F380. An even higher $[Ca^{2+}]_i$ peak was induced by the second application of caffeine, which indicated that the SR was loaded with Ca^{2+} during incubation in 80 K^+-PSS (lower panel). The experimental protocol was the same as above, except that thapsigargin (2 μM) was included in all the solutions used. Caffeine failed to induce a second peak in the presence of thapsigargin indicating that refilling was prevented. (b) Thapsigargin blocks the SR refilling by Ca^{2+} influx through the Na^+/Ca^{2+} exchanger (upper panel). The experimental protocol is similar to that in (a), but 0 Na^+, 10 mM Ca^{2+} solution was used instead of 80 K^+ solution during the refilling period. Ouabain (100 μM) and monensin (120 μM) were included in the solutions throughout the experiment in order to intensify the activity of Na^+/Ca^{2+} exchanger by loading the cell with Na^+. A caffeine-induced $[Ca^{2+}]_i$ signal peak was seen upon SR depletion. The large second peak indicates a high degree of SR loading upon Na^+ gradient reversal in the presence of 10 mM Ca^{2+}. (lower panel) Including 2 μM thapsigargin in an otherwise identical protocol blocked reloading of the SR as witnessed by the absence of a second caffeine-induced $[Ca^{2+}]_i$ signal peak. Thapsigargin completely blocked the second caffeine induced Ca^{2+} transient in 4 out of 4 experiments.

Mn^{2+} as a probe for Ca^{2+} influx in the rabbit inferior vena cava

Mn^{2+} ions have previously been shown to be a good substitute for Ca^{2+} ions in defining Ca^{2+} influx pathways (Missiaen *et al.*, 1990). They pass through almost all the Ca^{2+} channels in the plasmalemma, but cannot be taken into the SR by the SR Ca^{2+}-ATPase (Gomes da Costa & Madeira, 1986). In the rabbit inferior vena cava, Mn^{2+} entered the smooth muscle cells and quenched the fura-2 fluorescence in a linear manner, at least until 50% of the fluorescence was quenched (Figure 3). Thus, the slope of the first part of the quenching trace can be regarded as a measure of the rate of Mn^{2+} entry into the cells (Figure 3 legend).

Besides the leak pathway, Mn^{2+} also enters the plasmalemma through voltage-gated Ca^{2+} channels (VGC). As shown in Figure 4, high K^+ solution opened the VGC by depolarizing the membrane potential and caused an increase in the rate of Mn^{2+} influx. This effect was completely blocked by 1 μM diltiazem, a known VGC blocker (Figure 4).

NA is believed to stimulate opening of the receptor-operated channels (ROC) and facilitate the opening of VGC (reviewed by van Breemen & Saida, 1989). It also increased the rate of Mn^{2+} entry into the smooth muscle cells (Figure 5a). The VGC blocker, diltiazem, only partially inhibited the effect of NA (Figure 5b), but 2 mM Ni^{2+}, a blocker of both VGC and ROC, totally blocked the effect of NA on increasing the Mn^{2+} influx (Figure 5c).

The results above indicate that Mn^{2+} can enter the smooth muscle cells through the non-regulated leak pathway, VGC and ROC which are the three most important Ca^{2+} entry pathways in the smooth muscle plasmalemma.

Caffeine, ryanodine and thapsigargin do not increase the plasmalemmal permeability of divalent cations

As indicated above, caffeine, ryanodine and thapsigargin all enhanced the steady state $[Ca^{2+}]_i$. However none of these agents seemed to do so by increasing Ca^{2+} entry through the plasmalemma, as reflected by their failure to increase the rate of Mn^{2+} influx (Figure 6a,b,c). Therefore, we conclude that SR depletion by itself is not sufficient to cause an increase in plasmalemmal divalent cation permeability in the smooth muscle of the rabbit inferior vena cava.

We repeated each Mn^{2+} experiment 4 to 5 times and the average results are depicted in Figure 7.

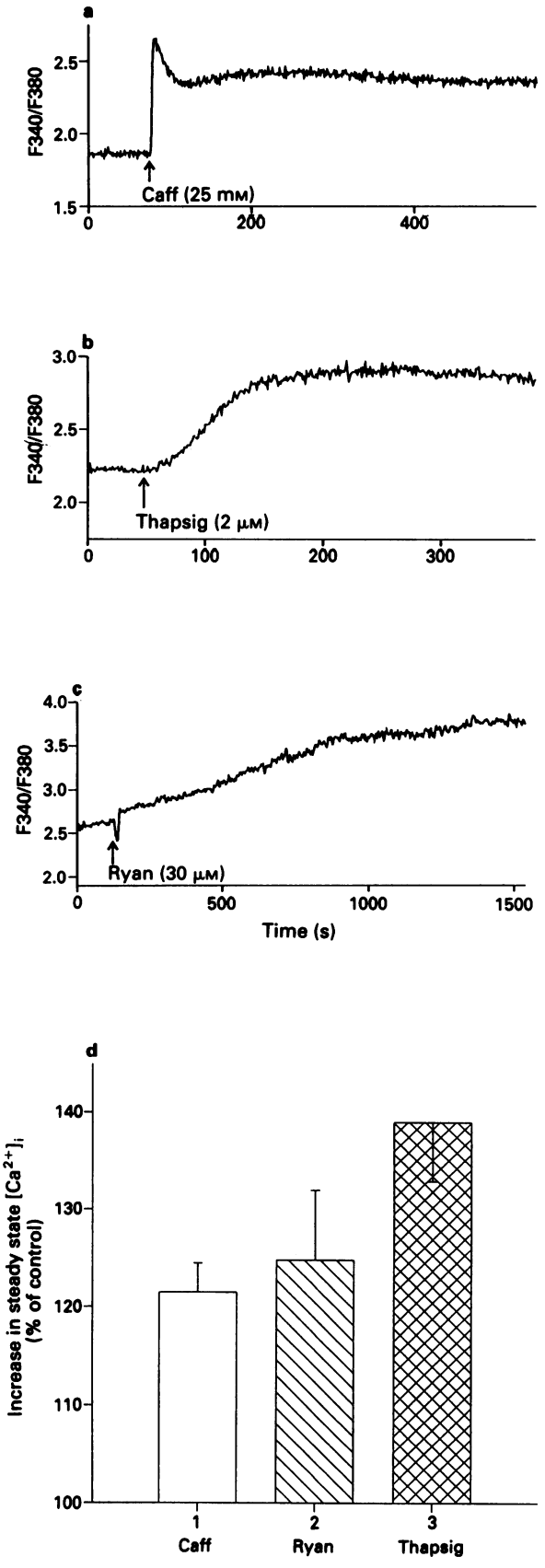

Figure 2 Three different agents which inhibit Ca^{2+} accumulation by sarcoplasmic reticulum (SR) shifted the steady state $[Ca^{2+}]_i$ seen in normal PSS to a higher value: (a) 25 mM caffeine (Caff); (b) 30 μM ryanodine (Ryan); (c) 2 μM thapsigargin (Thapsig). (d) A summary of the effects of above three agents on increasing the steady state $[Ca^{2+}]_i$. Values represent the percentage change in $[Ca^{2+}]_i$ compared with the respective control group. Each column represents the average of 4 experiments ± s.e. (1) Caff, 25 mM caffeine; (2) Ryan, 30 μM ryanodine; (3) Thapsig, 2 μM thapsigargin.

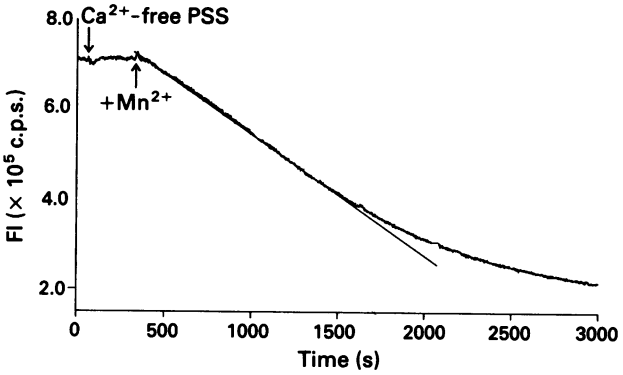

Figure 3 Mn^{2+} quenching of fura-2 fluorescence at excitation wavelength 360 nm. The incubating solution PSS was first replaced with Ca^{2+}-free PSS. The fluorescence intensity decayed immediately upon additon of 100 μM Mn^{2+}. After less than 1 min, the quenching trace appeared to be a straight line and finally levelled off when the fluorescence decayed to 50% of its original level. The slope of the straight line portion of the fura-2 quenching trace was assumed to be proportional to the rate of Mn^{2+} entry. All the subsequent Mn^{2+} quenching recordings were terminated before the fluorescence intensities decayed to 50% of their original values. (The ordinate scale indicates fura-2 fluorescence intensity excitation at 360 nm).

Discussion

After the SR Ca^{2+} has been depleted by exposure to a full agonist or caffeine in Ca^{2+}-free solution, it can be refilled by Ca^{2+} entering the cells from the ECS (Aaronson & van Breemen, 1981). Our data demonstrated that the SR Ca^{2+}-ATPase is essential for this process, since a blocker of the SR Ca^{2+}-ATPase, thapsigargin, completely prevented the SR refilling even if a large Ca^{2+} influx was induced through either excitable Ca^{2+} channels or the Na^+/Ca^{2+} exchanger (Figure 1a and b). These results suggest that during refilling of the SR, Ca^{2+} first enters the cytoplasm and is then actively transported into the SR lumen. On the other hand Casteels & Droogmans (1981) argued that since relatively large quantities of Ca^{2+} could be transferred from the ECS to the SR without contraction, there might be a direct Ca^{2+} transport pathway between these Ca^{2+} compartments. Their group has recently provided evidence for the participation of such a direct pathway in the refilling of the SR in A7r2 cells (a cell line derived from embryonic rat aorta) (Missiaen *et al.*,

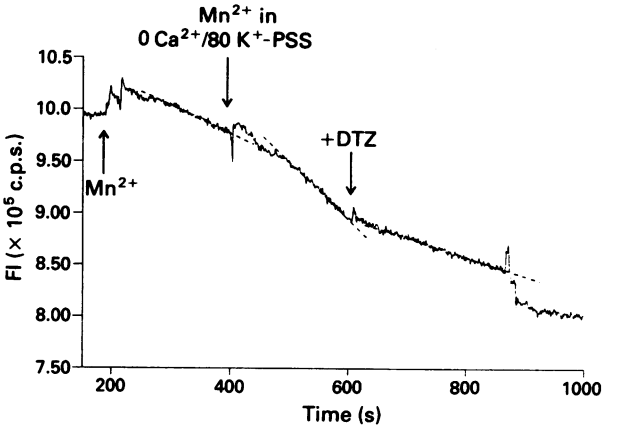

Figure 4 Effect of high K^+ solution on the rate of Mn^{2+} entry: the inferior vena cava was sequentially exposed to PSS, Ca^{2+}-free PSS, 100 μM Mn^{2+} added to Ca^{2+}-free PSS, Mn^{2+} added to 0 Ca^{2+}, 80 mM K^+-PSS and the same with the addition of 1 μM diltiazem (DTZ). High K^+ solution increased the rate of Mn^{2+} entry into the cells and this effect was completely blocked by 1 μM diltiazem. (The ordinate scale indicates fura-2 fluorescence intensity excitation at 360 nm).

1990). After depleting the SR of Ca^{2+} in the A7r5 cells, they incubated them in a Ca^{2+}-free, $^{54}Mn^{2+}$-containing medium for several minutes. Following subsequent saponin permeabilization, $^{54}Mn^{2+}$ efflux from the intracellular stores could be detected. Since Mn^{2+} permeates the plasmalemma but cannot be taken up by the SR Ca-ATPase (Gomes da Costa & Madeira, 1986), they concluded that the SR Ca^{2+} pump was not essential for SR refilling and that there must be a direct pathway for Ca^{2+} between the SR lumen and the ECS (Missiaen *et al.*,

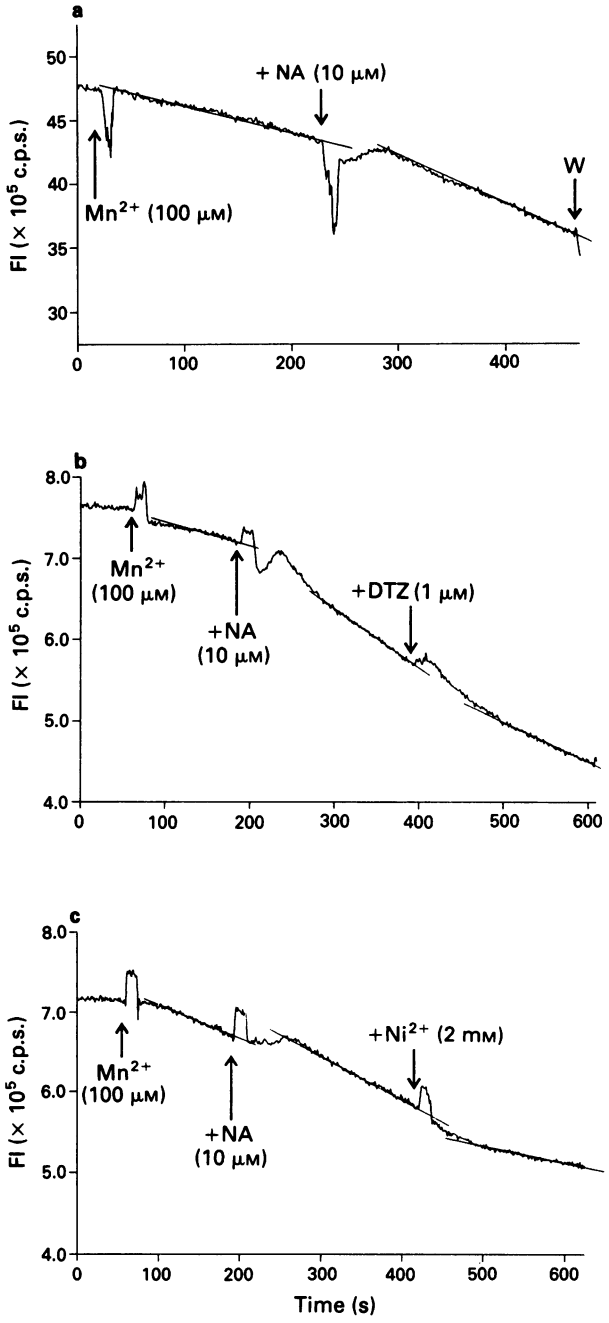

Figure 5 Effect of noradrenaline (NA) on the rate of Mn^{2+} entry. (a) After incubating the inferior vena cava in PSS, 25 mM caffeine in Ca^{2+}-free PSS was first applied to deplete the sarcoplasmic reticulum (SR) of Ca^{2+} in order to reduce the tissue mobility. The caffeine was then washed away with Ca^{2+}-free PSS. Mn^{2+} and NA were added consecutively at the indicated times. (b) The protocol was the same as above with the addition of one more step when 1 μM diltiazem (DTZ) was added in addition to Mn^{2+} and NA. Diltiazem partially inhibits the effect of NA on increasing the rate of Mn^{2+} entry. (c) The protocol was the same as that in (b) with the exception that 2 mM Ni^{+} instead of 1 μM diltiazem completely blocked the effect of NA on the rate of Mn^{2+} entry. (Ordinates indicate fura-2 fluorescence intensities excitation at 360 nm).

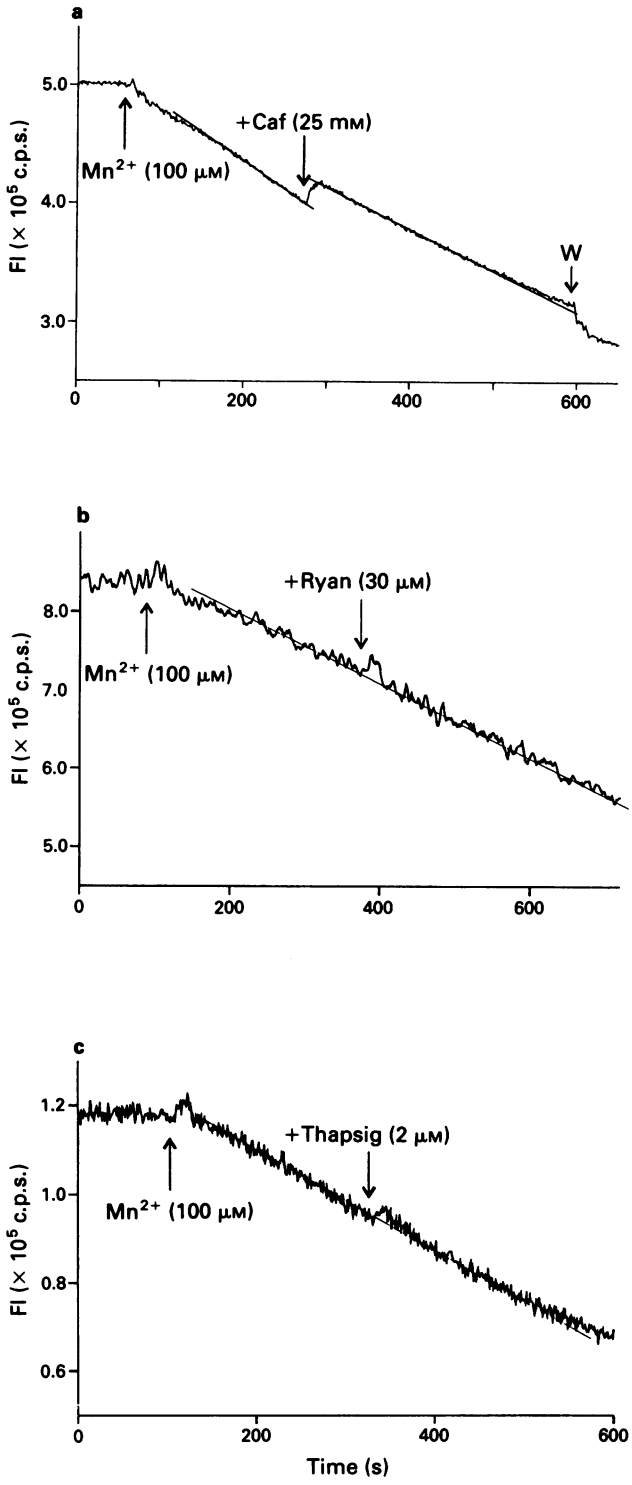

Figure 6 The effects of agents which inhibit Ca^{2+} accumulation by the sarcoplasmic reticulum (SR) on the rates of Mn^{2+} quenching of fura-2 fluorescence. (a) The rabbit inferior vena cava was exposed respectively to PSS, Ca^{2+}-free PSS, 100 μM Mn^{2+} added to Ca^{2+}-free PSS, addition of 25 mM caffeine to the preceding solution, and finally PSS. Caffeine (Caff) caused an initial jump in fluorescence due to its interaction with fura-2 but then decreased the rate of Mn^{2+} quenching of the fura-2 fluorescence. (b) The inferior vena cava was exposed respectively to PSS, Ca^{2+}-free PSS, 100 μM Mn^{2+} added to Ca^{2+}-free PSS and subsequent addition of 30 μM ryanodine (Ryan) to the same solution. Ryanodine did not affect the rate of Mn^{2+} quenching. (c) The protocol was the same as that in (b) with the exception that 2 μM thapsigargin (Thapsig) was added instead of ryanodine. Thapsigargin also had no effect on the rate of Mn^{2+} entry into fura-2 containing cells. (Ordinates indicate fura-2 fluorescence intensities excitation at 360 nm).

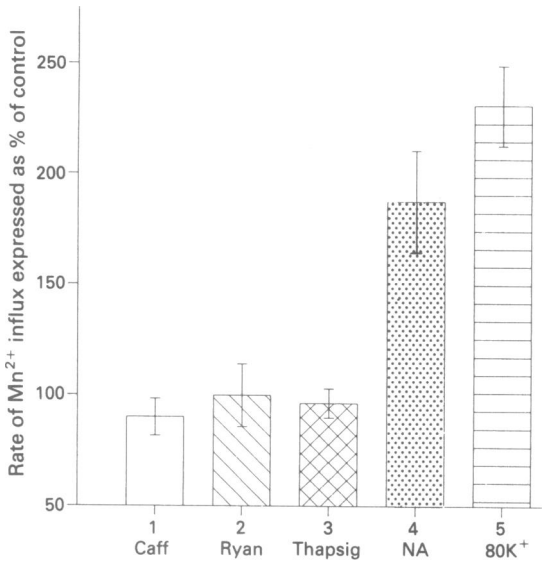

Figure 7 A summary of the effects of different agents and high K^+ solution on the rate of Mn^{2+} influx. The rate of Mn^{2+} influx was measured as described above. Values on the ordinate scale indicate the percentage change in the rate of Mn^{2+} influx compared with respective control group. Each column represents the average of four (five of the experiments with ryanodine) ± s.e. (1) Caff, 25 mM caffeine; (2) Ryan, 30 μM ryanodine; (3) Thapsig, 2 μM thapsigargin; (4) NA, 10 μM noradrenaline; (5) 80 K^+, 80 mM K^+ solution. For details, see the legends of Figure 4–Figure 6.

1990). The discrepancy between this conclusion and the one reached in the present paper may be due to the use of widely different preparations and experimental paradigms.

Electron microscopy of native smooth muscle, though showing close junctional areas between plasmalemma and SR, does not support the presence of any type of pore between the ECS and the SR lumen (Devine *et al.*, 1972; Kowarski *et al.*, 1985). The involvement of a restricted cytoplasmic space in the refilling of vascular smooth muscle SR was supported by a delay between the $[Ca^{2+}]_i$ signal and tension development if Ca^{2+} influx was stimulated after the SR had first been depleted (Rembold, 1989; Chen *et al.*, 1992a). This delay, which was abolished by caffeine, demonstrates the ability of the SR Ca^{2+} pump to establish intracellular Ca^{2+} gradients in the smooth muscle cell periphery (Chen *et al.*, 1992a). In agreement with this concept, Benham & Bolton (1986) observed that large numbers of Ca^{2+}-sensitive K^+ channels may be activated in the absence of force development. Recently Sturek and coworkers found that depletion of the SR in bovine aortic cells resulted in a 58% decrease in K^+ current compared to the resting K^+ current, without there being a difference in $[Ca^{2+}]_i$ as measured by fura-2 (Stehno-Bittel & Sturek, 1992). They also showed that unloading of the SR following a period of enhanced Ca^{2+} influx is accompanied by increased activity of Ca^{2+}-activated K^+ channels and a simultaneous decrease in average $[Ca^{2+}]_i$. These electrophysiological data not only provide strong support for the existence of Ca^{2+} gradients near the plasmalemma, but also suggest that SR Ca^{2+} may be released towards the plasmalemma. In other words, there may exist a continuous Ca^{2+} extrusion pathway from the SR lumen to the ECS which involves a transport process in both SR and cell membranes. The function of such a SR unloading mechanism may be to maintain the 'Ca^{2+} buffer barrier' under steady state conditions. Interruption of this process by prevention of SR Ca^{2+} accumulation would lead to an increase in the steady state $[Ca^{2+}]_i$ dependent on the inward Ca^{2+} leak, similar to the results shown in Figure 2 (see below and Figure 8). However an alternative explanation for the maintained elevation of $[Ca^{2+}]_i$ upon discharge of SR Ca^{2+} is provided by Putney's capacitive Ca^{2+} entry model. It states that depletion of an intracellular Ca^{2+} pool leads to opening of plasmalemmal Ca^{2+} channels (Putney, 1990). We tested the possible application of this hypothesis to venous smooth muscle with three different agents which inhibit Ca^{2+} accumulation by the SR in various ways and found that none of them increased the rate of Mn^{2+} entry through the plasmalemma (Figure 6a,b,c). Since we did record Mn^{2+} influx through the Ca^{2+} leak pathway, VGC and ROC (Figure 3a, Figure 4, Figure 5a,b,c), we suggest that the increase in $[Ca^{2+}]_i$ caused by the SR Ca^{2+} discharge cannot be explained by an increase in Ca^{2+} influx from the ECS under our conditions and that NA did not stimulate Ca^{2+} influx by virtue of discharging SR Ca^{2+}.

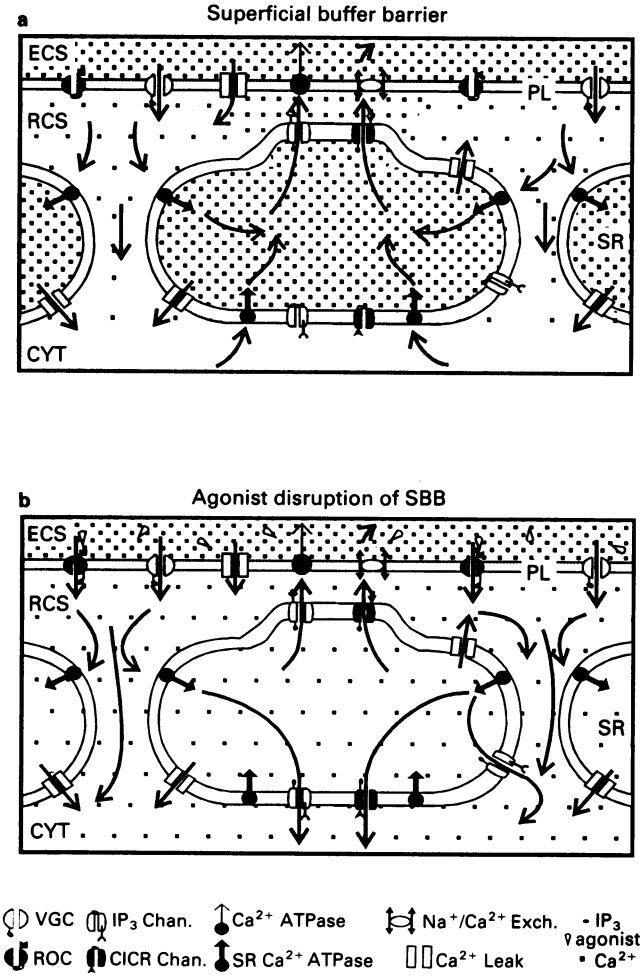

Figure 8 A diagrammatic representation of the Superficial Buffer Barrier (SBB) hypothesis (a) and disruption of the SBB by agonists (b). (a) Ca^{2+} transport in the plasmalemma and the sarcoplasmic reticulum (SR) membrane is mediated by a Ca^{2+} leak, Ca^{2+} channels and Ca^{2+} pumps. In the absence of agonists, Ca^{2+} enters the smooth muscle cell through a non-regulated leak and sporadically opening voltage-gated Ca^{2+} channels (VGC) into a restricted cytoplasmic space near the inner surface of the plasmalemma. A portion of the Ca^{2+} which has entered this space is taken up into the SR by the 100 kD Ca^{2+}-ATPase. The SR therefore buffers Ca^{2+} entry. To maintain this buffer function, SR Ca^{2+} is vectorially released towards the plasmalemma at the plasmalemma-SR junctional regions and extruded into the extracellular space by the 140 kD Ca^{2+}-ATPase and Na^+/Ca^{2+} exchanger (see text). In this model the SR Ca^{2+}-pump assists the plasmalemmal Ca^{2+}-pump in extruding Ca^{2+} from the cells. (b) Agonists stimulate inositol (1,4,5) trisphosphate (IP_3) generation, causing Ca^{2+} release from the SR into the myoplasm short circuiting SBB (see text). The dot density in the aqueous phase represents the $[Ca^{2+}]$. ECS: extracellular space; RCS: restricted cytoplasmic space; CYT: cytoplasm; PL: plasmalemma.

The results displayed in Figure 1 also confirm that the Ca^{2+} content of the SR at rest is well below its maximal capacity (Leijten & van Breemen, 1984), as indicated by the fact that the caffeine-induced $[Ca^{2+}]_i$ transients, which were obtained after Ca^{2+} influx was stimulated, were larger than the first ones obtained after a period of rest. Such would be a requirement for an organelle which at different times functions either as a source of activating Ca^{2+} or as a buffer promoting Ca^{2+} removal from the cytoplasm.

The results presented in this paper: namely, the prevention of SR refilling by thapsigargin and the increase in steady state $[Ca^{2+}]_i$ by this agent, caffeine and ryanodine without an increase in plasmalemmal Ca^{2+} permeability would be best explained by the 'Superficial Buffer Barrier Hypothesis' (see review by van Breemen & Saida, 1989). This hypothesis, which is graphically illustrated in Figure 8a holds that part of the Ca^{2+} which permeates the smooth muscle plasmalemma is taken up by the SR Ca^{2+} pump from a restricted cytoplasmic region before it diffuses into the deeper cytoplasm. In addition it proposes that the buffering is maintained by continuous unloading of the SR to the ECS. As mentioned above, the SR unloading process may involve vectorial Ca^{2+} release towards the inner plasmalemmal surface. A low basal rate of $Ins(1,4,5)P_3$ synthesis at the plasmalemma combined with an active cytoplasmic $Ins(1,4,5)P_3$-phosphatase could establish an $Ins(1,4,5)P_3$ gradient capable of activating only $Ins(1,4,5)P_3$ receptors on SR membranes in close proximity to the plasmalemma. Ca^{2+} released through the $Ins(1,4,5)P_3$ activated channels would activate the Ca^{2+}-sensitive channels (ryanodine receptors) to increase further the local $[Ca^{2+}]_i$ in the SR plasmalemmal junctional regions. This local elevation of $[Ca^{2+}]_i$ would facilitate Ca^{2+} extrusion by the Na^+/Ca^{2+} exchanger which is thought to be concentrated in the junctional regions (Moore *et al.*, 1991) as well as by the plasmalemmal Ca^{2+}-ATPase. Further experiments are required to elucidate the precise mechanism of the above SR unloading pathway. When stimulation with agonists keeps the SR Ca^{2+} channels in an open state (Figure 8b), the peripheral SR loses its ability to accumulate Ca^{2+} and therefore to function as a buffer barrier system. Consequently agonists, as well as pharmacological agents which interfere with SR Ca^{2+} accumulation, would abolish the established Ca^{2+} gradient and shunt out the vectorial extrusion pathway.

The above model for the Superficial Buffer Barrier is a specific example of the ways in which closely apposed areas of SR and plasmalemmal membranes, both having an active Ca^{2+} pump and a Ca^{2+} leak, would be able to interact. The resolution of the exact nature of this interaction will depend on the development of new methodology for measuring Ca^{2+} currents and concentrations in highly locallized regions of the smooth muscle cells.

It is tempting to speculate on possible functions of the hypothetical superficial buffer barrier, which was supported by new data in this paper. It clearly represents an additional element of control over intracellular Ca^{2+} signalling in smooth muscle. The buffering of Ca^{2+} entry may merely protect the cells from activation by a relatively large Ca^{2+} leak (due to a high surface to volume ratio of small cells). A more attractive idea is that the superficial buffer barrier enhances the informational content of Ca^{2+} signalling. For example the resulting Ca^{2+} gradients near the inner plasmalemmal surface would allow separate control over different Ca^{2+}-activated mechanisms which are spatially separated, such as Ca^{2+}-activated K^+ channels and protein kinase C located in the cell membrane and myofilaments and their regulatory kinase and phosphatases located in the cytoplasm.

This research was supported by the NIH grant No. HL 40184-05.

References

AARONSON, P. & VAN BREEMEN, C. (1981). Effects of Na gradient manipulation upon cellular Ca, ^{45}Ca fluxes and cellular Na in the guinea pig taenia coli. *J. Physiol.*, **319**, 443–461.

BENHAM, C.D. & BOLTON, T.B. (1986). Spontaneous transient outward currents in single visceral and vascular smooth muscle cells of the rabbit. *J. Physiol.*, **381**, 385–406.

BOURREAU, J.-P., ABELA, A.P., KWAN, C.Y. & DANIEL, E.E. (1992). Refilling of acetylcholine-sensitive internal Ca^{2+} store directly involves a dihydropyridine sensitive Ca^{2+}-channel in dog trachea. *Am. J. Physiol.*, (in press).

BRADING, A.F., BURNETT, M. & SNEDDON, P. (1980). The effect of sodium removal on the contractile responses of the guinea-pig taenia coli to carbachol. *J. Physiol.*, **306**, 411–419.

CASTEELS, R. & DROOGMANS, G. (1981). Exchange characteristics of the noradrenaline-sensitive calcium store in vascular smooth muscle cells of rabbit ear artery. *J. Physiol.*, **317**, 263–279.

CHEN, Q., CANNEL, M. & VAN BREEMEN, C. (1992a). The superficial buffer barrier in vascular smooth muscle. *Can. J. Physiol. Pharmacol.*, **70**, 509–514.

CHEN, Q. & VAN BREEMEN, C. (1992b). Function of smooth muscle sarcoplasmic reticulum. In *Inositol Phosphates and Calcium Signalling*. ed. Putney, J.W.Jr. pp. 335–350. New York: Raven Press.

DEVINE, C.E., SOMLYO, A.V. & SOMLYO, A.P. (1972). Sarcoplasmic reticulum and excitation-contraction coupling in mammalian smooth muscles. *J. Cell Biol.*, **52**, 690–718.

EGGERMONT, J.A., VROLIX, M., RAEYMAEKERS, L., WUYTACK, F. & CASTEELS, R. (1988). Ca^{2+} transport ATPase of vascular smooth muscle. *Circ. Res.*, **62**, 266–278.

GOMES DA COSTA, A.G. & MADEIRA, V.M.C. (1986). Magnesium and manganese ions modulate Ca^{2+} uptake and its energetic coupling in sarcoplasmic reticulum. *Arch. Biochem. Biophys.*, **249**, 199–206.

GRYNKIEWICZ, G., POENIE, M. & TSIEN, R.Y. (1985). A new generation of Ca^{2+} indicators with greatly improved fluorescence properties. *J. Biol. Chem.*, **260**, 3440–3450.

HWANG, K. & VAN BREEMEN, C. (1987). Ryanodine modulation of $^{45}Ca^{2+}$ efflux and tension in rabbit aortic smooth muscle. *Pflügers Arch. Eur. J. Pharmacol.*, **408**, 343–350.

KOWARSKI, D., SHUMAN, H., SOMLYO, A.P. & SOMLYO, A.V. (1985). Calcium release by noradrenaline from central sarcoplasmic reticulum in rabbit main pulmonary artery smooth muscle. *J. Physiol.*, **366**, 153–175.

LEIJTEN, P.A.A. & VAN BREEMEN, C. (1984). The effects of caffeine on the noradrenaline sensitive calcium store in rabbit aorta. *J. Physiol.*, **357**, 327–339.

MEISSNER, G., DARLING, E. & EVELETH, J. (1986). Kinetics of rapid Ca^{2+} release by sarcoplasmic reticulum. Effects of Ca^{2+}, Mg^{2+}, and adenine nucleotides. *Biochemistry*, **25**, 236–244.

MISSIAEN, L., DECLERCK, I., DROOGMANS, G., PLESSERS, L., DE SMEDT, H., RAEYMAEKERS, L. & CASTEELS, R. (1990). Agonist-dependent Ca^{2+} and Mn^{2+} entry dependent on state of refilling of Ca^{2+} stores in aortic smooth muscle cells of the rat. *J. Physiol.*, **427**, 171–186.

MOORE, E.D.W., FOGARTY, K.E. & FAY, F.S. (1991). Role of Na^+/Ca^{2+} exchanger in β-adrenergic relaxation of single smooth muscle cells. *Ann. N.Y. Acad. Sci.*, **639**, 543–549.

NISHIMURA, J., KHALIL, R.A. & VAN BREEMEN, C. (1989). Agonist-induced vascular tone. *Hypertension*, **13**, 835–844.

PUTNEY, J.W.Jr. (1986). A model for receptor-regulated calcium entry. *Cell Calcium*, **7**, 1–12.

PUTNEY, J.W.Jr. (1990). Capacitative calcium entry revisited. *Cell Calcium*, **11**, 611–624.

REMBOLD, C. (1989). Desensitization of swine arterial smooth muscle to transplasmalemmal Ca^{2+} influx. *J. Physiol.*, **416**, 273–290.

ROUSSEAU, E. & MEISSNER, G. (1987). Ryanodine modifies conductance and gating behavior of single Ca^{2+} release channels. *Am. J. Physiol.*, **253**, C364–C368.

ROUSSEAU, E. & MEISSNER, G. (1989). Single cardiac sarcoplasmic Ca^{2+}-release channels: activation by caffeine. *Am. J. Physiol.*, **253**, H328–H333.

SAIDA, K. (1982). Intracellular Ca release in skinned smooth muscle. *J. Gen. Physiol.*, **80**, 191–202.

SAIDA, K. & VAN BREEMEN, C. (1984). Characteristics of the norepinephrine-sensitive Ca^{2+} store in vascular smooth muscle. *Blood Vessels*, **21**, 43–52.

STEHNO-BITTEL, L. & STUREK, M. (1992). Spontaneous sarcoplasm reticulum calcium release and extrusion from bovine, not porcine, coronary artery smooth muscle. *J. Physiol.*, **451**, 49–78.

SUEMATSU, E., HIRATA, M., HASHIMOTO, T. & KURIYAMA, H. (1984). Inositol 1,4,5-trisphosphate releases Ca^{2+} from intracellular store sites in skinned single cells of porcine coronary artery. *Biochem. Biophys. Res. Commun.*, **120**, 481–485.

VAN BREEMEN, C. (1976). Transmembrane calcium transport in vascular smooth muscle. In *Vascular Neuroeffector Mechanism.* ed. Bevan, J.A. pp. 67–79. Basel: S. Karger.

VAN BREEMEN, C. (1977). Calcium requirement for activation of intact aortic smooth muscle. *J. Physiol.*, **272**, 317–329.

VAN BREEMEN, C. & SAIDA, K. (1989). Cellular mechanisms regulating $[Ca^{2+}]_i$ smooth muscle. *Annu. Rev. Physiol.*, **51**, 315–329.

(Received September 21, 1992
Revised January 24, 1993
Accepted January 26, 1993)

Br. J. Pharmacol. (1993), **109**, 344–352 © Macmillan Press Ltd, 1993

Characterization of propranolol-resistant (−)-[^{125}I]-cyanopindolol binding sites in rat soleus muscle

Susan J. Roberts, Peter Molenaar & [1]Roger J. Summers

Department of Pharmacology, University of Melbourne, Parkville, 3052 Victoria, Australia

1 The characteristics of a propranolol-resistant (−)-[^{125}I]-cyanopindolol (CYP) binding site in rat soleus muscle were determined.

2 Saturation studies performed on homogenates of rat soleus muscle showed two phases of (−)-[^{125}I]-CYP binding, a high affinity site (K_{D1} 30.5 ± 16.3 pM, B_{max} 9.4 ± 1.38 fmol mg^{-1} protein) and a lower affinity site (K_{D2} 522.5 ± 29.1 pM, B_{max} 62.19 ± 11.76 fmol mg^{-1} protein, $n = 4$).

3 In rat soleus muscle homogenates labelled with (−)-[^{125}I]-CYP (500 pM), (−)-propranolol competition curves were biphasic with pK_D values of 8.30 ± 0.19, and 5.33 ± 0.08, $n = 7$.

4 Competition between (−)-[^{125}I]-CYP (500 pM) and (±)-tertatolol, (±)-nadolol, (±)-alprenolol, (±)-CYP, and (−) and (+)-pindolol showed that these compounds competed for binding at the propranolol-resistant site with affinities lower than those displayed at typical β-adrenoceptors. The atypical β-adrenoceptor agonists BRL 37344, SR58611A and ICI D7114 and the partial agonist (±)-CGP 12177 also competed for (−)-[^{125}I]-CYP binding.

5 Stereoselectivity was demonstrated for the stereoisomers of alprenolol and tertatolol. The (−)-isomers of alprenolol and tertatolol had higher affinity than their corresponding (+)-isomers (3.1 and 2.6 fold respectively). These low stereoselectivity values are a characteristic of atypical β-adrenoceptors.

6 The β-adrenoceptor agonists, (−)-adrenaline, (−)-isoprenaline and (−)-noradrenaline, all showed lower affinity than the atypical β-adrenoceptor agonists and competition curves appeared biphasic in nature.

7 These results confirm the presence of a propranolol-resistant (−)-[^{125}I]-CYP binding site in rat soleus muscle. The affinities of the tested compounds at the propranolol-resistant (−)-[^{125}I]-CYP binding site show similarities to their affinities at 'atypical' β-adrenoceptors in adipocytes and gastrointestinal tissues and at the cloned β_3-adrenoceptor.

Keywords: Rat soleus muscle; (−)-[^{125}I]-cyanopindolol; receptor binding; atypical β-adrenoceptors; β_3-adrenoceptors

Introduction

The existence of β-adrenoceptors that differed from β_1- and β_2-subtypes was first indicated by functional studies on rat adipocytes. Isoprenaline-induced lipolysis was blocked by stereoisomers of β-adrenoceptor antagonists with lower stereoselectivity ratios than in tissues with predominantly β_1-(atrial) or β_2-(diaphragm) adrenoceptors (Harms *et al.*, 1977) and the affinity of β-adrenoceptor antagonists was lower at the adipocyte β-adrenoceptor than at typical β_1- and β_2-adrenoceptors (Bojanic *et al.*, 1985). This was further supported by the development of novel β-adrenoceptor agonists which selectively stimulated lipolysis in brown adipocytes (Arch *et al.*, 1984). These novel phenethanolamine analogues, BRL 37344, BRL 28410 and BRL 35113 were found to be more potent as stimulators of lipolysis than of either atrial rate (β_1-adrenoceptor mediated) or tracheal relaxation (β_2-adrenoceptor mediated).

Functional studies in gastrointestinal tissues such as guinea-pig gastric fundus (Coleman *et al.*, 1987) and ileum (Bond *et al.*, 1986; Bond & Clarke, 1988), rabbit stomach (Bristow *et al.*, 1970) and jejunum (Wikberg, 1977; Norman & Leathard, 1990), rat oesophageal muscle (Buckner & Christopherson, 1974), gastric fundus (Dettmar *et al.*, 1986; McLaughlin & McDonald, 1991), colon (Croci *et al.*, 1988; Bianchetti & Manara, 1990), distal colon (McLaughlin & McDonald, 1990), jejunum (Van der Vliet *et al.*, 1990), dog distal colon (Grivegnee *et al.*, 1984) and human colon (McLaughlin *et al.*, 1988) showed that adrenergic inhibition of tension development in these tissues was mediated by a β-adrenoceptor which was resistant to blockade by propranolol and other conventional β-adrenoceptor antagonists. In addition to brown and white fat cells there is evidence that other tissues such as heart (Kaumann, 1989), pancreas (Arch *et al.*, 1991) and liver (Emorine *et al.*, 1989) also contain atypical β-adrenoceptors, while functional studies in rat soleus muscle have identified a thermic response mediated by propranolol-resistant β-adrenoceptors (Challis *et al.*, 1988; see also Arch & Kaumann, 1993 for review).

The recent isolation and cloning of genes coding for β_3-adrenoceptors in man (Emorine *et al.*, 1989; Tate *et al.*, 1991), rat (Granneman *et al.*, 1991; Muzzin *et al.*, 1991) and mouse (Nahmias *et al.*, 1991) further supports the functional evidence that more than two subtypes exist. When expressed in cultured CHO cells the cloned β_3-adrenoceptors display a lower affinity for the radioligand (−)-[^{125}I]-cyanopindolol (CYP) than either β_1- and β_2-adrenoceptors. Identification of these receptors using receptor binding studies in tissues with atypical β-adrenoceptors has only recently been achieved in 3T3-F442A adipocytes with (−)-[^{125}I]-CYP and [^{3}H]-CGP 12177 (Feve *et al.*, 1991; 1992; Thomas *et al.*, 1992) and in rat brown adipose tissue membranes with [^{3}H]-CGP 12177 (Muzzin *et al.*, 1992).

Recent autoradiographic studies of β-adrenoceptors in rat skeletal muscle have revealed the presence of propranolol (1 μM)-resistant (−)-[^{125}I]-CYP binding (Molenaar *et al.*, 1991) distributed across the muscle bundle and most abundant in the soleus muscle. The present study was aimed at characterizing propranolol-resistant binding in rat soleus muscle with a view to the development of a receptor binding assay for atypical β-adrenoceptors.

[1] Author for correspondence.

Methods

Membrane preparation

Sprague-Dawley rats of either sex (250–450 *g*) were stunned by a blow to the back of the head and exsanguinated. The soleus muscle was dissected and homogenized (4 muscles per homogenate) in 20 vol of ice cold Krebs buffer containing phenylmethylsulphonylfluoride (PMSF) (10 μM) pH 7.4 or in Tris buffer pH 7.4 containing $MgCl_2$ (5 mM) and PMSF (10 μM) for competition studies with some agonists. Homogenates were filtered through a nylon filter (210 μm) and centrifuged twice at 4°C for 15 min at 50,000 *g* in a Sorvall RC-5 superspeed centrifuge. The final pellet was resuspended in 15 volumes of buffer and stored on ice until use. Protein was determined by the method of Lowry *et al.* (1951) with bovine serum albumin as a standard.

Kinetic studies

The association of (−)-[125I]-CYP (500 pM) with specific binding sites in 50 μl aliquots of soleus muscle homogenates incubated with 5-hydroxytryptamine (5-HT) at 10 μM to block 5-HT-sensitive (−)-[125I]-CYP binding sites (Molenaar *et al.*, 1991) and (−)-propranolol (0.1 μM) to block β_1- and β_2-adrenoceptors was determined at various times up to 90 min. Non-specific binding was determined with (±)-alprenolol (500 μM). Preliminary studies showed that this concentration identified maximal 'specific binding' and as it is approximately 200 × K_D value (2.2 μM, present study) it will therefore block 99.6% of the propranolol-resistant (−)-[125I]-CYP binding sites. The dissociation of (−)-[125I]-CYP was determined after a 60 min incubation with (−)-[125I]-CYP (500 pM) at 37°C at intervals up to 90 min after the addition of (±)-alprenolol (500 μM).

Saturation binding

Aliquots of membrane suspension (50 μl) were incubated with (−)-[125I]-CYP (10–1000 pM) and 5-HT (10 μM) at 37°C for 60 min in a final volume of 100 μl. Non-specific binding was defined by (±)-alprenolol (500 μM).

Competition binding

Aliquots of membrane suspension (50 μl) were incubated with (−)-[125I]-CYP (500 pM), 5-HT (10 μM), with or without (−)-propranolol (0.1 μM) and a range of concentrations of competing agent. Non-specific binding was defined by (±)-alprenolol (500 μM). In competition experiments using (−)-isoprenaline, (−)-adrenaline and (−)-noradrenaline the incubation mixture also contained 0.1 mM ascorbic acid to prevent catecholamine oxidation. Solutions were incubated in duplicate or triplicate for 60 min at 37°C in a final volume of 100 μl and incubation was terminated by the addition of 4 ml 20°C buffer solution followed by rapid vacuum filtration. Membranes were washed onto Whatman GF/B filters presoaked in 2% polyethylenimine and washed with 3 × 4 ml buffer (Brandel M-30R Cell Harvester). Radioactivity retained on the filters was measured in a Packard gamma counter (Model B5424) with 79% efficiency.

Analysis of results

Results are expressed as means ± standard error (s.e.) of *n* experiments. Kinetic constants were obtained using KINFIT (Williams & Summers, 1990). Saturation data were analysed with EBDA (McPherson, 1983) to obtain Hill coefficient and LIGAND (Munson & Rodbard, 1980) to obtain dissociation constant (K_D) and receptor density (B_{max}) values. Competition data were analysed with EBDA to obtain preliminary K_D values and the non-linear curve fitting programme GraphPad (Intuitive Software for Science) to obtain final K_D and pseudo Hill coefficient values. All curves were analysed for a one site fit (propranolol-resistant site) and tested for two sites where competition for typical β-adrenoceptors was also expected ((−)-[125I]-CYP saturation, propranolol, ICI 118551 and CGP 20712A competition binding curves). Significant line shifts were determined with ANCOVA which is part of the REAP package (Gamma Research Systems, Knoxfield, Australia).

Radioiodination of (−)-CYP

(−)-[125I]-CYP was prepared from (−)-CYP and Na125I as described by Lew & Summers (1985).

Materials

(−)-Propranolol, ICI D7114 ((S)-4-[2-hydroxy-3-phenoxypropylamino ethoxy]-*N*-(2-methoxyethyl)phenoxyacetamide), (±)-ICI 118551 (erythro-DL-1(7-methylindian-4-yloxy)-3-isopropylaminobutan-2-ol) (Imperial Chemical Industries, Wilmslow, Cheshire, England); 5-HT, (±)-nadolol, prazosin, (±)-alprenolol hydrochloride, (−)-alprenolol, (−)-isoprenaline, (−)-adrenaline (epinephrine), (−)-noradrenaline (norepinephrine) (Sigma, St Louis, U.S.A.); (+)-alprenolol (Professor B. Jarrott, Monash University); atropine sulphate (BDH Chemicals Ltd, Poole, Dorset); (±)-CGP 20712A (2-hydroxy-5(2-((2-hydroxy-3-(4-((1-methyl-4-trifluoromethyl) 1H-imidazole-2-yl)-phenoxy)propyl)amino)ethoxy)-benzamide monomethane sulphonate) (Ciba-Geigy AG Australia); (−)-CYP, (±)-CYP (Sandoz, Basel, Switzerland); Na [125I] (Amersham International, Buckinghamshire), BRL 37344 (sodium-4-[-2[-2-hydroxy-2-(-3-chloro-phenyl) ethylamino] propyl] phenoxyacetate) (Smith Kline Beecham, Great Burgh, Epsom, Surrey); (±)-tertatolol hydrochloride, (−)-tertatolol, (+)-tertatolol (Servier, Paris, France); SR58611A (**RS**-N-(7-carbethoxymethoxyl 1,2,3,4-tetrahydronaphth-2-yl)-2 hydroxy 2-(3-chlorophenyl)ethanamine) (SANOFI-MIDY S.p.A. Research Centre, Milan, Italy); (±)-CGP 12177 hydrochloride ((−)-4-)3-*t*-butylamino-2-hydroxypropoxy)benzimidazol-2-one) (Research Biochemicals Inc., Massachusetts, U.S.A.); (−)-pindolol, (+)-pindolol (Professor C. Raper, Victorian College of Pharmacy).

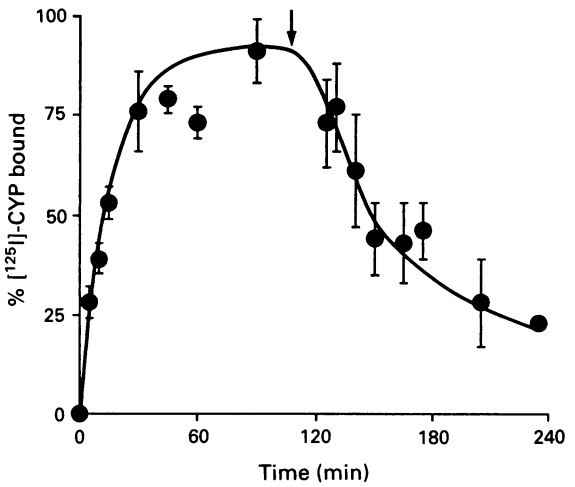

Figure 1 Association and dissociation of specific binding of (−)-[125I]-cyanopindolol ((−)-[125I]-CYP) to rat soleus muscle at 37°C. Dissociation curve represents specific binding at various times after the addition of (±)-alprenolol (arrow, 500 μM) to membranes incubated with (−)-[125I]-CYP for 60 min. Each point is expressed as a percentage of the binding occurring at equilibrium in association experiments. Points show mean ± s.e. ($n = 4$).

Results

Characterization of propranolol-resistant sites

Association kinetics of (−)-[^{125}I]-CYP binding to soleus muscle membranes Association kinetics of the site were determined at 37°C and showed that association of (−)-[^{125}I]-CYP to the propranolol-resistant site reached equilibrium in 60 min (Figure 1). The observed association rate constant, (K_{obs}) was 0.062/min. Dissociation kinetics determined at 37°C showed that binding was reversible on the addition of 500 μM (±)-alprenolol. Dissociation occurred in two phases, K_{-1} = 0.112/min (phase 1) and 0.008/min (phase 2) (Figure 1).

Saturation of (−)-[^{125}I]-CYP binding to soleus muscle membranes (−)-[^{125}I]-CYP bound to soleus muscle homogenates in a concentration-dependent manner. The specific binding defined by 500 μM (±)-alprenolol ranged from 45–80% at 10 pM, 76–86% at 160–180 pM and 71–78% at 530–580 pM. (−)-[^{125}I]-CYP bound with two affinities and analysis using LIGAND revealed a high affinity site with a K_D of 30.5 ± 16.3 pM (B_{max} = 9.4 ± 1.38 fmol mg^{-1} protein) (typical β-adrenoceptors) and a site of lower affinity with a K_D of 522.5 ± 29.1 pM (B_{max} = 62.19 ± 11.76 fmol mg^{-1} protein) (n = 4). A representative saturation isotherm is shown in Figure 2.

Competition by (−)-propranolol (−)-Propranolol competed for (−)-[^{125}I]-CYP binding in soleus muscle homogenates (Figure 3). The competition curve could be separated into high and low affinity components with pK_D values of 8.30 and 5.33 respectively. Using the mass action equation ([A]/[A] + K_D) we were able to establish that a concentration of 0.1 μM (−)-propranolol would block 95% of β_2-adrenoceptors but only 2% of the atypical site. Therefore subsequent competition studies were performed in the presence of (−)-propranolol (0.1 μM) to block the low density typical β-adrenoceptor sites so that competition for the more abundant atypical site could be examined.

In addition, competition between (−)-[^{125}I]-CYP and ICI 118551 (selective β_2-antagonist) in the absence of (−)-propranolol produced a biphasic curve with high and low affinity components (Table 1, Figure 4a) while competition with CGP 20712A (selective β_1-antagonist) showed a single low affinity binding site (Table 1, Figure 4b).

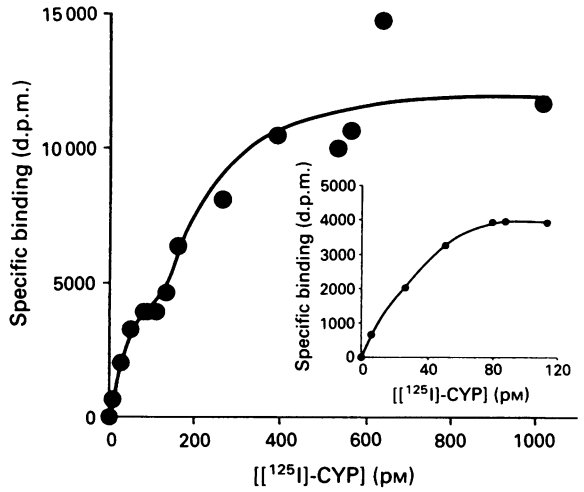

Figure 2 Representative saturation binding curve of specific (−)-[^{125}I]-cyanopindolol ((−)-[^{125}I]-CYP) binding to rat soleus muscle membranes. Non-specific binding was defined by 500 μM (±)-alprenolol. Two phases of binding were observed, a high affinity site K_{D1} 30.5 ± 16.3 pM (B_{max} = 9.4 ± 1.38 fmol mg^{-1} protein) and low affinity site K_{D2} 522.5 ± 29.1 pM (B_{max} = 62.19 ± 11.76 fmol mg^{-1} protein) (n = 4). Inset shows saturation binding data between 0–120 pM.

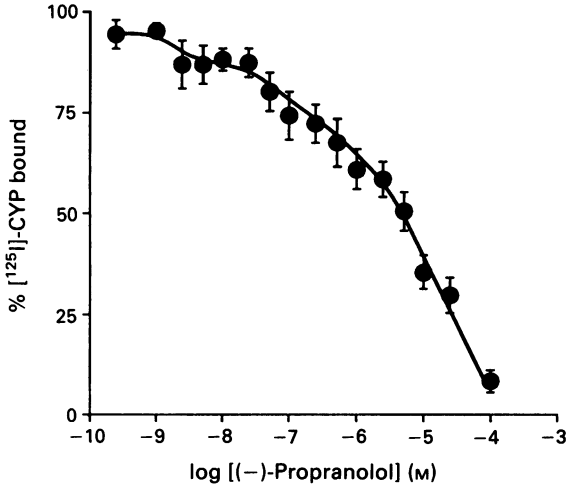

Figure 3 Competition between (−)-[^{125}I]-cyanopindolol ((−)-[^{125}I]-CYP) and (−)-propranolol for binding sites in homogenates of rat soleus muscle. Incubations were for 1 h at 37°C and non-specific binding was defined by 500 μM (±)-alprenolol. The biphasic curve indicates two sites. Corresponding affinity and pseudo Hill coefficient values are given in Table 1.

Table 1 Affinity and pseudo Hill coefficient values obtained in competition binding experiments against (−)-[^{125}I]-cyanopindolol ((−)-[^{125}I]-CYP) in rat soleus muscle

Competitor	n	*pK_D ± s.e.*	*nH ± s.e.*
(−)-Propranolol	7	8.30 ± 0.19[1] 5.33 ± 0.08	0.38 ± 0.03
(±)-ICI 118551	4	9.78 ± 0.33[1] 5.45 ± 0.09	0.40 ± 0.04
(±)-CGP 20712A	4	3.68 ± 0.06	1.44 ± 0.31
(±)-Cyanopindolol	6	7.63 ± 0.09	0.70 ± 0.11
(−)-[^{125}I]-CYP	4	10.52 ± 0.19[1] 9.28 ± 0.02	
(±)-Alprenolol	6	5.66 ± 0.05	0.62 ± 0.04
(±)-Tertatolol	6	6.70 ± 0.06	0.66 ± 0.06
(±)-Nadolol	6	5.09 ± 0.07	0.50 ± 0.04
(−)-Pindolol	7	4.61 ± 0.08	0.64 ± 0.07
(+)-Pindolol	7	4.48 ± 0.05	0.83 ± 0.07
(−)-Tertatolol	4	6.82 ± 0.04	0.70 ± 0.05
(+)-Tertatolol	4	6.40 ± 0.04	0.81 ± 0.06
(−)-Alprenolol	4	6.16 ± 0.03	0.88 ± 0.05
(+)-Alprenolol	4	5.67 ± 0.02	0.95 ± 0.03
Prazosin	3	3.71 ± 0.30	0.61 ± 0.22
Atropine	3	2.89 ± 0.20	0.62 ± 0.14
SR 58611A (Krebs)	4	5.50 ± 0.06	0.80 ± 0.08
SR 58611A (Tris)	8	5.34 ± 0.04	0.84 ± 0.05
ICI D7114 (Krebs)	5	5.12 ± 0.05	0.71 ± 0.05
ICI D7114 (Tris)	6	4.96 ± 0.07	0.64 ± 0.62
BRL 37344 (Krebs)	4	3.39 ± 0.10	0.56 ± 0.09
BRL 37344 (Tris)	6	3.95 ± 0.12	0.46 ± 0.06
(±)-CGP 12177A (Krebs)	4	5.11 ± 0.08	0.64 ± 0.69
(±)-CGP 12177A (Tris)	5	4.80 ± 0.04	0.68 ± 0.04
(−)-Isoprenaline	4	3.55 ± 0.10	0.68 ± 0.10
(−)-Adrenaline	4	3.57 ± 0.15	0.56 ± 0.10
(−)-Noradrenaline	4	3.20 ± 0.15	0.62 ± 0.14

[1]pK_D values obtained at classical β-adrenoceptors
Values are mean ± s.e. from n separate experiments.

Competition binding in the presence of (−)-propranolol

Antagonists Competition studies were performed to determine the affinities of the non-selective β-adrenoceptor antagonists (±)-alprenolol, (±)-nadolol and (±)-tertatolol

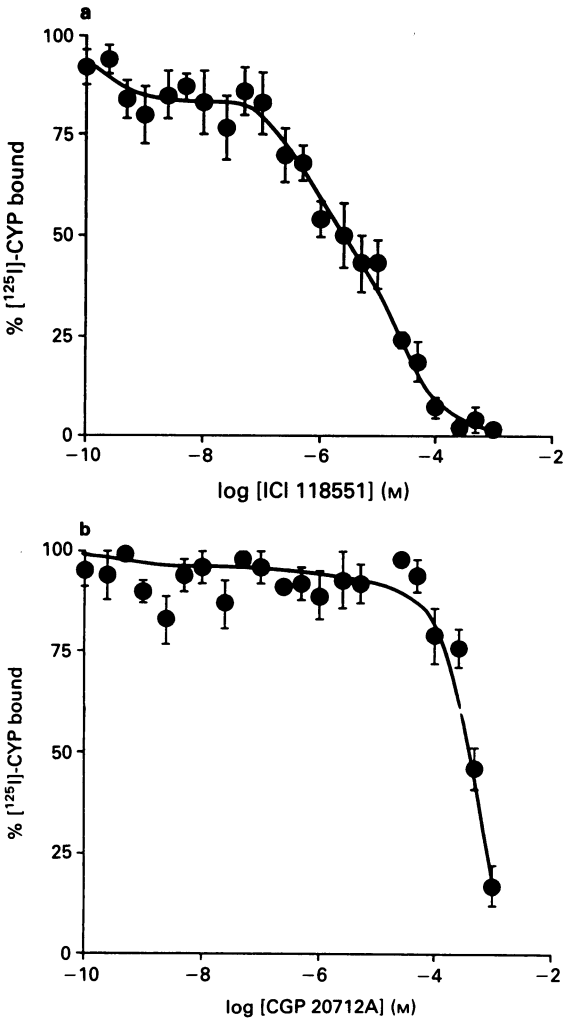

Figure 4 Competition between (−)-[^{125}I]-cyanopindolol ((−)-[^{125}I]-CYP) and (a) the selective β_2-adrenoceptor antagonist (±)-ICI 118551 and (b) the selective β_1-adrenoceptor antagonist (±)-CGP 20712A in the absence of (−)-propranolol. Note the biphasic nature of competition by (±)-ICI 118551. Corresponding affinity and pseudo Hill coefficient values are given in Table 1.

for the propranolol-resistant (−)-[^{125}I]-CYP binding site (Table 1). (±)-Tertatolol was the most effective compound, and the order of potency (pK_D) for these antagonists was (±)-tertatolol (6.70) > (±)-alprenolol (5.66) > (±)-nadolol (5.09) (Figure 5a).

The structurally related compounds (±)-cyanopindolol (CYP) and the isomers of pindolol competed for the propranolol-resistant site (Table 1, Figure 5b). These competitors showed the following order of potency (pK_D): (±)-CYP (7.63) > (−)-pindolol (4.61) ≥ (+)-pindolol (4.49). The site failed to show significant stereoselectivity ($P > 0.05$) for the stereoisomers of pindolol.

Stereoselectivity was further examined by use of stereoisomers of compounds with higher affinity for the atypical site (Table 1, Figure 5c). Stereoselective competition for (−)-[^{125}I]-CYP binding was demonstrated for (−)-tertatolol (pK_D 6.82) > (+)-tertatolol (pK_D 6.40) and (−)-alprenolol (pK_D 6.16) > (+)-alprenolol (pK_D 5.67). These isomers produced curves that were significantly different in position ($P < 0.05$) with stereoselectivity indices (pK_D (−)-isomer minus pK_D (+)-isomer) of 0.42 ± 0.09 for tertatolol and 0.49 ± 0.04 for alprenolol. Table 1 gives the mean pK_D values together with pseudo Hill coefficient values.

Agonists The agonists SR58611A, ICI D7114 and BRL 37344, which are active at atypical β-adrenoceptors, competed at the propranolol-resistant (−)-[^{125}I]-CYP binding site with an order of potency SR 58611A > ICI D7114 > BRL 37344. Table 1 gives mean pK_D and pseudo Hill coefficient values. The partial agonist (±)-CGP 12177 also competed for (−)-[^{125}I]-CYP binding with an affinity similar to that of ICI D7114 (Table 1). These studies were performed in both Krebs phosphate and Tris buffer and curves were not significantly different ($P > 0.05$) with the change of assay buffer (Figure 6).

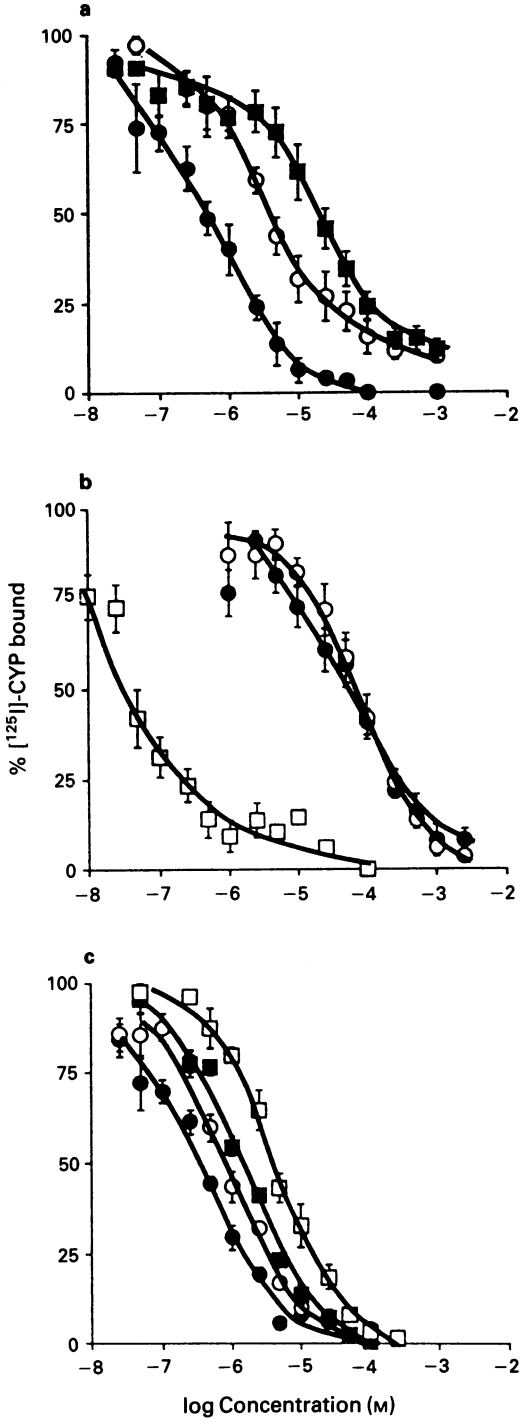

Figure 5 Mean curves for competition between (−)-[^{125}I]-cyanopindolol ((−)-[^{125}I]-CYP) and (a) the antagonists (±)-tertatolol (●); (±)-nadolol (■); and (±)-alprenolol (○); (b) (±)-CYP (□); (−)-pindolol (●); and (+)-pindolol (○); (c) the stereoisomers of alprenolol (−) (■); (+) (□); and tertatolol (−) (●); (+) (○); in the presence of 0.1 μM (−)-propranolol. Points show mean ± s.e. Corresponding affinity and pseudo Hill coefficient values are given in Table 1.

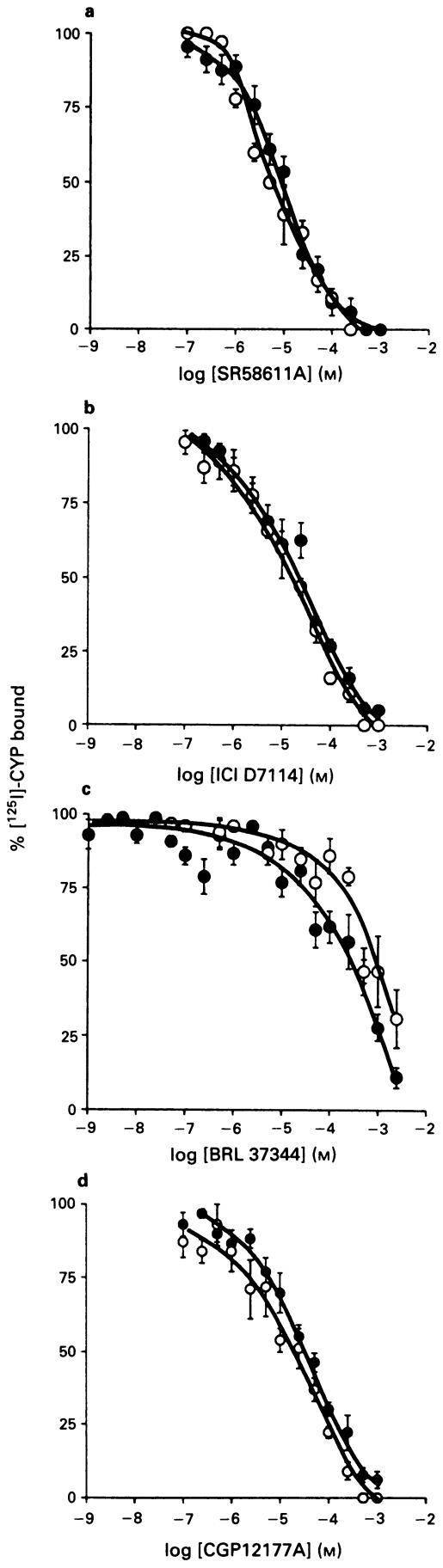

Competition between (−)-[^{125}I]-CYP and the catecholamines, (−)-adrenaline, (−)-noradrenaline and (−)-isoprenaline, was also examined. Table 1 shows that these agonists all had low affinity for the propranolol-resistant site and that the curves were distinctly biphasic in nature (Figure 7). The addition of GTP to the incubation mixture was found to have no effect (results not shown). Competition between (−)-[^{125}I]-CYP binding and the α-adrenoceptor antagonist, prazosin, and the muscarinic antagonist, atropine, were examined. Competition by these compounds was of extremely low affinity (Table 1, Figure 8).

Discussion

The rat soleus muscle contains at least four distinct binding sites for (−)-[^{125}I]-CYP, β_1- and β_2-adrenoceptors (Elfellah & Reid, 1987; Kim *et al.*, 1991), a highly localized 5-HT-sensitive site (Molenaar *et al.*, 1991) and a propranolol-resistant site. The affinity of (−)-[^{125}I]-CYP for the propranolol resistant site (K_D = 522 pM) has close similarities with its affinity at the cloned human β_3-adrenoceptor (K_D = 500 pM, Emorine *et al.*, 1989) and the β_3-adrenoceptor expressed in 3T3-F442A cells ($K_D \sim$ 500 pM, Thomas *et al.*, 1992). Other reports of K_D values for (−)-[^{125}I]-CYP at β_3-adrenoceptors have ranged from 1.3 nM for rat β_3-adrenoceptors expressed in CHO cells (Muzzin *et al.*, 1991) to 1.9 nM in 3T3-F442A adipocytes (Feve *et al.*, 1992). This variation in reported K_D values is not uncommon for binding studies performed in different laboratories under slightly different conditions and all show clearly the lower affinity of (−)-[^{125}I]-CYP for the β_3-adrenoceptor compared to typical β_1- and β_2-adrenoceptors (Neve *et al.*, 1986).

The existence of a low affinity β-adrenoceptor site on the muscle is further supported by the two affinity values obtained for (−)-propranolol in competition experiments. The pK_D value (8.30) for the high affinity site corresponds to the affinity of propranolol in tissues containing typical β-adrenoceptors (Molenaar *et al.*, 1987) while the low affinity site with a pK_D of 5.33 (Table 1) is indicative of a propranolol-resistant site similar in affinity to those described in adipocytes (Arch, 1989) and gastrointestinal tissues such as ileum (Blue *et al.*, 1990) and oesophagus (Ford *et al.*, 1992). In radioligand binding experiments, biphasic competition by (−)-propranolol has also been observed in intestinal membranes (Van der Vliet *et al.*, 1990). In the present study a biphasic curve was also seen with the selective β_2-adrenoceptor antagonist (±)-ICI 118551. The lower affinity pK_D values obtained for both of these antagonists correspond well with values obtained for (−)-[^{125}I]-CYP competition in adipocytes (Muzzin *et al.*, 1991) (Table 2). The low affinity shown by the selective β_1-adrenoceptor antagonist (±)-CGP 20712A suggests that few (Kim *et al.*, 1991) if any β_1-adrenoceptors exist in the preparation and only competition for the more abundant propranolol-resistant site is observed. (±)-CGP 20712A is a weak antagonist of BRL 37344-induced adenylate cyclase stimulation in adipocytes, producing a clear depression of the response only at 1 mM (Hollenga *et al.*, 1991).

Many of the compounds that compete with (−)-[^{125}I]-CYP for the propranolol-resistant site also have pharmacological activity at atypical β-adrenoceptors in adipocytes and gastrointestinal tissues (Table 2). The pharmacological tools for

Figure 6 Mean curves for competition between (−)-[^{125}I]-cyanopindolol ((−)-[^{125}I]-CYP) and various atypical β-adrenoceptor agonists: (a) SR 58611A; (b) ICI D7114; (c) BRL 37344, and (d) (±)-CGP 12177A in the presence of 0.1 μM (−)-propranolol. Curves are shown for competition in the two buffer systems Krebs (○) and Tris (●). Points show mean ± s.e. Corresponding affinity and pseudo Hill coefficient values are given in Table 1.

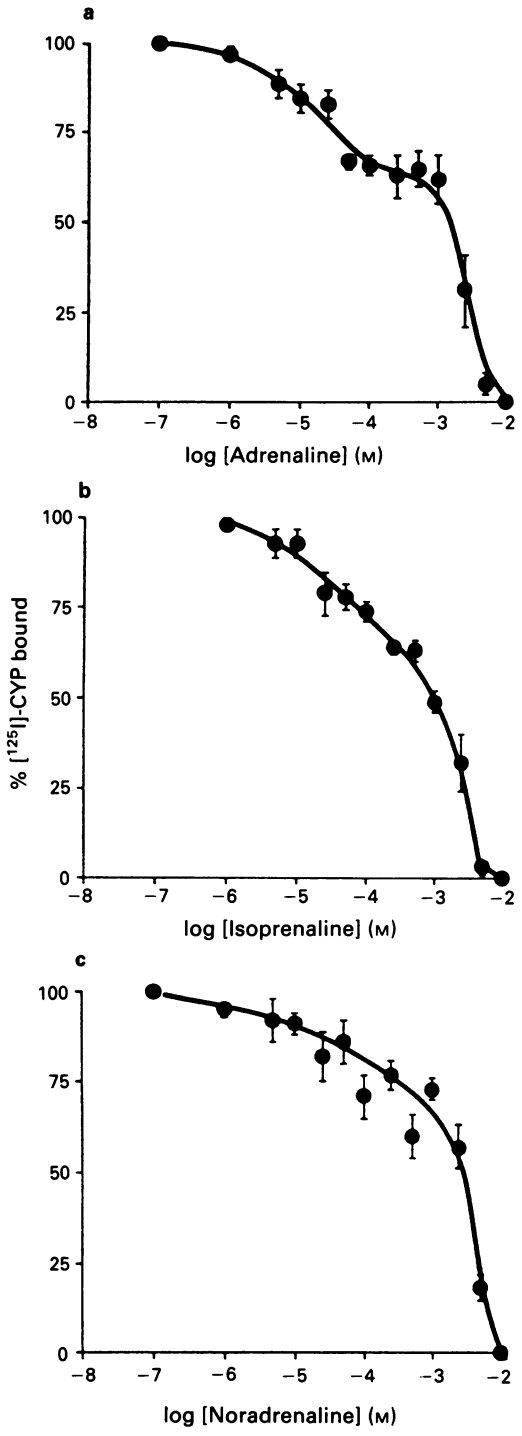

Figure 7 Mean curves for competition between (−)-[^{125}I]-cyanopindolol ((−)-[^{125}I]-CYP) and the typical β-adrenoceptor catecholamine agonists: (a) (−)-adrenaline; (b) (−)-isoprenaline; and (c) (−)-noradrenaline in the presence of 0.1 μM (−)-propranolol. Competition by each of these agonists is clearly biphasic. Points show mean ± s.e. Corresponding affinity and pseudo Hill coefficient values are given in Table 1.

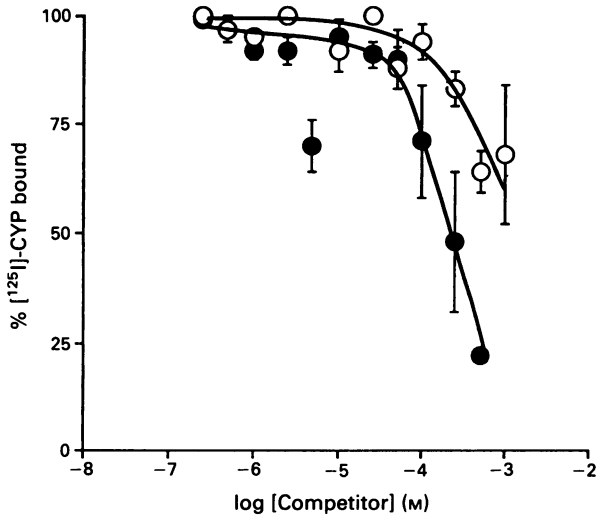

Figure 8 Mean competition binding curves between (−)-[^{125}I]-cyanopindolol ((−)-[^{125}I]-CYP) and the α_1-adrenoceptor antagonist prazosin (●) and the muscarinic antagonist atropine (○) in the presence of 0.1 μM (−)-propranolol. Points show mean ± s.e. Corresponding affinity and pseudo Hill coefficient values are given in Table 1.

atypical β-adrenoceptor identification include the typical β-adrenoceptor antagonists, alprenolol, nadolol and pindolol. Studies on guinea-pig ileum found that nadolol was an inhibitor of BRL 37344-induced relaxation, exhibiting a low affinity for the site with a pA_2 of 4.31 (Bond & Clarke, 1988). This value was 3 orders of magnitude lower than the pA_2 of 7.7 at typical β-adrenoceptors (Lee *et al.*, 1975), but compared favourably with the pA_2 value of 5.1 in rat oesophagus (Ford *et al.*, 1992) and the pK_D of 5.09 found in the present study for soleus muscle. The action of a novel β-adrenoceptor agonist, SR58306A on rat colon preparations was most effectively antagonized by alprenolol (pA_2 7) (Croci *et al.*, 1988). Alprenolol also has a higher affinity than nadolol in blocking atypical responses in guinea-pig ileum (pA_2 6.47) and rat oesophagus (pA_2 6.6) (Ford *et al.*, 1992). These values are lower than its affinity (pA_2 8.2) at typical β-adrenoceptors (Blue *et al.*, 1990).

The action of tertatolol as an antagonist varies from the typical β-adrenoceptor blockers. It has been suggested that tertatolol binds competitively to typical β-adrenoceptors and also modifies the receptor so that it is no longer available for ligand binding (De Blasi *et al.*, 1988). At atypical β-adrenoceptors tertatolol has a pA_2 value of 6.8 in guinea-pig ileum (Bond & Vanhoutte, 1992) and 6.1 in rat oesophagus which correspond to the value of 6.70 in this study, these values being 100 fold lower than the affinity of tertatolol at typical β-adrenoceptors. The affinity of (±)-CYP (pK_D 7.63) in this study is lower than its affinity at typical β-adrenoceptors (pK_D 9.4, Meunier & Labrie, 1982) but compares with the pA_2 values for (±)-CYP antagonism of isoprenaline responses in guinea-pig ileum in the presence of propranolol with a pA_2 value of 7.63 (Blue *et al.*, 1989) and more recently in rat oesophagus pA_2 7.3 (Ford *et al.*, 1992). These values are also similar to those found for the (±)-CYP antagonism of BRL 37344 mediated responses in rat gastric fundus (McLaughlin & MacDonald, 1991) and distal colon (McLaughlin & MacDonald, 1990) (Table 2).

Some authors argue that describing a new binding site as a receptor requires that the site fits certain criteria including:- affinity, reversibility, saturability, distribution, a rank order of potency of compounds and stereospecificity (Laduron, 1984). The above criteria have been satisfied in this study, for although the site showed a lack of stereoselectivity for the isomers of pindolol it shows small but significant selectivity for the stereoisomers of both tertatolol and alprenolol. One of the earliest differences reported which distinguished adipocyte adrenoceptors from typical β_1- (atrial) and β_2- (diaphragm) adrenoceptors was the lower stereoselectivity ratios of antagonists such as the isomers of alprenolol which showed a 10 fold difference for total β-adrenoceptors in adipocytes compared to a 200 fold difference for total β-adrenoceptors in atria (Harms *et al.*, 1977). The suggestion was that β-adrenoceptors existed as isoreceptors in different

Table 2 Comparison of affinities of various compounds for atypical β-adrenoceptors

Compound	*Soleus*[a*]	*Adipocytes*	*Gut*	*Oesophagus*[p]	*Cloned β_3-AR*
(−)-Propranolol	5.33	6.8[b], 5.8[c*]	6.1[g], 6.1[h]	5.9	6.35[q]
(±)-Alprenolol	5.66	6.8[b], 6.4[c*]	6.47[g], 7[i]	–	–
(−)-Alprenolol	6.16	–	–	6.6	–
(±)-Nadolol	5.09	–	4.68[g], 4.31[j]	5.1	–
(±)-Tertatolol	6.70	–	6.8[k]	6.1	–
(−)-Pindolol	4.61	–	–	–	–
(±)-Pindolol	–	–	–	5.9	–
(±)-CYP	7.63	7[b]	6.56[l], 6.67[m], 7.63[n]	7.3	–
(−)-[^{125}I]-CYP	9.28	8.82[d]	–	–	9.31[r] 9.06[q]
(±)-ICI 118551	5.45	5.3[c*], 5.3[d*]	5.5[h]	–	6.6[r*]
(±)-CGP 20712A	3.68	4.6[e], 5.3[d*]	–	–	5.6[r*]
ICI D7114	5.12	–	–	–	–
SR 58611A	5.50	–	8.4[o]	–	–
(±)-CGP 12177A	5.11	6.6[f], 6.8[d*]	–	–	6.86[r*]
BRL 37344	3.39	6.6[c*], 6.9[d*]	5.3[l]	–	6.7[r*]
(−)-Isoprenaline	3.55	4.2[c*], 5.2[d*]	6.3[l]	–	6.2[r*]
(−)-Adrenaline	3.57	3.8[c*], 3.6[d*]	5.8[h]	–	4.7[r*]
(−)-Noradrenaline	3.20	3.3[c*], 3.9[d*]	6.7[l]	–	6.3[r*]

*Values obtained from (−)-[^{125}I]-cyanopindolol ((−)-[^{125}I]-CYP) competition data; other values are functionally obtained EC_{50} or pK_A values.

[a]Present study; [b]Arch (1989); [c]Muzzin *et al.* (1991); [d]Feve *et al.* (1991); [e]Hollenga *et al.* (1991); [f]Granneman & Whitty (1991); [g]Blue *et al.* (1990); [h]Van der Vliet *et al.* (1990); [i]Croci *et al.* (1988); [j]Bond & Clarke (1988); [k]Bond & Vanhoutte (1992); [l]McLaughlin & McDonald (1991); [m]McLaughlin & McDonald (1990); [n]Blue *et al.* (1989); [o]Bianchetti & Manara (1990); [p]Ford *et al.* (1992); [q]Nahmias *et al.* (1991); [r]Emorine *et al.* (1989).

species and tissues. A different degree of stereoselectivity in two tissues is a strong indication for a difference between the receptors involved. A lower steroselectivity for antagonists is a feature of atypical β-adrenoceptors (Bojanic *et al.*, 1985; Zaagsma & Nahorski, 1990) and distinguishes a site from typical β-adrenoceptors. Autoradiographic studies of propranolol resistant (−)-[^{125}I]-CYP binding in rat skeletal muscle sections have also shown stereoselectivity for the isomers of alprenolol (Molenaar *et al.*, 1991).

A lower affinity displayed by agonists in receptor binding assays compared to their potency in functional assays is not unusual, as agonist binding prefers the high affinity state acquired in functional studies. In binding studies the receptors tend to be predominantly in the low affinity state, regardless of the assay buffer used, although agonist binding to typical β-adrenoceptors is affected by the change in assay buffer (McPherson *et al.*, 1985). However, competition by atypical agonists in this study for the propranolol-resistant site was not influenced by the choice of assay buffer (Krebs phosphate buffer or Tris-Mg^{2+} buffer). The agonist with the highest affinity for the skeletal muscle site was a phenylethanolaminotetraline, SR58611A which has previously been shown to have selective agonist activity at atypical β-adrenoceptors in rat colon (Croci *et al.*, 1988; Bianchetti & Manara, 1990) and in mediating adipocyte lipolysis (Manara & Bianchetti, 1990). The action of SR58611A in these tissues was blocked by alprenolol. BRL 37344 is a phenylethylamine analogue which stimulates lipolysis via an atypical β-adrenoceptor in rat adipocytes (Arch *et al.*, 1984; Wilson *et al.*, 1984). The action of BRL 37344 tends to be variable in different tissues. In rat gastric fundus (McLaughlin & MacDonald, 1991) and rat distal colon (McLaughlin & MacDonald, 1990) it produced tachyphylaxis to itself and to isoprenaline and was only weakly antagonized by propranolol (1 μM). ICI D7114 shows selectivity for effects on brown fat and in stimulating whole body oxygen consumption at doses which show no chronotropic effects in the heart (Holloway *et al.*, 1991). CGP 12177 appears to act as a partial agonist in brown adipose tissue where it stimulates adenylate cyclase activity (Granneman & Whitty, 1991). The partial agonist activity of CGP 12177 has also been described at the cloned β_3-adrenoceptor in rat (Granneman *et al.*, 1991) and mouse (Nahmias *et al.*, 1991). A comparison of atypical β-adrenoceptor agonist affinities obtained in various studies is given in Table 2.

Biphasic competition by the catecholamines, (−)-adrenaline, (−)-noradrenaline and (−)-isoprenaline, may be due to the low affinity that they show for this site. Table 2 shows however that low affinities for these catacholamines have also been reported in other binding studies. It is possible that the very high concentrations used could displace (−)-[^{125}I]-CYP from other sites and for this reason it is wise to limit the emphasis placed on displacement by exceptionally high concentrations of competitor. This is illustrated by the displacement by atropine and prazosin at concentrations in the millimolar range. This phenomenon may also be relevant to the displacement seen by (±)-CGP 20712A and BRL 37344 at very high concentrations.

The functional role of such receptors and their physiological significance has yet to be established. A different order of potency for endogenous agonists such as seen between β_1- and β_2- subtypes allows tissues to have different sensitivities to components of the sympathetic nervous system (Arch, 1989). The cloned β_3-adrenoceptor shows a higher sensitivity to noradrenaline than to adrenaline which has led to the suggestion that the sympathetic innervation in response to stress, high energy intake or cold acclimatization may modulate β_3-adrenoceptor activity (Emorine *et al.*, 1989). Evidence for sympathetic innervation of atypical β-adrenoceptors has been shown in guinea-pig ileum preparations (Taneja & Clarke, 1992). In these preparations the responses to para-arterial sympathetic stimulation in the presence of ICI 118551 and CGP 20712A were blocked by compounds such as (−)-alprenolol and nadolol indicating that the relaxant response could partly be attributed to the involvement of innervated atypical β-adrenoceptors.

Based on the differences in molecular structure of the β-adrenoceptor subtypes it has been suggested that the importance of a third β-adrenoceptor may relate to differences in regulation. Both β_1- and β_2-adrenoceptors are readily desensitized upon exposure to β-adrenoceptor agonists (Lefkowitz *et al.*, 1990) due to phosphorylation of Ser/Thr residues in the carboxy terminus. In contrast, the β_3-adrenoceptor is predicted to be less susceptible to desensitiza-

tion due to the presence of fewer phosphorylation sites (Emorine *et al.*, 1991).

The role of an atypical β-adrenoceptor in skeletal muscle has yet to be determined. Due to its bulk, skeletal muscle may be an important site of adrenergically induced thermogenesis (Yang & McElligott, 1989). BRL 26830A has been observed to stimulate lactate formation and inhibit glycogen synthesis in soleus muscle (Challiss *et al.*, 1988). This thermogenic response is resistant to blockade by propranolol. Also of interest is the propranolol resistance of clenbuterol-induced protein anabolism in rat soleus and plantaris muscle (Maltin *et al.*, 1989).

Taken together these functional data tend to suggest a family of β-adrenoceptors in skeletal muscle that are distinct from the β_1- and β_2-subtypes. Whether or not the receptors described in binding assays in this study are the same receptors as those identified functionally has yet to be established. However the affinity of (−)-[125I]-CYP, the resistance of (−)-[125I]-CYP binding to (−)-propranolol, the low affinity of other β-adrenoceptor antagonists, the low stereoselectivity ratios displayed by antagonists, the affinity of atypical β-adrenoceptor agonists and the potent competition shown by (±)-CYP suggests that the site present on soleus muscle is similar to atypical β-adrenoceptors described in adipocytes and gastrointestinal tissues.

This work was supported by the NH and MRC of Australia and Smith Kline Beecham Australia Pty Ltd under the Factor 'F' program. The isomers of tertatolol were kindly supplied by Dr Michel Dubar. S.J.R. is in receipt of an Australian postgraduate research scholarship. P.M. is an RD Wright Fellow (NH and MRC of Australia).

References

ARCH, J.R.S. (1989). The brown adipocyte β-adrenoceptor. *Proc. Nutr. Soc.*, **48**, 215–233.

ARCH, J.R.S., AINSWORTH, A.T., CAWTHORNE, M.A., PIERCY, V., SENNITT, M.V., THODY, V.E., WILSON, C. & WILSON, S. (1984). Atypical β-adrenoceptors on brown adipocytes as target for anti-obesity drugs. *Nature*, **309**, 363–365.

ARCH, J.R.S, CAWTHORNE, M.A., CONEY, K.A., GUSTERSON, B.A., PIERCY, V., SENNITT, M.V., SMITH, S.A., WALLACE, J. & WILSON, S. (1991). β-Adrenoceptor-mediated control of thermogenesis, body composition and glucose homeostasis. In *Obesity and Cachexia*, pp. 241–268, ed. Rothwell, N.J. & Stock, M.J. Chichester: John Wiley & Sons Ltd.

ARCH, J.R.S. & KAUMANN, A.J. (1993). β_3 and atypical β-adrenoceptors. *Med. Res. Rev.* (in press).

BIANCHETTI, A. & MANARA, L. (1990). *In vitro* inhibition of intestinal motility by phenylethanolaminotetralines: evidence of atypical β-adrenoceptors in rat colon. *Br. J. Pharmacol.*, **100**, 831–839.

BLUE, D.R., BOND, R.A., ADHAM, N., DELMENDO, R., MICHEL, A.D., EGLEN, R.M., WHITING, R.L. & CLARKE, D.E. (1989). Interaction of dihydroalprenolol and cyanopindolol with atypical β-adrenoceptors in guinea-pig ileum. *Br J. Pharmacol.*, **96**, 246P.

BLUE, D.R., BOND, R.A., ADHAM, N., DELMENDO, R., MICHEL, A.D., EGLEN, R.M., WHITING, R.L. & CLARKE, D.E. (1990). Antagonist characterisation of atypical beta adrenoceptors in guinea pig ileum: blockade by alprenolol and dihydroalprenolol. *J. Pharmacol. Exp. Ther.*, **252**, 1034–1042.

BOJANIC, D., JANSEN, J.D., NAHORSKI, S.R. & ZAAGSMA, J. (1985). Atypical characteristics of the β-adrenoceptor mediating cyclic AMP generation and lipolysis in the rat adipocyte. *Br. J. Pharmacol.*, **85**, 131–137.

BOND, R.A., CHARLTON, K.G. & CLARKE, D.E. (1986). Responses to norepinephrine resistant to inhibition by alpha and beta adrenoceptor antagonists. *J. Pharmacol. Exp. Ther.*, **236**, 408–415.

BOND, R.A. & CLARKE, D.E. (1988). Agonist and antagonist characterization of a putative adrenoceptor with distinct pharmacological properties from the α- and β-subtypes. *Br. J. Pharmacol.*, **95**, 723–734.

BOND, R.A. & VANHOUTTE, P.M. (1992). Interaction of tertatolol at the 'atypical' or beta$_3$-adrenoceptor in the guinea-pig ileum. *Gen. Pharmacol.*, **23**, 171–176.

BRISTOW, M., SHERROD, T.R. & GREEN, R.D. (1970). Analysis of beta receptor drug interactions in isolated rabbit atrium, aorta, stomach and trachea. *J. Pharmacol. Exp. Ther.*, **171**, 52–61.

BUCKNER, C.K. & CHRISTOPHERSON, R.C. (1974). Adrenergic receptors of rat esophageal smooth muscle. *J. Pharmacol. Exp. Ther.*, **189**, 467–475.

CHALLISS, R.A.J., LEIGHTON, B., WILSON, S., THURLBY, P.L. & ARCH, J.R.S. (1988). An investigation of the β-adrenoceptor that mediates metabolic responses to the novel agonist BRL28410 in rat soleus muscle. *Biochem. Pharmacol.*, **37**, 947–950.

COLEMAN, R.A., DENYER, L.H. & SHELDRICK, K.E. (1987). β-adrenoceptors in guinea-pig gastric fundus – are they the same as the atypical β-adrenoceptors in rat adipocytes? *Br. J. Pharmacol.*, **90**, 40P.

CROCI, T., CECCHI, R., TARANTINO, A., AUREGGI, G., BIANCHETTI, A., BOIGEGRAIN, R. & MANARA, L. (1988). Inhibition of rat colon motility by stimulation of atypical beta-adrenoceptors with new gut-specific agents. *Pharmacol. Res. Commun.*, **20**, 147–151.

DE BLASI, A., FRATELLI, M. & MARASCO, O. (1988). Certain β-blockers can decrease β-adrenergic receptor number: I. Acute reduction in receptor number by tertatolol and bopindolol. *Circ. Res.*, **63**, 273–278.

DETTMAR, P.W., KELLY, J. & MACDONALD, A. (1986). A non α- or β-adrenoceptor mediated effect of some catecholamines in the rat gastric fundus. *Br. J. Pharmacol.*, **89**, 498P.

ELFELLAH, M.S. & REID, J.L. (1987). Identification and characterisation of β-adrenoceptors in guinea-pig skeletal muscle. *Eur. J. Pharmacol.*, **139**, 67–72.

EMORINE, L.J., FEVE, B., PAIRAULT, J., BRIEND-SUTREN, M., MARULLO, S., DELAVIER-KLUTCHKO, C. & STROSBERG, D.A. (1991). Structural basis for functional diversity of β_1-, β_2- and β_3-adrenergic receptors. *Biochem. Pharmacol.*, **41**, 853–859.

EMORINE, L.J., MARULLO, S., BRIEND-SUTREN, M., PATEY, G., TATE, K., DELAVIER-KLUTCHKO, C. & STROSBERG, D.A. (1989). Molecular characterisation of the human β_3-adenergic receptor. *Science*, **245**, 1118–1121.

FEVE, B., BAUDE, B., KRIEF, S., STROSBERG, A.D., PAIRAULT, J. & EMORINE, L.J. (1992). Inhibition of dexamethasone of β_3-adrenergic receptor responsiveness in 3T3-F442A adipocytes. *J. Biol. Chem.*, **267**, 15909–15915.

FEVE, B., EMORINE, L.J., LASNIER, F., BLIN, N., BAUDE, B., NAHMIAS, C., STROSBERG, A.D. & PAIRAULT, J. (1991). Atypical β-adrenergic receptor in 3T3-F442A adipocytes. *J. Biol. Chem.*, **266**, 20329–20336.

FORD, A.P.D.W., TANEJA, D.T. & CLARKE, D.E. (1992). Atypical β-adrenoceptor-mediated relaxation and cyclic AMP formation in tunica muscularis mucosae (TMM) of the rat oesophagus. *Br. J. Pharmacol.*, **105**, 235P.

GRANNEMAN, J.G., LAHNERS, K.N. & CHAUDHRY, A. (1991). Molecular cloning and expression of the rat β_3-adrenergic receptor. *Mol. Pharmacol.*, **40**, 895–899.

GRANNEMAN, J.G. & WHITTY, C.J. (1991). CGP 12177A modulates brown fat adenylate cyclase activity by interacting with two distinct receptor sites. *J. Pharmacol. Exp. Ther.*, **256**, 421–425.

GRIVEGNEE, A.R., FONTAINE, J. & REUSE, J. (1984). Effect of dopamine on dog distal colon *in vitro*. *J. Pharm. Pharmacol.*, **36**, 454–457.

HARMS, H.H., ZAAGSMA, J. & DE VENTE, J. (1977). Differentiation of β-adrenoceptors in right atrium, diaphragm and adipose tissue of the rat, using stereoisomers of propranolol, alprenolol, nifenalol and practolol. *Life Sciences*, **21**, 123–128.

HOLLENGA, C.H., BROUWEAR, F. & ZAAGSMA, J. (1991). Relationship between lipolysis and cyclic AMP generation mediated by atypical β-adrenoceptors in rat adipocytes. *Br. J. Pharmacol.*, **102**, 577–580.

HOLLOWAY, B.R., HOWE, R., RAO, B.S., STRIBLING, D., MAYERS, R.M., BRISCOE, M.G. & JACKSON, J.M. (1991). ICI D7114 a novel selective β-adrenoceptor agonist selectively stimulates brown fat and increases whole-body oxygen consumption. *Br. J. Pharmacol.*, **104**, 97–104.

KAUMANN, A.J. (1989). Is there a third heart β-adrenoceptor? *Trends Pharmacol. Sci.*, **10**, 316–320.

KIM, Y.S., SAINZ, R.D., MOLENAAR, P. & SUMMERS, R.J. (1991). Characterisation of β_1- and β_2-adrenoceptors in rat skeletal muscles. *Biochem. Pharmacol.*, **42**, 1783–1789.

LADURON, P.M. (1984). Criteria for receptor sites in binding studies. *Biochem. Pharmacol.*, **33**, 833–839.

LEE, R.J., EVANS, D.B., BAKY, S.H. & LAFFAN, R.J. (1975). Pharmacology of nadolol (SQ 11725), a β-adrenergic antagonist lacking direct myocardial depression. *Eur. J. Pharmacol.*, **33**, 371–382.

LEFKOWITZ, R.J., HAUSDORFF, W.P. & CARON, M.G. (1990). Role of phosphorylation in desensitization of the β-adrenergic adrenoceptor. *Trends Pharmacol. Sci.*, **11**, 190–194.

LEW, R. & SUMMERS, R.J. (1985). Autoradiographic localization of β-adrenoceptor subtypes in guinea-pig kidney. *Br. J. Pharmacol.*, **85**, 341–348.

LOWRY, O.H., ROSEBROUGH, N.J., FARR, A.L. & RANDALL, R.J. (1951). Protein measurement with the folin phenol reagent. *J. Biol. Chem.*, **193**, 265–275.

MALTIN, C.A., HAY, S.M., DELDAY, M.I., REEDS, P.J. & PALMER, R.M. (1989). Evidence that the hypertrophic action of clenbuterol on denervated rat muscle is not propranolol-sensitive. *Br. J. Pharmacol.*, **96**, 817–822.

MANARA, L. & BIANCHETTI, A. (1990). The phenylethanolaminotetralines: new selective agonists for atypical β-adrenoceptors. *Trends Pharmacol. Sci.*, **11**, 229–230.

MCLAUGHLIN, D.P., FULTON, J.D., MACDONALD, A., MACDONALD, E. & SCOTT, P.J.W. (1988). Effects of catecholamines on human colonic circular smooth muscle. *Br. J. Pharmacol.*, **95**, 542P.

MCLAUGHLIN, D.P. & MACDONALD, A. (1990). Evidence for the existence of 'atypical' β-adrenoceptors (β_3-adrenoceptors) mediating relaxation in the rat distal colon *in vitro*. *Br. J. Pharmacol.*, **101**, 569–574.

MCLAUGHLIN, D.P. & MACDONALD, A. (1991). Characterisation of catecholamine-mediated relaxations in rat isolated gastric fundus: evidence for an atypical β-adrenoceptor. *Br. J. Pharmacol.*, **103**, 1351–1356.

MCPHERSON, G.A. (1983). A practical computer-based approach to the analysis of radioligand binding experiments. *Comput. Programs Biomed.*, **17**, 107–114.

MCPHERSON, G.A., MOLENAAR, P., MALTA, E. & RAPER, C. (1985). Influence of assay buffer on the dissociation constants of drugs at β-adrenoceptor subtypes. *Eur. J. Pharmacol.*, **119**, 93–100.

MEUNIER, H. & LABRIE, F. (1982). Specificity of the β_2-adrenergic receptor stimulating cyclic AMP accumulation in the intermediate lobe of rat pituitary gland. *Eur. J. Pharmacol.*, **81**, 411–420.

MOLENAAR, P., CANALE, E. & SUMMERS, R.J. (1987). Autoradiographic localization of beta-1 and beta-2 adrenoceptors in guinea-pig atrium and regions of the conducting system. *J. Pharmacol. Exp. Ther.*, **241**, 1048–1064.

MOLENAAR, P., ROBERTS, S.J., KIM, Y.S., PAK, H.S., SAINZ, R.D. & SUMMERS, R.J. (1991). Localisation and characterisation of two propranolol resistant (−)-[^{125}I]-cyanopindolol binding sites in rat skeletal muscle. *Eur. J. Pharmacol.*, **209**, 257–262.

MUNSON, P.J. & RODBARD, D. (1980). LIGAND: A versatile computerised approach for the characterisation of ligand binding systems. *Anal. Biochem.*, **107**, 220–239.

MUZZIN, P., REVELLI, J.-P., FRASER, C.M. & GIACOBINO, J.-P. (1992). Radioligand binding studies of the atypical β_3-adrenergic receptor in rat brown adipose tissue using [^{3}H]CGP 12177. *FEBS Lett.*, **298**, 162–164.

MUZZIN, P., REVELLI, J., KUHNE, F., GOCAYNE, J.D., MCCOMBIE, W.R., VENTER, J.C., GIACOBINO, J. & FRASER, C.M. (1991). An adipose tissue specific β-adrenergic receptor. *J. Biol. Chem.*, **266**, 24053–24058.

NAHMIAS, C., BLIN, N., ELALOUF, J.M., MATTEI, M.G., STROSBERG, A.D. & EMORINE, L.J. (1991). Molecular characterisation of the mouse β_3-adrenergic receptor: relationship with the atypical receptor of adipocytes. *EMBO J.*, **10**, 3721–3727.

NEVE, K.A., MCGONIGLE, P. & MOLINOFF, P.B. (1986). Quantitative analysis of the selectivity of radioligands for subtypes of beta adrenergic receptors. *J. Pharmacol. Exp. Ther.*, **238**, 46–53.

NORMAN, B.J. & LEATHARD, H.L. (1990). Evidence that an atypical β-adrenoceptor mediates the inhibition of spontaneous rhythmical contractions of rabbit isolated jejunum induced by ritodrine and salbutamol. *Br. J. Pharmacol.*, **101**, 27–30.

TANEJA, D.T. & CLARKE, D.E. (1992). Evidence for a noradrenergic innervation to 'atypical' beta adrenoceptors (or putative beta-3-adrenoceptors) in the ileum of guinea-pig. *J. Pharmacol. Exp. Ther.*, **260**, 192–200.

TATE, K.M., BRIEND-SUTREN, M.-M., EMORINE, L.J., DELAVIER-KLUTCHKO, C., MARULLO, S. & STROSBERG, A.D. (1991). Expression of three human β-adrenergic receptor subtypes in transfected chinese hamster ovary cells. *Eur. J. Biochem.*, **196**, 357–361.

THOMAS, R.F., HOLT, B.D., SCHWINN, D.A. & LIGGETT, S.B. (1992). Long-term agonist exposure induces upregulation of the β_3-adrenergic receptor expression via multiple cAMP response elements. *Proc. Natl. Acad. Sci. U.S.A.*, **89**, 4490–4494.

VAN DER VLIET, A., RADEMAKER, B. & BAST, A. (1990). A beta adrenoceptor with atypical characteristics is involved in the relaxation of the rat small intestine. *J. Pharmacol. Exp. Ther.*, **255**, 218–226.

WIKBERG, J. (1977). Localisation of adrenergic receptors in guinea-pig ileum and rabbit jejunum to cholinergic neurons and to smooth muscle cells. *Acta Physiol. Scand.*, **99**, 190–207.

WILLIAMS, D.W. & SUMMERS, R.J. (1990). A program for the estimation of kinetic parameters using two stage regression analysis. *Clin. Exp. Pharmacol. Physiol.*, **Suppl. 17**, 86.

WILSON, C., WILSON, S., PIERCY, V., SENNITT, M.V. & ARCH, J.R.S. (1984). The rat lipolytic β-adrenoceptor: studies using novel β-adrenoceptor agonists. *Eur. J. Pharmacol.*, **100**, 309–319.

YANG, Y.T. & MCELLIGOTT, M.A. (1989). Multiple actions of β-adrenergic agonists on skeletal muscle and adipose tissues. *Biochem. J.*, **261**, 1–10.

ZAAGSMA, J. & NAHORSKI, S.R. (1990). Is the adipocyte β-adrenoceptor a prototype for the recently cloned atypical 'β_3-adrenoceptor'? *Trends Pharmacol. Sci.*, **11**, 3–7.

(Received October 26, 1992
Revised January 15, 1993
Accepted January 27, 1993)

Br. J. Pharmacol. (1993), **109**, 353–359 © Macmillan Press Ltd, 1993

Desensitization of histamine H_1 receptor-mediated inositol phosphate production in HeLa cells

[1]David R. Bristow & M. Reza Zamani

Department of Physiological Sciences, University of Manchester, Stopford Building, Oxford Road, Manchester M13 9PT

1 Histamine stimulated the accumulation of total [^{3}H]-inositol phosphates (IP_n) in control HeLa cells with an EC_{50} of 3.7 ± 0.7 μM in the presence of 10 mM LiCl. The maximum response to histamine after 15 min incubation was $43 \pm 5\%$ over basal accumulation and occurred at a concentration of 1 mM histamine.

2 The histamine-induced IP_n production in HeLa cells was confirmed as H_1 receptor-mediated, since the H_1 antagonist mepyramine (10^{-6} M) inhibited the histamine response (10^{-4} M) by $83 \pm 7\%$, whereas the H_2 antagonist, ranitidine (10^{-4} M), and H_3 antagonist, thioperamide (10^{-6} M), were ineffective.

3 Histamine (10^{-4} M) pretreatment of HeLa cells for 30 min desensitized the subsequent histamine-induced IP_n accumulation. The desensitized cells accumulated IP_n in response to histamine with an EC_{50} of 1.7 ± 0.7 μM after 15 min incubation. The maximum histamine-induced IP_n accumulation at 10^{-4} M was $19 \pm 5\%$ over basal and was significantly lower ($P < 0.03$) than the maximum response in control cells.

4 The desensitization of histamine-induced IP_n accumulation was time-dependent and, at a desensitizing histamine concentration of 10^{-4} M, the half-maximal attenuation occurred after approximately 9 min and maximum desensitization was achieved by 15–20 min. The desensitization of the IP_n accumulation was a reversible phenomenon and full recovery of the response occurred 150 min after the removal of the desensitizing histamine-containing medium. The half-time for the recovery of the histamine-induced response was estimated at 120 min.

5 Bradykinin stimulated IP_n accumulation in HeLa cells, and the EC_{50} in control cells of 1.9 ± 0.2 nM was not significantly different from the EC_{50} value from histamine-pretreated cells of 1.6 ± 0.9 nM. The bradykinin response at 1 μM was $194 \pm 48\%$ over basal IP_n accumulation in control cells and this value was significantly different ($P < 0.04$) from the 1 μM bradykinin-induced IP_n accumulation in histamine-pretreated HeLa cells of $143 \pm 38\%$ over basal.

6 NaF stimulated IP_n accumulation in control HeLa cells in a dose-related manner, with the maximum effect occurring at 15–20 mM. The EC_{50} value for NaF-stimulated IP_n accumulation in control cells was 10.5 ± 1.1 mM and the maximum response was $136 \pm 41\%$ over basal after 20 min incubation. In histamine desensitized HeLa cells the EC_{50} value for NaF was 12.3 ± 0.4 mM after 20 min stimulation, which was not significantly different from the value obtained in control cells. The maximum NaF-stimulated IP_n formation in desensitized cells of $68 \pm 23\%$ over basal occurred at 15–20 mM and was significantly lower ($P < 0.01$) than that obtained in control cells.

7 We show here that the acute histamine pretreatment of HeLa cells results in the desensitization of histamine H_1 receptor-mediated IP_n production. The desensitization was not restricted to the H_1 receptor-mediated signal transduction pathway, but also includes both the bradykinin- and NaF-mediated responses, supporting a heterologous desensitization mechanism. Our results are consistent with the site of attenuation being at or distal to the G-protein and the underlying mechanism being a slowed time-course for the production of inositol phosphates.

Keywords: Histamine H_1 receptors; desensitization; heterologous desensitization; inositol phosphates; HeLa cells

Introduction

The prolonged exposure of many hormone and neurotransmitter receptors to agonists leads to an attenuation of the response to continued or subsequent agonist stimulation. This phenomenon, called desensitization, encompasses a number of distinct mechanisms, some or all of which may come into play depending on the severity of receptor stimulation (Lefkowitz *et al.*, 1990). In the early stages of agonist stimulation, this transient process is thought to prevent the consequences of excessive receptor stimulation. Additionally, long-term agonist-stimulation may result in an alteration in the rate of receptor production and degradation (Lefkowitz *et al.*, 1990). Thus, by exercising strict control over receptor function, desensitization has a pivotal role in the overall response of a cell to agonist stimulation, allowing a rapid modification of cellular response according to changing environmental conditions. Desensitization therefore has an important function in cellular homeostasis.

Receptor desensitization can be classified into two categories: homologous and heterologous. Homologous desensitization is a loss of responsiveness in the receptor that has been stimulated, whereas heterologous desensitization is where the prolonged stimulation of one receptor produces an attenuation both of its own response as well as the responses initiated by other receptors. The adenylate cyclase-coupled β-adrenoceptor has been extensively studied and many of the mechanisms of desensitization have been defined (Huganir & Greengard, 1990; Lefkowitz *et al.*, 1990). The salient features of short-term β-adrenoceptor desensitization involve receptor uncoupling and sequestration. Two protein kinases, β-adrenoceptor kinase (βARK) and protein kinase A, phosphorylate β-adrenoceptor proteins and appear to modulate the coupling between the receptor and G_s-protein. Protein kinase

[1] Author for correspondence.

A is adenosine 3':5'-cyclic monophosphate (cyclic AMP)-dependent, whilst βARK is cyclic AMP-independent and will posphorylate only the agonist occupied receptors. βARK-mediated desensitization is postulated to occur at high concentrations of agonist (at high receptor occupancy) and involves a 48 kD cytosolic protein, β-arrestin. β-Arrestin has a high affinity for the βARK-phosphorylated ternary complex and competes with the binding of guanine nucleotides, and thus sterically interrupts the transduction process. Interestingly, βARK is not as specific as its name would suggest, since it has also been shown to phosphorylate the α_2-adrenoceptor and the muscarinic receptor (Benovic *et al.*, 1989; Kwatra *et al.*, 1989). βARK is a member of the large family of related enzymes (Kwatra *et al.*, 1989), and therefore it is possible that a similar mechanism may be involved in the desensitization of other G-protein coupled receptors.

In contrast to the adenylate cyclase system, our understanding of the molecular mechanisms involved in the desensitization of phosphoinositidase C-coupled receptors is still rather poor. In essence, agonist occupation of a receptor of this class activates phosphoinositidase C, via a G-protein, with the formation of diacylglycerol (DAG) and inositol 1,4,5 trisphosphate (IP_3) from phosphatidylinositol 4,5-bisphosphate ($PtdInsP_2$) (Berridge & Irvine, 1989). IP_3 releases calcium from the endoplasmic reticulum (Streb *et al.*, 1984) by interaction with a specific receptor (Taylor *et al.*, 1988), while DAG acts by stimulating protein kinase C (PKC), which controls the activity of a variety of intracellular proteins (Nishizuka, 1988), presumably by phosphorylation. There are several examples of PKC activation regulating receptor function (Dillon-Carter & Chuang, 1989; Lai *et al.*, 1990; Cowlen *et al.*, 1990) and both phorbol ester-activated and receptor-activated PKC have been shown to phosphorylate receptor proteins (Bourvier *et al.*, 1987; Leeb-Lundberg *et al.*, 1987; Kwatra *et al.*, 1989; Haga *et al.*, 1990). Thus, PKC-mediated mechanisms appear to have a role in the desensitization process of phosphoinositidase C-coupled receptors. However, it may not be the only mechanism involved, since substance P and muscarinic receptors have also been shown to desensitize by a PKC-independent process (Sugiya & Putney, 1988; Cowlen *et al.*, 1990; Lai *et al.*, 1990).

The histamine H_1 receptor is an example of a receptor coupled to the hydrolysis of $PtdInsP_2$ (Hill, 1990). The desensitization of histamine-induced responses has been observed in tissue slices (Quach *et al.*, 1981) and cultured cells (Brown *et al.*, 1986; Dillon-Carter & Chuang, 1989; Driver *et al.*, 1989; Cowlen *et al.*, 1990), but the mechanisms that bring about this adaptive change have not been elucidated. Desensitization is thought to involve both short- and long-term changes (Quach *et al.*, 1981; Driver *et al.*, 1989), which may in part occur at the level of the H_1-receptor (Quach *et al.*, 1991; Brown *et al.*, 1986; Dillon-Carter & Chuang, 1989; Cowlen *et al.*, 1990). However, both homologous and heterologous types of H_1-receptor desensitization can be induced by prior agonist exposure (Brown *et al.*, 1986; Mitsuhashi & Payan, 1988; Dillon-Carter & Chuang, 1989), suggesting that in some circumstances the modulation occurs at a site common to several receptor systems. PKC has been implicated in H_1-receptor regulation. PKC activation by phorbol esters has been shown to down-regulate [^{3}H]-mepyramine binding sites in DDT_1 MF-2 smooth muscle cells (Mitsuhashi & Payan, 1988), increase [^{3}H]-mepyramine binding in human lymphoma cells (Driver *et al.*, 1989) and reduce histamine-mediated inositol phosphate production (Dillon-Carter & Chuang, 1989; Cowlen *et al.*, 1990). Interestingly, in human lymphoma cells that have a down-regulated PCK (24 h phorbol ester pretreatment), histamine could still induce receptor down-regulation, suggesting a PKC-independent process may be involved (Driver *et al.*, 1989).

HeLa cells, a human uterine carcinoma cell line, contain several receptors that are coupled to phosphoinositidase C, including histamine H_1, bombesin and bradykinin receptors (Tilly *et al.*, 1990). The H_1-receptor responses in these cells have been characterized (Hazama *et al.*, 1985; Volpi & Berlin, 1988; Tilly *et al.*, 1990; Bristow & Young, 1991; Bootman *et al.*, 1992) and suggest that these cells are a useful system to study the mechanisms underlying H_1 receptor activation and regulation. Previous studies have shown that the histamine H_1 receptor-induced Ca^{2+}-activated K^+ conductance (Hazama *et al.*, 1985), Ca^{2+} transients (Volpi & Berlin, 1988) and inositol phosphate production (Bristow & Young, 1991) in these cells are desensitized by acute histamine stimulation. We extend these studies and describe in this paper the effect of an acute histamine pretreatment of HeLa cells on the subsequent histamine H_1-, bradykinin- and sodium fluoride-induced inositol phosphate production and characterize the desensitization of the histamine H_1 receptor response.

Methods

Cell culture

HeLa cells were grown and maintained in a Dulbecco's modified Eagle's medium (DMEM, Gibco) containing 10% (v/v) newborn calf serum (Gibco) essentially as described before (Bristow *et al.*, 1991). When they reached near confluence (approximately 15×10^6 cells per 75 cm^2 culture flask), cells were washed with phosphate-buffered saline (PBS) (in mM: NaCl 137, Na_2HPO_4 8.1, KCl 2.7 and KH_2PO_4 1.5, pH 7.4) containing 0.6 mM ethylenediaminetetraacetic acid (EDTA), dissociated with 5 ml trypsin/EDTA (500–750 BAEE units ml^{-1}/0.6 mM, Sigma) for 5 min at 37°C, centrifuged (220 *g*, 5 min) and the resulting cell pellet resuspended in DMEM with sterile pipettes. Equal aliquots of this cell suspension were transferred into 6-well culture plates (approximately 300,000 cells per well, Greiner) using autoclaved 2.5 ml Eppendorf Combitips. Cells were then incubated in 1 ml of DMEM per well in a CO_2-incubator overnight.

Labelling of cells with [^{3}H]-inositol

The medium was aspirated off the 6-well plates and the cells immediately washed with PBS/EDTA (2 ml). This was removed by aspiration and replaced with 1 ml/35 mm well of inositol-free DMEM containing 10% dialysed calf serum (v/v, Gibco), *myo*-inositol (10^{-6} M, Sigma), and [^{3}H]-inositol (5 μCi ml^{-1}, 320 nM). Incubation was allowed to continue overnight (20–24 h) at 37°C in a CO_2-incubator. A number of early experiments were carried out on cell suspensions instead of monolayers. Here cells were maintained in 75 cm^2 culture flasks until they reached confluence. They were then labelled with 8 ml [^{3}H]-inositol-containing medium (with the same composition as described above) overnight, before trypsinisation and centrifugation as described under cell culture.

Desensitization of histamine H_1 receptors

[^{3}H]-inositol prelabelled cells were incubated with 10^{-4} M histamine (in Krebs-Henseleit medium (KHM) in mM: NaCl 116, KCl 4.7, $MgSO_4$ 1.2, KH_2PO_4 1.2, $NaHCO_3$ 25, $CaCl_2$ 2.5 and glucose 11, pH 7.4) for 30 min at 37°C. Control cells were incubated with KHM only for the same time period. After preincubation, the medium was removed from the monolayers by aspiration and both the histamine-treated and control cells were washed with PBS (3 × 2 ml) and then incubated in 1 ml of KHM containing LiCl (10 mM) for 30 min at 37°C. Agonists (histamine 10^{-7}–10^{-3} M, bradykinin 10^{-11}–10^{-6} M, or sodium fluoride 1–20 mM) were then added to the medium and the incubation continued at 37°C for 15–20 min in a CO_2-incubator. When antagonists were used (10^{-6} M mepyramine, 10^{-4} M ranitidine and 10^{-6} M thioperamide) these were added to the monolayers 15 min prior to agonist stimulation. During the experiment, when out of the incubator, culture plates were placed on an electrically-heated warm plate in order to maintain the temperature at

37°C. The incubation was terminated by rapid aspiration of KHM followed immediately by the addition of 0.5 ml per well of a 5% perchloric acid solution (PCA) containing 1 mM EDTA and 1 mg ml^{-1} phytic acid (4°C). In experiments measuring the histamine concentration-response in desensitized and control HeLa cells, cell suspensions were used and prepared as follows: [^{3}H]-inositol-labelled cells in 75 cm^2 flasks were desensitized with 10^{-4} M histamine for 30 min, washed three times with 30 ml PBS/EDTA, trypsinised, centrifuged (220 g, 5 min) and the cell pellet resuspended in 950 µl KHM. Aliquots of cell suspension (50 µl, 1×10^6 cells) were transferred to 1.5 ml microcentrifuge tubes containing 190 µl of LiCl-containing KHM. Cells were incubated for 30 min at 37°C. Cells were then stimulated with 10 µl histamine (10^{-7}–10^{-3} M final concentrations) for 20 min. The incubation was rapidly terminated by the addition of 250 µl ice-cold PCA (5% final) containing EDTA (1 mM) and phytic acid (1 mg ml^{-1}). Samples were kept at 4°C for a further 20 min and then analysed for the contents of their [^{3}H]-inositol phosphates.

Extraction and measurement of [^{3}H]-inositol phosphates

Total accumulated [^{3}H]-inositol phosphates (IP_n) were extracted from the PCA cell lysates by the trioctylamine-freon method described by Sharpes & McCarl (1982) and Downes *et al.* (1986). Briefly, 400 µl of trioctylamine: 1,1,2-trichlorotrifluoroethane (1:1 v/v) was added to each PCA cell lysate sample (0.5 ml), in microcentrifuge tubes, and the solutions thoroughly vortex mixed (15 s). After centrifugation (7000 g_{max} for 3 min), 375 µl of the upper phase was added to 3 ml of 100 mM HEPES buffer (pH 7.5), in insert vials, and the samples applied to Dowex AG1-X8 anion-exchange columns (1 ml of a 1:1 AG1-X8 resin:water slurry, Biorad, formate form, 100–200 mesh). Free [^{3}H]-inositol and [^{3}H]-glycerophosphoinositol were eluted with water (10 ml) and 60 mM ammonium formate/5 mM sodium tetraborate (10 ml), respectively. Total [^{3}H]-inositol phosphates (inositol mono, di, tris, and tetrakisphosphates, [^{3}H]-IP_n) were eluted with 10 ml of 1 M ammonium phosphate/100 mM formic acid and collected in scintillation vials. Quicksafe scintillation fluid (10 ml, Zinnser) was added to each vial and the amount of radioactivity determined by scintillation counting. The incorporation of [^{3}H]-inositol into phospholipids was measured in chloroform/methanol extracts.

Analysis of data

Mean d.p.m. values ± s.e.mean were calculated and [^{3}H]-IP_n expressed as a percentage of basal or maximum values. Concentration-response data for the histamine-induced [^{3}H]-IP_n accumulation were fitted to a Hill (logistic) equation using the Harwell Library non-linear regression programme VB01A as implemented on the Cambridge IBM 3040. The programme used the following equation:

$$\text{Total [}^3\text{H]-inositol phosphates accumulated} = \text{Maximum response} \times C^n/(C^n + EC^n_{50})$$

where C is the histamine concentration, EC_{50} is the concentration giving half-maximal response. Individual data were weighted according to the reciprocal of the variance associated with them.

Chemicals

[^{3}H]-*myo*-inositol (specific activity 15–18 Ci $mmol^{-1}$) was obtained from New England Nuclear and histamine dihydrochloride and mepyramine maleate were purchased from Sigma. Ranitidine was a gift from Glaxo and Thioperamide was purchased from Cookson Chemicals. All other compounds were analytical grade and purchased mainly from BDH and Sigma.

Results

Histamine-induced [^{3}H]-inositol phosphate accumulation in HeLa cells: effect of histamine pretreatment

Histamine stimulated the accumulation of total [^{3}H]-inositol phosphate (IP_n) in control HeLa cells with an EC_{50} of 3.7 ± 0.7 µM in the presence of 10 mM LiCl (Figure 1). The maximum response to histamine after 15 min incubation was 43 ± 5% ($n = 3$) over basal accumulation and occurred at a concentration of 1 mM (Figure 1). The histamine-induced IP_n production was confirmed as H_1-receptor mediated, since the H_1 antagonist, mepyramine (10^{-6} M) inhibited the histamine response (10^{-4} M) by 83 ± 7% ($n = 5$), whereas the H_2 antagonist, ranitidine (10^{-4} M), and H_3 antagonist, thioperamide (1 µM), were ineffective (Figure 2).

Histamine (10^{-4} M) pretreatment of HeLa cells for 30 min desensitized the subsequent histamine-induced IP_n accumulation (Figure 1). The desensitized cells accumulated IP_n in response to histamine with an EC_{50} of 1.7 ± 0.7 µM ($n = 3$) after 15 min incubation, which was consistently lower than the EC_{50} value obtained from control cells (3.7 µM), but the difference did not reach statistical significance (Student's t test). In an early experiment the effect of histamine-induced desensitization on [^{3}H]-inositol incorporation into phospholipids was assessed and no significant differences were observed between control and desensitized cells (results not shown). The maximum histamine-induced IP_n accumulation at 10^{-4} M was 19 ± 5% ($n = 3$) over basal and was significantly lower ($P < 0.03$, Student's t test) than the maximum response in control cells (Figure 1). The reduced maximum histamine-induced (15 min stimulation) IP_n accumulation after histamine pretreatment of the cells (Figure 1) was consistent with the slower time course of IP_n production in desensitized cells ($t_{0.5} = 15$ min) as compared to control cells ($t_{0.5} = 4.5$ min) shown in a previous report (Bristow & Young, 1991).

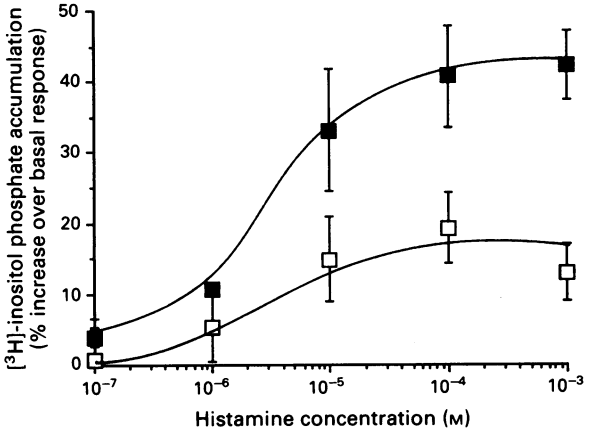

Figure 1 Concentration-response curve for histamine-induced total [^{3}H]-inositol phosphates ([^{3}H]-IP_n) formation in control (■) and desensitized (□) HeLa cells. Cells were prelabelled with [^{3}H]-inositol for 20–24 h, and were either pretreated with 10^{-4} M histamine (desensitized) or KHM (control) for 30 min. They were then extensively washed, trypsinized, and resuspended in KHM. Aliquots of cells (50 µl, 10^6 cells) were added to 240 µl KHM containing LiCl (10 mM) and stimulated with histamine (10^{-7} M–10^{-3} M) for 15 min. The accumulated [^{3}H]-IP_n were extracted and measured as described under Methods. In order to allow for variations in cellular response between experiments, values were standardized against [^{3}H]-IP_n accumulation in cells without histamine stimulation (basal). Each point is the mean ± s.e.mean of three independent experiments. The basal values for control and desensitized cells were 14990 ± 3027 d.p.m. and 15933 ± 1537 d.p.m. (mean ± s.e.mean, $n = 3$), respectively, and were not significantly different.

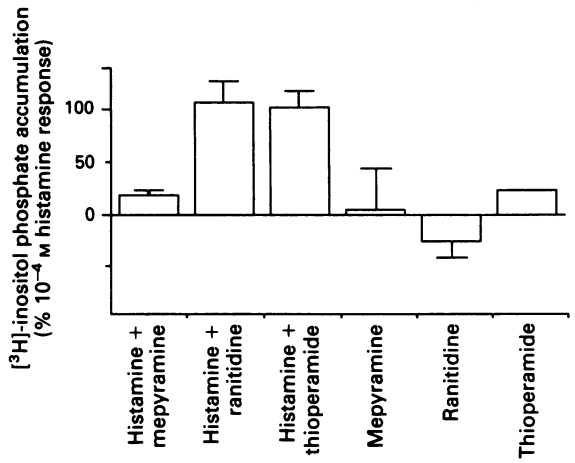

Figure 2 Histamine-induced accumulation of total [^{3}H]-inositol phosphates ([^{3}H]-IP$_n$) in HeLa cells in the presence of histamine receptor subtype antagonists. HeLa cells were prelabelled with [^{3}H]-inositol for 20–24 h and then incubated in KHM containing LiCl as described under Methods. Cell monolayers were given either antagonists and histamine (10^{-4} M) (with histamine being given 15 min after the addition of the antagonists), or the antagonist alone. The concentration of antagonists used were mepyramine, 10^{-6} M, ranitidine, 10^{-4} M, and thioperamide, 10^{-6} M. In order to allow for variations in cellular response between experiments, values were standardized against [^{3}H]-IP$_n$ accumulation in cells without histamine stimulation (basal). The [^{3}H]-IP$_n$ accumulation in cells in response to antagonists, both in the presence and the absence of histamine, is expressed as a percentage of [^{3}H]-IP$_n$ accumulation in cells stimulated with 10^{-4} M histamine. Each point is the mean ± s.e.mean of three independent experiments, except thioperamide alone which was a mean of 2 determinations.

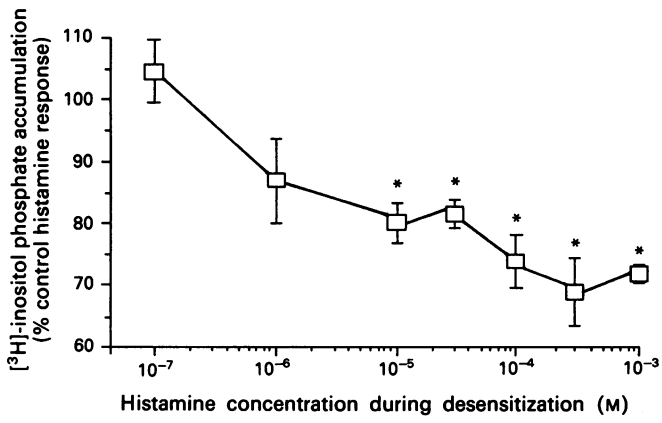

Figure 3 Concentration-response curve for histamine-induced desensitization in HeLa cells. Cells were prelabelled with [^{3}H]-inositol for 20–24 h and desensitized with varying concentrations of histamine (10^{-7}–10^{-3} M) for 30 min. They were then extensively washed, incubated in Li^+-containing KHM, and stimulated with 10^{-4} M histamine as described under Methods. In order to allow for variations in cellular response between experiments, values were standardized against total [^{3}H]-inositol phosphates ([^{3}H]-IP$_n$) accumulation in cells without histamine stimulation (basal). Data are expressed as a percentage of 10^{-4} M histamine-induced [^{3}H]-IP$_n$ accumulation in control cells (without histamine pretreatment). Each point is the mean ± s.e.mean of three independent experiments. Note that the ordinate and abcissa scales on the graph do not start at zero. *Statistically significant difference from cells desensitized with 10^{-7} M histamine (Student's t test, $P<0.008$).

Characterization of the histamine-mediated desensitization of IP$_n$ accumulation

The desensitization of histamine-induced IP$_n$ accumulation was a concentration-dependent effect (Figure 3). At a pretreatment histamine concentration of 3×10^{-4} M the maximum attenuation of IP$_n$ production was observed. The histamine-induced IP$_n$ production was not completely abolished by the histamine pretreatment, but was reduced by 31%. The concentration of histamine that causes half the maximum inhibition of response (IC_{50}) was estimated to be 2 μM (Figure 3).

The desensitization of histamine-induced IP$_n$ accumulation is time-dependent and, at a desensitizing histamine concentration of 10^{-4} M, the half-maximal attenuation occurs at approximately 9 min and maximum desensitization was achieved by 15–20 min (Figure 4). The desensitization of the IP$_n$ accumulation was a reversible phenomenon and total recovery of the response occurred 150 min after the removal of the desensitizing histamine-containing medium (Figure 5). The half-time for the recovery of the histamine-induced response was estimated as 120 min (Figure 5).

The maximum inhibition of IP$_n$ accumulation (Figure 3) and the first assessment of recovery from desensitization (Figure 5) were measured as soon as experimentally possible, but this was 60 min after the desensitizing concentration of histamine was removed. It should therefore be noted that during this time some degree of resensitization of the response may have occurred.

The homologous or heterologous nature of histamine H_1 receptor desensitization was determined by measuring the IP$_n$ accumulation induced by bradykinin and sodium fluoride (NaF). Bradykinin potently stimulated IP$_n$ accumulation in control HeLa cells (Figure 6). The EC_{50} for bradykinin in control cells of 1.9 ± 0.2 nM ($n = 3$) was not significantly different from the EC_{50} value from histamine-pretreated cells of 1.6 ± 0.9 nM ($n = 3$). The response to bradykinin in both

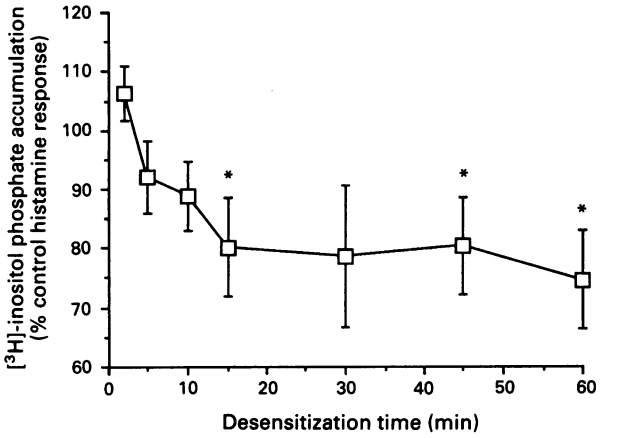

Figure 4 Time-course for histamine-induced desensitization in HeLa cells. Cells were prelabelled with [^{3}H]-inositol for 20–24 h and then desensitized with 10^{-4} M histamine for 2–60 min. The cells were extensively washed and then incubated in KHM containing LiCl and stimulated with histamine (10^{-4} M) as described under Methods. In order to allow for variations in cellular response between experiments, values were standardized against total [^{3}H]-inositol phosphates ([^{3}H]-IP$_n$) accumulation in cells without histamine stimulation (basal). Data are expressed as a percentage of 10^{-4} M histamine-induced [^{3}H]-IP$_n$ accumulation in control cells (without histamine pretreatment). Each point is the mean ± s.e.mean of three independent experiments. Note that the ordinate scale on the graph does not start at zero. *Statistically significant difference from cells desensitized for 2 min (Student's t test, $P<0.05$).

control and histamine pretreated cells reached a plateau phase at 0.1×10^{-6} M (Figure 6). The bradykinin response at 10^{-6} M was 194 ± 48% ($n = 3$) over basal IP$_n$ accumulation in control cells and this value was significantly different ($P<0.04$, paired t test) from the 10^{-6} M bradykinin-induced IP$_n$ accumulation in histamine-pretreated cells of 143 ± 38% ($n = 3$) over basal.

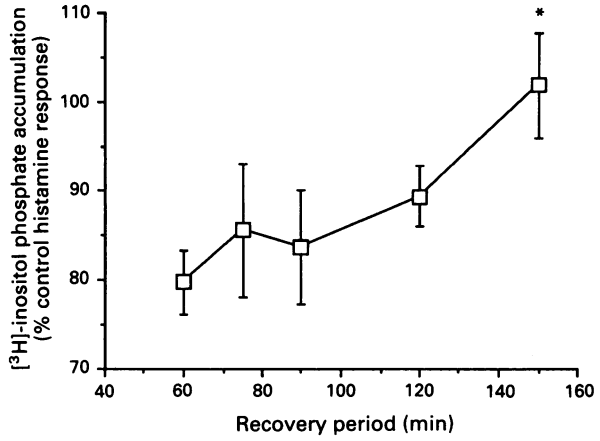

Figure 5 Time-course response for recovery from desensitization of total [^{3}H]-inositol phosphates ([^{3}H]-IP_n) accumulation in HeLa cells. Cells were prelabelled with [^{3}H]-inositol for 20–24 h and then desensitized with 10^{-4} M histamine for 30 min. The cells were extensively washed and then allowed to recover from desensitization in KHM containing LiCl at 37°C for between 60–150 min. Cells were then stimulated with histamine (10^{-4} M) for 30 min as described under Methods. Data are expressed as a percentage of 10^{-4} M histamine-induced [^{3}H]-IP_n accumulation in control cells (without histamine pretreatment). Each point is the mean ± s.e.mean of three to seven independent experiments. Note that the ordinate and abcissa scales on the graph do not start at zero. *Statistically significant difference from cells recovered from desensitization for 60 min (Student's t test, $P<0.006$).

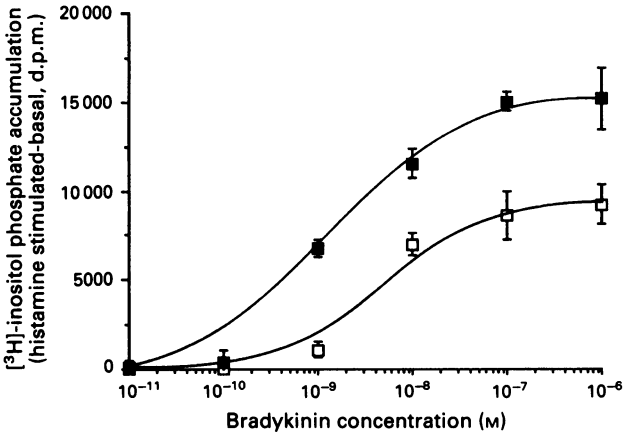

Figure 6 Concentration-response curve for bradykinin-induced total [^{3}H]-inositol phosphates ([^{3}H]-IP_n) accumulation in control (■) and desensitized (□) HeLa cells. Cells were prelabelled with [^{3}H]-inositol for 20–24 h, desensitized with 10^{-4} M histamine for 30 min, extensively washed and incubated in KHM containing LiCl as described under Methods. They were then stimulated with bradykinin (10^{-11}–10^{-6} M) for 20 min and the accumulated [^{3}H]-IP_n extracted and measured as described under Methods. Each point is the mean ± s.e.mean of triplicate samples from a representative experiment which was repeated on a further 2 occasions with similar results. Basal [^{3}H]-IP_n accumulation for control and desensitized samples were 12091 ± 749 d.p.m. and 11702 ± 523 d.p.m. (mean ± s.e.mean, $n = 3$), respectively.

NaF stimulates the G-protein directly by acting in the form of an aluminium fluoride anion (Bigay *et al.*, 1985), and thus bypasses the cell-surface receptor-mediated part of the transduction pathway. NaF stimulated IP_n accumulation in control HeLa cells in a dose-related manner (Figure 7), with a maximum effect occurring at 15–20 mM. In two experiments the IP_n accumulation at 20 mM was lower than that

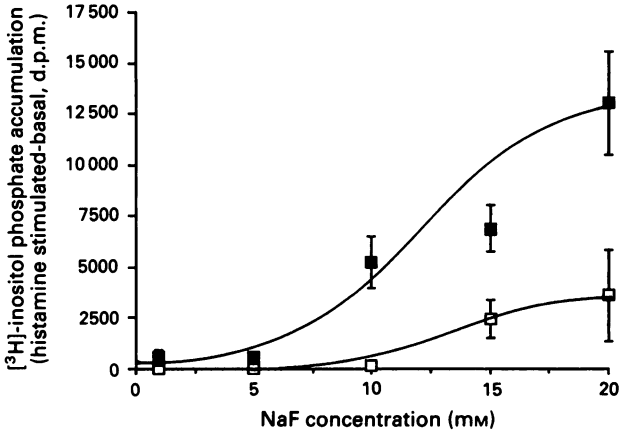

Figure 7 Concentration-response curve for NaF-induced total [^{3}H]-inositol phosphates ([^{3}H]-IP_n) accumulation in control (■) and desensitized (□) HeLa cells. Cells were prelabelled with [^{3}H]-inositol for 20–24 h, desensitized with 10^{-4} M histamine for 30 min, extensively washed and incubated in KHM containing LiCl as described under Methods. They were then stimulated with NaF (2–20 mM) for 20 min and the accumulated [^{3}H]-IP_n extracted and measured as described under Methods. Each point is the mean ± s.e.mean of triplicate samples from a representative experiment, which was repeated on a further 2 occasions with similar results. Basal [^{3}H]-IP_n accumulation for control and desensitized samples were 11308 ± 349 d.p.m. and 8359 ± 246 d.p.m. (mean ± s.e.mean, $n = 3$), respectively.

induced by 15 mM and a bell-shaped dose-response curve was obtained. The EC_{50} value for NaF-stimulated IP_n accumulation in control cells was estimated as 10.5 ± 1.1 mM ($n = 3$) and the maximum response was 136 ± 41% ($n = 3$) over basal after 20 min incubation. The EC_{50} value of NaF stimulation of control cells for 20 min was very simliar to the value of 11.5 mM obtained after 60 min NaF stimulation (results not shown). In histamine desensitized HeLa cells the EC_{50} value for NaF was 12.3 ± 0.4 mM ($n = 3$) after 20 min stimulation, which was not significantly different from the value obtained in control cells. The maximum NaF-stimulated IP_n formation in desensitized cells of 68 ± 23% ($n = 3$) over basal occurred at 15–20 mM and was significantly lower ($P<0.01$, paired t test over 15–20 mM) than that obtained in control cells.

Discussion

The results presented here show that the histamine H_1 receptor-mediated [^{3}H]-IP_n accumulation in HeLa cells can be desensitized by a prior acute treatment of the cells with histamine. The desensitization effect was manifest as a reduction in the maximum histamine-stimulated IP_n accumulation after 15 min stimulation, which was consistent with an attenuated time-course for IP_n production described previously (Bristow & Young, 1991). The desensitization of H_1 receptors was concentration- and preincubation time-dependent and was fully reversible upon removal of the agonist. The histamine pretreatment also partially reduced the bradykinin- and NaF-induced IP_n accumulation in these cells which support a heterologous type of desensitization mechanism.

Histamine H_1 receptor desensitization has been observed and studied in several tissues and cell lines (Hill, 1990). The type of desensitization mechanism shown in these previous studies is not consistent, with both homologous (Quach *et al.*, 1981; Cowlen *et al.*, 1990) and heterologous (Brown *et al.*, 1986; McDonough *et al.*, 1988) forms of H_1 receptor desensitization being reported. Homologous desensitization is thought to involve an alteration at the level of the receptor

molecules, perhaps by phosphorylation, although no evidence has been presented to date to support this contention for H_1 receptors. Some evidence does support the role of PKC in regulating H_1 receptor responsiveness (Cowlen *et al.*, 1990) and acute histamine stimulation of cells does appear to cause protein phosphorylation (Levin & Santell, 1991; Raymond *et al.*, 1991). Here we describe H_1 receptor desensitization in HeLa cells which involves a reduction in the maximum histamine-induced IP_n accumulation, an effect that has also been described in N1E-115 neuroblastoma cells (Taylor & Richelson, 1979), BC3H-1 muscle cells (Brown *et al.*, 1986) and DDT_1 MF-2 smooth muscle cell line (Cowlen *et al.*, 1990). This reduction in response may be due to a loss of functional H_1 receptors, an uncoupling of the receptor to the G-proteins, or a change in the activity of the transduction pathway distal to the G-protein. We did not observe a significant change in the EC_{50} for histamine-induced IP_n production as a result of desensitization, suggesting that the affinity of the H_1 receptor for histamine is unaltered by the desensitization process. However, additional radioreceptor binding studies would be needed to confirm this hypothesis.

The concentration of histamine required during pretreatment to induce a half-maximal desensitization (2 μM) is very similar to the EC_{50} value for histamine to stimulate IP_n production (3.7 μM). This implies that the extent of desensitization is directly proportional to the amount of receptor activity and also the intrinsic activity of the agonist. This finding is in agreement with that reported by Taylor & Richelson (1979) for histamine-stimulated cyclic GMP formation in mouse neuroblastoma cells, N1E-115.

In these studies we observe a maximum desensitization of the histamine-stimulated IP_n production that amounts to 31% inhibition of maximum response. This is substantially less than the degree of desensitization of response observed in mouse brain slices (Quach *et al.*, 1981), N1E-115 cells (Taylor & Richelson, 1979) and DDT_1 MF-2 smooth muscle cells (Cowlen *et al.*, 1990). However, in these previous studies the receptor activated response was measured between 6 and 35 min after removal of the desensitizing stimulus. Due to the inherent delay of the experimental procedure, IP_n accumulation was measured 60 min after the removal of the desensitizing stimulus and therefore considering our findings that the desensitization process is reversible, it is expected that the maximum extent of desensitization of this system will be much greater than 31%.

In the β-adrenoceptor system, desensitization is mediated by phosphorylation of the receptor (Huganir & Greengard, 1990), and loss of receptor activity and phosphorylation both occur with a half-time of 30 min, reaching maximum by 3 h (Sibley *et al.*, 1986). The desensitization of the H_1 receptor-induced IP_n accumulation observed here was time-dependent with a half-maximal effect in approximately 9 min. This time course for attenuation of the histamine response presented here corresponds with the time course for the histamine-induced phosphorylation of MARCKS protein (80 kD) in HeLa cells (Raymond *et al.*, 1991) and also p29 protein in human endothelial cells (Levin & Santell, 1991), suggesting that the desensitization process may involve protein phosphorylation. Indirect evidence to support this contention comes from the molecular cloning of the histamine H_1 receptor (Yamashita *et al.*, 1991). The amino acid sequence deduced from the cDNA encoding the H_1 receptor from bovine adrenal medulla is highly homologous with other G-protein coupled receptors, and includes several potential sites for protein phosphorylation in the third cytoplasmic loop (Yamashita *et al.*, 1991). Furthermore, the activation of protein kinases by phorbol esters are known to induce a desensitization of H_1 receptor-induced IP_n production within 10 min of exposure in cerebellar granule cells (Dillon-Carter & Chuang, 1989) and within 30 min in DDT_1 MF-2 cells (Cowlen *et al.*, 1990).

The heterologous desensitization of the H_1 receptor maybe inferred from the finding that the bradykinin- and NaF-stimulated IP_n accumulation were also attenuated after acute histamine pretreatment. NaF stimulated the production of IP_n in control and histamine-desensitized HeLa cells with similar EC_{50} values. However, the maximum IP_n production in desensitized cells was significantly lower than that of controls. It is known that NaF stimulates the transduction pathways by directly activating the G-protein in the form of an aluminium fluoride complex (Bigay *et al.*, 1985), thus bypassing the receptor-mediated process of this signal transduction pathway. Therefore, the mechanistic information that can be deduced from the NaF results is that the site of desensitization of the pathway must be located at or distal to the G-protein. However this does not preclude the possibility that the transduction pathway is regulated at more than one site.

In this study we also showed that the acute histamine stimulation of HeLa cells leads to the desensitization of the bradykinin-linked transduction pathway. Bradykinin potently stimulated IP_n production in HeLa cells and the EC_{50} value was unchanged as a result of H_1-receptor desensitization, but the maximum IP_n production was significantly attenuated. This profile parallels the features of H_1 receptor desensitization and suggests that the bradykinin recognition site on the receptor is unlikely to be involved in the desensitization process. From the heterologous nature of H_1 receptor desensitization it may be inferred that the site of regulation is common to both H_1 and bradykinin receptors and can be rationalised as follows. Histamine stimulation of H_1 receptors may initiate a cascade of cellular events, such as phosphorylation, which results not only in H_1 receptor desensitization but also in the desensitization of bradykinin receptors. In the analogous β-adrenoceptor system, protein kinase A is activated by acute agonist stimulation to phosphorylate the receptor molecule to cause β-adrenoceptor desensitization, but in addition it is thought to be responsible for heterologous desensitization (Huganir & Greengard, 1991). A similar mechanism could account for heterologous histamine H_1 receptor desensitization, or alternatively, the H_1 receptor may activate several different kinases one of which may phosphorylate the bradykinin receptor to desensitize its function. However, a caveat to this hypothesis is that in studies that observed histamine-mediated protein phosphorylation, the labelled products did not correspond to the estimated 56-kD size of the receptor protein (Raymond *et al.*, 1991; Levin & Santell, 1991).

We show here that the acute histamine pretreatment of HeLa cells results in the desensitization of histamine H_1 receptor-mediated IP_n production. The desensitization phenomenon was manifest as a reduction in the maximum receptor-mediated response, which was both time- and concentration-dependent and was fully reversible on removal of histamine. The desensitization was not restricted to the H_1 receptor-mediated signal transduction pathway, but also included both the bradykinin- and NaF-mediated responses, supporting a heterologous desensitization mechanism. Our results are consistent with the underlying mechanism being a slowed time-course for the production of inositol phosphates, which is the same as that observed in the desensitized P_{2x} purinoceptor-coupled phosphoinositidase C system (Martin & Harden, 1989), but the further characterization of this effect awaits the investigation of H_1 receptor-mediated events at the level of the calcium signal.

We are grateful to The Wellcome Trust, The Royal Society and the MRC for financial support of this project. We also thank Glaxo for the gift of ranitidine.

References

BENOVIC, J.L., DEBLASI, A., STONE, W.C., CARON, M.G. & LEFKOWITZ, R.J. (1989). β-adrenergic receptor kinase: primary structure delineates a multigene family. *Science*, **246**, 235–240.

BERRIDGE, M.J. & IRVINE, R.F. (1989). Inositol phosphates and cell signalling. *Nature*, **341**, 197–205.

BIGAY, J., DETERRE, P., PFISTER, C. & CHABRE, M. (1985). Fluoroaluminates activate transducin-GDP by mimicking the γ-phosphate of GTP in its binding site. *FEBS Lett.*, **191**, 181–185.

BOOTMAN, M.D., BERRIDGE, M.J. & TAYLOR, C.W. (1992). All-or-nothing Ca^{2+} mobilisation from the intracellular stores of single histamine-stimulated HeLa cells. *J. Physiol.*, **450**, 163–178.

BOURVIER, M., LEEB-LUNDBERG, L.M.F., BENOVIC, J.L., CARON, M.G. & LEFKOWITZ, R.J. (1987). Regulation of adrenergic receptor function by phosphorylation. II. Effects of agonist occupancy on phosphorylation of α_1- and β-adrenergic receptors by kinase C and the cyclic AMP-dependent protein kinase. *J. Biol. Chem.*, **262**, 3106–3113.

BRISTOW, D.R., ARIAS-MONTAÑO, J.A. & YOUNG, J.M. (1991). Histamine-induced inositol phosphate accumulation in HeLa cells: lithium sensitivity. *Br. J. Pharmacol.*, **104**, 677–684.

BRISTOW, D.R. & YOUNG, J.M. (1991). Characterisation of histamine-induced inositol phospholipid hydrolysis in HeLa cells. In *New Perspectives in Histamine Research: Agents and Actions Supplements*. ed. Timmerman, H. & van der Goot, H. pp. 387–392. Basel: Birkhauser Verlag.

BROWN, D.R., PRENDIVILLE, P. & CAIN, C. (1986). α_1-adrenergic and H_1-histamine receptor control of intracellular Ca^{2+} in a muscle cell line: the influence of prior agonist exposure on receptor responsiveness. *Mol. Pharmacol.*, **29**, 531–539.

COWLEN, M.S., BARNES, R.M. & TOEWS, M.L. (1990). Regulation of histamine H_1 receptor-mediated phosphoinositide hydrolysis by histamine and phorbol esters in DDT_1 MF-2 cells. *Eur. J. Pharmacol. Mol. Pharmacol. Sec.*, **188**, 105–112.

DILLON-CARTER, O. & CHUANG, D.-M. (1989). Homologous desensitisation of muscarinic cholinergic, histaminergic, adrenergic and serotonergic receptors coupled to phospholipase C in cerebellar granule cells. *J. Neurochem.*, **52**, 598–603.

DOWNES, C.P., HAWKINS, P.T. & IRVINE, R.F. (1986). Inositol 1,3,4,5-tetrakisphosphate and not phosphatidylinositol 3,4-bisphosphate stimulated parotid gland. *Biochem. J.*, **238**, 501–506.

DRIVER, A.G., KUKOLY, C.A. & BENNETT, T.E. (1989). Expression of histamine H_1 receptors on cultured histiocytic lymphoma cells. *Biochem. Pharmacol.*, **38**, 3083–3091.

HAGA, K., HAGA, T. & ICHIYAMA, A. (1990). Phosphorylation by protein kinase C of the muscarinic acetylcholine receptor. *J. Neurochem.*, **54**, 1639–1644.

HAZAMA, A., YADA, T. & OKADA, Y. (1985). HeLa cells have histamine H_1-receptors which mediate activation of the K^+ conductance. *Biochim. Biophys. Acta*, **845**, 249–253.

HILL, S.J. (1990). Distribution, properties, and functional characteristics of three classes of histamine receptor. *Pharmacol. Rev.*, **42**, 45–83.

HUGANIR, R.L. & GREENGARD, P. (1990). Regulation of neurotransmitter receptor desensitisation by protein phosphorylation. *Neuron*, **5**, 555–567.

KWATRA, M.M., BENOVIC, J.L., CARON, M.G., LEFKOWITZ, R.J. & HOSEY, M.M. (1989). Phosphorylation of chick heart muscarinic cholinergic receptors and the β-adrenergic receptor kinase. *Biochemistry*, **28**, 4543–4547.

LAI, WI. S., ROGERS, T.B. & EL-FAKAHANY, E.E. (1990). Protein kinase C is involved in desensitisation of muscarinic receptors induced by phorbol esters but not by receptor agonists. *Biochem. J.*, **267**, 23–29.

LEEB-LUNDBERG, L., COTECCHIA, S., DEBLASI, A., CARON, M.G. & LEFKOWITZ, R.J. (1987). Regulation of adrenergic receptor function by phosphorylation. *J. Biol. Chem.*, **262**, 3098–3105.

LEFKOWITZ, R.J., HAUSDORFF, W.P. & CARON, M.G. (1990). Role of phosphorylation in desensitisation of the β-adrenoceptor. *Trends Pharmacol. Sci.*, **11**, 190–194.

LEVIN, E.G. & SANTELL, L. (1991). Thrombin- and histamine-induced signal transduction in human endothelial cells. *J. Biol. Chem.*, **266**, 174–181.

MARTIN, M.W. & HARDEN, T.K. (1989). Agonist-induced desensitisation of a $P_{2\gamma}$-purinergic receptor-regulated phospholipase C. *J. Biol. Chem.*, **264**, 19535–19539.

MCDONOUGH, P.M., EUBANKS, H.J. & BROWN, J.H. (1988). Desensitisation and recovery of muscarinic and histaminergic Ca^{2+} mobilisation in 1321N1 astrocytoma cells. *Biochem. J.*, **249**, 135–141.

MITSUHASHI, M. & PAYAN, D.G. (1988). Phorbol ester-mediated desensitisation of histamine H_1 receptors on a cultured smooth muscle cell line. *Life Sci.*, **43**, 1433–1440.

NISHIZUKA, Y. (1988). The molecular heterogeneity of protein kinase C and its implications for cellular regulation. *Nature*, **334**, 661–665.

QUACH, T.T., DUCHEMIN, A., ROSE, C. & SCHWARTZ, J. (1981). Specific desensitisation of histamine H_1 receptor-mediated [^{3}H]-glycogen hydrolysis in brain slices. *Mol. Pharmacol.*, **20**, 331–338.

RAYMOND, J.R., ALBERS, F.J., MIDDLETON, J.P., LEFKOWITZ, R.J., CARON, M.G., OBEID, L.M. & DENNIS, V.W. (1991). 5-HT_{1A} and histamine H_1 receptors in HeLa cells stimulate phosphoinositide hydrolysis and phosphate uptake via distinct G protein pools. *J. Biol. Chem.*, **266**, 372–379.

SHARPES, E.S. & MCCARL, R.L. (1982). A high-performance liquid chromatographic method to measure ^{32}P incorporation into phosphorylated metabolites in cultured cells. *Anal. Biochem.*, **124**, 421–424.

SIBLEY, D.R., STRASSER, R.H., BENOVIC, J.L., DANIEL, K. & LEFKOWITZ, R.J. (1986). Phosphorylation/dephosphorylation of the β-adrenergic receptor regulates its functional coupling to adenylate cyclase and subcellular distribution. *Proc. Natl. Acad. Sci. U.S.A.*, **83**, 9408–9412.

STREB, H., BAYENDORFFER, E., HASSE, W., IRVINE, R.F. & SCHULZ, I. (1984). Effects of inositol-1,4,5-trisphosphate on isolated subcellular fractions of rat pancreas. *J. Membrane Biol.*, **81**, 241–253.

SUGIYA, H. & PUTNEY, J.W. (1988). Substance P receptor desensitisation requires receptor activation but not phospholipase C. *Am. J. Physiol.*, **255**, 149–154.

TAYLOR, C.W., BERRIDGE, M.J., BROWN, K., COOKE, A.M. & POTTER, B.V.L. (1988). DL-myo-inositol 1,4,5-trisphosphorothioate mobilises intracellular calcium in Swiss 3T3 cells and Xenopus oocytes. *Biochem. Biophys. Res. Commun.*, **150**, 626–632.

TAYLOR, J.E. & RICHELSON, E. (1979). Desensitisation of histamine H_1 receptor-mediated cyclic GMP formation in mouse neuroblastoma cells. *Mol. Pharmacol.*, **15**, 462–471.

TILLY, B.C., TERTOOLEN, G.J., LAMBRECHTS, A.C., REMORIE, R., DE LAAT, S.W. & MOOLENAAR, H.W. (1990). Histamine-H_1-receptor-mediated phosphoinositide hydrolysis, Ca^{2+} signalling and membrane-potential oscillations in human HeLa carcinoma cells. *Biochem. J.*, **266**, 235–243.

VOLPI, M. & BERLIN, R.D. (1988). Intracellular elevation of free calcium induced by activation of histamine H_1 receptors in interphase and mitotic HeLa cells: hormone signal transduction is altered during mitosis. *J. Cell Biol.*, **107**, 2533–2539.

YAMASHITA, M., FUKUI, H., SUGAMA, K., HORIO, Y., ITO, S., MIZUGUCHI, H. & WADA, H. (1991). Expression cloning of a cDNA encoding the bovine histamine H_1 receptor. *Proc. Natl. Acad. Sci. U.S.A.*, **88**, 11515–11519.

(Received October 19, 1992
Revised January 18, 1993
Accepted January 27, 1993)

Br. J. Pharmacol. (1993), **109**, 360–370 © Macmillan Press Ltd, 1993

Thermodynamics of antagonist binding to rat muscarinic M_2 receptors: antimuscarinics of the pridinol, sila-pridinol, diphenidol and sila-diphenidol type

M. Waelbroeck, J. Camus, M. Tastenoy, *G. Lambrecht, *E. Mutschler, †M. Kropfgans, †J. Sperlich, †F. Wiesenberger, †R. Tacke & [1]J. Christophe

Department of Biochemistry and Nutrition, Medical School, Université Libre de Bruxelles, Building G/E, CP 611, Route de Lennik 808, B-1070 Brussels, Belgium; *Department of Pharmacology, University of Frankfurt/M, Theodor-Stern-Kai 7, Geb. 75 A, D-6000 Frankfurt/M, Federal Republic of Germany, and †Institute of Inorganic Chemistry, University of Karlsruhe, Engesserstraße, Geb. 30.45, D-7500 Karlsruhe, Federal Republic of Germany

1 We studied the effect of temperature on the binding to rat heart M_2 muscarinic receptors of antagonists related to the carbon/silicon pairs pridinol/sila-pridinol and diphenidol/sila-diphenidol (including three germanium compounds) and six structurally related pairs of enantiomers [(**R**)- and (**S**)-procyclidine, (**R**)- and (**S**)-trihexyphenidyl, (**R**)- and (**S**)-tricyclamol, (**R**)- and (**S**)-trihexyphenidyl methiodide, (**R**)- and (**S**)-hexahydro-diphenidol and (**R**)- and (**S**)-hexbutinol]. Binding affinities were determined in competition experiments using [^{3}H]-N-methyl-scopolamine chloride as radioligand. The reference drugs were scopolamine and N-methyl-scopolamine bromide.

2 The affinity of the antagonists either increased or decreased with temperature. van 't Hoff plots were linear in the 278–310°K temperature range. Binding of all antagonists was entropy driven. Enthalpy changes varied from large negative values (down to -29 kJ mol^{-1}) to large positive values (up to $+30$ kJ mol^{-1}).

3 (**R**)-configurated drugs had a 10 to 100 fold greater affinity for M_2 receptors than the corresponding (**S**)-enantiomers. Enthalpy and entropy changes of the respective enantiomers were different but no consistent pattern was observed.

4 When silanols (R_3SiOH) were compared to carbinols (R_3COH), the affinity increase caused by C/Si exchange varied between 3 and 10 fold for achiral drugs but was negligible in the case of chiral drugs. Silanols induced more favourable enthalpy and less favourable entropy changes than the corresponding carbinols when binding. Organogermanium compounds (R_4Ge) when compared to their silicon counterparts (R_4Si) showed no significant difference in affinity as well as in enthalpy and entropy changes.

5 Exchange of a cyclohexyl by a phenyl moiety was associated with an increase or a decrease in drug affinity (depending on the absolute configuration in the case of chiral drugs) and generally also with a more favourable enthalpy change and a less favourable entropy change of drug binding.

6 Replacement of a pyrrolidino by a piperidino group and increasing the length of the alkylene chain bridging the amino group and the central carbon or silicon atom were associated with either an increase or a decrease of entropy and enthalpy changes of drug binding. However, there was no clear correlation between these structural variations and the thermodynamic effects.

7 Taken together, these results suggest that hydrogen bond-forming OH groups and, to a lesser extent, polarizable phenyl groups contribute significantly to the thermodynamics of interactions between these classes of muscarinic antagonists and M_2 muscarinic receptors.

Keywords: M_2 muscarinic receptors; binding; thermodynamics; van 't Hoff plot; enthalpy; entropy

Introduction

As recently reviewed by Raffa & Porreca (1989) as well as by Hitzemann (1988), thermodynamic analysis of drug-receptor interactions is often used to obtain new information on the differences between agonist and antagonist binding to their receptors. Interest in the temperature-dependence of drug binding was initiated by a study of Weiland *et al.* (1979). These authors observed that agonist binding to turkey erythrocyte β-adrenoceptors is far more temperature-dependent than antagonist binding. They interpreted this observation as indication that the processes leading to information transfer (conformational change of the receptor, receptor-effector interaction, etc.) are driven by enthalpy changes. In contrast with these results, we and others (Barlow *et al.*, 1979; Barlow & Burston, 1979; Waelbroeck *et al.*, 1985; Gies *et al.*, 1986; Muzio *et al.*, 1986) did not observe any coherent pattern when comparing agonist and antagonist binding to various muscarinic receptor subtypes: positive or negative enthalpy changes of binding were observed independently of the drugs' intrinsic efficacy. As explained below, we suspected that the great variation of $\Delta H°'$ and $\Delta S°'$ characterizing antagonist binding to cardiac M_2 muscarinic receptors might reflect differences in the forces driving the drug-receptor interaction (Waelbroeck *et al.*, 1985).

Hoping to identify the contribution of such forces, we investigated in this work the effect of temperature on the binding to rat cardiac muscarinic M_2 receptors of a family of muscarinic antagonists structurally related to the carbon/silicon pairs pridinol/sila-pridinol and diphenidol/sila-diphenidol (see Figure 1), including enantiomerically pure stereoisomers in the case of some chiral drugs. The selective binding and functional affinities of most of the drugs under investigation to M_1–M_4 receptors have been published elsewhere (Eltze *et al.*, 1988; Lambrecht *et al.*, 1988; 1989a,b; Feifel *et al.*, 1990; Dörje *et al.*, 1991; Waelbroeck *et al.*, 1989a,b; 1990a,b; 1991a,b; 1992). The results of functional

[1] Author for correspondence at: Department of Biochemistry and Nutrition, Medical School, Free University of Brussels, Building G/E. CP 611, Route de Lennik 808, B-1070 Brussels, Belgium.

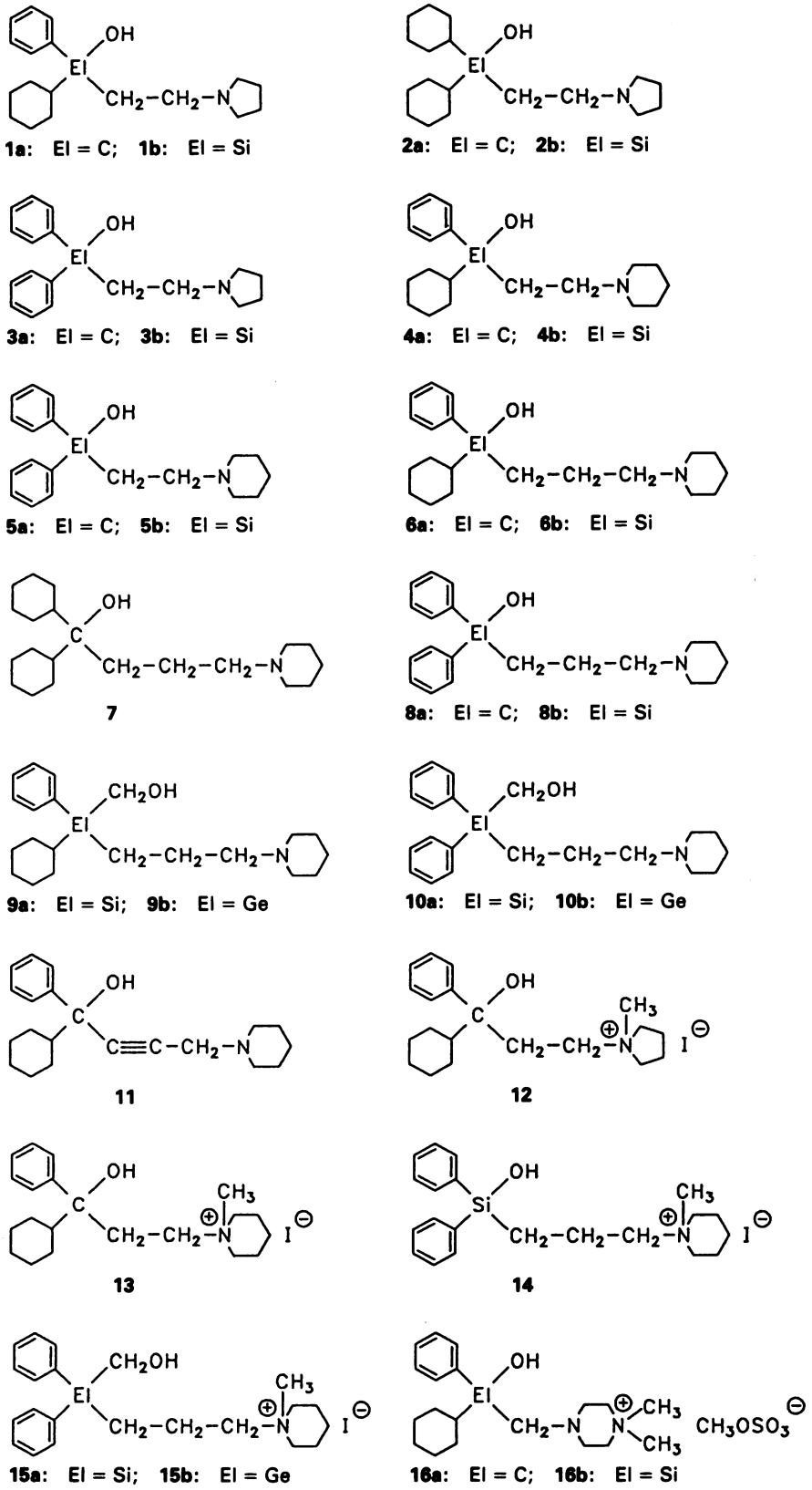

Figure 1 Chemical structure of the antagonists tested in this study (for drug names, see Tables 1 and 2).

studies (Eltze *et al.*, 1988; Lambrecht *et al.*, 1988; 1989a,b, and unpublished work; Waelbroeck *et al.*, 1989b; Feifel *et al.*, 1990) showed that all ligands used were devoid of any agonist activity. The studies described here are related to our systematic investigations on carbon/silicon bioisosterism (for a recent review, see Tacke & Linoh, 1989). Scopolamine and N-methyl-scopolamine bromide were used as reference drugs.

The compounds listed in Figure 1 were chosen to exemplify the chemical and physicochemical properties that might be of importance for enthalpy and entropy effects during drug-receptor interactions. Among the structural parameters were: absolute configuration, C/Si and Si/Ge exchange, cyclohexyl/phenyl exchange, variation in the amino group, variation of the side chain.

We chose to use a rat heart preparation for two reasons: (1) Rat heart contains only M_2 receptors, one of the five subtypes of muscarinic receptors which have been described in mammalian tissues (Hulme *et al.*, 1990; Dörje *et al.*, 1991). (2) The association and dissociation rate constants of antagonists binding to M_2 muscarinic receptors are greater than to other subtypes (M_1, M_3 or M_4) (Waelbroeck *et al.*, 1986; 1991c). It is therefore easier to achieve equilibrium binding in this system, especially at low temperatures. Binding affinities of antagonists were determined in competition experiments by the use of [^{3}H]-N-methyl-scopolamine chloride ([^{3}H]-NMS) as radioligand.

Methods

Cardiac homogenate preparation

Male Wistar Kyoto rats (200–250 g) were killed by decapitation, the heart immediately removed and rinsed in 150 mM NaCl. The homogenization buffer consisted of 20 mM Tris-HCl (pH 7.5) enriched with 250 mM sucrose. Each heart was homogenized in 2 ml of this buffer with an Ultraturrax homogenizer (maximal speed, 5 s at 4°C) followed by the addition of 13 ml of the same buffer, and 7 up and down strokes in a glass-Teflon homogenizer at 4°C. The resulting homogenate was filtered on two layers of medical gauze and either used fresh or stored in liquid nitrogen until use (with no change of muscarinic binding properties).

The protein concentration was determined according to Lowry *et al.* (1951) with bovine serum albumin as standard. The final protein concentration was 400 to 500 μg protein per assay, corresponding to about 250 pM muscarinic binding sites.

Binding assay

[^{3}H]-NMS binding was measured in a total volume of 1.2 ml, in a 50 mM sodium phosphate buffer (pH 7.4) enriched with 2 mM $MgCl_2$. The incubation periods chosen were 4 h at 4°C, 2 h at 12°C, 1 h at 25°C and 20 min at 37°C. [^{3}H]-NMS saturation curves were obtained with different tracer concentrations from 0.25 nM to 4.0 nM. The tracer concentration for competition experiments was 1.0 nM at all temperatures.

To terminate the incubation, each sample was diluted with 2 ml of ice-cold 50 mM sodium phosphate buffer (pH 7.4) and filtered on GF/C glass fibre filters (Whatman, Maidstone, England) presoaked in 0.05% polyethylenimine. The filters were rinsed three times with the same buffer, dried, and the radioactivity counted by liquid scintillation.

Non-specific binding was defined as [^{3}H]-NMS binding in the presence of 1 μM atropine.

Controls

As reported in our previous study using cardiac membranes rather than homogenates (Waelbroeck *et al.*, 1985), the total receptor concentration was not affected by temperature; the half-life of dissociation of the [^{3}H]-NMS-receptor complex varied between approximately 20 min at 5°C and less than 1 min at 37°C. The incubation times chosen in this study were well over 5 dissociation half-lives, and therefore sufficient to allow full equilibration of the binding reaction. The temperature varied by at most ± 1°C during the incubation.

Mathematical analysis and statistics

As found in our previous study (Waelbroeck *et al.*, 1985) the [^{3}H]-NMS Scatchard plots (Scatchard, 1949) were linear at all temperatures studied. The average K_D values of [^{3}H]-NMS were not significantly different from K_D values in our previous study, at the four temperatures used (Waelbroeck *et al.*, 1985).

The Hill coefficients of antagonist competition curves were not significantly different from 1.0, supporting the hypothesis that rat heart muscarinic receptors are homogeneous. Competition curves were therefore analysed assuming the existence of a single receptor class, by use of a computer assisted curve fitting procedure (Richardson & Humrich, 1984). K_i values were calculated from IC_{50} estimates using the Cheng & Prusoff (1973) equation. Affinity constants, as opposed to dissociation constants should be used to evaluate the enthalpy and entropy changes associated with binding; we therefore calculated the K_A values as $1/K_i$, the log K_A value being in fact equal to pK_i. All experiments were repeated 3 times at four temperatures. To estimate the values of the $\Delta H^{\circ\prime}$ and $\Delta S^{\circ\prime}$, we plotted the ln K_A values as a function of $1/T$, T being the absolute incubation temperature (van 't Hoff plots). All results were compatible with linear van 't Hoff plots. The enthalpy change ($\Delta H^{\circ\prime}$) due to the binding reaction was derived from the slope of this line, and the entropy change ($\Delta S^{\circ\prime}$) from its ordinate intercept, as shown by the following equation:

$$\ln K_A = -\frac{\Delta H^{\circ\prime}}{R}\frac{1}{T} + \frac{\Delta S^{\circ\prime}}{R}$$

We obtained very low standard deviations for some of the IC_{50} values; however, we felt that this is an underestimate of the true error, when taking into account the different IC_{50} value estimates obtained for a single drug in different batches of results (i.e. comparing four receptor subtypes rather than four temperatures). We therefore used the highest estimate of the standard deviation to evaluate the statistical significance of our results.

The standard deviation of each IC_{50} value was below 16% of the average value in all cases, corresponding to a ln K_A standard deviation of about 0.16, and are not mentioned in the Tables. Due to the relatively small temperature range accessible to experiment (278 to 310° K), this corresponds to large standard deviation values for enthalpy and entropy changes: ± 5.51 kJ mol^{-1} for $\Delta H^{\circ\prime}$ and ± 18.6 J mol^{-1} K^{-1} for $\Delta S^{\circ\prime}$ (assuming no error in tracers K_D values used to calculate K_A values). We used this standard deviation estimate to calculate the standard deviation of the slope and ordinate intercept of the van 't Hoff plot (proportional respectively to $\Delta H^{\circ\prime}$ and $\Delta S^{\circ\prime}$), as explained by Colquhoun (1971). Using these estimates, we considered the differences of $\Delta H^{\circ\prime}$ and $\Delta S^{\circ\prime}$ as statistically significant if they were, respectively, greater than 8.6 kJ mol^{-1} and 29.8 J mol^{-1} K^{-1} ($P > 0.90$); 11.0 kJ mol^{-1} and 37.3 J mol^{-1} K^{-1} ($P > 0.95$) or 13.2 kJ mol^{-1} and 44.7 J mol^{-1} K^{-1} ($P > 0.98$). This is indicated in the tables as (*$P > 0.90$), (**$P > 0.95$) or (***$P > 0.98$).

Compounds

Compounds were chosen to exemplify chemical and physicochemical properties which might determine the entropic and enthalpic effects of drug-receptor interactions.

Absolute configuration Some of the drugs listed in Figure 1 are chiral, containing a carbon, silicon or germanium atom as the center of chirality. We used the configurationally stable (**R**)- and (**S**)-enantiomers of the carbinols, $R^1R^2R^3COH$, to assess the importance of absolute configuration for the enthalpy and entropy changes of binding. Most of these carbinols were also studied as racemates. Since we have indications that structurally analogous silanols, $R^1R^2R^3SiOH$, may racemize in aqueous solution (Tacke *et al.*, 1987a) these drugs were only tested as racemates. The chiral (hydroxymethyl)silanes, $R^1R^2R^3SiCH_2OH$, and the chiral (hydroxymethyl)germanes, $R^1R^2R^3GeCH_2OH$, were also studied as racemates.

C/Si and Si/Ge exchange Carbon, silicon and germanium are members of Group IV of the Periodic Table. Carbon compounds $R^1R^2R^3R^4C$ may differ from their sila-analogues, $R^1R^2R^3R^4Si$, and germa-analogues, $R^1R^2R^3R^4Ge$, in several respects: (1) Due to the different covalent radii of carbon (0.77Å), silicon (1.17Å) and germanium (1.22Å), the analogues $R^1R^2R^3R^4El$ (El = C, Si, Ge) may differ in their surface (and thus in their lipophilicity) and in their conformational flexibility (C < Si < Ge); (2) Since carbon has a greater electronegativity than silicon and germanium (C > Si ≈ Ge), the carbon compounds may differ somewhat from their sila- and germa-analogues in their bond polarizations; (3) A special effect observed upon C/Si exchange (sila-substitution) of tertiary carbinols $R^1R^2R^3COH$ is an increase in OH acidity. Thus the silanols $R^1R^2R^3SiOH$ are more acidic than the carbinols and may form stronger hydrogen bonds with electron donors (Tacke & Linoh, 1989).

Generally, the chemical and physicochemical properties of silicon and germanium analogues are considerably closer to each other than to their carbon analogues (Lukevics & Ignatovich, 1992).

Cyclohexyl/phenyl exchange The cyclohexyl and phenyl group differ only slightly in size, but the phenyl moiety is considerably more polarizable than the cyclohexyl group.

Variation of the amino group Replacement of the pyrrolidino by a piperidino group as well as N-methylation leads to an increase in size.

Variation of the side chain Elongation of the El-CH_2CH_2-N chain (El = C, Si) by an additional methylene group (→El-$CH_2CH_2CH_2$-N) leads to an increase in size and conformational flexibility.

Scopolamine hydrobromide and N-methyl-scopolamine bromide were obtained from Merck (Darmstadt, Germany). Racemic procyclidine hydrochloride (*1a*.HCl) was provided by Deutsche Wellcome (Burgwedel, Germany). The (**R**)- and (**S**)-enantiomers of procyclidine [(**R**)- and (**S**)-*1a*] (Tacke *et al.*, 1986) as well as racemic sila-procyclidine (*1b*) (Tacke *et al.*, 1983; 1987b) were synthesized according to the literature. Dicyclidine (*2a*) and sila-dicyclidine (*2b*) were obtained by catalytic hydrogenation of pyrrinol (*3a*), and sila-pyrrinol (*3b*), respectively (Tacke *et al.*, unpublished work). Pyrrinol (*3a*) (Adamson, 1949), sila-pyrrinol (*3b*) (Tacke *et al.*, 1984), racemic sila-trihexyphenidyl (*4b*) (Tacke *et al.*, 1983; 1987b), pridinol (*5a*) (Adamson, 1949), sila-pridinol (*5b*) (Tacke *et al.*, 1980; 1984), racemic hexahydro-diphenidol hydrochloride (*6a*.HCl) (Tacke *et al.*, 1985), (**R**)- and (**S**)-hexahydro-diphenidol hydrochloride [(**R**)- and (**S**)-*6a*.HCl] (Tacke *et al.*, 1989a), and racemic hexahydro-sila-diphenidol hydrochloride (*6b*.HCl) (Tacke *et al.*, 1987b) were also synthesized according to published procedures. Racemic trihexyphenidyl hydrochloride (*4a*.HCl) was obtained from Sigma Chemical Co (St Louis, MO, U.S.A.), and (**R**)- and (**S**)-trihexyphenidyl hydrochloride [(**R**)- and (**S**)-*4a*.HCl] were a gift from Dr Aasen (Oslo, Norway). Dicyclidol hydrochloride (*7*.HCl) was obtained by analogy to the synthesis of (**R**)- and (**S**)-hexahydro-diphenidol hydrochloride, starting from dicyclohexyl ketone (Tacke *et al.*, unpublished work). Diphenidol (*8a*) (Miescher & Marxer, 1946) and sila-diphenidol (*8b*) (Steiling *et al.*, 1979; Tacke *et al.*, 1979) were prepared according to the literature. The racemic (hydroxymethyl)silane *9a*, the (hydroxymethyl)silane *10a*, the racemic (hydroxymethyl)germane *9b* and the (hydroxymethyl)germane *10b* were prepared (as hydrochlorides) according to the reaction sequence outlined in the literature (Tacke *et al.*, 1991) for the synthesis of *9a* (starting materials: trichloro(chloromethyl) silane and trichloro(chloromethyl)germane, respectively (Tacke *et al.*, unpublished work). (**R**)- and (**S**)-hexbutinol [(**R**)- and (**S**)-*11*] (Tacke *et al.*, 1989a) and (**R**)- and (**S**)-tricyclamol iodide [(**R**)- and (**S**)-*12*] (Tacke *et al.*, 1986) were synthesized according to the literature. (**R**)- and (**S**)-trihexyphenidyl methiodide [(**R**)- and (**S**)-N-methyl-trihexyphenidyl iodide, (**R**)- and (**S**)-*13*] were gifts from Dr Aasen (Oslo, Norway). Sila-diphenidol methiodide (N-methyl-sila-diphenidol iodide, *14*) (Steiling *et al.*, 1979) was synthesized according to the literature. The methiodides *15a* and *15b* were obtained by quaternization of the corresponding free bases *10a* and *10b*, respectively, with methyl iodide (Tacke *et al.*, unpublished work). Racemic hexocyclium methyl sulphate (*16a*) (Zaugg *et al.*, 1958) and racemic sila-hexocyclium methyl sulphate (*16b*) (Tacke *et al.*, 1989b) were synthesized according to the literature.

[^{3}H]-NMS (1-[N-methyl-^{3}H]-methyl-scopolamine chloride (74 Ci mmol^{-1}) was obtained from Amersham International (Bucks, England). Polyethylenimine was obtained from Sigma Chemicals Co (St Louis, MO, U.S.A.). All other chemicals were of the highest grade available and used as purchased.

Results

General remarks

As previously observed for selective muscarinic antagonists (Waelbroeck *et al.*, 1986; 1990b) the Hill coefficients of competition curves were not significantly different from 1.0 and [^{3}H]-NMS Scatchard plots were linear (not shown). This confirmed that rat heart muscarinic receptors were homogeneous (M_2) receptors. The log K_A values of the pridinol/sila-pridinol and diphenidol/sila-diphenidol type drugs studied

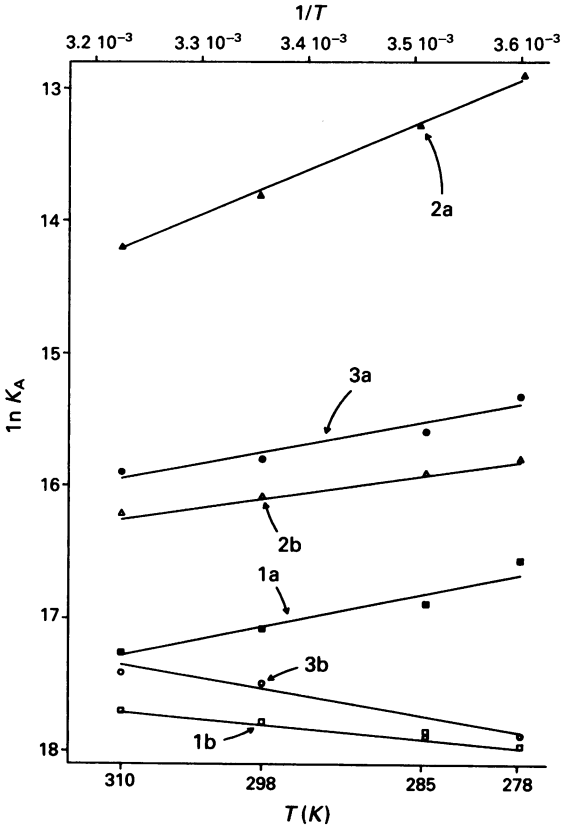

Figure 2 van 't Hoff plots of binding of procyclidine (*1a*), sila-procyclidine (*1b*), dicyclidine (*2a*), sila-dicyclidine (*2b*), pyrrinol (*3a*), and sila-pyrrinol (*3b*). The equilibrium association constants of procyclidine (*1a*) (■), sila-procyclidine (*1b*) (□), dicyclidine (*2a*) (▲), sila-dicyclidine (*2b*) (△), pyrrinol (*3a*) (●), and sila-pyrrinol (*3b*) (○) were calculated as explained in Methods, at four temperatures. ln (K_A) was then plotted as a function of the reciprocal of the absolute temperature. Each point is the average of three determinations in duplicate. The lines were drawn with the $\Delta H^{\circ\prime}$ and $\Delta S^{\circ\prime}$ values calculated as indicated in the Methods section.

here varied between 5.8 and 8.9, depending on the drug structure and, in the case of chiral compounds, on the absolute configuration (Tables 1 and 2).

When the effects of temperature on the binding of unlabelled drugs were plotted according to van 't Hoff, linear plots were obtained suggesting that $\Delta H^{\circ\prime}$ and $\Delta S^{\circ\prime}$ were constant in the temperature-range studied. This is illustrated in Figure 2 for representative antagonists. $\Delta H^{\circ\prime}$ and $\Delta S^{\circ\prime}$ values obtained from these van 't Hoff plots are summarized in Table 1 (racemic and achiral drugs) and 2 (enantiomerically pure chiral drugs). $\Delta H^{\circ\prime}$ values varied between -28.9 kJ mol^{-1} (for scopolamine binding) to $+29.6$ kJ mol^{-1} [for (**R**)-*6a*]. $\Delta S^{\circ\prime}$ values were all positive and varied between $+70$ J mol^{-1} K^{-1} (scopolamine) and $+236$ J mol^{-1} K^{-1} [(**R**)-*6a*]. There was no correlation between the affinity of antagonists for cardiac M_2 muscarinic receptors and the enthalpy or entropy changes due to drug-receptor interaction.

We already know that sila-substitution affects differently the affinity of the (**R**)- and (**S**)-enantiomers of procyclidine [(**R**)- and (**S**)-*1a*] for cardiac muscarinic receptors, and that silanol derivatives may racemize in aqueous solution (for functional studies with the enantiomers of sila-procyclidine [(**R**)- and (**S**)-*1b*] see: Tacke *et al.*, 1987a). The values of $\Delta H^{\circ\prime}$ and $\Delta S^{\circ\prime}$ of binding of the enantiomers of chiral silanols are therefore difficult to evaluate with precision. Theoretically, if the (**S**)-enantiomers are unable to recognize muscarinic receptors, the log K_A values of racemic compounds should be underestimated by 0.3 log units [as compared to the active (**R**)-enantiomers] at all temperatures. Since $\Delta H^{\circ\prime}$ measures the temperature dependence of ln K_A (slope of the van 't Hoff plot), the $\Delta H^{\circ\prime}$ of the racemic compounds and of the corresponding active (**R**)-enantiomer should be identical. By contrast, since all log K_A values could be underestimated by 0.3 log units, resulting in an error in the determination of the ordinate intercept of van 't Hoff plots, the $\Delta S^{\circ\prime}$ of racemic drugs could be underestimated by R.ln2 = 5.8 J mol^{-1} K^{-1}. In fact, the log K_A, $\Delta H^{\circ\prime}$ and $\Delta S^{\circ\prime}$ of binding of racemic procyclidine (*1a*), trihexyphenidyl (*4a*) and hexahydro-diphenidol (*6a*) were similar to the log K_A, $\Delta H^{\circ\prime}$ and $\Delta S^{\circ\prime}$ obtained using their (**R**)-enantiomers (Tables 1 and 2) and we did not observe the expected differences of log K_A and $\Delta S^{\circ\prime}$. This was probably due, in part, to the weak but significant binding affinity of (**S**)-enantiomers to cardiac muscarinic receptors: the stereoselectivity of cardiac receptors for these drugs was 'only' 10 to 100 fold (Table 2), suggesting that the less potent enantiomer could participate in drug binding.

By analogy with these results with carbinols (R_3COH), we considered that the experimental $\Delta H^{\circ\prime}$ and $\Delta S^{\circ\prime}$ of binding of analogous racemic silanols (R_3SiOH) were reasonable estimates for the thermodynamic parameters of binding of their active (**R**)-enantiomers.

Absolute configuration

Comparison of the binding properties of the corresponding (**R**)- and (**S**)-enantiomers indicated that the enthalpy and entropy changes associated with drug binding (Table 2) could be markedly affected by the absolute configuration of the drugs.

Effect of sila-substitution

Sila-substitution increased the drug affinity for the receptor (Table 3), with the exception of the carbon/silicon pairs trihexyphenidyl/sila-trihexyphenidyl (*4a/4b*), hexahydro-diphenidol/hexahydro-sila-diphenidol (*6a/6b*) and hexocyclium/sila-hexocyclium (*16a/16b*). In all cases, C/Si exchange led to negative $\Delta\Delta H^{\circ\prime}$ and $\Delta\Delta S^{\circ\prime}$ values, significantly so for five out of eight pairs.

Silicon/germanium exchange

Substitution of the silicon by a germanium atom was associated with small non-significant decreases of the drugs' affinities and of $\Delta H^{\circ\prime}$ and $\Delta S^{\circ\prime}$ values (Table 4).

Table 1 Values of log K_A data[a] at 25°C and of the enthalpy and entropy changes associated with the binding of several racemic or achiral antagonists to rat cardiac (M_2) muscarinic receptors, measured by van 't Hoff analysis

Drugs No.	*Name*	*log* K_A	*Enthalpy changes* ($\Delta H^{\circ\prime}$) (kJ mol^{-1})	*Entropy changes* ($\Delta S^{\circ\prime}$) (J mol^{-1} K^{-1})
1a	Procyclidine	7.42	+ 14.6	+ 191
1b	Sila-procyclidine	7.72	− 5.8	+ 128
2a	Dicyclidine	5.99	+ 28.1	+ 209
2b	Sila-dicyclidine	6.98	+ 9.5	+ 166
3a	Pyrrinol	6.85	+ 11.6	+ 170
3b	Sila-pyrrinol	7.61	− 8.8	+ 116
4a	Trihexyphenidyl	7.86	+ 8.9	+ 180
4b	Sila-trihexyphenidyl	7.61	+ 2.8	+ 155
5a	Pridinol	7.50	+ 3.9	+ 156
5b	Sila-pridinol	7.76	− 4.7	+ 130
6a	Hexahydro-diphenidol	6.85	+ 26.8	+ 222
6b	Hexahydro-sila-diphenidol	6.68	+ 10.0	+ 162
7	Dicyclidol	6.06	+ 22.5	+ 193
8a	Diphenidol	6.42	+ 15.2	+ 175
8b	Sila-diphenidol	7.01	− 4.8	+ 118
9a		6.81	+ 9.7	+ 164
9b		6.31	+ 7.5	+ 148
10a		6.16	+ 8.1	+ 146
10b		6.12	+ 4.9	+ 133
14	N-methyl-sila-diphenidol iodide	8.01	− 19.1	+ 90
15a		6.78	− 9.5	+ 98
15b		6.73	− 12.4	+ 87
16a	Hexocyclium methyl sulphate	7.61	+ 3.0	+ 154
16b	Sila-hexocyclium methyl sulphate	7.50	− 4.0	+ 130

[a]The standard deviation of log K_A was about 0.10 and the standard deviation of the estimates of $\Delta H^{\circ\prime}$ and $\Delta S^{\circ\prime}$ approximately $\pm$ 5.51 kJ mol^{-1} and $\pm$ 18.6 J mol^{-1} K^{-1}, respectively (see text: Mathematical analysis and statistics).

Table 2 Values of log K_A at 25°C and of the enthalpy and entropy changes associated with the binding of the (R)- and (S)-enantiomers of several antagonists to rat cardiac (M_2) muscarinic receptors, measured by van 't Hoff analysis[a]

Drugs No.	*Name*	log K_A	*Enthalpy changes* ($\Delta H^{\circ\prime}$) (kJ mol^{-1})	*Entropy changes* ($\Delta S^{\circ\prime}$) (J mol^{-1} K^{-1})
(R)-*1a*	(R)-Procyclidine	7.58	+ 13.6	+ 190
(S)-*1a*	(S)-Procyclidine	5.76	+ 18.5	+ 172
(R)-*4a*	(R)-Trihexyphenidyl	7.81	+ 8.5	+ 178
(S)-*4a*	(S)-Trihexyphenidyl	6.01	+ 13.8	+ 162
(R)-*6a*	(R)-Hexahydro-diphenidol	7.08	+ 29.6	+ 236
(S)-*6a*	(S)-Hexahydro-diphenidol	5.81	+ 21.4	+ 183***
(R)-*11*	(R)-Hexbutinol	7.98	− 5.4	+ 134
(S)-*11*	(S)-Hexbutinol	7.15	+ 23.8***	+ 217***
(R)-*12*	(R)-Tricyclamol iodide	8.38	+ 18.2	+ 221
(S)-*12*	(S)-Tricyclamol iodide	6.61	+ 12.1	+ 167***
(R)-*13*	(R)-N-methyl-trihexyphenidyl iodide	8.92	+ 14.3	+ 218
(S)-*13*	(S)-N-methyl-trihexyphenidyl iodide	6.98	+ 7.7	+ 159***
	Scopolamine	8.76	− 28.9	+ 70
	N-methyl-scopolamine bromide	9.53	− 26.9	+ 92

[a]The standard deviation of log K_A was about 0.10 and the standard deviation of the estimates of $\Delta H^{\circ\prime}$ and $\Delta S^{\circ\prime}$ approximately ± 5.51 kJ mol^{-1} and ± 18.6 J mol^{-1} K^{-1}, respectively (see text: Mathematical analysis and statistics).
***Significantly different ($P > 0.98$) from entropy (enthalpy) change associated with binding of the (R)-enantiomer.

Table 3 Differences between the log K_A, $\Delta H^{\circ\prime}$ and $\Delta S^{\circ\prime}$ values observed when comparing the binding of structurally analogous carbinols and silanols (C/Si exchange, sila-substitution)

Drugs	Δ log K_A	$\Delta\Delta H^{\circ\prime}$ (kJ mol^{-1})	$\Delta\Delta S^{\circ\prime}$ (J mol^{-1} K^{-1})
Procyclidine (*1a*)/ Sila-procyclidine (*1b*)	+ 0.30	− 20.4***	− 63***
Dicyclidine (*2a*)/ Sila-dicyclidine (*2b*)	+ 0.99	− 18.6***	− 43**
Pyrrinol (*3a*)/Sila-pyrrinol (*3b*)	+ 0.76	− 20.4***	− 54***
Trihexyphenidyl (*4a*)/ Sila-trihexyphenidyl (*4b*)	− 0.25	− 6.1	− 25
Pridinol (*5a*)/Sila-pridinol (*5b*)	+ 0.26	− 8.6*	− 26
Hexahydro-diphenidol (*6a*)/ Hexahydro-sila-diphenidol (*6b*)	− 0.17	− 16.8***	− 60***
Diphenidol (*8a*)/Sila-diphenidol (*8b*)	+ 0.59	− 20.0*	− 57***
Hexocyclium methyl sulphate (*16a*)/ Sila-hexocyclium methyl sulphate (*16b*)	− 0.11	− 7.0	− 24

Statistically significant: *$P > 0.90$; **$P > 0.95$; ***$P > 0.98$.

Table 4 Differences in log K_A, $\Delta H^{\circ\prime}$ and $\Delta S^{\circ\prime}$ values observed when comparing the binding of structurally analogous silanes and germanes (Si/Ge exchange)

Drugs	Δ log K_A	$\Delta\Delta H^{\circ\prime}$ (kJ mol^{-1})	$\Delta\Delta S^{\circ\prime}$ (J mol^{-1} K^{-1})
9a/9b	− 0.50	− 2.2	− 16
10a/10b	− 0.04	− 3.2	− 13
15a/15b	− 0.05	− 2.9	− 11

Cyclohexyl/phenyl exchange

Substitution of a cyclohexyl by a phenyl group increased or decreased the drug affinities, depending on the absolute configuration of the chiral compounds (Table 5). Except for the pair dicyclidol/(R)-hexahydro-diphenidol [*7*/(R)-*6a*], negative $\Delta\Delta H^{\circ\prime}$ values were observed when replacing the cyclohexyl by a phenyl moiety, significantly so in eight out of nineteen pairs of molecules. This was compensated by less favourable entropic effects (negative $\Delta\Delta S^{\circ\prime}$ values), statistically significant in seven out of nineteen pairs of drugs.

N-methylation of the cyclic amino group

The effect of N-methylation on log K_A, $\Delta H^{\circ\prime}$ and $\Delta S^{\circ\prime}$ values of (R)- and (S)-procyclidine [(R)- and (S)-*1a*], (R)- and (S)-trihexyphenidyl [(R)- and (S)-*4a*], sila-diphenidol [*8b*], *10a* and *10b*, is summarized in Table 6. The log K_A values were increased by up to one log unit, depending on the drugs' structure. The modifications of $\Delta H^{\circ\prime}$ and $\Delta S^{\circ\prime}$ were positive with the (R)-enantiomers, negative with the (S)-enantiomers and achiral compounds.

Pyrrolidino/piperidino exchange

Only small and non-significant modifications (of either sign) of the compounds' affinities, and of the $\Delta H^{\circ\prime}$ and $\Delta S^{\circ\prime}$ values of binding were observed (Table 7).

Table 5 Differences in log K_A, $\Delta H^{\circ\prime}$ and $\Delta S^{\circ\prime}$ values observed when comparing the binding of compounds with a cyclohexyl group and their corresponding phenyl analogues (cyclohexyl/phenyl exchange)

Drugs	Δ *log* K_A	$\Delta\Delta H^{\circ\prime}$	$\Delta\Delta S^{\circ\prime}$
1 Cyclohexyl/phenyl group		(kJ mol^{-1})	(J mol^{-1} K^{-1})
(R)-Procyclidine [(R)-*1a*]/Pyrrinol (*3a*)	− 0.73	− 2.0	− 20
(S)-Procyclidine [(S)-*1a*]/Pyrrinol (*3a*)	+ 1.09	− 6.9	− 2
Sila-procyclidine (*1b*)/ Sila-pyrrinol (*3b*)	− 0.11[a]	− 3.0	− 12
Dicyclidine (*2a*)/ (R)-Procyclidine [(R)-*1a*]	+ 1.59	− 14.5***	− 19
Dicyclidine (*2a*)/ (S)-Procyclidine [(S)-*1a*]	− 0.23	− 9.6*	− 37*
Sila-dicyclidine (*2b*)/ Sila-procyclidine (*1b*)	+ 0.74	− 15.3***	− 38*
(R)-Trihexyphenidyl [(R)-*4a*]/Pridinol (*5a*)	− 0.31	− 4.6	− 22
(S)-Trihexyphenidyl [(S)-*4a*]/Pridinol (*5a*)	+ 1.49	− 9.9*	− 6
Sila-trihexyphenidyl (*4b*)/ Sila-pridinol (*5b*)	+ 0.15[a]	− 7.5	− 25
(R)-Hexahydro-diphenidol [(R)-*6a*]/ Diphenidol (*8a*)	− 0.66	− 14.4*	− 61***
(S)-Hexahydro-diphenidol [(S)-*6a*]/ Diphenidol (*8a*)	+ 0.61	− 6.2	− 8
Hexahydro-sila-diphenidol (*6b*)/ Sila-diphenidol (*8b*)	+ 0.33[a]	− 14.8***	− 44**
Dicyclidol (*7*)/ (R)-Hexahydro-diphenidol [(R)-*6a*]	+ 1.02	+ 7.1	+ 43**
Dicyclidol (*7*)/ (S)-Hexahydro-diphenidol [(S)-*6a*]	− 0.25	− 1.1	− 10
9a/10a	− 0.65[a]	− 1.6	− 18
9b/10b	− 0.19[a]	− 2.6	− 15
2 Cyclohexyl/phenyl groups			
Dicyclidine (*2a*)/Pyrrinol (*3a*)	+ 0.86	− 16.5**	− 39*
Sila-dicyclidine (*2b*)/ Sila-pyrrinol (*3b*)	+ 0.63	− 18.3**	− 50***
Dicyclidol (*7*)/Diphenidol (*8a*)	+ 0.36	− 7.3	− 18

[a]One drug in each pair is a racemic mixture, the second an achiral molecule. The differences in log K_A, $\Delta H^{\circ\prime}$ and $\Delta S^{\circ\prime}$ shown in this Table are, therefore, approximate values only (see Results: general remarks).
Statistically significant: *$P>0.90$; **$P>0.95$; ***$P>0.98$.

Table 6 Differences in log K_A, $\Delta H^{\circ\prime}$ and $\Delta S^{\circ\prime}$ values observed when comparing the binding of tertiary and the corresponding quaternary (N-methylated) drugs (N-methylation)

Drugs	Δ *log* K_A	$\Delta\Delta H^{\circ\prime}$	$\Delta\Delta S^{\circ\prime}$
		(kJ mol^{-1})	(J mol^{-1} K^{-1})
(R)-Procyclidine [(R)-*1a*]/ (R)-Tricyclamol iodide [(R)-*12*]	+ 0.80	+ 4.6	+ 31*
(S)-Procyclidine [(S)-*1a*]/ (S)-Tricyclamol iodide [(S)-*12*]	+ 0.85	− 6.4	− 5
(R)-Trihexyphenidyl [(R)-*4a*]/ (R)-N-methyl-trihexyphenidyl iodide [(R)-*13*]	+ 1.11	+ 5.8	+ 40**
(S)-Trihexyphenidyl [(S)-*4a*]/ (S)-N-methyl-trihexyphenidyl iodide [(S)-*13*]	+ 0.97	− 6.1	− 3
Sila-diphenidol (*8b*)/ N-methyl-sila-diphenidol iodide (*14*)	+ 1.00	− 14.3***	− 28
10a/15a	+ 0.62	− 17.6***	− 48***
10b/15b	+ 0.61	− 17.3***	− 46***

Statistically significant: *$P>0.90$; **$P>0.95$; ***$P>0.98$.

Side-chain elongation

Elongation of the El-CH_2CH_2-N side chain (El = C,Si) by an additional methylene group led to a decrease by up to one log unit of log K_A values (Table 8). Except for the pair (R)-trihexyphenidyl/(R)-hexahydro-diphenidol [(R)-*4a*/(R)-*6a*] (statistically significant increases of the $\Delta H^{\circ\prime}$ and $\Delta S^{\circ\prime}$ values were found), only small and non-significant changes of either sign of $\Delta H^{\circ\prime}$ and $\Delta S^{\circ\prime}$ values were observed.

Table 7 Differences in log K_A, $\Delta H^{\circ\prime}$ and $\Delta S^{\circ\prime}$ values observed when comparing the binding of pyrrolidino-substituted compounds and their corresponding piperidino analogues (pyrrolidino/piperidino exchange)

Drugs	Δ *log* K_A	$\Delta\Delta H^{\circ\prime}$ (kJ mol^{-1})	$\Delta\Delta S^{\circ\prime}$ (J mol^{-1} K^{-1})
(R)-Procyclidine [(R)-*1a*]/ (R)-Trihexyphenidyl [(R)-*4a*]	+ 0.23	− 5.1	− 12
(S)-Procyclidine [(S)-*1a*]/ (S)-Trihexyphenidyl [(S)-*4a*]	+ 0.25	− 4.7	− 10
Sila-procyclidine (*1b*)/ Sila-trihexyphenidyl (*4b*)	− 0.11	+ 8.6	+ 27
Pyrrinol (*3a*)/Pridinol (*5a*)	+ 0.65	− 7.7	− 14
Sila-pyrrinol (*3b*)/ Sila-pridinol (*5b*)	+ 0.15	+ 4.1	+ 14
(R)-Tricyclamol iodide [(R)-*12*]/ (R)-N-methyl-trihexyphenidyl iodide [(R)-*13*]	+ 0.54	− 3.9	− 3
(S)-Tricyclamol iodide [(S)-*12*]/ (S)-N-methyl-trihexyphenidyl iodide [(S)-*13*]	+ 0.37	− 4.4	− 8

Table 8 Differences in log K_A, $\Delta H^{\circ\prime}$ and $\Delta S^{\circ\prime}$ values observed when comparing the binding of compounds with an El-CH_2CH_2-N chain (El = C, Si) and their corresponding analogues containing an El-$CH_2CH_2CH_2$-N moiety (elongation of the side chain)

Drugs	Δ *log* K_A	$\Delta\Delta H^{\circ\prime}$ (kJ mol^{-1})	$\Delta\Delta S^{\circ\prime}$ (J mol^{-1} K^{-1})
(R)-Trihexyphenidyl [(R)-*4a*]/ (R)-Hexahydro-diphenidol [(R)-*6a*]	− 0.73	+ 21.1***	+ 58***
(S)-Trihexyphenidyl [(S)-*4a*]/ (S)-Hexahydro-diphenidol [(S)-*6a*]	− 0.20	+ 7.6	+ 21
Sila-trihexyphenidyl (*4b*)/ Hexahydro-sila-diphenidol (*6b*)	− 0.93	+ 7.2	+ 7
Pridinol (*5a*)/ Diphenidol (*8a*)	− 1.08	+ 11.3	+ 19
Sila-pridinol (*5b*)/ Sila-diphenidol (*8b*)	− 0.75	− 0.1	− 12

Statistically significant: ***$P > 0.98$.

Discussion

The pioneering work of Weiland *et al.* (1979) on β-adrenoceptors led to the hope that agonists and antagonists would generally induce different enthalpy and entropy changes when associating with their receptors (independently of the drug structure or of the receptor studied), so that these differences could reflect the initiation or blockade of information transfer. Subsequent studies however indicated that this generalization was not tenable (Raffa & Porreca, 1989). Several authors therefore suggested that thermodynamic parameters of binding might reflect detailed molecular drug-receptor interactions (Kilpatrick *et al.*, 1986; Hitzemann, 1988; Miklavc *et al.*, 1990).

In an attempt to understand the enthalpic and entropic effects of non-covalent binding, the thermodynamic behaviour of simple model systems has been investigated in great detail (Edelhoch & Osborne, 1976). The forces driving the non-covalent association of two molecules are limited in number (Barrow, 1973; Ross & Subramanian, 1981).

(1) *Ionic bonds* are formed when two groups with opposite charges are brought into close contact. Since free ions interact strongly with water (ion-dipole interactions), the entropy changes associated with ionic bond formation in aqueous solutions are positive (Edelhoch & Osborne, 1976; Ross & Subramanian, 1981). The enthalpy changes are small (Ross & Subramanian, 1981) or positive (Edelhoch & Osborne, 1976). The molecular rearrangement of water being strongly temperature-dependent, the heat capacity change ($\Delta C_p^{\circ\prime}$, variation of $\Delta H^{\circ\prime}$ with temperature) associated with ionic bond formation is positive at 25°C (Edelhoch & Osborne, 1976).

(2) *van der Waals* interactions cover all dipole-dipole attractions. They can be divided into three contributions: (2a) a dipole-dipole attraction term (attraction between two molecules with a permanent dipole); (2b) an induction effect (caused by polarization of the electrons of a molecule when brought into contact with a permanent dipole); and (2c) London dispersion forces, which describe the induction effect of each 'instantaneous' dipole on the adjacent polarizable atom or molecule, allowing induced dipole-induced dipole interactions regardless of whether the interacting atoms or molecules have a permanent dipole or not (Barrow, 1973). In aqueous solution, these interactions are associated with negative enthalpy and entropy changes (Edelhoch & Osborne, 1976).

(3) *Hydrogen binding* occurs when a somewhat acidic hydrogen atom (carrying a partial positive charge) comes into contact with a lone electron pair of an atom, such as an oxygen or nitrogen atom, in a neighbouring molecule (Barrow, 1973). In aqueous solution, these interactions are also associated with negative enthalpy and entropy changes (Edelhoch & Osborne, 1976). Hydrogen bond formation, like hydrophobic interactions, is associated with a negative $\Delta Cp^{\circ\prime}$.

(4) *Hydrophobic interactions* appear when non-polar compounds are brought into contact from water. These binding interactions result from the molecular rearrangement of water, and are therefore strongly temperature-dependent. They are associated with positive enthalpy and entropy changes and (by contrast with ionic bond formation) negative heat capacity changes (Edelhoch & Osborne, 1976).

Our goal in this work was to test the hypothesis that differences in enthalpy and entropy changes, associated with antagonist binding to cardiac muscarinic M_2 receptors, could be explained by differences in hydrogen bonding or van der Waals interactions between the drug and its receptor. We therefore deliberately chose drugs with very similar chemical structures. Essential contributions to the solution of this problem was expected from the study of C/Si and Si/Ge pairs.

Binding of the muscarinic antagonists studied was driven by a large entropy increase, while the enthalpy change associated with binding varied between large positive values and large negative values (this work, Tables 1 and 2; see also Barlow *et al.*, 1979; Barlow & Burston, 1979; Waelbroeck *et al.*, 1985; Gies *et al.*, 1986; Muzio *et al.*, 1986). Few of the differences of $\Delta H^{\circ\prime}$ and $\Delta S^{\circ\prime}$ of binding ($\Delta\Delta H^{\circ\prime}$ and $\Delta\Delta S^{\circ\prime}$) observed in this work could be considered as statistically significant, due to the small temperature range accessible to experiment (5 to 37°C), and to the small structural variations studied. Nevertheless, we believe that the results of our thermodynamic analysis provides an insight into the molecular events underlying the interaction of antagonists with muscarinic receptors not obtainable by other experimental techniques. The following conclusions may be drawn:

(1) We did not observe any variation of values of $\Delta H^{\circ\prime}$ and $\Delta S^{\circ\prime}$ of binding with temperature. It is known that the cationic head of quaternary ammonium or protonated amino groups of muscarinic antagonists interacts with a negatively charged aspartate residue (Hulme *et al.*, 1990). This residue turns towards a relatively hydrophobic region of the receptor, formed by a bundle of seven transmembrane helices (Hulme *et al.*, 1990). Our results therefore suggest that the heat capacity changes due to hydrophobic, hydrogen, and ionic bond formation approximately compensated each other when the muscarinic antagonist binds to the receptor.

(2) The entropy and enthalpy changes associated with binding of the corresponding (**R**)- and (**S**)-enantiomers were often significantly different (Table 2). This is a reminder that these drugs interact with an asymmetric binding site: thermodynamic parameters reflect the drug-receptor interaction, not the drugs' chemical and physicochemical properties. The differences of affinity of the two enantiomers were below 100 fold for the compounds studied here. This corresponds either to a $\Delta\Delta H^{\circ\prime}$ value of 10.6 kJ mol^{-1} (assuming that the binding $\Delta S^{\circ\prime}$ of the two enantiomers are equal) or to a $\Delta\Delta S^{\circ\prime}$ value of 38 J mol^{-1} K^{-1} (assuming that the binding $\Delta H^{\circ\prime}$ of the two enantiomers are equal). These values would be barely significant. For compounds (**S**)-*1a* and (**S**)-*4a*, the binding $\Delta H^{\circ\prime}$ and $\Delta S^{\circ\prime}$ were both less favourable than those of (**R**)-*1a* or (**R**)-*4a* respectively: the $\Delta\Delta H^{\circ\prime}$ and $\Delta\Delta S^{\circ\prime}$ values were not statistically significant. In contrast, for the pairs of enantiomers of *6a*, *11*, *12* and *13*, the weaker (**S**)-enantiomer had either a more favourable $\Delta H^{\circ\prime}$ or a more favourable $\Delta S^{\circ\prime}$ as compared to the more potent (**R**)-enantiomer. This was overcompensated by a very large unfavourable change of $\Delta S^{\circ\prime}$ or $\Delta H^{\circ\prime}$, respectively.

(3) The enthalpy changes associated with binding of silanols (R_3SiOH) were more favourable than those associated with binding of the corresponding carbinols (R_3COH) (Table 3). On the other hand, sila-substitution resulted in less favourable entropic effects. This is in keeping with model systems (Edelhoch & Osborne, 1976; Ross & Subramanian, 1981): silanols are more acidic than carbinols and therefore susceptible to form stronger hydrogen bonds either with an electron donor atom of the receptor or with water, and hydrogen bond formation is associated with negative enthalpy and entropy changes.

(4) Since (hydroxymethyl)silanes (R_3SiCH_2OH) and (hydroxymethyl)germanes (R_3GeCH_2OH) do not differ significantly in OH acidity, lipophilicity and conformational flexibility, Si/Ge exchange did not lead to the thermodynamic effects observed upon C/Si exchange in the carbinol/silanol (R_3COH/R_3SiOH) structures (compare Tables 4 and 3). Generally, in accordance with the covalent radii ($C << Si < Ge$) and electronegativities ($C < Si \approx Ge$) of carbon, silicon and germanium, analogous silicon and germanium compounds are considerably closer by their chemical and physicochemical properties than to their corresponding carbon analogues (Lukevics & Ignatovich, 1992). These similarities in their chemical and physicochemical properties are reflected by the distinct bioisosteric relationships between analogous silicon and germanium compounds (see for example: Tacke *et al.*, 1992).

(5) The enthalpy change associated with binding of phenyl-substituted drugs was systematically more favourable than that of the corresponding cyclohexyl derivatives (Table 5). This was in keeping with results expected from model systems (Edelhoch & Osborne, 1976; Ross & Subramanian, 1981): a phenyl ring is more polarizable than a cyclohexyl group so that the contribution to van der Waals interactions via induction effects and London dispersion forces should be strengthened by substituting a cyclohexyl by a phenyl group.

(6) N-methylation of the tertiary amino group, as well as increasing the size of the heterocycle from pyrrolidino to piperidino, or lengthening the alkylene chain (i.e. changes increasing the hydrophobicity and conformational flexibility of the drugs) did not change the thermodynamic parameters of drug binding in a clear way (compare Tables 6, 7, 8). This is in keeping with model systems (Edelhoch & Osborne, 1976): dissolving hydrophobic molecules in water or their transfer from organic solvents into water (these reactions being equivalent to drug dissociation from the receptor) is associated with negative $\Delta H^{\circ\prime}$ and $\Delta S^{\circ\prime}$values, but there is no correlation between the absolute value of $\Delta H^{\circ\prime}$ and $\Delta S^{\circ\prime}$ and the size of the hydrophobic molecule (Edelhoch & Osborne, 1976).

Although not extensive, the list of studies which have applied thermodynamic analysis to pharmacological data is growing (Raffa & Porreca, 1989). The data obtained for various receptors demonstrate that there is a wide diversity in the thermodynamic profiles for agonist and antagonist ligands. For some receptors, such as the β-adrenoceptors, several reports are available (Raffa & Porreca, 1989).

As stated in the Introduction, binding of β-adrenoceptor agonists is driven by a large enthalpy decrease, while antagonist binding is associated with an entropy increase (Weiland *et al.*, 1979). This was interpreted as reflecting the receptor activation and interaction with a GTP-binding protein when an agonist is present.

More recently, Strader *et al.* (1989) identified two serine residues which are involved in agonist activation of the β-adrenoceptor. Agonist interaction with the receptor probably involves the formation of specific hydrogen bonds with these serine residues, causing the conformational changes in the receptor which lead to the activation of the GTP-binding protein. Since hydrogen bond formation is associated with the negative enthalpy and entropy changes, hydrogen bonds formation between the receptor and agonists but not between the receptor and antagonists might explain the observation that agonists but not antagonists binding to β-adrenoceptors is enthalpy driven.

Thus, thermodynamic analysis of pharmacological data potentially offers an insight into the molecular events underlying drug-receptor interactions not obtainable by other techniques. It offers the promise of measuring parameters that are more fundamental than equilibrium affinity constants. Implicit in thermodynamic analysis is quantitative measurement of the driving forces involved in the drug-receptor interaction and responsible for the affinity of an antagonist for a receptor and the efficacy of an agonist.

In conclusion, the thermodynamic analysis of the interactions of several muscarinic antagonists of the pridinol, sila-pridinol, diphenidol and sila-diphenidol type with M_2 cardiac receptors suggests that hydrogen bonds and polarizable groups play an important role in determining the enthalpy and entropy changes associated with ligand binding.

The sila-substitution approach (C/Si exchange) proved to be a valuable tool in these studies.

This work was supported by the Fund for Medical Scientific Research of Belgium (Grant 3.4525.91: J.C. and M.W.), by the Deutsche Forschungsgemeinschaft (G.L. and R.T.), by the Volkswagen-Stiftung (R.T.) and by the Fonds der Chemischen Industrie (G.L., E.M. and R.T.). In addition, this study was supported by gifts of chemicals from the Bayer AG (Leverkusen and Wuppertal – Elberfeld, Germany) (R.T.).

References

ADAMSON, D.W. (1949). Aminoalkyl tertiary carbinols and derived products. Part 1. 3-Amino-1:1-diphenylpropan-1-ols. *J. Chem. Soc.*, S144–S155.

BARLOW, R.B., BIRDSALL, N.J.M. & HULME, E.C. (1979). Temperature coefficients of affinity constants for the binding of antagonists to muscarinic receptors in the rat cerebral cortex. *Br. J. Pharmacol.*, **66**, 587–590.

BARLOW, R.B. & BURSTON, K.N. (1979). Temperature coefficients of affinity and entropies of adsorption for enantiomeric pairs of compounds acting at muscarinic receptors in the guinea-pig ileum. *Br. J. Pharmacol.*, **66**, 581–585.

BARROW, R.B. (1973). *Physical Chemistry* (International Student Edition), 3rd edn. Tokyo: McGraw Hill.

CHENG, Y. & PRUSOFF, W.H. (1973). Relationship between the inhibition constant (K_i) and the concentration of inhibitor which causes a 50 percent inhibition (I_{50}) of an enzymatic reaction. *Biochem. Pharmacol.*, **22**, 3099–3108.

COLQUHOUN, D. (1971). *Lectures in Biostatistics*. pp. 214–243. Oxford: Clarendon Press.

DÖRJE, F., WESS, J., LAMBRECHT, G., TACKE, R., MUTSCHLER, E. & BRANN, M.R. (1991). Antagonist binding profiles of five cloned human muscarinic receptor subtypes. *J. Pharmacol. Exp. Ther.*, **256**, 727–733.

EDELHOCH, H. & OSBORNE, J.C. (1976). The thermodynamic basis of the stability of proteins, nucleic acids, and membranes. *Adv. Prot. Chem.*, **30**, 183–250.

ELTZE, M., GMELIN, G., WESS, J., STROHMANN, C., TACKE, R., MUTSCHLER, E. & LAMBRECHT, G. (1988). Presynaptic muscarinic receptors mediating inhibition of neurogenic contractions in rabbit vas deferens are of the ganglionic M_1-type. *Eur. J. Pharmacol.*, **158**, 233–242.

FEIFEL, R., WAGNER-RÖDER, M., STROHMANN, C., TACKE, R., WAELBROECK, M., CHRISTOPHE, J., MUTSCHLER, E. & LAMBRECHT, G. (1990). Stereoselective inhibition of muscarinic receptor subtypes by the enantiomers of hexahydro-diphenidol and acetylenic analogues. *Br. J. Pharmacol.*, **99**, 455–460.

GIES, J.P., ILIEN, B. & LANDRY, Y. (1986). Muscarinic acetylcholine receptor: thermodynamic analysis of the interaction of agonists and antagonists. *Biochim. Biophys. Acta*, **889**, 103–115.

HITZEMANN, R. (1988). Thermodynamic aspects of drug-receptor interactions. *Trends Pharmacol. Sci.*, **9**, 408–411.

HULME, E.C., BIRDSALL, N.J.M. & BUCKLEY, N.J. (1990). Muscarinic receptor subtypes. *Annu. Rev. Pharmacol. Toxicol.*, **30**, 633–673.

KILPATRICK, G.J., EL TAYAR, N., VAN DE WATERBEEMD, H., JENNER, P., TESTA, B. & MARSDEN, C.D. (1986). The thermodynamics of agonist and antagonist binding to dopamine D-2 receptors. *Mol. Pharmacol.*, **30**, 226–234.

LAMBRECHT, G., FEIFEL, R., MOSER, U., AASEN, A.J., WAELBROECK, M., CHRISTOPHE, J. & MUTSCHLER, E. (1988). Stereoselectivity of the enantiomers of trihexyphenidyl and its methiodide at muscarinic receptor subtypes. *Eur. J. Pharmacol.*, **155**, 167–170.

LAMBRECHT, G., FEIFEL, R., MOSER, U., WAGNER-RÖDER, M., CHOO, L.K., CAMUS, J., TASTENOY, M., WAELBROECK, M., STROHMANN, C., TACKE, R., RODRIGUES DE MIRANDA, J.F., CHRISTOPHE, J. & MUTSCHLER, E. (1989a). Pharmacology of hexahydro-difenidol, hexahydro-sila-difenidol and related selective muscarinic antagonists. *Trends Pharmacol. Sci. Suppl.*, **10**, 60–64.

LAMBRECHT, G., FEIFEL, R., WAGNER-RÖDER, M., STROHMANN, C., ZILCH, H., TACKE, R., WAELBROECK, M., CHRISTOPHE, J., BODDEKE, H. & MUTSCHLER, E. (1989b). Affinity profiles of hexahydro-sila-difenidol analogues at muscarinic receptor subtypes. *Eur. J. Pharmacol.*, **168**, 71–80.

LOWRY, O.H., ROSEBROUGH, N.J., FARR, A.L. & RANDALL, R.J. (1951). Protein measurement with the Folin phenol reagent. *J. Biol. Chem.*, **193**, 265–275.

LUKEVICS, E. & IGNATOVICH, L. (1992). Comparative study of the biological activity of organosilicon and organogermanium compounds. *App. Organomet. Chem.*, **6**, 113–126.

MIESCHER, K. & MARXER, A. (1946). Amino alcohols. *U.S. Pat. 2,411,664*.

MIKLAVC, A., KOCJAN, D., MAVRI, J., KOLLER, J. & HADZI, D. (1990). On the fundamental difference in the thermodynamics of agonist and antagonist interactions with β-adrenergic receptors and the mechanism of entropy-driven binding. *Biochem. Pharmacol.*, **40**, 663–669.

MUZIO, F., MALANDRINO, S., FERRARI, M. & TONON, G. (1986). Temperature effect on subclasses of muscarinic receptors in rat colon, heart and cerebral cortex. *Life Sci.*, **39**, 365–371.

RAFFA, R.B. & PORRECA, F. (1989). Thermodynamic analysis of the drug-receptor interaction. *Life Sci.*, **44**, 245–258.

RICHARDSON, A. & HUMRICH, A. (1984). A microcomputer program for the analysis of radioligand binding curves and other dose-response data. *Trends Pharmacol. Sci.*, **5**, 47–49.

ROSS, P.D. & SUBRAMANIAN, S. (1981). Thermodynamics of protein association reactions: forces contributing to stability. *Biochemistry*, **20**, 3096–3102.

SCATCHARD, G. (1949). The attraction of proteins for small molecules and ions. *Ann. N.Y. Acad. Sci.*, **51**, 660–672.

STEILING, L., TACKE, R. & WANNAGAT, U. (1979). Diphenyl(3-piperidinopropyl)silanol, a sila-analogue of difenidol. *Liebigs Ann. Chem.*, 1554–1559.

STRADER, C.D., RIOS CANDELORE, M., HILL, W.S., SIGAL, I.S. & DIXON, R.A.F. (1989). Identification of two serine residues involved in agonist activation of the β-adrenergic receptor. *J. Biol. Chem.*, **264**, 13572–13578.

TACKE, R., BRAKMANN, S., KROPFGANS, M., STROHMANN, C., WUTTKE, F., LAMBRECHT, G., MUTSCHLER, E., PROKSCH, P., SCHIEBEL, H.-M. & WITTE, L. (1991). Bioorganosilicon chemistry – recent results. In *Frontiers of Organosilicon Chemistry*. ed. Bassindale, A.R. & Gaspar, P.P. pp. 218–228, Cambridge: Royal Chemistry Society.

TACKE, R., BECKER, B., BERG, D., BRANDES, W., DUTZMANN, S. & SCHALLER, K. (1992). Bis(4-fluorophenyl)methyl(1*H*-1,2,4-triazol-1-yl-methyl)germane, a germanium analogue of the agriculture fungicide flusilazole: synthesis and biological properties. *J. Organomet. Chem.*, **438**, 45–55.

TACKE, R. & LINOH, H. (1989). Bioorganosilicon chemistry. In *The Chemistry of Organic Silicon Compounds*, Part 2. ed. Patai, S. & Rappoport, Z. pp. 1143–1206. Chichester: John Wiley & Sons Ltd.

TACKE, R., LINOH, H., ERNST, L., MOSER, U., MUTSCHLER, E., SARGE, S., CAMMENGA, H.K. & LAMBRECHT, G. (1987a). Preparation and properties of the enantiomers of the antimuscarinic agents sila-procyclidine and sila-tricyclamol iodide: optically active silanols with silicon as the centre of chirality. *Chem. Ber.*, **120**, 1229–1237.

TACKE, R., LINOH, H., RAFEINER, K., LAMBRECHT, G. & MUTSCHLER, E. (1989b). Synthesis and properties of the selective antimuscarinic agent sila-hexocyclium methyl sulfate. *J. Organomet. Chem.*, **359**, 159–168.

TACKE, R., LINOH, H., SCHOMBURG, D., ERNST, L., MOSER, U., MUTSCHLER, E. & LAMBRECHT, G. (1986). On the absolute configuration of the enantiomers of the antimuscarinic agents procyclidine and tricyclamol iodide: X-ray structural analysis of (R)-1-[3-cyclohexyl-3-hydroxy-3-phenylpropyl]-1-methylpyrrolidinium iodide. *Liebigs Ann. Chem.*, 242–250.

TACKE, R., LINOH, H., ZILCH, H., WESS, J., MOSER, U., MUTSCHLER, E. & LAMBRECHT, G. (1985). Synthesis and properties of the selective antimuscarinic agent cyclohexylphenyl(3-piperidinopropyl)silanol. *Liebigs Ann. Chem.*, 2223–2228.

TACKE, R., PIKIES, J., LINOH, H., ROHR-AEHLE, R. & GÖNNE, S. (1987b). Sila-procyclidine: a new synthesis as well as investigations of the peripheral and central anticholinergic activity. *Liebigs Ann. Chem.*, 51–57.

TACKE, R., STRECKER, M., LAMBRECHT, G., MOSER, U. & MUTSCHLER, E. (1983). (2-Aminoethyl)cycloalkylphenylsilanols: bioisosteric C/Si exchange in parasympatholytics of the trihexyphenidyl, cycrimine, and procyclidine type. *Liebigs Ann. Chem.*, 922–930.

TACKE, R., STRECKER, M., LAMBRECHT, G., MOSER, U. & MUTSCHLER, E. (1984). Bioisosteric C/Si exchange in parasympatholytics of the pridinol type. *Arch. Pharm. (Weinheim)*, **317**, 207–214.

TACKE, R., STRECKER, M., SHELDRICK, W.S., ERNST, L., HEEG, E., BERNDT, B., KNAPSTEIN, C.-M. & NIEDNER, R. (1980). Silapridinol and pridinol: preparation and properties as well as structures in the solid state and in solution. *Chem. Ber.*, **113**, 1962–1980.

TACKE, R., STRECKER, M., SHELDRICK, W.S., HEEG, E., BERNDT, B. & KNAPSTEIN, K.M. (1979). Preparation and properties as well as crystal and molecular structure of sila-difenidol. *Z. Naturforsch.*, **34b**, 1279–1285.

TACKE, R., STROHMANN, C., SARGE, S., CAMMENGA, H.K., SCHOMBURG, E., MUTSCHLER, E. & LAMBRECHT, G. (1989a). Preparation and properties of the enantiomers of the selective antimuscarinic agent 1-cyclohexyl-1-phenyl-4-piperidino-1-butanol (hexahydro-difenidol). *Liebigs Ann. Chem.*, 137–143.

WAELBROECK, M., CAMUS, J., TASTENOY, M., LAMBRECHT, G., MUTSCHLER, E., TACKE, R. & CHRISTOPHE, J. (1990a). Stereoselectivity of procyclidine binding to muscarinic receptor subtypes M_1, M_2 and M_4. *Eur. J. Pharmacol.*, **189**, 135–142.

WAELBROECK, M., CAMUS, J., TASTENOY, M., MUTSCHLER, E., STROHMANN, C., TACKE, R., LAMBRECHT, G. & CHRISTOPHE, J. (1991a). Binding affinities of hexahydro-difenidol and hexahydro-sila-difenidol analogues at four muscarinic receptor subtypes: constitutional and stereochemical aspects. *Eur. J. Pharmacol.*, **206**, 95–103.

WAELBROECK, M., CAMUS, J., TASTENOY, M., MUTSCHLER, E., STROHMANN, C., TACKE, R., LAMBRECHT, G. & CHRISTOPHE, J. (1991b). Stereoselectivity of (R)- and (S)-hexahydro-difenidol binding to neuroblastoma M_1, cardiac M_2, pancreatic M_3, and striatum M_4 muscarinic receptors. *Chirality*, **3**, 118–123.

WAELBROECK, M., CAMUS, J., TASTENOY, M., MUTSCHLER, E., STROHMANN, C., TACKE, R., SCHJELDERUP, L., AASEN, A., LAMBRECHT, G. & CHRISTOPHE, J. (1992). Stereoselective interaction of procyclidine, hexahydro-difenidol, hexbutinol and oxyphencyclimine, and of related antagonists, with four muscarinic receptors. *Eur. J. Pharmacol.*, **227**, 33–42.

WAELBROECK, M., GILLARD, M., ROBBERECHT, P. & CHRISTOPHE, J. (1986). Kinetic studies of [^{3}H]-N-methylscopolamine binding to muscarinic receptors in the rat central nervous system: evidence for the existence of three classes of binding sites. *Mol. Pharmacol.*, **30**, 305–314.

WAELBROECK, M., ROBBERECHT, P., CHATELAIN, P., DE NEEF, P. & CHRISTOPHE, J. (1985). Effects of temperature and ethanol on agonist and antagonist binding to rat heart muscarinic receptors in the absence and presence of GTP. *Biochem. J.*, **231**, 469–476.

WAELBROECK, M., TASTENOY, M., CAMUS, J. & CHRISTOPHE, J. (1990b). Binding of selective antagonists to four muscarinic receptors (M_1 to M_4) in rat forebrain. *Mol. Pharmacol.*, **38**, 267–273.

WAELBROECK, M., TASTENOY, M., CAMUS, J., CHRISTOPHE, J., STROHMANN, C., LINOH, H., ZILCH, H., TACKE, R., MUTSCHLER, E. & LAMBRECHT, G. (1989b). Binding and functional properties of antimuscarinics of the hexocyclium/sila-hexocyclium and hexahydro-diphenidol/hexahydro-sila-diphenidol type to muscarinic receptor subtypes. *Br. J. Pharmacol.*, **98**, 197–205.

WAELBROECK, M., TASTENOY, M., CAMUS, J., FEIFEL, R., MUTSCHLER, E., STROHMANN, C., TACKE, R., LAMBRECHT, G. & CHRISTOPHE, J. (1989a). Stereoselectivity of the interaction of muscarinic antagonists with their receptors. *Trends Pharmacol. Sci. Suppl.*, **10**, 65–69.

WAELBROECK, M., TASTENOY, M., CAMUS, J., WINAND, J. & CHRISTOPHE, J. (1991c). Binding kinetics of QNB and methyl QNB enantiomers at neuronal (M_1), cardiac (M_2), and pancreatic (M_3) muscarinic receptors. *Mol. Pharmacol.*, **40**, 413–420.

WEILAND, G.A., MINNEMAN, K.P. & MOLINOFF, P.B. (1979). Fundamental difference between the molecular interactions of agonists and antagonists with the β-adrenergic receptor. *Nature*, **281**, 114–117.

ZAUGG, H.E., MICHAELS, R.J., GLENN, H.J., SWETT, L.R., FREIFELDER, M., STONE, G.R. & WESTON, A.W. (1958). Tertiary carbinols of the piperazine series. *J. Am. Chem. Soc.*, **80**, 2763–2768.

(Received September 21, 1992
Revised January 4, 1993
Accepted January 27, 1993)

Br. J. Pharmacol. (1993), **109**, 371-378 © Macmillan Press Ltd, 1993

Sodium modulation of ^{3}H-agonist and ^{3}H-antagonist binding to α_2-adrenoceptor subtypes

[1]A.C. MacKinnon, M. Spedding & C.M. Brown

Department of Pharmacology, Syntex Research Centre, Research Park, Riccarton, Edinburgh EH14 4AP

1 The α_2-adrenoceptors on human platelets and neonatal rat lung were characterized with the agonist and antagonist ligands [^{3}H]-adrenaline and [^{3}H]-RS-15385-197 respectively. A correlation of affinities for ^{3}H-antagonist binding showed the receptors to be of the α_{2A}-(platelet) and α_{2B}-(neonatal rat lung) adrenoceptor subtypes, whereas a correlation of affinities for ^{3}H-agonist binding showed the receptors to have similar characteristics ($r = 0.88$).

2 NaCl (100 mM) had no effect on [^{3}H]-RS-15385-197 binding in the human platelet, but increased the density of sites labelled with [^{3}H]-RS-15385-197 in neonatal rat lung by 52%. NaCl increased the density of sites labelled by [^{3}H]-adrenaline in neonatal rat lung, but there was a consequent 3.5 fold decrease in affinity. In the human platelet, no specific [^{3}H]-adrenaline binding was observed in the presence of 100 mM NaCl.

3 In the neonatal rat lung, NaCl had no significant effect on the affinity of prazosin for [^{3}H]-RS-15385-197 binding; however, imiloxan affinity was increased 13 fold. The affinity of the catecholamines, adrenaline and noradrenaline was significantly decreased, whereas the imidazolines, oxymetazoline and UK-14,304 were much less affected. The affinity of prazosin and imiloxan for [^{3}H]-adrenaline binding was significantly increased in the presence of 10 and 100 mM NaCl. Conversely, the affinity of adrenaline and noradrenaline was decreased in the presence of NaCl, and there was no change in the affinity of the imidazoline agonists.

4 In the human platelet, NaCl had no effect on the affinity of prazosin for [^{3}H]-RS-15385-197 binding but the affinity of imiloxan was significantly increased. NaCl significantly decreased the affinity of the catecholamines adrenaline and noradrenaline, whereas the affinity of UK-14,304 and oxymatazoline was much less affected. Competition experiments with [^{3}H]-adrenaline in the presence of NaCl in platelets were difficult to characterize as there was no specific binding under these conditions.

5 The results show that both the α_{2A}- and α_{2B}-adrenoceptor subtypes are allosterically regulated by Na^+, but only the α_{2B}-subtype showed a significant increase in density. Interestingly, there is a differential regulation of imidazoline (unchanged) and catecholamine (decreased affinity) agonist interactions with these subtypes. Na^+ may therefore critically affect receptor subtype selectivity of drugs. The implications for receptor subclassification are discussed.

Keywords: [^{3}H]-RS-15385-197; [^{3}H]-adrenaline; α_{2A}-adrenoceptor; α_{2B}-adrenoceptor; sodium

Introduction

Radioligand binding studies and molecular biology have identified multiple subtypes of α_2-adrenoceptors (for review see Ruffulo *et al.*, 1991). The α_{2A} subtype has low affinity for prazosin and high affinity for oxymetazoline whereas the α_{2B}-subtype has higher affinity for prazosin and lower affinity for oxymetazoline (Cheung *et al.*, 1982; Bylund, 1985; Nahorski *et al.*, 1985; Petrash & Bylund, 1986). The α_2-adrenoceptor on human platelets is considered as a pure population of the α_{2A}-adrenoceptor subtype (Cheung *et al.*, 1982) whereas neonatal rat lung contains a homogeneous population of the α_{2B}-adrenoceptor subtype (Latifpour *et al.*, 1982). A third subtype of α_2-adrenoceptor has been proposed to exist on a cell line from the opposum kidney (Murphy & Bylund, 1988). This subtype labelled by [^{3}H]-rauwolscine and [^{3}H]-yohimbine, had high affinity for prazosin and was termed α_{2C}. More recently, a fourth subtype (α_{2D}) has been proposed by Bylund and co-workers in membranes prepared from bovine pineal gland (Simmoneaux *et al.*, 1991). Recently, the selective α_2-adrenoceptor antagonist ligand, [^{3}H]-RS-15385-197 ((8a**R**, 12a**S**, 13a**S**)-5,8,8a,9,10,11,12,12a, 13, 13a-decahydro-3-methoxy-12-(methylsulphonyl)-6H-isoquino [2,1-g][1,6]-naphthyridine) has been shown to label α_{2A}- and α_{2B}-adrenoceptors on human platelet and neonatal rat lung membranes and a subtype on rat cortex which was most similar to the α_{2D}-adrenoceptor (Brown *et al.*, 1993; MacKinnon *et al.*, 1992). Differential binding to α_2-adrenoceptor subtypes has also been demonstrated with the antagonist ligands [^{3}H]-RX 821002 and [^{3}H]-MK 912 (Uhlen & Wikberg, 1991; Uhlen *et al.*, 1992).

The present definition of α_2-adrenoceptor heterogeneity, therefore, relies solely on the characteristics of the receptor labelled with ^{3}H-antagonists. However, an earlier study by Kahn *et al.* (1982) casts doubt on the use of ^{3}H-antagonist binding to describe adequately the nature of the α_2-adrenoceptor on the NG 108-15 cell line, a cell line considered by Bylund *et al.* (1988) as being of the α_{2B}-subtype. When the receptor was labelled by the agonists [^{3}H]-*p*-aminoclonidine or [^{3}H]-adrenaline it displayed high affinity for oxymetazoline and low affinity for prazosin, which was not consistent with the α_{2B}-adrenoceptor subtype. Using a range of subtype selective compounds, preliminary data from this laboratory have shown that [^{3}H]-adrenaline did not label the α_{2B}-adrenoceptor subtype on neonatal rat lung membranes (MacKinnon *et al.*, 1991). Other studies have shown that [^{3}H]-clonidine and [^{3}H]-UK-14,304 failed to discriminate between α_{2A}- and α_{2B}-adrenoceptor subtypes (Gleason & Hieble, 1991).

Agonist and antagonist interactions with the α_2-adrenoceptor have been shown to be differentially modulated by

[1] Author for correspondence.

Na^+ ions (Limbird *et al.*, 1982; Nunnari *et al.*, 1987). The effect of Na^+ is to increase antagonist affinity whilst agonist inhibition of [^{3}H]-yohimbine binding is reduced. It was the purpose of the present study, to investigate further, agonist and antagonist interactions with the α_{2A}- and α_{2B}-adrenoceptor subtypes using [^{3}H]-adrenaline and [^{3}H]-RS-15386-197 binding to human platelet and neonatal rat lung membranes, and to determine the effects of Na^+ on these interactions.

Methods

Preparation of human platelet membranes

Platelet membranes were prepared essentially as previously described (Cheung *et al.*, 1982; MacKinnon *et al.*, 1992). Blood was collected from male and female volunteers into 0.35% (w/v) trisodium citrate. Platelet rich plasma (PRP) was obtained by centrifugation at 200 *g* for 15 min. The PRP was centrifuged at 48000 *g* for 10 min at 4°C and the resulting pellet resuspended in cold lysing buffer (5 mM Tris HCl, 5 mM EDTA, pH 7.4). The pellet was washed once more in lysing buffer by resuspension and centrifugation followed by resuspension in 50 mM Tris HCl, 0.5 mM EDTA pH 7.4. The suspension was incubated at 37°C for 15 min before centrifugation (48000 *g* for 10 min) and the final pellet was resuspended in Tris HCl; pH 7.4 at a protein concentration of 1 mg ml^{-1}.

Preparation of neonatal rat lung membranes

Neonatal Sprague Dawley rats (<24 h old) of either sex were decapitated and the lungs dissected out and frozen under liquid nitrogen until use. Membranes were prepared as described previously (MacKinnon *et al.*, 1992). Briefly, lungs were homogenized in 25 volumes of ice cold homogenizing buffer (50 mM Tris HCl; 5 mM EDTA, pH 7.4 at 25°C), and centrifuged at 48000 *g* for 15 min at 4°C. The pellet was resuspended in the original volume of homogenizing buffer and recentrifuged. Membranes were washed twice more by resuspension and centrifugation in 50 mM Tris HCl; 0.5 mM EDTA, pH 7.4, and the final pellet resuspended in 3 ml 50 mM Tris HCl; pH 7.4 at an approximate protein concentration of 2 mg ml^{-1}.

[^{3}H]-RS-15385-197 binding

[^{3}H]-RS-15385-197 was synthesized to a specific activity of 57 Ci mmol^{-1} by Dr H. Parnes (Institute of Chemistry, Syntex, Palo Alto, U.S.A.). [^{3}H]-RS-15385-197 (0.01–2.0 nM) was incubated to equilibrium in 50 mM Tris HCl buffer, pH 7.4 containing 0.5 mM EDTA and 50–250 μg membrane protein. Incubations were carried out at 25°C for 60 min in a final volume of 1 ml. Competition experiments were carried out with 0.1–0.2 nM [^{3}H]-RS-15385-197 and 13 concentrations of competing drug. Bound ligand was separated from free by vacuum filtration over GF/B filters on a Brandell cell harvester. The filters were washed twice for 5 s with incubation buffer and the bound radioactivity determined by liquid scintillation counting. Non-specific binding was determined in the presence of 1 μM phentolamine.

[^{3}H]-adrenaline binding

[^{3}H]-(−)-adrenaline (65–75 Ci mmol^{-1}, Du Pont, UK) was incubated with 100–200 μg membrane protein in an assay volume of 0.5 ml to equilibrium (60 min at 25°C). The assay buffer (50 mM Tris HCl pH 7.4 at 25°C) contained 0.3 mM ascorbic acid, 5 mM $MgCl_2$, 0.8 mM dithiothreitol and 0.1 mM catechol to minimize degradation of the radioligand (Sénard *et al.*, 1988). For neonatal rat lung membranes the assay also contained 10 nM propranolol to prevent binding to β-adrenoceptors. Competition experiments were carried out with 2–3 nM [^{3}H]-adrenaline and 13 concentrations of competing drug. Non-specific binding was determined in the presence of 10 μM (−)-noradrenaline.

Data analysis

Binding isotherms from displacement studies were analysed by a non-linear least squares curve fitting programme capable of fitting to a one or two site model. The IC_{50} (concentration of drug displacing 50% specific binding) was converted to the inhibitory constant (K_i) by the equation of Cheng & Prusoff (1973) where $K_i = IC_{50}/1 + ([ligand]/K_d)$. The fits for a one and two site model were compared using the differential *F* value (Munson & Rodbard, 1980; Petrash & Bylund, 1986). A two site fit was assumed to be significantly better than a one site fit, if the determined F value was significant (95% confidence limits). Equilibrium binding parameters (K_d and B_{max}) were obtained by the iterative non-linear least squares curve fitting programme Ligand (Munson & Rodbard, 1980).

Chemicals and drugs

Yohimbine, clonidine, oxymetazoline, (−)-adrenaline, (−)-noradrenaline and prazosin from Sigma; phentolamine from Ciba Geigy; rauwolscine from Carl Roth; RS-15385-197 ((8a**R**, 12a**S**, 13a**S**)-5,8,8a,9,10,11,12,12a,13, 13a-decahydro-3-methoxy-12- (methylsulphonyl)-6H- isoquino [2,1-g][1,6]-naphthyridine), BRL 44409 (2-[(5-chloro-1, 3-dihydro-2H-isoindol-2-yl) methyl 1]- 4,5-dihydro-1H-imidazole dihydrochloride), idazoxan, imiloxan and UK-14,304 were synthesised by Dr R. Clark, Syntex, Palo Alto, U.S.A. All other chemicals were of the highest purity commercially available.

Results

Saturation analysis of [^{3}H]-RS-15385-197 binding revealed a single, high affinity binding site in human platelet membranes (Figure 1a) with an affinity (K_d) of 0.13 ± 0.01 nM and B_{max} = 111.6 ± 7.4 fmol mg^{-1} protein (n = 7). In neonatal rat lung membranes (Figure 1b), K_d = 0.081 ± 0.01 nM, B_{max} = 174 ± 20 fmol mg^{-1} protein (n = 4). Thus, [^{3}H]-RS-15385-197 labelled a single population of high affinity binding sites in human platelet and rat neonatal lung membranes. Saturation analysis of [^{3}H]-(−)-adrenaline binding (Figure 2a) revealed a single high affinity site in the human platelet (K_d = 2.62 ± 0.56 nM, B_{max} = 95.1 ± 17 fmol mg^{-1} protein, n = 3) and the neonatal rat lung (K_d = 3.04 ± 0.44 nM, B_{max} = 77.7 ± 11 fmol mg^{-1} protein, n = 7). Therefore, the percentage of sites labelled by the agonist, [^{3}H]-adrenaline, compared to that labelled by the antagonist, [^{3}H]-RS-15385-197, was 85% in the human platelet and 44% in the neonatal rat lung.

The affinities of a number of competing drugs for [^{3}H]-RS-15385-197 binding in human platelets and neonatal rat lung membranes are given in Table 1. The rank order of affinity of these compounds for [^{3}H]-RS-15385-197 binding, was consistent with their affinities for the α_{2A}- and α_{2B}-adrenoceptor subtypes respectively. Thus, in the human platelet, yohimbine = rauwolscine ≥ oxymetazoline > BRL 44409 > imiloxan ≥ prazosin; and in the neonatal rat lung, rauwolscine > yohimbine > prazosin ≥ imiloxan > oxymetazoline > BRL 44409. A correlation of the affinities of these compounds is presented in Figure 3a. In both tissues, adrenaline inhibition curves were shallow and better fitted to a 2 site model in the presence of 5 mM $MgCl_2$ (Table 2). In the presence of Gpp(NH)p (100 μM), adrenaline inhibition curves were shifted to the right and there was a steepening of the Hill slope, however, the magnitude of the shift was greater in the neonatal rat lung than the human platelet. In fact a significant shift in the affinity of adrenaline in the human platelet was only evident when compared to the response in the presence of $MgCl_2$. In contrast to adrenaline, inhibition curves to the antagonists prazosin and yohimbine were

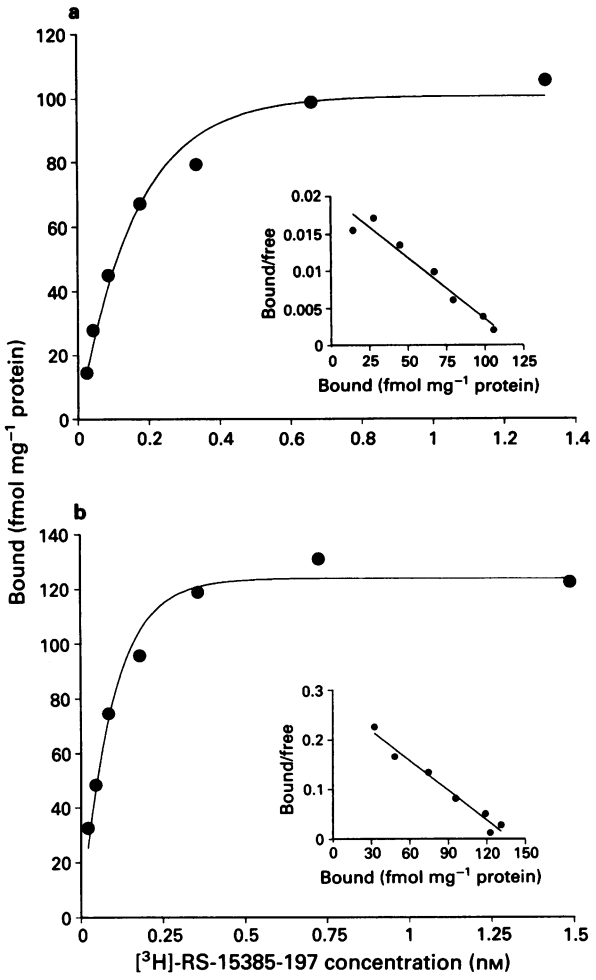

Figure 1 Saturation analysis of [^{3}H]-RS-15385-197 binding in human platelet (a) and neonatal rat lung (b) membranes. The insets show the Scatchard transformation of the data. The data represent a single experiment performed in triplicate. Essentially similar data were obtained in at least three other experiments on different preparations (see text for meaned values). The equilibrium binding constants K_d and B_{max} = 0.12 nM and 112 fmol mg^{-1} protein respectively in the human platelet (a), and 0.07 nM and 157 fmol mg^{-1} protein in the neonatal rat lung (b).

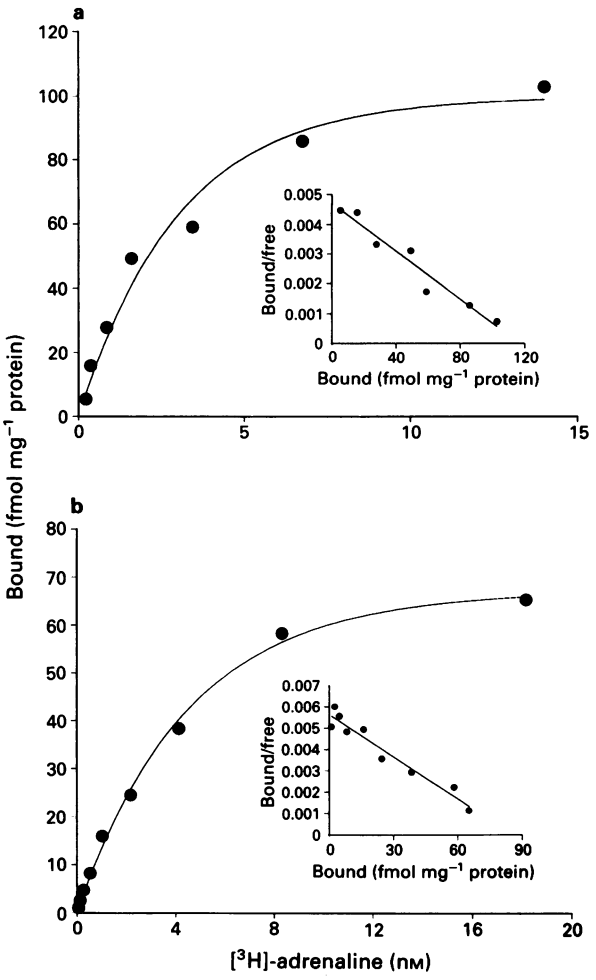

Figure 2 Saturation analysis of [^{3}H]-adrenaline binding in human platelet (a) and neonatal rat lung (b) membranes. The data represent a typical experiment performed in triplicate. Essentially similar data were obtained in at least two other experiments on different preparations (see text for meaned values). The equilibrium binding parameters K_d and B_{max} were 2.68 nM and 112 fmol mg^{-1} protein in the human platelet (a), and 2.75 nM and 82 fmol mg^{-1} protein in the neonatal rat lung (b).

Table 1 Affinity values (pK_i) for [^{3}H]-15385-197 binding in human platelet and neonatal rat lung membranes

	Human platelet			*Neonatal rat lung*		
	n	pK_i	nH	*n*	pK_i	nH
RS-15385-197	4	9.51 ± 0.10	0.99 ± 0.01	3	9.58 ± 0.31	1.01 ± 0.02
Yohimbine	4	8.98 ± 0.10	0.89 ± 0.04	3	8.16 ± 0.08	0.99 ± 0.01
Rauwolscine	4	8.91 ± 0.12	1.04 ± 0.09	3	8.62 ± 0.07	0.85 ± 0.02
Phentolamine	3	8.70 ± 0.22	1.25 ± 0.35	3	8.11 ± 0.08	1.01 ± 0.08
Idazoxan	4	8.22 ± 0.03	1.01 ± 0.04	3	7.46 ± 0.08	0.99 ± 0.01
Adrenaline	6	7.55 ± 0.11	0.81 ± 0.07	5	7.08 ± 0.04	0.75 ± 0.05
Noradrenaline	4	6.93 ± 0.04	0.75 ± 0.01	3	7.25 ± 0.03	0.68 ± 0.04
BHT 920	3	7.17 ± 0.03	1.05 ± 0.06	3	6.89 ± 0.04	0.83 ± 0.02
Clonidine	3	7.47 ± 0.06	1.01 ± 0.04	3	7.30 ± 0.01	1.05 ± 0.04
UK-14,304	3	7.87 ± 0.04	0.97 ± 0.13	3	7.04 ± 0.10	0.79 ± 0.05
Prazosin	4	6.13 ± 0.08	0.94 ± 0.15	4	7.49 ± 0.12	1.04 ± 0.09
Imiloxan	3	6.30 ± 0.04	1.30 ± 0.06	3	7.36 ± 0.02	1.03 ± 0.04
Oxymetazoline	4	8.49 ± 0.01	0.90 ± 0.06	3	6.91 ± 0.04	0.73 ± 0.07
BRL 44409	3	7.77 ± 0.05	0.98 ± 0.08	3	6.38 ± 0.05	1.07 ± 0.07

The affinity values were obtained from the displacement of 0.1 nM [^{3}H]-RS-15385-197 from human platelet and neonatal rat lung membranes as described in methods. Each value represents the mean ± s.e.mean of *n* determinations performed in duplicate. Where nH < 1.00 the pIC_{50} value corrected for receptor occupancy is given.

Table 2 Effect of Gpp(NH)p and $MgCl_2$ on the displacement of [^{3}H]-RS-15385-197 from human platelet and neonatal rat lung membranes

	1 site fit		*2 site fit*			
	pIC_{50}	nH	pIC_{50}	(%)	pIC_{50}	(%)
Human platelet						
Adrenaline	7.55 ± 0.11	0.81 ± 0.07	7.70 ± 0.37	(71 ± 12)	6.03 ± 0.43	(29 ± 12)
$MgCl_2$	8.00 ± 0.06*	0.58 ± 0.04*	8.09 ± 0.02	(65 ± 2)	6.08 ± 0.12	(35 ± 2)
Gpp (NH)p	7.34 ± 0.21§	0.73 ± 0.05§				
Yohimbine	8.98 ± 0.10	0.89 ± 0.04				
$MgCl_2$	8.72 ± 0.16	0.95 ± 0.07				
Gpp(NH)p	8.52 ± 0.29	0.97 ± 0.06				
Prazosin	6.13 ± 0.08	0.94 ± 0.15				
$MgCl_2$	5.76 ± 0.06	0.82 ± 0.15				
Gpp(NH)p	5.87 ± 0.12	0.83 ± 0.08				
Neonatal rat lung						
Adrenaline	7.08 ± 0.04	0.75 ± 0.05	7.36 ± 0.20	(46 ± 8)	6.07 ± 0.16	(54 ± 8)
$MgCl_2$	7.23 ± 0.03	0.56 ± 0.01*	8.25 ± 0.08	(35 ± 4)	6.41 ± 0.09	(65 ± 4)
Gpp(NH)p	6.60 ± 0.09§	0.79 ± 0.06§				
Yohimbine	8.16 ± 0.08	0.99 ± 0.01				
$MgCl_2$	8.02 ± 0.15	0.96 ± 0.01				
Gpp(NH)p	8.01 ± 0.08	1.01 ± 0.02				
Prazosin	7.49 ± 0.12	1.04 ± 0.09				
$MgCl_2$	7.26 ± 0.20	0.96 ± 0.08				
Gpp(NH)p	7.24 ± 0.13	1.04 ± 0.01				

The affinity values were determined from the displacement of specific binding of 0.1 nM [^{3}H]-RS-15385-197 in the absence and presence of 5 mM $MgCl_2$ or 100 μM Gpp(NH)p as shown. The results are expressed as pIC_{50} and Hill slope (nH) for a one site fit, and pIC_{50} and % contribution for a 2 site fit where appropriate. Values shown are the mean ± s.e.mean of at least 3 experiments. *Statistically significant difference ($P<0.05$) relative to corresponding control; §relative to $MgCl_2$.

unaltered by Gpp(NH)p. These data suggest that the α_{2A}- and α_{2B}-adrenoceptor subtypes exist in different affinity states for agonists, and that the expression of each state is influenced by the GTP analogue Gpp(NH)p and Mg^{2+}, consistent with an interaction at a G-protein linked receptor.

In contrast to [^{3}H]-RS-15385-197 binding, the rank order of affinity of these compounds for [^{3}H]-adrenaline binding was generally the same in both tissues (Table 3). The correlation (Figure 3b) showed that [^{3}H]-adrenaline did not discriminate between the subtypes ($r = 0.88$). When binding affinity for [^{3}H]-adrenaline and [^{3}H]-RS-15385-197 were compared within the same tissue, there was a poor correlation in the neonatal rat lung ($r = 0.001$, Figure 3c), and in the human platelet ($r = 0.53$, Figure 3d). The correlation in the human platelet was improved considerably when agonist affinities were removed from the analysis ($r = 0.99$), and although there was an improvement in the neonatal rat lung correlation ($r = 0.31$) there was still an obvious heterogeneity within the antagonists alone. This suggests that in the human platelet, [^{3}H]-RS-15385-197 and ^{3}H]-adrenaline label largely the same population of sites, and this is further substantiated by the similar number of sites labelled by the two ligands. In the neonatal rat lung, however, [^{3}H]-RS-15385-197 recognises additional, low affinity, agonist sites which have higher affinity for antagonists.

Previous studies by Limbird *et al.* (1982) have shown that Na^+ increases the affinity for antagonist binding to α_2-adrenoceptors whilst agonist binding is decreased. In the present study, saturation experiments showed that 100 mM NaCl had no effect on the affinity, but increased the density of sites labelled with [^{3}H]-RS-15385-197 in neonatal rat lung membranes by 52% (Table 4). NaCl (100 mM) also increased the density of sites labelled by [^{3}H]-adrenaline in neonatal rat lung membranes, and there was almost a 3 fold decrease in affinity. In the human platelet, 100 mM NaCl had no significant effect on [^{3}H]-RS-15385-197 binding but, [^{3}H]-adrenaline binding was abolished.

Table 5 shows the effect of 100 mM NaCl on the affinity of several competing drugs for [^{3}H]-adrenaline and [^{3}H]-RS-15385-197 binding. In the neonatal rat lung, there was no significant effect on the affinity of prazosin for [^{3}H]-RS-15385-197 binding, however, imiloxan affinity was increased 13 fold. The affinity of the catecholamine agonists adrenaline and noradrenaline for [^{3}H]-RS-15385-197 binding was significantly decreased, whereas oxymetazoline affinity was much less affected and there was no significant change in the affinity of UK-14,304. A lower concentration of NaCl (10 mM) also produced a significant decrease in adrenaline affinity ($pK_i = 6.68 \pm 0.08$, $n = 3$; $P<0.05$). The affinity of prazosin and imiloxan for [^{3}H]-adrenaline binding was significantly increased in the presence of 100 mM NaCl, whereas the affinity of adrenaline and noradrenaline was decreased, and there was no change in the affinity of oxymetazoline or UK-14,304. NaCl, 10 mM, was also effective in increasing the affinity of prazosin ($pK_i = 6.22 \pm 0.15$, $n = 4$; $P<0.05$), for [^{3}H]-adrenaline binding in the neonatal rat lung.

In platelet membranes, 100 mM NaCl had no effect on the affinity of prazosin for [^{3}H]-RS-15385-197 binding but the affinity of imiloxan was significantly increased. NaCl (100 mM) significantly decreased the affinity of the catecholamines, adrenaline and noradrenaline. There was a small decrease in the affinity of UK-14,304, whereas oxymetazoline affinity was unaffected. A lower concentration of NaCl (10 mM) did not significantly affect the affinity of adrenaline ($pK_i = 7.13 \pm 0.08$, $n = 3$). Competition experiments with [^{3}H]-adrenaline in the presence of NaCl in platelets were not carried out, as the specific binding was very low under these conditions.

Discussion

The ability of the agonist, [^{3}H]-adrenaline to label α_{2A}- and α_{2B}-adrenoceptors was assessed in human platelet and neonatal rat lung membranes, and compared wtih the antagonist [^{3}H]-RS-15385-197. Marked differences were noted in the nature of the sites labelled by the two radioligands. [^{3}H]-adrenaline labelled 85% and 44% of the sites labelled by [^{3}H]-RS-15385-197 in the human platelet and the neonatal rat

Table 3 Affinity values (pK_i) for [^{3}H]-adrenaline binding in human platelet and neonatal rat lung membranes

	Human platelets			*Neonatal rat lung*		
	n	pK_i	nH	*n*	pK_i	nH
Yohimbine	3	8.20 ± 0.28	0.78 ± 0.11	5	7.37 ± 0.20	0.98 ± 0.20
Rauwolscine	2	8.36	0.79	3	7.89 ± 0.12	0.80 ± 0.07
Phentolamine	2	7.99	1.20	3	7.84 ± 0.11	0.93 ± 0.07
Idazoxan	2	7.68	0.89	3	7.58 ± 0.06	0.98 ± 0.02
Imiloxan	3	5.68 ± 0.14	0.81 ± 0.09	3	5.61 ± 0.12	0.81 ± 0.10
Prazosin	3	5.12 ± 0.14	1.09 ± 0.09	4	5.68 ± 0.16	0.99 ± 0.01
Noradrenaline	3	8.15 ± 0.32	1.18 ± 0.31	4	8.42 ± 0.14	0.97 ± 0.03
Adrenaline	3	8.56 ± 0.15	0.89 ± 0.19	4	8.41 ± 0.16	1.00 ± 0.01
UK-14,304	2	8.21	0.94	3	7.83 ± 0.17	0.82 ± 0.13
Clonidine	2	7.92	0.88	3	7.45 ± 0.23	0.79 ± 0.11
BHT 920	2	7.79	0.79	3	7.97 ± 0.11	0.88 ± 0.09
Oxymetazoline	3	8.33 ± 0.13	0.78 ± 0.17	3	8.22 ± 0.09	0.90 ± 0.10
BRL 44409	3	7.19 ± 0.19	0.77 ± 0.07	3	6.67 ± 0.24	1.06 ± 0.06

The affinities are determined from competition experiments with [^{3}H]-adrenaline as described in Methods. The values represent the mean ($n = 2$) or the mean ± s.e.mean of n determinations from different preparations performed in duplicate.

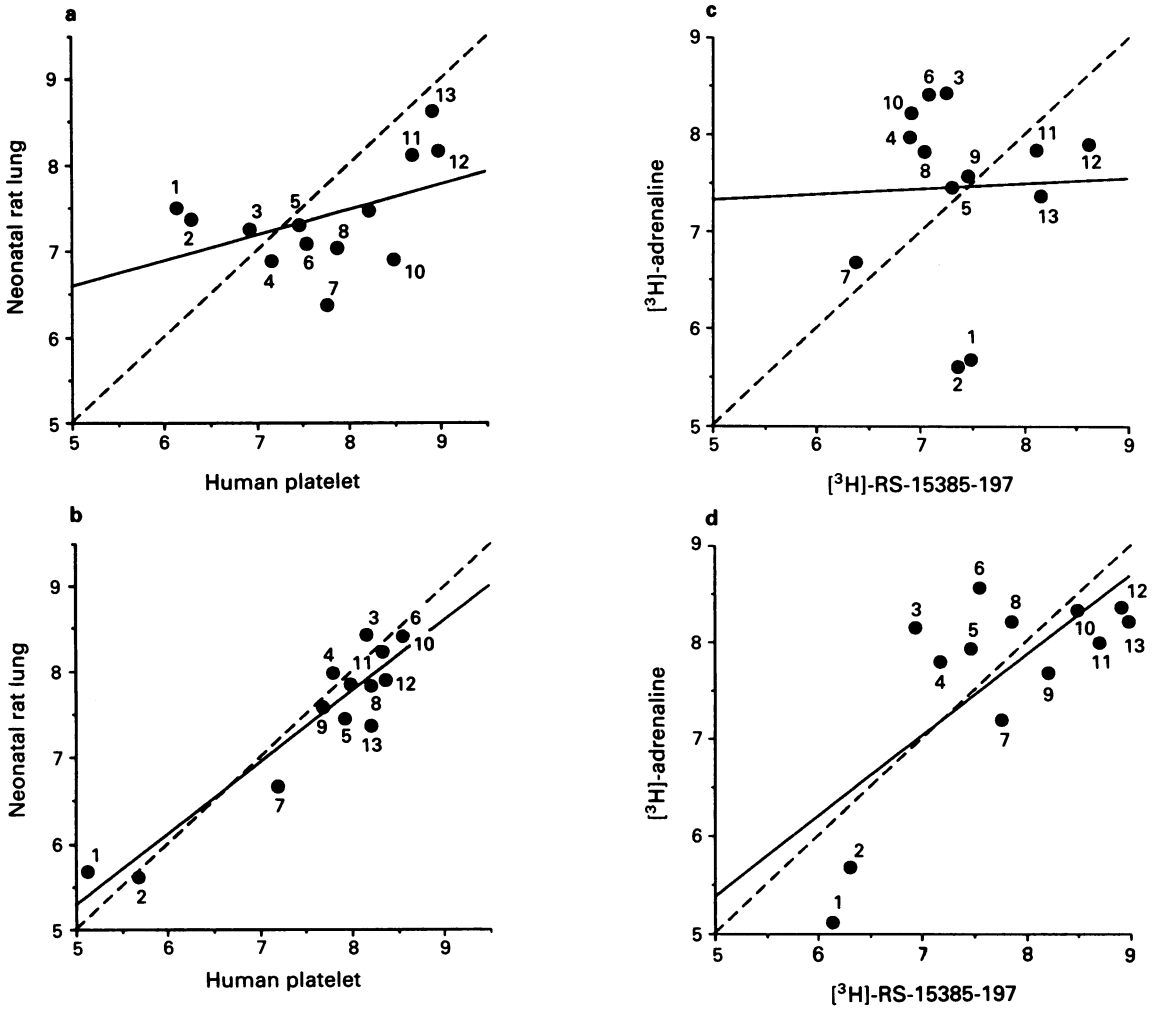

Figure 3 Correlation of affinities for [^{3}H]-RS-15385-197 and [^{3}H]-adrenaline binding to human platelet and neonatal rat lung membranes. Affinity values (pK_i) are taken from Tables 1 and 3. The solid line represents the line of best fit and the dotted line represents the line of identity. (a) [^{3}H]-RS-15385-197 binding in human platelet *vs* neonatal rat lung, slope = 0.29, $r = 0.20$; (b) [^{3}H]-adrenaline binding in human platelet *vs* neonatal rat lung, slope = 0.83, $r = 0.88$; (c) [^{3}H]-RS-15385-197 *vs* [^{3}H]-adrenaline binding in the neonatal rat lung, slope = 0.005, $r = 0.001$; (d) [^{3}H]-RS-15385-197 *vs* [^{3}H]-adrenaline binding in the human platelet, slope = 0.83, $r = 0.53$. (1) Prazosin, (2) imiloxan, (3) noradrenaline, (4) BHT 920, (5) clonidine, (6) adrenaline, (7) BRL 44409, (8) UK-14,304, (9) idazoxan, (10) oxymetazoline, (11) phentolamine, (12) rauwolscine, (13) yohimbine.

Table 4 Effect of 100 mM NaCl on [^{3}H]-RS-15385-197 and [^{3}H]-adrenaline binding

	Control		*NaCl* 100 mM	
	K_d	B_{max}	K_d	B_{max}
[^{3}H]-RS-15385-197 neonatal rat lung	0.08 ± 0.01	174 ± 20	0.09 ± 0.01	265.4 ± 3.2*
[^{3}H]-adrenaline neonatal rat lung	3.04 ± 0.44	77.7 ± 11	11.06 ± 1.73*	208.7 ± 37.5*
[^{3}H]-RS-15385-197 human platelet	0.13 ± 0.01	111.6 ± 7.4	0.16 ± 0.01	92.78 ± 10.8
[^{3}H]-adrenaline human platelet	2.62 ± 0.56	95.1 ± 17	No specific binding	

Saturation analysis of [^{3}H]-RS-15385-197 and [^{3}H]-adrenaline was carried out as described in methods. The results represent the mean ± s.e.mean of at least 3 separate determinations performed in triplicate. *Significantly different from corresponding control value, $P<0.05$.

Table 5 The effect of 100 mM NaCl on agonist and antagonist binding to α_2-adrenoceptors on neonatal rat lung and human platelet membranes

		Human platelet [^{3}H]-RS-15385-197		*Neonatal rat lung* [^{3}H]-adrenaline		[^{3}H]-RS-15385-197	
		Control	NaCl	Control	NaCl	Control	NaCl
Adrenaline	pIC_{50}	7.36 ± 0.01	6.48 ± 0.15*	8.41 ± 0.16	7.78 ± 0.20*	7.05 ± 0.04	6.25 ± 0.05*
	nH	0.80 ± 0.05	0.65 ± 0.04	1.00 ± 0.01	0.92 ± 0.07	0.82 ± 0.02	1.01 ± 0.03
Noradrenaline	pIC_{50}	6.93 ± 0.04	5.70 ± 0.05*	8.42 ± 0.14	8.00 ± 0.13*	7.25 ± 0.03	6.19 ± 0.06*
	nH	0.76 ± 0.07	0.85 ± 0.05	0.97 ± 0.03	0.82 ± 0.10	0.68 ± 0.04	0.94 ± 0.13
Oxymetazoline	pIC_{50}	8.49 ± 0.01	8.57 ± 0.08	8.22 ± 0.09	8.34 ± 0.25	6.91 ± 0.04	6.28 ± 0.04*
	nH	0.90 ± 0.06	0.81 ± 0.12	0.90 ± 0.10	0.75 ± 0.02	0.73 ± 0.07	1.06 ± 0.04
UK-14,304	pIC_{50}	7.87 ± 0.04	7.44 ± 0.06*	7.83 ± 0.17	7.82 ± 0.10	7.04 ± 0.10	6.81 ± 0.07
	nH	0.97 ± 0.13	0.82 ± 0.17	0.82 ± 0.13	0.87 ± 0.13	0.79 ± 0.05	0.92 ± 0.04
Prazosin	pIC_{50}	6.13 ± 0.08	6.13 ± 0.08	5.68 ± 0.16	6.70 ± 0.23*	7.49 ± 0.12	7.66 ± 0.02
	nH	0.94 ± 0.06	1.24 ± 0.14	0.99 ± 0.01	0.98 ± 0.04	1.04 ± 0.12	1.18 ± 0.09
Imiloxan	pIC_{50}	6.30 ± 0.04	7.00 ± 0.22*	5.61 ± 0.12	6.69 ± 0.27*	6.30 ± 0.04	7.40 ± 0.22*
	nH	1.30 ± 0.16	0.67 ± 0.12	0.81 ± 0.10	0.91 ± 0.12	1.03 ± 0.04	0.98 ± 0.13

The results represent the mean ± s.e.mean for at least 3 determinations performed in duplicate. *$P<0.05$ compared to corresponding control.

lung respectively. Unlike [^{3}H]-RS-15385-197 binding, however, the pharmacology of the agonist labelled site in both tissues was essentially similar ($r = 0.88$). Prazosin had low affinity and oxymetazoline had high affinity for the agonist labelled site in both tissues suggesting that an adrenoceptor characteristic of the α_{2B}-subtype could not be labelled with [^{3}H]-adrenaline. This is especially important as these two compounds are crucial ligands in differentiating α_2-adrenoceptor subtypes. In another study, [^{3}H]-clonidine and [^{3}H]-UK-14,304 failed to distinguish α_{2A}- and α_{2B}-adrenoceptor subtypes on HT29 and NG 108-15 cells ($r>0.9$, Gleason & Hieble, 1991), although it was suggested that closer examination of the slope of the plots revealed that prazosin and ARC 239 retained some selectivity for the α_{2B}-adrenoceptor subtype labelled by the agonists (slope <0.6). Correlations in the present study revealed slope values closer to unity for displacement of agonist binding to human platelet and neonatal rat lung membranes and no selectivity of prazosin and imiloxan for the α_{2B}-adrenoceptor was evident. Therefore, no marked differences were observed in the binding characteristics of the activated state of the α_{2A} and α_{2B}-adrenoceptor subtypes in the human platelet and neonatal rat lung. These studies have important implications in the development of selective antagonists.

The fact that prazosin had >100 fold lower affinity for the high affinity agonist state of the α_{2B}-adrenoceptor, as delineated by [^{3}H]-adrenaline binding, cannot explain why this compound exhibited monophasic inhibition curves for [^{3}H]-RS-15385-197, if it is assumed that the latter compound labels both high and low affinity states of the receptor. It cannot be explained by a non-competitive interaction of prazosin, as prazosin does not influence the dissociation rate of, or the number of sites labelled by [^{3}H]-RS-15385-197 (unpublished observations). Alternatively, [^{3}H]-adrenaline may label an additional high affinity state of the α_{2B}-adrenoceptor, which has low affinity for some antagonists, particularly prazosin and imiloxan. Multiple high affinity agonist states of the α_2-adrenoceptor on the human platelet have been previously suggested using [^{3}H]-adrenaline (U'Prichard *et al.*, 1983) and [^{3}H]-UK-14,304 (Neubig *et al.*, 1988). It is possible, therefore, that the same is true for the α_{2B}-adrenoceptor, and could be elucidated by a detailed kinetic analysis of [^{3}H]-adrenaline binding in the neonatal rat lung. The interaction of prazosin and RS-15385-197 with the various states of the α_2-adrenoceptor must therefore be more complicated than previously thought, and the difference in the ability of selective antagonists to inhibit [^{3}H]-antagonist and not [^{3}H]-agonist binding suggests additional differences in the interaction of these radioligands with the α_2-adrenoceptor subtypes.

By far the majority of functional experiments with α_2-adrenoceptors have had the characteristics of the α_{2A}-adrenoceptor subtype in that prazosin has had low affinity. A possible explanation for this is the greater pace of developments in the field of radioligand binding, coupled with fact that a high affinity for prazosin would have in the past been confused with an α_1-mediated event (see references cited in McGrath *et al.*, 1989; Wilson *et al.*, 1991b). Neubig *et al.*

(1988) demonstrated by a series of kinetic studies of [^{3}H]-yohimbine and [^{3}H]-UK-14,304 binding in the human platelet that approximately one third of the receptors were precoupled to G_i and bound agonist with high affinity to form a tightly coupled ternary complex (precoupled). Another third had low affinity for agonists and were unable to couple to G_i (free) while the remainder bound agonist with high affinity, were sensitive to guanyl nucleotides, and coupled with G_i following an agonist-induced conformational change and diffusional translocation in the membrane (couplable) (Neubig *et al.*, 1988: Gantzos & Neubig, 1988). If this model is correct then it could be assumed that ^{3}H-agonists would label the precoupled and couplable receptors, while ^{3}H-antagonists would label the precoupled and free receptors. Antagonists could not label the couplable receptors if it is assumed that antagonists, having no efficacy, cannot induce the conformational change required for diffusional-dependent G-protein coupling. This model therefore suggests, that not all states of the receptor are labelled by ^{3}H-antagonists, and can be used to explain some of the data in the present study. The idea that agonist labelled sites may not merely be a subset of those labelled by the antagonist could explain the vastly different affinities of prazosin for agonist and antagonist binding in the neonatal rat lung. Prazosin may not influence agonist-induced G-protein-coupling but may instead have high affinity for the free receptor. In the presence of Gpp NHp, agonist inhibition of ^{3}H-antagonist binding would be shifted to the right and the concentration-response curves would be steepened, but they may not reach unity if the precoupled receptors are less sensitive to GppNHp. The percentage of sites existing in the three states may be different in the human platelet and the neonatal lung. If, as suggested by Neubig *et al.* (1988), the proportion of precoupled, couplable and free receptors on the human platelet are 1:1:1, then the density of sites labelled by [^{3}H]-adrenaline (precoupled and couplable) would be approximately equal to the density of sites labelled by [^{3}H]-RS-15385-197 (precoupled and free). The present study showed that [^{3}H]-adrenaline labelled 85% of those sites labelled by [^{3}H]-RS-15385-197 which would be consistent with this model. However, in the neonatal rat lung the number of agonist labelled sites represented only 44%, suggesting that a large proportion of these receptors may be free receptors and show higher affinity for antagonists.

The finding that agonist affinities in the 2 tissues correlated well whilst antagonist affinities correlated poorly, suggests that the differences in the α_{2A} and α_{2B}-adrenoceptor reside in the characteristics of the free receptor. Antagonists such as prazosin and imiloxan may have higher affinity for the free α_{2B}-free adrenoceptor. The relationship of this selectivity to functional antagonism of the α_{2B}-adrenoceptor is however unclear. Based on these findings we would like to suggest that ^{3}H-antagonist binding may overestimate the postulated potency of antagonists in functional experiments and lead to a dubious estimation of receptor subtype selectivity. The combined use of ^{3}H-antagonist and ^{3}H-agonist binding data may better describe the physiological nature of the receptor. This may also be applicable to receptor systems other than the α_2-adrenoceptor.

The present study showed that modulation of agonist and antagonist binding occurred in the presence of NaCl in tissues containing the α_{2A} and α_{2B}-adrenoceptor subtypes. The effects were unlikely to be due to changes in osmolality, as previous studies have shown that the regulatory effects of NaCl on the porcine α_{2A}-adrenoceptor and the NG 108-15 cell α_{2B}-adrenoceptor were not produced by equimolar concentrations of N-methyl D-glucamine chloride-Cl (Guyer *et al.*, 1990; Wilson, *et al.*, 1991a). They are also not likely to be due to Cl^{-1}-ions as LiCl and KCl were much less effective (Nunnari *et al.*, 1987; Guyer *et al.*, 1990; Wilson *et al.*, 1991a).

NaCl, 100 mM, decreased the affinity of adrenaline by 4 fold in the neonatal rat lung and by 9 fold in the platelet. Therefore for both subtypes there was also a decrease in the affinity of [^{3}H]-adrenaline. In the human platelet, the decreased affinity was so great that no specific binding was observed with [^{3}H]-adrenaline. No change in the density of binding was seen for [^{3}H]-RS-15385-197 in the platelet; however, in the neonatal rat lung, an increase in the density of both [^{3}H]-RS-15385-197 and [^{3}H]-adrenaline was observed, suggesting that Na^+ brought about changes in the conformation of the receptor so that more sites in the low affinity agonist state were seen by both ligands.

A recent study has identified a specific residue (asp79) on the porcine α_{2A}-adrenoceptor to which Na^+ binds and exerts its allosteric effects (Horstman *et al.*, 1990). An aspartate residue reported to lie in a topographically identical position asp63) has been detected in the derived amino acid sequence from a rat cDNA encoding an α_{2B}-adrenoceptor (Zeng *et al.*, 1990). Thus, it appears that molecular biology has identified unique receptor proteins which correspond to the α_{2A}- and α_{2B}-adrenoceptor subtypes, and that Na^+ plays a crucial role in the regulation of α_{2A}- and α_{2B}-adrenoceptor function via an interaction with a specific amino acid residue. A previous study by Wilson *et al.* (1991a) showed, that although Na^+ decreased adrenaline affinity for [^{3}H]-yohimbine binding in the solubilized α_{2B}-adrenoceptor from NG 108-15 cells, it did not facilitate [^{3}H]-yohimbine dissociation. An increase in [^{3}H]-yohimbine dissociation rate has been demonstrated for the human and pig α_{2A}-adrenoceptor (Limbird *et al.*, 1982, Nunnari *et al.*, 1987). Therefore, these studies would support the results from the present study, that Na^+ modulates agonist and antagonist interactions with the α_{2A}- and α_{2B}-adrenoceptors via different mechanisms.

In the neonatal rat lung, competition experiments with [^{3}H]-adrenaline in the presence of Na^+, showed that the affinity of imiloxan and prazosin was increased more than 10 fold whilst adrenaline and noradrenaline affinity was decreased by a similar magnitude. The decreased agonist affinity was highlighted in that adrenaline and noradrenaline inhibition of [^{3}H]-RS-15385-197 binding was decreased by Na^+ and the Hill slopes were closer to unity, suggesting a predominance of a low affinity agonist state. Similar changes in the affinity of noradrenaline and adrenaline were observed in the human platelet. The affinity of the imidazoline agonists, oxymetazoline and UK-14,304, however, was unchanged by Na^+ when inhibiting [^{3}H]-adrenaline binding, and there was only a small decrease in the affinity of oxymetazoline for [^{3}H]-RS-15385-197 binding. These data suggest that the interaction of imidazoline and catecholamine agonists with the receptor may be different, and support an earlier hypothesis by Ruffulo *et al.* (1977).

The differential effects of Na^+ ions on ^{3}H-agonist and ^{3}H-antagonist binding to the α_{2A}- and α_{2B}-adrenoceptor subtypes suggests that the concentration of Na^+ around the vicinity of the receptor may affect its physiological characteristics. Given that the residue reputed to be responsible for Na^+ regulation of ligand binding faces intracellularly (Horstman *et al.*, 1990), the intracellular Na^+ concentration may be important for the final functional response. Studies in the human platelet (Limbird, 1984) and NG 108-15 cells (Isom *et al.*, 1987) have demonstrated that α_2-adrenoceptor activation can increase intracellular Na^+ by stimulating a Na^+/H^+ antiporter in the cell membrane. Further studies are required to determine what functional effects an increased intracellular Na^+ concentration has on the pharmacology of the α_2-adrenoceptor subtypes. Molecular biology shows that the structure of the α_{2A}- and α_{2B}-adrenoceptors are different; however, activation of these receptors may be greatly modulated by the local receptor environment.

References

BROWN, C.M., MACKINNON, A.C., KILPATRICK, A.T., REDFERN, W.S., RAMCHARAN, M., CLAGUE, R.U., SMALL, C., HICKS, P.E., CLARK, R., SPEDDING, M. & MACFARLANE, C.B. (1993). The pharmacology of RS-15385-197, a potent and selective alpha$_2$-adrenoceptor antagonist. *Br. J. Pharmacol.*, **108**, 516–525.

BYLUND, D.B. (1985). Heterogeneity of alpha$_2$-adrenergic receptors. *Pharmacol. Biochem. Behav*,. **22**, 835–843.

BYLUND, D.B., RAY-PRENGER, C. & MURPHY, T.J. (1988). Alpha$_{2A}$- and alpha$_{2B}$-adrenergic receptors: antagonist binding in tissues and cell lines containing only one subtype. *J. Pharmacol. Exp. Ther*,. **245**, 600–607.

CHENG, Y.C. & PRUSOFF, W.H. (1973). Relationship between the inhibition constant (Ki) and the concentration of inhibitor which caused 50 per cent inhibition (I_{50}) of an enzymic reaction. *Biochem. Pharmacol*,. **22**, 3099–3108.

CHEUNG, Y.D., BARNETT, D.B. & NAHORSKI, S.R. (1982). [^{3}H]-Rauwolscine and [^{3}H]-yohimbine binding to rat cerebral and human platelet membranes: possible heterogeneity of alpha$_2$-adrenoceptors. *Eur. J. Pharmacol.*, **84**, 79–85.

GANTZOS, R.D. & NEUBIG, R.R. (1988). Temperature effects on α_2-adrenergic receptor-Gi interactions. *Biochem. Pharmacol.*, **37**, 2815–2821.

GLEASON, M.M. & HIEBLE, J.P. (1991). Ability of SK&F 104078 and SK&F 104856 to identify alpha-$_2$ adrenoceptor subtypes in NCB 20 cells and guinea pig lung. *J. Pharmacol. Exp. Ther.*, **259**, 1124–1132.

GUYER, C.A., HORSTMAN, D.A., WILSON, A.L., CLARK, J.D., CRAGOE, E.J.Jnr. & LIMBIRD, L.E. (1990). Cloning, sequencing and expression of the gene encoding the porcine α_2-adrenergic receptor. *J. Biol. Chem.*, **265**, 17307–17317.

HORSTMAN, D.A., BRANDON, S., WILSON, A.L., GUYER, C.A., CRAGOE, E.J. & LIMBIRD, L.E. (1990). An aspartate conserved among G-protein receptors confers allosteric regulation of α_2-adrenergic receptors by sodium. *J. Biol. Chem*,. **265**, 21590– 21595.

ISOM, L.L., CRAGOE, E.J. & LIMBIRD, L.E. (1987). α_2-Adrenergic receptors accelerate Na^+/H^+ exchange in neuroblastoma x glioma cells. *J. Biol. Chem*,. **262**, 6750–6757.

KAHN, D.J., MITRIUS, J.C. & U'PRICHARD, D.C. (1982). Alpha$_2$-adrenergic receptors in neuroblastoma x glioma hybrid cells: characterisation with agonist and antagonist radioligands and relationship to adenylate cyclase. *Mol. Pharmacol.*, **21**, 17–26.

LATIFPOUR, J., JONES, S.B. & BYLUND, D.B. (1982). Characterization of [^{3}H]-yohimbine binding to putative alpha$_2$-adrenergic receptors in neonatal rat lung. *J. Pharmacol. Exp. Ther.*, **223**, 606–611.

LIMBIRD, L.E. (1984). GTP and Na^+ modulate receptor adenylate cyclase coupling and receptor-mediated function. *Am. J. Physiol.*, **247**, E59–E68.

LIMBIRD, L.E., SPECK, J.L. & SMITH, S.K. (1982). Sodium ion modulates agonist and antagonist interactions with the human platelet alpha$_2$-adrenergic receptor in membranes and solubilised preparations. *Mol. Pharmacol*,. **21**, 609–617.

MACKINNON, A.C., SPEDDING, M. & BROWN, C.M. (1991). [^{3}H]-adrenaline does not label an α_{2B}-adrenoceptor on rat neonatal lung. *Br. J. Pharmacol*,. **104**, 415P.

MACKINNON, A.C., KILPATRICK, A.T., KENNY, B.A., SPEDDING, M. & BROWN, C.M. (1992). [^{3}H]-RS-15385-197, a selective and high affinity radioligand for α_2-adrenoceptors: implications for receptor classification. *Br. J. Pharmacol.*, **106**, 1011–1018.

MCGRATH, J.C., BROWN, C.M. & WILSON, V.G. (1989). Alpha-adrenoceptors: a critical review. *Med. Res. Reviews*, **9**, 407–533.

MUNSON, P.J. & RODBARD, D. (1980). A versatile computerised approach for characterisation of ligand binding systems. *Anal. Biochem*, **107**, 220–239.

MURPHY, T.J. & BYLUND, D.B. (1988). Characterisation of alpha-$_2$ adrenergic receptors in the OK cell, an opposum kidney cell line. *J. Pharmacol. Exp. Ther.*, **244**, 571–578.

NAHORSKI, S.R., BARNETT, D.B. & CHEUNG, Y.D. (1985). Alpha-adrenoceptor-effector coupling: affinity states or heterogeneity of the alpha$_2$-adrenoceptor? *Clin. Sci.*, **68**, (Suppl. 10), 395–425.

NEUBIG, R.R., GANTZOS, R.D. & BRASIER, R.S. (1988). Agonist and antagonist binding to alpha-$_2$ adrenergic receptors in purified membranes from human platelets. *Mol. Pharmacol.*, **28**, 475–486.

NUNNARI, J.M., REPASKE, M.G., BRANDON, S., CRAGOE, E.J. & LIMBIRD, L.E. (1987). Regulation of porcine brain alpha$_2$-adrenergic receptors by Na^+,H^+ and inhibitors of Na^+/H^+ exchange. *J. Biol. Chem.*, **262**, 12387–12392.

PETRASH, A.C. & BYLUND, D.B. (1986). Alpha$_2$-adrenergic receptor subtypes indicated by [^{3}H]-yohimbine binding in human brain. *Life Sci.*, **38**, 2129–2137.

RUFFOLO, R.R.Jr., NICHOLS, A.J., STADEL, J.M. & HIEBLE, J.P. (1991). Structure and function of α-adrenoceptors. *Pharmacol. Rev.*, **43**, 475–505.

RUFFOLO, R.R.Jr., TUROWSKI, B.S. & PATIL, P.N. (1977). Lack of cross desensitisation between structurally dissimilar α-adrenoceptor agonists. *J. Pharm. Pharmacol.*, **29**, 378–380.

SENARD, J., MAURIEGE, P., DAVIAUD, D. & PARIS, H. (1988). α_2-adrenoceptor in HT29 human colon adenocarcinoma cell-line: study of [^{3}H]-adrenaline binding. *Eur. J. Pharmacol.*, **162**, 225–236.

SIMONNEAUX, V., EBADI, M. & BYLUND, D.B. (1991). Identification and characterisation of α_{2D}-adrenergic receptors in bovine pineal gland. *Mol. Pharmacol.*, **40**, 235–241.

UHLEN, S. & WIKBERG, J.E.S. (1991). Delineation of three pharmacological subtypes of α_2-adrenoceptor in the rat kidney. *Br. J. Pharmacol.*, **104**, 657–664.

UHLEN, S., XIA, Y,. CHHAJLANI, V., FELDER, C.C. & WIKBERG, J.E.S. (1992). [^{3}H]-MK 912 binding delineates two α_2-adrenoceptor subtypes in rat CNS one of which is identical with the cloned pA2d α_2-adrenoceptor. *Br. J. Pharmacol.*, **106**, 986–995.

U'PRICHARD, D.C., MITRIUS, J.C., KAHN, D.J. & PERRY, B.D. (1983). The α_2-adrenergic receptor: multiple affinity states and regulation of a receptor inversely coupled to adenylate cyclase. In *Molecular Pharmacology of Neurotransmitter Receptor Systems*. ed. Segawa, C.T., Yamamura, H.I. & Kuriyama, K. pp. 53–72. New York: Raven Press.

WILSON, A.L., SEIBERT, K., BRANDON, S., CRAGOE, E.J. & LIMBIRD, L.E. (1991a). Monovalent cation and amiloride analogue modulation of adrenergic ligand binding to the unglycosylated α_{2B}-adrenergic receptor subtype. *Mol. Pharmacol.*, **39**, 481–486.

WILSON, V.G., BROWN, C.M. & MCGRATH, J.C. (1991b). Are there more than two types of α-adrenoceptors involved in physiological responses. *Exp. Physiol.*, **76**, 317–346.

ZENG, D., HARRISON, J.K, D'ANGELO, D.D., BARBER, C.M., TUCKER, A.L., LU, K. & LYNCH, K.R. (1990). Molecular characterisation of a rat α_{2B}-adrenergic receptor. *Biochemistry*, **87**, 3102–3106.

(Received January 4, 1993
Revised January 18, 1993
Accepted January 28, 1993)

Br. J. Pharmacol. (1993), **109**, 379–385 © Macmillan Press Ltd, 1993

Excitatory amino acid receptor-stimulated phosphoinositide turnover in primary cerebrocortical cultures

Graham J. Birrell & Frank W. Marcoux

Parke-Davis Pharmaceutical Research Division, Warner-Lambert Company, 2800 Plymouth Road, Ann Arbor, MI 48106, U.S.A.

1 Characterization of excitatory amino acid-induced accumulation of [^{3}H]-phosphoinositides was carried out in primary cerebrocortical cultures isolated from foetal rats.

2 All of the excitatory amino acid receptor agonists examined caused concentration-dependent enhancement of phosphoinositide (PI) formation. The most potent excitatory amino acid receptor agonists were quisqualate, (1S,3**R**)-1-aminocyclopentane-1,3-dicarboxylic acid ((1S,3**R**)-ACPD), ibotenate and glutamate with mean EC_{50} values of $0.9 \pm 0.4\,\mu M$, $15 \pm 5\,\mu M$, $15 \pm 3\,\mu M$ and $41 \pm 8\,\mu M$ respectively.

3 The selective ionotropic receptor antagonists kynurenic acid (1 mM), 2,3-dihydroxy-6-nitro-7-sulphamoyl-benzo(F)quinoxaline (NBQX, 10 μM) and ($\pm$)-4-(3-phosphonopropyl)-2 piperazinecarboxylic acid (CPP, 100 μM), failed to block responses to quisqualate, (1S,3**R**)-ACPD or glutamate. D,L-2-Amino-3-phosphonopropionate (D,L-AP3) did not block 1S,3**R**-ACPD or quisqualate-induced PI turnover, but had an additive effect with quisqualate or (1S,3**R**)-ACPD.

4 Exposure of cultures to agonists in the absence of added extracellular calcium reduced the maximal quisqualate response by approximately 45%, revealing a two-component concentration-response curve. Concentration-response curves to ibotenate and glutamate became flattened by omission of extracellular calcium, whereas (1S,3**R**)-ACPD-stimulated PI turnover was unaffected.

5 Pretreatment of cultures with pertussis toxin markedly inhibited PI responses evoked by (1S,3**R**)-ACPD.

6 These results suggest that excitatory amino acid-stimulated PI turnover in cerebrocortical cultures is independent of ionotropic receptor activation and is mediated via specific G-protein-linked metabotropic receptors. The partial dependence of the responses to quisqualate, ibotenate and glutamate on the presence of extracellular calcium suggests that the effects of these agonists may be mediated by more than one receptor subtype.

Keywords: Glutamate metabotropic receptors; (1S,3**R**)-ACPD; quisqualate; ibotenate

Introduction

The amino acid, glutamate, is a major excitatory neurotransmitter in the mammalian central nervous system. Receptors for glutamate have been divided into four major classes including N-methyl-D-aspartate (NMDA), kainate, α-amino-hydroxy-5-methyl -4-isoxazolepropionic acid (AMPA), and metabotropic or (1S,3**R**)-1-aminocyclopentane-1,3-dicarboxylic acid ((1S,3**R**)-ACPD) receptors (Monaghan *et al.*, 1989; Watkins *et al.*, 1990). Stimulation of NMDA, AMPA and kainate receptors directly activates cation channels allowing the entry of Na^+ or Ca^{2+}, whereas excitatory amino acids acting via metabotropic receptors stimulate phosphoinositide turnover (see Schoepp *et al.*, 1990a).

Evidence from a large number of studies supports the involvement of excitatory amino acids and their receptors in a range of important processes including the neuronal cell injury associated with a variety of neurological disorders (see Meldrum & Garthwaite, 1990; Farooqui & Horrocks, 1991). Thus, characterization of the pharmacology of these receptors is essential for developing a greater understanding of the mechanisms mediating the effects of excitatory amino acids within the CNS.

Primary cerebrocortical cultures have been used extensively to study the excitotoxicity of excitatory amino acids and as a model system for hypoxia and hypoglycemia-induced cell death (see Choi & Rothman, 1990). Cerebrocortical cultures also provide a useful preparation for the study of the responses of isolated mammalian CNS neurones *in vitro*.

Although quisqualate, ibotenate and glutamate are potent agonists at the metabotropic receptor, complex interactions between ionotropic and metabotropic receptor-mediated responses may exist (Baudry *et al.*, 1986; Nicoletti *et al.*, 1986a; Baird & Nahorski, 1991; Morari *et al.*, 1991). Recently (1S,3**R**)-ACPD has been identified as a selective agonist for the metabotropic glutamate receptor (Palmer *et al.*, 1989). Characterization of excitatory amino acid stimulated phosphoinositide turnover in primary cerebrocortical cultures was examined using (1S,3**R**)-ACPD as a selective metabotropic receptor agonist, and 2,3-dihydroxy-6-nitro-7-sulphamoyl-benzo(F) quinoxaline (NBQX), ($\pm$)-4-(3-phosphonopropyl)-2-piperazinecarboxylic acid (CPP) and kynurenate as selective antagonists for glutamate ionotropic receptors. Dependency of the response on extracellular calcium and the possible involvement of a G-protein were also studied.

Methods

Cerebrocortical cultures

Primary cultures were prepared from foetal rat cerebral cortex as previously described (Marcoux *et al.*, 1990). Briefly, cortical hemispheres were sectioned from foetal rat brain and dissociated in Hank's Balanced salt solution (HBSS) containing 0.1% trypsin. The cells were then triturated and suspended in 50% Dulbecco's Modified Eagle's Medium (DME) and 50% Ham's Nutrient Mixture F-12 (F-12) supplemented with 10% horse serum and 6% foetal calf serum, and were plated out on 24 well plates at an approximate density of

200,000 cells cm^{-2}. After 4 days incubation additions of 5-fluoro-deoxyuridine (15 $\mu g\ ml^{-1}$) and uridine (35 $\mu g\ ml^{-1}$) were made to inhibit further division of non-neuronal cells (Ransom *et al.*, 1977). Feeding were performed as necessary with DME/F-12 with 10% horse serum.

Purified glial cultures were made by removing media from a plated well and exposing mixed culture preparations to air for 10 s. This procedure produced cultures which stained for glial fibrillary acidic protein with no residual neuronal cells (Marcoux *et al.*, 1989).

Comparisons between conditions within experiments were made by use of sister cultures from a single plating, thus maintaining matched cell densities and proportions of neuronal to non-neuronal cell types.

Measurement of [^{3}H]-inositol phosphate accumulation

After 15 days *in vitro* the medium was aspirated and cultures were labelled by adding 0.5 ml DME/F-12 with 10% horse serum containing 1 $\mu Ci\ ml^{-1}$ [^{3}H]-myo-inositol to each well. After 48 h, the medium was aspirated, and the cells washed twice with HBSS containing 10 mM LiCl (HBSS/LiCl). Cultures were then incubated at 37°C for 15 min in HBSS/LiCl to block inositol phosphate degradation (Allison *et al.*, 1976; Berridge *et al.*, 1982). Agonist exposures of 20 min duration were performed at 37°C, and were terminated by replacing the incubation medium with 0.5 ml ice-cold 5% trichloracetic acid (TCA). Each TCA extract was then applied to mini-columns containing Dowex-formate anion exchange resin. To remove free residual [^{3}H]-inositol, columns were washed four times with 3 ml 5 mM inositol. Total [^{3}H]-inositol phosphates were then eluted with two times 2 ml of 1 M ammonium formate containing 0.1 M formic acid. All fractions were collected, added to 15 ml of scintillation cocktail (Beckman Ready Gel), and counted for tritium on a scintillation spectrometer (Packard).

Some of the experiments in the present study were carried out in the absence of added calcium. In this case, cultures were washed twice with calcium-free HBSS/LiCl, and incubated for 15 min in this medium prior to agonist exposure. The same protocol was used for experiments carried out in the absence of added magnesium.

In those experiments involving pertussis toxin, cultures were incubated for 12 h before agonist exposure in media containing 1 $\mu g\ ml^{-1}$ of the toxin.

Data analysis

Agonist-stimulated accumulation of [^{3}H]-phosphoinositides was expressed as a percentage of basal control as determined from cultures exposed to vehicle alone. Mean values are expressed ± s.e.mean. Statistical analysis of differences between means was carried out with Student's *t*-test (two-tailed) and the null hypothesis rejected at $P<0.05$. EC_{50} and maximum response values for agonists were determined from logistic sigmoid plots generated by a curve fitting programme (Sigmaplot). Sigmoid plots were fitted to mean concentration-effect curves using the equation $f = (a-d)/[1 + (x/c)\ b]$, where a represents the maximum response, b the slope, c the EC_{50} and d the minimum response.

Materials

Myo-[2-^{3}H]-inositol: water/ethanol (9:1) solution was obtained from Amersham, Dowex AG1-X8 Anion exchange resin 100–200 mesh formate form was supplied by Biorad, and (1S,3R)-1-aminocyclopentane-1,3-dicarboxylate ((1S,3R)-ACPD) was from Tocris Neuramin Ltd. (2,3-Dihydroxy-6-nitro-7-sulphamoyl-benzo(F)quinoxaline (NBQX) and (±)-4-(3-phosphonopropyl)-2 piperazinecarboxylic acid (CPP) were obtained from Parke-Davis. Glutamic acid, quisqualic acid, kainic acid, ibotenic acid, N-methyl-D-aspartic acid (NMDA), α-amino-hydroxy-5-methyl-4- isoxazolepropionic acid (AMPA) and kynurenic acid were obtained from Sigma. Pertussis toxin (*Bordetella pertussis*) was purchased from Calbiochem. Drugs were dissolved in HBSS except NBQX which was dissolved in dimethyl sulphoxide (DMSO) and diluted in HBSS to produce a final concentration of <0.1% DMSO.

Results

Quisqualate, ibotenate, (1S,3R)-ACPD and glutamate caused concentration-dependent enhancement of [^{3}H]-phosphoinositide accumulation with EC_{50} values of 0.9 ± 0.4 μM, 15 ± 3 μM, 15 ± 5 μM and 41 ± 8 μM respectively. Results are summarized in Figure 1. Concentration-response curves to (1S,3R)-ACPD, ibotenate and glutamate had similar mean maximal values. The mean maximal response to quisqualate was higher than that of the other agonists. Concentration-response curves for quisqualate were often bell-shaped with concentrations above 3–10 μM producing progressively smaller responses. Only modest increases in phosphoinositide formation were evoked by NMDA (109 ± 3% of basal at 1 mM, $n = 9$), AMPA (131 ± 4% of basal at 1 mM, $n = 6$) or kainate (128 ± 5% of basal at 1 mM, $n = 6$), and estimated EC_{50} values were >1 mM.

In experiments with purified glial cell cultures, [^{3}H]-phosphoinositide accumulation from exposure to quisqualate ($n = 6$) or (1S,3R)-ACPD ($n = 6$), was increased significantly ($P<0.05$, Student's *t* test) above control levels. However, stimulated levels of [^{3}H]-phosphoinositide in glial cultures did not exceed those obtained for basal turnover in mixed neuronal sister cultures derived from the same plating.

Effects of excitatory amino acid receptor antagonists

The selective ionotropic receptor antagonists CPP at 100 μM, NBQX at 10 μM, or kynurenate at 1 mM, concentrations sufficient to block maximal NMDA or AMPA receptor-mediated effects in neuronal preparations *in vitro* (Bertolino *et al.*, 1989; Lodge *et al.*, 1990; Benveniste & Mayer, 1991), had no effect on the concentration-response curve for (1S,3R)-ACPD. Concentration-response curves for quisqualate or

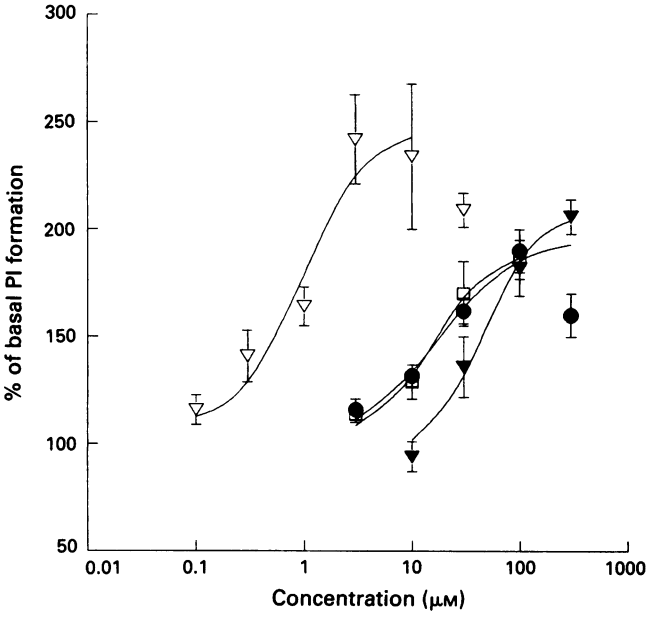

Figure 1 Concentration-dependent phosphoinositide (PI) formation in cerebrocortical cultures in response to quisqualate (▽, $n = 21$), (1S,3R)-ACPD (●, $n = 30$), ibotenate (□, $n = 9$), and glutamate (▼, $n = 6$). Values represent means ± s.e.mean of n determinations for each data point taken from between 2 and 10 separate experiments. Basal phosphoinositide accumulation was 738 ± 71 c.p.m.

Table 1 EC_{50} values for quisqualate, (1S,3R)-ACPD and glutamate in the absence and presence of various antagonists

Drugs	EC_{50} (μM)	n
Quisqualate	0.08 ± 0.02	9
Quisqualate + 100 μM CPP	0.18 ± 0.05	9
Quisqualate	0.05 ± 0.04	15
Quisqualate + 10 μM NBQX	0.1 ± 0.01	15
(1S,3R)-ACPD	11 ± 1.6	9
(1S,3R)-ACPD + 100 μM CPP	6 ± 0.8	9
(1S,3R)-ACPD	19 ± 3	6
(1S,3R)-ACPD + 10 μM NBQX	20 ± 0.4	6
(1S,3R)-ACPD	18 ± 8	6
(1S,3R)-ACPD + 1 mM kynurenate	12 ± 2	6
Glutamate	32 ± 3	9
Glutamate + 100 μM CPP	19 ± 1	9
Glutamate	25 ± 2	6
Glutamate + 10 μM NBQX	26 ± 1	6

Values represent the mean ± s.e.mean of *n* determinations for each data point taken from between 2 and 5 separate experiments. Comparisons between EC_{50} values were made between sister cultures in each experiment. For abbreviations, see text.

glutamate were not significantly altered by CPP (100 μM) or NBQX (10–100 μM). Results are summarized in Table 1. D,L-AP3, the reported glutamate metabotropic receptor antagonist, failed to inhibit (1S,3R)-ACPD or quisqualate-induced phosphoinositide turnover at concentrations up to 1 mM. AP3 alone at a concentration of 1 mM displayed agonist activity and had an additive effect with responses to (1S,3R)-ACPD and quisqualate (see Figure 2).

Calcium-dependence of phosphoinositide response

As illustrated in Figure 3, omission of calcium from the HBSS during agonist exposure caused a flattening of the concentration-response curves for ibotenate and glutamate, but had no effect on responses to (1S,3R)-ACPD. In approximately half of our experiments the quisqualate concentration-response curve appeared biphasic in nature. In these experiments the lower portion of the curve was unaffected by the absence of extracellular calcium, but the upper portion was abolished in medium lacking calcium. The remaining lower section of the curve had a mean maximum value comparable with that for (1S,3R)-ACPD.

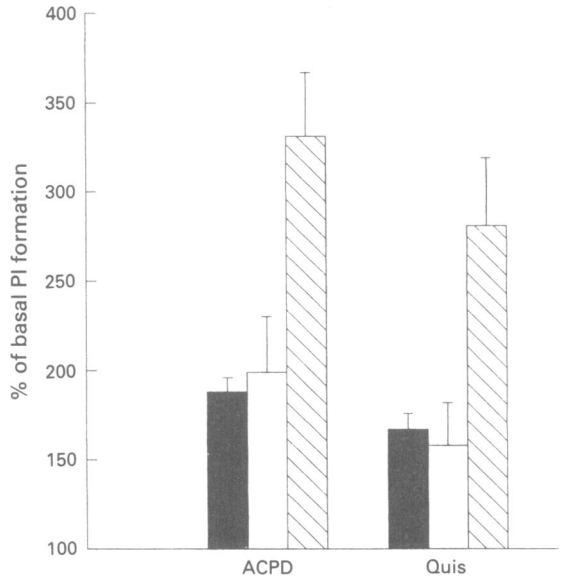

Figure 2 Phosphoinositide formation in response to (1S,3R)-ACPD (100 μM), quisqualate (Quis, 3 μM), or D,L-AP3 (1 mM). Columns represent either (1S,3R)-ACPD or quisqualate alone (solid columns), AP3 alone (open columns), or AP3 in combination with (1S,3R)-ACPD or quisqualate (hatched columns). Values are mean ± s.e.mean from 2 separate experiments with $n = 6$. Comparisons between conditions were made in sister cultures. Basal phosphoinositide formation was 640 ± 15 c.p.m. For abbreviations, see text.

Table 2 EC_{50} values for quisqualate, (1S,3R)-ACPD and glutamate in the presence and absence of magnesium in the exposure medium

Agonist	EC_{50} (μM) *HBSS*	EC_{50} (μM) Mg^{2+}-*free*	n
Quisqualate	1.4 ± 0.9	0.5 ± 0.05	21
1S,3R-ACPD	15 ± 5	18 ± 4	30
Glutamate	41 ± 8	52 ± 14	6

Values represent the mean ± s.e.mean of *n* determinations for each data point taken from between 2 and 10 separate experiments. Comparisons between EC_{50} values were made between sister cultures in each experiment.

Omission of magnesium from the extracellular medium, thus removing the voltage-dependent Mg^{2+} blockade of the NMDA receptor associated ion channel, resulted in an enhancement of the phosphoinositide accumulation evoked by NMDA. However, omission of calcium as well as magnesium from the exposure medium abolished this response (see Figure 4). Responses to glutamate, quisqualate or (1S,3R)-ACPD were not affected by magnesium-free medium. EC_{50} values obtained in the presence and absence of magnesium are shown in Table 2.

Effect of ionotropic receptor activation on the metabotropic response

The effects of selective activation of NMDA or AMPA receptors on (1S,3R)-ACPD-induced phosphoinositide accumulation were examined to determine whether any interaction occurs between ionotropic receptor-mediated and metabotropic receptor-stimulated phosphoinositide formation. As summarized in Figure 5, when NMDA or AMPA, at concentrations which alone evoked increases in phosphoinositide accumulation, were combined with a maximally effective concentration of (1S,3R)-ACPD, the response was no different from that caused by (1S,3R)-ACPD alone.

Sensitivity of phosphoinositide response to pertussis toxin pretreatment

Pre-incubation of cultures in pertussis toxin for 12 h before agonist exposure significantly reduced (1S,3R)-ACPD-stimulated [^{3}H]-phosphoinositide accumulation (Figure 6). Pertussis toxin pretreatment had no effect on basal phosphoinositide formation.

Discussion

The following rank-order of potency for excitatory amino acid receptor agonist-stimulated accumulation of [^{3}H]-phosphoinositides was obtained: quisqualate > (1S,3R)-ACPD = ibotenate > glutamate >> AMPA = kainate > NMDA. Although absolute potencies vary across neuronal preparations, this rank-order corresponds well with that described previously by others (Schoepp & Johnson, 1989; Schoepp *et al.*, 1990b; Watkins *et al.*, 1990; Masu *et al.*, 1991). Agonist-stimulated inositol phosphate formation was not inhibited by the ionotropic antagonists kynurenate, CPP or NBQX, suggesting that these responses are mediated by distinct glutamate metabotropic receptors, and are independent of ionotropic receptor activation. Similar findings have been

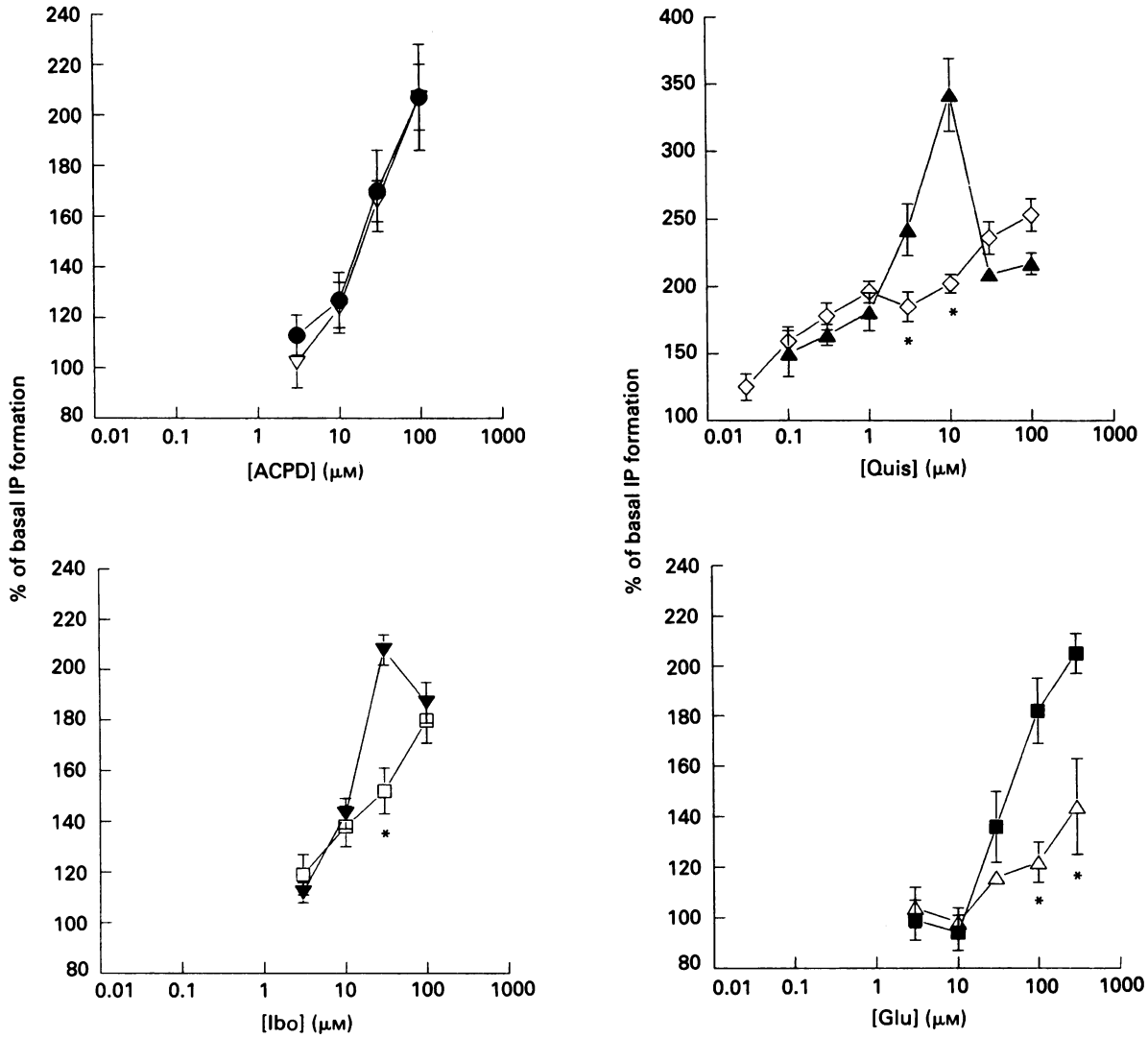

Figure 3 Phosphoinositide formation in cerebrocortical cultures in the presence (●) and absence (▽) of added extracellular calcium in response to (1S,3R)-ACPD ($n = 12$), quisqualate (Quis, $n = 12$), ibotenate (Ibo, $n = 6$) and glutamate (Glu, $n = 6$). Values represent the mean ± s.e.mean from n determinations for each data point taken from between 2 and 4 separate experiments. Values for nominally calcium-free media significantly less than those obtained with standard HBSS are shown by * when $P < 0.05$ (Student's t test). Basal phosphoinositide accumulation was 735 ± 16 c.p.m. and 561 ± 110 c.p.m. in the presence and absence of added extracellular calcium respectively.

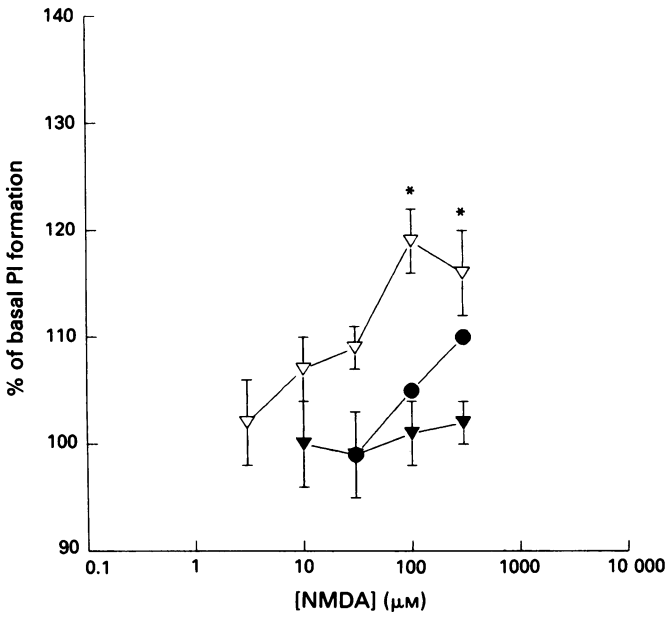

reported for metabotropic quisqualate or (1S,3R)-ACPD responses in other neuronal preparations (Nicoletti *et al.*, 1986b; Schoepp & Johnson, 1988; Palmer *et al.*, 1989; Furuya *et al.*, 1989). Stimulated phosphoinositide accumulation in purified glial cultures was lower than that for basal turnover in mixed cultures suggesting that the responses described in this study are associated primarily with neuronal cell populations.

In the absence of added calcium, a decrease in basal and (1S,3R)-ACPD- stimulated phosphoinositide accumulation was observed. However, the percentage increase above basal phosphoinositide turnover caused by (1S,3R)-ACPD was unaltered. In striatal slices (Doble & Perrier, 1989), synap-

Figure 4 Effects of extracellular magnesium and calcium on phosphoinositide formation in response to N-methyl-D-aspartate (NMDA). Concentration-response curves are shown for cultures exposed to normal medium (●), medium lacking magnesium (▽), or medium lacking magnesium and calcium (▼). Values are mean ± s.e.mean from 3 separate experiments with $n = 9$ for each data point. Values significantly greater than basal phosphoinositide formation are shown by * when $P < 0.05$ (Student's t test). Basal phosphoinositide accumulation was 727 ± 60 c.p.m. for normal HBSS and 721 ± 41 c.p.m. for magnesium-free medium.

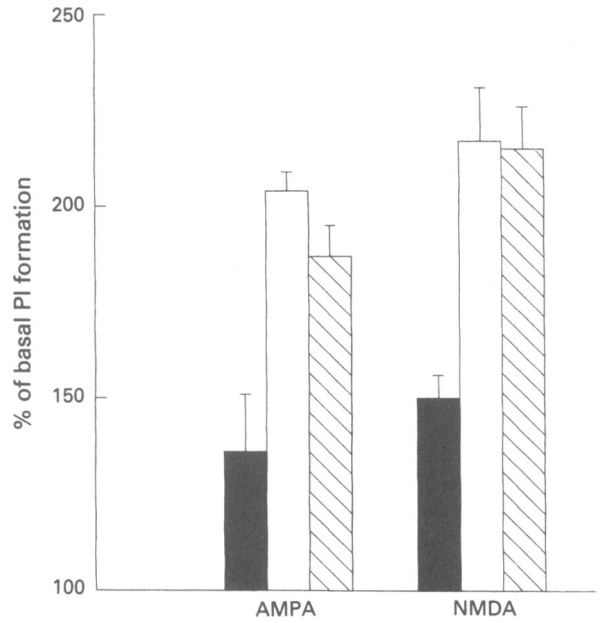

Figure 5 Effect of AMPA (300 μM) or NMDA (100 μM) on phosphoinositide (PI) formation stimulated by 100 μM (1S,3R)-ACPD. Columns represent the effects of AMPA or NMDA alone (solid columns), (1S,3R)-ACPD alone (open columns), or a combined exposure to (1S,3R)-ACPD with AMPA or NMDA (hatched columns). Exposures were performed using magnesium-free HBSS. Values are mean ± s.e.mean from 2 separate experiments with $n = 6$. Basal phosphoinositide accumulation was 819 ± 42 c.p.m. For abbreviations, see text.

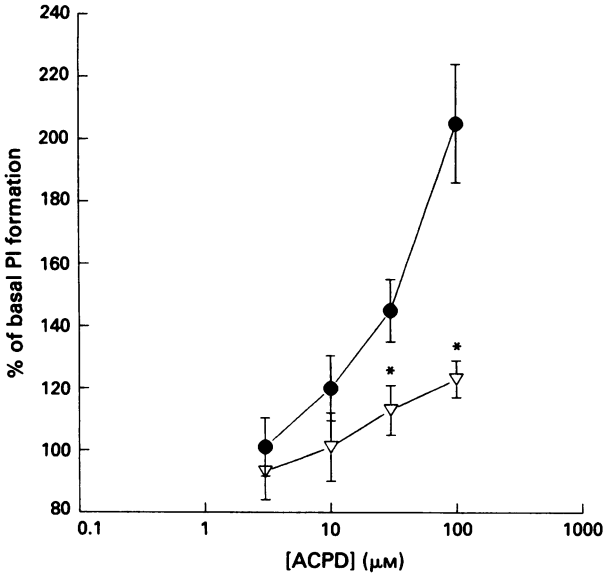

Figure 6 Effect of pertussis toxin pretreatment on phosphoinositide formation in response to (1S,3R)-ACPD. Concentration-response curves are shown for untreated cultures (●) and those exposed to pertussis toxin (PTX) (▽) for 12 h before agonist exposure. Values are mean ± s.e.mean from 3 separate experiments with $n = 9$ for each data point. Values for (1S,3R)-ACPD-stimulated phosphoinositide formation in PTX pretreated cultures significantly less than those obtained in control cultures are shown by * when $P < 0.05$ (Student's t test). Basal phosphoinositide accumulation was 583 ± 62 c.p.m. for control cultures and 631 ± 57 c.p.m. for pertussis pretreated cultures.

toneurosomes (Recasens *et al.*, 1987), and cerebellar granule cells (Nicoletti *et al.*, 1986c) similar results were obtained for quisqualate, ibotenate or glutamate. Reduced phosphoinositide accumulation probably reflects the calcium-dependency of phospholipase C activation, but the extent of stimulation by agonists is relatively calcium-independent (Bennet & Crooke, 1987; Berridge, 1987; Katan & Parker, 1987; Renard *et al.*, 1987). Our results suggest that (1S,3R)-ACPD-stimulated phosphoinositide metabolism is not dependent on influx of extracellular calcium and is mediated by a direct action rather than through calcium-dependent release of other neuroactive substances. However, the partial calcium-dependence of quisqualate, ibotenate and glutamate responses suggests these agonists may activate phosphoinositide metabolism via more than one mechanism.

Variations in the potency of quisqualate at the metabotropic receptor have been reported in different preparations, and may result from the presence of multiple metabotropic receptor subtypes. Evidence for multiple subtypes of metabotropic glutamate receptors also comes from cloning and expression of a family of metabotropic receptors (Tanabe *et al.*, 1992). In cortical neurones (Patel *et al.*, 1990), synaptoneurosomes (Recasens *et al.*, 1987; 1988; Guiramand *et al.*, 1989; Nakagawa *et al.*, 1990), striatal slices (Doble & Perrier, 1989) or retinal slices (Osborne, 1990), EC_{50} values for quisqualate range from 0.03–0.26 μM. However, in slices from hippocampus (Palmer *et al.*, 1988; Schoepp & Johnson, 1988; 1989), cerebellum (Blackstone *et al.*, 1989) or cerebral cortex (Godfrey *et al.*, 1988; Godfrey & Taghavi, 1990; Schoepp *et al.*, 1990b; Schoepp & Hillman, 1990), EC_{50} values range from 2–50 μM. Such variations in EC_{50} values are not reported for (1S,3R)-ACPD, suggesting that this agonist may act more selectively at a particular metabotropic receptor.

In the present study, EC_{50} values for quisqualate varied between experiments depending on the presence or absence of the calcium-sensitive portion of the concentration-response curve. Quisqualate was approximately ten fold less potent with regard to the calcium-sensitive response. This may correspond to the higher EC_{50} values seen in some of the preparations described above. The inconsistent nature and bell-shaped appearance of the upper section of the concentration-response curve suggests that this response may be susceptible to desensitization, responses becoming progressively smaller with increasing concentrations. Alternatively, quisqualate may be acting via a separate mechanism to inhibit calcium-sensitive phosphoinositide formation at these higher concentrations. Since combined activation of metabotropic and ionotropic receptors using (1S,3R)-ACPD with AMPA or NMDA did not produce an additive effect on total phosphoinositide formation, we propose that the upper portion of the quisqualate response is not mediated by ionotropic receptors. Although the effects of CPP or NBQX on the calcium-sensitive upper portion of the quisqualate response could not be determined in this study, further evidence against the involvement of ionotropic receptors comes from the finding that responses to glutamate or ibotenate, while partially sensitive to extracellular calcium, were not inhibited by these antagonists. Thus, the biphasic nature of the concentration-response curve for quisqualate supports the idea that multiple excitatory amino acid receptors, linked to the stimulation of phosphoinositide formation, are associated with cortical neurones in culture. These receptor subtypes may be associated with the same neurones or with different neuronal populations.

Responses to NMDA were enhanced by the omission of magnesium from the exposure medium suggesting that these effects were mediated via activation of NMDA receptors. Removal of calcium from magnesium-free medium abolished responses to NMDA confirming that ionotropic receptor-mediated calcium influx is required for NMDA-stimulated phosphoinositide formation in this preparation. In other systems NMDA produces weak or no effect on phosphoinositide metabolism (Sladeczek *et al.*, 1985; Nicoletti *et al.*, 1986b; 1987; Recasens *et al.*, 1987; 1988; Godfrey *et al.*, 1988; Schoepp & Johnson, 1988; Gonzales & Moerschbaecher, 1989), and its stimulatory effects can be blocked by NMDA receptor antagonists, supporting the involvement of ionotropic NMDA receptors in this response. Contrary to a number of previous studies showing an inhibitory effect of

NMDA on basal or stimulated phosphoinositide formation (Baudry *et al.*, 1986; Nicoletti *et al.*, 1986a; Schmidt *et al.*, 1987; Godfrey *et al.*, 1988; Gonzales & Moerschbaecher, 1989; Noble *et al.*, 1989; Morrisett *et al.*, 1990; Baird & Nahorski, 1991) in the present study NMDA had no inhibitory effect on basal or (1S,3R)-ACPD-stimulated phosphoinositide formation.

D,L-AP3 has been described as an antagonist of metabotropic receptors (Nicoletti *et al.*, 1986b; Schoepp & Johnson, 1989; Hwang *et al.*, 1990), although the high concentrations of AP3 required for blockade have cast some doubt on its selectivity (Baskys, 1992). In the present study D,L-AP3 failed to block (1S,3R)-ACPD responses at concentrations up to 1 mM, but at this concentration displayed agonist activity. In striatal neurones AP3 has been described as a partial agonist, inhibiting responses to quisqualate (Olivier *et al.*, 1991). Here, the drug had an additive effect with (1S,3R)-ACPD and quisqualate responses at 1 mM, with no evidence of inhibiting their effects, suggesting that AP3 is stimulating phosphoinositide formation by an alternative mechanism.

Exposure of cerebrocortical culture to pertussis toxin before agonist exposure in the present study greatly reduced phosphoinositide accumulation evoked by (1S,3R)-ACPD. In *Xenopus* oocytes injected with rat brain mRNA (Sugiyama *et al.*, 1987), in cerebellar granule cells (Nicoletti *et al.*, 1988), and in striatal or hippocampal neurones (Ambrosini & Meldolesi, 1989) pertussis toxin pretreatment also blocked glutamate metabotropic receptor-mediated events. These results suggest that glutamate metabotropic receptors in these preparations and in cerebrocortical neurones in culture are coupled with a pertussis toxin-sensitive G-protein. However, as a point of caution, pertussis toxin acts at several G-proteins (Gilman, 1987), and may be acting indirectly to modulate the phosphoinositide response associated with glutamate metabotropic receptor activation.

In conclusion, the present study has demonstrated that the stimulatory effects of glutamate on phosphoinositide metabolism in primary cerebrocortical cultures are mediated primarily by G-protein-linked metabotropic receptors distinct from ionotropic AMPA or NMDA receptors, and that these metabotropic receptors are associated with neuronal populations present in these cultures. Based on the inconsistent and sometimes biphasic nature of the quisqualate concentration-response curve and the partial sensitivity of the quisqualate response to removal of extracellular calcium, these effects are mediated by more than one receptor subtype. D,L-AP3 was not an effective antagonist of glutamate receptor-stimulated phosphoinositide formation, but had an additive stimulatory effect with quisqualate or (1S,3R)-ACPD. Thus, it is essential that more selective antagonists for glutamate metabotropic receptors be developed for further progress to be made in this important area of excitatory amino acid research.

References

ALLISON, J.H., BLISNER, M.E., HOLLAND, W.H., HIPPS, P.P. & SHERMAN, W.R. (1976). Increased brain myo-inositol-1-phosphate in lithium treated rats. *Biochem. Biophys. Res. Commun,*. **71,** 664–670.

AMBROSINI, A. & MELDOLESI, J. (1989). Muscarinic and quisqualate receptor-induced phosphoinositide hydrolysis in primary cultures of striatal and hippocampal neurones. Evidence for differential mechanisms of activation. *J. Neurochem.*, **53,** 825–833.

BAIRD, J.G. & NAHORSKI, S.R. (1991). Stimulatory and inhibitory effects of N-methyl-D-Aspartate on ^{3}H-inositol phosphate accumulation in rat cortical slices. *J. Neurochem*, **57,** 629–635.

BASKYS, A. (1992). Metabotropic receptors and 'slow' excitatory actions of glutamate agonists in the hippocampus. *Trends Neurosci.*, **15,** 92–96.

BAUDRY, M., EVANS, J. & LYNCH, G. (1986). Excitatory amino acids inhibit stimulation of phosphatidylinositol metabolism by aminergic agonist in hippocampus. *Nature*, **319,** 329–331.

BENNET, C.F. & CROOKE, S.T. (1987). Purification and characterization of a phosphoinositide-specific phospholipase C from guinea pig uterus. *J. Biol. Chem,*. **262,** 13789–13797.

BENVENISTE, M. & MAYER, M.L. (1991). Structure-activity analysis of binding kinetics for NMDA receptor competitive antagonists: the influence of conformational restriction. *Br. J. Pharmacol.*, **104,** 207–221.

BERRIDGE, M.J. (1987). Inositol triphosphate and diacylglycerol: two interacting second messengers. *Ann. Rev. Biochem.*, **56,** 159–193.

BERRIDGE, M.J., DOWNES, C.P. & HANLEY, M.R. (1982). Lithium amplifies agonist-dependent phosphatidylinositol responses in brain and salivary glands. *Biochem. J.*, **206,** 587.

BERTOLINO, M., VICINI, S. & COSTA, E. (1989). Kynurenic acid inhibits the activation of kainic and N-methyl-D-aspartic acid-sensitive ionotropic receptors by a different mechanism. *Neuropharmacology*, **28,** 453–457.

BLACKSTONE, C.D., SUPATTAPONE, S. & SNYDER, S.H. (1989). Inositol phospholipid-linked glutamate receptors mediate cerebellar parallel-fibre-purkinje-cell synaptic transmission. *Proc. Natl Acad. Sci. USA*, **86,** 463–467.

CHOI, D.W. & ROTHMAN, S.M. (1990). The role of glutamate neurotoxicity in hypoxic-ischemic neuronal death. *Annu. Rev. Neurosci.*, **13,** 171–182.

DOBLE, A. & PERRIER, M.L. (1989). Pharmacology of excitatory amino acid receptors coupled to inositol phosphate metabolism in neonatal rat striatum. *Neurochem. Int.*, **15,** 1–8.

FAROOQUI, A.A. & HORROCKS, L.A. (1991). Excitatory amino acid receptors, neural membrane phospholipid metabolism and neurological disorders. *Brain Res. Rev.*, **16,** 171–191.

FURUYA, S., OHMORI, H., SHIGEMOTO, T. & SUGIYAMA, H. (1989). Intracellular calcium mobilization triggered by a glutamate receptor in rat cultured hippocampal cells. *J. Physiol,*. **414,** 539–548.

GILMAN, A.G. (1987). G proteins: transducers of receptor generated signals. *Annu. Rev. Biochem.*, **56,** 615–649.

GODFREY, P.P., WILKINS, C.J., TYLER, W. & WATSON, S.P. (1988). Stimulatory and inhibitory actions of excitatory amino acids on inositol phospholipid metabolism in rat cerebral cortex. *Br. J. Pharmacol,*. **95,** 131–138.

GODFREY, P.P. & TAGHAVI, Z. (1990). The effect of non-NMDA antagonists and phorbol esters on excitatory amino acid-stimulated inositol phosphate formation in rat cerebral cortex. *Neurochem. Int.*, **16,** 65–72.

GONZALES, R.A. & MOERSCHBAECHER, J.M. (1989). A phencyclidine recognition site is associated with N-methyl-D-aspartate inhibition of carbachol-stimulated phosphoinositide hydrolysis in rat cortical slices. *Mol. Pharmacol,*. **35,** 787–794.

GUIRAMAND, J., SASSETTI, I. & RECASENS, M. (1989). Developmental changes in the chemosensitivity of rat brain synaptoneurosomes to excitatory amino acids, estimated by inositol phosphate formation. *Int. J. Dev. Neurosci.*, **7,** 257–266.

HWANG, P., BREDT, D.S. & SNYDER, S.H. (1990). Autoradiographic imaging of phosphoinositide turnover in the brain. *Science*, **249,** 802–804.

KATAN, M. & PARKER, P.J. (1987). Purification of phosphoinositide specific phospholipase C from a particulate fraction of bovine brain. *Eur. J. Biochem.*, **168,** 413–418.

LODGE, D., JONES, M.G. & PALMER, A.J. (1990). Excitatory amino acids: new tools for old stories or pharmacological subtypes of glutamate receptors: electrophysiological studies. *Can. J. Physiol. Pharmacol.*, **69,** 1123–1128.

MARCOUX, F.W., PROBERT, A.W. & WEBER, M.L. (1989). Hypoxic neuronal injury in cell culture: calcium accumulation blockade and neuroprotection by NMDA antagonists but not calcium channel antagonists. In *Cerebrovascular Diseases*. ed Ginsberg, M.D. & Dietrich, W.D. pp. 135–141. New York: Raven Press.

MARCOUX, F.W., PROBERT, A.W. & WEBER, M.L. (1990). Hypoxic neuronal injury in tissue culture is associated with delayed calcium accumulation. *Stroke*, **21** Suppl. III, 71–74.

MASU, M., TANABE, Y., TSUCHIDA, K., SHIGEMOTO, R. & NAKANISHI, S. (1991). Sequence and expression of a metabotropic glutamate receptor. *Nature*, **349,** 760–765.

MELDRUM, B. & GARTHWAITE, J. (1990). Excitatory amino acid neurotoxicity and neurodegeneratine disease. *Trends Pharmacol. Sci.*, **11,** 379–386.

MONAGHAN, D.T., BRIDGES, R.J. & COTMAN, C.W. (1989). The excitatory amino acid receptors: their classes, pharmacology and distinct properties in the function of the central nervous system. *Annu. Rev. Pharmacol. Toxicol.*, **29**, 365–402.

MORARI, M., CALO, G., ANTONELLI, T., GAIST, G., ACCIARRI, N., FABRIZI, A., BIANCHI, C. & BEANI, L. (1991). Inhibitory effect of NMDA receptor activation on quisqualate-stimulated phosphatidylinositol turnover in the human cerebral cortex. *Brain Res.*, **553**, 14–17.

MORRISETT, R.A., CHOW, C.C., SAKAGUCHI, T., SHIN, C. & MCNAMARA, J.O. (1990). Inhibition of muscarinic coupled phosphoinositide hydrolysis by N-methyl-D-aspartate is dependent on depolarization via channel activation. *J. Neurochem.*, **54**, 1517–1525.

NAKAGAWA, Y., SAITOH, K., ISHIHARA, M.J. & SHINOZAKI, H. (1990). (1S,3S,4S) α (carboxycyclopropyl) glycine is a novel agonist of metabotropic glutamate receptors. *Eur. J. Pharmacol.*, **184**, 205–206.

NICOLETTI, F., IADAROLA, M.J., WROBLESKI, J.T. & COSTA, E. (1986a). Excitatory amino acid recognition sites coupled with inositol phospholipid metabolism: developmental changes and interaction with α_1 adrenoceptors. *Proc. Natl. Acad. Sci. USA*, **83**, 1931–1935.

NICOLETTI, F., MEEK, J.L., IADORALA, M.J., CHUANG, D.M., ROTH, B.L. & COSTA, E. (1986b). Coupling of inositol phospholipid metabolism with excitatory amino acid recognition sites in rat hippocampus. *J. Neurochem*, **46**, 40–46.

NICOLETTI, F., WORLEWSKI, J.T. & COSTA, E. (1987). Magnesium ions inhibit the stimulation of inositol phospholipid hydrolysis in primary culture of cerebellar granule cells. *J. Neurochem.*, **48**, 967–973.

NICOLETTI, F., WROBLEWSKI, J.T., FADDA, E. & COSTA, E. (1988). Pertussis toxin inhibits signal transduction at a specific metabotropic glutamate receptor in primary cultures of cerebellar granule cells. *Neuropharmacology*, **27**, 551–556.

NICOLETTI, F., WROBLEWSKI, J.T., NOVELLI, A., ALHO, H., GUILOTTI, A. & COSTA, E. (1986c). The activation of inositol phospholipid metabolism as a signal-transducing system for excitatory amino acids in primary cultures of cerebellar granule cells. *J. Neurosci.*, **6**, 1905–1911.

NOBLE, E.P., SINCINI, E., BERGMANN, D. & BRUGGENCATE, G.T. (1989). Excitatory amino acids inhibit stimulated phosphoinositide hydrolysis in rat prefrontal cortex. *Life Sci.*, **44**, 19–26.

OLIVIER, J.J., POULAT, F., DO, E., SAHUQUET, A., SASSETTI, I., BOCKAERT, J. & SLAECZEK, F.A.J. (1991). Pharmacological characterization of the quisqualate receptor coupled to phospholipase C (Qp) in striatal neurones. *Eur. J. Pharmacol.*, **207**, 231–241.

OSBORNE, N.N. (1990). Stimulatory and inhibitory actions of excitatory amino acids on inositol phospholipid metabolism in rabbit retina. Evidence for a specific quisqualate receptor subtype associated with neurones. *Exp. Eye. Res.*, **50**, 397–405.

PALMER, E., MONAGHAN, D.T. & COTMAN, C.W. (1988). Glutamate receptors and phosphoinositide metabolism: stimulation via quisqualate receptors is inhibited by N-methyl-D-aspartate receptor activation. *Mol. Brain Res*, **4**, 161–165.

PALMER, E., MONAGHAN, D.T. & COTMAN, C.W. (1989). Trans-ACPD, a selective agonist of the phosphoinositide-coupled excitatory amino acid receptor. *Eur. J. Pharmacol.*, **166**, 585–587.

PATEL, J., MOORE, W.C., THOMPSON, C., KEITH, R.A. & SALAMA, A.I. (1990). Characterization of the quisqualate receptor linked to phosphoinositide hydrolysis in neurocortical cultures. *J. Neurochem,*. **54**, 1461–1466.

RANSOM, B.R., NEALE, E., HENKART, M., BULLOCK, P.N. & NELSON, P.G. (1977). Mouse spinal cord in cell culture. I. Morphology and intrinsic neuronal electrophysiologic properties. *J. Neurophysiol,*. **40**, 1132–1150.

RECASENS, M., GUIRAMAND, J., NOURIGAT, A., SASSETTI, I. & DEVILLIERS, G. (1988). A new quisqualate receptor subtype (sAA_2) responsible for the glutamate-induced inositol phosphate formation in rat brain synaptoneurosomes. *Neurochem. Int.*, **13**, 463–467.

RECASENS, M., SASSETTI, I., NOURIGAT, A., SLADECZEK, F. & BOCKAERT, J. (1987). Characterization of subtypes of excitatory amino acid receptors involved in the stimulation of inositol phosphate synthesis in rat brain synaptoneurosomes. *Eur. J. Pharmacol.*, **141**, 87–93.

RENARD, D., POGGIOLI, J., BERTHON, B. & CLARET, M. (1987). How far does phospholipase C activity depend on the cell calcium concentration. *Biochem. J.*, **243**, 391–398.

SCHMIDT, B.H., WEISS, S., SEBBEN, M., KEMP, D.E., BOCKAERT, J. & SLADECZEK, F. (1987). Dual action of excitatory amino acids on the metabolism of inositol phosphates in striatal neurons. *Mol. Pharmacol.*, **32**, 364–368.

SCHOEPP, D.D., BOCKAERT, J. & SLADECZEK, F. (1990a). Pharmacological and functional characteristics of metabotropic excitatory amino acid receptors. *Trends Pharmacol. Sci.*, **11**, 508–515.

SCHOEPP, D.D. & HILLMAN, C.C. (1990). Developmental and pharmacological characterization of quisqualate, ibotenate, and trans-1-amino-1, 3-cyclopentane dicarboxylic acid stimulation of phosphoinositide hydrolysis in rat cortical brain slices. *Biogenic Amines*, **7**, 331–340.

SCHOEPP, D.D. & JOHNSON, B.G. (1988). Excitatory amino acid agonist-antagonist interactions at 2-amino-4-phosphonobutyric acid sensitive quisqualate receptors coupled to phosphoinositide hydrolysis in slices of rat hippocampus. *J. Neurochem.*, **50**, 1605–1613.

SCHOEPP, D.D. & JOHNSON, B.G. (1989). Inhibition of excitatory amino acid-stimulated phosphoinositide hydrolysis in the neonatal rat hippocampus by 2-amino-3-phosphonopropionate. *J. Neurochem.*, **53**, 1865–1870.

SCHOEPP, D.D., JOHNSON, B.G., SMITH, E.C. & MCQUAID, L.A. (1990b). Stereoselectivity and mode of inhibition of phosphoinositide-coupled excitatory amino acid receptors by 2-amino-3-phosphonopropionoic acid. *Mol. Pharmacol,*. **38**, 222–228.

SLADECZEK, F., PIN, J.-P., RECASENS, M., BOCKAERT, J. & WEISS, S. (1985). Glutamate stimulates inositol phosphate formation in striatal neurones. *Nature*, **317**, 717–719.

SUGIYAMA, H., ITO, I. & HIRONO, C. (1987). A new type of glutamate receptor linked to inositol phospholipid metabolism. *Nature*, **325**, 531–533.

TANABE, Y., MASU, M., ISHII, T., SHIGEMOTO, R. & NAKANISHI, S. (1992). A family of metabotropic glutamate receptors. *Neuron*, **8**, 169–179.

WATKINS, J.C., KROGSGAARD-LARSEN, P. & HONORE, T. (1990). Structure activity relationships in the development of excitatory amino-acid receptor agonists and competitive antagonists. *Trends Pharmacol. Sci.*, **11**, 25–33.

(Received October 27, 1992
Revised January 25, 1993
Accepted January 28, 1993)

Br. J. Pharmacol. (1993), **109**, 386–393 © Macmillan Press Ltd, 1993

Modulation of vasodilatation to levcromakalim by hypoxia and EDRF in the rabbit isolated ear: a comparison with pinacidil, sodium nitroprusside and verapamil

[1]Michael D. Randall & Tudor M. Griffith

Department of Diagnostic Radiology, University of Wales College of Medicine, Heath Park, Cardiff CF4 4XN

1 We have used an isolated buffer-perfused preparation of the rabbit ear to investigate the effects of hypoxia and inhibition of endothelium-derived relaxing factor (EDRF) synthesis on the vasodilator responses to the potassium channel opener, levcromakalim (the active (−)-enantiomer of cromakalim). The results obtained with levcromakalim have been compared with those for pinacidil, sodium nitroprusside and verapamil.

2 Levcromakalim relaxed preconstricted preparations with an $EC_{50} = 343 \pm 41$ nM and $R_{max} = 80.3 \pm 6.4\%$. Under hypoxic conditions the concentration-response curve was significantly ($P < 0.01$) shifted to the left with an $EC_{50} = 118 \pm 16$ nM and $R_{max} = 89.9 \pm 2.7\%$. Hypoxia did not influence relaxation to either pinacidil, sodium nitroprusside or verapamil.

3 Inhibition of EDRF synthesis with 100 μM N^G-nitro-L-arginine methyl ester (L-NAME) also significantly ($P < 0.001$) increased the vasodilator potency of levcromakalim ($EC_{50} = 56 \pm 5$ nM), and caused a similar shift in the concentration-response curve to sodium nitroprusside. It did not influence vasodilatation to either verapamil or pinacidil. The potentiation of vasodilator responses to levcromakalim by L-NAME was reversed by an excess of L-arginine.

4 Impairment of oxidative phosphorylation with 400 nM carbonyl cyanide *m*-chlorophenylhydrazone significantly ($P < 0.05$) increased the potency of levcromakalim ($EC_{50} = 120 \pm 20$ nM) but did not influence vasodilatation to pinacidil or endothelium-dependent relaxations to acetylcholine.

5 Vasodilatation to levcromakalim was augmented both by hypoxia and by inhibition of EDRF activity. Since impairment of oxidative phosphorylation increased the potency of levcromakalim but did not alter EDRF activity then the mechanism responsible for hypoxic facilitation of responses to levcromakalim is likely to be due to reduced ATP levels in hypoxic smooth muscle cells rather than a change in EDRF activity. These results suggest that levcromakalim may selectively dilate both hypoxic vessels and vessels with impaired EDRF activity. The results also point to important differences in the pharmacology of levcromakalim and pinacidil.

Keywords: Levcromakalim; sodium nitroprusside; verapamil; pinacidil; N^G-nitro-L-arginine methyl ester; L-arginine; hypoxia; endothelium-derived relaxant factor; potassium channel opener-sensitive potassium channels (KCO-channels); rabbit ear

Introduction

Levcromakalim (formerly BRL 38227), the active enantiomer of cromakalim, is a member of the novel class of vasodilators (Edwards & Weston, 1990) and hypotensive agents (Buckingham *et al.*, 1986) which are thought to act via the activation of potassium channels (Standen *et al.*, 1989) leading to hyperpolarization (Hamilton *et al.*, 1986; see Edwards & Weston, 1990). The potassium channel subtypes involved are thought to be regulated by both intracellular ATP and ADP concentrations (Noma, 1983; Misler *et al.*, 1986). In this respect, intracellular ATP closes these channels and high ADP favours opening, while potassium channel openers reduce channel sensitivity towards ATP thereby promoting channel opening (see Nichols & Lederer, 1991). These channels are selectively blocked by the hypoglycaemic sulphonylureas (Sturgess *et al.*, 1985).

In a recently developed model of acute collateral perfusion in the rabbit ear, we have previously shown that levcromakalim substantially improves collateral flow after acute arterial occlusion (Randall & Griffith, 1992). In this respect, levcromakalim had appreciably greater effects than sodium nitroprusside, while verapamil was without effect. Accordingly, we hypothesized that the selectivity shown by levcromakalim may relate to differences in the distribution of potassium channel opener-sensitive channels (KCO-channels) between pre-existing collateral vessels and non-collateral vessels, or alternatively that the collateral vessels may potentially be hypoxic and this could influence the action of vasodilators. Impairment of oxidative metabolism in hypoxia may reduce intracellular ATP levels, and could theoretically promote the opening of KCO channels. Indeed, this mechanism is thought to be responsible for hypoxic vasodilatation in the guinea-pig coronary vasculature, which is blocked by glibenclamide and mimicked by cromakalim and inhibition of oxidative phosphorylation with dinitrophenol (Daut *et al.*, 1990). That the activity of potassium channel activators may be influenced by hypoxia has also been proposed by Cook & Quast (1990). To test this hypothesis we have now examined the influence of hypoxia on vasodilatation to levcromakalim in the intact perfused ear of the rabbit and compared the results with those obtained with three other vasodilators, namely pinacidil which also acts via the opening of potassium channels, sodium nitroprusside (which acts via the generation of nitric oxide) and verapamil (which acts through blockage of voltage-sensitive calcium channels).

Hypoxia also influences vasorelaxation to endothelium-dependent vasodilators through either a reduction in EDRF synthesis or vascular smooth muscle sensitivity (Furchgott & Zawadzki, 1980; DeMey & Vanhoutte, 1983; Johns *et al.*, 1989; Warren *et al.*, 1989; Randall *et al.*, 1990). We have accordingly investigated the effects of inhibition of EDRF synthesis with N^G-nitro-L-arginine methyl ester (L-NAME)

[1] Author for correspondence.

on vasodilatation to levcromakalim, pinacidil, sodium nitroprusside and verapamil. Additionally, we have also used carbonyl cyanide *m*-chlorophenylhydrazone (CCCP), an uncoupler of oxidative phosphorylation, to examine whether responses to levcromakalim and pinacidil are influenced by impaired ATP generation.

Part of this work was communicated to the January 1993 meeting of the British Pharmacological Society (Randall & Griffith, 1993).

Methods

Preparation of the rabbit ear vascular bed

Male New Zealand White rabbits (2–2.5 kg) were killed by cervical dislocation. An ear was removed and the central artery cannulated and perfused with Holman's solution (composition mM: NaCl 120, KCl 5, $CaCl_2$ 2.5, NaH_2PO_4 1.3, $NaHCO_3$ 25, sucrose 10 and D-glucose 11) at a flow rate of 3.5 ml min^{-1}. The physiological buffer also contained 5% (w/v) dextran (mol. wt. 80,000) to increase its viscosity (to ca. 2.3 mPas) and 10 μM indomethacin to eliminate prostanoid activity. The buffer was gassed with either 95% O_2/5% CO_2 (normoxia, Po_2 = 500–600 mmHg) or 95% N_2/CO_2 (hypoxia, Po_2 = 20–30 mmHg) and maintained at 35°C from the start of the experiments.

Experimental protocols

The perfusion pressure of the intact preparation was continuously monitored by means of a pressure transducer placed close to the inflow cannula. The pressure drop across the cannula was determined at the end of each experiment and subtracted from the recorded pressure in order to determine the actual perfusion pressures across the vascular bed.

To characterize the vasodilator responses, preparations were equilibrated for 1 h. Perfusion pressure was raised pharmacologically with the combination of 5-hydroxytryptamine and histamine in equimolar concentrations to achieve submaximal tone (ca. 60% of maximal tone, Randall & Griffith, 1991). Cumulative concentration-response curves were obtained in different preparations for levcromakalim, pinacidil, sodium nitroprusside and verapamil by addition of each agent to the reservoir containing the perfusion fluid in volumes less than 100 μl and perfusion pressure was monitored continuously. The results obtained under hypoxic perfusion were compared with control responses obtained from different preparations perfused under normoxic conditions.

In order to investigate the influence of EDRF on relaxation to these agents, different preparations were perfused with 100 μM N^G-nitro-L-arginine methyl ester (L-NAME) which was included in the perfusion fluid 30 min before the construction of the concentration-response curves. We have previously shown that perfusion with L-NAME selectively abolishes endothelium-dependent relaxations to acetylcholine and inhibits basal EDRF activity (Randall & Griffith, 1991). The ability of excess L-arginine (10 mM) to reverse the effects of L-NAME on the relaxations to levcromakalim was investigated by its inclusion in the perfusion fluid 30 min after addition of L-NAME. Concentration-response curves to levcromakalim were then constructed after a further 30 min. The effects of L-arginine alone on vasodilatation to levcromakalim were also investigated by perfusion with 10 mM L-arginine prior to (30 min) and during preconstriction with 5-hydroxytryptamine and histamine. In the case of levcromakalim, experiments were performed to investigate the effects of L-NAME in combination with hypoxic perfusion which was carried out as described above.

The effects of impaired oxidative phosphorylation on vasodilatation to levcromakalim and pinacidil were also investigated. In these experiments, normoxic preparations were equilibrated and then preconstricted with supramaximal concentrations of 5-hydroxytryptamine and histamine (both 3 μM) and once maximal pressor effects had been achieved, carbonyl cyanide *m*-chlorophenylhydrazone (CCCP) was added to the perfusion fluid to achieve a concentration of 400 nM which resulted in a reduction in established tone. Once the level of established tone had stabilized at a constant value (after ca. 30 min) concentration-response curves were constructed for levcromakalim and pinacidil in different preparations. Since vasodilator responses may be influenced by the level of preconstriction (White *et al.*, 1986) the control concentration-response curves for levcromakalim and pinacidil were constructed against an equivalent level of induced tone. To achieve a level of tone comparable to that observed in the presence of 400 nM CCCP, it was found necessary to reduce the equimolar concentrations of 5-hydroxytryptamine and histamine to 300 nM. Subsequent analysis of the potencies of levcromakalim and pinacidil indicated that this reduction in the concentrations of vasoconstrictor agents did not influence vasodilatation to either agent.

To determine whether the chosen concentration of CCCP influenced EDRF activity, concentration-response curves were constructed for the endothelium-dependent vasodilator, acetylcholine, in the presence of CCCP and in control preparations preconstricted to a level of tone comparable to that in preparations receiving the metabolic inhibitor.

Data and statistical analysis

All data are given as the mean ± s.e.mean and were compared by either paired or unpaired Student's *t* tests or analysis of variance, as appropriate. EC_{50} values for vasodilator responses were obtained from individual concentration-response curves as the concentration at which half-maximal reduction in established tone occurred. These values were converted to the logarithmic values (pD_2) for statistical analysis.

Drugs

All solutions were prepared on the day of the experiment. N^G-nitro-L-arginine methyl ester, L-arginine hydrochloride, 5-hydroxytryptamine as creatinine sulphate complex, histamine dihydrochloride, acetylcholine chloride and sodium nitroprusside (all from Sigma Chemical Company, Poole, Dorset), were dissolved in saline. Verapamil hydrochloride (Sigma) glibenclamide (Hoescht, Hounslow, Middlesex) and carbonyl cyanide *m*-chlorophenylhydrazone (Sigma) were dissolved in abolute ethanol. Levcromakalim (a generous gift from Smith Kline Beecham, Surrey) and pinacidil (a generous gift from Leo, Bucks.) were dissolved in 70% (v/v) ethanol. All drugs were then diluted to the required concentrations in the Holman's solution.

Results

Vasodilator responses to levcromakalim, pinacidil, sodium nitroprusside and verapamil

The concentration-response curve for the vasoconstrictor effects of 5-hydroxytryptamine and histamine under control conditions is shown in Figure 1 and is described by an EC_{50} of 895 ± 190 nM and R_{max} value of 174 ± 8 mmHg.

In different preparations all 4 vasodilator agents used caused concentration-related reductions in submaximal (ca. 60%) tone induced by 1 μM 5-hydroxytryptamine and 1 μM histamine. Table 1 and Figures 2a, 3, 4 and 5 indicate that verapamil was the most potent vasodilator, levcromakalim and sodium nitroprusside were equipotent and pinacidil was considerably less potent. The vasodilator effects of both maximum concentrations of levcromakalim and pinacidil were reversed by addition of 10 μM glibenclamide (Table 1).

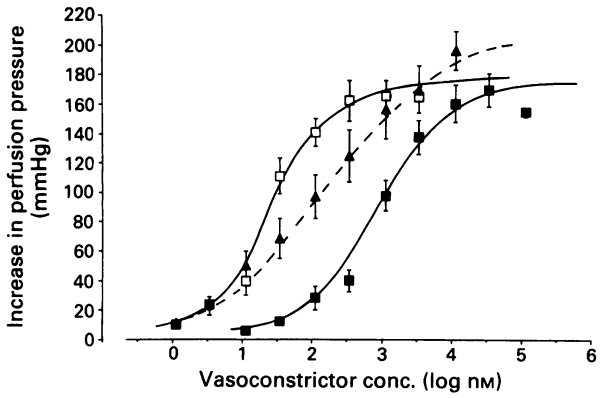

Figure 1 Concentration-response curves for the increase in perfusion pressure induced by the equimolar combination of 5-hydroxytryptamine and histamine during normoxia (■, $n = 8$), hypoxia (▲, $n = 5-7$), and in the presence of 100 μM N^G-nitro-L-arginine methyl ester (□, $n = 4-5$) in isolated perfused ear preparations of rabbit.

Effects of hypoxia on vascular responses

The concentration-response curve for 5-hydroxytryptamine plus histamine constructed during hypoxic perfusion is shown in Figure 1. In these 7 preparations, basal perfusion pressure was 40.1 ± 4.8 mmHg. Addition of equimolar amounts of vasoconstrictors (1 nM–10 μM) resulted in concentration-related increases in perfusion pressure, with an R_{max} of 191 ± 11 mmHg and the EC_{50} value of 407 ± 210 nM (Figure 1). Therefore, under hypoxic conditions the combination of vasoconstrictors was significantly ($P < 0.05$) more potent. To achieve a comparable level of tone in the vasodilator experiments to that used under normoxic conditions (ca. 60% of maximum), the equimolar concentration used to preconstrict the rabbit ear preparations under hypoxic conditions was 100 nM.

In the preconstricted preparations perfused with hypoxic buffer, all four vasodilators induced concentration-related reductions in established tone. It can be seen from Table 2 and Figure 2a that the EC_{50} value for the relaxation of tone by levcromakalim was significantly ($P < 0.001$) less than that under normoxic conditions. The maximum reduction in tone was 89.9 ± 2.7% and not significantly different from that obtained in normoxic control preparations. However, the EC_{50} values and the R_{max} values obtained for pinacidil, sodium nitroprusside and verapamil did not differ from their respective values obtained under normoxic perfusion (Table 2, Figures 3, 4 and 5). Once again, addition of 10 μM glibenclamide reversed the relaxation of tone induced by levcromakalim and pinacidil (Table 2).

Effects of inhibition of EDRF activity on vasodilator responses

Concentration-response curves were constructed for the combination of 5-hydroxytryptamine and histamine in 5 preparations pretreated with 100 μM L-NAME (Figure 1). Prior to the addition of L-NAME, basal perfusion pressure was 30.9 ± 4.1 mmHg and afterwards was 41.8 ± 7.6 mmHg. The EC_{50} value for the vasoconstrictor effects was 29.0 ± 8.6 nM and maximum increase in perfusion pressure was 166 ± 12 mmHg. The EC_{50} value was significantly ($P < 0.01$) lower than under normoxic conditions. To achieve a comparable level of tone to that used under normoxic control conditions (ca 60% of maximum), the equimolar concentration used to preconstrict the rabbit ear preparations in the presence of L-NAME was reduced to 100 nM.

In the presence of 100 μM L-NAME, all of the vasorelaxants caused concentration-related decreases in tone (Figures 2a, 3 and 4, Table 3). In the case of both verapamil and pinacidil, their potencies were not significantly different from those obtained under control conditions in the absence of the inhibitor. In the presence of L-NAME there were significant increases in the potency for both levcromakalim ($P < 0.001$) and sodium nitroprusside ($P < 0.001$). Furthermore, the EC_{50} value obtained for levcromakalim in the presence of L-NAME was also significantly ($P < 0.05$) less than that obtained under hypoxic conditions.

In order to characterize further the effects of L-NAME on vasorelaxation to levcromakalim, excess L-arginine (10 mM) was added to a further 7 preparations 30 min after the addition of 100 μM L-NAME. In the preparations treated with both L-NAME and L-arginine the concentration-response curve was shifted back to a similar position to that obtained under normoxic conditions (Table 3; Figure 2b). In the absence of L-NAME, treatment with L-arginine alone did not influence vasodilatation by levcromakalim, when the concentration-response curve was described by an EC_{50} value of 300 ± 84 nM and R_{max} of 76.2 ± 0.6% ($n = 5$). These parameters were not significantly different from those obtained in control preparations.

Table 1 Vasodilator properties of levcromakalim, pinacidil, sodium nitroprusside and verapamil under control conditions

	Levcromakalim	*Pinacidil*	*Sodium nitroprusside*	*Verapamil*
n	8	8	5	5
Basal perfusion pressure (mmHg)	40.3 ± 8.5	34.1 ± 5.9	18.8 ± 2.6	36.6 ± 12.6
Increase in tone (mmHg)	112 ± 19	101 ± 11	91.4 ± 15.4	109 ± 31
EC_{50} (nM)	343 ± 41	3,360 ± 850	488 ± 75	72.6 ± 32.0
Maximum relaxation (%)	80.3 ± 6.4	95.3 ± 3.5	81.9 ± 5.6	63.8 ± 11.4
% reversal of maximum relaxation by 10 μM glibenclamide	118 ± 14	78.2 ± 14.6		

Table 2 Vasodilator properties of levcromakalim, pinacidil, sodium nitroprusside and verapamil under hypoxic conditions

	Levcromakalim	*Pinacidil*	*Sodium nitroprusside*	*Verapamil*
n	12	8	6	4
Basal perfusion pressure (mmHg)	27.8 ± 6.2	38.1 ± 3.1	34.4 ± 8.1	24.8 ± 11.8
Increase in tone (mmHg)	111 ± 4	102 ± 12	94.0 ± 14.0	84.0 ± 19.0
EC_{50} (nM)	118 ± 16	2,950 ± 580	518 ± 130	95 ± 19
Maximum relaxation (%)	89.9 ± 2.7	94.9 ± 2.7	87.6 ± 3.2	64.8 ± 6.8
% reversal of maximum relaxation by 10 μM glibenclamide	96.2 ± 4.7	72.9 ± 11.0		

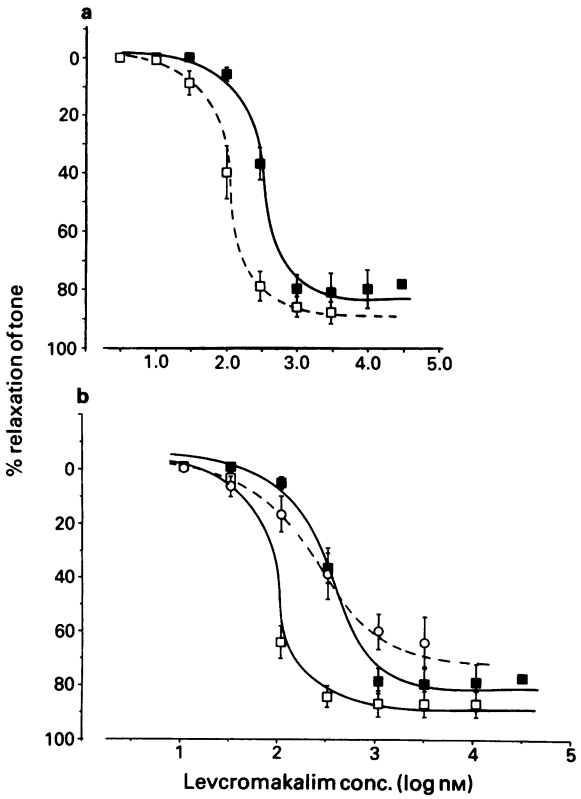

Figure 2 Concentration-response curves for the relaxation of established tone by levcromakalim in isolated perfused ear preparations of rabbit. (a) Under normoxic (■, $n = 8$) and hypoxic (□, $n = 12$) conditions. (b) In the presence of 100 μM N^G-nitro-L-arginine methyl ester (L-NAME) under normoxic conditions (□, $n = 7$), in the presence of L-NAME and 10 mM L-arginine (○, $n = 7$) and in the absence of L-NAME under normoxic conditions (■) (taken from a).

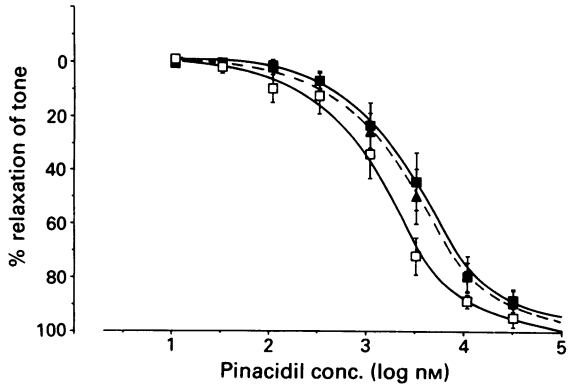

Figure 3 Vasodilatation to pinacidil in the preconstricted isolated perfused ear of preparations of rabbit under control conditions (■, $n = 8$), during hypoxic perfusion (▲, $n = 8$) and in the presence of 100 μM N^G-nitro-L-arginine methyl ester (□, $n = 8$).

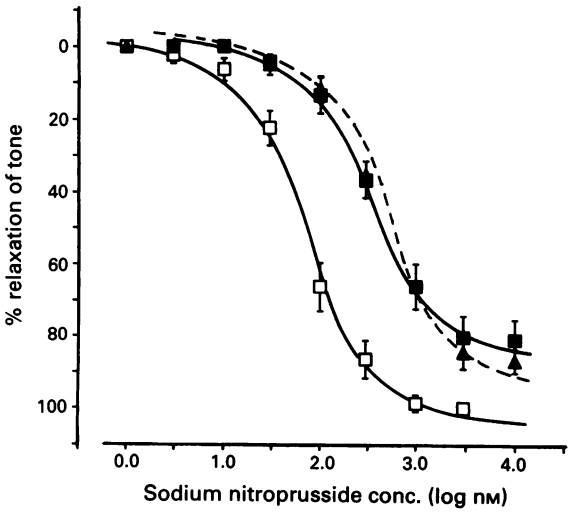

Figure 4 Concentration-response curves for the relaxation of established tone by sodium nitroprusside under normoxic conditions (■, $n = 5$), hypoxic conditions (▲, $n = 6$) and preparations perfused with 100 μM N^G-nitro-L-arginine methyl ester (□, $n = 6$).

Effects of combined inhibition of EDRF synthesis and hypoxia on vasodilatation to levcromakalim

In 8 preparations perfused with hypoxic buffer, resting perfusion pressure was 37.1 ± 7.1 mmHg and this was not significantly affected by addition of 100 μM L-NAME (43.5 ± 11.1 mmHg). Following addition of 5-hydroxytryptamine and histamine (both 100 nM) perfusion pressure rose by 151 ± 11 mmHg to 195 ± 15 mmHg. In these preparations the vasodilator responses to levcromakalim were described by an EC_{50} of 71 ± 13 nM and $R_{max} = 95.3 \pm 8.2\%$. Under these conditions levcromakalim was therefore significantly more potent than under hypoxic conditions alone ($P < 0.05$) or normoxic conditions ($P < 0.001$) alone, but not different from that in the presence of L-NAME under normoxia. The maximum reactivity was not significantly different under any of the above conditions.

Effects of impairment of oxidative phosphorylation with CCCP on vasodilatation to levcromakalim and pinacidil

In 7 preparations, perfusion pressure was 30.9 ± 10.6 mmHg and this was increased by 118 ± 13 mmHg to 149 ± 14 mmHg after addition of the combination of vasoconstrictors (both 3 μM). Following addition of 400 nM CCCP, the level of induced tone fell by 66.2 ± 13.1 mmHg so that total perfusion pressure was 82.7 ± 14.7 mmHg. Levcromakalim (10 nM–3 μM) in the presence of CCCP brought about concentration-related reductions in induced tone (EC_{50} = 120 ± 20 nM, R_{max} was 91.4 ± 2.9%) (Figure 6). In 3 preparations 10 μM glibenclamide was added in the presence of 3 μM levcromakalim and returned the level of tone to 96.1 ± 14.4% of the preconstricted level in the presence of CCCP.

Table 3 Vasodilator properties of levcromakalim, pinacidil, sodium nitroprusside and verapamil in the presence of 100 μM N^G-nitro-L-arginine methyl ester (L-NAME)

	Levcromakalim	*Levcromakalim + L-arginine*	*Pinacidil*	*Sodium nitroprusside*	*Verapamil*
n	7	7	8	6	5
Basal perfusion pressure (mmHg)	20.7 ± 1.9	27.1 ± 14.0	55.0 ± 8.9	17.2 ± 2.5	22.2 ± 2.8
Change in tone (+L-NAME, mmHg)	5.5 ± 5.7	23.4 ± 9.3	17.5 ± 10.0	13.3 ± 9.5	13.0 ± 9.4
Increase in tone (mmHg)	119 ± 9	130 ± 6	133 ± 18	127 ± 12	99.0 ± 16.1
EC_{50} (nM)	56 ± 5	273 ± 47	1,740 ± 370	71 ± 12	91 ± 19
Maximum relaxation (%)	86.3 ± 4.6	70.9 ± 10.0	95.9 ± 3.0	100 ± 2	62.7 ± 4.7

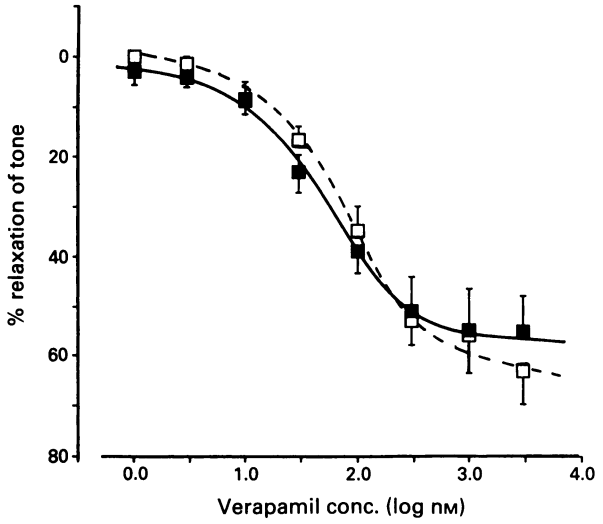

Figure 5 Concentration-response curves for vasodilatation to verapamil in the preconstricted isolated perfused ear preparations of rabbit under control conditions (■, $n = 5$) and during hypoxic perfusion (□, $n = 4$).

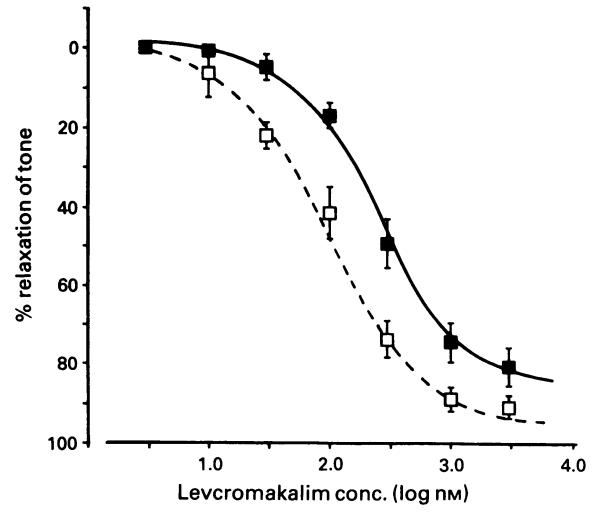

Figure 6 Concentration-response curves for the relaxation of established tone by levcromakalim in the absence (■, $n = 8$) and presence (□, $n = 7$) of 400 nM carbonyl cyanide *m*-chlorophenylhydrazone in isolated perfused ear preparations of rabbit.

As a control to these experiments, the vasodilator responses to levcromakalim were determined against a level of established tone comparable to that observed in the presence of CCCP. In these 8 control preparations, resting perfusion pressure was 23.4 ± 5.6 mmHg and following addition of 5-hydroxytryptamine and histamine (both 300 nM) rose by 50.9 ± 6.6 mmHg to 74.3 ± 7.3 mmHg. This increase in tone was not significantly different from that in the preparations receiving CCCP (51.8 ± 5.4 v 50.9 ± 6.6 mmHg). In these control preparations, where induced tone was ca. 30% of maximum, levcromakalim (10 nM–3 μM) brought about concentration-related reductions in established tone with an EC_{50} = 242 ± 42 nM, which is significantly greater ($P < 0.05$) than that observed in the presence of CCCP and with an R_{max} = 78.0 ± 5.4% which is significantly ($P < 0.05$) less than that in the presence of CCCP (Figure 6). In the 4 preparations which received 10 μM glibenclamide in the presence of 3 μM levcromakalim established tone returned to 126 ± 25% of control values.

In another group of control preparations basal perfusion pressure was 62.2 ± 8.4 mmHg and addition of 300 nM 5-hydroxytryptamine and histamine increased tone by a further 58.6 ± 8.1 mmHg to 121 ± 14 mmHg. In these preparations, pinacidil (10 nM–30 μM) relaxed tone with an EC_{50} value of 2.89 ± 0.87 μM and the R_{max} value was 87.4 ± 6.5% ($n = 8$). Subsequent addition of 10 μM glibenclamide partially reversed the vasodilator effects of 30 μM pinacidil such that induced tone was returned to 74.1 ± 6.1% of control. In the 11 preparations treated with CCCP, basal perfusion pressure was 38.6 ± 5.4 mmHg and was increased by 160 ± 10 mmHg to 198 ± 10 mmHg. After addition of CCCP the level of established tone was reduced to 55.0 ± 6.9 mmHg. In these preparations the vasodilator responses of pinacidil (10 nM–300 μM) were described by an EC_{50} value of 5.25 ± 1.26 μM and the R_{max} was 102 ± 6%. These values did not differ significantly from those obtained in the controls.

Effects of CCCP on endothelium-dependent vasodilatation to acetylcholine

In 6 different control preparations, perfusion pressure was 37.0 ± 9.4 mmHg and 5-hydroxytryptamine and histamine (both 300 nM) increased this by 71.7 ± 11.8 mmHg to 109 ± 12 mmHg. In these preparations, acetylcholine (3 nM–10 μM) induced concentration-related relaxations of established tone which were described by an EC_{50} = 91 ± 33 nM and a maximum inhibition of 90.2 ± 5.0%. In the experimental preparations, basal perfusion pressure was 35.0 ± 9.7 mmHg and was increased by 166 ± 18 mmHg to 201 ± 19 mmHg following addition of 3 μM 5-hydroxytryptamine and 3 μM histamine. Subsequent addition of CCCP (400 nM) caused perfusion pressure to fall by 75.7 ± 6.4 mmHg to 125 ± 15 mmHg after 30 min. In these preparations, acetylcholine (3 nM–10 μM) caused concentration-related relaxations of tone with an EC_{50} of 87 ± 17 nM and a maximum reduction in tone of 81.7 ± 8.8%. These values were not significantly different from those obtained in the absence of CCCP.

Discussion

The present investigation demonstrates that the vasodilator potency of levcromakalim is increased 3 fold under hypoxic conditions, compared to normoxia, while responses to pinacidil, sodium nitroprusside and verapamil are unaffected. To our knowledge this is the first demonstration that the vasodilator properties of levcromakalim are influenced by acute hypoxia. Furthermore, the differential effects of hypoxia on vasodilatation to levcromakalim and pinacidil are interesting in view of the common action of these agents on potassium channels.

That the potency of levcromakalim is augmented by hypoxia is not entirely unexpected, as levcromakalim is thought to act on potassium channels sensitive to intracellular ATP as glibenclamide, which has been shown to block ATP-sensitive potassium channels in other cell types, blocked the action of cromakalim (Standen *et al.*, 1989). It should be noted, however, that there is recent evidence that potassium channel openers may also act on other potassium channels including the calcium-activated subtypes (see Kajioka *et al.*, 1991). Furthermore, high intracellular ATP levels have previously been reported to depress the channel opening activity of pinacidil in guinea-pig isolated myocytes (Fan *et al.*, 1990). It is therefore conceivable that a reduction in metabolic activity leading to reduced ATP promotes the actions of potassium channel openers.

In addition to hypoxia, impairment of oxidative phosphorylation with CCCP, an uncoupler of oxidative metabolism, selectively increased the potency of levcromakalim without influencing vasodilator responses to either acetylcholine or pinacidil. In the present study, perfusion with CCCP resulted in reductions of established tone, an effect previously reported by Griffith *et al.* (1986) in both endothelium-intact and endothelium-denuded rabbit aorta. This is

consistent with a reduced supply of ATP for smooth muscle contraction or alternatively a non-specific vasodilator action. The present results indicate that under conditions associated with a reduction in ATP generation, the vasodilator properties of levcromakalim are augmented. This accords with findings in pancreatic β cells where metabolic inhibitors promote the opening of ATP-sensitive potassium channels (Misler *et al.*, 1986). We have therefore established a link between impaired oxidative metabolism and increased vasodilator potency for levcromakalim which may account for the hypoxic augmentation of vasodilatation.

That the responses to levcromakalim but not those to pinacidil were affected by hypoxia requires explanation. Despite their widely different chemical structures these agents are generally assumed to have a common mechanism of action through the activation of KCO-sensitive potassium channels. However, there is some evidence in the literature pointing to differences in the pharmacology of these agents (see Cook & Quast, 1990). Early studies indicated subtle haemodynamic differences between cromakalim and pinacidil. In the cat, for example, the hypotensive actions of cromakalim but not those of pinacidil are accompanied by reductions in renal vascular resistance (Longman *et al.*, 1988). McPherson & Angus (1990) also identified differences in the pharmacology of cromakalim and pinacidil, in that glibenclamide, phentolamine and alinidine non-competively inhibited the actions of cromakalim on the canine coronary artery while having competitive actions against pinacidil. More recently Lawson *et al.* (1992) have demonstrated that endothelin-1 discriminates between the actions of levcromakalim and that of pinacidil. In their study, subcontractile concentrations of endothelin-1 prevented the vasodilator actions of low concentrations of levcromakalim but not those of pinacidil, observations which led to them proposing that levcromakalim and pinacidil interact with different sites on the potassium channel. In the present context, hypoxia may be associated with increased endothelin-1 release (Rakugi *et al.*, 1990), but this would not account for the specific increase in the potency of levcromakalim, since an increase in endothelin-1 would be expected to reduce its dilator activity. The differences between levcromakalim and pinacidil identified in the current study may therefore be related to differences in the way these agents interact with potassium channels as suggested by Lawson *et al.* (1992).

Hypoxia may influence vascular responses in other ways, for example we have previously shown that it reduces the potency of acetylcholine as an endothelium-dependent vasodilator in the rabbit ear preparation (Randall *et al.*, 1990). This effect can be ascribed to either a reduction in either EDRF production or attenuation of its relaxant effects on vascular smooth muscle, or both (DeMey & Vanhoutte, 1983; Johns *et al.*, 1989; Warren *et al.*, 1989). The present results indicate that in hypoxia, vasodilatation to sodium nitroprusside is unaltered. Since this agent acts via stimulation of soluble guanylyl cyclase, and may be regarded as an analogue of EDRF, altered vascular smooth muscle responsiveness to EDRF does not appear to occur under the present experimental conditions. The impairment of endothelium-dependent relaxations in hypoxia that we have previously reported in the rabbit ear (Randall *et al.*, 1990) is therefore likely to be due to reduced EDRF synthesis.

Loss of basally released EDRF augments vasodilatation to endothelium-independent vasodilators (Shirasaki & Su, 1985; White *et al.*, 1986; Moncada *et al.*, 1991). To investigate whether hypoxia-induced changes in EDRF activity could account for the increase in potency for levcromakalim, experiments were carried out under normoxic conditions in which both agonist-stimulated and basal EDRF activity were abolished by perfusion with L-NAME (Randall & Griffith, 1991). Under these conditions the vasodilator potency of levcromakalim was increased 6 fold, a change greater than that in hypoxia (3 fold). In the absence of EDRF activity, sodium nitroprusside underwent a similar 7 fold increase in potency, while vasodilatation to verapamil and pinacidil were unaffected. That vasodilatation to nitrovasodilators is enhanced in the absence of EDRF has been known for sometime (Shirasaki & Su, 1985) and has been ascribed to increased sensitivity of guanylyl cyclase on loss of the basal EDRF input (Moncada *et al.*, 1991). Alternatively, basal EDRF activity has a tonic vasodilator input which is abolished, thus enabling other vasodilators to have greater impact. This idea is supported by augmented responses to the endothelium-independent agent isoprenaline in the rabbit aorta after endothelial loss (White *et al.*, 1986). In the present study loss of EDRF activity was accompanied by increased potency for both levcromakalim and sodium nitroprusside but not verapamil or pinacidil. The observation that the responses to verapamil and pinacidil were unaffected, suggests that non-specific augmentation through loss of tonic vasodilator input is not a contributory factor. Therefore, the increased potency of sodium nitroprusside observed in the present study is probably due to increased sensitivity of guanylyl cyclase on loss of the basal input of EDRF (Moncada *et al.*, 1991).

The increased potency of levcromakalim after inhibition of EDRF activity requires explanation. Since cromakalim acts independently of guanylyl cyclase (Taylor *et al.*, 1988) and the vasodilatation to levcromakalim in the present study was fully reversed by glibenclamide, then increased sensitivity of guanylyl cyclase presumably cannot account for this change. Non-specific effects of L-NAME are unlikely since destruction of the endothelium also results in increased potency of levcromakalim in the isolated rat mesenteric arterial bed (C.R. Hiley, personal communication). The possibility that L-NAME acts to uncouple oxidative phosphorylation in a manner akin to CCCP can be excluded because vasoconstrictor responses are augmented rather than impaired in the presence of L-NAME (Randall & Griffith, 1991). Nitric oxide, in some (Tare *et al.*, 1990; Garland & McPherson, 1992) but not all (Komori *et al.*, 1988) vascular preparations may exert a hyperpolarizing effect. If nitric oxide exerts a hyperpolarizing effect in the rabbit ear then inhibition of this input may lead to vascular smooth muscle depolarization, which might enable a potassium channel opener to have a greater hyperpolarizing effect leading to augmented vasodilatation. However, since only relaxations to levcromakalim and not those to pinacidil were augmented after L-NAME, such a mechanism would appear unlikely.

Associated with the hyperpolarizing effects of nitric oxide on vascular smooth muscle is the cyclic GMP-dependent activation of calcium-sensitive potassium channels leading to hyperpolarization and relaxation (Fujino *et al.*, 1991). This action of nitric oxide may account for its synergism with cromakalim reported by others (Rae & Corrêa, 1992). In the present experiments, loss of EDRF activity after inhibition with L-NAME may potentially enable levcromakalim to have greater impact through the above mechanism but why the responses to pinacidil are not similarly influenced is at present unclear.

Although hypoxia results in impaired endothelium-dependent relaxations (Randall *et al.*, 1990), it did not, in the present study, augment vasodilatation to sodium nitroprusside. This suggests that the level of hypoxia used did not alter basal EDRF activity for reductions in basal EDRF activity are known to augment relaxations to nitrovasodilators through supersensitivity of guanylate cyclase (Shirasaki & Su, 1985; Moncada *et al.*, 1991). That hypoxia does not substantially alter the basal release of EDRF accords with previous findings in bovine aorta endothelial cells (Richards *et al.*, 1991). Furthermore, previous studies have indicated that basal, but not stimulated, EDRF release is resistant to the effects of full inhibition of oxidative metabolism (Griffith *et al.*, 1986; 1987). CCCP, at the concentration used, did not impair endothelium-dependent vasodilatation to acetylcholine while previous work has shown that higher concentrations of CCCP do reduce agonist-stimulated but not basal EDRF activity (Griffith *et al.*, 1986). Therefore the experiments with

CCCP have effectively dissociated a reduction in oxidative metabolism and altered basal EDRF synthesis, indicating that a reduction in oxidative metabolism may augment relaxations to levcromakalim without influencing EDRF activity. This enables the conclusion to be drawn in that hypoxia, the augmentation of vasodilatation to levcromakalim is likely to be due to reduced oxidative metabolism leading to reduced ATP content in the vascular smooth muscle favouring the action of potassium channel activators.

The results of the present study indicate that the vasodilator potency of levcromakalim, but not that of pinacidil, is increased both in hypoxia and the absence of EDRF activity. That hypoxia may promote the action of levcromakalim is a novel and important finding and may indicate that this compound may be effective at increasing blood flow to acutely ischaemic organs. This complements previous work showing that cromakalim can increase blood flow to chronically ischaemia tissues (Angersbach & Nicholson, 1988). Our findings may also explain the selectivity shown by levcromakalim in substantially improving collateral flow after acute arterial occlusion (Randall & Griffith, 1992). The increase in potency found in hypoxia would appear independent of EDRF activity, and is probably related to a reduction in intracellular ATP levels in vascular smooth muscle. In addition to these findings is the observation that the potency of levcromakalim is also enhanced in the absence of basal EDRF, which may enable levcromakalim to dilate selectively vessels where endothelial activity is impaired, for example through various disease states eg. hypertension (Lüscher & Vanhoutte, 1986; Mayhan *et al.*, 1987), atherosclerosis (Harrison *et al.*, 1987) or hypercholesterolemia (Verbeuren *et al.*, 1986). The results also indicate differences in the pharmacology of levcromakalim and pinacidil, the significance of which remains to be determined.

This work was funded by a grant from the British Heart Foundation. The authors thank Professor G.M. Roberts of the University of Wales College of Medicine for his support and interest.

References

ANGERSBACH, D. & NICHOLSON, C.D. (1988). Enhancement of muscle blood cell flux and pO_2 by cromakalim (BRL 34915) and other compounds enhancing K^+ conductance, but not Ca^{2+} antagonists or hydralazine, in an animal model of occlusive arterial disease. *Naunyn-Schmiedebergs Arch. Pharmacol.*, **337**, 341–346.

BUCKINGHAM, R.E., CLAPHAM, J.C., HAMILTON, T.C., LONGMAN, S.D., NORTON, J. & POYSNER, R.H. (1986). BRL 34915, a novel antihypertensive agent: comparison of effects on blood pressure and other haemodynamic parameters with those of nifedipine in animal models. *J. Cardiovasc. Pharmacol.*, **8**, 798–804.

COOK, N.S. & QUAST, U. (1990). Potassium channel pharmacology. In *Potassium Channels: Structure, Classification, Function and Therapeutic Potential.* pp. 181–255, ed. Cook, N.S. Chichester, West Sussex: Halstead Press.

DAUT, J., MAIER-RULDOLPH, W., VON BECKERATH, N., MEHRKE, G., GÜNTHER, K. & GOEDEL-MEINEN, L. (1990). Hypoxic dilation of coronary arteries is mediated by ATP-sensitivie potassium channels. *Science*, **247**, 1341–1344.

DEMEY, J.G. & VANHOUTTE, P.M. (1983). Anoxia and endothelium-dependent reactivity in the canine femoral artery. *J. Physiol.*, **335**, 65–74.

EDWARDS, G. & WESTON, A.H. (1990). Potassium channel openers and vascular smooth muscle relaxation. *Pharmacol. Ther.*, **48**, 237–258.

FAN, Z., NAKAYAMA, K. & HIRAOKA, M. (1990). Multiple actions of pinacidil on adenosine triphosphate-sensitive potassium channels in guinea-pig ventricular myocytes. *J. Physiol.*, **430**, 273–295.

FUJINO, K., NAKAYA, S., NAKATSUKI, T., MIYOSHI, Y., NAKAYA, Y., MORI, H. & INOUE, I. (1991). Effects of nitroglycerin on ATP-induced Ca^{++}-mobilization, Ca^{++}-activated K channels and contraction of cultured smooth muscle cells of porcine coronary artery. *J. Pharmacol. Exp. Ther.*, **256**, 371–377.

FURCHGOTT, R.F. & ZAWADZKI, J.V. (1980). The obligatory role of endothelial cells in the relaxation of vascular smooth muscle by acetylcholine. *Nature*, **288**, 373–376.

GARLAND, C.J. & MCPHERSON, G.A. (1992). Evidence that nitric oxide does not mediate the hyperpolarization and relaxation to acetylcholine in the rat small mesenteric artery. *Br. J. Pharmacol.*, **105**, 429–435.

GRIFFITH, T.M., EDWARDS, D.H. & HENDERSON, A.H. (1987). Unstimulated release of endothelium-derived relaxing factor is independent of mitochondrial ATP generation. *Cardiovasc. Res.*, **21**, 565–568.

GRIFFITH, T.M., EDWARDS, D.H., NEWBY, A.C., LEWIS, M.J. & HENDERSON, A.H. (1986). Production of endothelium-derived relaxant factor is dependent on oxidative phosphorylation and extracellular calcium. *Cardiovasc. Res.*, **20**, 7–12.

HAMILTON, T.C., WEIR, S.W. & WESTON, A.H. (1986). Comparison of the effects of BRL 34915 and verapamil in the electrical and mechanical activity in rat portal vein. *Br. J. Pharmacol.*, **88**, 103–111.

HARRISON, D.G., FREIMAN, P.C., ARMSTRONG, M.L., MARCUS, M.L. & HEISTAD, D.D. (1987). Alterations of vascular reactivity in atherosclerosis. *Cir. Res.*, **61**, II-74–II-80.

JOHNS, R.A., LINDEN, J.M. & PEACH, M.J. (1989). Endothelium-dependent relaxation and cyclic GMP accumulation in rabbit pulmonary artery are selectively impaired by moderate hypoxia. *Circ. Res.*, **65**, 1508–1515.

KAJIOKA, S., NAKASHIMA, M., KITAMURA, K. & KURIYAMA, H. (1991). Mechanisms of vasodilatation induced by potassium channel activators. *Clin. Sci.*, **81**, 129–139.

KOMORI, K., LORENZ, R.R. & VANHOUTTE, P.M. (1988). Nitric oxide, Ach, and electrical and mechanical properties of canine arterial smooth muscle. *Am. J. Physiol.*, **255**, H207–H212.

LAWSON, K., BARRAS, M., ZAZZI-SUDRIEZ, E., MARTIN, D.J., ARMSTRONG, M. & HICKS, P.E. (1992). Differential effects of endothelin-1 on the vasorelaxant properties of benzopyran and non-benzopyran potassium channel openers. *Br. J. Pharmacol.*, **107**, 58–65.

LONGMAN, S.D., CLAPHAM, J.C., WILSON, C. & HAMILTON, T.C. (1988). Cromakalim, a potassium channel activator: a comparison of its cardiovascular haemodynamic profile and tissue specificity with those of pinacidil and nicorandil. *J. Cardiovasc. Pharmacol.*, **12**, 535–542.

LÜSCHER, T.F. & VANHOUTTE, P.M. (1986). Endothelium-dependent contractions to acetylcholine in the aorta of the spontaneously hypertensive rat. *Hypertension*, **8**, 344–348.

MAYHAN, W.G., FARACI, F.M. & HEISTAD, D.D. (1987). Impairment of endothelium-dependent responses of cerebral arterioles in chronic hypertension. *Am. J. Physiol.*, **253**, H1453–1440.

MCPHERSON, G.A. & ANGUS, J.A. (1990). Characterization of responses to cromakalim and pinacidil in smooth and cardiac muscle by use of selective antagonists. *Br. J. Pharmacol.*, **100**, 201–206.

MISLER, D.S., FALKE, L.C., GILLIS, K. & MCDANIEL, M.L. (1986). A metabolite regulated potassium channel in rat pancreatic B cells. *Proc. Natl. Acad. Sci. U.S.A.*, **83**, 7119–7123.

MONCADA, S., REES, D.D., SHULZ, R. & PALMER, R.M.J. (1991). Development and mechanisms of a specific supersensitivity to nitrovasodilators following inhibition of vascular nitric oxide synthesis in vivo. *Proc. Natl. Acad. Sci. U.S.A.*, **88**, 2166–2170.

NICHOLS, C.G. & LEDERER, W.J. (1991). Adenosine triphosphate-sensitive potassium channels in the cardiovascular system. *Am. J. Physiol.*, **261**, H1675–1686.

NOMA, A. (1983). ATP regulated K^+ channels in cardiac muscle. *Nature*, **305**, 147–148.

RAE, G.A. & CORRÊA, D.S. (1992). Effect of cromakalim on endothelium-dependent vasodilation in rat aortic rings. *J. Vasc. Res.*, **29**, 185.

RAKUGI, H., TABUCHI, Y., NAKAMARU, M., NAGANO, M., HIGASHIMORI, H., MIKAMI, H., OGIHARA, T. & SUZUKI, N. (1990). Evidence for endothelin-1 release from resistance vessels of rats in response to hypoxia. *Biochem. Biophys. Res. Commun.*, **169**, 973–977.

RANDALL, M.D., EDWARDS, D.H. & GRIFFITH, T.M. (1990). Activities of endothelin-1 in the vascular network of the rabbit ear: a microangiographic study. *Br. J. Pharmacol.*, **101**, 781–788.

RANDALL, M.D. & GRIFFITH, T.M. (1991). Differential effects of L-arginine on the inhibition of N^G-nitro-L-arginine methyl ester of basal and agonist-stimulated EDRF activity. *Br. J. Pharmacol.*, **104**, 743–749.

RANDALL, M.D. & GRIFFITH, T.M. (1992). Effects of 38227, sodium nitroprusside and verapamil on collateral perfusion following acute arterial occlusion in the isolated rabbit ear. *Br. J. Pharmacol.*, **106**, 315–323.

RANDALL, M.D. & GRIFFITH, T.M. (1993). The effects of hypoxia on vasodilatation to BRL 38227 in the isolated perfused rabbit ear. *Br. J. Pharmacol.* (in press).

RICHARDS, J.M., GIBSON, I.F. & MARTIN, W. (1991). Effects of hypoxia and metabolic inhibitors on production of prostacyclin and endothelium-derived relaxing factor by pig aortic endothelial cells. *Br. J. Pharmacol.*, **102**, 203–209.

SHIRASAKI, Y. & SU, C. (1985). Endothelium removal augments vasodilatation by sodium nitroprusside and sodium nitrite. *Eur. J. Pharmacol.*, **114**, 93–96.

STANDEN, N.B., QUAYLE, J.M., DAVIES, N.W., BRAYDEN, J.E., HUANG, Y. & NELSON, M.T. (1989). Hyperpolarizing vasodilators activate ATP-sensitive K^+ channels in arterial smooth muscle. *Science*, **245**, 177–180.

STURGESS, N.C., ASHFORD, M.J.L., COOK, D.L. & HALES, C.N. (1985). The sulphonylurea receptor may be an ATP-sensitive potassium channel. *Lancet*, **ii**, 474–475.

TARE, M., PARKINGTON, H.C., COLEMAN, H.A., NEILD, T.O. & DUSTING, G.J. (1990). Hyperpolarization and relaxation of arterial smooth muscle caused by nitric oxide derived from endothelium. *Nature*, **346**, 69–71.

TAYLOR, S.G., SOUTHERTON, J.S., WESTON, A.H. & BAKER, J.R.L. (1988). Endothelium-dependent effects of acetylcholine in rat aorta. A comparison with sodium nitroprusside and cromakalim. *Br. J. Pharmacol.*, **94**, 853–863.

VERBEUREN, T.J., JORDAENS, F.H., ZONNEKEYN, L.L., VAN HOVE, C.E., COENE, M.C. & HERMAN, A.G. (1986). Effect of hypercholesterolemia on vascular reactivity in the rabbit. *Circ. Res.*, **58**, 552–554.

WARREN, J.B., MALTBY, N.H., MACCORMACK, D. & BARNES, P.J. (1989). Pulmonary endothelium-derived relaxing factor is impaired in hypoxia. *Clin. Sci.*, **77**, 671–676.

WHITE, D.G., LEWIS, M.J., GRIFFITH, T.M., EDWARDS, D.H. & HENDERSON, A.H. (1986). Influence of endothelium on drug-induced relaxation of rabbit aorta. *Eur. J. Pharmacol.*, **121**, 19–23.

(Received November 16, 1992
Revised January 15, 1993
Accepted January 29, 1993)

Br. J. Pharmacol. (1993), **109**, 394–404 © Macmillan Press Ltd, 1993

Interactions between responses mediated by activation of adenosine A_2 receptors and α_1-adrenoceptors in the rabbit isolated aorta

*†Harvey L. Wiener, [2]*George P. Thalody & †‡Saul Maayani

*Department of Pharmaceutical Sciences, College of Pharmacy and Allied Health Professions, St. John's University, Jamaica, New York 11439, U.S.A., and Departments of †Anesthesiology and ‡Pharmacology, Mount Sinai School of Medicine of the City University of New York, New York, New York 10029, U.S.A.

1 This paper describes aspects of the functional antagonism between the responses mediated by activated α_1-adrenoceptors and adenosine A_2 receptors in the adventitia- and endothelium-denuded aorta of the rabbit.

2 Adenosine A_2 receptor agonists relaxed aortic rings pre-contracted with phenylephrine. The relaxation response was agonist concentration-dependent and saturable. The respective contractile and relaxation responses were stable, reproducible, and reversible.

3 Increasing the phenylephrine concentration caused a progressive attenuation of the action of adenosine A_2 receptor agonists, consisting of a decreased maximal response and a dextral shift of the adenosine agonist concentration-response curve. This functional antagonism could be completely reversed upon removal of adenosine by either the addition of adenosine deaminase or by wash-out of the adenosine agonist from the tissue. The relaxation response to the adenosine A_2 receptor partial agonists, N^6-cyclohexyladenosine and **R**-(−)-N^6-(2-phenylisopropyl)adenosine, was abolished at higher phenylephrine concentrations (e.g. 30 EC_{50}).

4 A 1000 fold increase in the adenosine concentration was required to shift the value of the EC_{50} of phenylephrine six fold, while a similar increase in the value of the EC_{50} of adenosine could be elicited by only a 32 fold increase in the phenylephrine concentration. A 30 fold increase in the phenylephrine concentration shifted the value of the EC_{50} of 5'-N-ethylcarboxamidoadenosine four fold.

5 Analysis of the functional antagonism between the responses mediated by these receptors using the Black & Leff (1983) operational model of agonism allowed for the estimation of the agonist dissociation constant, K_A, and the apparent efficacy, τ, for both phenylephrine and adenosine A_2 receptor agonists. Increasing the concentration of phenylephrine reduced the value of τ for adenosine agonists in a concentration-dependent and saturable manner. Similarly, increasing the concentration of adenosine reduced the value of τ for phenylephrine in a concentration-dependent and saturable manner. The phenylephrine K_A value obtained by the method of functional antagonism (1.9 μM) was similar to that obtained by the receptor inactivation method (2.1 μM).

6 Partial occlusion of the α_1-adrenoceptor by the alkylating agent, dibenamine, demonstrated that the magnitude of the adenosine A_2 receptor-mediated relaxation was inversely proportional to the number of functional α_1-adrenoceptors.

7 It is concluded that the magnitude of functional antagonism is proportional to the stimulus elicited through either receptor. We propose that this tissue preparation and pair of receptors is a good model to study quantitative aspects of functional antagonism between activated receptors.

Keywords: Adenosine; adenosine A_2 receptor; alkylation; α_1-adrenoceptor; functional antagonism; operational model of agonism; rabbit aorta

Introduction

Blood vessel tone is regulated *in vivo* by the action of different endogenous substances. For example, one of the neuronal controls of vascular tone is mediated through activation of α_1-adrenoceptors and β_2-adrenoceptors which mediate constriction and relaxation, respectively (Hoffman & Lefkowitz, 1990). Blood vessel tone can also be modulated by a variety of peptides, such as angiotensin II and vasoactive intestinal polypeptide. Similar opposing responses were reported for endothelin and nitric oxide, two factors released from the endothelium. This functional or physiological antagonism, which appears to be ubiquitous in all excitable tissues, was the impetus for the development of models attempting to quantify the relationship between the two opposing stimuli.

Although functional antagonism has been used extensively to determine agonist dissociation constants when an irreversible antagonist is not available (Buckner & Saini, 1975; Emmerson & Mackay, 1981; Henry *et al.*, 1985; Molenaar & Malta, 1986; Eglen *et al.*, 1991) and several mathematical models have been proposed to study functional antagonism (Van den Brink, 1973a,b; Mackay, 1981), its applicability has been questioned when its use is compared to the results obtained with an irreversible antagonist (Leff *et al.*, 1985). Buckner & Saini (1975) and more recently, Lemoine & Overlack (1992) studied functional antagonism of cholinergic contraction in the guinea-pig isolated trachea by β-adrenoceptor agonists of different efficacies and showed that in tracheal smooth muscle there is an inverse relationship between the magnitude of contraction and the maximum relaxation. They also demonstrated that a maximal response to carbachol

[1] Author for correspondence: Department of Pharmaceutical Sciences, College of Pharmacy and Allied Health Professions, St. John's University, Grand Central and Utopia Parkways, Jamaica, New York 11439, U.S.A.

[2] Present address: Central Nervous System Neuropharmacology, Bristol-Myers Squibb Co., Pharmaceutical Research Institute, Wallingford, Connecticut 06492, U.S.A.

attenuated the relaxation responses to partial β-adrenoceptor agonists more than that to full β-adrenoceptor agonists. This phenomenon enabled Buckner & Saini (1975) to use functional antagonism, under the appropriate conditions, to determine agonist dissociation constants.

In the present paper we describe the interactions between adenosine A_2 receptors and α_1-adrenoceptors in the adventitia- and endothelium-denuded aorta of the rabbit. The cardiovascular effects of adenosine have recently been reviewed (Belardinelli *et al.*, 1989). Adenosine-mediated vasodilatation results from its action on the adenosine A_2 receptor subtype, which is linked to the stimulation of adenylyl cyclase through a cholera toxin-sensitive stimulatory G-protein, G_S (Sabouni *et al.*, 1989). Adenosine A_2 receptor agonists were reported to mediate relaxation of the rabbit aorta (Ghai & Mustafa, 1982; Balwierczak *et al.*, 1991), guinea-pig aorta (Collis & Brown, 1983; Headrick & Berne, 1990), bovine left anterior descending coronary artery (Cushing *et al.*, 1991), porcine carotid artery (Herlihy *et al.*, 1976; King *et al.*, 1990), and human pulmonary artery (McCormack *et al.*, 1989) and left anterior descending coronary artery (Sabouni *et al.*, 1990). All of these investigators employed functional antagonism of a pre-contracted tissue to assay the response to adenosine. Herlihy *et al.* (1976) demonstrated that the concentration-response curve for adenosine undergoes a dextral shift as the concentration of noradrenaline was increased from 0.3 to 1 μM; they also demonstrated that the magnitude of adenosine-mediated relaxation decreased as the concentration of K^+ was increased from 20 to 60 mM.

The present paper describes the influence of α_1-adrenoceptor fractional occupancy and density on adenosine A_2 receptor-mediated relaxation for a series of adenosine receptor agonists of different efficacies, as well as the influence of adenosine A_2 receptor fractional occupancy on α_1-adrenoceptor-mediated contraction. We now show that the magnitude of functional antagonism was proportional to the stimulus elicited through either receptor. In addition, we describe the use of the Black & Leff (1983) operational model of agonism to estimate the agonist dissociation constant, K_A, for phenylephrine and five adenosine A_2 receptor agonists. The availability of an irreversible α_1-adrenoceptor antagonist allowed for the comparison of K_A values estimated by the receptor inactivation method to those estimated by use of functional antagonism. Use of the Black & Leff (1983) operational model of agonism also allowed for the estimation of and characterization of the mutual changes in τ, the efficacy parameter, for both phenylephrine and adenosine A_2 receptor agonists. A preliminary account of some of these findings has appeared in abstract form (Wiener *et al.*, 1991).

Methods

Animals and tissue preparation

Male New Zealand white rabbits (1.5–2.0 kg) were purchased from H.A.R.E.-Marland Rabbits for Research, a Division of Marland Breeding Farms (Hewitt, NJ, U.S.A.), or from Buckshire Corporation (Perkasie, PA, U.S.A.), and were cared for in the St. John's University Animal Care Center, which is accredited by the American Association for the Accreditation of Laboratory Animal Care. All animals were housed at 68–72°F and 30–70% relative humidity with a 12 h light/12 h dark cycle (lights on 07 h 00 min). Food (Purina high fibre rabbit chow) and water were provided *ad libitum*. All experiments were approved by the St. John's University Institutional Animal Care and Use Committee and were performed in accordance with the *Guide for the Care and Use of Laboratory Animals* as adopted and promulgated by the National Institutes of Health. The rabbits were killed by asphyxiation with carbon dioxide. The thoracic aortae were removed, cut into rings approximately 7–8 mm in length and trimmed of connective tissue, fat, and adventitia by the method of Maxwell *et al.* (1968). The endothelium was removed by rubbing the intima with a moistened glass rod. The lack of endothelium function was verified as the absence of relaxation to 30 μM carbachol in rings precontracted with 0.1 μM phenylephrine. The rings were suspended overnight, at room temperature, between two stainless steel hooks in 20 ml organ baths containing Krebs-bicarbonate buffer (having the following composition in mM: NaCl 110, KCl 5, $CaCl_2$ 2.35, KH_2PO_4 1.2, $MgSO_4$ 1.2, $NaHCO_3$ 14.7, glucose 11 and Na_2EDTA 0.03), and were continuously bubbled with 95% oxygen and 5% carbon dioxide. Suspending the tissue overnight at room temperature before use allowed the tissues to stabilize more rapidly on the morning of the experiment and this practice has been described by us previously (Keitz *et al.*, 1990; Wiener *et al.*, 1992). The following morning the buffer was replaced, the temperature was adjusted to 37 ± 0.5°C, and the rate of bubbling was adjusted to maintain the pH at 7.4 ± 0.1. Two grams of basal tension were applied to all rings, and the tissues were allowed to stabilize for at least 1 h. When a stable response was reached, 2.0 ± 0.2 g tension were reapplied and the rings were conditioned by priming the tissue once with 10 μM phenylephrine, which was approximately twenty times the EC_{50}. The tension developed was measured with isometric force displacement transducers (Grass Instrument Company, Quincy, MA, U.S.A., model FT-03C) connected to a multichannel polygraph (Grass Instrument Company, model 7D or 79E). Drugs were washed from the organ bath by emptying and refilling the bath at least thrice rapidly and 60 min were allowed to elapse between experimental trials. During each experimental trial one ring from each rabbit was used as a paired-control to correct for any spontaneous changes in the tissue throughout the course of the experiment.

Logistic curve-fitting

Concentration-response curves were analyzed by non-linear regression analysis (Sigmaplot, Jandel Scientific, Corte Madera, CA, U.S.A.) by fitting the observed response and drug concentration to the following three-parameter logistic equation modified from De Lean *et al.* (1978):

$$E = \frac{E_{max}}{1 + \left(\frac{EC_{50}}{A}\right)^b} \quad (1)$$

where E was the observed response, E_{max} was the maximal response, EC_{50} was the concentration producing one-half maximal response, A was the agonist concentration, and b was the slope index. For studying relaxation responses, the fractional relaxation (relaxation/contraction; R/C) was an adequate description of the graded response to the tested drug (Keitz *et al.*, 1990). Therefore, equation 1 was adapted to reflect this observation:

$$\frac{R}{C} = \frac{\left(\frac{R}{C}\right)_{max} - \left(\frac{R}{C}\right)_{min}}{1 + \left(\frac{EC_{50}}{A}\right)^b} + \left(\frac{R}{C}\right)_{min} \quad (2)$$

where R/C was the observed fractional relaxation (relaxation/contraction) response, $(R/C)_{max}$ was the maximal fractional relaxation response, $(R/C)_{min}$ was the minimal fractional relaxation response (which was only used when describing an agonist concentration-response curve in the presence of a partial agonist; e.g. Figure 9), EC_{50} was the concentration producing one-half maximal response, A was the agonist concentration, and b was the slope index.

Operational model-fitting

Concentration-response curves were also analyzed by non-linear regression analysis to the Black & Leff (1983) operational model of agonism according to the following equation:

$$E = \frac{E_m \ \tau^n \ A^n}{(K_A + A)^n + \tau^n \ A^n} \quad (3)$$

where E was the observed response, E_m was the theoretical maximal response in the system, A was the agonist concentration, K_A was the agonist dissociation constant, τ was the efficacy parameter, and n was the slope factor. When a family of concentration-response curves for an individual tissue were fitted assuming a common E_m, K_A, and n, only the efficacy, τ, was allowed to vary between the individual curves. In fitting fractional relaxation concentration-response curves, such as those in Figures 3a, 5a, 6, and 8a, the value of E_m was constrained to $\leqslant 1$ to maintain physiological relevance, since the maximal relaxation response cannot exceed the maximal contractile response.

Receptor inactivation method

After first constructing a concentration-response curve to phenylephrine, tissues were contracted with 10 times the EC_{50} of phenylephrine and alkylated with 0.6 μM dibenamine for 10 min. Although a significant proportion of the α_1-adrenoceptors would be occupied at this concentration of phenylephrine, this method was employed in our laboratories since it consistently inactivated approximately 80% of the α_1-adrenoceptors. After the dibenamine was washed out, a concentration-response curve to phenylephrine was constructed. Operational model-fitting of concentration-response curves for the receptor inactivation method (e.g. Figure 7) was performed using Eq. 3 above as described by Leff *et al.* (1990).

Determination of the dissociation constant for competitive antagonism by adenosine partial agonists

The dose-ratio (DR) of the dextral shift for an adenosine agonist concentration-response curve in the presence of an adenosine partial agonist was used to calculate the dissociation constant, K_B, for the partial agonist by the method of Arunlakshana & Schild (1959) according to the following equation:

$$\log (DR - 1) = \log [\textit{partial agonist}] - \log K_B \quad (4)$$

A plot of log (DR − 1) versus log [partial agonist] was fitted by linear regression and the K_B was calculated from the y-axis intercept.

Statistical evaluation

All numerical values given are the arithmetic means ± s.e.mean, except for EC_{50} (Fleming *et al.*, 1972) and τ (Leff *et al.*, 1990) values which are the geometric means. Statistical evaluation was by one-way analysis of variance followed by Duncan's multiple-range test, two-way analysis of variance, or correlation analysis. The accepted level of significance was $P \leqslant 0.05$.

Reagents

N^6-cyclohexyladenosine (CHA), N^6-methyladenosine (MeAD), and **R**-(−)-N^6-(2-phenylisopropyl)adenosine (**R**-PIA) were purchased from Research Biochemicals Incorporated (Natick, MA, U.S.A.). Dibenamine was purchased from ICN Biomedicals Incorporated (Costa Mesa, CA, U.S.A.) and was prepared immediately before use. All other chemicals were purchased from Sigma Chemical Co. (St. Louis, MO, U.S.A.) and were of the highest grade available.

Results

Effect of adenosine A_2 receptor agonists on tissue tone in naive and phenylephrine-pre-contracted aortic rings

Adenosine and other adenosine agonists (5'-N-ethylcarboxamidoadenosine (NECA), MeAD, CHA, and **R**-PIA) did not alter basal tissue tone in naive adventitia- and endothelium-denuded aortic rings (data not shown). Therefore, relaxation of pre-contracted tissue was used to visualize the effects of adenosine agonists (Figure 1). The contractile response elicited by phenylephrine was stable throughout the time period required to construct the cumulative concentration response. The apparent lack of a contractile response to **R**-PIA or CHA in naive denuded rings suggested that the rabbit aorta does not contain adenosine A_1 receptors, in contrast to the guinea-pig isolated aorta (Stoggall & Shaw, 1990). As shown in Figure 1, the relaxation response to 3 or 100 μM adenosine did not fade for over 30 min after addition, in contrast to the rapid desensitization of the relaxation response to a β-adrenoceptor agonist (Keitz *et al.*, 1990).

To determine if prior exposure to adenosine agonists affects the concentration-response curve of phenylephrine the following experiment was performed: a cumulative concentration-response curve for phenylephrine was constructed, the phenylephrine was washed out and the rings were then exposed to an adenosine agonist for 30 min, and a second concentration-response curve for phenylephrine was constructed after the adenosine agonist was washed out. In all cases the phenylephrine concentration-response curves were superimposible (data not shown). The pEC_{50}, EC_{50} (μM), and slope index for phenylephrine (in the absence of adenosine agonists) were 6.31 ± 0.02, 0.49, and 1.46 ± 0.02, respectively, for 214 rings from 51 rabbits. Since aortic rings prepared from different rabbits had slightly different EC_{50} values for phenylephrine, a concentration-response curve for phenylephrine was constructed for each aortic ring and the tested concentration of phenylephrine used was expressed as the ratio [phenylephrine]/EC_{50}.

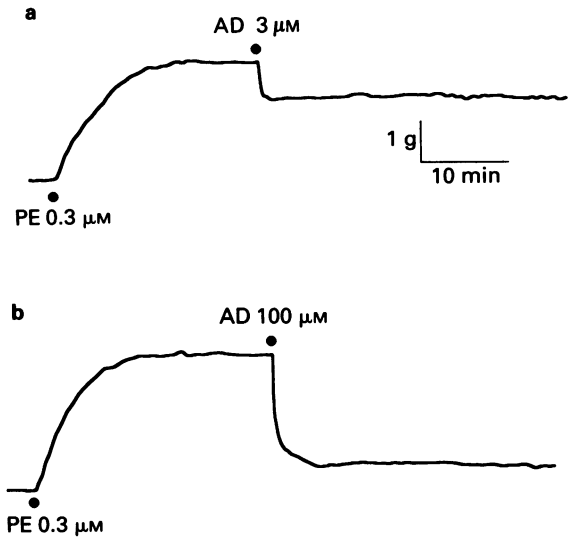

Figure 1 Representative tracing of a polygraph recording demonstrating that the relaxation mediated by adenosine is stable for over 30 min. Phenylephrine (PE) (0.3 μM; [phenylephrine]/EC_{50} = 1) was added to the organ bath at time indicated by the dot; when the contraction stabilized, adenosine (AD, 3 or 100 μM, a or b respectively) was added where indicated. The observed fractional relaxation (R/C) responses were 0.31 or 0.79 for 3 or 100 μM adenosine, respectively. Both tracings were from the same aortic ring. Control rings (phenylephrine alone, data not shown) were stable over this time period. These experiments were replicated using 9 rings from 3 rabbits (a) and 18 rings from 6 rabbits (b) with similar results.

Adenosine and its congeners (NECA, MeAD, CHA, or R-PIA) relaxed aortic rings precontracted with phenylephrine in a concentration-dependent and saturable manner (Figure 2). Repetitive cumulative concentration-response curves for an adenosine agonist in the same aortic ring were superimposible (data not shown). The agonist concentrations and mean observed R/C were fitted to the logistic equation (Eq. 2) to give the following values for $(R/C)_{max}$, pEC_{50}, EC_{50} (μM), and slope index: for NECA, 0.89 ± 0.02, 6.73 ± 0.07, 0.19, and 0.78 ± 0.02; for adenosine, 0.986 ± 0.002, 5.45 ± 0.02, 3.5, and 0.91 ± 0.02; for MeAD, 1.000 ± 0.000, 4.59 ± 0.09, 26, and 1.24 ± 0.05; for R-PIA, 0.79 ± 0.03, 5.57 ± 0.04, 2.7, 1.14 ± 0.04; and for CHA, 0.73 ± 0.02, 5.21 ± 0.06, 6.1, and 1.12 ± 0.02, respectively. The $(R/C)_{max}$, pEC_{50} and slope indices were compared by one-way analysis of variance followed by Duncan's multiple range test. For $(R/C)_{max}$: $F(4,82) = 83.3$, $P < 0.0001$; adenosine = MeAD > NECA > R-PIA > CHA. For pEC_{50}: $F(4, 82) = 209$, $P < 0.0001$; NECA > R-PIA = adenosine > CHA > MeAD. For slope index: NECA < 1 ($P < 0.01$); adenosine = 1 ($P > 0.05$); CHA > 1 ($P < 0.05$); MeAD > 1 ($P < 0.01$); R-PIA > 1 ($P < 0.01$). The observed rank order of agonist potency NECA > adenosine = R-PIA > CHA > MeAD was consistent with that of an adenosine A_2 receptor subtype (Williams, 1989) (see Figure 2). The addition of adenosine deaminase (4 u ml^{-1}), which converts adenosine to inosine, rapidly reversed the adenosine relaxation, restoring the contraction to the level observed before addition of adenosine. Adenosine deaminase did not reverse the relaxation produced by NECA, CHA, R-PIA, or MeAD, since these compounds are not substrates for adenosine deaminase (data not shown).

Mutual attenuation of the responses to adenosine A_2 agonists and phenylephrine

When the [phenylephrine]/EC_{50} was increased from 1 to 64, a dextral shift of the adenosine concentration-response curve (Figure 3a, Table 1) was observed; all pEC_{50} values were statistically different than each other ($F(6, 97) = 215.8$, $P < 0.0001$). In addition the maximal fractional relaxation response was inversely proportional to the [phenylephrine]/EC_{50} (F (6, 97) = 154.8, $P < 0.0001$; Figure 3a); the $(R/C)_{max}$ for adenosine (Table 1) markedly decreased by 67%, as the [phenylephrine]/EC_{50} increased from 1 to 64. All $(R/C)_{max}$ values were statistically different from each other with the exception of those obtained at a [phenylephrine]/EC_{50} of 1 and 2. The decrease in the fractional relaxation response for adenosine at phenylephrine concentrations greater than or equal to 8 times its EC_{50} (Figure 3a) was most likely due to a decrease in the magnitude of the adenosine agonist-mediated relaxation response (R) and not to an increased force of contraction, since a phenylephrine concentration greater than 8 times its EC_{50} would produce a response that was greater than 95% of the maximal response, when the slope index of the three-parameter logistic equation (Eq. 1) was 1.46.

To test if stimulation of β-adrenoceptors by high concentrations of phenylephrine affected the adenosine con-

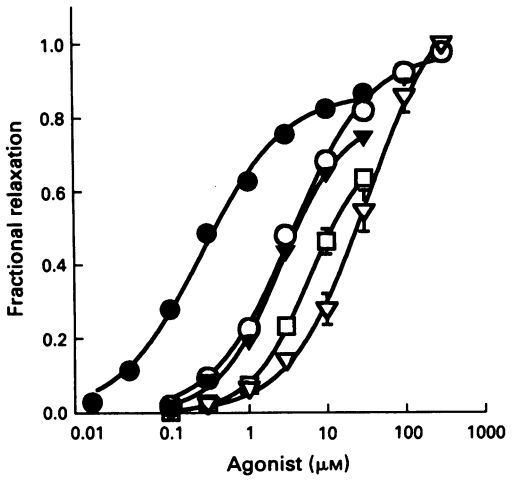

Figure 2 Cumulative concentration-response curves to 5'-N-ethylcarboxamidoadenosine (NECA, ●), adenosine (○), N^6-methyladenosine (MeAD, ▽), R-(−)-N^6-2-phenylisopropyladenosine (R-PIA, ▼), and N^6-cyclohexyladenosine (CHA, □). Following contraction with phenylephrine ([phenylephrine]/EC_{50} = 1), NECA, adenosine, MeAD, R-PIA or CHA was added in a cumulative manner and the fractional relaxation response (R/C) observed at each concentration was calculated. The agonist concentrations and mean observed R/C were fitted to the logistic equation (Eq.2) to estimate the values of $(R/C)_{max}$, EC_{50}, and slope index (see Results). The results shown in this figure were collected from 15 rings from 5 rabbits for NECA, 46 rings from 15 rabbits for adenosine, 10 rings from 4 rabbits for MeAD, 10 rings from 5 rabbits for R-PIA, and from 6 rings from 2 rabbits for CHA.

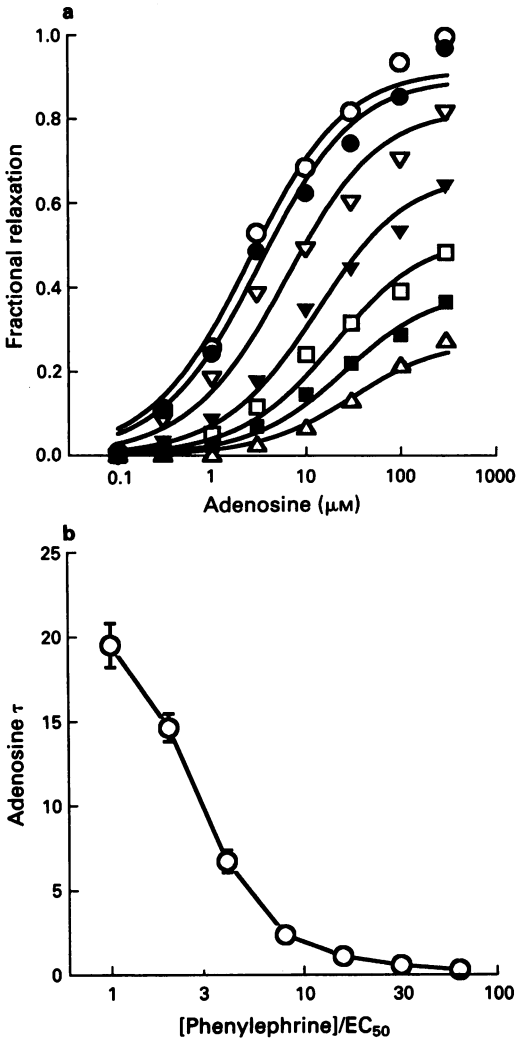

Figure 3 Attenuation of the responses to adenosine by phenylephrine. Illustrated in (a) is the effect of increased phenylephrine concentration (○, ●, ▽, ▼, □, ■, and △, represent 1, 2, 4, 8, 16, 32, and 64 times the EC_{50} of phenylephrine, respectively) on the fractional relaxation response to adenosine, where each curve represents the mean ± s.e.mean of 14–15 rings from 5 rabbits. A cumulative concentration-response curve to phenylephrine was first constructed for each ring. Each ring was then contracted with the indicated concentration of phenylephrine and a cumulative concentration-response curve to adenosine was constructed. For each ring, the adenosine concentration-response curves were fitted to Eq. 3 (Methods) simultaneously using non-linear regression. The pK_A for adenosine was 4.25 ± 0.05 ($K_A = 56$ μM). The value of n was 0.80 ± 0.02. (b) Represents the changes in the adenosine τ for the curves in (a) as a function of the phenylephrine concentration.

Table 1 Mutual attenuation of the responses to phenylephrine or adenosine in the isolated adventitia- and endothelium-denuded aorta of the rabbit

Adenosine (μM)	*Phenylephrine concentration-response curve parameters*[a]			
	E/E_{max}[b]	*Slope index*	pEC_{50}	EC_{50} *(μM)*
0	1.00 ± 0.00	1.98 ± 0.20	6.54 ± 0.05	0.29
0.1	1.00 ± 0.00	1.98 ± 0.20	6.54 ± 0.05	0.29
0.3	1.00 ± 0.00	1.74 ± 0.15	6.47 ± 0.05	0.34
1	1.00 ± 0.01	1.54 ± 0.11	6.38 ± 0.05	0.42
3	0.97 ± 0.01	1.49 ± 0.08	6.20 ± 0.05	0.63
10	0.96 ± 0.03	1.26 ± 0.07	6.02 ± 0.07	0.95
30	0.90 ± 0.03	1.32 ± 0.08	5.92 ± 0.06	1.21
100	0.82 ± 0.03	1.51 ± 0.10	5.84 ± 0.06	1.46
300	0.74 ± 0.02	1.77 ± 0.13	5.73 ± 0.06	1.86
[Phenylephrine]/EC_{50}	*Adenosine concentration-response curve parameters*[a]			
	$(R/C)_{max}$	*Slope index*	pEC_{50}	EC_{50} *(μM)*
1	0.99 ± 0.00	0.82 ± 0.02	5.47 ± 0.02	3.5
2	0.97 ± 0.01	0.73 ± 0.02	5.37 ± 0.02	4.3
4	0.84 ± 0.02	0.69 ± 0.02	5.25 ± 0.03	5.6
8	0.69 ± 0.03	0.77 ± 0.01	4.95 ± 0.03	11
16	0.53 ± 0.03	0.76 ± 0.01	4.82 ± 0.02	15
32	0.43 ± 0.03	0.80 ± 0.03	4.61 ± 0.05	24
64	0.33 ± 0.02	0.95 ± 0.02	4.34 ± 0.02	46

[a]Results are the mean ± s.e.mean for 14–15 rings from 5 rabbits. For statistical evaluation which was by one-way analysis of variance followed by Duncan's multiple-range test see Results.
[b]E/E_{max} represents the maximal response obtained by fitting the phenylephrine concentration-response curve to the three-parameter logistic equation (Eq.1) in the presence of adenosine as a ratio to the maximal response obtained in the absence of adenosine.

centration-response curve, the following experiment was performed: cumulative concentration-response curves to adenosine were constructed at different phenylephrine concentrations in the absence and presence of 1 μM (±)-propranolol to block the β-adrenoceptor. Adenosine concentration-response curves constructed in the presence and absence of propranolol were superimposible at all phenylephrine concentrations tested suggesting that there was no β-adrenoceptor component in the response to phenylephrine.

Analysis of the adenosine concentration-response curves by simultaneous curve fitting using the Black & Leff (1983) operational model of agonism (Eq. 3) allowed estimation of three shared parameters, E_m (the maximal fractional relaxation response), K_A (the agonist dissociation constant), and n (the slope factor). Simultaneous curve fitting also allowed the estimation of τ (the efficacy parameter) for each individual curve. Increasing the phenylephrine concentration resulted in a concentration-dependent and saturable decrease in the value of τ for adenosine (Figure 3b). Since the value of τ was assumed to be log-normally distributed (Leff *et al.*, 1990) the values of log τ were statistically evaluated by one-way analysis of variance (F (6, 97) = 315, $P < 0.0001$) followed by Duncan's multiple-range test and this testing indicated that all log τ values were statistically different than each other. The K_A for adenosine was also estimated, it was 56 μM ($pK_A = 4.25 \pm 0.05$) in rings pre-contracted with phenylephrine. The lack of an irreversible adenosine A_2 receptor antagonist prevented determination of the agonist dissociation constant by the receptor inactivation method.

Construction of adenosine concentration-response curves at multiple concentrations of phenylephrine also allowed us to calculate the contractile concentration-response curves in the absence or presence of eight different concentrations of adenosine. Phenylephrine (Figure 4a) contracted adventitia- and endothelium-denuded aortic rings of rabbit in a concentration-dependent and saturable manner. Increasing the adenosine concentration attenuated the response to phenylephrine (Figure 4a) in a concentration-dependent and saturable manner as was observed by the dextral shift and attenuation of the maximal response for the concentration-response curve to phenylephrine. The E_{max} for phenylephrine decreased by a modest 26% as the adenosine concentration increased by over three orders of magnitude from 0.1 to 300 μM (Table 1), with the majority of the decrease occurring at the highest concentrations of adenosine tested (100 or 300 μM). The responses at 30, 100, and 300 μM adenosine were statistically different from the responses at all other adenosine concentrations tested (F (8, 117) = 26.93, $P < 0.0001$). The EC_{50} for phenylephrine increased 6.4 fold as the adenosine concentration increased from 0.1 to 300 μM (Table 1); however, the phenylephrine concentration had to be increased only 32 fold to cause a similar increase in the EC_{50} for adenosine (Table 1).

Analysis of the contractile agonist concentration-response data using Eq.3 allowed for the estimation of operational parameters for phenylephrine. The K_A for phenylephrine, when estimated by the method of functional antagonism was 1.9 μM ($pK_A = 5.71 \pm 0.14$) and was comparable to that obtained by the receptor inactivation method (2.1 μM, $pK_A = 5.69 \pm 0.06$; Figure 7). The efficacy parameter, τ, for phenylephrine decreased in a concentration-dependent and saturable manner as the adenosine concentration increased (Figure 4b); these data were fitted to a four-parameter logistic equation using ALLFIT (De Lean *et al.*, 1978) to estimate the values of the maximal value of τ (8.8 ± 0.3), the IC_{50} (1.66 ± 0.02 μM), the slope index (0.78 ± 0.09), and the minimal value of τ (1.8 ± 0.2).

Phenylephrine also attenuated the concentration-response curves to NECA (Figure 5a). A 30 fold increase in phenylephrine concentration resulted in a 3.75 fold increase in the EC_{50} for NECA (Table 2) and decreased the $(R/C)_{max}$ from 0.86 to 0.21. The efficacy parameter, τ, for NECA decreased in a concentration-dependent and saturable manner as the concentration of phenylephrine increased (Figure 5b). The values of log τ were statistically evaluated by one-way analysis of variance (F (3, 32) = 65.5, $P < 0.0001$) followed by Duncan's multiple-range test and this testing indicated that all log τ values were statistically different from each other, except for those at 10 and 30 times the EC_{50} of phenylephrine. The efficacy of MeAD, CHA, or **R**-PIA was also inversely proportional to the phenylephrine concentration (Figure 6) and the relaxation responses to CHA or **R**-PIA were abolished when the phenylephrine concentration was 30 times its EC_{50} value. The dissociation constants for these adenosine agonists, estimated by the method of functional antagonism, are reported in Table 3.

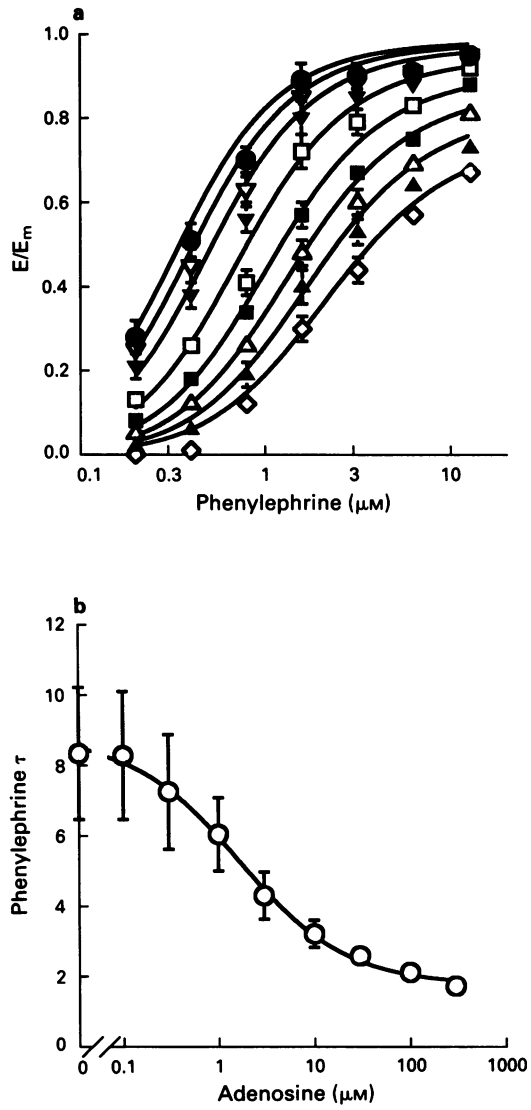

Figure 4 Attenuation of the responses to phenylephrine by adenosine. Illustrated in (a) is the effect of increased adenosine concentration (○, ●, ▽, ▼, □, ■, △, ▲, and ◇, represent 0, 0.1, 0.3, 1, 3, 10, 30, 100, and 300 μM adenosine, respectively) on the contractile response to phenylephrine, where each curve represents the mean ± s.e.mean of 14–15 rings from 5 rabbits and was calculated from the adenosine concentration-response curves illustrated in Figure 3a. For each ring, the phenylephrine concentration-response curves were fitted to Eq. 3 (Methods) simultaneously using non-linear regression. The pK_A for phenylephrine was 5.71 ± 0.14 (K_A = 1.9 μM). The value of n was 2.16 ± 0.27. (b) Represents the changes in the phenylephrine τ for the curves in (a) as a function of the adenosine concentration.

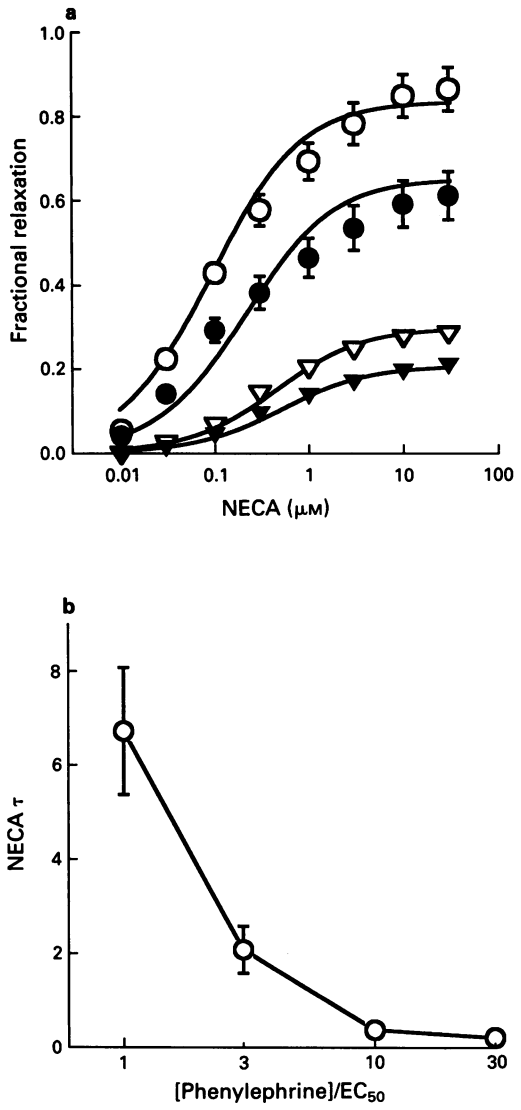

Figure 5 Attenuation of the responses to 5'-N-ethylcarboxamidoadenosine (NECA) by phenylephrine. Illustrated in (a) is the effect of increased phenylephrine concentration (○, ●, ▽, and ▼ represent 1, 3, 10, and 30 times the EC_{50} of phenylephrine, respectively) on the fractional relaxation response to NECA, where each curve represents the mean ± s.e.mean of 9 rings from 3 rabbits. The pK_A for NECA was 6.08 ± 0.06 (K_A = 0.82 μM). The value of n was 0.86 ± 0.04. (b) Represents the changes in the NECA τ for the curves in (a) as a function of the phenylephrine concentration.

Table 2 Attenuation of the responses to 5'-N-ethylcarboxamidoadenosine (NECA) by phenylephrine in the isolated adventitia- and endothelium-denuded aorta of the rabbit

[Phenylephrine]/EC_{50}	*NECA concentration-response curve parameters*[a]			
	$(R/C)_{max}$	*Slope index*	*pEC_{50}*	*EC_{50} (μM)*
1	0.86 ± 0.05	0.81 ± 0.03	6.91 ± 0.02	0.12
3	0.61 ± 0.06	0.71 ± 0.02	6.80 ± 0.03	0.16
10	0.28 ± 0.02	0.95 ± 0.04	6.46 ± 0.01	0.34
30	0.21 ± 0.02	0.87 ± 0.04	6.35 ± 0.01	0.45

[a]Results are the mean ± s.e.mean for 9 rings from 3 different rabbits. For statistical evaluation which was by one-way analysis of variance followed by Duncan's multiple-range test see Results.

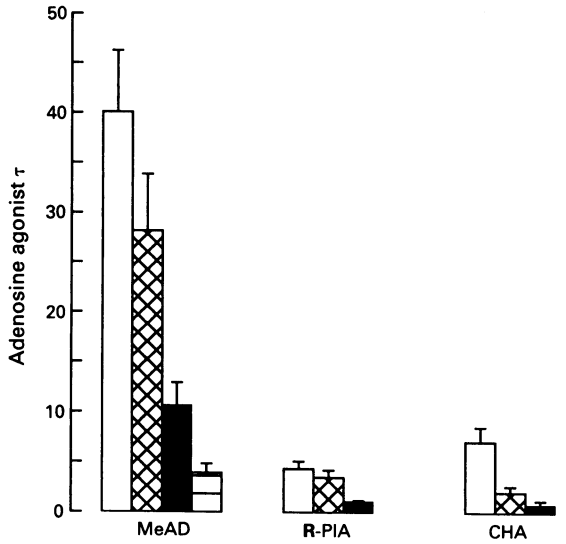

Figure 6 The value of τ for N^6-methyladenosine (MeAD), **R**(−)-N^6-(2-phenylisopropyl)adenosine (**R**-PIA), or N^6-cyclohexyladenosine (CHA) was inversely proportional to the phenylephrine concentration. Illustrated is the effect of increased phenylephrine concentration (the open, cross-hatched, solid and horizontally-hatched columns represent 1, 3, 10, and 30 times the EC_{50} of phenylephrine, respectively) on the value of τ for MeAD, **R**-PIA, or CHA where each column represents the mean ± s.e.mean of 6 rings from 3 different rabbits. The values of the K_A for MeAD, **R**-PIA, and CHA are listed in Table 3. The values of n for MeAD, **R**-PIA, and CHA were 0.91 ± 0.03, 1.19 ± 0.08, and 1.06 ± 0.08, respectively. The values of E_m for MeAD, **R**-PIA, and CHA were 1 (constrained, see Methods), 0.97 ± 0.02, and 0.91 ± 0.04, respectively. No relaxation response was observed for **R**-PIA or CHA in rings precontracted with 30 times the EC_{50} of phenylephrine.

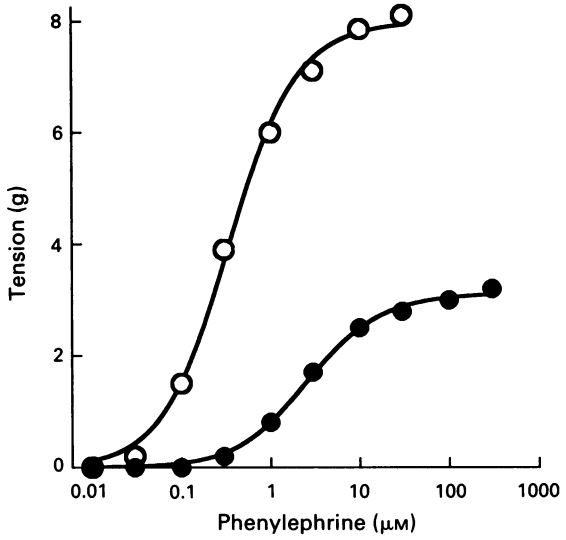

Figure 7 Effect of dibenamine treatment on phenylephrine concentration-response curves. Phenylephrine curves were obtained before (○) and following (●) 10 min exposure to 0.6 μM dibenamine. The symbols represent the data obtained from a single aortic ring and the lines drawn through them are the results of operational model-fitting. For this particular tissue the estimated model parameters were as follows: $E_m = 8.57$; $n = 1.19$; τ_1 (control) = 9.1; τ_2 (0.6 μM dibenamine) = 0.63; $pK_A = 5.50$. For full results see text.

Table 3 Adenosine agonist dissociation constants estimated by functional antagonism

Agonist	pK_A	K_A (μM)
Adenosine	4.25 ± 0.05	56
CHA	4.58 ± 0.16	26
NECA	6.08 ± 0.06	0.82
MeAD	3.56 ± 0.12	273
R-PIA	4.72 ± 0.08	19

The results for adenosine and NECA were from the experiments illustrated in Figures 3 and 5, respectively. For CHA, MeAD, and **R**-PIA the results were from the experiments illustrated in Figure 6. See text for abbreviations.

The response to adenosine was inversely proportional to the fraction of functional α_1-adrenoceptors remaining after partial irreversible occlusion with the alkylating agent dibenamine

Concentration-response curves to phenylephrine were constructed before and after partial irreversible occlusion with the alkylating agent dibenamine. The contractile response to phenylephrine was attenuated after partial receptor occlusion with dibenamine (Figure 7). Analysis of the concentration response curves by the operational model (Black & Leff, 1983) allowed for the estimation of the agonist dissociation constant, K_A, and the efficacy. As was expected, the efficacy of phenylephrine decreased following partial irreversible α_1-adrenoceptor occlusion with dibenamine. The values of log τ before and after alkylation with dibenamine were 0.99 ± 0.04 (τ = 9.7) and 0.22 ± 0.04 (τ = 1.7), respectively for 35 rings from 9 rabbits; statistical evaluation by a paired sample Student's *t* test indicated that log τ was statically decreased following alkylation (*t* test statistic = 7.90, 34 degrees of freedom, $P < 0.0001$). The values of the pK_A and n were 5.69 ± 0.06 (K_A = 2.1 μM) and 1.49 ± 0.04, respectively for 35 rings from 9 rabbits.

Concentration-response curves to adenosine were also constructed before and after partial irreversible α_1-adrenoceptor occlusion. The pEC_{50} of phenylephrine before alkylation was 6.67 ± 0.04 (EC_{50} = 0.21 μM) and the K_A/EC_{50} ratio was approximately 10 indicating that there was substantial α_1-adrenoceptor reserve in this preparation. The concentration-response curves to adenosine constructed at the EC_{50} of phenylephrine were superimposible before and after alkylation (Figure 8a) and the efficacy of adenosine was, therefore, unchanged (Figure 8b) before and after alkylation in rings pre-contracted with the EC_{50} of phenylephrine. In contrast to the response observed at the EC_{50} of phenylephrine, the relaxation responses to adenosine were potentiated, as was its operational efficacy parameter, τ, following partial α_1-adrenoceptor occlusion with dibenamine in rings pre-contracted with 30 times the EC_{50} of phenylephrine (Figure 8). Statistical evaluation by two-way analysis of variance followed by Bonferroni *post-hoc* testing (Godfrey, 1985) indicated that the value of τ for adenosine was significantly reduced as the phenylephrine concentration increased ($P < 0.001$). A similar statistical evaluation indicated that the value of τ for adenosine was significantly increased following partial irreversible occlusion of the α_1-adrenoceptor in rings pre-contracted with 30 EC_{50} of phenylephrine ($P < 0.01$).

Antagonistic nature of adenosine A_2 receptor partial agonists

Construction of cumulative concentration-response curves to adenosine agonists (adenosine, NECA, MeAD) was also performed in the presence of adenosine partial agonists (**R**-PIA, CHA). As expected, the addition of an adenosine partial agonist resulted in an agonist response and a dextral and surmountable shift of the agonist concentration-response curve as illustrated for NECA and CHA in Figure 9a. Schild analysis (Arunlakshana & Schild, 1959) of a family of NECA concentration-response curves constructed in the presence of

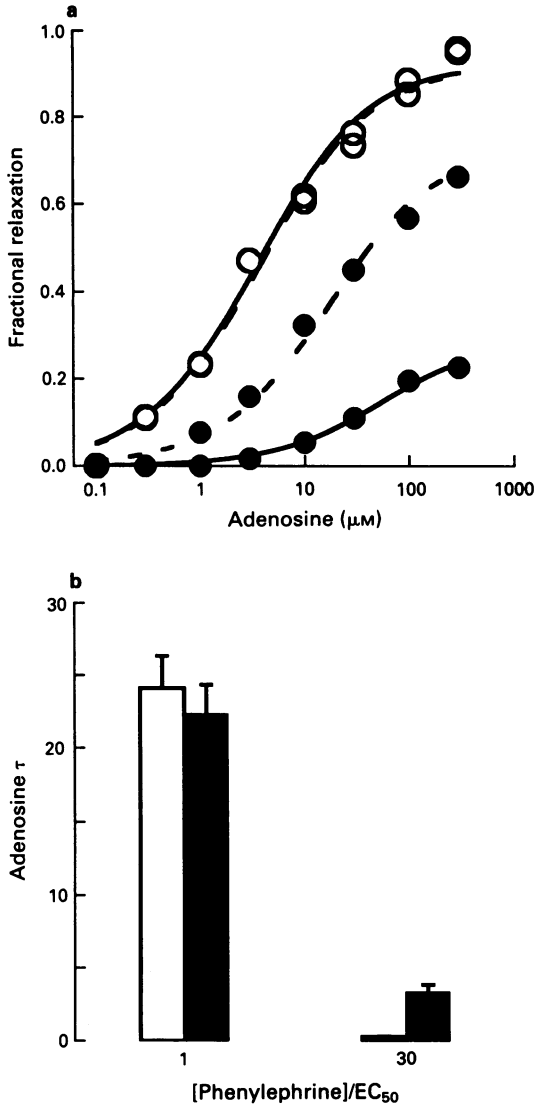

Figure 8 The fractional relaxation response to adenosine in rings pre-contracted with 30 times the EC_{50} of phenylephrine was potentiated following partial occlusion of the α_1-adrenoceptor with dibenamine. Illustrated in (a) are concentration-response curves to adenosine at 1 (○) and 30 (●) times the EC_{50} of phenylephrine, before (——) and after (------) partial irreversible receptor occlusion by exposure to 0.6 μM dibenamine for 10 min. Illustrated are the mean ± s.e.mean of 9 rings from 3 rabbits fitted using the operational model. The pK_A was 4.00 ± 0.03 (K_A = 100 μM). The value of the slope factor, n, was 0.77 ± 0.01. (b) Indicates the changes in the efficacy parameter, τ, for adenosine before (open column) and after (solid column) partial α_1-adrenoceptor occlusion with dibenamine. For statistical evaluation see Results.

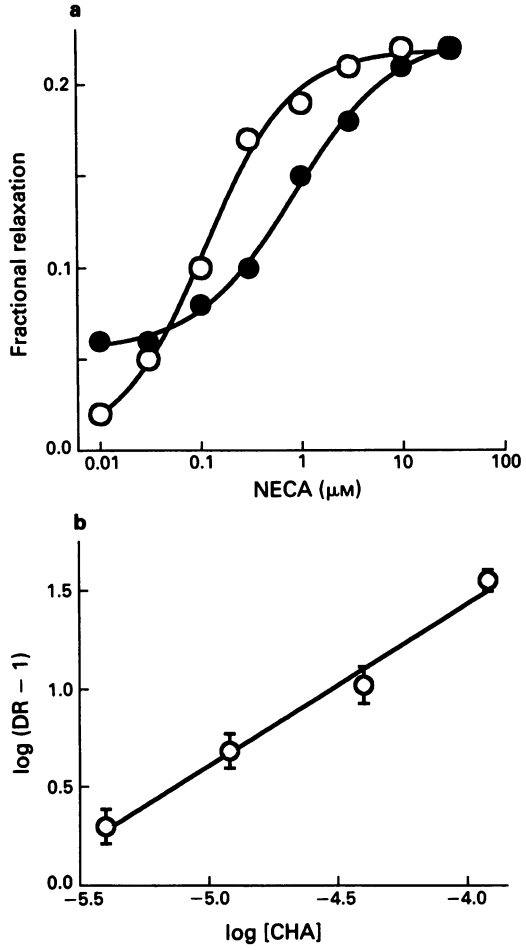

Figure 9 (a) Representative effect of an adenosine partial agonist N^6-cyclohexyladenosine, (CHA) on the cumulative concentration-response curve of an adenosine agonist 5'-N-ethylcarboxamidoadenosine, (NECA). An aortic ring was contracted with 4 μM phenylephrine ([phenylephrine]/EC_{50} = 10) and a cumulative concentration-response curve to NECA was constructed in the absence (○) or presence (●) of CHA (12 μM). The agonist concentrations and observed R/C were fitted to the logistic equation (Eq.2) to give the following values for $(R/C)_{max}$, $(R/C)_{min}$, EC_{50} (μM), and slope index: in the absence of CHA, 0.22, 0.002, 0.11, and 1.00; in the presence of 12 μM CHA, 0.23, 0.055, 0.88, and 0.87, respectively. This experiment was repeated on 6 rings from 3 rabbits. Each ring was exposed to 4 different concentrations of CHA (4–120 μM), allowing construction of a Schild plot (Arunlakshana & Schild, 1959). (b) Schild plot for the competitive antagonism of CHA against NECA. Shown are the mean ± s.e.mean for 6 rings from 3 rabbits. The slope, y-axis intercept, and R^2 were 0.824, 4.73, and 0.988, respectively. The K_B for CHA against NECA at [phenylephrine]/EC_{50} = 10 was 18.6 μM.

4 different concentrations of CHA had slopes approximately equal to unity (0.82), suggesting that NECA and CHA compete for the same adenosine A_2 receptor binding site (Figure 9b). As expected for partial agonists, the calculated K_B was similar to the EC_{50} value observed at the same concentration of phenylephrine. In addition, the K_B values obtained from the Schild analysis (Arunlakshana & Schild, 1959) were similar to the K_A values determined by the Black & Leff (1983) analysis of the functional antagonism data. (See Table 3).

Discussion

Functional interactions in vasculature are an integral component in maintaining blood vessel tone, which in turn participates in controlling blood pressure. The present paper characterizes aspects of the interactions between responses mediated by two activated receptors, the adenosine A_2 receptor and the α_1-adrenoceptor, in the adventitia- and endothelium-denuded aorta of the rabbit. Adenosine triphosphate (ATP) is co-packaged and co-released with numerous neurotransmitters, including noradrenaline (Burnstock, 1991a,b). That ATP and noradrenaline are co-released necessitates the development of physiological control mechanisms to attenuate their contractile responses, which are mediated through their action on either the P_{2x} purinoceptor or the α_1-adrenoceptor, respectively. In addition to selective reuptake mechanisms, other mechanisms may participate in attenuating these contractile responses. A plausible mechanism is the rapid metabolism of ATP by ectonucleotidases to produce adenosine, which can mediate vasodilatation by interacting with the adenosine A_2 receptor. This modulates tissue tone at the smooth muscle level. Other mechanisms proposed to attenuate contractile responses in-

clude the production and release of relaxing factors from endothelial cells (Furchgott, 1984). We chose to study one of these mechanisms, namely the functional antagonism between α_1-adrenoceptor-mediated vasoconstriction and adenosine A_2 receptor-mediated vasodilatation in the denuded rabbit aorta. The use of the denuded aorta preparation affords several advantages: we are essentially studying only a vascular smooth muscle preparation, removal of the endothelium excludes any influence it may possess by eliminating its ability to release agents that alter muscle tone (Furchgott, 1984), and removal of the adventitia eliminates its participation as a diffusion barrier (Wiener & Sehba, 1993) and as a source of sympathetic nerve endings which may release agents that can also alter muscle tone (Maxwell et al., 1968). Although both α_{1A}- and α_{1B}-adrenoceptor subtypes may coexist in the rabbit aorta, we assumed that phenylephrine activated only one type of α_1-adrenoceptor in this preparation since Oriowo & Ruffolo (1992) concluded that it was impossible to subclassify reliably the α_1-adrenoceptor in the mammalian aorta with the currently available pharmacological antagonists.

Analysis of functional antagonism between the responses mediated by the α_1-adrenoceptor and the β_2-adrenoceptor in the adventitia- and endothelium-denuded rabbit aorta is complicated by desensitization of the β_2-adrenoceptor (Keitz et al., 1990; Osman et al., 1990). In contrast, functional antagonism between responses mediated by the α_1-adrenoceptor and the adenosine A_2 receptor was less complex in that activation of the adenosine A_2 receptor was not associated with any detectable desensitization, as the steady-state relaxation response remained virtually unchanged for over 30 min (Figure 1). This permitted construction of *cumulative* concentration-response curves for several agonists on the same piece of tissue during the course of a single experiment, the response parameters ($(R/C)_{max}$, EC_{50}, and slope index) of adenosine A_2 agonists being stable throughout the course of an experiment.

The $(R/C)_{max}$ of the response mediated by adenosine A_2 receptor activation was inversely proportional to the [phenylephrine]/EC_{50} which was proportional to the α_1-adrenoceptor fractional occupancy (Table 4) and presumably, therefore, to the stimulus mediated by this receptor. As the [phenylephrine]/EC_{50} was increased it caused a progressive attenuation of the magnitude of the response to adenosine (Figure 3) and to NECA (Figure 5). These effects were also observed for the other adenosine agonists tested (Figure 6). The observed K_A/EC_{50} ratio for phenylephrine was approximately 11 (Figure 7, Tables 1 and 4), which may indicate that this preparation contains a large receptor reserve for this α_1-adrenoceptor agonist. If the highest theoretical EC_{50} value equals the K_A (Kenakin, 1987), it could be anticipated that adenosine concentrations greater than 300 μM should shift the concentration-response curves to phenylephrine even further to the right (Figure 4). However, this was not practical due to solubility limitations of adenosine. The six fold increase in the value of the phenylephrine EC_{50} resulting from a 1000 fold increase in adenosine concentration (Figure 4) indicates that the interaction between the two responses cannot be described by simple competitive behaviour. Intriguingly, only a 32 fold increase in the phenylephrine concentration was required to produce a six fold dextral shift in the adenosine concentration-response curve. These results suggest that a greater inhibitory stimulus results from α_1-adrenoceptor occupancy than from adenosine A_2 receptor occupancy in this preparation. This may reflect differences in absolute receptor density but, unfortunately, this cannot be confirmed directly due to the lack of a high specific activity radiolabelled adenosine A_2 antagonist.

Table 4 Comparison of [phenylephrine]/EC_{50} and [phenylephrine]/K_A ratios and fractional occupancies

[Phenylephrine]/EC_{50}[a]	*[Phenylephrine]/K_A*[b]	*Fractional occupancy*[c]
1	0.14	0.12
2	0.28	0.22
3	0.41	0.29
4	0.55	0.36
8	1.1	0.52
10	1.4	0.58
16	2.2	0.69
30	4.1	0.81
32	4.4	0.82
64	8.8	0.90

[a]The EC_{50} value for phenylephrine, in the absence of adenosine, was from table 1 and was 0.29 μM.
[b]The K_A value for phenylephrine, estimated by the receptor inactivation method (Figure 7), was 2.1 μM.
[c]The fractional occupany was calculated from the equation $[A]/([A] + K_A)$, where A was the phenylephrine concentration and K_A was the agonist dissociation constant.

Interestingly, the relaxation responses observed for the adenosine A_2 partial agonists (CHA and **R**-PIA) were abolished at [phenylephrine]/EC_{50} = 30. This finding was in agreement with that of Buckner & Saini (1975) who reported that the maximal relaxation response of the guinea-pig isolated trachea to the β-adrenoceptor partial agonist, (−)-soterenol, was reduced to a much greater extent than the maximal response to the β-adrenoceptor agonist, isoprenaline, was by carbachol. We also studied the antagonistic nature of the adenosine A_2 receptor partial agonists (**R**-PIA and CHA) on the concentration-response curve to an adenosine A_2 receptor agonist (NECA, adenosine, and MeAD). As would be expected, the partial agonist induced a dextral shift in the agonist concentration-response curve, and since the K_B and EC_{50} were equal one can conclude that there was no receptor reserve for the partial agonist (illustrated for CHA against NECA in Figure 9).

To investigate further the relationship between the stimulus mediated by the α_1-adrenoceptor and the adenosine A_2 receptor, we reduced the number of functional α_1-adrenoceptors by partial occlusion using the irreversible alkylating agent dibenamine. Decreasing the number of functional α_1-adrenoceptors did not alter the inverse relationship between R/C and [phenylephrine]/EC_{50} (Figure 8); it did, however, act to potentiate the response to adenosine as reflected by the increased maximal fractional relaxation response observed after alkylation. These alkylation experiments suggested that a crucial factor determining the magnitude of functional antagonism may be the ratio of the densities of the two receptors, which is directly proportional to the ratio of the two stimuli.

Analysis of the data presented in the present communication by the Black & Leff (1983) operational model of agonism allowed for the estimation of the agonist dissociation constant (K_A) for phenylephrine and the adenosine A_2 receptor agonists, adenosine, NECA, MeAD, CHA, and **R**-PIA (Table 3). The lack of an irreversible adenosine A_2 receptor antagonist prevented a direct comparison of the K_A values estimated by the functional antagonism method and the receptor inactivation method. However, this was not the case for phenylephrine. A comparison of the results obtained from the functional antagonism method (Figure 4) with those obtained from the receptor inactivation method (Figure 7) revealed similar K_A values for phenylephrine (1.9 and 2.1 μM respectively).

The Black & Leff (1983) operational model also allowed for the estimation of the mutual changes in the agonist efficacy parameter, τ, as a function of the fractional occupancy of the other receptor. The majority of the decrease in the value of τ for adenosine (Figure 3) occurred as the fractional occupancy of the α_1-adrenoceptor by phenylephrine increased from 0.12 to 0.52. Similar changes were observed for NECA (Figure 5), MeAD (Figure 6), **R**-PIA (Figure 6), and CHA (Figure 6). In contrast, adenosine was less able to decrease the value of τ for phenylephrine.

In summary, the results of this study demonstrated that the relaxation mediated by the adenosine A_2 receptor in the adventitia- and endothelium-denuded rabbit aorta was inversely proportional to both the fractional occupancy and density of the α_1-adrenoceptor. Furthermore, this study also demonstrated that the response to adenosine A_2 receptor partial agonists was reduced to a much greater extent than that observed for adenosine A_2 receptor agonists as the [phenylephrine]/EC_{50} and, therefore, α_1-adrenoceptor fractional occupany was increased. The changes in the values of the operational efficacy parameter, τ, induced by functional antagonism was reported for five adenosine A_2 receptor and one α_1-adrenoceptor agonist. We propose that this tissue preparation and pair of receptors is a good model to study quantitative aspects of functional antagonism between activated receptors.

We are grateful to Drs Joseph Goldfarb and Roman Osman for their many stimulating discussions and critical evaluation of the manuscript. Supported by grants from St. John's University (Awards 050-91-002-4/6 and 050-92-002-2/6 to H.L.W.) and the United States Public Health Service (Grant GM 34852 to S.M.).

References

ARUNLAKSHANA, O. & SCHILD, H.O. (1959). Some quantitative uses of drug antagonists. *Br. J. Pharmacol Chemother.*, **14**, 48–58.

BALWIERCZAK, J.L., SHARIF, R., KRULAN, C.M., FIELD, F.P., WEISS, G.B. & MILLER, M.J.S. (1991). Comparative effects of a selective adenosine A_2 receptor agonist, CGS 21680, and nitroprusside in vascular smooth muscle. *Eur. J. Pharmacol.*, **196**, 117–123.

BELARDINELLI, L., LINDEN, J. & BERNE, R.M. (1989). The cardiac effects of adenosine. *Prog. Cardiovasc. Dis.*, **32**, 73–97.

BLACK, J.W. & LEFF, P. (1983). Operational models of pharmacological agonism. *Proc. R. Soc.*, **B, 220**, 141–162.

BUCKNER, C.K. & SAINI, R.K. (1975). On the use of functional antagonism to estimate dissociation constants for *beta* adrenergic receptor agonists in isolated guinea-pig trachea. *J. Pharmacol. Exp. Ther.*, **194**, 565–574.

BURNSTOCK, G. (1991a). Overview: purinergic mechanisms. *Ann. N.Y. Acad. Sci.*, **603**, 1–17.

BURNSTOCK, G. (1991b). Dual control of local blood flow by purines. *Ann. N.Y. Acad. Sci.*, **603**, 31–44.

COLLIS, M.G. & BROWN, C.M. (1983). Adenosine relaxes the aorta by interacting with an A_2 receptor and an intracellular site. *Eur. J. Pharmacol.*, **96**, 61–69.

CUSHING, D.J., BROWN, G.L., SABOUNI, M.H. & MUSTAFA, S.J. (1991). Adenosine-receptor-mediated coronary artery relaxation and cyclic nucleotide production. *Am. J. Physiol.*, **261**, H343–H348.

DE LEAN, A., MUNSON, P.J. & RODBARD, D. (1978). Simultaneous analysis of families of sigmoidal curves: application to bioassay, radioligand assay, and physiological dose-response curves. *Am. J. Physiol*, **235**, E97–E102.

EGLEN, R.M., MONTGOMERY, W.W. & WHITING, R.L. (1991). Desensitization and functional antagonism by β-adrenoceptor and muscarinic receptor agonists, respectively: a comparison with receptor alkylation for calculation of apparent agonist affinity. *Br. J. Pharmacol.*, **103**, 1951–1957.

EMMERSON, J. & MACKAY, D. (1981). A test of the null equation for functional antagonism. *Br. J. Pharmacol.*, **73**, 135–141.

FLEMING, W.W., WESTFALL, D.P., DE LA LANDE, I.S. & JELLETT, L.B. (1972). Log-normal distribution of equieffective doses of norepinephrine and acetylcholine in several tissues. *J. Pharmacol. Exp. Ther.*, **181**, 339–345.

FURCHGOTT, R.F. (1984). The role of endothelium in the responses of vascular smooth muscle to drugs. *Annu. Rev. Pharmacol. Toxicol.*, **24**, 175–197.

GHAI, G. & MUSTAFA, S.J. (1982). Demonstration of a putative adenosine receptor in rabbit aorta. *Blood Vessels*, **19**, 117–125.

GODFREY, K. (1985). Statistics in practice: comparing the means of several groups. *N. Engl. J. Med.*, **313**, 1450–1456.

HEADRICK, J.P. & BERNE, R.M. (1990). Endothelium-dependent and -independent relaxations to adenosine in guinea pig aorta. *Am. J. Physiol.*, **259**, H62–H67.

HENRY, P.J., LULICH, K.M. & PATERSON, J.W. (1985). Experimental testing of Mackay's model for functional antagonism in the isolated costo-uterus of the rat. *Br. J. Pharmacol.*, **86**, 131–139.

HERLIHY, J.T., BOCKMAN, E.L., BERNE, R.M. & RUBIO, R. (1976). Adenosine relaxation of isolated vascular smooth muscle. *Am. J. Physiol.*, **230**, 1239–1243.

HOFFMAN, B.B. & LEFKOWITZ, R.J. (1990). Catecholamines and sympathomimetic drugs. In *Goodman and Gilman's The Pharmacological Basis of Therapeutics*. ed. Gilman, A.G., Rall, T.W., Nies, A.S. & Taylor, P. pp. 187–220. Elmsford, NY: Pergamon Press.

KEITZ, S.A., OSMAN, R., CLARKE, W.P., GOLDFARB, J. & MAAYANI, S. (1990). Functional interactions in smooth muscle: kinetic characterization of the relaxation and desensitization responses to a *beta* adrenergic agonist in the rabbit aorta. *J. Pharmacol. Exp. Ther.*, **255**, 650–656.

KENAKIN, T.P. (1987). *Pharmacologic Analysis of Drug-Receptor Interaction*. New York: Raven Press.

KING, A.D., MILAVEC-KRIZMAN, M. & MULLER-SCHWEINITZER, E. (1990). Characterization of the adenosine receptor in porcine coronary arteries. *Br. J. Pharmacol.*, **100**, 483–486.

LEFF, P., MARTIN, G.R. & MORSE, J.M. (1985). Application of the operational model of agonism to establish conditions when functional antagonism may be used to estimate agonist dissociation constants. *Br. J. Pharmacol.*, **85**, 655–663.

LEFF, P., PRENTICE, D.J., GILES, H., MARTIN, G.R. & WOOD, J. (1990). Estimation of agonist affinity and efficacy by direct, operational model-fitting. *J. Pharmacol. Meth.*, **23**, 225–237.

LEMOINE, H. & OVERLACK, C. (1992). Highly potent *beta*-sympathomimetics convert to less potent partial agonists as relaxants of guinea pig tracheae maximally contracted by carbachol. Comparison of relaxation with receptor binding and adenylate cyclase stimulation. *J. Pharmacol. Exp. Ther.*, **261**, 258–270.

MACKAY, D. (1981). An analysis of functional antagonism and synergism. *Br. J. Pharmacol.*, **73**, 127–134.

MAXWELL, R.A., ECKHARDT, S.B. & WASTILA, W.B. (1968). Concerning the distribution of endogenous norepinephrine in the adventitial and media-intimal layers of the rabbit aorta and the capacity of these layers to bind tritiated norepinephrine. *J. Pharmacol. Exp. Ther.*, **161**, 34–39.

MCCORMACK, D.G., CLARKE, B. & BARNES, P.J. (1989). Characterization of adenosine receptors in human pulmonary arteries. *Am. J. Physiol.*, **256**, H41–H46.

MOLENAAR, P. & MALTA, E. (1986). Analysis of agonist dissociation constants as assessed by functional antagonism in guinea pig left atria. *J. Pharmacol. Meth.*, **15**, 105–117.

ORIOWO, M.A. & RUFFOLO, R.R. Jr. (1992). Heterogeneity of postjunctional α_1-adrenoceptors in mammalian aortae: subclassification based on chlorethylclonidine, WB-4101 and nifedipine. *J. Vasc. Res.*, **29**, 33–40.

OSMAN, R., KEITZ, S.A., GOLDFARB, J. & MAAYANI, S. (1990). Kinetics of response and drug action. *Neuropsychopharmacology*, **3**, 417–425.

SABOUNI, M.H., BROWN, G.L., KOTAKE, A.N., DOUGLAS, F.L. & MUSTAFA, S.J. (1990). Effects of CGS-15943A on the relaxations produced by adenosine analogs in human blood vessels. *Eur. J. Pharmacol.*, **187**, 523–530.

SABOUNI, M.H., CUSHING, D.J. & MUSTAFA, S.J. (1989). Adenosine-receptor-mediated relaxation in coronary artery: evidence for a guanyl nucleotide-binding regulatory protein involvement. *J. Pharmacol. Exp. Ther.*, **251**, 943–948.

STOGGALL, S.M. & SHAW, J.S. (1990). The coexistence of adenosine A1 and A2 receptors in guinea-pig aorta. *Eur. J. Pharmacol.*, **190**, 329–335.

VAN DEN BRINK, F.G. (1973a). The model of functional interaction. I. Development and first check of a new model of functional synergism and antagonism. *Eur. J. Pharmacol.*, **22**, 270–278.

VAN DEN BRINK, F.G. (1973b). The model of functional interaction. II. Experimental verification of a new model. The antagonism of β-adrenoceptor stimulants and other agonists. *Eur. J. Pharmacol.*, **22**, 279–286.

WIENER, H.L. & SEHBA, F.A. (1993). Kinetics of relaxation responses to vasorelaxants in intact and adventitia- and endothelium-denuded isolated rabbit thoracic aorta. *Gen. Pharmacol.*, (in press).

WIENER, H.L., MURRAY, J.M., THALODY, G.P. & MAAYANI, S. (1992). Kinetics of relaxation responses to vasorelaxants in isolated rabbit aorta. *Eur. J. Pharmacol.*, **220,** 131–140.

WIENER, H.L., THALODY, G.P. & MAAYANI, S. (1991). Interactions between responses mediated by simultaneous activation of adenosine A2 and alpha$_1$ adrenergic receptors. *Soc. Neurosci. Abstr.*, **17,** 989.

WILLIAMS, M. (1990). Purine receptors. In *Receptor Pharmacology and Function*. ed. Williams, M., Glennon, R.A. & Timmermans, P.B.M.W.M. pp. 503–525. New York: Marcel Dekker.

(Received May 27, 1992
Revised December 22, 1992
Accepted January 29, 1993)

Br. J. Pharmacol. (1993), **109**, 405–410 © Macmillan Press Ltd, 1993

Interaction between the effects of 5-hydroxytryptamine and adrenaline on the growth of platelet thrombi in the coronary artery of the anaesthetized dog

*S.J.G. McAuliffe, *[1]H.M. Snow, *B. Cox, †C.C.T. Smith & ‡M.I.M. Noble

*Bioscience II, ICI Pharmaceuticals, Macclesfield; †Department of Clinical Pharmacology, University College and Middlesex Medical School and ‡Academic Unit of Cardiovascular Medicine, Charing Cross and Westminster Medical School, London

1 The interaction between adrenaline and 5-hydroxytryptamine (5-HT) has been quantitated on the rate of thrombus formation, in the stenosed coronary artery with damaged endothelium of the anaesthetized dog.

2 Changes in the plasma concentration of adrenaline were produced by varying the rate of an intravenous infusion of adrenaline and in the effects of 5-HT, by intravenous injections of the selective 5-HT_2 receptor antagonist, ICI 170809.

3 Increases in the plasma concentration of adrenaline, which did not cause significant changes in blood pressure and heart rate, increased the rate of thrombus formation.

4 Antagonism of the 5-HT_2 receptor by ICI 170809, in the absence of an infusion of adrenaline, abolished thrombus formation (mean ED_{50} 0.41 $\mu g\,kg^{-1}$, i.v.).

5 The effects of adrenaline were non-competively antagonized by ICI 170809; maximum effects were obtained in the dose-range 50–200 $\mu g\,kg^{-1}$, i.v., when the mean dose-ratio increase in adrenaline required to restore equivalent rates of thrombus formation was 39 fold.

6 These results are consistent with a synergism between adrenaline and 5-HT and emphasize the importance of both on thrombus formation.

Keywords: Platelet; coronary artery; 5-hydroxytryptamine; adrenaline

Introduction

Platelet thrombi form at sites of arterial stenosis and endothelial denudation or damage. The presence of such sites in the coronary arteries of patients dying suddenly has led to the suggestion that the acute formation of platelet thrombi plays an important role in coronary artery disease (Haerem, 1972).

Folts and co-workers (1976, 1982) developed a model of thrombus formation in the stenosed coronary artery of the dog with damaged endothelium. In this model, coronary blood flow declines as a thrombus forms, until occlusion or near occlusion occurs, when the platelet thrombus dislodges and flow is restored. Thus a cyclical pattern of flow reductions is established (CFRs). This pattern of CFRs has now been observed in human coronary arteries (Eichorn *et al.*, 1991). The arterial thrombi contain platelets, fibrin and red and white blood cells. Arterial thrombus formation appears to be initiated by activation of platelets and the subsequent release of 5-hydroxytryptamine (5-HT) and thromboxane A_2, both of which promote further aggregation (Ashton *et al.*, 1986; De Clerck *et al.*, 1988). This positive feedback promotion of thrombus formation can be potentiated by adrenaline (Ashton *et al.*, 1989).

The aim of the present experiments, in anaesthetized dogs, was to quantify the interaction between the effects of adrenaline and 5-HT on thrombus formation, in a stenosed and damaged coronary artery, using the rate of decline of coronary blood flow as an index of the rate of thrombus formation. A preliminary communication of the results has been given (Cox *et al.*, 1991a,b).

[1] Author for correspondence at: H.M. Snow, Zeneca Limited, Research Department, Mereside, Alderley Park, Macclesfield, Cheshire SK10 4TG.

Methods

General

Experiments were carried out in 19 beagle dogs weighing between 15.0–19.0 kg. The dogs were sedated with morphine sulphate (10 mg, i.m.) and 30 min later were anaesthetized with pentobarbitone (induction 30 mg kg^{-1}, i.v., maintenance 3 mg kg^{-1}, i.v., every 30 min) through a cannula inserted into the long saphenous vein under local anaesthesia.

Ventilation was delivered via a tracheotomy with a mixture of 40% oxygen in room air supplied by a Harvard animal ventilator. When the chest was open a resistance to expiration was produced by placing the expiratory output of the pump under 3 cm of water. Samples of arterial blood were withdrawn at intervals throughout each experiment and pH, P_{O_2} and P_{CO_2} measured with a Corning EEL blood gas analyser. End-tidal P_{CO_2} was continuously measured by aspirating expired air from the trachea into an infra-red CO_2 analyser (P.K. Morgan Ltd.). The arterial P_{CO_2} was kept within the limits 34–42 mmHg and the arterial blood pH between 7.33 and 7.43 either by adjustment of respiration or the intravenous injection of 1.0 M $NaHCO_3$ solution. Oesophageal temperature was recorded and maintained at 37 ± 1°C (range) by heating lamps above and a thermostatically controlled heating blanket below the animal.

The ECG lead II was recorded and the signal used to drive a cardiotachometer. Systemic arterial pressure was recorded through a cannula inserted into the left femoral artery. All pressures were measured with strain gauge manometers (Hewlett Packard 4-442-001) attached to d.c. bridge amplifiers (Electromed). Blood flow in the left circumflex coronary artery was measured with either an electromagnetic flowmeter (Carolina Instruments Inc.) or an ultra-sound flowmeter (Transonic Inc.). The ECG, heart rate (HR), systemic arterial pressure and the mean and pulsatile coronary artery blood flow were recorded with a thermal array recorder (Gould TA4000).

Surgical procedures

The chest was opened in the 5th intercostal space, the left phrenic nerve divided and the pericardium opened to expose the left circumflex artery and vein. The circumflex coronary artery was damaged and stenosed as described by Folts *et al.* (1976). Briefly, about 2 cm of the left circumflex coronary artery was dissected free of surrounding tissue and the endothelium of a 5 mm length of artery damaged by crushing with a pair of Spencer Wells forceps. The damaged section of the artery was stenosed by a stiff plastic cuff which occluded the artery by about 60%. A flow probe was placed proximal to and a snare distal to the stenosis. Fine adjustment of the degree of stenosis was accomplished by passing a tapered nylon fishing line through the cuff. The degree of stenosis was adjusted until a 20 s occlusion with the distal snare did not produce a reactive hyperaemia, i.e. the distal vascular bed was fully dilated and therefore changes in blood flow (at constant heart rate and blood pressure) indicated changes in resistance at the stenosis.

In the above preparation the combination of stenosis and damaged endothelium induces platelet aggregation and the formation of a thombus, increasing the resistance to blood flow. When blood flow approached zero, thrombi embolised either spontaneously or after gentle vibration of the plastic cuff; blood flow and thrombus formation then restarted and a pattern of cyclic flow reductions (CFRs) began, e.g. Figure 3 (Folts *et al.*, 1976; Folts, 1982).

Experimental protocol

In 10 dogs cumulative intravenous doses of the selective 5-HT_2 antagonist ICI 170809 (Blackburn *et al.*, 1990) in the range 0.1–100 $\mu g\ kg^{-1}$ were given at 10 min intervals. Heart rate, arterial blood pressure and coronary blood flow were recorded throughout and measurements made 10 min after each dose.

In 10 dogs the effects of infusions of adrenaline (range 0.2–20 $\mu g\ kg^{-1}\ min^{-1}$, i.v.) on CFRs were obtained in the absence and presence of cumulative doses of ICI 170809 (range 1–1000 $\mu g\ kg^{-1}$, i.v.). In five of these dogs samples of arterial blood were taken 10 min after the start of adrenaline infusion for measurement of adrenaline concentration.

Adrenaline assay

The concentration of adrenaline in the plasma was assayed as described by Smith & Betteridge (1984) and Smith *et al.* (1985). Blood was taken into EDTA (1 mg ml^{-1}) and centrifuged immediately, the plasma was removed and stored at − 70°C. Following thawing, centrifugation was performed to remove fibrous protein and 1.5 ml of plasma added to an LP3 tube containing 10–20 mg of acid alumina; 10 μl BHBA (equivalent to 1000 pg) internal standard was then added, together with 1 M Tris buffer, pH 8.6. After shaking, mixing and washing of the alumina, 110 μl of eluent (acetic acid, EDTA, sodium disulphite solution) was added. After centrifugation 75 μl of alumina-free supernatant was assayed by high performance liquid chromatography (h.p.l.c.).

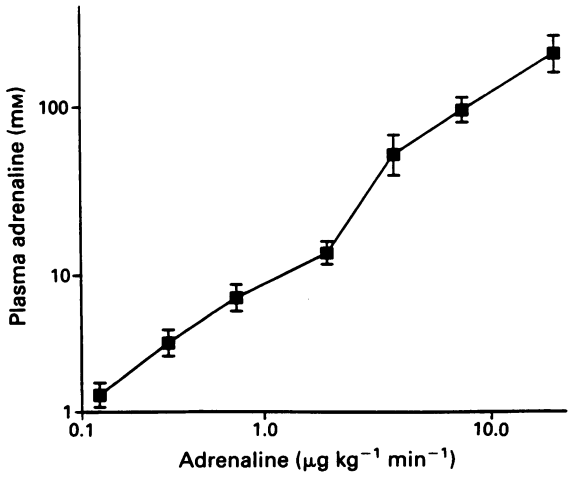

Figure 1 The measured plasma concentration of adrenaline (± s.e.mean) as a function of the rate of infusion of adrenaline.

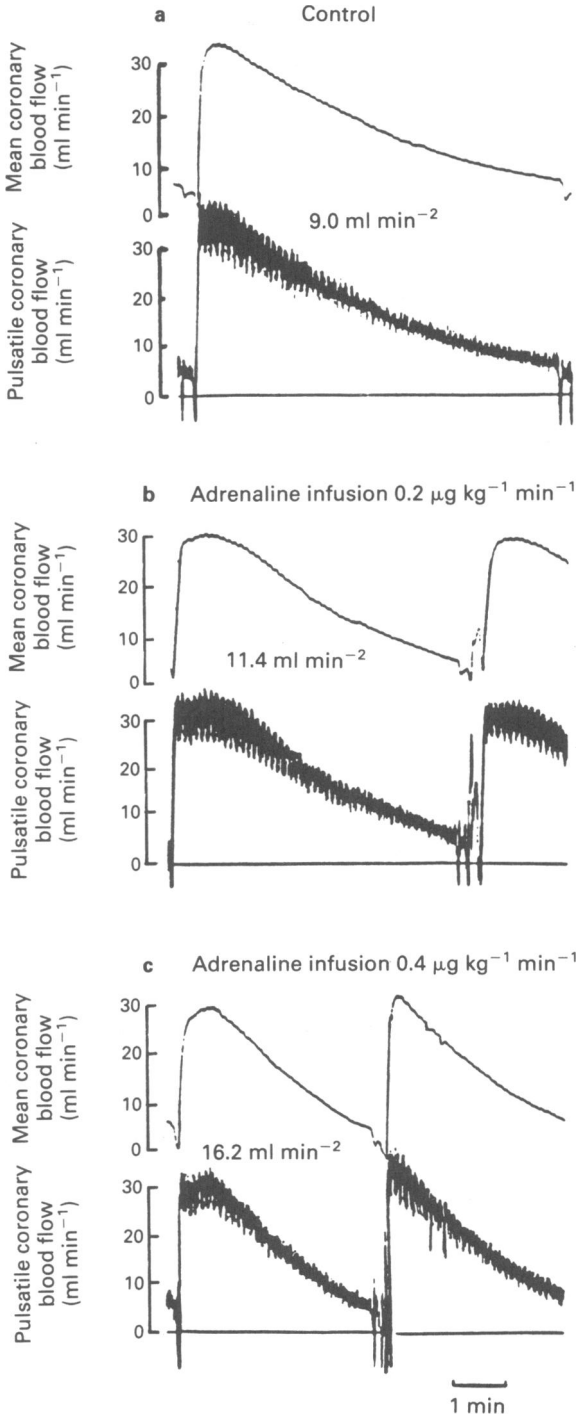

Figure 2 Records of mean and pulsatile blood flow in the stenosed left circumflex coronary artery showing the effects of adrenaline on the rate of thrombus formation as indicated by the rate of decline of coronary blood flow. Increasing the rate of adrenaline infusion to 0.2 (b) and 0.4 (c) $\mu g\ kg^{-1}\ min^{-1}$, i.v. had no effects on blood pressure and heart rate; the rate of decline of blood flow was increased from 9.0 (a) to 11.4 (b) and 16.2 (c) ml min^{-2}.

Drugs

The following were used: adrenaline bitartrate (Sigma UK); ICI 170809 2-[[3-(dimethylthylamino)ethyl]thio]-3-phenylquinoline (Zeneca Limited). All drugs were dissolved in sterile pyrogen-free 0.85% sodium chloride solution.

Results

About 1 h after the completion of surgical procedures, reproducible records of CFRs were usually obtained. In nine dogs, analysis of variance gave a within-dog standard error of the mean control estimate of the rate of decline of coronary blood flow of ± 6% (Snedecor & Cochran, 1989).

When control CFR's were obtained in all 19 dogs the heart rate and mean systemic arterial blood pressure were respectively: 161 ± 20 beats min^{-1} (mean ± s.d.) and 120 ± 10 mmHg. The pH, P_{CO_2} and P_{O_2} of the arterial blood were respectively: 7.394 ± 0.05, 37.4 ± 4.0 mmHg and 196 ± 26 mmHg (mean ± s.d.). The oesophageal temperature was 38.0 ± 0.3°C.

The mean curve relating the infusion rate of adrenaline to the plasma concentration of adenaline is shown in Figure 1. During the control period a measurable plasma concentration of adrenaline (0.2 nM) was found in only one dog. The two lowest rates of adrenaline infusion (0.2 and 0.4 μg kg^{-1} min^{-1}) produced plasma concentrations of 2.16 ± 0.2 nM and 4.04 ± 0.61 nM (mean ± s.d.). At these levels, after an initial transient fall in blood pressure and increase in heart rate, no significant changes from control value were observed. At higher rates of infusion (mean plasma concentration above 7.64 ± 1.38 nM) arterial blood pressure increased with variable changes in heart rate.

The effects of intravenous infusions of adrenaline on blood flow in the stenosed circumflex coronary artery in one dog is shown in Figure 2. Ten minutes after the start of each infusion, the rate of decline of coronary blood flow (the index of the rate of thrombus formation) was increased from 9.0 ml min^{-2} to 11.4 ml min^{-2} and 16.2 ml min^{-2}. Similar results were obtained in 10 dogs; the control decline in blood flow was 8.7 ± 1.4 ml min^{-2} and was decreased to 12.0 ± 1.5 ml min^{-2} and 14.2 ± 2.2 ml min^{-2} respectively.

Records of coronary blood flow in one dog (Figure 3), in the absence of an infusion of adrenaline, show the effects of antagonism of the 5-HT_2 receptor by ICI 170809. The rate of thrombus formation was progressively reduced and at a dose of 10 μg kg^{-1}, i.v., spontaneous embolization occurred and further thombus formation ceased. Similar results were obtained in 10 dogs and the mean dose-response curve is shown in Figure 4. We normalized the response in each dog; complete prevention of thrombus formation was taken as 100% response. The mean ED_{50} for this intitial effect of 5-HT_2 antagonism in the absence of adrenaline was 0.41 μg kg^{-1}, i.v. (95% CI 0.2–0.8). The variation of the ED_{50} between individual dogs was large with an overall range from a minimum of 0.1 to 5.0 μg kg^{-1}, i.v. The slope of the dose-response curve is unusually steep, from threshold to maximum effect takes place over a dose-range of less than one order of magnitude.

The interaction between 5-HT and adrenaline on thrombus formation was investigated by obtaining dose-response curves to adrenaline in the absence and in the presence of increasing doses of the 5-HT_2 antagonist, ICI 170809. In the presence of the 5-HT_2 receptor antagonist, increased amounts of adrenaline are required to restore equivalent rates of thrombus

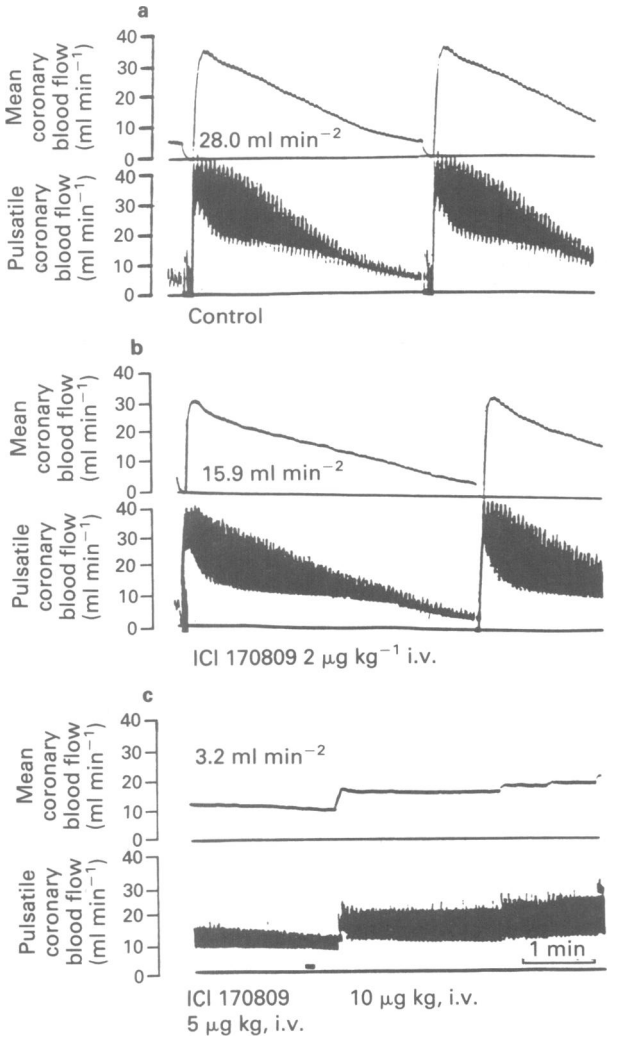

Figure 3 Records of mean and pulsatile coronary blood flow in the stenosed left coronary artery showing the effects of antagonism, of the platelet 5-HT_2 receptor by ICI 170809. The doses of 2 (b) and 5 μg kg^{-1}, i.v. (c) successively reduced the decline of blood flow from 28.0 (a) to 15.9 (b) and 3.2 (c) ml min^{-2}. After 10 μg kg^{-1}, i.v. (c) spontaneous embolization occurred and thrombus formation was abolished.

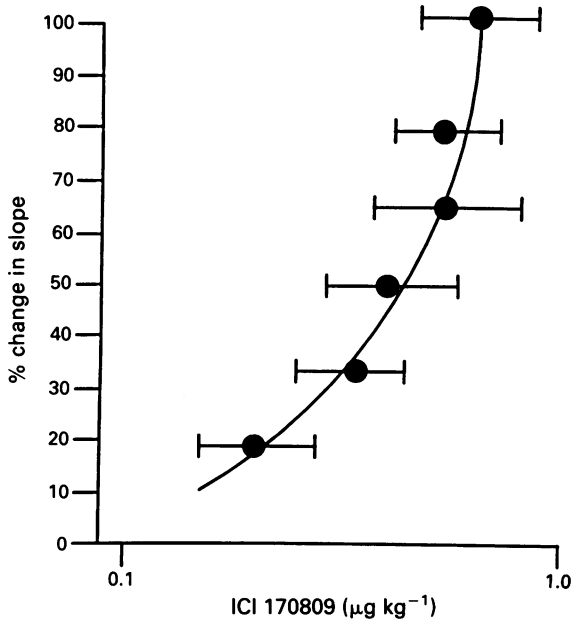

Figure 4 Dose-response curve obtained in nine dogs relating the dose of ICI 170809 (μg kg^{-1} i.v., mean ± s.e.mean) to the percentage change in the rate of decline of coronary blood flow (% change in slope). The curve was obtained by averaging the doses required to give the indicated responses, by interpolation on each individual dose-response curve.

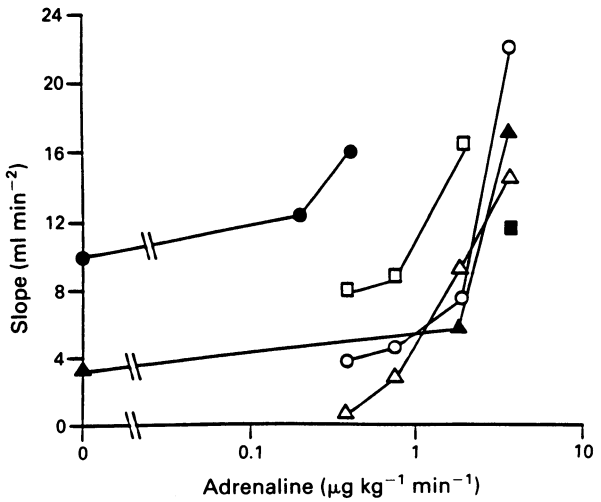

Figure 5 Dose-response curves obtained in one dog, in the absence and presence of increasing doses of ICI 170809 (●, control; □ 10; ▲ 50; ○ 70; △ 200 and ■ 500 μg kg^{-1} min^{-1}, i.v.) relating the infusion rate of adrenaline (μg kg^{-1} min^{-1}, i.v.) to the rate of decline of coronary blood flow (ml min^{-2}) as an index of thrombus formation. Doses of 10 and 50 μg kg^{-1}, i.v., cause a rightward shift of the dose-response curve; 70–200 μg kg^{-1}, i.v., have no further detectable effect.

formation. However in this particular experiment, at doses of ICI 170809 of 50 μg kg^{-1}, i.v. and above no further effects on the adrenaline dose-response curve occurred. This inhibitory effect of ICI 170809 on the ability of adrenaline to increase the rate of thrombus formation in four dogs is shown in Figure 5. In each dog the dose-ratio (DR) of adrenaline measured at the same rate of thrombus formation, was calculated and plotted as log(DR-1) against the dose of ICI 170809. All the slopes are less than the theoretical slope of one for competitive inhibition, as might be expected for an interaction between adrenaline and 5-HT, acting as they do at different receptor sites. There is a tendency for the inhibitory effects of ICI 170809 to remain constant at doses above 50 μg kg^{-1}, i.v., at which dose the DR increase to adrenaline was 39 fold (12–126) (mean ± 95% CI).

In five dogs the effects of antagonism of the 5-HT$_2$ receptor on thrombus formation were obtained after the inhibition of the enzyme, cyclo-oxygenase, by aspirin (5 mg kg^{-1}, i.v.), thus removing the effects of arachidonic acid metabolites on platelet aggregation. Aspirin alone abolished thrombus formation which was then restarted by an infusion of adrenaline (4.0 μg kg^{-1} min^{-1}, i.v.; plasma concentration 53.1 ± 13.9 nM, mean ± s.d.), an infusion rate which caused significant increases in arterial pressure. In these circumstances, ICI 170809 was still capable of preventing thrombus formation at doses of 50–100 μg kg^{-1}, i.v.

Discussion

This study shows that ICI 170809, a selective 5-HT$_2$ antagonist lacking effects at adrenoceptors (Blackburn *et al.*, 1988; 1990), inhibits both thrombus formation and also the potentiating effects of adrenaline, thereby implicating 5-HT in platelet aggregation.

The low plasma concentration of 5-HT coupled with low potency as a platelet aggregatory agent *in vitro* has raised doubts about the role of platelet-derived 5-HT in pathological states involving platelet aggregation (Robertson & Andrews, 1961; De Clerck & Herman, 1983; Van Neuton *et al.*, 1986).

However, 5-HT is concentrated in dense granules in the platelet and is released on activation, resulting in a relatively high concentration of 5-HT at the site of platelet aggregation. Ashton *et al.* (1986) measured an 18 fold increase in 5-HT concentration between damaged and normal sections of the left circumflex cororonary artery of the dog. Also 5-HT markedly amplifies the effects of other agonists, such as ADP, adrenaline, noradrenaline, collagen and thromboxane A$_2$ (TXA$_2$), as demonstrated by De Clerck *et al.* (1984), using the 5-HT$_2$ antagonist, ketanserin. Furthermore there is some evidence that disease processes increase the sensitivity of tissues to 5-HT and that plasma 5-HT concentration is increased after myocardial infarction. Constituents of the atheromatous plaque, such as low density lipoprotein, have been reported to amplify 5-HT-induced platelet aggregation (Fetkovska *et al.*, 1989) and endothelial damage has been shown to enhance arterial contractile responses to 5-HT (Orlandi *et al.*, 1990).

In our experiments the steepness of the antagonist dose-response curve, in the absence of an adrenaline infusion (Figure 4) suggests that activation of only a small proportion of the available 5-HT$_2$ receptors is required to cause aggregation. These observations, demonstrating the importance of 5-HT in the formation of a platelet thrombus, are supported by clinical evidence that ketanserin may be effective for the prevention of intracoronary events in patients with ischaemic heart disease (Noble & Drake-Holland, 1990).

It has been demonstrated that adrenaline potentiates, and aspirin, thromboxane receptor antagonists, thromboxane synthase inhibitors and 5-HT$_2$ antagonists all inhibit thrombus formation in this dog model of coronary artery thrombosis (Sheng-Kun Yao *et al.*, 1990; McAuliffe *et al.*, 1992). In experiments reported here and elsewhere (Cox *et al.*, 1991a,b), it was shown that the effects of all of the above agents, whether present alone or in combination, can eventually be overcome by increasing the stimulus to thrombus formation in terms of adrenaline, degree of stenosis and endothelial damage.

Adrenaline is able to cause platelet aggregation directly and to potentiate the effects of other agonists (Grant & Scrutton, 1979; Peety & Scrutton, 1989). In the present experiments both mechanisms could have been responsible for the effects of adrenaline. The stepwise removal of the effects of 5-HT, caused by increasing doses of the 5-HT$_2$ antagonist, resulted in a rightward shift in the adrenaline dose-response curve (Figure 5), demonstrating the synergism between adrenaline and 5-HT on platelet aggregation and

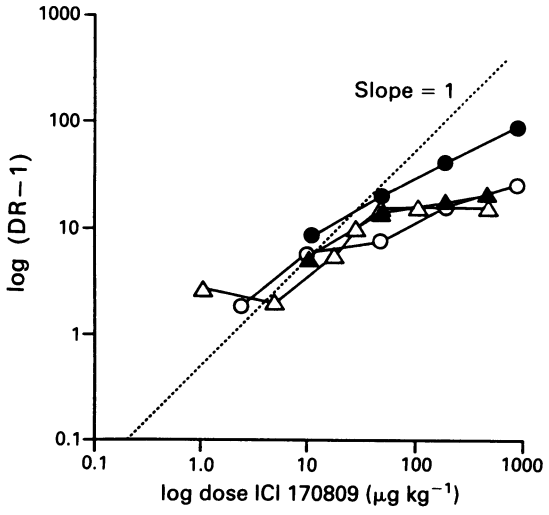

Figure 6 The effect of ICI 170809 (μg kg^{-1}, i.v.), in four dogs, on adrenaline dose-response curves (see Figure 5); measured as the dose ratio (DR) of adrenaline required to give equal rates of decline of coronary blood flow (plotted as log DR − 1). In all four dogs the slope of the relationship is less than one. At doses above 50–100 μg kg^{-1}, i.v., ICI 170809 tends to become less effective in antagonizing the effects of adrenaline.

thrombus formation. However the maximum effects of 5-HT_2 antagonism were limited to about a 30 fold increase in the plasma concentration of adrenaline (Figure 6), such that doses of ICI 170809 above 100 $\mu g\,kg^{-1}$, i.v., had no further antagonistic effects on the ability of adrenaline to cause platelet aggregation. Assuming that there is an upper limit to the amount of 5-HT released by platelets on activation, it should be possible to antagonize completely the effects of 5-HT with the highest doses of ICI 170809 used in this study. Thus the inability to prevent platelet aggregation, in the presence of a high concentration of adrenaline, is likely to be the result of both the direct effect of adrenaline and synergism with other aggregants, e.g. TXA_2 and platelet activating factor (PAF). In a previous study (Torr *et al.*, 1990), another specific 5-HT_2 antagonist, ritanserin, appeared to antagonize completely the effects of infused adrenaline. A similar result (Belcher *et al.*, 1992) has been obtained for the 5-HT_2 receptor antagonist, MDL 11,939 (Dudley *et al.*, 1988). In these studies the maximum rate of infusion of adrenaline was only 0.4 $\mu g\,kg^{-1}\,min^{-1}$, a rate of infusion much less than the maximum rate used in the present study.

The present approach has provided a more detailed and quantitative examination of the interaction between 5-HT and adrenaline in coronary artery thrombus formation and shown that in an experimental situation plasma concentrations of adrenaline, well above the normal physiological range, are required to cause platelet aggregation *in vivo* after the removal of the effects of 5-HT.

Recently we have shown that the amount of adrenaline required to offset the maximum effects of aspirin, ICI 192605 a thromboxane A_2 antagonist and ICI 170809 are all similar (Snow *et al.*, 1992). Further the anti-aggregating effects of a 5-HT_2 antagonist and aspirin are additive, whereas those of a cyclo-oxygenase inhibitor (aspirin) and any other drug acting on the arachidonic acid/thromboxane pathway such as a TXA_2 receptor antagonist or a TXA_2 synthase inhibitor are obviously not. These results allow the speculation that ICI 170809 may be of clinical use in the treatment of coronary artery thrombosis, since Blackburn *et al.* (1990) have shown that ICI 170809 inhibits aggregation of human platelets *ex-vivo*, indicating that the effects of a specific 5-HT_2 antagonist in patients with a coronary thrombosis may be similar to those suggested for ketanserin (Noble & Drake-Holland, 1990).

References

ASHTON, J.H., BENEDICT, C.R. & FITZGERALD, C. (1986). Serotonin as a mediator of cyclical flow variations in stenosed canine coronary arteries. *Circulation*, **73**, 572–578.

ASHTON, J.H., GOLINO, P., MCNATT, J.M., BUJA, L.M. & WILLERSON, J.T. (1989). Serotonin S_2 and thromboxane A_2 prostaglandin H_2 receptor blockade provide protection against epinepherine induced cyclic flow variations in severely narrowed canine coronary arteries. *J. Am. Coll. Cardiol.*, **13**, 755–763.

BELCHER, P.R., DRAKE-HOLLAND, A.J., HYND, J. & NOBLE, M.I.M. (1992). Dispersion of coronary artery thrombi by antagonism of platelet serotonin receptor. *Cardiovascular Res.*, (in press).

BLACKBURN, T.P., HAWORTH, S.J., JESSUP, C.L., MORTON, P.B. & WILLIAMS, C. (1990). ICI 170809, a selective 5-hydroxytryptamine antagonist, inhibits human platelet aggregation in vivo and ex-vivo. In *Cardiovascular Pharmacology of 5-hydroxytryptamine*. ed. Saxena, P.R., Wallis, D.I., Wouters, W. & Bevan, P. pp. 459–463. Kluwer: Academic Publishers.

BLACKBURN, T.P., THORNBER, C.W., PEARCE, R.J. & COX, B. (1988). In-vitro pharmacology of ICI 170809 – a new 5-HT_2 antagonist. *FASEB*, **A1404**, 6441.

COX, B., MCAULIFFE, S.J.G., NOBLE, M.I.M. & SNOW, H.M. (1991a). Inhibition of coronary artery thrombosis in the anaesthetized dog by antagonism of the 5-HT_2 receptors. *J. Physiol.*, **438**, 54P.

COX, B., MCAULIFFE, S.J.G., MOORS, J.A., NOBLE, M.I.M. & SNOW, H.M. (1991b). The effects of adrenaline and serotonin on the rate of formation of platelet thrombi in a stenosed coronary artery of the anaesthetized dog. *J. Physiol.*, **438**, 169P.

DE CLERCK, F. & HERMAN, G.G. (1983). 5-Hydroxytryptamine and platelet aggregation. *Fed. Proc.*, **42**, 228–232.

DE CLERCK, F., XHONNEUX, B. & DE COURCELLES, D. (1988). Functional expression of the amplification reaction between serotonin and epinepherine on platelets. *J. Cardiovasc. Pharmacol.*, **11**, S1–5.

DE CLERCK, F., XHONNEUX, B., LEYSEN, J.E. & JANNSEN, P.A.J. (1984). Evidence for functional 5-HT_2 receptor sites on human blood platelets. *Biochem. Pharmacol.*, **33**, 2808–2811.

DUDLEY, M.W., WIECH, N.L., MILLERE, F.P., CARR, A.A., CHENG, H.C., ROEBEL, L.E., DOHERTY, N.S., YAMAMURA, H.I., URSILLO, R.C. & PALFREYMAN, M.G. (1988). Pharmacological effects of MDL 11,939: a selective, centrally acting antagonist of $5HT_2$ receptors. *Drug Development Res.*, **13**, 29–43.

EICHORN, E.J., GRAYBURN, P.A., WILLARD, J.E., ANDERSON, H.V., BEDOTTO, J.B., CARRY, M., KAHN, J.K. & WILLERSON, J.T. (1991). Spontaneous alterations in coronary blood flow velocity before and after coronary artery angioplasty in patients with severe angina. *J. Am. Coll. Cardiol.*, **17**, 43–52.

FETKOVSKA, N., FETOVSKA, V. & DZURIK, R. (1989). Low density lipoprotein amplifies the platelet response to serotonin in human plasma. *J. Hypertens.*, **7** (suppl. 6), S164–165.

FOLTS, J.D. (1982). Experimental arterial platelet thrombosis, platelet inhibitors, and their possible clinical relevance. *Cardiovasc. Rev. Rep.*, **3**, 270–382.

FOLTS, J.D., CROWELL, E.B. & ROWE, G.G. (1976). Platelet aggregation in partially obstructed vessels and its elimination with aspirin. *Circulation*, **54**, 365–370.

GRANT, J.A. & SCRUTTON, M.C. (1979). Novel alpha$_2$-adrenoceptors primarily responsible for inducing human platelet aggregation. *Nature*, **277**, 659–661.

HAEREM, J.W. (1972). Platelet aggregates in intramyocardial vessels of patients dying suddenly and unexpectedly of coronary artery disease. *Atherosclerosis*, **15**, 199–213.

MCAULIFFE, S.J.G., SNOW, H.M., MOORS, J.A., WAYNE, M. & NOBLE, M.I.M. (1992). Inhibition of arachidonic acid metabolism by aspirin can promote thrombus formation in a stenosed coronary artery of the anaesthetized dog. *J. Physiol.*, **446**, 413P.

NOBLE, M.I.M. & DRAKE-HOLLAND, A.J. (1990). The involvement of serotonin in the formation of thrombi at critical stenoses in humans. *Coronary Artery Dis.*, **1**, 675–679.

ORLANDI, C., HUMPHREY, W.R., HOLLENBERG, N.K. & SCHAUB, R.G. (1990). In-vivo demonstration of enhanced platelet arterial constrictor response to serotonin following local endothelial loss. *Exp. Mol. Pathol.*, **52**, 192–201.

PEETY, A.C. & SCRUTTON, M.C. (1989). Platelet aggregation in whole blood: is the response to adrenaline, 5-hydroxytryptamine and PAF a direct consequence of stimulation by these agonists? *Thrombosis Res.*, **54**, 151–159.

ROBERTSON, J.I.S. & ANDREWS, T.M. (1961). Free serotonin in human plasma: quantitative and qualitative estimation. *Lancet*, **1**, 578–580.

SHENG-KUN YAO, ROSOLOWSY, M., ANDERSON, H.V., GOLINO, P., MCNATT, J.M., DE CLERCK, K., BUJA, L.M., WILLERSON, J.T. (1990). Combined thromboxane A_2 synthase inhibition and receptor blockade are effective in preventing spontaneous and epinephrine induced canine coronary cyclic flow variations. *J. Am. Coll. Cardiol.*, **16**, 705–713.

SMITH, C.C.T. & BETTERIDGE, D.J. (1984). Improved liquid chromatographic determination of catecholamines in platelets. *Clin. Chem.*, **30**, 1432–1433.

SMITH, C.C.T., CURTIS, L.D., DELAMONTHE, A.P., PRITCHARD, B.N.C. & BETTERIDGE, D.J. (1985). The distribution of catecholamines between platelets and plasma in normal human subjects. *Clin. Sci.*, **69**, 1–6.

SNEDECOR, G.W. & COCHRAN, W.G. (1989). Statistical Methods. 8th edition. Iowa State University Press, Ames, Iowa.

SNOW, H.M., MCAULIFFE, S.J.G., JESSUP, R., WAYNE, M. & NOBLE, M.I.M. (1992). Prevention of coronary thrombosis in the dog by inhibitors of platelet aggregation. *Br. J. Pharmacol. Proc. Suppl.* (in press).

TORR, S., NOBLE, M.I.M. & FOLTS, J.D. (1990). Inhibition of acute platelet thrombosis formation in the stenosed canine coronary arteries by the specific serotonin 5-HT_2 receptor antagonist ritanserin. *Cardiovasc. Res.*, **24**, 465–470.

VAN NEUTON, J.M., XHONNEUX, R. & JANSSENS, W.J. (1986). Interaction between S_2-serotonergic and $alpha_1$-adrenergic receptors and the control of blood pressure. In *Mechanisms of Vasodilatation* IV. Rochester, Minn.

(Received December 8, 1992
Revised January 26, 1993
Accepted January 29, 1993)

Br. J. Pharmacol. (1993), **109**, 411–414 © Macmillan Press Ltd, 1993

Selective MPP^+ uptake into synaptic dopamine vesicles: possible involvement in MPTP neurotoxicity

[1]M. Del Zompo, M.P. Piccardi, S. Ruiu, *M. Quartu, G.L. Gessa & A. Vaccari

Department of Neuroscience 'B. Brodie', University of Cagliari, Via Porcell 4, and *Department of Cytomorphology, Via Porcell 2, 09124 Cagliari, Italy

1 In the present study we provide evidence for a saturable, Mg^{2+}/ATP- and temperature-dependent, tetrabenazine-, dopamine-, and amphetamine-sensitive uptake of 1-methyl-4-phenylpyridinium ion (MPP^+) in synaptic vesicles from mouse striatum.

2 Similarity in the properties of the vesicular uptake suggests that in the striatum dopamine and MPP^+ share the vesicular carrier.

3 The presence of MPP^+ vesicular uptake in dopamine-rich regions such as striatum, olfactory, tubercles and hypothalamus, as well as its absence in cerebellum, cortex and pons-medulla, suggest that monoamine vesicular carriers differ between highly and poorly dopamine-innervated regions.

4 The restriction of active MPP^+ uptake to the dopaminergic regions, which reflects the previously shown distribution of [^{3}H]-MPP^+ binding sites in mouse brain membranes, indicates MPP^+ as a marker of the vesicular carrier for dopamine in dopaminergic neurones.

5 A role in MPP^+ neurotoxicity is suggested for this region-specific, vesicular storage of the toxin.

Keywords: 1-Methyl-4-phenylpyridinium ion (MPP^+) uptake; synaptic vesicles; dopamine carrier; neurotoxicity; 1-methyl-4-phenyl-1,2,3,6-tetrahydropyridine

Introduction

MPTP (1-methyl-4-phenyl-1,2,3,6-tetrahydropyridine) is a neurotoxin that produces a persistent Parkinson-like disorder in man, primates and rodents (Davis *et al.*, 1979; Burns *et al.*, 1983; Heikkila *et al.*, 1984) causing degeneration of the substantia nigra. The discovery of these effects of MPTP has highlighted the possibility that some unknown environmental or endogenous toxins contribute to the pathogenesis of Parkinson' s disease (Calne & Langston, 1983; Barbeau *et al.*, 1987). Evidence exists that in rodents, MPP^+ (1-methyl-4-phenylpyridinium ion), the neurotoxic metabolite of MPTP, is actively taken up into dopaminergic neurones via the catecholamine transporter (Javitch *et al.*, 1985). The long-term storage of MPP^+ after MPTP exposure would distinguish MPTP-sensitive from MPTP-refractory species, and could be required to express MPTP toxicity (Johannessen *et al.*, 1985). MPP^+ is actively accumulated by mitochondria (Ramsay & Singer, 1986) where it blocks NADH dehydrogenase of complex I, thus resulting in a reduction of ATP synthesis, which may ultimately kill the neurones (Nicklas *et al.*, 1985; Ramsay & Singer, 1986). Whereas the uptake of MPP^+ into dopaminergic neurones appears to be a necessary step to select neurotoxicity, the site for long-term MPP^+ storage in the brain of sensitive species is unknown. We recently demonstrated a vesicular location of high affinity [^{3}H]-MPP^+ binding sites in dopaminergic nigrostriatal terminals of the mouse, which is a MPTP-sensitive species (Del Zompo *et al.*, 1992). This site may represent a specific marker of striatal dopamine storage vesicles. Moreover, we showed a functional interaction of MPP^+ with the tyramine-labelled, putative vesicular transporter of dopamine in rat striatal membranes (Vaccari *et al.*, 1991). Similarly, it had been previously shown that MPP^+ is a substrate for the monoamine transporter in adrenal chromaffin granules (Scherman *et al.*, 1988).

This study was designed to characterize MPP^+ uptake into purified striatal vesicles, and to ascertain whether this mechanism may be involved in the neurotoxicity of MPTP.

[1] Author for correspondence.

Methods

Male, Swiss-Webster mice (22–25 g) were killed by cervical dislocation and the brains quickly removed and placed on a cold plate.

Preparation of synaptic vesicles

The striatum, cerebellum, pons-medulla and hypothalamus were dissected according to Glowinski & Iversen (1966). The frontal cortex was taken at the level of the olfactory tubercle anterior pole (Heffner *et al.*, 1980). Purified synaptic vesicles from brain regions were obtained according to Erickson *et al.* (1990). Briefly, freshly-dissected tissues were homogenized in 0.32 M sucrose with 10 up and down strokes with a Teflon pestle (clearance approx 0.009 inches) at 800 r.p.m. The homogenate was centrifuged at 2,000 *g* for 10 min and the resulting supernatant removed and centrifuged at 10,000 *g* for 30 min to obtain a crude synaptosomal fraction. The synaptosome-containing pellet was resuspended by gentle swirling in 2 ml of 0.32 M sucrose, then was subjected to an osmotic shock by addition of distilled water and homogenized with 5 up and down strokes. Osmolarity was restored by addition of 0.25 M HEPES and neutral potassium tartrate buffer (pH 6.5). The suspension was centrifuged at 20,000 *g* for 20 min. The resulting supernatant was centrifuged at 55,000 *g* for 60 min, the pellet discarded, and the supernatant treated with 1 mM $MgSO_4$ was centrifuged at 100,000 *g* for 45 min. The final pellet (synaptic vesicles) was gently resuspended in the assay buffer immediately before use.

Vesicular uptake of [^{3}H]-MPP^+ and [^{3}H]-dopamine

The standard uptake medium (pH 7.4) contained 25 mM HEPES, 100 mM potassium tartrate, 50 μM EGTA, 100 μM EDTA and 2 mM ATP-Mg^{2+}. Duplicate aliquots (8–12 μg protein) of the synaptic vesicle fractions were incubated in 100 μl of medium for an appropriate period (usually 5 min) at 37°C with 0.05–4 μM [^{3}H]-MPP^+ or [^{3}H]-dopamine. The reaction was stopped by filtering the samples through Whatman GF/F filters pre-soaked for 1 h in a 0.5% polyethylenimine solution to prevent binding of [^{3}H]-MPP^+ to the filters.

The filters were then washed with 3 × 4 ml aliquots of ice-cold buffer containing 2 mM $MgSO_4$ and counted.

The values of [^{3}H]-MPP^+ or [^{3}H]-dopamine uptake obtained from vesicles incubated at 4°C were subtracted from corresponding samples at 37°C and all measurements of transport are given as temperature-sensitive uptake.

Electron microscopy

Synaptic vesicle pellets from mouse striatum were processed for electron microscopy. The pellet was fixed with 6% glutaraldehyde in 0.1 M phosphate buffer (PB), pH 7.3, for 2 h. After a brief rinse in PB, the pellet was postfixed in 1% osmium tetroxide in PB buffer for 2 h, and then stained *en bloc* overnight in an aqueous solution of 0.2% uranyl-acetate. The pellet was then dehydrated in graded acetone, and embedded in Epon (glycine-ether 100; Merck, Darmstadt, Germany). Ultrathin sections were collected on copper grids and stained with uranyl acetate and bismuth subnitrate (Riva, 1974). The grids were finally viewed in a Jeol 100S electron microscope.

Materials

The labelled ligands [^{3}H]-MPP^+ (82.8 Ci $mmol^{-1}$), and [^{3}H]-dopamine (35.1 Ci $mmol^{-1}$) were from Dupont-NEN, Boston, U.S.A.

Results

Vesicular uptake of [^{3}H]-MPP^+

The optimal conditions for the standard assay of [^{3}H]-MPP^+ were determined by using a virtually homogeneous preparation of synaptic vesicles from the mouse striatum. Electron microscopic examination of this preparation revealed synaptic vesicle profiles of approx 50 nm in diameter as the predominant membrane structures (Figure 1).

The vesicular uptake was temperature-dependent, as it was four fold higher at 37°C than at 0°C. Furthermore, it was time-related ($t_{1/2}$ approx 36 s), reaching the peak after 90 s and remaining stable up to 10 min of incubation (data not shown). When the vesicular fraction was diluted and washed with water instead of the standard buffer (osmotic shock), uptake was reduced by 72%.

[^{3}H]-MPP^+ uptake was highly dependent on the presence of ATP/Mg^{2+} in the incubation medium. In the absence of ATP, [^{3}H]-MPP^+ uptake was reduced by 98%, indicating the involvement of a Mg^{2+}-ATPase. Ouabain (250 μM) had no effect on MPP^+ uptake, thus excluding the presence of any plasma membrane contamination in our samples (data not shown).

Chloride-ions increased [^{3}H]-MPP^+-uptake in a concentration-related manner. The half-maximal stimulation was observed with approx 5 mM Cl^- and a plateau was reached at 10 mM Cl^- (data not shown).

The uptake of [^{3}H]-MPP^+ (0.05–4 μM) under optimum assay conditions in striatal vesicles is shown in Figure 2. Kinetic analysis of Lineweaver-Burk plots revealed a single uptake component, with a K_m value of 0.58 μM with a corresponding V_{max} of 14.7 pmol min^{-1} mg^{-1} protein (Table 1). Thus, the Mg^{2+}/ATP-dependent vesicular uptake system for MPP^+ operates with a higher affinity mechanism.

Brain regional distribution of [^{3}H]-MPP^+ vesicular uptake

The uptake of [^{3}H]-MPP^+ into synaptic vesicles isolated from different brain regions showed the highest concentration of uptake sites in the striatum, the olfactory tubercles and the hypothalamus. The V_{max} values in the hypothalamus and olfactory tubercles were respectivly 3 and 7 fold lower than in the striatum. No uptake could be detected in the cerebellum and pons-medulla, with [^{3}H]-MPP^+ concentrations between 0.05 and 4 μM (Table 2).

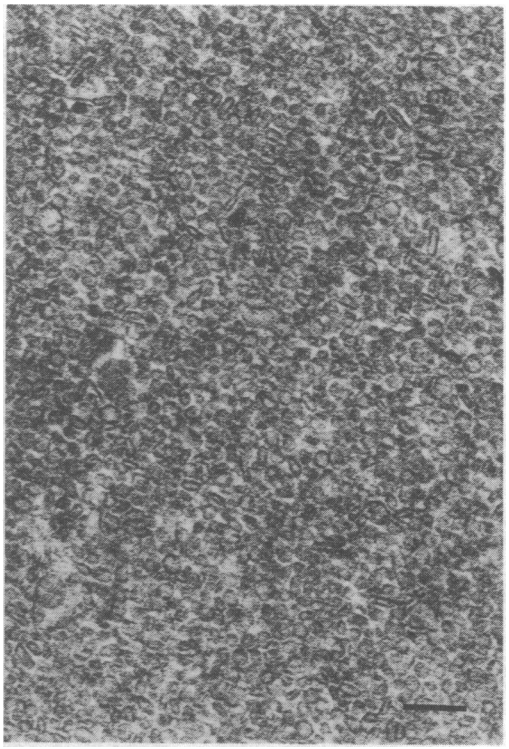

Figure 1 Electron micrograph of purified striatal synaptic vesicles. Scale bar = 200 nm.

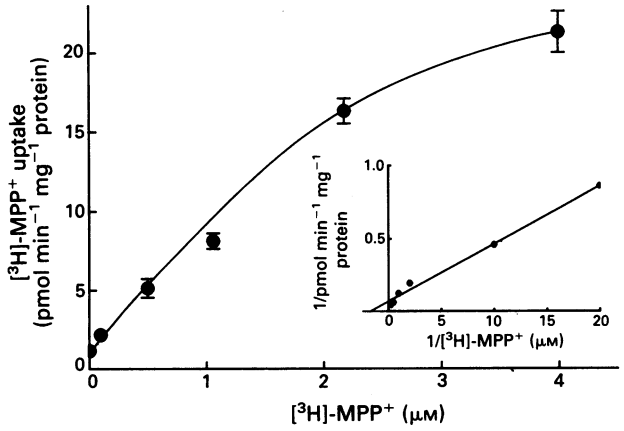

Figure 2 Rate of ATP/Mg^{2+}-dependent vesicular uptake of 1-methyl-4-phenylpyridinium ion (MPP^+) as a function of MPP^+ concentration. Duplicate aliquots of striatal synaptic vesicles were incubated at 37°C for 5 min with increasing concentrations (0.05–4 μM) of [^{3}H]-MPP^+. The inset shows a Lineweaver-Burk plot of the kinetic data.

[^{3}H]-dopamine vesicular uptake

The vesicular uptake of [^{3}H]-dopamine showed similar K_m values in the striatum and in the cerebellum. The V_{max} was approximately 30 fold higher in the striatum (Table 1).

Table 1 Comparison between [^{3}H]-1-methyl-4-phenylpyridinium ion ([^{3}H]-MPP$^+$) and [^{3}H]-dopamine uptake in striatal and cerebellar purified synaptic vesicles

Regions	*MPP+* K_m(μM)	*Dopamine* K_m(μM)	*MPP+* V_{max} (pmol min^{-1} mg^{-1} protein)	*Dopamine* V_{max} (pmol min^{-1} mg^{-1} protein)
Striatum	0.58 ± 0.22	0.40 ± 0.15	14.7 ± 2	83.0 ± 11
Cerebellum	ND	0.40 ± 0.26	ND	2.85 ± 0.2

ND = not detectable.
The uptake process into synaptic vesicles was measured at 37°C for 5 min in the presence of increasing concentrations (0.05–4 μM) of [^{3}H]-MPP$^+$ or [^{3}H]-dopamine. Data were analysed as Lineweaver-Burk plots. Values are means ± s.e. mean of three different experiments performed in duplicate.

Table 2 Uptake of [^{3}H]-1-methyl-4-phenylpyridinium ion ([^{3}H]-MPP$^+$) into synaptic vesicles isolated from different mouse brain regions

Regions	K_m (μM)	V_{max} (pmol min^{-1} mg^{-1} protein)
Striatum	0.58 ± 0.22	14.7 ± 2
Hypothalamus	0.68 ± 0.19	5.05 ± 1.7
Olfactory tubercles	0.60 ± 0.31	2.12 ± 0.6
Frontal cortex	ND	ND
Cerebellum	ND	ND
Pons-Medulla	ND	ND

ND = not detectable.
Aliquots of synpatic vesicle fractions were incubated at 37°C for 5 min in 100 μl of medium with increasing concentrations of [^{3}H]-MPP$^+$ (0.05–4 μM). Values are means ± s.e. mean from three different experiments performed in duplicate. Data were analysed as Lineweaver-Burk plots.

Drug specificity of [^{3}H]-MPP$^+$ uptake

The pharmacological characterization of [^{3}H]-MPP$^+$ uptake into striatal vesicles is shown in Table 3. Both dopamine and amphetamine were fairly potent inhibitors, with IC_{50} values in the low μM range; tetrabenazine was the most potent antagonist, with an IC_{50} approx 100 fold lower than that observed with dopamine and amphetamine. Mazindol and cocaine were poor inhibitors of [^{3}H]-MPP$^+$ uptake, while MPTP showed no affinity for the carrier of MPP$^+$ into striatal vesicles.

Table 3 Pharmacological inhibition of [^{3}H]-1-methyl-4-phenylpyridinium ion ([^{3}H]-MPP$^+$) uptake into mouse striatal synaptic vesicles

Drug	*IC_{50} (μM)*	n
Tetrabenazine	0.022 ± 0.001	4
Dopamine	2.0 ± 0.3	3
Amphetamine	2.7 ± 0.5	5
Mazindol	15 ± 2	2
Cocaine	28 ± 5	4
MPTP	> 1000	3

Synaptic vesicles, prepared from freshly-obtained mouse striatum, were incubated at 37°C for 5 min with [^{3}H]-MPP$^+$ (1 μM), in the absence or presence of at least 6 concentrations of competing drugs (10^{-9}–10^{-4} M) in duplicate. Values are means ± s.e.mean from *n* different experiments. MPTP = 1-methyl-4-phenyl-1,2,3,6-tetrahydropyridine.

Discussion

The present study provides evidence for a saturable, temperature-, Mg^{2+}/ATP-, and Cl^--dependent uptake system for MPP$^+$ into purified synaptic vesicles isolated from the mouse striatum. The decrease of MPP$^+$ uptake caused by osmotic shock confirms that we are dealing with an uptake process into osmotically-sensitive particles, rather than with membrane binding. Moreover, the plasma membrane Na^+/K^+-ATPase is not involved in MPP$^+$ uptake, since its inhibitor, ouabain, is inactive. This uptake is potently inhibited by the vesicular marker, tetrabenazine and to a lesser extent, by dopamine and amphetamine. The vesicular uptake of MPP$^+$ is localized in dopamine-innervated regions such as the striatum, the hypothalamus and the olfactory tubercles, the same areas where binding sites for [^{3}H]-MPP$^+$ are distributed (Del Zompo *et al.*, 1992), and is absent in regions with poor dopaminergic innervation, such as the cerebellum and the pons-medulla. Finally, similarities in kinetic characteristics (K_m), sensitivity to competing drugs, and dependency on Cl^- ions, of striatal vesicular uptake of MPP$^+$ and dopamine, (Philippu & Beyer, 1973; Erickson *et al.*, 1990), all suggest that in this area MPP$^+$ and dopamine use the same vesicular carrier.

The regional differences in the capability of vesicles to take up MPP$^+$ with high affinity are of interest. Contrasting evidence suggests that the cerebellum contains very few dopaminergic terminals (Panagopoulos *et al.*, 1991), and is consistently innervated by noradrenergic fibres coming from the locus coeruleus (Westerink & De Vries, 1985). Thus, the absence of MPP$^+$ uptake in the cerebellum suggests that MPP$^+$ can be recognized only by the vesicular carrier which is specific for dopaminergic neurones. Dopamine itself is less specific, since it can be taken up even by vesicular carriers located in non-dopaminergic regions. Our finding that the striatum is the area with the highest vesicular uptake of MPP$^+$ fits with the hypothesis that the vesicular depot of MPP$^+$ in dopaminergic neurones, may represent a source of toxin towards neuronal targets (Johannessen, 1991). Thus, when the vesicular storage capacity is exceeded, the release of MPP$^+$ might determine a rise in cytoplasmic levels, which would result in toxin accumulation within the mitochondria and subsequent inhibition of mitochondrial respiration (Ramsay & Singer, 1986). This study also indicates that brain region specificity of MPP$^+$ uptake might be involved in the mechanism of brain regional sensitivity to MPP$^+$ neurotoxic effects.

References

BARBEAU, A., ROY, M., BERNIER, G., CAMPANELLA, G. & PARISI, S. (1987). Ecogenetics of Parkinson's disease: prevalence and environmental aspects in rural areas. *Can. J. Neurol. Sci.*, **14**, 36–41.

BURNS, R.S., CHIUEH, C.C., MARKEY, S.P., EBERT, M.H., JACOBOWITZ, D.M. & KOPIN, I.J. (1983). A primate model of Parkinsonism: selective destruction of dopaminergic neurons in the pars compacta of the substantia nigra by N-methyl-4-phenyl-1,2,3,6 tetrahydropyridine. *Proc. Natl. Acad. Sci. U.S.A.*, **80**, 4546–4550.

CALNE, P.B. & LANGSTON, J.W. (1983). Aetiology of Parkinson's disease. *Lancet*, **i**, 1457–1459.

DAVIS, G.C., WILLIAMS, A.C., MARKEY, S.P., EBERT, M.H., CAINE, E.D., REICHERT, C.M. & KOPIN, I.J. (1979). Chronic Parkisonism secondary to intravenous injection of meperidine analogues. *Psychiatry Res.*, **1**, 249–254.

DEL ZOMPO, M., PICCARDI M.P., RUIU, S., CORSINI, G.U. & VACCARI, A. (1992). Characterization of a putatively vesicular binding site for ^{3}H-MPP$^+$ in mouse striatal membranes. *Brain Res.*, **571**, 354–357.

ERICKSON, J.D., MASSERANO, J.M., BARNES, E.M., RUTH, J.A. & WEINER, N. (1990). Chloride ion increases [^{3}H]-dopamine accumulation by synaptic vesicles purified from rat striatum: thiocyanate ion. *Brain Res.*, **516**, 155–160.

GLOWINSKI, J. & IVERSEN, L.L. (1966). Regional studies of catecholamines in the rat brain. *J. Neurochem.*, **13**, 655–669.

HEFFNER, T.G., HARTMAN, J.A. & SEIDEN, L.S. (1980). A rapid method for the regional dissection of the rat brain. *Pharmacol. Biochem. Behav.*, **13**, 453–456.

HEIKKILA, R.E., HESS, A. & DUVOISIN, R.C. (1984). Dopaminergic neurotoxicity of 1-methyl-4-phenyl 1,2,3,6-tetrahydropyridine in mice. *Science*, **224**, 1451–1453.

JAVITCH, J.A., D'AMATO, R.J., STRITMATTER, S.M. & SNYDER, S.H. (1985). Parkinsonism-inducing neurotoxin, N-methyl-4-phenyl-1,2,3,6-tetrahydropyridine: uptake of the metabolite N-methyl-4-phenylpyridine by dopamine neurons explains selective toxicity. *Proc. Natl. Acad. Sci. U.S.A.*, **82**, 2173–2177.

JOHANNESSEN, J.N. (1991). A model of chronic neurotoxicity: long-term retention of the neurotoxin 1-methyl-4-phenylpyridinium (MPP^+) within catecholaminergic neurons. *Neurotoxicology*, **12**, 285–302.

JOHANNESSEN, J.N., CHIUEH, C.C., BURNS, R.S. & MARKEY, S.P. (1985). Differences in metabolism of MPTP in the rodent and primate parallel differences in sensitivity to its neurotoxic effects. *Life Sci.*, **36**, 219–224.

NICKLAS, W.J., VYAS, I. & HEIKKILA, R.E. (1985). Inhibition of NADH-linked oxidation in brain mitochondria by 1-methyl-4-phenylpyridine, a metabolite of the neurotoxin 1-methyl-4-phenyl-1,2,3,6-tetrahydropyridine. *Life Sci.*, **36**, 2503–2508.

PANAGOPOULOS, N.T., PAPADOPOULOS, G.C. & MATSOKIS, N.A. (1991). Dopaminergic innervation and binding in the rat cerebellum. *Neurosci. Lett.*, **130**, 208–212.

PHILIPPU, A. & BEYER, J. (1973). Dopamine and noradrenaline transport into subcellular vesicles of the striatum. *Naunyn Schmied. Arch. Pharmacol.*, **278**, 387–402.

RAMSAY, R.R. & SINGER, T.P. (1986). Energy-dependent uptake of N-methyl-4-phenylpyridinium, the neurotoxic metabolite of 1-methyl-4-phenyl-1,2,3,6-tetrahydropyridine, by mitochondria. *J. Biol. Chem.*, **261**, 7585–7587.

RIVA, A. (1974). A simple and rapid staining method for enhancing the contrast of tissue previously treated with uranyl acetate. *J. Microscopie, (Paris)*, **19**, 105–108.

SCHERMAN, D., DARCHEN, F., DESNOS, C. & HENRY, J.P. (1988). 1-Methyl-4-phenylpyridinium is a substrate of the vesicular monoamine uptake system of chromaffin granules. *Eur. J. Pharmacol.*, **146**, 359–360.

VACCARI, A., DEL ZOMPO, M., MELIS, F., GESSA, G.L. & ROSSETTI, Z.L. (1991). Interaction of 1-methyl-4-phenyl-pyridinium ion and tyramine with a site putatively involved in the striatal vesicular release of dopamine. *Br. J. Pharmacol.*, **104**, 573–574.

WESTERINK, B.H.C. & DE VRIES, J.B. (1985). On the origin of dopamine and its metabolite in predominantly noradrenergic innervated brain areas. *Brain Res.*, **330**, 164–166.

(Received September 16, 1992
Revised January 20, 1993
Accepted January 29, 1993)

Br. J. Pharmacol. (1993), **109**, 415–423 © Macmillan Press Ltd, 1993

S-nitrosocysteine, but not sodium nitroprusside, produces apamin-sensitive hyperpolarization in rat gastric fundus

[1]Kenji Kitamura, [2]Qishen Lian, [3]Andreas Carl & Hirosi Kuriyama

Department of Pharmacology, Faculty of Medicine, Kyushu University, Fukuoka 812, Japan.

1 To investigate the pharmacological properties of the membrane hyperpolarization induced by electrical field stimulation (EFS), sodium nitroprusside (SNP) and S-nitrosocysteine (NO-Cys) in circular smooth muscle cells of the rat gastric fundus (forestomach), the effects of various potassium channel blockers on these hyperpolarizations were investigated.

2 EFS (50 μs, 20 Hz, 3 pulses, 10–50 V) produced inhibitory junction potentials (i.j.ps), in the presence of atropine (1 μM) and guanethidine (1 μM). NO-Cys and SNP produced hyperpolarization of the membrane in the rat gastric fundus. L-N^G-nitroarginine (L-NNA) inhibited the i.j.ps, but not the hyperpolarization induced by NO-Cys and SNP. This inhibitory action of L-NNA on the i.j.ps was partly reversed by subsequent application of L-arginine (1 mM) but not by D-arginine.

3 Oxyhaemoglobin (Oxy-Hb; 5 μM) inhibited these hyperpolarizations, although a higher concentration of Oxy-Hb was required to inhibit the SNP-induced hyperpolarization. Hydroquinone (50 μM) inhibited only the hyperpolarization induced by NO-Cys.

4 Apamin (1 μM) partly inhibited i.j.ps and NO-Cys-induced hyperpolarization, but not the SNP-induced hyperpolarization. Tetraethylammonium (TEA; 1 mM), 4-aminopyridine (4-AP; 1 mM) or glibenclamide (1 μM) did not affect hyperpolarization induced by NO-Cys and SNP.

5 8-Bromo cyclic guanosine 3′:5′-monophosphate (1 mM) also produced hyperpolarization. Apamin (1 μM), TEA (1 mM) and glibenclamide (5 μM) all failed to inhibit this hyperpolarization.

6 These results indicate that NO-Cys and EFS hyperpolarize the membrane by activating apamin-sensitive and TEA-resistant K^+ channels and favour the hypothesis that a NO-liberating substance may act as a neurotransmitter in non-adrenergic, non-cholinergic (NANC) neurones in the rat forestomach. Our results also suggest that increase in cyclic GMP may cause apamin-resistant hyperpolarization but the apamin-sensitive hyperpolarization is mediated by another mechanism.

Keywords: S-nitrosocysteine; sodium nitroprusside; apamin; Ca^{2+}-dependent K^+ channel; nitric oxide; cyclic GMP; inhibitory junction potential

Introduction

It has been proposed that nitric oxide (NO) and NO-liberating substances are likely candidates for the endothelium-dependnet relaxing factor and neurotransmitter of non-adrenergic, non-cholinergic (NANC) neurones (Ignarro *et al.*, 1987; Li & Rand, 1989; Bult *et al.*, 1990; Moncada *et al.*, 1991). In dog ileocolonic sphincter, inhibitory junction potentials (i.j.ps) were inhibited by L-N^G-nitroarginine methylester and N^G-monomethyl L-arginine (Ward *et al.*, 1992b) and exogenous application of NO and S-nitrocysteine (NO-Cys), a NO-liberating compound, mimicked the i.j.ps in the dog colon and small intestine (Thornbury *et al.*, 1991; Stark *et al.*, 1991; Ward *et al.*, 1992a). Ward *et al.* (1992a) also demonstrated that NO enhanced synthesis of guanosine 3′:5′-cyclic monophosphate (cyclic GMP) and 8-bromo cyclic GMP mimicked the membrane hyperpolarization in the dog colon. Although actions of 8-bromo cyclic GMP in the rat tail artery were not related to membrane hyperpolarization or inhibition of membrane excitability (Cheung & MacKay, 1985), cyclic GMP seemed a key substance for generation of i.j.ps in dog visceral tissues.

Fujino *et al.* (1991) and Thornbury *et al.* (1991) showed that nitroglycerin and NO augmented the open probability of the maxi-K^+ channel in porcine coronary artery and canine colon, respectively. On the other hand, Garland & McPherson (1992) found that NO-induced hyperpolarization was blocked by glibenclamide, a blocker of the adenosine 5′-triphosphate (ATP)-sensitive K^+ channel, in the rat mesenteric artery. The maxi-K^+ channel is known to be insensitive to apamin, a selective blocker of small-conductance Ca^{2+}-dependent K^+ channels (Romy & Lazdunski, 1984; Blatz & Magleby, 1986). Furthermore, apamin did not block the nicorandil (an activator of the ATP-sensitive K^+ channel)-induced hyperpolarization in smooth muscle cells of the guinea-pig small intestine (Yamanaka *et al.*, 1985; Kajioka *et al.*, 1990). On the other hand i.j.ps are blocked by apamin in many preparations (Banks *et al.*, 1979; Bauer & Kuriyama, 1982; Yamanaka *et al.*, 1985; Nakao *et al.*, 1986; Komori & Suzuki, 1986). Therefore, it is important to determine the properties of the hyperpolarization induced by NO-liberating substances for elucidation of a putative neurotransmitter in NANC neurones. We chose the rat gastric fundus (forestomach) to study effects of NO-Cys and sodium nitroprusside (SNP), a spontaneous releaser of NO, because the membrane potential of the rat gastric fundus is more stable than that of the small intestine. Furthermore the presence of NANC neurones with similar properties to those in dog colon and small intestine has been reported in rat gastric fundus (Boeckxstaens *et al.*, 1991).

Methods

Male rats (Wister King A, 250–300 g) were anaesthetized with diethyl ether and exsanguinated from the carotid artery. The fundus region of the rat stomach was excised and the mucosa layer was removed in Krebs solution at room temperature (27°C). The strips of circular muscle layer (3 mm in width and 2 cm in length) attached to the longitudinal

[1] Author for correspondence.
Present address: [2]Department of Pharmacology, Gannan Medical College, Ganzhou 341000, Jiangxi, China; [3]Department of Physiology, University of Nevada, School of Medicine, Reno, NV 89557, U.S.A.

muscle layer were mounted on a rubber plate with insect pins in the experimental chamber (2 ml in volume). The tissue was superfused with warmed Krebs solution (35°C) at a flow rate of 2–3 ml min^{-1} and were equilibrated for more than 90 min before the experiments were started.

For recording of the membrane potential, a conventional microelectrode method was used. The glass capillary microelectrode was filled with 3 M KCl (electrode resistance was 40–60 MΩ) and inserted into the cell from the mucosa side. The electrical responses were monitored by an oscilloscope (VC-10; Nihon Kohden, Tokyo, Japan) and displayed on a thermo-writing pen recorder (RJG-4102; Nihon Kohden). Electrical field stimulation (EFS) was applied through a chloride-coated silver wire (0.5 mm in diameter) placed on the tissue close to the microelectrode (≤ 0.1 mm). Electrical stimulation (50 μs, 20 Hz, 3 pulses) of 10–50 V in intensity was supplied from an electric stimulator (SEN-7102; Nihon Kohden).

The ionic composition of the Krebs solution was as follows (mM): Na^+ 137.4, K^+ 5.9, Mg^{2+} 1.2, Ca^{2+} 2.5, HCO_3^- 15.5, $H_2PO_4^-$ 1.2, Cl^- 134 and glucose 11.5. The pH of the solution was adjusted to 7.4 with 97% O_2:3% CO_2.

Drugs used were S-nitrosocysteine (NO-Cys), sodium nitroprusside (SNP), atropine (Nakarai Chem., Kyoto, Japan), dibutyryl guanosine 3′:5′-cyclic monophosphate (dibutyryl cyclic GMP; Sigma Chem., St. Louis, MO, U.S.A.), 8-bromo cyclic GMP (Sigma Chem.), oxyhaemoglobin (Oxy-Hb; made from haemoglobin, Sigma Chem.), L-N^G-nitroarginine (L-NNA; gift from Dr T.X. Watanabe, Peptide Inst., Osaka, Japan), L-arginine (Ishizu Seiyaku, Osaka, Japan), D-arginine, methylene blue, guanethidine (Tokyo Kasei, Tokyo, Japan), apamin (Serva, Heidelberg, Germany), glibenclamide (Sigma Chem.), hydroquinone (Hayashi Pure Chem., Osaka, Japan) and tetrodotoxin (Sankyo, Tokyo, Japan). NO-Cys was prepared from L-cysteine (Sigma Chem.) and sodium nitrite (Ishizu Seiyaku) as described by Field *et al.* (1978). A small amount of NO-Cys stock solution (1 ml; concentration approximately 100 mM) was equilibrated with N_2 gas, stored in a tightly-sealed test tube at − 20°C and used within 6 h. NO-Cys solution was diluted with the Krebs solution to an appropriate concentration just before application to the tissue. The reactant solution of NO-Cys containing 1 N HCl, methanol and concentrated sulphuric acid, was tested in experiments. No effect of the reactant solution was detected on membrane potential of the same cell used for NO-Cys. L-NNA, L-arginine and D-arginine were dissolved in 0.1 N HCl solution or in deionized water. No difference in the pH of the Krebs solution in the presence of these drugs from the normal Krebs solution was found before superfusion of the solution. Other drugs were dissolved in the deionized water. All drugs except NO-Cys were diluted with Krebs solution to the desired concentration and superfused in the bath. The final concentrations of these drugs are stated in the text and figures. Since NO-Cys rapidly breaks down at high temperature (36°C), small amounts of NO-Cys solution (200 μl; diluted with the Krebs solution) was applied from a fine tube located at the upper reaches of the chamber. Dibutyryl cyclic GMP and 8-bromo cyclic GMP were also applied in the same way as NO-Cys. Therefore, the stated concentrations of NO-Cys, dibutyryl cyclic GMP and 8-bromo cyclic GMP do not indicate the final concentrations of these drugs applied to the tissue.

Statistical significance was estimated by the Student's *t* test for paired data and *P* less than 0.05 was considered to be significant.

Results

The resting membrane potential of the circular smooth muscle cells of the rat gastric fundus was − 46.2 ± 1.6 mV ($n = 40$) and most of cells were electrically quiescent. Electrical field stimulation (EFS; 50 ms, 3 pulses; 20 Hz, 50V) produced a cholinergic-excitatory junction potential (e.j.p) which was followed by an i.j.p. In these experiments, to avoid the influence of the adrenergic and cholinergic nerve activation in excitation the NANC neurones, 1 μM atropine and 1 μM guanethidine were added in the superfusate throughout the experiments. The resting membrane potential was not influenced by application of 1 μM atropine and 1 μM

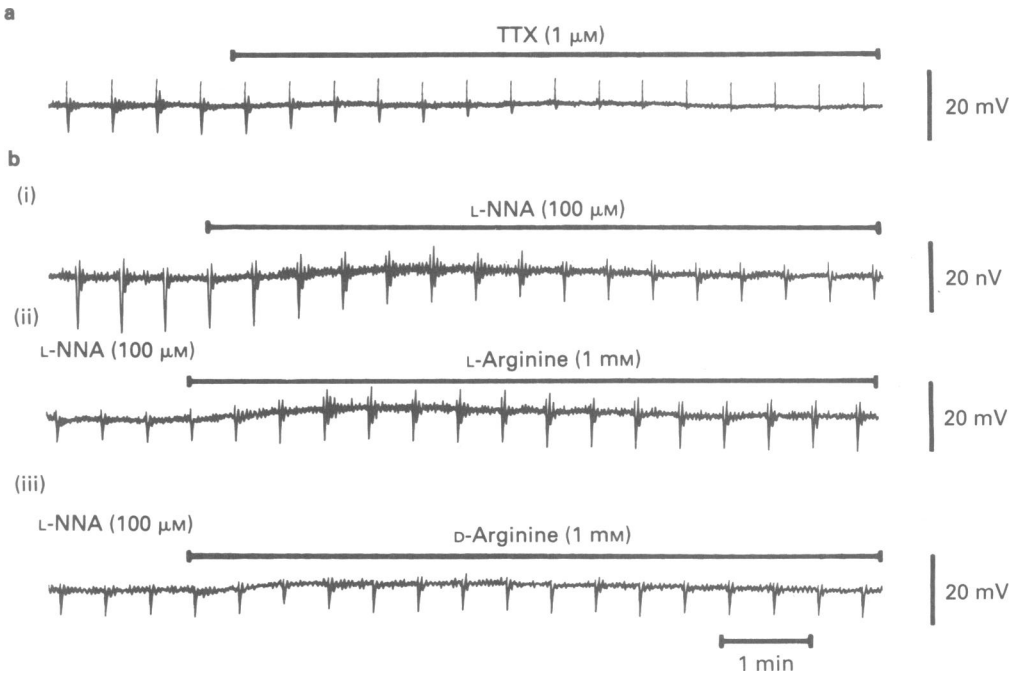

Figure 1 Effects of tetrodotoxin (TTX), L-N^G-nitroarginine (L-NNA), L-arginine and D-arginine on i.j.ps evoked by a constant intensity electrical field stimulation with an interval of 30 s (see Methods). (a) TTX (1 μM) was applied at the time indicated by bar (b) (i) L-NNA (100 μM) was applied at the time indicated by bar. (ii) L-Arginine (1 mM) was applied in the presence of L-NNA (3 min after the end of trace (i)). (iii) Effects of D-arginine (1 mM) on i.j.ps in the presence of L-NNA (100 μM). D-Arginine was applied at the time indicated by bar and L-NNA was applied 10 min before application of D-arginine. Traces (i) and (ii) but not (iii) were obtained from the same cell.

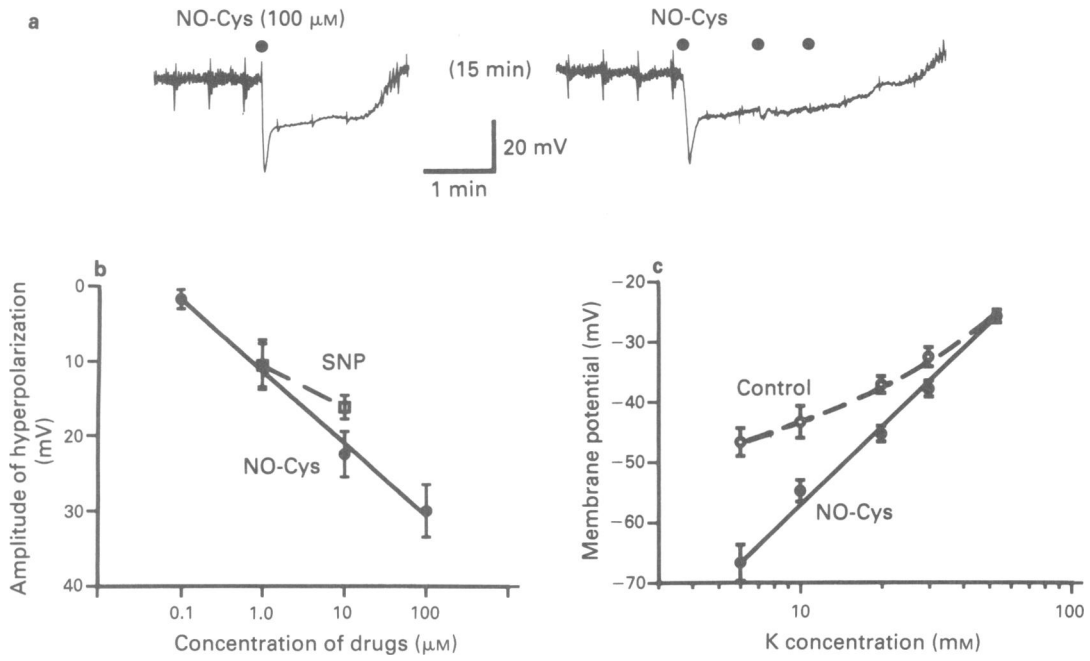

Figure 2 Effects of S-nitrosocysteine (NO-Cys) on membrane potential of the rat gastric fundus. (a) Comparison of the hyperpolarizations induced by single (left trace) and repetitive (right trace) application of 100 μM NO-Cys. Time of the NO-Cys application is indicated by (●). Two traces were recorded from the same cell with intervals of 15 min. I.j.ps were recorded by constant intensity electrical field stimulation with an interval of 30 s (see Methods). (b) Relationships between amplitude of the hyperpolarization and concentrations of NO-Cys and SNP. Lines are drawn by eye. Each symbol indicates mean value of 4–7 observations with s.d. (c) Relationship between the concentration of extracellular potassium and the membrane potential in the presence (●) and absence (○) of 10 μM NO-Cys. Each symbol indicates mean value of 5–11 observations with s.d.

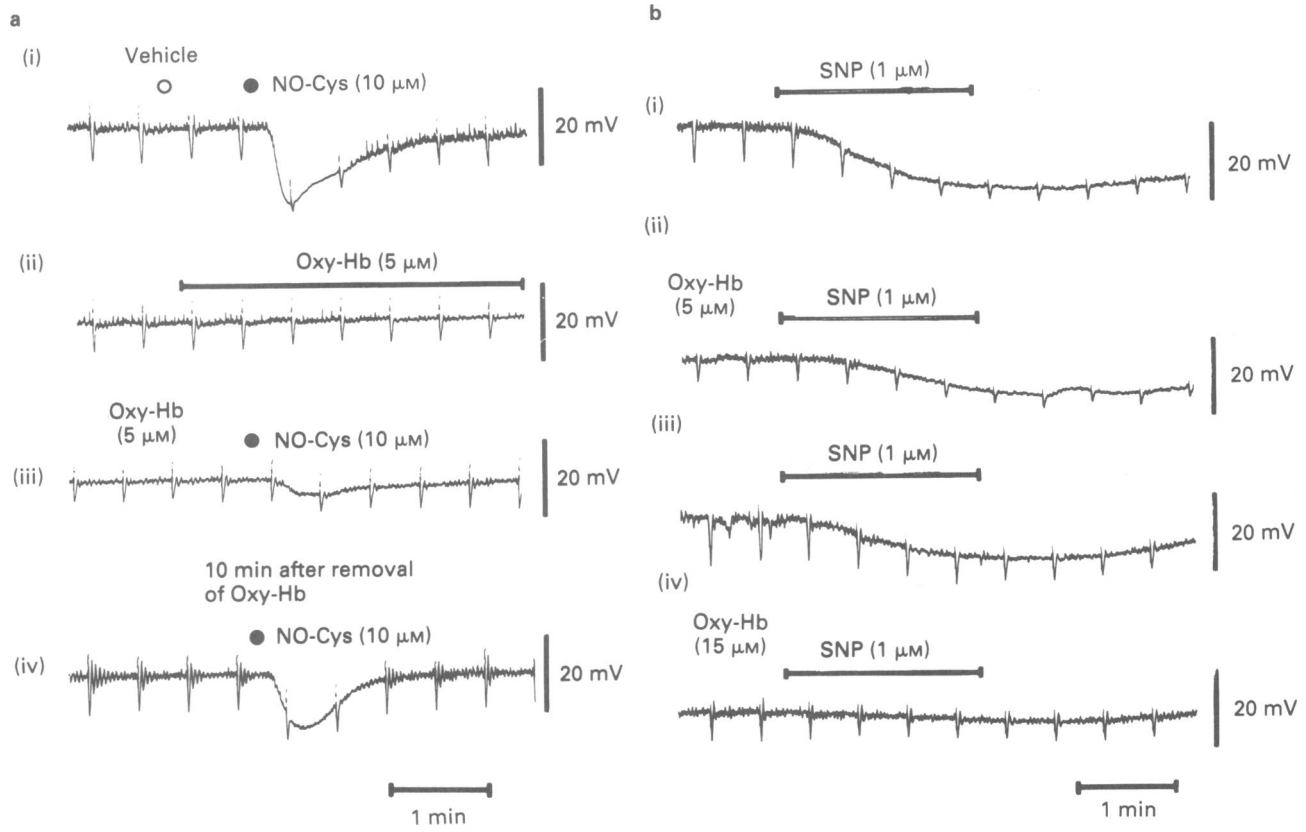

Figure 3 Effects of oxy-haemoglobin (Oxy-Hb) on the i.j.p. and hyperpolarization induced by S-nitrosocysteine (NO-Cys) (a) or sodium nitroprusside (SNP) (b). I.j.ps were recorded by constant intensity electrical field stimulation with an interval of 30 s. (a) As a control, the same amount and concentration of vehicle (methanol + acids) as those of NO-Cys was applied, and the vehicle had no action on the membrane potential (trace (i) (○)). NO-Cys (10 μM) was applied at the time indicated by (●). Oxy-Hb (5 μM) was applied at the time indicated by bar in trace (ii). In traces (iii) and (iv), NO-Cys (10 μM) was applied in the presence of Oxy-Hb (10 min after the end of trace (ii)) and at 10 min after removal of Oxy-Hb, respectively. All traces were recorded from the same cell. (b) SNP (1 μM) was applied at the time indicated by the bar in each trace; (i) Control. (ii) In the presence of 5 μM Oxy-Hb. Oxy-Hb superfusion was started 10 min before recording of trace (ii). Traces (i) and (ii) were obtained from the same cell. (iii) and (iv) Before and after application of 15 μM Oxy-Hb, respectively. Other conditions were the same as those of traces (i) and (ii).

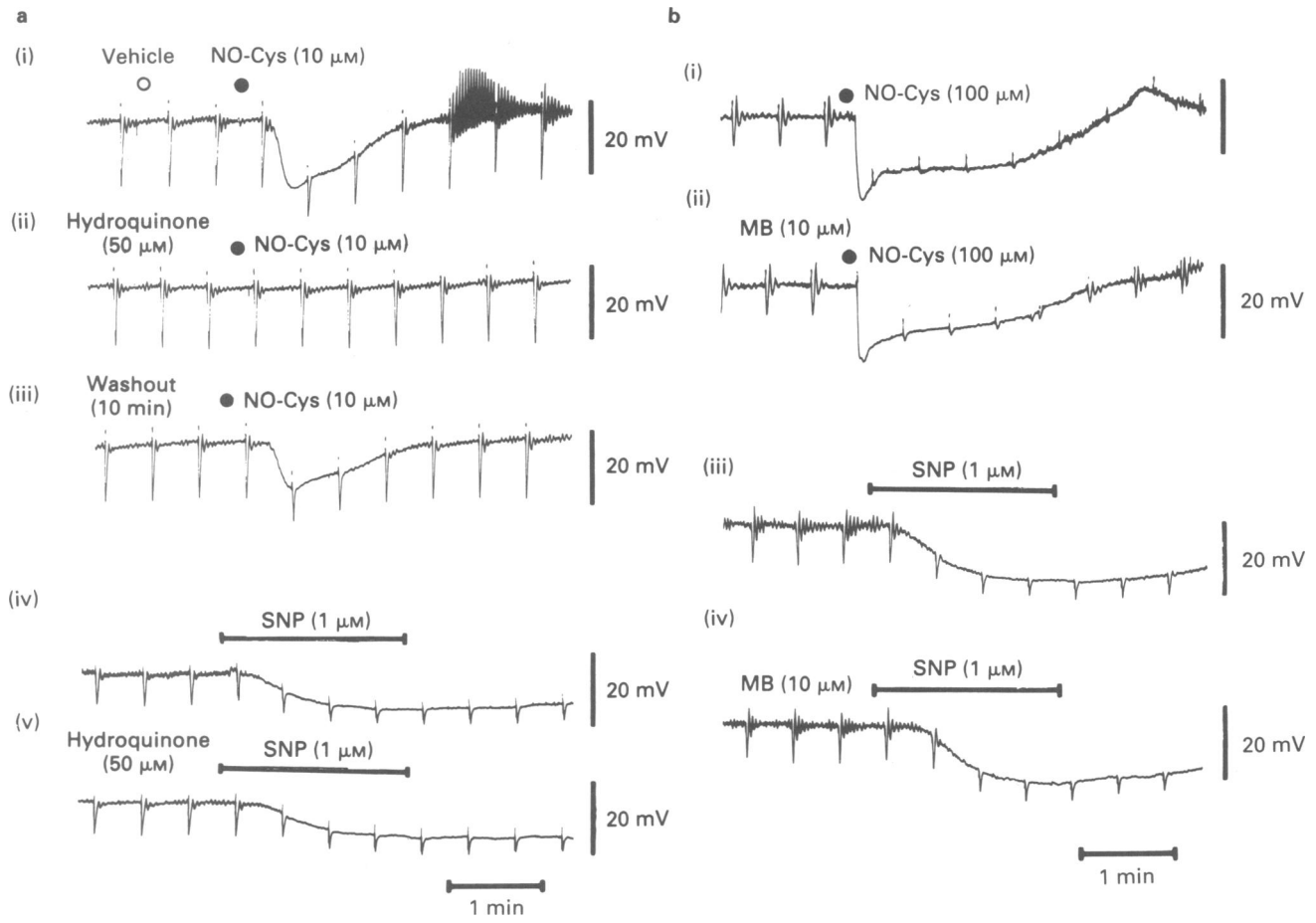

Figure 4 Effects of hydroquinone (50 μM) and methylene blue (MB; 10 μM) on i.j.ps and hyperpolarization induced by S-nitrosocysteine (NO-Cys) or sodium nitroprusside (SNP). I.j.ps were recorded by constant intensity electrical field stimulation with interval of 30 s. (a) Effects of hydroquinone: (i) Vehicle (○) and NO-Cys (10 μM; ●) were successively applied. (ii) Hydroquinone (50 μM) was applied 10 min before recording trace (ii). (iii) Trace was obtained 10 min after removal of hydroquinone. Traces (i)–(iii) were obtained from the same cell. (iv) SNP (1 μM) was applied at the time indicated by bar. (v) Hydroquinone was superfused 10 min before recording trace (v). Traces (iv) and (v) were obtained from the same cell. (b) Effects of methylene blue (10 μM) on the hyperpolarization induced by 100 μM NO-Cys ((i) and (ii)) and 1 μM SNP ((iii) and (iv)). (i) and (iii) Control. (ii) and (iv) Methylene blue was superfused 10 min before recording of traces (ii) and (iv).

guanethidine (-46.7 ± 2.3 mV, $n = 40$; $P > 0.05$). Application of tetrodoxotin (100 nM) abolished the i.j.ps evoked by EFS (Figure 1a). L-NNA (100 μM) did not produce a significant depolarization of smooth muscle membranes in the rat gastric fundus but inhibited the amplitude of i.j.ps from a control value of 10.2 ± 3.4 mV to 4.2 ± 2.2 mV after L-NNA ($n = 9$; $P < 0.01$; Figure 1b(i)). Simultaneous application of L-arginine (1 mM) with L-NNA partly restored the amplitude of i.j.ps (7.0 ± 2.3 mV, $n = 9$; $P < 0.01$; Figure 1b(ii)). On the other hand, simultaneous application of D-arginine with L-NNA did not restore i.j.ps (control, 9.6 ± 2.1 mV; L-NNA, 4.0 ± 2.2 mV; D-arginine + L-NNA, 4.2 ± 2.5 mV, $n = 5$; Figure 1b(iii)).

A bolus application of NO-Cys (200 μl, 100 μM; chamber volume of 2 ml) produced a transient hyperpolarization of 30.0 ± 3.5 mV ($n = 7$) and the membrane potential was slowly restored to the control level. The reactant solution (methanol and acids) for NO-Cys at equivalent concentrations had no effect on the membrane potentials of the rat gastric fundus. Consecutive applications of NO-Cys did not restore the maximum hyperpolarization, suggesting the decay of the hyperpolarization was not due to diffusion or rapid decomposition of NO-Cys (Figure 2a). The minimum concentration of NO-Cys required to hyperpolarize the membrane by a single application was 100 nM and the amplitude of the hyperpolarization was increased in a concentration-dependent manner (Figure 2b). Elevation of the K concentration depolarized the membrane and reduced the amplitude of the NO-Cys induced hyperpolarization (Figure 2c). In a solution containing 54 mM K^+, NO-Cys (10 μM) did not hyperpolarize the membrane. The slope of the K^+-depolarization plotted against various concentrations of K^+ in the presence of 10 μM NO-Cys became steeper than that obtained in the absence of NO-Cys and the maximum slope of the potential change obtained by a 10 fold change in K^+-concentration was 54 mV, suggesting that the NO-Cys-induced hyperpolarization depends on the K^+ equilibrium potential. Figure 2b also shows the amplitude of hyperpolarization induced by SNP (1 μM, 10.6 ± 2.9 mV, $n = 5$; 10 μM, 16.2 ± 1.6 mV, $n = 4$). L-NNA (100 μM) had no effect on the amplitude of hyperpolarization induced by NO-Cys or SNP (1 μM NO-Cys, 13.9 ± 4.4 mV, $n = 6$; 1 μM SNP, 11.4 ± 3.8 mV, $n = 5$).

Effects of oxyhaemoglobin on the hyperpolarization induced by EFS, NO-Cys and SNP

Since Oxy-Hb is commonly used as an inhibitor of the actions induced by NO due to its scavenger action in the extracellular medium (Martin *et al.*, 1985; Moncada *et al.*, 1991), we compared the inhibitory effects of Oxy-Hb on the hyperpolarizations induced by EFS, NO-Cys and SNP. Oxy-Hb (5 μM) reduced i.j.ps without change in the resting membrane potential. Increasing the Oxy-Hb concentration to 15 μM, however, did not further reduce the amplitude of i.j.ps (5 μM Oxy-Hb, 68 ± 11% of control, $n = 13$; 15 μM Oxy-Hb, 72 ± 8% of control, $n = 6$; $P \geqslant 0.05$). The hyperpolarization induced by 1 μM NO-Cys was strongly inhibited by 5 μM Oxy-Hb (control, 14.2 ± 6.6 mV, $n = 7$; Oxy-Hb, $0.7 \pm$

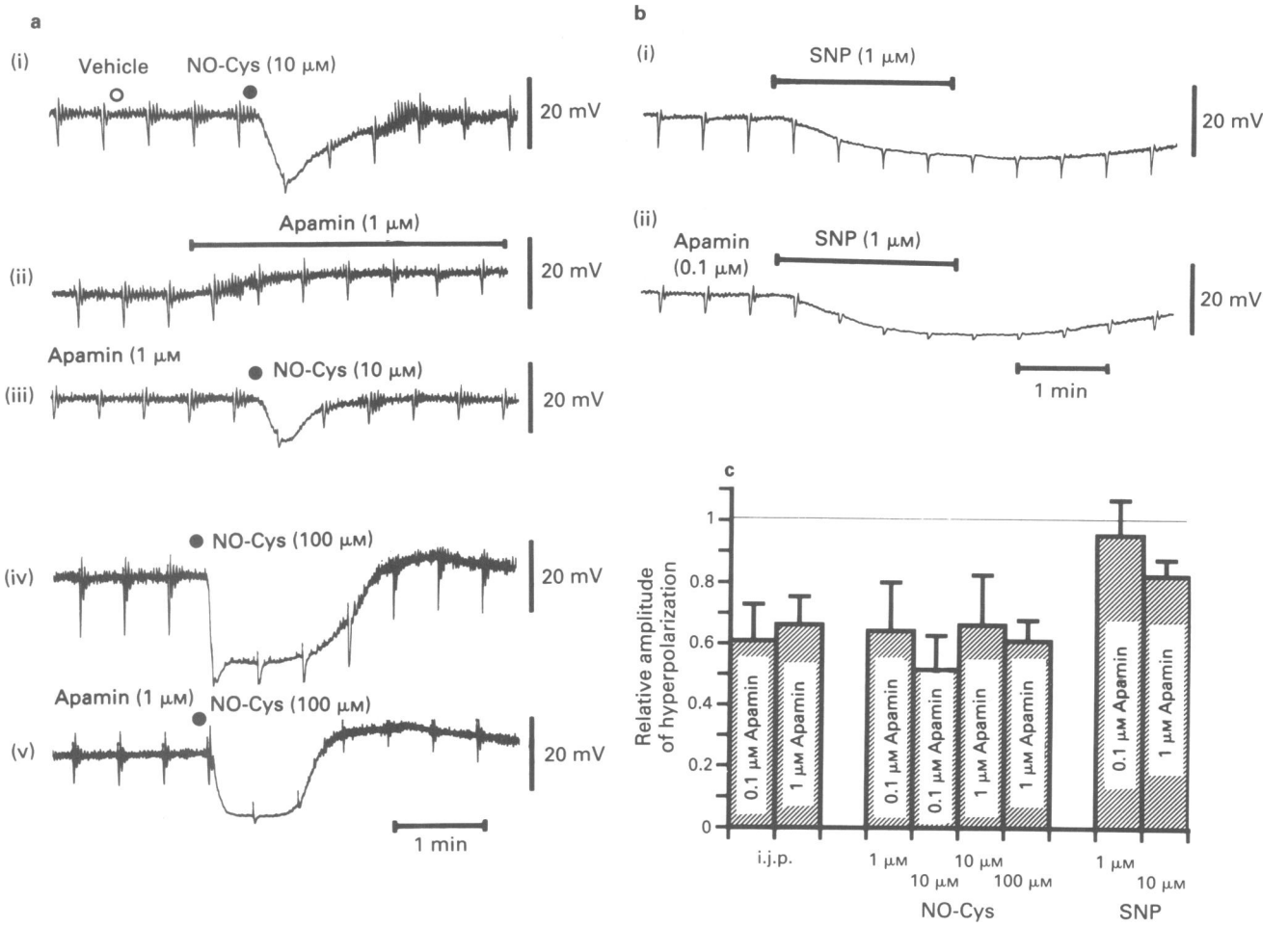

Figure 5 Effects of apamin on i.j.ps and hyperpolarizations induced by S-nitrosocysteine (NO-Cys) (a) and sodium nitroprusside (SNP) (b). I.j.ps were recorded by constant intensity electrical field stimulation with an interval of 30 s. (a) (i) As a control, vehicle was applied (○). NO-Cys (10 μM) was applied at the time indicated by (●). (ii) Apamin (1 μM) was applied at the time indicated by bar. (iii) NO-Cys (10 μM) was applied in the presence of apamin (10 min after the end of trace (ii)). Traces (i)–(iii) were obtained from the same cell. (iv) and (v) NO-Cys (100 μM) was applied at the time indicated by (●). Apamin (1 μM) superfusion was started 10 min before recording trace (v). Traces (iv) and (v) were obtained from the same cell. (b) SNP (1 μM) was applied at the time indicated by the bar in each trace. (i) Control. (ii) In the presence of 1 μM apamin. Apamin superfusion was started 10 min before recording of trace (ii). (c) Summary of inhibitory actions of apamin (0.1 and 1 μM) on i.j.ps and hyperpolarizations induced by various concentrations of NO-Cys and SNP. The amplitudes of i.j.ps and NO-Cys- or SNP-induced hyperpolarizations before application of apamin were normalized as 1.0, each. Each column indicates the mean value of 3–10 observations with s.d.

1.3 mV, $n = 7$; $P < 0.01$; Figure 3a). On the other hand, Oxy-Hb (5 μM) suppressed the hyperpolarization induced by SNP to a lesser extent (control, 14.1 ± 3.5 mV, $n = 6$; Oxy-Hb, 7.5 ± 1.4 mV, $n = 6$; $P < 0.01$) and 15 μM Oxy-Hb further inhibited the hyperpolarization induced by SNP (control, 11.1 ± 3.5 mV, $n = 6$; Oxy-Hb, 2.9 ± 1.2 mV, $n = 6$; $P < 0.01$; Figure 3b).

Figure 4a shows the effects of hydroquinone, a radical scavenger (Mittal & Murad, 1977; Gillespie & Sheng, 1990), on the hyperpolarization induced by EFS, NO-Cys and SNP in the rat gastric fundus. Hydroquinone (50 μM) completely inhibited the hyperpolarization induced by 10 μM NO-Cys, but no effect on the hyperpolarization induced by 1 μM SNP or EFS. On the other hand, 10 min pretreatment with methylene blue (10 μM), an inhibitor of soluble guanylate cyclase (Gruetter *et al.*, 1981; Martin *et al.*, 1985), did not modify the hyperpolarization induced by NO-Cys (100 μM), SNP (1 μM) or EFS (Figure 4b). Long exposure to methylene blue (40 min; 10 μM) did not inhibit the amplitudes of i.j.ps or the hyperpolarization induced by NO-Cys.

Effects of apamin on the hyperpolarizations induced by EFS, NO-Cys and SNP

As shown in Figure 5a and c, apamin (0.1 μM) partly inhibited i.j.ps (control, 10.1 ± 3.2 mV, $n = 17$; 0.1 μM apamin, 6.2 ± 2.1 mV, $n = 17$, $P < 0.01$). Reduction of the i.j.p. amplitude by 0.1 μM apamin was 61 ± 12% of the control and a higher concentration of apamin (1 μM) inhibited i.j.ps to the same extent (66 ± 9% of the control). the hyperpolarization induced by NO-Cys was also reduced by 0.1 μM apamin. Apamin (1 μM) reduced amplitudes of the hyperpolarizations induced by 10 μM and 100 μM NO-Cys (Figure 5a). On the other hand, apamin did not significantly inhibit the amplitude of the hyperpolarization induced by SNP (Figure 5b). In Figure 5c, inhibitory effects of apamin (0.1 μM and 1 μM) on the i.j.p. and hyperpolarization induced by NO-Cys and SNP are summarized. Both concentrations of apamin inhibited the amplitude of i.j.ps and the NO-Cys-induced hyperpolarizations to the same extent.

It is known that apamin inhibits a small conductance Ca^{2+}-dependent K^+ channel in neuronal cells (Romy & Lazdunski, 1984; Blatz & Magleby, 1986). Therefore, we investigated whether or not the hyperpolarization induced by NO-Cys and SNP were sensitive to extracellular Ca^{2+} concentration.

When a nominally Ca^{2+}-free Krebs solution was superfused in the bath, the membrane was depolarized to − 40 mV and the amplitude of the hyperpolarization induced by NO-Cys (100 μM) decreased gradually. The maximum amplitude of hyperpolarization induced by 100 μM NO-Cys was reduced to 44% of control at 30 min after superfusion of Ca^{2+}-free

solution (Figure 6a (i, iii), b; Krebs solution, 32.8 ± 3.1 mV, $n = 6$; Ca^{2+}-free solution, 14.4 ± 3.8 mV, $n = 5$; $P < 0.01$). With superfusion of normal Krebs solution, the amplitude of hyperpolarizations induced by NO-Cys was restored to control level. The amplitude of hyperpolarizations induced by 1 μM SNP was also inhibited by superfusion of nominally Ca^{2+}-free solution (Figure 6b; Krebs solution, 10.8 ± 1.9 mV, $n = 5$; Ca^{2+}-free solution, 4.2 ± 1.6 mV, $n = 5$; $P < 0.01$).

Effects of TEA, 4-AP and glibenclamide on hyperpolarizations induced by NO-Cys and SNP

TEA (10 mM), but not 1 mM TEA depolarized the membrane (control, − 46.7 ± 2.3 mV; 1 mM TEA, − 43.7 ± 3.6 mV, $n = 10$; $P > 0.05$; 10 mM TEA, − 40.3 ± 4.0, $n = 6$; $P < 0.05$). The amplitude of hyperpolarizations induced by NO-Cys was not inhibited by 1 mM TEA (Figure 7a). A higher concentration of TEA (10 mM) inhibited the amplitude of the hyperpolarizations induced by 10 μM NO-Cys (Figure 7a). TEA (1 mM) did not inhibit the amplitude of hyperpolarizations induced by 1 μM or 10 μM SNP (Figure 7b). On the other hand, 10 mM TEA reduced the amplitude of hyperpolarization induced by 1 μM SNP (Figure 7b).

Application of 4-AP (< 10 mM) did not reduce the amplitude of hyperpolarizations induced by 10 μM NO-Cys (Figure 7a; control, 16.0 ± 0.5 mV, $n = 3$; 1 mM 4-AP, 17.5 ± 1.7 mV, $n = 3$; $P > 0.05$; 10 mM 4-AP, 17.0 ± 2.5 mV, $n = 3$; $P > 0.05$). Glibenclamide (1 μM) also had no inhibitory action on the hyperpolarizations induced by NO-Cys and SNP (Figure 7a,b; NO-Cys, control 15.0 ± 2.8 mV, $n = 3$; glibenclamide, 14.0 ± 3.0 mV, $n = 3$; $P > 0.05$; SNP, control, 11.0 ± 2.7 mV, $n = 3$; glibenclamide, 10.5 ± 1.5 mV, $n = 3$; $P > 0.05$).

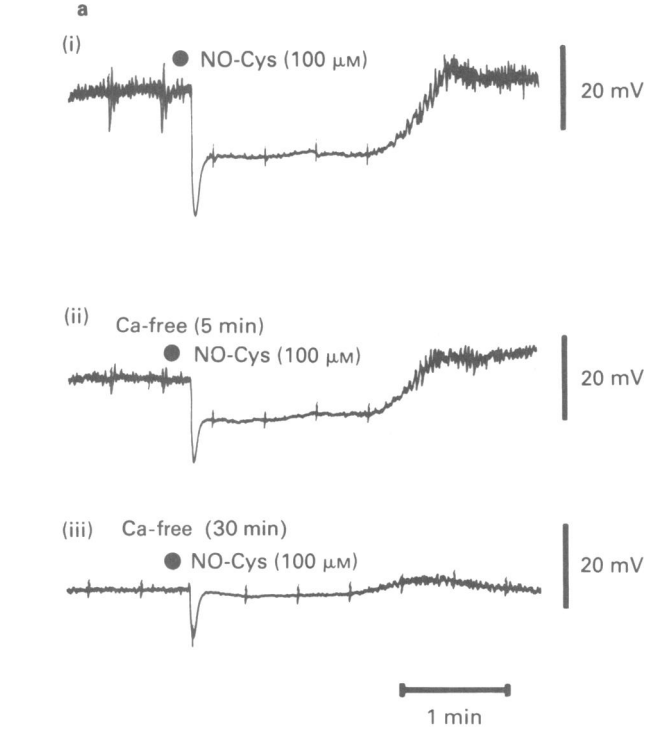

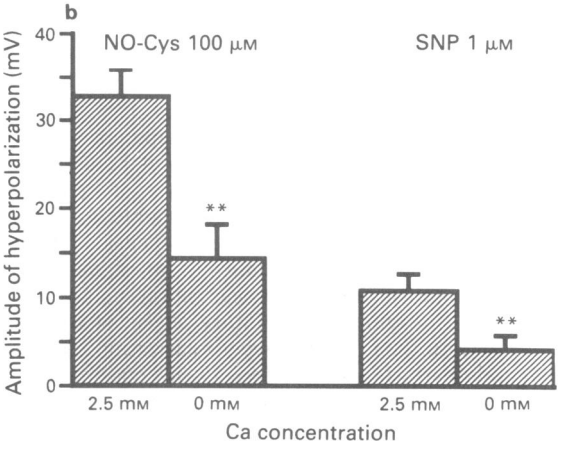

Figure 6 Influences of nominally Ca^{2+}-free solution on the hyperpolarization induced by S-nitrosocysteine (NO-Cys) (100 μM) and sodium nitroprusside (SNP) (1 μM). (a) Examples of the NO-Cys-induced hyperpolarization recorded before (i) and during ((ii) and (iii)) superfusion of nominally Ca^{2+}-free solution. Traces (ii) and (iii) were obtained 5 min and 30 min after starting superfusion of the Ca^{2+}-free solution. NO-Cys (100 μM) was applied at the time indicated by (●). I.j.ps were recorded by constant intensity electrical field stimulation with an interval of 30 s. (b) Relationships between Ca concentration and the amplitude of the hyperpolarization induced by NO-Cys (100 μM) or SNP (1 μM). Each column indicates the mean value of 5–6 observations with s.d. $^{**}P < 0.01$.

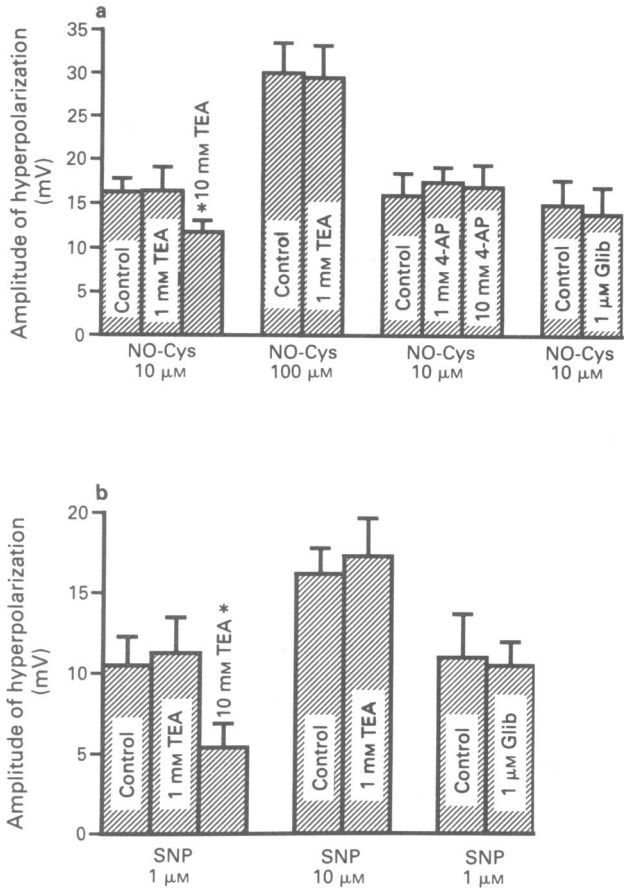

Figure 7 Effects of various K^+ channel blockers on the hyperpolarizations induced by S-nitrosocysteine (NO-Cys) and sodium nitroprusside (SNP). (a) Effects of tetraethylammonium (TEA), 4-aminopyridine (4-AP) and glibenclamide (Glib) on the hyperpolarizations induced by 10 μM and 100 μM NO-Cys. Each column indicates the mean value of the absolute amplitude of the hyperpolarization (4–6 observations) with s.d. (b) Effects of TEA and glibenclamide on the hyperpolarizations induced by 1 μM and 10 μM SNP. Each column indicates the mean value of the absolute amplitude of the hyperpolarization (4–6 observations) with s.d. $^{*}P < 0.05$.

Effects of cyclic GMP on the membrane of the rat gastric fundus

Application of a high concentration of dibutyryl cyclic GMP (1 mM) did not produce a significant hyperpolarization in smooth muscle membranes of the rat gastric fundus (control, − 46.3 ± 2.6 mV, $n = 4$; dibutyryl cyclic GMP, − 49.3 ±

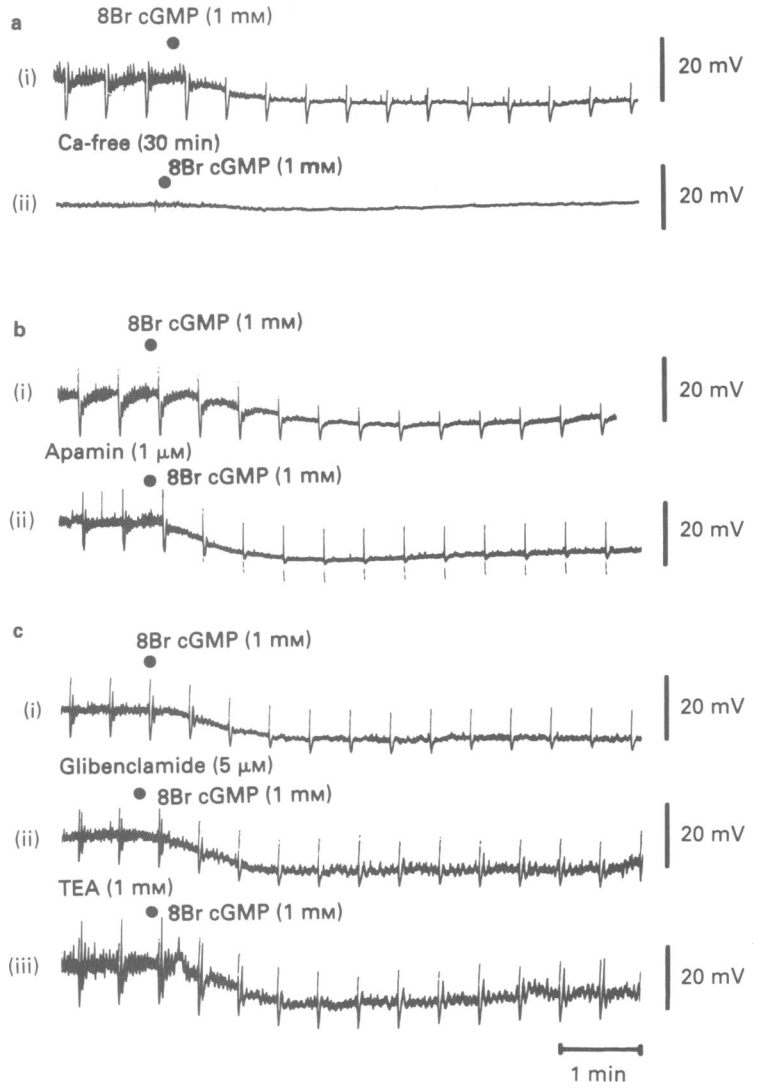

Figure 8 Effects of nominally Ca^{2+}-free solution and several K^+ channel blockers on the hyperpolarization induced by 8-bromo cyclic GMP (8Br cGMP). I.j.ps were recorded by constant intensity electrical field stimulation with an interval of 30 s. (a) An example of the 8-bromo cyclic GMP-induced hyperpolarization recorded before (i) and during (ii) superfusion of nominally Ca^{2+}-free solution. Traces (ii) was obtained 30 min after starting superfusion of the Ca^{2+}-free solution. 8-Bromo cyclic GMP (1 mM) was applied at the time indicated by (●). (b) Effects of apamin (1 μM) on the hyperpolarization induced by 1 mM 8-bromo cyclic GMP. (i) Control. (ii) In the presence of 1 μM apamin. Trace (ii) was obtained 15 min after application of apamin. (c) Effects of glibenclamide (5 μM) and TEA (1 mM) on the hyperpolarization induced by 8-bromo cyclic GMP (1 mM): (i) Control. (ii) In the presence of glibenclamide. (iii) In the presence of TEA. Trace (ii) was obtained 10 min after application of glibenclamide and trace (iii) was obtained 15 min after application of TEA.

2.5 mV, $n = 4$; $P > 0.05$). The same concentration of 8-bromo cyclic GMP produced hyperpolarization (control, -44.3 ± 2.1 mV, $n = 7$; 8-bromo cyclic GMP, -54.4 ± 2.6 mV, $n = 18$; $P < 0.01$), while application of 1 mM Br^- did not produce any change in the membrane potential and amplitude of i.j.ps. Development of the hyperpolarization induced by 1 μM 8-bromo cyclic GMP was slower than that induced by NO-Cys and the hyperpolarization was persistent for more than 30 min. As shown in Figure 8a, when the Ca^{2+}-free solution was superfused in the bath, the hyperpolarization induced by 8-bromo cyclic GMP was completely abolished ($n = 3$). Neither pretreatment with apamin (1 μM) nor TEA (1 mM) inhibited the hyperpolarization induced by 8-bromo cyclic GMP (Figure 8b and c; control, 9.1 ± 2.0 mV, $n = 8$; apamin, 8.5 ± 3.1 mV, $n = 4$; $P > 0.05$; TEA, 8.0 ± 1.0, $n = 3$; $P > 0.05$). Furthermore, 1 mM 8-bromo cyclic GMP also produced membrane hyperpolarization with an amplitude of 10 mV in the presence of glibenclamide (Figure 8c(iii), $n = 1$).

Discussion

In smooth muscle cells of the rat gastric fundus (forestomach), when cholinergic and adrenergic nerves were blocked by atropine and guanethidine, respectively, EFS produced solely i.j.ps. Since tetrodotoxin (TTX) completely blocked the i.j.ps evoked by EFS, it can be concluded that i.j.ps in this preparation are purely nerve-mediated. Komori & Suzuki (1986) and Nakao *et al.* (1986) reported that the i.j.ps were completely inhibited by 0.1 μM apamin in the guinea-pig stomach and ileum, while in the present study apamin (1 μM) inhibited only 40% of the i.j.p. amplitude in the rat stomach. A higher concentration of apamin (1 μM) did not produce further inhibition of i.j.p. in the rat gastric fundus, suggesting that both apamin-sensitive and resistant ion channels are involved.

Evidence has accumulated to support the idea that NO or NO-liberating substances are neurotransmitters released from NANC neurones (Gillespie & Sheng, 1990; Boeckxstaens *et*

al., 1991; Stark et al., 1991; Thornbury et al., 1991; Osthaus & Galligan, 1992; Ward et al., 1992b). We obtained similar results in smooth muscle cells of the rat gastric fundus, i.e. (1) L-NNA inhibited the i.j.p., (2) L-arginine but not D-arginine attenuated the actions of L-NNA on the i.j.p. and (3) Oxy-Hb inhibited the i.j.p. as well as the hyperpolarization induced by NO-Cys. SNP is known to liberate NO spontaneously and activates soluble guanylate cyclase (Martin et al., 1985); however, higher concentrations of Oxy-Hb were required to inhibit the hyperpolarization induced by SNP than that induced by NO-Cys or the i.j.ps. Thornbury et al. (1991) reported that development of the SNP-induced hyperpolarization was slower than those induced by NO-Cys or NO, probably due to a slower liberation of NO from SNP. In the present experiments, we also observed a slower development of hyperpolarization induced by SNP than that by EFS or NO-Cys. These results may indicate that NO from NO-liberating substances produces the hyperpolarization. However, in the present experiments hydroquinone, a hydroxy radical scavenger, completely inhibited the hyperpolarization induced by NO-Cys but not i.j.ps, while Oxy-Hb inhibited i.j.ps and the hyperpolarization induced by NO-Cys to the same extent. Differences observed in actions of Oxy-Hb and hydroquinone on i.j.ps were not solved and, therefore, it is uncertain whether NO itself is a neurotransmitter of the NANC nerve in the present experiments.

Apamin inhibited the hyperpolarization induced by NO-Cys. The effectiveness of inhibition of the hyperpolarization obtained by applications of apamin was very similar to that of i.j.ps. This means that both the EFS- and NO-Cys-induced hyperpolarizations can be classified into the apamin-sensitive and resistant components. NO-Cys, SNP and other NO compounds are known to activate guanylate cyclase in smooth muscle cells and generate cyclic GMP (Moncada et al., 1991). However, neither SNP nor 8-bromo cyclic GMP produced an apamin-sensitive hyperpolarization. Furthermore, TEA and glibenclamide failed to block, but superfusion of Ca^{2+}-free solution abolished the hyperpolarization induced by both substances. Recently, Ward et al. (1992a) reported that there is a close relation between cyclic GMP concentration and membrane hyperpolarization or muscle tone in the dog colon and they proposed that actions of NO and NANC nerve stimulation were mediated by cyclic GMP. Our results obtained in the present experiments were consistent with such an idea and we speculate that NO-Cys and SNP activate apamin-resistant K^+ channels through synthesis of cyclic GMP. On the other hand, the apamin-sensitive component was only seen in hyperpolarization induced by NO-Cys and NANC nerve stimulation. Therefore, it is unlikely that activation of guanylate cyclase or production of cyclic GMP is essential for activation of apamin-sensitive K^+ channels.

Although we failed to see an inhibitory action of apamin on the SNP-induced hyperpolarization, Osthaus & Galligan (1992) reported that the relaxation induced by SNP was partly apamin-sensitive in the longitudinal muscle layer of the guinea-pig ileum. Bauer & Kuriyama (1982) and Nakao et al. (1986) reported that apamin (0.1 μM) did not depolarize the membrane but increased the frequency of action potentials in the longitudinal and circular smooth muscle cells of the guinea-pig ileum. Therefore, apamin might inhibit the relaxation induced by SNP without affecting the amplitude of the hyperpolarization. It is also possible that ion channels with different sensitivities to apamin are present in guinea-pig ileum and rat stomach.

In the present experiments, we found that methylene blue, an inhibitor of soluble guanylate cyclase (Gruetter et al., 1981; Martin et al., 1985), produced no attenuation of the hyperpolarization induced by NO-Cys, SNP and EFS. The same effect of methylene blue has been reported on the hyperpolarization induced by NO in the dog proximal colon (Ward et al., 1992a). Both NO-Cys and SNP have been reported to activate particulate guanylate cyclase, an effect which was not inhibited by methylene blue, as well as soluble guanylate cyclase in various preparations (Waldman & Murad, 1987; Horio & Murad, 1991). Furthermore, Kowaluk et al. (1992) estimated that a low molecular weight protein in the membrane fraction (5–11 kDa) generated NO from SNP. Our results observed in the present experiments may indicate that the hyperpolarization induced by NO-Cys and SNP is related to activation of particulate rather than cytosolic guanylate cyclase.

It is known that apamin blocks the small conductance Ca^{2+}-dependent K^+ channel (Romy & Lazdunski, 1984; Blatz & Magleby, 1986). In the present experiments, we have shown that removal of Ca^{2+} in the bath reduced the amplitude of the NO-Cys, SNP- 8-bromo cyclic GMP-induced hyperpolarization, suggesting that both the apamin-sensitive and resistant components of the hyperpolarization were Ca^{2+}-dependent. Thornbury et al. (1991) and Fujino et al. (1991) reported that NO and nitroglycerin activated the large conductance Ca^{2+}-dependent K^+ channel (maxi-K^+ channel) in the canine colon and pig coronary artery, respectively. Since dibutyryl cyclic GMP opened maxi-K^+ channel in vascular cells (Williams et al., 1988), cyclic GMP, produced by these substances, might activate maxi-K^+ channels and produce hyperpolarization. With single channel current recording, maxi-K^+ channels in smooth muscle cells are blocked by charybdotoxin or low concentrations of TEA (<1 mM) but neither by apamin nor glibenclamide (Inoue et al., 1985; Standen et al., 1989; Kajioka et al., 1990). In the present experiments, since TEA (1 mM) did not inhibit the hyperpolarization induced by NO-Cys, SNP or 8-bromo cyclic GMP, it is unlikely that maxi-K^+ channels contribute to the hyperpolarization induced by NO-Cys, SNP and 8-bromo cyclic GMP in the rat gastric fundus.

Garland & McPherson (1992) reported that NO produced a glibenclamide-sensitive hyperpolarization in the rat mesenteric artery. On the other hand, in the present experiments, hyperpolarizations induced by EFS (i.j.ps), NO-Cys, SNP or 8-bromo cyclic GMP were not inhibited by glibenclamide. Therefore, we conclude that NO and NO-liberating substances do not activate the glibenclamide-sensitive K^+ channel in the rat gastric fundus.

In conclusion, although many questions still remain unsolved, NO-Cys and SNP produced an apamin-resistant hyperpolarization presumably through activation of guanylate cyclase. In addition to activation of the apamin-resistant K^+ channels, we found that NO-Cys also activates apamin-sensitive K^+ channels in the rat gastric fundus via a cyclic GMP-independent process. Our results also indicate that a putative neurotransmitter for NANC neurones in the rat gastric fundus may be a NO-liberating substance.

The authors are grateful to Dr S.M. Ward, University of Nevada, Reno, Nevada, U.S.A. for giving us many valuable comments on the manuscript. The authors also thank Dr T.X. Watanabe, The Peptide Institute, Osaka, Japan, for providing L-NNA. This work was supported by a Grant-in-Aid for Scientific Research from the Ministry of Science, Education and Culture, Japan.

References

BANKS, B.E.C., BROWN, C., BURGESS, G.M., BURNSTOCK, G., CLARET, M., COCKS, T.M. & JENKINSON, D.H. (1989). Apamin blocks certain neurotransmitter-induced increase in potassium permeability. *Nature*, **282**, 415–417.

BAUER, V. & KURIYAMA, H. (1982). Evidence for non-cholinergic, non-adrenergic transmission in the guinea-pig ileum. *J. Physiol.*, **330**, 95–110.

BLATZ, A.L. & MAGLEBY, K.L. (1986). Single apamin-blocked Ca-activated K^+ channels of small conductance in rat cultured skeletal muscle. *Nature*, **323**, 718–720.

BOECKXSTAENS, G.Y., PELCKMANS, P.A., BOGERS, J.J., BULT, H. DE MAN, J.G., OOSTERBOSCH, L., HERMAN, A.G. & VAN MAERCKE, Y.M. (1991). Release of nitric oxide upon stimulation of nonadrenergic nerves in the rat gastric fundus. *J. Pharmacol. Exp. Ther.*, **256**, 441–447.

BULT, H., BOECKXSTAENS, G.Y., PELCKMANS, P.A., JORDAENS, F.H., VAN MAERCKE, Y.M. & HERMAN, A.G. (1990). Nitric oxide as an inhibitory nonadrenergic noncholinergic neurotransmitter. *Nature*, **345**, 346–347.

CHEUNG, D.W. & MACKAY, M.J. (1985). The effects of sodium nitroprusside and 8-bromo-cyclic GMP on electrical and mechanical activities of the rat tail artery. *Br. J. Pharmacol.*, **86**, 117–124.

FIELD, L., DILTS, R.V., RAVICHANDAN, R., LEHNERT. P.G. & CARNAHAN, G.E. (1978). An unusually stable thionitrite from N-acetyl-D, L-penicillamine: X-ray crystal and molecular structure of 2-(acetylamino)-2-carboxy-1,1-dimethylethyl thionitrite. *J.S.C. Chem. Commun.*, 249–250.

FUJINO, K., NAKAYA, S., WAKATSUKI, T., MIYOSHI, Y., NAKAYA, Y., MORI, H. & INOUE, I. (1991). Effects of nitroglycerin on ATP-induced Ca^{++}-mobilization, Ca^{++}-activated K channels and contraction of cultured smooth muscle cells of porcine coronary artery. *J. Pharmacol. Exp. Ther.*, **256**, 371–377.

GARLAND, C.J. & MCPHERSON, G.A. (1992). Evidence that nitric oxide does not mediate the hyperpolarization and relaxation to acetylcholine in the rat small mesenteric artery. *Br. J. Pharmacol.*, **105**, 429–435.

GILLESPIE, J.S. & SHENG, H. (1990). The effects of pyrogallol and hydroquinone on the response to NANC nerve stimulation in the rat anococcygeus and the bovine retractor penis muscle. *Br. J. Pharmacol.*, **99**, 194–196.

GRUETTER, C.A., KADWITZ, P.J. & IGNARRO, L.J. (1981). Methylene blue inhibits coronary arterial relaxation and guanylate cyclase activation by nitroglycerin, sodium nitrite and amylnitrite. *Can. J. Physiol. Pharmacol.*, **59**, 150–162.

HORIO, Y. & MURAD, F. (1991). Purification of guanylate cyclase from rod outer segments. *Biochem. Biophys. Acta.*, **1133**, 81–88.

IGNARRO, L.J., BUGA, G.M., AOOD, K.S., BYRNS, R.E. & CHAUSHURI, G. (1987). Endothelium-derived relaxing factor produced and released from artery and vein is nitric oxide. *Proc. Natl. Acad. Sci. U.S.A.*, **84**, 9265–9269.

INOUE, T., KANMURA, Y., FUJISAWA, K., ITOH, T. & KURIYAMA, H. (1984). Effects of 2-nicrotinaminoethyl nitrate (nicorandil; SG-75) and its derivatives on smooth muscle cells of the canine mesenteric artery. *J. Pharmacol. Exp. Ther.*, **229**, 793–802.

KAJIOKA, S., OIKE, M. & KITAMURA, K. (1990). Nicorandil opens a calcium-dependent potassium channel in smooth muscle cells of the rat portal vein. *J. Pharmacol. Exp. Ther.*, **254**, 905–913.

KOMORI, K. & SUZUKI, H. (1986). Distribution and properties of excitatory and inhibitory junction potentials in circular muscle of the guinea-pig stomach. *J. Physiol.*, **370**, 339–355.

KOWALUK, E.A., SETH, P. & FUNG, H. (1992). Metabolic activation of sodium nitroprusside to nitric oxide in vascular smooth muscle. *J. Pharmacol. Exp. Ther.*, **262**, 916–922.

LI, C.G. & RAND, M.J. (1989). Evidence for a role of nitric oxide in the neurotransmitter system mediating relaxation of the rat anococcygeus muscle. *Clin. Exp. Pharmacol. Physiol.*, **16**, 933–938.

MARTIN, W., VILLANI, G.M., JOTHIANANDAN, D. & FURCHGOTT, R.F. (1985). Selective blockade of endothelium-dependent and glyceryl trinitrate-induced relaxation by hemoglobin and methylene blue in the rabbit aorta. *J. Pharmacol. Exp. Ther.*, **232**, 708–716.

MITTAL, C.K. & MURAD, F. (1977). Activation of guanylate cyclase by superoxide dismutase and hydroxy free radical: a physiological regulator of guanosine 3'5'-monophosphate formation. *Proc. Natl. Acad. Sci. U.S.A.*, **75**, 4360–4364.

MONCADA, S., PALMER, R.M.J. & HIGGS, E.A. (1991). Nitric oxide: physiology, pathophysiology, and pharmacology. *Pharmacol. Rev.*, **43**, 109–142.

NAKAO, K., INOUE, R., YAMANAKA, K. & KITAMURA, K. (1986). Actions of guinidine and apamin on after-hyperpolarization of the spike in circular smooth muscle cells of the guinea-pig ileum. *Naunyn-Schmiedebergs Arch. Pharmacol.*, **334**, 508–513.

OSTHAUS, L.E. & GALLIGAN, J.J. (1992). Antagonists of nitric oxide synthesis inhibit nerve-mediated relaxations of longitudinal muscle in guinea pig ileum. *J. Pharmacol. Exp. Ther.*, **260**, 140–145.

ROMY, G. & LAZDUNSKI, M. (1984). The coexistence in rat muscle cells of two distinct classes of Ca^{2+}-dependent K^+ channels with different pharmacological properties and different physiological functions. *Biochem. Biophys. Res. Commun.*, **118**, 669–674.

STANDEN, N.B., QUAYLE, J.M., DAVIES, N.W., BRAYDEN, J.E., HUANG, Y. & NELSON, M.T. (1989). Hyperpolarizing vasodilators activate ATP-sensitive K^+ channels in arterial smooth muscle. *Science*, **245**, 177–180.

STARK, M.E., BAUER, A.J. & SZURSZEWSKI, J.H. (1991). Effects of nitric oxide on circular muscle of the canine small intestine. *J. Physiol.*, **444**, 743–761.

THORNBURY, K.D., WARD, S.M., DALZIEL, H.H., CARL, A., WESTFALL, D.P. & SANDERS, K.M. (1991). Nitric oxide and nitrosocysteine mimic nonadrenergic, noncholinergic hyperpolarization in canine proximal colon. *Am. J. Physiol.*, **261**, G553–G557.

WALDMAN, S.A. & MURAD, F. (1987). Cyclic GMP synthesis and function. *Pharmacol. Rev.*, **39**, 163–196.

WARD, S.M., DALZIEL, H.H., BRADLEY, M.E., BUXTON, I.L.O., KEEF, K., WESTFALL, D.P. & SANDERS, K.M. (1992a). Involvement of cyclic GMP in non-adrenergic, non-cholinergic inhibitory neurotransmission in dog proximal colon. *Br. J. Pharmacol.*, **107**, 1075–1082.

WARD, S.M., MCKEEN, E.S. & SANDERS, K.M. (1992b). Role of nitric oxide in non-adrenergic, non-cholinergic inhibitory junction potentials in canine ileocolonic sphincter. *Br. J. Pharmacol.*, **105**, 776–782.

WILLIAMS, D.L., KATZ, G.M., ROY-CONTANCIN, L. & REUBEN, J.P. (1988). Guanosine 5'-monophosphate modulates gating of high-conductance Ca^{2+}-activated K^+ channels in vascular smooth muscle cells. *Proc. Natl. Acad. Sci. U.S.A.*, **85**, 9360–9364.

YAMANAKA, K., FURUKAWA, K. & KITAMURA, K. (1985). The different mechanisms of action of nicorandil and adenosine triphosphate on potassium channels of circular smooth muscle of the guinea-pig small intestine. *Naunyn-Schmiedebergs Arch. Pharmacol.*, **331**, 96–103.

(Received November 9, 1992
Revised January 15, 1993
Accepted February 1, 1993)

Br. J. Pharmacol. (1993), **109**, 424–429 © Macmillan Press Ltd, 1993

A_2-purinoceptor-mediated relaxation in the guinea-pig coronary vasculature: a role for nitric oxide

Amanda Vials & [1]Geoffrey Burnstock

Department of Anatomy and Developmental Biology and Centre for Neuroscience, University College London, Gower Street, London WC1E 6BT

1 The Langendorff heart preparation was used to investigate the mechanism of action of the endothelium-dependent vasodilatation evoked by adenosine and its analogues in the guinea-pig coronary vasculature.

2 The relative order of potency of adenosine and its analogues in causing a reduction in perfusion pressure was D-5'-(N-ethylcarboxamide)adenosine (NECA) = 2-[*p*-(2-carboxyethyl)phenylethylamino]-5'-N-ethylcarboxamidoadenosine (CGS 21680)>**R**-N^6-(2-phenylisopropyl)adenosine (**R**-PIA) = adenosine = 2-chloroadenosine (2-CA)>**S**-N^6-(2-phenylisopropyl)adenosine (**S**-PIA) = N^6-cyclopentyl-adenosine (CPA); thus suggesting the presence of A_2-purinoceptors in this preparation.

3 8-(*p*-Sulphophenyl)theophylline (8-PSPT; 3×10^{-5} M) significantly reduced both the maximum amplitude and area of the vasodilatation produced in response to adenosine (5×10^{-10}–5×10^{-8} mol) without having any effect on the response to the P_2-purinoceptor agonist, 2-methylthioATP. The relaxation induced by adenosine (5×10^{-12}–5×10^{-8} mol) was unaffected by the selective A_1-purinoceptor antagonist 1,3-dipropyl-8-cyclopentylxanthine (DPCPX; 10^{-8} M). This antagonist profile suggests that only A_2-purinoceptors are present in the guinea-pig coronary vasculature.

4 The areas of the vasodilator response to adenosine (5×10^{-10}–5×10^{-7} mol), NECA (5×10^{-12}–5×10^{-7} mol) and CGS 21680 (5×10^{-12}–5×10^{-10} mol) were significantly reduced by N^G-nitro-L-arginine methyl ester (L-NAME; 3×10^{-5} M). The amplitude of the responses to low concentrations of adenosine (5×10^{-10}–5×10^{-9} mol), NECA (5×10^{-11} mol) and CGS 21680 (5×10^{-11}–5×10^{-9} mol) were significantly reduced by L-NAME (3×10^{-5} M).

5 L-Arginine (1.5×10^{-3} M) significantly reversed the inhibition, by L-NAME (3×10^{-5} M), of the relaxant response to adenosine (5×10^{-8} mol), NECA (5×10^{-9} mol) and CGS 21680 (5×10^{-11} mol).

6 Indomethacin (10^{-6} M) did not inhibit the response to adenosine, except at low doses (5×10^{-11}–5×10^{-10} mol).

7 It is concluded that in the guinea-pig coronary vasculature, while a major part of the vasodilator action of adenosine is probably directly via A_2-receptors on the smooth muscle, activation of a subpopulation of A_2-purinoceptors on endothelial cells by adenosine and its analogues induces relaxation via production of nitric oxide; prostanoids appear to play a minimal role in the relaxation induced by adenosine as in most other preparations.

Keywords: Nitric oxide; A_2-purinoceptors; coronary vasculature; adenosine; endothelium

Introduction

Adenosine, a potent vasodilator (Drury & Szent-Györgyi, 1929), has been proposed as a regulator of coronary flow (Berne, 1963; 1980). The pharmacological effects of adenosine are mediated by specific receptors specified as P_1-purinoceptors (Burnstock, 1978). P_1-purinoceptors have been subdivided into A_1 and A_2 receptors on the basis of different structure-activity relationships for agonists and antagonists. At A_1 receptors, N^6-substituted adenosine analogues such as N^6-cyclopentyladenosine (CPA) and N^6-phenylisopropyl-adenosine (PIA) are more potent than 5'-N-ethyl-carboxamido-adenosine (NECA), whereas, on A_2 receptors the potency order is reversed (Bruns, 1990a,b; Daly, 1990).

On the basis of the relative order of potency of NECA, **R**- and **S**-PIA it has been determined that the vasodilator action of adenosine in the guinea-pig coronary vasculature is mediated via the A_2 subclass of the P_1-purinoceptor (Leung *et al.*, 1985). In most blood vessels the vasodilator effect of adenosine has been shown to be largely due to action at A_2-purinoceptors on the vascular smooth muscle and not the endothelium (Collis & Brown, 1983; White & Angus, 1987). Adenosine has been shown to be released from coronary endothelial cells (Deussen *et al.*, 1986) and at low doses it has been shown to induce relaxation via receptors on endothelial cells (Corr & Burnstock, 1990; Balcells *et al.*, 1992). Des Rosiers & Nees (1987) have provided functional evidence for the presence of A_2-purinoceptors on cultured coronary endothelial cells. The action at such receptors on the endothelium could stimulate the synthesis and release of endothelium-derived relaxing factors, such as prostacyclin (Moncada & Vane, 1979) or nitric oxide (NO; Furchgott & Zawadzki, 1980; Ignarro *et al.*, 1986; Moncada *et al.*, 1991).

The purpose of this study was to investigate the possible mechanisms of action of the endothelial response to adenosine and some of its analogues by using inhibitors of the enzymatic synthesis of NO and prostaglandins. N^G-nitro-L-arginine methyl ester (L-NAME) is a competitive inhibitor of the synthesis of NO from L-arginine (Rees *et al.*, 1990) and is effective in inhibiting vasodilator responses to various agents in the guinea-pig coronary vasculature (Vials & Burnstock, 1992), while indomethacin is a prostaglandin-synthetase inhibitor (Vane, 1971) which will therefore prevent the formation of prostanoids. In addition, studies of the relative order of potency of adenosine analogues in the guinea-pig coronary vasculature have been expanded upon to include more specific adenosine analogues such as 2-[*p*-(2-carboxyethyl) phenylethylamino] - 5' - N - ethylcarboxamidoadenosine

[1] Author for correspondence.

(CGS 21680). CGS 21680 is an adenosine agonist which is 140 fold more selective for A_2-purinoceptors than A_1-purinoceptors (Hutchison *et al.*, 1989).

Methods

Guinea-pigs (250–400 g) of either sex were injected with heparin (2,500 units i.p.) 15 min before being killed by cervical dislocation. The heart was quickly removed and placed in cold Krebs solution (4°C) to arrest the beating. Extraneous fat and large vessels were removed, the heart was cannulated via the aorta, and the coronary circulation perfused by the method of Langendorff with a modified Krebs-Henseleit solution containing (mM): NaCl 115.3, KCl 4.6, $MgSO_4$. $7H_2O$ 1.1, $NaHCO_3$ 22.1, KH_2PO_4 1.1, $CaCl_2$ 2.5 and glucose 11.1; equilibrated with 95% O_2:5% CO_2. Albumin (0.5 g l^{-1}) was also added to the solution to increase the osmotic pressure and reduce oedema. A water-filled latex balloon, connected to a pressure transducer (Viggo-Spectramed, model P23XL), was placed in the left ventricle for the measurement of left ventricular pressure. The left ventricular diastolic pressure did not exceed 10 mmHg. It was found that the average starting left ventricular systolic pressure was 27.3 ± 1.3 mmHg ($n = 71$). Perfusion pressure was monitored with a pressure transducer connected via a side arm to the cannula. A pair of platinum electrodes were placed in the right ventricle and the heart was paced at 4 Hz with electrical pulses of 5 ms duration at supramaximal voltage (usually around 20 V). The flow rate was gradually increased to obtain a starting perfusion pressure of 50–60 mmHg, using a Masterflex constant flow roller pump (Cole-Palmer Instruments Co., Chicago, U.S.A.). The flow rate was determined by collecting the effluent, over a period of time, and the average rate was 14.1 ± 0.28 ml min^{-1} ($n = 71$). The heart was left to equilibrate for at least 20 min before the experiment was started. When the perfusion pressure had reached a steady state, adenosine and its analogues were given as 50 µl boluses, injected over 3 s into the superfused solution close to the heart. The duration of each individual experiment was no longer than 3 h. Due to this time restriction the effects of all the agonists could not be tested on the same heart. For this reason the agonists were chosen randomly and not more than three agonists were used on a particular heart. The order of exposure of the agonists to the heart was also random to minimize differences due to time-dependent changes in the preparation. At least 5 min was left between the administration of each dose of agonist. When the effect of antagonists was examined, control dose-response relationships for adenosine and its analogues were first obtained and L-NAME, indomethacin, 8-(*p*-sulphophenyl)theophylline (8-PSPT) or 1,3-dipropyl-8-cyclopentylxanthine (DPCPX) added to the perfusing solution and allowed to equilibrate for 20 min. The dose-responses were then repeated in the presence of the antagonist. After inhibition by L-NAME, L-arginine was added to the perfusing solution after the dose-response relationship had been established to determine whether the inhibition could be reversed. The preparations were allowed to equilibrate for a further 20 min before a submaximal dose (in terms of area of response) was repeated. DPCPX was not used above 10^{-8} M as the purpose of using this antagonist was to establish if there are any A_1-purinoceptors present in the guinea-pig coronary vasculature and it has been shown on guinea-pig tissue that above this concentration, DPCPX also inhibits effects mediated via A_2-purinoceptors (Collis *et al.*, 1989). When the effects of adenosine were examined before and after an antagonist the highest dose used to obtain the dose-response curve (Figure 1) was not used as the resting perfusion pressure tended to find a new lower level after this high dose was applied. For a given response, both its maximum amplitude and area were measured. The area of the vasodilator response was calculated by a measurement and analysis programme on an Apple II Computer. Student's

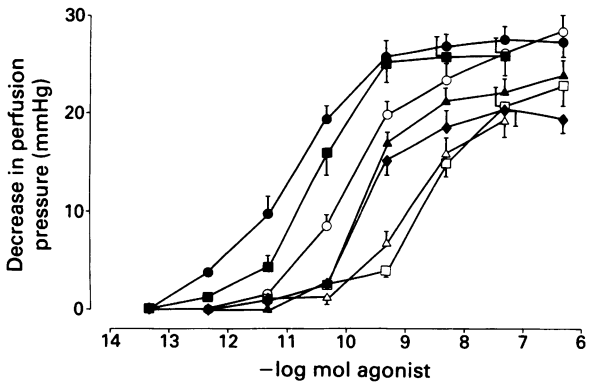

Figure 1 The amplitude of the vasodilatation evoked by NEC A (●), CGS 21680 (■), R-PIA (○), adenosine (▲), 2-CA (◆), S-PIA (□) and CPA (△) in the guinea-pig isolated perfused heart. The graph shows the mean ($n \geq 10$) with s.e. mean. For abbreviations, see text.

t tests were used to assess statistical significance between responses obtained before and after antagonist, $P < 0.05$ being taken as significant. Analysis of variance and Tukey's test were used to assess relative order of potency of the adenosine analogues. These tests were used on both the pD_2 ($-\log EC_{50}$) values and the responses to individual concentrations of the agonists. At the end of the experiment the heart was removed from the cannula, blotted and weighed. The mean wet weights were 1.54 ± 0.02 g ($n = 71$).

Adenosine hemisulphate, 2-chloroadenosine (2-CA), NECA, R-PIA, S-PIA, bradykinin, indomethacin and L-NAME were all obtained from Sigma Chemical Co. Ltd. CPA, 2-methylthioATP (2MeSATP), 8-PSPT and CGS 21680 were obtained from RBI. DPCPX was obtained from Cookson Chemicals. S-PIA, R-PIA, 2-CA, D-NECA, CPA, CGS 21680 and DPCPX were made up as stock solutions (10^{-2} M) in dimethyl sulphoxide (DMSO) and diluted in distilled water. A 50 µl bolus injection of distilled water or DMSO caused no change in perfusion pressure other than a small injection artefact.

Results

Dose-response to adenosine and analogues

Bolus injections of NECA, CGS 21680, CPA, 2-CA, R-PIA, S-PIA and adenosine produced dose-dependent vasodilatation in the guinea-pig coronary vasculature. Dose-response curves for the 7 agonists are illustrated in Figure 1. The maximum responses produced by NECA and CGS 21680 were similar and the pD_2 values for both were not significantly different from one another (6.25 ± 0.16 ($n = 21$) and 6.16 ± 0.11 ($n = 11$) respectively). The pD_2 values for adenosine and 2-CA were 5.38 ± 0.03 ($n = 23$) and 5.44 ± 0.06 ($n = 11$) respectively. The pD_2 values for R-PIA, S-PIA and CPA were 5.54 ± 0.09 ($n = 23$), 4.35 ± 0.08 ($n = 13$) and 4.68 ± 0.1 ($n = 10$) respectively, although there are limitations in the accuracy of these values as the maximum responses were not always achieved in all the preparations due to the limited solubility of these agents. Their potency expressed relative to the pD_2 value of adenosine was in the ratio 7:6:1.4:1.2:1:0.2:0.1 respectively. A similar range order of potency was obtained when individual doses of agonists were compared by analysis of variance and Tukey's tests. There was a small but unsignificant fall in the left ventricular systolic pressure on bolus administration of agonists at the high doses.

Effect of 8-PSPT and DPCPX

8-PSPT (3×10^{-5} M) significantly reduced the maximum amplitude and area of the vasodilatation produced in response to adenosine (5×10^{-10}–5×10^{-8} mol, Figure 2a; data for area not shown). As a control, neither the maximum amplitude nor the area of the response to 2MeSATP (5×10^{-13}–5×10^{-9} mol, Figure 2b; data for area not shown) were affected by 8-PSPT (3×10^{-5} M). DPCPX (10^{-8} M) did not have any effect on the response to adenosine (5×10^{-12}–5×10^{-8} mol; data not shown). 8-PSPT (3×10^{-5} M) did not significantly affect the resting perfusion pressure of left ventricular pressure of the preparations.

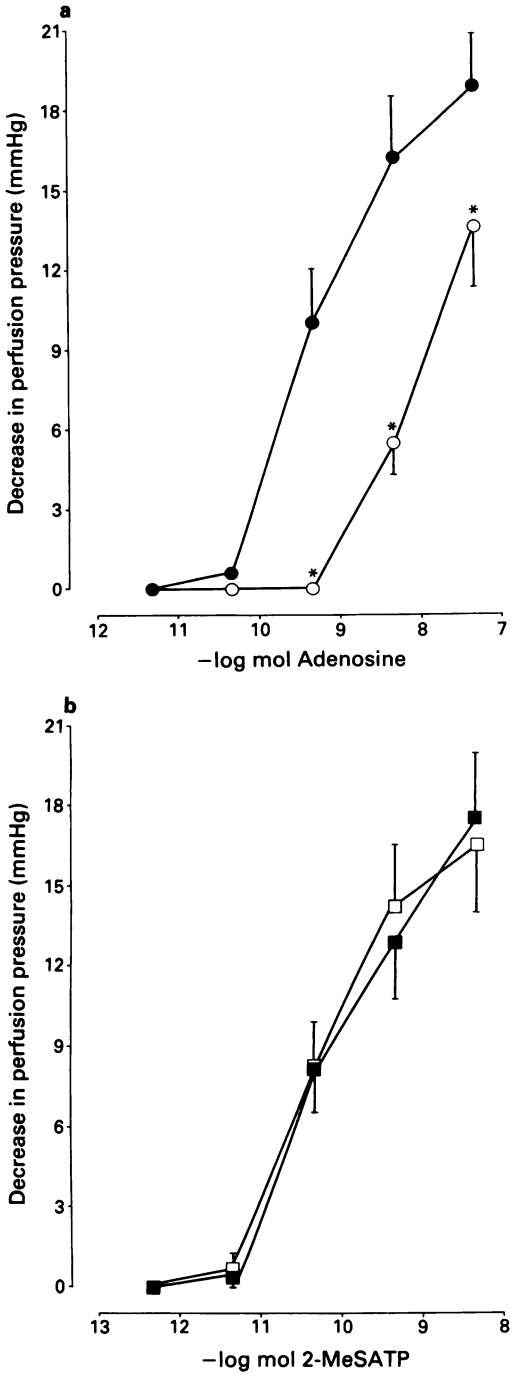

Figure 2 The amplitude of the vasodilator responses evoked by (a) adenosine and (b) 2-methylthioATP (2-MeSATP), in the absence (● and ■ respectively) and presence (○ and □ respectively) of 8-(p-sulphophenyl)theophylline (8-pSPT, 3×10^{-5} M), in the guinea-pig isolated perfused heart. The graph shows the mean ($n \geqslant 6$) with s.e. mean. The significant differences are $^{*}P < 0.05$.

Effect of L-NAME and L-arginine

L-NAME (3×10^{-5} M) significantly reduced the amplitude of the response to adenosine (5×10^{-10}–5×10^{-9} mol, Figure 3a). However, L-NAME (3×10^{-5} M) had a greater effect and significantly attenuated the area of the response to adenosine

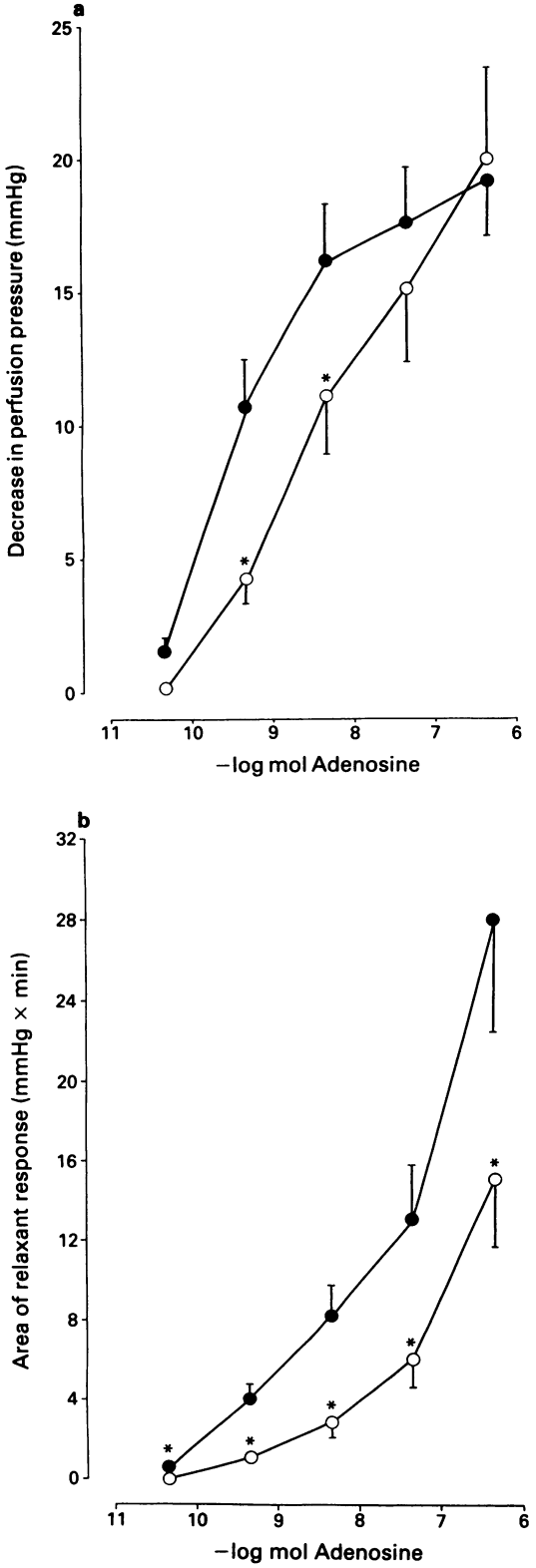

Figure 3 The (a) amplitude and (b) area of the vasodilatation obtained in response to adenosine, in the absence (●) and presence (○) of N^{G}-nitro-L-arginine methyl ester (L-NAME) (3×10^{-5} M), in the guinea-pig isolated perfused heart. The graph shows the mean ($n \geqslant 6$) with s.e. mean. The significant differences are $^{*}P < 0.05$.

(5×10^{-10}–5×10^{-7} mol, Figure 3b). The inhibition of the response to adenosine (5×10^{-8} mol, Table 1), by L-NAME (3×10^{-5} M), was significantly reversed in the presence of L-arginine (1.5×10^{-3} M). L-NAME (3×10^{-5} M) only significantly reduced the amplitude of the response to a low concentration of NECA (5×10^{-11} mol, data not shown) and two concentrations of CGS 21680 (5×10^{-12} and 5×10^{-9} mol, data not shown). In the case of both NECA (5×10^{-12}–5×10^{-7} mol, Figure 4a) and CGS 21680 (5×10^{-12}–5×10^{-9} mol, Figure 4b) the area of the responses were significantly attenuated by L-NAME (3×10^{-5} M). The attenuation of the area of the response to NECA (5×10^{-9} mol, Table 1) and CGS 21680 (5×10^{-11} mol, Table 1) by L-NAME (3×10^{-5} M) was significantly reversed in the presence of L-arginine (1.5×10^{-3} M). There was only partial reversal but the concentration of L-arginine could not be increased because a higher dose reduced the perfusion pressure of the preparation and therefore affected the degree of relaxation that could be obtained. The concentration of NECA and CGS 21680 used to show reversal of inhibition of L-NAME by L-arginine was chosen as a dose that gave a similar submaximal response in terms of area. The resting perfusion and left ventricular pressure of the preparations were unaffected by the addition of L-NAME (3×10^{-5} M) to the perfusate.

Effect of indomethacin

Indomethacin (10^{-6} M) significantly reduced the amplitude and area of the response to only two low concentrations of adenosine (5×10^{-11} and 5×10^{-10} mol, Figure 5; data for area not shown). As a control, both the maximum amplitude and area of the vasodilatation produced in response to bradykinin (5×10^{-12}–5×10^{-9} mol, data not shown) were significantly reduced by indomethacin (10^{-6} M). Indomethacin (10^{-6} M) did not significantly affect either the resting perfusion pressure or the left ventricular pressure of the preparations.

Discussion

The relative order of potency of adenosine and its analogues, in the guinea-pig coronary vasculature is a characteristic of P_1-purinoceptors of the A_2 sub-type (Collis, 1985; Burnstock & Kennedy, 1986; Williams, 1987). 8-PSPT inhibited the response to adenosine whereas DPCPX had no effect. This also suggests the presence of A_2-purinoceptors. The response to adenosine is at least in part mediated via nitric oxide, whereas prostaglandins play a minimal role.

Previous work involving the use of NECA, R- and S-PIA has shown that A_2-purinoceptors are present in the guinea-pig coronary vasculature (Leung *et al.*, 1985). Additional information obtained with the selective A_2-purinoceptor agonist CGS 21680 (Hutchison *et al.*, 1989) and A_1-purinoceptor agonist CPA (Moos *et al.*, 1985) has provided a clearer picture of the receptor profile in the guinea-pig coronary vasculature. CPA is significantly less potent than adenosine and 2-CA whereas R-PIA is not, and CGS 21680 is equipotent with NECA. The agonist profile of CGS 21680 and CPA strongly implies the involvement of A_2-purinoceptors. The nonselective P_1-purinoceptor antagonist, 8-PSPT (Collis *et al.*, 1987) inhibited the response to adenosine at a concentration that had no effect on the response to 2MeSATP, confirming the fact that adenosine was acting on P_1-purinoceptors. DPCPX has been shown at low concentrations to be a highly selective A_1-purinoceptor antagonist (Haleen *et al.*, 1987; Lohse *et al.*, 1987) in guinea-pig and rat tissues (Collis *et al.*, 1987; 1989; Collis, 1990). In the guinea-pig coronary vasculature, DPCPX had no effect on the response to adenosine suggesting that the relaxation was not mediated by A_1-purinoceptors. The effects of the antagonists also suggest the presence of A_2-purinoceptors. Thus, it can be concluded that even with the use of more selective agonists there does not appear to be a role for A_1-purinoceptors in the relaxation of the guinea-pig coronary vasculature by adenosine analogues.

L-NAME inhibited the area, although not the maximum amplitude (except at low concentrations of adenosine, NECA and CGS 21680), of the responses to adenosine, NECA and CGS 21680. This suggests that at least part of the response induced by these vasodilators is mediated via nitric oxide. It has been shown in guinea-pig isolated perfused hearts that the endothelium is a highly active metabolic barrier for adenosine (Nees *et al.*, 1985), such that at low concentrations adenosine would be avidly metabolized and therefore unable to reach the smooth muscle. Therefore the response to low doses of adenosine would be due to action on the endothelium. There is evidence for the presence of adenosine A_2-purinoceptors in cultured coronary endothelial cells (Des Rosiers & Nees, 1987), although in the guinea-pig coronary artery, P_1-purinoceptors appear to be limited to the smooth muscle (Keef *et al.*, 1992). In contrast, in the rabbit coronary artery an endothelial role to part of the response to adenosine has been reported (Corr & Burnstock, 1990). This information suggests that at least some A_2-purinoceptors are located on endothelial cells on resistance vessels in the guinea-pig coronary bed which when activated induced relaxation via nitric oxide. The fact that L-arginine at least partially reversed the inhibition of the response to adenosine, NECA and CGS 21680 by L-NAME substantiates these claims in that it shows that L-NAME was selectively inhibiting the enzyme NO synthase. NO synthase converts L-arginine into L-citrulline with the additional production of NO (Palmer *et al.*, 1988; Schmidt *et al.*, 1988; Mayer *et al.*, 1989; Palmer & Moncada, 1989). It has been demonstrated in the rabbit perfused heart that inhibition by the nitric oxide synthase inhibitor N^G-monomethyl-L-arginine of the effect of acetylcholine (ACh) was due to shortening of the response rather than to an effect on peak fall in perfusion pressure

Table 1 The area of relaxation obtained in response to adenosine, NECA and CGS 21680 in the guinea-pig isolated perfused heart

		Area of relaxant response (mmHg × min)		
			After addition of	
Agonist	*Dose* (mol)	*Control*	*L-NAME*	*L-NAME + L-Arg*
Adenosine	5×10^{-8}	26.17 ± 6.3	10.41 ± 2.0*	18.20 ± 3.8†
NECA	5×10^{-9}	109.63 ± 15.2	43.04 ± 9.9*	56.91 ± 12.8†
CGS 21680	5×10^{-11}	117.27 ± 26.7	10.98 ± 4.3*	39.02 ± 5.8†

The effect of N^G-nitro-L-arginine methyl ester (L-NAME, 3×10^{-5} M; in the perfusate) on the response to these agonists and the effect of L-arginine (L-Arg (1.5×10^{-3} M); in the perfusate along with L-NAME) on the inhibition by L-NAME is demonstrated. The areas are expressed as the mean ± s.e. mean ($n \geq 6$).
Significant differences from control are $^*P < 0.05$. Significant differences from responses obtained in presence of L-NAME are $^\dagger P < 0.05$.
For abbreviations, see text.

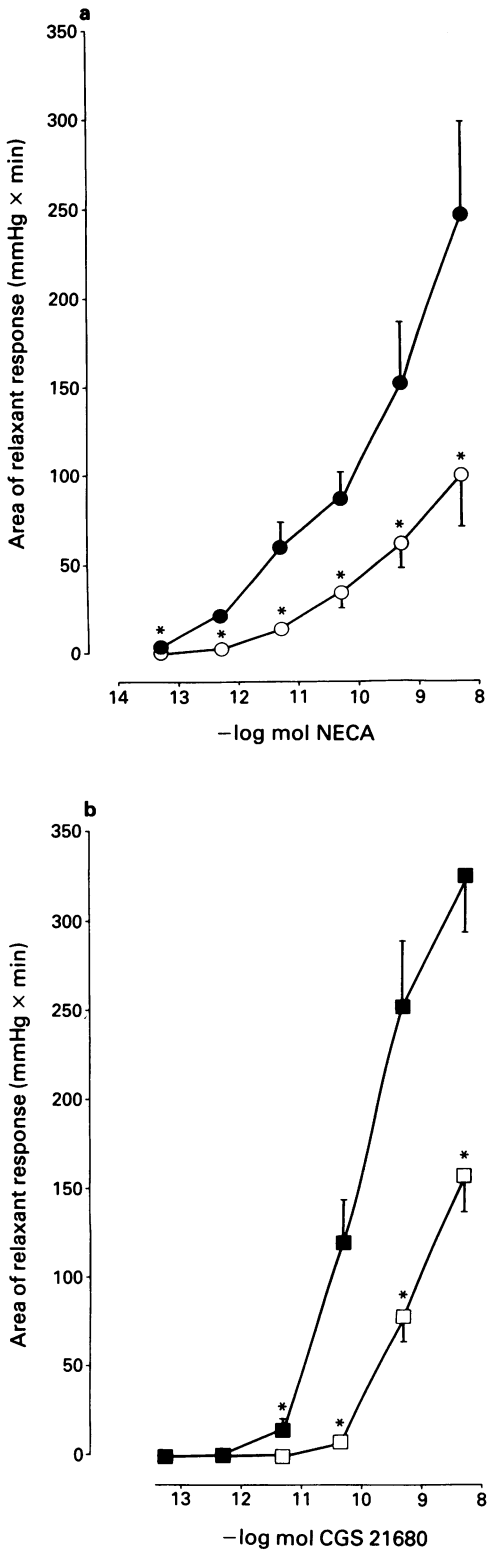

Figure 4 The area of the relaxant response to (a) D-5′-(N-ethylcarboxamide) adenosine (NECA) and (b) 2-[*p*-(2-carboxyethyl)-phenylethylamino]-5′-N-ethylcarboxamidoadenosine (CGS 21680), in the guinea-pig isolated perfused heart, in the absence (● and ■ respectively) and presence (○ and □ respectively) of N^G-nitro-L-arginine methyl ester (3×10^{-5} M). The graph shows the mean ($n \geqslant 6$) with s.e. mean. The significant differences are $^*P < 0.05$.

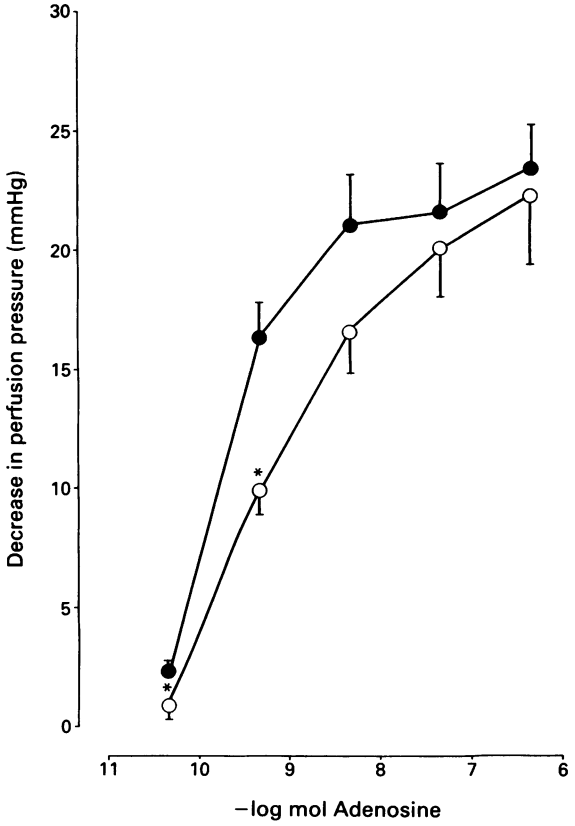

Figure 5 The amplitude of the vasodilatation obtained in response to adenosine in the guinea-pig isolated perfused heart, in the absence (●) and presence (○) of indomethacin (10^{-6} M). The graph shows the mean ($n \geqslant 6$) with s.e. mean. The significant differences are $^*P < 0.05$.

(Smith *et al.*, 1992). It was suggested that NO was involved in the sustained relaxation induced by ACh but not in the initial event. Similarly, in the anaesthetized guinea-pig, L-N^G-methylarginine decreased the duration of the hypotensive response to ACh without affecting the magnitude of the response (Aisaka *et al.*, 1989). The same might be suggested about the vasodilator action of these A_2-receptor agonists in that there appears to be two overlapping phases, a brief early one which appears to be insensitive to L-NAME and is responsible for the initial peak depressor response, followed by a second phase of longer duration that is abbreviated by L-NAME.

Prostacyclin is a powerful vasodilator and platelet anti-aggregatory compound (Gryglewski *et al.*, 1976). In the perfused guinea-pig heart the endothelium-dependent dilatation to acetylcholine was significantly attenuated by indomethacin (Lee *et al.*, 1990), suggesting that prostanoid production can be induced. In the rabbit isolated heart the same adenosine receptors that elicit relaxation also induce release of prostacyclin (Karwatowska-Prokopoczuk *et al.*, 1988). Therefore it could be conceivable that adenosine induced relaxation via release of prostanoids. However indomethacin, at a concentration that significantly inhibited the response to bradykinin, only attenuated the area and maximum amplitude of the responses to a few individual doses of adenosine. Therefore it is apparent that prostanoids do not play a major role in the relaxation induced by adenosine.

In conclusion it can be stated that there is a population of A_2 purinoceptors present in the guinea-pig coronary vasculature which when activated by adenosine, NECA and CGS 21680 induce relaxation that is partly mediated via nitric oxide. Prostanoids play only a minor role if any in the relaxation induced by administration of adenosine.

This work was supported with a grant from the Science and Engineering Research Council. Dr C.H.V. Hoyle is thanked for helpful discussion during the course of this work.

References

AISAKA, K., GROSS, S.S., GRIFFITH, O.W. & LEVI, R. (1989). L-Arginine availability determines the duration of acetylcholine-induced systemic vasodilatation *in vivo*. *Biochem. Biophys. Res. Commun.*, **163**, 710–717.

BALCELLS, E., SUAREZ, J. & RUBIO, R. (1992). Functional role of intravascular coronary endothelial adenosine receptors. *Eur. J. Pharmacol.*, **210**, 1–9.

BERNE, R.M. (1980). The role of adenosine in the regulation of coronary blood flow. *Circ. Res.*, **47**, 807–813.

BERNE, R.M. (1963). Cardiac nucleotides in hypoxia: possible role in regulation of coronary blood flow. *Am. J. Physiol.*, **204**, 317–322.

BRUNS, R.F. (1990a). Structure-activity relationships for adenosine antagonists. In *Purines in Cellular Signalling*. ed. Jacobson, K.A., Daly, J.W. & Manganiello, V. pp. 126–135. New York: Springer-Verlag.

BRUNS, R.F. (1990b). Adenosine receptors: role and pharmacology. *Ann. N.Y. Acad. Sci.*, **603**, 211–226.

BURNSTOCK, G. (1978). A basis for distinguishing two types of purinergic receptor. In *Cell and Membrane Receptors for Drugs and Hormones: A Multidisciplinary Approach*. ed. Bolis, L. & Straub, R.W. pp. 107–118. New York: Raven Press.

BURNSTOCK, G. & KENNEDY, C. (1986). Purinergic receptors in the cardiovascular system. *Prog. Pharmacol.*, **6**, 111–132.

COLLIS, M.G. (1985). Are there two types of adenosine receptors in peripheral tissues? In *Purines: Pharmacology and Physiological Roles*. ed. Stone, T.W. pp. 75–84. London: Macmillan press.

COLLIS, M.G. (1990). Adenosine receptor sub-types in isolated tissues: antagonist studies. In *Purines in Cellular Signalling*. ed. Jacobson, K.A., Daly, J.W. & Manganiello, V. pp. 48–53. New York: Springer-Verlag.

COLLIS, M.G. & BROWN, C.M. (1983). Adenosine relaxes the aorta by interacting with an A_2 receptor and an intracellular site. *Eur. J. Pharmacol.*, **96**, 61–69.

COLLIS, M.G., JACOBSON, K.A. & TOMKINS, D.M. (1987). Apparent affinity of some 8-phenyl-substituted xanthines at adenosine receptors in guinea-pig aorta and atria. *Br. J. Pharmacol.*, **92**, 69–75.

COLLIS, M.G., STOGGALL, S.M. & MARTIN, F.M. (1989). Apparent affiity of 1,3-dipropyl-8-cyclopentylxanthine for adenosine A_1 and A_2 receptors in isolated tissues from guinea-pigs. *Br. J. Pharmacol.*, **97**, 1274–1278.

CORR, L.A. & BURNSTOCK, G. (1990). Purinoceptor subtypes in the coronary artery. *Circulation*, **82**, 408.

DALY, J.W. (1990). Adenosine agonsits and antagonists. In *Purines and Cellular Signalling*. ed. Jacobson, K.A., Daly, J.W. & Manganiello, V. pp. 3–12. New York: Springer-Verlag.

DES ROSIERS, C. & NESS, S. (1987). Functional evidence for the presence of adenosine A_2-receptors in cultured coronary endothelial cells. *Naunyn Schmiedebergs Arch. Pharmacol.*, **336**, 94–98.

DEUSSEN, A., MÖSER, G. & SCHRADER, J. (1986). Contribution of coronary endothelial cells to cardiac adenosine production. *Pflügers Arch.*, **406**, 608–614.

DRURY, A.N. & SZENT-GYÖRGYI, A. (1929). The physiological activity of adenine compounds with especial reference to their action upon the mammalian heart. *J. Physiol.*, **68**, 213–237.

FURCHGOTT, R.F. & ZAWADZKI, J.V. (1980). The obligatory role of endothelial cells in the regulation of arterial smooth muscle by acetylcholine. *Nature*, **288**, 373–376.

GRYGLEWSKI, R.J., BUNTING, S., MONCADA, S., FLOWER, R.J. & VANE, J.R. (1976). Arterial walls are protected against deposition of platelet thrombi by a substance (Prostaglandin X) which they make from prostaglandin endoperoxides. *Prostaglandins*, **12**, 685–713.

HALEEN, S.J., STEFFAN, R.P. & HAMILTON, H.W. (1987). DPCPX, a highly selective A_1 adenosine receptor antagonist. *Life Sci.*, **40**, 555–563.

HUTCHISON, A.J., WEBB, R.L., OEI, H.H., GHAI, G.R., ZIMMERMAN, M.B. & WILLIAMS, M. (1989). CGS 21680C, an A_2 selective adenosine receptor agonist with preferential hypotensive activity. *J. Pharmacol. Exp. Ther.*, **251**, 47.

IGNARRO, L.J., WOOD, K.S. & BYRNS, R.E. (1986). Pharmacological and biochemical properties of EDRF: evidence that EDRF is closely related to nitric oxide (NO) radical. *Circulation*, **74**, 287.

KARWATOWSKA-PROKOPCZUK, E., CIABATTONI, G. & WENNMALM, Å. (1988). Effect of adenosine on the formation of prostacyclin in the rabbit isolated heart. *Br. J. Pharmacol.*, **94**, 721–728.

KEEF, K.D., PASCO, J.S. & ECKMAN, D.M. (1992). Purinergic relaxation and hyperpolarization in guinea-pig and rabbit coronary artery: role of the endothelium. *J. Pharmacol. Exp. Ther.*, **260**, 592–600.

LEE, L., BRUNER, C.A. & WEBB, R.C. (1990). Prostanoids contribute to endothelium-dependent coronary vasodilatation in guinea-pigs. *Blood Vessels*, **27**, 341–351.

LEUNG, E., JOHNSTON, C.I. & WOODCOCK, E.A. (1985). An investigation of the receptors involved in the coronary vasodilatory effect of adenosine analogues. *Clin. Exp. Pharmacol. Physiol.*, **12**, 515–519.

LOHSE, M.J., KLOTZ, K.-N., LINDENBORN-FOTINOS, J., REDDINGTON, M., SCHWABE, V. & OLSSON, A. (1987). 8-Cyclopentyl-1,3-dipropylxanthine (DPCPX) – a selective high affinity radioligand for A_1 adenosine receptors. *Naunyn-Schmiedebergs. Arch. Pharmacol.*, **336**, 204–210.

MAYER, B., SCHMIDT, K., HUMBERT, P. & BOHME, E. (1989). Biosynthesis of endothelium-derived relaxing factors: a cytosolic enzyme in porcine aortic endothelial cells Ca^{2+}-dependently converts L-arginine into an activator of soluble guanylate cyclase. *Biochem. Biophys. Res. Commun.*, **164**, 678–685.

MONCADA, S., PALMER, R.M.J. & HIGGS, E.A. (1991). Nitric oxide: physiology, pathophysiology and pharmacology. *Pharmacol. Rev.*, **43**, 109–142.

MONCADA, S. & VANE, J.R. (1979). Pharmacology and endogenous roles of prostaglandin endoperoxides, thromboxane A_2 and prostacyclin. *Pharmacol. Rev.*, **30**, 293–331.

MOOS, W.H., SZOTEK, D.L. & BRUNS, R.F. (1985). N^6-Cycloalkyladenosines. Potent A_1-selective adenosine agonists. *J. Med. Chem.*, **28**, 1383.

NEES, S., HERZOG, V., BECKER, B.F., BÖCK, M., DES ROSIERS, C. & GERLACH, E. (1985). The coronary endothelium: a highly active metabolic barrier for adenosine. *Basic. Res. Cardiol.*, **80**, 515–529.

PALMER, R.M.J. & MONCADA, S. (1989). A novel citrulline-forming enzyme implicated in the formation of nitric oxide by vascular endothelial cells. *Biochem. Biophys. Res. Commun.*, **158**, 348–352.

PALMER, R.M.J., REES, D.D., ASHTON, D.S. & MONCADA, S. (1988). L-Arginine is the physiological precursor for the formation of nitric oxide in endothelium-dependent relaxation. *Biochem. Biophys. Res. Commun.*, **153**, 1251–1256.

REES, D.D., PALMER, R.M.J., SCHULZ, R., HODSON, H.F. & MONCADA, S. (1990). Characterization of three inhibitors of endothelial nitric oxide synthase *in vitro* and *in vivo*. *Br. J. Pharmacol.*, **101**, 746–752.

SCHMIDT, H.H.H.W., NAU, H., WITTPOHT, W., GERLACH, J., PRESCHER, K.-E., KLEIN, M.N., NIROOMAND, F. & BOHME, E. (1988). Arginine is a physiological precursor of endothelium-derived nitric oxide. *Eur. J. Pharmacol.*, **154**, 213–216.

SMITH, R.E.A., PALMER, R.M.J., BUCKNALL, C.A. & MONCADA, S. (1992). Role of nitric oxide synthesis in the regulation of coronary vascular tone in the isolated perfused rabbit heart. *Cardiovasc. Res.*, **26**, 508–512.

VANE, J.R. (1971). Inhibition of prostaglandin synthesis as a mechanism of action of aspirin like drugs. *Nature*, **231**, 232.

VIALS, A. & BURNSTOCK, G. (1992). Effects of nitric oxide synthase inhibitors L-N^G-nitroarginine and L-N^G-nitroarginine methyl ester on responses to vasodilators of the guinea-pig coronary vasculature. *Br. J. Pharmacol.*, **107**, 604–609.

WHITE, T.D. & ANGUS, J.A. (1987). Relaxant effects of ATP and adenosine on canine large and small coronary arteries *in vitro*. *Eur. J. Pharmacol.*, **143**, 119–126.

WILLIAMS, M. (1987). Purine receptors in mammalian tissues: pharmacology and functional significance. *Annu. Rev. Pharmacol. Toxicol.*, **27**, 315–345.

(Received September 28, 1992
Revised January 26, 1993
Accepted February 2, 1993)

Br. J. Pharmacol. (1993), **109**, 430–436 © Macmillan Press Ltd, 1993

Release of nitric oxide from glyceryl trinitrate by captopril but not enalaprilat: *in vitro* and *in vivo* studies

[1]Daniela Salvemini, [2]Alessandra Pistelli & *Vincenzo Mollace

The William Harvey Research Institute, St. Bartholomews Hospital Medical College, Charterhouse Square, London EC1M 6BQ and *Department of Biology, University of Rome Tor Vergata, Via orazio Raimondo, 00173 Rome, Italy

1 The hypotensive effects of glyceryl trinitrate (GTN, 0.5 mg kg^{-1}) but not of 3-morpholino-sydnonimine (SIN-1, 0.125 mg kg^{-1}) in anaesthetized rats were attenuated following a seven day (using a q.i.d. dosing schedule) oral treatment with isosorbide-5-mononitrate (IS-5-MN; 5 mg kg^{-1}) indicative of the induction of tolerance to GTN but not to SIN-1. The hypotensive effects of GTN did not decline when the sulphydryl (SH) containing angiotensin converting enzyme inhibitor (ACE-I), captopril (CPT, 5 mg kg^{-1}) or the structurally unrelated SH-containing, N-acetylcysteine (NAC, 10 mg kg^{-1}) but not the non-SH-containing ACE-I, enalaprilat (ENA, 5 mg kg^{-1}) were given together with IS-5-MN for the seven days treatment.

2 The attenuated hypotensive effects of GTN (0.5 mg kg^{-1}) in rats treated with IS-5-MN were also restored when CPT (1 mg kg^{-1}) or NAC (2.5 mg kg^{-1}) but not ENA (1 mg kg^{-1}) was administered intraperitoneally (i.p.) 30 min before GTN. Furthermore, in control rats, CPT or NAC but not ENA given i.p. 30 min before GTN, potentiated its haemodynamic effects. These effects were blocked by methylene blue (10 mg kg^{-1}). At the same doses, CPT or NAC did not affect the hypotensive effects of SIN-1.

3 The reduced ability of cultured tolerant smooth muscle cells (SMC, 24×10^3 cells) or endothelial cells (EC, 40×10^3 cells) to potentiate the anti-platelet effects of GTN (44 μM) was restored by CPT or NAC but not by ENA or glutathione (all at 0.5 mM). Potentiation of the anti-platelet effects of tolerant SMC or EC by CPT or NAC was abolished by co-incubation with oxyhaemoglobin (Oxy-Hb, 10 μM) indicative of nitric oxide (NO) formation.

4 When GTN (150–2400 μM) was incubated with CPT, NAC or glutathione but not ENA (all at 0.1 mM) for 30 min in Krebs buffer at 37°C a concentration-dependent increase in nitrite (NO_2^-) formation was observed.

5 The antiplatelet effects of GTN (5.5–352 μM) were potentiated by co-incubation with CPT or NAC but not with ENA or glutathione (all at 0.5 mM). The concentration of GTN required to inhibit platelet aggregation by 50% (IC_{50}) was 110 ± 2 μM for GTN alone, 14 ± 2 μM for GTN in the presence of NAC and 30 ± 2 μM for GTN in the presence of CPT. The potentiation of the effects of GTN by CPT or NAC was inhibited by co-incubation with Oxy-Hb (10 μM). By themselves, CPT or NAC did not inhibit platelet aggregation.

6 The ability of CPT to restore (a) the haemodynamic effects of GTN in tolerant rats and (b) the reduced capacity of tolerant SMC or EC to potentiate the anti-platelet effects of GTN is not related to its ACE inhibitory activity.

7 CPT also potentiated the hypotensive effects of GTN in non-tolerant rats, and *in vitro* CPT released NO from GTN in the absence of a GTN to NO converting cell, so that it is unlikely that reversal of tolerance by CPT is due to the replenishment of intracellular thiols. Rather it can be explained by the ability of CPT to release NO from GTN in the extracellular space. This extracellular formation of NO from GTN by CPT would then compensate for the impaired enzymic biotransformation of GTN to NO that develops during tolerance as was originally proposed for NAC.

Keywords: Glyceryl trinitrate; nitric oxide; tolerance; smooth muscle cells; endothelial cells; captopril; enalaprilat

Introduction

Glyceryl trinitrate (GTN) requires bioconversion to nitric oxide (NO) by various cells including smooth muscle cells (SMC) and endothelial cells (EC) in order to elicit vasodilatation (Ignarro *et al.*, 1981; Murad, 1986) and inhibition of platelet aggregation (Benjamin *et al.*, 1991; Salvemini *et al.*, 1992). This bioconversion is mediated by an enzyme not yet characterized (Chung & Fung, 1990; Feelisch & Kelm, 1991; Salvemini *et al.*, 1992). Enzymes such as the glutathione-S-transferase or cytochrome P_{450} which metabolize GTN in the liver or kidney (Needleman & Johnson, 1973; Yeates *et al.*, 1989; Servent *et al.*, 1989; Schröder & Schrör, 1992) are not involved in the biotransformation of GTN to NO by SMC or EC (Gruetter & Lemke, 1985; Sakanashi *et al.*, 1991; Salvemini *et al.*, 1993). One hypothesis explains the action of GTN by denitration followed by interaction in vascular smooth muscle cells with reduced sulphydryl (SH) groups (Needleman *et al.*, 1973) to form NO or a S-nitrosothiol (Ignarro *et al.*, 1981). The mechanism by which SH-containing molecules form NO from GTN is not known but may involve nucleophilic attack by thiolate anions on the nitrogen atom of the ester group of GTN (Feelisch, 1991).

The development of tolerance to nitrates in patients after continuous treatment for either chronic stable angina (Parker & Fung, 1984; Parker *et al.*, 1987) or congestive heart failure (Jordan *et al.*, 1985) is not completely understood. Desensitization of soluble guanylate cyclase or increased phosphodiesterase activity are not involved (see Ahlner *et al.*,

[1] Author for correspondence at present address: Monsanto Company, Department of Molecular Pharmacology, 800 North Lindbergh Boulevard, St. Louis, Missouri 63137, U.S.A.

[2] Present address: Department of Preclinical and Clinical Pharmacology 'M. Aiazzi Mancini', Viale G.B. Morgagni 65, 50134 Florence, Italy.

1991; Elkayam, 1991 for reviews). Elevation of catecholamines and plasma renin activity have been observed in GTN-tolerant patients (Packer *et al.*, 1981; 1987) suggesting that neurohormonal compensation may play a role. However, the most widely-held hypothesis to explain nitrate tolerance is based on the work of Needleman and coworkers who demonstrated that the induction of GTN tolerance *in vivo* and *in vitro* was associated with a reduction of intracellular thiols thereby limiting the bioconversion of GTN. This explanation is supported by the finding that thiols, such as N-acetylcysteine (NAC), prevent or reverse tolerance to GTN both in *in vivo* and *in vitro* (Needleman & Johnson, 1973; Packer *et al.*, 1987). In addition, thiol-containing angiotensin converting enzyme inhibitors (ACE-I), such as captopril (CPT), prevent the development of nitrate tolerance and potentiate GTN-mediated vasorelaxations (Halon *et al.*, 1988; de Graeff *et al.*, 1989; Lawson *et al.*, 1991). Although these experiments favour the concept that tolerance to GTN is due to loss of intracellular thiols, this concept is not universally accepted (see Ahler *et al.*, 1991; Elkayam, 1991 for reviews).

Clearly, at least in cultured SMC and EC, tolerance is the result of impaired enzymic bioconversion of GTN to NO (Brien *et al.*, 1986; Feelisch & Kelm, 1991; Salvemini *et al.*, 1993). In addition we have proposed that reversal of tolerance to GTN by thiols such as NAC could not be explained solely by replenishment of intracellular thiols, for NAC was able to form NO from GTN in Krebs buffer and in the absence of metabolizing cells. Thus reversal of tolerance to GTN by thiols such as NAC may simply be due to extracellular formation of NO from GTN which would in turn compensate for the reduced metabolism by the enzymatic pathway.

Long-term administration of isosorbide-5-mononitrate (IS-5-MN) *in vitro* and *in vivo* induces tolerance to GTN (this is the so-called cross-tolerance; see Ahlner *et al.*, 1991; Elkayam, 1991, for reviews). Here we have studied the effects of CPT, NAC or ENA on the *in vivo* responses to GTN after long-term treatment of rats with IS-5-MN. In addition, we have compared the effects of CPT, ENA or glutathione to those of NAC on the anti-platelet effects of GTN in the absence or presence of tolerant cultured SMC or EC and on NO_2^- production from GTN in Krebs buffer.

Methods

Preparation of washed platelets

Human washed platelets were prepared as described by Radomski & Moncada (1983). Indomethacin (10 μM) was added to the final platelet suspension to prevent the formation of cyclo-oxygenase products. The platelet count was adjusted to approximately $1.5-2 \times 10^8$ ml^{-1}.

Preparation of endothelial cells or smooth muscle cells

Bovine aortic EC were harvested and grown on cytodex 3 microcarrier beads (Pharmacia/LKB, Ltd.) in Dulbecco's modifed Eagle's medium (DMEM, Flow Laboratories) supplemented with 4 mM L-glutamine and 10% (v/v) foetal calf serum (Gibco) as described previously (de Nucci *et al.*, 1988). The approximate cell number was 3.5×10^7 ml^{-1} of beads. Bovine aortic SMC were characterized by the presence of specific alpha actin using a Sigma kit and were prepared as previously described (Mollace *et al.*, 1991a). Indomethacin (10 μM) was added to all final cell suspensions. In some experiments, GTN (600 μM) was incubated for 18 h with SMC or EC in culture (referred to as 'tolerant' cells; Salvemini *et al.*, 1993). The cell supernatant was removed and cells washed at least 3 times with warm Krebs buffer containing indomethacin (10 μM) before exposure to lower concentrations of GTN.

Platelet aggregation

A suspension of washed platelets was incubated at 37°C for 4 min in a Payton dual channel aggregometer (Born & Cross, 1963) with continuous stirring at 1,000 r.p.m. and then stimulated with thrombin (40 mu ml^{-1}) to give a submaximal aggregation (80–90%). The decrease in optical density was recorded for 5 min. After a 3 min incubation period with platelets, the inhibitory effects of GTN on platelet aggregation induced by thrombin were measured either alone or in the presence of captopril, NAC, glutathione, ENA or tolerant SMC or EC. When using cells of oxyhaemoglobin, the calibrations were performed in the presence of these agents to compensate for possible changes in light transmission (Salvemini *et al.*, 1989). Inhibition of platelet aggregation was calculated as described previously (Salvemini *et al.*, 1989).

Nitrite analysis

Nitrite (NO_2^-) was measured by the Griess reaction. GTN (150–2400 μM) was incubated in Krebs buffer containing SOD (100 u ml^{-1}) and CPT, NAC, glutathione or ENA (all at 0.1–1 mM). The samples were incubated in a shaking water bath for 30 min at 37°C and then allowed to react with the Griess reagent (1% sulphanilamide/0.1% naphthylethylenediamine dihydrochloride/2.5% H_3PO_4) to form a chromophore absorbing at 546 nm. Nitrite concentration was determined with sodium nitrite as a standard. Results are expressed as nmol NO_2^- ml^{-1} and each experiment was performed in triplicate.

In vivo *measurements*

Adult male Wistar Morini (S. Polo d'Enza, Reggio Emilia, Italy) normotensive rats (approx weight 200–300 g) were used throughout. The animals were divided into 2 groups: the first group received IS-5-MN (5 mg kg^{-1}) orally for 7 days using a q.i.d. dosing schedule treatment (08 h 00 min, 11 h 00 min, 14 h 00 min and 17 h 00 min) and the second group received saline at the same time periods. CPT (5 mg kg^{-1}), NAC (10 mg kg^{-1}) or ENA (5 mg kg^{-1}) were administered orally once daily (08 h 00 min) to a subgroup of IS-5-MN- or saline-treated rats. After 7 days, the animals were anaesthetized with sodium pentobarbitone (55 mg kg^{-1}) before surgical preparation. A catheter (PE50), filled with heparinized saline (200 u ml^{-1}) was inserted into the left common carotid artery to record blood pressure (BP) and heart rate (HR). The jugular vein was cannulated for i.v. injections of drugs. The animals were allowed to stabilize for at least 20 min after surgery. BP and HR were monitored on a Gemini polygraph via Bentley transducers (Ugo Basile, Comerio Vares, Italy). Each rat was used for only one dose of either GTN or SIN-1; GTN was given as a short 30 s infusion of 100 μl at a dose of 0.5 mg kg^{-1} (i.e. 1 mg kg^{-1} min^{-1}) and SIN-1 at 0.125 mg kg^{-1} (i.e. 0.25 mg kg^{-1} min^{-1}). In some experiments, CPT (1 mg kg^{-1}), NAC (2.5 mg kg^{-1}) or ENA (1 mg kg^{-1}) were given intraperitoneally to the IS-5-MN or saline-treated rats 30 min before the intravenous administration of GTN. When required methylene blue (MeB, 10 mg kg^{-1}, i.v.) was given 30 min before GTN or SIN-1. The mean arterial pressure (MAP) was calculated as the diastolic blood pressure plus one third of the pulse pressure. Results are expressed as changes in mean arterial pressure taken at the peak fall of the response (MAP changes, mmHg).

Materials

The composition of the modified (Sneddon & Vane, 1988) Krebs bicarbonate buffer was (mM): NaCl 137, KCl 2.7, $NaHCO_3$ 11.9, NaH_2PO_4 0.3, $MgSO_4$ 0.8, glucose 5.6, and $CaCl_2$ 1. Human thrombin, haemoglobin (from bovine

blood), N-acetylcysteine (NAC), reduced glutathione, superoxide dismutase (SOD, from bovine erythrocytes), indomethacin, sulfanilic acid, N-1-naphthylethylenediamine dihydrochloride, Na_2CO_3, sodium nitrite and kits for characterizing alpha smooth muscle actin (procedure number S1H903) were obtained from Sigma (Poole, Dorset). Phosphoric acid was obtained from BDH Analar (Essex). Oxyhaemoglobin (Oxy-Hb) was prepared by reduction of bovine haemoglobin with sodium hydrosulphite as described previously (Salvemini *et al.*, 1989). Glyceryl trinitrate (Nitronal) was obtained from Lipha Pharmaceuticals Ltd. (West Drayton, Middlesex). Prostacyclin was a gift from the Wellcome Research Laboratories (Beckenham, Kent), captopril a gift from Squibb (U.S.A.), enalaprilat (ENA) a gift from Sigma-Tau (Rome, Italy) and 3-morpholinosydnonimine (SIN-1) a gift from Hoeschst. For the *in vivo* experiments, pentobarbitone and N-acetyl-cysteine were obtained from Sigma (Milan, Italy), glyceryl trinitrate (Venitrin) from Simes (Milan, Italy) and isosorbide-5-mononitrate (Nitrosorbide) from Lusofarmaco (Milan, Italy).

Statistics

Results are expressed as mean ± s.e.mean for (n) experiments. The results were analysed by Student's unpaired t test to determine the significance of differences between means, or by a two-way analysis of variance (ANOVA) followed by a least significance procedure to determine the nature of this response. A P value of <0.05 was taken as significant.

Results

Haemodynamic responses to glyceryl trinitrate in non-treated rats or in rats treated with isosorbide-5-mononitrate

Baseline blood pressure and heart rate in rats receiving IS-5-MN (5 mg kg^{-1}) were not different from those receiving saline (102.0 ± 2.0 or 104.0 ± 3.2 mmHg for MAP and 380.0 ± 4.0 or 374 ± 5.2 b.p.m. for HR in animals receiving saline or IS-5-MN, $n = 10$). Intravenous administration of GTN (0.5 mg kg^{-1}) produced a fall in MAP in control rats (− 31 ± 2.8 mmHg, $n = 10$) which was larger than that seen in rats pretreated with IS-5-MN (− 12 ± 2.2 mmHg, $P<0.05$, $n = 5$; Figure 1a and b). Thus, the IS-5-MN treatment induced tolerance to the hypotensive action of GTN. CPT (5 mg kg^{-1}) or NAC (10 mg kg^{-1}) when given together with IS-5-MN for 7 days prevented the blunted hypotensive response to GTN (− 30.2 ± 3.2 mmHg or − 33.0 ± 3.6 mmHg for CPT- or NAC-treated rats, $n = 5$ for each group). However, ENA (5 mg kg^{-1}) did not prevent tolerance to GTN (− 18.0 ± 3.2 mmHg, $n = 4$). Chronic (7 days) administration of CPT, NAC or ENA did not affect resting blood pressure and heart rate ($n = 4$, data not shown). In control rats (non-treated with IS-5-MN), CPT, NAC or ENA treatment did not modify the fall in blood pressure elicited by verapamil (2 mg kg^{-1}, i.v.; from − 35 ± 4 to − 30 ± 2.5, − 36 ± 3 or − 38 ± 4 mmHg respectively, $n = 4$), phentolamine (0.5 mg kg^{-1}, i.v.; from − 42 ± 16 to − 38 ± 2.6, − 38 ± 3.1 or − 40 ± 3.2 mmHg respectively, $n = 4$) or SIN-1 (0.125 mg kg^{-1}; from − 32 ± 3 to − 35 ± 2, − 31 ± 3 or − 36 ± 3 mmHg respectively, $n = 4$). The haemodynamic changes obtained with verapamil, phentolamine or SIN-1 in rats treated with IS-5-MN were identical to those obtained in non-treated rats ($n = 4$, data not shown). CPT (1 mg kg^{-1}) or NAC (2.5 mg kg^{-1}), but not ENA (1 mg kg^{-1}) when given intraperitoneally 30 min before GTN restored the haemodynamic responses to GTN (0.5 mg kg^{-1}) in the IS-5-MN-treated rats (Figure 1b). The ability of CPT or NAC to restore the reduced responses to GTN in rats treated with IS-5-MN was abrogated by MeB (10 mg kg^{-1}, i.v.) (from − 34 ± 3 mmHg for GTN + CPT to − 6 ± 1.2 mmHg for GTN + CPT + MeB, $n = 4$, $P<0.05$ and from − 30 ± 2.5 mmHg for GTN + NAC to − 5 ± 2.1 mmHg for GTN + NAC + MeB, $n = 4$, $P<0.05$). In control, saline-treated rats, CPT (1 mg kg^{-1}) or NAC (2.5 mg kg^{-1}) but not ENA (1 mg kg^{-1}) when given i.p. 30 min before GTN (0.5 mg kg^{-1}) potentiated the haemodynamic responses to GTN (Figure 1b). This potentiating effect was abrogated by MeB (from − 45 ± 3 mmHg for GTN + CPT to − 2 ± 1 mmHg for GTN + CPT + MeB, $n = 4$, $P<0.05$ and from − 40 ± 4 mmHg for GTN + NAC to − 3 ± 1 mmHg for GTN + NAC + MeB, $n = 4$, $P<0.05$). MeB also attenuated the fall

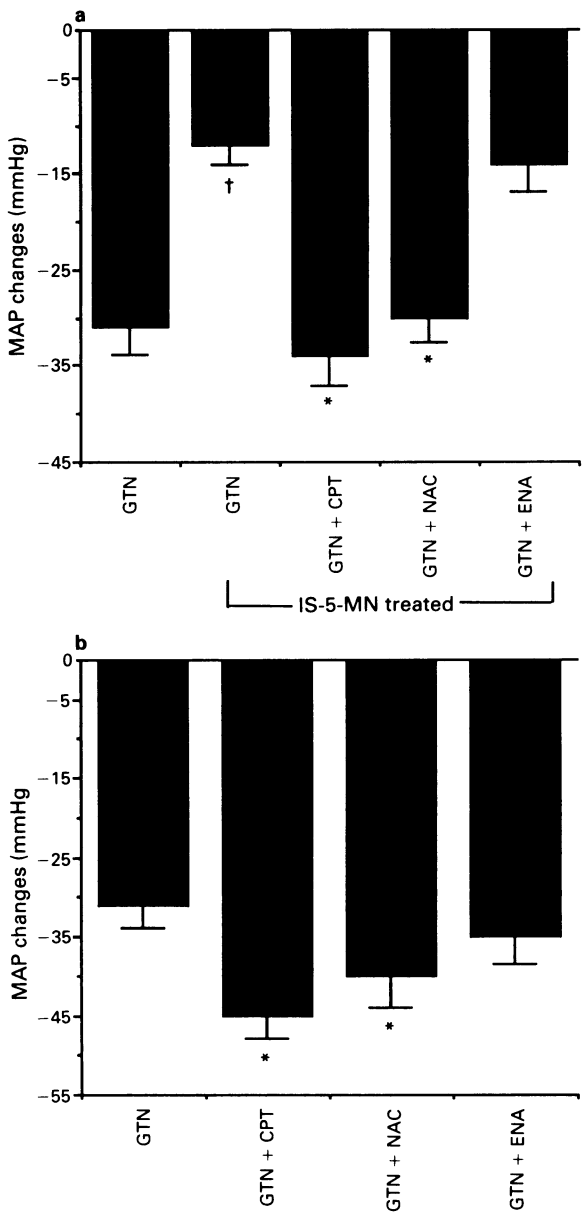

Figure 1 (a) The hypotensive effects of glyceryl trinitrate (GTN, 0.5 mg kg^{-1}) were reduced in rats rendered tolerant by treatment for seven days with isosorbide-5-mononitrate (IS-5-MN, 5 mg kg^{-1}). This effect was restored when captopril (CPT, 1 mg kg^{-1}) or N-acetylcysteine (NAC, 2.5 mg kg^{-1}) but not enalaprilat (ENA, 1 mg kg^{-1}) were given 30 min before the administration of GTN. (b) When given 30 min before GTN (0.5 mg kg^{-1}), CPT (1 mg kg^{-1}) or NAC (2.5 mg kg^{-1}) but not ENA (1 mg kg^{-1}) potentiated the hypotensive effects of GTN in control non-tolerant rats. The results are expressed as mean arterial pressure (MAP) changes (mmHg). Each point is the mean ± s.e.mean for the changes in five rats. *$P<0.05$ when compared to the values obtained in the absence of CPT, NAC or ENA. †$P<0.05$ when compared to the value obtained in control non-tolerant rats.

in blood pressure elicited by GTN (0.5 mg kg^{-1}; from -31 ± 2.8 mmHg to -12 ± 2 mmHg, $n = 5$, $P < 0.05$). At the doses used, CPT, NAC, ENA or MeB did not modify basal MAP (102 ± 2 mmHg for control rats, 102 ± 4 mmHg in the presence of CPT, 100 ± 4 mmHg in the presence of NAC, 106 ± 4 mmHg in the presence of ENA and 107 ± 3 mmHg in the presence of MeB).

Effects of captopril, N-acetylcysteine, glutathione or enalaprilat on nitrite production from glyceryl trinitrate

Exposure of GTN (150–2400 μM) to CPT, NAC or glutathione (0.1 mM) for 30 min led to a concentration-dependent increase in the formation of NO_2^- (Figure 2). Glutathione was more potent than CPT or NAC whereas CPT and NAC produced similar amounts of NO_2^- from GTN (Figure 2). Enalaprilat (1 mM) failed to release NO_2^- from GTN ($n = 4$, not shown). GTN, CPT, NAC or glutathione by themselves did not produce NO_2^-.

Comparison of the effects of captopril, glutathione or enalaprilat to those of N-acetylcysteine on the antiplatelet effect of glyceryl trinitrate in the absence or presence of tolerant SMC or EC

Salvemini *et al.* (1993) found that NAC (0.5 mM) when incubated for 3 min in the presence of platelets and GTN increased the anti-platelet effects of GTN (44 μM). Here, we compared the effects of NAC to those of CPT, ENA or glutathione and found that CPT (0.5 mM) potentiated, but to a lesser extent than NAC, the anti-platelet effects of GTN (5.5–352 μM) (Figure 3). The concentration of GTN required to inhibit platelet aggregation by 50% (IC_{50}) was 110 ± 2 μM for GTN alone, 30 ± 2 μM for GTN in the presence of CPT and 14 ± 2 μM for GTN in the presence of NAC ($n = 4$). Therefore, NAC enhanced 8 fold and CPT 4 fold the anti-platelet effect of GTN making NAC at least 2 fold more potent than CPT. Potentiation of the antiplatelet effects of GTN by CPT or NAC was abolished by co-incubation with OxyHb (10 M; Figure 3). By itself NAC or CPT (both at 0.5 mM) did not modify platelet aggregation induced by thrombin. Enalaprit or glutathione at a dose up to 2 mM failed to modify the inhibition of platelet aggregation by GTN (5.5–352 μM; $n = 4$, not shown). SMC or EC treated with GTN (600 μM) for 18 h became tolerant to GTN and lost their ability to potentiate the anti-platelet effects of GTN; this loss was restored by NAC (Salvemini *et al.*, 1993). In this study, loss of the potentiation of the anti-platelet effects of GTN (44 μM) by tolerant SMC (24×10^3 cells) or EC (40×10^3 cells) was restored by CPT but not by ENA or glutathione (all at 0.5 mM; Figure 4a and b). The effect of CPT was abolished by co-incubation with OxyHb (10 μM; Figure 4a and b).

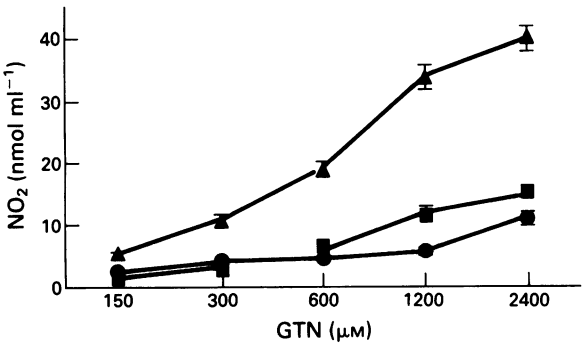

Figure 2 A 30 min exposure of glyceryl trinitrate (GTN, 150–2400 μM) in Krebs buffer at 37°C to 0.1 mM captopril (CPT, ●), N-acetylcysteine (NAC, ■) or glutathione (▲) produced a concentration-dependent increase in the formation of NO_2^-. Results are expressed in nmol NO_2^- ml^{-1}. GTN, CPT, NAC or glutathione alone did not produce NO_2^-. Each point is the mean ± s.e.mean of 3 experiments each performed in triplicate.

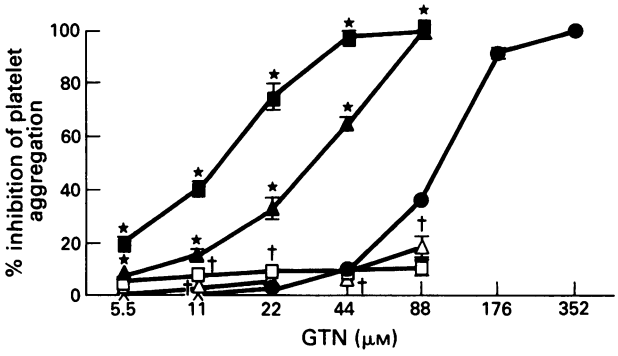

Figure 3 The antiplatelet effects of glyceryl trinitrate (GTN, 5.5–352 μM, ●) were potentiated by a 3 min co-incubation with captopril (CPT, ▲, 0.5 mM) or N-acetylcysteine (NAC, ■, 0.5 mM). Oxyhaemoglobin (OxyHb, 10 μM) abolished the potentiation of the antiplatelet effects of GTN by CPT (△) or NAC (□). Points represent the mean ± s.e.mean of 4 experiments. Results are expressed as % inhibition of platelet aggregation. *$P < 0.001$ for GTN + NAC vs GTN alone or for GTN + CPT vs GTN alone and †$P < 0.001$ for GTN + NAC + OxyHb vs GTN + NAC or GTN + CPT + OxyHb vs GTN + CPT. Statistical analysis was performed using the ANOVA test followed by a least significant test.

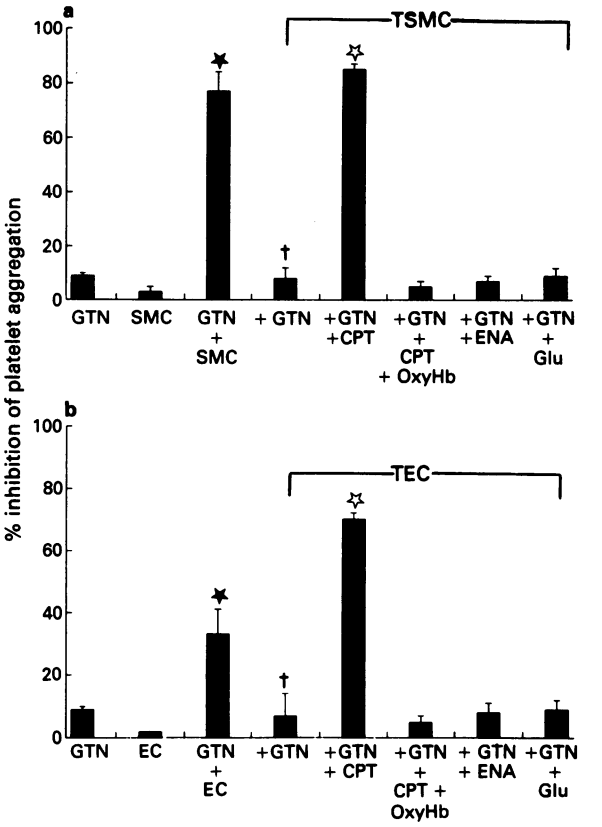

Figure 4 (a) Tolerant smooth muscle cells (TSMC, 24×10^3 cells) or (b) tolerant endothelial cells (TEC, 40×10^3 cells) did not potentiate the anti-platelet effects of glyceryl trinitrate (GTN, 44 μM). These effects were however potentiated when captopril (CPT) but not enalaprilat (ENA) or glutathione (Glu) (all at 0.5 mM) was co-incubated for 3 min with (a) TMSC and GTN or (b) TEC and GTN. This potentiation is abolished by oxyhaemoglobin (OxyHb, 10 μM). Platelet aggregation was initiated by thrombin (40 mu ml^{-1}). Each point is the mean ± s.e.mean of 4 experiments. *$P < 0.005$ when compared to the value obtained in the presence of GTN and non-tolerant SMC or EC if the effect was an additive one; †$P < 0.005$ when compared to the value obtained with GTN in the presence of non-tolerant SMC or EC and *$P < 0.005$ when compared to the value obtained with GTN in the presence of tolerant SMC or EC.

Discussion

It has been recognized for many years that the continuous administration of GTN or other organic nitrates such as IS-5-MN leads to the development of tolerance as evidenced by reduced vasodilator and anti-platelet effects of GTN, and that cross tolerance between GTN and IS-5-MN exists (Zelis & Mason, 1975; Thadani *et al.*, 1980). NAC partially reverses nitrate tolerance *in vitro* (Torresi *et al.*, 1985; Winniford *et al.*, 1986; Fung *et al.*, 1988; Lawson *et al.*, 1991) and *in vivo* as demonstrated by animal (Fung *et al.*, 1988; Boesgard *et al.*, 1991; Bauer & Fung, 1991) and human (Horowitz *et al.*, 1983) studies. In addition NAC potentiates the haemodynamic responses to GTN (Lawson *et al.*, 1991), restores the decreased anti-platelet responses to GTN during tolerance (Loscalzo, 1985; Folts *et al.*, 1989; Salvemini *et al.*, 1993) and increases the anti-platelet effects of GTN (Loscalzo, 1985; Salvemini *et al.*, 1993).

In the present study we have demonstrated that the development of tolerance to GTN in IS-5-MN treated rats can be restored by CPT or NAC when given together with the IS-5-MN during the seven day dosing period. The non-SH-containing ACE-I, ENA, failed to alter the development of tolerance. This supports previous studies which demonstrated that the beneficial effects of CPT were related to the presence of the SH-moiety and not to inhibition of ACE (van Gilst *et al.*, 1987; 1988; Cooke *et al.*, 1989; Lawson *et al.*, 1991). *In vitro*, the decreased ability of tolerant SMC or EC to potentiate the anti-platelet effects of GTN was restored by co-incubation with CPT or NAC but not by ENA. In addition, CPT or NAC but not ENA prevented the reduced haemodynamic effects of GTN in tolerant rats when given 30 min before GTN and they augmented the haemodynamic effects of GTN in saline-treated rats. SIN-1 releases NO spontaneously without metabolic activation (Feelisch, 1991). In the present study, the findings that neither NAC or CPT enhanced the hypotensive response of SIN-1 indicates that their *in vivo* effects on GTN are not likely to be due to increased survival of NO.

Incubation of cultured SMC or EC with high concentrations of GTN for 18 h leads to the development of tolerance as shown by reduced pharmacological and biochemical responses upon subsequent exposure to GTN (Salvemini *et al.*, 1993). Tolerance was found to be the result of impaired enzymic biotransformation of GTN to NO, and NAC by directly forming NO from GTN, compensating for this failing mechanism (Salvemini *et al.*, 1993). In the present study, the decreased ability of tolerant SMC or EC to potentiate the anti-platelet effects of GTN was restored by co-incubation with CPT but not ENA. The possibility that this reversal is due to replenishment of intracellular SH groups is unlikely, for CPT also increased the levels of NO_2^-. The potentiation by CPT in the absence or presence of tolerant SMC or EC was reversed by OxyHb indicating that an extracellular interaction between GTN and CPT took place with subsequent NO formation. Although the release of NO_2^- from GTN by CPT was similar to that by NAC, CPT was less effective in potentiating the anti-platelet effects of GTN. This indicates that CPT and NAC release the same amounts of NO_2^- but NAC releases more NO. Since in tolerant SMC or EC, the soluble guanylate cyclase (GC) activity is not affected (Kukowetz & Holzman, 1986; Mulsch *et al.*, 1988; Salvemini *et al.*, 1993), NO release from GTN by thiols would stimulate the soluble GC, increase the levels of cyclic GMP and restore both vasodilator and anti-platelet effects of GTN. This effect would compensate for the failing enzymatic mechanism that converts GTN to NO (Salvemini *et al.*, 1993).

Glutathione interacts with GTN to form NO_2^- which lacks biological activity (Feelisch, 1991). In our experiments we have demonstrated that although glutathione is more potent than CPT or NAC in releasing NO_2^-, it fails to potentiate the anti-platelet effects of GTN, indicating that glutathione does not form NO from GTN. In our study, the effects of various thiols on NO release from GTN indicate that a non-enzymic pathway exists for the bioconversion of GTN to NO and NO_2^-. This strengthens and supports earlier work by Feelisch and co-workers who demonstrated that, depending on the structure of the thiol used, two pathways independent of each other are involved in the formation of either NO or NO_2^-. Thus, although 54 different thiols were capable of releasing NO_2^- from GTN in aqueous solution only 3 (namely thiosalycylic acid, NAC and cysteine) were able to release NO as well (Feelisch & Noack, 1987; Feelisch *et al.*, 1988). From our study, CPT fits into the category of a non-enzymic releaser of NO from GTN. Our experiments also favour the concept that the higher the catalytic capacity of the thiol to form NO from GTN, the better their ability to counteract tolerance (Chung & Fung, 1991; Salvemini *et al.*, 1993).

The experiments presented in this study reinforce the concept that *in vitro* reversal of tolerance by thiols is due to a direct interaction between GTN and the thiol and that subsequent NO formation is required in order to prevent or reverse tolerance.

MeB an inhibitor of the soluble guanylate cyclase prevented the potentiating effects of NAC or CPT in control rats and prevented the ability of these thiol donors to restore the responses to GTN in tolerant rats. MeB does not prevent the hypotensive effects of verapamil or phentolamine which act in a NO-independent way (Salvemini *et al.*, 1993). This suggests that the effects of NAC or CPT on GTN responses *in vivo* involve release of NO from GTN which subsequently stimulates the soluble guanylate cyclase. Such possible mechanism of action is supported by the *in vitro* results. However, whether this is the exact mechanism by which NAC or CPT potentiate the effects of GTN or reverse GTN tolerance *in vivo* remains to be evaluated further.

The presence of an SH group on CPT is responsible for the superoxide anion scavenging properties attributed to CPT (Goldschmidt & Tallarida, 1991). In this way, CPT preserves or enhances the biological activity of NO and prostacyclin released from the endothelium (Mollace *et al.*, 1991b), the actions of which can be affected by superoxide anions (see Salvemini & Botting, 1990 for review) generated during reperfusion of ischaemic tissues. This, together with the fact that CPT releases NO directly from the molecule of GTN and thus enhances the haemodynamic and anti-platelet effects of GTN, indicates that CPT may confer particular therapeutic benefits on patients with ischaemic heart disease or congestive heart failure who are undergoing concomitant therapy with GTN. It should, however, be kept in mind that since plasma levels of the ACE-I used in this study were not measured, extrapolation from *in vitro* to *in vivo* should be made with some caution.

This work was supported by a grant from Glaxo Research Ltd. We thank Dr R. Botting for editorial help and L. Wood for culturing the cells used in this study.

References

AHLNER, J., ANDERSSON, R.G.G., TORFGARD, K. & AXELSSON, K.L. (1991). Organic nitrate esters: clinical use and mechanisms of actions. *Pharmacol. Rev.*, **43**, 351–423.

BAUER, J.A. & FUNG, H.L. (1991). Differential hemodynamic effects and tolerance properties of nitroglycerin and S-nitrosothiol in experimental heart failure. *J. Pharmacol. Exp. Ther.*, **256**, 249–254.

BENJAMIN, N., DUTTON, J.A.E. & RITTER, J.M. (1991). Human vascular smooth muscle cells inhibit platelet aggregation when incubated with glyceryl trinitrate: evidence for generation of nitric oxide. *Br. J. Pharmacol.*, **102**, 847–851.

BOESGAARD, S., PETERSEN, J.S., ALDERSHVILE, J., POULSEN, H.E. & FLACHS, H. (1991). Nitrate tolerance: effect of thiol supplementation during prolonged nitroglycerin infusion in an in vivo rat model. *J. Pharmacol. Exp. Ther.*, **258**, 851–856.

BORN, G.V.R. & CROSS, M.J. (1963). The aggregation of blood platelets. *J. Physiol.*, **168**, 178–195.

BRIEN, J.F., MCLAUGHLIN, B.E., BREEDON, T.H., BENNET, B.M., NAKATSU, K. & MARKS, G.S. (1986). Biotransformation of glyceryl trinitrate occurs concurrently with relaxation of rabbit aorta. *J. Pharmacol. Exp. Ther.*, **237**, 608–614.

CHUNG, S.J. & FUNG, H.L. (1990). Identification of the subcellular site for nitroglycerin metabolism to nitric oxide in bovine coronary smooth muscle cells. *J. Pharmacol. Exp. Ther.*, **253**, 614–619.

COOKE, J.P., ANDON, N. & LOSCALZO, J. (1989). S-nitrosocaptopril II: effects on vascular reactivity. *J. Pharmacol. Exp. Ther.*, **249**, 730–734.

DE GRAEFF, P.A., DE LEEUW, M.J., VAN GILST, W.H. & WESSELING, H. (1989). Antianginal effects of captopril during chronic nitrate treatment. *Circulation*, **80**, II11–II14.

DENUCCI, G., GRYGLEWSKI, R.J., WARNER, T.D. & VANE, J.R. (1988). Receptor-mediated release of endothelium-derived relaxing factor and prostacyclin from bovine aortic endothelial cells is coupled. *Proc. Natl. Acad. Sci. U.S.A.*, **85**, 2334–2338.

ELKAYAM, U. (1991). Tolerance to organic nitrates: evidence, mechanisms, clinical relevance and strategies for prevention. *Ann. Intern. Med.*, **114**, 667–677.

FEELISCH, M. (1991). The biochemical pathways of nitric oxide formation from vasodilators: appropriate choice of exogenous NO donors and aspects of preparation and handling of aqueous NO solutions. *J. Cardiovasc. Pharmacol.*, **17**, S25–S33.

FEELISCH, M. & KELM, M. (1991). Biotransformation of organic nitrates to nitric oxide by vascular smooth muscle and endothelial cells. *Biochem. Biophys. Res. Commun.*, **180**, 286–293.

FEELISCH, M. & NOACK, E.A. (1987). Correlation between nitric oxide formation during degradation of organic nitrates and activation of guanylate cyclase. *Eur. J. Pharmacol.*, **139**, 19–30.

FEELISCH, M., NOACK, E. & SCHRODER, H. (1988). Explanation of the discrepancy between the degree of organic nitrate decomposition, nitrite formation and guanylate cyclase stimulation. *Eur. Heart J.*, **9**, 57–62.

FOLTS, J.D., STAMLER, J. & LOSCALZO, J. (1989). N-acetylcysteine potentiates intravenous nitroglycerin in inhibiting periodic platelet thrombus formation in stenosed dog coronary arteries. *J. Am. Coll. Cardiol.*, **13**, 145A.

FUNG, H.L., CHONG, S., KOWALUK, E., HOUGH, K. & KAKEMI, M. (1988). Mechanisms for the pharmacologic interaction of organic nitrates with thiols. Existence of an extracellular pathway for the reversal of nitrate vascular tolerance by N-acetylcysteine. *J. Pharmacol. Exp. Ther.*, **245**, 524–530.

GOLDSCHMIDT, J.E. & TALLARIDA, R.J. (1991). Pharmacological evidence that captopril possesses an endothelium-mediated component of vasodilatation: effect of sulfhydryl groups on endothelium-derived relaxing factor. *J. Pharmacol. Exp. Ther.*, **257**, 1136–1145.

GRUETTER, C.A. & LEMKE, S.M. (1985). Dissociation of cysteine and glutathione levels from nitroglycerin-induced relaxation. *Eur. J. Pharmacol.*, **111**, 85–95.

HALON, D.A., ROSENFELD, T., HARDOFF, R. & LEWIS, B.S. (1988). Advantage of combined therapy with captopril and nitrates in severe congestive heart failure. *Isr. J. Med. Sci.*, **24**, 664–670.

HOROWITZ, J.D., ANTMAN, E.M., LORELL, B.H., BARRY, W.H. & SMITH, T.W. (1983). Potentiation of the cardiovascular effects of nitroglycerin by N-acetylcysteine. *Circulation*, **68**, 1247–1253.

IGNARRO, L.J., LIPPTON, H., EDWARDS, J.C., BARICOS, W.H., HYMAN, A.L., KADOWITZ, P.J. & GRUETTER, C.A. (1981). Mechanism of vascular smooth muscle relaxation by organic nitrates, nitrites, nitroprusside and nitric oxide: evidence for involvement of S-nitrosothiols as active intermediates. *J. Pharmacol. Exp. Ther.*, **218**, 739–749.

JORDAN, R.A., SETH, L., HENRY, D.A., WILEN, M.M. & FRANCIOSA, J.A. (1985). Dose requirements and hemodynamic effects of transdermal nitroglycerin compared with placebo in patients with congestive heart failure. *Circulation*, **71**, 980–986.

KUKOVETZ, W.R. & HOLZMANN, S. (1986). Mode of action of nitrates with regard to vasodilatation and tolerance. *Z. Kardiol.*, **75** Suppl. 3, 8–11.

LAWSON, D.L., NICHOLS, W.W., MEHTA, P. & MEHTA, J.L. (1991). Captopril-induced reversal of nitroglycerin tolerance: role of sulfhydryl group vs ACE-inhibitory activity. *J. Cardiovasc. Pharmacol.*, **17**, 411–418.

LOSCALZO, J. (1985). N-acetylcysteine potentiates inhibition of platelet aggregation by nitroglycerin. *J. Clin. Invest.*, **76**, 703–708.

MOLLACE, V., SALVEMINI, D., ANGGARD, E. & VANE, J. (1991a). Nitric oxide from vascular smooth muscle cells: regulation of platelet reactivity and smooth muscle cells guanylate cyclase. *Br. J. Pharmacol.*, **104**, 633–638.

MOLLACE, V., SALVEMINI, D., SESSA, W.C. & VANE, J.R. (1991b). Inhibition of human platelet aggregation by endothelium-derived relaxing factor, sodium nitroprusside or iloprost is potentiated by captopril and reduced thiols. *J. Pharmacol. Exp. Ther.*, **258**, 820–823.

MULSCH, A., BUSSE, R. & BASSENGE, E. (1988). Desensitization of guanylate cyclase in nitrate tolerance does not impair endothelium-dependent responses. *Eur. J. Pharmacol.*, **158**, 191–198.

MURAD, F. (1986). Cyclic guanosine monophosphate as a mediator of vasodilation. *J. Clin. Invest.*, **78**, 1–5.

NEEDLEMAN, P. & JOHNSON, E.M. JR. (1973). Mechanism of tolerance development to organic nitrates. *J. Pharmacol. Exp. Ther.*, **84**, 709–715.

NEEDLEMAN, P., JAKSCHIK, B. & JOHNSON, E.M. JR. (1973). Sulphydryl requirement for relaxation of vascular smooth muscle. *J. Pharmacol. Exp. Ther.*, **187**, 324–331.

PACKER, M., LEE, W.H., KESSLER, P.D., GOTTLIEB, S.S., MEDINA, N. & YUSHAK, M. (1987). Prevention and reversal of nitrate tolerance in patients with congestive heart failure. *N. Engl. J. Med.*, **317**, 799–804.

PACKER, M., MELLER, J., MEDINA, N., YUSHAK, M. & GORLIN, R. (1981). Determinants of drug response in severe chronic heart failure. 1. Activation of vasoconstrictor forced during vasodilator therapy. *Circulation*, **64**, 506–514.

PARKER, J.O. & FUNG, H.L. (1984). Transdermal nitroglycerin in angina pectoris. *Am. J. Cardiol.*, **54**, 471–476.

PARKER, J.O., FARRELL, B., LAHEY, K.A. & ROSE, B.F. (1987). Nitrate tolerance: the lack of effect of N-acetylcysteine. *Circulation*, **76**, 572–576.

PURI, R.N. & MEISTER, A. (1983). Transport of glutathione, as gamma-glutamylcysteinylglycyl ester into liver and kidney. *Proc. Natl. Acad. Sci. U.S.A.*, **80**, 5258–5260.

RADOMSKI, M.W. & MONCADA, S. (1983). An improved method for the washing of human platelets with prostacyclin. *Thromb. Res.*, **30**, 383–389.

SAKANASHI, M., MATSUZAKI, T. & ANIYA, Y. (1991). Nitroglycerin relaxes coronary artery of the pig with no change in glutathione content of glutathione S-transferase activity. *Br. J. Pharmacol.*, **103**, 1905–1908.

SALVEMINI, D. & BOTTING, R. (1990). The effect of free radical scavengers on platelet adhesion and aggregation. In *Drug News and Perspectives*. ed. Prous, J.R. Science Publishers, **3**, 202–212.

SALVEMINI, D., DE NUCCI, G., GRYGLEWSKI, R.J. & VANE, J.R. (1989). Human neutrophils and mononuclear cells inhibit platelet aggregation by releasing a nitric oxide-like factor. *Proc. Natl. Acad. Sci. U.S.A.*, **86**, 6328–6332.

SALVEMINI, D., MOLLACE, V., PISTELLI, A., ANGGARD, E. & VANE, J. (1992). Metabolism of glyceryl trinitrate to nitric oxide by endothelial cells and smooth muscle cells and its induction by E. coli lipopolysaccharide. *Proc. Natl. Acad. Sci. U.S.A.*, **89**, 982–986.

SALVEMINI, D., PISTELLI, A. & VANE, J. (1993). Conversion of glyceryl trinitrate to nitric oxide in tolerant and non-tolerant smooth muscle and endothelial cells. *Br. J. Pharmacol.*, **108**, 162–169.

SCHRÖDER, H. & SCHRÖR, K. (1992). Cytochrome P_{450} mediates bioactivation of glyceryl trinitrate in cultured cells. In *'Biology of Nitric Oxide'* ed. Moncada, S., Marletta, M., Hibbs, H. Jr. & Higgs, E.A. London: Portland Press.

SERVENT, D., DELAFORGE, M., DUCROCQ, C., MANSUY, D. & LENFANT, M. (1989). Nitric oxide formation during microsomal hepatic degradation of glyceryl trinitrate: involvement of cytochrome P_{450}. *Biochem. Biophys. Res. Commun.*, **163**, 1210–1216.

SNEDDON, J.M. & VANE, J.R. (1988). Endothelium-derived relaxing factor reduces platelet adhesion to bovine endothelial cells. *Proc. Natl. Acad. Sci. U.S.A.*, **85**, 2800–2804.

THADANI, U., MANYARI, D., PARKER, J.O. & FUNG, H.L. (1980). Tolerance to the circulatory effects of oral isosorbide dinitrate. Rate of development and cross tolerance to glyceryl trinitrate. *Circulation*, **61**, 526–535.

TORRESI, J., HOROWITZ, J.D. & DUSTING, G.J. (1985). Prevention and reversal of tolerance to nitroglycerine with N-actylcysteine. *J. Cardiovasc. Pharmacol.*, **7**, 777–783.

VAN GILST, W.H., DE GRAEFF, P.A., SCHOLTENS, E., DE LANGEN, C.D.J. & WESSELING, H. (1987). Potentiation of isosorbide dinitrate-induced coronary dilatation by captopril. *J. Cardiovasc. Pharmacol.*, **9**, 254–255.

VAN GILST, W.H., SCHOLTENS, E., DE GRAEFF, P.A., DE LANGEN, C.D.J. & WESSELING, H. (1988). Differential influences of angiotensin converting-enzyme inhibitors on the coronary circulation. *Circulation*, **77**, I24–29.

WINNIFORD, M.D., KENNEDY, P.L., WELLS, P.J. & HILLIS, L.D. (1986). Potentiation of nitroglycerin-induced coronary dilatation by N-acetylcysteine. *Circulation*, **73**, 138–142.

YEATES, R.A., SCHMID, M. & LEITOLD, M. (1989). Antagonism of glyceryl trinitrate activity by an inhibitor of glutathione S-transferase. *Biochem. Pharmacol.*, **38**, 1749–1753.

ZELIS, R. & MASON, D.T. (1975). Isosorbide dinitrate. Effect on the vasodilator response to nitroglycerin. *J. Am. Med. Assoc.*, **234**, 166–170.

(Received August 17, 1992
Revised January 27, 1993
Accepted February 2, 1993)

Br. J. Pharmacol. (1993), **109**, 437–442 © Macmillan Press Ltd, 1993

Changes in [^{3}H]-PK 11195 and [^{3}H]-8-OH-DPAT binding following forebrain ischaemia in the gerbil

[1]B.A. Kenny, A.C. MacKinnon, [2]Michael Spedding & [3]Christine M. Brown

Department of Pharmacology, Syntex Research Centre, Heriot-Watt University Research Park, Riccarton, Edinburgh. EH14 4AP

1 A high density of [^{3}H]-PK 11195 binding sites was present in gerbil cortical membranes (B_{max} [^{3}H]-PK 11195 1360 ± 71 fmol mg^{-1} protein) in comparison to rat cortical membranes (254 ± 21 fmol mg^{-1} protein). This effect was species-specific as similar findings were obtained with hippocampal membranes (B_{max} 1430 ± 111 fmol mg^{-1} protein in gerbil, compared to 196 ± 31 in rat).

2 RO 5-4864, also a peripheral type benzodiazepine compound, displayed low affinity for the [^{3}H]-PK 11195 site in the gerbil (pK_i 6.57 ± 0.02 and 6.70 ± 0.12 in hippocampus and cortex respectively) compared to rat (pK_i 8.16 ± 0.07 and 8.48 ± 0.02). Central benzodiazepine compounds, diazepam and flunitrazepam, also displayed this trend.

3 RO 5-4864 displaced [^{3}H]-PK 11195 binding from gerbil and rat cortical membranes through a competitive interaction with Hill slopes close to unity. In both tissues, saturation isotherms of [^{3}H]-PK 11195 binding indicated that the presence of RO 5-4864 caused changes in K_d without any effect on B_{max}. In kinetic experiments, the presence of RO 5-4864 failed to modify the rate of dissociation of [^{3}H]-PK 11195 from equilibrium in both rat and gerbil cortical membranes.

4 Forebrain ischaemia in the Mongolian gerbil (5 min bilateral carotid artery occlusion) with 7 days recovery caused a significant ($P<0.05$) decrease in the density of hippocampal 5-HT$_{1A}$ binding sites labelled by [^{3}H]-8-OH-DPAT (B_{max} control, 393 ± 33 fmol mg^{-1} protein; ischaemic, 289 ± 21 fmol mg^{-1} protein) and an increase ($P<0.01$) in [^{3}H]-PK 11195 binding sites (B_{max} control, 1430 ± 111 fmol mg^{-1} protein; ischaemic, 2160 ± 170 fmol mg^{-1} protein). Ischaemia and recovery had no effect on the affinity of either ligand.

5 Autoradiography experiments in gerbil brain sections revealed that the ischaemia-induced increase in [^{3}H]-PK 11195 binding was consistent and significant in the CA$_1$ subfield on the hippocampus (control, 152 ± 42 fmol mg^{-1} tissue; ischaemic, 314 ± 43 fmol mg^{-1} tissue).

Keywords: [^{3}H]-PK 11195; [^{3}H]-8-OH-DPAT; hippocampus; forebrain ischaemia; gerbil

Introduction

The Mongolian gerbil (*Meriones unguiculatus*) has been extensively used as an experimental model of cerebral ischaemia, the majority of animals being predisposed to complete forebrain ischaemia due to a lack of posterior communicating arteries (Levine & Payan, 1966; Kahn, 1972). Histological studies have demonstrated that following bilateral occlusion of the common carotid arteries for 5 min and recovery beyond 72 h, selective neuronal loss of pyramidal cells in the CA$_1$ subfield of the hippocampus occurs (Kirino, 1982). This phenomenon of delayed neuronal death is now well documented (Kirino, 1982; Pulsinelli *et al.*, 1982; Kirino & Sano, 1984a), the protection of which has been demonstrated by a variety of putative neuroprotective agents (Gill *et al.*, 1987; Foster *et al.*, 1988; Alps *et al.*, 1988). In addition to neuronal cell death, cerebral ischaemia results in the proliferation of astrocytes and glia (reactive gliosis) and an invasion of macrophages into ischaemic brain tissue (Dolman, 1986). The cell types, in particular microglia, have been shown to possess a high density of peripheral type benzodiazepine (PTB) binding sites in comparison to healthy neurones (Syapin & Skolnick, 1979; Zavala & Lenfant, 1987; Benavides *et al.*, 1988). PTB binding sites have since been classified as ω_3, to distinguish them from the sites of action of centrally acting benzodiazepines (Langer & Arbilla, 1988). Whilst termed peripheral, sites for these agents are located throughout the CNS, but are distinct from the site of action of centrally acting agents in terms of their pharmacology, subcellular and anatomical distribution (Benavides *et al.*, 1983; Anholt *et al.*, 1986) and although their function is unclear, a role in the regulation of mitochondrial function in neuronal cells has been postulated (Anholt, 1986; Larcher *et al.*, 1989).

Previous studies have indicated that in neuronal disease states associated with macrophage invasion and proliferation of glia and astrocytes, the selective ω_3 ligands [^{3}H]-PK 11195 and [^{3}H]-RO 5-4864 may be useful markers of neuronal damage. Intrastriatal injection of excitotoxic compounds has been shown to increase the density of ω_3 sites in the rat (Benavides *et al.*, 1987; Dubois *et al.*, 1988). The level of ω_3 sites has also been shown to be markedly elevated following focal ischaemia in the cat and rat (Dubois *et al.*, 1988) and in the mouse (Gotti *et al.*, 1989; Kenny *et al.*, 1992). Furthermore, it has been postulated that ω_3 ligands may be sensitive indicators of neuronal disease states such as multiple sclerosis and cerebrovascular disease in man (Benavides *et al.*, 1988).

In this paper we have characterized the binding properties of [^{3}H]-PK 11195 in gerbil brain and have examined the effect of brief forebrain ischaemia on binding site parameters. For comparison we have also examined the effect of ischaemia on 5-HT$_{1A}$ receptors labelled by [^{3}H]-8-hydroxy-2-(di-n-propylamino)tetralin ([^{3}H]-8-OH-DPAT) as evidence indicates that a high density of these receptors exist on pyramidal cells in the CA$_1$ region of the hippocampus (Pazos & Palacios, 1985). Thus, we have examined the effect of ischaemia on neuronal and non-neuronal cells in the hippocampus. Some of these data have previously been published in abstract form (Kenny *et al.*, 1990).

[3] Author for correspondence.
Present address: [1]Pfizer Central Research, Sandwich, Kent, CT13 9NJ; [2]Institut de Recherches Servier, 92150 Suresnes, Paris, France.

Methods

Forebrain ischaemia in the gerbil

Adult male gerbils (*Meriones unguiculatus*; Tumblebrook Farms) weighing 60–80 *g* were anaesthetised with 5% halothane (Halothane, BP, May & Baker, Dagenham, Essex) in a 70% nitrous oxide/30% oxygen gas mixture. Halothane was then reduced to 1.5–2.0% and maintained at this level throughout remaining surgical procedures. The left and right common carotid arteries were exposed through a midline paratracheal incision, freed of connective tissue and the vago-sympathetic nerve trunks, and simultaneously occluded with microvascular clips (Ackland C2V, Weiss, London) for 5 min. Following release of the artery clips the wound was dusted with antibiotic powder and surgically closed. On regaining consciousness (less than 2 min) the animals were caged singly with free access to food and water. Animals were recovered for a period of 7 days, decapitated, and the hippocampus and cerebral cortex dissected free from the rest of the brain over ice and stored in liquid nitrogen until prepared for assay. Sham-operated animals were subject to identical procedures with the exception of artery occlusion.

Ligand binding assays

[^{3}H]-8-OH-DPAT binding in gerbil hippocampus Hippocampal tissue was homogenized (Polytron, setting 10, two bursts of 10 s duration) in ice cold 50 mM Tris-HCl (pH 7.4 at 4°C) and centrifuged at 48,000 *g* for 15 min. The resulting pellet was resuspended at 50 mM Tris-HCl and the homogenization and centrifugation steps repeated three times. The final pellet was resuspended in 50 mM Tris HCl (pH 7.4) containing 5 mM $MgSO_4$ and 0.5 mM EDTA, and stored in liquid nitrogen prior to assay. Aliquots of membrane homogenate (assayed in triplicate, 300 μg protein per assay) were incubated in 50 mM Tris-HCl (pH 7.4) containing 5 mM $MgSO_4$, 0.5 mM EDTA, with [^{3}H]-8-OH-DPAT (0.2–12 nM) for 10 min at 37°C in a total volume of 2.0 ml. Non-specific binding was determined in the presence of 3.0 μM buspirone. Membrane bound radioligand was recovered by vacuum filtration over Whatman GF/B glass fibre filters. The filters were washed twice with buffer and bound radioactivity determined by liquid scintillation counting.

[^{3}H]-PK 11195 binding in rat and gerbil hippocampus and cerebral cortex Hippocampal and cortical tissue was homogenized (Polytron, setting 10, two bursts of 10 s duration) in ice cold 50 mM Tris HCl (pH 7.4 at 4°C) and centrifuged as described above. The final pellet was resuspended in 50 mM Tris-HCl and stored in liquid nitrogen until required for assay.

Aliquots of membrane homogenate (30–60 μg protein per assay) were incubated in 50 mM Tris-HCl (pH 7.4 at 25°C) with 0.01–2.0 nM [^{3}H]-PK 11195 (0.2 nM for competition studies) for 30 min at 25°C in a total volume of 1.0 ml. Non-specific binding was determined in the presence of 10 μM RO 5-4864. Assay protein was determined with BSA protein assay reagent (Pierce, UK).

In vitro *receptor autoradiography*

Following 7 days recovery gerbil brains were rapidly removed and placed in isopentane maintained at − 50°C. Brains were then mounted onto orientating microtome chucks with Tissue Tek and embedded in Lipshaw Embedding Matrix. Frozen brains were equilibrated at − 30°C for 20 min in a cryostat prior to sectioning. Sections were cut at 20 μm and thaw mounted onto slides previously subbed in 1% gelatin, 0.05% chromic potassium sulphate and dried. Sections were cut in the rostrocaudal plane and stored dessicated at − 20°C for 48–72 h.

Sections were preincubated in 0.17 M Tris-HCl buffer for 30 min and then in buffer containing 1.0 nM [^{3}H]-PK 11195 for 45 min at 25°C. Parallel sections were incubated in the presence of 10 μM RO 5-4864 to define non-specific binding. Following the incubation period, sections were washed for 5 min in ice-cold 0.17 M Tris HCl and then briefly dipped in ice-cold distilled water to remove salts and facilitate drying under a stream of cold air for 60 min. Sections were then dried at room temperature overnight and exposed in X-ray cassettes with ^{3}H-sensitive Hyperfilm (Amersham plc) for 6 weeks at 4°C, before development and fixation. ^{3}H radiolabelled brain sections were analysed quantitatively by a Quantimet-970 image analysis system.

Drugs and chemicals

The following drugs were used: PK 11195 (1-(2-chlorophenyl-*N*-methyl-*N*-(1-methylpropyl)-3-isoquinolinecarboxamide) and RO 5-4864 (7-chloro-1,3-dihydro-1-methyl-5- (*p*-chlorophenyl)-2H-1,4-benzodiazepine-2-one) were synthesized by the Chemistry department (Recherche Syntex France, Paris) and buspirone was synthesized by the Institute of Organic Chemistry (Syntex, Palo Alto, U.S.A.). [^{3}H]-8-OH-DPAT (140 Ci mmol^{-1}) and [^{3}H]-PK 11195 (83 Ci mmol^{-1}) were obtained from DuPont UK Ltd. Dipyridamole was obtained from Boehringer Ingelheim Ltd. Diazepam, flunitrazepam and all other chemicals were obtained from Sigma at the highest grade available. Drug solutions were prepared daily, as stock solutions of 1 mM in ethanol or distilled water. Subsequent dilutions were made in the appropriate assay buffer.

Data analysis

Equilibrium binding parameters (K_d and B_{max}) were obtained with the non-linear least square curve fitting programme 'LIGAND' (Munson & Rodbard, 1980). Inhibition of specific binding by competing drugs were analysed by a non-linear least squares fitting programme capable of defining IC_{50} (concentration of drug displacing 50% specific binding) and the Hill slope of the displacement curve. The IC_{50} was converted to pK_i by the equation of Cheng & Prusoff (1973): $pK_i = IC_{50}/(1 + [L]/K_d)$ where [L] represents free radioligand concentration and K_d represents the equilibrium dissociation constant.

In kinetic experiments dissociation rate was determined from the slope of the plot ln Bt/Be against time, where Be is specific binding at equilibrium and Bt is specific binding at time t.

Data were tested for significance by Student's unpaired *t* test and significance taken at $P < 0.05$.

Results

Pharmacological specificity

In cortical and hippocampal membrane homogenates from both rat and gerbil, [^{3}H]-PK 11195 binding was of high affinity, rapid, saturable and reversible. At 25°C the $t_{1/2}$ for association was <2.0 min. In both hippocampal and cerebrocortical membranes a greater number of binding sites was labelled in gerbil tissue than in the rat, although all sites were labelled with similar affinity (Table 1). In displacement studies, sites labelled by [^{3}H]-PK 11195 in both rat and gerbil membranes showed selectivity for PK 11195 (Table 2). The structurally related PTB compound RO 5-4864 inhibited [^{3}H]-PK 11195 binding in rat hippocampus with nanomolar affinity but was more than a log order less potent in gerbil hippocampus. This effect appeared to be species-specific as the selectivity expressed in cortical membranes was even greater (pK_i 8.48 in rat; pK_i 6.70 in gerbil). Centrally acting benzodiazepines displayed lower affinity for this site (rank order: PK 11195 > RO 5-4864 > diazepam > flunitrazepam)

Table 1 Saturation binding parameters in rat and gerbil brain

	Hippocampus	
	Rat	*Gerbil*
K_d (nM)	0.26 ± 0.03	0.31 ± 0.02
B_{max} (fmol mg^{-1} protein)	196 ± 31	1430 ± 111
	Cerebral Cortex	
	Rat	*Gerbil*
K_d (nM)	0.21 ± 0.05	0.17 ± 0.02
B_{max} (fmol mg^{-1} protein)	254 ± 21	1360 ± 71

Saturation binding parameters for [^{3}H]-PK 11195 in gerbil and rat hippocampal and cerebral cortical membrane homogenates were determined over the concentration range (0.01–2.0 nM) and equilibrium binding parameters, determined as in Methods. The data represent the mean ± s.e. mean of at least 4 experiments.

Table 2 Affinities of central and peripheral type benzodiazepine compounds for the [^{3}H]-PK 11195 binding site in rat and gerbil brain

	Hippocampus			
	Rat		*Gerbil*	
Compound	pK_i	nH	pK_i	nH
PK 11195	8.90 ± 0.06	0.83	9.06 ± 0.11	1.05
RO 5-4864	8.16 ± 0.07	0.96	6.57 ± 0.02	0.97
Dipyridamole	7.24 ± 0.06	0.93	6.64 ± 0.05	1.11
Diazepam	6.90 ± 0.09	1.06	5.44 ± 0.10	1.10
Flunitrazepam	6.65 ± 0.03	1.26	5.44 ± 0.08	1.05
	Cerebral Cortex			
	Rat		*Gerbil*	
Compound	pK_i	nH	pK_i	nH
PK 11195	9.28 ± 0.08	1.02	9.38 ± 0.15	1.13
RO 5-4864	8.48 ± 0.02	0.92	6.70 ± 0.12	0.83
Dipyridamole	7.19 ± 0.12	0.92	7.55 ± 0.10	1.03
Diazepam	7.25 ± 0.15	0.90	5.45 ± 0.11	0.90
Flunitrazepam	6.95 ± 0.09	0.93	5.42 ± 0.03	0.87

Displacement of 0.2 nM [^{3}H]-PK 11195 from Tris HCl washed hippocampal and cortical membranes. Assays were carried out in duplicate with at least 10 concentrations of competing drug. Hill slopes for all compounds did not deviate significantly from unity. Values represent mean ± s.e.mean of at least 4 experiments.

consistent with [^{3}H]-PK 11195 binding to a PTB binding site, although these agents also expressed higher affinity for the site in rat brain compared to gerbil brain (Table 2). In all displacement studies Hill slopes did not deviate significantly from unity indicating that these compounds appeared to displace [^{3}H]-PK 11195 from a single site.

Competitive interactions of RO 5-4864

The interaction of RO 5-4864 with rat and gerbil cortical membranes was examined further by investigating the effect of RO 5-4864 on [^{3}H]-PK 11195 binding kinetics and equilibrium parameters. The effect on saturation binding parameters was examined using concentrations of RO 5-4864 in the particular tissue respective to its K_i, producing a similar quantifiable shift in saturation parameters. Dissociation rate experiments were performed at 4°C in order to slow the rapid rate of dissociation of [^{3}H]-PK 11195 that occurs at 25°C. For these experiments membranes were left for 100 min to reach equilibrium, prior to dissociation with 1 μM PK 11195 in the absence (control) or presence of RO 5-4864. Preliminary experiments showed that the affinity for RO 5-4864 was unaffected by the reduction in temperature (data not shown).

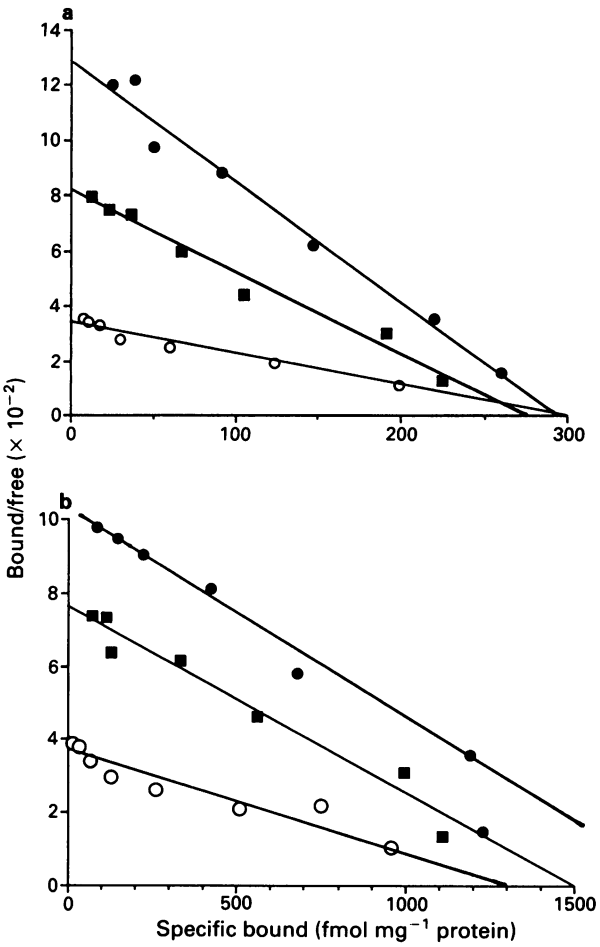

Figure 1 A representative experiment of the effect of RO 5-4864 on [^{3}H]-PK 11195 saturation binding parameters in (a) rat and (b) gerbil cerebral cortex. Saturation binding parameters (B_{max} and K_d) were determined in the absence of RO 5-4864, control (●), and in the presence of 5.0 nM (■) and 10.0 nM (○) RO 5-4864 in rat cortex (a) and in gerbil cortex 0.1 μM (■) and 0.5 μM (○) RO 5-4864 (b). Mean values as in text.

The effect of RO 5-4864 on [^{3}H]-PK 11195 saturation binding parameters in rat and gerbil cortical membranes is shown in Figure 1. Scatchard transformation of saturation data (Table 3) indicated that in both rat and gerbil cortex, RO 5-4864 caused a decrease in receptor affinity (measured by the equilibrium dissociation constant K_d) but no effect on the density of binding sites (B_{max}). In both cases these results indicated an apparently competitive interaction of RO 5-4864

Table 3 The effect of RO 5-4864 on [^{3}H]-PK 11195 saturation binding parameters in rat and gerbil cortical membranes

Rat cortex	B_{max} *(fmol mg^{-1})*	K_d *(nM)*
Control	303 ± 42	0.23 ± 0.02
+ 5.0 nM RO 5-4864	269 ± 31	0.72 ± 0.09**
+ 10.0 nM RO 5-4864	287 ± 46	1.07 ± 0.04**
Gerbil cortex	B_{max} *(fmol mg^{-1})*	K_d *(nM)*
Control	1102 ± 72	0.24 ± 0.02
+ 0.1 nM RO 5-4864	935 ± 75	0.41 ± 0.06*
+ 0.5 nM RO 5-4864	960 ± 44	0.77 ± 0.05**

Saturation binding parameters in the absence (control) and presence of RO 5-4864. Values represent the mean ± s.e. mean of 4 separate determinations.
*$P<0.05$, **$P<0.01$, statistical decrease in K_d from control no significant statistical changes in B_{max}.

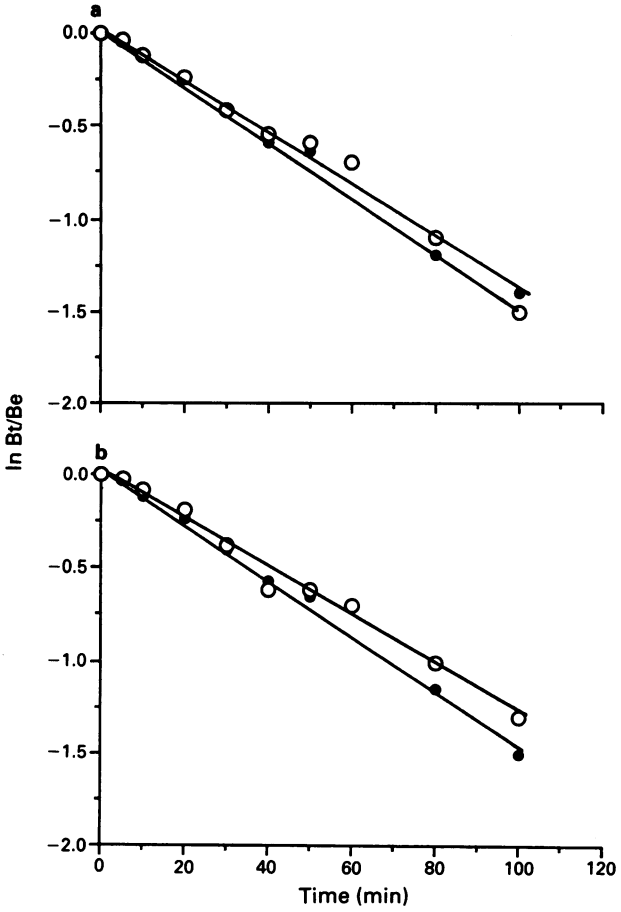

Figure 2 A representative experiment of the effect of RO 5-4864 on the rate of dissociation of [^{3}H]-PK 11195 from (a) rat and (b) gerbil cerebral cortex. Dissociation was initiated from equilibrium at 4°C by the addition of 1 μM PK 11195, control (●), or in presence of 0.1 μM RO 5-4864 (○) in rat cortex (a) and in the presence of 10 μM RO 5-4864 (○) in gerbil cortex (b).

at the [^{3}H]-PK 11195 binding site in rat and gerbil cortical membranes.

In kinetic experiments (Figure 2) the presence of excess RO 5-4864 did not change the rate of dissociation (initiated by 1 μM cold PK 11195) of the [^{3}H]-PK 11195-receptor complex from equilibrium. In rat cortex the control dissociation rate was $0.014 \pm 0.002\ min^{-1}$, and $0.015 \pm 0.004\ min^{-1}$ in the presence of 0.1 μM RO 5-4864. In gerbil cortex the control rate of dissociation was $0.015 \pm 0.0017\ min^{-1}$, and $0.014 \pm 0.002\ min^{-1}$ in the presence of 10 μM RO 5-4864. These results further confirm the competitive nature of the interaction of RO 5-4864 at the [^{3}H]-PK 11195 binding site in both rat and gerbil cortex.

Table 5 Autoradiographical analysis of the effect of forebrain ischaemia on the density of [^{3}H]-PK 11195 binding to gerbil brain sections

Brain region	*Sham control*	*Ischaemic*
Hippocampal CA_1	152 ± 42	314 ± 43*
Hippocampal CA_3	202 ± 28	231 ± 30
Frontoparietal cortex (I–II)	191 ± 28	247 ± 18

Densimetric [^{3}H]-PK 11195 (1.0 nM) binding parameters (fmol mg^{-1} tissue) were determined from duplicate measurements of total and non-specific binding from at least 6 sections for each animal, consisting of 4–5 animals per group. The specific binding represented 85–90% of the total binding and values represent mean ± s.e.mean.
*$P<0.05$ against non-ischaemic sham control.

The effect of forebrain ischaemia on [^{3}H]-PK 11195 and [^{3}H]-8-OH-DPAT binding

The effect of 5 min forebrain ischaemia followed by 7 days recovery on [^{3}H]-PK 11195 binding parameters in gerbil brain membranes is shown in Table 4. Ischaemia with recovery resulted in a significant increase ($P<0.01$) in the density of binding sites for [^{3}H]-PK 11195 in gerbil hippocampus with no significant change in cerebral cortex. Conversely, the $5\text{-}HT_{1A}$ selective ligand, [^{3}H]-8-OH-DPAT showed a significant decrease ($P<0.05$) in hippocampal binding (Table 4). Ischaemia and subsequent recovery had no effect on binding affinity for either of the ligands used.

Autoradiographic analysis of [^{3}H]-PK 11195 binding to 20 μm coronal brain sections showed that 5 min forebrain ischaemia followed by 7 days recovery resulted in an increase in binding density in ischaemic animals (CA_1, CA_3, frontoparietal cortex layers I–II) compared to sham controls (Table 5). This effect was only consistent and significant in the CA_1 region of the hippocampus, although cortical changes were apparent in those sections in which the largest increases in hippocampal CA_1 binding density were detected.

Discussion

In this paper we have demonstrated high affinity binding of [^{3}H]-PK 11195 to a site in rat brain consistent with the pharmacology of PTB (or ω_3) binding sites (Benavides *et al.*, 1983; Schoemaker *et al.*, 1983; Doble *et al.*, 1987; Langer & Arbilla, 1988). The affinities of PTB and non-PTB compounds is in agreement with previously reported data with the rank order of potency PK 11195 > RO 5-4864 > diazepam > flunitrazepam (LeFur *et al.*, 1983). Thus far, ω_3 binding sites have not been characterized in gerbil brain even though this animal has been extensively used as an ischaemic model, and on the basis of data in these studies we have shown them to be clearly different from those in rat. A previous study has reported species differences in the density,

Table 4 The effect of 5 min forebrain ischaemia on [^{3}H]-8-hydroxy-2-(di-n-propylamino)tetralin ([^{3}H]-8-OH-DPAT) and [^{3}H]-PK 11195 binding parameters in gerbil brain

	Non ischaemic		*Ischaemic*	
Radioligand (tissue)	K_d (nM)	B_{max} (fmol mg^{-1} protein)	K_d (nM)	B_{max} (fmol mg^{-1} protein)
[^{3}H]-8-OH-DPAT Gerbil hippocampus	4.29 ± 0.31	393 ± 33	3.98 ± 0.62	289 ± 21*
[^{3}H]-PK 11195 Gerbil hippocampus	0.32 ± 0.02	1430 ± 111	0.29 ± 0.10	2160 ± 170**
[^{3}H]-PK 11195 Gerbil cortex	0.18 ± 0.07	1560 ± 70	0.22 ± 0.05	1740 ± 150

Forebrain ischaemia was induced by occlusion of right and left common carotid arteries for 5 min followed by recovery for 7 days. Saturation experiments ($n = 4–5$) were carried out as described in Methods and statistical significance is given for ischaemic against non-ischaemic sham-operated animals: *$P<0.05$; **$P<0.01$.

and the affinity of RO 5-4864 for ω_3 sites labelled in the cerebral cortex of various species (Award & Gavish, 1987). The results from our experiments confirm those findings, with RO 5-4864 having an affinity in gerbil brain comparable to that in human brain tissues (Doble *et al.*, 1987). Furthermore, we have shown that these differences appear to be highly species-, as opposed to tissue-specific, as the properties in gerbil hippocampus are similar to those in cerebral cortex. Some studies have indicated differences between [^{3}H]-RO 5-4864 and [^{3}H]-PK 11195 based on thermodynamic binding studies, indicating that these agents may be an agonist and antagonist respectively (LeFur *et al.*, 1983). Indeed RO 5-4864 has been shown to decrease cardiac contractility and the duration of the intracellular action potential, and this effect can be selectively antagonized by PK 11195 (Mestre *et al.*, 1984). In our studies however, we could find no evidence for this interaction or of heterogeneity of binding sites based on the interaction of RO 5-4864 in competition studies as previously reported (Awad & Gavish, 1987), since Hill slopes did not deviate significantly from unity and a competitive interaction for RO 5-4864 was confirmed in equilibrium and kinetic experiments. The low affinity expressed by RO 5-4864 for ω_3 sites in gerbil brain is an important finding however, as both [^{3}H]-PK 11195 and [^{3}H]-RO 5-4864 have been used as markers of neuronal damage (Benavides *et al.*, 1987).

The location of ω_3 sites is thought to be on the outer mitochondrial membrane (Basile & Skolnick, 1986; Doble *et al.*, 1987) and associated with non-neuronal cell types such as glia, astrocytes and macrophages. It is unclear if the abundance of ω_3 sites in gerbil tissue homogenates compared to rat is a reflection of differential labelling of subcellular components or of a difference in the abundance of specific cell types in the different species, although the increased density of sites between species may be an indication of a preferential neuronal location (Benavides *et al.*, 1984). The use of more specific cell type markers such as glial fibrillary acidic protein (Petito *et al.*, 1989) would characterize these differences more clearly.

Changes in CA_1 pyramidal cells following forebrain ischaemia have been well documented, and whilst cell changes become immediately apparent (Suzuki *et al.*, 1983), it is a feature of this model that morphological cell damage is gradual and takes several days to become established (Kirino 1982; Kirino *et al.*, 1984b). In this study we have examined the density of ω_3 sites at 7 days post-ischaemia in order to achieve maximal changes in [^{3}H]-PK 11195 binding due to reactive gliosis, astrocyte proliferation and infiltration of macrophages following ischaemia-induced cell loss. The increase in cortical ω_3 sites following focal ischaemia in the mouse is also maximal at 4–7 days (Gotti *et al.*, 1989; Benavides *et al.*, 1990; Kenny *et al.*, 1992). In a recent study using a four vessel occlusion model of forebrain ischaemia in the rat by Demerlé-Pallardy *et al.* (1991) it was shown that the post-ischaemic increase in hippocampal ω_3 density is maximal after 4–7 days, although following forebrain ischaemia, cortical ω_3 binding increased over longer post-ischaemic periods. In a similar model of forebrain ischaemia, Morioka *et al.* (1991) demonstrated a similar temporal relationship for the post-ischaemic increase in microglia using a specific lectin stain. However, whilst it has been demonstrated that macrophages appear to be the predominant cell type elevated post-ischaemia and claimed to represent the increase in ω_3 density (Myers *et al.*, 1991) reactive microglia and macrophages are difficult to distinguish because they have similar cell surface antigens and phagocytotic properties. The decrease in the density of $5\text{-}HT_{1A}$ sites at this time presumably reflects the loss of CA_1 neurones on which they are located (Pazos & Palacios, 1985). Indeed a similar profile for the selective post-ischaemic loss of muscarinic, dihydropyridine and adenosine uptake sites on hippocampal pyramidal cells has been demonstrated following forebrain ischaemia in the rat (Onodera & Kogure, 1990).

In the present studies, whilst autoradiographic analysis indicated that a 5 min period of ischaemia and 7 days recovery resulted in a consistent increased ω_3 density in hippocampal CA_1 layers, moderate cortical increases were detected in those sections with the greatest extent of CA_1 damage. This finding is consistent with previous histological evidence in this gerbil model which points to an involvement of other brain areas in those animals severely symptomatic of the ischaemic insult (i.e. complete loss of CA_1 neurones) following bilateral carotid occlusion (Alps *et al.*, 1988). Other studies have shown that forebrain ischaemia in the gerbil involves not only morphological cell loss of CA_1 pyramidal neurones, but other pathological processes involving chromatolysis of some neuronal cells in deep cortical layers and the paramedian area of the hippocampus (Brown *et al.*, 1979), and such effects will be variable, probably due to the extent to which the circulus arteriosus is complete in any given animal (Berry *et al.*, 1975). Furthermore, other studies using this model (Brown *et al.*, 1988) have demonstrated decreases in the density of $5\text{-}HT_2$ sites in the frontal cortex at a time when there is no apparent change in the level of 5-HT or evidence for histological cell changes (Kirino & Sano, 1984b). [^{3}H]-PK 11195 would therefore appear to be a sensitive indirect index of neuronal damage, indicative of cellular injury in the absence of obvious histological changes. Thus, cortical cell injury assessed by histological means appears to be associated with prolonged unilateral occlusion (Ito *et al.*, 1975) or longer periods of forebrain ischaemia (Pulsinelli *et al.*, 1982; Wieloch, 1985).

In conclusion, we have demonstrated the use of [^{3}H]-PK 11195 as a sensitive marker of neuronal damage following forebrain ischaemia and, in this model, have further illustrated the selective vulnerability of certain brain regions to ischaemic damage by non-histological means. This ligand represents a useful means of assessing damage, because it is an indirect measure of ischaemic events and may provide another useful method for the detection of neuroprotective agents in forebrain ischaemia models and avoids the histological assessment of neuronal cell loss.

References

ALPS, B.J., CALDER, C., HASS, W.K. & WILSON, A. (1988). Comparative protective effects of nicardipine, flunarizine, lidoflazine and nimodipine against ischaemic injury in the hippocampus of the Mongolian gerbil. *Br. J. Pharmacol.*, **93**, 877–883.

ANHOLT, R.H. (1986). Mitochondrial benzodiazepine receptors as potential modulators of intermediary metabolism. *Trends Pharmacol. Sci.*, **7**, 506–511.

ANHOLT, R.H., PEDERSEN, E.B. DE SOUZA, E.B. & SYNDER, S.H. (1986). The peripheral-type benzodiazepine receptor. Localisation to the outer mitochondrial membrane. *J. Biol. Chem.*, **261**, 576–583.

AWAD, M. & GAVISH, M. (1987). Binding of [^{3}H] RO 5-4864 and [^{3}H]-PK 11195 to cerebral cortex and peripheral tissues of various species: Species differences and heterogeneity in peripheral benzodiazepine binding sites. *J. Neurochem.*, **49**, 1407–1414.

BASILE, A.S. & SKOLNICK, P. (1986). Subcellular distribution of 'peripheral type' benzodiazepine binding sites for benzodiazepines in rat brain. *J. Neurochem.*, **46**, 305–308.

BENAVIDES, J., CAPDEVILLE, C., DAUPHIN, F., DUBOIS, A., DUVERGER, D., FAGE, D., GOTTI, B., MACKENZIE, E.T. & SCATTON, B. (1990). The quantification of brain lesions with an ω_3 site ligland: a critical analysis of animal models of cerebral ischaemia and neurodegeneration. *Brain Res.*, **522**, 275–289.

BENAVIDES, J., CORNU, P., DENNIS, T., HAUW, J.J., MACKENZIE, E.T., SAZDOVITCH, V. & SCATTON, B. (1988). Imaging of human brain lesions with an ω_3 site radioligand. *Ann. Neurol.*, **24**, 708–712.

BENAVIDES, J., FAGE, D., CARTER, C. & SCATTON, B. (1987). Peripheral type benzodiazepine binding sites are a sensitive indirect index of neuronal damage. *Brain Res.*, **421**, 167–172.

BENAVIDES, J., QUARTERONET, D., IMBAULT, F., MALGOURIS, C., UZAN, A., RENAULT, C., DUBROEUCQ, M.C., GUEREMY, C. & LEFUR, G. (1983). Labelling of 'peripheral type' benzodiazepine binding sites in the rat brain. Kinetic studies and autoradiographic localisation. *J. Neurochem.*, **41**, 1744–1750.

BENAVIDES, J., SAVAKI, H.E., MALGOURIS, C., LAPLACE, C., DANIEL, M., UZAN, A., DUBROUECQ, M.C., RENAULT, C., GUEREMY, C. & LEFUR, G. (1984). Autoradiographic localization of peripheral benzodiazepine binding sites in the cat brain with [^{3}H]-PK 11195. *Brain Res. Bull.*, **13**, 69–77.

BERRY, K., WISNIEWSKI, H.M., SVARZBAIN, L. & BAEZ, S. (1975). On the relationship of brain vasculature to production of neurological deficit and morphological changes following acute unilateral common carotid artery ligation in gerbil. *J. Neurol. Sci.*, **25**, 75–92.

BROWN, A.W., LEVY, D.E., KUBLIK, M., HARROW, J., PLUM, F. & BRIERLEY, J.B. (1979). Selective chromatolysis of neurons in the gerbil brain: A possible consequence of 'epileptic' activity produced by common carotid artery occlusion. *Ann. Neurol.*, **1**, 519–527.

BROWN, C.M., KILPATRICK, A.T., MARTIN, A. & SPEDDING, M. (1988). Cerebral ischaemia reduces the density of 5-HT_2 binding sites in the frontal cortex of the gerbil. *Neuropharmacol.*, **27**, 831–836.

CHENG, Y.C. & PRUSOFF, W.H. (1973). Relationship between the inhibition constant (Ki) and the concentration of inhibitor which caused 50 per cent inhibition (IC50) of an enzymic reaction. *Biochem. Pharmacol.*, **22**, 3099–3108.

DEMERLÉ-PALLARDY, DUVERGER, D., SPINNEWYN, B., PIROTZKY, E. & BRAQUET, P. (1991). Peripheral type benzodiazepine binding sites following transient forebrain ischaemia in the rat: effect of neuroprotective drugs. *Brain Res.*, **565**, 312–320.

DOBLE, A., MALGOURIS, J., DANIEL, M., DANIEL, N., IMBAULT, F., BASBAUN, A., UZAN, A., GUEREMY, C. & LEFUR, G. (1987). Labelling of peripheral-type benzodiazepine binding sites in human brain with [^{3}H]-PK 11195: anatomical and subcellular distribution. *Brain Res. Bull.*, **18**, 4961.

DOLMAN, C.L. (1986). Microglia, In *Textbook of Neuropathology* (ed) Davis, R.L. & Robertson, D.M., 117–137 (Williams and Wilkins, Baltimore).

DUBOIS, A.J., BENAVIDES, J., PENY, B., DUVERGER, D., FAGE., GOTTI, B., MACKENZIE, E.T. & SCATTON, B. (1988). Imaging of primary and remote ischaemic and excitotoxic brain lesions. An autoradiographic study of peripheral type benzodiazepine binding sites in the rat and cat. *Brain Res.*, **445**, 77–90.

FOSTER, A.C., GILL, R. & WOODRUFF, G.N. (1988). Neuroprotective effects of MK-801 in vivo: selectivity and evidence for delayed degeneration mediated by NMDA receptor activation. *J. Neurosci.*, **8**, 4745–4754.

GILL, R., FOSTER, A.C. & WOODRUFF, G.N. (1987). Systemic administration of MK-801 protects against ischaemia-induced hippocampal neurodegeneration in the gerbil. *J. Neurosci.*, **7**, 3343–3349.

GOTTI, B., BENAVIDES, J., DUBOIS, A., MACKENZIE, E.T., SCATTON, B. & THERAULAZ, M. (1989). Quantification of experimental focal ischaemic lesions with an ω_3 site radioligand in mouse brain. *J. Cereb. Blood Flow Metab.*, **9**, S258.

ITO, U., SPATZ, M., WALKER, J.T. & KLATZO, I. (1975). Experimental cerebral ischaemia in Mongolian gerbils. 1. Light microscopic observations. *Acta Neuropathol.*, **32**, 209–223.

KAHN, K. (1972). The natural course of experimental cerebral infarction in the gerbil. *Neurology*, **22**, 510–515.

KENNY, B.A., MACKINNON, A.C., KILPATRICK, A.T. & SPEDDING, M. (1990). Species differences in the sensitivity to [^{3}H]-PK 11195, a potential marker of neuronal damage. *Br. J. Pharmacol.*, **100**, 355P.

KENNY, B.A., CALDER, C. & BROWN, C.M. (1992). Neuroprotective properties of phenytoin in a mouse model of focal cerebral ischaemia. *Br. J. Pharmacol.*, **107**, 60P.

KIRINO, T. (1982). Delayed neuronal death in the gerbil hippocampus following ischaemia. *Brain Res.*, **239**, 57–90.

KIRINO, T. & SANO, K. (1984a). Selective vulnerability in the gerbil hippocampus following transient ischaemia. *Acta Neuropathol.*, **62**, 201–208.

KIRINO, T. & SANO, K. (1984b). Fine structural nature of delayed neuronal death following ischaemia in the gerbil hippocampus. *Acta Neuropathol.*, **62**, 209–218.

LANGER, S.Z. & ARBILLA, S. (1988). Imidazopyridines as a tool for the characterisation of benzodiazepine receptors: a proposal for a pharmacological classification as ω_3 receptor. *Pharmacol. Biochem. Behav.*, **29**, 763–766.

LARCHER, J.C., VAYSSIERE, J.L. LEMARQUER, F.J., CORDEAU, L.T., KEANE, P.E., BACHY, A., GROS, F. & CROISAT, B.P. (1989). Effects of peripheral benzodiazepines upon the O_2 consumption of neuroblastoma cells. *Eur. J. Pharmacol.*, **161**, 197–202.

LEFUR, G., VAUCHER, N., PERRIER, A., FLAMIER, A., BENAVIDES, J., RENAULT, C., DUBROEUCQ, M.C., GUEREMY, C. & UZAN, A. (1983). Differentiation between 2 ligands for peripheral benzodiazepine binding sites, [^{3}H] RO 5-4864 and [^{3}H]-PK 11195 by thermodynamic studies. *Life Sci.*, **33**, 449–457.

LEVINE, S. & PAYAN, H. (1966). Effects of ischaemia and other processes on the brain and retina of the gerbil (Meriones unguiculatus). *Exp. Neurol.*, **16**, 255–262.

MESTRE, M., CARRIOT, T., BELIN, C., UZAN, A., RENAULT, C., DUBROEUCQ, C., GUEREMY, C. & LEFUR, G. (1984). Electrophysiological and pharmacological characterisation of peripheral benzodiazepine receptors in a guinea pig heart preparation. *Life Sci.*, **35**, 953–962.

MORIOKA, T., KALEHUA, A.N. & STREIT, W.J. (1991). The microglial reaction in rat dorsal hippocampus following transient forebrain ischaemia. *J. Cereb. Blood Flow Metab.*, **11**, 966–973.

MUNSON, P.J. & RODBARD, D. (1980). LIGAND: a versatile computerised approach for characterisation of ligand binding systems. *Anal. Biochem.*, **107**, 220–239.

MYERS, R., MANJIL, L.G., CULLEN, B.M., PRICE, G.W., FRACKOWIAK, R.S. & CREMER, J.E. (1991). Macrophage and astrocyte populations in relation to [^{3}H]-PK 11195 binding in rat cerebral cortex following a local ischaemic lesion. *J. Cereb. Blood Flow Metab.*, **11**, 314–322.

ONODERA, H. & KOGURE, K. (1990). Calcium antagonist, adenosine A_1, and muscarinic binding in rat hippocampus after transient ischemia. *Stroke*, **21**, 771–776.

PAZOS, A. & PALACIOS, J.M. (1985). Quantitative autoradiographic mapping of serotonin receptors in rat brain. I. Serotinin-1 receptors. *Brain Res.*, **346**, 205–230.

PETITO, C.K., CHUNG, H.M., MORGELLO, S., FELIX, J.C. & LESSER, M.L. (1989). Post-ischaemic increases in astrocyte glutamine synthetase and intermediate filament proteins. In *Cerebrovascular Diseases*. ed. Ginsberg, M.D. & Dalton, W. New York: Raven Press.

PULSINELLI, W.A., BRIERLEY, J.B. & PLUM, F. (1982). Temporal profile of neuronal damage in a model of transient forebrain ischaemia. *Ann. Neurol.*, **11**, 491–498.

SCHOEMAKER, H., BOLES, R.G. HORST, W.D. & YAMAMURA, H.I. (1983). Specific high affinity binding sites for [^{3}H] RO 5-4864 in rat brain and kidney. *J. Pharmacol. Exp. Ther.*, **225**, 61–69.

SUZUKI, R., YAMAGUCHI, T., KIRINO, T., ORZI, F. & KLATZO, I. (1983). The effects of 5 minute ischemia on mongolian gerbils: 11. Changes of spontaneous neuronal activity in cerebral cortex and CA_1 sector of hippocampus. *Acta Neuropathol.*, **60**, 217–222.

SYAPIN, P.J. & SKOLNICK, P. (1979). Characterisation of benzodiazepine binding sites in cultured cells of neuronal origin. *J. Neurochem.*, **32**, 1047–1051.

WIELOCH, T. (1985). Neurochemical correlates to selective neuronal vulnerability. *Prog. Brain. Res.*, **63**, 69–85.

ZAVALA, F. & LENFANT, M. (1987). Benzodiazepines and PK 11195 exert immunomodulating activities by binding on a specific receptor on macrophages. *Ann. N.Y. Acad. Sci.*, **496**, 240–249.

(Received November 6, 1992
Revised February 1, 1993
Accepted February 3, 1993)

Br. J. Pharmacol. (1993), **109**, 443–448 © Macmillan Press Ltd, 1993

Effects of prolonged application of isoprenaline on intracellular free magnesium concentration in isolated heart of rat

H. Nishimura, T. Matsubara, Y. Ikoma, [1]*S. Nakayama & N. Sakamoto

Departments of Internal Medicine III and *Physiology, School of Medicine, Nagoya University, Nagoya 466, Japan

1 The effect of prolonged application of isoprenaline on intracellular free-Mg^{2+} concentration ($[Mg^{2+}]_i$) was examined by use of ^{31}P-nuclear magnetic resonance (^{31}P-n.m.r.) in rat isolated hearts. Left ventricular pressure (LVP) was simultaneously measured.

2 $[Mg^{2+}]_i$ was estimated from the separation of the α- and β-ATP peaks, using the dissociation constant of MgATP 38 μM (established previously). In normal (phosphate-free, Krebs-Henseleit) solution, $[Mg^{2+}]_i$ was approximately 0.4 mM.

3 When isoprenaline was applied for 100 min, a transient increase in $[Mg^{2+}]_i$ was observed during the initial 25 min, whilst concentrations of ATP ([ATP]) and phosphocreatine ([PCr]) decreased and $[P_i]$ correspondingly increased. During the subsequent 75 min of isoprenaline application, $[Mg^{2+}]_i$ decreased below its resting levels. Washout of isoprenaline restored $[Mg^{2+}]_i$ and [PCr], but [ATP] remained low. These changes elicited by isoprenaline were not observed in the presence of propranolol, a typical α-adrenoceptor blocker.

4 Isoprenaline increased both LVP and heart rate. The increased LVP and heart rate slowly returned to lower values during prolonged application of isoprenaline, but remained higher than those before application.

5 The transient rise in $[Mg^{2+}]_i$ elicited by isoprenaline could be attributed to the decrease in [ATP] resulting in a release of Mg^{2+}. The subsequent decrease in $[Mg^{2+}]_i$ during the prolonged applications suggests that β-adrenoceptor stimulation itself facilitates Mg^{2+}-extruding mechanism(s).

Keywords: Rat heart; Mg^{2+}; nuclear magnetic resonance; isoprenaline; β-adrenoceptors; phosphorous compounds

Introduction

It is generally believed that changes in intracellular magnesium can modify cardiac function. By use of material isolated from heart, e.g. skinned fibres (Kusuoka & Marban, 1992) and single cells and cell membranes in patch clamp recordings (White & Hartzell, 1989; Matsuda, 1991; Agus & Morad, 1991), possible effects of magnesium ions on contractility have been assessed.

In diseased hearts, the importance of the effects of intracellular magnesium on cardiac function has been emphasized: epidemiological studies (Stitt *et al.*, 1973; Anderson *et al.*, 1975) have indicated that in soft water areas, relatively high mortality from cardiovascular disease may be due to magnesium deficiency. On the other hand, it has been suggested that Mg^{2+} deficiency in cardiovascular disease is due to the action of catecholamines (Ebel & Günther, 1983).

Recently, conflicting results have been published on the regulation of intracellular free Mg^{2+} concentration ($[Mg^{2+}]_i$) in rat isolated hearts. Romani & Scarpa (1990) found that Mg^{2+} efflux was increased by a short (approx. 10 min) application of noradrenaline and the increase was not observed in the presence of propranolol, suggesting a decrease in $[Mg^{2+}]_i$ by β-adrenoceptor stimulation. On the other hand, using ^{31}P-nuclear magnetic resonance (^{31}P-n.m.r.), Headrick & Willis (1989) estimated that $[Mg^{2+}]_i$ was *increased* by application of isoprenaline for a similar short duration (20 min). In the present study, we measured $[Mg^{2+}]_i$ during prolonged (100 min) applications of isoprenaline using the same n.m.r. techniques, and obtained results which can explain the discrepancy between these two studies.

[1] Author for correspondence at present address: University Department of Pharmacology, Mansfield Road, Oxford, OX1 3QT.

Methods

Preparation and solution

Male Wistar rats weighing 350–400 g were anaesthetized with sodium pentobarbitone. Hearts were rapidly excised and arrested in ice-cold saline. The aorta was cannulated for retrograde perfusion, and a water-filled balloon was placed in the left ventricle for monitoring developed pressure. The heart preparation was mounted in an n.m.r. tube of 25 mm diameter, and perfused at a constant flow rate of 15–16 ml min^{-1} with a peristaltic pump. The perfusate was a phosphate-free, Krebs-Henseleit solution (KH) of the following composition (mM): NaCl 118, KCl 5.9, $CaCl_2$ 2.5, $MgSO_4$ 1.2, $NaHCO_3$ 25, glucose 12, Na_2EDTA 0.5 and was oxygenated with a mixture of 95% O_2 and 5% CO_2. The temperature in the sample tube was 37°C. The perfusing set-up was approximately 3 m from the main magnet. The temperature and oxygen tension were maintained using a triple-walled vinyl tube (Nakayama *et al.*, 1988). The inner tube was used for perfusing solution pre-warmed to 40°C, the middle and outer tubes were for circulation of the gas mixture and warmed water (40°C), respectively. After inserting the sample into the bore, the proton signal from water was used to improve the homogeneity of the magnetic field.

^{31}P-n.m.r.

The methods employed for measurements of ^{31}P-n.m.r. spectra and estimation of $[Mg^{2+}]_i$ were essentially the same as those described previously (Nakayama & Tomita, 1990). An n.m.r. spectrometer (JEOL GSX270W) was operated at 109.4 MHz. Radiofrequency pulses corresponding to a 30° flip angle were repeated at 0.6 s intervals. Spectra were usually obtained by accumulating 2500 signals over 25 min. In some experiments, a 5 min accumulation period was tested, but was judged to be inappropriate because of large

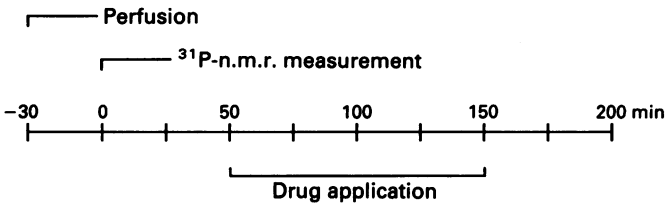

Figure 1 Time table of experiment. Perfusion of the heart preparation starts at −30 min. ^{31}P-n.m.r. measurement starts at 0 min and lasts for 200 min. Spectra are obtained by 25 min accumulation periods of n.m.r. signals. Drugs are applied from 50 to 150 min.

variation in the spectral peak analysis. Before Fourier transformation, a line broadening factor of 15 Hz was applied to enhance the signal-to-noise ratio. Spectral peak resonances were measured relative to that of PCr (phosphocreatine) in parts per million (p.p.m.). Digital resolution of the spectrum was set to be approximately 0.005 p.p.m. by zero-filling to free induction decay.

Definition of the experimental periods

The experimental protocol is shown in Figure 1. ^{31}P-n.m.r. measurements were performed for 200 min after the heart preparation has been equilibrated by normal (KH) solution for approx. 30 min. Each spectrum required a 25 min accumulation of n.m.r. signals, thus afforded eight during the 200 min measurement. After two spectra had been obtained in normal (KH) solution (50 min total accumulation), drugs (isoprenaline and/or propranolol) were applied for 100 min. Thus, four spectra were obtained during the application of drugs. Recovery was assessed by observing the two spectra (50 min total accumulation) during the subsequent washout of the drugs.

In some heart preparations, ^{31}P-n.m.r. measurements were performed during continuous perfusion of normal solution (200 min, 8 spectra) without any drugs, to assess the stability of the preparation.

Estimation of intracellular Mg^{2+} and pH

$[Mg^{2+}]_i$ was estimated from the separation of the α- and β-peaks of ATP (δ_x), using the following equations (Gupta & Moore, 1980; Gupta *et al.*, 1984; Nakayama & Tomita, 1990):

$$[Mg^{2+}]_i = K_D\ (\Phi^{-1}-1), \quad (1)$$

$$\Phi = [ATP]_{free}/[ATP]_{total} = (\delta_x-\delta_1)/(\delta_2-\delta_1), \quad (2)$$

where K_D is the dissociation constant of MgATP, and δ_1 and δ_2 are the resonance separations of the α- and β-peaks in MgATP and free ATP, respectively. We used the values of 8.35 and 10.85 p.p.m. for δ_1 and δ_2, respectively, and 38 μM for K_D (Gupta & Moore, 1980).

Intracellular pH (pH_i) was estimated from the chemical shift of inorganic phosphate (P_i) (Moon & Richards, 1973). The pK_a value for $H_2PO_4^-$ used in the estimation was 6.65, and the chemical shifts used of $H_2PO_4^-$ and HPO_4^{2-} were 3.14 and 5.61 p.p.m., respectively (Eisner *et al.*, 1987).

Statistics

Numerical data are expressed as means ± standard deviation (s.d.). Differences between means were evaluated by paired *t* tests, and a test value of less than 0.05 was taken as a statistically significant difference.

Drugs

Isoprenaline hydrochloride and propranolol hydrochloride were purchased from Sigma. Stock solutions of the drugs,

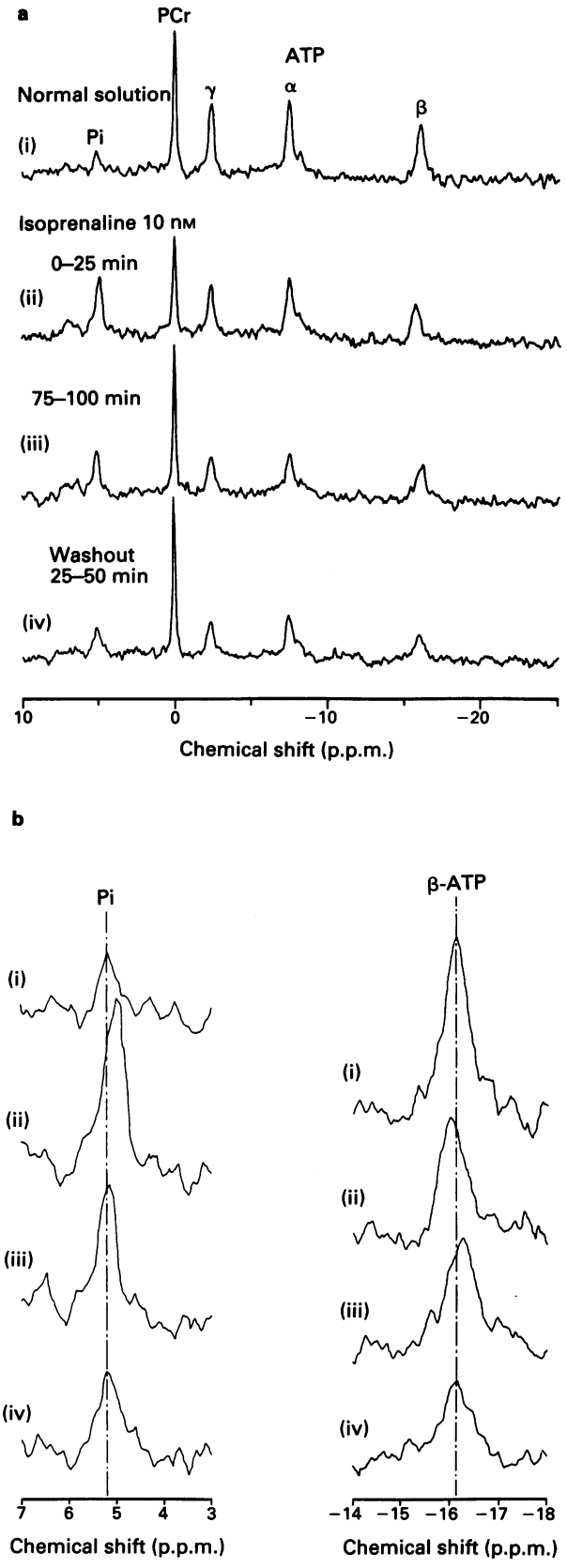

Figure 2 Effects of isoprenaline on ^{31}P-n.m.r. spectra. (a) After obtaining the second spectrum ((i); $t = 25-50$ min) in normal (KH) solution, isoprenaline (10 nM) was added for 100 min, then washed out for 50 min. The spectra (ii) and (iii) were obtained during 0–25 and 75–100 min for isoprenaline application, respectively, and (iv) was obtained during 25–50 min washout. In (a), the whole spectra are shown. Each spectrum was taken by accumulation of 2500 signals (25 min). Spectral peaks were assigned as P_i, PCr and three ATP peaks (i). In (b), the P_i and β-ATP peaks are shown expanded. Vertical lines indicate the initial values of each peak.

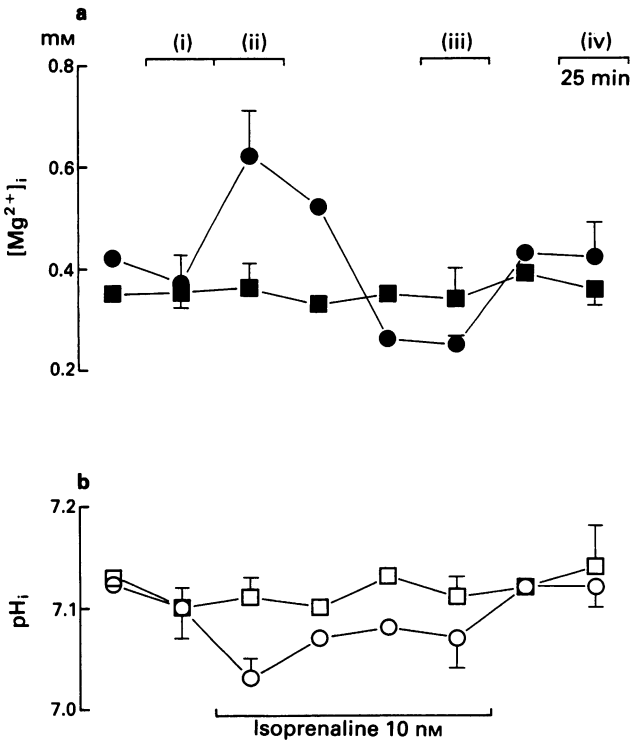

Figure 3 Changes in $[Mg^{2+}]_i$ (a) and pH_i (b). After two spectra were obtained over 50 min in KH solution, isoprenaline was applied for 100 min (●, ○). Each point represents averaged estimates from spectra obtained by accumulation over 25 min. The values of $[Mg^{2+}]_i$ and pH_i obtained by continuous perfusion (200 min) of KH solution (■, □) are shown for comparison. (i)–(iv) correspond to those in Figure 1. Vertical bars represent s.d. values ($n = 6$, isoprenaline; $n = 5$, control); for clarity, some of the s.d. values were omitted. $[Mg^{2+}]_i$ during exposure of isoprenaline, was statistically significantly different (larger or smaller) from that in (i) ($P < 0.05$). pH_i significantly decreased during the first 25 min application.

which were prepared on the same day, were kept cold and protected from the light, before use.

Results

^{31}P-n.m.r. spectra from rat isolated hearts

Acquisitions of ^{31}P-n.m.r. started after the heart preparations had been equilibrated by perfusing with a KH solution for approximately 30 min. Spectra were subsequently taken every 25 min. In normal (KH) solutions, five major peaks were observed (P_i, PCr and γ-, α- and β-ATP: Figure 2a(i)). In the spectra obtained during the 25–50 min acquisition period, the chemical shifts of P_i, α- and β-ATP peaks were 4.98 ± 0.03, −7.53 ± 0.03 and −16.12 ± 0.02 p.p.m. ($n = 16$), respectively. The pH_i and $[Mg^{2+}]_i$ estimated from these chemical shifts were 7.12 ± 0.03 and 0.38 ± 0.06 mM, respectively. To assess the stability of this preparation, five hearts were continuously perfused with KH solution for 200 min in five independent experiments. The mean values ($n = 5$) of pH_i and $[Mg^{2+}]_i$ corresponded to within 0.05 pH units and 0.07 mM, respectively, during the continuous perfusion of KH solution (Figure 3). [PCr] and [ATP] gradually decreased by 15 and 10%, respectively, over 200 min.

Effects of isoprenaline on $[Mg^{2+}]_i$ and phosphorous compounds

In Figure 2, changes in ^{31}P-n.m.r. spectra on application and washout of isoprenaline (10 nM) are shown. As changes in pH_i and $[Mg^{2+}]_i$ are most strongly expressed in the chemical shifts of the P_i and β-ATP peaks, respectively, these peaks are expanded in Figure 2b. After the two spectra had been obtained during the 50 min perfusion with KH solution alone, isoprenaline was added for 100 min. During the first 25 min of application of isoprenaline, the β-ATP peak was shifted to the higher p.p.m. (leftwards) by 0.08 ± 0.03 p.p.m. ($n = 6$). However, the β-ATP peak shifted in the opposite direction during the subsequent 75 min in the presence of isoprenaline, and reached lower frequencies than the chemical shift of the β-ATP peak observed before the application. The chemical shift of the β-ATP peak was −16.22 ± 0.01 p.p.m. in the last (4th) spectra obtained during application of isoprenaline (during 75–100 min of the application). The subsequent washout of isoprenaline restored the chemical shift of the β-ATP peak to its normal values. These changes in the chemical shift of the β-ATP peak revealed that $[Mg^{2+}]_i$ transiently increased from 0.37 ± 0.05 to 0.63 ± 0.09 mM during the initial 25 min application of isoprenaline and then gradually decreased to 0.25 ± 0.02 mM during the subsequent 75 min in the presence of isoprenaline (Figure 3a). The subsequent washout of isoprenaline recovered $[Mg^{2+}]_i$ to its normal concentrations in 25 min.

The P_i peak was shifted to lower p.p.m. (rightwards) by 0.09 ± 0.02 p.p.m. in the first spectra of the four obtained during application of isoprenaline, and gradually returned towards its normal chemical shift value during continued application (Figure 2b). Thus, the largest intracellular acidosis (pH_i 7.03 ± 0.02) was observed during the first 25 min application of isoprenaline, whence the estimated pH_i was gradually restored in the continued presence of isoprenaline (Figure 3b).

The concentrations of phosphorus compounds correspond to the integrals of the peaks. The intracellular concentration of ATP ([ATP]) is estimated from the integral of the β-ATP peak, because the γ- and α-ATP peaks have a contribution from ADP. When isoprenaline (10 nM) was applied, during the first 25 min, [PCr] and [ATP] significantly decreased to 56 ± 6 and 57 ± 4% of each control value (estimated from the 2nd of the initial spectra before the application), respectively, while $[P_i]$ correspondingly increased. During the subsequent 75 min application of isoprenaline, [PCr] recovered to 95 ± 18%, whereas [ATP] was further decreased to 49 ± 9% (Table 1). Like the β-ATP peak, the areas of the γ- and α-peaks decreased simultaneously during application of isoprenaline (Figure 2a), indicating further degradation of ADP. When isoprenaline was washed out, [ATP] was not restored. The lack of restoration in [ATP] is presumably due to deamination of adenosine and adenylate (Jennings & Steenbergen, 1985), and/or release of adenosine (Headrick & Willis, 1990).

Effects of propranolol

In five hearts, after observing two spectra during 50 min perfusion of normal (KH) solutions, 1 μM propranolol was simultaneously applied with isoprenaline (10 nM) for 100 min. The simultaneous application of propranolol eliminated both

Table 1 Effects of isoprenaline on phosphorus compounds ($n = 6$)

	Normal (KH)	*Isoprenaline* (10 nM)		*Washout*
	25–50	0–25	75–100	25–50 min
[PCr]	100	56 ± 6*	95 ± 18	115 ± 8*
[ATP]	100	57 ± 4*	49 ± 9*	46 ± 8*
$[P_i]$	100	274 ± 105*	228 ± 108*	117 ± 60

The concentrations of phosphorus compounds are expressed as percentages of respective initial concentrations in normal solution.
*Significantly different from the concentrations in normal solutions (25–50 min).

Table 2 Effects of isoprenaline and propranolol on developed pressure (A) and heart rate (B)

	Normal (KH) 25–50	*Drug application* 0–25	75–100	*Washout* 25–50 min
A *Developed pressure* (mmHg)				
Control ($n = 5$)	121 ± 9	115 ± 7	115 ± 9	119 ± 4
Isoprenaline (10 nM) ($n = 6$)	114 ± 6	207 ± 18*	140 ± 11*	118 ± 15
Isoprenaline (10 nM) + propranolol (1 μM) ($n = 5$)	114 ± 9	130 ± 14	110 ± 9	117 ± 9
B *Heart rate* (beats min^{-1})				
Control ($n = 5$)	219 ± 7	214 ± 9	216 ± 7	215 ± 8
Isoprenaline (10 nM) ($n = 6$)	229 ± 12	367 ± 18*	285 ± 10*	220 ± 19
Isoprenaline (10 nM) + propranolol (1 μM) ($n = 5$)	232 ± 32	278 ± 16*	241 ± 8	219 ± 10

Contractility was simultaneously monitored during ^{31}P-n.m.r. measurements for 200 min. After 50 min perfusion of normal (KH) solutions, isoprenaline alone, or isoprenaline and propranolol were applied for 100 min. In control experiments, no drug was applied during these periods.
*Significantly different from the values in normal solution (25–50 min).

of the changes in $[Mg^{2+}]_i$ and pH_i observed during applications of isoprenaline alone (Figure 4a and b). The concentrations of high energy phosphates, however, changed little throughout the experiments.

When propranolol (1 μM) alone was applied for 100 min, no significant changes were observed in $[Mg^{2+}]_i$, pH_i and phosphate concentrations.

Contractility

Contractility was simultaneously monitored during the ^{31}P-n.m.r. measurements, by a water-filled balloon in the left ventricle. Changes in developed pressure and heart rate are summarised in Table 2A and 2B, respectively. During 200 min continuous perfusion of KH solution neither developed pressure, nor heart rate changed significantly ($n = 5$). When isoprenaline (10 nM, 100 min) was applied, both developed pressure and heart rate increased by 82 and 60% ($n = 6$), respectively, during the first 25 min of drug application, and gradually decreased during the subsequent 75 min. Both of the values towards the end of isoprenaline application were still higher than those before application. Propranolol (1 μM) inhibited both the inotropic and chronotropic effects of isoprenaline. In the presence of propranolol, the contractility towards the end of isoprenaline application was nearly the same as in KH solution (control values).

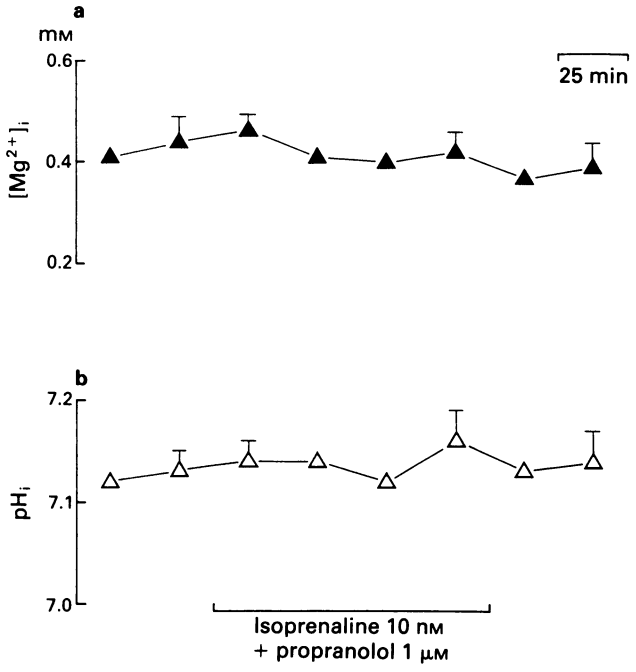

Figure 4 Effects of propranolol on $[Mg^{2+}]_i$ (a) and pH_i (b). After observing spectra in normal solutions for 50 min, propranolol (1 μM) was applied simultaneously with isoprenaline (10 nM) for 100 min. Vertical bars represent s.d. values ($n = 5$).

Discussion

In heart muscle, reported values of $[Mg^{2+}]_i$ vary considerably (0.4–3 mM), however, recent estimated values are mostly less than 1 mM (reviewed by McGuigan *et al.*, 1991). Our estimation of $[Mg^{2+}]_i$ (approx. 0.4 mM) using ^{31}P-n.m.r. in normal (KH) solutions agrees with these values. In the present study, we measured changes in $[Mg^{2+}]_i$ during prolonged applications of isoprenaline (over 100 min). $[Mg^{2+}]_i$ increased transiently (0.63 mM), but significant decreases in $[Mg^{2+}]_i$ (0.25 mM) were observed during the subsequent 75 min of drug applications (Figure 3a). These changes in $[Mg^{2+}]_i$ were markedly diminished by propranolol (Figure 4a), suggesting a hormonal regulation of $[Mg^{2+}]_i$ through a β-adrenoceptor effect.

We also measured changes in pH_i during application of isoprenaline. The pH_i estimated was approximately 7.1 in normal solutions, and transiently decreased by 0.1 units during the first 25 min application of isoprenaline (Figure 3b). Changes in pH_i are known to perturb the estimation of $[Mg^{2+}]_i$ (London, 1991). According to an equation described by Bock *et al.* (1985), the decrease in pH_i by 0.1 units from 7.1 leads to an increase in the estimation of $[Mg^{2+}]_i$ by less than 5%. Thus, in the present study, estimation of $[Mg^{2+}]_i$ does not seem to be perturbed significantly. Recently, Freudenrich *et al.* (1992) have reported that intracellular pH_i modulates $[Mg^{2+}]_i$ probably by affecting cytosolic Mg^{2+}-binding and/or the transport of Mg^{2+} across subcellular organelles. In cultured chicken heart cells, acidification of 0.9 pH units caused an increase in $[Mg^{2+}]_i$ of 0.1 mM. This modulation by pH_i of $[Mg^{2+}]_i$ is too small to explain the transient rise in $[Mg^{2+}]_i$ by applications of isoprenaline.

Adenosine triphosphate (ATP) is known as an important intracellular Mg^{2+} buffer. Headrick & Willis (1989) reported that inotropic stimulation using isoprenaline or ouabain results in a decrease in [ATP] and subsequently in an increase in $[Mg^{2+}]_i$ caused by dissociation of Mg^{2+} from ATP. The authors also showed an inverse relationship between $[Mg^{2+}]_i$ and [ATP]. Our results, a transient rise in $[Mg^{2+}]_i$ observed during the initial 25 min of isoprenaline application, accompanied by a marked decrease in [ATP], support their notion on regulation of $[Mg^{2+}]_i$ through a Mg^{2+}-buffering effect on ATP. However, in the present study, $[Mg^{2+}]_i$ decreased below its normal concentrations during the prolonged application of isoprenaline (over 100 min), while [ATP] decreased fur-

ther. If there were no other regulation except Mg^{2+} buffering by ATP, $[Mg^{2+}]_i$ would be expected to remain at the high concentration which was observed during the first 25 min of isoprenaline application, so long as [ATP] is not restored. On the other hand, Romani & Scarpa (1990) showed that 20% of total cellular Mg^{2+} was extruded by noradrenaline within a few minutes, and that this very large efflux of Mg^{2+} was inhibited by the preapplication of propranolol. They proposed a hormonal control of $[Mg^{2+}]_i$ and that β-adrenoceptor stimulation decreases $[Mg^{2+}]_i$. This β-adrenoceptor effect on Mg^{2+} efflux is in accordance with our observations of decreases in $[Mg^{2+}]_i$ in the latter half of isoprenaline application, whereas it seems likely that during short-term applications of isoprenaline, $[Mg^{2+}]_i$ would only increase due to the 'release' of Mg^{2+} from ATP. Ouabain, which is also known to have positive inotropic action, increased $[Mg^{2+}]_i$ in 25 min, accompanied by reduction of [ATP]. In contrast to isoprenaline, during the subsequent 75 min application, the increase in $[Mg^{2+}]_i$ was either sustained or increased gradually (unpublished observation, Nishimura & Nakayama). These results are consistent with the interpretation that the late decrease in $[Mg^{2+}]_i$ induced by isoprenaline is specific to β-adrenoceptor stimulation.

Intracellular Mg^{2+} buffers are also likely to have a binding affinity to Ca^{2+}. Therefore an increase in $[Ca^{2+}]_i$ may increase $[Mg^{2+}]_i$ due to competition. This effect has been investigated by use of n.m.r. techniques (Rotevatn *et al.*, 1989) and fluorescent dyes (Murphy *et al.*, 1989). In heart cells, it has been reported that $[Mg^{2+}]_i$ was increased by the removal of extracellular Na^+ in the presence of Ca^{2+}, whether extracellular Mg^{2+} is present or not, suggesting that the increase in $[Mg^{2+}]_i$ was induced through an increase in $[Ca^{2+}]_i$ via Na^+-Ca^{2+} exchange. In the present study, isoprenaline increased cardiac contractility throughout application. One would suspect that an increase in $[Ca^{2+}]_i$ by isoprenaline may modulate $[Mg^{2+}]_i$. The increase in $[Mg^{2+}]_i$ observed in the first 25 min after application of isoprenaline may in part be due to an increase in $[Ca^{2+}]_i$. However, in the latter half of prolonged application of isoprenaline, decreases in $[Mg^{2+}]_i$ were observed. Thus, modulation of $[Mg^{2+}]_i$ elicited by changes in $[Ca^{2+}]_i$ appears not to be significant when the physiological Na^+-gradient is maintained. When isoprenaline was applied together with propranolol, a small transient increase in $[Mg^{2+}]_i$ (Figure 4a, statistically not significant) was observed during the initial 25 min, accompanied by little change in [ATP]. This may be explained by intracellular competition between Mg^{2+} and Ca^{2+}.

There are many papers concerning the effects of extracellular Mg^{2+} on cardiac function (Shine, 1979). In contrast, little is known about changes in cardiac function upon increases or decreases in $[Mg^{2+}]_i$. However, according to the results obtained using material isolated from heart tissue, we can postulate the effects of $[Mg^{2+}]_i$ on cardiac function. In skinned muscle experiments, increases in $[Mg^{2+}]_i$ shift the $[Ca^{2+}]_i$-tension relation towards higher $[Ca^{2+}]_i$ (Godt, 1974; Fabiato & Fabiato, 1975; Best *et al.*, 1977). Furthermore, patch clamp techniques have recently revealed that increases in $[Mg^{2+}]_i$ inhibit L-type Ca^{2+} channel currents, whilst decreases in $[Mg^{2+}]_i$ facilitate such currents, especially when stimulated by adenosine 3':5'-cyclic monophosphate (cyclic AMP) (White & Hartzell, 1988). These results suggest that the decreases in $[Mg^{2+}]_i$ observed during prolonged applications of isoprenaline contribute to the inotropic effect of β-adrenoceptor stimulation. On the other hand, in S49 murine lymphoma cells, it has been shown that the guanine nucleotide-binding regulatory component of adenylyl cyclase is activated only by high concentrations of Mg^{2+} (Cech & Maguire, 1982), but that hormonal stimulation reduces the Mg^{2+} requirement below the normal concentrations of $[Mg^{2+}]_i$ (Iyengar & Birnbaumer, 1982). If cardiac cells possess similar mechanisms for the regulation of adenylyl cyclase, a fall of $[Mg^{2+}]_i$ would reduce cyclic AMP production and subsequently may diminish the effects of β-adrenoceptor stimulation. In this case, our observation of a fall in $[Mg^{2+}]_i$ during the prolonged application, may be interpreted as a feedback mechanism of desensitization, and would correlate with a reduction in ventricular pressure and heart rate (Table 2). At present, it is difficult to address the role of $[Mg^{2+}]_i$ in such mechanisms. Thus, the physiological implications of changes in $[Mg^{2+}]_i$ on contractility as well as regulatory mechanism(s) of $[Mg^{2+}]_i$ during applications of isoprenaline merit further investigation.

In the present study, a transient increase and subsequent decrease in $[Mg^{2+}]_i$ were observed during prolonged applications of isoprenaline. These changes can be explained by apparently conflicting evidence which has been reported in short-term stimulation of β-adrenoceptors: $[Mg^{2+}]_i$ is transiently increased by Mg^{2+} 'release' via reduction of MgATP through a positive inotropic effect (Headrick & Willis, 1989); a large efflux of Mg^{2+} may be due to an $[Mg^{2+}]_i$ regulatory mechanism activated by cyclic AMP (Romani & Scarpa, 1990).

The authors are greatly indebted to Prof. Sadayuki Sakuma and Dr Kengo Itoh, Nagoya University, for pertinent help and advice, and are also grateful to Drs Andrew Cook, Narelle Bramich and Derek Terrar, Oxford University, for their useful comments and critical reading of this manuscript.

References

AGUS, Z.S. & MORAD, M. (1991). Modulation of cardiac ion channels by magnesium. *Annu. Rev. Physiol.*, **53**, 299–307.

ANDERSON, T.W., NERI, L.C., SCHREIBER, G.B., TALBOT, F.D.F. & ZDROJESKI, A. (1975). Ischemic heart disease, water hardness and myocardial magnesium. *Can. Med. Assoc. J.*, **113**, 199–203.

BEST, P.M., DONALDSON, S.K.B. & KERRICK, W.G.L. (1977). Tension mechanically disrupted mammalian cardiac cells: effects of magnesium adenosine triphosphate. *J. Physiol.*, **256**, 1–17.

BOCK, J.L., WENZ, B. & GUPTA, R.K. (1985). Changes in intracellular Mg adenosine triphosphate and ionized Mg^{2+} during blood storage: detection by ^{31}P nuclear magnetic resonance spectroscopy. *Blood*, **65**, 1526–1530.

CECH, S.Y. & MAGUIRE, M.E. (1982). Magnesium regulation of the beta-receptor-adenylate cyclase complex. 1. Effects of manganese on receptor binding and cyclase activation. *Mol. Pharmacol.*, **22**, 267–273.

EBEL, H. & GÜNTHER, T. (1983). Role of magnesium in cardiac disease. *J. Clin. Chem. Clin. Biochem.*, **21**, 249–265.

EISNER, D.A., ELLIOTT, A.C. & SMITH, G.L. (1987). The contribution of intracellular acidosis to the decline of developed pressure in ferret hearts exposed to cyanide. *J. Physiol.*, **391**, 99–108.

FABIATO, A. & FABIATO, F. (1975). Effects of magnesium on contractile activation of skinned cardiac cells. *J. Physiol.*, **249**, 497–517.

FREUDENRICH, C.C., MURPHY, E., LEVY, L.A., LONDON, R.E. & LIEBERMAN, M. (1992). Intracellular pH modulates cytosolic free magnesium in cultured chicken heart cells. *Am. J. Physiol.*, **262**, C1024–1030.

GODT, R.E. (1974). Calcium-activated tension of skinned muscle fibers of the frog: dependence on magnesium adenosine triphosphate concentration. *J. Gen. Physiol.*, **63**, 722–739.

GUPTA, R.K., GUPTA, P. & MOORE, R.D. (1984). NMR studies of intracellular metal ions in intact cells and tissues. *Annu. Rev. Biophys. Bioeng.*, **13**, 221–246.

GUPTA, R.K. & MOORE, R.D. (1980). ^{31}P NMR studies of intracellular free Mg^{2+} in intact frog skeletal muscle. *J. Biol. Chem.*, **255**, 3987–3993.

HEADRICK, J.P. & WILLIS, R.J. (1989). Effects of inotropic stimulation on cytosolic Mg^{2+} in isolated rat heart. ^{31}P magnetic resonance study. *Magn. Reson. Med.*, **12**, 328–338.

HEADRICK, J.P. & WILLIS, R.J. (1990). Adenosine formation and energy metabolism: a ^{31}P-NMR study in isolated rat heart. *Am. J. Physiol.*, **258**, H617–624.

IYENGAR, R. & BIRNBAUMER, L. (1982). Hormone receptor modulates the regulatory component of adenylyl cyclase by reducing its requirement for Mg^{2+} and enhancing its extent of activation by guanine nucleotides. *Proc. Natl. Acad. Sci. U.S.A.*, **79**, 5179–5183.

JENNINGS, R.B. & STEENBERGEN, C. (1985). Nucleotide metabolism and cellular damage in myocardial ischemia. *Annu. Rev. Physiol.*, **47**, 729–749.

KUSUOKA, H. & MARBAN, E. (1992). Cellular mechanisms of myocardial stunning. *Annu. Rev. Physiol.*, **54**, 243–256.

LONDON, R.E. (1991). Methods for measurement of intracellular magnesium: NMR and fluorescence. *Annu. Rev. Physiol.*, **53**, 241–258.

MATSUDA, H. (1991). Magnesium gating of the inwardly rectifying K^+ channel. *Annu. Rev. Physiol.*, **53**, 289–298.

McGUIGAN, J.A.S., BLATTER, L.A. & BURI, A. (1991). Use of ion selective microelectrodes to measure intracellular free Mg^{2+}. In *Mg^{2+} and Excitable Membranes*. ed. Strata, P. & Carbone, E. pp. 1–19. Berlin Heidelberg: Springer-Verlag.

MOON, R.B. & RICHARDS, J.H. (1973). Determination of intracellular pH by P-31 magnetic resonance. *J. Biol. Chem.*, **248**, 7276–7278.

MURPHY, E., FREUDENRICH, C.C., LEVY, L.A., LONDON, R.E. & LIEBERMAN, M. (1989). Monitoring cytosolic free magnesium in cultured chicken heart cells by use of the fluorescent indicator Furaptra. *Proc. Natl. Acad. Sci. U.S.A.*, **86**, 2981–2984.

NAKAYAMA, S., SEO, Y., TAKAI, A., TOMITA, T. & WATARI, H. (1988). Phosphorous compounds studied by ^{31}P nuclear magnetic resonance spectroscopy in the taenia of guinea-pig caecum. *J. Physiol.*, **402**, 565–578.

NAKAYAMA, S. & TOMITA, T. (1990). Depletion of intracellular free Mg^{2+} in Mg^{2+}- and Ca^{2+}-free solution in the taenia isolated from guinea-pig caecum. *J. Physiol.*, **421**, 363–378.

ROMANI, A. & SCARPA, A. (1990). Hormonal control of Mg^{2+} transport in the heart. *Nature*, **346**, 841–844.

ROTEVATN, S., MURPHY, E., LEVY, L.A. RAJU, B., LIEBERMAN, M. & LONDON, R.E. (1989). Cytosolic free magnesium concentration in cultured chick heart cells. *Am. J. Physiol.*, **257**, C141–146.

SHINE, K.I. (1979). Myocardial effects of magnesium. *Am. J. Physiol.*, **237**, H413–423.

STITT, F.W., CLAYTON, D.G., CRAWFORD, M.D. & MORRIS, J.N. (1973). Clinical and biochemical indicators of cardiovascular disease among men living in hard and soft water area. *Lancet*, **i**, 122–126.

WHITE, R.E. & HARTZELL, H.C. (1988). Effects of intracellular free magnesium on calcium current in isolated cardiac myocytes. *Science*, **239**, 778–780.

WHITE, R.E. & HARTZELL, H.C. (1989). Magnesium ions in cardiac function. *Biochem. Pharmacol.*, **38**, 859–867.

(Received October 13, 1992
Revised December 16, 1992
Accepted February 4, 1993)

Br. J. Pharmacol. (1993), **109**, 449–458 © Macmillan Press Ltd, 1993

Anion transport blockers inhibit DL-2-amino-4-phosphonobutyrate responses induced by quisqualate in the rat cerebral cortex

[1]Jonathan P. Turner

Department of Neurology, Institute of Psychiatry, De Crespigny Park, Denmark Hill, London SE5 8AF

1 Depolarizing responses to DL-2-amino-4-phosphonobutyrate (AP4) and related amino acids have been studied in the rat cerebral cortex slice following the application of quisqualate (Quis).

2 Before exposure to Quis, 500 μM DL-AP4 had little or no effect. However, following a single application of 40 μM Quis for 2 min, DL-AP4 produced depolarizing responses. With repeated applications of DL-AP4, there was a decline in response amplitude. A second application of Quis restored the depolarizing potency of DL-AP4 to a level above that for the first DL-AP4 response after the first Quis application. With a sequence of alternate applications of Quis and DL-AP4, the amplitude of DL-AP4 responses became maximal after the second Quis application. Responses to DL-AP4 could also be induced by the application of 1 μM Quis for 60 min, but were smaller in amplitude.

3 Responses to the normally inactive amino acids L-cysteine (Cys), L-cystathionine (CTN) and L-α-aminoadipate (AA) were also induced once Quis was applied. These responses were also maximized after a second application of Quis, except those to L-Cys, which failed to reach a plateau after three Quis applications.

4 The co-application of DL-AP4 with the first Quis application depressed the subsequent mean DL-AP4 response by 47%. Re-application of Quis restored the amplitude of DL-AP4 responses to levels comparable to control. L-α-AA also suppressed the induction of DL-AP4 responses, when co-applied with the first Quis exposure, reducing mean response amplitude by 98%. Unlike DL-AP4, however, the effect with L-α-AA persisted so that DL-AP4 responses were significantly suppressed compared to control, even after further applications of Quis.

5 The effects of the anion transport blockers, 4,4′-diisothiocyanatostilbene-2,2′-disulphonic acid (DIDS) and 4-acetoamido-4′-isothiocyanatostilbene-2,2′-disulphonic acid (SITS) on the induction process and the DL-AP4 responses themselves were examined. DIDS (100 μM) significantly inhibited the DL-AP4 responses, and to a lesser extent the induction of the responses by 40 μM Quis (2 min), while SITS (300 μM) only inhibited the DL-AP4 responses. However, the induction of responses by 1 μM Quis (60 min) was significantly affected by this concentration of SITS.

6 DIDS (100 μM) had no effect on responses to α-amino-3-hydroxy-5-methyl-4-isoxazolepropionate (AMPA), but selectively potentiated those to Quis. Examination of the full concentration-response curve for Quis revealed that, while the R_{max} remained constant, the Hill slope was increased and the EC_{50} was decreased in the presence of DIDS. SITS (300 μM), however, antagonized responses to AMPA, and had little effect on responses to Quis except at the highest concentration of Quis tested (20 μM), where a potentiation was observed, suggesting that it is a non-NMDA receptor antagonist.

7 These observations indicate that the production of depolarizing responses to a number of amino acids, including DL-AP4, in the cerebral cortex is mediated via an anion transport mechanism sensitive to DIDS and SITS, and that the exchange of DL-AP4 for a sequestered excitatory amino acid receptor agonist, probably Quis, could underlie the production of these responses. Indeed, Quis is apparently sequestered via a similar process. However, the involvement of such a process in the induction of these responses remains inconclusive.

Keywords: DL-2-Amino-4-phosphonobutyrate; quisqualate; anion transport; cerebral cortex

Introduction

There is evidence for a novel interaction between the excitatory amino acid (EAA) receptor agonist quisqualate (Quis) and L-2-amino-4-phosphonobutyrate (AP4). Before exposure to Quis, L-AP4 has little or no direct action on the electrophysiological properties of the consistuents of hippocampal and neocortical slices. However, the application of AP4 subsequent to Quis in these tissues produces a depolarizing response (Harris *et al.*, 1987; Sheardown, 1988) and/or suppression of synaptic responses (Robinson *et al.*, 1986; Harris *et al.*, 1987). Since α-amino-3-hydroxy-5-methyl-4-isoxazolepropionate (AMPA), kainate (KA) and N-methyl-D-aspartate (NMDA) do not induce responses to AP4, this effect is unlikely to depend on the activation of any of the three ionotropic EAA receptor subtypes for which these compounds are selective agonists (Watkins & Evans, 1981; Monaghan *et al.*, 1989) during the exposure to Quis. However, since the AMPA/KA receptor antagonist 6-cyano-7-nitroquinoxaline-2,3-dione, but not NMDA antagonists, blocks the L-AP4 response in the cortex (Sheardown, 1988; Lodge & Zeman, 1989), the production of these responses would appear to be dependent on the activation of non-NMDA rather than NMDA receptors.

Both L-AP4 and Quis displace Cl^--dependent L-[^{3}H]-glutamate and DL-[^{3}H]-AP4 binding, with inhibition constants in the 0.1–10 μM range (Butcher *et al.*, 1983; Foster & Fagg, 1984). The Cl^--dependent L-[^{3}H]-glutamate binding is heterogeneous, composed of at least two components with different sensitivities to Quis. The relatively Quis-sensitive component

[1] Present address: Department of Physiology, University of Wales College of Cardiff, P.O. Box 902, Museum Avenue, Cardiff CF1 1SS.

and DL-[^{3}H]-AP4 binding have very similar pharmacological profiles, indicating that they probably represent the same site (Werling *et al.*, 1983). These binding correlates have been suggested to represent Cl^--dependent L-glutamate sequestration (Pin *et al.*, 1984), mediated via an anion transport mechanism sensitive to 4,4'-diisothiocyanatostilbene-2-2'-disulphonic acid (DIDS) (Recasens *et al.*, 1987; Zaczek *et al.*, 1987a). These uptake/transport sites differ from the Cl^--dependent L-[^{3}H]-glutamate binding sites which represent the metabotrophic L-glutamate receptor (Cha *et al.*, 1990), when their pharmacological profiles are compared. The Quis effect could, therefore, represent an electrophysiological manifestation of this sequestration process, as proposed by Harris *et al.* (1987), with sequestered Quis being released via a heterogeneous exchange with L-AP4. An alternative explanation is that Quis 'sensitizes' neuronal tissue to AP4 as proposed by Whittemore & Koerner (1991). Since agonists selective for receptors coupled to phosphoinositide (PI) turnover are also able to induce responses to AP4 (Whittemore & Cotman, 1991), the induction of these responses by Quis could result from the stimulation of PI turnover via its agonist action at the metabotropic L-glutamate receptor.

Methods

Male Wistar rats (200–300 g) were killed by decapitation and their brains rapidly removed. Wedges of anterior cingulate cortex 500 μm thick were prepared from coronal slices (corresponding to plates 13–22, Paxinos & Watson, 1986) with a Vibroslice (Camden Instruments) as a modification to the method of Harrison & Simmonds (1985). The wedges were set up in two-compartment baths so that the cortical tissue projected through a greased gap in a two piece barrier separating the two compartments. The majority of the cortex was in one compartment and the underlying white matter was in the other. The compartments were perfused independently with Krebs medium of the following composition (mM): NaCl 118, $NaHCO_3$ 25, KCl 2.1, KH_2PO_4 1.2, $CaCl_2$ 2.5, $MgSO_4$ 1, glucose 11; and gassed with 95% O_2/5% CO_2. The flow rate was approximately 2 ml min^{-1} and the temperature maintained at 21–23°C. All drugs were dissolved in the Krebs medium and perfused through the cortical compartment only. The d.c. potential difference between the two compartments was recorded continuously using Ag/AgCl bath electrodes, amplified and displayed on a pen recorder. Negativity induced in the cortical compartment was interpreted as a depolarization of the neuronal tissue passing through the barrier. Responses were measured at their peak amplitude.

In experiments where responses to DL-AP4 and related amino acids were induced by Quis, all drugs were applied for 2 min, except where stated. These amino acids were selected for study on their ability to displace either Cl^--dependent L-[^{3}H]-glutamate or [^{3}H]-AP4 but not AMPA, KA and NMDA receptor binding (Simon *et al.*, 1976; Butcher *et al.*, 1983; Werling *et al.*, 1983; Kessler *et al.*, 1987; Murphy *et al.*, 1987; Pullan *et al.*, 1987; Olverman *et al.*, 1988). L-α-Aminoadipate (AA), L-cysteine (Cys) and L-cystathionine (CTN), fulfilled this criterion, although the first two are weakly active at NMDA receptor binding sites. Paradigms for the examination of the effects of L-α-AA, of DL-AP4 itself, and of the anion transport blockers 4,4'-diisothiocyanatostilbene-2,2'-disulphonic acid (DIDS) and 4-acetoamido-4'-isothiocyanatostilbene-2,2'-disulphonic acid (SITS) on the induction by Quis, and the DL-AP4 responses themselves, are detailed in the results. In a few experiments, the influence of DIDS and SITS on responses to AMPA and Quis was also examined. Concentrations of 2.5 and 5 μM AMPA; and 5, 10 and 20 μM Quis were perfused for 2 min to produce depolarizing responses which are on the lower halves of the linear portions of their respective DR curves. Either DIDS or SITS was then perfused for 30 min prior to and during the re-determination of agonist responses, bridging the same response range as the control DR lines. The slopes of DR lines were calculated by linear regression analysis. From parallel shifts of the DR lines, equi-effective dose-ratios for each agonist could be calculated. In these experiments, AMPA and Quis DR lines were obtained from the same slices so that a direct comparison of the two AMPA receptor agonists could be made. In addition, the effect of DIDS on the full concentration-response curve to Quis was examined. One concentration-response curve was obtained from one experiment, either in the absence or in the presence of DIDS to eliminate the problem of desensitization. The curves were compared by measuring all responses relative to an initial response to 20 μM Quis = 1 recorded in the absence of DIDS. These initial responses to Quis were also compared to a response to 5 μM AMPA obtained under the same conditions. This analysis did not reveal any significant difference ($P > 0.1$, Student's t test) in the sensitivities of control and drug applied slices to AMPA and Quis. Each full concentration-response curve was fitted using the log concentration-response relationship:

$$y = R_{max}/1 + (EC_{50}/x)^H$$

where x = agonists concentration producing response amplitude y, R_{max} = maximal response, EC_{50} = agonist concentration producing half maximal response, H = Hill coefficient.

DIDS and SITS were dissolved directly into the Krebs medium just before use. All other drugs were made up as stock stolutions at 10 mM and diluted in the Krebs medium just before use. Drugs were purchased from the following sources: α-amino-3-hydroxy-5-methyl-4-isoxazolepropionate, DL-2-amino-4-phosphonobutyrate and quisqualate from Tocris; L-α-aminoadipate, L-cysteine, L-cystathionine, 4,4'-diisothiocyanatostilbene-2,2'-disulphonic acid and 4-acetoamido-4'-isothiocyanatostilbene-2,2'-disulphonic acid from Sigma.

Results

Induction of responses to amino acid analogues

Prior to the application of Quis, 500 μM DL-AP4 had little or no effect on the baseline (Figure 1). In some slices small depolarizations were observed, but these never exceeded 0.04 when measured relative to the subsequent 40 μM Quis response = 1. This concentration of Quis was used in order to maximize the amplitude of DL-AP4 depolarizing responses. It was just above the EC_{50} value for Quis (22.3 μM, cf. Figure 8 and Table 4), consistent with a previous study (24.0 μM, Horne & Simmonds, 1989). Four consecutive DL-AP4 applications subsequent to Quis produced responses of progressively diminishing amplitude (Figure 1 and Table 1). A second application of Quis restored the DL-AP4 response amplitude to a level above that found initially after the first Quis application. These results clearly indicate that the induction of DL-AP4 responses in cortical tissue is readily reversible. However, whether this loss of responsiveness is time- or use-dependent was not determined. In addition, this loss of responsiveness is also readily counteracted by a further application of Quis, indicating that the mechanism underlying the induction of responsiveness of cortical tissue to DL-AP4 can undergo reactivation. This loss of responsiveness precluded a more detailed examination of DL-AP4 responses involving the construction of concentration-effect curves.

In a second set of experiments Quis and DL-AP4 or one of the selected amino acids were applied alternately (Figures 2 and 3). Prior to the application of Quis, 50 μM L-Cys, 500 μM L-α-AA (Figure 2) and 100 μM CTN (data not shown) had little or no effect on the baseline. This is consistent with binding data (Simon *et al.*, 1976; Kessler *et al.*, 1987; Murphy *et al.*, 1987; Pullan *et al.*, 1987; Olverman *et al.*, 1988), which indicated that these compounds are relatively inactive at AMPA, KA, and NMDA receptors. However, once the

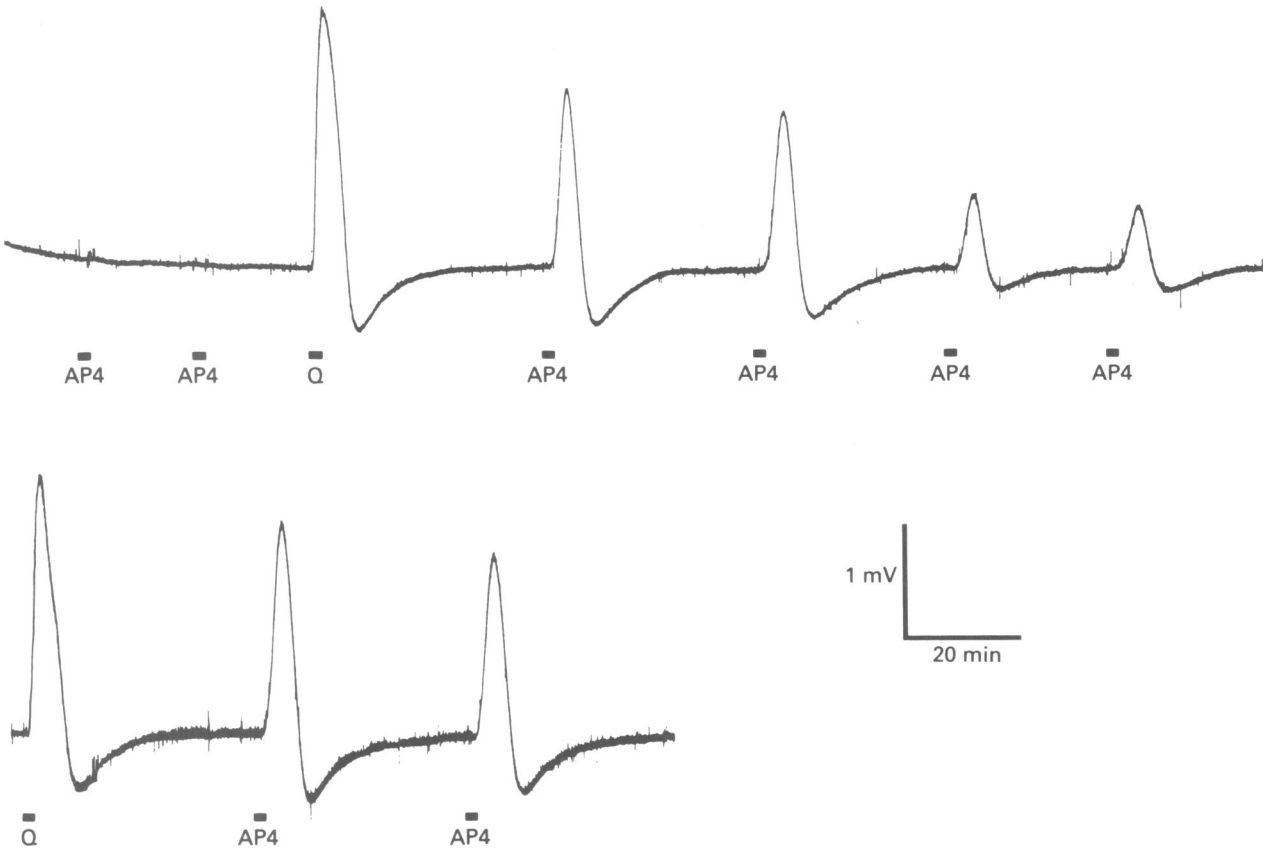

Figure 1 A continuous recording of d.c. potential showing the induction of depolarizing responses to 500 μM DL-AP4 by 40 μM Quis (Q) and their subsequent decline in amplitude upon repeated applications of DL-AP4. Both Quis and DL-AP4 were perfused for 2 min. For abbreviations in this and subsequent figures, see text.

Table 1 Sequential responses to quisqualate (Quis) 40 μM and DL-2-amino-4-phosphonobutyrate (DL-AP4) 500 μM

$Quis_1$	$AP4_1$	$AP4_2$	$AP4_3$	$AP4_4$	$Quis_2$	$AP4_5$	$AP4_6$
1.00	0.61 ±0.042	0.53 ±0.024	0.33[a] ±0.021	0.27[a] ±0.022	1.06[b] ±0.018	0.74[a] ±0.035	0.64[c] ±0.036

Response amplitude was measured relative to the initial response to Quis = 1. Values are mean ± s.e.mean from 16 experiments. [a]$P<0.001$ compared to $AP4_1$ response, [b]$P<0.01$ compared to $Quis_1$ response; [c]$P<0.01$ compared to $AP4_5$ response (paired t test).

tissue had been exposed to Quis all three compounds produced depolarizing responses. The mean amplitudes for these responses in the sequence of alternating applications with Quis are shown in Figure 3. The amplitude of these amino acid responses became maximal after two Quis applications, except for those to L-Cys, which failed to plateau after three Quis applications. A second application of these amino acids after the third Quis response produced a response of comparable amplitude to the first. These results indicate that Quis is able to induce responses to a number of amino acids, that are highly selective ligands for Cl^--dependent L-[^{3}H]-glutamate and L-[^{3}H]-AP4 binding sites, other than DL-AP4.

Responses to 500 μM DL-AP4 were also induced following perfusion of 1 μM Quis for 60 min (Figure 4a). However, these responses were of smaller amplitude than those initially induced by 40 μM Quis for 2 min (Table 2). The subsequent application of 40 μM Quis resulted in a larger response to DL-AP4 comparable in amplitude to that of responses in the previous experiments, where alternate applications of 40 μM Quis and DL-AP4 were used (Table 2). The fact that a low concentration of Quis, applied for a relatively long period of time, is able to induce responses to DL-AP4 indicates that this effect is not solely dependent on the level of depolarization produced by Quis, but on a combination of concentration and time course of application.

The effect of DL-AP4 and L-α-AA on induction by Quis

In an attempt to determine whether the sites underlying the production of the responses to DL-AP4 also underlie the induction process as predicted by the exchange hypothesis, the influence of DL-AP4 and L-α-AA on the induction of DL-AP4 responses by Quis was studied using a paradigm based on the design in Figure 3. DL-AP4 and L-α-AA (both 500 μM) were perfused for 10 min before and then during the first application of 40 μM Quis. There then followed a 60 min re-equilibration period in control Krebs medium. Responses to alternate applications of 500 μM DL-AP4 and 40 μM Quis were obtained and compared to the data in Figure 3 (recalculated relative to the third Quis responses = 1) as shown in Table 2. DL-AP4 partially suppressed the induction of responses by Quis in a readily reversible manner (Figure 5a), while L-α-AA suppressed induction almost completely, an effect that showed only a small reversal after several Quis applications (Figure 5b). The persistent suppression of DL-AP4 responses by L-α-AA applied for a relatively short

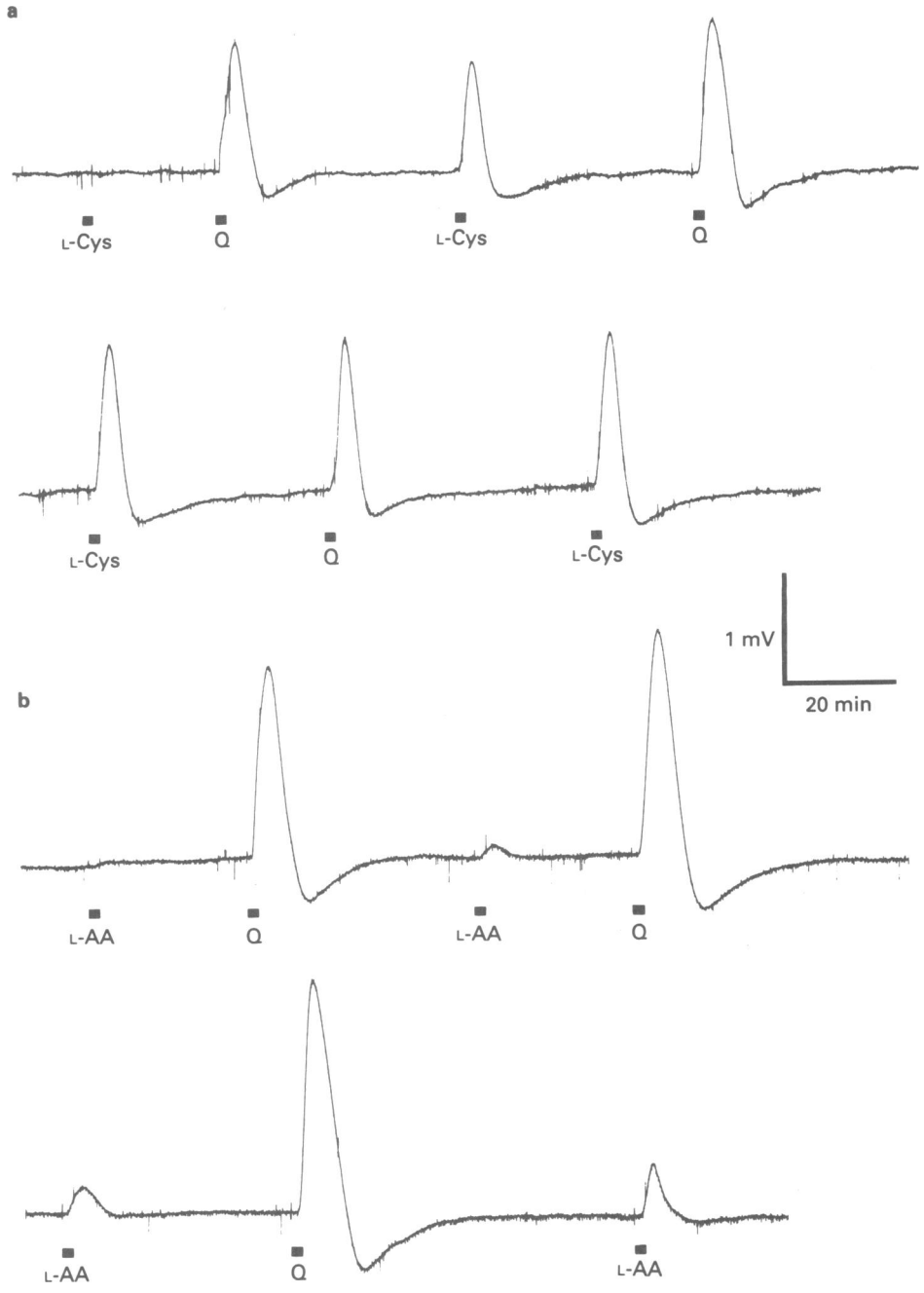

Figure 2 Continuous recordings of d.c. potential showing the induction of depolarizing responses to (a) 50 μM L-Cys and (b) 500 μM L-α-AA by 40 μM Quis (Q) and their subsequent enhancement upon repeated applications of Quis. Both Quis and L-Cys or L-α-AA were perfused for 2 min.

period of time during induction indicated that there was a slow recovery for its effect on induction. This could explain the relatively small responses obtained for L-α-AA in Figure 3, as the L-α-AA applied before the Quis could be blocking the induction process. In addition, since the same concentration of L-α-AA and DL-AP4 were used in these experiments, and these compounds are almost equipotent as displacers of Cl^--dependent L-glutamate/AP4 binding sites (Butcher *et al.*, 1983; Werling *et al.*, 1983), the data would suggest that it is unlikely that these sites are involved in the induction of responses. However, without either comparing the DL-AP4 concentration-effect curve for control induction with those for induction in the presence of DL-AP4 or L-α-AA, or using different concentrations of DL-AP4 and L-α-AA during the induction process, it is impossible to measure the difference in potency with respect to the inhibition of induction.

The effect of the anion transport blockers DIDS and SITS

A similar paradigm based on the design in Figure 3 was used to study the influence of DIDS on Quis-induced DL-AP4 responses (Figure 6a). In a similar sequence of alternating applications of Quis and DL-AP4, medium containing 100 μM DIDS was perfused 20 min before and during the first Quis and third DL-AP4 applications, and 60 min allowed for re-equilibration with normal Krebs medium. The amplitude of the DL-AP4 responses was measured relative to the third Quis response = 1, and compared with the data in Figure 3 (Tables 2 and 3). DIDS had no effect on the baseline, but produced a suppression of the first DL-AP4 response following the priming application of Quis, and almost completely abolished the responses once they had been induced. There was a significant recovery of the DL-AP4 responses after their

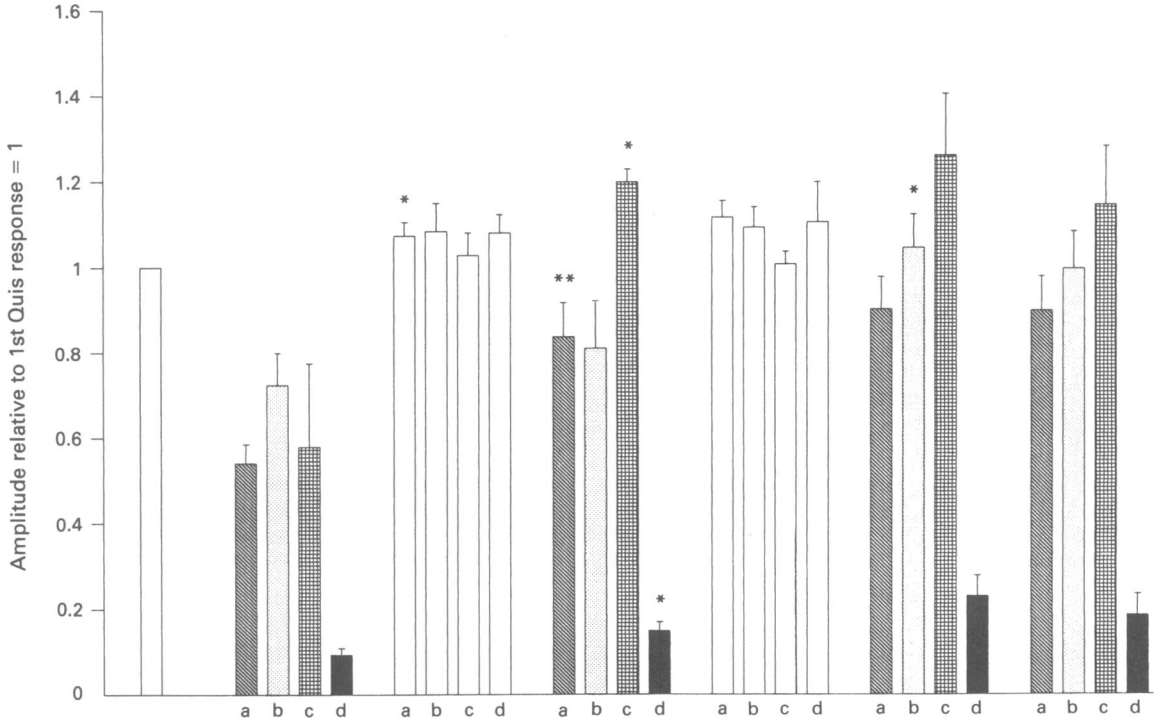

Figure 3 The mean ± s.e.mean amplitude of depolarizing responses to alternate applications of 500 μM DL-AP4 ($n = 9$) (a), 50 μM L-Cys ($n = 6$) (b), 100 μM L-CTN ($n = 3-4$) (c) and 500 μM L-α-AA ($n = 6$) (d) with 40 μM Quis measured relative to the first priming Quis response = 1. Open columns, Quis; hatched column, DL-AP4; stippled columns, L-Cys; checkered column, L-CTN; solid columns, L-α-AA. $^*P < 0.05$; $^{**}P < 0.01$ (paired t test) when compared with the preceding response to the same compound.

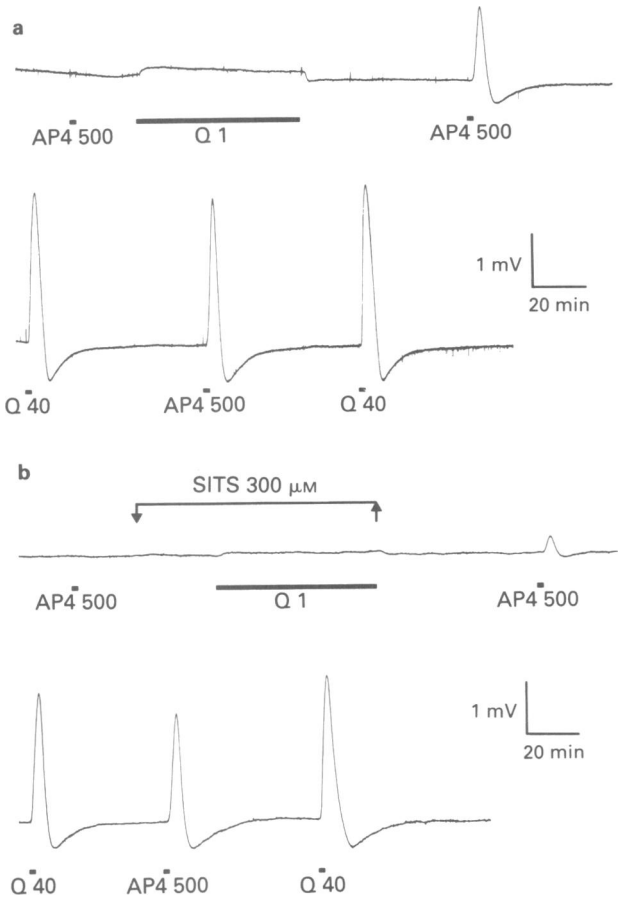

Figure 4 Continuous recordings of d.c. potential showing (a) the induction of depolarizing responses to 500 μM DL-AP4 by 1 μM quisqualate (Q) and (b) the effect of 300 μM SITS on this induction. Quis 1 μM was perfused for 60 min, 40 μM Quis and 500 μM DL-AP4 for 2 min. SITS 300 μM was perfused for the time period indicated by the bar above the record.

depression by DIDS, but the mean amplitude of the response was only 52% of that prior to the application of DIDS. This is less than would be predicted for the control experiments (Figure 3) as shown in Table 3, probably indicating that there is a very slow recovery from the effects of DIDS in these experiments, casting doubt on the interpretation of the effect of DIDS on the induction of DL-AP4 responses. This is consistent with previous observations which have indicated that the effects of DIDS are difficult to reverse (White & Miller, 1979).

As a result, a second anion transport blocker, SITS, which is known to be reversible (White & Miller, 1979), was used. In a design like that for DIDS, 300 μM SITS was applied 20 min before and during the first Quis and third DL-AP4 applications in an alternating sequence, and 60 min allowed for re-equilibration with control medium (Figure 6b). SITS had no effect on baseline, and unlike DIDS had no effect on the induction of DL-AP4 responses by 40 μM Quis (Table 2), although it blocked the induced DL-AP4 responses in a reversible manner (Figure 6b and Table 3). This finding supports the suggestion that the poor washout of DIDS is responsible for the apparent suppression of induction in the DIDS experiments. Therefore, the apparent lack of effect of the anion transport blockers on the induction of DL-AP4 responses by Quis indicates that a process other than anion exchange underlies induction, when 40 μM Quis is used. Binding studies show that Quis inhibits Na^+-dependent L-[^{3}H]-glutamate binding to whole brain synaptosomes (Ogita & Yoneda, 1986) and Na^+-dependent D-[^{3}H]-aspartate binding to brain slices (Anderson *et al.*, 1990), with approximated IC_{50}s in the 10–100 μM range. Therefore, with 40 μM Quis, there may well be sufficient sequestration by Na^+-dependent transport to provide an anion transport blocker-resistant source of Quis for heterogeneous exchange with AP4. A study of uptake of Quis by hippocampal tissue reveals that negligible amounts of Quis are sequestered via a Na^+-dependent mechanism at a concentration of 16 μM (Harrison & Kilpatrick, 1991). Therefore, the experiments with SITS were repeated using 1 μM Quis applied for 60 min as the sensitiz-

Table 2 The influence of amino acid analogues and anion transport blockers on the induction of DL-2-amino-4-phosphonobutyrate (DL-AP4, 500 μM) responses, by their application prior to and during the first quisqualate (Quis) exposure

	$Quis_1$	$AP4_1$	$Quis_2$	$AP4_2$
Quis 40 μM (2 min) ($n = 9$)	0.904 ± 0.031	0.47 ± 0.046	0.973 ± 0.047	0.76 ± 0.077
+ DL-AP4 500 μM ($n = 5$)	1.031 ± 0.119	0.25 ± 0.076**	0.926 ± 0.051	0.69 ± 0.082
+ L-α-AA 500 μM ($n = 5$)	0.931 ± 0.052	0.01 ± 0.006***	0.880 ± 0.050	0.11 ± 0.050***
+ DIDS 100 μM ($n = 7$)	1.140 ± 0.055**	0.22 ± 0.053***	1.014 ± 0.043	0.54 ± 0.069
+ SITS 300 μM ($n = 5$)	0.993 ± 0.074	0.36 ± 0.103	0.900 ± 0.065	0.78 ± 0.117
Quis 1 μM (60 min) ($n = 7$)	–	0.35 ± 0.055	0.987 ± 0.025	0.70 ± 0.096
+ SITS 300 μM ($n = 5$)	–	0.14 ± 0.047*	0.966 ± 0.076	0.65 ± 0.095

Response amplitude was measured relative to the third Quis response = 1. Values are mean ± s.e.mean of the number of experiments in parentheses.
*$P < 0.05$, **$P < 0.01$, ***$P < 0.005$; compared to control (Student's t test).

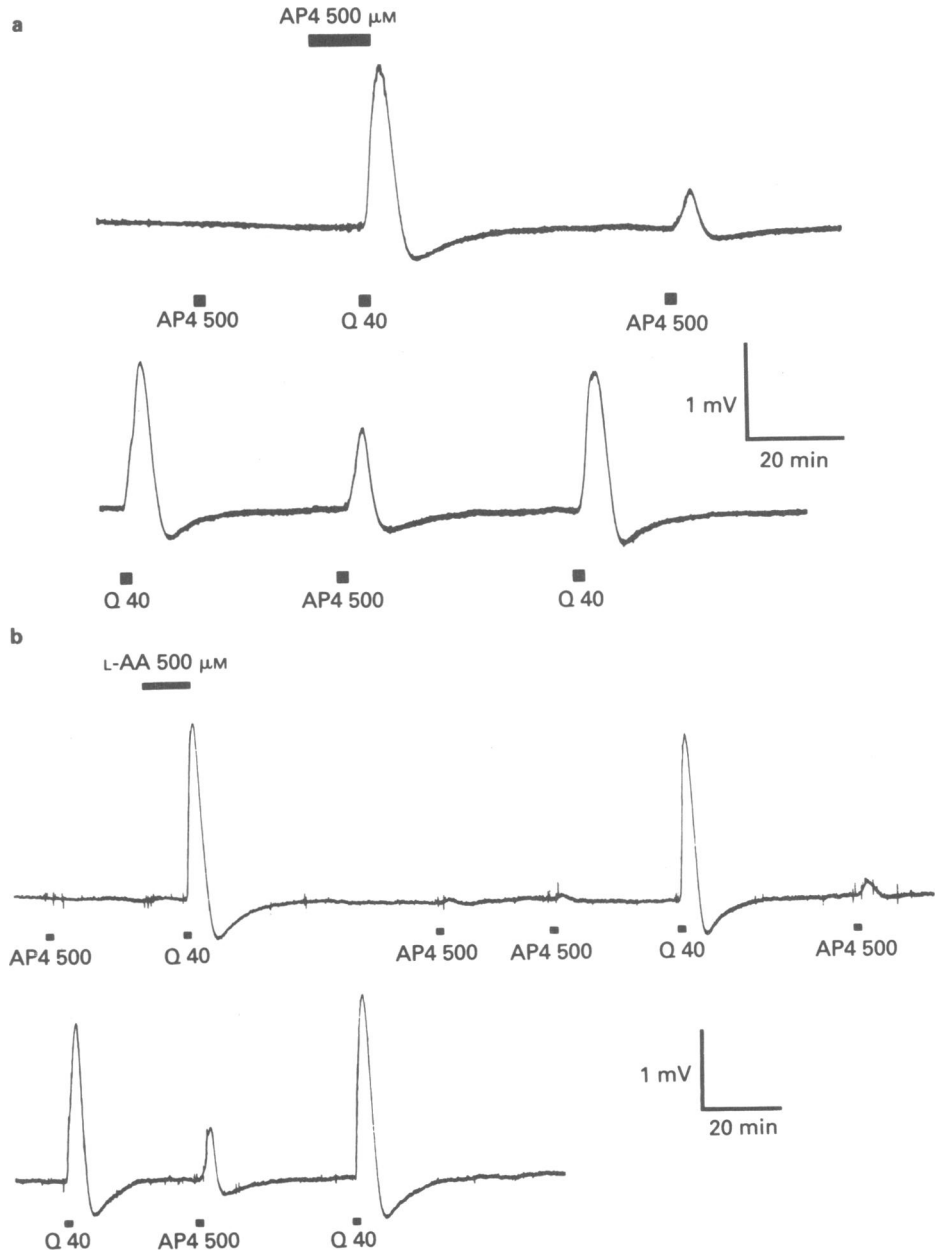

Figure 5 Continuous recordings of d.c. potential showing the effects of (a) 500 μM DL-AP4 and (b) 500 μM L-α-AA on depolarizing responses to 500 μM DL-AP4 and their induction by 40 μM Quis (Q). All drugs were perfused for the time periods indicated by the bars above and below the records at the concentrations indicated in μM.

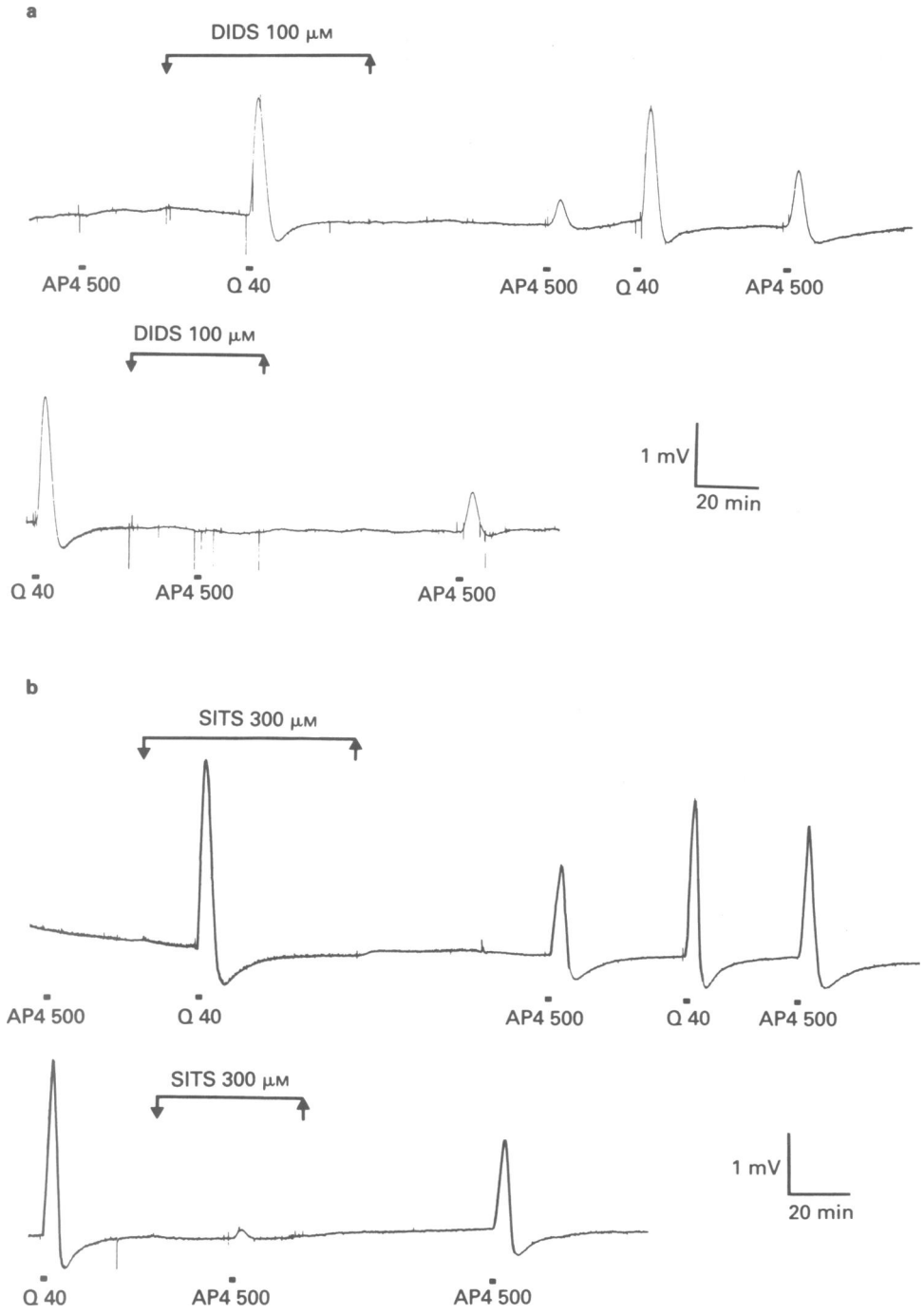

Figure 6 Continuous recordings of d.c. potential showing the effects of (a) 100 μM DIDS and (b) 300 μM SITS on depolarizing responses to 500 μM DL-AP4 and their induction by 40 μM Quis (Q). Both DL-AP4 and Quis were perfused for 2 min. DIDS and SITS were perfused for the time period indicated by the bars above the record.

ing pulse, and 60 min allowed for the re-equilibration in control Krebs medium. As demonstrated in Figure 4b and Table 2, under these conditions 300 μM SITS was able to suppress the induction of DL-AP4 responses by 60%.

Since the production of DL-AP4 responses is apparently dependent on the activation of non-NMDA receptors, DIDS and SITS were tested against responses to AMPA and Quis. DIDS (100 μM) produced a leftward shift of the Quis DR line, with a dose-ratio range of 0.64–0.44 (1.6–2.2 fold leftward shift, Figure 7a), with no significant effects on responses to AMPA (Figure 7b). This enhancement of Quis responses is consistent with the significantly larger 40 μM Quis responses observed in the presence of DIDS in Table 2. Indeed, examination of the full concentration-response curve for Quis in the absence and presence of 100 μM DIDS (Figure 8) indicate that, while R_{max} is unaffected, the EC_{50} and Hill slope of the concentration-response curve are decreased and increased, respectively, in the presence of DIDS (Table 4). On the other hand, SITS (300 μM) had no significant effect on responses to 5 and 10 μM Quis, and only potentiated those to 20 μM, with an increased amplitude of 36 ± 10% (Figure 7c). In addition, it antagonized responses to AMPA, shifting the DR line to the right 1.71 fold in a parallel manner (Figure 7d). This would suggest that as well as the DIDS-like potentiation of Quis responses, there is also an underlying non-NMDA receptor antagonism. Therefore, examination of the effect of SITS on the full Quis concentration-response curve was not performed. These results are

Table 3 The influence of anion transport blockers on the production of DL-2-amino-4-phosphonobutyrate (DL-AP4) response induced by quisqualate (Quis)

	DL-AP4 responses in relation to third Quis response		
	Prior	*Subsequent*	
	Control	*Drug*	*Wash*
Control	0.76	0.81	0.81
($n = 9$)	± 0.077	± 0.066	± 0.081
DIDS 100 μM	0.54	0.03*	0.28*[a]
($n = 7$)	± 0.069	± 0.011	± 0.036
SITS 300 μM	0.78	0.06*	0.77
($n = 5$)	± 0.117	± 0.015	± 0.171

Response amplitude was measured relative to the third Quis response = 1. Values are mean ± s.e.mean of the number of experiments in parentheses, and are a continuation of those experiments shown under the conditions stated used with 40 μM Quis as the inducing pulse in Table 2.
*$P < 0.005$ compared to Control; [a]$P < 0.05$ compared to DL-AP4 response prior to third Quis response (Student's t test).

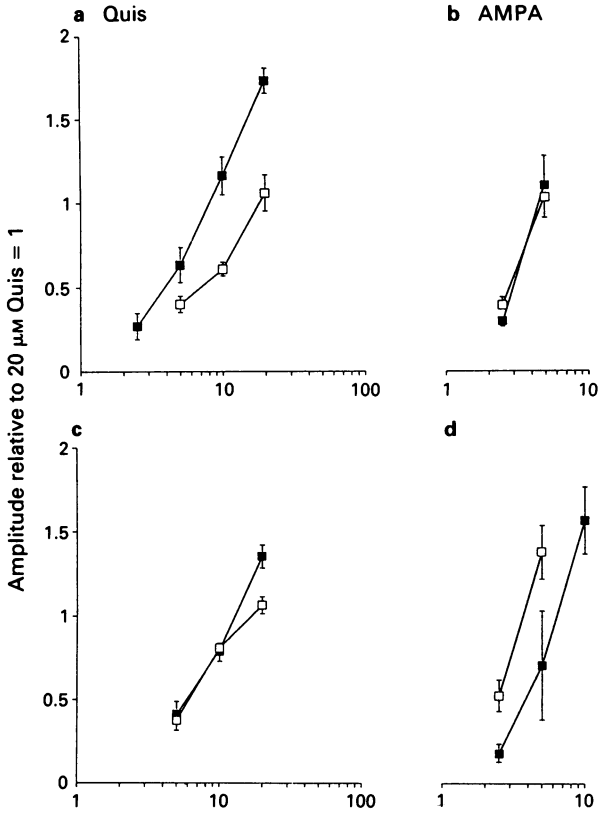

Figure 7 Log concentration-response lines for the non-NMDA receptor agonists Quis and AMPA in the absence (□) and presence (■) of 100 μM DIDS (a and b) or 300 μM SITS (c and d). Each point is the mean ± s.e.mean of response values calculated relative to an initial response to 20 μM Quis = 1 in the absence of anion transport blocker from 5 individual experiments for both DIDS and SITS, with data for Quis and AMPA being collected from the same slice.

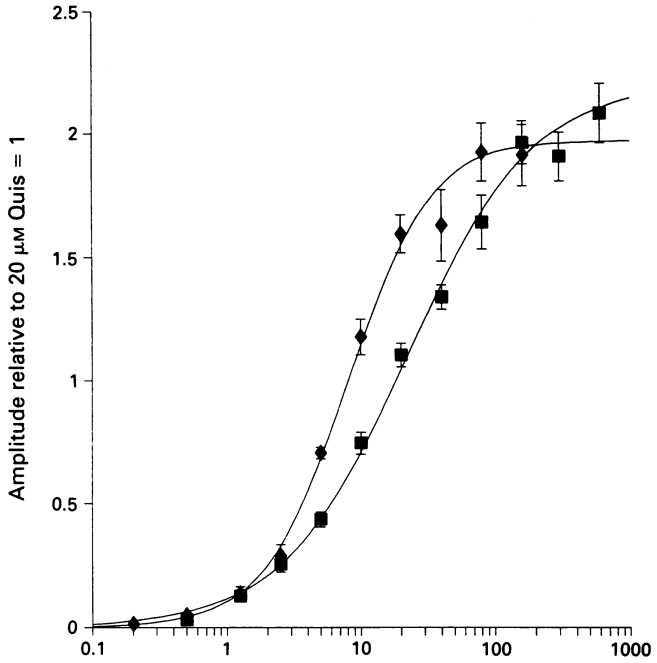

Figure 8 Full log concentration-response curves for Quis in the absence (■) and presence of 100 μM DIDS (◆), obtained from 6 and 4 experiments, respectively. Each point is the mean ± s.e.mean of response values calculated relative to the mean of two initial responses to 20 μM Quis = 1 obtained in the control conditions.

consistent with the proposed selective uptake of Quis over AMPA by a Cl^--dependent anion transport/sequestration mechanism. However, there is a block of non-NMDA receptors by SITS, indicating that the suppression of the production of DL-AP4 responses by SITS may in part, at least, be the result of the antagonism of non-NMDA receptor activation, which probably underlies these responses, and if washout were incomplete, cast doubt on the suppression of induction using 1 μM Quis as the sensitizing pulse. Therefore, it is evident that the use of either of these drugs has its limitations, and that while the effect on the production of responses is clear for DIDS, and although it is evident that Quis could be sequestered by a mechanism sensitive to anion transport blockers, the effects on the induction by Quis remain inconclusive.

Discussion

The present study has clearly shown that Quis is able to sensitize the cerebral cortex to amino acids other than DL-AP4, so that they produce depolarizing responses. All these amino acids are highly selective for L-glutamate/AP4 binding sites, with an order of potency consistent with that found here, except for L-α-AA, but this probably reflects the ability of L-α-AA to inhibit strongly its own induction. In addition, the block of DL-AP4 responses by the anion transport

Table 4 Mean values ± s.e.mean of maximum response (R_{max}), log EC_{50} and Hill slope coefficient from log concentration-response curves for quisqualate (Quis) in Figure 8, fitted to the equation given in the text, for the number of experiments given in parentheses

Condition	*R_{max}*	*log EC_{50}*	*Hill slope*
Control ($n = 6$)	2.20 ± 0.154	−4.65 ± 0.080 [22.3 μM]	0.96 ± 0.070
DIDS 100 μM ($n = 4$)	1.97 ± 0.148	−5.10 ± 0.076** [7.9 μM]	1.50 ± 0.217*

R_{max} is expressed relative to a response to 20 μM Quis obtained in the control condition, and the log EC_{50} in log [M].
*$P < 0.05$; **$P < 0.005$ compared to control (Student's t test).

blockers DIDS and SITS demonstrated in the present study is consistent with the sensitivity of Cl^--dependent L-[^{3}H]-glutamate binding to these agents (Recasens *et al.*, 1987; Hollmann *et al.*, 1988). This evidence supports the idea that Cl^--dependent L-[^{3}H]-glutamate/AP4 binding sites are the biochemical correlate of the sites involved in the production of responses to these amino acids. DIDS and SITS block a number of anion transport processes across neural cell membranes (Kimelberg, 1981), and the production of the Quis-induced DL-AP4 responses would appear superficially to be due to an anion exchange process similar to that described for the uptake of L-glutamate in glial cells by Waniewski & Martin (1983). However, Quis/AP4-sensitive L-[^{3}H]-glutamate binding represents a Cl^--dependent Na^+-independent uptake site located on neuronal membranes (Zaczek *et al.*, 1987b), and L-AP4 has little or no affinity for the Cl^--dependent L-[^{3}H]-glutamate binding to astrocyte membranes that corresponds to glial uptake sites (Bridges *et al.*, 1987). Since these sites are believed to be exchange transport sites for amino acids, the exchange uptake of these amino acids for a neuroactive one could be responsible for the production of the depolarizing responses, lending support to the exchange hypothesis. In addition, the location of the processes underlying DL-AP4 responses would appear to be neuronal rather than glial. If the AP4 responses are the result of heterogeneous amino acid exchange, one would expect that the sequestered EAA agonist would be released close to AMPA receptor sites, so a neuronal location is not surprising.

The role these transport/L-glutamate/AP4 sites play in the induction of AP4 responses remains unresolved, primarily owing to the problems of poor reversibility for DIDS, and the antagonism of non-NMDA receptors by SITS. However, the proposed sequestration of Quis via these sites (Zaczek *et al.*, 1987b) is supported in the present study by the fact that responses to Quis rather than AMPA are relatively selectively enhanced by anion transport blockers, consistent with the >60 fold greater potency of Quis over AMPA to displace Ca^{2+} and Cl^--dependent L-[^{3}H]-glutamate and DL-[^{3}H]AP4 binding (Butcher *et al.*, 1983; Werling *et al.*, 1983). This is circumstantial evidence indicating that the exchange hypothesis is possible, but there is no direct evidence that Quis has indeed been sequestrated by the cortical tissue, although this has been demonstrated in the hippocampus (Harrison & Kilpatrick, 1991). However, the marked difference in the suppression of induction by DL-AP4 and L-α-AA points away from the exchange hypothesis, and the evidence that these amino acids are also potential antagonists of the metabotropic L-glutamate receptor (Schoepp & Johnson, 1989) suggests that PI turnover may also be involved in the induction process, supporting the sensitization hypothesis. Indeed, it has been established that agonists for receptors coupled to PI turnover are able to sensitize the responses to DL-AP4 (Whittemore & Cotman, 1991), and that calmodulin and gangliosides are able to modulate Cl^-/Ca^{2+}-dependent L-[^{3}H]-glutamate binding (Yoneda *et al.*, 1989; Hollmann & Seifert, 1989), indicating that these sites are under the control of inducible intracellular mechanisms. Therefore, the inconclusive evidence concerning the effect of DIDS and SITS on the induction process, but the clear block of DL-AP4 responses suggest that the combination of the two hypotheses would provide the ultimate solution to this problem. Certainly, the number of Cl^--dependent L-[^{3}H]-glutamate binding sites is known to increase following exposure to Quis (Kessler *et al.*, 1986), supporting the notion of a sensitized exchange uptake site being responsible. In addition, while Quis remains the prime candidate for the sequestered EAA released during exchange, another possibility is L-glutamate as it is known to be tightly sequestered into pools associated with a Cl^--dependent, AP4-sensitive mechanism in the retina (Mitchell & Redburn, 1988).

I wish to thank the M.R.C. for financial support (Project Grant: Prof. B.S. Meldrum and Dr J.F. Collins), Prof. M.A. Simmonds for his helpful comments, and Mr R. Jones for helping to prepare the manuscript.

References

ANDERSON, K.J., MONAGHAN, D.T., BRIDGES, R.J., TAVOULARIS, A.L. & COTMAN, C.W. (1990). Autoradiographic characterization of putative excitatory amino acid transport sites. *Neuroscience*, **38**, 311–322.

BRIDGES, R.J., NIETO-SAMPEDRO, M., KADRI, M. & COTMAN, C.W. (1987). A novel chloride-dependent L-[^{3}H]glutamate binding site in astrocyte membranes. *J. Neurochem.*, **48**, 1709–1715.

BUTCHER, S.P., COLLINS, J.F. & ROBERTS, P.J. (1983). Characterization of the binding of DL-[^{3}H]-2-amino-4-phosphonobutyrate to L-glutamate sensitive sites on rat brain synaptic membranes. *Br. J. Pharmacol.*, **80**, 355–364.

CHA, J.-H.J., MAKOWIEC, R.L., PENNEY, J.B. & YOUNG, A.B. (1990). L-[^{3}H]-glutamate labels the metabotropic excitatory amino acid receptor in rodent brain. *Neurosci. Lett.*, **113**, 78–83.

FOSTER, A.C. & FAGG, G.E. (1984). Acidic amino acid binding sites in mammalian neuronal membranes: their characteristics and relationship to synaptic receptors. *Brain Res. Rev.*, **7**, 103–164.

HARRIS, E.W., STEVENS, D.R. & COTMAN, C.W. (1987). Hippocampal cells primed with quisqualate are depolarized by AP4 and AP6, ligands for a putative glutamate uptake site. *Brain Res.*, **418**, 361–365.

HARRISON, N.L. & SIMMONDS, M.A. (1985). Quantitative studies on some antagonists of N-methyl-D-aspartate in slices of rat cerebral cortex. *Br. J. Pharmacol.*, **84**, 381–391.

HARRISON, P.S. & KILPATRICK, I.C. (1991). Hippocampal slices do not appear to accumulate low micromolar concentrations of quisqualate by an active uptake mechanism. *Neurosci. Lett.*, **127**, 177–180.

HOLLMANN, M., HARNECKER, J. & SEIFERT, W. (1988). Calcium ions induce glutamate transport into rat brain membrane vesicles in the absence of sodium and chloride. Evidence for a novel uptake site? *F.E.B.S. Lett.*, **228**, 74–78.

HOLLMANN, M. & SIEFERT, W. (1989). Glutamate transport and not glutamate receptor binding is stimulated by gangliosides in a Ca^+-dependent manner in rat brain synaptic plasma membranes. *J. Neurochem.*, **53**, 716–723.

HORNE, A.L. & SIMMONDS, M.A. (1989). The pharmacology of quisqualate and AMPA in the cerebral cortex of the rat *in vitro*. *Neuropharmacology*, **28**, 1113–1118.

KESSLER, M., BAUDRY, M., CUMMINS, J.T., WAY, S. & LYNCH, G. (1986). Induction of glutamate binding sites in hippocampal membranes by transient exposure to high concentrations of glutamate or glutamate analogues. *J. Neurosci.*, **6**, 355–363.

KESSLER, M., BAUDRY, M. & LYNCH, G. (1987). Use of cystine to distinguish glutamate binding from glutamate sequestration. *Neurosci. Lett.*, **81**, 221–226.

KIMELBERG, H.K. (1981). Active accumulation and exchange transport of chloride in astroglial cells in culture. *Biochim. Biophys. Acta*, **646**, 179–184.

LODGE, D. & ZEMAN, S. (1989). Pharmacology of quisqualate-induction of depolarizing responses to L-amino-4-phosphonobutyrate (L-AP4) in rat cortical wedges. *Br. J. Pharmacol.*, **97**, 375P.

MITCHELL, C.K. & REDBURN, D.A. (1988). AP4 inhibits chloride-dependent binding and uptake of [^{3}H]glutamate in rabbit retina. *Brain Res.*, **459**, 298–311.

MONAGHAN, D.T., BRIDGES, R.J. & COTMAN, C.W. (1989). The excitatory amino acid receptors: their classes, pharmacology, and distinct properties in the function of the central nervous system. *Annu. Rev. Pharmacol. Toxicol.*, **29**, 365–402.

MURPHY, D.E., SNOWHILL, E.W. & WILLIAMS, M. (1987). Characterization of quisqualate recognition sites in rat brain tissue using DL-[^{3}H]α-amino-3-hydroxy-5-methylisoxazole-4-propionic acid (AMPA) and a filtration assay. *Neurochem. Res.*, **12**, 775–782.

OGITA, K. & YONEDA, Y. (1986). Characterization of Na^+-dependent binding sites of [^{3}H]glutamate in synaptic membranes from rat brain. *Brain Res.*, **397**, 137–144.

OLVERMAN, H.J., JONES, A.W., MEWETT, K.N. & WATKINS, J.C. (1988). Structure/activity relations of *N*-methyl-d-aspartate receptor ligands as studied by their inhibition of [^{3}H]D-2-amino-5-phosphonopentanoic acid binding in rat brain membranes. *Neuroscience*, **26**, 17–31.

PAXINOS, G. & WATSON, C. (1986). *The Rat Brain in Stereotaxic Coordinates*. 2nd edition. San Diego: Academic Press.

PIN, J.-P., BOCKAERT, J. & RECASENS, M. (1984). The Ca^{2+}/Cl^--dependent L-[^{3}H]glutamate: a new receptor or a particular transport process? *F.E.B.S. Lett.*, **175**, 31–36.

PULLAN, L.M., OLNEY, J.W., PRICE, M.T., COMPTON, R.P., HOOD, W.F., MICHEL, J. & MONAGHAN, J.B. (1987). Excitatory amino acid receptor potency and subclass specificity of sulfur containing amino acids. *J. Neurochem.*, **49**, 1301–1307.

RECASENS, M., PIN, J.-P. & BOCKAERT, J. (1987). Chloride transport blockers inhibit the chloride-dependent glutamate binding to rat brain membranes. *Neurosci. Lett.*, **74**, 211–216.

ROBINSON, M.B., WHITTEMORE, E.R., MARKS, R.L. & KOERNER, J.F. (1986). Exposure of hippocampal slices to quisqualate sensitizes synaptic responses to phosphonate-containing analogues of glutamate. *Brain Res.*, **381**, 187–190.

SCHOEPP, D.D. & JOHNSON, B.G. (1989). Comparison of excitatory amino acid stimulated phosphoinositide hydrolysis and *N*-[^{3}H] acetylaspartylglutamate binding in the rat brain: selective inhibition of phosphoinositide hydrolysis by 2-amino-3-phosphonopropionate. *J. Neurochem.*, **53**, 273–278.

SHEARDOWN, M.J. (1988). A new and specific non-NMDA receptor antagonist FG9065 blocks L-AP4-evoked depolarizations in rat cerebral cortex. *Eur. J. Pharmacol.*, **148**, 471–474.

SIMON, J.R., CONTRERA, J.F. & KUHAR, M.J. (1976). Binding of [^{3}H]kainic acid, an analogue of L-glutamate, to brain membranes. *J. Neurochem.*, **26**, 141–147.

WANIEWSKI, R.A. & MARTIN, D.L. (1983). Selective inhibition of glial versus neuronal uptake of L-glutamic acid by SITS. *Brain Res.*, **268**, 390–394.

WATKINS, J.C. & EVANS, R.H. (1981). Excitatory amino acid transmitters. *Annu. Rev. Pharmacol. Toxicol.*, **21**, 165–204.

WERLING, L.L., DOMAN, K.A. & NADLER, J.V. (1983). L-[^{3}H] glutamate binding to hippocampal synaptic membranes: two binding sites discriminated by their differing affnities for quisqualate. *J. Neurochem.*, **41**, 586–593.

WHITE, M.M. & MILLER, C. (1979). A voltage-gated anion channel from the electric organ of *Torpedo californica*. *J. Biol. Chem.*, **254**, 10161–10166.

WHITTEMORE, E.R. & COTMAN, C.W. (1991). Agonists selective for phosphoinositide-coupled receptors sensitize neurons to depolarization by L-2-amino-4-phosphonobutanoic acid (L-AP4). *Brain Res.*, **555**, 215–219.

WHITTEMORE, E.R. & KOERNER, J.F. (1991). Pre-exposure to L-homocysteinesulfinic acid blocks quisqualate-induced sensitization to L-2-amino-4-phosphonobutanoic acid. *Eur. J. Pharmacol.*, **192**, 435–438.

YONEDA, Y., OGITA, K., YAMADA, K., KOUDA, T., OHGAKI, T., UCHIDA, S. & MEGURI, H. (1989). High concentrations of calmodulin antagonists inhibit accumulation and binding activities of [^{3}H]glutamate in rat brain. *Neurochem. Int.*, **15**, 17–23.

ZACZEK, R., ARLIS, S., MARKL, A., MURPHY, T., DRUCKER, H. & COYLE, J.T. (1987a). Characteristics of chloride-dependent incorporation of glutamate into brain membranes argue against a receptor binding site. *Neuropharmacology*, **26**, 281–287.

ZACZEK, R., BALM, M., ARLIS, S., DRUCKER, H. & COYLE, J.T. (1987b). Quisqualate-sensitive chloride-dependent transport of glutamate into rat brain synaptosomes. *J. Neurosci. Res.*, **18**, 425–431.

(Received July 13, 1992
Revised January 25, 1993
Accepted February 5, 1993)

Br. J. Pharmacol. (1993), **109**, 459–465 © Macmillan Press Ltd, 1993

Caffeine and related compounds block inhibitory amino acid-gated Cl^- currents in freshly dissociated rat hippocampal neurones

Hisayuki Uneyama, Nobutoshi Harata & [1]Norio Akaike

Department of Neurophysiology, Tohoku University School of Medicine, Sendai 980, Japan

1 The effects of caffeine and related compounds on responses mediated by inhibitory amino acids were investigated in freshly dissociated rat hippocampal pyramidal neurones by conventional and nystatin perforated patch-clamp techniques.

2 Glycine and γ-aminobutyric acid (GABA) evoked Cl^- currents in hippocampal neurones. The half-maximum effective concentrations (EC_{50}) of glycine and GABA were 8.5×10^{-5} and 5×10^{-6} M, respectively.

3 Caffeine reversibly inhibited both 10^{-4} M glycine- and 10^{-5} M GABA-induced Cl^- currents in a concentration-dependent manner. The half-maximum inhibitory concentrations (IC_{50}) of caffeine were 4.5×10^{-4} M for the glycine response and 3.6×10^{-3} M for the GABA response.

4 Caffeine shifted the concentration-response curve of I_{Gly} to the right without affecting the maximum response.

5 The inhibitory action of caffeine did not show voltage-dependency.

6 The blocking action of caffeine was not affected by intracellular perfusion with 5 mM BAPTA or by pretreatment with the protein kinase A inhibitor, H-8. This excludes the participation of Ca^{2+} or cyclic AMP in the inhibitory action of caffeine.

7 Caffeine failed to inhibit the augmentations of aspartate- and *N*-methyl-D-aspartate (NMDA) -gated current by glycine, suggesting that caffeine has no effect on the allosteric glycine binding site on the NMDA receptor.

8 The inhibitory effects of some xanthine derivatives on I_{Gly} were compared. The inhibitory potency of those compounds on I_{Gly} was in the order of pentoxifylline > theophylline ≥ caffeine > paraxanthine > IBMX ≥ theobromine > dyphylline. Xanthine had no effect.

9 The results indicate that methylxanthines including caffeine may act directly on the glycine receptor Cl^- channel complex in rat hippocampal pyramidal neurones. The blockade of the inhibitory amino acid response by methylxanthines may be involved in the excitatory side effects of methylxanthines in the mammalian central nervous system.

Keywords: Caffeine; methylxanthines; glycine; GABA; rat hippocampus; dissociated neurones; whole-cell recording

Introduction

Caffeine and related compounds are widely consumed throughout the world as psycho-stimulant drugs. The consumption of caffeine in the UK is approximately 165 mg per person per day and that in the USA is around 246 mg. Caffeine has a wide variety of pharmacological actions of therapeutic interest, such as stimulation of cardiac muscle and the central nervous system (CNS), relaxation of smooth muscle and diuresis (Rall, 1985). Increasing ingestion of caffeine produces multiple signs of progressive CNS stimulation including nervousness, anxiety and restlessness. At higher doses, convulsions are elicited (Clementz & Dailey, 1988). However, the molecular mechanisms for the CNS stimulant effects of caffeine are unclear, because caffeine has multiple actions at the cellular level. For instance, caffeine antagonizes adenosine (Day *et al.*, 1991) and GABA receptor-mediated effects (Izquierdo, 1986; Lopez *et al.*, 1989), inhibits phosphodiesterase (Butcher & Sutherland, 1962), and stimulates Ca^{2+} release from the endoplasmic reticulum (Endo *et al.*, 1970).

Glycine and GABA are established as inhibitory neurotransmitters in the CNS of vertebrates and invertebrates. The release of inhibitory amino acids (IAAs) from presynaptic terminals inhibits postsynaptic neuronal firing by increasing the membrane Cl^- conductance (Hamill *et al.*, 1983). We have previously recorded IAA-gated Cl^- currents in neurones dissociated from the rat brain, and used this technique to clarify the mechanisms of some CNS stimulants (Akaike *et al.*, 1991; Shirasaki *et al.*, 1991). In the present study, we examined the effects of caffeine and related compounds on IAA-induced Cl^- currents in dissociated rat hippocampal pyramidal neurones under voltage-clamp conditions. We report for the first time that these compounds potently blocked the response mediated by glycine.

[1] Author for correspondence.

Methods

Preparation

The dissociation technique of rat hippocampal CA1 neurones has been described previously (Nakagawa *et al.*, 1991). Briefly, 2-week-old Wistar rats were decapitated under ether anaesthesia. The brain was sliced at a thickness of 400 μm with a microslicer (D.S.K. DTK-1000). The brain slices were incubated in the external solution with pronase (1 mg 6 ml^{-1}) at 31°C for 15 min and subsequently with thermolysin (1 mg 6 ml^{-1}) under the same conditions. After the enzyme treatments, the slices were washed with Ca^{2+}-free external solution containing EGTA and incubated for a few minutes in the normal external solution. The CA1 area of the hippocampus was removed by micro-punching and triturated with fire-polished pasteur pipettes. The dissociated CA1 neurones were used for experiments within 9 h.

Solutions

The ionic composition of normal external solution was (in mM): NaCl 150, KCl 5, $MgCl_2$ 1, $CaCl_2$ 2, N-2-hydroxyethylpiperazine-*N'*-2-ethanesulphonic acid (HEPES) 10 and glucose 10. The pH was adjusted to 7.4 with tris(hydroxymethyl)aminomethane (Tris-OH). For Ca^{2+}-free external solution, $CaCl_2$ was replaced with equimolar $MgCl_2$ and 2 mM ethylene glycol-*bis*(β-aminoethyl ether)-*N,N,N',N'*-tetraacetic acid (EGTA) was added.

The composition of the perforated patch-pipette solution was (in mM): KCl 150 and HEPES 10. The pH was adjusted to 7.2 with Tris-OH. The conventional patch-pipette solution contained (in mM): NaCl 30, KCl 70, K-gluconate 70, $CaCl_2$ 0.25, $MgCl_2$ 1, ATP-Mg 5, EGTA 5 and HEPES 10. The pH was adjusted to 7.2 with Tris-OH. When the current-voltage relationship for glycine-induced Cl^- currents was examined 70 mM CsCl and 70 mM Cs-gluconate were used as the pipette solution instead of KCl and K-gluconate, respectively. Nystatin was dissolved in acidified methanol (adjusted with 1N HCl to pH 2.0). Immediately after dissolving nystatin, the pH was adjusted to 7.2 with 1N KOH (nystatin stock solution; 10 mg ml^{-1}). The stock solution was diluted with the perforated patch-pipette solution to a final concentration of 50 μg ml^{-1}.

Electrical measurements

Electrical measurements were performed in a whole-cell mode using a conventional patch-clamp technique (Hamill *et al.*, 1981). Some experiments were performed with the nystatin perforated patch-clamp technique (Horn & Marty, 1988). The pipettes were pulled from 1.5 mm capillary glass (Narishige) in two stages on a vertical pipette puller (Narishige, PB-7). The pipette tip was fire polished before use. The resistance between the recording electrode filled with internal solution and reference electrode in external solution was 4–6 MΩ. The current and voltage were measured with a patch-clamp amplifier (List Medical, EPC-7), and monitored on both a storage oscilloscope (Tektronix, R5113) and a pen recorder (San-ei, RECTI-HORIZ-8K), and stored on video tapes after digitization with a PCM processor (Nihon kohden, PCM501ESN). When the series resistance was measured by a circuit for series resistance compensation in the amplifier, the values ranged between 16 and 19 MΩ. The value of compensation of the series resistance was between 30 and 80%. All experiments were performed at room temperature (20–22°C).

Drugs

The drugs used in the present study were 1,2-*bis*(o-aminophenoxy)ethane-*N,N,N',N'*-tetraacetic acid (BAPTA) [Dojin]; 6-cyano-7-nitroquinoxaline-2,3-dione (CNQX) [Tocris]. Other drugs were purchased from Sigma. Drugs were dissolved in the internal or external solution just before use. Drugs were applied by a rapid application method termed the 'Y-tube' method, as described elsewhere (Murase *et al.*, 1990). With the use of this technique, the drugs could be applied to the neurone within 20 ms.

Statistical analysis

Experimental values are presented as mean ± standard error of the mean (s.e.mean). Results were analyzed by Student's *t* test (unpaired or paired comparison), and a *P* value of less than 0.05 was considered to be significant. For evaluation of half-maximal effective concentration (EC_{50}) and Hill coefficient (n) in concentration-response curve, data were fitted to the Michaelis-Menten equation using a least-squares fitting,

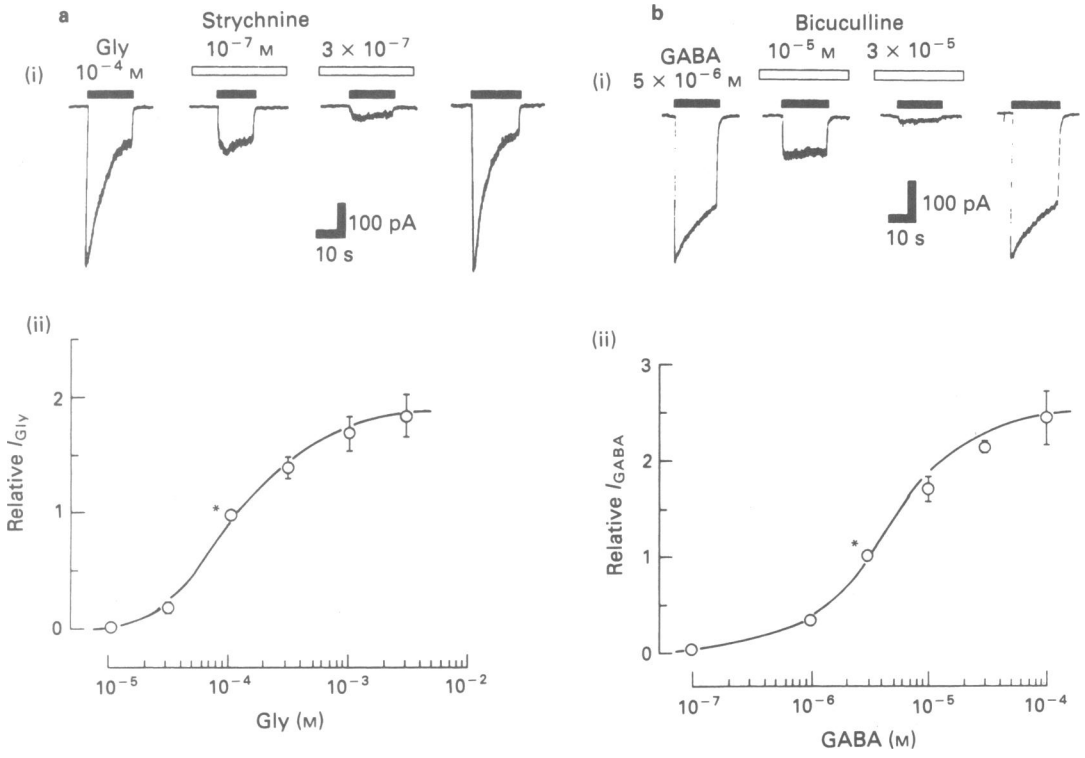

Figure 1 Glycine- and GABA-induced Cl^- currents in hippocampal neurones. (a) Glycine-induced responses: (i) 10^{-4} M glycine evoked an inward current (I_{Gly}). The inward current was reversibly depressed in a concentration-dependent manner by pretreatment with strychnine. (ii) Concentration-response relationship for I_{Gly}. All currents induced by glycine at various concentrations were normalised to that induced by 10^{-4} M glycine (see symbol marked with asterisk). (b) GABA-induced responses: (i) 5×10^{-6} M GABA-induced inward current (I_{GABA}) was inhibited by pretreatment with bicuculline. (ii) Concentration-response curve for I_{GABA}. All currents induced by GABA were normalized to that induced by 3×10^{-6} M GABA (see symbol marked with asterisk). Strychnine and bicuculline were applied for 15 s before the simultaneous application of each amino acid. Neurones were voltage-clamped at −60 mV. Each point represents mean ± s.e.mean from 5–7 experiments.

$I = (I_{max} \times C^n)/(C^n + K_d^n)$ (Eqn. 1), where I is current, I_{max} is the maximum response, and C is the concentration of agonist. The equation for the concentration-inhibition curve is the mirror image of the Michaelis-Menten equation; $I/I_{max} = 1 - (1/I_{max}) \cdot (I_{max} \times C^n)/(C^n + K_d^n)$ (Eqn. 2), where C is the concentration of antagonist. Assuming that the value of I_{max} is 1, then $I = 1 - C^n/(C^n + K_d^n)$ (Eqn. 3), $I = K_d^n/(C^n + K_d^n)$ (Eqn. 4). The data for the concentration-inhibition curve were fitted to Eqn. 4 by the use of a least-squares fitting to obtain the half-maximal inhibition concentration (IC_{50}).

Results

Effects of caffeine on glycine- and GABA-evoked Cl^- currents

The dissociated CA1 pyramidal neurones were perfused with normal external and internal solutions containing 161 and 82.5 mM Cl^-, respectively. Under these conditions, glycine and γ-aminobutyric acid (GABA) evoked Cl^- inward curents (I_{Gly} and I_{GABA}) at a holding potential (V_H) of −60 mV, as previously observed (Shirasaki *et al.*, 1991; Nakagawa *et al.*, 1991). Glycine and GABA were applied every 2 min, at which interval no desensitization occurred. To confirm that the I_{Gly} and I_{GABA} were mediated by their specific receptors, the selective antagonists for glycine and GABA were examined (Figure 1a(i) and 1b(i)). The I_{Gly} and I_{GABA} were inhibited in a concentration-dependent manner by a glycine receptor antagonist, strychnine and a $GABA_A$ receptor antagonist, bicuculline, respectively. Figure 1a(ii) and 1b(ii) summarize the concentration-response curves for glycine and GABA. The half-maximum effective concentrations (EC_{50}) were 8.5×10^{-5} M for glycine and 5.0×10^{-6} M for GABA.

Applications of caffeine inhibited both 10^{-4} M glycine- and 10^{-5} M GABA-induced currents in a concentration-dependent manner (Figure 2a). Current amplitudes induced by these concentrations of glycine and GABA were 592 ± 117 and 805 ± 228 pA ($n = 8$), respectively. Neurones were pretreated with caffeine 15 s before simultaneous application with one of the IAAs. The half-maximum inhibitory concentrations (IC_{50}) of caffeine on 10^{-4} M glycine- and 10^{-5} M GABA-induced responses were 4.5×10^{-4} and 3.6×10^{-3} M, respectively (Figure 2b). The following experiments were confined to the inhibitory action of caffeine on the glycine response since the antagonistic effects of caffeine on GABA responses has been described previously (Izquierdo, 1986; Lopez *et al.*, 1989).

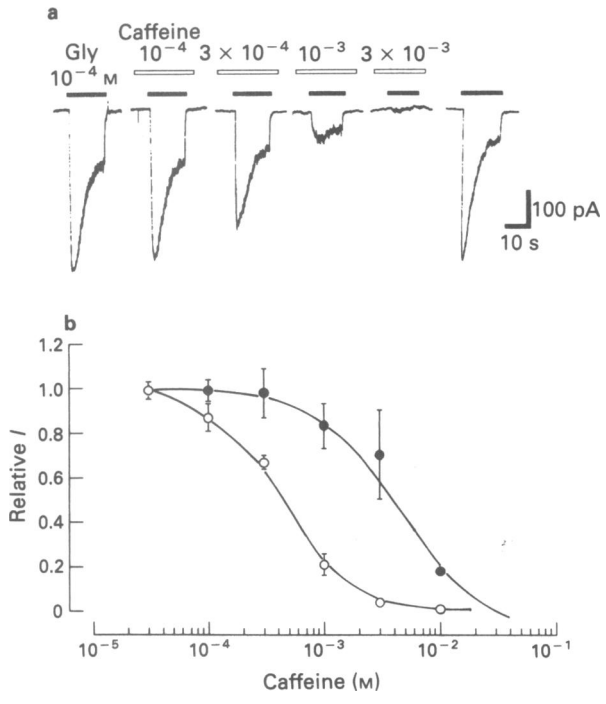

Figure 2 Effect of caffeine on glycine- and GABA-induced currents. (a) Caffeine depressed 10^{-4} M glycine-induced Cl^- current in a concentration-dependent manner. V_H was −60 mV. All recordings were obtained from the same neurone. (b) Concentration-inhibition curves of caffeine for I_{Gly} and I_{GABA}. Concentrations of glycine (○) and GABA (●) were 10^{-4} and 10^{-5} M, respectively. Each point represents mean ± s.e.mean from 5–8 experiments.

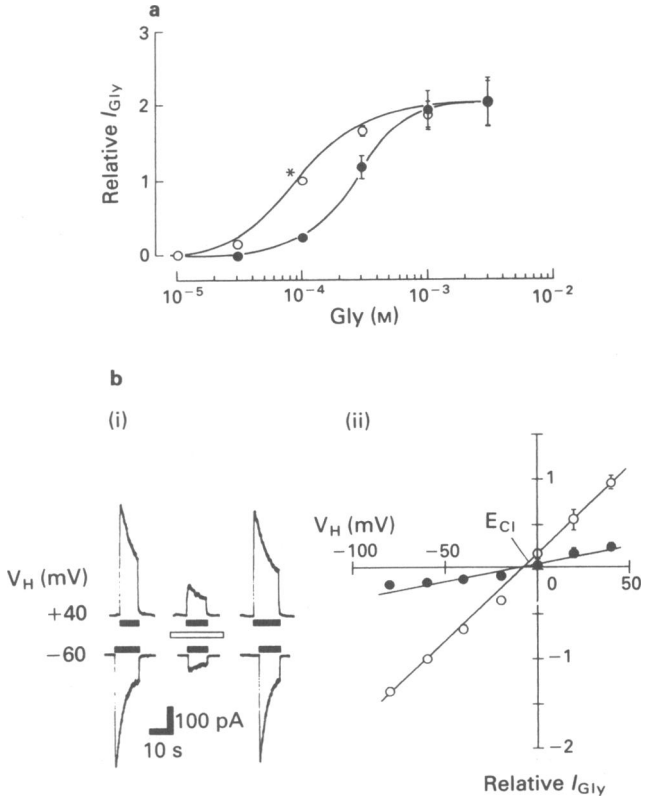

Figure 3 Inhibitory effect of caffeine on I_{Gly}. (a) Concentration-response curve for I_{Gly} in the presence (●) or absence (○) of 1 mM caffeine. Neurones were voltage-clamped at −60 mV. All responses were normalized to the peak amplitude induced by 10^{-4} M glycine alone (see symbol marked with asterisk). Each point shows mean ± s.e.mean from 6 experiments. (b) Effect of V_H on the blocking action of caffeine: (i) Current traces at V_Hs of −60 and +40 mV. All traces were obtained from the same neurone. Solid bar: 10^{-4} M glycine; open bar, 10^{-3} M caffeine. (ii) Current-voltage (I–V) relationships for I_{Gly} in the presence (●) or absence (○) of 1 mM caffeine. All responses were normalized to the peak amplitude induced by glycine at a V_H of −60 mV (*). Each point shows mean ± s.e.mean from 5–7 experiments. E_{Cl}, Cl^- equilibrium potential.

To investigate the mechanism of the blocking action of caffeine on glycine response, the influence of caffeine on the concentration-response relationship for the I_{Gly} was examined (Figure 3a). In the presence of 1 mM caffeine, the concentration-response curve was shifted to the right without affecting the maximum value, indicating that caffeine acts as a competitive antagonist. The EC_{50} values in the presence and absence of 10^{-3} M caffeine were 6.3×10^{-4} and 0.9×10^{-4} M, respectively. The inhibitory effect of caffeine was examined at various V_Hs (Figure 3b). To suppress the voltage-dependent K^+ channels, K^+ in the pipette solution was replaced with equimolar Cs^+ and to suppress Ca^{2+} and Na^+ channels, 10^{-5} M $LaCl_3$ and 10^{-7} M tetrodotoxin (TTX) were added to the external solution. Figure 3b(ii) shows the current-voltage (I-V) relationships for I_{Gly} in the presence and absence of 10^{-3} M caffeine. In both conditions, I_{Gly} reversed the current

direction at − 11 mV. The reversal potential for I_{Gly} (E_{Gly}) was close to Cl^--equilibrium potential (− 15.5 mV) calculated using the Nernst equation from the given intra- and extracellular Cl^- concentrations and their Cl^- activities. In addition, I_{Gly} was equally depressed by 75–85% at V_Hs between − 80 and + 40 mV, suggesting that the inhibitory action of caffeine on I_{Gly} has no voltage-dependency. These results make it unlikely that caffeine acts as a channel blocker of glycine-gated Cl^- channels. In keeping with this, the inhibitory potency of caffeine did not depend on the current amplitudes induced by glycine, but on the concentrations of the applied agonist (data not shown).

Lack of participation of intracellular cyclic AMP-protein kinase A cascade in the blocking action of caffeine

Several lines of evidence suggest that the GABA- and glycine-induced currents are modulated by second messengers such as Ca^{2+} and adenosine 3′:5′-cyclic monophosphate (cyclic AMP) (Inoue *et al.*, 1986; Diatlov, 1989; Porter *et al.*, 1990; Song & Huang, 1990). Since methylxanthines including caffeine elevate the cellular contents of these two substances (Butcher & Sutherland, 1962; Edno *et al.*, 1970), we assessed the involvement of these second messengers on the blocking action of caffeine. In a conventional whole-cell mode, it has been reported that the second messenger-mediated responses almost disappear with diffusional exchange between the cytoplasm and the pipette solution (Fernandez *et al.*, 1984). In order to prevent the diffusion, the nystatin perforated-patch technique was devised, and this technique allowed us to record successfully neurotransmitter-mediated responses in the brain neurones (Uneyama *et al.*, 1992; Wakamori *et al.*, 1993). We compared the blocking potency of caffeine on I_{Gly} with the conventional and the perforated whole-cell patch techniques, and there was no significant difference between the data obtained with the two techniques ($n = 5$, data not shown). It seems, therefore, reasonable to suppose that the blocking action of caffeine was not mediated by diffusible intracellular molecules. To confirm this, the experiments in Figure 4 were performed. Figure 4a(i) and (ii) show the effect of a potent Ca^{2+} chelator, BAPTA, on the inhibitory action of caffeine for I_{Gly}. We recorded I_{Gly} under the cell-attach condition using a pipette solution containing both 5×10^{-3} M BAPTA and nystatin, and successively ruptured the cell membrane to let BAPTA diffuse into the cell. Intracellular perfusion with 5×10^{-3} M BAPTA did not affect the inhibitory action of caffeine on I_{Gly}. We also examined the possibility that cyclic AMP was involved in the blocking effect of caffeine on I_{Gly} (Figure 4b). The blocking action of caffeine was not affected by pretreatment with 10^{-5} M N-[2-(methylamino)ethyl]-5-isoquinoline sulphonamide (H-8), an inhibitor of protein kinase A (Figure 4b(i)). Moreover, I_{Gly} itself was not depressed by the pre-administration of forskolin (FK, 10^{-5} M), a potent activator of adenylate cyclase, or of isobutyl-methylxanthine (IBMX, 3×10^{-4} M) a methylxanthine derivative having potent phosphodiesterase inhibitory activity, (Figure 4b(ii)).

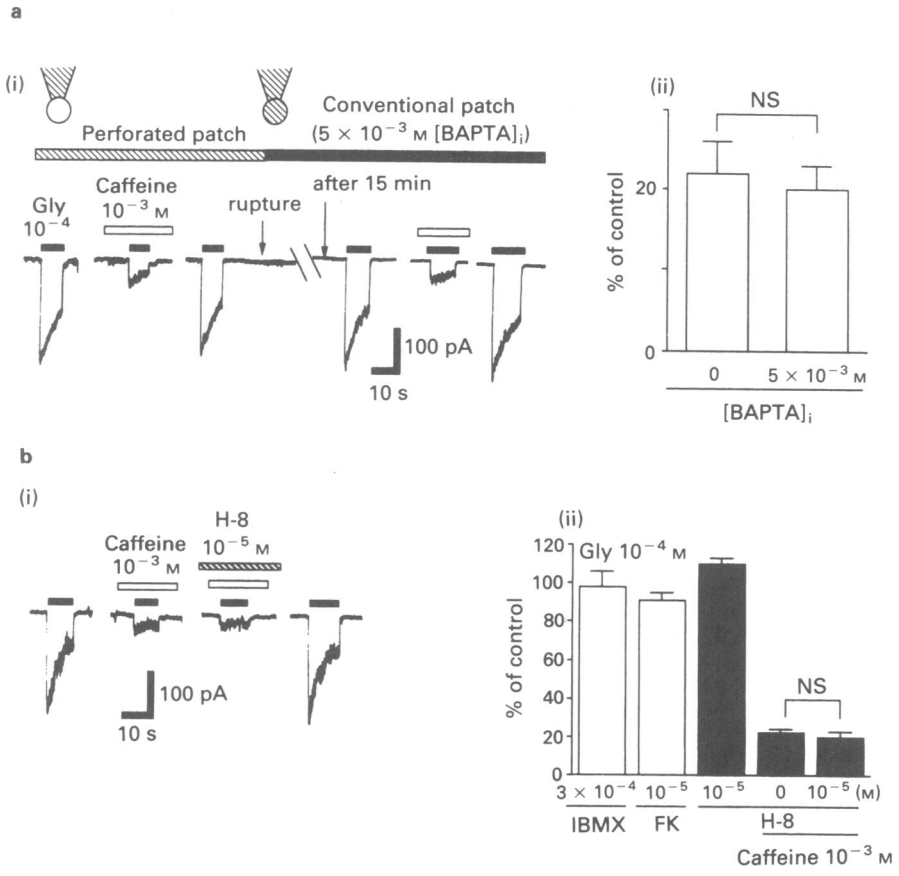

Figure 4 The lack of involvement of 2nd messengers in the blocking action of caffeine. (a) Effect of internal perfusion with 5×10^{-3} M BAPTA. (i) Current traces before and 15 min after the rupture of the patch membrane with a pipette containing 5×10^{-3} M BAPTA. V_H was − 60 mV. Current before rupture of patch membrane was monitored using the nystatin-perforated patch-clamp technique. The blocking action of caffeine on I_{Gly} was not affected by intracellular perfusion with BAPTA. (ii) Quantitative analysis of the results obtained in (i). (b). Effect of cyclic AMP elevation in the blocking action of caffeine. (i) Effect of protein kinase A inhibitor, H-8. V_H was − 60 mV. All traces were obtained in the same neurone. (ii) Neurones were pretreated by IBMX and forskolin for 2 min. Each column and vertical bar represents mean and ± s.e.mean from 5 experiments. NS, not significant. For abbreviations, see text.

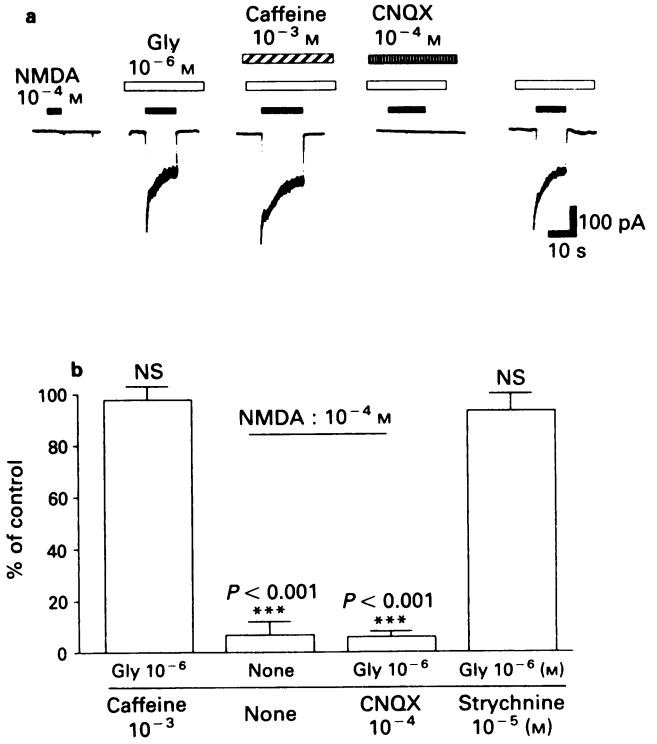

Figure 5 Effect of caffeine on the strychnine-insensitive glycine site on the NMDA receptor. (a) Current traces obtained in the same neurone. V_H was − 60 mV. Each horizontal bar indicates the period of drug application. Glycine 10^{-6} M potently augmented the NMDA response, and CNQX 10^{-4} M failed to suppress the augmentation. (b) Data obtained in (a) are summarized. Pretreatment time for all drugs was 15 s. Data are shown as percentages of the current amplitudes induced by NMDA 10^{-4} M plus glycine 10^{-6} M (control). Each column represents mean ± s.e.mean from 5–7 experiments. NS, not significant. For abbreviations, see text.

Effect of caffeine on strychnine-insensitive glycine binding site

The effect of caffeine on the glycine-binding site of the *N*-methyl-D-aspartate (NMDA) receptor was examined (Figure 5a). In glycine-free external solutions (concentrations below 10^{-8} M glycine), 10^{-4} M NMDA evoked only small transient peak and sustained steady-state currents (15.9 ± 3.4 and 7.3 ± 1.2 pA, respectively: $n = 6$). In the presence of 10^{-6} M glycine, 10^{-4} M NMDA induced large transient peak and steady-state currents (373.3 ± 72.8 and 202.5 ± 24.1 pA, respectively; $n = 6$). The augmentation of NMDA response by glycine was reversibly abolished by co-administration of CNQX (10^{-4} M), an inhibitor at the glycine binding site on the NMDA receptor, suggesting that glycine potently augmented NMDA responses via the allosteric sites on the NMDA receptor (Harris & Miller, 1989; Ito *et al.*, 1991). However, caffeine failed to depress the augmentation of NMDA responses by glycine even at a concentration of 10^{-3} M. These results are summarized in Figure 5b. Strychnine also failed to depress the augmentation at 10^{-5} M (93 ± 7% of control, $n = 4$), which is high enough to abolish 10^{-4} M glycine-induced responses. Similar results were obtained when aspartic acid was used instead of NMDA (data not shown).

Inhibitory effects of caffeine-related compounds on I_{Gly}

Table 1 lists a group of xanthine derivatives modified at positions 1, 3 and 7 with corresponding IC_{50} values when glycine was used at a concentration of 10^{-4} M as an agonist. Xanthine did not inhibit I_{Gly}. Methyl substitution at position 1 had weak inhibitory activity, whereas a similar substitution at position 3 had no effect. Methyl substitution at positions 1 and 3 (theophylline) enhanced the inhibitory potency for I_{Gly}, but its isobutyl substitution at position 3 reduced the potency. 1,3,7-Trimethylxanthine (caffeine) had an inhibitory potency almost equal to 1,3-dimethylxanthine (theophylline). Oxohexyl substitution at position 1 of caffeine showed about three times more potent inhibitory activity for I_{Gly} than caffeine. Dihydroxyl substitution at position 7 (dyphylline) of caffeine resulted in a loss of inhibitory activity.

Discussion

We have shown here that methylxanthines inhibit IAA-mediated responses in dissociated rat hippocampal pyramidal neurones. To date, there have been some reports of the inhibitory effect of methylxanthines on GABA-benzodiazepine receptors (Izquierdo, 1986; Lopez *et al.*, 1989), but there has been no report concerning the effect on glycine receptors.

Methylxanthines such as caffeine have at least two well-documented actions at intracellular sites: (1) mobilization of Ca^{2+} from intracellular stores (Endo *et al.*, 1970) and (2) inhibition of cyclic nucleotide phosphodiesterase (Butcher & Sutherland, 1962). In the present study, neither internal perfusion with a potent Ca^{2+} chelator, BAPTA (5 mM), nor external application of a potent protein kinase A inhibitor, H-8 (10 μM), could reverse the suppression of I_{Gly} by caffeine. Moreover, the concentration-response curve for I_{Gly} was shifted to the right in the presence of caffeine (Figure 3a), and the inhibitory potency of caffeine showed no voltage-

Table 1 Effects of caffeine-related compounds on glycine-induced current

Derivatives	R_1	R_2	R_3	n	IC_{50} ($\times 10^{-3}$)
Xanthine	H	H	H	4	–
1-Methylxanthine	CH_3	H	H	5	6.90
3-Methylxanthine	H	CH_3	H	4	–
Paraxanthine	CH_3	H	CH_3	5	0.84
Theobromine	H	CH_3	CH_3	5	1.49
Theophylline	CH_3	CH_3	H	7	0.39
Caffeine	**CH_3**	**CH_3**	**CH_3**	**8**	**0.45**
IBMX	CH_3	$CH_2CH(CH_3)_2$	H	5	1.43
Pentoxifylline	$CH_2CH_2CH_2CH_2C(=O)CH_3$	CH_3	CH_3	7	0.20
Dyphylline	CH_3	CH_3	$CH_2CH(OH)CH(OH)$	5	4.10

Inhibitory potencies of methylxanthine derivatives on I_{Gly} were investigated with the conventional whole-cell configuration. The concentration of glycine was 10^{-4} M. IC_{50} of each derivative was calculated as described in Methods.

dependency (Figure 3b). These results strongly indicate that caffeine competitively interacts with the glycine receptor-Cl^- channel complex on the plasma membrane, but not with the intracellular signal pathway. In the present study, the inhibitory potency of methylxanthines for I_{Gly} was in the order of pentoxifylline > theophylline ≥ caffeine > paraxanthine > IBMX ≥ theobromine > dyphylline (Table 1). This order is different from that of the inhibitory activity on phosphodiesterase and that of the affinity for adenosine receptors (Rall, 1985; Martinson *et al.*, 1986; Choi *et al.*, 1988; Day *et al.*, 1991). These findings consolidate our view that the inhibitory action of caffeine and related methylxanthines is directly exerted on the glycine receptor-channel complex.

Glycine-binding sites in the CNS are classified into 2 types by their affinities for strychnine and their effects on neuronal excitability. One is the glycine-binding site which forms a part of the receptor-Cl^- channel complex, which has inhibitory effects on CNS neurones and is strongly depressed by nanomolar concentrations of strychnine (Curtis *et al.*, 1968; Barron & Guth, 1987; Shirasaki *et al.*, 1991). The other is a site on NMDA receptors, which has excitatory effects on the neurones by potentiating NMDA responses and is inhibited by micromolar concentrations of 7-chloro kynurenic acid or CNQX, but not by strychnine (Harris & Miller, 1989; Ito *et al.*, 1991). In the present experiments, 10^{-6} M glycine strongly augmented the NMDA responses, but caffeine failed to depress that augmentation (Figure 5). Thus, the inhibitory effect of caffeine on glycine responses is selective to those at the strychnine-sensitive site. The results suggest that caffeine could act as an excitatory modulator by inhibiting glycine-gated Cl^- currents, without affecting Ca^{2+} or Na^+ influx through the NMDA receptor-channel complex.

Caffeine easily passes through the blood-brain barrier and accumulates in the brain (Rall, 1985). When a convulsive dose of caffeine (20 mg kg^{-1}) is administered intravenously in rats, the concentration of caffeine in the brain exceeds 10^{-4} M (Stahle *et al.*, 1991). In the present study, this concentration inhibited the glycine-induced Cl^- current. The finding that the inhibitory action of caffeine on I_{Gly} is competitive suggests that the inhibitory potency of caffeine is determined by the concentration of glycine in the synaptic cleft. Indeed, in the present study, when the concentration of applied glycine was reduced to 2×10^{-5} M, 5×10^{-5} M caffeine abolished the I_{Gly} (data not shown). Further quantitative research is anticipated to elucidate the actual concentration of glycine in synaptic clefts, in order for us to determine whether the inhibitory action of caffeine on I_{Gly} is operative in the physiological range of concentrations occurring during glycinergic transmission *in vivo*.

It is well-established the glycine is one of the major inhibitory neurotransmitters in the lower regions of CNS in vertebrates, such as the spinal cord and brain stem. However, in the higher regions of the mammalian CNS the role of glycine has been controversial. In the hippocampus, for instance, the major inhibitory neurotransmitter is believed to be GABA, not glycine, because radiolabelling and immunohistochemical studies showed few strychnine-sensitive glycine binding sites whereas GABA binding sites were very dense in the region (Zarbin *et al.*, 1981; Araki *et al.*, 1988). However, there are several lines of evidence to support the idea that strychnine-sensitive glycine receptors play an important role in the higher regions including the hippocampus. (1) Recent *in situ* hybridization experiments have shown that the mRNAs encoding strychnine-sensitive glycine receptors were expressed throughout the higher regions of the CNS (Malosio *et al.*, 1991). (2) In addition to the present experiments, our and other laboratories have shown that neurones freshly dissociated from the rat hippocampus and cortex exhibited a Cl^- current in response to glycine (Krishtal *et al.*, 1988; Shirasaki *et al.*, 1991; Ebihara *et al.*, 1992). In experiments on hippocampal slices, application of glycine enhanced noradrenaline release from the hippocampus without involving the augmentation of the NMDA receptor (Raiteri *et al.*, 1990).

Recently, subunits constituting the glycine receptor have been revealed (Betz & Becker, 1988; Crenningloh *et al.*, 1990). Glycine receptors are now known to be expressed heterogeneously in the CNS and to change ontogenetically (Akagi & Miledi, 1988; Malosio *et al.*, 1991). It is possible that the inhibitory potency of methylxanthines might show regional or developmental changes in the CNS, reflecting the possible difference in affinities of caffeine for each of the subtypes of glycine receptor. The present study on structure-activity relationship of methylxanthines, together with future investigations concerning possible variation in glycine receptor subunit compositions, may provide further evidence that inhibitory actions of methylxanthines on I_{Gly} is one of the factors underyling the CNS stimulant effects of these drugs.

This study was supported by a Grant-in-Aid for Scientific Research (Nos. 02557005, 0330426, 04404023 and 0404429) to N. A. from the Ministry of Education, Science and Culture, Japan.

References

AKAGI, H. & MILEDI, R. (1988). Heterogeneity of glycine receptors and their messenger RNAs in rat brain and spinal cord. *Science*, **242**, 270–273.

AKAIKE, N., SHIRASAKI, T. & YAKUSHIJI, T. (1991). Quinolones and fenbufen interact with $GABA_A$ receptor in dissociated hippocampal cells of rat. *J. Neurophysiol.*, **66**, 497–504.

ARAKI, T., YAMANO, M., MURAKAMI, T., WANAKA, A., BETZ, H. & THOYAMA, M. (1988). Localization of glycine receptors in the rat central nervous system: an immunocytochemical analysis using monoclonal antibody. *Neurosci.*, **25**, 613–624.

BARRON, S.E. & GUTH, P.S. (1987). Uses and limitations of strychnine as a probe in neurotransmission. *News Physiol. Sci.*, **8**, 204–206.

BETZ, H. & BECKER, C.M. (1988). The mammalian glycine receptor: biology and structure of a neuronal chloride channel protein. *Neurochem. Int.*, **13**, 137–146.

BUTCHER, R.W. & SUTHERLAND, E.W. (1962). Adenosine 3',5'-phosphate in biological material. I. purification and properties of cyclic 3',5'-nucleotide phosphodiesterase and use of this enzyme to characterize adenosine 3',5'-phosphate in human urine. *J. Biol. Chem.*, **237**, 1244–1250.

CHOI, O.H., SHAMIM, M.T., PADGETT, W.L. & DALY, J.W. (1988). Caffeine and theophylline analogues: correlation of behavioral effects with activity as adenosine receptor antagonists and as phosphodiesterase inhibitors. *Life Sci.*, **43**, 387–398.

CLEMENTZ, G.L. & DAILEY, J.W. (1988). Psychotropic effects of caffeine. *Am. Fam. Physician*, **37**, 167–172.

CRENNINGLOH, G., PRIBILLA, I., PRIOR, P., MULTHAUP, G., BEYERUTHER, K., TALEB, O. & BETZ, H. (1990). Cloning and expression of the 58 kd β subunit of the inhibitory glycine receptor. *Neuron*, **4**, 963–970.

CURTIS, D.R., HOSLE, L. & JOHNSTON, G.A.R. (1968). A pharmacological study of the depression of spinal neurons by glycine and related amino acids. *Exp. Brain Res.*, **6**, 1–18.

DAY, J.W., HIDE, I., MULLER, C.E. & SHAMIM, M. (1991). Caffeine analogs: structure-activity relationships at adenosine receptors. *Pharmacol.*, **42**, 309–321.

DIATLOV, V.A. (1989). Serotonin modulation of glycine-induced ionic currents in mollusk neurons. *Neirofiziologiia*, **21**, 413–416.

EBIHARA, S., TAKISHIMA, T., SHIRASAKI, T. & AKAIKE, N. (1992). Regional variation of excitatory and inhibitory amino acid-induced responses in rat dissociated CNS neurons. *Neurosci. Res.*, **14**, 61–71.

ENDO, M., TANAKA, M. & OGAWA, Y. (1970). Calcium induced release of calcium from the sarcoplasmic reticulum of skinned skeletal muscle fibers. *Nature*, **228**, 34–36.

FERNANDEZ, J.M., NEHER, E. & GOMPERTS, B.D. (1984). Capacitance measurements reveal stepwise fusion events in degranulating mast cells. *Nature*, **312**, 453–455.

HAMILL, O.P., BORMANN, J. & SAKMANN, B. (1983). Activation of multiple-conductance state chloride channel in spinal neurones by glycine and GABA. *Nature*, **305**, 805–808.

HAMILL, O.P., MARTY, A., NEHER, E., SAKMANN, B. & SIGWORTH, F.J. (1981). Improved patch-clamp technique for high resolution current recording from cells and cell-free membrane patch. *Pflügers Arch. Eur. J. Physiol.*, **391**, 85–100.

HARRIS, K.M. & MILLER, J.R. (1989). CNQX (6-cyano-7-nitro-quinoxaline-2,3-dione) antagonizes NMDA-evoked [^{3}H]GABA release from cultured cortical neurons via an inhibitory action at the strychnine-insensitive glycine sites. *Brain Res.*, **489**, 185–189.

HORN, R. & MARTY, A. (1988). Muscarinic activation of ionic currents measured by a new whole-cell recording method. *J. Gen. Physiol.*, **92**, 145–159.

INOUE, M., OOMURA, Y., YAKUSHIJI, T. & AKAIKE, N. (1986). Intracellular calcium ions decrease the affinity of the GABA receptor. *Nature*, **324**, 156–158.

ITO, C., WAKAMORI, M. & AKAIKE, N. (1991). Dual effect of glycine on isolated rat suprachiasmatic neurons. *Am. J. Physiol.*, **260**, C213–C218.

IZQUIERDO, I. (1986). Interactions between methylxanthines and benzodiazepine binding sites. *Trends Pharmacol. Sci.*, **7**, 256.

KRISHTAL, O.A., OSIPCHUK, Y.V. & VRUBLEVSKY, S.V. (1988). Properties of glycine-activated conductances in rat brain neurones. *Neurosci. Lett.*, **84**, 271–276.

LOPEZ, F., MILLER, L.G., GREENBLATT, D.J. KAPLAN, G.B. & SHADER, R.I. (1989). Interaction of caffeine with the $GABA_A$ receptor complex: alterations in receptor function but not ligand binding. *Eur. J. Pharmacol.*, **172**, 453–459.

MALOSIO, M.L., MARQUEZE-POUEY, B., KUHSE, J. & BETZ, H. (1991). Widespread expression of glycine receptor subunit mRNAs in the adult and developing rat brain. *EMBO J.*, **10**, 2401–2409.

MARTINSON, E.A., JOHNSON, R.A. & WELLS, J.N. (1986). Potent adenosine receptor antagonists that are selective for the A_1 receptor subtype. *Mol. Pharmacol.*, **31**, 247–252.

MURASE, K., RANDIC, M., SHIRASAKI, T., NAKAGAWA, T. & AKAIKE, N. (1990). Serotonin suppresses *N*-methyl-D-aspartate response in acutely isolated spinal dorsal horn neurons of the rat. *Brain Res.*, **525**, 84–91.

NAKAGAWA, T., WAKAMORI, M., SHIRASAKI, T., NAKAYE, T. & AKAIKE, N. (1991). γ-Aminobutyric acid-induced response in acutely isolated nucleus tractus solitarii neurons of the rat. *Am. J. Physiol.*, **260**, C745–C749.

PORTER, N.M., TWYMAN, R.E., UHLER, M.D. & MACDONALD, R.L. (1990). Cyclic AMP-dependent protein kinase decreases $GABA_A$ receptor current in mouse spinal neurons. *Neuron*, **5**, 789–796.

RAITERI, M., FEDELE, E., FONTANA, G. & PITTALUGA, A. (1990). Glycine enhances [^{3}H] noradrenaline release from slices of rat hippocampus. *Neurosci. Lett.*, **116**, 352–356.

RALL, T.W. (1985). Central nervous system stimulants: the methylxanthines. In *Goodman and Gilman's the Pharmacological Basis of Therapeutics*, ed. Gilman, A.G., Goodman, L.S., Rall, T.W. & Murad, F. 7th edn. pp. 589–603. New York: Macmillan.

SHIRASAKI, T., KLEE, M.R., NAKAYE, T. & AKAIKE, N. (1991). Differential blockade of bicuculline and strychnine on GABA- and glycine-induced responses in dissociated rat hippocampal pyramidal cells. *Brain Res.*, **561**, 77–83.

SONG, Y.M. & HUANG, L.Y. (1990). Modulation of glycine receptor chloride channels by cAMP-dependent protein kinase in spinal trigeminal neurons. *Nature*, **348**, 242–245.

STAHLE, L., SEGERSVARD, S. & UNGERSTEDT, U. (1991). Drug distribution studies with microdialysis: II. caffeine and theophylline in blood and other tissues in rats. *Life Sci.*, **49**, 1843–1852.

UNEYAMA, H., MUNAKATA, M. & AKAIKE, N. (1992). 5-HT response of rat hippocampal pyramidal cell bodies. *NeuroReport*, **3**, 633–636.

WAKAMORI, M., HIDAKA, H. & AKAIKE, N. (1993). Hyperpolarizing muscarinic responses of freshly dissociated rat hippocampal CA1 neurones. *J. Physiol.*, (in press).

ZARBIN, M.A., WAMSLEY, J.K. & KUHAR, M.J. (1981). Glycine receptor: light microscopic autoradiographic localization with [^{3}H]strychnine. *J. Neurosci.*, **1**, 532–547.

(Received September 15, 1992
Revised February 1, 1993
Accepted February 5, 1993)

Br. J. Pharmacol. (1993), **109**, 466–472 © Macmillan Press Ltd, 1993

Blockade by glibenclamide of the flow-evoked endothelial release of ATP that contributes to vasodilatation in the pulmonary vascular bed of the rat

Haroutioun Hasséssian, Philippe Bodin & [1]Geoffrey Burnstock

Department of Anatomy and Developmental Biology, University College London, Gower Street, London WC1E 6BT

1 The effect of step augmentation of flow rate on the level of adenosine -5'-triphosphate (ATP) measured in the Krebs perfusate was investigated, and the effect of glibenclamide on the release of ATP was tested in the rat pulmonary vascular bed.

2 For flow rates between 10.38 ± 1.18 and 28.88 ± 2.08 ml min^{-1} ($n = 8$) 1 μM suramin, a P_2-purinoceptor antagonist, significantly ($P < 0.05$) increased vascular resistance under conditions of step augmentation of flow rate. This suggests that endogenous ATP released during increases in flow rate dilates pulmonary vessels.

3 In response to a step augmentation in flow rate from 9.13 ± 0.97 to 18.3 ± 1.69 ml min^{-1} ($n = 4$) ATP levels were up to 23 fold higher ($P < 0.05$) for 15 s, and gradually dropped to a level of about half the initial rise. Once the ATP levels had stabilized, another step augmentation of flow rate to 27.00 ± 3.49 ml min^{-1} was able to evoke a corresponding increase of ATP release. The ability of the vascular bed to respond with increased ATP release after the initial ATP responses had tapered, demonstrates that the drop in ATP levels after the initial rise is not due to depletion of ATP. Furthermore, the maximal ATP response directly precedes the vasodilatation observed following each jump in perfusion pressure produced with each step increase in flow rate.

4 In response to two 3 fold step augmentations of flow rate (8.41–27.29 ml min^{-1}) spaced 30 min apart there were two increases in the level of ATP which were not significantly different from each other. However, perfusion with 1 μM glibenclamide between the first and the second step augmentation of flow rate (8.08–24.67 ml min^{-1}) significantly ($P < 0.05$; $n = 6$) blocked the increase in ATP release. This suggests that the release of intracellular ATP is mediated by glibenclamide-sensitive K^+ channels.

5 A concentration of 1 μM glibenclamide perfused for 30 min was without effect on vascular pressure at constant flow. However, under conditions where flow was augmented in a stepwise manner (between 11.50 and 36.45 ml min^{-1}) perfusing with 1 μM glibenclamide increased vascular resistance ($P < 0.10$).

6 It is concluded that flow-induced ATP release is mediated by a glibenclamide-sensitive K^+ channel, and that the release of ATP from endothelial cells probably functions to vasodilate the pulmonary vascular bed of the rat.

Keywords: Flow evoked ATP release; endothelium; glibenclamide; pulmonary vascular bed

Introduction

Blood flow through the pulmonary vascular bed changes more than 100 fold during each cardiac cycle resulting in proportionately large variations in flow-derived forces (Milnor, 1990). In blood vessels, flow-derived forces can be resolved into two vectors of which pressure acts perpendicular to the long axis, and shear stress acts tangentially (Davies, 1989). Hence, flow-induced shear stress acts primarily on vascular endothelial cells.

Haemodynamic shear stress is known to activate a K^+ conductance in vascular endothelial cells (Olesen *et al.*, 1988) which has not been completely characterized. The functional consequence of increases in flow through arteries is known to be vasodilatation, which was found to be resistant to inhibitors of cyclo-oxygenase (Holtz *et al.*, 1984a; Rubanyi *et al.*, 1986), and abolished by removal of the endothelium (Holtz *et al.*, 1984b; Smiesko *et al.*, 1985). In addition to nitric oxide (Moncada *et al.*, 1991), a large number of vasoactive substances, including adenosine-5'-triphosphate (ATP) are present in the endothelium, and are released in response to various stimuli (Ralevic *et al.*, 1992).

The objective of the present study was to investigate if suramin, a P_2-purinoceptor antagonist, has an effect on perfusion pressure in the pulmonary vascular bed of the rat, and if so, to measure ATP release with an attempt to block it with glibenclamide, a blocker of intracellular ATP-sensitive K^+ channels.

[1] Author for correspondence.

Methods

Isolation and perfusion of pulmonary vascular beds

All experiments were conducted on male Wistar rats of 300–400 g weight. The rats were stunned and exsanguinated to perform a median sternotomy. The trachea was quickly catheterized, and the lungs were removed, together with the heart, to be placed in a Petri dish containing Krebs solution (composition in mM: NaCl 118.0, KCl 5.0, $NaH_2PO_4.2H_2O$ 1.22, $NaHCO_3$ 25.47, $MgSO_4.7H_2O$ 1.22, D-glucose 5.61, $CaCl_2.2H_2O$ 2.52 and 4% bovine serum albumin). The lungs were superfused with Krebs solution, and the left atrium was removed with scissors, after which a Krebs-filled catheter was inserted into and fixed to the main pulmonary artery.

The preparation was transferred to a chamber which was at room temperature (23.96 ± 0.32°C), where the preparation was kept moist by gently superfusing with Krebs solution from a Pasteur pipette. Inside the chamber, the tracheal catheter was connected to a custom-built respirator (Hammersmith Hospital Engineering Unit), and ventilated with air at a frequency of 1 Hz. The mean tidal volume was 7.14 ± 0.86 ml min^{-1} and a positive end expiratory pressure of 7.69 ± 0.66 mmHg was maintained throughout the experiment. The preparation was perfused with Krebs (mean temperature: 23.53 ± 0.42°C) via the main pulmonary artery. The Krebs was bubbled with carbogen (95% O_2:5% CO_2) to maintain pH at 7.25 ± 0.01 by adjusting the carbogen pressure. The pH of the Krebs was measured at the start of each event in the experiments.

Flow-pressure relationship

The tracheal and the main pulmonary artery catheters were connected to separate pressure transducers (Grass model T4), to allow continuous monitoring of airway as well as vascular pressure during the length of the experiments. At the start of each day, before connecting the pulmonary vascular bed preparation, the perfusion pressure of the organ bath apparatus was measured at multiple flow rate settings between 12 and 36 ml min^{-1} at about 6 ml min^{-1} intervals. The perfusion pressure of the organ bath measured in this way was subtracted from the apparent pressure measured once the pulmonary vascular bed was connected to obtain the actual perfusion pressure of the pulmonary vascular bed. The Masterflex pump (Cole Parmer Instrument Co., Chicago, Illinois 60648) delivered a constant flow; near square wave changes in flow rate could be produced using the apparatus.

Once the preparation had stabilized, after 15–30 min, the flow rate was increased to preset levels in a step-wise manner at 30 s intervals. The perfusion pressure stabilized within the 30 s period at the new flow rate. After the peak flow rate of 36.45 ± 0.31 ml min^{-1}, the flow was reduced with the same flow rate steps. The suramin or glibenclamide was introduced, and following 15–30 min of perfusion with drug, the same step increases in flow rate were repeated. Perfusion pressure values were taken at the end of 30 s intervals during ascents in flow. At a constant flow the changes in vascular perfusion pressure reflect changes in vascular resistance. For a fixed volume perfusion with air, a sustained change in the pulse pressure reflects a change in the compliance of the airways. An increase in the compliance of the airways indicates oedema, and throughout the experiments in this study pulse pressure was constant.

Release experiments

To study the kinetics of ATP release, after a 30 min stabilization period with the Krebs solution perfusing at low flow, three 1 ml samples of the effluent were collected into prechilled micro-eppendorf tubes. The perfusion rate was then instantaneously raised and the preparation was subjected to high flow. After a 45 s period and once the perfusion pressure had dropped, the flow rate was raised yet higher. Samples of 1 ml volume were continually collected during the length of the experiment.

Once the preparation had stabilized with the Krebs solution perfusing at low flow, four 1 ml samples were collected before instantaneously raising the flow rate, to investigate the effect of glibenclamide on the ATP response. After the 30 s high flow episode, the perfusion rate was returned to low flow. If necessary, glibenclamide was introduced into the perfusate at this time. Following a 30 min period of perfusion, either with or without glibenclamide, four 1 ml samples of the effluent were collected before repeating the high flow episode. At the end of each trial, effluent was collected into a graduated cylinder for 1 min to determine the flow rate at the low and high flow settings.

Lactate dehydrogenase (LDH) assay

Using the Sigma lactate dehydrogenase (LDH) colorimetric assay procedure, triplicate measures of LDH activity were made from samples of the effluent collected during the low flow (9.5 ml min^{-1}), a 30 s episode of high flow (28.0 ml min^{-1}) and 5 min after the flow rate was lowered to low flow. A 100 µl aliquot of the sample was incubated at 37°C with 0.75 mM pyruvate and 1.28 mM nicotinamide-adenine-dinucleotide (NADH) for 30 min. The reaction was stopped with 1.0 ml of Sigma colour reagent and left for 20 min before adding 5 ml of 0.4 mM NaOH. The absorbance was read at 450 nm. The samples tested had LDH activity below or close to the 40 units ml^{-1} sensitivity of the assay consistent with there being no cell lysis during fast flow experiments.

ATP assays

ATP was measured with the luciferin-luciferase assay essentially as described by Kirkpatrick & Burnstock (1987). Bubbled Krebs solution with or without glibenclamide was collected to determine the background level of ATP which was subtracted from the values obtained in the experimental samples. A 100 µl aliquot of the sample to be assayed was transferred to polypropylene tubes and left at 4°C for 2 h. The samples were then passed through a Packard luminometer for spectrometric analysis during which 200 µl (3.33 mg ml^{-1}) of luciferin-luciferase was added to each sample. By use of linear regression, a standard curve was prepared with samples containing known quantities of ATP, from which ATP quantities in the samples were measured. The limit of detection for ATP was 25 fmol.

Materials

The salts used to prepare the Krebs solution were purchased from BDH Chemicals Ltd. (Poole, Dorset, U.K.), while adenosine-5′-triphosphate (sodium salt, ATP), glibenclamide, and the luciferin-luciferase as well as the LDH colour reagent assay were from Sigma (St. Louis, MO 63178, U.S.A.). Suramin was a kind gift from Bayer, Pharma Research Centre (Newbury, Berkshire).

Statistical analysis

Various parametric and non-parametric tests were conducted after the distribution of the data was examined using GB-STAT (Dynamic Microsystems, Silver Spring, Maryland). For the results shown in Figure 1, the hypothesis that there is no linear trend relating the two variables was tested for each curve using the parametric estimate and the standard error of the parametric estimate in the t-statistic. The data represented in Figure 2 were analysed by a paired Student's *t* test for point analysis. The maximal ATP release during each

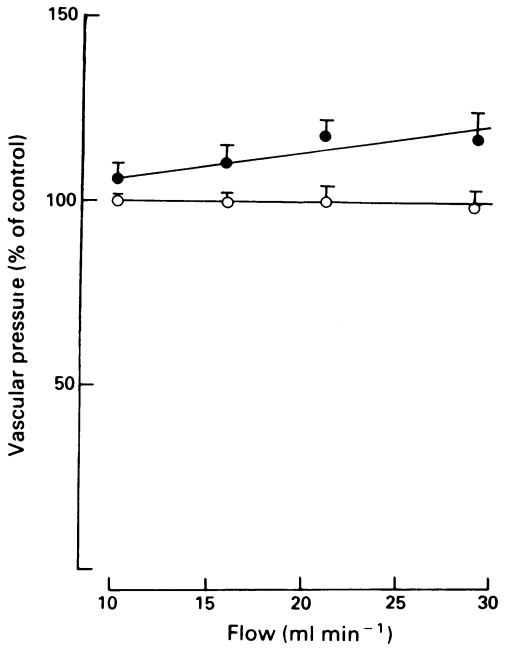

Figure 1 The effect of suramin on vascular perfusion pressure. A second trial of step augmentation of flow rate, in the absence (○) or presence of 1 µM suramin (●) was compared to its control first trial ($n = 8$). The curve representing the experiments without suramin is described by $y = -0.03x + 100.17$ (corr = −0.47), and the slope is not significantly different from zero, indicating that repeating the trial has no effect on the perfusion pressure. The curve representing the experiments with suramin is described by $y = 0.71x + 98.70$ (corr = 0.91), and the slope is significantly ($P < 0.05$) greater than zero indicating that suramin has increased perfusion pressure.

of the high flow episodes were compared with the ATP release measured just before the fast flow and the ATP release during the two episodes of fast flow were compared with each other. For data depicted in Figure 3, a Wilcoxon Rank-Sum test was used to compare the ATP release during the high flow with the corresponding low flow, and the ATP release during high flow between the first and second high flow episodes. The curves shown in Figure 4 and 6 were compared with the appropriate control by testing for statistical significance between the difference of regression line slopes and the standard error of difference of regression slopes in the t-statistic. All values are expressed as means ± s.e.mean, and a probability $P<0.10$ was considered significant.

Results

Effect of suramin on vascular perfusion pressure

Before the effect of drugs on the flow to perfusion pressure relationship could be investigated, it was necessary to examine whether repeating a trial of step augmentation in flow rate produced any change in the perfusion pressure response. In a group of rats, step augmentation of the flow rate between 10.38 ± 1.18 ml min^{-1} and 28.88 ± 2.08 ml min^{-1} produced proportionate increases in vascular perfusion pressure between 23.0 ± 4.55 mmHg and 36.20 ± 4.45 mmHg respectively. After a 15 min rest period, repeating the experiment produced increases in perfusion pressure between 21.80 ± 4.58 mmHg and 35.0 ± 4.18 mmHg. When the perfusion pressure measured during the first and the second trials were compared, the test trial values were close to 100% of their respective control from the first trial and were not significantly different (Figure 1), indicating that repeating the trial by itself did not modify the response.

In a separate group of rats 1 μM suramin was perfused for 15 min between the first and second trials. At the end of the 15 min constant flow rate perfusion, 1 μM suramin was without significant effect on the vascular perfusion pressure (20.50 ± 2.77 mmHg, before; 21.13 ± 3.63 mmHg, after). Step augmentation of the flow rate (9.75 ± 2.21–28.25 ± 3.04 ml min^{-1}) produced, during the second trial, greater increases in perfusion pressure (21.13 ± 3.63–38.63 ± 5.02 mmHg) than were observed during the control trials in the absence of suramin (Figure 1). In the presence of suramin, the perfusion pressure was significantly ($P<0.05$) higher than during the control trial for that group and the effect of suramin on the perfusion pressure was greater with increasing flow rate (Figure 1).

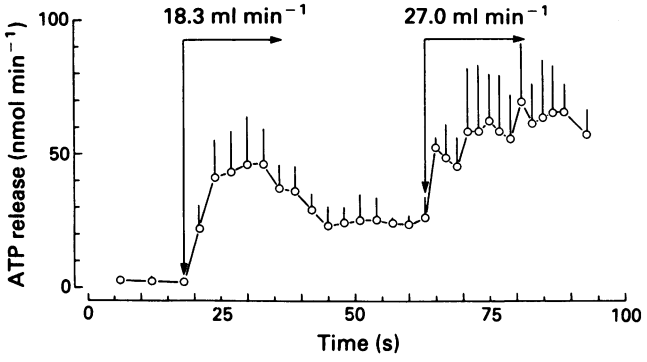

Figure 2 Kinetics of the ATP response to step-augmented flow rate. The flow rate was raised from 9.13 ml min^{-1} to 18.3 ml min^{-1} maintained for 45 s before being raised yet higher to 27.0 ml min^{-1}. The level of ATP measured in samples collected during the 9.13 ml min^{-1} flow rate were not significantly different from each other ($n=4$). The maximal level of ATP measured at each flow rate is significantly ($P<0.05$) greater than the ATP level just prior to augmenting flow rate.

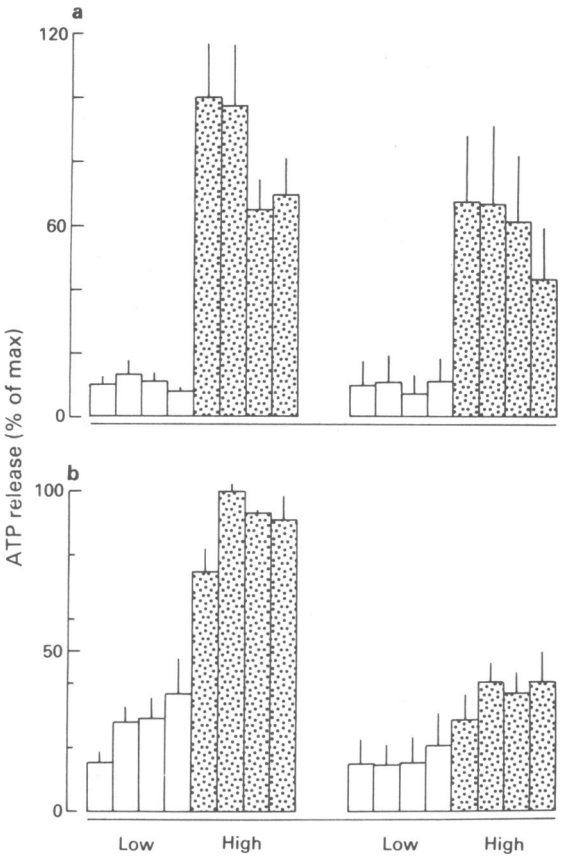

Figure 3 Blockade by glibenclamide of the ATP release in response to step augmentation of flow rate. (a) Release of ATP during two trials of step augmentation of flow rate from 8.41 (open columns) to 27.29 (stippled columns) ml min^{-1} spaced 30 min apart was not significantly different. (b) In the presence of 1 μM glibenclamide, the level of ATP measured during the second step augmentation of flow rate (8.08–24.67 ml min^{-1}) was significantly lower ($P<0.05$, $n=6$) than that measured during the first control trials in the same rats.

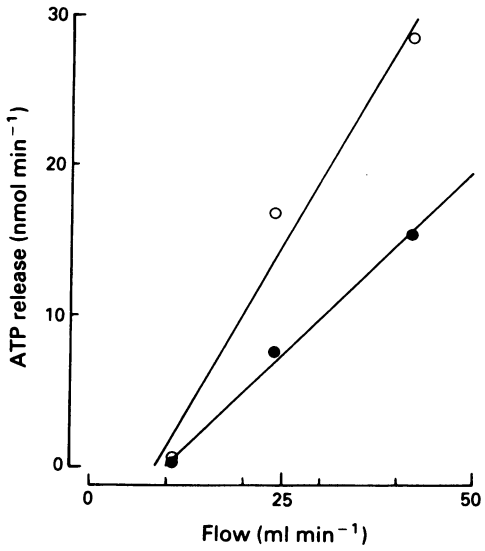

Figure 4 Flow-related blockade by 1 μM glibenclamide of the ATP response to step-augmented flow rate. Blockade of the ATP response is greater with higher flow rate. The curve produced in the absence of glibenclamide is described by $y=0.85x-6.15$ (corr = 0.99) and the curve produced in the presence of 1 μM glibenclamide is described by $y=0.44x-3.16$ (corr = 1.00). The two curves are significantly ($P<0.05$, $n=12$) different.

Kinetics of ATP release

To establish the profile of ATP release during a step increase in flow, multiple samples were collected at short intervals. At low flow (9.13 ± 0.97 ml min^{-1}) ATP release was measured to be about 0.2 ± 0.1 nmol min^{-1} (Figure 2). A sudden augmentation of flow rate to 18.3 ± 1.69 ml min^{-1} for 45 s produced a significant ($P<0.05$) increase in the level of ATP which reached 23 fold that at low flow measured just before increasing flow rate (Figure 2). The level of ATP measured was highest within the first 15 s after high flow, and subsequently was gradually less. Augmenting the flow rate yet higher, to 27.0 ± 3.49 ml min^{-1}, evoked another significant ($P<0.05$) increase in the level of ATP which was maximal within 20 s, and was of greater magnitude than that observed after the first step augmentation of flow rate (Figure 2). In response to a step increase in flow rate, the maximal ATP levels were measured in samples collected within the first 15 s irrespective of the flow step (Figure 2).

Effect of glibenclamide on augmented flow-evoked ATP release

To determine the effect of glibenclamide on ATP release, samples were collected during the first 15 s of augmented flow rate where ATP levels were found to be maximal. Following a 30 min recovery period from a 30 s episode of high flow (27.29 ± 3.74 ml min^{-1}), augmenting the flow rate from the low flow (8.41 ± 1.01 ml min^{-1}) a second time, evoked an ATP response which appeared slightly decreased but was not significantly different (Figure 3a). Perfusing with glibenclamide at constant flow for 30 min between the first and second trials had no effect on basal release of ATP (0.12 ± 0.05 nmol min^{-1}, before; 0.12 ± 0.05 nmol min^{-1}, after). However, after perfusion with 1 μM glibenclamide for 30 min, challenging the vascular bed with a step to the high flow rate (24.67 ± 4.08 ml min^{-1}) from the low flow rate (8.08 ± 1.0 ml min^{-1}) evoked ATP release which was significantly ($P<0.05$) less than the ATP response measured during the control episode of high flow in the absence of glibenclamide (Figure 3b). The effect of glibenclamide to significantly ($P<0.05$) block ATP release in response to a step augmentation of flow rate from 8.88 ± 2.28 ml min^{-1} was observed over a range of flow rate augmentation steps (Figure 4). Furthermore, the greater the augmentation step, the greater was the quantity of ATP which was measured. Under conditions of constant flow glibenclamide was without effect on levels of ATP, unlike the drop in ATP levels observed in the presence of glibenclamide under conditions of step augmentation of flow rate.

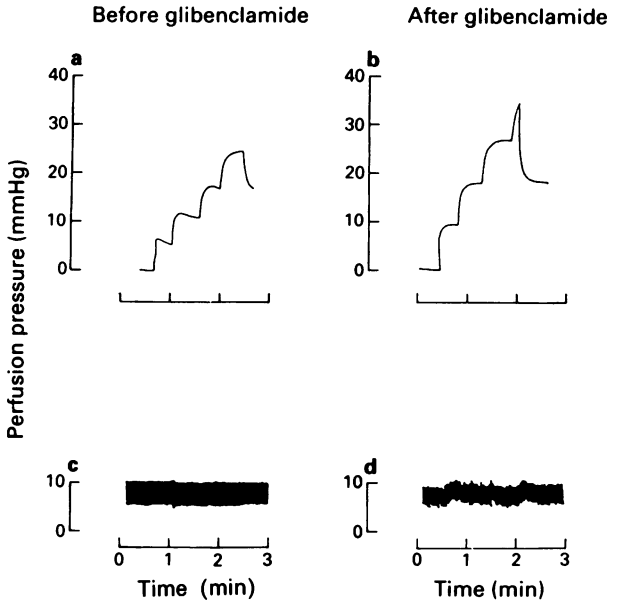

Figure 5 Polygraph traces showing the change in vascular perfusion pressure in (a) and (b), and the airway perfusion pressure in (c) and (d). Step augmentation of the Krebs flow rate (11.5–17.44–23.0–30.11–36.45 ml min^{-1}) produced corresponding step increases in vascular perfusion pressure without affecting the airways. In the presence of 1 μM glibenclamide the drop in perfusion pressure after the initial jump at each step has been blocked (b). In addition, the pressure jumps are to higher levels with each step augmentation of flow rate.

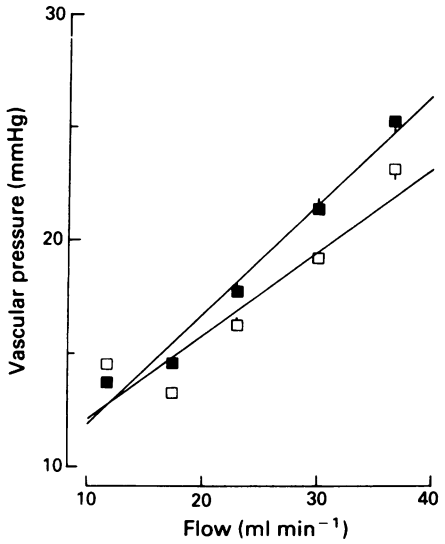

Figure 6 The effect of glibenclamide on the flow rate to perfusion pressure relationship of the vascular bed. The curve produced without perfusion of glibenclamide (□) is described by $y = 0.35x + 8.91$ (corr = 0.91) and the curve produced with perfusion of 1 μM glibenclamide (■) is described by $y = 0.61x + 3.38$ (corr = 1.0, $n = 6$). Glibenclamide increased the resistance in the vascular bed as indicated by the significantly ($P<0.10$) larger slope.

Effect of glibenclamide on the vascular perfusion pressure

Correlated with the inhibition of ATP release produced by glibenclamide under conditions of augmenting flow rate was an increase in vascular resistance. As observed with ATP levels, at a constant flow rate (8.45 ± 1.03 ml min^{-1}) perfusion with 1 μM glibenclamide was without effect on the perfusion pressure (20.0 ± 2.88 mmHg, before; 19.20 ± 3.10 mmHg, after). However, step augmentation of the flow rate produced corresponding increases in the perfusion pressure which jumped to a higher level and within 30 s gradually stabilized at a lower level than the initial jump (Figure 5). After perfusing with 1 μM glibenclamide for 30 min, when the flow rate was augmented in steps similar to the first trial, the perfusion pressure jumped to higher levels with each step and furthermore, with each jump, the perfusion pressure did not drop to a lower level after the initial jump (Figure 5). Examination of the flow to perfusion pressure relationship with and without 1 μM glibenclamide perfusion demonstrated that glibenclamide increased the vascular resistance as indicated by the significant ($P<0.10$) increase in the slope of this curve (Figure 6).

Discussion

During experiments with step augmentation of flow rate, the increase in resistance brought about by suramin indicates that under such conditions of increasing haemodynamic shear stress, endogenous ATP functions to vasodilate the pulmonary vascular bed. In addition, the effect of suramin appears to be greater the higher the flow rate, suggesting that

the higher the flow rate and consequently the shear stress, the greater the vasodilator role of ATP. Suramin was reported to antagonize the response of mouse vas deferens to the P_{2x}-purinoceptor agonist, α,β-MeATP (Dunn & Blakeley, 1988) and has been shown to block the P_{2y}-purinoceptor as well (Hoyle et al., 1990). Suramin has been used as a P_2-purinoceptor antagonist and has been shown to block both the membrane currents as well as the formation of inositol tetrakisphosphate evoked by extracellular ATP (Hoiting et al., 1990).

The source of ATP measured in our study is likely to be the pulmonary vascular endothelial cells. Endothelial cells are capable of rapidly synthesizing ATP from adenosine following the uptake of this nucleoside (Pearson et al., 1978; Pearson & Gordon, 1985). Release of ATP in response to increased flow has been shown in endothelial cell cultures from non-pulmonary vascular beds (Milner et al., 1990a,b; Bodin et al., 1992) and ATP release could not be evoked, in response to augmented flow rate, from cultured vascular smooth muscle cells (Bodin et al., 1991). The release of ATP in response to step augmentation of flow rate is not likely to be due to damage of cells in the pulmonary vascular bed. We could repeat the step augmentation of flow rate without significant change in the ATP response, and furthermore, LDH activity in the effluent was below 40 units ml^{-1} even following episodes of augmented flow rate, suggesting that there is not a massive liberation of LDH from endothelial cells. In addition, upon electron microscopic examination of pulmonary vessels subjected to augmented flow rate, we could not find any change in the ultrastructure of pulmonary vessels compared to controls (Dr A. Loesch, personal communication). The sum of these observations are reassuring that the release of ATP is a physiological phenomenon and not a consequence of destruction of cell membranes and indiscriminate liberation of intracellular ATP.

The kinetics of the ATP response are consistent with the ATP release being evoked from endothelial cells by the increased shear stress produced by the augmented flow rate. The formula for haemodynamic shear stress is $32\mu Q/\pi d^3$ (Olesen et al., 1988), where μ represents the coefficient of viscosity, Q the flow rate of Krebs solution, π the ratio of the circumference of a circle to its diameter and is the diameter of the vessels through which the Krebs solution is flowing. In our experiments, augmenting Q produced an instantaneous increase in shear stress, which would be followed by changes in d. The increase in shear stress brought about by the sudden augmentation of flow rate will liberate vasoactive substances (Pohl et al., 1986; Rubanyi et al., 1986; Christie et al., 1989), which can then alter the shear stress endothelial cells are subjected to by modifying the diameter of vessels (Rubanyi et al., 1986). An increase in the diameter of vessels in the pulmonary vascular bed, and a drop in shear stress can explain why the initial burst of ATP release tapers off to a lower level. An alternative explanation could be the presence of two pools of ATP. One pool which is activated during changes in shear stress to release ATP in a short pulse and a second pool which releases ATP in proportion to the degree of shear stress. Further investigation is required to identify the mechanism responsible for the time course of the ATP release. However, the drop in ATP release is not a result of depletion of intracellular ATP, because a second challenge, by augmenting flow rate yet higher, is able to evoke a corresponding ATP release.

The ATP levels increased within seconds after augmentation of flow rate, and the maximal ATP release directly preceded the drop in perfusion pressure which was observed following the step augmentation in flow rate and the initial increase in perfusion pressure. Mo and colleagues (1991) have reported that adenine nucleotides are required in the extracellular medium to produce the biphasic increase of $[Ca^{2+}]_i$ that was observed in response to haemodynamic shear stress. In this respect, the rank order of potency for adenine nucleotides was found to be ADP>ATP>>>AMP and, adenosine was without effect on $[Ca^{2+}]_i$ (Mo et al., 1991). There is now clear evidence that elevation of $[Ca^{2+}]_i$ is required for the release of endothelium-derived relaxing factor (EDRF) (Long & Stone, 1985; Lewis & Smith, 1991). Hence, ATP may function to produce $[Ca^{2+}]_i$ increases that are necessary for the release of EDRF. In pulmonary vessels of man (Liu et al., 1989), cat (Neely et al., 1989) and rat (Liu et al., 1989), ATP will produce an endothelial P_{2y}-purinoceptor mediated vasodilatation. Activation of P_{2y}-purinoceptors by ATP has been shown to release nitric oxide from cultured endothelial cells (Kelm et al., 1988), and the vasodilator response to P_{2y}-purinoceptor activation in the rat is blocked by N^G-nitro-L-arginine methyl ester an inhibitor of nitric oxide synthase (Moncada et al., 1991). Therefore, shear stress-induced release of ATP from endothelial cells can evoke the release of EDRF from endothelial cells further downstream. Previous studies demonstrated that haemodynamic shear stress activated a K^+ conductance in endothelial cells (Olesen et al., 1988; Davies, 1989), although the nature and the role of this conductance was not elucidated. Other investigators have proposed that efflux of K^+ and hyperpolarization of the endothelial cell, producing a rise in $[Ca^{2+}]_i$, is necessary for the release of EDRF (Busse et al., 1992). In a similar manner, efflux of K^+ through glibenclamide-sensitive channels, activated by augmented shear stress, appears from the present study to be necessary for the release of intracellular ATP from endothelial cells in response to haemodynamic shear stress.

Glibenclamide, an antagonist of intracellular ATP-sensitive K^+ channels (Cook, 1988; Quast & Cook, 1989), increased the resistance in the pulmonary vascular bed under conditions of augmenting flow rate and glibenclamide was found to block the ATP response to augmented flow rate. Therefore, blockade of ATP release by glibenclamide is likely to contribute to the increased vascular resistance which was observed with this drug. However, when measured during a constant flow rate, glibenclamide had no effect on the resting pulmonary arterial pressure nor the levels of ATP. This suggests that two pools of intracellular ATP are present in the rat pulmonary vascular bed. One ATP pool which is sensitive to glibenclamide and another which is not.

The lack of effect of glibenclamide at constant flow is consistent with a previous study in the cat where it was found that glibenclamide did not significantly alter the pulmonary arterial pressure measured during constant flow, although glibenclamide blocked vasodilator responses to cromakalim, a K^+ channel opener (Minkes et al., 1991). Other studies have shown that glibenclamide blocks vasodilator responses to RP52891 (Hood et al., 1991a), an opener of K^+ channels and furthermore, that lemakalim, another opener of K^+ channels, produces vasodilatation in the cat (Hood et al., 1991b). Hence, K^+ channels mediate vasodilatation in the pulmonary vascular bed of the rat. Furthermore, intracellular ATP-sensitive K^+ channels are implicated in the maintenance of the resting potential of pulmonary arteries of the rabbit (Clapp & Gurney, 1992). It is reported that the intracellular ATP concentration is about 1.5 mM (Post & Jones, 1991), which is consistent with intracellular ATP-sensitive K^+ channels being partly functional under resting conditions (Clapp & Gurney, 1992).

In the healthy rat, breathing air, pulsatile increases in blood flow would evoke release of ATP from endothelial cells, which would partly contribute to maintain the pulmonary vascular bed in a dilated state. Therefore, by blocking ATP released in this way, glibenclamide would increase pulmonary vascular resistance. During hypoxia, shear stress is increased as the diameter of vessels is reduced (Davies, 1989). In consequence, more ATP would be released and the endothelium-mediated vasodilator effect of ATP would partly counteract hypoxic vasoconstriction in the pulmonary vascular bed. Release of ATP during hypoxia has been shown in other vascular beds (Paddle & Burnstock, 1974; Forrester & Williams, 1977; Clemens & Forrester, 1981; Hopwood et al.,

1989). However, the intracellular ATP content of pulmonary arteries has been shown to be reduced by prolonged hypoxia (Ohe *et al.*, 1986), and it is known that glibenclamide-sensitive K^+ channels are closed by high intracellular ATP (Cook, 1988). Therefore, ATP can be released in response to increases in flow during hypoxia until the stores of endothelial ATP are depleted. Prolonged hypoxia may even facilitate the flow induced release of ATP by removing the intracellular ATP-mediated inhibition of ATP sensitive K^+ channels. Therefore, the mechanism of the flow-induced release of ATP is likely to be functional in normoxia and hypoxia as long as there is ATP in endothelial cells.

We would like to thank Dr A. Loesch for kindly assisting with the electron microscopy. H.H. is a postdoctoral fellow of the Medical Research Council of Canada and P.B. is a postdoctoral fellow of the British Heart Foundation. This project was conducted with a grant to G.B. from the British Heart Foundation.

References

BODIN, P., BAILEY, D. & BURNSTOCK, G. (1991). Increased flow-induced ATP release from isolated vascular endothelial cells but not smooth muscle cells. *Br. J. Pharmacol.*, **103,** 1203–1205.

BODIN, P., MILNER, P., WINTER, R. & BURNSTOCK, G. (1992). Chronic hypoxia changes the ratio of endothelin to ATP release from rat aortic endothelial cells exposed to high flow. *Proc. R. Soc.* B., **247,** 131–135.

BUSSE, R., LUCKHOFF, A. & POHL, U. (1992). Role of membrane potential in the synthesis and release of EDRF. In *Endothelial Regulation of Vascular Tone*. ed. Ryan, U.S. & Rubanyi, G.M. pp. 105–120. New York: Marcell Dekker Inc.

CHRISTIE, M.T., GRIFFITH, T.M. & LEWIS, M.J. (1989). A comparison of basal and agonist-stimulated release of endothelium-derived relaxing factor from different arteries. *Br. J. Pharmacol.*, **98,** 397–406.

CLAPP, L.H. & GURNEY, A.M. (1992). ATP-sensitive K^+ channels regulate resting potential of pulmonary arterial smooth muscle cells. *Am. J. Physiol.*, **262,** H916–H920.

CLEMENS, M.G. & FORRESTER, T. (1981). Appearance of adenosine triphosphate in the coronary sinus effluent from isolated working rat heart in response to hypoxia. *J. Physiol.*, **312,** 143–158.

COOK, N.S. (1988). The pharmacology of potassium channels and their therapeutic potential. *Trends Pharmacol. Sci.*, **8,** 209–211.

DAVIES, P.F. (1989). How do vascular endothelial cells respond to flow? *News Physiol. Sci.*, **4,** 22–25.

DUNN, P.M. & BLAKELEY, A.G.H. (1988). Suramin: a reversible P_2-purinoceptor antagonist in the mouse vas deferens. *Br. J. Pharmacol.*, **93,** 243–245.

FORRESTER, T. & WILLIAMS, C.A. (1977). Release of adenosine triphosphate from isolated adult heart cells in response to hypoxia. *J. Physiol.*, **268,** 371–390.

HOITING, B., MOLLEMAN, A., NELEMANS, A. & HERTOG, A.D. (1990). P_2-purinoceptor-activated membrane currents and inositol tetrakisphosphate formation are blocked by suramin. *Eur. J. Pharmacol.*, **181,** 127–131.

HOLTZ, J., FORSTERMANN, U., POHL, U., GIESLER, M. & BASSENGE, E. (1984a). Flow-dependent, endothelium mediated dilation of epicardial coronary arteries in conscious dogs: effects of cyclo-oxygenase inhibition. *J. Cardiovasc. Pharmacol.*, **6,** 1161–1169.

HOLTZ, J., POHL, U., KELLNER, C. & BUSSE, R. (1984b). Effect of endothelial removal or damage on the flow-dependent dilation of canine femoral arteries in vivo and in vitro (abstract). *Pflügers Arch.*, **400,** R9.

HOOD, J.S., MCMAHON, T.J. & KADOWITZ, P.J. (1991a). Pulmonary vasodilator responses to RP52891 are mediated by activation of glibenclamide-sensitive K^+_{ATP} channel. *Eur. J. Pharmacol.*, **202,** 121–124.

HOOD, J.S., MCMAHON, T.J. & KADOWITZ, P.J. (1991b). Influence of lemakalim on the pulmonary vascular bed of the cat. *Eur. J. Pharmacol.*, **202,** 101–104.

HOPWOOD, A.M., LINCOLN, J., KIRKPATRICK, K.A. & BURNSTOCK, G. (1989). Adenosine 5'-triphosphate, adenosine and endothelium-derived relaxing factor in hypoxic vasodilation of the heart. *Eur. J. Pharmacol.*, **165,** 323–326.

HOYLE, C.H.V., KNIGHT, G.E. & BURNSTOCK, G. (1990). Suramin antagonizes responses to P_2-purinoceptor agonists and purinergic nerve stimulation in the guinea-pig urinary bladder and taenia coli. *Br. J. Pharmacol.*, **99,** 617–621.

KELM, M., FEELISCH, M., SPAHR, R., PIPER, H.M., NOACK, E. & SCHRADER, J. (1988). Quantitative and kinetic characterization of nitric oxide and EDRF released from cultured endothelial-cells. *Biochem. Biophys. Res. Commun.*, **154,** 236–244.

KIRKPATRICK, K.A. & BURNSTOCK, G. (1987). Sympathetic nerve-mediated release of ATP from the guinea-pig vas deferens is unaffected by reserpine. *Eur. J. Pharmacol.*, **138,** 207–214.

LEWIS, M.J. & SMITH, J.A. (1991). Factors regulating the release of endothelium-derived relaxing factor. In *Endothelial Regulation of Vascular Tone*. ed. Ryan, U.S. & Rubanyi, G.M. pp. 139–154. New York: Marcell Dekker Inc.

LIU, S.F., MCCORMACK, D.G., EVANS, T.W. & BARNES, P.J. (1989). Evidence for two P_2-purinoceptor subtypes in human small pulmonary arteries. *Br. J. Pharmacol.*, **98,** 1014–1020.

LONG, C.J. & STONE, T.W. (1985). The release of endothelium-derived relaxant factor is calcium dependent. *Blood Vessels*, **22,** 205–208.

MILNER, P., BODIN, P., LOESCH, A. & BURNSTOCK, G. (1990a). Rapid release of endothelin and ATP from isolated aortic endothelial cells exposed to increased flow. *Biochem. Biophys. Res. Commun.*, **160,** 93–100.

MILNER, P., KIRKPATRICK, K.A., RALEVIC, V., TOOTHILL, V., PEARSON, J. & BURNSTOCK, G. (1990b). Endothelial cells cultured from human umbilical vein release ATP, substance P and acetylcholine in response to increased flow. *Proc. R. Soc.* B, **241,** 245–248.

MILNOR, W.R. (1990). Pulmonary circulation. In *Cardiovascular Physiology*, pp. 357–386. Oxford: University Press.

MINKES, R.K., KVAMME, P., HIGUERA, T.R., NOSSAMAN, B.D. & KADOWITZ, P.J. (1991). Analysis of pulmonary and systemic vascular responses to cromakalim, an activator of K^+_{ATP} channels. *Am. J. Physiol.*, **260,** H957–H966.

MO, M., ESKIN, S.G. & SCHILLING, W.P. (1991). Flow-induced changes in Ca^{2+} signalling of vascular endothelial cells: effect of shear stress and ATP. *Am. J. Physiol.*, **260,** H1698–H1707.

MONCADA, S., PALMER, R.M.J. & HIGGS, E.A. (1991). Nitric oxide: physiology, pathophysiology and pharmacology. *Pharmacol. Rev.*, **43,** 109–142.

NEELY, C.F., KADOWITZ, P.J., LIPPTON, H., NEIMAN, M. & HYMAN, A.L. (1989). Adenosine does not mediate the pulmonary vasodilator response of adenosine 5'-triphosphate in the feline pulmonary vascular bed. *J. Pharmacol. Exp. Ther.*, **250,** 170–176.

OHE, M., MIMATA, T., HANEDA, T. & TAKISHIM, T. (1986). Time course of pulmonary vasoconstriction with repeated hypoxia and glucose depletion. *Rep. Physiol.*, **63,** 177–186.

OLESEN, S.-P., CLAPHAM, D.E. & DAVIES, P.F. (1988). Haemodynamic shear stress activates a K^+ current in vascular endothelial cells. *Nature*, **331,** 168–170.

PADDLE, B.M. & BURNSTOCK, G. (1974). Release of ATP from perfused heart during coronary vasodilation. *Blood Vessels*, **11,** 110–119.

PEARSON, J., CARLETON, J.S., HUTCHINGS, A. & GORDON, J.L. (1978). Uptake and metabolism of adenosine by pig aortic endothelial and smooth-muscle cells in culture. *Biochem. J.*, **170,** 265–271.

PEARSON, J.D. & GORDON, J.L. (1985). Nucleotide metabolism by endothelium. *Annu. Rev. Physiol.*, **47,** 617–627.

POHL, U., BUSSE, R., KUON, E. & BASSENG, E. (1986). Pulsatile perfusion stimulates the release of endothelial autocoids. *J. Appl. Cardiol.*, **1,** 215–235.

POST, J.M. & JONES, A.W. (1991). Stimulation of arterial ^{42}K efflux by ATP depletion and cromakalim is antagonized by glibenclamide. *Am. J. Physiol.*, **260,** H848–H854.

QUAST, U. & COOK, N.S. (1989). Moving together: K^+ channel openers and ATP sensitive K^+ channels. *Trends Pharmacol. Sci.*, **10,** 431–435.

RALEVIC, V., LINCOLN, J. & BURNSTOCK, G. (1992). Release of vasoactive substances from endothelial cells. In *Endothelial Regulation of Vascular Tone*. ed. Ryan, U.S. & Rubanyi, G.M. pp. 297–328. New York: Marcell Dekker Inc.

RUBANYI, G.M., ROMERO, J.C. & VANHOUTTE, P.M. (1986). Flow-induced release of endothelium-derived relaxing factor. *Am. J. Physiol.*, **250**, H1145–H1149.

SMIESKO, V., KOZIK, J. & DOLEZEL, S. (1985). Role of endothelium in the control of arterial diameter by blood flow. *Blood Vessels*, **22**, 247–251.

(Received August 26, 1992
Revised January 5, 1993
Accepted February 8, 1993)

Br. J. Pharmacol. (1993), **109**, 473–479 © Macmillan Press Ltd, 1993

Functional importance of cholinergic and purinergic neurotransmission for micturition contraction in the normal, unanaesthetized rat

[1]*†Yasuhiko Igawa, *Anders Mattiasson & **Karl-Erik Andersson

Departments of *Urology and **Clinical Pharmacology, Lund University Hospital, Lund, Sweden, and †Department of Urology, Shinshu University School of Medicine, Matsumoto, Japan

1 The cholinergic and purinergic neurotransmission involved in micturition in the normal, unanaesthetized rat was investigated by means of continuous cystometry.

2 ATP (1 and 5 mg kg^{-1}), administered intra-arterially (i.a.) close to the bladder, produced rapid, phasic, dose-dependent increases in bladder pressure with micturition immediately after injection. The micturition pressure of the following spontaneous voidings increased, and bladder capacity, micturition volume, and residual volume decreased. Pretreatment with α,β-methylene ATP (1 mg kg^{-1}, i.a.) blocked the effects of ATP (5 mg kg^{-1}).

3 α,β-Methylene ATP (0.25, 0.5 and 1 mg kg^{-1}, i.a.) produced rapid, phasic, increases in bladder pressure with micturition immediately after injection. The effects of α,β-methylene ATP (0.25 mg kg^{-1}, i.a.) were not affected by pretreatment with indomethacin (0.5–2 mg kg^{-1}, i.a.). The micturition pressure of the subsequent spontaneous voidings decreased, and bladder capacity and residual volume increased.

4 Carbachol (5–50 μg kg^{-1}, i.a.) produced rapid, sustained, dose-dependent increases in bladder pressure with micturition, and then increased basal pressure, threshold pressure, and micturition pressure, and decreased bladder capacity and micturition volume during the following spontaneous voidings.

5 Atropine (1 mg kg^{-1}, i.a.) decreased micturition pressure and micturition volume, but did not induce dribbling incontinence. Micturition contractions still occurred after the injection, but changed in appearance and were of shorter duration than before. In the presence of atropine (1 mg kg^{-1}, i.a.), α,β-methylene ATP (1 mg kg^{-1}, i.a.) produced initially a phasic increase in bladder pressure with micturition and then dribbling incontinence in all animals tested.

6 After blockade of the micturition reflex with morphine (10 μg intrathecally), ATP (5 mg kg^{-1}, i.a.), α,β-methylene ATP (0.25–1 mg kg^{-1}, i.a.), and carbachol (5–500 μg kg^{-1}, i.a.) were unable to empty the bladder.

7 The results suggest that drug-induced bladder emptying in the normal, unanaesthetized rat requires an intact micturition reflex and they support the view that the two physiologically important transmitters involved in micturition are acetylcholine and ATP.

Keywords: Micturition in rat; cholinergic transmission; purinergic transmission; cystometry; α,β-methylene ATP

Introduction

It is generally agreed that reflex activation of the parasympathetic nerve supply to the bladder is responsible for bladder emptying. It is also accepted that acetylcholine is one of the transmitters released during activation, but the well known occurrence of atropine resistance has led to the suggestion that other, non-adrenergic, non-cholinergic (NANC) transmitters may also be involved (Ambache & Zar, 1970). In the rat bladder, for example, the NANC component of contraction seems to be the quantitatively dominating (Carpenter, 1977). Stimulation of NANC-nerves in the guinea-pig bladder evokes contractions that can be mimicked by exogenous adenosine-5′-triphosphate (ATP) and studies on the NANC component of bladder contraction in this and several other species, including rat and man (Burnstock *et al.*, 1972; 1978a,b; Dean & Downie, 1978; Dahlén & Hedqvist, 1980; Kasakov & Burnstock, 1983; Sibley, 1984; Hoyle & Burnstock, 1985; Kasakov & Vlaskova, 1985; Fujii, 1988; Bhat *et al.*, 1989; Brading & Mostwin, 1989; Hoyle *et al.*, 1989; Brading & Williams, 1990; Luheshi & Zar, 1990; Parija *et al.*, 1991) have supported the view that ATP is an excitatory NANC transmitter. The contractile response of guinea-pig, rat, and human detrusor strips to field stimulation was shown to be blocked almost completely by a combination of atropine and desensitization of bladder P_2-purinoceptors with α,β-methylene ATP (Kasakov & Burnstock, 1983; Brading, 1987; Brading & Mostwin, 1989; Hoyle *et al.*, 1989; Brading & Williams, 1990). In the rat bladder, a cholinergic (slow) and a non-cholinergic (fast) contractile component in response to single pulse stimulation could be distinctly separated (Maggi *et al.*, 1985). The slow component was abolished by atropine, and the fast component was reduced, but not abolished, by α,β-methylene ATP (Luheshi & Zar, 1990; Parija *et al.*, 1991; Maggi, 1991). These results suggest that ATP and acetylcholine are the main contractile activators of the rat detrusor.

However, investigations using field stimulation of the nerves of isolated whole bladders or strips of detrusor muscle give no information on the importance of the released transmitters for bladder emptying *in vivo*. In the present investigation, we have studied by continuous cystometry, the cholinergic and the purinergic neurotransmission involved in micturition in normal, unanaesthetized rats.

Methods

Surgical procedures

Female Sprague-Dawley rats weighing 200–250 g were anaesthetized with ketamine (75 mg kg^{-1}, i.m.) and xylazine (15 mg kg^{-1}, i.m.). The abdomen was opened through a mid-

[1] Author for correspondence at: Department of Urology, Lund University Hospital, S-221 85 Lund, Sweden.

line incision, and a polyethylene catheter (Clay-Adams PE-50, NJ, U.S.A.) was implanted into the bladder through the dome as described previously (Malmgren *et al.*, 1987b). Two days after this operation, the animals were again anaesthetized, and a femoral artery was exposed through an inguinal incision. A poleythylene catheter (Clay-Adams PE-10, NJ, U.S.A.) filled with heparinized saline (30 iu ml^{-1}) was inserted into the vessel, and advanced proximally until the tip of the catheter reached the abdominal aortic bifurcation. In order to increase the amount of drug reaching the bladder, both femoral arteries were tied. The catheter was tunnelled subcutaneously and an orifice was made on the back of the animal. In some animals, a polyethylene catheter (Clay-Adams PE-10, NJ, U.S.A.) was implanted into the subarachnoid space at the level of L_6-S_1 spinal cord segments for intrathecal (i.t.) administration of drugs as described in detail previously (Igawa *et al.*, 1992a,b). Neither the placement of the i.t. catheter itself, nor i.t. injection of saline, affects the cystometric pattern (Igawa *et al.*, 1992a,b). After the experiment, the position of the catheter in the abdominal aorta and in the spinal subarachnoid space was confirmed in each animal.

Cystometric investigations

Cystometric investigations were performed without any anaesthesia the day after the intra-arterial (i.a.) catheterization. The bladder catheter was connected via a T-tube to a pressure transducer (P23 DC, Statham Instrument Inc., CA, U.S.A.) and a microinjection pump (CMA 100, Carnegie Medicine AB, Sweden). The conscious rat was placed, without any restraint, in a metabolic cage which also enabled measurements of micturition volumes by means of a fluid collector connected to a Grass force displacement transducer (FT 03C, Grass Instrument Co., Quincy, Mass, U.S.A.). Room-temperature saline was infused into the bladder at a rate of 10 ml h^{-1}. Intravesical pressure and micturition volumes were recorded continuously on a Grass polygraph (Model 7E, Grass Instrument Co., Quincy, Mass, U.S.A.; recording speed: 10 mm min^{-1}). Three reproducible micturition cycles, corresponding to a 20 min period, were recorded before drug administration. After each drug administration, recording was continued for another 60 min. The following cystometric parameters were investigated (Malmgren *et al.*, 1987b): basal pressure (the lowest bladder pressure during filling), threshold pressure (bladder pressure immediately prior to micturition), micturition pressure (the maximum bladder pressure during micturition), bladder capacity (residual volume at the latest previous micturition plus volume of infused saline at the micturition), micturition volume (volume of expelled urine), residual volume (bladder capacity minus micturition volume), and duration of micturition contraction. Analysis was performed for a 20 min period before drug administration. Drug effects on cystometric parameters were assessed for 60 min, and the most effective two micturition cycles were subjected to analysis. When a rapid bladder contraction was observed immediately after drug injection, the amplitude, and duration of the contraction, and percentage volume expelled (i.e. volume of expelled urine/volume of infused saline) were also analysed.

Administration of drugs

The following drugs were used for i.a. or i.t. administration: carbamylcholine chloride (carbachol), adenosine 5'-triphosphate (ATP disodium salt), α,β-methylene ATP (lithium salt), indomethacin (Sigma Chemical Co., St. Louis, MO, U.S.A.), atropine sulphate (Kabi-Pharmacia, Stockholm, Sweden), and morphine sulphate (Gacell Laboratories, Malmö, Sweden). Drugs were dissolved in redistilled water, and then stored at −70°C. Subsequent dilutions of the drugs were made on the day of experiments in saline. Drugs were injected through the i.a. catheter in a volume of 1 ml kg^{-1} (0.20–0.25 ml), and were followed by 0.1 ml of heparinized saline for less than 5 s. To evaluate the micturition induced directly by drugs *per se*, the drugs, except atropine and morphine, were given at the time when the volume of infused saline reached half the bladder capacity during the preceding micturition cycles. Atropine and morphine were injected immediately after micturition. Administration of the vehicles had no effects on the cystometric pattern.

Statistical analysis

The results are given as mean values ± s.e.mean. Student's paired *t* test was used for comparison between before and after treatments. Comparison between the drugs was performed by use of factorial analysis of variance. A probability level <0.05 was accepted as significant.

Results

Repeated cystometries gave reproducible results. The bladder pressure was low and almost devoid of spontaneous fluctuations during filling. The micturition contractions generally had a biphasic appearance (biphasic in 19 out of 23 animals; 83%, monophasic in 4 animals; 17%).

ATP, administered i.a. close to the bladder in a dose of 0.1 mg kg^{-1} ($n = 5$), had no clear-cut effects. In doses of 1 ($n = 9$) and 5 mg kg^{-1} ($n = 10$), ATP produced rapid, phasic, dose-dependent increases in bladder pressure with micturition immediately after the injection. The amplitude and duration of the drug-induced contractions after injection of 5 mg kg^{-1} were 26 ± 6 cmH_2O and 15 ± 2 s, respectively. The percentage volume expelled after 5 mg kg^{-1} was 75 ± 6% (Table 1). The micturition pressure of the following spontaneous voidings increased dose-dependently, and bladder capacity, micturition volume, and residual volume decreased (Figure 1a; Table 2). The duration of the effects was approximately 15 min. Pretreatment with α,β-methylene ATP (1 mg kg^{-1}, i.a., 2–3 min before administration of ATP) blocked the effects of ATP (5 mg kg^{-1}, $n = 6$; Figure 1b).

α,β-Methylene ATP, administered i.a. in doses of 0.25 ($n = 9$), 0.5 ($n = 4$) and 1 mg kg^{-1} ($n = 8$), produced rapid, phasic, dose-dependent increases in bladder pressure with micturition immediately after the injections (Figure 2a). The amplitude and duration of the drug-induced contractions after injection of 0.25 and 1 mg kg^{-1} were 49 ± 8 and 64 ± 3 cmH_2O, and 36 ± 12 and 54 ± 7 s, respectively. The percentage volume expelled after 0.25 and 1 mg kg^{-1} was 76 ± 3 and 77 ± 8%, respectively (Table 1). The effects of α,β-methylene ATP (0.25 mg kg^{-1}, i.a.) were not affected by pretreatment with indomethacin (0.5–2 mg kg^{-1}, i.a.; $n = 5$; data not shown). After injection of 0.25 mg kg^{-1} α,β-methylene ATP, there were no consistent effects on the subsequent spontaneous voidings. After 0.5 and 1 mg kg^{-1} α,β-methylene ATP, on the other hand, the micturition pressure of the subsequent spontaneous voidings decreased, and bladder capacity and residual volume increased (Figure 2a; Table 2). However, dribbling incontinence was not induced. Repeated injections of α,β-methylene ATP (0.25–0.5 mg kg^{-1}, i.a. every 5–7 min × 5–8; $n = 4$) decreased the micturition pressure of the following spontaneous voidings, and changed the micturition contractions in those cases where it was monophasic into a biphasic pattern (Figure 2b). However, the duration of the micturition contractions did not change, and dribbling incontinence was not observed. Five to 10 min after the last of the repeated administrations of α,β-methylene ATP, atropine (1 mg kg^{-1}, i.a.; $n = 4$) was administered. Atropine abolished the second tonic part of the micturition contractions, but did not affect the initial phasic component (Figure 2b). Dribbling incontinence was not produced after the injection of atropine. In 2 animals, α,β-methylene ATP (0.5–1.0 mg kg^{-1}, i.a.) was administered again 10 min after atropine. Small bladder contractions still remained after the injection, but dribbling incontinence was now observed in both animals.

Table 1 The amplitude and duration of the bladder contractions and expelled volume induced by ATP, α,β-methylene ATP, and carbachol given intra-arterially to the rat

	Amplitude (cmH_2O)	*Duration* (s)	*% vol. exp.* (%)
ATP			
5 mg kg^{-1}, $n = 10$	26 ± 6	15 ± 2**	75 ± 6
α,β-Methylene ATP			
0.25 mg kg^{-1}, $n = 9$	49 ± 8	36 ± 12**	76 ± 3
1 mg kg^{-1}, $n = 8$	64 ± 3	54 ± 7**	77 ± 8
1 mg kg^{-1}, $n = 8$ (in the presence of atropine)	22 ± 5†††	24 ± 6††	23 ± 8†††
Carbachol			
5 μg kg^{-1}, $n = 7$	63 ± 16	76 ± 36**	90 ± 4
50 μg kg^{-1}, $n = 8$	65 ± 15	458 ± 108	90 ± 4

Results are expressed as mean ± s.e.mean.
Amplitude; amplitude of the bladder contraction induced by the drugs. Duration; duration of the bladder contraction induced by the drugs. % vol. exp.; percentage volume expelled by the drug-induced bladder contraction compared to carbachol (50 μg kg^{-1}): **$P<0.01$; compared to the corresponding values in the absence of atropine: ††$P<0.01$; †††$P<0.001$.

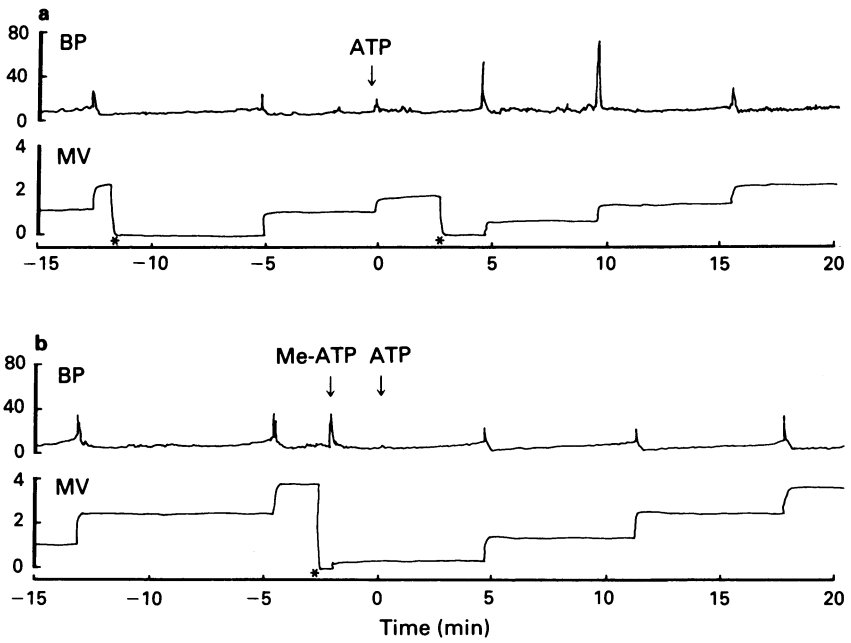

Figure 1 Effects of ATP administered intra-arterially (i.a.) in the absence and presence of α,β-methylene ATP on bladder pressure (BP; cmH_2O) and micturition volume (MV; ml) during cystometry performed in a normal rat. (a) In the absence of α,β-methylene ATP, ATP (5 mg kg^{-1}, i.a.) produced a rapid, phasic rise in bladder pressure with micturition, and then increased micturition pressure during the following spontaneous voidings. (b) α,β-Methylene ATP (Me-ATP; 1 mg kg^{-1}, i.a.), administered 2 min before ATP, by itself produced a rapid, phasic increase in micturition pressure with micturition. In the presence of α,β-methylene ATP, the effects of ATP (5 mg kg^{-1}, i.a.) were blocked. *indicates adjustment to baseline position.

Carbachol, administered i.a. in a dose of 1 μg kg^{-1} ($n = 4$), had no clear-cut effects. Carbachol, in doses of 5 ($n = 7$) and 50 μg kg^{-1} ($n = 8$), produced rapid, sustained, dose-dependent increases in bladder pressure, and micturition (Figure 3). The amplitude and duration of the drug-induced contractions after injection of 5 and 50 μg kg^{-1} were 63 ± 16 and 65 ± 15 cmH_2O, and 76 ± 36 and 458 ± 108 s, respectively (Table 1). The duration of the contraction after carbachol 50 μg kg^{-1} was longer than that after ATP (5 mg kg^{-1}), α,β-methylene ATP (0.25 and 1.0 mg kg^{-1}), and carbachol 5 μg kg^{-1}. The percentage volume expelled after 5 or 50 μg kg^{-1} was 90 ± 4% (Table 1). After 5 and 50 μg kg^{-1}, the basal pressure, threshold pressure, and micturition pressure increased during the following spontaneous voidings. Bladder capacity and micturition volume also decreased (Figure 3; Table 2). The duration of the effects was approximately 15 min.

Atropine (1 mg kg^{-1}, i.a., $n = 9$) decreased micturition pressure (by 54%) and micturition volume, and increased residual volume for about 30 min, but did not induce dribbling incontinence (Figure 4; Table 2). Micturition contractions still occurred after the injection, but changed appearance (biphasic in 7, monophasic in 2 out of 9 animals before administration, monophasic in 9 out of 9 animals after administration) and were of shorter duration than before (Figure 4). The mean duration of the micturition contraction after administration was 6.0 ± 0.6 s, which was significantly shorter ($P<0.001$) than the corresponding value (12.0 ± 0.6 s) before administration. In the presence of atropine (1 mg kg^{-1}, i.a., 8–15 min before administration of α,β-methylene ATP), α,β-methylene ATP (1 mg kg^{-1}, i.a.; $n = 8$) produced initially a phasic increase in bladder pressure with micturition. The amplitude and duration of the drug-induced contraction after injection of α,β-methylene were

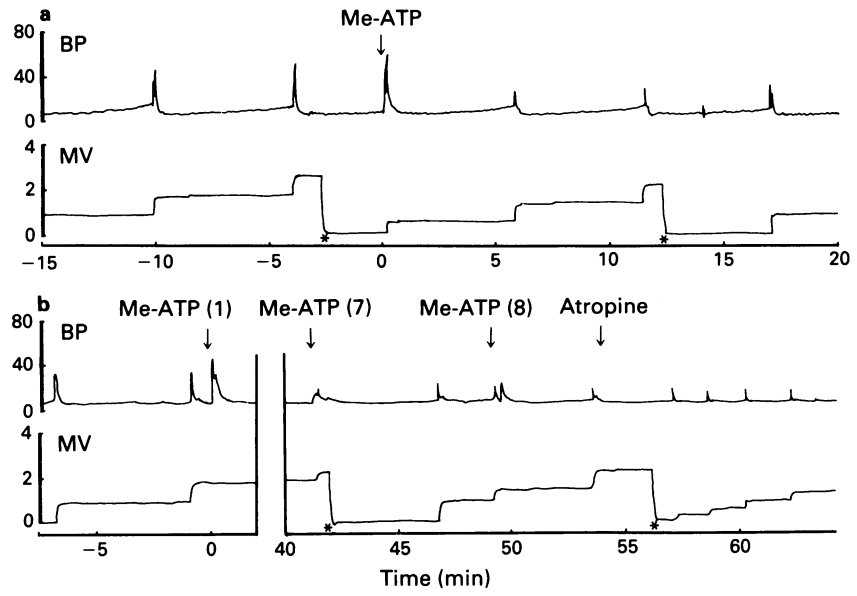

Figure 2 Original recordings of bladder pressure (BP; cmH_2O) and micturition volume (MV; ml) during cystometry performed in a normal rat before and after intra-arterial (i.a.) single injection (a), and repeated injections (b) of α,β-methylene ATP. (a) α,β-Methylene ATP (Me-ATP; 1 mg kg^{-1}, i.a.) induced a phasic pressure rise with micturition, and suppressed the following micturition contractions. (b) Repeated administration of α,β-methylene ATP (Me-ATP; 0.5 mg kg^{-1}, i.a., 8 times, 7 min intervals) produced a decrease in micturition pressure, and changed the micturition contractions from a mono- to a biphasic pattern. Atropine (1 mg kg^{-1}, i.a.) abolished the second tonic component of the biphasic contraction. *indicates adjustment to baseline position. Number of α,β-methylene ATP administrations given in parentheses.

Table 2 Effects of intra-arterial administration of ATP (5 mg kg^{-1}, $n = 10$), α,β-methylene ATP (1 mg kg^{-1}, $n = 8$), carbachol (50 μg kg^{-1}, $n = 8$), and atropine (1 mg kg^{-1}, $n = 9$) on cystometric parameters during the following spontaneous voidings

	MP	*BC*	*MV*	*RV*
ATP				
before	47.8 ± 5.7	1.15 ± 0.08	1.03 ± 0.08	0.11 ± 0.02
after	73.9 ± 9.6***	0.83 ± 0.09***	0.78 ± 0.08***	0.05 ± 0.02*
α,β-Methylene ATP				
before	54.2 ± 5.8	0.82 ± 0.07	0.76 ± 0.06	0.06 ± 0.02
after	30.8 ± 5.8**	1.04 ± 0.09*	0.66 ± 0.07	0.37 ± 0.04***
Carbachol				
before	44.0 ± 9.6	1.00 ± 0.11	0.94 ± 0.09	0.06 ± 0.04
after	62.0 ± 12.9*	0.41 ± 0.06***	0.39 ± 0.05***	0.02 ± 0.01
Atropine				
before	46.0 ± 4.0	0.80 ± 0.08	0.75 ± 0.08	0.05 ± 0.02
after	21.1 ± 3.3***	0.95 ± 0.11	0.48 ± 0.02***	0.47 ± 0.09***

MP: micturition pressure (cmH_2O); BC: bladder capacity (ml); MV: micturition volume (ml); RV residual volume (ml).
Results are expressed as mean ± s.e.mean.
Values before vs after administration: *$P<0.05$; **$P<0.01$; ***$P<0.001$.

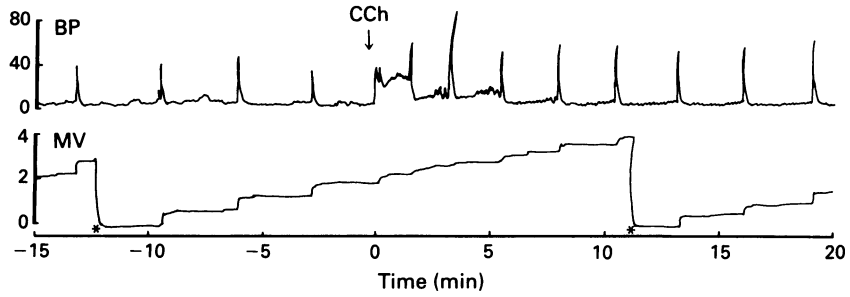

Figure 3 Effects of carbachol administered intra-arterially on bladder pressure (BP; cmH_2O) and micturition volume (MV; ml) during cystometry performed in a normal rat. Immediately after injection of carbachol (CCh; 50 μg kg^{-1}), a rapid, sustained increase in bladder pressure with micturition was observed. Then, the basal, threshold, and micturition pressures increased, and micturition volume decreased during the following spontaneous voidings. *indicates adjustment to baseline position.

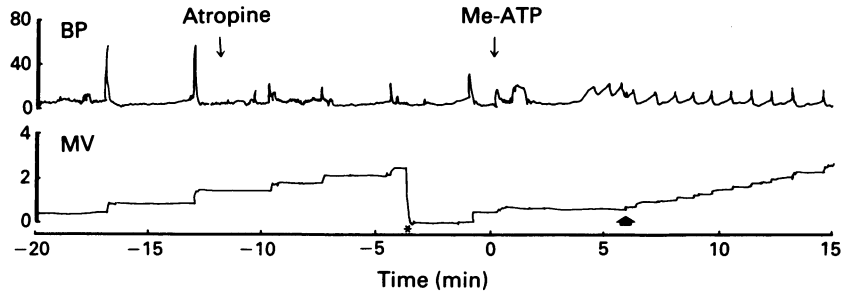

Figure 4 Effects of atropine, and α,β-methylene ATP in the presence of atropine on bladder pressure (BP; cmH_2O) and micturition volume (MV; ml) during cystometry performed in a normal rat. Atropine (1 mg kg^{-1}), administered intra-arterially (i.a.), by itself decreased micturition pressure and micturition volume, and shortened the micturition contraction. In the presence of atropine, α,β-methylene ATP (Me-ATP; 1 mg kg^{-1}, i.a.) produced a rapid, transient increase in bladder pressure, and then dribbling incontinence. * and ↑ indicate adjustment to baseline position and initiation of dribbling incontinence, respectively.

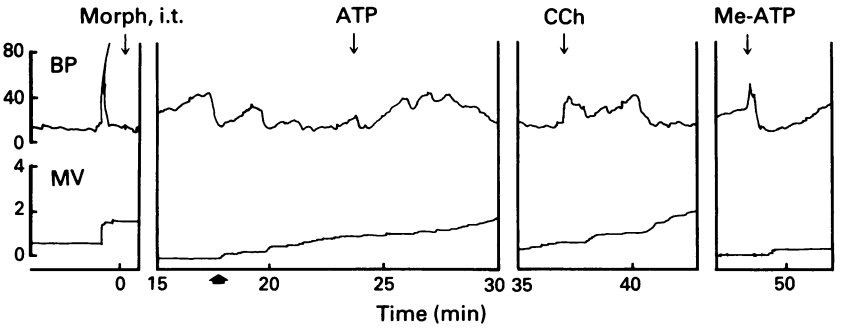

Figure 5 Effects of carbachol, ATP, and α,β-methylene ATP, administered intra-arterially (i.a.), in the presence of morphine on bladder pressure (BP; cmH_2O) and micturition volume (MV; ml) during cystometry performed in a normal rat. Morphine, administered intrathecally (Morph. i.t.; 10 μg), blocked micturition contractions and produced dribbling incontinence. Carbachol (CCh; 50 μg kg^{-1}, i.a.) ATP (5 mg kg^{-1}, i.a.), and α,β-methylene ATP (Me-ATP; 1 mg kg^{-1}, i.a.) produced small increases in bladder pressure, but did not induce micturition. ↑ indicates initiation of dribbling incontinence.

22 ± 5 cmH_2O and 24 ± 6 s, respectively. The percentage volume expelled was $23 \pm 8\%$ (Table 1). The micturition contractions were abolished in 3 animals out of 8, and the amplitude of the bladder pressure increase was reduced from 18.6 ± 2.4 to 7.6 ± 2.6 cmH_2O ($P < 0.05$) in the remaining 5 animals. Dribbling incontinence was observed in all animals (Figure 4).

Intrathecal administration of morphine (10 μg) blocked micturition contractions and produced dribbling incontinence, which persisted for more than 2 h. In the presence of morphine (10 μg, i.t.), carbachol (5–500 μg kg^{-1}, i.a.; $n = 6$), ATP (5 mg kg^{-1}, i.a.; $n = 6$), and α,β-methylene ATP (0.25–1 mg kg^{-1}, i.a.; $n = 6$) were all unable to produce bladder emptying, i.e. the percentage volume expelled was less than 10%, even if bladder contractions were noted after the injections (Figure 5).

Discussion

The present study showed that ATP and α,β-methylene ATP were able to induce bladder contraction and micturition in the normal, unanaesthetized rat. Even when the purinoceptors were desensitized by repeated exposure to α,β-methylene ATP, the micturition contraction, although decreased, was not abolished. This is in line with the results of several other investigations supporting the view that ATP is a NANC transmitter in the rat (Dahlén & Hedqvist, 1980; Brading & Williams, 1990; Luheshi & Zar, 1990; Parija *et al.*, 1991), but casts some doubt about its functional predominance under *in vivo* conditions (cf. *in vitro*; Carpenter, 1977). Also carbachol induced bladder contractions leading to bladder emptying. The volumes expelled by these contractions were about 75% of the bladder content after ATP or α,β-methylene ATP, and 90% after carbachol. These results suggest that not only cholinergic but also purinergic transmission is of importance for both pressure generation and emptying of the bladder *in vivo* in rats.

Based on their studies on field-stimulated rabbit and cat whole bladder preparations *in vitro*, Levin *et al.* (1986; 1990) and Chancellor *et al.* (1992) suggested that non-cholinergic transmission may initiate bladder contraction, but that the ability to empty the bladder in these two species is primarily a function of cholinergic transmission. This conclusion may be valid also for the rat, but factors not possible to study in the *in vitro* preparation come into play *in vivo*. Thus, Chancellor *et al.* (1992) found ATP unable to empty the rabbit isolated bladder with moderate outlet resistance, whereas bethanechol and electrical field stimulation could. *In vivo*, we found that exogenous ATP could empty the bladder. Downie *et al.* (1983) found that the ability of bethanechol to empty the bladder in cats was dependent on an intact micturition reflex. This may also be the case for the contractions induced by ATP, α,β-methylene ATP, and carbachol in the rat. When the micturition reflex was blocked by morphine administered i.t., none of these agents produced bladder emptying. Durant & Yaksh (1988) also found that neither bethanechol, nor α-adrenoceptor agonists, were able to empty the bladder when micturition was blocked by i.t. morphine. These findings suggest that an intact micturition reflex is necessary for efficient bladder emptying *in vivo*. It may be that both ATP, α,β-methylene ATP, and carbachol, when administered *in vivo*, by increasing tone of the detrusor muscle cells, elicit a micturition reflex leading to synchronized detrusor contraction and outlet relaxation with consequent bladder emptying. An increase in bladder pressure alone does not seem to be sufficient for bladder emptying *in vivo*. A direct stimulating effect of bethanechol on the central nervous system (locus caeruleus) has been suggested also to contribute to initiation of micturition (O'Donnell, 1990; Stephenson, 1991). This may also be the case for carbachol.

As shown previously in the rat (Malmgren *et al.*, 1987a), atropine did not abolish the micturition contractions. However, atropine changed their characteristics. They became more rapid and shortlasting than previously, and similar to the contractions induced by ATP. The bladder contraction induced by carbachol lasted longer than that induced by ATP or α,β-methylene ATP. In addition, repeated injections of α,β-methylene ATP, which antagonized the effects of ATP, reduced the amplitude of the micturition contractions, and disclosed a second, tonic component of the contraction. The second component, but not the first, was abolished by atropine. This is in agreement with findings in rat isolated detrusor strips (Maggi *et al.*, 1985; Parija *et al.*, 1991), which responded to single pulse stimulation with a biphasic contractile response consisting of an initial, fast, and an ensuing slow component. α,β-Methylene ATP abolished ATP-induced contractions, and inhibited the fast component by 38%, but did not alter the slow component, whereas atropine selectively abolished the slow component. Also in the cat, Theobald (1983) reported two distinct bladder responses to parasympathetic nerve stimulation. The initial response was a sharp, transient rise in intravesical pressure, and the second consisted of a tonic maintenance during stimulation. The photoaffinity analogue of ATP, $ANAPP_3$, which blocked ATP-induced contractions, partially blocked the first phase, and atropine, which had no effect on the first response, blocked the second phase of the contraction.

The observation that the contractile responses of guinea-pig and rat detrusor strips to field stimulation was blocked to a minor extent when atropine and α,β-methylene ATP were given separately, but was almost abolished by a combination of the two drugs (Brading, 1987; Brading & Mostwin, 1989; Brading & Williams, 1990), suggests that interaction between the two transmitters may be important for normal micturition. This view was supported by the present study, since in the normal, unanaesthetized rat, the combination of atropine and desensitization of bladder P_2-purinoceptors with α,β-methylene ATP induced retention and dribbling incontinence. However, neither atropine, nor α,β-methylene ATP, when given alone, produced dribbling incontinence in any animal tested.

Even if this and previous studies support a role for ATP in NANC neurotransmission, ATP may not be the sole NANC transmitter. Based on their findings in rabbit and guinea-pig bladders, Creed *et al.* (1991) suggested that either the desensitization with α,β-methylene ATP is not complete, or other NANC nerves contribute to the innervation. Luheshi & Zar (1990) found that the responses to electrical stimulation in the rat bladder were reduced following α,β-methylene ATP desensitization, but that a sizable proportion of the response persisted in the presence of atropine and indomethacin. They concluded therefore that ATP is unlikely to be the sole non-cholinergic motor transmitter in the rat detrusor. Choo & Mitchelson (1980), using ATP as the desensitizing nucleotide, had previously arrived at a similar conclusion.

The present study demonstrated that in the presence of atropine, α,β-methylene ATP produced dribbling incontinence, even if some animals still showed small bladder contractions, which did not lead to bladder emptying. On the other hand, atropine added 5–10 min after repeated injections of α,β-methylene ATP did not produce dribbling incontinence. When α,β-methylene ATP was given again after atropine to these animals, dribbling incontinence was induced. Considering the short duration of action of α,β-methylene ATP, and the fact that the maximum action of atropine was seen after 5–10 min, the possibility cannot be excluded that the contractions remaining after desensitization with α,β-methylene ATP and addition of atropine were mediated via purinoceptors. However, even if transmitters other than acetylcholine and ATP may be released from bladder nerves, their functional relevance for bladder emptying may be questioned, at least in the rat. Obviously, when these two main transmitters were blocked, no effective emptying contraction could be elicited, resulting in dribbling incontinence in all animals tested.

In conclusion, the results of the present study suggest that drug-induced bladder emptying in the normal, unanaesthetized rat requires an intact micturition reflex, and they support the view that the two physiologically important transmitters involved in micturition are acetylcholine and ATP.

This study was supported by the Swedish Medical Research Council (grants no. 6837 & 10399), and the Medical Faculty, University of Lund.

References

AMBACHE, N. & ZAR, M.A. (1970). Non-cholinergic transmission by post-ganglionic motor neurones in the mammalian bladder. *J. Physiol.*, **210**, 761–783.

BHAT, M.B., MISHRA, S.K. & RAVIPRAKASH, V. (1989). Differential susceptibility of cholinergic and noncholinergic neurogenic responses to calcium channel blockers and low Ca^{2+} medium in rat urinary bladder. *Br. J. Pharmacol.*, **96**, 837–842.

BRADING, A.F. (1987). The physiology of bladder smooth muscle. In *The Physiology of the Lower Urinary Tract*. ed. Torrens, M. & Morrison, J. pp. 161–191. Berlin: Springer-Verlag.

BRADING, A.F. & MOSTWIN, J.L. (1989). Electrical and mechanical responses of guinea-pig bladder muscle to nerve stimulation. *Br. J. Pharmacol.*, **98**, 1083–1090.

BRADING, A.F. & WILLIAMS, J.H. (1990). Contractile responses of smooth muscle strips from rat and guinea-pig urinary bladder to transmural stimulation: effects of atropine and α,β-methylene ATP. *Br. J. Pharmacol.*, **99**, 493–498.

BURNSTOCK, G., COCKS, T., CROWE, R. & KASAKOV, L. (1978a). Purinergic innervation of the guinea-pig urinary bladder. *Br. J. Pharmacol.*, **63**, 125–138.

BURNSTOCK, G., COCKS, T., KASAKOV, L. & WONG, A. (1978b). Direct evidence for ATP release from non-adrenergic, non-cholinergic ('purinergic') nerves in the guinea-pig taenia coli and bladder. *Eur. J. Pharmacol.*, **49**, 145–149.

BURNSTOCK, G., DUMSDAY, B. & SMYTHE, A. (1972). Atropine-resistant excitation of the urinary bladder: the possibility of transmission via nerves releasing a purine nucleotide. *Br. J. Pharmacol.*, **44**, 451–461.

CARPENTER, F.G. (1977). Atropine resistance and muscarinic receptors in the rat urinary bladder. *Br. J. Pharmacol.*, **59**, 43–49.

CHANCELLOR, M.B., KAPLAN, S.A. & BLAIVAS, J.G. (1992). The cholinergic and purinergic components of detrusor contractility in a whole rabbit bladder model. *J. Urol.*, **148**, 906–909.

CHOO, L.K. & MITCHELSON, F. (1980). The effect of indomethacin and adenosine 5'-triphosphate on the excitatory innervation of the rat urinary bladder. *Can. J. Physiol. Pharmacol.*, **58**, 1042–1048.

CREED, K.E., ITO, Y. & KATSUYAMA, H. (1991). Neurotransmission in the urinary bladder of rabbits and guinea pigs. *Am. J. Physiol.*, **261**, C271–C277.

DAHLÉN, S.E. & HEDQVIST, P. (1980). ATP, β,γ-methylene ATP and adenosine inhibit non-cholinergic, non-adrenergic transmission in the rat urinary bladder. *Acta Physiol. Scand.*, **109**, 137–142.

DEAN, D.M. & DOWNIE, J.W. (1978). Contribution of adrenergic and 'purinergic' neurotransmission to contraction in the rabbit detrusor. *J. Pharmacol. Exp. Ther.*, **207**, 431–445.

DOWNIE, J.W., MOOCHALA, S.M. & BIALIK, G.J. (1983). The role of reflexes in modifying the response to bethanechol chloride: a basis for selectivity of action on the bladder. *Neurourol. Urodyn.*, **2**, 301–309.

DURANT, P.A.C. & YAKSH, T. (1988). Drug effects on urinary bladder tone during spinal morphine-induced inhibition of the micturition reflex in unanaesthetized rats. *Anesthesiol.*, **68**, 325–334.

FUJII, K. (1988). Evidence for adenosine triphosphate as an excitatory transmitter in guinea-pig, rabbit and pig urinary bladder. *J. Physiol.*, **404**, 39–52.

HOYLE, C.H.V. & BURNSTOCK, G. (1985). Atropine-resistant excitatory junction potential in rabbit bladder are blocked by α,β-methylene ATP. *Eur. J. Pharmacol.*, **114**, 239–240.

HOYLE, C.H.V., CHAPPLE, C. & BURNSTOCK, G. (1989). Isolated human bladder: evidence for an adenosine dinucleotide acting on P_{2x}-purinoceptors and for purinergic transmission. *Eur. J. Pharmacol.*, **174**, 115–118.

IGAWA, Y., ANDERSSON, K.-E., POST, C., UVELIUS, B. & MATTIASSON, A. (1992a). A rat model for investigation of spinal mechanisms in detrusor instability associated with infravesical outflow obstruction. *J. Urol.*, **147**, 349A (abstract no. 546).

IGAWA, Y., PERSSON, K., ANDERSSON, K.-E., UVELIUS, B. & MATTIASSON, A. (1992b). Facilitatory effect of vasoactive intestinal polypeptide on spinal and peripheral micturition reflex pathways in conscious rats with and without detrusor instability. *J. Urol.*, (in press).

KASAKOV, L. & BURNSTOCK, G. (1983). The use of the slowly degradable analogue, α,β-methylene ATP to produce desensitisation of the P_2-purinoceptor: effect on non-adrenergic, non-cholinergic responses of the guinea-pig urinary bladder. *Eur. J. Pharmacol.*, **86**, 291–294.

KASAKOV, L. & VLASKOVA, M.V. (1985). Profile of prostaglandins generated in the detrusor muscle of rat urinary bladder: effects of adenosine triphosphate and adenosine. *Eur. J. Pharmacol.*, **113**, 431–436.

LEVIN, R.M., LONGHURST, P.A., KATO, K., MCGUIRE, E.J., EL-BADAWI, A. & WEIN, A.J. (1990). Comparative physiology and pharmacology of the cat and rabbit urinary bladder. *J. Urol.*, **143**, 848–852.

LEVIN, R.M., RUGGIERI, M.R. & WEIN, A.J. (1986) Functional effects of purinergic innervation of the rabbit urinary bladder. *J. Pharmacol. Exp. Ther.*, **236**, 452–460.

LUHESHI, G. & ZAR, A. (1990). Purinoceptor desensitization impairs but does not abolish the non-cholinergic motor transmission in rat isolated urinary bladder. *Eur. J. Pharmacol.*, **185**, 203–208.

MAGGI, C.A. (1991). Omega conotoxin and prejunctional modulation of the biphasic response of the rat isolated urinary bladder to single pulse electrical field stimulation. *J. Autonom. Pharmacol.*, **11**, 295–304.

MAGGI, C.A., SANTICIOLI, P. & MELI, A. (1985). Pharmacological evidence for the existence of two components in the twitch response to field stimulation of detrusor strips from the rat urinary bladder. *J. Autonom. Pharmacol.*, **5**, 221–230.

MALMGREN, A., SJÖGREN, C., ANDERSSON, K.-E. & ANDERSSON, P.O. (1987a). Effects of atropine on bladder capacity and instability in rats with bladder hypertrophy. *Neurourol. Urodyn.*, **6**, 331–338.

MALMGREN, A., SJÖGREN, C., UVELIUS, B., MATTIASSON, A., ANDERSSON, K.-E. & ANDERSSON, P.O. (1987b). Cystometrical evaluation of bladder instability in rats with infravesical outflow obstruction. *J. Urol.*, **137**, 1291–1294.

O'DONNELL, P.D. (1990). Central actions of bethanechol on the urinary bladder in dogs. *J. Urol.*, **143**, 634–637.

PARIJA, S.C., RAVIPRAKASH, V. & MISHRA, S.K. (1991). Adenosine- and α,β-methylene ATP-induced differential inhibition of cholinergic and non-cholinergic neurogenic responses in rat urinary bladder. *Br. J. Pharmacol.*, **102**, 396–400.

SIBLEY, G.N.A. (1984). A comparison of spontaneous and nerve-mediated activity in bladder muscle from man, pig and rabbit. *J. Physiol.*, **354**, 431–443.

STEPHENSON, J.D. (1991). Pharmacology of the central control of micturition. *Funct. Neurol.*, **6**, 211–217.

THEOBALD JR., R.T. (1983). The effect of arylazido aminopropionyl ATP on atropine resistant contractions of the cat urinary bladder. *Life Sci.*, **32**, 2479–2484.

(Received November 20, 1992
Revised January 4, 1993
Accepted February 8, 1993)

Br. J. Pharmacol. (1993), **109**, 480–485 © Macmillan Press Ltd, 1993

Nitric oxide and arachidonic acid modulation of calcium currents in postganglionic neurones of avian cultured ciliary ganglia

G. Khurana & [1]M.R. Bennett

The Neurobiology Laboratory, Physiology Department, University of Sydney, N.S.W. 2006, Australia

1 A study has been made of the modulation of high-voltage activated transient and sustained calcium currents in cultured neurones of avian ciliary ganglia by nitric oxide (NO) and arachidonic acid.

2 Sodium nitroprusside (100 μM) reduced the transient calcium current (I_{Ca}) on average by 31% and the sustained I_{Ca} by 32% during a test depolarization to +20 mV from a holding potential of −100 mV. This reduction was maintained for at least 30 min following a single application of sodium nitroprusside.

3 L-Arginine (270 μM) reduced the transient I_{Ca} on average by 28% and the sustained I_{Ca} by 22% and these effects were prevented by the presence of the NO-synthase competitive blocker N^G-nitro-L-arginine methylester (L-NAME; 100 μM) in the bathing solution.

4 Arachidonic acid (50 μM) reduced the transient I_{Ca} on average by 28% and the sustained I_{Ca} by 33%. When added together, arachidonic acid (50 μM) and L-arginine (270 μM) produced the same effects as arachidonic acid alone.

5 Blocking the conversion of arachidonic acid to prostaglandins by addition of indomethacin (20 μM) to the bathing solution did not prevent the depression of either the transient or the sustained calcium current during application of arachidonic acid (50 μM). The effects of arachidonic acid were also not occluded by L-NAME (100 μM) when present in the bathing solution.

6 Inhibiting the biosynthesis of leukotrienes by applying L-663,536 (MK-886; 3 μM) to the bathing solution prevented the depression of both components of I_{Ca} during application of arachidonic acid (50 μM).

7 These results indicate that endogenous NO and arachidonic acid pathways are present in parasympathetic ciliary neurones, and that both act to depress high-voltage, gated, calcium channel activity.

Keywords: Nitric oxide; arachidonic acid; calcium current; postganglionic neurones; avian ciliary ganglia

Introduction

Nitric oxide synthase (NOS; Bredt & Snyder, 1992) is present in the cell bodies of avian ciliary ganglia and NO enhances transmitter secretion in the ganglion (Scott *et al.*, 1992). One possible mechanism by which NO may modulate transmitter release is through an action on calcium channels. NO can elevate levels of guanosine 3′:5′-cyclic monophosphate (cyclic GMP) in smooth muscle cells to produce a hyperpolarization that closes voltage-sensitive calcium channels (Clapp & Gurney, 1991). NO can also act through cyclic GMP to prevent the noradrenaline-induced increase in cytosolic calcium levels via an inhibition of both calcium influx and intracellular calcium release (Tare *et al.*, 1990). It should also be noted that elevated cyclic GMP levels are known to depress the calcium current through high-voltage-activated calcium channels in acutely isolated hippocampal neurones (Doerner & Alger, 1988).

Ciliary neurones possess high-voltage-activated calcium channels that mediate a rapidly inactivating calcium current and a slowly inactivating calcium current (Bennett *et al.*, 1992), which may be referred to as 'transient' and 'sustained' currents, respectively (Schroeder *et al.*, 1990; Sher & Clementi, 1991). Both transient and sustained calcium currents are reduced by the dihydropyridine antagonist nifedipine as well as by ω-conotoxin (Bennett *et al.*, 1992), so that these currents cannot be assigned to distinct types of high-threshold calcium channels (Fox *et al.*, 1987a,b; for reviews see Scott *et al.*, 1991; Swandulla *et al.*, 1991). In the present work both transient and sustained currents have been recorded from nine to twelve day old chick embryo ciliary neurones and their relative sensitivity to NO determined.

Arachidonic acid has been shown to inhibit calcium current in *Aplysia* sensory neurones (Piomelli *et al.*, 1987) and also in neurones of the chick sympathetic ganglion (Bug *et al.*, 1989) and the guinea-pig hippocampus (Keyser & Alger, 1990). Furthermore, it has recently been demonstrated that arachidonic acid can modulate NO production as the cyclooxygenase pathway of arachidonic acid metabolism gives rise to prostaglandins which can activate the L-arginine:NO pathway (Gray *et al.*, 1991). It was therefore of interest to determine if arachidonic acid or one of its prostaglandin metabolites could modulate the transient or sustained calcium currents in parasympathetic neurones of the chick ciliary ganglion and, if so, whether this was due to an action on the L-arginine:NO pathway.

Methods

Ciliary ganglion cell preparation and recording

Neurones from ciliary ganglia dissected from 9–12 day old white leghorn chick embryos were cultured and whole-cell patch-clamped according to the methods described in Bennett *et al.* (1992). Cells were held at a potential of −100 mV for 4 s prior to depolarization to the test potential. Different ciliary neurones showed the peak currents occurring between 0 and +20 mV, although for any single neurone the peak current in control stimulations occurred consistently at the same voltage. Drug effects were consistent between neurones.

[1] Author for correspondence.

Solutions

Ciliary neurones were placed in a bathing solution at 21°C which consisted of (in mM): $CaCl_2$ 10, TEACl 5, NaCl 125, glucose 10, HEPES 10, and tetrodotoxin (TTX) 300 nM, with the pH adjusted to 7.3 with NaOH. Pipettes of boro-silicate capillary tubing (resistance 4 to 10 MΩ; Hamill *et al.*, 1981) were filled with a solution which consisted of (in mM): CsCl 100, EGTA 10, $MgCl_2$ 5, HEPES 40, ATP 2 and GTP 0.35, with the pH adjusted to 7.3 with CsOH.

Drugs

Sodium nitroprusside, L-arginine, N^G-nitro-L-arginine methylester (L-NAME), and indomethacin (all from Sigma Chemical Co.) were dissolved in recording medium, while arachidonic acid, oleic acid (Sigma Chemical Co.) and L-663,536 (MK-886; 3-[1(4-chloro-benzyl)-3-*t*-butyl-thio-5-isopropylindol-2-yl]-2, 2-dimethylpropanoic acid, the kind gift of Dr A.W. Ford-Hutchinson, Merck Frosst Canada Inc.) were dissolved in dimethylsulphoxide (DMSO; 0.05% v/v concentration). Sodium nitroprusside, L-arginine and arachidonic acid were applied by pressure ejection (2 to 7 kPA) from puffer micropipettes with tip diameters of approximately 10 μm. Puffer pipettes were positioned between 20–50 μm from the cell bodies of ciliary neurones during a puff application and then removed.

Statistics

Data are expressed as mean ± standard error of the mean (s.e.mean) and n gives the number of experiments. The significance of the difference between the n pairs of observations made before and after application of a drug was calculated by Student's paired t test. P values of 0.05 or less were considered to represent significant differences.

Results

The puffing of bathing solution onto ciliary neurones produced a small but significant decrease in the transient calcium current (I_{Ca}) of 2.2 ± 2% (mean ± s.e.mean; $n = 11$ neurones; $P > 0.25$ using Student's paired t test) for test depolarization

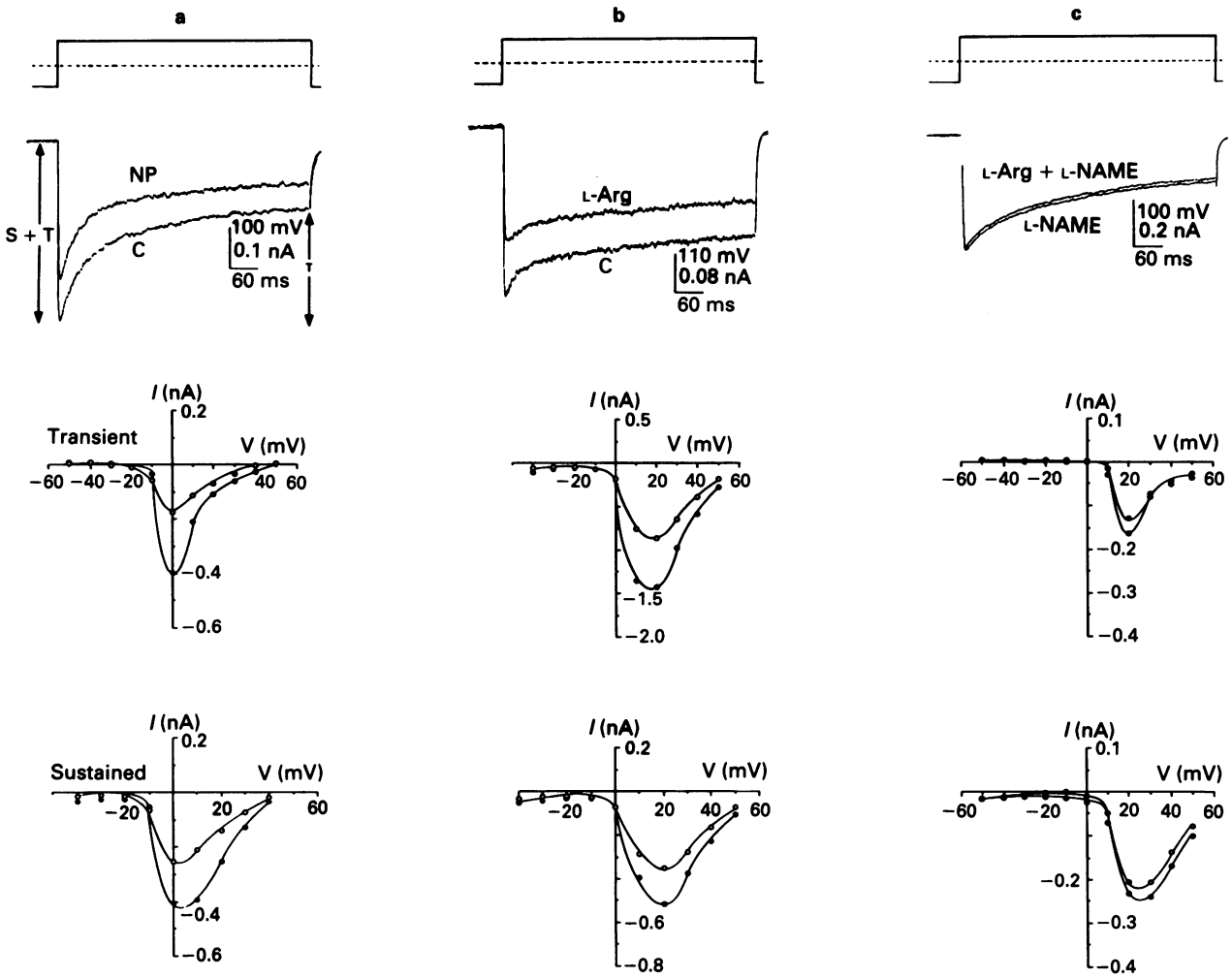

Figure 1 The action of sodium nitroprusside and L-arginine on whole-cell calcium current. The upper panels give the effects of the drugs on the currents generated at + 20 mV from a holding potential of − 100 mV; the broken line indicates the level of − 50 mV. The middle and lower panels give the effects of the drugs on the transient and sustained currents respectively both before (●) and after (○) their puffer application; the voltages are the test potentials. (a) Effect of sodium nitroprusside (100 μM) on whole-cell transient and sustained calcium currents; the upper panel shows the currents evoked both before (C) and after (NP) exposure to sodium nitroprusside; T refers to the transient component of the calcium current and S + T to the sustained plus transient components of the current. (b) Effect of L-arginine (270 μM) on whole-cell transient and sustained calcium currents; in the upper panel are shown the currents evoked both before (C) and after (L-Arg) exposure to L-arginine. (c) Effect of L-arginine (L-Arg; 270 μM) on whole-cell calcium current in the presence of L-N^G-nitroarginine methylester (L-NAME; 100 μM); the upper panel shows the currents evoked in the presence of L-NAME alone (L-NAME) and after exposure to a puff of L-arginine (L-Arg + L-NAME) given 10 s before the observation was made in the presence of L-NAME.

to + 20 mV from a holding potential, V_h, of − 100 mV. A small but significant decrease in the sustained I_{Ca} of 4.9 ± 1% ($n = 11$; $P < 0.002$) occurred under the same conditions.

Nitric oxide

Sodium nitroprusside (100 μM) puffed onto ciliary neurones before a depolarization to + 20 mV from a V_h of − 100 mV, significantly reduced both the transient and sustained components of I_{Ca} (Figure 1a). The transient I_{Ca} was reduced from − 233 ± 37 pA to − 169 ± 33 pA, that is a reduction of 31 ± 8% ($n = 9$; $P < 0.01$), and the sustained I_{Ca} was reduced from − 267 ± 57 pA to − 147 ± 15 pA, that is a reduction of 32 ± 12% ($n = 9$; $P < 0.05$). This depression in I_{Ca} was maintained for at least 30 min following a single puff of sodium nitroprusside. Both sustained and transient I_{Ca} were clearly reduced over the test potential range from − 10 mV to + 30 mV. These results suggest the presence of a nitric oxide-sensitive cyclic GMP system in ciliary neurones that controls the activity of calcium channels.

In order to test whether a nitric oxide synthase system using L-arginine as substrate is likely to be functioning in the ciliary ganglion, the effect of L-arginine puffed onto ganglion cells 10 s before a test depolarization to + 20 mV from a V_h of − 100 mV, was determined (Figure 1b). L-Arginine (270 μM) significantly decreased the transient I_{Ca} from − 355 ± 62 pA to − 250 ± 44 pA, that is a reduction of 28 ± 5% ($n = 16$; $P < 0.01$). L-Arginine also caused a significant reduction in the sustained current, decreasing it by 22 ± 4% ($n = 16$; $P < 0.001$) from − 315 ± 27 pA to − 241 ± 23 pA. The reduction in both components of I_{Ca} occurred over the test potential range from 0 mV to + 50 mV. These effects of

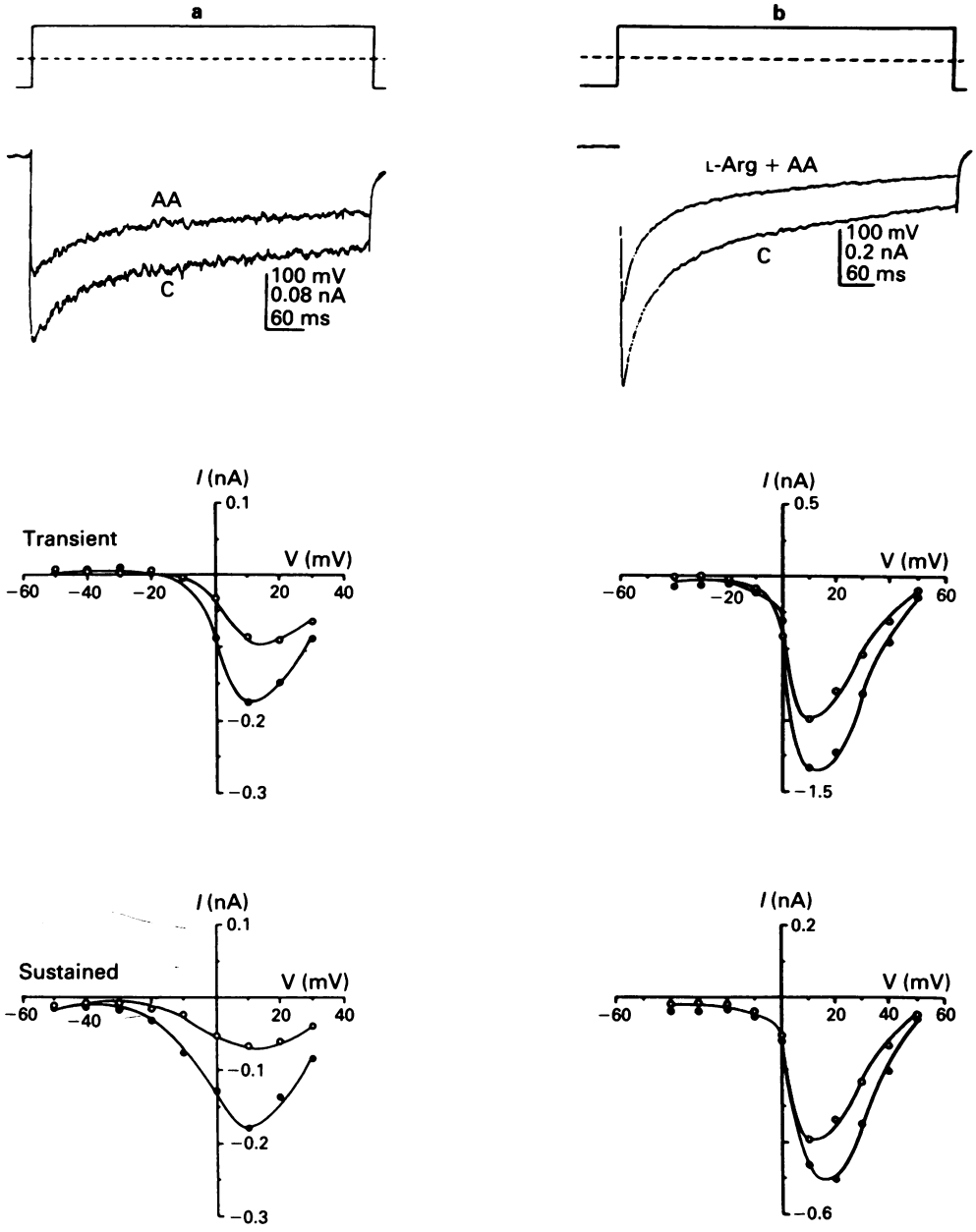

Figure 2 The action of arachidonic acid alone and arachidonic acid and L-arginine together on whole-cell calcium current. The upper panels give the effects of the drugs on the currents generated at + 10 mV from a holding potential of − 100 mV; the broken line indicates the level of − 50 mV. The middle and lower panels give the effects of the drugs on the transient and sustained currents respectively both before (●) and after (○) their puffer application; the voltages are the test potentials. (a) Effect of arachidonic (50 μM) on whole-cell transient and sustained calcium currents; the upper panel shows the currents evoked both before (C) and after (AA) exposure to arachidonic acid. (b) Effect of L-arginine (270 μM) and arachidonic acid (50 μM) on whole-cell transient and sustained calcium currents; in the upper panel are shown the currents evoked both before (C) and after (L-Arg + AA) exposure to the combined puff of L-arginine and arachidonic acid.

L-arginine were occluded by the nitric oxide synthase inhibitor, N^G-nitro-L-arginine methylester (L-NAME; Figure 1c). After bathing the ganglion cells for at least 5 min in L-NAME (100 μM), a puff of L-arginine (270 μM) produced only a marginal decrease in the transient current, shifting it from -352 ± 57 pA to -335 ± 51 pA ($4 \pm 2\%$; $n = 6$; $P < 0.05$) during depolarization to +20 mV from a V_h of −100 mV. Under the same conditions, the sustained I_{Ca} was also only reduced by L-arginine to a small extent, namely from -235 ± 32 pA to -219 ± 28 pA ($7 \pm 2\%$; $n = 6$; $P < 0.05$). L-NAME clearly prevented the large depression in I_{Ca} due to L-arginine over the entire range of test potentials from −20 mV to +50 mV. These results indicate that a nitric oxide synthase system using L-arginine as a substrate can control both the transient and sustained components of high-voltage activated calcium current in parasympathetic ciliary neurones.

Arachidonic acid

Arachidonic acid also has an effect in reducing the whole-cell I_{Ca} in ciliary neurones (Figure 2a). During depolarization to +10 mV from a V_h of −100 mV, a puff of arachidonic acid (50 μM) reduced the transient I_{Ca} from -212 ± 40 pA to -153 ± 31 pA ($28 \pm 5\%$; $n = 13$; $P < 0.002$). Under the same conditions, arachidonic acid (50 μM) decreased the sustained I_{Ca} from -218 ± 43 pA to -162 ± 37 pA ($33 \pm 4\%$; $n = 13$; $P < 0.001$). The reductions in I_{Ca} occurred over the test potential range from −20 mV to +30 mV.

To exclude possible non-specific membrane effects of arachidonic acid, another fatty acid, oleic acid, was used as a control. During depolarization to +10 mV from a V_h of −100 mV, a puff of oleic acid (50 μM) reduced the transient I_{Ca} from -263 ± 11 pA to -255 ± 10 pA ($4 \pm 1\%$; $n = 6$; $P < 0.05$) and the sustained from -170 ± 7 pA to -165 ± 8 pA ($4 \pm 1\%$; $n = 6$; $P < 0.1$). These reductions in I_{Ca} occurred over the test potential range from −30 mV to +30 mV.

Possible interaction between NO and arachidonic acid

It has recently been shown that the cyclo-oxygenase-mediated prostaglandin metabolites of arachidonic acid can interact with the L-arginine:NO pathway via the activation of nitric oxide synthase (Gray *et al.*, 1991). It was therefore of interest to see whether or not the effects of arachidonic acid and L-arginine were additive. It was found that puffing arachidonic acid (50 μM) together with L-arginine (270 μM) onto ciliary neurones had the same effect on the sustained current as puffing arachidonic acid alone (Figure 2b): the sustained I_{Ca} was reduced from -346 ± 34 pA to -251 ± 32 pA ($29 \pm 3\%$; $n = 15$; $P < 0.001$); this is compared with a reduction of $33 \pm 4\%$ caused by a puff of arachidonic acid on its own. The transient I_{Ca} was reduced from -369 ± 44 pA to -273 ± 29 pA ($20 \pm 4\%$, $n = 15$; $P < 0.001$). These effects occurred over a test potential range from 0 mV to +50 mV, and suggest that arachidonic acid, or one of its metabolites, and L-arginine may be acting through a final common pathway to modulate I_{Ca}. To investigate this possibility further, indomethacin (20 μM), a specific inhibitor of cyclo-oxygenase, was introduced into the bathing solution prior to the puffing of arachidonic acid. Under these conditions, during depolarization to +20 mV from a V_h of −100 mV, a puff of arachidonic acid (50 μM) still caused a significant reduction in both the transient and sustained components of ciliary neurone I_{Ca} (Figure 3a): the transient I_{Ca} was reduced from -367 ± 88 pA to -253 ± 50 pA, a reduction of $28 \pm 2\%$ ($n = 7$; $P < 0.01$); the sustained was reduced from -414 ± 96 pA to -277 ± 49 pA, a reduction of $31 \pm 3\%$ ($n = 7$; $P < 0.02$). Similarly, the presence in the bathing solution of the specific nitric oxide synthase inhibitor, L-NAME (100 μM), also had no effect upon the depression of I_{Ca} caused by arachidonic acid (Figure 3b). Under these conditions, a puff of arachidonic acid reduced the transient I_{Ca} by $32 \pm 4\%$, shifting it from -237 ± 36 pA to -162 ± 25 pA ($n = 5$, $P < 0.001$), and reduced the sustained by $35 \pm 3\%$, decreasing it from -428 ± 55 pA to -275 ± 29 pA ($n = 5$; $P < 0.001$), effects which occurred during depolarizations to +10 mV from a V_h of −100 mV, and over the range of test potentials from 0 mV to +40 mV. Although the results indicate that in ciliary neurones arachidonic acid or one of its cyclo-oxygenase metabolites does not regulate nitric oxide synthase, the question as to whether the modulatory effects of arachidonic acid on calcium channels might be exerted through one of its leukotriene metabolites remained to be addressed. Using L-663,536 (MK-886), an inhibitor of leukotriene biosynthesis, the effects of arachidonic acid were then investigated (Figure 3c). With L-663,536 (3 μM) present in the bathing solution, a puff of arachidonic acid (50 μM) produced no significant change in the transient current, shifting it from -290 ± 13 pA to -291 ± 14 pA ($n = 6$; $P > 0.25$) during depolarization to +20 mV from a V_h of −100 mV. Under the same conditions, the sustained I_{Ca} was also only reduced by arachidonic acid to a small extent, namely from -323 ± 25 pA to -302 ± 24 pA ($6 \pm 2\%$; $n = 6$; $P < 0.05$). These results suggest that in ciliary neurones, the depression of whole-cell calcium current caused by arachidonic acid is in fact mediated by one of its leukotriene metabolites.

Discussion

The NO synthase present in avian ciliary neurones (Scott *et al.*, 1992) has been shown to be enzymatically active in the present work, converting L-arginine to NO (Garthwaite, 1991; for a review of the pathway see Moncada *et al.*, 1991) which then acts to modulate calcium currents. This enzyme has been shown to be active in all parts of the nervous system in which it has been found (Bredt & Snyder, 1991), whether by using antibodies to the synthase (Bredt *et al.*, 1990; Young *et al.*, 1992), or through localization of the mRNA for the enzyme (Bredt *et al.*, 1991), or via localization of NADPH diaphorase which is now known to be nitric oxide synthase (Dawson *et al.*, 1991; Hope *et al.*, 1991). Thus, the enteric inhibitory neurones to the gastrointestinal tract (Bennett *et al.*, 1963), which release neither noradrenaline nor acetylcholine (Bennett *et al.*, 1966), are now known to contain NO synthase and to release NO (see for example Li & Rand, 1990; Bult *et al.*, 1990; for a review see Rand, 1992). Likewise, the granule cells of the hippocampus are known to contain NO synthase (Bredt *et al.*, 1990) and here there is evidence that transmitter secretion from the perforant pathway is enhanced by the release of NO from the granule cells after activation of NMDA receptors on these cells (Errington *et al.*, 1991).

The action of NO on ciliary neurone calcium currents was to depress these uniformly, as it depresses the high-voltage activated calcium currents of the hippocampal neurones (Doerner & Alger, 1988). If similar effects occurred on presynaptic calcium currents, then a depression in transmitter secretion would be expected. However, as sodium nitroprusside is known to potentiate transmitter secretion in parasympathetic ganglia (Scott *et al.*, 1992) as well as in rat sympathetic ganglia (Briggs, 1992), this apparent dichotomy may be due to differences in the properties of postsynaptic calcium channels as compared with the presynaptic channels that mediate transmitter release. These calcium channels, which display transient calcium currents with a voltage-dependent inactivation different from that observed in the present work, have been identified at the preganglionic terminals of avian ciliary ganglia (Brosius *et al.*, 1990; Stanley & Goping, 1991; Stanley, 1992). It will therefore be necessary to examine the effects of NO on these presynaptic channels in order to determine whether NO is likely to enhance transmitter release by acting differentially on calcium channels present in nerve terminals.

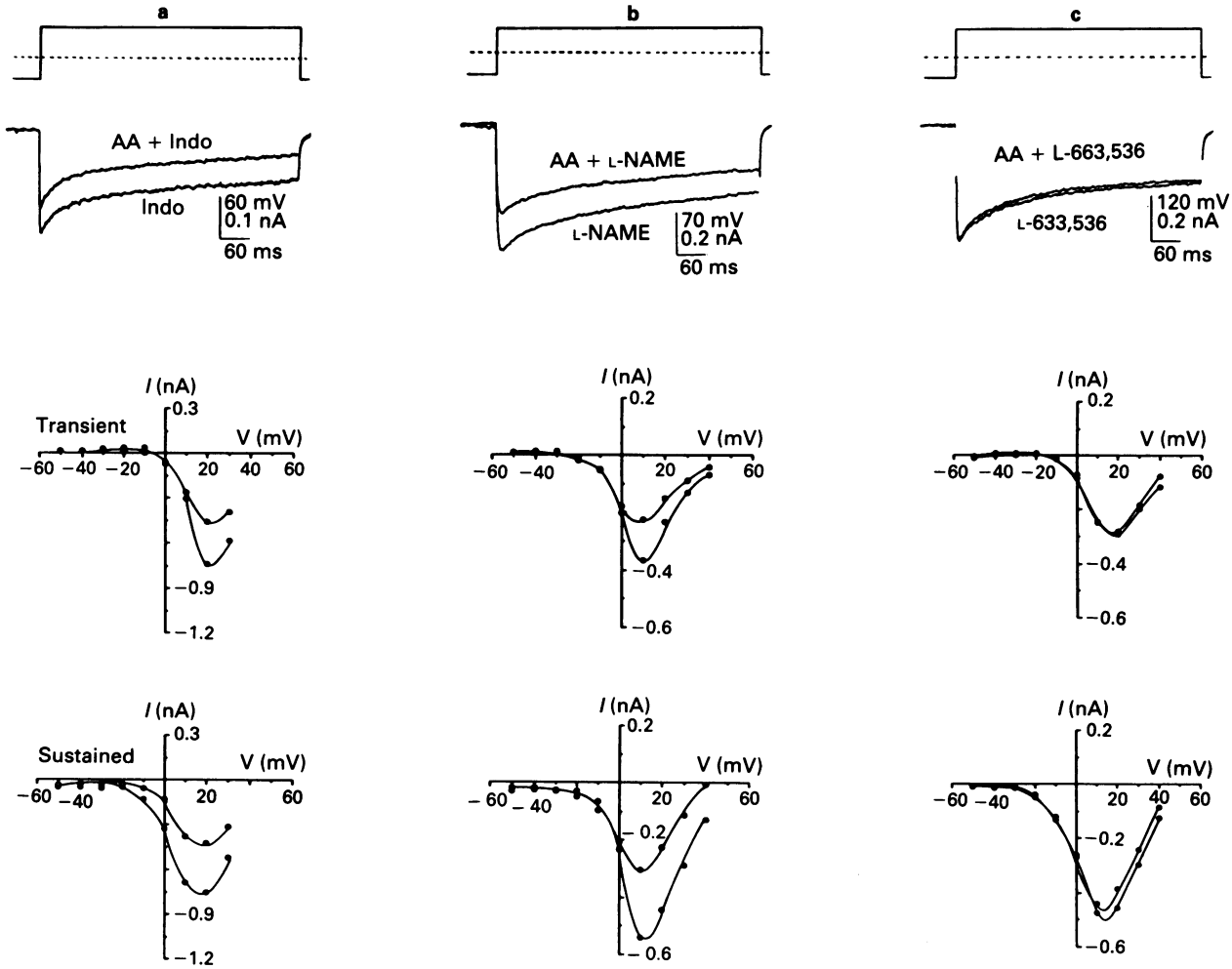

Figure 3 The effects of arachidonic acid on whole-cell calcium current in the presence of indomethacin, L-N^G-nitroarginine methylester (L-NAME) and L-663,536. The upper panels in (a) and (c) give the effects on the currents generated at + 20 mV from a holding potential (V_h) of − 100 mV; in (b) is shown the effect on the currents generated at + 10 mV from a V_h of − 100 mV; the broken line in each case indicates the level of − 50 mV. The middle and lower panels give the effects of arachidonic acid on the transient and sustained currents respectively both before (●) and after (○) its puffer application; the voltages are the test potentials. (a) Effect of arachidonic acid (50 μM) on whole-cell transient and sustained calcium currents in the presence of indomethacin (20 μM) in the bathing solution; the upper panel shows the currents evoked in the presence of indomethacin alone (Indo) and after exposure to a puff of arachidonic acid (AA + Indo) given 10 s before the observation was made in the presence of indomethacin. (b) Effect of arachidonic acid (50 μM) on transient and sustained calcium currents in the presence of L-NAME (100 μM) in the bathing solution; the upper panel shows the currents evoked in the presence of L-NAME alone (L-NAME) and after exposure to a puff of arachidonic acid (AA + L-NAME) given 10 s before the observation was made in the presence of L-NAME. (c) Effect of arachidonic acid (50 μM) on transient and sustained calcium currents in the presence of L-663,536 (3 μM) in the bathing solution; the upper panel shows the currents evoked in the presence of L-663,536 alone (L-663,536) and after exposure to a puff of arachidonic acid (AA + L-663,536) given 10 s before the observation was made in the presence of L-663,536.

The effect of arachidonic acid on transmission in the ciliary ganglion has not been determined. Arachidonic acid increases the efficacy of transmission between the perforant pathway and granule cells in the hippocampus (Williams *et al.*, 1988) and this effect can be blocked by the phospholipase A_2 and lipoxygenase inhibitor, nordihydroguaiaretic acid (Lynch *et al.*, 1989). This suggests that endogenous arachidonic acid or one of its lipoxygenase metabolites is responsible for the increased efficacy of transmission, perhaps by facilitating the NO synthase system (O'Dell *et al.*, 1991). However arachidonic acid or one of its lipoxygenase metabolites depresses the high-voltage activated L-type calcium currents in hippocampal neurones (Keyser & Alger, 1990). In the present study, arachidonic acid also reduced the high-voltage activated calcium current, and by use of L-663,536 (MK-886; see Gillard *et al.*, 1989) this effect was shown to be mediated by its leukotriene metabolites. A depression of calcium current is not to be expected if the action of arachidonic acid is to enhance transmitter release by increasing the efficacy of presynaptic calcium channels. Again, it would seem that a direct analysis of the effects of arachidonic acid on presynaptic calcium channels is required.

Arachidonic acid is converted to prostaglandins by cyclooxygenase (for a review see Piomelli & Greengard, 1990), and these are known to potentiate or even initiate the events leading to activation of the L-arginine:NO pathway (Gray *et al.*, 1991). In the present study, the inhibition of calcium current caused by arachidonic acid was found not to be additive with that caused by nitric oxide, and this suggested that both may work through a final common pathway in ciliary neurones. However, as neither indomethacin nor L-NAME affected the depression of whole-cell calcium current caused by arachidonic acid, it seems likely that in these parasympathetic neurones, arachidonic acid and nitric oxide act via independent pathways to modulate high-voltage activated calcium channels.

References

BENNETT, M.R., BURNSTOCK, G. & HOLMAN, M.E. (1963). The effect of potassium and chloride ions on the inhibitory potential recorded in the guinea-pig taenia coli. *J. Physiol.*, **169**, 33P.

BENNETT, M.R., BURNSTOCK, G. & HOLMAN, M.E. (1966). Transmission from intramural inhibitory nerves to the smooth muscle of the guinea-pig taenia coli. *J. Physiol.*, **182**, 541–558.

BENNETT, M.R., KERR, R. & KHURANA, G. (1992). Adenosine modulation of calcium currents in postganglionic neurones of cultured avian ciliary ganglia. *Br. J. Pharmacol.*, **106**, 25–32.

BREDT, D.S., HWANG, P.M., GLATT, C.E., LOWENSTEIN, C., REED, R.R. & SNYDER, S.H. (1991). Cloned and expressed nitric oxide synthase structurally resembles cytochrome P-450 reductase. *Nature*, **351**, 714–718.

BREDT, D.S., HWANG, P.M. & SNYDER, S.H. (1990). Localization of nitric oxide synthase indicating a neural role for nitric oxide. *Nature*, **347**, 768–770.

BREDT, D.S. & SNYDER, S.H. (1992). Nitric oxide, a novel neuronal messenger. *Neuron*, **8**, 3–11.

BRIGGS, C.A. (1992). Potentiation of nicotinic transmission in the rat superior cervical sympathetic ganglion: effects of cyclic GMP and nitric oxide generators. *Brain Res.*, **573**, 139–146.

BROSIUS, D.C., HACKETT, J.T. & TUTTLE, J.B. (1990). Pre-synaptic calcium currents evoking quantal transmission from avian ciliary ganglion neurons. *Synapse*, **5**, 313–323.

BUG, W., ROLE, L., SIEGELBAUM, S.A. & SIMMONS, L. (1989). Arachidonic acid inhibits calcium current in chick sympathetic neurons. *Neurosci. Soc. Abstr.*, **15**, 177.

BULT, H., BOECKXSTAENS, G.E., PELCKMANS, P.A., JORDAENS, F.H. VAN MAERCKE, Y.M. & HERMAN, A.G. (1990). Nitric oxide as an inhibitory non-adrenergic non-cholinergic neurotransmitter. *Nature*, **345**, 346–347.

CLAPP, L.H. & GURNEY, A.M. (1991). Modulation of calcium movements by nitroprusside in isolated vascular smooth muscles. *Eur. J. Physiol.*, **418**, 462–470.

DAWSON, T.M., BREDT, D.S., FOTUHI, M., HWANG, P.M. & SNYDER, S.H. (1991). Nitric oxide synthase and neuronal NADPH diaphorase are identical in brain and peripheral tissues. *Proc. Natl. Acad. Sci. U.S.A.*, **88**, 7797–7801.

DOERNER, D. & ALGER, B.E. (1988). Cyclic GMP depresses hippocampal Ca^{2+} current through a mechanism independent of cGMP-dependent protein-kinase. *Neuron*, **1**, 693–699.

ERRINGTON, M.L., LI, Y.G., MATTHIES, H., WILLIAMS, J.H. & BLISS, T.V.P. (1991). The nitric oxide synthase inhibitor N^{ω}-nitro-L-arginine reduces the magnitude of long-term potentiation in the dentate gyrus but not in area CA1 of the hippocampus *in vitro*. *Neurosci. Soc. Abstr.*, **17**, 951.

FOX, A.P., NOWYCKY, M.C. & TSIEN, R.W. (1987a). Kinetic and pharmocological properties distinguishing three types of calcium current in chick sensory neurones. *J. Physiol.*, **394**, 149–172.

FOX, A.P., NOWYCKY, M.C. & TSIEN, R.W. (1987b). Single-channel recordings of three types of calcium channels in chick sensory neurones. *J. Physiol.*, **394**, 173–200.

GARTHWAITE, J. (1991). Glutamate, nitric oxide and cell-cell signalling in the nervous system. *Trends Neurosci.*, **14**, 60–67.

GILLARD, J., FORD-HUTCHINSON, A.W., CHAN, C., CHARLESON, S., DENIS, D., FOSTER, A., FORTIN, R., LEGER, S., MCFARLANE, C.S., MORTON, H., PIECHUTA, H., REINDEAU, D., ROUZER, C.A., ROKACH, J., YOUNG, R., MACINTYRE, D.E., PETERSON, L., BACH, T., EIERMANN, G., HOPPLE, S., HUMES, J., HUPE, L., LUELL, S., METZGER, J., MEURER, R., MILLER, D.K., OPAS, E. & PACHOLOK, S. (1989). L-663,536 (MK-886) (3-[1-(4-chlorobenzyl)-3-*t*-butyl-thio-5-isopropylindol-2-yl]-2,2-dimethylpropanoic acid), a novel, orally active leukotriene biosynthesis inhibitor. *Can. J. Physiol. Pharmacol.*, **67**, 456–464.

GRAY, G.A., SCHOTT, C., JULOU-SCHAEFFER, G., FLEMING, I., PARRATT, J.R. & STOCLET, J.C. (1991). The effect of inhibitors of the L-arginine-nitric oxide pathway on endotoxin induced loss of vascular responsiveness in anaesthetized rats. *Br. J. Pharmacol.*, **103**, 1210–1224.

HAMILL, O.P., MARTY, A., NEHER, E., SAKMANN, G. & SIGWORTH, F.J. (1981). Improved patch-clamp techniques for high-resolution current recording from cells and cell-free membrane patches. *Pflügers Arch.*, **391**, 85–100.

HOPE, B.T., MICHAEL, G.J., KNIGGE, K.M. & VINCENT, S.R. (1991). Neuronal NADPH diaphorase is a nitric oxide synthase. *Proc. Natl. Acad. Sci. U.S.A.*, **88**, 2811–2814.

KEYSER, D.O. & ALGER, B.E. (1990). Arachidonic acid modulates hippocampal calcium current via protein kinase C and oxygen radicals. *Neuron*, **5**, 545–553.

LI, G.G. & RAND, M.J. (1990). Nitric oxide and vasoactive intestinal polypeptide mediate non-adrenergic, non-cholinergic inhibitory transmission to smooth muscle of the rat gastric fundus. *Eur. J. Pharmacol.*, **191**, 303–309.

LYNCH, M.A., ERRINGTON, M.L. & BLISS, T.V.P. (1989). Nordihydroguiaretic acid blocks the synaptic component of long-term potentiation and the associated increases in release of glutamate and arachidonate: an *in vivo* study in the dentate gyrus of the rat. *Neurosci.*, **30**, 693–701.

MONCADA, S., PALMER, R.M.J. & HIGGS, E.A. (1991). Nitric oxide: physiology, pathophysiology and pharmacology. *Pharmacol. Rev.*, **43**, 109–143.

O'DELL, T.J., HAWKINS, R.D., KANDEL, E.R. & ARANCIO, I. (1991). Tests of the roles of two diffusible substances in long-term potentiation: evidence for nitric oxide as a possible early retrograde messenger. *Proc. Natl. Acad. Sci. U.S.A.*, **88**, 11285–11289.

PIOMELLI, D. & GREENGARD, P. (1990). Lipoxygenase metabolites of arachidonic acid in neuronal transmembrane signalling. *Trends Pharmacol. Sci.*, **11**, 367–373.

PIOMELLI, D., VOLTERRA, A., DALE, N., SIEGELBAUM, S.A., KANDEL, E.R., SCHWARTZ, J.H. & BELARDETTI, F. (1987). Lipoxygenase metabolites of arachidonic acid as second messengers for pre-synaptic inhibition of *Aplysia* sensory cells. *Nature*, **328**, 38–43.

RAND, M.J. (1992). New perspectives in neurotransmission: nitric oxide, the mediator of nitergic transmission. *Proc. Aust. Physiol. Pharmacol. Soc.*, **23**, 1–16.

SCHROEDER, J.E., FISCHBACH, P.S., MAMO, M. & MCCLOSKEY, E.W. (1990). Two components of high-threshold Ca^{2+} current inactivate by different mechanisms. *Neuron*, **5**, 445–452.

SCOTT, T.R.D., NICHOL, K., CHAN, N. & BENNETT, M.R. (1992). Nitric oxide synthase localization in autonomic ciliary ganglia and its participation in long-term potentiation. *Proc. Aust. Physiol. Pharmacol. Soc.*, **23**, 191P.

SCOTT, R.H., PEARSON, H.A. & DOLPHIN, A.C. (1991). Aspects of vertebrate neuronal voltage-activated calcium currents and their regulation. *Prog. Neurobiol.*, **36**, 485–520.

SHER, E. & CLEMENTI, F. (1991). ω-conotoxin-sensitive voltage-operated calcium channels in vertebrate cells. *Neurosci.*, **42**, 301–307.

STANLEY, E.F. (1992). Single calcium channels in a cholinergic presynaptic nerve terminal. *Neuron*, **7**, 585–591.

STANLEY, E.F. & GOPING, G. (1991). Characterization of a calcium current in a vertebrate cholinergic nerve terminal. *J. Neurosci.*, **11**, 985–993.

SWANDULLA, D., CARBONE, E. & LUX, H.D. (1991). Do calcium channel classifications account for neuronal calcium diversity? *Trends Neurosci.*, **14**, 46–51.

TARE, M., PARKINGTON, H.C., COLEMAN, H.A., NEILD, T.O. & DUSTING, G.J. (1990). Hyperpolarization and relaxation of arterial smooth muscle caused by nitric oxide derived from the endothelium. *Nature*, **346**, 69–71.

WILLIAMS, J.H., ERRINGTON, M.L., LYNCH, M.A. & BLISS, T.V.P. (1988). Arachidonic acid induces long-term activity-dependent enhancement of synaptic transmission in the hippocampus. *Nature*, **341**, 739–742.

YOUNG, H.M., FURNESS, J.B., SHUTTLEWORTH, C.W.R., BREDT, D.S. & SNYDER, S.H. (1992). Co-localization of nitric oxide synthase immunoreactivity and NADPH diaphorase staining in neurones of the guinea-pig intestine. *Proc. Aust. Physiol. Pharmacol Soc.*, **23**, 45P.

(Received July 7, 1992
Revised January 4, 1993
Accepted February 8, 1993)

Br. J. Pharmacol. (1993), **109**, 486–490 © Macmillan Press Ltd, 1993

Induction of endothelium-dependent relaxation in the rat aorta by IRL 1620, a novel and selective agonist at the endothelin ET_B receptor

[1]Hideaki Karaki, Sri Agus Sudjarwo, Masatoshi Hori, *Michihiro Takai, *Yoshihiro Urade & *Toshikazu Okada

Department of Veterinary Pharmacology, Faculty of Agriculture, The University of Tokyo, Tokyo 113 and *International Research Laboratories, CIBA-GEIGY (Japan), Takarazuka 665, Japan

1 The effects of a novel and selective agonist at the endothelin ET_B receptor, IRL 1620 (Suc-[Glu^9, Ala^{11,15}] endothelin-1 (8-21)), were examined in the isolated aorta of the rat.

2 IRL 1620 (1–300 nM) changed neither the resting tone nor the cytosolic Ca^{2+} level ($[Ca^{2+}]_i$) of the aorta without endothelium. In the presence of endothelium, however, IRL 1620 increased endothelial $[Ca^{2+}]_i$ with little effect on the muscle tone. In the absence of external Ca^{2+}, IRL 1620 still induced a transient increase in endothelial $[Ca^{2+}]_i$.

3 Noradrenaline (100 nM) increased both muscle $[Ca^{2+}]_i$ and tension. IRL 1620 (1–300 nM) relaxed the muscle with an increase in endothelial $[Ca^{2+}]_i$ only in the presence of endothelium. An inhibitor of nitric oxide synthase, 100 μM N^G-monomethyl-L-arginine, inhibited the relaxant effect of IRL 1620 but not the increase in endothelial $[Ca^{2+}]_i$.

4 In resting and noradrenaline-stimulated aorta, the effects of IRL 1620 were inhibited by a selective antagonist of the ET_B receptor, IRL 1038 (0.3–3 μM), although a selective antagonist of the ET_A receptor, BQ-123 (3 μM), was ineffective. Verapamil (10 μM) did not alter the effects of IRL 1620.

5 A muscarinic receptor agonist, carbachol (1 μM), also induced endothelium-dependent relaxation with an increase in endothelial $[Ca^{2+}]_i$. However, the effects of carbachol were not inhibited by the ET_B antagonist, IRL 1038 (3 μM).

6 These results suggest that IRL 1620 is a selective agonist at the ET_B receptor which increases endothelial $[Ca^{2+}]_i$ by releasing Ca^{2+} from storage sites and by opening non-L type Ca^{2+} channels, activates nitric oxide synthase, releases nitric oxide, and relaxes vascular smooth muscle.

Keywords: IRL 1620; ET_B receptor agonist; IRL 1038; ET_B receptor antagonist; endothelin-3; endothelium-dependent relaxation; cytosolic Ca^{2+} level; rat aorta

Introduction

It has been shown that three isoforms of endothelin, endothelin-1, endothelin-2 and endothelin-3 (Yanagisawa *et al.*, 1988; Inoue *et al.*, 1989), activate ET_B receptors at similar concentrations (Sakurai *et al.*, 1990) whereas endothelin-1 and endothelin-2 activate ET_A receptors at concentrations lower than endothelin-3 (Arai *et al.*, 1990). In blood vessels, ET_A receptors are found in smooth muscle whereas ET_B receptors are found in endothelium (Fujitani *et al.*, 1992). Endothelins relax vascular smooth muscle (De Nucci *et al.*, 1988; Sakata *et al.*, 1989) by activating ET_B receptors (Sakurai *et al.*, 1992) which cause release of endothelium-derived relaxing factor (EDRF; Furchgott, 1984) recently identified as nitric oxide (Moncada *et al.*, 1991). Thus, endothelins have a vasoconstrictor action via the activation of ET_A receptors and a vasodilator action via the activation of ET_B receptors. Recently, Takai *et al.* (1992) found that IRL 1620 specifically binds to ET_B receptors on porcine lung membrane and induces contraction of guinea-pig trachea. If IRL 1620 is a selective agonist at ET_B receptors, it will prove useful in elucidating the role of these receptors in various biological systems. In the present experiments we examined the effects of IRL 1620 on the functions of endothelium and smooth muscle in the isolated aorta of the rat. The results indicate that IRL 1620 is a selective agonist of the ET_B receptors.

[1] Author for correspondence at: Department of Veterinary Pharmacology, Faculty of Agriculture, The University of Tokyo, Bunkyo-ku, Tokyo 113, Japan.

Methods

Thoracic aortae were isolated from male Wistar rats (200–250 g), cut into spiral strips (1–2 mm in width and 5–7 mm in length) and placed in normal physiological salt solution which contained (mM): NaCl 136.9, KCl 5.4, $CaCl_2$ 1.5, $MgCl_2$ 1.0, $NaHCO_3$ 23.8, ethylenediamine tetraacetic acid 0.01 and glucose 5.5. In some experiments, endothelium was removed by gently rubbing the intimal surface with a finger moistened with the above solution. A high K^+ solution was made by substituting 68.5 mM NaCl with equimolar KCl. Ca^{2+}-free solution was made by omitting $CaCl_2$ and adding 0.5 mM EGTA. These solutions were saturated with a mixture of 95% O_2 and 5% CO_2 at 37°C and pH 7.4. Muscle tension was recorded isometrically with a force displacement transducer. Each muscle strip was attached to a holder under a resting tension of 10 mN and equilibrated for 60–90 min in a 10 ml muscle bath until the contractile response to the high K^+ solution became stable.

The functional integrity of the vascular endothelium was assessed by determining whether carbachol (1 μM) induced almost complete relaxation (>90%) in aortae stimulated with noradrenaline (100 nM) (Karaki & Nagase, 1987).

For the simultaneous measurement of muscle tension and cytosolic Ca^{2+} level, muscle strips were incubated with 5 μM of the acetoxymethyl ester of fura-2 (fura-2/AM) for 3–5 h at room temperature. The noncytotoxic detergent, cremophor EL (0.02%), was also added to increase the solubility of fura-2/AM. Experiments were performed with a fluorimeter (CAF-100, Japan Spectroscopic, Tokyo, Japan) as described previously (Sato *et al.*, 1988; 1990). The muscle strip was held horizontally in a temperature-controlled organ bath. One end of the muscle strip was connected to the force displacement

transducer to monitor the mechanical activity. The endothelial surface of the strip was excited by 340 nm and 380 nm light alternately (48 Hz) and the intensity of fluorescence at 500 nm (F340 and F380) at the endothelial surface was measured. The Ca^{2+} signals thus obtained were derived from both endothelial and smooth muscle cells. In some experiments the endothelium was removed in order to measure $[Ca^{2+}]_i$ in smooth muscle cells alone. By comparing the total and the smooth muscle $[Ca^{2+}]_i$, it is possible to speculate about the changes in endothelial $[Ca^{2+}]_i$ (Sato *et al.*, 1990). Absolute $[Ca^{2+}]_i$ was not calculated because the dissocation constant of fura-2 for Ca^{2+} might be different from that obtained *in vitro* (Karaki, 1989) and also because we simultaneously measured $[Ca^{2+}]_i$ in different tissues (smooth muscle and endothelium) with different fura-2 contents. The ratio of F340 to F380 (R340/380) was used as an indicator of $[Ca^{2+}]_i$, and the quantitative comparison of $[Ca^{2+}]_i$ was made by taking resting and high K^+-stimulated $[Ca^{2+}]_i$ as 0% and 100%, respectively, unless otherwise stated.

IRL 1620 (Suc-[Glu^9,$Ala^{11,15}$] endothelin-1 [8-21]; Takai *et al.*, 1992), IRL 1038 ([Cys^{11}-Cys^{15}] endothelin-1 [11-21]; Urade *et al.*, 1992) and BQ-123 (cyclo[-Asp-Pro-Val-Leu-Trp-]; Ihara *et al.*, 1992) were synthesized at Ciba-Geigy (Japan), Takarazuka, Japan. Other chemicals used were endothelin-3 (Peptide Institute, Osaka, Japan), verapamil hydrochloride, N^G-monomethyl-L-arginine (L-NMMA) (Sigma Chemicals, St. Louis, MO, U.S.A.), and noradrenaline bitartrate (Wako Pure Chemicals, Tokyo, Japan). In a preliminary experiment, it was confirmed that these chemicals did not interfere with fura-2 fluorescence.

Results of the experiments are expressed as mean ± s.e.mean of n individual determinations. Student's t test was used to evaluate the significance of difference between group means.

Results

As shown in Figure 1, 100 nM IRL 1620 increased $[Ca^{2+}]_i$ without changing muscle tone in spiral strips of aorta with endothelium. Carbachol (1 μM) showed similar effects to IRL 1620. In contrast, high K^+ increased both $[Ca^{2+}]_i$ and muscle tension. In strips without endothelium, high K^+ also increased $[Ca^{2+}]_i$ and muscle tension. However, IRL 1620 and carbachol were ineffective. These results suggest that IRL 1620 and carbachol increase $[Ca^{2+}]_i$ in endothelium but not in smooth muscle.

Figure 2 shows the effects of IRL 1620 and carbachol on $[Ca^{2+}]_i$ in the absence of external Ca^{2+}. Addition of 100 nM IRL 1620 induced a transient increase in $[Ca^{2+}]_i$ (58.8 ± 5.9%, $n = 4$). Sequential addition of 100 nM IRL 1620 (data not shown) or 100 nM endothelin-3 (Figure 2) did not change $[Ca^{2+}]_i$. In contrast, sequential addition of 1 μM carbachol again transiently increased $[Ca^{2+}]_i$ (65.2 ± 7.3%, $n = 4$). When applied in the absence of IRL 1620, 100 nM endothelin-3 increased $[Ca^{2+}]_i$ to 64.8 ± 6.2% ($n = 4$) and 1 μM carbachol to 80.3 ± 12.8% ($n = 4$).

As shown in Figure 3, 100 nM noradrenaline increased both $[Ca^{2+}]_i$ and muscle tension. Addition of 100 nM IRL 1620 transiently relaxed the sustained contraction induced by noradrenaline. This change was associated with a transient increase in $[Ca^{2+}]_i$. Sequential addition of 1 μM carbachol almost completely relaxed the muscle with an increase in $[Ca^{2+}]_i$. In strips without endothelium, noradrenaline increased both $[Ca^{2+}]_i$ and muscle tension; however, neither IRL 1620 nor carbachol had any effect ($n = 4$ each).

Figure 4 shows the concentration-response curves for the relaxant effect of IRL 1620 in noradrenaline-stimulated aorta. As shown in Figure 4a, an ET_B antagonist, 0.3–3.0 μM IRL 1038, inhibited the response to IRL 1620 shifting the curve to the right and downwards. IRL 1038 itself changed neither the tone of the muscle nor $[Ca^{2+}]_i$ in the absence or presence of noradrenaline (data not shown). As shown in Figure 4b, an inhibitor of nitric oxide synthase, 100 μM L-NMMA (Moncada *et al.*, 1991), almost completely inhibited the relaxation induced by IRL 1620. However, an ET_A antagonist, 3 μM BQ-123, did not change the response to IRL 1620. In a preliminary experiment, we confirmed that the same concentration of BQ-123 almost completely inhibited the contractile effect of 10 nM endothelin-1 in rat isolated aorta.

Figure 5 shows the effects of 100 nM IRL 1620 on endothelial $[Ca^{2+}]_i$ and on the relaxation of noradrenaline-induced contraction. Verapamil, 10 μM, changed neither the relaxation nor the increase in $[Ca^{2+}]_i$ produced by IRL 1620. In contrast, 100 μM L-NMMA inhibited the relaxation without changing the increase in $[Ca^{2+}]_i$ whereas 3 μM IRL 1038 strongly inhibited both of these changes produced by IRL 1620.

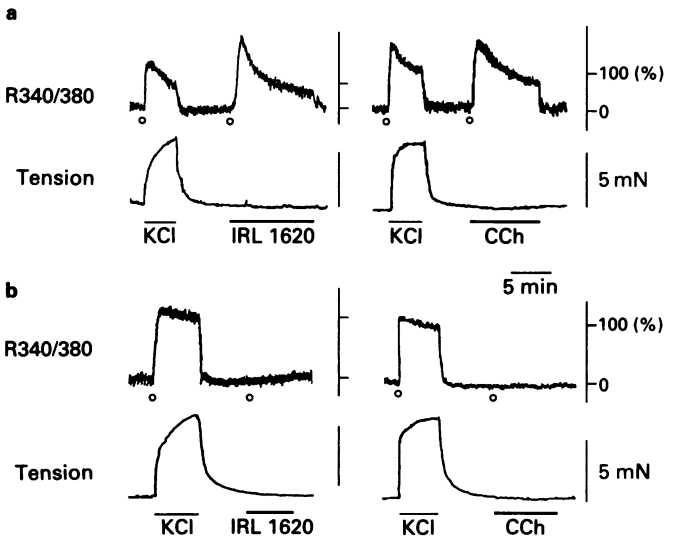

Figure 1 Effects of IRL 1620 (100 nM) and carbachol (CCh, 1 μM) on cytosolic Ca^{2+} level (upper trace, expressed as R340/380) and muscle tension (lower trace) in rat aorta with (a) and without (b) endothelium. 100% represents cytosolic Ca^{2+} stimulated by high K^+. The trace shown is typical of 4 experiments.

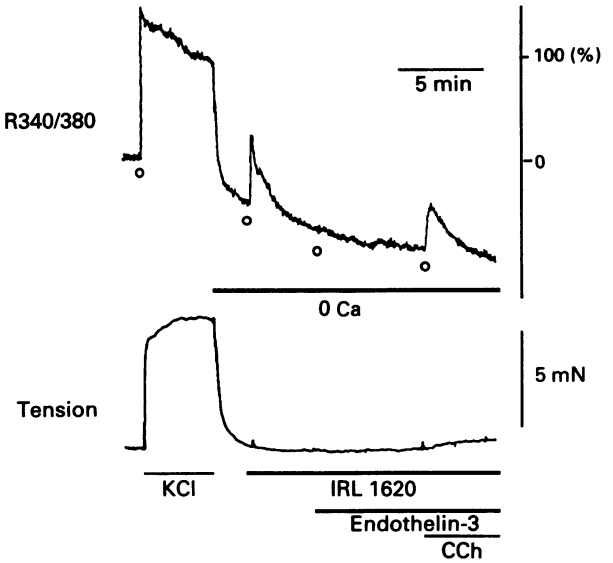

Figure 2 Effects of IRL 1620 (100 nM), endothelin-3 (100 nM) and carbachol (CCh) (1 μM) on cytosolic Ca^{2+} level (upper trace, expressed as R340/380) and muscle tension (lower trace) in rat aorta with endothelium in the absence of external Ca^{2+} (0 Ca; with 0.5 mM EGTA). 100% represents cytosolic Ca^{2+} stimulated by high K^+. The trace shown is typical of 4 experiments.

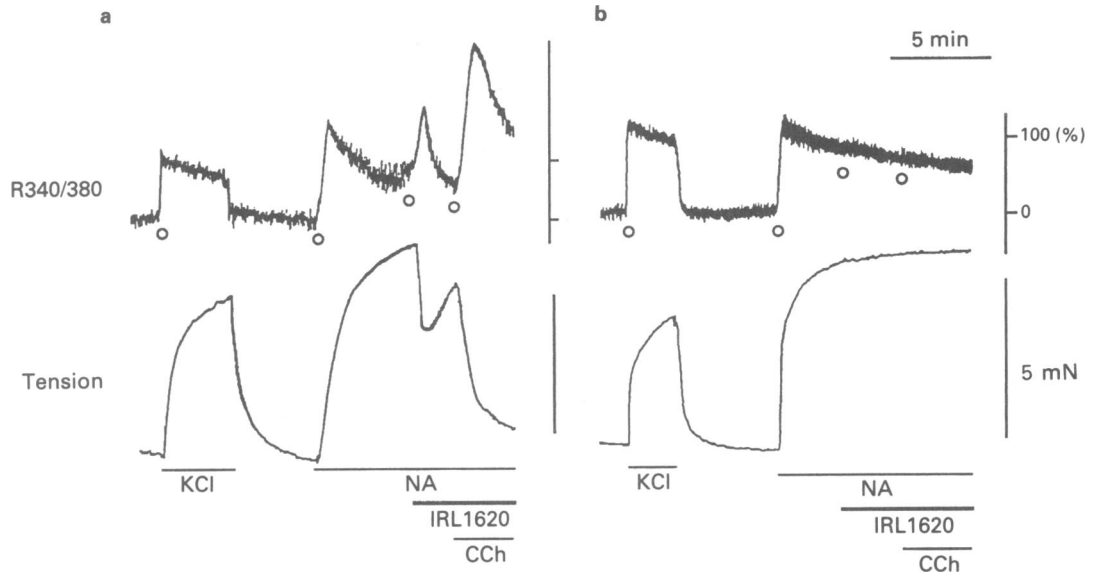

Figure 3 Effects of IRL 1620 (100 nM) and carbachol (CCh, 1 μM) on cytosolic Ca^{2+} level (upper trace, expressed as R340/380) and muscle tension (lower trace) in rat aorta with (a) and without endothelium (b) in the presence of 100 nM noradrenaline. 100% represents cytosolic Ca^{2+} stimulated by high K^+. The trace shown is typical of 4 experiments.

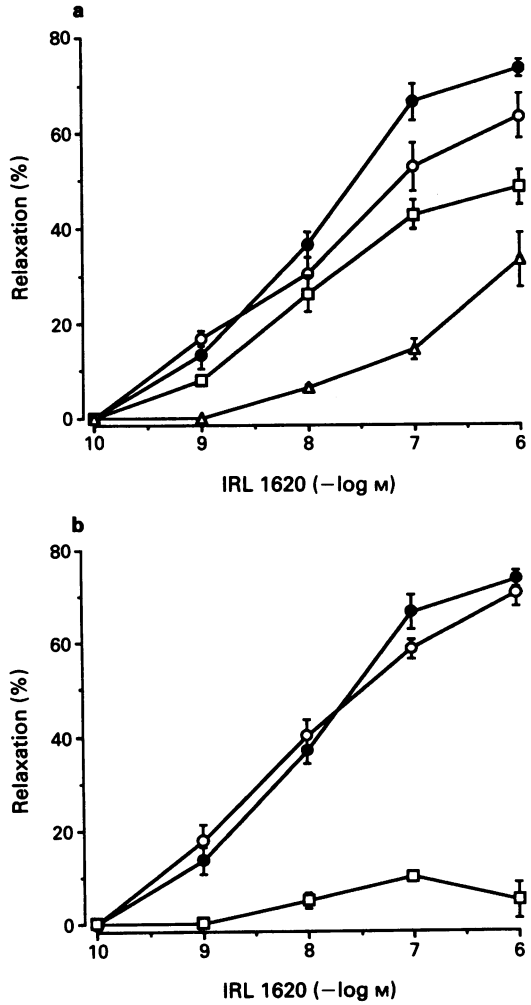

Figure 4 Effects of IRL 1038 (a), BQ-123 and N^G-monomethyl-L-arginine (L-NMMA) (b) on the concentration-response curve for the relaxant effect of IRL 1620. IRL 1620 was added during the sustained contraction induced by 100 nM noradrenaline. Only one concentration of IRL 1620 was applied to one muscle strip. The inhibitor was added 20 min before the addition of IRL 1620. (a) In the absence (●) and in the presence of 0.3 μM (○), 1 μM (□) or 3 μM (△) IRL 1038. (b) In the absence (●) and in the presence of 3 μM BQ-123 (○) or 100 μM L-NMMA (□). Each point represents mean (with s.e.mean) of 4 experiments.

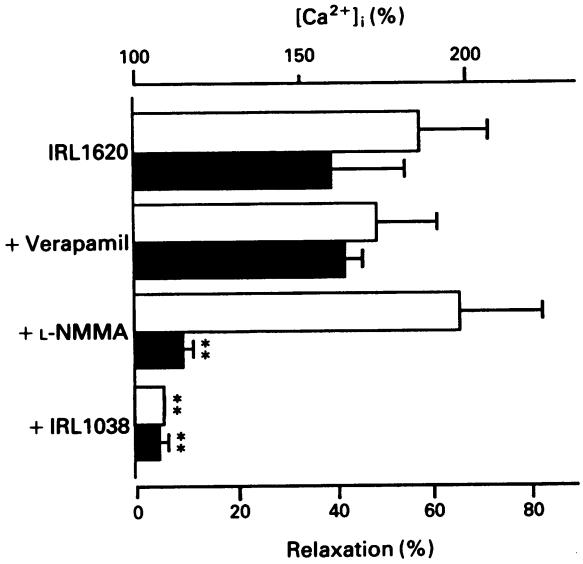

Figure 5 Effects of verapamil, N^G-monomethyl-L-arginine (L-NMMA) and IRL 1038 on 100 nM IRL 1620-induced muscle relaxation (solid column) and cytosolic Ca^{2+} level ($[Ca^{2+}]_i$: open column) in the rat aorta stimulated with 100 nM noradrenaline. Verapamil (10 μM), L-NMMA (100 μM) or IRL 1038 (3 μM) was added 20 min before the addition of IRL 1620. Each point represents the mean (with s.e.mean) of 4 experiments. Upper scale: 100% represents cytosolic Ca^{2+} stimulated by 100 nM noradrenaline. Lower scale: 100% represents complete inhibition of the contraction induced by 100 nM noradrenaline.

Discussion

In the present experiments, it was found that IRL 1620 increased $[Ca^{2+}]_i$ without changing muscle tone in the rat aorta. This effect was abolished by removal of the endothelium. The ET_B antagonist, IRL 1038 (Urade *et al.*, 1992), non-competitively inhibited the effect of IRL 1620. However, an ET_A antagonist, BQ-123 (Ihara *et al.*, 1992) was ineffective. These results suggest that IRL 1620 acts on ET_B receptors and increases endothelial $[Ca^{2+}]_i$.

Previously, Sudjarwo *et al.* (1992) found that endothelin-3 also induced an endothelium-dependent increase in $[Ca^{2+}]_i$ without changing muscle tone. In contrast, in the absence of endothelium, or in the presence of the ET_B antagonist IRL

1038, endothelin-3 increased both $[Ca^{2+}]_i$ and muscle tension, both of which effects were abolished by the ET_A antagonist BQ-123 at 3 μM. The difference between IRL 1620 and endothelin-3 is explained by the fact that although IRL 1620 selectively binds to ET_B receptors, endothelin-3 binds to both ET_B and ET_A receptors (Takai *et al.*, 1992).

In noradrenaline-stimulated aortae, IRL 1620 increased endothelial $[Ca^{2+}]_i$ followed by an inhibition of contraction. These effects were inhibited by the ET_B antagonist, IRL 1038. In contrast, relaxation but not the increase in $[Ca^{2+}]_i$ was inhibited by L-NMMA, an inhibitor of nitric oxide synthase. These findings suggest that activation of ET_B receptors by IRL 1620 increases endothelial $[Ca^{2+}]_i$, activates nitric oxide synthase to increase synthesis and release of nitric oxide, and relaxes the smooth muscle. It has been reported that endothelin-3 also increases endothelial $[Ca^{2+}]_i$ and relaxes noradrenaline-stimulated aortae and these effects are inhibited by the ET_B antagonist IRL 1038 (Sudjarwo *et al.*, 1992).

IRL 1620 transiently increased $[Ca^{2+}]_i$ in the absence of external Ca^{2+} although the duration of the $[Ca^{2+}]_i$ increase was shorter in the absence of external Ca^{2+}. This result suggests that IRL 1620 mobilized Ca^{2+} from cellular storage sites and also increased Ca^{2+} influx. The pathway of Ca^{2+} influx does not seem to be the L-type Ca^{2+} channels because verapamil did not inhibit the IRL 1620-induced increase in $[Ca^{2+}]_i$. This result is consistent with the suggestion that endothelins open non-selective cation channels in vascular endothelium (Colden-Stanfield *et al.*, 1987; Adams *et al.*, 1989; Lückoff & Busse, 1990). Sato *et al.* (1990) have shown that carbachol and histamine increase endothelial $[Ca^{2+}]_i$ also by the release of cellular Ca^{2+} and the opening of non-L type Ca^{2+} channels. In strips pretreated with 100 nM IRL 1620 in the absence of external Ca^{2+}, the second application of 100 nM IRL 1620 or 100 nM endothelin-3 was ineffective, possibly because Ca^{2+} stores had been depleted. However, 1 μM carbachol released Ca^{2+} in the muscle pretreated with IRL 1620. These results suggest that carbachol releases Ca^{2+} from stores which are not depleted by IRL 1620.

Previously, it has been shown that sarafotoxin S6c (Williams *et al.*, 1991) and [$Ala^{1,3,11,15}$] endothelin-1 (Hiley *et al.*, 1990; Saeki *et al.*, 1991) are selective agonists of ET_B receptors. However, the effects of these agonists on endothelium-dependent relaxation are different. In the methoxamine-precontracted rat mesenteric bed, sarafotoxin S6c induced endothelium-dependent relaxation (Clozel *et al.*, 1992) although [$Ala^{1,3,11,15}$] endothelin-1 was ineffective (Douglas & Hiley, 1991). In contrast, [$Ala^{1,3,11,15}$] endothelin-1 induced endothelium-dependent relaxation in noradrenaline-precontracted porcine pulmonary artery (Saeki *et al.*, 1991) although sarafotoxin S6c failed to relax the phenylephrine-precontracted rabbit carotid artery (Moreland *et al.*, 1992). In the present experiments, we found that IRL 1620 induced endothelium-dependent relaxation in the noradrenaline-precontracted rat aorta. These differences may be attributable to the presence of vasoconstrictor ET_B receptors in some blood vessels (Moreland *et al.*, 1992), selectivity of these antagonists to the vasoconstrictor ET_A receptors and vasodilator ET_B receptors, and/or regional differences in the coupling of ET_B receptors to the synthesis of nitric oxide.

These results suggest that IRL 1620 acts selectively on ET_B receptors, increases endothelial $[Ca^{2+}]_i$ by releasing Ca^{2+} and also by opening of non-L type Ca^{2+} channels, activates nitric oxide synthase, releases nitric oxide and relaxes vascular smooth muscle.

We are grateful to Dr A. James, Ciba Geigy (Japan), for helpful discussion and critical reading of the manuscript. This work was supported by Grant-in-Aid for Scientific Research from the Ministry of Education, Science and Culture, Japan.

References

ADAMS, D.J., BARAKEH, J. & VAN BREEMEN, C. (1989). Ion channels and regulation of intracellular calcium in vascular endothelial cells. *FASEB J.*, **3**, 2389–2400.

ARAI, H., HORI, S., ARAMORI, I., OHKUBO, H. & NAKANISHI, S. (1990). Cloning and expression of a cDNA encoding an endothelin receptor. *Nature*, **348**, 730–732.

CLOZEL, M., GRAY, G.A., BREU, V., LÖFFLER, B.-M. & OSTERWALDER, R. (1992). The endothelin ET_B receptor mediates both vasodilatation and vasoconstriction *in vivo*. *Biochem. Biophys. Res. Commun.*, **186**, 867–873.

COLDEN-STANFIELD, M., SCHILLING, W.P., RITCHIE, A.K., ESKIN, S.G., NAVARRO, L.T. & KUNZE, D.L. (1987). Bradykinin-induced increase in cytosolic calcium and ion currents in cultured bovine aortic endothelial cells. *Circ. Res.*, **61**, 632–640.

DE NUCCI, G., THOMAS, R., D'ORLEANS-JUSTE, P., ANTUNES, E., WALDER, C., WARNER, T.D. & VANE, J.R. (1988). Pressor effects of circulating endothelin are limited by its removal in the pulmonary circulation and by the release of prostacyclin and endothelium-derived relaxing factor. *Proc. Natl. Acad. Sci. U.S.A.*, **85**, 9797–9800.

DOUGLAS, S.A. & HILEY, C.R. (1991). Endothelium-dependent mesenteric vasorelaxant effect and systemic actions of endothelin (16-21) and other endothelin-related peptides in the rat. *Br. J. Pharmacol.*, **104**, 311–320.

FUJITANI, Y., ODA, K., TAKIMOTO, M., INUI, T., OKADA, T. & URADE, Y. (1992). Autocrine receptors for endothelins in the primary culture of endothelial cells of human umbilical vein. *FEBS Lett.*, **298**, 79–83.

FURCHGOTT, R.F. (1984). The role of endothelium in the responses of vascular smooth muscle to drugs. *Annu. Rev. Pharmacol. Toxicol.*, **24**, 175–197.

HILEY, C.R., JONES, C.R., PELTON, J.T. & MILLER, R.C. (1990). Binding of [^{125}I]endothelin-1 to rat cerebellar homogenates and its interactions with some analogues. *Br. J. Pharmacol.*, **101**, 319–324.

IHARA, M., NOGUCHI, K., SAEKI, T., FUKURODA, T., TSUCHIDA, S., KIMURA, S., FUKAMI, T., ISHIKAWA, K., NISHIKIBE, M. & YANO, M. (1992). Biological profiles of highly potent novel endothelin antagonists selective for the ET_A receptor. *Life Sci.*, **50**, 247–255.

INOUE, A., YANAGISAWA, M., KIMURA, S., KASUYA, Y., MIYAUCHI, T., GOTO, K. & MASAKI, T. (1989). The human endothelin family; three structurally and pharmacologically distinct isopeptides predicted by three separate genes. *Proc. Natl. Acad. Sci. U.S.A.*, **86**, 2863–2867.

KARAKI, H. (1989). Ca^{2+} localization and sensitivity in vascular smooth muscle. *Trends Pharmacol. Sci.*, **10**, 320–325.

KARAKI, H. & NAGASE, H. (1987). Low temperature augments the endothelium-dependent relaxation in isolated rat aorta. *Eur. J. Pharmacol.*, **142**, 129–132.

LÜCKHOFF, A. & BUSSE, R. (1990). Calcium influx into endothelial cells and formation of EDRF is controlled by membrane potential. *Pflügers Arch.*, **416**, 305–311.

MONCADA, S., PALMER, R.M.J. & HIGGS, E.A. (1991). Nitric oxide; physiology, pathophysiology, and pharmacology. *Pharmacol. Rev.*, **43**, 109–142.

MORELAND, S., MCMULLEN, D.M., DELANEY, C.L., LEE, V.G. & HUNT, J.T. (1992). Venous smooth muscle contains vasoconstrictor ET_B-like receptors. *Biochem. Biophys. Res. Commun.*, **184**, 100–106.

SAEKI, T., IHARA, M., FUKURODA, T., YAMAGIWA, M. & YANO, M. (1991). [Ala 1,3,11,15] endothelin-1 analogs with ET_B agonistic activity. *Biochem. Biophys. Res. Commun.*, **179**, 286–292.

SAKATA, K., OZAKI, H., KWON, S.-C. & KARAKI, H. (1989). Effects of endothelin on the mechanical activity and cytosolic calcium levels of various types of smooth muscle. *Br. J. Pharmacol.*, **98**, 483–492.

SAKURAI, T., YANAGISAWA, M. & MASAKI, T. (1992). Molecular characterization of endothelin receptors. *Trends Pharmacol. Sci.*, **13**, 103–108.

SAKURAI, T., YANAGISAWA, M., TAKUWA, Y., MIYAZAKI, H., KIMURA, S., GOTO, K. & MASAKI, T. (1990). Cloning of cDNA encoding a non-isopeptide-selective subtype of the endothelin receptor. *Nature*, **348**, 732–735.

SATO, K., OZAKI, H. & KARAKI, H. (1988). Changes in cytosolic calcium level in vascular smooth muscle strip measured simultaneously with contraction using fluorescent calcium indicator. Fura 2. *J. Pharmacol. Exp. Ther.*, **246**, 294–300.

SATO, K., OZAKI, H. & KARAKI, H. (1990). Differential effects of carbachol on cytosolic calcium levels in vascular endothelium and smooth muscle. *J. Pharmacol. Exp. Ther.*, **255**, 114–119.

SUDJARWO, S.A., HORI, M. & KARAKI, H. (1992). Effect of endothelin-3 on cytosolic calcium level in vascular endothelium and smooth muscle contraction. *Eur. J. Pharmacol.*, **229**, 137–142.

TAKAI, M., UMEMURA, I., YAMASAKI, K., WATAKABE, T., FUJITANI, Y., ODA, K., URADE, Y., INUI, T., YAMAMURA, T. & OKADA, T. (1992). A potent and specific agonist, Suc-[Glu^{9}-Ala^{11,15}] endothelin-1 (8-21), IRL 1620, for the ET_B receptor. *Biochem. Biophys. Res. Commun.*, **184**, 953–959.

URADE, Y., FUJITANI, Y., ODA, K., WATAKABE, T., UMEMURA, I., TAKAI, M., OKADA, T., SAKATA, K. & KARAKI, H. (1992). An endothelin B receptor-selective antagonist: IRL 1038, [Cys^{11}-Cys^{15}]-endothelin-1 (11-21). *FEBS Lett.*, **311**, 12–16.

WILLIAMS, D.L., JONES, K.L., PETTIBONE, D.J., LIS, E.V. & CLINE-SCHMIDT, B.V. (1991). Sarafotoxin S6c: an agonist which distinguishes between endothelin subtypes. *Biochem. Biophys. Res. Commun.*, **175**, 556–561.

YANAGISAWA, M., KURIHARA, H., KIMURA, S., TOMOBE, Y., KOBAYASHI, M., MITSUI, Y., YAZAKI, Y., GOTO, K. & MASAKI, T. (1988). A novel potent vasoconstrictor peptide produced by vascular endothelial cells. *Nature*, **332**, 411–415.

(Received September 18, 1992
Revised February 2, 1993
Accepted February 9, 1993)

Br. J. Pharmacol. (1993), **109**, 491–494 © Macmillan Press Ltd, 1993

Reciprocal interaction of 5-hydroxytryptamine and cholecystokinin in the control of feeding patterns in rats

Giuliano Grignaschi, Barbara Mantelli, Claudia Fracasso, Marina Anelli, Silvio Caccia & [1]Rosario Samanin

Istituto di Ricerche Farmacologiche 'Mario Negri' Via Eritrea 62, 20157 Milan, Italy

1 The effect of the CCK_A receptor antagonist, devazepide (100 mg kg^{-1}) on meal parameters during the initial phase of the dark period was studied in free-feeding rats by use of a procedure for continuously monitoring feeding patterns.

2 In a second experiment, the effect of devazepide on the reduction in meal parameters induced by the 5-hydroxytryptamine (5-HT) releaser and uptake inhibitor, (+)-fenfluramine (1.5 mg kg^{-1}) in 4 h food-deprived rats was examined.

3 The hypophagic effect of an intraperitoneal injection of cholecystokinin (CCK-8, 4 μg kg^{-1}) was studied in rats treated with the 5-HT receptor antagonist, metergoline (1 and 2 mg kg^{-1}).

4 Devazepide increased the size of the first meal in free-feeding, but not in 4 h food-deprived rats and partially antagonized the effect of (+)-fenfluramine on the size and duration of the first meal. The reduction in eating rate induced by (+)-fenfluramine was not modified by devazepide. No changes in (+)-fenfluramine or (+)-norfenfluramine levels were found in the brain of rats treated with devazepide.

5 The effect of CCK-8 on meal size was completely antagonized by 2 mg kg^{-1} metergoline. A significant interaction was also found between 2 mg kg^{-1} metergoline and CCK-8 as regards their effect on the inter-meal interval.

6 The results suggest a reciprocal interaction between 5-HT and CCK-8 in enhancing the satiating effect of food in rats.

Keywords: (+)-fenfluramine; cholecystokinin; feeding patterns; satiety; 5-hydroxytryptamine

Introduction

Exogenous cholecystokinin (CCK-8) has been largely studied for its ability to reduce feeding in rats but only recently has the development of potent and selective agonists and antagonists made possible research into the roles of CCK_A and CCK_B receptors on feeding behaviour.

The anorectic effect of intracerebroventricularly or peripherally administered CCK-8 seems to be mediated by CCK_A receptors (Crawley *et al.*, 1991; Dourish *et al.*, 1989a), while the ability of CCK_A and CCK_B receptor antagonists to increase feeding in pre-satiated or free-feeding rats is still debated. One study (Dourish *et al.*, 1989b) proposed that the blockade of CCK_A or CCK_B receptors could increase food intake in pre-satiated rats, but two others subsequently reported an increase in food consumption after CCK_A but not CCK_B receptor blockade both in pre-satiated rats tested with a liquid diet (Corwin *et al.*, 1991) and in free-feeding rats (Reidelberger *et al.*, 1991).

Of particular interest were findings (Cooper *et al.*, 1990) that the CCK_A receptor antagonist devazepide (formerly known as L-374,718) (Chang & Lotti, 1986; Evans *et al.*, 1986) blocked the reduction in sweet-mash consumption and in nocturnal feeding induced by the 5-hydroxytryptamine (5-HT) releaser and uptake inhibitor (+)-fenfluramine (Garattini *et al.*, 1987). Thus 5-HT-dependent anorexia may be partially mediated by CCK_A receptors. On the other hand, the 5-HT receptor antagonist, metergoline (Hoyer, 1988) antagonized the reduction in food intake induced in food-deprived rats by an intraperitoneal injection of CCK-8 (Stallone *et al.*, 1989). There seems, therefore, to be a reciprocal functional interaction between CCK and 5-HT in the control of food intake.

Should 5-HT mediate the effect of CCK-8 on feeding, one would expect similar effects on meal patterns of CCK-8 and drugs enhancing 5-hydroxytryptaminergic transmission. (+)-Fenfluramine and CCK-8 reduce meal size, suggesting that both enhance the state of satiety in rats (Hsiao *et al.*, 1979; West *et al.*, 1987; Grignaschi *et al.*, 1992). (+)-Fenfluramine had no effect on the inter-meal interval (Grignaschi *et al.*, 1992) and the effect of CCK-8 on this parameter is not clear (Hsiao *et al.*, 1979; West *et al.*, 1987). In order to clarify the interaction between CCK and 5-HT, a meal pattern analysis of the effects of (+)-fenfluramine and CCK-8 in the presence of CCK and 5-HT receptor antagonists respectively has been carried out.

By use of a procedure for continuously monitoring feeding patterns in free-feeding and 4 h food-deprived rats (Blundell *et al.*, 1976; Grignaschi *et al.*, 1992), the changes in meal parameters induced by devazepide in free-feeding rats and the drug's effect on the reduction in meal parameters induced by (+)-fenfluramine in 4 h food-deprived rats (Grignaschi *et al.*, 1992) have been studied. Finally, the effect of an intraperitoneal injection of CCK-8 on meal parameters was studied in 4 h food-deprived rats treated with the 5-HT receptor antagonist, metergoline.

Methods

Animals

Male Sprague-Dawley rats (CD-COBS, Charles River, Italy), housed in groups of four in an animal colony maintained at 21 ± 1°C and 60% relative humidity, with a 12 h light-12 h dark cycle (light off at 18 h 00 min) and water and food *ad libitum* were used for testing. At the beginning of the experiment each animal, weighing 220–250 g, was housed in an individual box and allowed seven days' habituation to the pelleted food.

[1] Author for correspondence.

Apparatus

The apparatus consisted of eight cages (Perspex boxes, 280 × 210 × 210 mm) and a cage supervisor apparatus connected to a MS-DOS computer for long-term data storage and analysis (Microsystem, Milan, Italy). The cages were equipped with a food hopper and a drinking bottle fixed to one wall. A single 45 mg food pellet (Noyes improved formula A) was always available in the hopper. Removal of the pellet activated an infra-red photo-beam system and another pellet was delivered in 3 s. Removal of each pellet was recorded by the cage supervisor apparatus with a timing resolution of 1 s and stored on a computer hard disc for long-term data storage.

Analysis

Feeding parameters were analysed essentially as described previously (Grignaschi *et al.*, 1992). A meal consisted of two or more pellets and 10 min was adopted as the minimum inter-response interval separating two meals. These choices were based on preliminary experiments showing that the pattern of meals did not differ when the inter-response interval was between 2 and 15 min and a minimum of one or two pellets was adopted as the criterion for a meal. Meal size (g), duration (min), eating rate (g min^{-1}) and inter-meal interval (min) were measured over different periods.

Effect of devazepide on meal patterns of free-feeding rats

During the seven days' habituation the animals were handled gently, weighed and injected subcutaneously (s.c.) with saline at 17 h 50 min, 10 min before the dark period. On the test day, devazepide (0.1 mg kg^{-1}, s.c.) was injection at 17 h 50 min and the test started at 18 h 00 min. The dose of devazepide was chosen on the basis of previous studies (Dourish *et al.*, 1989a,b; Reidelberger *et al.*, 1991) and preliminary experiments indicated it to be the most appropriate.

Effect of devazepide on the changes in meal parameters induced by (+)-fenfluramine in 4 h food-deprived rats

Since previous studies (Grignaschi & Samanin, 1992) had shown that the effect of (+)-fenfluramine is studied better in 4 h food-deprived rats, at the beginning of the seven days' habituation, delivery of pellets was stopped from 14 h 00 min to 18 h 00 min. During the habituation period before this study the animals were handled gently, weighed and injected intraperitoneally (i.p.) with saline at 17 h 30 min, 30 min before food was made available. On the test day, devazepide (0.1 mg kg^{-1}, s.c.) was injected at 17 h 20 min, 10 min before (+)-fenfluramine (1.5 mg kg^{-1}, i.p.). The test started at 18 h 00 min.

Measurement of brain concentrations of (+)-fenfluramine and (+)-norfenfluramine

Each animal was housed individually and allowed seven days' habituation with food available from 18 h 00 min to 14 h 00 min. On the test day the animals were injected with devazepide (0.1 mg kg^{-1}, s.c.) at 17 h 20 min, 10 min before (+)-fenfluramine (1.5 mg kg^{-1}, i.p.). The animals were killed 30, 60 or 90 min after (+)-fenfluramine and the brains were immediately removed and stored at − 20°C.

Brain concentrations of (+)-fenfluramine and (+)-norfenfluramine were extracted and analysed by electron capture gas liquid chromatography as previously described (Fracasso *et al.*, 1988; Spinelli *et al.*, 1988).

Effect of metergoline on the changes of meal parameters induced by CCK-8 in 4 h food-deprived rats

Since preliminary studies had indicated that the action of exogenous CCK-8 was rapid and short-lasting, delivery of pellets was stopped from 14 h 00 min to 18 h 00 min to facilitate analysis of drug effects at early times. During the habituation period the animals were handled gently, weighed and injected i.p. with saline at 17 h 45 min, 15 min before food was made available. On the test days, metergoline (1.0 and 2.0 mg kg^{-1}, i.p.) was injected at 15 h 00 min, 2 h 45 min before CCK-8 (4 μg kg^{-1}, i.p.). The test started at 18 h 00 min.

Drugs

Devazepide (Merck Sharp & Dohme Research Laboratories, West Point, PA, U.S.A.) was suspended in 0.5% carboxymethylcellulose and injected s.c. 10 min before the test or 10 min before (+)-fenfluramine. Metergoline base (Farmitalia Carlo Erba, Milan, Italy) was dissolved in 1% ascorbic acid and injected i.p. 3 h before the test. (+)-Fenfluramine hydrochloride (Servier, Neuilly-sur-Seine, France) and CCK-8 sulphate (Sigma, St. Louis, U.S.A.) were dissolved in saline and injected i.p. respectively 30 min and 15 min before the test. All drugs were injected in a volume of 2 ml kg^{-1}.

Statistical analysis

The effect of devazepide in free-feeding animals was analysed by Student's *t* test; a two-way analysis of variance (ANOVA 2 × 2) followed by Tukey's test was used to analyse the effect of (+)-fenfluramine in devazepide-treated rats and the effect of CCK-8 in metergoline-treated rats. Brain concentrations of (+)-fenfluramine and (+)-norfenfluramine in vehicle and devazepide treated rats were analysed by Student's *t* test.

Results

Effect of devazepide on meal patterns of free-feeding rats

As shown in Table 1, 100 μg kg^{-1} devazepide significantly increased the size of the first meal without modifying the eating rate. Devazepide increased the duration of the first meal, although the effect was not statistically significant. The CCK_A antagonist had no effect on the interval between the first and the second meal or any parameter of the second meal.

Effect of devazepide on the changes in meal parameters induced by (+)-fenfluramine in 4 h food-deprived rats

As shown in Table 2, devazepide when injected alone did not modify any parameter of the first meal but partially antagonized the reduction in meal size and duration caused by (+)-fenfluramine (F interaction $(1,23) = 6.4$ and 6.7 respectively; $P < 0.05$). It did not significantly modify the reduction in eating rate induced by (+)-fenfluramine (F interaction $(1,23) < 2.1$; $P > 0.05$). The parameters of the second meal were not affected by any treatment (data not shown).

There were no significant differences between (+)-fenfluramine and devazepide + (+)-fenfluramine groups in the brain levels of (+)-fenfluramine and (+)-norfenfluramine 30, 60 and 90 min after injection of (+)-fenfluramine (results not shown).

Effect of metergoline on the changes in meal parameters induced by CCK-8 in 4 h food-deprived rats

Preliminary studies showed that CCK-8, 4 μg kg^{-1}, reduced the size of the first meal and the interval between the first

Table 1 Effect of devazepide on meal parameters of free-feeding rats

	Vehicle	*Devazepide*
First meal:		
Size (g)	2.49 ± 0.59	4.09 ± 0.43*
Duration (min)	11.0 ± 3.2	14.1 ± 1.60
Eating rate (g min^{-1})	0.27 ± 0.03	0.30 ± 0.01
Second meal		
Size (g)	3.02 ± 0.75	3.17 ± 0.77
Duration (min)	12.4 ± 3.64	12.1 ± 2.91
Eating rate (g min^{-1})	0.27 ± 0.02	0.28 ± 0.02
Inter-meal interval (min)	55.4 ± 10.8	51.5 ± 8.90

Mean ± s.e.mean of eight animals per group.
Devazepide (100 μg kg^{-1}) was injected subcutaneously 10 min before the test.
*$P<0.05$ vs vehicle; Student's t test.

and the second meal. The other parameters were not modified, although the meal duration was clearly shorter in CCK-8-treated rats (data not shown).

As shown in Table 3, metergoline did not modify the size of the first meal but significantly antagonized the effect of 4 μg kg^{-1} CCK-8 on this parameter (F interaction (2,47) = 3.3; $P<0.05$). Further analysis by Tukey's test showed that only 2 mg kg^{-1} metergoline completely antagonized the effect of CCK-8. The interval between the first and the second meal was significantly reduced by CCK-8 ($P<0.05$, Tukey's test) and there was a statistically significant interaction (F interaction (2,47) = 6.5; $P<0.01$) between metergoline and CCK-8. Metergoline, at the dose of 2 mg kg^{-1}, significantly reduced the inter-meal interval ($P<0.01$, Tukey's test) and the treatment with CCK-8 did not modify this measure in the animals treated with the higher dose of metergoline.

Discussion

The CCK_A antagonist devazepide, at the dose of 100 μg kg^{-1}, increased the size of the first meal consumed during the initial phase of the dark period in free-feeding rats, with no effect on subsequent meals. Cooper *et al.* (1990) found that devazepide did not increase nocturnal feeding by free-feeding rats but the longer period considered in that study (2, 4 and

Table 2 Effect of devazepide on the changes of first-meal parameters induced by (+)-fenfluramine in 4 h food-deprived rats

	Saline	*(+)-fenfluramine*
Size (g)		
Vehicle	8.1 ± 0.7	1.4 ± 0.4**
Devazepide	6.7 ± 0.4	3.5 ± 0.8** [b]
Duration (min)		
Vehicle	28.2 ± 3.7	6.7 ± 1.5**
Devazepide	20.6 ± 2.6	14.0 ± 3.0 [b]
Eating rate (g min^{-1})		
Vehicle	0.30 ± 0.02	0.19 ± 0.02*
Devazepide	0.34 ± 0.03	0.25 ± 0.03*

Mean ± s.e.mean of at least six animals per group.
(+)-fenfluramine (1.5 mg kg^{-1}) was injected intraperitoneally 30 min before the test session.
Devazepide (100 μg kg^{-1}) was injected subcutaneously 10 min before (+)-fenfluramine.
F interaction (1,23) = 6.4 and 6.7 respectively for meal size and meal duration.
**$P<0.01$; *$P<0.05$ vs their respective saline group: Tukey's test.
[b]$P<0.05$ F interaction: 2-way ANOVA.

Table 3 Effect of metergoline on the changes in meal parameters induced by cholecystokinin (CCK-8) in 4 h food-deprived rats

	Dose (mg kg^{-1})	*Saline*	*CCK-8*
First meal (g)			
Vehicle		6.3 ± 0.5	3.1 ± 0.4*
Metergoline	1.0	6.4 ± 1.1	3.0 ± 0.6*
Metergoline	2.0	5.7 ± 0.6	6.0 ± 1.3[b]
Inter-meal interval (min)			
Vehicle		84.6 ± 8.5	52.9 ± 8.3*
Metergoline	1.0	78.8 ± 10.8	41.3 ± 4.5**
Metergoline	2.0	41.6 ± 6.4°°	54.8 ± 6.2[a]

Mean ± s.e.mean of eight animals per group.
Metergoline (1 and 2 mg kg^{-1}) and CCK-8 (4 μg kg^{-1}) were injected intraperitoneally respectively 3 h and 15 min before the test.
F interaction (2,47) = 3.3 and 6.5 respectively for meal size and inter-meal interval.
[b]$P<0.05$; [a]$P<0.01$: 2-way ANOVA
*$P<0.05$; **$P<0.01$ vs saline treated group: Tukey's test.
°°$P<0.01$ vs vehicle: Tukey's test.

6 h) may account for this difference. In 4 h food-deprived rats devazepide did not modify the parameters of the first meal, confirming that the animals' deprivation status may be important for revealing the ability of CCK_A antagonists to increase feeding.

Devazepide significantly antagonized the reduction in meal size and duration induced by (+)-fenfluramine confirming that endogenous CCK appears to mediate partially the reduction in food intake induced by (+)-fenfluramine (Cooper *et al.*, 1990). This antagonism could not be attributed to an interference of devazepide with the distribution and metabolism of (+)-fenfluramine since the brain levels of (+)-fenfluramine and its main metabolite (+)-norfenfluramine were not modified. Since the reduction in meal size by (+)-fenfluramine seems to be mediated by 5-HT_{1B} receptors (Grignaschi & Samanin, 1992), these receptors probably interact with CCK to reduce feeding.

5-HT appears to act as a potent releaser of CCK-like immunoreactivity in the rat through activation of the 5-HT_3 receptor type (Paudice & Raiteri, 1991). In that study the $5\text{-HT}_1/5\text{-HT}_2$ receptor antagonist methiothepin (Hoyer, 1988) did not modify the release of CCK-like immunoreactivity caused by 5-HT but the study employed synaptosomes prepared from rat cerebral cortex and nucleus accumbens. It therefore remains open whether stimulation of 5-HT_{1B} receptors enhance the release of CCK or increases the sensitivity of CCK receptors in the hypothalamus, a region playing a major role in monoamine- or peptide-induced changes in feeding (Leibowitz, 1989).

The decrease in eating rate by (+)-fenfluramine was not modified by devazepide, suggesting that the effect of (+)-fenfluramine on meal size and eating rate can be separated. This agrees with previous findings that the reduction in eating rate disappears more rapidly than the effect on meal size after repeated treatment with (+)-fenfluramine (Grignaschi *et al.*, 1992), and (±)-cyanopindolol antagonized the effect of (+)-fenfluramine on meal size but not on eating rate (Grignaschi & Samanin, 1992). It seems therefore that after changes in 5-HT transmission the duration rather than the rate of eating varies in relation to changes in meal size.

The hypothesis of an interaction between 5-HT and CCK in the control of feeding behaviour is further supported by the fact that, in agreement with previous findings on 3 h food-deprived rats (Stallone *et al.*, 1989), the 5-HT receptor antagonist metergoline completely antagonized the reduction in the size of the first meal induced by CCK-8. In rats used

to eating for 5 h daily, no interaction between metergoline and CCK-8 has been found (Garattini et al., 1992) confirming the importance of animals' deprivation status in feeding studies.

Dense CCK-8-like immunoreactivity has been found in the rat dorsal raphe (Vanderhaegen et al., 1980; Van Der Koy et al., 1981), an important site of origin of 5-HT-containing neurones innervating the forebrain, and a recent study (Boden et al., 1991) showed that CCK-8 excited some 5-HT-containing cells in this region. Possibly therefore part of the satiating effect of CCK-8 is due to its ability to activate 5-HT neurones in the raphe nuclei.

While (+)-fenfluramine reduced meal size with no effect on inter-meal interval, suggesting that it prolongs the satiating effect of a given amount of food (Samanin et al., 1991; Grignaschi et al., 1992), CCK-8 did not prevent the compensatory decrease in inter-meal interval which usually follows the reduction in meal size. The relatively short-acting effect of CCK-8 in our conditions may have contributed to this since when administered by continuous infusion CCK-8 had no effect on inter-meal interval (West et al., 1987). However, the fact that the rats ate more frequently to compensate for the CCK-8-induced reduction of meal size (West et al., 1987) suggests that the main action of CCK is to hasten the onset of satiety.

In conclusion, this study confirmed that the CCK_A antagonist, devazepide, at the dose of $100\,\mu g\,kg^{-1}$ increases the size of the first meal in free-feeding rats. That 5-HT and CCK interact reciprocally was shown by the finding that devazepide and metergoline attenuated the reduction in meal size caused respectively by (+)-fenfluramine and CCK-8.

This study was supported by CNR contract No. 91.01513.CT04 and by Convenzione Psicofarmacologia CNR.

References

BLUNDELL, J.E., LATHAM, C.J. & LESHEM, M.B. (1976). Differences between the anorexic actions of amphetamine and fenfluramine-possible effects on hunger and satiety. *J. Pharm. Pharmacol.*, **28**, 471–477.

BODEN, P.R., WOODRUFF, G.N. & PINNOCK, R.D. (1991). Pharmacology of a cholecystokinin receptor on 5-hydroxytryptamine neurones in the dorsal raphe of the rat brain. *Br. J. Pharmacol.*, **102**, 635–638.

CHANG, R.S.L. & LOTTI, V.J. (1986). Biochemical and pharmacological characterization of an extremely potent and selective nonpeptide cholecystokinin antagonist. *Proc. Natl. Acad. Sci. U.S.A.*, **83**, 4923–4926.

COOPER, S.J., DOURISH, C.T. & BARBER, D.J. (1990). Reversal of the anorectic effect of (+)-fenfluramine in the rat by the selective cholecystokinin receptor antagonist MK-329. *Br. J. Pharmacol.*, **99**, 65–70.

CORWIN, R.L., GIBBS, J. & SMITH, G.P. (1991). Increased food intake after type A but not type B cholecystokinin receptor blockade. *Physiol. Behav.*, **50**, 255–258.

CRAWLEY, J.N., FISKE, S.M., DURIEUX, C., DERRIEN, M. & ROQUES, B.P. (1991). Centrally administered cholecystokinin suppresses feeding through a peripheral-type receptor mechanism. *J. Pharmacol. Exp. Ther.*, **257**, 1076–1080.

DOURISH, C.T., RUCKERT, A.C., TATTERSALL, F.D. & IVERSEN, S.D. (1989a). Evidence that decreased feeding induced by systemic injection of cholecystokinin is mediated by CCK-A receptors. *Eur. J. Pharmacol.*, **173**, 233–234.

DOURISH, C.T., RYCROFT, W. & IVERSEN, S.D. (1989b). Postponement of satiety by blockade of brain cholecystokinin (CCK-B) receptors. *Science*, **245**, 1509–1511.

EVANS, B.E., BOCK, M.G., RITTLE, K.E., DIPARDO, R.M., WHITTER, W.L., VEBER, D.F., ANDERSON, P.S. & FREIDINGER, R.M. (1986). Design of potent, orally effective nonpeptidal antagonists of the peptide hormone cholecystokinin. *Proc. Natl. Acad. Sci. U.S.A.*, **83**, 4918–4922.

FRACASSO, C., GUISO, G., GARATTINI, S. & CACCIA, S. (1988). Disposition of d-fenfluramine in lean and obese rats. *Appetite*, **10**, 45–55.

GARATTINI, S., MENNINI, T. & SAMANIN, R. (1987). From fenfluramine racemate to d-fenfluramine: specificity and potency of the effects on the serotoninergic system and food intake. *Ann. N.Y. Acad. Sci.*, **409**, 156–166.

GARATTINI, S., BIZZI, A., CACCIA, S. & MENNINI, T. (1992). Progress report on the anorectic effect of fenfluramine, fluoxetine and sertraline. *Int. J. Obes.*, (in press).

GRIGNASCHI, G., NEILL, J.C., PETRINI, A., GARATTINI, S. & SAMANIN, R. (1992). Feeding pattern studies suggest that d-fenfluramine and sertraline specifically enhance the state of satiety in rats. *Eur. J. Pharmacol.*, **211**, 137–142.

GRIGNASCHI, G. & SAMANIN, R. (1992). Role of 5-HT receptors in the effect of d-fenfluramine on feeding patterns in the rat. *Eur. J. Pharmacol.*, **212**, 287–289.

HOYER, D. (1988). Functional correlates of serotonin 5-HT 1 recognition sites. *J. Receptor Res.*, **8**, 59–81.

HSIAO, S., WANG, C.H. & SCHALLERT, T. (1979). Cholecystokinin, meal pattern, and the intermeal interval: can eating be stopped before it starts? *Physiol. Behav.*, **23**, 909–914.

LEIBOWITZ, S.F. (1989). Hypothalamic neuropeptide Y, galanin, and amines. Concepts of coexistence in relation to feeding behavior. *Ann. N.Y. Acad. Sci.*, **575**, 221–235.

PAUDICE, P. & RAITERI, M. (1991). Cholecystokinin release mediated by $5\text{-}HT_3$ receptors in rat cerebral cortex and nucleus accumbens. *Br. J. Pharmacol.*, **103**, 1790–1794.

REIDELBERGER, R.D., VARGA, G. & SOLOMON, T.E. (1991). Effects of selective cholecystokinin antagonists L364,718 and L365,260 on food intake in rats. *Peptides*, **12**, 1215–1221.

SAMANIN, R., NEILL, J.C., GRIGNASCHI, G., MARTIN PADURA, I., BIZZI, A. & GARATTINI, S. (1991). Role of 5-HT receptors in the effect of d-fenfluramine on gastric emptying and feeding behaviour as examined in the runway test. *Eur. J. Pharmacol.*, **197**, 69–73.

SPINELLI, R., FRACASSO, C., GUISO, G., GARATTINI, S. & CACCIA, S. (1988). Disposition of (−)-fenfluramine and its active metabolite, (−)-norfenfluramine in rat: a single dose-proportionality study. *Xenobiotica*, **18**, 573–584.

STALLONE, D., NICOLAIDIS, S. & GIBBS, J. (1989). Cholecystokinin-induced anorexia depends on serotoninergic function. *Am. J. Physiol.*, **256**, R1138–R1141.

VANDERHAEGEN, J.J., LOSTRA, F., DEMAY, J. & GILLES, C. (1980). Immunohistochemical localisation of cholecystokinin and gastrin-like peptides in the brain and hypophysis of the rat. *Proc. Natl. Acad. Sci. U.S.A.*, **77**, 1190–1194.

VAN DER KOY, D., HUNT, S., STEINBUSCH, H.W.M. & VERHOFSTAD, A.A.J. (1981). Separate populations of cholecystokinin and 5-HT containing cells in the rat dorsal raphe and their contribution to its ascending projections. *Neurosci. Lett.*, **26**, 25–31.

WEST, D.B., GREENWOOD, M.R.C., SULLIVAN, A.C., PRESCOD, L., MARZULLO, L.R. & TRISCARI, J. (1987). Infusion of cholecystokinin between meals into free-feeding rats fails to prolong the intermeal interval. *Physiol. Behav.*, **39**, 111–115.

(Received September 28, 1992
Revised January 18, 1993
Accepted February 9, 1993)

Br. J. Pharmacol. (1993), **109**, 495–501 © Macmillan Press Ltd, 1993

Interactions of nitric oxide synthase inhibitors and dexamethasone with α-adrenoceptor-mediated responses in rat aorta

[1]Ayotunde S.O. Adeagbo & Christopher R. Triggle

Department of Pharmacology and Therapeutics, University of Calgary, 3330 Hospital Drive N.W., Calgary, Alberta, Canada T2N 4N1

1 The effects of N^G-nitro-L-arginine methyl ester (L-NAME) and N^G-monomethyl-L-arginine (L-NMMA), their D-isomers, and dexamethasone on noradrenaline (NA)-induced contractions and antagonism by α-adrenoceptor antagonists, have been investigated in rat isolated thoracic aortic rings with/without endothelium.

2 NA produced concentration-dependent contractions of isolated aortic rings with EC_{50} values of 2.41 ± 0.54 ($n = 21$) and 28.00 ± 8.50 ($n = 25$) nM for endothelium-denuded and -intact preparations respectively. Acetylcholine (ACh) relaxed NA-precontracted rings with intact, but not those denuded of endothelium.

3 Treatment with L-NAME (1–30 μM), or L-NMMA (10–500 μM), but not their D-isomers, resulted in an endothelium-dependent enhancement of NA-induced contractions. Pre-treatment, *in vitro*, with 0.5 μM dexamethasone neither directly potentiated, nor influenced L-NAME-induced potentiation of NA-mediated contractions in endothelium-intact rings; however, dexamethasone pretreatment reduced EC_{50} values for NA, and also prevented L-NAME-induced potentiation, in denuded rings equilibrated for 5 h under resting tension.

4 In both intact and denuded rings, phentolamine, prazosin and WB 4101 shifted NA concentration-response curves to the right; L-NAME, and also L-NMMA, but not their D-isomers, reversed the blockade as indicated by significant decreases in NA dose-ratios. In denuded rings, reversal by L-NAME or L-NMMA was prevented following pretreatment with dexamethasone.

5 Following treatment with 5 or 50 nM phenoxybenzamine (PBZ), NA concentration-response (C-R) curves were shifted to the right with marked depression of maximal responses; 100 μM L-NAME reversed the antagonism in both endothelium intact and denuded rings. However, 500 nM PBZ treatment resulted in complete abolition of the responses to NA, and contractions were not restored by either L-NAME or L-NMMA.

6 5-Hydroxytryptamine (5-HT)-induced contractions of aortic rings were potentiated by endothelium denudation and also by L-, but not D-, NAME. 5-HT-induced contractions were non-competitively antagonized by 10 nM ritanserin, and 100 μM L-NAME partially reversed the antagonism in intact but not denuded rings.

7 It is concluded that the inhibition of constitutive endothelial NO synthase and inducible smooth muscle NO synthase accounts for the ability of L-NAME, and L-NMMA, to potentiate the effects of agonists and reduce α-adrenoceptor antagonism in endothelium-intact and denuded rings. Furthermore, endothelial cell removal/damage triggers the induction of a smooth muscle NO synthase.

Keywords: Rat aorta; α-adrenoceptors; NO synthase inhibitors; inducible NO synthase; dexamethasone

Introduction

It is widely accepted that vascular endothelial cells (Palmer *et al.*, 1988; Palmer & Moncada, 1989; Ignarro, 1989), and a variety of other mammalian tissues and cell types such as cerebellum (Garthwaite *et al.*, 1988), stomach (Desai *et al.*, 1991), rat isolated aortae (Schini & Vanhoutte, 1991) and macrophages (Moncada *et al.*, 1989; Collier & Vallance, 1989), synthesize nitric oxide (NO) from L-arginine. Furthermore, it is also recognized that NO is the principal mediator of the actions of endothelium-derived relaxing factor (EDRF) on vascular smooth muscle (Palmer *et al.*, 1987). In rat isolated aortic rings, the presence of a functional endothelium has been shown to depress the contractile actions of α-adrenoceptor agonists (Allan *et al.*, 1983; Egleme *et al.*, 1984; Lues & Schumann, 1984; Carrier & White, 1985); an action attributed to the spontaneous release of EDRF and subsequent physiological antagonism of the contractile process. Thus endothelial denudation, and inhibitors of EDRF, such as methylene blue and oxyhaemoglobin, usually augment vascular contractions to a variety of agonists (Martin *et al.*, 1986; Miller *et al.*, 1988).

The role of the endothelium in the modulation of the binding of subtype-specific adrenoceptor radioligands to vascular α_1- and α_2-adrenoceptor sites was first described by Carman-Krzan (1985). It was reported that the removal of endothelium caused an increase in the density of specific α_1-adrenoceptor binding, with little effect on the affinity of the ligand for the receptor. Carman-Krzan (1985) concluded that the loss of endothelial cells may uncover otherwise undetectable receptor sites in the bovine thoracic aorta. Subsequently, Alosachie & Godfraind (1988) showed that the vascular endothelium modified prazosin-mediated antagonism of noradrenaline action: noncompetitive in the presence, and competitive in the absence of endothelium; a finding that was explained in terms of their earlier proposal (Alosachie & Godfraind, 1986) i.e. reduction in agonist efficacy and receptor reserve by EDRF. Perhaps more surprising was the demonstration by Mostaghim *et al.* (1988) that α-antagonists such as phentolamine, prazosin and yohimbine, caused endothelium-dependent relaxations of rat

[1] Author for correspondence.

thoracic aortic rings; one interpretation of these data is that a component of what had been interpreted as adrenoceptor blockade may in fact be due to release of one or more bioactive substance(s) from the endothelium. If this interpretation is correct, the following hypothesis can be formulated: the degree of α-adrenoceptor antagonism produced by phentolamine, prazosin, yohimbine, or related compounds, should be less in endothelium-intact, compared to endothelium-denuded vascular tissue.

In the present study, we have tested this hypothesis, by examining the effects of endothelial denudation, and of the NO synthase inhibitors, N^G-nitro-L-arginine methyl ester (L-NAME) and N^G-monomethyl-L-arginine (L-NMMA) on noradrenaline-induced contractions, and antagonism by a variety of α-adrenoceptor antagonists, in aortic rings with intact or denuded endothelium.

Methods

Male Sprague-Dawley rats (Charles River, PQ, Canada; 200–300 g) were stunned by a blow to the head and exsanguinated. Thoracic aortae were excised, cleaned of all connective tissue and cut into rings of approximately 3–4 mm length. Each ring was suspended between platinum hooks and mounted under 2 g passive tension in 10 ml organ baths containing physiological salt solution (PSS), maintained at 37°C and bubbled with 95% O_2/5% CO_2. Isometric tension was recorded with a force displacement transducer (Grass FT .03) coupled to a Grass polygraph model 7E. The PSS used had the following composition (in mM): NaCl 118, KCl 4.7, $CaCl_2$ 2.5, KH_2PO_4 1.2, $MgSO_4$ 1.2, $NaHCO_3$ 12.5 and glucose 11.1. The pH of the solution after saturation with 95% O_2/5% CO_2 gas mixture was 7.4. As a routine, tissues were allowed to equilibrate for 1 h before the start of the experiments and where endothelial denudation was required, this was achieved mechanically by rubbing a piece of PE 90 tubing against the intimal surface of the aortic rings.

Experimental procedure

Protocol 1: This series of experiments was carried out to characterize the effects of L-NAME, L-NMMA, and their D-isomers on noradrenaline (NA) concentration-response (C-R) curves in aortic rings with/without endothelium. Control C-R curves were performed to NA and, upon reaching the maximal contractile response, 1 μM acetylcholine (ACh) was applied to ascertain the functional integrity of the endothelium; preparations which did not show >85% relaxation of the active tone were not included in our data. Thereafter, the tissues were washed and similar C-R curves performed 30 min after the addition of different concentrations of a NO synthase inhibitor.

Protocol 2: Three series of experiments were carried out under this protocol, all of which involved construction of C-R curves to NA before and after incubation with desired concentrations of: (a) α-adrenoceptor antagonists and, (b) α-adrenoceptor antagonists + NO synthase inhibitor L-NAME, L-NMMA, or their D-isomers, in aortic rings with/without endothelium. The first series examined the ability of the reversible antagonists, phentolamine, prazosin and WB 4101 to antagonize NA-induced contractions, and the influence of L-, and D-, NAME and NMMA on such effects. In these studies, tissues were equilibrated in PSS for 1 h, followed by control NA C-R curves (routinely performed twice to ensure consistency), and, then, incubation with each of the antagonists for 30 min before reestablishing C-R curves and calculations of dose-ratios for NA. Tissues were subsequently washed and incubated with a combination of the antagonist under study plus a desired concentration of either L-NAME and L-NMMA. The second series of experiments was designed to study the influence of the glucocorticoid, dexamethasone, on the interaction of L-NAME with NA-induced contractions, and the effects of prazosin thereon. The procedure was identical to that described in the first series above, except that experiments were performed in PSS with or without 0.5 μM dexamethasone, and tissues were equilibrated for either a 1- or a 5-h period. In the third series, the α-adrenoceptor alkylating agent phenoxybenzamine (PBZ) was used instead of the reversible antagonists. Thus, NA C-R curves were established, the aortic rings were then incubated with the alkylating agent for 30 min, washed in PBZ-free PSS for 2 h, and agonist responses alone, and in the presence of L-NAME (100 μM), reestablished.

Protocol 3: Experiments in this series examined the influence of L-, or D-NAME, on 5-hydroxytryptamine (5-HT) C-R curves and on the 5-HT/ritanserin interactions in aortic rings with/without endothelium. The procedure was as described for the first series of experiments in protocol 2 above.

Drugs

Noradrenaline hydrochloride, acetylcholine hydrobromide, N^G-nitro-L-arginine methyl ester, 5-hydroxytryptamine maleate, and dexamethasone were purchased from Sigma Chem. Co. (St. Louis, MO, U.S.A.); ritanserin, phenoxybenzamine hydrochloride and WB 4101 (2-(2,6-dimethoxyphenoxyethyl)-aminomethyl-1,4-benzodioxane hydrochloride) were purchased from Research Biochemicals, Inc. (Natick, MA, U.S.A.); N^G-nitro-D-arginine methyl ester (Bachem Inc., Torrance, CA, U.S.A.); N^G-monomethyl-L-arginine (Chemical Dynamics Corp., Plainfield, NJ, U.S.A.). Phentolamine hydrochloride (Regitine) and prazosin hydrochloride were generously supplied by Ciba-Geigy Corp. (Summit, NJ, U.S.A.) and Pfizer Canada Inc. (Arnprior, Ont., Canada) respectively. N^G-monomethyl-D-arginine acetate hemihydrate was a gift from Dr S. Moncada, The Wellcome Research Laboratories, Kent, U.K.

Stock solutions of NA, 5-HT, and ritanserin were prepared in 0.1 M HCl; all other compounds dissolved freely in PSS except for prazosin which required sonication.

Data analysis

Results are presented as means ± s.e.mean of either the percentage maximal responses or absolute tension measurements. Differences between the mean values were determined by Student's *t* test for paired and unpaired observations, and were regarded as significant when $P<0.05$. NA dose-ratios, defined as the ratios of NA EC_{50} values in the presence to values in the absence of a competitive antagonist, were calculated from plots of individual experiments under the various applicable experimental conditions.

Results

Effects of endothelial denudation, L-NAME and L-NMMA on NA-induced contractions

NA (0.1–1000 nM) produced concentration-dependent contraction of rat isolated aortic ring segments with AC_{50} values (in nM) of 2.41 ± 0.54 ($n=21$) and 28.00 ± 8.50 ($n=25$) nM for endothelium-denuded and intact preparations respectively. Although the EC_{50} values were significantly ($P<0.05$) different, no differences in the E_{max} were apparent. Neither L-NAME nor L-NMMA, within the concentration range 1–30 μM and 10–500 μM respectively, affected basal aortic tone, however, the L- but not the D-isomers of these inhibitors caused a leftward shift of NA concentration-response curves with marked increases in the maximal response in endothelium-intact aortic rings (Figure 1). No enhancement was observed in endothelium-denuded rings.

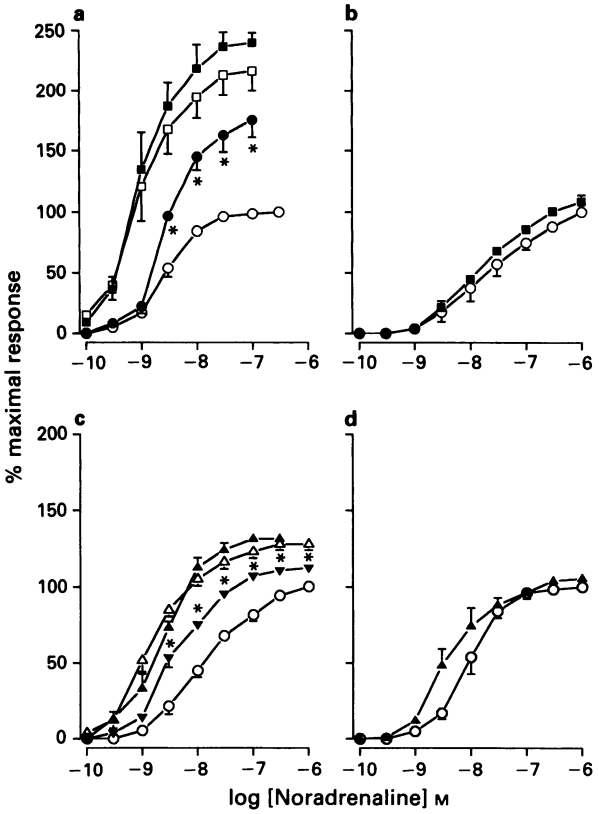

Figure 1 The effects of N^G-nitro-L-arginine methyl ester (L-NAME) (a) N^G-monomethyl-L-arginine (L-NMMA) (c) and their corresponding D-isomers (b,d) on concentration-response curves to noradrenaline (NA) in rat aortic rings with an intact endothelium. In all panels, (○) represent control responses, while (●), (□) and (■) respectively represent the responses in the presence of 1, 10 and 30 μM L-, or D-NAME in (a) and (b); and, (▼), (△) and (▲) respectively represent the responses in the presence of 10, 100 and 500 μM L-, or D-NMMA in (c) and (d). Each point on the graph represents the mean ± s.e. ($n = 5-12$). *Denotes statistically significant difference ($P < 0.05$) from corresponding control values.

NA antagonism by phentolamine, prazosin and WB 4101: influence of NO synthase inhibitors

Regardless of whether the endothelium was intact or denuded, the concentration-response curves to NA were shifted to the right by 0.3 μM phentolamine, 3.0 nM prazosin and 5 nM WB 4101 without a change in the maximal responses. L- but not D-NAME, at either 10 or 100 μM caused significant decreases in the ability (measured at dose-ratios) of prazosin (Table 1), and also phentolamine and WB 4101 (Figure 2), to inhibit NA-induced contractions. NA concentration-response curves, in the presence of the antagonist and L-NAME, were shifted leftwards, towards the control curve, and this effect occurred both in endothelium-intact and denuded rings, L-NMMA, at 100 or 500 μM, also reduced the dose-ratios of phentolamine and prazosin on NA C-R curves (Figure 3).

Effects of dexamethasone

Treatment with 0.5 μM dexamethasone did not significantly alter the EC_{50} values for NA in either endothelium-intact or denuded rings, equilibrated in PSS for 1 h. For example, NA EC_{50} values (in nM) in the absence, and presence, of dexamethasone pretreatment were: 23.8 ± 7.0 ($n = 31$) versus

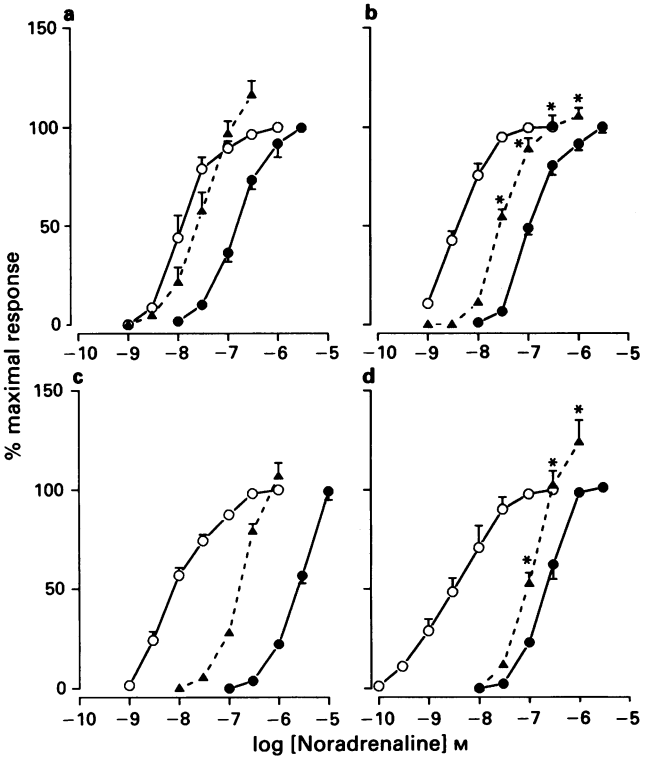

Figure 2 The effects of N^G-nitro-L-arginine methyl ester (L-NAME) on the antagonism of concentration-response curves to noradrenaline (NA) by 0.3 μM phentolamine (a,b) and 5 nM WB 4101 (c,d) in rat isolated aortic rings with intact (a,c) or denuded (b,d) endothelium. In all panels, (○), represent NA control responses, while (●) and (▲) respectively represent the responses to NA in the presence of the antagonists alone and antagonist + 100 μM L-NAME. Each data point on the graphs represents the mean ± s.e. ($n = 8$). *Denote statistically significant difference ($P < 0.05$) from the corresponding responses in the presence of the antagonist alone.

Table 1 Effects of N^G-nitro-L-arginine methyl ester (L-NAME) and D-NAME, and prazosin, on noradrenaline (NA)-mediated responses (expressed as dose-ratios) in rat isolated aortic rings with/without endothelium and in the absence/presence of 0.5 μM dexamethasone (Dex)

	Prazosin (3 nM)	+ *L-NAME* (10 μM)	+ *L-NAME* (100 μM)	+ *D-NAME* (100 μM)
+ Endo	95.60 ± 14.77 ($n = 12$)	31.05 ± 5.06* ($n = 8$)	7.97 ± 2.77* ($n = 8$)	87.75 ± 13.46 ($n = 5$)
+ Endo, + Dex	117.68 ± 30.88 ($n = 6$)	12.99 ± 4.74* ($n = 6$)	4.05 ± 2.07* ($n = 6$)	
(−) Endo	105.35 ± 20.65 ($n = 11$)	52.49 ± 20.08* ($n = 8$)	19.89 ± 8.01* ($n = 8$)	112.96 ± 34.30 ($n = 5$)
(−) Endo, + Dex	106.78 ± 15.47 ($n = 6$)	120.65 ± 31.74 ($n = 6$)	114.19 ± 33.04 ($n = 6$)	

*Denote significant ($P < 0.05$) differences from corresponding controls.

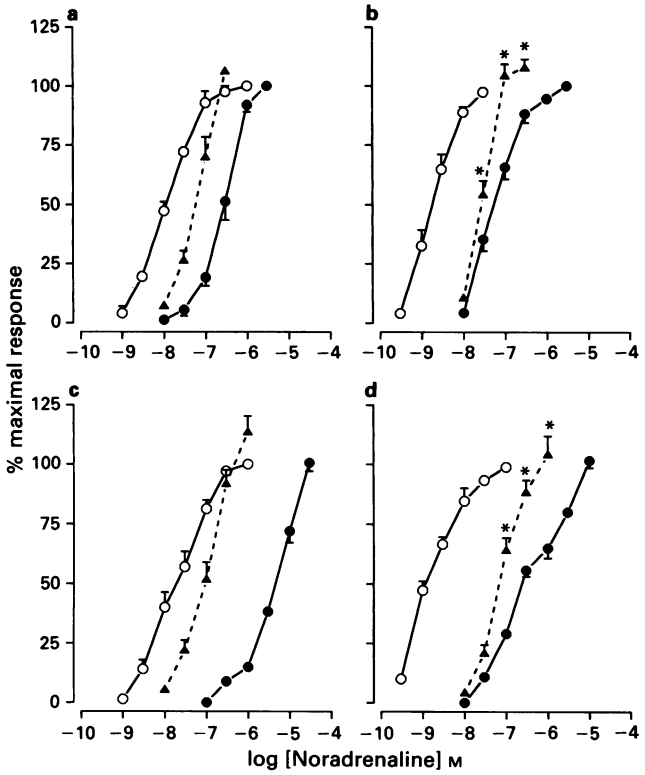

Figure 3 The effects of N^G-monomethyl-L-arginine (L-NMMA) on the antagonism of concentration-response curves to noradrenaline (NA) by 0.3 μM phentolamine (a,b) and 3 nM prazosin (c,d) in aortic rings with intact (a,c) or denuded (b,d) endothelium. In all panels, (○), represent NA control responses, while (●) and (▲) respectively represent the responses to NA in the presence of the antagonist alone, and antagonist + 500 μM L-NMMA. Each data point on the graphs represents the mean ± s.e. ($n = 5$). *Denote statistically significant difference from the corresponding responses in the presence of the antagonist alone.

16.1 ± 4.6 ($n = 6$) respectively in endothelium-intact rings; and, 2.4 ± 0.4 ($n = 21$) versus (1.9 ± 0.5 ($n = 11$) respectively in endothelium-denuded rings. However, following 5 h of tissue pre-equilibration in PSS, EC_{50}s for NA were significantly ($P < 0.05$) higher than comparative values obtained during shorter-term pre-equilibration (Table 2). EC_{50}s for NA in denuded, but not intact rings, pre-equilibrated for 5 h with PSS containing 0.5 μM dexamethasone were significantly lower. Treatment with L-NAME (100 μM) potentiated NA-induced contractions in 5 h PSS pre-equilibrated, endothelium-intact and denuded rings; however, there was no such potentiation in denuded rings equilibrated in PSS for only 1 h. The presence of dexamethasone in the PSS selectively antagonized L-NAME-induced potentiation in denuded rings (Figure 4). Regardless of whether the endothelium was intact or denuded, NA dose-ratios, with prazosin as the antagonist, were similar in control versus dexamethasone-treated rings (see Table 1); L-NAME at 100 μM, still significantly reduced the dose-ratios in dexamethasone-treated rings with intact endothelium, but, it had no significant effect in endothelium-denuded rings (see Table 1).

Table 2 EC_{50} values (nM) for noradrenaline (NA) in endothelium-intact or denuded aortic rings, and pre-equilibrated for 1 or 5 h, in physiological salt solution with/without 0.5 μM dexamethasone (Dex)

	− *Dex*		+ *Dex*	
	1 h	5 h	1 h	5 h
+ Endo	23.8 ± 7.0 ($n = 31$)	114.0 ± 19.1[a] ($n = 5$)	16.1 ± 4.6 ($n = 6$)	82.3 ± 19.2[a] ($n = 4$)
− Endo	2.4 ± 0.4 ($n = 21$)	33.6 ± 7.8[a] ($n = 6$)	1.9 ± 0.5 ($n = 11$)	14.4 ± 3.3[a,b] ($n = 5$)

Data are expressed as means ± s.e., (n).
[a] and [b] respectively denote statistically significant differences ($P < 0.05$) from corresponding values obtained after 1 h pre-equilibration, and in the absence of dexamethasone.

Interaction of L-NAME with NA after treatment with PBZ

In aortic rings with/without endothelium, and treated with 5 or 10 nM PBZ, to alkylate α_1-adrenoceptors, contractions initiated by NA had a reduced E_{max}. Pretreatment with L-NAME (100 μM) restored responsiveness to NA in rings with/without endothelium (Figure 5). However, following treatment with 0.5 μM PBZ, both endothelium intact and denuded rings failed to respond to NA; L-NAME, in concentrations up to 1 mM, failed to reverse this inhibition (see Figure 5).

Are the effects of L-NAME specific for α-adrenoceptor-mediated events?

We also examined the effects of L-NAME on 5-HT-mediated contractions in the absence and presence of the 5-HT_2 antagonist, ritanserin, in both endothelium-intact and denuded aortic rings. 5-HT (0.1–30 μM) initiated concentration-related contractions of rat aortic rings with E_{max} of 0.64 ± 0.09 and 1.46 ± 0.18 g tension respectively for endothelium-intact and denuded rings. L-NAME (100 μM) potentiated the 5-HT contractions in intact but not in denuded

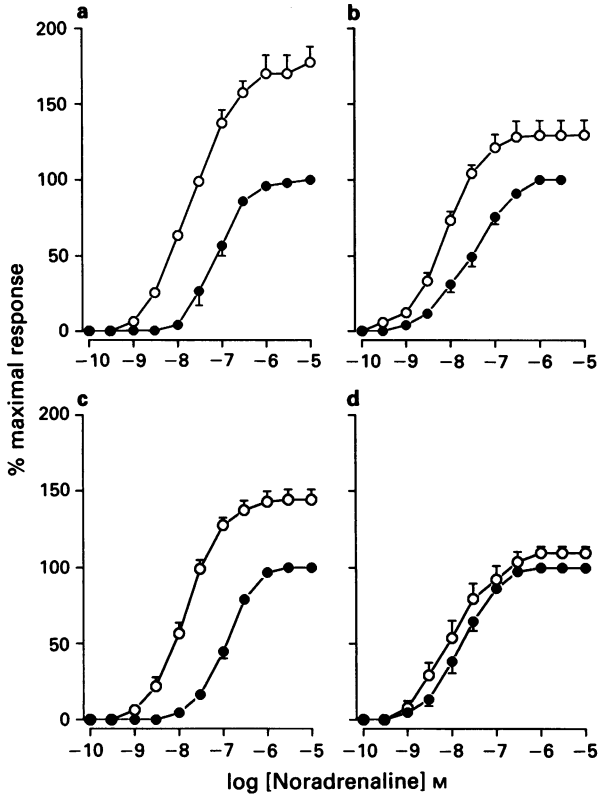

Figure 4 Potentiating effect of N^G-nitro-L-arginine methyl ester (L-NAME, 100 μM) on concentration-response curves to noradrenaline (NA) in endothelium-intact (a,c) and denuded (b,d) aortic rings after 5 h equilibration in normal PSS (a,b) or PSS containing 0.5 μM dexamethasone (c,d). In both panels, (●) and (○) respectively represent the responses to NA in the absence and presence of 100 μM L-NAME. Each data point is mean ± s.e. ($n = 5$).

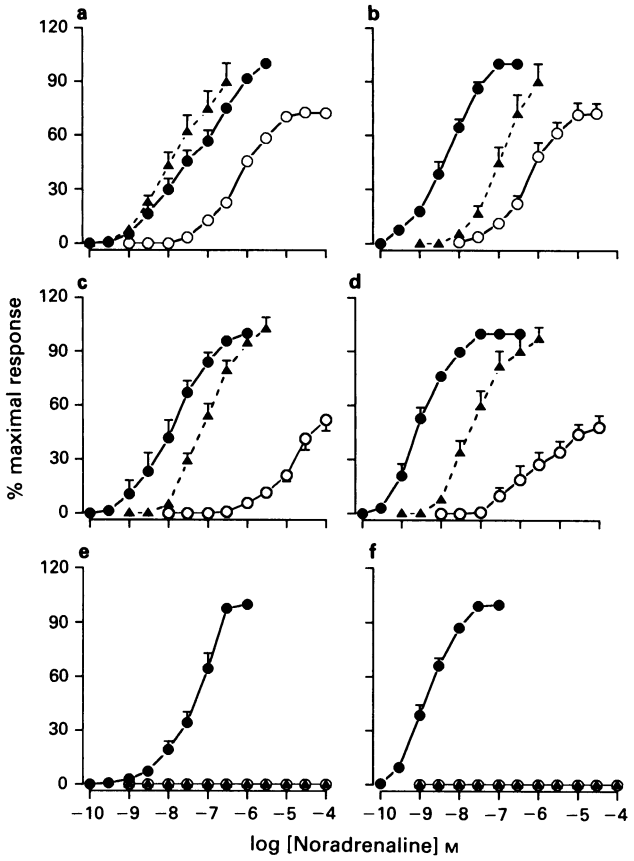

Figure 5 Effects of N^G-nitro-L-arginine methyl ester (L-NAME) after antagonism of contractions to noradrenaline (NA) by 5 (a,b), 50 (c,d) and 500 (e,f) nM phenoxybenzamine (PBZ) in endothelium-intact (a,c,e), and denuded (b,d,f) aortic rings. In all panels, (●) represent control responses to NA, while (○) indicate NA responses after treatment with the antagonist alone, and (▲), antagonist treatment + 100 μM L-NAME. Each data point represents the mean ± s.e. ($n = 5$).

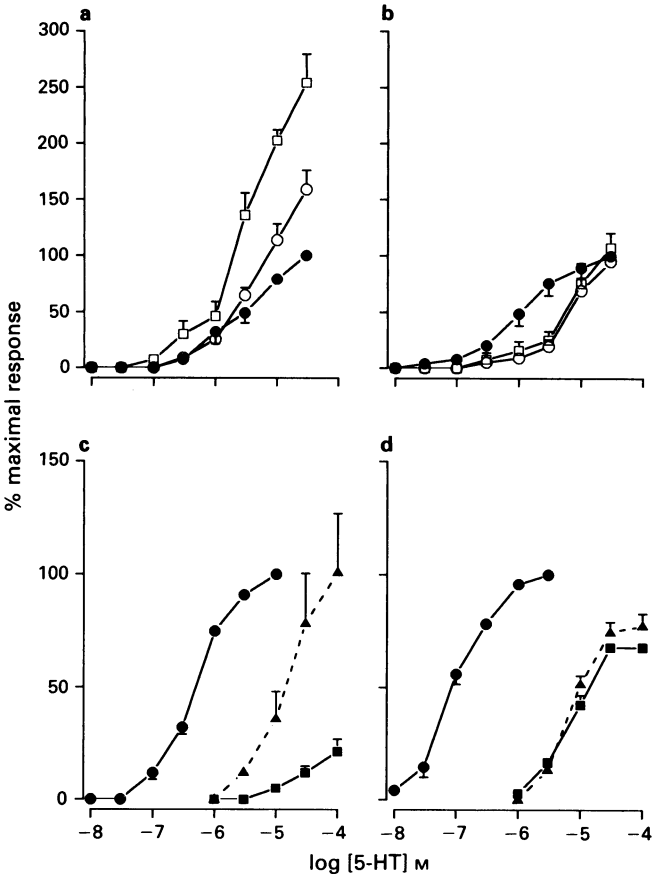

Figure 6 Effect of N^G-nitro-L-arginine methyl ester (L-NAME) (a) and D-NAME (b) on the concentration-response curves to 5-hydroxytryptamine (5-HT), and, of L-NAME on the antagonism of 5-HT responses by ritanserin (c,d) in aortic rings with (c) or without (d) endothelium. For (a,b), (●), represents the control responses, while (○) and (□) respectively represent responses in the presence of 10 and 100 μM L-, or D-NAME. In (c,d), (●), represents the control 5-HT responses, while (■) and (▲) respectively represent 5-HT responses in the presence of 10 nM ritanserin alone, and ritanserin + 100 μM L-NAME. Each data point represents the mean ± s.e. ($n = 4$).

rings (Figure 6a). Ritanserin, 10 nM, non-competitively antagonized responses to 5-HT, and treatment with 100 μM L-NAME resulted in a partial restoration of 5-HT contractions in endothelium-intact, but not in denuded rings (Figure 6b).

Discussion

The ability of endothelium-derived nitric oxide (EDNO) to mediate vascular relaxation (Moncada *et al.*, 1987) and to modulate agonist-induced contractile responses of the vasculature (Miller *et al.*, 1988) is very well documented. The data from the present study, are in accord with these established facts. However, this study has also provided evidence that constitutive, as well as inducible, NO synthase(s) contribute to the actions of L-NAME and L-NMME, viz enhancement of NA contractions, and reduction of the effects of α-adrenoceptor antagonists in endothelium-denuded rings. Evidence that a smooth muscle NO synthase contributed to the effects of NO synthase inhibition was provided by the ability of dexamethasone to inhibit the enhancement of responses to NA following either L-NAME or L-NMMA treatment, and to reverse antagonism of NA by α-adrenoceptor antagonists in denuded rings.

The role of the rat aortic endothelium as a generator of NO, and modulator of contractile response, is clearly evident in the present study: the NO synthase inhibitors produced an endothelium-dependent enhancement of NA-, and also 5-HT-, induced contractions, with L-NAME, being more potent than L-NMMA. As expected, the D-isomers of both of these NO synthase inhibitors were ineffective. It has previously been demonstrated that L-arginine, but not its D-enantiomer, is the substrate for NO synthesis (Palmer *et al.*, 1988) and that L-NMMA, but not its D-isomer (Rees *et al.*, 1989) and L-NAME are competitive inhibitors of the endothelial NO synthase (Rees *et al.*, 1990b); the latter having been shown to be an irreversible inhibitor of the brain NO synthase (Dwyer *et al.*, 1991).

A second aspect of our study relates to the interaction between NO synthase inhibitors and α-adrenoceptor antagonists in aortic rings with/without endothelium. The dose-ratios for NA in the presence of the competitive α-adrenoceptor antagonists, phentolamine, prazosin and WB 4101 were significantly reduced by L-NAME and L-NMMA in rings with intact or denuded of endothelium. It might be argued that the reduction of NA dose-ratios in endothelium-intact rings results from the inhibition of endothelial NO production by L-NAME, or L-NMMA. However, this does not explain the stereospecific reversal of α-adrenoceptor blockade that occurred in denuded rings. The latter data suggest the involvement of an inducible smooth muscle NO synthase in denuded rings. The ability of L-NAME/L-NMMA to reverse α-adrenoceptor blockade may thus relate to the approximately 5 h incubation period in PSS following the initial equilibration of the aortic rings and the completion of the

experiment (see protocol 2). Evidence implicating the inducible vascular smooth muscle (VSM) NO synthase in the reversal phenomenon include: (a) the significant increases in NA EC_{50} values for tissues equilibrated in PSS for 5 h versus 1 h; treatment with L-NAME restored the EC_{50}s to near control values. (b) Dexamethasone prevented the effects of L-NAME on NA C-R curves and also on the reversal phenomenon in denuded rings. The induction of smooth muscle NO synthase, which can be prevented by the glucocorticoids (Rees *et al.*, 1990a), has previously been demonstrated to require a lag period of 2 h, with maximal inducible enzyme activity detectable in 6–12 h (Radomski *et al.*, 1990). Furthermore, Schini & Vanhoutte (1991) have also shown that rat thoracic aorta is endowed with an inducible NO synthase which can be detected after prolonged (8 h) equilibration in PSS.

The ineffectiveness of dexamethasone on both potentiation and reversal phenomenon in endothelium-intact rings is surprising in view of the findings by Radomski *et al.* (1990) that the vascular endothelium also expresses an inducible, Ca^{2+}-independent NO synthase after activation *in vitro* with lipopolysaccharide (LPS) and interferon-γ (IFN-γ). In our study, no such activation of the inducible NO synthase was apparent, except in denuded rings, thus suggesting that endothelial denudation, or damage, may, in addition to LPS and IFN-γ, serve as a trigger for the induction of the smooth muscle NO synthase and also that this enzyme system may function as a physiological safeguard when there is a dysfunction in the constitutive synthase system.

It has been known for some time that glucocorticoids can potentiate the responses of vascular smooth muscle to the effects of catecholamines (Kalsner, 1969; Yard & Kadowitz, 1972). Glucocorticoid receptors, which bind dexamethasone, have been demonstrated in VSM cells (Dural *et al.*, 1977; Kornel *et al.*, 1981) thus suggesting a direct effect of glucocorticoids on VSMs as the basis, at least in part, for the pathogenesis of glucocorticoid-induced hypertension (Romas-Frendo *et al.*, 1985). Our data also indicate a significant reduction of the EC_{50} value for NA in the presence of dexamethasone in endothelium-denuded aortic rings, but not in the endothelium-intact rings where active synthesis of NO mediated by a constitutive enzyme population is presumably uninterrupted. Thus, considering that the period of time following dissection was comparable for both endothelium-denuded and intact tissues, it is compelling to conclude that the effects of dexamethasone are mediated, in denuded tissues, by an inhibition of the production of an inducible aortic smooth muscle NO synthase rather than a direct receptor effect.

The contractile effect of NA on the rat thoracic aorta is mediated by the activation of α_1-adrenoceptors, possibly coupled to two different signal transduction processes, one of which mobilizes intracellular Ca^{2+} and the other activates the translocation of extracellular Ca^{2+} (Mir & Fozard, 1989; Oriowo & Ruffolo, 1992; Oriowo *et al.*, 1992). Our study of the effect(s) of L-NAME in PBZ-treated tissues was designed to determine the dependency, or otherwise, of NO synthase activation on the α_1-adrenoceptor-mediated contractile process. In aortic rings with/without endothelium, contractions occurred to NA, and L-NAME evoked a reversal of the inhibition of NA contractile responses in aortic rings with/without endothelium. L-NAME reversed the antagonism of NA contractions induced by PBZ treatment, and, when PBZ concentration was sufficiently high to cause total abolition of NA-induced contractions, treatment with L-NAME failed to reverse the inhibition in rings with/without endothelium. It thus seems that the reversal of α-adrenoceptor blockade by L-NAME is related to the ability of the agonist to evoke aortic contractions. It is unclear, however, why L-NAME should fail to reverse the antagonism of 5-HT_2 receptors by ritanserin, in endothelium-denuded rings. Our expectation was that within the time frame of these experiments, 4–5 h, vascular NO synthase activity should have been induced.

In conclusion, the current data has produced evidence in support of two types of NO synthase activities in rat isolated aortic rings: (a) endothelial NO synthase, the action of which modulates contractile responses to NA and 5-HT; and (b) an inducible smooth muscle NO synthase(s), the induction of which is enhanced by endothelial cell removal and can be prevented by preequilibration with dexamethasone. Both enzymes are inhibited in a stereospecific manner by either L-, NAME or NMMA, with resultant increased response and sensitivity to vasoconstrictor influences.

We are grateful to the Alberta Heart and Stroke Foundation for financial support, and to Ciba-Geigy Corp. (Summit, NJ, U.S.A.), Pfizer Canada Inc. (Arnprior, Ontario, Canada) and Dr S. Moncada (Wellcome Research Laboratories, Kent, U.K.) for generous gifts of phentolamine, prazosin and D-NMMA respectively. We also thank Dr Meg Kargacin for useful suggestions during the preparation of this manuscript.

References

ALLAN, G., BROOKS, C.D., CAMBRIDGE, D. & HLADKIWSKYJ, J. (1983). Enhanced responsiveness of vascular smooth muscle to vasoconstrictor agents after removal of endothelial cells. *Br. J. Pharmacol.*, **79**, 334P.

ALOSACHIE, I. & GODFRAIND, T. (1986). Role of cyclic GMP in the modulation by endothelium of the adrenolytic action of prazosin in the rat isolated aorta. *Br. J. Pharmacol.*, **89**, 525–532.

ALOSACHIE, I. & GODFRAIND, T. (1988). The modulatory role of vascular endothelium in the interaction of agonists and antagonists with α-adrenoceptors in the rat aorta. *Br. J. Pharmacol.*, **95**, 619–629.

CARMAN-KRZAN, M. (1985). Role of endothelium in the binding of [^{3}H] prazosin to the aortic α_1-adrenergic receptors. *Eur. J. Pharmacol.*, **111**, 137–138.

CARRIER, G.O. & WHITE, R.E. (1985). Enhancement of alpha-1 and alpha-2 adrenergic agonist-induced vasoconstriction by removal of endothelium in rat aorta. *J. Pharmacol. Exp. Ther.*, **232**, 682–687.

COLLIER, J. & VALLANCE, P. (1989). Second messenger role for NO widens to nervous and immune systems. *Trends Pharmacol. Sci.*, **10**, 427–431.

DESAI, K.M., SESSA, W.C. & VANE, J.R. (1991). Involvement of nitric oxide in the reflex relaxation of the stomach to accomodate food or fluid. *Nature*, **351**, 477–479.

DURAL, D., FUNDER, J.W., DEVYNCK, M. & MEYER, P. (1977). Arterial glucocorticoid receptors: the binding of tritiated dexamethasone in rabbit aorta. *Cardiovasc. Res.*, **11**, 529–535.

DWYER, M.A., BREDT, D.S. & SNYDER, S.H. (1991). Nitric oxide synthase: irreversible inhibition by L-N^G-nitroarginine in brain in vitro and in vivo. *Biochem. Biophys. Res. Commun.*, **176**, 1136–1141.

EGLEME, C., GODFRAIND, T. & MILLER, R.C. (1984). Enhanced responsiveness of rat isolated aorta to clonidine after removal of the endothelial cells. *Br. J. Pharmacol.*, **81**, 016–018.

GARTHWAITE, J., CHARLES, S.L. & CHESS-WILLIAMS, R. (1988). Endothelium-derived relaxing factor release on activation of NMDA receptors suggests role as intracellular messenger in the brain. *Nature*, **336**, 385–388.

IGNARRO, L.J. (1989). Endothelium-derived nitric oxide: actions and properties. *FASEB J.*, **3**, 31–36.

KALSNER, S. (1969). Mechanism of hydrocortisone potentiation of responses to epinephrine and norepinephrine in rabbit aorta. *Circ. Res.*, **24**, 383–395.

KORNEL, L., KANARMARLAPUDI, N., TRAVVERS, T., TAFF, D., PATEL, N., CHEN, C., BAUM, R. & RAYNOR, W. (1981). Studies on high affinity binding of mineralo- and glucocorticoids in rabbit aorta cytosol. *J. Steroid Biochem.*, **16**, 282–293.

LUES, I. & SCHUMANN, H.J. (1984). Effect of removing the endothelial cells on the reactivity of rat aortic segments to different α-adrenoceptor agonists. *Naunyn-Schmiedebergs Arch. Pharmacol.*, **328**, 160–163.

MARTIN, W., FURCHGOTT, R.F., VILLANI, G.M. & JOTHIANANDAN, D. (1986). Depression of contractile responses in rat aorta by spontaneously released endothelium-derived relaxing factor. *J. Pharmacol. Exp. Ther.*, **237**, 529–538.

MILLER, R.C., SCHINI, V. & SCHOEFFTER, P. (1988). Modulation by the endothelium of agonist-induced contractions of vascular smooth muscle. In *Relaxing and Contracting Factors, Biological and Clinical Research*. ed. Vanhoutte, P.M., pp. 241–265. Clifton, N.J., Humana Press Inc.

MIR, A.K. & FOZARD, J.R. (1989). A single α_1-adrenoceptor, distinct from the α_{1A}- and α_{1B}-subtypes, may initiate contraction of the rat aorta to phenylephrine. *Br. J. Pharmacol.*, **98**, 651P.

MONCADA, S., HERMAN, A.G. & VANHOUTTE, P.M. (1987). Endothelium-derived relaxing factor is identified as nitric oxide. *Trends Pharmacol. Sci.*, **8**, 365–367.

MONCADA, S., PALMER, R.M.J. & HIGGS, E.A. (1989). Biosynthesis of nitric oxide from L-arginine, a pathway for the regulation of cell function and communication. *Biochem. Pharmacol.*, **38**, 1709–1715.

MOSTAGHIM, R., THOMAS, G. & RAMWELL, P.W. (1988). Endothelial potentiation of relaxation response to phentolamine in rat thoracic aorta. *J. Pharmacol. Exp. Ther.*, **244**, 475–478.

ORIOWO, M.A., NICHOLS, A.J. & RUFFOLO Jr., R.R. (1992). Receptor protection studies with phenoxybenzamine indicate that a single α_1-adrenoceptor may be coupled to two signal transduction processes in vascular smooth muscle. *Pharmacology*, **45**, 17–26.

ORIOWO, M.A. & RUFFOLO Jr., R.R. (1992). Activation of a single alpha-1-adrenoceptor subtype in rat aorta mobilizes intracellular and extracellular pools of calcium. *Pharmacology*, **44**, 139–149.

PALMER, R.M.J., ASHTON, D.S. & MONCADA, S. (1988). Vascular endothelial cells synthesize nitric oxide. *Nature*, **333**, 664–666.

PALMER, R.M.J. & MONCADA, S. (1989). A novel citrulline-forming enzyme implicated in the formation of nitric oxide by vascular endothelial cells. *Biochem. Biophys. Res. Commun.*, **158**, 348–352.

PALMER, R.M.J., FERRIGE, A.G. & MONCADA, S. (1987). Nitric oxide release accounts for the biological activity of endothelium-derived relaxing factor. *Nature*, **327**, 524–526.

RADOMSKI, M.W., PALMER, R.M.J. & MONCADA, S. (1990). Glucocorticoids inhibit the expression of an inducible, but not the constitutive, nitric oxide synthase in vascular endothelial cells. *Proc. Natl. Acad. Sci. U.S.A.*, **87**, 10043–10047.

REES, D.D., CELLEK, S., PALMER, R.M.J. & MONCADA, S. (1990a). Dexamethasone prevents the induction by endotoxin of a nitric oxide synthase and the associated effects on vascular tone: an insight into endotoxin shock. *Biochem. Biophys. Res. Commun.*, **173**, 541–547.

REES, D.D., PALMER, R.M.J., HODSON, H.F. & MONCADA, S. (1990b). Characterization of three inhibitors of endothelial nitric oxide synthase *in vitro* and *in vivo*. *Br. J. Pharmacol.*, **101**, 746–752.

REES, D.D., PALMER, R.M.J. & MONCADA, S. (1989). Role of endothelium-derived nitric oxide in the regulation of blood pressure. *Proc. Natl. Acad. Sci. U.S.A.*, **86**, 3375–3378.

ROMAS-FRENDO, B., ELOY, L. & GRUNFELD, J.P. (1985). Methylprednisolone-induced hypertension in the rat: evidence against the role of plasma volume changes in vasopressin and renal prostaglandin E_2. *J. Hypertens.*, **3**, 461–467.

SCHINI, V.B. & VANHOUTTE, P.M. (1991). L-arginine evokes both endothelium-dependent and -independent relaxations in L-arginine-depleted aortas of the rat. *Circ. Res.*, **68**, 209–216.

YARD, A.C. & KADOWITZ, P.J. (1972). Studies on the mechanism of hydrocortisone potentiation of vasoconstrictor responses to epinephrine in the anesthetized animal. *Eur. J. Pharmacol.*, **20**, 1–9.

(Received December 21, 1992
Revised February 1, 1993
Accepted February 9, 1993)

Br. J. Pharmacol. (1993), **109**, 502–509 © Macmillan Press Ltd, 1993

Investigations of the dual contractile/relaxant properties showed by antioquine in rat aorta

M. Dolores Ivorra, *Claire Lugnier, Maria Catret, Elsa Anselmi, Diego Cortes & [1]Pilar D'Ocon

Laboratorio de Farmacognosia y Farmacodinamia, Departamento de Farmacologia, Facultad de Farmacia, Universidad de Valencia, Avda Vicent Andrés Estelles, s/n 46100 Burjasot, Valencia, Spain and *Laboratoire de Pharmacologie Cellulaire et Moleculaire, Faculté de Pharmacie, Université Louis Pasteur CNRS URA 600, BP 24, 67401 Illkirch, France

1 In the present study we assessed the activity of antioquine, a bisbenzyltetrahydroisoquinoline alkaloid isolated from *Pseudoxandra sclerocarpa*, by examining its effects on the contractile activity of rat isolated aorta, specific binding of [^{3}H]-(+)-*cis*-diltiazem, [^{3}H]-nitrendipine and [^{3}H]-prazosin to cerebral cortical membranes and the different molecular forms of cyclic nucleotide phosphodiesterases (PDE) isolated from bovine aorta.

2 Contractions in rat aorta induced by high concentrations of KCl (80 mM) and noradrenaline (1 μM) were inhibited by antioquine in a concentration-dependent manner (0.1 μM– 300 μM). The alkaloid appeared more potent against KCl-induced contractions. This inhibitory effect was observed at both 37°C and 25°C.

3 Paradoxically, at the highest concentration tested (300 μM) antioquine induced a contractile response of similar magnitude in the presence and absence of extracellular calcium, at 37°C. This activity was greatly attenuated at 25°C. Antioquine-induced contractions were not inhibited by prazosin (0.1 μM), nifedipine (1 μM) or diltiazem (100 μM). On the contrary, prazosin and nifedipine slightly increased the contractions in the presence of extracellular calcium. Papaverine (100 μM) partially inhibited the contractile response to antioquine both in the presence and absence of extracellular calcium.

4 At 25°C, in Ca^{2+}-free solution, antioquine (300 μM) did not modify the contractile response (phasic and tonic) evoked by noradrenaline, but increased the phasic contraction induced by caffeine. At 37°C, the contraction elicited by antioquine made it impossible to observe the noradrenaline-induced one.

5 Antioquine showed affinity for the [^{3}H]-prazosin binding site and for the [^{3}H]-(+)-*cis*-diltiazem binding site of the Ca^{2+}-channel receptor complex, but had no effect at the dihydropyridine binding site in rat cerebral cortex.

6 Antioquine weakly inhibited some PDE forms isolated from bovine aorta: a CaM-PDE (PDE I) which preferentially hydrolyzes cyclic GMP and is activated by calmodulin, and a rolipram-sensitive cyclic AMP-PDE (PDE IV) which hydrolyzed cyclic AMP. Antioquine did not exert any inhibitory effect on the other forms of PDE, a cyclic GMP selective form (PDE V) and a low K_m cyclic AMP-PDE that is inhibited by cyclic GMP (CGI-PDE, PDE III).

7 The present work provides evidence that antioquine has properties both as a calcium entry blocker (possibly through the benzothiazepine recognition site in the calcium channel) and as a contractile agent. Its mechanism of action as a contractile agent is not related to Ca^{2+}-entry and is hypothetically similar to that of calyculin-A or okadaic acid. The possible involvement of α-adrenoceptors in this paradoxical effect cannot be excluded. The rigidity of the molecule provides an interesting model for analyzing this contractile mechanism and the intracellular processes involved.

Keywords: Antioquine; α_1-adrenoceptors; calcium antagonists; rat aorta; intracellular calcium

Introduction

Antioquine, a bisbenzyltetrahydroisoquinoline (BBTHIQ) alkaloid, was isolated from the stem bark of an endemic Columbian plant *Pseudoxandra sclerocarpa* (Cortes *et al.*, 1985; 1986). It is the main alkaloid from this species and is closely related structurally to tetrandrine (Figure 1), another BBTHIQ alkaloid isolated from *Stephania tetrandra*, that has been reported to possess effects on heart rate (*in vitro* and *in vivo*) and blood pressure, as does verapamil (Wang & Liu, 1985) which is consistent with tetrandrine being a calcium channel blocker (Wang & Liu, 1985; Fang & Jiang, 1986a,b; Yao *et al.*, 1987; Triggle *et al.*, 1989; Chen & Liu, 1990). Recently, other BBTHIQs, including dauricine (Dongke *et al.*, 1987) and (−)-daurisoline (Lu & Liu, 1990) have also been shown to have Ca^{2+} channel blocking properties.

It has been suggested that the mechanism of action of tetrandrine is related to an allosteric modulation of phenylalkylamine and 1,4-dihydropyridine binding, apparently through interactions at the benzothiazepine receptor site at the L-channel (King *et al.*, 1988; Triggle *et al.*, 1989; Glossman *et al.*, 1991). Structurally, tetrandrine is unique among the known chemical classes of calcium entry blockers (Triggle *et al.*, 1989; Dong *et al.*, 1992). It is a dimer of two benzylisoquinoline subunits condensed in a head to head, tail to tail fashion with 1S, 1'S, stereochemistry at the chiral isoquinoline carbons. Antioquine (Figure 1), shows a peculiar linkage by a biphenyl bond between the monomer BIQ rings (C11–C11') and the second bridge, a diaryl ether (C7–C7'), is more common in nature and it also appears in tetrandrine.

Preliminary studies (D'Ocon *et al.*, 1989; Ivorra *et al.*, 1992a) have shown that antioquine and several BBTHIQ alkaloids preferentially relax sustained contractions induced by KCl and induce a displacement to the right of the dose-response curves to $CaCl_2$ in rat isolated uterus. These results suggest that the relaxant effects of antioquine may be due to the blockade of calcium movements across the cell membrane in a similar way to the action of tetrandrine. The aim of the present study was to examine the mechanism of action of

[1] Author for correspondence.

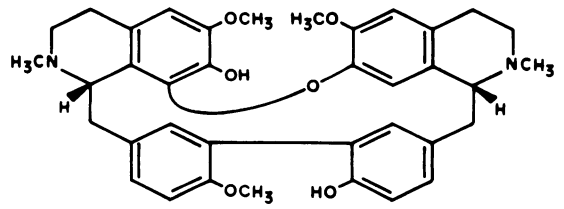

Antioquine

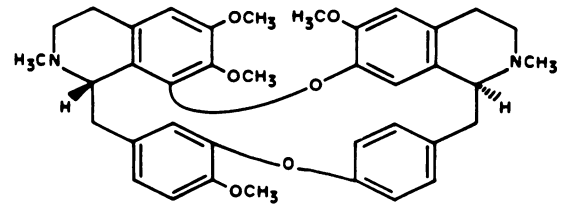

Tetrandrine

Figure 1 Chemical structures of antioquine and tetrandrine.

antioquine by means of functional studies on rat aorta contracted by addition of noradrenaline, caffeine and KCl; radioligand binding studies using [^{3}H]-(+)-*cis*-diltiazem, [^{3}H]-nitrendipine, [^{3}H]-prazosin, and determination of inhibitory effects on cyclic nucleotide phosphodiesterase (PDE) activity.

We have examined the inhibitory effect of antioquine on the following cytosolic molecular forms of PDE isolated from bovine aorta: a PDE form called CaM-PDE, which preferentially hydrolyzes guanosine 3':5'-cyclic monophosphate (cyclic GMP) and is activated by calmodulin (CaM); a cyclic GMP selective form (cGMP-PDE) insensitive to the stimulatory effect of CaM; and two PDE forms, one belonging to the cyclic GMP-inhibited family (CGI-PDE, type III) and the other a rolipram-sensitive form (cAMP-PDE, type IV) (Lugnier *et al.*, 1986; Ivorra *et al.*, 1992b), which specifically hydrolyze adenosine 3':5'-cyclic monophosphate (cyclic AMP) with a low K_m and not stimulated by the addition of Ca^{2+}-CaM.

Methods

Functional study

Helically cut strips of thoracic aorta (denuded of endothelium) of male Wistar rats (200–220 g) were prepared and mounted as described by Furchgott & Zawadzki (1980). Each preparation was suspended in a 10 ml organ bath containing Krebs-bicarbonate solution (KBS), maintained at 37°C and gassed with 95% O_2 and 5% CO_2. An initial load of 1 g was applied to each preparation and maintained throughout a 75–90 min equilibration period before agonist addition. Tension was recorded isometrically on a Phillips recorder (PM 8222) coupled to a Hewlett Packard amplifier (8805D) via force-displacement transducers (Gould Statham UC2).

A series of experiments was performed in KBS in order to determine if and to what extent antioquine induced a contractile response and/or relaxed rat aorta precontracted by noradrenaline or KCl. Contractions were expressed in mg (noradrenaline- or KCl-induced contractions) or as a percentage of the previous noradrenaline-induced contraction (antioquine-induced contractile response). Concentration-response curves of relaxation were obtained by the addition of cumulative concentrations of antioquine following the achievement of sustained contractions with noradrenaline (1 μM) or KCl (80 mM). Relaxations were expressed as a percentage of the maximum tension obtained by agonist addition. E_{max} values representing the maximal relaxation obtained after addition of the highest dose of antioquine were calculated. The concentration needed to produce 50% inhibition (IC_{50}) was also calculated for each preparation from a least squares regression analysis of all points between 20–80% of the maximal response.

Figure 3a shows the experimental procedure used to study the action of antioquine on noradrenaline-induced contraction in the absence of extracellular calcium at 37°C or 25°C. In order to clarify the intracellular action of antioquine, similar experimental procedures were performed but noradrenaline was replaced by caffeine (Figure 3b). Caffeine yielded a contraction only at 25°C in Ca-free medium, so in protocols using caffeine as agonist, the temperature was decreased to 25°C.

After incubation for 1 h in KBS to stabilize the preparation, 1 μM noradrenaline or 10 mM caffeine were administered to contract the muscle, and the amplitude of the resultant contraction was monitored as a reference. The solution was then replaced by Ca^{2+}-free solution and left for 15 min before 1 μM noradrenaline or 10 mM caffeine was added and the contractile response monitored as a measure of the amount of Ca^{2+} released from the store sensitive to the agonist. After washing, a new addition of the agonist, noradrenaline or caffeine, did not elicit any contractile response. The solution was then replaced by normal KBS and left 20 min to refill the depleted Ca^{2+} stores. Noradrenaline or caffeine were again administered after 15 min in Ca^{2+}-free solution.

In rat aorta, contractile response to noradrenaline in Ca-free medium is associated with two different internal Ca-pools, one of which is common to caffeine (Noguera & D'Ocon, 1992). Further experiments were performed at 37°C and 25°C to test the effects of antioquine on Ca^{2+} release from the intracellular storage site sensitive only to noradrenaline. Figure 4 shows the experimental procedure used.

Contractions induced by antioquine in Ca^{2+}-free KBS were also obtained after addition of noradrenaline in Ca^{2+}-containing solution. The time of exposure to antioquine was 45 min in all cases. All contractile responses in Ca^{2+}-free medium were expressed as a percentage of the noradrenaline or caffeine-induced contraction in normal KBS.

Statistical analysis

Results are expressed as the mean ± s.e.mean of n preparations obtained from different animals. Statistical significance of differences between the means was assessed by Student's t test for unpaired data. P values of less than 0.05 were considered to represent significant differences.

Radioligand binding experiments

Binding of [^{3}H]-prazosin to rat cerebral cortex was saturable, reversible and showed high affinity, with a dissociation constant K_d of 0.14 nM (Schott *et al.*, 1988). [^{3}H]-nitrendipine and [^{3}H]-*cis*-diltiazem also bound to a single class of binding site in rat cortical membrane homogenate, with K_d values of 0.7 nM and 50 nM, respectively (Schaeffer *et al.*, 1988).

Membranes were prepared from cerebral cortex of male Wistar rats as previously described (Schott *et al.*, 1988). Briefly, the tissue was homogenized in 10 vol (w/v) of ice-cold buffer (50 mM Tris-HCl, pH 7.5) in an Ultra-turrax (twice, 15 s). The homogenate was centrifuged at 40,000 *g* at 4°C for 10 min and the resulting pellet was washed by resuspension and centrifugation under the same conditions. The final pellet was resuspended in incubation buffer to give a final protein concentration of about 1 mg ml^{-1}. Membrane aliquots (250 μl) were incubated in a final volume of 500 μl in 50 mM Tris-HCl (pH 7.5) with [^{3}H]-prazosin (0.1–0.2 nM) or [^{3}H]-nitrendipine (0.3–0.4 nM) or in 50 mM Tris-HCl pH 7.5 containing 1 mg ml^{-1} of bovine serum albumin (BSA) with [^{3}H]-

(+)-*cis*-diltiazem (3–4 nM), in the absence or in the presence of drugs at various concentrations.

Incubations were carried out at 25°C for 30 min ([^{3}H]-prazosin), 90 min ([^{3}H]-nitrendipine) or 120 min ([^{3}H]-(+)-*cis*-diltiazem), after which the reaction was terminated by the addition of 3.0 ml ice-cold buffer and rapid filtration over Whatman GF/B filters that were washed with 9 ml (3 × 3 ml) of ice-cold buffer. For [^{3}H]-(+)-*cis*-diltiazem binding experiments, filters were pretreated for 120 min with polyethylenimine 0.3%. The radioactivity bound to the filters was determined by liquid scintillation counting. Non-specific binding was determined in the presence of 10^{-6} M phentolamine, 10^{-6} M nifedipine or 10^{-5} M diltiazem, respectively. All experiments were performed in triplicate.

Displacement curves were analyzed by a computerized non-linear curve-fitting program and K_i values were calculated from the formula of Cheng & Prussoff (1973).

Phosphodiesterase inhibition

Cytosolic cyclic nucleotide phosphodiesterase activities were isolated from the media layer of bovine aorta by a modification of the methods of Lugnier *et al.* (1986). Briefly, the tissue was homogenized in 10 vol (w/v) isotonic buffer A (25 mM sodium phosphate pH 6.6, 250 mM saccharose, 2 mM magnesium acetate (MgAc), 1 mM dithiothreitol, 5 mM EGTA, 2000 u ml^{-1} aprotinin, 10 μg ml^{-1} soya bean trypsin inhibitor and 10 μg ml^{-1} leupeptin) using an Ultra-turrax (six times, 10 s) and a glass pestle homogenizer, and then centrifuged at 105,000 *g* for 60 min. The resulting supernatant fraction (40 ml) was applied to a DEAE-Sephacel ion-exchange column (15 cm × 1.5 cm) and first eluted by buffer B (25 mM phosphate pH 6.6, MgAc 2 mM and dithiothreitol 1 mM) until no more absorbance was detected in the eluate at 280 nm. Elution was then continued with a linear gradient of 0–0.55 M of NaCl in buffer B (flow rate 25 ml h^{-1}). Each fraction was tested for PDE activity.

Since DEAE-Sephacel did not allow the separation of CaM-PDE from cGMP-PDE, as did DEAE-Trisacryl chromatography (Lugnier *et al.*, 1986) a further higher performance liquid chromatography (h.p.l.c.) repurification was carried out. The first peak was then injected into an h.p.l.c. column (TSK-DEAE-5PW), washed for 20 min with elution buffer (25 mM phosphate pH 6.6) and eluted (0.8 ml min^{-1}) by a linear NaCl gradient (0.05–0.3 M) in elution buffer. Fractions under each PDE activity peak were pooled, dialyzed against buffer (20 mM Tris-HCl, 2 mM MgAc pH 7.5) and stored in aliquots at – 80°C with bovine serum albumin (BSA).

PDE activities were measured by the two-step assay described by Wells *et al.* (1975) at a substrate ([^{3}H]-cyclic AMP or [^{3}H]-cyclic GMP) concentration of 1 μM, in the following buffer: 50 mM Tris-HCl pH 7.5, 2 mM MgAc, 1 mg ml^{-1} BSA and in the presence of 10 μM $CaCl_2$ and 18 nM calmodulin (CaM) or in the absence of calcium and CaM but with 1 mM EGTA. To prevent the influence of cross-contamination between CGI-PDE (PDE III) and cAMP-PDE (PDE IV), the studies performed with these forms were always carried out in the presence of 100 μM rolipram or 100 μM cyclic GMP, respectively.

The IC_{50} (concentration which produced 50% inhibition of substrate hydrolysis) for the compounds studied was determined from the concentration-response curves obtained with five concentrations of inhibitor and calculated by a non-linear regression. The apparent K_i values were obtained according to Cheng & Prusoff (1973). Results are expressed as mean ± s.e.mean of three determinations made in duplicate with three different enzymatic preparations.

Drugs and solutions

The following drugs were used: (–)-noradrenaline L-tartrate and acetylcholine (Merck; Darmstadt, FRG); nifedipine, diltiazem, prazosin, papaverine, caffeine, cyclic AMP, cyclic GMP and phentolamine (Sigma Chemical Co.; St. Louis, U.S.A.); rolipram (Schering AG). Antioquine was isolated by the method of Cortes *et al.* (1985) from *Pseudoxandra sclerocarpa* (Annonaceae).

The composition of KBS was as follows (mM): NaCl 118, KCl 4.75, $CaCl_2$ 1.8, $MgCl_2$ 1.2, KH_2PO_4 1.2, $NaHCO_3$ 25 and glucose 11. Ca-free solution had the same composition except that $CaCl_2$ was omitted and EDTA (0.1 mM) was added.

[^{3}H]-prazosin (20.2 Ci mmol^{-1}), [^{3}H]-nitrendipine (70 Ci mmol^{-1}), [8-^{3}H]-cyclic AMP (30–50 Ci mmol^{-1}) and [8-^{3}H]-cyclic GMP (5–15 Ci mmol^{-1}) were purchased from New England Nuclear. [^{3}H]-(+)-*cis*-diltiazem (154 Ci mmol^{-1}) was obtained from Amersham. Other reagents were of analytical grade.

Caffeine was dissolved in Ca^{2+}-free KBS. Nifedipine was dissolved in ethanol (10^{-2} M) before being diluted in distilled water. The other drugs were dissolved in distilled water. All solutions were prepared daily and pH adjusted to 7.0.

Results

Vasorelaxant response to antioquine

The contractile responses of rat aorta elicited by depolarizing solution (KCl 80 mM) at 37°C or 25°C, were 600.8 ± 48.8 mg ($n = 10$) and 638.3 ± 97.8 mg ($n = 6$) respectively. The same contraction elicited in the presence of phentolamine 10^{-5} M at 37°C, was lower (358.3 ± 33.7 mg, 59.7% of the first one).

Antioquine (0.1–300 μM) produced concentration-dependent relaxations of KCl-depolarized rat aorta at 37°C both in the presence and absence of phentolamine. Experiments performed at 25°C gave similar results (Table 1).

Noradrenaline (1 μM) produced a sustained contraction of rat isolated thoracic aorta incubated in KBS at 37°C (584.2 ± 45.2 mg, $n = 10$) and a similar contraction at 25°C (623.3 ± 86.4 mg, $n = 10$). This dose of noradrenaline has proved to be the maximal for contraction in rat aorta (Noguera & D'Ocon, 1992).

Addition of cumulative concentrations of antioquine (0.1–300 μM) on the sustained contraction induced by noradrenaline 1 μM in KBS induced concentration-dependent relaxations. The E_{max} and IC_{50} values are shown in Table 1. No differences were observed at 37°C or 25°C.

Vasoconstrictor response to antioquine

Noradrenaline (1 μM) produced a sustained contraction in rat isolated thoracic aorta incubated in KBS (see above). After washing, subsequent addition of antioquine 30 μM did not modify the basal tone in KBS or Ca^{2+}-free KBS at 37°C or 25°C. A higher concentration of this alkaloid (300 μM) induced a sustained contractile response in the presence (61.6 ± 2.2%, with respect to noradrenaline-induced contraction in KBS, $n = 6$) or absence (61.0 ± 1.7%, $n = 4$) of extracellular Ca^{2+}, at 37°C (Figure 2). This contractile response

Table 1 Inhibitory potencies of antioquine on contractions induced by noradrenaline, KCl and KCl + phentolamine 10^{-5} M (Phen) at 37°C or 25°C

Temperature		*Noradrenaline*	*KCl*	*KCl + Phen*
37°C	E_{max} (%)	46.7 ± 2.7	63.0 ± 3.7	63.3 ± 4.7
		$n = 14$	$n = 10$	$n = 6$
	IC_{50} (μM)	> 300	185.1 ± 53.9	187.0 ± 65.0
25°C	E_{max} (%)	50.8 ± 3.2	66.4 ± 6.7	
		$n = 6$	$n = 6$	
	IC_{50} (μM)	> 300	154.1 ± 25.3	

Values are mean ± s.e.mean; n = number of experiments.

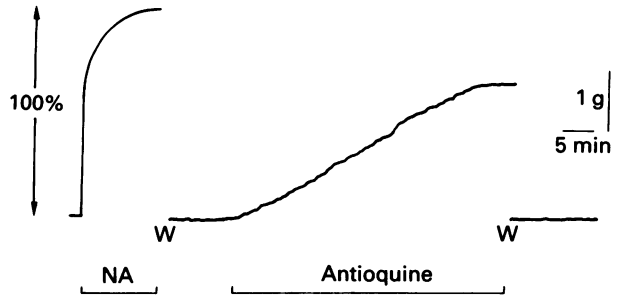

Figure 2 Typical recording of the effects of 300 μM antioquine (ATQ) on rat isolated aorta in the presence or absence of calcium. NA: 1 μM noradrenaline; W: wash.

was significantly less ($P<0.002$) when the experiments were carried out at 25°C (26.0 ± 4.8%, $n=9$ in the presence and 24.3 ± 4.2% in the absence, of extracellular Ca^{2+}).

Prazosin, nifedipine and diltiazem did not inhibit the contractile response to antioquine in the presence or absence of calcium (Table 2). Moreover, prazosin and nifedipine slightly increased the contraction in the presence of extracellular calcium. Papaverine partially inhibited the contractile response to antioquine under both experimental conditions (Table 2).

Effect of antioquine on noradrenaline- or caffeine-induced contractions in a Ca^{2+}-free medium

After 15 min in Ca^{2+}-free solution, addition of noradrenaline 1 μM induced a phasic contraction followed by a tonic one. However, after washing, the contraction was not evoked upon the second application of noradrenaline in Ca^{2+}-free solution. After a 20 min resting period in KBS, the application of noradrenaline after 15 min in Ca^{2+}-free solution induced a contraction similar in magnitude to that produced by its first application, thereby indicating that loading 1.8 mM Ca^{2+} for 20 min had refilled the calcium storage sites.

Addition of antioquine (300 μM) 10 min before addition of noradrenaline, elicited a slowly developed and sustained contraction (14.15 ± 2.06%, $n=7$, with respect to noradrenaline-induced contraction in KBS) at 37°C, but no contractile response to antioquine was observed at 25°C. Subsequent addition of noradrenaline in the presence of antioquine did not modify the profile of the antioquine-induced contraction at 37°C. This response was similar to that obtained when only antioquine (300 μM) was added to Ca^{2+}-free or Ca^{2+}-containing medium. The alkaloid did not modify the contractile response to noradrenaline at 25°C (Table 3).

At 25°C, caffeine 10 mM induced a rapid transient contraction in Ca^{2+} 1.8 mM solution (Table 3, Figure 3b). Addition of caffeine after 15 min of exposure to a Ca^{2+}-free solution yielded a phasic contraction. After washing, addition of caffeine did not induce any contractile response. After a loading period (20 min) in KBS to refill the intracellular Ca^{2+}-stores, the caffeine-induced contraction in Ca^{2+}-free medium (15 min) was restored. Preincubation (10 min) with antioquine (300 μM) increased the phasic contractile response induced by caffeine in Ca^{2+}-free medium after refilling of the intracellular Ca^{2+} stores (Table 3).

Table 2 Effects of different agents on the contractile response induced by antioquine (300 μM) in KBS and Ca^{2+}-free solution

Agent	*Concentration*	*% contraction in KBS*	*% contraction in Ca-free solution*
Control		61.6 ± 2.2	61.0 ± 1.7
		$n=6$	$n=4$
Prazosin	0.1 μM	83.5 ± 3.8*	64.2 ± 4.3
		$n=6$	$n=5$
Nifedipine	1 μM	72.8 ± 3.7*	52.7 ± 4.3
		$n=9$	$n=6$
Diltiazem	100 μM	64.0 ± 3.9	66.8 ± 7.7
		$n=6$	$n=3$
Papaverine	100 μM	32.2 ± 5.1*	21.3 ± 1.6*
		$n=4$	$n=4$

The concentrations of prazosin, nifedipine, diltiazem and papaverine completely inhibited noradrenaline- or KCl-induced contraction in KBS.
% contractions are calculated from the initial contraction by noradrenaline in Krebs solution.
Values are mean ± s.e.mean; n = number of experiments.
*$P<0.002$ compared with control.

Table 3 Effect of antioquine 300 μM (ATQ) on phasic contraction of rat aorta induced by noradrenaline or caffeine in Ca^{2+}-free medium (see Figures 3a and b)

Agonist (A)	*Temperature (°C)*	*A_1 (%)*	*A_2 + ATQ (%)*	n
NA	37°	22.0 ± 1.8	51.1 ± 2.6*[s]	7
NA	25°	26.4 ± 3.5	24.1 ± 2.7	6
Caff	25°	27.5 ± 5.0	48.1 ± 5.4*	5

% are calculated from the initial contraction by noradrenaline (NA) or caffeine (Caff) in Krebs solution.
Values are mean ± s.e.mean; n = number of experiments.
*$P<0.005$ compared with A_1.
[s]Sustained contraction after 45 min of exposure to antioquine.
A_1: addition of agonist after 15 min in Ca^{2+}-free medium.
A_2: addition of agonist after depletion, complete refilling of internal Ca^{2+}-stores and subsequent loading for 15 min in Ca^{2+}-free medium.

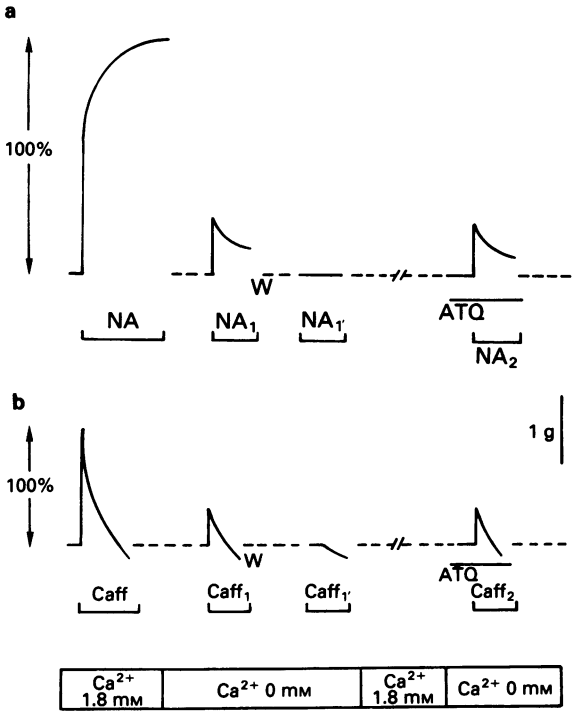

Figure 3 Schematic representation of the effect of antioquine on noradrenaline (NA)-induced contraction (a) or caffeine (Caff)-induced contraction (b) in the absence of extracellular calcium. NA_1 or $Caff_1$: addition of the agonist after 15 min incubation in Ca^{2+}-free medium. $NA_{1'}$ of $Caff_{1'}$: second addition of the agonist after washing (W) in Ca^{2+}-free medium. NA_2 or $Caff_2$: addition of the agonist in presence of antioquine (ATQ) 300 μM, after a 15 min resting period in KBS (Ca^{2+} 1.8 mM) and 20 min in Ca^{2+}-free solution.

Addition of noradrenaline (1 μM) in Ca^{2+}-free medium (NA_1, Figure 4) elicited a contractile response and depleted intracellular stores sensitive to this agonist. A refilling of these internal Ca^{2+}-pools was obtained by subsequent loading in Ca^{2+}-containing solution (20 min). After 15 min in Ca^{2+}-free medium, application of caffeine (10 mM) evoked a transient contractile response at 25°C but not at 37°C ($Caff_1$, Figure 4). No contraction was evoked when caffeine was added a second time ($Caff_{1'}$, Figure 4), which suggests that the intracellular Ca^{2+}-stores sensitive to caffeine were emptied. After washing, addition of noradrenaline (NA_2, Figure 4) in Ca^{2+}-free medium induced a small and tonic contractile response at 25°C and 37°C in the absence of antioquine, and a similar response at 25°C in the presence of antioquine (Table 4). At 37°C, addition of antioquine in Ca^{2+}-free medium, induced a contractile response and addition of noradrenaline (10 min later) did not modify this contraction with respect to that obtained when only antioquine was added in Ca^{2+}-free medium (Table 4).

Binding assays

The interactions of antioquine with [^{3}H]-prazosin and [^{3}H]-(+)-*cis*-diltiazem binding are shown in Figure 5. Antioquine fully inhibited [^{3}H]-prazosin binding to cortical membranes, with an inhibition constant of 0.90 ± 0.34 μM. The fact that the pseudo-Hill coefficient (slope factor) was not significantly different from unity (n_H = 0.98 ± 0.07) suggests direct competition between antioquine and the radioligand for a single common binding site. In addition, antioquine inhibited binding of [^{3}H]-(+)-*cis*-diltiazem but with a lower potency (K_i = 20.58 ± 4.39 μM) and with a similar pseudo-Hill slope (n_H = 0.89 ± 0.19). This suggests that the interaction between antioquine and [^{3}H]-(+)-*cis*-diltiazem is also a simple competition for a single common binding site.

[^{3}H]-nitrendipine binding was not affected by antioquine in concentrations up to 100 μM (results not shown).

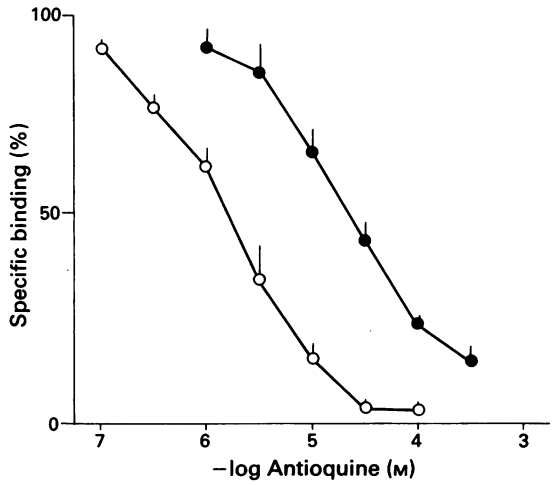

Figure 5 Displacement curves of [^{3}H]-prazosin (○) or [^{3}H]-(+)-*cis*-diltiazem specific binding (●) by antioquine. Each point is the mean (with s.e.mean) from three experiments made in triplicate.

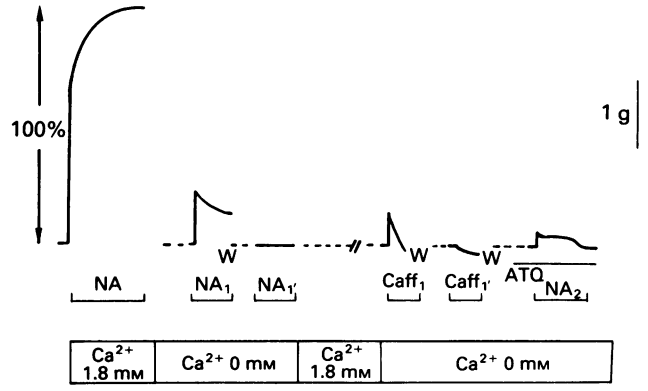

Figure 4 Experimental procedure used to study the effect of antioquine in the absence of extracellular calcium on noradrenaline (NA)-induced contraction after depletion of caffeine (Caff)-sensitive intracellular calcium pools. NA_1: addition of 1 μM noradrenaline after 15 min incubation in Ca^{2+}-free medium. $NA_{1'}$: second addition of the agonist after washing (W) in Ca^{2+}-free medium. $Caff_1$: addition of 10 mM caffeine after a 15 min resting period in KBS (Ca^{2+} 1.8 mM) and 20 min in Ca^{2+}-free solution. $Caff_{1'}$: second addition of the agonist after washing (W) in Ca^{2+}-free medium. NA_2: addition of noradrenaline in the presence of antioquine (ATQ) 300 μM, after depletion of caffeine-sensitive intracellular calcium stores and washing (W) in Ca^{2+}-free solution.

Inhibition of bovine aorta cyclic nucleotide phosphodiesterase enzymes

As shown in Table 5, antioquine has a weak inhibitory effect on PDE I and IV forms but did not have a significant action on the other forms (PDE III and V). In contrast, papaverine exerted a relatively non-selective inhibitory effect on all PDE forms, although the inhibition of the calmodulin-sensitive form (PDE I) appeared weaker than that of the other forms.

Discussion

The present experiments have demonstrated that antioquine, an alkaloid isolated from *Pseudoxandra sclerocarpa*, has a dual effect on the contractile mechanism of rat aorta: lower concentrations inhibit contractile responses whereas the highest concentration tested elicited a contraction that is not dependent on extracellular calcium.

Antioquine inhibited the contractile responses of rat aorta to the adrenoceptor agonist, noradrenaline, and high-potassium depolarization at 37°C and 25°C in the absence of vascular endothelium. Therefore, the vasorelaxation caused by antioquine was not mediated by either endothelium-derived relaxing factor (EDRF) or prostacyclin (PGI_2) (Jaffe, 1985; Vanhoutte *et al.*, 1986).

Table 4 Influence of temperature on contractile responses to noradrenaline (NA) and caffeine (Caff) in Ca-free solution in presence (b) and absence (a) of antioquine 300 μM (ATQ) (see Figure 4)

Temperature	n	*NA_1*	*Caff*	*ATQ*	*NA_2*
(a) 37°C	7	21.6 ± 3.2	NR	–	7.3 ± 0.8
(b) 37°C	4	19.5 ± 3.6	NR	13.8 ± 3.0	62.8 ± 4.3
(a) 25°C	6	28.1 ± 3.5	12.3 ± 2.1	–	8.6 ± 0.7
(b) 25°C	5	26.3 ± 4.8	13.3 ± 3.1	NR	9.7 ± 3.5

% contractions are calculated from the initial contraction by noradrenaline in Krebs solution.
Values are mean ± s.e.mean; *n* = number of experiments.
NR = no response.

Table 5 Effects of agents on cyclic nucleotide phosphodiesterases (PDE) isolated from bovine aorta

PDE activity	*^3H substrate*	K_i (μM) *Antioquine*	*Papaverine**
CaM-PDE type I	Cyclic GMP + EGTA	97.4	8
	Cyclic GMP + CaM	45.8 ± 3.0	27.5 ± 2.2
cGMP-PDE type V	Cyclic GMP + EGTA	>300	1.08 ± 0.36
CGI-PDE type III	Cyclic AMP + EGTA	>300	0.76
cAMP-PDE type IV	Cyclic AMP + EGTA	62.3 ± 12.7	1.68

Data shown are mean ± s.e.mean from three determinations obtained in different enzymatic preparations. See text for abbreviations.
*Data from Ivorra *et al.* (1992c).

In order to determine to what extent inhibition of PDE is involved in the vasorelaxant response to antioquine, we tested the effect of this compound on PDE activities isolated from bovine aorta as a model for vascular smooth muscle. Our results show that antioquine did not exhibit any potent inhibitory action on the different PDE forms. It only weakly inhibits CaM-PDE (PDE I) and cAMP-PDE (PDE IV), and unlike papaverine, has no inhibitory effect on the other forms (PDEs III and V). Therefore, it is probable that inhibition of some PDE form is not a major mechanism responsible for the relaxant response to antioquine.

Analysis of the results obtained in the binding assays indicates that antioquine inhibited binding of [^{3}H]-(+)-*cis*-diltiazem and [^{3}H]-prazosin with a similar pseudo-Hill slope (0.89 ± 0.19 and 0.98 ± 0.07 respectively). This suggests that the interaction between antioquine and [^{3}H]-(+)-*cis*-diltiazem or [^{3}H]-prazosin is a simple competition for a single common binding site. These results could suggest a direct action of antioquine at α_1-adrenoceptors and or the benzothiazepine receptor site at the calcium channel.

The fact that antioquine relaxes rat aorta may be interpreted as an antagonistic action with respect to a noradrenaline- or KCl-induced contraction. Analysis of the IC_{50} values of concentration-response curves of relaxation indicates that antioquine exhibits greater activity on the contractile response induced by KCl. Thus, the relaxant effects of antioquine may be due to the blockade of calcium movements through potential operated channels. The fact that the IC_{50} of antioquine on the contractile response induced by KCl was similar in the presence and absence of phentolamine indicates that the relaxant action shown by this alkaloid is not dependent on α-adrenoceptor blocking activity.

Results were different when antioquine was added at 37°C at the higher concentration tested (300 μM). In this case, antioquine induced a slow-developing sustained contraction in both Ca^{2+}-containing and Ca^{2+}-free medium. The magnitude of this contraction after 45 min of exposure to antioquine was about 60% with respect to that of noradrenaline in Ca^{2+}-containing solution. The contractile response was similar both in the presence and absence of extracellular calcium but was clearly attenuated at 25°C. Therefore, it is mediated by a temperature-dependent process. This contraction was reduced by papaverine (with and without calcium in the medium); and, as expected, contractile responses to antioquine were not modified by the presence of calcium antagonists (nifedipine and diltiazem), the absence of external calcium, or prazosin. Paradoxically, nifedipine and prazosin increased contractions in Ca^{2+}-containing solution.

Thus, our present results showed that the antioquine-induced contraction was not mediated by α_1-adrenoceptor activation or entry of external cations through voltage-operated channels. These findings also rule out the possibility of an involvement of noradrenaline release from perivascular adrenergic nerve endings. We suggest that this contraction is more likely due to an intracellular action of antioquine. The fact that prazosin and nifedipine, in Ca-containing solution, increase this contractile response to antioquine means that a possible participation of α-adrenoceptors or voltage-dependent calcium channels cannot be excluded. Moreover, the evidence that only papaverine inhibits the antioquine-induced contractions confirms the peculiarity of this process and suggests an intracellular mechanism related to the contractile apparatus.

In order to examine the possible intracellular action of antioquine, functional studies were performed in Ca^{2+}-free medium and noradrenaline- or caffeine-induced contractile responses were elicited in the presence or absence of antioquine. The results obtained demonstrated that in rat isolated aorta, at 25°C, antioquine did not elicit any contractile response, did not modify the contraction induced by noradrenaline and increased caffeine-induced contraction. At 37°C, antioquine induced a contractile response in all the experimental procedures used and previous addition of caffeine or subsequent addition of noradrenaline did not modify this contraction.

Recent studies have shown that the alkaloid, ryanodine, has a contractile action on smooth muscle cells, selectively acts on the Ca^{2+} channel in the sarcoplasmic reticulum membrane when it is in the open state and depletes the Ca^{2+} in both caffeine- and noradrenaline-sensitive stores (Meissner, 1986; Herrman-Frank *et al.*, 1991). The compound behaves as a functional Ca^{2+} store blocker and inhibits contractile responses to caffeine and noradrenaline in Ca^{2+}-free medium (Sato *et al.*, 1988; Hisayama *et al.*, 1990). It, therefore, seems clear that antioquine and ryanodine do not act by a common mechanism.

Antioquine-evoked contraction in Ca^{2+}-free medium may be induced by intracellular Ca^{2+} release from noradrenaline- and caffeine-insensitive sources; alternatively this contraction may not be due to an intracellular Ca^{2+} mobilization but to a direct action on the contractile machinery.

A possible source of intracellular Ca^{2+} responsible for antioquine-induced contraction could be the mitochondria. Autoradiographic and electron microscopic studies have confirmed that diltiazem, verapamil and dihydropyridines all accumulate within the mitchondrial matrix (Sato *et al.*, 1971; Nakajima *et al.*, 1975; Lullman *et al.*, 1979; Pang & Sperelakis, 1983; Tagami *et al.*, 1985) and have the ability to alter Ca^{2+} transport into the mitochondria. These findings support the hypothesis that antioquine, which binds selectively to the benzothiazepine receptor site at the plasma membrane calcium channel, also acts in the same way at the mitochondrial membrane. It would them inhibit Ca^{2+} uptake and the capacity of mitochondria to regulate the intracellular free Ca^{2+} level.

Another explanation for the present findings is a direct sensitization of the contractile machinery to Ca^{2+}. This sensitization could result from an action on the contractile proteins *via* an effect on protein kinases, as occurs with phorbol esters and endothelin-1 (Salaices *et al.*, 1990; Itoh *et al.*, 1991), or *via* phosphatase inhibition. With respect to the latter mechanism, it should be noted that two known potent inhibitors of type 1 and type 2A phosphatases, okadaic acid and calyculin-A (Ishihara *et al.*, 1989; Obara *et al.*, 1989), induce a similar contraction of smooth muscle, which is also independent of extracellular calcium. Moreover, Karaki *et al.* (1989) demonstrated that okadaic acid at concentrations lower than that needed to induce a contractile response, has

an inhibitory effect on smooth muscle contraction, as does antioquine. In any case, further work will be required to establish the exact mechanism of the antioquine-elicited contraction in rat aorta.

Structurally, antioquine is closely related to tetrandrine and, as stated earlier, tetrandrine is a calcium channel blocker that interacts at the benzothiazepine receptor site at the L-channel. However, antioquine and tetrandrine appear to act in different ways at the intracellular level: tetrandrine does not elicit any contractile response and inhibits noradrenaline-induced contraction in Ca^{2+}-free medium (unpublished results). The different behaviour shown by the two alkaloids can be explained on the basis of their different structural features. The structural modifications found in antioquine with respect to tetrandrine are the presence of an unusual linkage by a biphenyl bond between the monomer BIQ rings ($C_{11}-C_{11'}$) and the absolute configuration at the chiral centres (1S,1'**R** antioquine and 1S,1'S tetrandrine). In the benzylisoquinoline group containing the chiral carbon with absolute configuration 1S, the phenyl ring must remain orthogonal to the plane defined by the isoquinoline system. In contrast, in the benzylisoquinoline containing the chiral carbon with absolute configuration 1**R**, the phenyl and the heterocyclic rings are nearly coplanar. These different topological characteristics could determine the different behaviour of the two alkaloids.

Only compounds such as antioquine have a temperature-dependent contractile activity of apparent intracellular origin. This means that antioquine could be an interesting compound for studying this process, due to the presence of the biphenyl linkage that restricts conformational mobility in this molecule..

In summary, these data show that antioquine can relax smooth muscle cells in the rat aorta previously contracted by noradrenaline or KCl, probably due to activity as a calcium antagonist. However, at the highest concentration tested, it elicits a slow-developing and sustained contraction independent of extracellular calcium and is not inhibited by prazosin, nifedipine or diltiazem. Antioquine exhibits an affinity for [^{3}H]-prazosin and [^{3}H]-(+)-*cis*-diltiazem binding sites and selectively inhibits, although weakly, some PDE forms (PDE I and IV) isolated from bovine aorta; however, the mechanism for its contractile action requires further investigation.

References

CHEN, S.H. & LIU, G.Z. (1990). Calcium antagonists from traditional chinese herbs. *Drug New Perspectives*, **3**, 425–428.

CHENG, Y.G. & PRUSOFF, W.H. (1973). Relationship between the inhibition constant (K_i) and the concentration of inhibitor which causes 50 per cent inhibition (IC_{50}) of an enzymatic reaction. *Biochem. Pharmacol.*, **22**, 3099–3108.

CORTES, D., SAEZ, J., HOCQUEMILLER, R., CAVE, A. & CAVE, A. (1985). Alcaloïdes des Annonacées: alcaloïdes du *Pseudoxandra off. lucida*: etude de l'antioquine et de ses derivés. *J. Nat. Prod.*, **48**, 76–85.

CORTES, D., HOCQUEMILLER, R., CAVE, A. & SAEZ, J. (1986). Annonaceae alkaloids. Part 64. Minor alkaloids from the bark of *Pseudoxandra sclerocarpa*. *J. Nat. Prod.*, **49**, 854–858.

D'OCON, M.P., CANDENAS, M.L., ANSELMI, E., ZAFRA-POLO, M.C. & CORTES, D. (1989). Antioquine: a new bisbenzylisoquinoline alkaloid with calcium antagonist activity. *Arch. Int. Pharmacodyn. Ther.*, **297**, 205–216.

DONG, H., LEE, C.M., HUANG, W.L. & PENG, S.X. (1992). Cardiovascular effects of substituted tetrahydroisoquinolines in rats. *Br. J. Pharmacol.*, **107**, 262–268.

DONGKE, Z., GENG, S.Z. & PEI, L.Q. (1987). Effect of dauricine on the auricle of guinea pig. *Chin. Pharmacol. Bull.*, **3**, 100–103.

FANG, D. & JIANG, M. (1986a). Studies on tetrandrine calcium antagonistic action. *Chin. Med. J.*, **99**, 638–644.

FANG, D. & JIANG, M. (1986b). A new calcium antagonist of chinese medicinal origin: tetrandrine. *J. Hypertens.*, **4** (suppl. 6), S150–S152.

FURCHGOTT, R.F. & ZAWADZKI, J.V. (1980). The obligatory role of endothelial cells in the relaxation of arterial smooth muscle by acetylcholine. *Nature*, **288**, 373–376.

GLOSSMAN, H., ZECH, C., STRIESSING, J., STAUDINGER, R., HALL, L., GREENBERG, R. & ARMAH, B.I. (1991). Very high affinity interaction of DPI 201–106 and BDF 8784 enantiomers with the phenylalkylamine sensitive Ca^{2+} channel in *Drosophila* head membranes. *Br. J. Pharmacol.*, **102**, 446–452.

HERRMANN-FRANK, A., DARLING, E. & MEISSNER, G. (1991). Functional characterization of the Ca^{2+} release channel of vascular smooth muscle sarcoplasmic reticulum. *Pflügers Arch.*, **418**, 353–359.

HISAYAMA, T., TAKAYANAGI, I. & OKAMOTO, Y. (1990). Ryanodine reveals multiple contractile and relaxant mechanisms in vascular smooth muscle: simultaneous measurements of mechanical activity and of cytoplasmic free Ca^{2+} level with fura-2. *Br. J. Pharmacol.*, **100**, 677–684.

ISHIHARA, H., OZAKI, H., SATO, K., MASATOSHI, H., KARAK, H., WATAB, S., KATO, Y., FUSETANI, N., HASHIMOTO, K., VEMURA, D. & HARTSHORNE, D.J. (1989). Calcium-independent activation of contractile apparatus in smooth muscle by calyculin-A. *J. Pharmacol. Exp. Ther.*, **250**, 388–396.

ITOH, H., HIGUCHI, H., HIRAOKA, N., ITO, M., KONICHI, T., NAKANO, T. & LEDERIS, K. (1991). Contraction of rat thoracic aorta strips by endothelin-1 in the absence of extracellular Ca^{2+}. *Br. J. Pharmacol.*, **104**, 847–852.

IVORRA, M.D., CERCOS, A.C., ZAFRA-POLO, M.C., PEREZ-PRIETO, J., SAEZ, J., CORTES, D. & D'OCON, M.P. (1992a). Selective chiral inhibition of calcium entry promoted by bisbenzyltetrahydroisoquinolines in rat uterus. *Eur. J. Pharmacol.*, **219**, 303–309.

IVORRA, M.D., LE BEC, A. & LUGNIER, C. (1992b). Characterization of membrane-bound cyclic nucleotide phosphodiesterases from bovine aortic smooth muscle. *J. Cardiovasc. Pharmacol.*, **19**, 532–540.

IVORRA, M.D., LUGNIER, C., SCHOTT, C., CATRET, M., NOGUERA, M.A., ANSELMI, E. & D'OCON, P. (1992c). Multiple actions of glaucine on cyclic nucleotide phosphodiesterases, α_1-adrenoceptor and benzothiazepine binding site at the calcium channel. *Br. J. Pharmacol.*, **106**, 387–394.

JAFFE, E.A. (1985). Physiological function of normal endothelial cells. *Ann. N.Y. Acad. Sci.*, **454**, 279–291.

KARAKI, H., MITSUI, M., NAGASE, H., OZAKI, H., SHIBATA, S. & UEMURA, D. (1989). Inhibitory effect of a toxin okadaic acid, isolated from the black sponge on smooth muscle and platelets. *Br. J. Pharmacol.*, **98**, 590–596.

KING, V.F., GARCIA, M.L., HIMMEL, D., REUBEN, J.P., LAM, Y.T., PAN, J., HAN, G. & KACZOROWSKI, G.J. (1988). Interaction of tetrandrine with slowly inactivating calcium channels. *J. Biol. Chem.*, **263**, 2238–2244.

LU, M.Y. & LIU, G.Q. (1990). The effects of (−)-daurisoline on Ca^{2+} influx in presynaptic nerve terminals. *Br. J. Pharmacol.*, **101**, 45–48.

LUGNIER, C., SCHOEFFTER, P., LE BEC, A., STROUTHON, E. & STOCLET, J.C. (1986). Selective inhibition of cyclic nucleotide phosphodiesterases of human, bovine and rat aorta. *Biochem. Pharmacol.*, **35**, 1743–1751.

LULLMANN, H.M., TIMMERMANS, P.B. & ZIEGLER, A. (1979). Accumulation of drugs by resting or beating cardiac tissues. *Eur. J. Pharmacol.*, **60**, 277–285.

MEISSNER, G. (1986). Ryanodine activation and inhibition of the Ca^{2+} release channel of sarcoplasmic reticulum. *J. Biol. Chem.*, **261**, 6300–6306.

NAKAJIMA, H., HOSHIYAMA, M., YAMASHITA, K. & KIYOMOTO, A. (1975). Effect of diltiazem on electrical and mechanical activity of isolated cardiac ventricular muscle of guinea-pig. *Jpn. J. Pharmacol.*, **25**, 383–392.

NOGUERA, M.A. & D'OCON, M.P. (1992). Different and common intracellular calcium-stores mobilized by noradrenaline and caffeine in vascular smooth muscle. *Naunyn-Schmied. Arch. Pharmacol.*, **345**, 333–341.

OBARA, K., TAKAI, A., RUEGG, J.C. & DE LANEROLLE, P. (1989). Okadaic acid, a phosphatase inhibitor, produces a Ca^{2+} and calmodulin-independent contraction of smooth muscle. *Pflügers Arch.*, **414**, 134–138.

PANG, D.C. & SPERELAKIS, N. (1983). Uptake of [^{3}H]-nitrendipine into cardiac and smooth muscle. *Biochem. Pharmacol.*, **32**, 1660–1663.

SALAICES, M., BALFAGON, G., ARRIBAS, S., DE SAGARRA, M. & MARIN, J. (1990). Effects of phorbol 12,13-dibutyrate on the vascular tone and on norepinephrine- and potassium- induced contractions of cat cerebral arteries. *J. Pharmacol. Exp. Ther.*, **255**, 66–73.

SATO, M., NAGAO, T., YAMAGUCHI, I., NAKAJIMA, H. & KIYOMOTO, A. (1971). Pharmacological studies on a new 1,5-benzothiazepine derivative (CRD-401 = Diltiazem). *Arzneim. Forsch. Drug. Res.*, **21**, 1338–1343.

SATO, K., OZABE, H. & KARAKI, H. (1988). Multiple effects of caffeine on contractions and cytosolic free Ca levels in vascular smooth muscle of rat aorta. *Naunyn-Schmied. Arch. Pharmacol.*, **333**, 443–448.

SCHAEFFER, P., LUGNIER, C. & STOCLET, J.C. (1988). Interaction of calmodulin and calcium antagonist with [^{3}H]-diltiazem and [^{3}H]-nitrendipine binding sites. *J. Cardiovasc. Pharmacol.*, **12**, (Suppl. 4) S102–S103.

SCHOTT, C., TETSI, L., HEITZ, C., STAMBACH, J.F., JUNG, L. & STOCLET, J.C. (1988). Stereoselective blockade of α-adrenoceptors by berbine derivatives. *Arzneim-Forsch. Drug Res.*, **38**, 1567–1571.

TAGAMI, M., NARA, Y., KUBOTA, A., SUNAGA, T., MAELZAWA, H., HORIE, R. & YAMORI, Y. (1985). Electromicroscopic autoradiographic study of the distribution of [^{3}H]-diltiazem in myocardial cells. *Jpn. Heart J.*, **65**, 823–832.

TRIGGLE, D.J., LANGS, D.A. & JANIS, R.A. (1989). Ca-channels ligands: structure-function relationships of the 1,4-dihydropyridines. *Med. Res. Rev.*, **9**, 123–180.

VANHOUTTE, P.M., RUBANY, G.M., MELLER, U.M. & HOUSTON, D.S. (1986). Modulation of vascular smooth muscle contraction by endothelium. *Annu. Rev. Physiol.*, **48**, 307–320.

WANG, Z.G. & LIU, G.Z. (1985). Advances in natural products in China. *Trends Pharmacol. Sci.*, **6**, 423D–426D.

WELLS, J.W., BAIRD, C.E., WU, V.J. & HARDMAN, J.C. (1975). Cyclic nucleotide phosphodiesterase activity of pig coronary arteries. *Biochem. Biophys. Acta*, **384**, 430–442.

YAO, W., XIA, G., FANG, D. & JIANG, M. (1987). Studies on the calcium antagonistic action of tetrandrine: influence of tetrandrine and verapamil on hemodynamic action of ouabain in guinea-pig. *J. Tonqji Med. Univ.*, **7**, 80–83.

(Received October 2, 1992
Revised January 23, 1993
Accepted February 10, 1993)

Br. J. Pharmacol. (1993), **109**, 510–517 © Macmillan Press Ltd, 1993

Activation by calcium alone of chloride secretion in T_{84} epithelial cells

Udom Kachintorn, Mana Vajanaphanich, Alexis E. Traynor-Kaplan, the late Kiertisin Dharmsathaphorn & [1]Kim E. Barrett

Department of Medicine, University of California, San Diego, School of Medicine, San Diego, CA 92103, U.S.A.

1 The goal of this study was to determine if an increase in cytoplasmic calcium concentration ($[Ca^{2+}]_i$), in the absence of additional second messengers derived from membrane phospholipid turnover, is a sufficient signal to induce chloride secretion across monolayers of the human colonic epithelial line, T_{84}.

2 Thapsigargin was used to increase $[Ca^{2+}]_i$ by inhibiting the endomembrane Ca^{2+}-ATPase. $[Ca^{2+}]_i$ was monitored in monolayers by fura-2 fluorescence spectroscopy, chloride secretion by measuring changes in short circuit current (I_{sc}) in modified Ussing chambers, and inositol phosphates were measured by radio-h.p.l.c. of extracts of cells prelabelled with [^{3}H]-inositol.

3 Thapsigargin increased $[Ca^{2+}]_i$ and I_{sc} in parallel, without increasing any inositol phosphates. The effect of thapsigargin on I_{sc} was abolished by the intracellular calcium chelator, *bis*-(*o*-aminophenoxy)-ethane-*N*,*N*,*N*′,*N*′-tetraacetic acid (BAPTA).

4 Increasing $[Ca^{2+}]_i$ with thapsigargin did not prevent a subsequent calcium response to carbachol or histamine if extracellular calcium was available. In the absence of extracellular calcium, only one such release of calcium to hormonal stimulation occurred when cells were pretreated with thapsigargin, and a second response to either carbachol or histamine was essentially abolished.

5 Addition of carbachol or histamine to thapsigargin-treated cells mounted in Ussing chambers caused a transient further increase in I_{sc} followed by termination of the response, even though $[Ca^{2+}]_i$ continued to rise.

6 We conclude that an elevation in $[Ca^{2+}]_i$ is a sufficient signal to induce chloride secretion in T_{84} cells. Rather than being required to stimulate secretory responses, additional second messengers induced by hormonal secretagogues (such as inositol phosphates) may in fact serve to limit the secretory response.

Keywords: Epithelium; chloride secretion; calcium; inositol phosphates; thapsigargin; carbachol; histamine

Introduction

Active secretion of chloride is thought to be an important driving force for secretion of fluid across a number of epithelial surfaces, including the lung and intestine (McCann & Welsh, 1990; Barrett & Dharmsathaphorn, 1991). Disregulation of this process occurs in a number of diseases, including secretory diarrhoea and cystic fibrosis. There are accordingly clinical as well as basic reasons for wishing to understand fully the control of chloride secretion. Studies with the tranformed human colonic epithelial cell line T_{84}, which permits precise correlations of biochemical events with the physiological response of chloride secretion, have revealed three primary signal transduction pathways linking receptor occupancy to the final response of chloride secretion (Barrett & Dharmsathaphorn, 1990). These involve elevations in cellular levels of adenosine 3′:5′-cyclic monophosphate (cyclic AMP), guanosine 3′:5′-cyclic monophosphate (cyclic GMP) or free cytosolic calcium ($[Ca^{2+}]_i$). However, particularly for the last of these named second messengers, the precise steps which constitute the coupling between stimulus and secretion have not been fully elucidated.

$[Ca^{2+}]_i$ is widely recognized to be involved in the control of chloride secretion in a number of cell types (Bolton & Field, 1977; Frizzell, 1977; Chase, 1984; Cartwright *et al.*, 1985; Dharmsathaphorn & Pandol, 1986; Donowitz & Welsh, 1986; Mandel *et al.*, 1986; Welsh, 1987; Wasserman *et al.*, 1988; Dharmsathaphorn *et al.*, 1989a; Wong *et al.*, 1989). However, a definition of its exact role in the process has been difficult because most hormones which elevate $[Ca^{2+}]_i$ also have numerous other biochemical effects on the cell. For example, stimulation of T_{84} cells with the prototype calcium-dependent chloride secretagogue, carbachol, results in phosphatidylinositol turnover, elevations in a number of phospholipid metabolites including inositol (1,4,5) trisphosphate, inositol (1,3,4) trisphosphate, inositol tetrakisphosphates, diacylglycerol and phosphatidic acid, synergistic enhancement of responsiveness to cyclic nucleotide-dependent stimuli, and phosphorylation of substrates of protein kinase C (Cartwright *et al.*, 1985; Cohn, 1990; Vajanaphanich *et al.*, 1993; Kachintorn *et al.*, 1993). Moreover, it has been postulated that some of the biochemical events, or others as yet unidentified, might be required for the effect of calcium on chloride secretion, and that calcium acting alone is insufficient to activate the secretory response (Dharmsathaphorn *et al.*, 1989a). The primary evidence for this hypothesis rests on the observation that there is a very poor correlation between the ability of various substances to increase $[Ca^{2+}]_i$ and stimulate chloride secretion. Calcium ionophores can have marked and sustained effects on $[Ca^{2+}]_i$ while being relatively ineffective as transient chloride secretagogues, whereas histamine and carbachol stimulate more marked chloride secretion in association with a modest rise in $[Ca^{2+}]_i$ (Dharmsathaphorn *et al.*, 1989a).

Part of the difficulty in fully delineating the role of calcium in chloride secretion across T_{84} cells arose from the previous lack of an experimental means of elevating $[Ca^{2+}]_i$ in the absence of the biochemical changes described above. Calcium ionophores such as ionomycin and A23187, which have been widely employed as experimental tools in this regard, are now well-recognized to be capable of stimulating phospholipase C and consequent inositol phosphate metabolism. In the present study, we have employed another means of elevating cytoplasmic calcium concentrations, thapsigargin.

[1] Author for correspondence at: UCSD Medical Center, 8414, 225 Dickinson Street, San Diego, CA 92103-8414, U.S.A.

This sesquiterpene lactone has been shown to induce a sustained $[Ca^{2+}]_i$ signal in many cells, including platelets, hepatocytes, parotid acinar cells and lymphocytes (Thastrup *et al.*, 1987; 1990; Takemura *et al.*, 1989; Mason *et al.*, 1991). The rise in calcium, which is derived from both intracellular and extracellular sources, is reportedly independent of inositol phosphate generation (Jackson *et al.*, 1988; Takemura *et al.*, 1989; Law *et al.*, 1990). It is thought to act directly on intracellular stores of calcium as an inhibitor of the endomembrane Ca^{2+}-ATPase (Thastrup *et al.*, 1990). Secondarily, this agent also stimulates influx from the extracellular compartment, presumably because the internal stores are in some way linked to the plasma membrane calcium permeability pathway (Takemura *et al.*, 1989). We therefore reasoned that this might be a useful agent to settle the question of whether calcium, acting alone in the absence of products derived from membrane phospholipid turnover, was capable of stimulating transepithelial chloride secretion. We have also examined the possible links between the agonist-(i.e. inositol (1,4,5) trisphosphate-) sensitive pool of calcium that is mobilized by agents such as carbachol or histamine in T_{84} cells, with the calcium pool that is mobilized by thapsigargin.

Methods

Measurement of Cl^- secretion and $[Ca^{2+}]_i$

Growth and maintenace of the human colonic epithelial cell line, T_{84}, transepithelial electrolyte transport studies (using Ussing chambers modified for use with cultured cells), and free cytosolic Ca^{2+} measurements followed procedures similar to those described previously (Dharmsathaphorn *et al.*, 1989b; Dharmsathaphorn & Madara, 1990). Short-circuit current (I_{sc}) was used to quantitate transepithelial Cl^- secretion. Previous studies have demonstrated that T_{84} cells secrete Cl^- in response to carbachol and histamine, and that the resulting changes in I_{sc} are wholly reflective of the amounts of Cl^- secretion induced by these secretagogues (Dharmsathaphorn & Pandol, 1986; Wasserman *et al.*, 1988). In this study, I_{sc} measurements were carried out in Ringer solution containing (in mM); Na^+ 140, K^+ 5.2, Ca^{2+} 1.2, Cl^- 119.8, HCO_3^- 25, $H_2PO_4^-$ 2.4, HPO_4^{2-} 0.4, and glucose 10. Free cytosolic Ca^{2+} measurements had to be carried out in a bathing medium that was relatively low in HCO_3^- to avoid interference caused by precipitation. Therefore, we have modified the Ringer solution used in I_{sc} studies for optimal $[Ca^{2+}]_i$ measurements. This was essentially accomplished by reducing the concentration of HCO_3^- and adding N-[2-hydroxyethyl] piperazine-N'-[2-ethane sulphonic acid] (HEPES) as a buffer; the solution resembles standard Hanks' buffer. This buffer contained (in mM): Na^+ 141.6, K^+ 5.8, Ca^{2+} 1.2, Mg^{2+} 0.8, Cl^- 144.7, $H_2PO_4^-$ 0.3; SO_4^{2-} 0.8, HCO_3^- 4.1, HEPES 10 and glucose 5.6, with the pH adjusted to 7.4 with NaOH. Preliminary testing indicated that the actions of each secretagogue on I_{sc} in both media were similar (data not shown). Therefore, the I_{sc} measurements which have been obtained with the standard Ringer solution are compared to $[Ca^{2+}]_i$ data obtained with the modified solution. In some experiments, I_{sc} measurements were made in T_{84} monolayers which had been preincubated for 45 min with the acetoxymethyl ester of the intracellular Ca^{2+} chelator, *bis*-(*o*-aminophenoxy)-ethane-*N*,*N*,*N*',*N*'-tetraaceticacid (BAPTA) (0.15 mM). This concentration of BAPTA is sufficient to abolish completely agonist-stimulated increases in $[Ca^{2+}]_i$ in T_{84} cells (Kachintorn *et al.*, 1992).

Determination of inositol phosphates

T_{84} cells were labelled with *myo*-[2-^{3}H]-inositol to study the generation of inositol phosphates following stimulation. T_{84} cells were grown to confluency (about 10^6 cells/well) in 6-well tissue culture plates (35 mm diameter wells). The culture medium was removed and the cells were then washed once with 0.22% trypsin/0.72 mM EDTA solution, which remained on the cells for 5 min. The trypsin/EDTA solution was replaced with 1 ml of inositol-free DMEM/F12 medium (1:1, v/v) supplemented with dialyzed newborn calf serum (5%) and *myo*-[2-^{3}H]-inositol (12.8 Ci mmol^{-1}, 50 μCi ml^{-1}). Cells were then incubated for 24 h after which time an additional 1 ml of medium containing dialyzed serum was added. The cells were then incubated for another 48 h (72 h total). Control experiments indicated that growth of cells in inositol-free medium did not alter their ability to display ion transport responses (data not shown). After labelling, the medium containing any unincorporated radioisotope was removed and the cells were washed 4 times with Ringer solution containing glucose. The cells were incubated for varying periods of time at 37°C in 500 μl Ringer solution containing thapsigargin (1 μM). The incubations were terminated by addition of 1 ml of ice cold methanol and the cells were then sonicated at 4°C until they were detached from the tissue culture plate. The suspension of sonicated cells in methanol was pooled with one methanol wash (in 1 ml) of the well into a polypropylene test tube. Inositol phosphates were extracted by a slight modification of a procedure described by Berridge and co-workers (1983). Briefly, HCl (300 μl, 0.5 N), 1 mM $CaCl_2$ plus 10 mM mannitol (600 μl), and chloroform (800 μl) were added to the extracts and the tubes were then centrifuged. After collecting the upper phase, the interface was washed twice with 1 ml of the upper phase of chloroform/methanol/0.1 M sodium cyclohexone-1,2-diaminetetra-acetic acid (16:8:5 v/v/v). The combined upper phases were then dried and the product was dissolved in 500 μl of double-

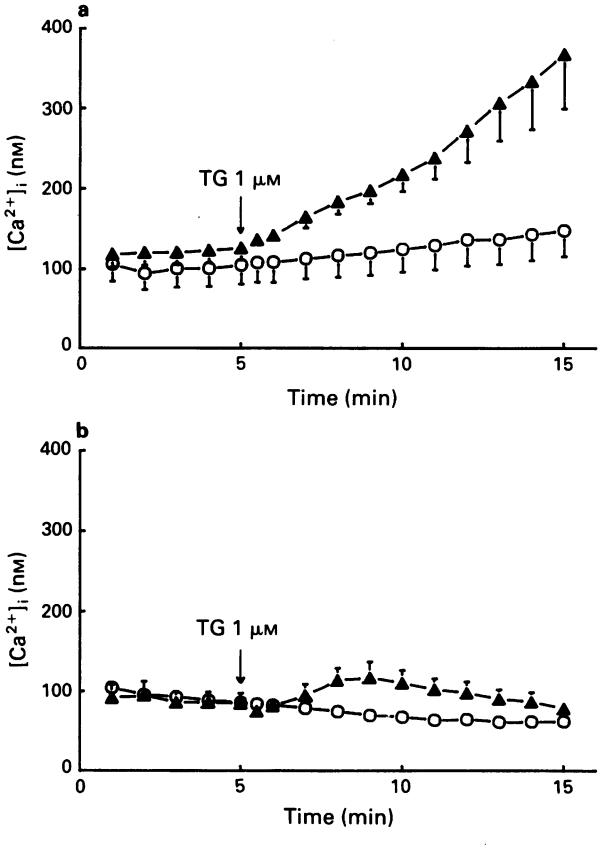

Figure 1 Effect of thapsigargin (TG) on free cytoplasmic calcium concentrations ($[Ca^{2+}]_i$) in T_{84} cell monolayers in the presence (a) or absence (b) of extracellular calcium. In (a) and (b) (○) show the time course of changes in $[Ca^{2+}]_i$ in control monolayers with no additions. In experiments denoted by (▲) TG (1 μM) was added at 5 min. Values are means ± s.e.mean for 4 experiments.

distilled water and filtered before being applied to an anion-exhange column.

Inositol phosphates were resolved by anion-exchange high performance liquid chromatography (h.p.l.c.) as described by Auger *et al.* (1989) on a 4.6 × 250 mm Partisil 10 SAX column (Whatman, Clifton, New Jersey, U.S.A). Elution was performed with a three stage gradient: water for 15 min, followed by a linear gradient to 0.25 M $NH_4H_2PO_4$ (pH 3.8) over 60 min, followed by a linear gradient to 1 M $NH_4H_2PO_4$ (pH 3.8) over 50 min, at a flow rate of 1 ml min^{-1}. The column was washed with water (1 ml min^{-1}) for 10 min between application of samples. The radioactivity of the effluent was continuously measured by a 171 radioisotope detector (Beckman, San Ramon, California), which performed automatic peak integration with Beckman System Gold Program software. Identification of the inositol phosphates was based on comparison of their elution times with those of authentic radiolabelled standards (New England Nuclear, Boston, MA, U.S.A.).

Materials

Thapsigargin was kindly provided by Dr O. Thastrup, University Hospital, Copenhagen, Denmark and vasoactive intestinal polypeptide (VIP) was donated by Dr J. Rivier, Salk Institute, La Jolla, California, U.S.A. Carbachol (ICN, Irvine, California, U.S.A.), histamine dihydrochloride (Sigma Chemical Co., St. Louis, Missouri, U.S.A.), fura-2/AM and *bis*-(*o*-aminophenoxy)-ethane-*N*,*N*,*N*',*N*'tetraacetic acid tetraacetoxymethyl ester (BAPTA/AM) (Calbiochem Biochemical, La Jolla, California, U.S.A.) and *myo*-[2-^{3}H]inositol, (+)-[inositol-2-^{3}H(N)]-inositol 1-phosphate, (+)-[inositol-2-^{3}H(N)]-inositol 1,4-bisphosphate, (+)-[inositol-2-^{3}H(N)]-inositol 1,3,4-trisphosphate, and (+)-[inositol-2-^{3}H(N)]-inositol tetrakisphosphate (New England Nuclear, Boston, Massachusetts, U.S.A.), were purchased from the sources indicated.

Results

Effect of thapsigargin on $[Ca^{2+}]_i$

First, we tested whether thapsigargin had an effect on $[Ca^{2+}]_i$ in T_{84} cells. Figure 1 shows that when cells were bathed in Ca^{2+}-containing medium (Figure 1a) the addition of 1 μM thapsigargin gradually and progressively increased $[Ca^{2+}]_i$. In Ca^{2+}-free medium (Figure 1b) the increase in $[Ca^{2+}]_i$ caused by thapsigargin was of lesser magnitude and not progressive. Next, we tested whether breakdown of phosphoinositides and the resulting production of inositol phosphates was involved in the Ca^{2+}-mobilizing activity of thapsigargin. T_{84} monolayers prelabelled with [^{3}H]-*myo*-inositol were stimulated with 1 μM thapsigargin and the levels of [^{3}H]-inositol phosphates were analyzed by h.p.l.c. As shown in Figure 2, none of the [^{3}H]-inositol phosphates measured (including inositol 1,4,5-trisphosphate ((1,4,5)IP_3), inositol 1,3,4-trisphosphate, inositol 1,4-bisphosphate, inositol 1,3,4,5-tetrakisphosphate, inositol pentakisphosphate and inositol hexakisphosphate) were increased by thapsigargin. In contrast, we have previously reported that increases in a number of inositol phosphates can be readily demonstrated when T_{84} cells are treated with the calcium-mobilizing secretagogues histamine or carbachol (Kachintorn *et al.*, 1993).

Effect of thapsigargin on I_{sc}

Having confirmed in the cell type under study that the effects of thapsigargin on $[Ca^{2+}]_i$ are not accompanied by the generation of inositol phosphates, we were next able to test whether $[Ca^{2+}]_i$ mobilized in the absence of phosphatidylinositol turnover can stimulate chloride secretion. Figure 3 shows that addition of thapsigargin to T_{84} monolayers mounted in Ussing chambers caused an increase in I_{sc}. The increase in I_{sc} appeared to correlate well with the increase in $[Ca^{2+}]_i$ induced by thapsigargin in the presence of extracellular calcium (compare Figure 1a with Figure 3). It should be noted that it is not possible to perform Ussing chamber experiments in the nominal absence of extracellular calcium, so whether a direct correlation exists between the data presented in Figure 1b with changes in I_{sc} cannot be tested. As an alternative strategy, we employed the intracellular calcium chelator, BAPTA. We have previously shown that preloading of T_{84} monolayers with this agent is able to suppress completely both the increase in $[Ca^{2+}]_i$ and I_{sc} induced by carbachol, in a parallel fashion (Kachintorn *et al.*, 1992). As shown in Figure 3, the current experiments revealed that the effect of thapsigargin on I_{sc} was likely to be dependent on its ability to increase intracellular calcium levels. When thapsigargin was added to T_{84} cell monolayers that had been preloaded with the chelator, no increase in I_{sc} was observed (Figure 3). This inhibition was not the result of non-specific

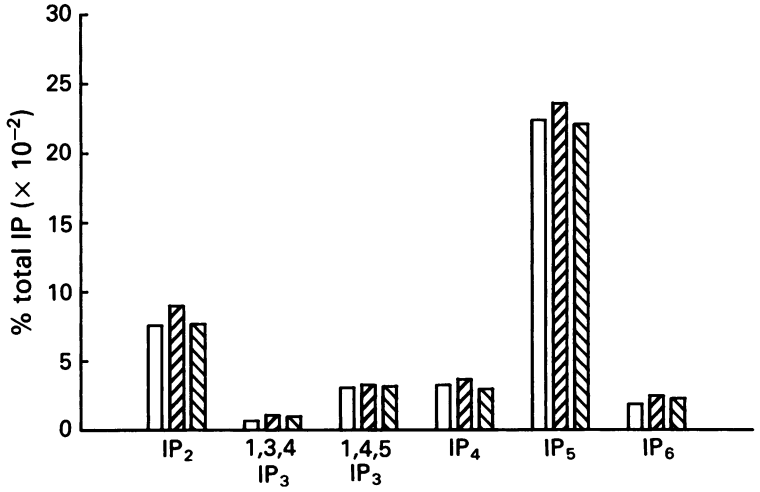

Figure 2 Effect of thapsigargin on levels of ^{3}H-labelled inositol phosphates (IP) in T_{84} cell monolayers. Levels of IP_2, 1,4,5-IP_3, 1,3,4-IP_3, IP_4, IP_5, and IP_6 are expressed as a percentage of the total counts in inositol phosphates. Standards for IP_5 and IP_6 are not commerically available so their identification is accordingly tentative. Open columns denote levels of each inositol phosphate in control, unstimulated cells. Hatched columns denote levels of each inositol phosphate in cells stimulated with thapsigargin for 1 (▨) or 5 (▧) min. Values are means for 1 experiment performed in duplicate.

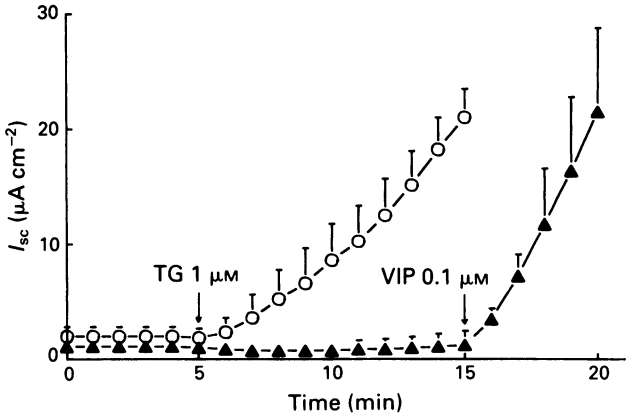

Figure 3 Effect of thapsigargin on chloride secretion (measured as I_{sc}) across T_{84} cell monolayers in the presence (▲) or absence (○) of BAPTA. Thapsigargin (TG) was added at 5 min. Cells were preincubated with BAPTA, when used, for 45 min prior to mounting. When BAPTA was used, vasoactive intestinal polypeptide (VIP) was added at 15 min to confirm that the chelator did not have nonspecific antisecretory effects. Values are means ± s.e.mean for 4 experiments.

cytotoxicity of BAPTA, since the same cells responded normally to subsequent addition of the cyclic AMP-dependent secretagogue, VIP.

Interaction between thapsigargin and agonists stimulating phospholipid turnover

Carbachol and histamine have been shown to increase $[Ca^{2+}]_i$ in T_{84} and other cell types by an inositol 1,4,5-trisphosphate-dependent mechanism. We therefore added both thapsigargin and carbachol or histamine to T_{84} cells to see if their effects on $[Ca^{2+}]_i$ were additive. Figure 4a shows that the addition of 100 μM carbachol alone caused an immediate increase in $[Ca^{2+}]_i$ with a slow return to baseline after the first minute. In monolayers where 1 μM thapsigargin and 100 μM carbachol were added simultaneously, the initial increase in $[Ca^{2+}]_i$ attributable to carbachol was the same, but subsequently $[Ca^{2+}]_i$ continued to increase. Figure 4b shows similar additive effects when 1 μM thapsigargin and 100 μM histamine were added simultaneously. Thus the effects of thapsigargin plus a (1,4,5)IP_3-dependent stimulus on $[Ca^{2+}]_i$ are additive (compare Figures 1 and 4).

Because the Ca^{2+}-releasing effect of thapsigargin was gradual, we attempted to empty the thapsigargin-sensitive Ca^{2+} pool, before the addition of carbachol or histamine, by pretreating T_{84} monolayers with 1 μM thapsigargin for 10 min. The results are shown in Figures 5 and 6. In either the presence (Figure 5a) or absence (Figure 6a) of extracellular calcium, pretreatment for 10 min with thapsigargin did not significantly alter the change in $[Ca^{2+}]_i$ induced by carbachol. Similarly, the effect of histamine on $[Ca^{2+}]_i$ was not attenuated by thapsigargin in either Ca^{2+}-containing medium (Figure 5) or Ca^{2+}-free medium (Figure 6).

We further investigated a possible relationship between the thapsigargin-sensitive Ca^{2+} pool and the (1,4,5)IP_3-sensitive Ca^{2+} pool by treating cell monolayers with thapsigargin, and then adding carbachol followed by histamine (or *vice versa*). When experiments were carried out in the absence of extracellular Ca^{2+} (Figure 6), pretreatment with thapsigargin prevented the rise in $[Ca^{2+}]_i$ produced by a second stimulation with a (1,4,5)IP_3-mobilizing agonist. Thus when histamine followed carbachol, the small rise in $[Ca^{2+}]_i$ induced by histamine was totally abolished by thapsigargin pretreatment. Similarly, when carbachol followed histamine, carbachol stimulation had no effect on $[Ca^{2+}]_i$ in the presence of thapsigargin.

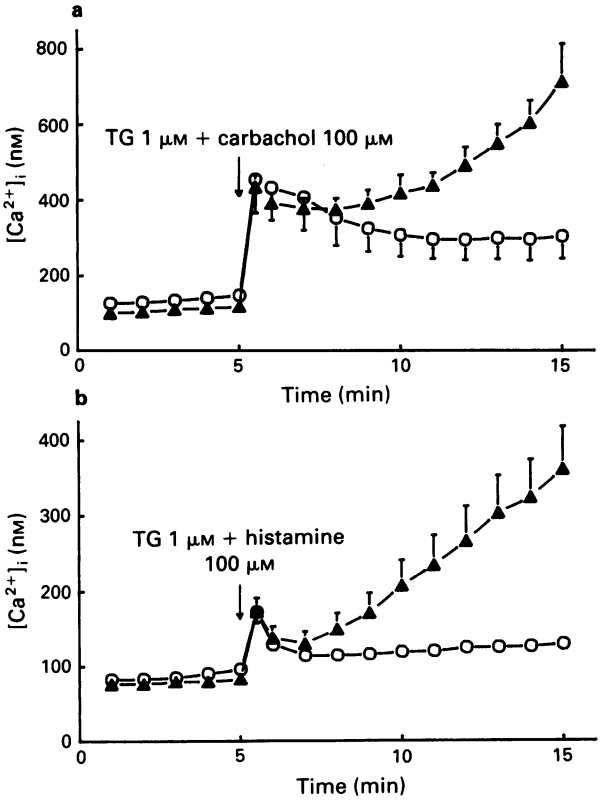

Figure 4 Effect of thapsigargin on $[Ca^{2+}]_i$ in T_{84} cell monolayers when added simultaneously with either carbachol (a) or histamine (b), and in the presence of extracellular calcium: (○) changes in $[Ca^{2+}]_i$ when carbachol or histamine were added alone; (▲) indicate the time course of changes in $[Ca^{2+}]_i$ following addition of thapsigargin (TG) plus carbachol or histamine at 5 min. Values are means ± s.e. mean for 4 experiments.

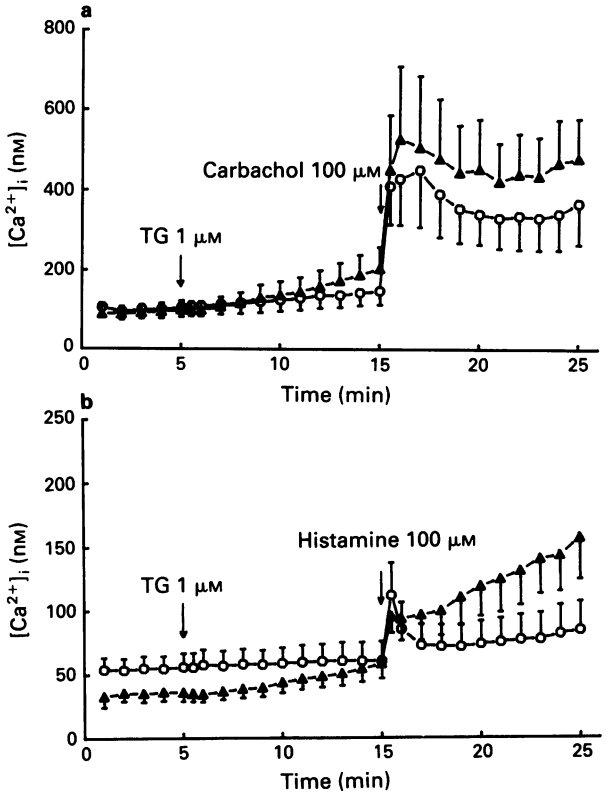

Figure 5 Effects of sequential addition of thapsigargin and either carbachol or histamine on $[Ca^{2+}]_i$ in T_{84} cell monolayers in the presence of extracellular calcium: (○) denote results when either carbachol or histamine were added in the absence of thapsigargin (TG); (▲) depict experiments where thapsigargin was added at 5 min, followed by carbachol or histamine at 15 min. Values are means ± s.e.mean for 4–6 experiments.

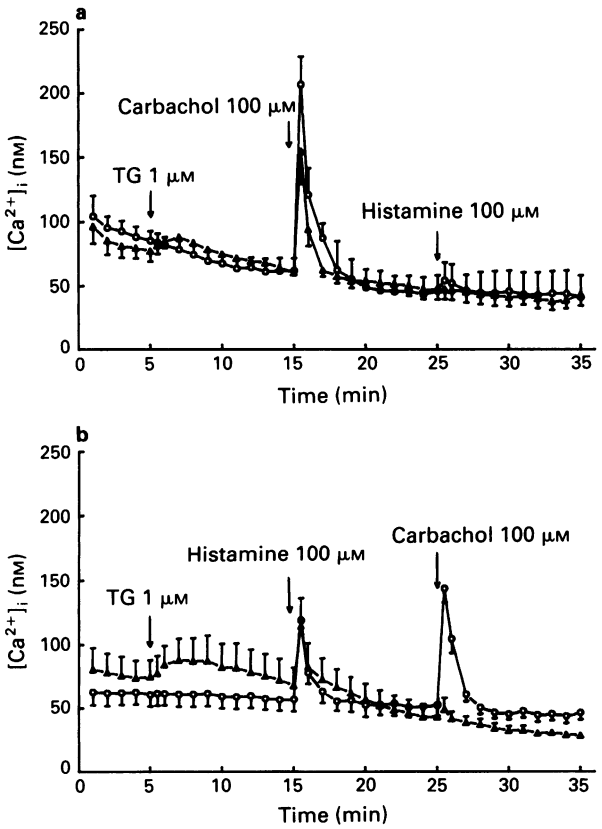

Figure 6 Effect of thapsigargin on $[Ca^{2+}]_i$ responses in T_{84} cells induced by sequential addition of carbachol followed by histamine (a) or histamine followed by carbachol (b) in the absence of extracellular calcium: (O) depict responses in the absence of thapsigargin (TG) while (▲) depict experiments where thapsigargin was added 10 min pior to carbachol or histamine. Values are means ± s.e.mean for 4 experiments.

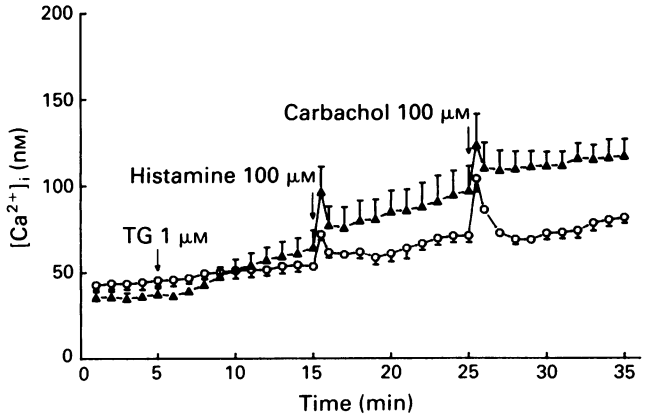

Figure 7 Effect of thapsigargin (TG) on $[Ca^{2+}]_i$ responses in T_{84} cells induced by sequential addition of histamine and carbachol in the presence of extracellular calcium: (O) denote responses in the absence of thapsigargin while (▲) depict experiments where thapsigargin was added at 5 min. Values are mean ± s.e.mean for 4 experiments.

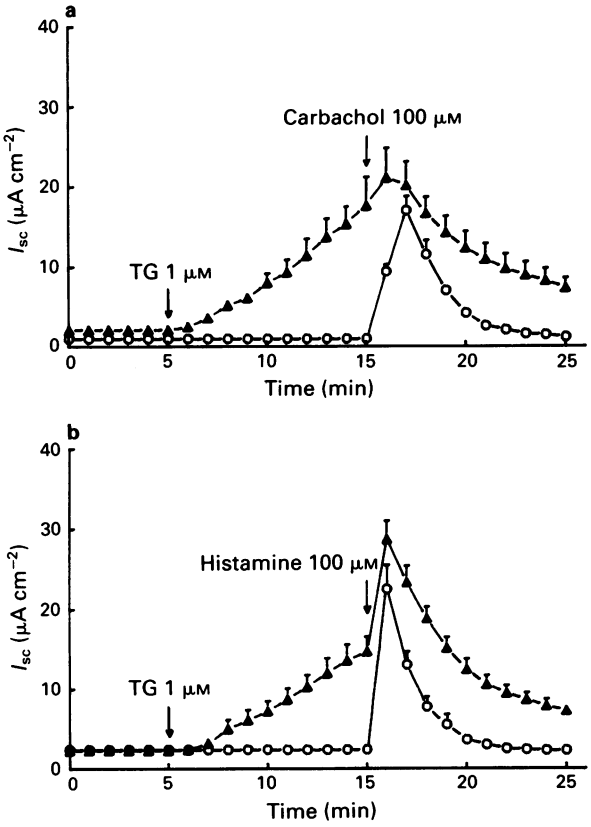

Figue 8 Effect of sequential addition of thapsigargin (TG) and carbachol (a) or histamine (b) on chloride secretion across T_{84} cell monolayers: (O) denote the response to carbachol or histamine alone; (▲) depict experiments where thapsigargin was added at 5 min, which was 10 min before carbachol or histamine addition. Values are means ± s.e.mean for 5 (carbachol) or 7 (histamine) experiments.

The same experimental design was employed in the presence of extracellular calcium to examine possible mechanisms of calcium pool refilling following stimulation. As shown in Figure 7, when calcium was available in the medium, thapsigargin could not prevent a second response to a (1,4,5)IP_3-dependent stimulus. Thus, when histamine addition was followed 10 min later by carbachol, the latter agent produced essentially equivalent increases in $[Ca^{2+}]_i$ whether or not thapsigargin was present. These finding contrast with the findings of experiments carried out in the absence of extracellular Ca^{2+} (see Figure 6 for comparison). Also of note is the finding that, in cells treated with the sequence of thapsigargin followed by histamine followed by carbachol, $[Ca^{2+}]_i$ still continued to rise significantly compared with cells treated with only the inositol phosphate-dependent stimuli, even after the addition of both carbachol and histamine. This observation suggests that even after treatment with maximal doses of carbachol and histamine, sufficient calcium remains in intracellular stores to be mobilized by thapsigargin and/or the emptying of these stores triggers continued influx of extracellular calcium in the presence of thapsigargin. It was therefore of interest to examine I_{sc} responses when cells were stimulated with sequences of agonists.

As shown in Figure 8, if addition of thapsigargin to the Ussing chamber was followed by either carbachol or histamine addition, the cells were able to display a further increase in I_{sc} which is consistent with the initial spike in $[Ca^{2+}]_i$ that is induced by carbachol or histamine under similar circumstances. This is in keeping with the $[Ca^{2+}]_i$ data shown in Figures 5 and 7. However, pretreament with thapsigargin appeared to reduce the ability of the cells to display an I_{sc} response to carbachol somewhat, though responsiveness to histamine was essentially unaffected. Furthermore, the response to histamine or carbachol was rapidly resolved either in the presence or absence of thapsigargin, even though, in the former case, $[Ca^{2+}]_i$ levels remained elevated (Figure 5).

Discussion

This study was designed to address whether calcium, acting in the absence of any additional second messengers derived

from the turnover of membrane phospholipids, is capable of stimulating transepithelial chloride secretion across a line of human colonic epithelial cells, T_{84}. We had previously demonstrated that such auxiliary second messengers, including diacylglycerol and phosphatidic acid, are likely to contribute to the magnitude of the secretory response stimulated by increases in $[Ca^{2+}]_i$ (Kachintorn *et al.*, 1992; Vajanaphanich *et al.*, 1993). In this study, we confirmed that thapsigargin was without effect on the accumulation of any inositol phosphates, and in particular on the levels of inositol 1,4,5-trisphosphate and inositol 1,3,4,5-tetrakisphosphate, molecules that are widely recognized as being intracellular mediators of calcium mobilization and/or influx (Hansen *et al.*, 1991; Luckhoff & Clapham, 1992). Thapsigargin was able to increase calcium levels within T_{84} cells in both the presence and absence of extracellular calcium, though the response was smaller in the nominal extracellular absence of the cation. The smaller response occurring when calcium was not present in the bathing medium may suggest that emptying of an intracellular store directly stimulates calcium influx from the extracellular environment, as has been reported by a number of authors (Takemura *et al.*, 1989; Mason *et al.*, 1991), or might simply reflect the fact that changes in intracellular calcium that are induced by thapsigargin might be more readily dissipated in the absence of extracellular calcium, and therefore less readily detectable via the fura-2 technique.

Overall, qualitatively similar events to those presented here for the effect of thapsigargin on intracellular calcium levels have been described in a number of cell types (Thastrup *et al.*, 1987; 1990; Cheek *et al.*, 1988; Okuchi *et al.*, 1988; Scharff *et al.*, 1988; Benton *et al.*, 1989; Takemura *et al.*, 1989; Foder *et al.*, 1990; Kwan *et al.*, 1990; Law *et al.*, 1990), including another human colonic adenocarcinoma cell line, HCA-7 (Brayden *et al.*, 1989). However, there are some quantitative differences between our findings and those of workers using other cell types. Chief among these was the observation that thapsigargin caused a progressive increase in $[Ca^{2+}]_i$ in our cells, whereas in a number of other systems it has been reported to have more rapid and transient effects on $[Ca^{2+}]_i$. This might suggest that the rates of calcium leakage from intracellular stores are different among cell types, or that rates of calcium influx or extrusion across the plasma membrane are likewise variable.

In this study using T_{84} cells, as well as in most other cell types, a sustained elevation in $[Ca^{2+}]_i$ after thapsigargin treatment is dependent on the presence of extracellular Ca^{2+}. There is an exception in NG115-401L neuronal cells which only show a transient Ca^{2+} signal (Jackson *et al.*, 1988). Recently, by using extracellular Mn^{2+} as a marker for Ca^{2+}-influx induced by thapsigargin, it has been shown that Ca^{2+} entry is responsible for sustaining increased $[Ca^{2+}]_i$ (Foder *et al.*, 1990). Furthermore, it has been shown by others that the sustained increase in $[Ca^{2+}]_i$ seen with thapsigargin is not due to inhibition of the rate of Ca^{2+} extrusion across the plasma membrane (Takemura *et al.*, 1990). Other inhibitors of endomembrane Ca^{2+}-ATPases, such as 2,5-di-(*tert*-butyl)-1,4-hydroquinone (BHQ) may have an additional side effect on plasma membrane calcium permeability, which complicates the interpretation of studies with these drugs (Mason *et al.*, 1991).

Thapsigargin failed to increase inositol phosphate production in T_{84} cells, confirming previous reports that thapsigargin releases Ca^{2+} from an intracellular store by a mechanism independent of the hydrolysis of phosphoinositides (Jackson *et al.*, 1988; Takemura *et al.*, 1989; Law *et al.*, 1990). In addition Takemura and co-workers (1989) reported that thapsigargin had no effect on levels of phosphatidic acid, a product which results from the degradation of phospholipids other than phosphoinositides by phospholipase C or phospholipase D. Our preliminary data also showed that thapsigargin did not increase phosphatidic acid production in T_{84} cells (data not shown). Thapsigargin did inhibit resolution of the increase in $[Ca^{2+}]_i$ induced by carbachol and histamine, and therefore most likely inhibits Ca^{2+}-recycling into intracellular Ca^{2+} stores, via the endoplasmic reticulum Ca^{2+}-ATPase, as reported by others (Thastrup *et al.*, 1990).

Notwithstanding the source of the $[Ca^{2+}]_i$ elevation induced by thapsigargin, the ability of this drug to increase I_{sc} suggests that calcium alone can be a stimulus of chloride secretion. Thus the primary objective of our study was achieved. Our findings stand in contrast to those of Pickles & Cuthbert (1992) who showed that calcium alone was not sufficient to activate ion transport in a human absorptive epithelium. This discrepancy may reflect differences in the control of absorption *vs* secretion or tissue-specific mechanisms, and is deserving of additional study. Thapsigargin induced chloride secretion from T_{84} cells in parallel with its effect on $[Ca^{2+}]_i$. The importance of the mobilized calcium in mediating the observed secretory response was demonstrated with BAPTA; this intracellular chelator abolished the change in I_{sc} induced by thapsigargin without affecting the response of the cells to a cyclic AMP-dependent stimulus. Thus calcium is a primary mediator of chloride secretion which is effective in the absence of other messengers generated via phospholipid metabolism. In fact, rather than providing evidence that phospholipid metabolites are required to stimulate chloride secretion, we are led to the opposite conclusion by the observations reported here. The data presented in Figure 8 imply that secretagogues which stimulate both a rise in $[Ca^{2+}]_i$ and turnover of phosphatidylinositol induce the formation of auxiliary second messengers which actually uncouple chloride secretion from elevated levels of cytoplasmic calcium. This conclusion is drawn from a comparison of the I_{sc} responses shown in Figure 8 with the $[Ca^{2+}]_i$ responses depicted in Figures 5 and 7. Similarly, the fall in $[Ca^{2+}]_i$ after its elevation by carbachol or histamine is unlikely to be the sole reason for the rapid termination of the Cl^- secretory response to these agents. The mechanism of the uncoupling of chloride secretion from $[Ca^{2+}]_i$ is the subject of current studies in our laboratory, which have preliminarily implicated inositol tetrakisphosphate as a candidate negative second messenger (Kachintorn *et al.*, 1993).

Our studies also addressed whether there is any correspondence between the intracellular pools of calcium within T_{84} cells that are mobilized by thapsigargin *vs* those mobilized by stimulation with carbachol or histamine. Thapsigargin did not abolish an initial $[Ca^{2+}]_i$ response induced by these secretagogues in either the presence or absence of extracellular Ca^{2+} (Figures 5 and 6). This might suggest that different pools of calcium are being mobilized by thapsigargin and carbachol or histamine. However, these pools at least appear to be linked in some way because, in the absence of extracellular Ca^{2+}, pretreatment with thapsigargin could abolish the histamine-induced $[Ca^{2+}]_i$ response following addition of carbachol; similarly, thapsigargin pretreatment abolished the carbachol response following the addition of histamine (Figure 6). In human platelets, the thrombin-sensitive Ca^{2+} pool (a (1,4,5)IP_3-sensitive pool) was not completely included in the thapsigargin-sensitive pool (Thastrup, 1990). The present findings are, however, in contrast to those of other studies showing that thapsigargin and (1,4,5)IP_3 affect the same or substantially overlapping pools of sequestered Ca^{2+}, e.g. methacholine as examined in adrenal chromaffin cells and parotid acinar cells, and bradykinin as examined in NG115-401L neuronal cells and chondrocytes (Cheek *et al.*, 1988; Jackson *et al.*, 1988; Benton *et al.*, 1989; Takemura *et al.*, 1989). It is possible that thapsigargin and the IP_3-dependent agonists also access the same calcium store in T_{84} cells, if the rate of spontaneous leakage from this store is low, so that thapsigargin treatment could only deplete a small fraction of the stored calcium under the conditions studied. This possibility is supported by the data presented in Figure 1, which show that, unlike the effects of thapsigargin in many other cell types, this drug has a progressive effect on $[Ca^{2+}]_i$ in T_{84} cells.

We found that prior release of Ca^{2+} from intracellular stores by thapsigargin and histamine did not affect a subsequent $[Ca^{2+}]_i$ response induced by carbachol, provided that extracellular Ca^{2+} was present (Figure 6). This contrasts with the findings of experiments carried out in the absence of extracellular Ca^{2+}, when the $[Ca^{2+}]_i$ response to a second IP_3-dependent agent was essentially abolished (Figure 5). The results suggest that, in the presence of extracellular Ca^{2+}, depletion of intracellular Ca^{2+} stores by the action of thapsigargin and carbachol or histamine stimulates refilling of Ca^{2+} stores directly, thereby allowing a second $[Ca^{2+}]_i$ response to carbachol or histamine. This is consistent with the theory that emptying of an intracellular Ca^{2+} pool can serve as a signal for Ca^{2+} entry as described previously (Berridge *et al.*, 1983; Scharff *et al.*, 1988; Takemura *et al.*, 1989). However, it is as yet unclear whether the extracellular Ca^{2+} flows directly into the cytoplasm or via the endoplasmic reticulum. From our observations, it seems reasonable to suggest that Ca^{2+} entry may occur through an endoplasmic reticulum pool before entering the cytoplasm, because the apparent refilling was not accompanied by a change in $[Ca^{2+}]_i$.

In summary, thapsigargin mobilizes calcium in T_{84} cells, as in other cell types, in a manner that is apparently independent of phosphatidylinositol breakdown and utilizes both intracellular and extracellular calcium. This increased cytoplasmic calcium can stimulate chloride secretion without a requirement for additional auxiliary second messengers. Indeed, our data suggest that calcium-dependent hormonal secretagogues actually induce the production of inhibitory second messengers which serve to uncouple chloride secretion from calcium elevations. This is in keeping with our current working model of calcium-dependent chloride secretion across T_{84} cells, where events subsequent to, or occurring in parallel with calcium mobilization, such as protein kinase C activation (Kachintorn *et al.*, 1992) or the generation of inositol tetrakisphosphate (Kachintorn *et al.*, 1993) actually serve to limit, rather than promote, the secretory response.

This study would not have been possible without the generosity of Dr O. Thastrup in providing the thapsigargin used here. We also thank Dr J. Rivier for his gift of vasoactive intestinal polypeptide, Dr S. Pandol for helpful suggestions and Mrs Glenda Wheeler for her assistance in manuscript preparation. The studies were supported by grants number DK28305 and AI24992 from the National Institutes of Health (U.S.A.).

References

AUGER, K.R., SERUNIAN, L.A., SOLTOFF, S.P., LIBBY, P. & CANTLEY, L.C. (1989). PDGF-dependent tyrosine phosphorylation stimulates production of novel phosphoinositides in intact cells. *Cell*, **57**, 167–175.

BARRETT, K.E. & DHARMSATHAPHORN, K. (1990). Mechanisms of chloride secretion in a colonic epithelial cell line. In *Textbook of Secretory Diarrhea*. ed. Lebenthal, E. & Duffey, M.E. pp. 59–66. New York: Raven Press, Inc.

BARRETT, K.E. & DHARMSATHAPHORN, K. (1991). Secretion and absorption: small intestine and colon. In *Textbook of Gastroenterology*. ed. Yamada, T. pp. 265–294. Philadelphia: J.B. Lippincott Company.

BENTON, H., JACKSON, T.R. & HANLEY, M.R. (1989). Identification of a novel inflammatory stimulant of chondrocytes. Early events in cell activation by bradykinin receptors on pig articular chondrocytes. *Biochem. J.*, **258**, 861–867.

BERRIDGE, M.J., DAWSON, R.M.C., DOWNES, C.P., HESLOP, J.P. & IRVINE, R.F. (1983). Changes in the level of inositol phosphates after agonist-dependent hydrolysis of membrane phosphoinositides. *Biochem. J.*, **211**, 473–482.

BOLTON, J.E. & FIELD, M. (1977). Ca ionophore-stimulated chloride secretion in rabbit ileal mucosa: relation to action of cyclic 3',5'-AMP and carbamylcholine. *J. Membrane Biol.*, **35**, 159–173.

BRAYDEN, D.J., HANLEY, M.R., THASTRUP, O. & CUTHBERT, A.W. (1989). Thapsigargin, a new calcium dependent epithelial anion secretagogue. *Br. J. Pharmacol.*, **98**, 809–816.

CARTWRIGHT, C.A., MCROBERTS, J.A., MANDEL, K.G. & DHARMSATHAPHORN, K. (1985). Synergistic action of cyclic adenosine monophosphate- and calcium-mediated secretion in a colonic epithelial cell line. *J. Clin. Invest.*, **76**, 1837–1842.

CHASE, H.S. (1984). Does calcium couple the apical and basolateral membrane permeabilities in epithelia? *Am. J. Physiol.*, **247**, F869–F876.

CHEEK, T.R., MORETON, R.B., BERRIDGE, M.J. & THASTRUP, O. (1988). Effects of the Ca^{2+}-mobilizing tumor promoter thapsigargin and an inositol trisphosphate mobilizing agonist on cytosolic Ca^{2+} in bovine adrenal chromaffin cells. *Biochem. Soc. Trans.*, **17**, 94–95.

COHN, J.A. (1990). Protein kinase C mediates cholinergically-regulated protein phosphorylation in a Cl^--secreting epithelium. *Am. J. Physiol.*, **258**, C227–C233.

DHARMSATHAPHORN, K., COHN, J. & BEUERLEIN, G. (1989a). Multiple calcium-mediated effector mechanisms regulate chloride secretory responses in T_{84} cells. *Am. J. Physiol.*, **256**, C1224–C1230.

DHARMSATHAPHORN, K., HUOTT, P.A., VONGKOVIT, P., BEUERLEIN, G., PANDOL, S. & AMMON, H.V. (1989b). Cl^- secretion induced by bile salts. A study of the mechanism of action based on a cultured colonic epithelial cell line. *J. Clin. Invest.*, **84**, 945–953.

DHARMSATHAPHORN, K. & MADARA, J.L. (1990). Established intestinal cell lines as model systems for electrolyte transport studies. In *Methods of Enzymology: Biomembranes and Biological Transport*, Vol. 5: *Cellular and Subcellular Transport: Epithelial Cells*. ed. Fleischer, S. & Fleischer, B. pp. 354–389. San Diego: Academic Press.

DHARMSATHAPHORN, K. & PANDOL, S.J. (1986). Mechanisms of chloride secretion induced by carbachol in a colonic epithelial cell line. *J. Clin. Invest.*, **77**, 348–354.

DONOWITZ, M. & WELSH, M.J. (1986). Ca^{2+} and cyclic AMP in regulation of intestinal Na, K, and Cl transport. *Annu. Rev. Physiol.*, **48**, 135–150.

FODER, B., SCHARFF, O. & THASTRUP, O. (1990). Ca^{2+} transients and Mn^{2+} entry in human neutrophils induced by thapsigargin. *Cell Calcium*, **10**, 477–490.

FRIZZELL, R.A. (1977). Active chloride secretion by rabbit colon: calcium-dependent stimulation by ionophore A23187. *J. Membrane Biol.*, **35**, 175–187.

HANSEN, C.A., YANG, L.J. & WILLIAMSON, J.R. (1991). Mechanisms of receptor-mediated Ca^{2+} signalling in rat hepatocytes. *J. Biol. Chem.*, **266**, 18573–18579.

JACKSON, T.R., PATTERSON, S.I., THASTRUP, O. & HANLEY, M.R. (1988). A novel tumor promoter, thapsigargin, transiently increases cytoplasmic free Ca^{2+} without generation of inositol phosphates in NG 115–401L neuronal cells. *Biochem. J.*, **353**, 81–86.

KACHINTORN, U. VAJANAPHANICH, M., BARRETT, K.E. & TRAYNOR-KAPLAN, A.E. (1993). Elevation of inositol tetrakisphosphate parallels inhibition of calcium-dependent chloride secretion in T_{84} colonic epithelial cells. *Am. J. Physiol.*, (in press).

KACHINTORN, U., VONGKOVIT, P., VAJANAPHANICH, M., DINH, S., BARRETT, K.E. & DHARMSATHAPHORN, K. (1992). Dual effects of a phorbol ester on calcium-dependent chloride secretion by T_{84} human colonic epithelial cells. *Am. J. Physiol.*, **262**, C15–C22.

KWAN, C.Y., TAKEMURA, H., OBIE, J.F., THASTRUP, O. & PUTNEY, J.W. Jr. (1990). Effects of MeCh, thapsigargin and La^{3+} on plasmalemmal and intracellular Ca^{2+} transport in lacrimal acinar cells. *Am. J. Physiol.*, **258**, C1006–C1015.

LAW, G.J., PACHTER, J.A., THASTRUP, P., HANLEY, M.J. & DANNIES, P.S. (1990). Thapsigargin, but not caffeine, blocks the ability of thyrotropin-releasing hormone to release Ca^{2+} from an intracellular store in GH4C1 pituitary cells. *Biochem. J.*, **267**, 359–364.

LUCKHOFF, A. & CLAPHAM, D.E. (1992). Inositol 1,3,4,5-tetrakisphosphate activates an endothelial Ca^{2+} permeable channel. *Nature*, **355**, 356–358.

MANDEL, K.G., MCROBERTS, J.A., BEUERLEIN, G., FOSTER, E.S. & DHARMSATHAPHORN, K. (1986). Ba^{2+} inhibition of VIP-and A23187-stimulated Cl^- secretion by T_{84} cell monolayers. *Am. J. Physiol.*, **250**, C486–C494.

MASON, M.J., GARCIA-RODRIGUEZ, C. & GRINSTEIN, S. (1991). Coupling between intracellular Ca^{2+} stores and the Ca^{2+} permeability of the plasma membrane. Comparison of the effects of thapsigargin, 2,5-di-(*tert*-butyl)-1,4-hydroquinone, and cyclopiazonic acid in rat thymic lymphocytes. *J. Biol. Chem.*, **266**, 20856–20862.

MCCANN, J.D. & WELSH, M.J. (1990). Regulation of Cl^- and K^+ channels in airway epithelium. *Annu. Rev. Physiol.*, **52**, 115–135.

OKUCHI, K., SUGAWARA, T., WATANABE, N., HIRASAWA, N., TSURRUFUJI, S., FUJIKI, H., CHRISTENSEN, S.B. & SUGIMURA, T. (1988). Analysis of the stimulative effect of thapsigargin, a non-TPA-type tumour promoter, on arachidonic acid metabolism in rat peritoneal macrophages. *Br. J. Pharmacol.*, **94**, 917–923.

PICKLES, R.J. & CUTHBERT, A.W. (1992). Failure of thapsigargin to alter ion transport in human sweat gland epithelia while intracellular Ca^{2+} concentration is raised. *J. Biol. Chem.*, **267**, 14818–14825.

SCHARFF, O., FODER, B., THASTRUP, O., HOFMANN, B., MOLLER, J., RYDER, L.P., JACOBSON, K.D., LANGHOFF, E., DICKMEISS, E., CHRISTENSEN, S., SKINHOJ, P. & SVEJGAARD, A. (1988). Effect of thapsigargin on cytosplasmic Ca^{2+} and proliferation of human lymphocytes in relation to AIDS. *Biochim. Biophys. Acta*, **972**, 257–264.

TAKEMURA, H., HUGHES, A.R., THASTRUP, O. & PUTNEY, J.W. Jr. (1989). Activation of calcium entry by the tumor promoter, thapsigargin, in parotid acinar cells. Evidence that an intracellular calcium pool, and not an inositol phosphate, regulates calcium fluxes at the plasma membrane. *J. Biol. Chem.*, **264**, 12266–12271.

TAKEMURA, H., THASTRUP, O. & PUTNEY, J.W. Jr. (1990). Calcium efflux across the plasma membrane of rat parotid acinar cells is unaffected by receptor activation or by the microsomal calcium. ATPase inhibitor, thapsigargin. *Cell Calcium*, **11**, 11–17.

THASTRUP, O. (1990). Role of Ca^{2+}-ATPase in regulation of cellular Ca^{2+} signalling, as studied with the selective microsomal Ca^{2+}-ATPase inhibitor, thapsigargin. *Agents Actions*, **29**, 8–15.

THASTRUP, O., CULLEN, P.J., DROBAK, B.K., HANLEY, M.R. & DAWSON, A.P. (1990). Thapsigargin, a tumor promoter, discharges intracellular Ca^{2+} stores by specific inhibition of the endoplasmic reticulum Ca^{2+}-ATPase. *Proc. Natl. Acad. Sci. U.S.A.*, **87**, 2466–2470.

THASTRUP, O., FODER, B. & SCHARFF, O. (1987). The calcium mobilizing and tumor promoting agent, thapsigargin, elevates the platelet cytoplasmic free calcium concentration to a higher steady state level. A possible mechanism for action for the tumor promoter. *Biochem. Biophys. Res. Commun.*, **142**, 654–660.

VAJANAPHANICH, M., KACHINTORN, U., BARRETT, K.E., COHN, J.A., DHARMSATHAPHORN, K. & TRAYNOR-KAPLAN, A.E. (1993). Phosphatidic acid modulates Cl^- secretion in T_{84} cells; varying effects depending on mode of stimulation. *Am. J. Physiol.*, (in press).

WASSERMAN, S.I., BARRETT, K.E., HUOTT, P.A., BEUERLEIN, G., KAGNOFF, M. & DHARMSATHAPHORN, K. (1988). Immune-related intestinal Cl^- secretion. I. Effect of histamine on the T_{84} cell line. *Am. J. Physiol.*, **254**, C53–C62.

WELSH, M.J. (1987). Effect of phorbol ester and calcium ionophore on chloride secretion in canine tracheal epithelium. *Am. J. Physiol.*, **253**, C828–C834.

WONG, S.M.E., LINDEMAN, R.P., PARANGI, S. & CHASE, H.S. Jr. (1989). Role of calcium in mediating action of carbachol in T_{84} cells. *Am. J. Physiol.*, **257**, C976–C985.

(Received November 10, 1992
Revised January 27, 1993
Accepted February 11, 1993)

Br. J. Pharmacol. (1993), **109**, 518–523 © Macmillan Press Ltd, 1993

On the high affinity binding site for [^{3}H]-1,3-dipropyl-8-cyclopentylxanthine in frog brain membranes

J.C. Oliveira, A.M. Sebastião & [1]J.A. Ribeiro

Laboratory of Pharmacology, Gulbenkian Institute of Science, 2781 Oeiras, Portugal

1 Radioligand binding properties of the adenosine receptor ligands, [^{3}H]-1,3-dipropyl-8-cyclopentylxanthine ([^{3}H]-DPCPX), and [^{3}H]-**R**-phenylisopropyladenosine ([^{3}H]-**R**-PIA) were investigated in frog brain membranes.

2 The specific binding of the adenosine antagonist, [^{3}H]-DPCPX to frog brain membranes showed one binding site with K_d and B_{max} values of 43.8 nM and 0.238 ± 0.016 pmol mg^{-1} protein, respectively. Guanosine 5'-triphosphate (GTP, 100 μM) decreased to 72 ± 7% and Mg^{2+} (8 mM) increased to 121 ± 3% [^{3}H]-DPCPX (40 nM) binding to frog brain membranes.

3 [^{3}H]-DPCPX saturation binding experiments performed in the presence of Mg^{2+} (8 mM), or in the presence of GTP showed that Mg^{2+} ions decreased the K_d value of [^{3}H]-DPCPX to 14 nM, and GTP increased this value to 65.6 nM. B_{max} values were not significantly ($P > 0.05$) modified (0.261 ± 0.018 pmol mg^{-1} protein, with Mg^{2+}, and 0.266 ± 0.026 pmol mg^{-1} protein, in presence of GTP) by the presence of Mg^{2+} or GTP.

4 The specific binding of [^{3}H]-**R**-PIA (15 nM) was decreased to 37 ± 6% by GTP (100 μM) and increased to 123 ± 4% by Mg^{2+} (8 mM). [^{3}H]-**R**-PIA saturation binding experiments performed in the presence of Mg^{2+} (8 mM) showed one binding site with K_d and B_{max} values of 0.9 nM and 0.229 ± 0.008 pmol mg^{-1} of protein, respectively.

5 The concentration-inhibition curves of adenosine agonists and antagonists versus [^{3}H]-DPCPX binding showed the following order of potencies: CPA > **R**-PIA ≃ NECA > **S**-PIA >> CGS 21680, for the agonists, and XAC ≃ DPCPX >> XCC > PACPX, for the antagonists.

6 The present results suggest that the adenosine binding site in the frog brain membranes is G-protein coupled, but that the antagonist affinities and the pharmacological profile is different from the A_1 or A_2 adenosine receptors.

Keywords: Frog brain membranes; adenosine; adenosine receptors; [^{3}H]-1,3-dipropyl-8-cyclopentylxanthine ([^{3}H]-DPCPX) binding; [^{3}H]-**R**-phenylisopropyladenosine ([^{3}H]-**R**-PIA) binding

Introduction

Different subtypes of adenosine receptors have been proposed based on pharmacological and biochemical criteria (see e.g. Ribeiro & Sebastião, 1986). The adenosine receptor antagonist 1,3-dipropyl-8-cyclopentylxanthine (DPCPX), is a good tool to distinguish between adenosine receptor subtypes. The K_i value for this adenosine antagonist, at the rat neuromuscular junction (K_i = 0.54 nM; Sebastião *et al.*, 1990) is about the same as that obtained in the rat hippocampus (K_i = 0.45; Sebastião *et al.*, 1990), and very close to the A_1 high affinity binding site detected in the rat brain membranes ($K_d \leqslant 1$ nM; Bruns *et al.*, 1987). Besides this binding site, another high affinity binding site for [^{3}H]-DPCPX (K_d = 10.7–13.5 nM) was detected in solubilized rat brain preparations; this binding site appears to be neither an A_1 nor an A_2 adenosine receptor (Oliveira *et al.*, 1991). At the frog neuromuscular junction the K_i value (35 nM) determined for DPCPX is about seventy times higher than that detected at the rat neuromuscular junction and within the same order of magnitude (2–3 times higher) as that found for the second high affinity binding site for [^{3}H]-DPCPX in the solubilized rat brain membranes. It, therefore, is of interest to investigate the binding characteristics of [^{3}H]-DPCPX to the frog brain membranes, as well as the potency of several adenosine agonists and antagonists in inhibiting [^{3}H]-DPCPX binding. The involvement of G-proteins in the binding of the agonist, [^{3}H]-phenylisopropyladenosine ([^{3}H]-**R**-PIA), as well as in the binding of the antagonist [^{3}H]-DPCPX was also investigated.

Brief accounts of some of this work already appeared (Oliveira *et al.*, 1992a,b).

[1] Author for correspondence.

Methods

Brain membrane preparation

Membranes were prepared according to Ruegg *et al.* (1981) with some modifications. Briefly, the frogs (*Rana ridibunda*) were killed by decapitation and brain membranes were prepared by homogenization with 20 ml of Buffer A per gram of tissue (Buffer A: Tris/HCl 50 mM (pH 7.4), NaCl 100 mM, $MgCl_2$, 10 mM, ethylenediaminetetraacetic acid (EDTA) 1 mM, diethylenetriaminepentaacetic acid (DTPA) 0.1 mM and a cocktail of proteinase inhibitors containing: dithiothreitol 1 mM, phenylmethylsulphonyl fluoride 0.1 mM and pepstatin A, leupeptin, chymostatin, antipain and aprotinin all at 1 μg ml^{-1}) and centrifuged at 2,000 r.p.m., (600 *g*) for 10 min (4°C). The supernatant was centrifuged at 15,000 r.p.m. (27,000 *g*), for 20 min (4°C), washed 3 times with the same buffer, and stored in fractions of 1 ml (~5 mg of protein) at − 85°C. Protein content was measured according the method of Lowry as modified by Peterson (1977).

Binding assay

In all the experiments, membranes were thawed, centrifuged at 15,000 r.p.m. to remove Buffer A and resuspended in Buffer B (50 mM Tris/HCl, pH 7.4). The effects of GTP on [^{3}H]-DPCPX or [^{3}H]-**R**-PIA binding were studied with membranes preincubated with 10 mM EDTA in Buffer B, for 30 min, at 25°C, washed twice and finally resuspended in Buffer B. In all experiments preparations were incubated with the ligands for 2 h, at 25°C, in presence of 2 u ml^{-1} of adenosine deaminase. In each experiment the assays were always performed in triplicate, in a final volume of 100 μl, using 12 × 75 mm polypropylene tubes.

[^{3}H]-DPCPX saturation binding studies (0.5–150 nM) were performed in control conditions (i.e. in the absence of added Mg^{2+} or GTP), in the presence of 8 mM $MgCl_2$, or in the presence of 100 μM GTP; nonspecific binding was determined in the presence of 10 mM theophylline; some experiments were performed with **R**-PIA (30 μM) to determine nonspecific binding. [^{3}H]-**R**-PIA saturation binding studies in the frog brain membranes were performed, in the presence of 8 mM Mg^{2+}, or in the presence of 100 μM GTP; nonspecific binding was determined in the presence of 10 μM xanthine amine congener (XAC). Concentration-inhibition curves for adenosine agonists (i.e. N^6-cyclopentyladenosine (CPA), 5'-N-ethylcarboxamido adenosine (NECA), **R**- and **S**-phenylisopropyladenosine (**R**- and **S**-PIA), and 2-[4-(2-carboxyethyl) phenethylamino]-5'-N-ethylcarboxamidoadenosine, (CGS 21680)), and the antagonists, xanthine amine congener (XAC), DPCPX, 1,3-dipropyl-8-(carboxymethyloxyphenyl)xanthine (XCC), and 1,3-dipropyl-8-(2-amino-4-chlorophenyl)xanthine, (PACPX) *versus* [^{3}H]-DPCPX (15 nM) binding were performed in the presence of 8 mM Mg^{2+}; nonspecific binding was determined in the presence of 30 μM **R**-PIA.

Incubations were initiated by the addition of the tissue at a final protein concentration of about 80–100 μg/tube (0.8–1.0 μg ml^{-1}). Protein concentrations were determined by the method of Lowry as modified by Peterson (1977). After incubation, the binding was stopped by rapid filtration under reduced pressure over Whatman GF/C glass fibre filters; the preparation was then washed 3 times with 5 ml Buffer B containing 0.01% 3-[(3-cholamidepropyl)dimethylammonio]-1-propane sulphonate (CHAPS) and dried. After gentle shaking overnight in a liquid-scintillation cocktail, the radioactivity was measured in a liquid-scintillation counter Beckman LS 6000 LL, for 1 min, with an efficiency of about 50%.

Data analysis

Binding parameters (K_d and B_{max} values) were determined from analysis of the binding data of all the experiments treated simultaneously with the LIGAND computer-assisted nonlinear curve fitting programme (Munson & Rodbard, 1980).

Statistics

Unless otherwise specified, data are expressed as means ± s.e.mean, and n represents the number of experiments. Because the K_d values are log normally distributed their confidence limits were calculated from the log of the K_d values. The significance of the differences between means was calculated by Student's t test, and was considered significant at $P<0.05$.

Materials

Dithiothreitol, diethylenetriaminepentaacetic acid, ethylediaminetetraacetic acid, phenylmethylsulphonyl fluoride, aprotinin, leupeptin, pepstatin A, adenosine deaminase (type VI), guanosine triphosphate, and theophylline were obtained from Sigma. [^{3}H]-DPCPX (108.3 Ci $mmol^{-1}$) was obtained from Nen Dupont and [^{3}H]-**R**-PIA (45.9 Ci $mmol^{-1}$) from Amersham. CPA, **R**- and **S**-PIA, NECA, CGS 21680, DPCPX, XAC and PACPX were from RBI (Research Biochemicals Inc., U.S.A.). All other chemicals were analytical grade.

Results

Figure 1 shows a typical binding experiment for [^{3}H]-DPCPX, used in a range of concentrations between 5 and 100 nM. Concentrations of [^{3}H]-DPCPX below 5 nM were used in two other experiments but specific binding was not detected. Concentrations up to 125 nM were used in three other experiments and the specific binding was not appreciably greater than that obtained with 100 nM [^{3}H]-DPCPX. In the [^{3}H]-DPCPX binding experiments only one binding site was detected and the averaged K_d and B_{max} values for [^{3}H]-DPCPX were 43.8 nM and 0.238 ± 0.016 pmol mg^{-1} protein ($n = 4$), respectively (see Table 1). Nonspecific binding determined in the presence of 10 mM theophylline was 65 ± 3% of the total binding at the K_d value for [^{3}H]-DPCPX binding. This high nonspecific binding was not reduced when **R**-PIA (30 μM) was used as cold ligand instead of theophylline (see below).

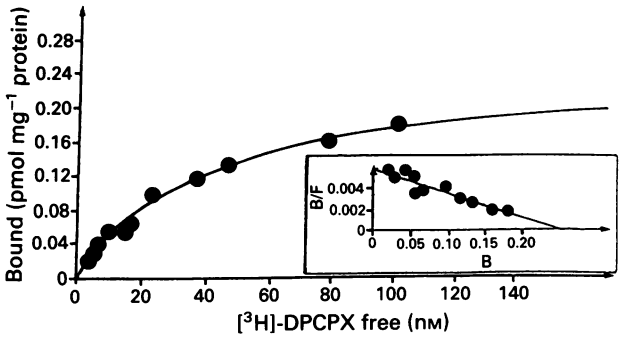

Figure 1 Specific [^{3}H]-1,3-dipropyl-8-cyclopentylxanthine ([^{3}H]-DPCPX) binding to frog brain membranes in control conditions (i.e. in the absence of added Mg^{2+} or GTP). Specific [^{3}H]-DPCPX binding was determined by subtracting nonspecific binding from the total binding. Nonspecific binding was determined in the presence of 10 mM theophylline, and for a [^{3}H]-DPCPX concentration equal to its K_d value was 65 ± 3% of the total binding. The points correspond to one representative experiment performed in triplicate, out of four experiments with similar results. Inset: Scatchard plot of the specific [^{3}H]-DPCPX binding. Binding parameters (K_d and B_{max} values) for the experiment showed in the figure were obtained by computer-assisted nonlinear curve fitting and were 40.8 nM and 0.245 ± 0.015 pmol mg^{-1} of protein. B, bound (pmol mg^{-1} protein) (i.e. specific binding); F, free [^{3}H]-DPCPX in the incubation medium (nM) after occupation of the binding sites.

Figure 2 illustrates a typical experiment on [^{3}H]-**R**-PIA binding to frog brain membranes performed in the presence

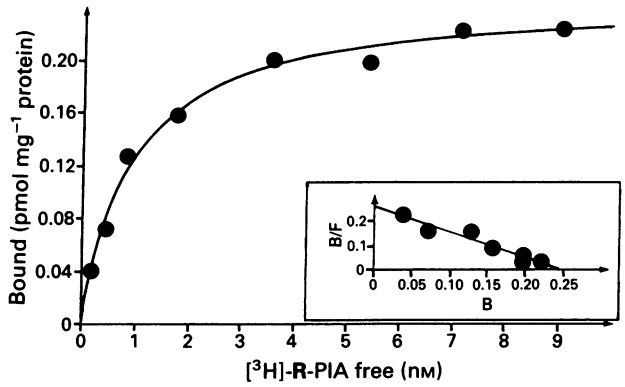

Figure 2 Specific [^{3}H]-**R**-phenylisopropyladenosine ([^{3}H]-**R**-PIA) binding to frog brain membranes in the presence of 8 mM $MgCl_2$. Specific [^{3}H]-**R**-PIA binding was determined by subtracting nonspecific binding from the total binding. Nonspecific binding was determined in the presence of 10 μM xanthine amine congener (XAC), and at the K_d values for [^{3}H]-**R**-PIA was 12 ± 0.5% of the total binding. The points correspond to one representative experiment performed in triplicate, out of three experiments with similar results. Inset: Scatchard plot of the specific [^{3}H]-**R**-PIA binding. Binding parameters (K_d and B_{max} values) for the experiment showed in the figure were obtained by computer-assisted nonlinear curve fitting and were 0.94 nM and 0.245 ± 0.243 pmol mg^{-1} of protein. B, bound (pmol mg^{-1} protein) (i.e. specific binding); F, free [^{3}H]-**R**-PIA in the incubation medium (nM) after occupation of the binding sites.

of Mg^{2+} (8 mM). Only one [^{3}H]-**R**-PIA binding site was detected with a K_d value of 0.94 nM and a B_{max} value of 0.245 ± 0.024 pmol mg^{-1} of protein. Similar results were obtained in two other experiments, and K_d and B_{max} values calculated for the three experiments (treated simultaneously by LIGAND; Munson & Rodbard, 1980) were 0.9 nM and 0.229 ± 0.08 pmol mg^{-1} of protein, respectively. Nonspecific binding determined in the presence of 10 μM XAC represented 12 ± 0.5% of the total binding at the K_d value concentration of [^{3}H]-**R**-PIA.

It is well known that GTP modifies receptor G-protein interactions in an opposite manner to the changes induced by Mg^{2+}; Mg^{2+} elicits the formation of R-G-complexes with high affinity for agonists, whereas GTP dissociates the R-G-complexes revealing the low affinity conformation for the agonists (Gilman, 1987). To investigate if the adenosine receptor present in frog brain membranes behaves as a receptor-G-protein complex, the effects of GTP (100 μM) or Mg^{2+} (8 mM) on the binding of the agonist, [^{3}H]-**R**-PIA (15 nM), were studied. The effects of these agents on the binding of the antagonist, [^{3}H]-DPCPX (40 nM), to frog brain membranes were also investigated. Figure 3 shows that

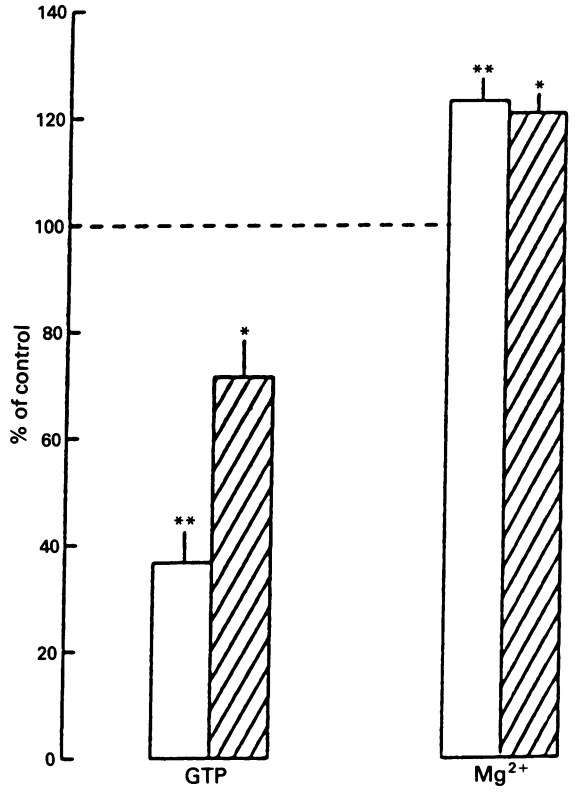

Figure 3 Effect of GTP (100 μM) and Mg^{2+} (8 mM) on the specific [^{3}H]-**R**-phenylisopropyladenosine ([^{3}H]-**R**-PIA, 15 nM) (open columns) and [^{3}H]-1,3-dipropyl-8-cyclopentylxanthine ([^{3}H]-DPCPX, 40 nM) (hatched columns) binding to frog brain membranes. Membranes were pretreated wtih EDTA (10 mM) for 30 min, at 25°C, centrifuged, washed twice with 50 mM Tris/HCl (pH 7.4), and resuspended in the same buffer. In each experiment the incubations were performed in triplicate, in control conditions (i.e. no added Mg^{2+} or GTP), in the presence of 8 mM $MgCl_2$, and in the presence of 100 μM GTP. Nonspecific binding for the antagonist was determined in presence of 10 mM theophylline, and for the agonist was determined with 10 μM xanthine amine congener (XAC). In each experiment the binding obtained in the presence of Mg^{2+} or GTP was calculated as a percentage of the binding obtained in control conditions, which was taken as 100%. Note that GTP decreased and Mg^{2+} increased the specific [^{3}H]-**R**-PIA and [^{3}H]-DPCPX binding to the frog brain membranes, when compared with the controls. Values are means ± s.e.mean obtained in $n = 3$ experiments. *$P < 0.05$ (Student's t test), when compared with the control (100%). **$P < 0.01$ (Student's t test), when compared with the control (100%).

GTP, and Mg^{2+} ions modified, in an opposite manner, the specific binding for [^{3}H]-**R**-PIA, as well as that of [^{3}H]-DPCPX. GTP decreased to 36.7 ± 6% (mean ± s.e.mean; $n = 3$) and Mg^{2+} increased to 123 ± 4.2% ($n = 3$) the specific binding of [^{3}H]-**R**-PIA; the binding of [^{3}H]-DPCPX was reduced by GTP to 71.5 ± 7.4% ($n = 3$), and increased by Mg^{2+} to 120.7 ± 3.4% ($n = 3$). The binding of ligands in the presence of Mg^{2+} was significantly different ($P < 0.05$) from their binding in the presence of GTP. In one experiment several concentrations of Mg^{2+} (1–15 mM) were tested, and it was found that the specific binding of [^{3}H]-DPCPX (40 nM) increased as the concentrations of Mg^{2+} increased up to 4 mM; with concentrations of Mg^{2+} higher than 4 mM there was no further increase in the [^{3}H]-DPCPX binding (results not shown).

To ascertain whether K_d or B_{max} values were modified by Mg^{2+} or GTP, [^{3}H]-DPCPX and [^{3}H]-**R**-PIA saturation binding experiments were carried out in which we tested the influence of these agents. Typical [^{3}H]-DPCPX saturation binding experiments are shown in Figure 4; the K_d value found for [^{3}H]-DPCPX in the presence of Mg^{2+} was 12 nM, and in the presence of GTP was 77 nM. Similar values were obtained in two other experiments, and K_d values obtained for the three experiments treated simultaneously were 14 and 65.6 nM, for the [^{3}H]-DPCPX binding in the presence of Mg^{2+} and GTP, respectively. With the individual K_d values determined by LIGAND for each experiment, confidence limits of the K_d values for each group of experiments were determined, using the logarithms of the individual K_d values. The K_d values obtained in the presence of Mg^{2+} were significantly different ($P < 0.05$) from the K_d values obtained in the presence of GTP (Table 1). B_{max} values determined in both conditions are presented in Table 1, and were not significantly different ($P > 0.05$).

In the assays performed with GTP, nonspecific [^{3}H]-DPCPX binding determined in the presence of 10 mM theophylline was 72.2% of the total binding, and in the presence of Mg^{2+} ions (8 mM) it was 41 ± 3% of the total binding. [^{3}H]-DPCPX binding parameters were not markedly modified (i.e. $K_d = 15.8$ nM; $B_{max} = 0.260 \pm 0.024$ pmol mg^{-1}

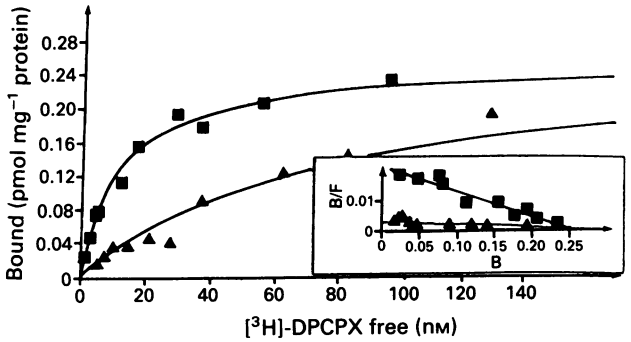

Figure 4 Specific [^{3}H]-1,3-dipropyl-8-cyclopentylxanthine ([^{3}H]-DPCPX) binding to frog brain membranes in the presence of 8 mM $MgCl_2$ (■), and in the presence of 100 μM GTP (▲). Specific [^{3}H]-DPCPX binding was determined by subtracting nonspecific binding from the total binding. Nonspecific binding was determined in the presence of 10 mM theophylline, and at the K_d value for [^{3}H]-DPCPX was 41 ± 3% of the total binding in the presence of Mg^{2+}, and of 72.2 ± 2.1% of the total binding, in the presence of GTP. For each curve, the points correspond to one representative experiment performed in triplicate, out of three experiments with similar results. Inset: Scatchard plot of the specific [^{3}H]-DPCPX binding. Binding parameters (K_d and B_{max} values) for the experiment showed in the figure were obtained by computer-assisted nonlinear curve fitting and were 12 nM and 0.253 ± 0.103 pmol mg^{-1} of protein in the presence of Mg^{2+}, and 77 nM and 0.264 ± 0.059 pmol mg^{-1} of protein in the presence of GTP. B, bound (pmol mg^{-1} protein) (i.e. specific binding); F, free [^{3}H]-DPCPX in the incubation medium (nM) after occupation of the binding sites.

Table 1 Binding parameters for [^{3}H]-1,3-dipropyl-8-cyclopentylxanthine ([^{3}H]-DPCPX) to frog brain membranes

	K_d (nM)	B_{max} (pmol mg^{-1} prot)
Control ($n = 4$)	43.8 (27–63)	0.238 ± 0.016
Mg^{2+} (8 mM, $n = 3$)	14.0 (10–21)[a]	0.261 ± 0.018[c]
GTP (100 μM, $n = 3$)	65.6 (54–83)[b]	0.266 ± 0.026[c]

K_d and B_{max} (means ± s.e.mean) values were determined with the LIGAND computer-assisted non-linear curve-fitting programme (Munson & Rodbard, 1980). In parentheses are shown the confidence limits of the means of the K_d values obtained from the individual experiments to allow statistical comparison.

[a]Statistically different from the control ($P < 0.05$; Student's t test).

[b]Statistically different from the K_d value obtained in the presence of Mg^{2+} ($P < 0.05$; Student's t test).

[c]Not statistically different from the control ($P > 0.05$; Student's t test).

of protein, in the presence of Mg^{2+}, $n = 3$) when **R**-PIA (30 μM) instead of theophylline (10 mM) was used to define nonspecific binding. When **R**-PIA was used instead of theophylline, nonspecific [^{3}H]-DPCPX binding in the presence of Mg^{2+} (8 mM) was 51 ± 3% of the total binding at the K_d value for [^{3}H]-DPCPX; this nonspecific binding was not significantly different ($P > 0.05$) from that obtained with theophylline (10 mM).

One [^{3}H]-**R**-PIA binding experiment was performed in the presence of 100 μM-GTP using concentrations of [^{3}H]-**R**-PIA up to 200 nM. With concentrations below 10 nM, no measurable specific [^{3}H]-**R**-PIA binding was observed, and with higher concentrations of [^{3}H]-**R**-PIA (i.e. 200 nM) the saturation was not yet achieved. This made impossible an accurate determination of the K_d value for [^{3}H]-**R**-PIA binding in the presence of GTP. Though the K_d of [^{3}H]-**R**-PIA in the presence of GTP could not be determined by this method, the need of the high concentrations of [^{3}H]-**R**-PIA to obtain a measurable specific binding in the presence of GTP suggests that GTP affected mainly the affinity of the agonist for the binding sites.

Because Mg^{2+} increased the affinity of [^{3}H]-DPCPX for the binding sites, we performed concentration-inhibition curves for adenosine agonists and antagonists *versus* [^{3}H]-DPCPX (15 nM) binding in the presence of 8 mM $MgCl_2$. The inhibition of [^{3}H]-DPCPX binding showed the following order of potencies (K_i): CPA (0.8 nM) > **R**-PIA (3.2 nM) ≃ NECA (4.8 nM) > S-PIA (19.8 nM) >> CGS 21680 (1749 nM), for the agonists (Figure 5, and Table 2), and XAC (12.7 nM) ≃ DPCPX (13.7 nM) >> XCC (2047 nM) > PACPX (> 10000 nM), for the antagonists (Figure 6 and Table 2). Nonspecific binding determined in the presence of 30 μM-**R**-PIA was about 40% of the total binding. Computer analysis revealed that all the inhibition binding curves (except for PACPX) were best described by one site binding model. The Hofstee plots for all these compounds were linear, and the Hill coefficients were near 1.0, a result also suggesting the presence of only one binding site (see Table 2). Problems with the solubility of PACPX made impossible its use in concentrations higher than 10^{-4} M; thus, complete concentration-inhibition curves for PACPX and determination of the Hill coefficient could not be obtained.

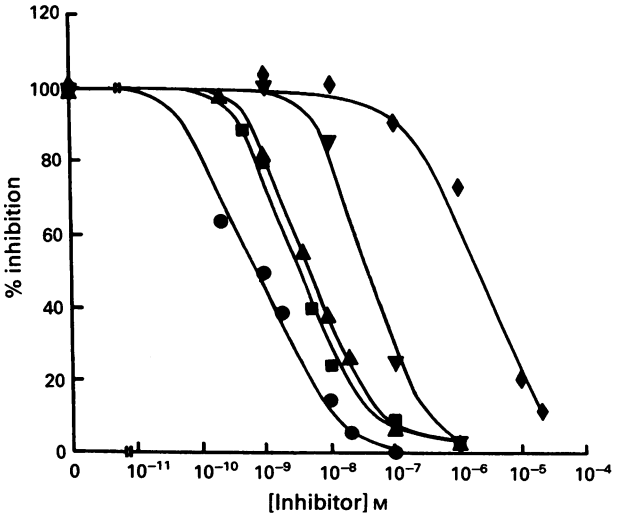

Figure 5 Concentration-inhibition curves for adenosine agonists versus specific binding of [^{3}H]-1,3-dipropyl-8-cyclopentylxanthine ([^{3}H]-DPCPX, 15 nM) to frog brain membranes: (●) CPA, (■) **R**-PIA, (▲) NECA, (▼) S-PIA and (◆) CGS 21680. For abbreviations, see text. Incubations were performed, as described in Methods, in the presence of 8 mM Mg^{2+}. For each curve, the points correspond to one representative experiment out of two to four with similar results. K_i values for each agonist are in Table 2. Curves were generated using the best fit parameters from the computer LIGAND programme.

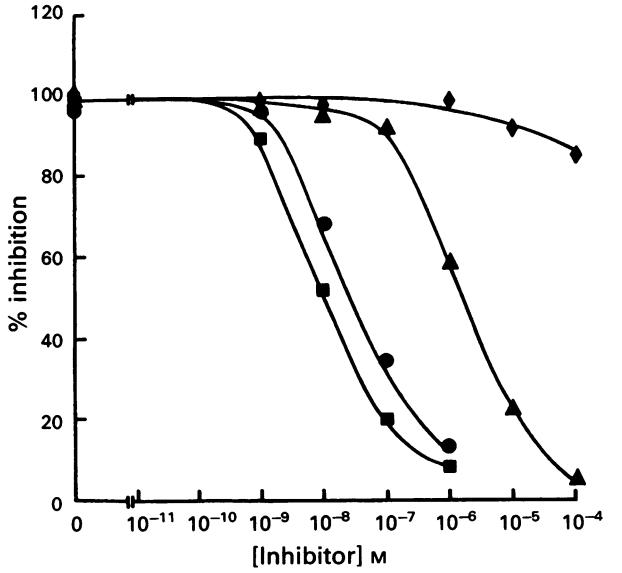

Figure 6 Concentration-inhibition curves for adenosine antagonists versus specific binding of [^{3}H]-1,3-dipropyl-8-cyclopentylxanthine ([^{3}H]-DPCPX, 15 nM) to frog brain membranes: (■) XAC, (●) DPCPX, (▲) XCC, and (◆) PACPX. For abbreviations, see text. Incubations were performed, as described in Methods, in the presence of 8 mM Mg^{2+}. For each curve, the points correspond to one representative experiment out of three with similar results. K_i values for each antagonist are in Table 2. Curves were generated using the best fit parameters from the computer LIGAND programme.

Discussion

The results obtained in the present work show that the frog brain membranes possess a high affinity binding site for [^{3}H]-DPCPX, whose affinity is different either from the A_1 ($K_i \leq 1$ nM, Bruns *et al.*, 1987) or the A_2 ($K_d = 340$ nM, Lohse *et al.*, 1987) adenosine receptors obtained in rat brain membranes. The K_d value now obtained for the binding of [^{3}H]-DPCPX to the frog brain membranes in the absence of added Mg^{2+} or GTP (i.e. control conditions, $K_d = 43.8$ nM) suggests that this site could be equivalent to the receptor detected in the functional studies in the frog neuromuscular

Table 2 K_i values for the inhibition of [^{3}H]-1,3-dipropyl-8-cyclopentylxanthine ([^{3}H]-DPCPX) binding (15 nM) to frog brain membranes by agonists and antagonists of adenosine receptors

	n	K_i (nM)	n_H
Agonists			
CPA	2	0.8	1.00 ± 0.02
R-PIA	4	3.2	1.00 ± 0.02
NECA	2	4.8	1.03 ± 0.03
S-PIA	3	19.8	1.10 ± 0.15
CGS 21680	3	1749	1.08 ± 0.07
Antagonists			
XAC	3	12.7	0.99 ± 0.07
DPCPX	3	13.7	0.99 ± 0.06
XCC	3	2047	1.01 ± 0.05
PACPX[a]	3	>10000	-

Membranes were incubated with 15 nM [^{3}H]-DPCPX, for 2 h, at 25°C, in the presence of 8 mM Mg^{2+}, and competitors in a range of 1 nM to 300 μM, as described in Methods. K_i values were determined by the computer LIGAND programme, assuming a K_d value for [^{3}H]-DPCPX binding of 14.0 nM. In all cases the one site-model fitted the data better than the two site model ($P<0.05$). *n* represents the number of experiments; n_H is the Hill coefficient (means ± s.d.). For abbreviations, see text.

[a]Problems with the solubilization of PACPX made impossible the accurate determination of the K_i of PACPX, as well as of its n_H.

Table 3 Comparison of the activity of various agonists and antagonists for the A_1 and A_2 adenosine receptor of rat brain membranes with that for the adenosine receptor of frog brain membranes

	K_i (nM)		
	Frog brain membranes	A_1	A_2
Agonists			
CPA	0.8	0.6[a]	462[a]
R-PIA	3.2	1.17[a]	124[a]
NECA	4.8	6.3[a]	10.3[a]
S-PIA	19.8	49.3[a]	1820[a]
CGS 21680	1749	2600[b]	15[b]
Antagonists			
XAC	12.7	4[b]	44[b]
DPCPX	13.7 (43.8)*	0.5[c]	340[c]
XCC	2047	42[a]	1500[a]
PACPX	>10000	2.5[a]	91.9[a]

Mean K_i values for the activity of adenosine ligands in the A_1 [^{3}H]-CHA and in the A_2 [^{3}H]-NECA (+ 50 nM CPA) binding assays were obtained from [a]Bruns *et al.* (1986), [b]Jarvis *et al.* (1989), and [c]Bruns *et al.* (1987). Agonist and antagonist K_i values for the adenosine receptor in the frog brain membranes were obtained by inhibition of [^{3}H]-DPCPX binding (15 nM), in the presence of 8 mM Mg^{2+}, which increased the affinity of the binding of the antagonist, DPCPX.

*The K_d value for [^{3}H]-DPCPX in conditions similar to that used in the studies for the A_1 and A_2 receptor is shown in parentheses.

junction where the K_i value obtained for DPCPX was 35 nM (Sebastião & Ribeiro, 1989).

[^{3}H]-DPCPX binding to the frog brain membranes was displaced by adenosine analogues with the rank order of potency CPA (K_i = 0.8 nM) > **R**-PIA (3.2 nM) ≥ NECA (4.8 nM) > S-PIA (19.8 nM) >> CGS 21680 (1.7 μM), which, except for the near equipotency between NECA and **R**-PIA and the small (≈6) stereoselectivity for the PIA isomers, is not markedly different from what one could expect for the rank order of potency for binding to A_1 adenosine receptors to rat brain membranes (see Table 3, and references therein).

Several adenosine receptor antagonists were used to perform concentration-inhibition curves *vs* [^{3}H]-DPCPX binding in the presence of Mg^{2+}. The rank order of potency of the 1,3,8-substituted xanthine derivatives was XAC (K_i = 13 nM) ≈ DPCPX (14 nM) >> XCC (2 μM) > PACPX (> 10 μM). This profile conforms with the data obtained for the adenosine receptor mediating the adenosine-induced presynaptic inhibition of neuromuscular transmission in the innervated frog sartorius muscle, where XAC (K_i = 23 nM) ≥ DPCPX (35 nM) >> XCC (1.9 μM) ≥ PACPX (2.3 μM) (Sebastião & Ribeiro, 1989). The order of antagonist potency found in the present work is different from that described either for the A_1 or the A_2 adenosine receptors (see Table 3). The main differences related to the A_1 receptor are, besides the low potency of DPCPX, the very low potency of PACPX and XCC.

The finding that the agonist affinities, in contrast to the antagonist affinities for the adenosine receptor in frog brain membranes did not exhibit great differences from the agonist affinities reported for the A_1 adenosine receptor might indicate that the adenosine receptor in the frog brain membranes is a variety of the A_1 adenosine receptor. Indeed, species differences between ligand affinities are more intense for adenosine receptor antagonists, than for adenosine receptor agonists (Ukena *et al.*, 1986; Klotz *et al.*, 1991). For example, sheep, bovine (Klotz *et al.*, 1991) and calf (Ukena *et al.*, 1986) brains have A_1 adenosine receptors highly sensitive to DPCPX (K_d = 0.2 nM), whereas guinea-pig brain has an A_1 adenosine receptor with a relatively low affinity for DPCPX (K_d = 2 nM: Klotz *et al.*, 1991; 5 nM: Ukena *et al.*, 1986). If the adenosine receptor in the frog brain membranes belongs to the A_1 subtype it has thus an even lower affinity for DPCPX, with a K_d value of 43.8 nM, when we used experimental conditions (i.e. absence of added Mg^{2+} or GTP) similar to those used by Ukena *et al.* (1986) or Klotz *et al.* (1991). Thus, considering that the adenosine receptor in the frog brain membranes belongs to the A_1 subtype, one has to assume that one of the more selective antagonists for this receptor, DPCPX, has more than a 200 fold difference in its affinity for the A_1 receptor according to the animal species used. This issue becomes even more complicated when in the same animals species, the rat, some A_1 adenosine receptors have subnanomolar affinities for DPCPX (Bruns *et al.*, 1987), whereas other non A_2-DPCPX sensitive receptors have considerably lower affinity, i.e. intermediate affinity between the typical A_1 and the A_2 adenosine receptor subtypes for this xanthine (Alexander *et al.*, 1989; Oliveira *et al.*, 1991).

Modulation by Mg^{2+} and GTP of the [^{3}H]-**R**-PIA binding showed that, as occurs with the A_1-adenosine receptors from rat brain (Perez-Reyes *et al.*, 1987), or rat adipocytes (Ukena *et al.*, 1984), GTP decreased and Mg^{2+} increased specific binding of this agonist to the frog brain membranes. The [^{3}H]-**R**-PIA saturation binding studies indicate that the effects of Mg^{2+} and GTP are probably on the affinity of the agonist for the binding site. In the solubilized rat brain membranes, the non-A_1 non-A_2 binding site for [^{3}H]-**R**-PIA is also enhanced by Mg^{2+} and inhibited by GTP (Oliveira *et al.*, 1991). It thus appears that the binding of agonists to the non-A_1 non-A_2 adenosine receptor is influenced by GTP and Mg^{2+} in the same manner as the binding of agonists to the A_1 adenosine receptor. There is a consensus that this is a general characteristic of receptors coupled to G-proteins (Gilman, 1987).

Another point of interest in the present results is that the K_d value of this newly detected binding site for [^{3}H]-DPCPX was increased by GTP. High Mg^{2+} decreased the K_d for [^{3}H]-DPCPX, an effect common in adenosine agonist binding, but usually not seen in the adenosine antagonist binding. Thus, DPCPX seems to discriminate between two conformations of the adenosine receptor in frog brain membranes, the high affinity form induced by Mg^{2+}, and the low

affinity form induced by GTP, suggesting that a guanine nucleotide binding protein regulates the currently described adenosine antagonist binding in the same manner as it regulates adenosine agonist binding in other situations. This differs from the [^{3}H]-DPCPX binding to the A_1 adenosine receptor (Weber *et al.*, 1990; Klotz *et al.*, 1990). In some receptor systems, e.g. D_2-dopamine (De Lean *et al.*, 1982), muscarinic (Burgisser *et al.*, 1982) and opioid (Simon *et al.*, 1984) receptors, it has been found that the antagonists could discriminate between two different conformations of the receptor molecule, with GTP increasing and Mg^{2+} decreasing antagonist affinity. This contrasts with what was found in the present work, where GTP decreased and Mg^{2+} increased antagonist binding. Whether this behaviour of DPCPX means that this xanthine has some agonist properties needs to be elucidated in functional studies. However, in the same animal species, at the frog neuromuscular junction, DPCPX was a consistent competitive adenosine receptor antagonist (Sebastião & Ribeiro, 1989). The same occurs at the rat neuromuscular junction and the rat hippocampus (Sebastião *et al.*, 1990).

In solubilized rat brain preparations, the K_d for the second high affinity site for [^{3}H]-DPCPX ($K_d = 11-14$ nM), in the presence of Mg^{2+} (Oliveira *et al.*, 1991), is similar to the K_d value (14 nM) for [^{3}H]-DPCPX binding to the frog brain membranes also obtained in the presence of Mg^{2+}. Although the GTP-sensitivity of the second binding site for [^{3}H]-DPCPX in rat brain is not known, the similarity between its K_d value and the K_d value of the [^{3}H]-DPCPX binding site in frog brain membranes, in similar conditions (i.e. in the presence of Mg^{2+}), might suggest that the binding site similar to that now detected in frog brain membranes is also present in a mammalian preparation.

In summary, besides functional studies establishing the existence of a non-A_1 non-A_2 adenosine receptor at the frog motor nerve terminals (Ribeiro & Sebastião, 1985; Sebastião & Ribeiro, 1989), the present work suggests that the frog brain also possesses this adenosine receptor. This new entity behaves as a receptor G-protein complex, where G-protein coupling regulates its affinity for the agonist, **R**-PIA, as well as for the antagonist, DPCPX.

J.C.O. is in receipt of a JNICT Ph.D. studentship (BD/821/90-ID). The help of Mr Artur Costa is acknowledged.

References

ALEXANDER, S.P.H., KENDALL, D.A. & HILL, S.J. (1989). Differences in the adenosine receptors modulating inositol phosphates and cyclic AMP accumulation in mammalian cerebral cortex. *Br. J. Pharmacol.*, **98**, 1241–1248.

BRUNS, R.F., LU, G.H. & PUGSLEY, T.A. (1986). Characterization of the A_2 adenosine receptor labelled by [^{3}H]-NECA in rat striatal membranes. *Mol. Pharmacol.*, **29**, 331–346.

BRUNS, R.F., FERGUS, J.H., BADBER, E.W., BRISTOL, J.A., SANTAY, L.A., HARTMAN, J.D., HATS, S.J. & HUANG, C.C. (1987). Binding of the A_1-selective adenosine antagonist [^{3}H]-8-cyclopentyl-1,3-dipropylxanthine to rat brain membranes. *Naunyn Schmiedebergs Arch. Pharmacol.*, **335**, 59–63.

BURGISSER, E., DE LEAN, A. & LEFKOWITZ, R.J. (1982). Reciprocal modulation of agonist and antagonist binding to muscarinic cholinergic receptor by guanine nucleotide. *Proc. Natl. Acad. Sci. U.S.A.*, **79**, 1732–1736.

DE LEAN, A., HANCOCK, A.A. & LEFKOWITZ, R.J. (1982). Validation and statistical analysis of a computer modeling method for quantitative analysis of radioligand binding data for mixtures of pharmacological receptor subtypes. *Mol. Pharmacol.*, **21**, 5–16.

GILMAN, A.G. (1987). G proteins: transducers of receptor-generated signals. *Annu. Rev. Biochem.*, **56**, 615–649.

JARVIS, M.F., SCHULZ, R., HUTCHISON, A.J., DO, U.H., SILLS, M.A. & WILLIAMS, M. (1989). [^{3}H]-CGS 21680, a selective A_2 adenosine receptor agonist directly labels A_2 receptors in rat brain. *J. Pharmacol. Exp. Ther.*, **251**, 888–893.

KLOTZ, K.-N., VOGT, H. & TAWFIK-SCHLIEPER, H. (1991). Comparison of A_1 adenosine receptors in brain from different species by radioligand binding and photoaffinity labelling. *Naunyn-Schmiedebergs Arch. Pharmacol.*, **343**, 196–201.

LOHSE, M.J., KLOTZ, K.-N., LINDERBORN-FOTINOS, J., REDDINGTON, M., SCHWABE, U. & OLSSON, R.A. (1987). 8-cyclopentyl-1,3-dipropylxanthine (DPCPX) – a selective high affinity radioligand for A_1 adenosine receptors. *Naunyn Schmiedebergs Arch. Pharmacol.*, **336**, 204–210.

MUNSON, P.J. & RODBARD, D. (1980). LIGAND: a versatile computerized approach for characterization of ligand-binding systems. *Anal. Biochem.*, **107**, 220–239.

OLIVEIRA, J.C., SEBASTIÃO, A.M. & RIBEIRO, J.A. (1991). Solubilized rat brain adenosine receptors have two high affinity binding sites for [^{3}H]-1,3-dipropyl-8-cyclopentylxanthine. *J. Neurochem.*, **57**, 1165–1171.

OLIVEIRA, J.C., SEBASTIÃO, A.M. & RIBEIRO, J.A. (1992a). The frog brain possesses one binding site different from the A_1 or the A_2 adenosine receptors. *Br. J. Pharmacol.*, **105**, 176P.

OLIVEIRA, J.C., SEBASTIÃO, A.M. & RIBEIRO, J.A. (1992b). Binding characteristics and molecular weight of the A_3 adenosine receptor in the frog brain membranes. *Neurochem. Int.* (Supplement), **21**, C6(22).

PEREZ-REYES, E., YEUNG, S.-M., LASHER, R.L. & COOPER, D.M.F. (1987). Structural studies on adenosine R_i receptors from rat brain cerebral cortex. In *Topics and Perspectives in Adenosine Research*. ed. Gerlach, E. & Becker, B.F. pp. 37–48. Springer-Verlag: Berlin.

PETERSON, G.L. (1977). A simplification of the protein assay method of Lowry et al., which is more generally applicable. *Anal. Biochem.*, **83**, 346–356.

RIBEIRO, J.A. & SEBASTIÃO, A.M. (1985). On the type of receptor involved in the inhibitory action of adenosine at the neuromuscular junction. *Br. J. Pharmacol.*, **84**, 911–918.

RIBEIRO, J.A. & SEBASTIÃO, A.M. (1986). Adenosine receptors and Ca^{2+}: basis for proposing a third (A_3) adenosine receptor. *Prog. Neurobiol.*, **26**, 179–209.

RUEGG, U.T., CUENOD, S., HILLER, J.M., GIOANNINI, T., HOWELLS, R.D. & SIMON, E.J. (1981). Characterization and partial purification of solubilized active opiate receptors from toad brain. *Proc. Natl. Acad. Sci. U.S.A.*, **78**, 4635–4638.

SEBASTIÃO, A.M. & RIBEIRO, J.A. (1989). 1,3,8- and 1,3,7-substituted xanthines: relative potency as adenosine receptor antagonists at the frog neuromuscular junction. *Br. J. Pharmacol.*, **96**, 211–219.

SEBASTIÃO, A.M., STONE, T.W. & RIBEIRO, J.A. (1990). The inhibitory adenosine receptor at the neuromuscular junction and hippocampus of the rat: antagonism by 1,3,8-substituted xanthines. *Br. J. Pharmacol.*, **101**, 453–459.

SIMON, J., SZUCS, M., BENYHE, S., BORSODI, A., ZEMAN, P. & WOLLEMANN, M. (1984). Solubilization and characterization of opioid binding sites from frog (*Rana esculenta*) brain. *J. Neurochem.*, **43**, 957–963.

UKENA, D., POESCHLA, E. & SCHWABE, U. (1984). Guanine nucleotide and cation regulation of radioligand binding to R_i adenosine receptors of rat fat cells. *Naunyn-Schmiedebergs Arch. Pharmacol.*, **326**, 241–247.

UKENA, D., JACOBSON, K.A., PADGETT, W.L., AYALA, C., SHAMIM, M.T., KIRK, K.L., OLSSON, R.O. & DALY, J.W. (1986). Species differences in structure-activity relationships of adenosine agonists and xanthine antagonists at brain A_1 adenosine receptors. *FEBS Lett.*, **209**, 122–128.

WEBER, R.G., JONES, C.R., LOHSE, M.J. & PALACIOS, J.M. (1990). Autoradiographic visualization of A_1 adenosine receptors in rat brain with [^{3}H]8-cyclopentyl-1,3-dipropylxanthine. *J. Neurochem.*, **54**, 1344–1353.

(Received November 20, 1992
Revised February 9, 1993
Accepted February 11, 1993)

Br. J. Pharmacol. (1993), **109**, 524–529 © Macmillan Press Ltd, 1993

Roles of prostacyclin, EDRF and active oxygens in leukocyte-dependent platelet adhesion to endothelial cells induced by platelet-activating factor *in vitro*

Masahiko Hirafuji & Hisashi Shinoda

Department of Pharmacology, Tohoku University School of Dentistry, 4–1 Seiryo-machi, Sendai 980, Japan

1 The mechanism of polymorphonuclear leukocyte (PMN)-dependent platelet adhesion to cultured endothelial cells induced by platelet-activating factor (PAF) was investigated to determine whether PMNs release or generate any factor(s) capable of inducing platelet adhesion, and the roles of prostacyclin and endothelium-derived relaxing factor (EDRF).

2 Cell-free supernatants, sonicates or rapid filtrates of PAF-stimulated PMN suspensions did not induce platelet adhesion to endothelial cells, but the PMN sonicates induced platelet adhesion when endothelial cells were pretreated with both aspirin and N^G-nitro-L-arginine (L-NOARG). Its microphotograph showed that mainly platelet aggregates adhered to the endothelial cell surface.

3 Platelet adhesion induced by the PMN sonicates to aspirin- and L-NOARG-pretreated endothelial cells was dose-dependently prevented by OP-41483 (1–100 nM), and slightly by L-arginine (1 mM). The inhibition of platelet adhesion by OP-41483 and L-arginine was potentiated by their combination.

4 WEB 2170 (3 μM), a PAF antagonist, inhibited platelet adhesion induced by the PMN sonicates. However, PAF alone did not induce significant platelet adhesion to aspirin- and L-NOARG-treated endothelial cells.

5 Platelet adhesion induced by the PMN sonicates was not suppressed by AA-861 and indomethacin. However, both superoxide dismutase and catalase significantly inhibited platelet adhesion, and, in combination, their inhibitory effect was synergistically potentiated. Mannitol had no effect. It was also significantly inhibited by α_1-antitrypsin, whereas chymostatin and elastatinal had no effect.

6 PAF-induced platelet adhesion to endothelial cells in the presence of intact PMNs was not suppressed by indomethacin and AA-861, or by protease inhibitors. SOD alone, and in combination with catalase, caused a slight but significant inhibition, while catalase and mannitol by themselves had no effect.

7 PMN-induced platelet adhesion was slightly inhibited by OP-41483 (100 nM). L-Arginine (1 mM) alone had no effect, but slightly potentiated the effect of OP-41483. This platelet adhesion was not accompanied by suppression of prostacyclin synthesis.

8 The results with the PMN sonicates show that prostacyclin, EDRF and active oxygens are important modulators of intercellular interactions between platelets and endothelial cells. These results further suggest that the mechanism of intact PMN-dependent platelet adhesion is primarily through platelet-endothelial cell interactions in which leukocyte-derived active oxygens play a role, but does not involve platelet-platelet interactions inhibitable by prostacyclin.

Keywords: Active oxygens; prostacyclin; EDRF; platelet adhesion; endothelial cells; leukocytes; platelet-activating factor (PAF)

Introduction

Interaction of platelets and polymorphonuclear leukocytes (PMNs) with the blood vessel walls at sites of vascular injury is considered to be an essential early event in the pathogenesis of inflammation, thrombosis and atherosclerosis. In a previous report, we demonstrated that platelet-activating factor (PAF) induced platelet adhesion to endothelial cells in the presence of PMNs *in vitro*, and had no effect in the absence of PMNs (Hirafuji & Shinoda, 1991a). Another potent PMN activator, N-formyl-methionyl-leucyl-phenylalanine also induced platelet adhesion to endothelial cells when PMNs were present, while leukotriene B_4 had no effect, suggesting that the induction of platelet adhesion is not a general property of PMN activators (Hirafuji & Shinoda, 1991b). Although there are several possible mechanisms for the platelet adhesion, microscopic examination has suggested the possibility that some factor(s) released from PAF-stimulated PMNs mediate(s) platelet adhesion by acting on platelets or/and endothelial cells. Activated PMNs are known to generate and release various bioactive substances, including arachidonate metabolites, proteases and active oxygens, which can modulate not only platelets but also endothelial cell functions (Harlan, 1987).

On the other hand, endothelial cells normally have highly anti-thrombogenic properties which can be attributed to their capacity to synthesize and release a variety of substances, including prostacyclin and endothelium-derived relaxing factor (EDRF) which have been shown to inhibit platelet aggregation and adhesion (Moncada *et al.*, 1976; Azuma *et al.*, 1986; Furlong *et al.*, 1987; Radomski *et al.*, 1987a,b; Sneddon & Vane, 1988). Therefore, PMN-dependent platelet adhesion induced by PAF would also occur due to the loss of these anti-thrombogenic properties. In the present study, to clarify the mechanism of PMN-dependent platelet adhesion, we investigated whether PAF-stimulated PMNs release or generate any factor(s) capable of inducing platelet adhesion to endothelial cells. We also examined the role of prostacyclin and EDRF released from endothelial cells in this mechanism.

Methods

Endothelial cells, platelets and PMNs

Endothelial cells, platelets and PMNs were prepared as described previously (Hirafuji & Shinoda, 1991a). In brief, endothelial cells were isolated from human umbilical cord veins by collagenase digestion. Primary endothelial cells were seeded into 24-well culture plates (Primaria, Falcon), and grown until confluent (4–6 days) in Ham's F-12 medium containing 15% foetal calf serum, 25 $\mu g\ ml^{-1}$ endothelial cell mitogen, 90 $\mu g\ ml^{-1}$ heparin, 50 $u\ ml^{-1}$ penicillin and 50 $\mu g\ ml^{-1}$ streptomycin. Just prior to experiments, endothelial cells were washed 3 times with Hanks' balanced salt solution containing 10 mM HEPES (pH 7.4) and 0.25% bovine serum albumin (BSA; HBSS).

Washed platelets were prepared from freshly collected rabbit blood with EDTA (5 mM) as anticoagulant. Platelets were finally resuspended in HBSS at 5×10^8 platelets ml^{-1}. To radio-label platelets, platelets in platelet-rich plasma were incubated with [^{3}H]-adenine, 0.5 $\mu Ci\ ml^{-1}$ for 30 min at 37°C, according to the method of Curwen *et al.* (1982). After washing out free radioactivity, cold adenine (100 μM) was added to the final platelet suspension.

Methods for rabbit PMN preparation included dextran sedimentation of erythrocytes, hypotonic shock to eliminate erythrocyte contamination, and purification by centrifugation on Lymphoprep solution. PMNs were finally suspended in calcium- and magnesium-free HBSS at 1×10^7 cells ml^{-1}. Calcium (1.3 mM) and magnesium (1.0 mM) were added just prior to the experiments.

Platelet adhesion assay

Platelet adhesion to endothelial cells was determined in the presence of either intact PMNs or their cell-free preparations. When intact PMNs were used, radiolabelled platelets (7.5×10^7 per well) and/or PMNs (7.5×10^5 per well) were added to endothelial cell monolayers, and incubated for 20 min at 37°C with gentle shaking in a total volume of 400 μl. Platelets and endothelial cells were also incubated with various cell-free preparations derived from PMN suspensions. In some experiments, platelets and PMN preparations were incubated with endothelial cells that had been pretreated with aspirin (500 μM) and/or N^G-nitro-L-arginine (L-NOARG; 300 μM) for 15 min. Following incubation, the wells were gently washed 3 times with HBSS to remove non-adherent cells. Distilled water containing 1% Triton X-100 was added to each well to lyse the remaining cells, and the radioactivity in the wells was counted.

Cell-free preparations of PMNs

To prepare cell-free supernatants, PMN suspensions (1×10^7 ml^{-1}) were incubated for 10 min at 37°C with or without 26.7 nM PAF, and then centrifuged at 230 *g* for 10 min at 4°C. To obtain PMN sonicates, PMN suspensions were sonicated for 20 s (Tomy UR-20P, Japan) at 0°C after PAF stimulation. To obtain rapid filtrates, PMNs were stimulated for 10 min with PAF in a disposable syringe. Following incubation, PMN suspensions were rapidly filtered through a 0.22 μM membrane filter (Millipore, Japan) attached to the syringe, and the filtrates were immediately (within 1 s) added to endothelial cell monolayer and platelets.

Determination of prostacyclin

Following incubation of endothelial cells, platelets or PMNs for 20 min at 37°C as indicated in the text, the medium in the well was transferred to microvials containing indomethacin (10 μM, final concentration), chilled on ice and then centrifuged at 8,000 *g* for 2 min. The supernatants were stored at − 20°C until use. Prostacyclin was determined as 6-keto-prostaglandin $F_{1\alpha}$ (6-keto-$PGF_{1\alpha}$) by a specific radioimmunoassay (Hirafuji & Shinoda, 1992).

Materials

PAF (1-O-hexadecyl -2-acetyl-*sn*-glycero-3-phosphocholine), bovine serum albumin, adenine, indomethacin, N^G-nitro-L-arginine, α_1-antitrypsin, superoxide dismutase, and catalase were purchased from Sigma; Ham's F-12 culture medium, foetal calf serum, penicillin and streptomycin from Gibco; endothelial cell mitogen from Biomedical Technologies Inc.; Lymphoprep (9.6% sodium metrizoate and 5.6% Ficoll) from Nycomed AS; collagenase (*Clostridium histolyticum*), mannitol, L-arginine and HEPES from Wako Chemicals; chymostatin and elastatinal from Peptide Institute Inc.; Hanks' balanced salt solution from Nissui Pharmaceut.; aspirin (DL-lysin salt) from Midorijuhji Co.; [^{3}H]-adenine (24 $Ci\ mmol^{-1}$) from Amersham, Buckinghamshire; [^{3}H]-6-keto-$PGF_{1\alpha}$ from NEN, U.S.A. AA-861 (2-(12-hydroxydodeca-5, 10-dinyl)-3,5,6-trimethyl-1,4-benzoquinone) and WEB 2170 (6-(2-chloro-phenyl)-8,9-dihydro-1-methyl-8-(4-morpholinyl-carbonyl)-4H, 7H-cyclopenta[4,5]thieno[3,2-f][1,2,4]-triazolo-[4,3-a][1,4]daizepine) were gifts from Takeda Chemical Indust., Japan, and Dr H. Heuer, Boehringer-Ingelheim KG, Germany, respectively. OP-41483-α-cyclodextrin (5(E)-6,9α-methylene-15-cyclopentyl-16, 17, 18, 19, 20-pentanor-prostaglandin I_2·α-cyclodextrin clathrate), 6-keto-$PGF_{1\alpha}$ and its antiserum were also kindly provided by Ono Pharmaceuticals Indust., Ltd., Japan.

Statistical analysis

Platelet adhesion was expressed as a percentage of the total radioactivity in cell suspension added to the wells. Results are expressed as mean ± s.e.mean of *n* experiments performed in triplicate which agreed within 10% or of replicate determinations. Statistical analysis was made by Student's *t* test, and *P* values less than 0.05 were considered as significant.

Results

Effects of cell-free preparations of PMNs

Platelets and endothelial cells were incubated with various cell-free preparations from PMNs stimulated without or with PAF (26.7 nM) for 10 min to determine if PMNs generate or release any factor(s) capable of inducing platelet adhesion. However, as shown in Table 1, neither the cell-free supernatants, the sonicates, nor the rapid filtrates, of PMN suspensions stimulated with or without PAF caused significant platelet adhesion to endothelial cells.

Effects of pretreatment of endothelial cells with aspirin and L-NOARG

Endothelial cells were pretreated for 15 min with aspirin (500 μM) and/or L-NOARG (300 μM), and incubated with platelets in the presence of the sonicates of PAF-stimulated PMNs. As shown in Figure 1, when endothelial cells were pretreated with either aspirin or L-NOARG, the PMN sonicates did not induce significant platelet adhesion to the endothelial cells. However, when endothelial cells were pretreated with both aspirin and L-NOARG, the PAF-stimulated sonicates significantly ($P < 0.01$) induced platelet adhesion (from 2.8 ± 0.3 to 8.4 ± 0.6% platelet adhesion, mean ± s.e.mean, $n = 4$ experiments performed in triplicate). As demonstrated in Figure 2, microscopic examination showed that some single platelets and mainly aggregates of platelets adhered to endothelial cell surfaces without any gaps or retraction of endothelial cell monolayers. The sonicates of unstimulated PMNs did not induce platelet adhesion to the aspirin- and/or L-NOARG-pretreated endo-

Table 1 Effects of various cell-free preparations from PMNs on platelet adhesion to endothelial cells

Additions	*Platelet adhesion* (%)
Basal	2.6 ± 0.2
Cell-free supernatants[a]	
Unstimulated PMNs	2.3 ± 0.1
PAF-stimulated PMNs	2.2 ± 0.3
Sonicates[b]	
Unstimulated PMNs	2.4 ± 0.2
PAF-stimulated PMNs	2.3 ± 0.1
Rapid filtrates[c]	
Unstimulated PMNs	3.0 ± 0.2
PAF-stimulated PMNs	2.9 ± 0.4

[^{3}H]-adenine-labelled platelets and cell-free preparations of PMN suspension, either unstimulated or stimulated with 26.7 nM PAF for 10 min, were added to endothelial cell monolayers and incubated for 20 min. Mean ± s.e.mean of 3 experiments performed in triplicate.

[a]After PAF stimulation, PMN suspensions (1×10^7 cells ml^{-1}) were centrifuged at 230 *g* for 10 min at 4°C.

[b]After PAF stimulation, PMN suspensions were sonicated for 5 × 4 s at 0°C.

[c]After PAF stimulation, PMN suspensions were rapidly filtered through a 0.22 μm membrane filter, and the filtrates were immediately (within 1 s) added to platelets and the endothelial cell monolayer.

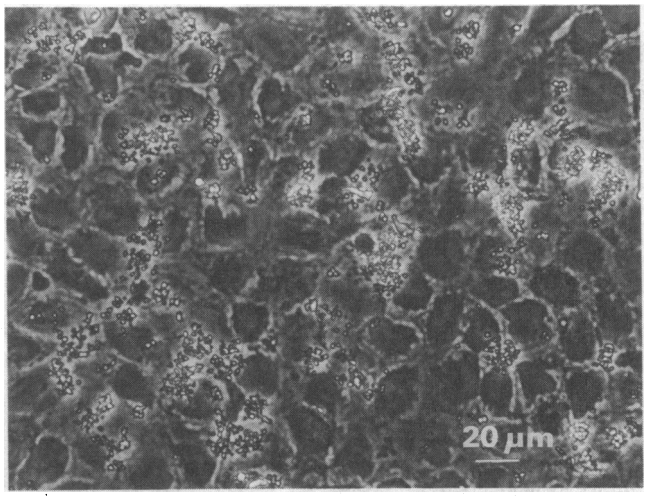

Figure 2 Phase-contrast photomicrograph (original magnification; × 200) of platelet adhesion to endothelial cells. Platelets and sonicates of PAF-stimulated PMNs were incubated for 20 min with aspirin- and N^G-nitro-L-arginine (L-NOARG)-pretreated endothelial cells. Details are the same as described in the legend of Figure 1. Following three washings, the well was fixed with 2% paraformaldehyde-2% glutaraldehyde. Scale bar = 20 μm.

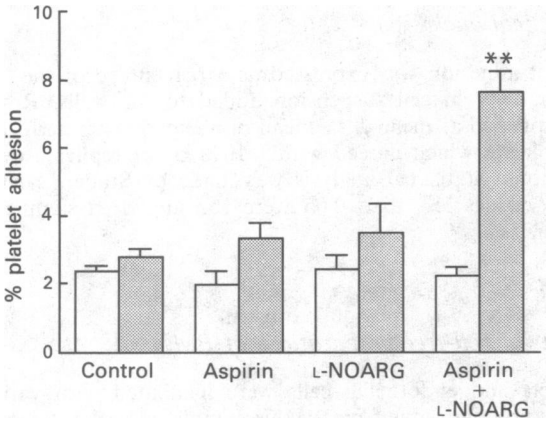

Figure 1 Effects of aspirin- and N^G-nitro-L-arginine (L-NOARG)-pretreatment of endothelial cells on platelet adhesion in the presence of PMN sonicates. Endothelial cells were pretreated with 500 μM aspirin and/or 300 μM L-NOARG for 15 min at 37°C. After aspirating the incubation medium, radiolabelled platelets and sonicates of PMNs stimulated (stippled columns) or unstimulated (open columns) with PAF were added to endothelial cells and incubated for 20 min at 37°C. Mean with s.e.mean of 4 experiments performed in triplicate. $^{**}P < 0.01$.

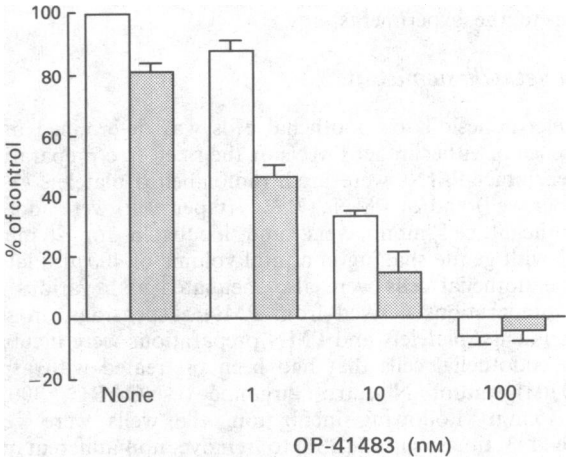

Figure 3 Effects of L-arginine and OP-41483 on platelet adhesion to aspirin- and N^G-nitro-L-arginine (L-NOARG)-pretreated endothelial cells induced by sonicates of PAF-stimulated PMNs. Endothelial cells were pretreated with aspirin and L-NOARG in the presence (stippled columns) or the absence (open columns) of L-arginine (1 mM). Following the pretreatment, endothelial cells were incubated with platelets and the sonicates in the presence or the absence of OP-41483 at the indicated concentrations. Results are expressed as a percentage of the control platelet adhesion induced without L-arginine and OP-41483. Mean with s.e.mean of 4 experiments in triplicate. All treatments were statistically significant ($P < 0.05$).

thelial cells. The cell-free supernatants of the PAF-stimulated and unstimulated PMNs also did not induce platelet adhesion to the thrombogenic endothelial cells (data not shown).

Effects of L-arginine and OP-41483 on platelet adhesion

Figure 3 demonstrates the effects of L-arginine and OP-41483 on platelet adhesion to aspirin- and L-NOARG-pretreated endothelial cells induced by sonicates of PAF-stimulated PMNs. When endothelial cells were pretreated with aspirin and L-NOARG in the presence of L-arginine (1 mM), platelet adhesion induced by PMN sonicates was slightly prevented (20.5 ± 5.1% inhibition, $n = 4$ in triplicate, $P < 0.05$). Platelet adhesion induced by the PMN sonicates was dose-dependently prevented by OP-41483 with complete prevention at 100 nM. The effect of OP-41483 was potentiated when combined with L-arginine, which was remarkable at lower concentration. OP-41483 alone at 1 nM caused 12.2 ± 3.6% inhibition ($n = 4$, $P < 0.05$) of platelet adhesion, while it caused 46.6 ± 4.0% inhibition ($n = 4$, $P < 0.01$) in combination with L-arginine.

Effects of PAF and PAF antagonist on platelet adhesion

As illustrated in Figure 4, a potent PAF antagonist, WEB 2170 (3 μM) completely inhibited platelet adhesion to aspirin-

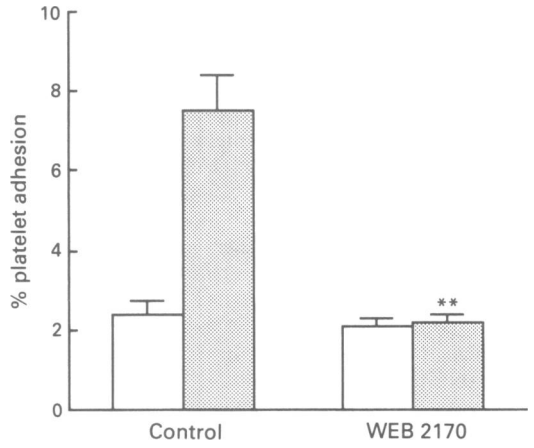

Figure 4 Effects of WEB 2170 on platelet adhesion to aspirin- and N^G-nitro-L-arginine (L-NOARG)-pretreated endothelial cells induced by sonicates of PAF-stimulated PMNs. Radiolabelled platelets without (open columns) or with (stippled columns) sonicates of PAF-stimulated PMNs were added to the aspirin- and L-NOARG-pretreated endothelial cells in the presence of a PAF antagonist, WEB 2170 (3 μM), and incubated for 20 min. Mean with s.e.mean of 3 experiments in triplicate. $^{**}P<0.01$.

and L-NOARG-pretreated endothelial cells induced by sonicates of PAF-stimulated PMNs, but had no effect on the basal adhesion.

On the other hand, PAF (10 nM) alone without the sonicates did not induce platelet adhesion to aspirin- and/or L-NOARG-pretreated endothelial cells (data not shown).

Effects of various inhibitors on platelet adhesion induced by PMN sonicates

Table 2 shows the effects of inhibitors of arachidonate metabolism and proteases, and of scavengers of active oxygens on the sonicates-induced platelet adhesion to thrombogenic endothelial cells. Platelet adhesion induced by the sonicates of PAF-stimulated PMNs was not suppressed when PMNs were stimulated in the presence of AA-861 (3 μM), a 5-lipoxygenase inhibitor (Ashida *et al.*, 1983), or indomethacin (3 μM). However, both superoxide dismutase (SOD; 300 u ml^{-1}) and catalase (1000 u ml^{-1}) significantly ($P<0.05$) inhibited platelet adhesion, and their inhibitory effect was potentiated by their combination. Mannitol (1 mM) had no effect. Platelet adhesion was also significantly ($P<0.05$) inhibited by α_1-antitrypsin (1 mg ml^{-1}), whereas chymostatin (10 μg ml^{-1}) and elastatinal (10 μg ml^{-1}) had no effect.

Effects of various inhibitors on platelet adhesion induced by intact PMNs

PAF induces platelet adhesion to endothelial cells when intact PMNs were coincubated (Hirafuji & Shinoda, 1991a). The effects of various inhibitors and scavengers of active oxygens were also evaluated on PAF-induced platelet adhesion to endothelial cells in the presence of intact PMNs (Table 2). Indomethacin and AA-861 again had no effect on platelet adhesion. Furthermore, α_1-antitrypsin, chymostatin and elastatinal had no significant effect. Among scavengers of active oxygens, SOD alone, and in combination with catalase, caused a slight but significant ($P<0.05$) inhibition of platelet adhesion. However, catalase and mannitol by themselves were without effect.

Effects of L-arginine and OP-41483 on intact PMN-induced platelet adhesion

PAF (10 nM) caused a significant ($P<0.01$) platelet adhesion to endothelial cells when intact PMNs were present (3.9 ± 0.5 in basal and 9.9 ± 0.6 in PAF-stimulated group, $n=6$ in triplicate). As illustrated in Figure 5, OP-41483 at 100 nM slightly inhibited platelet adhesion induced by PAF in the presence of PMNs (92.5 ± 1.5% of control, $n=4$, $P<0.05$), whereas the lower concentrations had no effect. L-Arginine at 1 mM alone had no effect (94.7 ± 5.7% of control, $n=4$), but slightly potentiated the effect of OP-41483 (77.6 ± 3.9% of control, $n=4$, $P<0.05$).

Prostacyclin production during intact PMN-induced platelet adhesion

Table 3 demonstrates a representative result of the effect of PAF on prostacyclin production during platelet adhesion. Incubation of endothelial cells with platelets but not PMNs remarkably increased the basal prostacyclin production. Addition of PAF (10 nM) caused 2, 3.2 and 3.5 fold increase in prostacyclin production by endothelial cells alone, with platelets and with PMNs, respectively, when compared with each basal production. PAF also caused a 3.6 fold increase in

Table 2 Effects of scavengers of active oxygens and various inhibitors on platelet adhesion to endothelial cells induced by sonicates of PAF-stimulated PMNs and by intact PMNs

Additions	*Platelet adhesion induced by* PMN sonicates[a]	Intact PMNs[b]
	% of control (n)	
Indomethacin (3 μM)	97.6 ± 3.4 (3)	104.6 ± 5.0 (3)
AA-861 (3 μM)	98.9 ± 2.9 (3)	90.1 ± 15.8 (3)
α_1-Antitrypsin (1 mg ml^{-1})	34.7 ± 5.1 (3)*	89.7 ± 8.4 (3)
Chymostatin (10 μg ml^{-1})	95.6 ± 3.2 (3)	92.4 ± 5.5 (3)
Elastatinal (10 μg ml^{-1})	93.0 ± 4.7 (3)	95.7 ± 4.0 (3)
SOD (300 u ml^{-1})	78.7 ± 7.5 (4)*	87.9 ± 2.8 (4)*
Catalase (1000 u ml^{-1})	59.9 ± 9.8 (4)*	96.6 ± 1.4 (4)
SOD + catalase	19.8 ± 4.8 (4)**	81.0 ± 4.5 (4)*
Mannitol (1 mM)	92.7 ± 5.6 (3)	93.5 ± 5.5 (3)

For abbreviations, see text.

[a]Endothelial cells were pretreated with 500 μM aspirin and 300 μM N^G-nitro-L-arginine for 15 min. After aspirating the incubation medium, [^{3}H]-adenine-labelled platelets and sonicates of PAF-stimulated PMNs were incubated for 20 min with endothelial cells in the presence of the indicated agent, except that indomethacin and AA-861 were added to PMN suspensions during the PAF stimulation.

[b]Radio-labelled platelets and intact PMNs were incubated for 20 min with untreated endothelial cells in the presence of PAF (10 nM) and the indicated agent.

Mean ± s.e.mean of n experiments performed in triplicate. $^*P<0.05$, $^{**}P<0.01$.

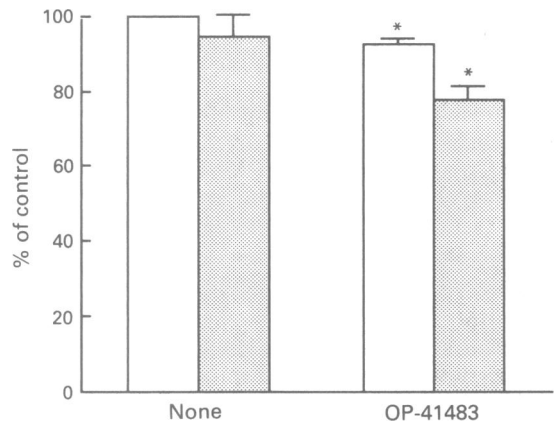

Figure 5 Effects of L-arginine and OP-41483 on platelet adhesion induced by PAF in the presence of intact PMNs. Radiolabelled platelets, endothelial cells and intact PMNs were stimulated by PAF (10 nM) for 20 min without or with OP-41483 (100 nM) in the absence (open columns) or presence (stippled columns) of L-arginine (1 mM). Results are expressed as a percentage of the control platelet adhesion induced by PAF. Mean with s.e.mean of 4 experiments in triplicate. $*P < 0.05$.

Table 3 Effect of PAF on prostacyclin production by intercellular interactions among endothelial cells (ECs), platelets and PMNs

	Prostacyclin (ng per well)	
Conditions	*Basal*	*PAF* (10 nM)
ECs	0.06 ± 0.005	0.12 ± 0.003
ECs + platelets	3.62 ± 0.26	11.68 ± 0.62
ECs + PMNs	0.06 ± 0.003	0.21 ± 0.07
ECs + platelets + PMNs	3.60 ± 0.30	13.07 ± 0.51

Endothelial cells without or with platelets and/or PMNs were incubated in the absence (Basal) or the presence of PAF (10 nM) for 20 min at 37°C. At the end of incubation, the medium was added with indomethacin (10 μM) and centrifuged at 8,000 *g* for 2 min. Prostacyclin in the supernatants was determined by radioimmunoassay as 6-keto-$PGF_{1\alpha}$. Mean ± s.e.mean of a representative of 3 experiments performed in triplicate.

prostacyclin production by endothelial cells with platelets and PMNs, a condition under which platelet adhesion to endothelial cells occurred. The experiment was repeated three times with essentially similar results, although the basal levels and response to PAF of prostacyclin productions in each condition were very variable depending on the experiment, possibly due to the variation in batches of endothelial cells.

Discussion

In a previous paper, we demonstrated that PAF induced platelet adhesion to endothelial cell surfaces only in the presence of PMNs *in vitro* (Hirafuji & Shinoda, 1991a). In the present study, to determine whether PMNs release or generate any factor(s) capable of inducing platelet adhesion, the effects of various cell-free preparations from PMNs on platelet adhesion were first examined. However, neither the cell-free supernatants containing released factors, the sonicates containing various factors and their generating systems, nor the rapid filtrates containing stable and unstable released factors, of PMN suspensions stimulated with or without PAF, caused platelet adhesion to endothelial cells. This indicates that PMN-dependent platelet adhesion cannot be simply explained by factor(s) released or generated by activated PMNs. As platelet adhesion occurs only in the presence of intact PMNs, it may require the concomitant intercellular interactions among these cells.

However, when endothelial cells were depleted of prostacyclin and EDRF by pretreatment with both aspirin, a cyclo-oxygenase inhibitor, and L-NOARG, a potent inhibitor of EDRF production (Ishii *et al.*, 1990; Moore *et al.*, 1990), the sonicates of PAF-stimulated PMNs induced platelet adhesion. Pretreatment with either aspirin or L-NOARG alone had no effect. Furthermore, L-arginine partially prevented platelet adhesion induced by the PMN sonicates, possibly antagonizing the effect of L-NOARG, and the inhibitory effect was potentiated in combination with OP-41483, a stable prostacyclin analogue (Fujitani & Wakitani, 1990). However, these results may not necessarily imply that prostacyclin and EDRF prevent platelet adhesion to endothelial cells by acting in concert as in platelet aggregation (Radomski *et al.*, 1987b; MacDonald *et al.*, 1988). Platelet adhesion seems to be regulated by elevation of guanosine 3′:5′-cyclic monophosphate (cyclic GMP) but not adenosine 3′:5′-cyclic monophosphate (cyclic AMP) (Radomski *et al.*, 1987a; Sneddon & Vane, 1988; Venturini *et al.*, 1992), while OP-41483 elevates cyclic AMP level in platelets like prostacyclin (Fujitani & Wakitani, 1990), and this compound alone effectively inhibited platelet adhesion induced by the PMN sonicates. Furthermore, since photomicrographs of sonicate-induced platelet adhesion showed that mainly platelet aggregates adhered to the endothelial cell surface, platelet adhesion cannot be readily separated from platelet aggregation in this system. Therefore, the inhibition of platelet adhesion by OP-41483 may be due to dissociation of adherent platelet aggregates which have formed in the presence of PAF-stimulated PMN sonicates. The synergism between endogenous prostacyclin and EDRF in preventing platelet adhesion may be also due to inhibition of platelet aggregate formation rather than platelet-endothelial cell interactions.

Platelet adhesion to aspirin- and L-NOARG-pretreated endothelial cells induced by sonicates of PAF-stimulated PMNs was completely inhibited by a PAF antagonist, WEB 2170 (Heuer *et al.*, 1990). This result indicates that the sonicates contain PAF which was not inactivated by acetylhydrolase (Lee *et al.*, 1982), and that platelet adhesion to thrombogenic endothelial cells requires, at a minimum, the activation of both, or either, the platelets and/or endothelial cells by PAF. Since PAF is a potent agonist in rabbit platelets and a weak agonist in human endothelial cells (Hirafuji & Shinoda, 1992), platelets may be the target cells of PAF. However, PAF alone at a concentration (10 nM) that induces full aggregation did not induce platelet adhesion even to the thrombogenic endothelial cells without the sonicates, suggesting that some factor(s) in the sonicates are prerequisite to the ultimate platelet-endothelial cell interactions. Since the platelet adhesion was significantly inhibited by SOD, catalase and mostly by their combination, active oxygens in the PMN sonicates may be those factors. Likewise, Salvemini *et al.* (1989) have found that SOD inhibits thrombin-stimulated platelet aggregation and adhesion to gelatin-coated plastic, although catalase has no effect, suggesting that superoxide anions enhance platelet aggregation and adhesion. Therefore, in our system, active oxygens may potentiate both aggregation and adhesion, resulting in the deposition of platelet aggregates on the endothelial cells. Certain proteases also seem to play minor roles, because the platelet adhesion was also significantly inhibited by a non-specific protease inhibitor, α_1-antitrypsin.

Thus, an experimental system using the PMN sonicates suggested that prostacyclin, EDRF and active oxygens were important modulators of intercellular interactions between platelets and endothelial cells. Therefore, we also evaluated the involvements of these factors in platelet adhesion to endothelial cells induced by intact PMNs. The results suggest that alteration of prostacyclin synthesis, at least, is not

involved in this system for the following reasons. First, OP-41483 at 100 nM caused a minimal inhibition of platelet adhesion induced by intact PMNs, whereas this concentration of OP-41483 completely inhibited the sonicate-induced platelet adhesion. Second, when prostacyclin production during the intercellular interactions was determined, PMN-dependent platelet adhesion induced by PAF was not accompanied by a suppression in prostacyclin synthesis. Furthermore, single platelets are the predominant adhering cells in intact PMN-induced platelet adhesion (Hirafuji & Shinoda, 1991a), while aggregates of platelets are mainly adhering in the sonicate-induced platelet adhesion (Figure 2). Hence, the mechanism by which intact PMNs induce platelet adhesion is probably different from that of the sonicate-induced platelet adhesion. It may be primarily platelet-endothelial cell interactions mediated by activated PMNs, but does not involve platelet-platelet interactions inhibitable by prostacyclin.

Since the platelet adhesion induced by intact PMNs was significantly inhibited by scavengers of active oxygens, active oxygens derived from activated PMNs may play a role in the platelet-endothelial cell interactions. However, these scavengers had less of an effect in this system than in the system using the PMN sonicates. This minor effect could be explained by recent electron microscopic-histochemical studies (Vissers *et al.*, 1985; Hirai *et al.*, 1991). These studies have demonstrated that PMNs, activated by specific agonists, release active oxygens only at the area of contact between PMNs and nonphagocytosable surfaces or phagocytosable particles, which is hence inaccessible to macromolecules such as scavenger proteins. Since pharmacological studies seem to possess such a limitation, further studies with other approaches may be required to clarify the involvement of active oxygens.

It is also not clear from the present study whether EDRF is involved in the PMN-dependent platelet adhesion. EDRF, in contrast to prostacyclin, strongly inhibits platelet adhesion by stimulating guanylate cyclase (Radomski *et al.*, 1987a; Sneddon & Vane, 1988; Venturini *et al.*, 1992). Furthermore, a possible mechanism by which active oxygens increase platelet adhesion may be through inhibition of guanylate cyclase (Salvemini *et al.*, 1989). Therefore, it is conceivable that PMN-derived active oxygens decrease the cyclic GMP level in platelets by inhibiting guanylate cyclase and by destroying EDRF released from endothelial cells (Gryglewski *et al.*, 1986) ultimately cause platelet adhesion. It would be of interest to determine levels of cyclic GMP or EDRF during the intercellular interactions to clarify these possibilities.

The authors are grateful to Dr T. Adachi and the staff at the Adachi Maternity Hospital for kindly providing the umbilical cords. This study was supported in part by a Grant-in-Aid for Scientific Research from the Ministry of Education, Science and Culture, and NISHINOMIYA Basic Research Fund, Japan.

References

ASHIDA, Y., SAIJO, T., KURIKI, H., MAKINO, H., TERAO, S. & MAKI, Y. (1983). Pharmacological profile of AA-861, a 5-lipoxygenase inhibitor. *Prostaglandins*, **26**, 955–972.

AZUMA, H., ISHIKAWA, M. & SEKIZAKI, S. (1986). Endothelium-dependent inhibition of platelet aggregation. *Br. J. Pharmacol.*, **88**, 411–415.

CURWEN, K.D., KIM, H.-Y., VAZQUEZ, M., HANDIN, R.I. & GIMBRONE, M.A.Jr. (1982). Platelet adhesion to cultured vascular endothelial cells. A quantitative monolayer adhesion assay. *J. Lab. Clin. Med.*, **100**, 425–436.

FUJITANI, B. & WAKITANI, K. (1990). Studies on antiplatelet effect of OP-41483, a prostaglandin I_2 analog, in experimental animals. II. Mechanism of its antiplatelet effect. *Jpn. J. Pharmacol.*, **52**, 123–130.

FURLONG, B., HENDERSON, A.H., LEWIS, M.J. & SMITH, J.A. (1987). Endothelium-derived relaxing factor inhibits *in vitro* platelet aggregation. *Br. J. Pharmacol.*, **90**, 687–692.

GRYGLEWSKI, R.J., PALMER, R.M.J. & MONCADA, S. (1986). Superoxide anion is involved in the breakdown of endothelium-derived relaxing factor. *Nature*, **308**, 645–647.

HARLAN, J.M. (1987). Consequence of leukocyte-vessel wall interactions in inflammatory and immune reactions. *Semin. Thromb. Hemost.*, **13**, 434–444.

HEUER, H.O., CASALS-STENZEL, J., MUACEVIC, G. & WEBER, K.H. (1990). Pharmacological activity of bepafant (WEB 2170), a new and selective hetrazepinoic antagonist of platelet-activating factor. *J. Pharmacol. Exp. Ther.*, **255**, 962–968.

HIRAFUJI, M. & SHINODA, H. (1991a). Platelet-leukocyte interaction in adhesion to endothelial cells induced by platelet-activating factor *in vitro*. *Br. J. Pharmacol.*, **136**, 1356–1377.

HIRAFUJI, M. & SHINODA, H. (1991b). PAF-mediated platelet adhesion to endothelial cells induced by FMLP-stimulated leukocytes. *J. Lipid Mediat.*, **4**, 347–352.

HIRAFUJI, M. & SHINODA, H. (1992). Antagonism of platelet-activating factor-induced increase in cytosolic free calcium concentration in human endothelial cells. *Jpn. J. Pharmacol.*, **58**, 231–241.

HIRAI, K., MORIGUCHI, K. & WANG, G.-Y. (1991). Human neutrophils produce free radicals from the cell-zymosan interface during phagocytosis and from the whole plasma membrane when stimulated with calcium ionophore A23187. *Exp. Cell Res.*, **194**, 19–27.

ISHII, K., CHANG, B., KERWIN, J.F.Jr., HUANG, Z.-J. & MURAD, F. (1990). N^G-nitro-L-arginine: a potent inhibitor of endothelium-derived relaxing factor formation. *Eur. J. Pharmacol.*, **176**, 219–223.

LEE, T.-C., MALONE, B., WASSERMAN, S.I., FITZGERALD, V. & SYNDER, F. (1982). Activities of enzyme that metabolize platelet-activating factor (1-alkyl-2-acetyl-*sn*-glycero-3-phosphocholine) in neutrophils and eosinophils from humans and the effect of a calcium ionophore. *J. Biol. Chem.*, **256**, 175–178.

MACDONALD, P.S., READ, M.A. & DUSTING, G.J. (1988). Synergistic inhibition of platelet aggregation by endothelium-derived relaxing factor and prostacyclin. *Thromb. Res.*, **49**, 437–449.

MONCADA, S., GLYGLEWSKI, R., BUNTING, S. & VANE, J.R. (1976). An enzyme isolated from arteries transforms prostaglandin endoperoxides to an unstable substance that inhibits platelet aggregation. *Nature*, **263**, 663–665.

MOORE, P.K., AL-SWAYEH, O.A., CHONG, N.W.S., EVANS, R.A. & GIBSON, A. (1990). N^G-nitro-L-arginine, a novel, L-arginine-reversible inhibitor of endothelium-dependent vasodilatation *in vitro*. *Br. J. Pharmacol.*, **99**, 408–412.

RADOMSKI, M.W., PALMER, R.M.J. & MONCADA, S. (1987a). The role of nitric oxide and cGMP in platelet adhesion to vascular endothelium. *Biochem. Biophys. Res. Commun.*, **148**, 1482–1489.

RADOMSKI, M.W., PALMER, R.M.J. & MONCADA, S. (1987b). The anti-aggregating properties of vascular endothelium: interactions between prostacyclin and nitric oxide. *Br. J. Pharmacol.*, **92**, 639–646.

SALVEMINI, D., DE NUCCI, G., SNEDDON, J.M. & VANE, J.R. (1989). Superoxide anions enhance platelet adhesion and aggregation. *Br. J. Pharmacol.*, **97**, 1145–1150.

SNEDDON, J.M. & VANE, J.R. (1988). Endothelium-derived relaxing factor reduces platelet adhesion to bovine endothelial cells. *Proc. Natl. Acad. Sci. U.S.A.*, **85**, 2800–2804.

VENTURINI, C.M., WESTON, L.K. & KAPLAN, J.E. (1992). Platelet cGMP, but not cAMP, inhibits thrombin-induced platelet adhesion to pulmonary vascular endothelium. *Am. J. Physiol.*, **263**, H606–H612.

VISSERS, M.C.M., DAY, W.A. & WINTERBOURN, C.C. (1985). Neutrophils adherent to a nonphagocytosable surface (glomerular basement membrane) produce oxidants only at the site of attachment. *Blood*, **66**, 161–166.

(Received December 21, 1992
Revised February 5, 1993
Accepted February 15, 1993)

Br. J. Pharmacol. (1993), **109**, 530–534 © Macmillan Press Ltd, 1993

Mediation of endothelin-1-induced inhibition of platelet aggregation via the ET_B receptor

Lorraine McMurdo, Paul S. Lidbury, [1]Christoph Thiemermann & John R. Vane

The William Harvey Research Institute, St. Bartholomew's Hospital Medical College, Charterhouse Square, London EC1M 6BQ

1 The effects of FR139317 (ET_A antagonist) or PD145065 (non-selective ET_A/ET_B antagonist) on endothelin-1 (ET-1)-induced changes in blood pressure and inhibition of *ex vivo* platelet aggregation were investigated in the anaesthetized rabbit.

2 ET-1 (1 nmol kg^{-1}, i.a. bolus) caused a sustained increase in mean arterial pressure (MAP) (peak increase 47 ± 5 mmHg, $n = 8$). Intravenous infusion of FR139317 at 0.2 ($n = 4$) or 0.6 mg kg^{-1} min^{-1} ($n = 4$) inhibited the ET-1 pressor response by 83 or 89%, respectively. Infusion of PD145065 at 0.2 ($n = 4$) or 0.6 mg kg^{-1} min^{-1} ($n = 4$) inhibited the ET-1-induced increase in MAP by 79 or 75%, respectively.

3 The transient depressor response (− 16 ± 3 mmHg) which preceded the rise in blood pressure induced by ET-1 (1 nmol kg^{-1}, i.a., $n = 8$) was enhanced by an intravenous infusion of FR139317 (0.6 mg kg^{-1} min^{-1}) to − 35 ± 5 mmHg ($P < 0.05$, $n = 4$). This enhancement was abolished by indomethacin (5 mg kg^{-1}, i.v.) pretreatment (− 17 ± 1 mmHg, $n = 4$). PD145065 (0.2 mg kg^{-1} min^{-1}, i.v.) attenuated the ET-1-induced fall in blood pressure to − 9 ± 1 mmHg ($n = 4$), while a higher dose of this antagonist (0.6 mg kg^{-1} min^{-1}, i.v.) completely abolished the ET-1-mediated depressor response.

4 ET-1 (1 nmol kg^{-1}, $n = 8$) inhibited *ex vivo* platelet aggregation by 96% at 5 min after injection of the peptide. FR139317 (0.2 or 0.6 mg kg^{-1} min^{-1}, i.v.) or PD145065 (0.2 mg kg^{-1} min^{-1}, i.v.) did not affect the inhibition of *ex vivo* platelet aggregation in response to ET-1. In contrast, intravenous infusion of PD145065 (0.6 mg kg^{-1} min^{-1}) abolished the anti-aggregatory effects of ET-1.

5 Thus, FR139317 inhibits the pressor, but not the depressor actions of ET-1 and has no effect on the ET-1-induced inhibition of *ex vivo* platelet aggregation. In contrast, PD145065 antagonizes the pressor and depressor responses to ET-1 and abolishes the anti-aggregatory effects of the peptide.

6 These results strongly suggest that ET-1-induced vasoconstriction in the anaesthetized rabbit is primarily mediated via the ET_A receptor while the depressor and antiaggregatory actions of ET-1 are due to activation of the ET_B receptor.

Keywords: Endothelin; prostacyclin; ET_A antagonist; ET_A/ET_B antagonist; *ex vivo* platelet aggregation

Introduction

Endothelin-1 (ET-1) is a potent 21 amino acid vasoconstrictor peptide produced by vascular endothelial cells (Yanagisawa *et al.*, 1988). ET-1 stimulates the release of a variety of endothelium-derived vasodilator autacoids including prostacyclin (PGI_2), prostaglandin E_2 and nitric oxide (NO) (De Nucci *et al.*, 1988; Rae *et al.*, 1989; Warner *et al.*, 1989a,b; see Thiemermann, 1991). The release of PGI_2 into the circulation ameliorates the pressor effects brought about by systemic application of ET-1 (de Nucci *et al.*, 1988; Thiemermann *et al.*, 1990) and inhibits platelet aggregation when measured *ex vivo* (Thiemermann *et al.*, 1989) and *in vivo* (Herman *et al.*, 1989; Thiemermann *et al.*, 1990).

At present two endothelin receptors have been cloned and expressed, namely ET_A and ET_B. Each receptor contains seven trans-membrane domains and shows remarkable similarity to the rhodopsin receptor and other G protein coupled receptors (see Webb, 1991). The ET_A receptor is highly selective for ET-1 and is characterized by the rank order of binding affinities: ET-1 > sarafotoxin 6b > ET-3 (Arai *et al.*, 1990), while the ET_B receptor is non-isopeptide selective (ET-1 = ET-3) (Sakurai *et al.*, 1990). The discovery of distinct endothelin receptors has prompted the development of selective endothelin receptor antagonists, two of which (FR 139317 and PD145065) have been used in this study. FR 139317 is a potent, highly specific ET_A antagonist *in vitro* and *in vivo* (Sogabe *et al.*, 1992). PD145065 is a non-selective ET_A/ET_B receptor antagonist (Cody *et al.*, 1993).

Intravenous injection of ET-1 in several species including man (see Thiemermann, 1991) causes a transient vasodilatation followed by a sustained vasoconstriction. The vasoconstrictor/pressor effects of ET-1 are mainly due to activation of the ET_A receptor, for they are attenuated by selective ET_A receptor antagonists *in vitro* and *in vivo* (Ihara *et al.*, 1991; McMurdo *et al.*, 1993). The ET-1 induced fall in blood pressure is not inhibited by ET_A receptor antagonists, suggesting that this response may be mediated via the ET_B receptor (Ihara *et al.*, 1991; McMurdo *et al.*, 1993). However, the receptor(s) through which ET-1 stimulates the release of PGI_2 and, hence inhibits platelet aggregation, have not been characterized, although the non-selectivity to the endothelins (Lidbury *et al.*, 1990) suggests it is an ET_B type.

Here, we investigate the effects of FR139317 and PD 145065 on blood pressure changes induced by ET-1 in the anaesthetized rabbit. In addition, we have studied the effects of these antagonists on ET-1-induced inhibition of *ex vivo* platelet aggregation.

Methods

Surgical procedure

Male New Zealand White rabbits (2–3 kg) were premedicated with Hypnorm (fentanyl citrate at 0.1 ml kg^{-1} and fluanisone at 10 mg ml^{-1}, i.m.). General anaesthesia was then induced with sodium pentobarbitone (30 mg kg^{-1}, i.v.) and anaesthesia was maintained with supplementary doses of

[1] Author for correspondence.

sodium pentobarbitone as required. The rabbits were intubated and ventilated with room air from a Harvard ventilator at 36–40 strokes min^{-1} and a tidal volume of 6 ml kg^{-1}. Body temperature was monitored and maintained at 38 ± 1°C by means of a rectal probe thermometer attached to a homeothermic blanket control unit (Harvard, Edenbridge, Kent). The left femoral vein was cannulated for drug administration. The left femoral artery was cannulated for the measurement of blood pressure from which mean arterial pressure (MAP) and heart rate (HR) were derived. Another catheter was placed in the left ventricle via the right common carotid artery for measurement of left ventricular pressure (LVP) and injection of ET-1.

Platelet aggregation ex vivo

Ex vivo platelet aggregation was measured as previously described (Thiemermann *et al.*, 1988). Briefly, arterial blood samples were collected from the left femoral artery into 3.15% tri-sodium citrate (9:1 v/v) and immediately centrifuged at 1400 *g* (4000 r.p.m.) for 20 s (Heraeus, Biofuge 15) to produce platelet rich plasma (PRP). The blood was further centrifuged at 14900 *g* (12000 r.p.m.) for 1 min to obtain platelet poor plasma (PPP). Platelet aggregation was studied with a dual channel aggregometer (Payton) calibrated using PRP (0%) and PPP (100%) with respect to the degree of light transmission. Aliquots of PRP (0.4 ml) were added to siliconised cuvettes, warmed to 37°C and stirred at 1000 r.p.m. After incubation for 30 s, a sub-maximal dose of adenosine-5'-diphosphate (ADP; 2 μg ml^{-1}) was added and the extent of aggregation measured as peak increase in light transmission.

The inhibition of platelet aggregation induced by ET-1 (1 nmol kg^{-1}) was calculated from peak increase in light transmission observed over a 4 min period after addition of a sub-maximal dose (70–80% maximum response) of ADP, as compared to that of control.

Experimental design

After surgery, all animals were allowed to stabilize for 20 min before the first arterial blood sample was withdrawn. Antagonists (FR139317 or PD145065) were administered as an infusion of 0.2 or 0.6 mg kg^{-1} min^{-1} (preceded by loading doses of 1 or 3 mg kg^{-1}, respectively) for 30 min prior to and continued for a further 30 min after a bolus injection of ET-1 (1 nmol kg^{-1}, intra-ventricular). In some experiments, indomethacin (5 mg kg^{-1}, i.v. bolus) was given 20 min before ET-1 injection. *Ex vivo* platelet aggregation was measured 5 min before antagonist infusion, 5 min before ET-1 injection (control) and 1, 5, 15 and 30 min after injection of ET-1.

Materials

Hypnorm was bought from Janssen Pharmaceutical Co., (Oxford, UK). Sodium pentobarbitone (Sagatal) was purchased from May and Baker (Dagenham, Essex, UK). Adenosine-5'- diphosphate, indomethacin and dimethylsulphoxide were obtained from Sigma Chem. Co., (Poole, Dorset, UK). Tri-sodium citrate was bought from B.D.H. Chem. Co., (Essex, UK). ET-1 was supplied by Scientific Marketing Associates (London, UK) and was reconstituted in 0.1% acetic acid and diluted in 0.9% w/v saline containing 1% w/v bovine serum albumin and 0.06% sodium bicarbonate. FR 139317 ((**R**)-2[(**R**)-2-[(**S**)-2-[[1-(hexahydro-1H-azepinyl)] carbonyl] amino-4-methylpentanoyl]amino-3[3-(1-methyl-1H-indolyl]propionyl] amino-3-(2-pyridyl)proprionic acid) and PD 145065 [Ac-(D-5H-dibenzyl[a,d] cyclo-heptene-10,11-dihydroglycine-L-Leu-L-Asp-L-Ile-L-Ile-L-Trp)] were provided by Dr Annette M. Doherty and Dr Wayne L. Cody of the Medicinal Chemistry Department at Parke-Davis Pharmaceutical Research Division of Warner-Lambert Co. (Ann Arbor, U.S.A.). The antagonists were dissolved in 20% dimethylsulphoxide. Aliquots of ET-1 and of the ET antagonists were stored frozen (– 20°C) until use.

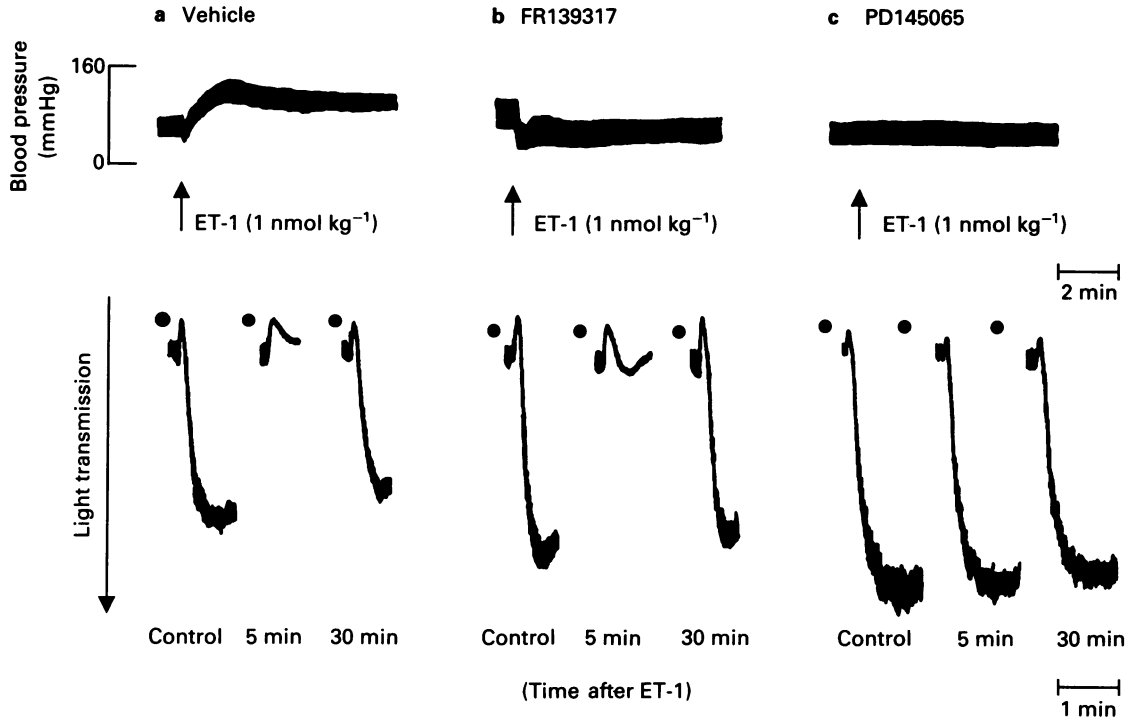

Figure 1 The figure shows 3 representative traces comparing endothelin-1 (ET-1, 1 nmol kg^{-1}, i.a., bolus)-induced changes in blood pressure (upper panel) and *ex vivo* platelet aggregation (lower panel) in rabbits treated with (a) ET-1 at 30 min after the start of an infusion of vehicle (20% DMSO) for 60 min; (b) ET-1 at 30 min after the start of an infusion of FR139317 (loading dose of 3 mg kg^{-1} then 0.6 mg kg^{-1} min^{-1} for 60 min, i.v.) and (c) ET-1 at 30 min after the start of an infusion of PD145065 (loading dose of 3 mg kg^{-1} then 0.6 mg kg^{-1} min^{-1} for 60 min, i.v.). The solid circle signifies an injection of ADP (2 μg ml^{-1}).

Statistical analysis

All values in the figures and text are expressed as mean ± s.e.mean of n observations. Statistical evaluation of the data was by Student's t test for unpaired determinations. A P value of <0.05 was considered significant.

Results

Mean resting values for MAP were 59 ± 1 mmHg and for HR were 246 ± 4 beats min^{-1} ($n = 24$). ET-1 (1 nmol kg^{-1}, i.a., bolus) caused an initial transient depressor response (− 16 ± 3 mmHg, $n = 8$) which was succeeded by a sustained increase in MAP (peak: 47 ± 5 mmHg) ($n = 8$, Figure 1a, Figure 2 and Figure 3). There was no change in ADP-induced platelet aggregation over a period of 30 min in rabbits treated with vehicle ($n = 3$). ET-1 (1 nmol kg^{-1}, i.a., bolus) caused a 96 ± 2% inhibition of *ex vivo* platelet aggregation at 5 min after injection which returned towards control levels within 30 min (15 ± 8% inhibition, $n = 8$) (Figure 1a and Figure 4).

The effect of FR139317 on haemodynamics and platelet aggregation

FR139317 (0.2 mg kg^{-1} min^{-1}, i.v.) had no significant effect on the ET-1 depressor response ($n = 4$, Figure 2b). However, a higher dose of FR139317 (0.6 mg kg^{-1} min^{-1}, i.v.) enhanced the ET-1-induced fall in MAP from − 16 ± 3 mmHg to − 35 ± 5 mmHg ($n = 4$, $P<0.05$; Figure 1b and Figure 2b). The fall in blood pressure remained at control levels (− 17 ± 1 mmHg) after pretreatment with indomethacin (5 mg kg^{-1}, i.v., bolus; $n = 4$). Infusions of FR139317 at 0.2 or 0.6 mg kg^{-1} min^{-1} significantly attenuated the pressor response produced by ET-1 from 47 ± 5 mmHg (control) to 8 ± 2 mmHg or 5 ± 4 mmHg, respectively ($n = 4$, $P<0.05$; Figure 1b and Figure 2a). In contrast, inhibition of *ex vivo* platelet aggregation in response to ET-1 (control: 96 ± 2% at 5 min after injection) was not affected by FR139317 (0.2 mg kg^{-1} min^{-1}: 92 ± 5%; 0.6 mg kg^{-1} min^{-1}: 92 ± 3%) (Figure 1b and Figure 4). Pretreatment with indomethacin (5 mg kg^{-1}, i.v. bolus) in the presence of FR139317 (0.6 mg kg^{-1} min^{-1}, i.v.) attenuated the ET-1-induced inhibition of platelet aggregation (18 ± 3%; $n = 4$).

The effect of PD145065 on haemodynamics and platelet aggregation

PD145065 (0.2 mg kg^{-1} min^{-1}, i.v.) reduced (by 47%) the ET-1-induced fall in blood pressure ($n = 4$, Figure 3b). The fall in MAP produced by ET-1 was abolished by pretreat-

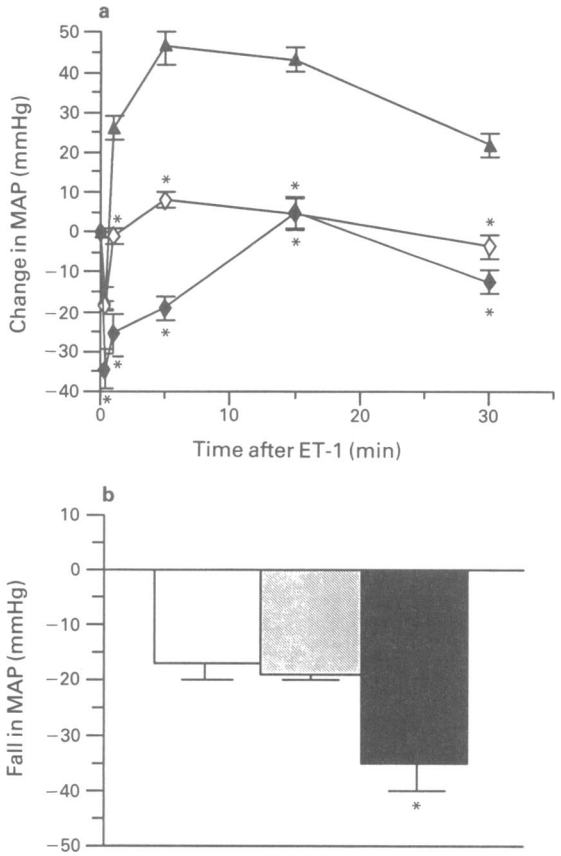

Figure 2 (a) Time course of the effect of endothelin-1 (ET-1, 1 nmol kg^{-1}, i.a., bolus given at time = 0 min) on mean arterial pressure (MAP) in the anaesthetized rabbit. ET-1 was given 30 min after the start of a 60 min infusion of either vehicle (▲, $n = 8$), FR139317 (loading dose of 1 mg kg^{-1} then 0.2 mg kg^{-1} min^{-1}, i.v., ◇, $n = 4$) or FR139317 (loading dose of 3 mg kg^{-1} then 0.6 mg kg^{-1} min^{-1}, i.v., ◆, $n = 4$). (b) Depicted are the ET-1 induced falls in MAP in rabbits given either vehicle (open column, $n = 8$), FR139317 (loading dose of 1 mg kg^{-1} then 0.2 mg kg^{-1} min^{-1}, i.v., hatched column, $n = 4$) or FR139317 (loading dose of 3 mg kg^{-1} then 0.6 mg kg^{-1} min^{-1}, i.v., solid column, $n = 4$). Data are expressed as mean ± s.e.mean of n observations. $^*P<0.05$ when compared to vehicle control.

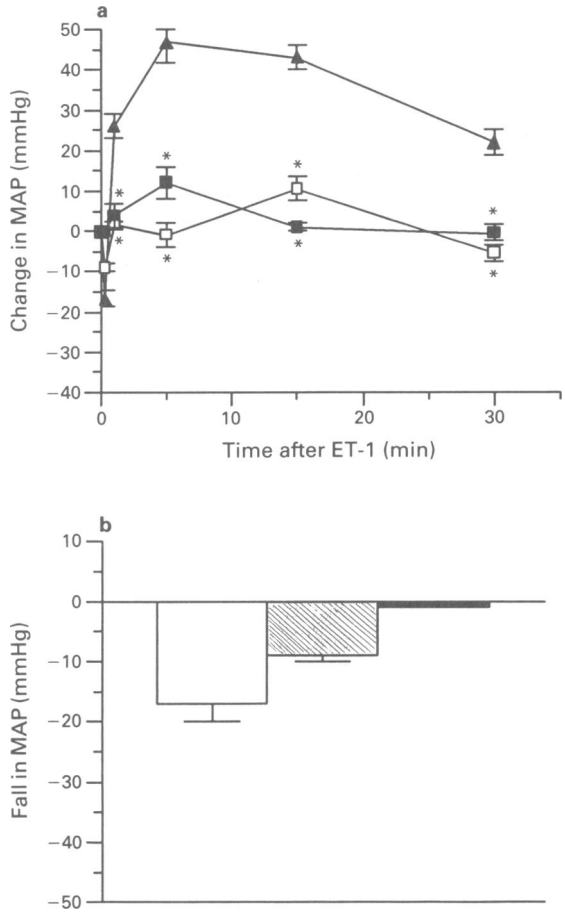

Figure 3 (a) Time course of the effect of endothelin-1 (ET-1, 1 nmol kg^{-1}, i.a., bolus given at time = 0 min) on mean arterial pressure (MAP) in the anaesthetized rabbit. ET-1 was given 30 min after the start of a 60 min infusion of either vehicle (▲, $n = 8$), PD145065 (loading dose of 1 mg kg^{-1} then 0.2 mg kg^{-1} min^{-1}, i.v., □, $n = 4$) or PD145065 (loading dose of 3 mg kg^{-1} then 0.6 mg kg^{-1} min^{-1}, i.v., ■, $n = 4$). (b) Depicted are the ET-1-induced falls in MAP in rabbits given either vehicle (open column, $n = 8$), PD145065 (loading dose of 1 mg kg^{-1} then 0.2 mg kg^{-1} min^{-1}, i.v., hatched column, $n = 4$) or PD145065 (3 mg kg^{-1} then 0.6 mg kg^{-1} min^{-1}, i.v., solid column, $n = 4$). Data are expressed as mean ± s.e.mean of n observations. $^*P<0.05$ when compared to vehicle control.

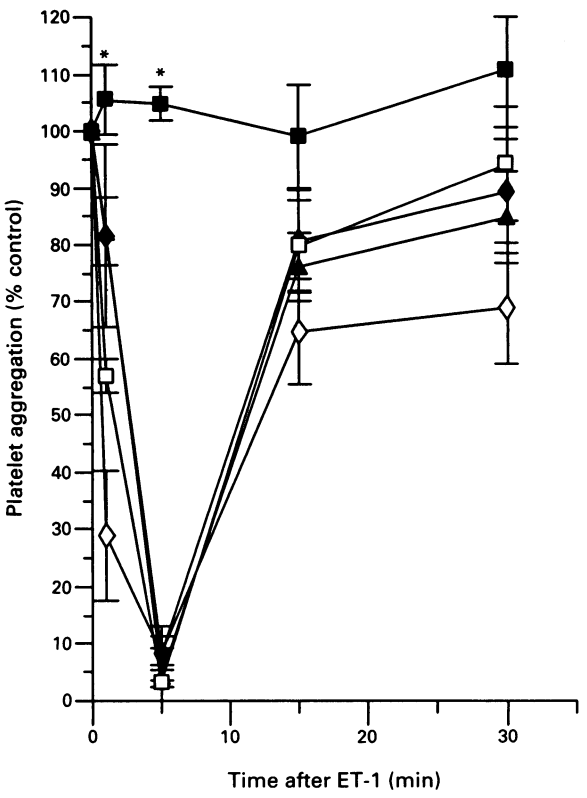

Figure 4 Time course of the effects of endothelin-1 (ET-1, 1 nmol kg^{-1}, i.a., bolus) on *ex vivo* platelet aggregation induced by ADP (2 $\mu g\,ml^{-1}$) in anaesthetized rabbits given either vehicle (▲, $n = 8$), FR139317 (loading dose of 1 $mg\,kg^{-1}$ then 0.2 $mg\,kg^{-1}\,min^{-1}$, i.v., ◇, $n = 4$), FR139317 (loading dose of 3 $mg\,kg^{-1}$ then 0.6 $mg\,kg^{-1}\,min^{-1}$, i.v., ◆, $n = 4$), PD145065 (loading dose of 1 $mg\,kg^{-1}$ then 0.2 $mg\,kg^{-1}\,min^{-1}$, i.v., □, $n = 4$) or PD145065 (loading dose of 3 $mg\,kg^{-1}$ then 0.6 $mg\,kg^{-1}\,min^{-1}$, i.v., ■, $n = 4$). Data are expressed as mean ± s.e.mean of n observations. $^*P < 0.05$ when compared to vehicle control.

ment with a higher dose (0.6 $mg\,kg^{-1}\,min^{-1}$, i.v.) of this antagonist (Figure 1c and Figure 3b). The peak pressor effect of ET-1 was significantly reduced from 47 ± 5 mmHg (control) to 10 ± 3 mmHg or 12 ± 4 mmHg by PD145065 (0.2 or 0.6 $mg\,kg^{-1}\,min^{-1}$, i.v.) respectively, ($n = 4$, Figure 3a). PD 145065 (0.2 $mg\,kg^{-1}\,min^{-1}$, i.v.) had no effect on ET-1-induced inhibition of *ex vivo* platelet aggregation (Figure 4). In contrast, pretreatment with PD145065 (0.6 $mg\,kg^{-1}\,min^{-1}$, i.v.) abolished the anti-aggregatory effects of ET-1 ($n = 4$, Figure 1c and Figure 4).

Discussion

This study demonstrates that the non-selective ET_A/ET_B receptor antagonist PD145065, but not the selective ET_A receptor antagonist FR139317, abolished the ET-1-induced inhibition of *ex vivo* platelet aggregation in the anaesthetized rabbit. In addition, PD145065 abolished the transient fall in blood pressure produced by ET-1 and largely attenuated the ET-1-induced pressor response. FR139317 also strongly attenuated the pressor response to ET-1, but in contrast to PD145065 enhanced the vasodilator response to the peptide.

Intravenous injection of ET-1 is associated with a release of PGI_2 which ameliorates the vasoconstrictor/pressor effects of the peptide and inhibits platelet aggregation (Thiemermann *et al.*, 1988; 1990; Herman *et al.*, 1989; Lidbury *et al.*, 1990). A variety of pressor agents including angiotensin II, vasopressin, noradrenaline and the thromboxane A_2-mimetic, U46619, stimulate vascular PGI_2 synthesis (see: Thiemermann, 1991) suggesting that PGI_2 release may occur as a defence mechanism in response to elevation of arterial blood pressure. However, this study demonstrates that the ET_A receptor antagonist, FR139137, attenuates the rise in blood pressure produced by ET-1 in the anaesthetized rabbit without affecting the ET-1-induced inhibition of *ex vivo* platelet aggregation. Thus, it seems unlikely that the ET-1-induced release of PGI_2 occurs as a response to elevated blood pressure, but rather is a direct receptor-mediated event.

Which receptor, then, mediates the stimulation by ET-1 of endogenous PGI_2 formation? The finding that the ET_A receptor antagonist BQ-123 markedly reduced the release of PGI_2 in response to ET-1 in rat isolated perfused lungs, suggested that this effect of ET-1 in the rat is due to selective activation of ET_A receptors (D'Orleans-Juste *et al.*, 1992). However, we demonstrate here that the non-selective ET_A/ET_B antagonist PD145065, but not the ET_A antagonist FR139137, abolished the inhibition of *ex vivo* platelet aggregation produced by ET-1 in the anaesthetized rabbit. These findings clearly demonstrate that ET-1-stimulated release of PGI_2 in the anaesthetized rabbit is not due to activation of the ET_A receptor. The finding that the inhibition of *ex vivo* platelet aggregation in response to ET-1 was abolished by the non-selective ET_A/ET_B receptor antagonist, PD145065, strongly suggests that the ET-1-induced release of PGI_2 and, hence, inhibition of platelet aggregation in the anaesthetized rabbit is due to activation of the ET_B receptor. PD145065 (1 $mg\,ml^{-1}$) did not influence the inhibition of platelet aggregation produced by PGI_2 (10 $ng\,ml^{-1}$) *in vitro* (unpublished observation). Thus, it is unlikely that PD145065 abolishes the antiaggregatory effects of PGI_2 by acting at the platelet prostaglandin receptor.

The hypothesis that the vasodilator effects of ET-1, which are partly mediated by the release of NO and PGI_2 (see Thiemermann, 1991), are due to activation of the ET_B receptor (Ihara *et al.*, 1991) is strongly supported by the finding that PD145065 abolishes the transient vasodilator response to ET-1. In contrast, FR139317 enhanced the ET-1 induced depressor response probably by inhibiting the vasoconstrictor (ET_A) without affecting the vasodilator (ET_B) properties of the peptide. The finding that this augmentation of the depressor response to ET-1 in the presence of FR139317 was largely, but not completely, inhibited by indomethacin supports the view that the ET-1-induced vasodilatation is mediated by the release of prostanoids, principally PGI_2, and to a lesser degree by NO (Whittle *et al.*, 1989; Fozzard & Part, 1992).

There is increasing evidence pointing to the existence of multiple ET receptor subtypes (Emori *et al.*, 1990; Samson *et al.*, 1990; Fukuroda *et al.*, 1992; Harrison *et al.*, 1992). The hypothesis that ET_A receptors exclusively mediate ET-1-induced vasoconstriction was recently challenged by findings demonstrating that activation of non-ET_A (ET_B ?) receptors causes vasoconstriction (Williams *et al.*, 1991; Bigaud & Pelton, 1992; Cristol *et al.*, 1993). The notion that the contraction of vascular and non-vascular smooth muscle is not solely due to activation of the ET_A receptor is also supported by *in vitro* studies demonstrating that the selective ET_A antagonist BQ-123 does not affect ET-1-induced contractions in the guinea-pig bronchus, rabbit pulmonary artery and rat stomach strip (Hay, 1992; Warner *et al.*, 1992). Moreover, BQ-123 does not completely inhibit the pressor responses to ET-1, big ET-1, sarafotoxin 6b or sarafotoxin 6c in the anaesthetized, ganglion-blocked rat (McMurdo *et al.*, 1993). The results of the present study suggest that the ET-1 pressor response in the anaesthetized rabbit is mediated almost entirely via the ET_A receptor. FR139317 (ET_A antagonist) and PD145065 (ET_A/ET_B antagonist) were equipotent at inhibiting the ET-1-induced rise in blood pressure. Thus, it is unlikely that a regional, ET_B-mediated vasoconstriction substantially contributes to the pressor response produced by ET-1 in the anaesthetized rabbit. These findings also suggest that there are species-related differences in the ET-receptors

responsible for mediating vasoconstriction and PGI_2 release (D'Orleans-Juste *et al.*, 1992; in this study).

This work was supported by the Parke-Davis Pharmaceutical Research Division of Warner-Lambert Co. We thank Drs A. Doherty and W. Cody of the Medicinal Chemistry Department for providing FR139317 and PD145065. The authors would like to thank Dr T.D. Warner and Dr R. Corder for helpful discussion.

References

ARAI, H., HORI, S., ARAMORI, I., OHKUBA, H. & NAKANISHI, S. (1990). Cloning and expression of a cDNA encoding an endothelin receptor. *Nature*, **348**, 730–732.

BIGAUD, M. & PELTON, J.T. (1992). Discrimination between ETA- and ETB-receptor-mediated effects of endothelin-1 and [$Ala^{1,3,11,15}$] endothelin-1 by BQ-123 in the anasthetized rat. *Br. J. Pharmacol.*, **107**, 912–918.

CODY, W.L., DOHERTY, A.M., HE, J.X., TOPLISS, J., HALEEN, S., LADOUCEUR, D., HILL, K.E,. FLYNN, M.A. & REYNOLDS, E.E. (1993). Structure-activity relationships in the C-terminus of endothelin-1 (ET-1): the discovery of Potent Antagonists. In *Proceedings of the 22nd European Peptide Symposium.* ed. Scheider, C.H. & Eberle, A.N. The Netherlands, ESCOM Science, (in press).

CRISTOL, J.P., WARNER, T.D., THIEMERMANN, C.T. & VANE, J.R. (1993). Vasoconstrictor effects of endothelins and sarafotoxins in the systemic circulation and renal vasculature are mediated via different receptors. *Br. J. Pharmacol.*, (in press).

DE NUCCI, G., THOMAS, R., D'ORLEANS-JUSTE, P., ANTUNES, E., WALDER, C., WARNER, T.D. & VANE, J.R. (1988). Pressor effects of circulating endothelin are limited by its removal in the pulmonary circulation and by the release of prostacyclin and endothelium-derived relaxing factor. *Proc. Natl. Acad. Sci. U.S.A.*, **85**, 9797–9800.

D'ORLEANS-JUSTE, P., TELEMAQUE, S., CLAING, A., IHARA, M. & YANO, M. (1992). Human big-endothelin-1 and endothelin-1 release prostacyclin via the activation of ET_1 receptors in the rat perfused lung. *Br. J .Pharmacol.*, **105**, 773–775.

EMORI, T., HIRATA, Y. & MARUMO, F. (1990). Specific receptors for endothelin-3 in cultured bovine endothelial cells and its cellular mechanism of action. *FEBS Lett,*. **263**, 261–264.

FOZZARD, J.R. & PART, M. (1992). The role of nitric oxide in the regional vasodilator effects of endothelin-1 in the rat. *Br. J. Pharmacol.*, **105**, 744–750.

FUKURODA, T., NISHIKIBE, M., OHTA, Y, IHARA, M., YANO, M., ISHIKAWA, K., FUKAMI, T. & IKEMOTO, F. (1992). Analysis of responses to endothelins in isolated porcine blood vessels by using a novel endothelin antagonist, BQ-153. *Life Sci,*. **50**, 107–111.

HARRISON, V.J., RANDRIANTSOA, A. & SCHOEFFTER, P. (1992). Heterogeneity of endothelin-sarafotoxin receptors mediating contraction of pig coronary artery. *Br. J. Pharmacol.*, **105**, 511–513.

HAY, D.W.P. (1992). Pharmacological evidence for distinct endothelin receptors in guinea-pig bronchus and aorta. *Br. J. Pharmacol,*. **106**, 759–761.

HERMAN, F., MAGYAR, K., CHABRIER, P.E., BRAQUET, P. & FILEP, J. (1989). Prostacyclin mediates antiaggregatory and hypotensive actions of endothelin in anaesthetized beagle dogs. *Br. J. Pharmacol.*, **98**, 38–40.

IHARA, M., FUKURODA, T., SAEKI, T., NISHIKIBE, M., KOJIRI, K., SUDA, H. & YANO, M. (1991). An endothelin receptor (ET_A) antagonist isolated from *Streptomyces misakiensis*. *Biochem. Biophys. Res. Commun.*, **178**, 132–137.

LIDBURY, P.S., THIEMERMANN, C., KORBUT, R. & VANE, J.R. (1990). Endothelins release tissue plasminogen activator and prostanoids. *Eur. J. Pharmacol.*, **186**, 205–212.

McMURDO, L., CORDER, R., THIEMERMANN, C. & VANE, J.R. (1993). Incomplete inhibition of ET-1 and related peptides in the anaesthetized rat with BQ-123 provides evidence for more than one vasoconstrictor receptor. *Br. J. Pharmacol.*, **108**, 557–561.

RAE, G.A., TRYBULEC, M., DE NUCCI, G. & VANE, J.R. (1989). Endothelin-1 releases eicosanoids from rabbit isolated perfused kidney and spleen. *J. Cardiovasc. Pharmacol.*, **13**, (Suppl. 5) S89–S92.

SAKURAI, T., YANAGISAWA, M., TAKUWA, Y., MIYAZAKI, H., KIMURA, S., GOTO, K. & MASAKI, T. (1990). Cloning of a cDNA encoding a non-isopeptide selective subtype of the endothelin receptor. *Nature*, **348**, 732–735.

SAMSON, W.K., SKALA, K.D., ALEXANDER, B.D. & HUANG, F.L.S. (1990). Pituitary site of action of endothelin: selective inhibition of prolactin release in vitro. *Biochem. Biophys. Res. Commun.*, **169**, 737–743.

SOGABE, K., NIREI, H., SHOUBO, M., HAMADA, K., NOMOTO, A., HENMI, K., NOTSU, Y. & ONU, T. (1992). A novel endothelial receptor antagonist: studies with FR139317. *J. Vasc. Res,*. **29**, 201–202.

THIEMERMANN, C., LIDBURY, P.S., THOMAS, R. & VANE, J.R. (1988). Endothelin inhibits *ex vivo* platelet aggregation in the rabbit. *Eur. J. Pharmacol.*, **158**, 181–182.

THIEMERMANN, C., LIDBURY, P.S., THOMAS, G.R. & VANE, J.R. (1989). Endothelin-1 releases prostacyclin and inhibits *ex vivo* platelet aggregation in the anaesthetized rabbit. *J. Cardiovasc. Pharmacol*, **13** (Suppl. 5), S138–S141.

THIEMERMANN, C., MAY, G.R., PAGE, C.P. & VANE, J.R. (1990). Endothelin-1 inhibits platelet aggregation *in vivo*: a study with ^{111}indium-labelled platelets. *Br. J. Pharmacol,*. **99**, 303–308.

THIEMERMANN, C. (1991). Biosynthesis and interaction of endothelium-derived vasoactive mediators. *Eicosanoids*, **4**, 187–202.

WARNER, T.D., ALLCOCK, G.H., CORDER, R. & VANE, J.R. (1992). BQ-123 and different isolated tissue preparations reveal heterogeneity in the receptors mediating contractions to endothelin-1. *Br. J. Pharmacol.*, **107**, 103P.

WARNER, T.D., DE NUCCI, G. & VANE, J.R. (1989a). Rat endothelin is a vasodilator in the isolated perfused mesentery of the rat. *Eur. J. Pharmacol*, **159**, 325–326.

WARNER, T.D., MITCHELL, J.A., DE NUCCI, G. & VANE, J.R. (1989b). Endothelin-1 and endothelin-3 release EDRF from isolated perfused arterial vessels of the rat and rabbit. *J. Cardiovasc. Pharmacol.*, **13** (Suppl. 5), S85–S88.

WEBB, D.J. (1991). Endothelin receptors cloned, endothelin converting enzyme characterised and pathophysiological roles for endothelin proposed. *Trends Pharmacol. Sci.*, **12**, 43–46.

WHITTLE, B.J.R., LOPEX-BELMONTE, J. & REES, D.D. (1989). Modulation of the vasodepressor actions of acetylcholine, bradykinin, substance P and endothelin in the rat by a specific inhibitor of nitric oxide formation. *Br. J. Pharmacol.*, **98**, 646–652.

WILLIAMS, Jr, D.L., JONES, K.L., PETTIBONE, D.J., LIS, E.V. & CLINESCHMIDT, B.V. (1991). Sarafotoxin S6c: an agonist which distinguishes between endothelin receptor subtypes. *Biochem. Biophys. Res. Commun.*, **175**, 556–561.

YANAGISAWA, M., KURIHARA, H., KIMURA, S., TOMOBE, Y., KOBAYASHI, M., MITSUI, Y., YAZAKI, Y., GOTO, K. & MASAKI, T. (1988). A novel potent vasoconstrictor peptide produced by vascular endothelial cells. *Nature*, **332**, 411–415.

(Received January 14, 1993
Revised February 8, 1993
Accepted February 15, 1993)

Br. J. Pharmacol. (1993), **109**, 535–538 © Macmillan Press Ltd, 1993

Action of α-dendrotoxin on K^+ currents in nerve terminal regions of axons in rat olfactory cortex

J. McGivern, [1]C.N. Scholfield & *J.O. Dolly

School of Biomedical Science, Queen's University, 97 Lisburn Road, Belfast, BT9 7BL, UK and *Department of Biochemistry, Imperial College, London SW7 2AZ

1 In the rat olfactory cortex, unmyelinated axons give rise to synapses *en passant*. This tissue was used to study the pharmacology of axonal K^+-currents. Responses were measured from a group of these axons as unclamped field currents, with a polarizable suction electrode.

2 A single stimulus to the axons elicited a tetrodotoxin-sensitive Na^+-dependent transient. K^+-currents were revealed by positive polarization of the suction electrode and were manifest as a negative current following the Na^+-component.

3 In the presence of tetraethylammonium (TEA, 5 mM) and Cd^{2+} (100 μM), the K^+-component was depressed by 3,4-diaminopyridine (3,4-DAP; 1 to 20 μM; IC_{50} 2.0 ± 0.4 μM). α-Dendrotoxin (DTX; 15–1500 nM) also attenuated the aminopyridine-sensitive component (IC_{50} 93 ± 4 nM). At the highest DTX concentration, depression of the K^+-current was incomplete, the residual K^+ current being reduced by 3,4-DAP (0.1 to 5 μM).

4 These results indicate the presence of two aminopyridine-sensitive K^+ currents in this preparation distinguished by their susceptibility to DTX.

Keywords: Dendrotoxin; aminopyridine; K^+-current; axons; axonal currents; unmyelinated; rat olfactory cortex

Introduction

α-Dendrotoxin (DTX) is a basic protein with a molecular weight of around 7 kD derived from the venom of the snake, *Dendroaspis angusticeps* (Halliwell *et al.*, 1986). It inhibits the voltage-dependent aminopyridine-sensitive 'A' like K^+-current in rodent hippocampal neurones (Dolly *et al.*, 1984; Halliwell *et al.*, 1986) but DTX is more effective on the slowly inactivating K^+ current found in ganglia (Penner *et al.*, 1986; Stansfeld *et al.*, 1986), frog motor nerve terminals (Weller *et al.*, 1985; Dreyer & Penner, 1987) and myelinated axons (Brau *et al.*, 1990).

DTX is convulsant (Mehraban *et al.*, 1986) and it increases transmitter release (Harvey & Karlsson, 1982; Tibbs *et al.*, 1989a) as a consequence of the K^+-channel blockade. This idea is confirmed by the inhibition of ^{86}Rb efflux from synaptosomes (Benishin *et al.*, 1988). In the hippocampus, high densities of DTX binding sites are found in the synaptic regions (Halliwell *et al.*, 1986). Therefore, it would be useful to study electrophysiologically the action of DTX on central nerve terminals. Many synapses in the central nervous system are of the *en passant* type produced from unmyelinated axons and typical are those axons in the olfactory cortex. Direct intracellular recordings of membrane currents in central nerve terminals are not possible because of their very small size (about 0.2 μm in diameter in olfactory cortex; Gracey & Scholfield, 1990). However, field current recordings can give some idea of the various conductances present (Mallart, 1983). In the olfactory cortex, K^+-currents can be revealed by current clamping using suction electrodes (Scholfield, 1990). Since voltage clamping is not possible, the information obtained is limited to pharmacological rather than kinetic characteristics. Notwithstanding this limitation, DTX has been shown to block partially an aminopyridine-sensitive K^+-current; a preliminary report of this work has been published (McGivern & Scholfield, 1991).

[1] Author for correspondence.

Methods

Female Wistar rats of 200–250 g were decapitated and their brains removed. The brain was trimmed to produce a 3–5 mm thick slab incorporating the olfactory cortex. Pial surface slices of olfactory cortex were cut with a bow cutter and guide (Scholfield, 1980) to give a thickness of 150–200 μm. The slices were maintained in a reservoir of Krebs solution agitated by bubbling with 95%O_2/5%CO_2 before experimentation. They were divided along the axonal radiations (Scholfield, 1987) by a clean cut made with a razor blade. Immediately before recording, another vertical cut was made at right angles to the axons. The slices were placed in a 0.3 ml recording bath through which Krebs solution flowed at 5 ml min^{-1}; this solution was recirculated from a 20 ml reservoir. The recording pipette was filled with Krebs solution and connected to 10 cm of water vacuum. The tip diameter of the electrode was 30 μm and this was offered up to the freshly cut face of the slice so drawing in the severed ends of the axons. The electrode was connected to a current amplifier having a 10 kΩ input resistance. Voltage commands (400 ms) were applied to the non-inverting input of the amplifier so the electrode could be simultaneously polarized by ± 200 mV. These commands began 300 ms before the stimulus. Current waveforms were captured by analogue-to-digital conversion, displayed and stored on computer. Stimuli (20 V, 1 ms) were applied to the axons 2 mm away from the recording electrode. The action potential invaded the axons within the recording electrode to elicit the recorded currents.

Drug solutions were applied directly to the bathing solution superfusing the slice. To economize on the DTX, it was necessary to reduce the circulating volume of Krebs solution to 5 ml. With large volumes of solution, gassing the reservoir with 95%O_2/5%CO_2 was adequate while for smaller reservoir volumes it was also necessary to pass the gas mixutre over the surface of the recording bath. The Krebs solution had the following composition (mM): Na^+ 144, K^+ 5.0, Ca^{2+} 2.5, Mg^{2+} 1.3, Cl^- 128, HCO_3 25, D-glucose 11 and it was equilibrated with 95%O_2/5%CO_2. The DTX was purified from crude snake venom by a combination of conventional chromatograpy and high performance liquid chromatography (h.p.l.c.) cation-exchange (Black *et al.*, 1986).

Results

A single stimulus delivered to the unmyelinated axons produced a positive transient (Figure 1) which was tetrodotoxin-sensitive (10–100 nM, McGivern & Scholfield, 1990). When the recording electrode was positively polarized, a negative current was also observed (Figure 1). Only the negative current showed a polarization dependency and it was blocked by aminopyridines (Scholfield, 1990). Since the electrode resistance and electrode potential remained constant, the recordings were of the current clamp type and as such they gave little information about the kinetics of the respective currents; thus their characterization was limited to the pharmacological properties. To avoid any confusion with voltage clamp records, these positive-negative currents are termed the Na^+- and K^+-components, respectively.

The negative current was depressed by the application of the 3,4-diaminopyridine (3,4-DAP), a more potent analogue of 4-aminopyridine (Kirsch & Narahashi, 1978; Berger *et al.*, 1989). The depression was dose-dependent in the concentration range of 1 to 20 μM: the half-maximal effect (IC_{50}) was at 2.0 ± 0.4 μM in 12 slices (Figure 3b). The above experiments were performed in the presence of tetraethylammonium (TEA) (5 mM) and Cd^{2+} (100 μM) to block the K-currents which were resistant to aminopyridine. Unless otherwise noted all experiments below were done with TEA and Cd^{2+}.

DTX attenuated the K^+-component (Figures 1 and 2) in a manner similar to 3,4-DAP. The action of DTX was concentration-dependent over the range 15–1500 nM, with a IC_{50} of 93 ± 4 nM (Figure 3a). At lower concentrations, the depression was similar to that produced by 3,4-DAP but at the highest concentration, the effect was incomplete. Another series of experiments was conducted in the absence of TEA and Cd^{2+}. DTX also produced a dose-dependent depression although the potency was less (IC_{50} 550 ± 60 nM) and the depression was also incomplete at the highest concentration.

With DTX, the amplitude of the Na^+-component was slightly decreased in some preparations, as in Figure 1, whereas in other cases, the Na^+-component was increased somewhat (Figure 3). These small effects on the Na^+-component were also seen with 3,4-DAP (Figure 3).

3,4-DAP was tested in the presence of 300 nM DTX (TEA and Cd^{2+} were also included); under these conditions, 3,4-DAP (0.1–5.0 μM) depressed the residual K-component in a concentration-dependent manner (Figure 3b). The shape of the dose-effect curve was similar to that seen without DTX but 3,4-DAP was slightly more potent (IC_{50} = 0.75–0.10 μM in DTX compared to 2.0 ± 0.4, $P = 0.006$ by unpaired Student's t test comparing effect of 3,4-DAP alone and in TEA/Cd^{2+}). Neither the effect of DTX nor 3,4-DAP could be readily reversed by washing out (over a period of 60 min).

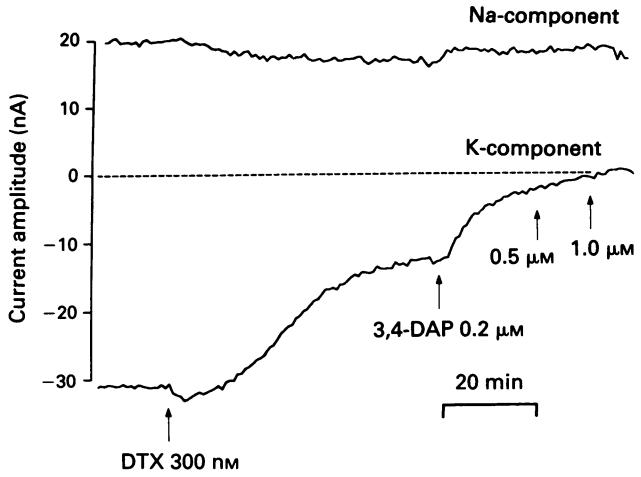

Figure 2 Time course for the action of α-dendrotoxin (DTX, 300 nM, added at the first arrow) followed by 3,4-diaminopyridine (3,4-DAP, 0.2, 0.5 and 1.0 μM added at the points indicated). Throughout the experiment, the axons were electrically stimulated at 0.05 Hz. At each stimulus cycle, the electrode was polarized by + 100 mV and the maximum amplitudes of the positive transient (labelled Na component) and negative transient measured (labelled K-component). Each point was joined to the next to produce a continuous time course. The dashed line indicates the recording base-line.

Although the potency of DTX was around 20 fold greater than that of 3,4-DAP, its IC_{50} in this preparation was lower than in some tissues and its onset of action was slow (Figure 2). Thus, the possibility exists that degradation by proteolytic enzymes in interstitial spaces, uptake, absorption or restricted penetration may reduce the effectiveness as it does with some drugs in this preparation (Brown & Scholfield, 1984). Therefore, a series of experiments was performed to investigate the possibility of binding and enzymatic breakdown. This was done by comparing the effect of 70 nM DTX in normal solution and in the presence of various test agents. Bovine serum albumin (0.02 mg ml^{-1}) was added to offset any non-specific binding. Brystatin (50 μM), captopril (1 mM) or N-carboxymethyl-phe-leu (0.12 mM) for protease inhibition were applied 20 min before DTX and during toxin application. To reduce the hindrance of extracellular matrix to DTX diffusion, collagenase (type 1, 1 mg ml^{-1}), trypsin (type 3, 0.8 units ml^{-1}) and hyaluronidase (1 mg ml^{-1}) were applied for 30 min and then washed out for 30 min before the application of DTX. The enzyme concentrations were the highest that could be used without attenuation of the current responses. None of these treatments had any influence on the

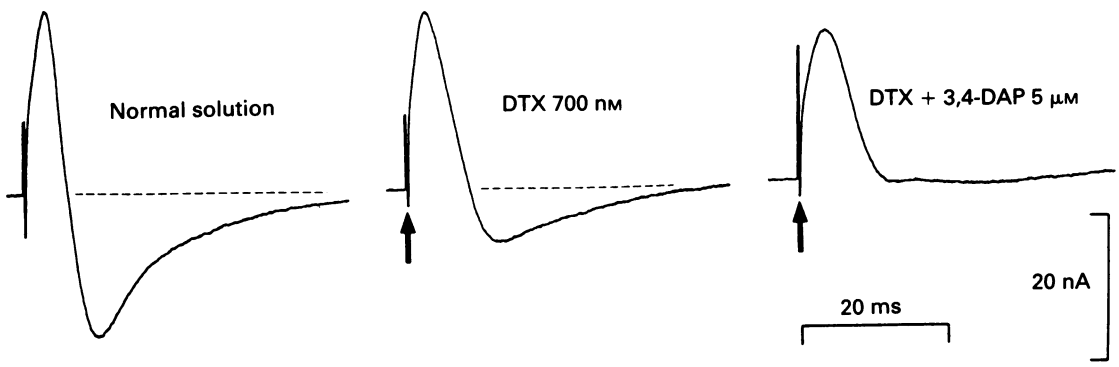

Figure 1 Single responses recorded from the unmyelinated axons of the rat olfactory cortex. Throughout the experiment, the electrode was polarized by + 100 mV to reveal the negative current component. In the first response, the slice was bathed in normal solution followed by 700 nM α-dendrotoxin (DTX) for 30 min and by DTX and 5 μM 3,4-diaminopyridine (3,4-DAP) for 30 min. The arrows indicate the point of stimulus application.

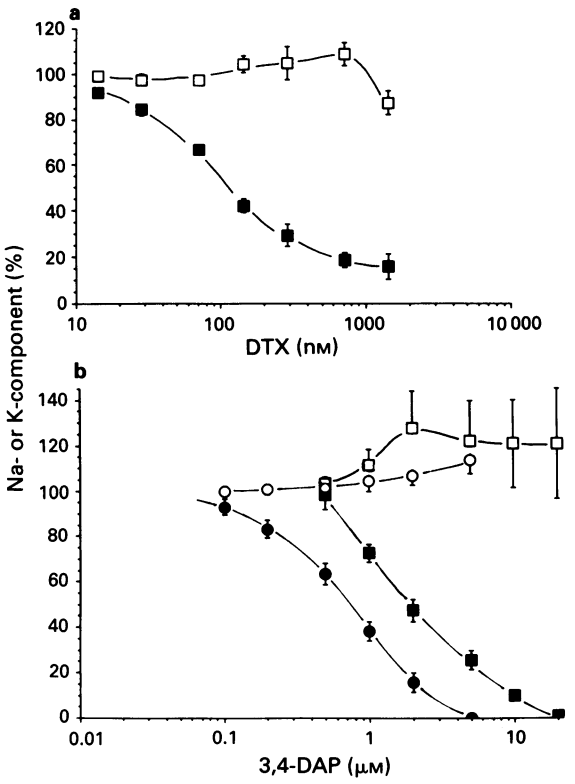

Figure 3 Concentration-depression curves for 3,4-diaminopyridine (3,4-DAP) and α-dendrotoxin (DTX). For each plot, the Na component is the open symbols (□, ○) and K-component during + 100 mV electrode polarization the solid symbols (■, ●). (a) Slices were treated with increasing concentrations of DTX (15–1500 nM). (b) This shows two series of experiments where slices were either pretreated with 700 nM DTX for 30 min and with DTX still present, 0.1 to 5 μM 3,4-DAP tested (circles) or tested with 3,4-DAP in the absence of DTX (squares). All experiments were conducted in the presence of tetraethylammonium (TEA, 5 mM) and Cd (100 μM). The ordinate scale is the peak amplitude of the respective ionic current component expressed as a percentage of that in normal solution. Each point represents the mean (with s.e.mean) of 7–12 slices.

time-course or magnitude of DTX action. Although this list of substances cannot be considered exhaustive, it does suggest that the effect of DTX was not attenuated by the above influences.

Discussion

The present results clearly show that DTX depresses the aminopyridine-sensitive K^+-current in unmyelinated axons of the rat olfactory cortex. In some other preparations, DTX has been shown to affect more than one channel or binding sites. For *Xenopus* myelinated axons, it has an IC_{50} of 70 nM and 1.8 μM (Brau *et al.*, 1990) whereas in nodose ganglion A cells it is much more potent (IC_{50} of 2 nM for slowly inactivating current, Penner *et al.*, 1986; Dolly *et al.*, 1987). For ^{86}Rb fluxes in synaptosomes, the IC_{50} for DTX is 1.7 to 20 nM (Benishin *et al.*, 1988; Tibbs *et al.*, 1989a,b) whilst inhibition of voltage-dependent K^+ currents in hippocampal neurones (Halliwell *et al.*, 1986) and axons (Schauf, 1987; Brau *et al.*, 1990) lies between 50 and <800 nM. In contrast, the K_D for binding is around 0.3 nM (Halliwell *et al.*, 1986; Bidard *et al.*, 1987). In cloned K^+ channels, DTX also has high potency (Stuhmer *et al.*, 1989; Kirsch *et al.*, 1991) although these K^+ channels are also sensitive to TEA (Schroter *et al.*, 1990; Kirsch *et al.*, 1991) in contrast to the present study. For the olfactory cortex, the IC_{50} was 93 nM which suggests that they are of the fast inactivating type seen in the hippocampus and in myelinated axons. There was no evidence for a second DTX-sensitive component in the olfactory cortex although very high concentrations were not tested.

We also considered that the potency might have been attenuated by restricted access of the extracellular space. Our experiments suggest that this was unlikely. Furthermore, 3,4-DAP appeared to be very potent in our experiments having an IC_{50} at 2 μM. In other tissues somewhat higher 3,4-DAP concentrations of 4 μM upwards are required: the neuromuscular junction (Hong & Chang, 1990), squid giant axon nerve terminal (Augustine, 1990), pituicytes (Racke *et al.*, 1988; Rogawski, 1988), smooth muscle (Berger *et al.*, 1989). Thus, the observed IC_{50} for DTX appears to be a true reflection of K^+ channel potency.

The blockade of the K^+-current by DTX was incomplete, the residual being blocked by 3,4-DAP. This suggests the presence of two aminopyridine-sensitive currents, as seen in some other tissues (see Introduction). The residual negative current after DTX was significantly more sensitive to 3,4-DAP than the DTX sensitive component which is opposite to the results with other preparations (see Dolly *et al.*, 1987). This suggests that the two 3,4-DAP binding sites are not identical. Thus DTX was selective for part of the aminopyridine-sensitive component and had a negligible effect on the Na component.

We thank the Wellcome Trust for financial support.

References

AUGUSTINE, G.J. (1990). Regulation of transmitter release at the squid giant synapses by presynaptic delayed rectifier potassium current. *J. Physiol.*, **431**, 343–364.

BENISHIN, C.G., SORENSEN, R.G., BROWN, W.E., KRUEGER, B.K. & BLAUSTEIN, M.P. (1988). Four polypeptide components of green mamba venom selectively block certain potassium channels in rat brain synaptosomes. *Mol. Pharmacol.*, **34**, 152–159.

BERGER, S.C., WASER, P.G. & HOFMANN, A. (1989). Effects of new 4-aminopyridine derivatives on neuromuscular transmission and on smooth muscle contractility. *Arzneimittelforschung*, **39**, 762–765.

BIDARD, J.N., MOURRE, C. & LAZDUNSKI, M. (1987). Two potent central convulsant peptides, a bee venom toxin, the MCD peptide, and a snake venom toxin, dendrotoxin I, known to block K^+ channels, have interacting receptor sites. *Biochem. Biophys. Res. Commun.*, **143**, 383–389.

BLACK, A.R., BREEZE, A.L., OTHMAN, I.B. & DOLLY, J.O. (1986). Involvement of neuronal acceptors for dendrotoxin in its convulsive action in rat brain. *Biochem. J.*, **237**, 397–404.

BRAU, M.E., DREYER, F., JONAS, P., REPP, H. & VOGEL, W. (1990). A K channel in *Xenopus* nerve fibres selectively blocked by bee and snake toxins: binding and voltage clamp experiments. *J. Physiol.*, **420**, 365–385.

BROWN, D.A. & SCHOLFIELD, C.N. (1984). Inhibition of GABA uptake potentiates the conductance increase produced by GABA-mimetic compounds on single neurones in isolated olfactory cortex of the guinea-pig. *Br. J. Pharmacol.*, **83**, 195–202.

DOLLY, J.O., HALLIWELL, J.V., BLACK, J.D., WILLIAMS, R.S., PELCHEN-MATTHEWS, S.J., BREEZE, A.L., MEHRABAN, F., OTHMAN, I.B. & BLACK, A.R. (1984). Botulinum neurotoxin and dentrotoxin as probes for studies on transmitter release. *J. Physiol. (Paris)*, **79**, 280–303.

DOLLY, J.O., STANSFELD, C.E., BREEZE, A., PELCHEN-MATTHEWS, S.J. & BROWN, D.A. (1987). Neuronal receptors subtypes for dendrotoxin and their relation to K^+ channels. In *Neurotoxins and their Pharmacological Implications* pp. 81–96, ed. Jenner, P., New York: Raven Press.

DREYER, F. & PENNER, R. (1987). The actions of presynaptic snake toxins on membrane currents of mouse motor nerve terminals. *J. Physiol.*, **386**, 455–463.

GRACEY, A. & SCHOLFIELD, C.N. (1990). Studies on unmyelinated axons and *en passant* synapses in the olfactory cortex. *Expl. Brain Res.*, **80**, 436–440.

HALLIWELL, J.V., OTHMAN, I.B., PELCHEN-MATTHEWS, A. & DOLLY, J.O. (1986). Central action of dendrotoxin: selective reduction of a transient K conductance in hippocampus and binding to localized acceptors. *Proc. Natl. Acad. Sci. U.S.A.*, **83**, 493–497.

HARVEY, A.L. & KARLSSON, E. (1982). Protease inhibitor homologues from mamba venoms: facilitation of acetylcholine release and interactions with prejunctional blocking toxins. *Br. J. Pharmacol.*, **77**, 153–161.

HONG, S.J. & CHANG, C.C. (1990). Facilitation by 3,4-diaminopyridine of regenerative acetylcholine release from mouse motor nerve. *Br. J. Pharmacol.*, **101**, 793–798.

KIRSCH, G.E., DREWE, J.A., VERMA, S., BROWN, A.M. & JOHO, R.H. (1991). Electrophysiological characterization of a new member of the RCK family of rat brain K + channels. *FEBS Letts.*, **278**, 55–60.

KIRSH, G.E. & NARAHASHI, T. (1978). 3,4-diaminopyridine: a potent new potassium channel blocker. *Biophys. J.*, **22**, 507–512.

MALLART, A. (1983). Electric current flow inside perineural sheaths of mouse motor nerves. *J. Physiol.*, **368**, 565–575.

McGIVERN, J. & SCHOLFIELD, C.N. (1990). General anaesthetics and field current in unclamped, unmyelinated axons of rat olfactory cortex. *Br. J. Pharmacol.*, **101**, 217–223.

McGIVERN, J. & SCHOLFIELD, C.N. (1991). Dendrotoxin partially blocks potassium 'A' current of nerve terminals in slices of rat brain. *J. Physiol.*, **432**, 20P.

MEHRABAN, F., HAINES, A. & DOLLY, J.O. (1986). Monoclonal and polyclonal antibodies against dendrotoxin: their effects on its convulsant activity and interaction with neuronal acceptors. *Neurochem. Int.*, **9**, 11–22.

PENNER, R., PETERSEN, M., PIERAU, F.K. & DREYER, F. (1986). Dendrotoxin: a selective blocker of a non-activating potassium current in guinea-pig dorsal root ganglion neurones. *Pflügers Arch.*, **407**, 365–369.

RACKE, K., ALTES, U., BAUR, A.M., HOBBACH, H.P., JOST, D., SCHAFER, J. & WAMMACK, R. (1988). Differential effects of potassium channel blockers on neurohypophysial release of oxytocin and vasopressin. Evidence for frequency-dependent interaction with the endogenous opioid inhibition of oxytocin release. *Naunyn Schmiedebergs Arch. Pharmacol.*, **338**, 560–566.

ROGAWSKI, M.A. (1988). Transient outward current (I_A) in clonal anterior pituitary cells: blockade by aminopyridine analogs. *Naunyn Schmiedebergs Arch. Pharmacol.*, **338**, 125–132.

SCHAUF, C.L. (1987). Dendrotoxin blocks potassium channels and slows sodium inactivation in *Myxicola* giant axons. *J. Pharmacol. Exp. Ther.*, **241**, 793–796.

SCHOLFIELD, C.N. (1980). Intracellular and extracellular recordings in the isolated olfactory cortex slice and some problems associated with assessing drug action. In *Electrophysiology of Isolated Mammalian CNS Preparations*. ed. Kerkut, G.A. & Wheal, H. pp. 133–151, London: Academic Press.

SCHOLFIELD, C.N. (1987). Presynaptic Na/Ca action potentials in unmyelinated axons of olfactory cortex. *Pflügers Arch.*, **411**, 180–187.

SCHOLFIELD, C.N. (1990). Properties of K-currents in unmyelinated presynaptic axons of brain revealed by extracellular polarisation. *Brain Res.*, **507**, 121–128.

SCHROTER, K.H., SAKMANN, B., STOCKER, M., SEWING, S. & PONGS, O. (1990). Heteromultimeric channels formed by rat brain potassium-channel proteins. *Nature*, **345**, 535–537.

STANSFELD, C.E., MARSH, S.J., HALLIWELL, J.V. & BROWN, D.A. (1986). 4-Aminopyridine and dendrotoxin induce repetitive firing in rat visceral sensory neurones by blocking a slowly inactivating outward current. *Neurosci. Lett.*, **64**, 299–304.

STUHMER, W., RUPPERSGERG, J.P. SCHRÖTER, K.H., SAKMANN, B., STOCKER, M., GIESE, K.P., PERSCHKE, A., BAUMANN, A. & BORGS, O. (1989). Molecular basis of functional diversity of voltage-gated potassium channels in mammalian brain. *EMBO J.*, **8**, 3235–3244.

TIBBS, G.R., NICHOLLS, D.G. & DOLLY, J.O. (1989a). Dendrotoxin, 4-aminopyridine and beta-bungarotoxin act at common loci but by two distinct mechanisms to induce Ca^{2+} dependent release of glutamate from guinea-pig cerebrocortical synaptosomes. *J. Neurochem.*, **52**, 201–206.

TIBBS, G.R., NICHOLLS, D.G. & DOLLY, J.O. (1989b). Dendrotoxin and charybdotoxin increase the cytosolic concentration of free Ca^{2+} in cerebrocortical synaptosomes: an effect not shared by apamin. *FEBS Letts.*, **255**, 159–162.

WELLER, U., BERNHARDT, U., SIEMEN, D., DREYER, F., VOGEL, W. & HABERMANN, E. (1985). Electrophysiological and neurobiochemical evidence for the blockade of a K^+-channel by dendrotoxin. *Naunyn Schmiedebergs Arch. Pharmacol.*, **330**, 77–83.

(Received October 26, 1992
Revised February 5, 1993
Accepted February 17, 1993)

Br. J. Pharmacol. (1993), **109**, 539–543 © Macmillan Press Ltd, 1993

Activation by *Phoneutria nigriventer* (armed spider) venom of tissue kallikrein-kininogen-kinin system in rabbit skin *in vivo*

Rossana A. Marangoni, [1]Edson Antunes, *Susan D. Brain & Gilberto de Nucci

Department of Pharmacology, Faculty of Medical Sciences, UNICAMP, PO Box 6111, 13081, Campinas, São Paulo, Brazil and *Pharmacology Group, Biomedical Sciences Division, King's College, Manresa Road, London SW3 6LX

1 The purpose of the present study was to investigate the mechanisms by which venom from *Phoneutria nigriventer* spider induces increases in vascular permeability in rabbit skin.

2 Local oedema formation, in response to intradermally-injected agents, was measured in male New Zealand white rabbits as the local accumulation of i.v. injected ^{125}I-labelled human serum albumin into skin sites.

3 *Phoneutria nigriventer* venom (10–30 μg/site) increased vascular permeability, which was inhibited by trasylol (10 μg/site) and the bradykinin B_2 receptor antagonists D-Arg,[Hyp^3,Thi^{5,8},D-Phe^7]-BK (3 nmol/site) and Hoe 140 (0.3 nmol/site). In addition, the oedema induced by the venom was potentiated by the kinase II inhibitor, captopril (1 nmol/site). The lipoxygenase inhibitor, BWA4C (10 nmol/site) and the PAF antagonist, WEB 2086 (100 nmol/site) had no effect on the venom-induced increase in vascular permeability.

4 Incubation of rabbit plasma with *Phoneutria nigriventer* venom *in vitro* did not cause bradykinin formation. Further, the plasma kallikrein inhibitor, soybean trypsin inhibitor (10 μg/site), had no effect on the venom-induced increase in vascular permeability in rabbit skin.

5 These results indicate that the oedema produced by *Phoneutria nigriventer* venom is dependent on the activation of the tissue kallikrein-kinin system.

Keywords: Trasylol; bradykinin; kallidin; soybean trypsin inhibitor; captopril; oedema; *Phoneutria nigriventer*

Introduction

Phoneutria nigriventer is a spider responsible for most human accidents involving spider bites in South America, mainly in Brazil (Lucas, 1988). The human victim presents several signs and symptoms including intense and radiating local pain, neurogenic shock, cardiac disturbances, pulmonary oedema and priapism (Schenberg & Pereira-Lima, 1971). *Phoneutria nigriventer* venom contains neurotoxin(s) which activates sodium channels leading to either neuromuscular blockade on the phrenic nerve-diaphragm muscle preparation (Fontana & Vital-Brazil, 1985) or release of acetylcholine and noradrenaline by the autonomic nerve endings in the guinea-pig auricles (Vital-Brazil *et al.*, 1988). This venom also contains substance(s), probably peptides, which induce rabbit vascular smooth muscle contractions (Antunes *et al.*, 1990; 1993; Marangoni *et al.*, 1993) and local oedema formation in rat and rabbit skin (Antunes *et al.*, 1992). The oedema formation observed in animal skin is mainly due to an increase in microvascular permeability and not to an increased microvascular blood flow, as it is markedly potentiated by the co-injection of the prostanoid vasodilator, prostaglandin E_1, or the peptide vasodilator, calcitonin gene-related peptide (Antunes *et al.*, 1992). The venom from *Phoneutria nigriventer* contains histamine and 5-hydroxytryptamine (5-HT) (Schenberg & Pereira-Lima, 1971) but oedema formation is still clearly observed in rabbit skin after removal of these amines (Antunes *et al.*, 1992). In this study we describe the mechanisms by which this venom increases microvascular permeability in rabbit skin.

Methods

Measurement of local oedema formation in rabbit skin

Local oedema formation was measured in male New Zealand White rabbits (1.5–2.5 kg; provided by Cemib-UNICAMP, Brazil) as the local accumulation of i.v. injected ^{125}I-labelled human serum albumin into skin sites as described previously (Williams, 1979; Brain & Williams, 1985). The rabbits were anaesthetized with pentobarbitone sodium (Sagatal, 30–40 mg kg^{-1}) injected via the marginal ear vein and maintenance doses were given when required. ^{125}I-human serum albumin (2 μCi kg^{-1}) and Evans blue dye (0.5 ml kg^{-1}, 2.5% w/v) were injected by the same route. The agents under test were made up in sterile saline and injected intradermally in 100 μl volumes into the shaved dorsal skin according to a balanced site pattern with six replicates per dose. After 30 min, a 5 ml cardiac blood sample was taken into heparin and the animal killed by a Sagatal overdose. The dorsal skin was removed and the injection sites punched out (15 mm diameter) and counted for radioactivity in a gamma counter. Oedema formation at each site was expressed as plasma volume, calculated from the counts in 1 ml plasma.

Kinin-generating system in rabbit plasma in vitro

Rabbit blood was collected in siliconized tubes in presence of heparin (20 iu ml^{-1}) and centrifuged at 3000 r.p.m. for 15 min. An aliquot of plasma (0.2 ml) was added to an 0.1% acetic acid solution (1.8 ml). The mixture was boiled for 30 min and pH was adjusted to 7.4–7.8. Tris buffer solution (0.2 M, pH 7.8, 0.5 ml) and trypsin (2000 u contained in 0.1 ml) were added to the mixture and then incubated at 37°C for 30 min. The reaction was stopped by adding 0.2% acetic acid solution (0.1 ml) and the mixture was boiled (10 min) again in order to destroy trypsin (Diniz & Carvalho, 1963). Similar experiments were carried out with either saline or *Phoneutria nigriventer* venom (0.2 mg) instead of trypsin. Bradykinin formation *in vitro* was assayed by the contractions obtained in the guinea-pig isolated ileum in a selective bioassay using Krebs solution containing the histamine H_1 antagonist, mepyramine (0.35 μM), the 5-HT antagonist, methysergide (0.60 μM), the acetylcholine antagonist, atropine (0.35 μM), the β-adrenoceptor antagonist, propranolol (6.5

[1] Author for correspondence.

μM), the α-adrenoceptor antagonist, phenoxybenzamine (0.05 μM) and the prostanoid cyclo-oxygenase inhibitor, indomethacin (5.6 μM; see Gilmore *et al.*, 1968; Eckenfels & Vane, 1972).

Dialysis of Phoneutria nigriventer *venom*

Phoneutria nigriventer venom [3–4 ml of a 2 mg ml^{-1} 0.9% (w/v) saline solution] was dialyzed for up to 48 h at 4–6°C against two litres of 0.9% saline in order to remove histamine and 5-HT. The dialyzing solution was changed four times during this period. A venom sample was withdrawn prior to dialysis for subsequent comparison with the dialyzed material. Efficient removal (>99.9%) of histamine and 5-HT was confirmed by bioassay on rabbit mesenteric artery strip. Dialyzed *Phoneutria nigriventer* venom was used throughout the study in order that we could investigate mechanisms of oedema formation induced by the venom that are independent of histamine and 5-HT.

Venom and reagents

Lyophilized *Phoneutria nigriventer* venom (PNV) was purchased from the Butantan Institute (São Paulo, Brazil). The venom was collected from the spiders by electrical stimulation.

Trasylol (aprotinin), soybean trypsin inhibitor, arachidonic acid, bradykinin, des-Arg^9-bradykinin, histamine, L-α-phosphatidylcholine β-acetyl-γ-O-alkyl (platelet-activating factor, PAF), bradykinin B_2 receptor antagonist (D-Arg,[Hyp^3,Thi^{5,8}, D-Phe^7]-BK), propranolol, atropine, indomethacin and porcine pancreas kallikrein were obtained from Sigma (St. Louis, U.S.A.). Pentobarbitone sodium (Sagatal) was obtained from May & Baker (Dagenham, Essex, U.K.). Prostaglandin E_1 was kindly provided by Dr John Pike (Upjohn Co., Kalamazoo, U.S.A.). Evans blue dye and mepyramine maleate were obtained from Merck (Darmstadt, Germany) and May & Baker (Dagenham, Essex, U.K.), respectively. BWA4C (N-(3-phenoxycinnamyl) acetohydroxamic acid) and captopril were kindly provided by Wellcome Research Laboratories (Beckenham, U.K.) and Squibb Inc. (U.S.A.), respectively. Methysergide maleate and phenoxybenzamine were a gift from Sandoz Ltd (Basel, Switzerland) and Smith, Kline & French (Stevenage, U.K.). Hoe 140 (D-Arg-[Hyp^3,Thi^5,DTic^7, Oic^8]-BK) was kindly provided by Hoechst AG (Frankfurt, Germany). ^{125}I-human serum albumin (50 μCi ml^{-1}, 20 mg albumin ml^{-1}) was bought from Amersham International (Amersham, U.K.). Dialysis tubing (mol. wt. cutoff 12000–14000) was bought from Philip Harris Scientific (London, U.K.). WEB 2086 (3-(4-(2-chlorophenyl)-9-methyl-6H-thieno-(3,2f) (1,2,4)-triazolo-(4,3-a) (1,4)-diazepine-2-yl)-(4-morpholinyl)-1-propanone) was obtained from Boehringer-Ingelheim (Germany).

Statistical analysis

Data are presented as the mean ± s.e.mean and have been analysed by Analysis of Variance and Student's paired *t* test for within animal treatments. A *P* value of less than 0.05 was considered as significant.

Results

Figure 1 shows that tissue kallikrein (5.7 mu/site), bradykinin (0.1 nmol/site) and PNV (30 μg/site) induced local skin oedema formation which were all potentiated when injected with the vasodilator PGE_1 (0.1 nmol/site). In further experiments PGE_1 was routinely used to potentiate oedema formation. The protease inhibitor trasylol (10 μg/site), known to inhibit bradykinin synthesis, significantly inhibited both kallikrein- and PNV-induced oedema, without affecting the oedema induced by bradykinin (Figure 1).

Soybean trypsin inhibitor (SBTI, 10 μg/site), an inhibitor of plasma kallikrein, failed to affect significantly the increased vascular permeability induced by tissue kallikrein (180 ± 7.0 μl and 237 ± 24.0 μl for control and SBTI-treated sites, respectively, mean ± s.e.mean, $n = 3$), bradykinin (108 ± 17.0 μl and 132 ± 9.3 μl for control and SBTI-treated sites, respectively, mean ± s.e.mean, $n = 3$) and PNV (121 ± 9.8 μl and 136 ± 19.0 μl for control and SBTI-treated sites, respectively, mean ± s.e.mean, $n = 4$).

The bradykinin B_2 receptor antagonist D-Arg,[Hyp^3,Thi^{5,8}, D-Phe^7]-BK (3 nmol/site) significantly reduced bradykinin-

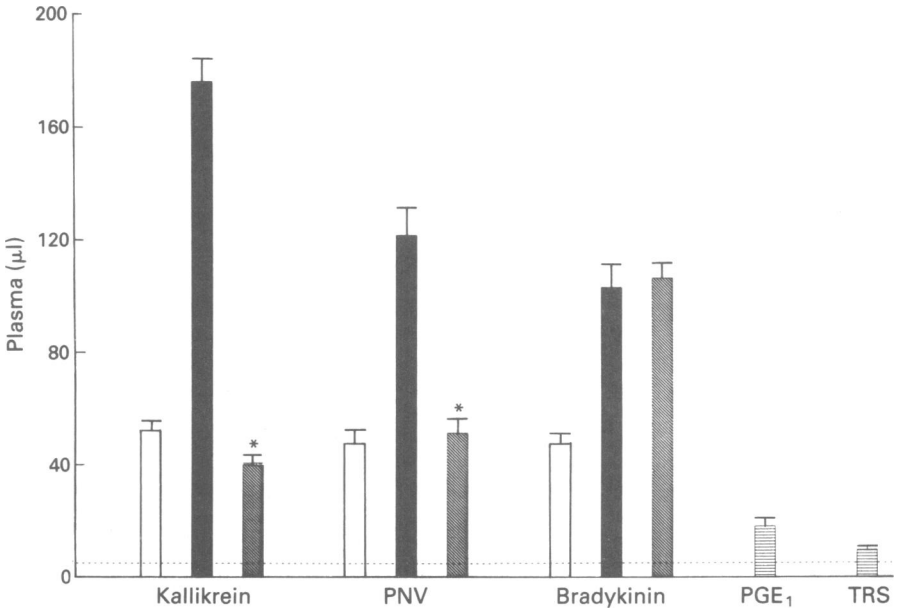

Figure 1 Increased vascular permeability induced by *Phoneutria nigriventer* venom (PNV) is inhibited by trasylol in rabbit skin. Kallikrein (5.7 mu/site), bradykinin (0.1 nmol/site) and PNV (30 μg/site) were injected alone (open columns) and co-injected with prostaglandin (PGE_1, 0.1 nmol/site; solid columns). The hatched columns represent the co-injection of the inflammatory agents (kallikrein, PNV or bradykinin) + PGE_1 + trasylol (10 μg/site). The dashed line represents sites injected with saline alone. Oedema response induced by PGE_1 and trasylol (TRS) injected alone is also shown (striped columns). The results are expressed as mean (with s.e.mean) values from 6–7 rabbits. *$P < 0.001$ when compared with oedema in the absence of trasylol.

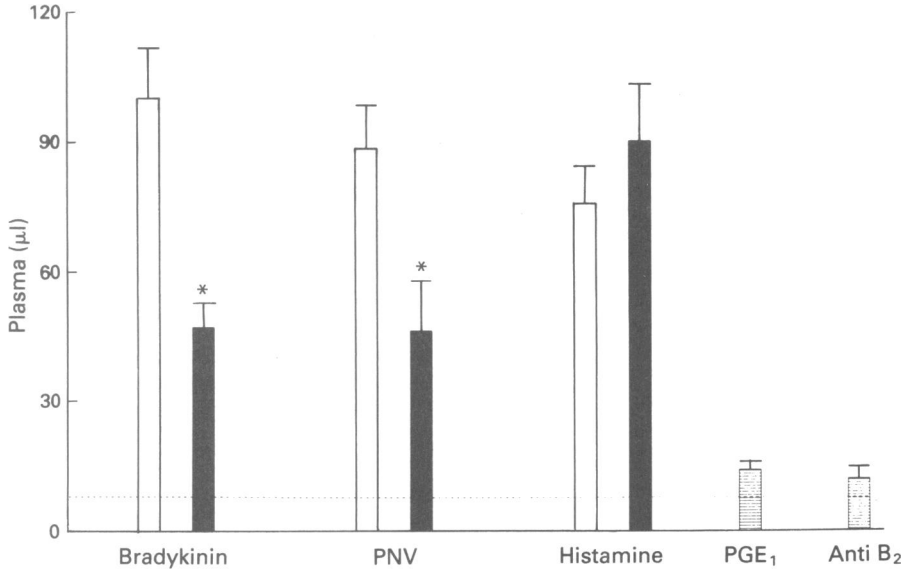

Figure 2 Bradykinin B_2 receptor antagonist reduces the increased vascular permeability induced by *Phoneutria nigriventer* venom (PNV) in rabbit skin. Bradykinin (0.1 nmol/site), PNV (30 μg/site) and histamine (3 nmol/site) were co-injected with prostaglandin E_1 (PGE_1, 0.1 nmol/site) in the absence (open columns) or presence (solid columns) of the bradykinin B_2 receptor antagonist D-Arg,[Hyp^3,Thi^{5,8},D-Phe^7]-BK (3 nmol/site). The dashed line represents sites injected with saline alone. Oedema response induced by PGE_1 and bradykinin B_2 receptor antagonist (Anti-B_2) injected alone is shown by the striped columns. Results are expressed as the mean (with s.e.mean) values from 4 rabbits. $^*P<0.01$ and $^{**}P<0.05$.

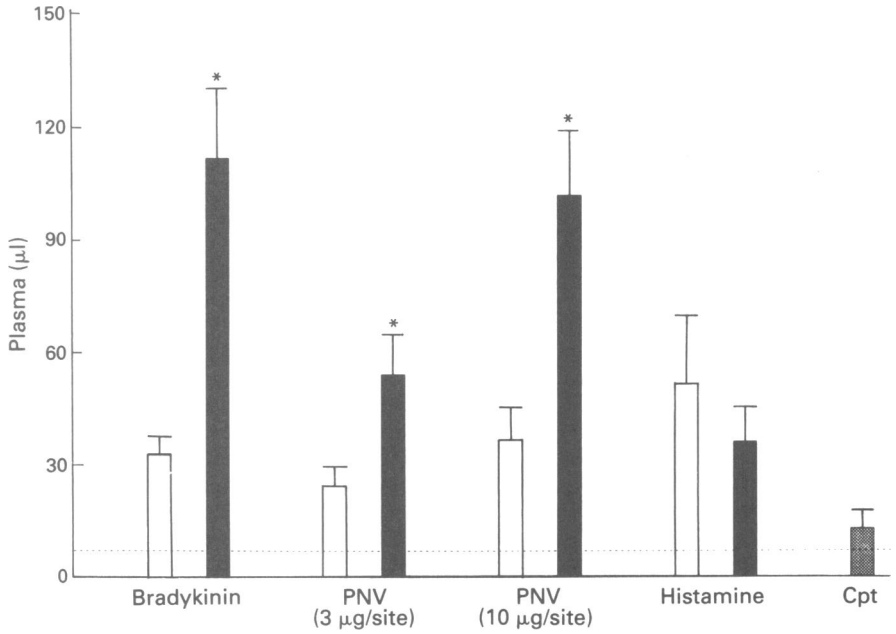

Figure 3 Captopril potentiates *Phoneutria nigriventer* venom (PNV)-induced oedema in rabbit skin. Bradykinin (0.1 nmol/site), PNV (3 and 10 μg/site) and histamine (10 nmol/site) were injected alone (open columns) and in combination with captopril (1 nmol/site; solid columns). The dashed line represents sites injected with saline alone. Oedema response induced by captopril (Cpt) alone (hatched column) is also shown. Results are expressed as the mean (with s.e.mean) values from 4 rabbits. $^*P<0.05$.

and PNV-induced oedema (when in the presence of PGE_1) but not that induced by the combination of histamine (3 nmol/site) and PGE_1 (0.1 nmol/site; Figure 2). The stable B_2 receptor antagonist, D-Arg-[Hyp^3,Thi^5,DTic^7,Oic^8]-BK (Hoe 140; 0.3 nmol/site) also significantly reduced the oedema induced by bradykinin (104 ± 19 μl and 49.8 ± 4.1 μl for control and Hoe-treated sites, respectively, mean ± s.e.mean, $n = 3$, $P<0.05$) and virtually abolished that induced by PNV (111 ± 16.2 μl and 19.3 ± 1.3 μl for control and Hoe-treated sites, respectively, mean ± s.e.mean, $n = 3$, $P<0.05$). At the dose used above, Hoe 140 did not significantly affect histamine (3 nmol/site)-induced oedema (115 ± 20 μl and 108 ± 21.7 μl for control and Hoe-treated sites, respectively, mean ± s.e.mean., $n = 3$). The selective bradykinin B_1 receptor agonist, des-Arg^9-BK (0.1 nmol/site) caused a small oedematous response when compared to an equimolar dose of BK (31 ± 5.4 μl and 92 ± 7.2 μl, respectively, $n = 3$, $P<0.05$). The increased vascular permeability induced by both bradykinin and PNV were significantly potentiated by the kininase II inhibitor, captopril (1 nmol/site, $n = 4$; Figure 3). At the dose used, captopril did not affect histamine (10 nmol/site)-induced oedema (Figure 3).

In further experiments we investigated whether other mediators of increased microvascular permeability could also be

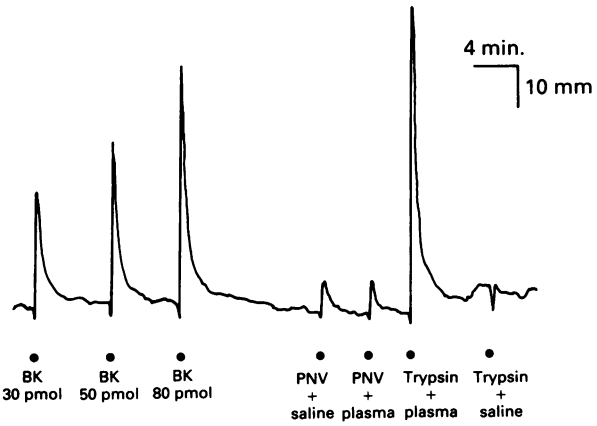

Figure 4 *Phoneutria nigriventer* venom (PNV) does not induce bradykinin formation in rabbit plasma *in vitro*. Guinea-pig isolated ileum strips were previously treated with mepyramine (0.35 μM), methysergide (0.6 μM), atropine (0.35 μM), phenoxybenzamine (0.05 μM), propranolol (6.5 μM) and indomethacin (5.6 μM). Both trypsin and PNV were incubated with either denatured rabbit plasma or saline (as described in Methods) and given as bolus injection (100 μl) in the guinea-pig ileum strips. Similar results were obtained in another four experiments.

involved in the response to intradermal PNV. The platelet-activating factor antagonist WEB 2086 (100 nmol/site) significantly reduced (44.0 ± 8.7%, $n = 4$, $P < 0.05$) the oedema caused by the co-injection of PAF (3 nmol/site) and PGE_1 (0.1 nmol/site) without affecting the oedema induced by PNV and PGE_1 (111 ± 5.9 μl and 120 ± 9.3 μl for control and WEB 2086-treated sites respectively, mean ± s.e.mean, $n = 4$). Similarly, the lipoxygenase inhibitor BWA4C (10 nmol/site) did not significantly affect the oedema formation induced by either BK (82 ± 6.9 μl and 103 ± 6.5 μl, for control and BWA4C-treated sites, respectively; mean ± s.e.mean, $n = 4$) or PNV (110 ± 10.7 μl and 120.7 ± 11.6 μl, for control and BWA4C-treated sites, respectively; mean ± s.e.mean, $n = 4$) in presence of PGE_1. BWA4C (10 nmol/site) significantly inhibited the oedema resulting from the co-injection of bradykinin (0.1 nmol/site) and arachidonic acid (3 nmol/site; 42.0 ± 9.4% of inhibition, $n = 4$, $P < 0.05$).

The bradykinin formation *in vitro* obtained by incubation of rabbit plasma with trypsin was confirmed by contractions obtained in guinea-pig ileum previously treated with a mixture of antagonists (phenoxybenzamine, propranolol, mepyramine, methysergide and atropine; Figure 4). These contractile responses were abolished when plasma was pre-incubated (10 min) with SBTI (100–500 μg) before adding trypsin (not shown). The contractions were compared to standard doses of bradykinin (1 –100 ng). However, guinea-pig ileum contractions were not observed when PNV or saline were used instead of trypsin to stimulate bradykinin formation (Figure 4).

Discussion

Phoneutria nigriventer venom causes increased vascular permeability in rabbit and rat skin independently of its 5-HT or histamine content and mast cell activation (Antunes *et al.*, 1992). Here we demonstrate that the oedema observed in the rabbit skin occurs mainly due to tissue kallikrein-kinin system activation.

Several mediators can interact to induce inflammatory oedema formation. For instance, PAF increases vascular permeability in rabbit (Wedmore & Williams, 1981), rat (Hwang *et al.*, 1985), guinea-pig (Morley *et al.*, 1983) and human (McGivern & Basran, 1984) skin. Since the PAF antagonist, WEB 2086 (Casals-Stenzel *et al.*, 1986) had no effect on PNV-induced oedema, we may assume that this mediator does not participate in the oedema observed. Similarly, the leukotrienes B_4, C_4 and D_4 induce oedema formation (Ueno *et al.*, 1981; Bray *et al.*, 1981). However, the failure of the lipoxygenase inhibitor BWA4C (Higgs *et al.*, 1988) to inhibit PNV-induced oedema indicates that leukotrienes do not appear to be involved.

Locally generated prostaglandins, such as prostaglandin E_2 and I_2, are known to increase oedema formation as a consequence of their vasodilator activity (Williams & Morley, 1973; Williams & Peck, 1977; Williams, 1979). Interestingly, the *Phoneutria nigriventer* bite is characterized by intense local pain (Schenberg & Pereira-Lima, 1971) and prostaglandins have a potent hyperalgesic effect on peripheral nerve terminals (Ferreira, 1972; Ferreira *et al.*, 1978). Thus, it is possible that prostaglandins could be involved in both potentiating the oedema formation and sensitizing the nerve terminals. However in the rabbit skin it is necessary to inject vasodilator doses of PGE_1 to allow full observation of oedema potential. This suggests that either pain producing amounts of prostaglandins are below the threshold for increasing blood flow, or that *Phoneutria nigriventer* venom does not release prostaglandins in the rabbit skin, as happens in guinea-pig isolated lungs (Antunes *et al.*, 1993).

Another important mediator implicated in the modulation of vascular permeability and pain is bradykinin (Spector & Willoughby, 1968; Bathon & Proud, 1991). Kinins can be formed by kallikreins acting on kininogens of either low or high molecular weight, the latter are considered to occur mainly in plasma. Interestingly, the kallikrein inhibitor, trasylol (Vogel, 1979) and the bradykinin B_2 receptor antagonists (Vavrek & Stewart, 1985; Wirth *et al.*, 1991) caused a significant reduction on the venom-induced oedema. Furthermore, captopril which inhibits the breakdown of bradykinin, potentiated PNV- but not histamine-induced increased vascular permeability, indicating that this effect was not linked to its vasodilator activity. These results indicate that the oedema induced by PNV in rabbit skin is dependent mostly on kallikrein activation and consequent kinin formation. Although we did not observe kinin formation in rabbit plasma when it was incubated with venom, this apparent discrepancy could be explained by considering that the venom may be activating tissue and not plasma kallikrein. In this aspect, it is interesting to note that the plasma kallikrein inhibitor SBTI (Spector & Willoughby, 1968) has no effect on PNV-induced increased vascular permeability.

Kallikreins derived from tissue sources are acidic glycoproteins (mol. wt. 25,000–43,000) which act locally near their site of origin and greatly differ from plasma kallikreins (Fukushima *et al.*, 1985; Evans *et al.*, 1988; Proud & Kaplan, 1988; Margolius, 1989). A fragment of 24 amino acids is removed from human pancreatic kallikrein to form the activate enzyme (Fukushima *et al.*, 1985), but the endogenous protease responsible for this reaction has not been identified. Tissue kallikreins act specifically on low molecular weight kininogen causing local formation of the decapeptide kallidin (Lys-bradykinin) which acts at bradykinin B_2 receptors (de Nucci *et al.*, 1988; Regoli *et al.*, 1990). The physiological role of kallidin has not yet been established. However, in traumas such as spider bites, it is likely that extravascularly generated kinins such as kallidin may be more important modulators of vascular permeability and pain than intravascular ones, such as bradykinin. It would be worth investigating whether clinical use of trasylol or the B_2 antagonists under present development could alleviate the local symptoms as well as perhaps some of the systemic ones (e.g. pulmonary oedema) induced by *Phoneutria* bites.

Wasp and ant venoms are known to contain kinins (Piek, 1991); however, no tissue kallikrein activator has been described in venoms so far. The biochemical identification of the peptide(s) responsible for this activity in *Phoneutria* venom might provide a useful tool to understand further the role of the tissue kallikrein-kinin system.

G.D.N. thanks Fundação de Amparo à Pesquisa do Estado de São Paulo (FAPESP) and E.A. thanks Fundo de Apoio à Pesquisa da UNICAMP (FAEP).

References

ANTUNES, E., MARANGONI, R.A., BORGES, N.C.C., FONTANA, M.D. & DE NUCCI, G. (1990). Pharmacological profile of *Phoneutria nigriventer* venom on rabbit vascular smooth muscle. *Br. J. Pharmacol.*, **101,** 508P.

ANTUNES, E., MARANGONI, R.A., BORGES, N.C.C., HYSLOP, S., FONTANA, M.D. & DE NUCCI, G. (1993). Effects of *Phoneutria nigriventer* venom on rabbit vascular smooth muscle. *Braz. J. Med. Biol. Res.*, **26,** 81–91.

ANTUNES, E., MARANGONI, R.A., BRAIN, S.D. & DE NUCCI, G. (1992). *Phoneutria nigriventer* (armed spider) venom induces increased vascular permeability in rat and rabbit skin *in vivo*. *Toxicon.*, **30,** 1011–1016.

BATHON, J.M. & PROUD, D. (1991). Bradykinin antagonists. *Annu. Rev. Pharmacol. Toxicol.*, **31,** 129–162.

BRAIN, S.D. & WILLIAMS, T.J. (1985). Inflammatory oedema induced by synergism between calcitonin gene-related peptide (CGRP) and mediators of increased vascular permeabiltiy. *Br. J. Pharmacol.*, **86,** 855–860.

BRAY, M.A., CUNNINGHAM, F.M., FORD-HUTCHINSON, A.W. & SMITH, M.J.H. (1981). Leukotriene B_4: a mediator of vascular permeability. *Br. J. Pharmacol.*, **72,** 483–486.

CASALS-STENZEL, J.G., MUACEVIC, G. & WEBER, K.H. (1986). WEB 2086, a new and specific antagonist of platelet-activating factor (PAF) in vitro and in vivo. *Naunyn-Schmiedebergs Arch. Pharmacol.*, **334,** R44.

DE NUCCI, G., GRYGLEWSKI, R.G., WARNER, T.D. & VANE, J.R. (1988). The receptor-mediated release of endothelium-derived relaxing factor and prostacyclin from bovine aortic endothelial cells is coupled. *Proc. Natl. Acad. Sci. U.S.A.*, **85,** 2334–2338.

DINIZ, C.R. & CARVALHO, I.F. (1963). A micromethod for determination of bradykininogen under several conditions. *Ann. New York Acad. Sci.*, **104,** 77–89.

ECKENFELS, A. & VANE, J.R. (1972). Prostaglandins, oxygen tension and smooth muscle tone. *Br. J. Pharmacol.*, **45,** 451–462.

EVANS, B.A., YUN, Z.X., CLOSE, J.A., FREGEAR, G.W., KITAMURA, N., NAKANISHI, S., CALLEN, D.F., BAKER, E., HYLAND, V.J. & RICHARDS, R.I. (1988). Structure and chromosomal localization of the human renal kallikrein gene. *Biochemistry*, **27,** 3124–3129.

FERREIRA, S.H. (1972). Prostaglandins, aspirin-like drugs and analgesia. *Nature*, **240,** 200–203.

FERREIRA, S.H., NAKAMURA, M. & CASTRO, M.S.A. (1978). The hyperalgesic effects of prostacyclin and prostaglandin E_2. *Prostaglandins*, **16,** 31–39.

FONTANA, M.D. & VITAL-BRAZIL, O. (1985). Mode of action of *Phoneutria nigriventer* spider venom at the isolated phrenic nerve-diaphragm of the rat. *Braz. J. Med. Biol. Res*,. **18,** 557–565.

FUKUSHIMA, D., KITAMURA, N. & NAKANISHI, S. (1985). Nucleotide sequence of cloned cDNA from human pancreatic kallikrein. *Biochemistry*, **24,** 8037–8043.

GILMORE, N., VANE, J.R. & WYLLIE, J.H. (1968). Prostaglandins released by the spleen. *Nature*, **218,** 1135–1140.

HIGGS, G.A., FOLLENFANT, R.L. & GARLAND, L.G. (1988). Selective inhibition of arachidonate 5-lipoxygenase by novel acetohydroxamic acids: effects on acute inflammatory responses. *Br. J. Pharmacol.*, **94,** 547–551.

HWANG, S.-B., LI, C.-L., LAM, M.-H. & SHEN, T.-Y. (1985). Characterization of cutaneous vascular permeability induced by platelet-activating factor in guinea-pigs and rats and its inhibition by a platelet-activating factor receptor antagonist. *Lab. Invest.*, **52,** 617–630.

LUCAS, S. (1988). Spiders in Brazil. *Toxicon*,. **26,** 759–772.

MARANGONI, S., BORGES, N.C.C., MARANGONI, R.A., ANTUNES, E., VIEIRA, C.A., NOVELLO, J.C., DOMONT, G.B., GIGLIO, J.R., OLIVEIRA, B. & DE NUCCI, G. (1993). Biochemical characterization of a vascular smooth muscle contracting polypeptide purified from *Phoneutria nigriventer* (armed spider) venom. *Toxicon*, (in press).

MARGOLIUS, H.S. (1989). Tissue kallikrein and kinins: regulation and roles in hypertensive and diabetic diseases. *Annu. Rev. Pharmacol. Toxicol.*, **29,** 343–364.

MCGIVERN, D.V. & BASRAN, G.S. (1984). Synergism between platelet-activating factor (PAF-acether) and prostaglandin E_2 in man. *Eur. J. Pharmacol.*, **102,** 183–185.

MORLEY, J., PAGE, C.P. & PAUL, W. (1983). Inflammatory actions of platelet-activating factor (Paf-acether) in guinea-pig skin. *Br. J. Pharmacol.*, **80,** 503–509.

PIEK, T. (1991). Neurotoxic kinins from wasp and ant venoms. *Toxicon*, **29,** 139–149.

PROUD, D. & KAPLAN, A.P. (1988). Kinin formation: mechanisms and role in inflammatory disorders. *Annu. Rev. Immunol.*, **6,** 49–83.

REGOLI, D., RHALEB, N.-E., DION, S. & DRAPEAU, G. (1990). New selective bradykinin receptor antagonists and bradykinin B_2 receptor characterization. *Trends Pharmacol. Sci.*, **11,** 156–161.

SCHENBERG, S. & PEREIRA-LIMA, F.A. (1971). *Phoneutria nigriventer* venom. Pharmacology and biochemistry of its components. In *Venomous Animals and Their Venoms*, vol. 3, pp. 279–297. New York: Academic Press.

SPECTOR, W.G. & WILLOUGHBY, D.A. (1968). Endogenous mediators of increased vascular permeability in inflammation. In *The Pharmacology of Inflammation*. pp. 22–54. London: The English Universities Press Ltd.

UENO, A., TANAKA, K., KATORI, M., HAYASHI, M. & ARAI, Y. (1981). Species differences in increased vascular permeability by synthetic leukotrienes C_4 and D_4. *Prostaglandins*, **21,** 637–648.

VAVREK, R.J. & STEWART, J.M. (1985). Development and modification of competitive antagonists of bradykinin. In *Peptides, Structure and Function. Proc. 9th American Peptide Symp*,. ed. Deber, C.M., Hruby, V.L. & Kopple, K.D. pp. 655–658. Rockford IL: Pierce Chem. Comp.

VITAL-BRAZIL, O., LEITE, G.B. & FONTANA, M.D. (1988). Modo de ação da peçonha da aranha armadeira, *Phoneutria nigriventer* (Keyserling, 1981), nas aurículas isoladas de cobaia. *Ciência Cult*, **40,** 181–185.

VOGEL, R. (1979). Kallikrein inhibitors. In *Bradykinin, Kallidin and Kallikrein. Handb. Exp. Pharmacol.*, Vol. XXV, Suppl. pp. 163–225, Berlin, Heidelberg: Springer-Verlag.

WEDMORE, C.V. & WILLIAMS, T.J. (1981). Platelet-activating factor (PAF), a secretory product of polymorphonuclear leukocytes, increases vascular permeability in rabbit skin. *Br. J. Pharmacol.*, **74,** 916–917P.

WILLIAMS, T.J. (1979). Prostaglandin E_2, prostaglandin I_2 and the vascular changes in inflammation. *Br. J. Pharmacol.*, **65,** 517–524.

WILLIAMS, T.J. & MORLEY, J. (1973). Prostaglandins as potentiators of increased vascular permeability in inflammation. *Nature*, **246,** 215–217.

WILLIAMS, T.J. & PECK, M.J. (1977). Role of prostaglandin-mediated vasodilatation in inflammation. *Nature*, **270,** 530–532.

WIRTH, K., HOCK, F.J., ALBUS, U., LINZ, W., ALPERMANN, H.G., ANAGNOSTOPOULOS, H., HENKE, St., BREIPOHL, G., KÖNIG, W., KNOLLE, J. & SCHÖLKENS, B.A. (1991). Hoe 140 a new potent and long acting bradykinin-antagonist: *in vivo* studies. *Br. J. Pharmacol.*, **102,** 774–777.

(Received September 15, 1992
Revised January 14, 1993
Accepted February 17, 1993)

Br. J. Pharmacol. (1993), **109**, 544–552 © Macmillan Press Ltd, 1993

Differential localization of endothelin ET_A and ET_B binding sites in human placenta

Richard A.D. Rutherford, [1]John Wharton, *Andrew McCarthy, Lee Gordon, *Mark H.F. Sullivan, *Murdoch G. Elder & Julia M. Polak

Departments of Histochemistry and *Obstetrics and Gynaecology, Royal Postgraduate Medical School, Hammersmith Hospital, London W12 0NN

1 The localization and differential distribution of endothelin (ET) receptor subtypes (ET_A and ET_B) was investigated in sections of human placenta by use of quantitative *in vitro* autoradiography and receptor selective ligands.

2 Specific, high density [^{125}I]-ET-1 binding sites were localized to the decidua and foetal membranes as well as to arteries and veins in the chorionic plate and throughout the villous tree. Moderate to low density binding was found in the extravillous and villous trophoblast respectively.

3 [^{125}I]-ET-1 binding sites exhibited a rank order of inhibition by unlabelled peptide sequences (ET-1 > ET-3 > [Ala^{3,11,18}Nle^7]-ET-1 > BQ123 ⩾ sarafotoxin 6c). However, in contrast to the monophasic inhibition curve of ET-1, the other sequences produced a significantly better fit to a two component inhibition curve suggesting the presence of a heterogeneous population of ET binding sites.

4 ET_A and ET_B receptors were distinguished by competitive inhibition of [^{125}I]-ET-1 binding with increasing concentrations of unlabelled ET-3, [Ala^{3,11,18}Nle^7]-ET-1, sarafotoxin 6c and BQ123 and by incubating sections with the ET_B agonist, [^{125}I]-BQ3020. ET receptor subtypes exhibited a differential distribution in the placenta. ET_A type binding sites predominated (~80% of the total) on veins and arteries in the chorionic plate. Veins in stem villi, blood vessels in distal regions of the villous tree and decidual cells displayed a high density (~60–70% of the total) of the ET_B receptor subtype.

5 No difference was detected in either the relative density of [^{125}I]-ET-1 binding sites or the proportion of ET_A to ET_B sites in placentae from pregnancies complicated by pre-eclampsia compared with normal term controls.

6 ET may have a local autocrine or paracrine role in the placenta, acting via specific receptors to influence foetoplacental blood flow and other aspects of placental function.

Keywords: Endothelin; ET-receptor subtypes; *in vitro* autoradiography; placenta

Introduction

Due to the lack of autonomic innervation, the regulation of foetoplacental blood flow is dependent on locally released or circulating vasoactive substances (Reilly & Russell, 1977). The precise mediators are not known, however, a number of vasoactive substances have been suggested including the 21 amino acid peptide, endothelin (Howard, 1987; Wilkes *et al.*, 1990). Endothelin (ET) has been shown to be a potent vasoconstrictor of the human isolated foetoplacental cotyledon (Wilkes *et al.*, 1990) and foetoplacental blood vessels (MacLean *et al.*, 1992) and has the potential to influence placental blood flow either directly or in concert with other vasoactive agents including thromboxane A_2, prostaglandin $F_{2\alpha}$, prostacyclin, nitric oxide and atrial natriuretic peptide (De Nucci *et al.*, 1988; Hu *et al.*, 1988; Rae *et al.*, 1989; Wilkes *et al.*, 1990; Cameron *et al.*, 1991). Circulating ET levels have been shown to increase during pregnancy and labour (Mastrogiannis *et al.*, 1991); however, conflicting evidence exists concerning the possible role of ET in the pathogenesis of pre-eclampsia. While some reports have indicated a further elevation of plasma ET levels in this condition (Nova *et al.*, 1991; Clark *et al.*, 1992), more recent studies have not found a significant difference in plasma ET levels between pre-eclamptic and normal pregnancies (Benigni *et al.*, 1992) nor any correlation between plasma ET-1 concentration, blood pressure or renal function during toxaemic pregnancy (Otani *et al.*, 1991).

Three ET isoforms ET-1, ET-2 and ET-3 have been isolated and the mRNA encoding ET-1 and ET-3 detected in placental tissues (Sunnergren *et al.*, 1989; Onda *et al.*, 1990; Benigni *et al.*, 1991). Endothelin-like immunoreactivity has also been localized to vascular and avascular regions of the placenta including the endothelium of stem villous blood vessels, decidual cells and the epithelium of the amniotic membrane (Hemsén *et al.*, 1991; van Pappendorp *et al.*, 1991). High affinity binding sites for [^{125}I]-ET have been identified in whole placental membrane preparations by affinity cross-linking (Fischli *et al.*, 1989; Nakajo *et al.*, 1989; Wada *et al.*, 1990), whilst the use of molecular cloning techniques has demonstrated the expression of two ET-receptor subtypes in placental tissues which display distinct affinities for ET isoforms (Adachi *et al.*, 1991; Ogawa *et al.*, 1991). The selective (ET_A) subtype exhibits a high affinity for ET-1 and ET-2, and ~1000 fold lower affinity for ET-3, whereas the non-selective (ET_B) receptor subtype binds all three isoforms with a similar affinity. A number of ET_A and ET_B selective peptide sequences have been identified, including the cyclic pentapeptide BQ123, a potent ET_A antagonist (Ihara *et al.*, 1991), and BQ3020, an alanine substituted truncated ET-1 analogue which is a potent ET_B agonist (Saeki *et al.*, 1991; Ihara *et al.*, 1992). ET_B type binding sites may also be distinguished on the basis of their high affinity for the agonists, sarafotoxin 6c (Williams *et al.*, 1991) and [Ala^{3,11,18}Nle^7]-ET-1 (Hunt *et al.*, 1991).

In view of the relatively high level expression of ET and ET-receptor subtypes in the human placenta, it may be postulated that endothelin plays a local regulatory role in this organ. In the present studies, we have employed the technique of quantitative *in vitro* autoradiography and used receptor selective ligands to localize ET binding sites in human

[1] Author for correspondence.

placental tissues and to determine the differential distribution of receptor subtypes.

Methods

Tissues

Placentae were obtained from normal term pregnancies, immediately following transvaginal delivery or elective caesarean section, and from cases complicated by pre-eclampsia following caesarean section (Table 1). Pregnancies in the latter group were characterized by proteinurea, a sustained rise (> 30 mmHg) in the maternal diastolic blood pressure from the initial measurement made in the first half of the pregnancy and the absence of systemic disease or pre-existing hypertension. Four of the pre-eclamptic pregnancies were further complicated by (intrauterine) foetal growth retardation, the birth weight being below the 10th centile for gestational age. Tissue samples were taken through the whole placenta to include the chorionic plate, the placental villi, basal plate (decidua) and foetal membranes. The tissues were placed on cork mats, surrounded in mounting medium (Tissue-Tek™, Miles Inc., Elkhart, Indiana, U.S.A.) and frozen in melting dichlorodifluoromethane (Arcton-12, I.C.I., Cheshire) suspended in liquid nitrogen.

In vitro *autoradiography*

Cryostat sections (10 μm thick) were cut at − 25°C, thaw mounted onto Vectabond (Vector Laboratories, Peterborough)-treated glass slides and stored at − 20°C. Sections were preincubated at room temperature for 15 min in 50 mM Tris HCl buffer (pH 7.2) containing, NaCl 100 mM, $MgCl_2$ 5 mM and bacitracin 28 μM and then incubated in fresh buffer containing bovine serum albumin 0.5%, phosphoramidon 1 μM and 3-([^{125}I]-iodotyrosyl)-ET-1 150 pM, for up to 180 min at 20°C. The slices were then washed twice for 5 min in fresh buffer at 4°C, rinsed briefly in distilled water and dried under a stream of cold air. Non-specific binding was assessed by incubating serial sections in the presence of 10^{-6} M unlabelled ET-1. Depletion of ligand binding capacity was assessed by reapplying the incubation medium to fresh sections, under identical conditions. In order to distinguish ET_A and ET_B receptor subtypes in the placenta, sections were co-incubated with 150 pM [^{125}I]-ET-1 in the presence of either the ET_A selective antagonist, BQ123 (10^{-6} M–10^{-8} M) or the ET_B selective agonist, [Ala^{3,11,18}Nle^7]-ET-1 (10^{-7} M). Further localization of the ET_B receptor subtype was provided by incubating sections with the ET_B agonist [^{125}I]-BQ3020 (150 pM) for 120 min at 20°C. The specificity of binding was also investigated by co-incubation of the ligands with 1 μM of unrelated peptides including vasoactive intestinal polypeptide (VIP), calcitonin gene-related peptide (CGRP), atrial natriuretic peptide (ANP), neuropeptide tyrosine (NPY) and substance P. Macroautoradiographic images were produced by exposing the dry labelled sections to Hyperfilm-^{3}H together with ^{125}I-microsales (Amersham, Bucks) for 18 h at 4°C. The autoradiographic film was developed in Kodak D-19 developer for 5 min, fixed in Amfix and rinsed in running water for at least 30 min.

Microautoradiography, immunohistochemistry and histochemistry

Greater anatomical resolution was obtained when labelled sections were fixed in Bouin's solution for 1 h at 4°C, washed twice in cold phosphate buffer (2–3 min), rinsed in distilled water at 4°C, dried under a stream of cold air and dipped in LM-1 emulsion (Amersham, Bucks) at 43°C. Slides were then stored in the dark at 4°C for up to 5 days, developed for 2.5 min in Kodak D-19 at 20°C, fixed, stained with haematoxylin and eosin and mounted in DPX mounting medium. Fixation of labelled sections in Bouin's solution and rapid washing at 4°C, prior to dipping dried sections in emulsion, retains regional differences in ligand binding, inhibits the dissociation of ligand and preserves tissue morphology for microscopic examination. The localization of ET binding sites to the media and endothelium of placental blood vessels was further examined by comparing the distribution of [^{125}I]-ET-1 binding sites with immunofluorescence staining in adjacent sections of placenta. Vascular smooth muscle and endothelial cells were identified with monoclonal antisera to α-smooth muscle actin (IA4, Sigma) and the endothelium associated CD31 glycoprotein (JC70A, Dako) respectively. Cryostat sections were post fixed in acetone at − 20°C for 10 min, rinsed and incubated with either IA4 (1/1000) or JC70A (1/40) antibodies overnight at 4°C. Immunoreactivity was visualized by incubating sections in fluorescein isothiocyanate-labelled goat anti-mouse IgG (1/100, Miles) for 60 min at room temperature and the sections examined with an Olympus AH2 microscope. Controls included the omission of the primary antisera and replacement with non-immune serum. Differential binding of [^{125}I]-ET-1 to trophoblast and decidual cells was demonstrated by the histochemical localization of glucose-6-phosphate dehydrogenase activity in adjacent sections (Bancroft, 1975). Briefly, sections were incubated in a Tris buffer solution (pH 7.4) containing the specific substrate glucose-6-phosphate, nitro-blue tetrazolium and nicotinamide adenine dinucleotide phosphate, for 60–90 min at 37°C. Sections were subsequently fixed in 10% formol saline, washed and counterstained with 2% methyl green.

Quantification and characterization of ET binding sites

Quantitative image analysis of the film autoradiographic images was carried out by means of computer assisted microdensitometry using an IBAS 386 Image Analysis System

Table 1 Clinical features of pregnancies

Pregnancies	*Birth weight* (kg)	*Gestational age* (weeks)	*Maternal age* (years)	*Blood pressure at birth* (mmHg) *systolic*	*diastolic*
Normal					
Transvaginal delivery ($n = 8$)	3.4 (2.9–4.0)	39 (38–40)	28 (24–32)	119 (110–127)	74 (68–80)
Caesarean section ($n = 5$)	3.6 (3.1–4.1)	40 (39–41)	28 (23–34)	120 (111–128)	75 (69–81)
Pre-eclampsia ($n = 6$)	1.4 (0.6–2.3)**[a]	32 (28–36)*	28 (22–33)	149 (138–160)*	103 (96–109)**

[a]In 4 of the pre-eclampsia cases the pregnancies were further complicated by (intrauterine) foetal growth retardation, the birth weight being below the 10th centile for gestational age. Values are expressed as the mean and 95% confidence interval.
Significant difference (**$P < 0.001$ and *$P < 0.01$) in pregnancies complicated by pre-eclampsia compared with normal-term transvaginal and caesarean deliveries.

(Kontron Elektronic, Watford, UK). The density of ligand binding (amol mm^{-2}) was determined for placental villi, decidua and blood vessels of the chorionic plate and stem villi. Specific binding was determined by subtracting the non-specific binding, obtained by incubating sections with an excess (1 μM) of unlabelled ET-1, from the total binding obtained by incubating sections with 150 pM [^{125}I]-ET-1 or [^{125}I]-BQ3020 alone. Competitive inhibition of specific [^{125}I]-ET-1 binding was examined in the presence of increasing concentrations (10^{-13}–10^{-6} M) of unlabelled ET-1, ET-3, [Ala^{3,11,18}Nle^{7}]-ET-1 and sarafotoxin 6c (S6c). Association kinetics of ET-1 binding were examined by incubating placental sections with [^{125}I]-ET-1 (150 pM) for up to 180 min. Dissociation of the ligand was assessed by removing the incubation medium after 120 min, applying excess (1 μM) unlabelled ET-1 and reincubating for up to 300 min. The possible role of guanosine nucleotides in endothelin binding was determined by examining the effect of the non-hydrolysable analogue, guanosine 5'-O-(thiotriphosphate) (GTP-γ-s), on the association and dissociation of [^{125}I]-ET-1 binding. The non-linear curve fitting programme, GraphPad InPlot version 3.1 (GraphPad Software, San Diego, U.S.A.) was used to analyse the binding data and a four parameter logistic equation used to describe the relationship between the percentage of [^{125}I]-ET-1 bound and the concentration of ET-1, ET-3, [Ala^{3,11,18}Nle^{7}]-ET-1 and S6c in competitive inhibition experiments. A one or two component competitive binding curve was fitted to the data and the 'best fit' sums of squares compared statistically by an *F*-test. The concentration of peptide which inhibited 50% of the specific ligand binding (IC_{50}) to the high and low affinity ET binding sites was calculated for each competing peptide and the values expressed as a geometric mean with 95% confidence interval (95% CI), being derived from logarithmically transformed data.

Statistics

Binding data were analysed using one way analysis of variance and differences considered to be significant if the P value was less than 0.05. The IC_{50} values of competitive inhibition data for villi, decidua and blood vessels were used as three separate dependent variables and the competing peptides as within subject factors. To reduce the probability of significant differences arising by chance a Bonferroni correction was applied to the data (Wallenstein *et al.*, 1980).

Drugs

Drugs used were 3-([^{125}I]-iodotyrosyl)-ET-1 and ^{125}I-labelled [Ala^{1,3,11,15}]-endothelin-7(16–21) ([^{125}I]-BQ3020) (2~2000 Ci mmol^{-1}; Amersham, Bucks.), bacitracin, GTP-γ-S, bovine serum albumin (fraction V) and phosphoramidon (Na salt) (Sigma Chemical Co., UK). Cyclo(-D-Asp-Pro-D-Val-Leu-D-Trp) (BQ123) was a generous gift from the Banyu Pharmaceutical Co. Ltd., Japan. ET-1, ET-3, [Ala^{3,11,18}Nle^{7}]-ET-1, S6c, VIP, CGRP, ANP, NPY and substance P (Peninsula Laboratories).

Results

Specific, high density binding sites for [^{125}I]-ET-1 were localized to placental villi, decidua, foetal blood vessels in the chorionic plate and stem villi and to foetal membranes (Figure 1, Table 2). Co-incubation of [^{125}I]-ET-1 with an excess (1 μM) of unlabelled ET-1 resulted in a complete inhibition of binding to all placental sites (Figure 1) whereas co-incubation with an excess of either unlabelled ET-3, S6c, BQ123 or the ET_B receptor agonist, [Ala^{3,11,18}Nle^{7}]-ET1, produced a differential inhibition. ET-3 completely inhibited binding to the decidua and distal regions of the villous tree whilst not completely inhibiting [^{125}I]-ET-1 binding to blood vessels in the stem villi and chorionic plate (Figure 1). Coincubation with an excess of either of the ET_B selective agonists, S6c or [Ala^{3,11,18}Nle^{7}]-ET-1 (10^{-7} M) had a minimal effect on binding of [^{125}I]-ET-1 to foetal blood vessels in stem and intermediate villi, but inhibited the ligand binding to terminal villi, decidua and foetal membranes (Figure 1). In contrast, coincubation with 1 μM BQ123, significantly inhibited [^{125}I]-ET-1 binding to foetal blood vessels in the chorionic plate and stem villi, whilst only slightly reducing the density of binding to the decidua, distal regions of the villous tree and foetal membranes. The differential distribution of ET receptor subtypes in foetoplacental blood vessels, decidua and villi was further investigated using the ET_B selective ligand [^{125}I]-BQ3020. Unlike [^{125}I]-ET-1 this ligand demonstrated regional differences in the distribution of binding sites on foetoplacental arteries and veins. Arteries in the chorionic plate, intermediate and stem villi and veins in the chorionic plate exhibited relatively low binding whereas a higher density of binding sites was observed on veins in distal regions of the stem villi (Table 2). As expected from the differential inhibition of [^{125}I]-ET-1 binding by ET_B selective ligands, a relatively high density of [^{125}I]-BQ3020 binding sites was detected in the decidua, distal regions of the villous tree and foetal membranes (Table 2). Specific [^{125}I]-ET-1 binding in all regions of the placenta was unaffected by coincubation of radiolabelled ligands with an excess (1 μM) of the unrelated peptides CGRP, VIP, NPY, ANP and substance P. No significant difference was found between the relative density of vascular and villous [^{125}I]-ET-1 binding sites in placentae obtained after elective caesarean section and normal transvaginal delivery ($P > 0.365$) or between placentae from normal pregnancies and those complicated by pre-eclampsia ($P > 0.144$). Binding sites were further resolved by micro-

Table 2 Relative binding density of [^{125}I]-endothelin-1 ([^{125}I]-ET-1) and [^{125}I]-BQ3020 in human placenta

	Binding density (amol mm^{-2})	
Region	*[^{125}I]-ET-1* (ET_A and ET_B sites)	*[^{125}I]-BQ3020* (ET_B sites)
Chorionic plate		
Arteries ($n = 5$)	415 (289–541)	81 (60–102)
Veins ($n = 5$)	306 (190–422)	67 (23–111)
Stem villi		
Arteries ($n = 8$)	370 (312–428)	41 (28–54)
Veins ($n = 8$)	401 (290–512)	226 (148–304)*
Decidua ($n = 7$)	466 (390–542)	362 (291–433)*
Villi ($n = 11$)	252 (216–288)	153 (131–175)*

Binding density values expressed as the mean and 95% Confidence Interval (CI) for *n* separate normal term placentae, obtained following either transvaginal delivery or elective caesarean section. All sections were incubated for 120 min at 20°C with either [^{125}I]-ET-1 (150 pM) or [^{125}I]-BQ3020 (150 pM).

*Significantly greater binding site density compared to vessels in the chorionic plate and arteries in stem villi ($P < 0.01$).

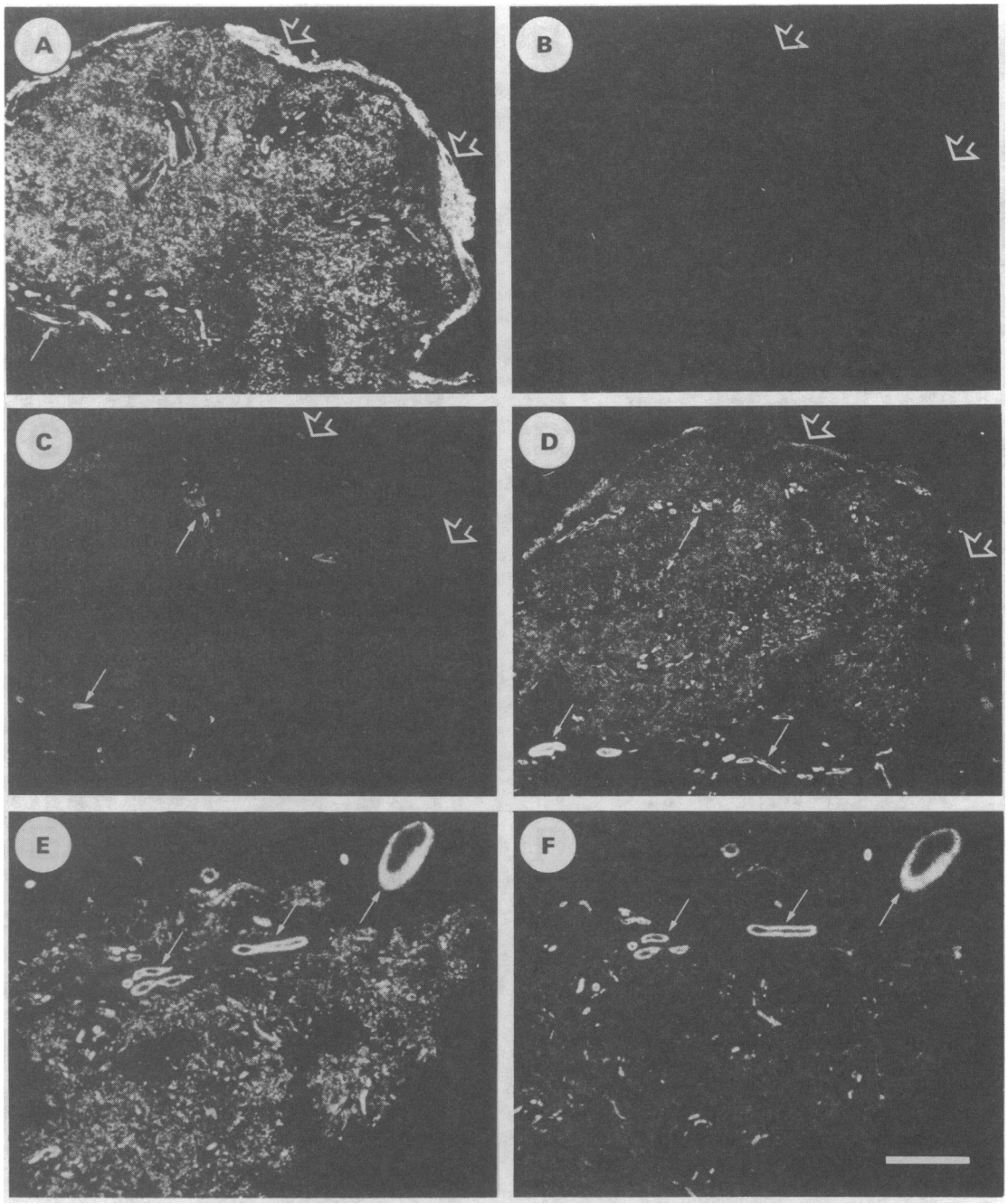

Figure 1 Darkfield images of film autoradiograms demonstrating the localization of [^{125}I]-endothelin-1 ([^{125}I]-ET-1) binding sites in serial sections (A–D, E–F) of human placenta incubated in the absence (A,E) or presence of an excess of unlabelled ET-1 (B), ET-3 (C), S6c (D) or [Ala^{3,11,18}Nle^{7}]-ET1 (F). Binding is completely inhibited in the presence of 1 μM unlabelled ET-1 (B) and selectively inhibited in the decidua (open arrows) and placental villi by ET-3 (C), S6c (D) and [Ala^{3,11,18}Nle^{7}]-ET-1 (F). [^{125}I]-ET-1 binding sites on blood vessels in the chorionic plate and stem villi (arrows) display a low affinity for ET_B receptor selective ligands. Bar = 2 mm.

scopic examination of emulsion-coated sections and comparison with immunohistochemical and histochemical preparations. Enzyme histochemistry for glucose-6-phosphate dehydrogenase discriminated between trophoblast and decidual cells, strong enzyme activity being detected in villous and extravillous trophoblast cells, as well as amnion cells, whilst decidual cells were faintly stained (Figure 2). Moderate or low level [^{125}I]-ET-1 binding was localized in the villous trophoblast and extravillous cytotrophoblast (X-cells) whereas decidual cells in the basal plate and those attached to the chorion in the foetal membranes exhibited a relatively high density of binding sites (Figure 2). No specific binding was observed to chorionic mesenchyme or amnion cells. Microscopic examination of villous [^{125}I]-ET-1 binding demonstrated that binding sites were localized to the media in arteries, arterioles, veins and venules at all levels of the villous tree (Figure 3). Due to the limited resolution of the autoradiographic images obtained with ^{125}I-labelled ET-1 and the high density of binding sites on the media, a distinct receptor subtype could not be identified in the endothelium. Vascular smooth muscle and endothelial cells were, however, distinguished by immunofluorescence staining and [^{125}I]-ET-1 binding sites localized microscopically to the endothelial layer in foetoplacental blood vessels (Figure 3).

[^{125}I]-ET-1 binding sites were characterized by association, dissociation and competitive inhibition studies. The time

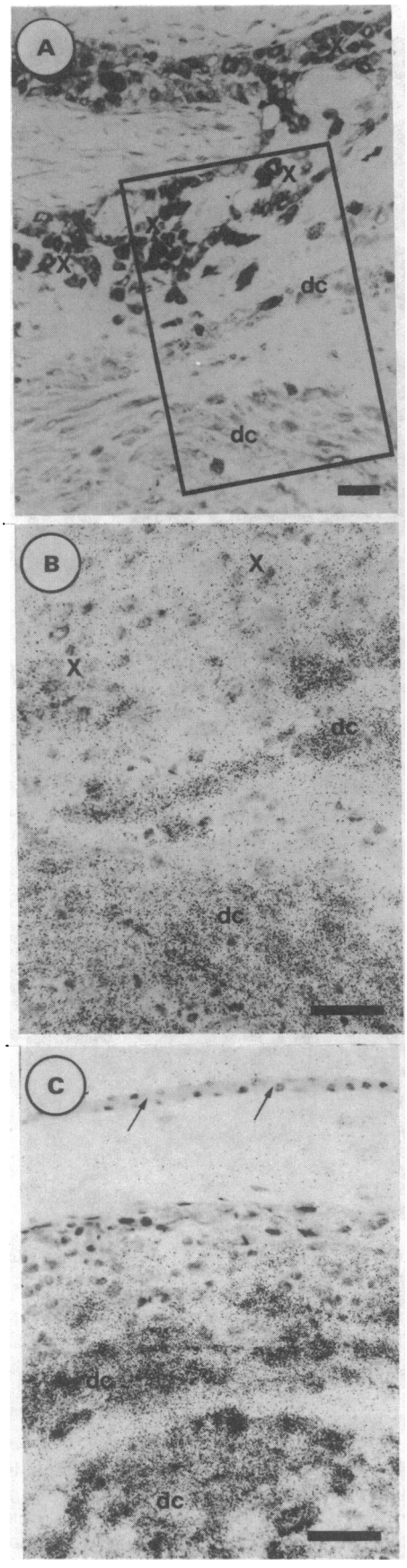

Figure 2 Photomicrographs of sections of decidua (A–B) and foetal membranes (C) showing the microscopic localization of glucose-6-phosphate dehydrogenase activity (A) and [^{125}I]-endothelin-1 ([^{125}I]-ET-1) binding sites (B–C). Decidual cells (dc) exhibit a high binding site density and lack enzyme activity whereas the extravillous trophoblast (X-cells) display strong enzyme staining and a moderate amount of [^{125}I]-ET-1 binding (A–B). Amnion epithelial cells (arrows) and underlying chorionic mesenchyme show no specific ligand binding sites (C). Box (A) corresponds to the area in an adjacent section showing the distribution of [^{125}I]-ET-1 binding sites (B). Bar = 50 μm.

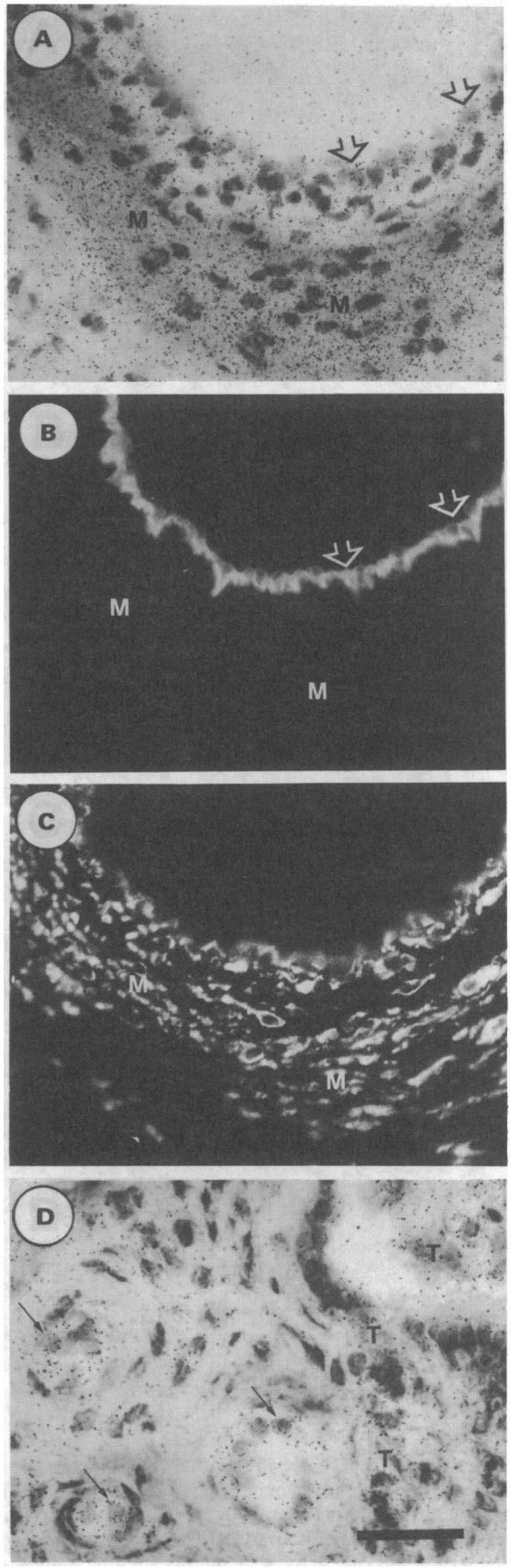

Figure 3 Photomicrographs of serial section of an artery in a stem villous demonstrating the microscopic localization of [^{125}I]-endothelin-1 ([^{125}I]-ET-1) binding sites (A) to the endothelium (open arrows) and media (m), which exhibit immunofluorescence staining for CD31 (B) and α-smooth muscle actin (C) respectively. Silver grains are also shown localized to the vascular endothelium (arrows) and trophoblast in a tertiary stem villous (D). T, villous trophoblast. Bar = 50 μm.

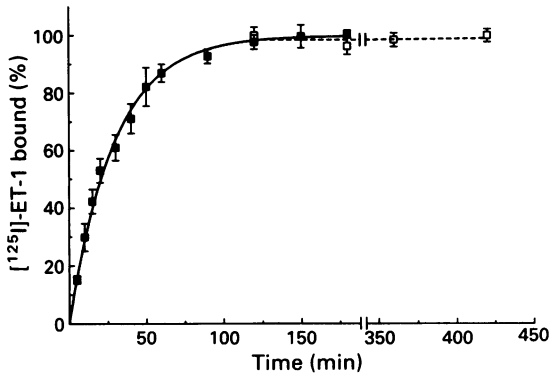

Figure 4 Association (■) and dissociation (□) of [^{125}I]-endothelin-1 ([^{125}I]-ET-1) to decidual binding sites in the human placenta. Each point represents the mean ± s.e.mean derived from six normal-term placentae expressed as a percentage of maximum specific binding. A similar time course was observed for placental villi and vessels of the chorionic plate and stem villi.

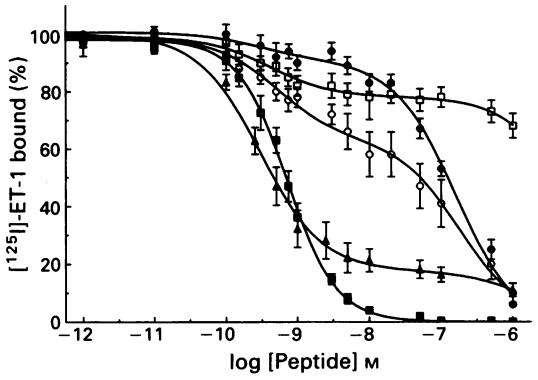

Figure 5 Competitive inhibition curves of specific [^{125}I]-endothelin-1 ([^{125}I]-ET-1) binding to blood vessels in the chorionic plate and stem villi. Each point represents the mean ± s.e.mean derived from six separate normal-term placentae expressed as a percentage of ligand binding in the presence of increasing concentrations of unlabelled ET-1 (■), ET-3 (○), [Ala^{3,11,18}Nle^{7}]-ET-1 (●), BQ123 (▲) and S6c (□).

course of association for 150 pM [^{125}I]-ET-1 at 20°C binding to the decidua gave a rate constant (k_{+1}) of 2.245×10^{8} M^{-1} min^{-1}, reaching an apparent equilibrium by 120 min, with no detectable dissociation after 5 h (Figure 4). Similar binding characteristics were observed in the placental villi and foetal blood vessels. Preincubation for 30 min and coincubation of the ligand with 10^{-5} M GTP-γ-S had no apparent effect on either the association or dissociation of [^{125}I]-ET-1 binding to decidua, villi or blood vessels (data not shown). Re-application of the incubation medium after 120 min to fresh sections of placenta and incubation for a further 120 min showed a ~40% decrease in the binding density over the total incubation period. The apparent depletion in ligand binding was not inhibited by inclusion of the enzyme inhibitors bacitracin (28 μM) and phosphoramidon (1 μM). Unlabelled peptides exhibited a similar rank order of inhibitory potency (ET-1 > ET-3 > [Ala^{3,11,18}Nle^{7}]-ET-1 > BQ123 ⩾ S6c) for [^{125}I]-ET-1 binding sites. In contrast to the single phase sigmoid curve obtained with ET-1, however, the data produced a significantly better fit to a two component than a one component inhibition curve for unlabelled ET-3 ($P<0.05$), [Ala^{3,11,18}Nle^{7}]-ET-1 ($P<0.05$), BQ123 ($P<0.001$) and S6c ($P<0.001$) (Figures 5–6). Analysis of the inhibition curves indicated a heterogeneous population of binding sites displaying high affinity for ET-1 and a differential affinity for ET-3, [Ala^{3,11,18}Nle^{7}]-ET-1, BQ123 and S6c (Table 3). S6c was found to be the most selective ET_B-receptor ligand displaying a significantly lower inhibitory potency for ET_A type binding sites than either ET-3 or [Ala^{3,11,18}Nle^{7}]-ET-1 whilst exhibiting a high affinity for ET_B type binding sites in all regions of the placenta. BQ123, on the other hand, displayed the lowest

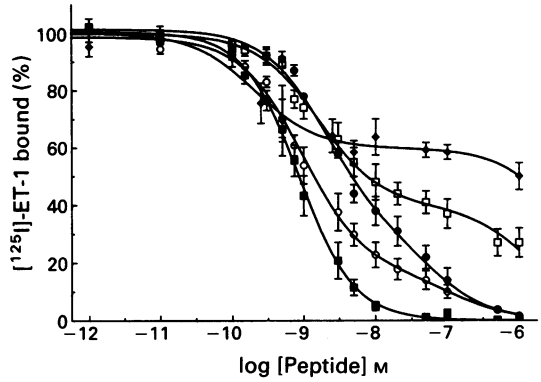

Figure 6 Competitive inhibition curves of specific [^{125}I]-endothelin-1 ([^{125}I]-ET-1) binding to the decidua. Each point represents the mean ± s.e.mean derived from six separate normal-term placentae expressed as a percentage of ligand binding in the presence of increasing concentrations of unlabelled ET-1 (■), ET-3 (○), [Ala^{3,11,18}Nle^{7}] (●), BQ123 (◆) and S6c (□). Competitive inhibition studies for binding to the placental villi gave very similar inhibition curves.

affinity for ET_B type binding sites and was equipotent with ET-1 for high affinity ET_A type sites (Table 3). Placental tissues displayed a heterogeneous population of ET binding sites and exhibited marked regional differences in the relative proportion of ET_A and ET_B type binding sites. ET_A sites predominated in proximal regions of foetal vessels in the

Table 3 Selective inhibition of specific [^{125}I]-endothelin-1 ([^{125}I]-ET-1) binding to receptor subtypes in human placenta by unlabelled peptide sequences

Region	*ET-1*[a] *IC_{50} (nM)*	*Receptor subtype*	*BQ123 IC_{50} (nM)*	*ET-3 IC_{50} (nM)*	*[Ala^{3,11,18}Nle^{7}]ET-1 IC_{50} (nM)*	*S6c IC_{50} (nM)*
Foetal vessels‡	0.67 (0.44–1.01)	ET_B	2400 (1500–3900)*	0.19 (0.08–0.41)	0.16 (0.01–1.82)	0.29 (0.09–0.89)
		ET_A	0.41 (0.20–0.85)	96 (18.2–512.9)	149 (94.0–237.1)	7311 (3199–16749)*
Villi	0.45 (0.32–0.63)	ET_B	3300 (1300–8300)*	0.42 (0.30–0.61)	0.97 (0.72–1.31)	1.02 (0.66–1.58)
		ET_A	0.21 (0.09–0.51)	104 (49.0–218.8)	128 (69.8–233.9)	3785 (1230–11455)*
Decidua	0.90 (0.51–1.61)	ET_B	5300 (2080–13500)*	0.96 (0.54–1.70)	2.37 (1.49–3.78)	1.62 (0.97–2.71)
		ET_A	0.29 (0.07–1.14)	219 (81.3–588.8)	105 (73.6–150.3)	1954 (822–4645)*

IC_{50} values derived from non-linear regression analysis of inhibition binding data fitted to a one (ET-1) or two component inhibition curve. Data are expressed as the geometric mean and 95% Confidence Interval (CI) for six separate placentae.
‡Blood vessels in the chorionic plate and proximal stem villi.
*Significantly lower ($P<0.01$) inhibitory potency of the receptor selective ligands S6c and BQ123 for ET_A and ET_B binding sites respectively, compared with the other unlabelled peptide sequences. [a]Inhibition of total [^{125}I]-ET-1 binding to ET_A and ET_B subtypes.

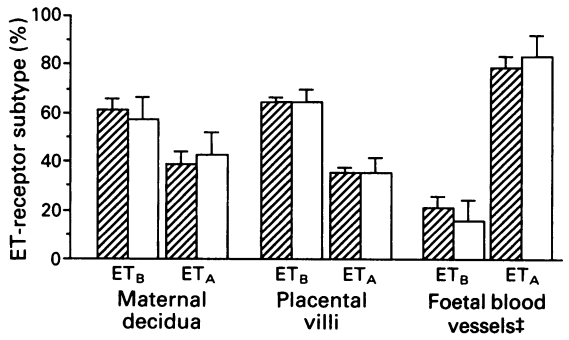

Figure 7 Relative proportion of ET_A to ET_B binding sites in the normal-term human placenta calculated from the competitive inhibition of 150 pM [^{125}I]-endothelin-1 ([^{125}I]-ET-1) binding by S6c (hatched columns) and BQ123 (open columns), after fitting a two component competitive binding curve to the data. Each column represents the mean ± s.e.mean derived from six placentae. ‡Blood vessels in the chorionic plate and proximal stem villi.

chorionic plate and stem villi whereas ET_B sites were concentrated on intermediate and terminal villi, the decidua and foetal membranes. The relative proportion of ET-receptor subtypes was calculated by fitting a two component binding curve to the S6c and BQ123 inhibition data and indicates that in the decidua and terminal villi 60–70% of the total [^{125}I]-ET-1 binding sites are of the ET_B subtype while in vessels in the chorionic plate and stem villi the proportion is less than 20% (Figure 7).

Discussion

Two populations of specific, high affinity ET binding sites were demonstrated in human placental sections by the use of selective agonist and antagonist sequences, displaying differential, tissue-specific distribution patterns. This corresponds with the recent molecular cloning of nucleotide sequences from human placental cDNA libraries encoding both ET_A and ET_B receptor subtypes (Ogawa *et al.*, 1991; Adachi *et al.*, 1991). These latter studies did not, however, determine the cellular localization of ET receptor subtype expression.

The decidua and blood vessels in placental villi contained a high proportion of ET_B type binding sites whereas ET_A sites predominated in vessels in the chorionic plate. A differential distribution of ET receptor subtypes has also been demonstrated in the human foetal heart (Wharton *et al.*, 1991) and porcine pulmonary tissues (Nakamichi *et al.*, 1991). The present investigation of placental [^{125}I]-ET-1 and [^{125}I]-BQ 3020 binding sites further indicates that the proportion of ET_A/ET_B receptors varies between different regions of the placental vascular bed. In particular, arteries in stem villi and chorionic plate, as well as veins in the chorionic plate, contain a high proportion of ET_A sites whereas veins in stem villi and vessels in distal regions of the villous tree possess mainly ET_B sites. The current findings support and extend the results obtained by ligand binding to membrane preparations (Robaut *et al.*, 1991) whilst the localization of [^{125}I]-ET-1 binding sites to vessels which also contain ET-like immunoreactive endothelial cells (Hemsén *et al.*, 1990; van Papendorp *et al.*, 1991) suggests a local autocrine or paracrine role for ET in the foetoplacental vasculature. The combined microautoradiographic and immunohistochemical observations suggest that [^{125}I]-ET isoforms bind to both endothelial and smooth muscle cells. Furthermore, it was apparent from quantitative analysis of film autoradiographs that both ET_A and ET_B type binding sites are localized to the media in foetoplacental blood vessels. ET_B receptors have previously been considered only to occur on endothelial cells and may mediate the transient vasodilator effect of ET via the release of nitric oxide (Takayanagi *et al.*, 1991; Namiki *et al.*, 1992). The present observations are, however, consistent with recent reports which demonstrate that both ET_B and ET_A receptors occur on vascular smooth muscle cells and mediate the ET-induced vasopressor response (Ihara *et al.*, 1991; Fukurodoa *et al.*, 1992; Moreland *et al.*, 1992; Panek *et al.*, 1992). Studies on mammalian isolated blood vessels indicate that ET_A receptors mediate the ET-induced vasoconstriction of arterial smooth muscle whereas ET_B receptors are responsible for the contractile response in veins (Moreland *et al.*, 1992). [^{125}I]-ET-1 binding sites on veins and arteries in the chorionic plate display a similar relative density and affinity for ET isoforms, as ascertained by autoradiographic and membrane binding techniques (Robaut *et al.*, 1991), but it has been reported that the veins in the chorionic plate are some ten times more sensitive to ET-1 than the corresponding arteries (MacLean *et al.*, 1992). It is uncertain to what extent regional variation in the relative density of ET receptor subtypes may influence the vasopressor response of different foetoplacental blood vessels, but this may also be dependent on factors such as differences in the transduction mechanisms of the two receptors (Aramori & Nakanishi, 1992).

The relationship between ET and other vasoactive peptides in the placenta, has not been determined but binding sites for [^{125}I]-ET-1, [^{125}I]-ANP-(1-28) (Salas *et al.*, 1991) and [^{125}I]-[Sar^{1}Ile^8]-angiotensin II (unpublished observations) have been localized to foetoplacental blood vessels and both ANP and angiotensin II modulate placental blood flow (McQueen *et al.*, 1990a) and ET-1 secretion from umbilical endothelial cells (Kohno *et al.*, 1991). Elevated levels of circulating ANP and the activation of the foetal renin-angiotensin system have been associated with a reduction in the affinity or density of ANP and angiotensin II receptors in placentae from pregnancies complicated by pre-eclampsia and intrauterine growth retardation (IUGR) (McQueen *et al.*, 1990b; Malee *et al.*, 1992). The role of ET in pre-eclampsia is unclear, however, as contradictory reports exist concerning circulating ET levels in normotensive patients and those exhibiting this condition. Some reports have shown that prepro-ET-1 gene expression and plasma ET-1 levels are similar in both normal pregnancy and pre-eclampsia (Benigni *et al.*, 1992; Otani *et al.*, 1991), whilst others have reported elevated maternal plasma ET-1 levels in pre-eclampsia implicating ET in the impaired renal function and placental blood flow associated with the disease (Mastrogiannis *et al.*, 1991; Nova *et al.*, 1991; Clark *et al.*, 1992). In the present study, we were unable to detect a difference in either the relative density or proportion of vascular and villous ET receptor subtypes in placentae from pregnancies exhibiting pre-eclampsia compared with normal-term controls. The possibility that endogenously bound ligand influenced the demonstration of ET binding cannot be excluded, but these observations suggest that a modulation of placental [^{125}I]-ET-1 binding site density does not occur in pregnancies complicated by pre-eclampsia.

A high density of [^{125}I]-ET-1 binding sites was also found on non-vascular tissues in the placenta, suggesting that ET may affect other aspects of placental function. These sites predominated on decidual cells, occurring to a lesser extent on the extravillous trophoblast and were mainly of the ET_B subtype. The localization of [^{125}I]-ET-1 binding sites and ET-like immunoreactivity to human decidual cells (van Pappendorp *et al.*, 1991) suggests a local function. ET is considered to be a putative growth factor and stimulates mitogenesis in human placental fibroblasts (Fant *et al.*, 1992) which implies a potential role as a growth factor in the placenta.

Analysis of [^{125}I]-ET-1 binding to placental sections at 20°C indicated an association constant (k_{+1}) of 2.245×10^8 M^{-1} min^{-1}, but the lack of any detectable dissociation precluded the calculation of a dissociation constant from kinetic data. Binding of [^{125}I]-ET-1 to placental sections was apparently irreversible with no significant dissociation being found up to 5 h after addition of an excess of unlabelled ligand. Estimating the equilibrium dissociation constant from saturation

data obtained under these conditions was therefore considered inappropriate. Nonetheless, the ligands used, inhibited binding in a competitive manner and displayed selective affinity for ET receptor subtypes. Cloning of cDNA sequences encoding ET receptors indicates that they are members of the G-protein coupled family of receptors (Ogawa *et al.*, 1991). However, in contrast to other G-protein coupled receptors, the binding affinity of ET receptors is not necessarily reduced in the presence of non-hydrolysable GTP analogues. In the present study, GTP-γ-S elicited no effect on [^{125}I]-ET-1 binding to placental sections. Previous studies have shown that GTP-γ-S did not inhibit [^{125}I]-ET-1 binding to membrane preparations of human placenta (Wilkes *et al.*, 1990) or tissues such as porcine cerebellum (Ihara *et al.*, 1992), whereas an inhibitory effect was demonstrated in human bronchial smooth muscle (Mattoli *et al.*, 1991). It is apparent that the interaction of ET receptors and G-proteins is complex (Sokolovsky, 1991) and variations between tissues may reflect differences in the distribution of ET receptor subtypes and their coupling to distinct G-proteins (Aramori & Nakanishi, 1992). Although an apparent reduction in ligand binding activity was observed after two consecutive incubation periods of 120 min each, it is unlikely that even a 40% depletion would substantially affect the IC_{50} values derived from the competitive inhibition studies. ET isoforms are substrates for neutral endopeptidase (Vijayaraghavan *et al.*, 1990), but the inclusion of the specific and non-specific enzyme inhibitors, phosphoramidon and bacitracin, had no detectable effect on [^{125}I]-ET-1 binding density. Possible reasons for the apparent loss in binding activity, other than enzymatic degradation, may include the adherence of ligand to the glass slides, inactivation of constituents in the buffer and release of inhibitory factors from tissue sections.

In conclusion, the localization of [^{125}I]-ET-1 binding sites in human placenta suggests that ET may play a local role in the modulation of foetoplacental blood flow as well as in other aspects of placental function. The action of ET may be dependent on the relative proportion of ET_A and ET_B receptor subtypes which varies in different regions of the placenta. The significance of ET and ET receptors in the pathophysiology of pre-eclampsia remains to be established.

The authors would like to thank Patricia Harley for excellent technical assistance. The work was supported in part by the British Heart Foundation and the Council for Tobacco Research, U.S.A.

References

ADACHI, M., YANG, Y., FURUICHI, Y. & MIYAMOTO, C. (1991). Cloning and characterization of cDNA encoding human A-type endothelin receptor. *Biochem. Biophys. Res. Commun.*, **180**, 1265–1272.

ARAMORI, I. & NAKANISHI, S. (1992). Coupling of two endothelin receptor subtypes to differing signal transduction in transfected chinese hamster ovary cells. *J. Biol. Chem.*, **267**, 12468–12474.

BANCROFT, J.D. (1975). Chapter 18; Oxidoreductases II: Dehydrogenases. In *Histochemical Techniques*. ed. Bancroft, J.D. pp. 278–287. London: Butterworth & Co.

BENIGNI, A., GASPARI, F., ORISIO, S., BELLIZI, L., AMUSO, G., TIZIANA, F. & REMUZZI, G. (1991). Human placenta expresses endothelin gene and corresponding protein is excreted in urine in increasing amounts during normal pregnancy. *Am. J. Obstet. Gynecol.*, **164**, 844–848.

BENIGNI, A., ORISIO, S., GASPARI, F., FRUSCA, T., AMUSO, G. & REMUZZI, G. (1992). Evidence against a pathogenetic role for endothelin in pre-eclampsia. *Br. J. Obstet. Gynaecol.*, **99**, 798–802.

CAMERON, I.T., DAVENPORT, A.P., BROWN, M.J. & SMITH, S.K. (1991). Endothelin-1 stimulates prostaglandin $F_{2\alpha}$ release from human endometrium. *Prostaglandins*, **42**, 155–157.

CLARK, B.A., HALVORSON, L., SACHS, B. & EPSTEIN, F.H. (1992). Plasma endothelin levels in preeclampsia: elevation and correlation with uric acid levels and renal impairment. *Am. J. Obstet. Gynecol.*, **166**, 962–968.

DE NUCCI, G., THOMAS, R., D'ORLEANS-JUSTE, P., ANTUNES, E., WALDER, C., WARNER, T.D. & VANE, J.R. (1988). Pressor effects of circulating endothelin are limited by its removal in the pulmonary circulation and by the release of prostacyclin and endothelium-derived relaxing factor. *Proc. Natl. Acad. Sci. USA*, **85**, 9797–9800.

FANT, M.E., NANU, L. & WORD, R.A. (1992). A potential role for endothelin-1 in human placental growth: interactions with the insulin-like growth factor family of peptides. *J. Clin. Endocrinol. Metab.*, **74**, 1158–1163.

FISCHLI, W., CLOZEL, M. & GUILLY, C. (1989). Specific receptors for endothelin on membranes from human placenta. Characterization and use in a binding assay. *Life Sci.*, **44**, 1429–1436.

FUKURODA, T., NISHIKIBE, M., OHTA, Y., IHARA, M., YANO, M., ISHIKAWA, K., FUKAMI, T. & IKEMOTO, F. (1992). Analysis of responses to endothelins in isolated porcine blood vessels by using a novel endothelin antagonist, BQ-153. *Life Sci.*, **50**, PL107–PL102.

HEMSÉN, A., GILLIS, C., LARSSON, O., HAEGERSTRAND, A. & LUNDBERG, J.M. (1991). Characterization, localisation and actions of endothelins in umbilical vessels and placenta of man. *Acta Physiol. Scand.*, **143**, 395–404.

HOWARD, R.B. (1987). Control of human placental blood flow. *Med. Hypoth.*, **23**, 51–58.

HU, J.R., BERNINGER, U.G. & LANE, R.E. (1988). Endothelin stimulates atrial natriuretic peptide (ANP) release from rat atria. *Eur. J. Pharmacol.*, **158**, 177–178.

HUNT, J.T., LEE, V.G., STEIN, P.D., HEDBERG, A., LIU, E.C., MCMULLEN, D. & MORELAND, S. (1991). Structure-activity relationships of monocyclic endothelin analogs. *Bio. Med. Chem. Lett.*, **1**, 33–38.

IHARA, M., NOGUCHI, K., SAEKI, T., FUKURODA, T., TSUCHIDA, S., KIMURA, S., FUKAMI, T., ISHIKAWA, K., NISHIKIBE, M. & YANO, M. (1991). Biological profiles of highly potent novel antagonists selective for the ET_A receptor. *Life Sci.*, **50**, 247–255.

IHARA, M., SAEKI, T., FUKURODA, T., KIMURA, S., OZAKI, S., PATEL, A.C. & YANO, M. (1992). A novel radioligand [^{125}I]BQ-3020 selective for endothelin (ET_B) receptors. *Life Sci.*, **51**, PL47–PL52.

KOHNO, M., YASUNARI, K., YOKOKAWA, K., MURAKAWA, K., HORIO, T. & TAKEDA, T. (1991). Inhibition by atrial and brain natriuretic peptides of endothelin-1 secretion after stimulation with angiotensin II and thrombin of cultured human endothelial cells. *J. Clin. Invest.*, **87**, 1999–2004.

MACLEAN, M.R., TEMPLETON, A.G.B. & MCGRATH, J.C. (1992). The influence of endothelin-1 on human foeto-placental blood vessels: a comparison with 5-hydroxytryptamine. *Br. J. Pharmacol.*, **106**, 937–941.

MALEE, M.P., MALEE, K.M., AZUMA, S.D., TAYLOR, R.N. & ROBERTS, J.M. (1992). Increases in plasma atrial natriuretic peptide concentrations antedate clinical evidence of preeclampsia. *J. Clin. Endocrinol. Metab.*, **74**, 1095–1100.

MASTROGIANNIS, D.S., O'BRIEN, W.F., KRAMMER, J. & BENOIT, R. (1991). Potential role of endothelin-1 in normal and hypertensive pregnancies. *Am. J. Obstet. Gynecol.*, **165**, 1711–1716.

MATTOLI, S., SOLOPERTO, M., MEZZETTI, M. & FASOLI, A. (1991). Mechanisms of calcium mobilization and phosphoinositide hydrolysis in human bronchial smooth muscle cells by endothelin 1. *Am. J. Respir. Cell Mol. Biol.*, **5**, 424–430.

MCQUEEN, J., JARDINE, A., KINGDOM, J., TEMPLETON, A., WHITTLE, M. & CONNELL, J.M.C. (1990a). Interaction of angiotensin II and atrial natriuretic peptide in the human fetoplacental unit. *Am. J. Hypertens*, **3**, 641–644.

MCQUEEN, J., KINGDOM, J.C.P., JARDINE, A.G., CONNELL, J.M.C. & WHITTLE, M.J. (1990b). Vascular angiotensin II and atrial natriuretic peptide receptors in normal and growth-retarded human placentae. *J. Endocrinol.*, **126**, 341–347.

MORELAND, S., MCMULLEN, D.M., DELANEY, C.L., LEE, V.G. & HUNT, J.T. (1992). Venous smooth muscle contains vasoconstrictor ET_B-like receptors. *Biochem. Biophys. Res. Commun.*, **184**, 100–106.

NAKAJO, S., SUGIURA, M., SNAJDAR, R.M., BOEHM, F.H. & INAGAMI, T. (1989). Solubilization and identification of human placental endothelin receptor. *Biochem. Biophys. Res. Commun.*, **164**, 205–211.

NAKAMICHI, K., IHARA, M., KOBAYASHI, M., SAEKI, T., ISHIKAWA, K. & YANO, M. (1992). Different distribution of endothelin receptor subtypes in pulmonary tissues revealed by the novel selective ligands BQ-123 and [$Ala^{1,3,11,15}$]ET-1. *Biochem. Biophys. Res. Commun.*, **182**, 144–150.

NAMIKI, A., HIRATA, Y., ISHIKAWA, M., MOROI, M., AIKAWA, J. & MACHII, K. (1992). Endothelin-1 and endothelin-3-induced vasorelaxation via common generation of endothelium derived nitric oxide. *Life Sci.*, **50**, 677–682.

NOVA, A., SIBAI, B.M., BARTON, J.R., MERCER, B.M. & MITCHELL, M.D. (1991). Maternal plasma level of endothelin is increased in preeclampsia. *Am. J. Obstet. Gynecol.*, **165**, 724–727.

OGAWA, Y., NAKAO, K., ARAI, H., NAKAGAWA, O., HOSODA, K., SUGA, S., NAKANISHI, S. & IMURA, H. (1991). Molecular cloning of a non-isopeptide-selective human endothelin receptor. *Biochem. Biophys. Res. Commun.*, **178**, 248–255.

ONDA, H., OHKUBO, S., OGI, K., KOSAKA, T., KIMURA, C., MATSUMOTO, H., SUZUKI, N. & FUJINO, M. (1990). One of the endothelin family, endothelin 3 gene, is expressed in the placenta. *FEBS*, **261**, 327–330.

OTANI, S., USUKI, S., SAITOH, T., YANAGISAWA, M., IWASAKI, H., TANAKA, J., SUZUKI, N., FUJINO, M., GOTO, K. & MASAKI, T. (1991). Comparison of endothelin-1 concentrations in normal and complicated pregnancies. *J. Cardiovasc. Pharmacol.*, **17** (Suppl. 7), S308–S312.

PANEK, R.L., MAJOR, R.C., HINGORANI, G.P., DOHERTY, A.M., TAYLOR, D.G. & RAPUNDALO, S.T. (1992). Endothelin and structurally related analogs distinguish between endothelin receptor subtypes. *Biochem. Biophys. Res. Commun*, **183**, 566–571.

RAE, G.A., TRYBULEC, M., DE NUCCI, G. & VANE, J.R. (1989). Endothelin-1 releases eicosanoids from isolated perfused kidney and spleen. *J. Cardiovasc. Pharmacol.*, **13** (Suppl. 5), S89–S92.

REILLY, F.D. & RUSSELL, P.T. (1977). Neurohistochemical evidence supporting an absence of adrenergic and cholinergic innervation in the human placenta and umbilical cord. *Anat. Rec.*, **188**, 277–286.

ROBAUT, C., MONDON, F., BANDET, J., FERRE, F. & CAVERO, I. (1991). Regional distribution and pharmacological characterization of [^{125}I]Endothelin-1 binding sites in human fetal placental vessels. *Placenta*, **12**, 55–67.

SAEKI, T., IHARA, M., FUKURODA, T., YAMAGIWA, M. & YANO, M. (1991). [$Ala^{1,3,11,15}$]Endothelin-1 analogs with ET_B agonistic activity. *Biochem. Biophys. Res. Commun.*, **179**, 286–292.

SALAS, S.P., POWER, R.F., SINGLETON, A., WHARTON, J., POLAK, J.M. & BROWN, J. (1991). Heterogeneous binding sites for α-atrial natriuretic peptide in human umbilical cord and placenta. *Am. J. Physiol*, **261**, R633–R638.

SOKOLOVSKY, M. (1991). Endothelin and sarafotoxins: receptor subtypes and transmembrane signaling. *Trends Biochem. Sci.*, **16**, 261–264.

SUNNERGREN, K.P., WORD, A.R., SAMBROOK, J.F., MACDONALD, P.C. & CASEY, L. (1989). Expression and regulation of endothelin precursor mRNA in avascular human amnion. *Mol. Cell. Endocrinol.*, **68**, R7–R14.

TAKAYANAGI, R., KITAZUMI, K., TAKASAKI, C., OHNAKA, K., AIMOTO, S., TASAKA, K., OHASHI, M. & NAWATA, H. (1991). Presence of non-selective type of endothelin receptor on vascular endothelium and its linkage to vasodilatation. *FEBS*, **282**, 103–106.

VAN PAPPENDORP, C.L., CAMERON, I.T., DAVENPORT, A.P., KING, A., BARKER, P.J., HUSKISSON, N.S., GILMOUR, R.S., BROWN, M.J. & SMITH, S.K. (1991). Localization and endogenous concentration of endothelin-like immunoreactivity in human placenta. *J. Endocrinol.*, **131**, 507–511.

VIJAYARAGHAVAN, J., SCILI, A.G., CARRETERO, O.A., SLAUGHTER, C., MOOMAW, C. & HERSCH, L.B. (1990). The hydrolysis of endothelins by neutral endopeptidase 24.11 (enkephalinase). *J. Biol. Chem.*, **265**, 14150–14155.

WADA, K., TABUCHI, H., OHBA, R., SATOH, M., TACHIBANA, Y., AKIYAMA, N., HIROAKA, O., ASAKURA, A., MIYAMOTO, C. & FURUICHI, Y. (1990). Purification of an endothelin receptor from human placenta. *Biochem. Biophys. Res. Commun.*, **167**, 251–257.

WALLENSTEIN, S., ZUCKER, C. & FLEISS, J.L. (1980). Some statistical methods useful in circulation research. *Circ. Res.*, **47**, 1–9.

WHARTON, J., RUTHERFORD, R.A.D., GORDON, L., MOSCOSO, G., SCHIEMBERG, I., GAER, J.A.R., TAYLOR, K.M. & POLAK, J.M. (1991). Localization of endothelin binding sites and endothelin-like immunoreactivity in human fetal heart. *J. Cardiovasc. Pharmacol.*, **17** (Suppl. 7), S378–S384.

WILKES, B.M., MENTO, P.F., HOLLANDER, A.M., MAITA, M.E., SUNG, S. & GIRARDI, E.P. (1990). Endothelin receptors in human placenta: relationship to vascular resistance and thromboxane release. *Am. J. Physiol.*, **258**, E864–E870.

WILLIAMS, D.L., JONES, K.L., PETTIBONE, D.J., LIS, E.V. & CLINE-SCHMIDT, B.V. (1991). Sarafotoxin S6c: an agonist which distinguishes between endothelin receptor subtypes. *Biochem. Biophys. Res. Commun.*, **175**, 556–561.

(Received December 21, 1992
Revised February 12, 1993
Accepted February 18, 1993)

Br. J. Pharmacol. (1993), **109**, 553–561 © Macmillan Press Ltd, 1993

A comparison of the effects of polyarginine and stimulated eosinophils on the responsiveness of the bovine isovolumic bronchial segment preparation

Taher Omari, Malcolm P. Sparrow, *Martin K. Church, *Stephen T. Holgate & [1]†Clive Robinson

[1]Department of Physiology, University of Western Australia, Nedlands 6009, Western Australia; *Immunopharmacology Group, Southampton General Hospital, Southampton SO9 4XY and †Department of Pharmacology & Clinical Pharmacology, St George's Hospital Medical School, Cranmer Terrace, London SW17 0RE

1 The bovine isovolumic bronchial segment preparation has been used to study the sensitivity and responsiveness of bronchial smooth muscle after various manipulations.

2 Addition of acetylcholine (ACh) to the lumen of the segments elicited an increase in intraluminal pressure as a result of contraction of the airway smooth muscle. However, the increases in intraluminal pressure were greater when the ACh was added to the adventitial surface of the preparation.

3 Addition of polyarginine to the bronchial lumen for 60–120 min resulted in an increased magnitude of response and greater than 100 fold increase in sensitivity to ACh administered into the lumen. Depolarizations induced by KCl were similarly enhanced when the solution was added into the lumen. In contrast, the sensitivity and responsiveness to ACh or K^+-induced depolarization administered adventitially was unchanged.

4 The mechanical disruption of the epithelium produced a 32 fold increase in sensitivity to ACh introduced via the lumen, whereas the sensitivity to ACh added adventitially remained unaltered.

5 Addition of polyarginine to the adventitial bathing medium resulted in no change in the responsiveness or sensitivity to ACh, irrespective of whether the ACh was given intraluminally or adventitially.

6 Histological examination revealed that polyarginine caused extensive disordering of the normal architecture of the bronchial epithelium. Taken together with the unaltered responsiveness to adventitial ACh (i.e. lack of change in intrinsic muscle sensitivity) these observations suggest that the effect of polyarginine was most likely due to disruption of a diffusion barrier.

7 In contrast to the effects of polyarginine, the only effect of stimulated eosinophils was to produce a small diminution in the responsiveness to ACh that had been added adventitially.

Keywords: Polyarginine; bronchial responsiveness; eosinophil; bronchial segment preparation

Introduction

In diseases such as bronchial asthma or following certain viral infections, the consequences of the mucosal immune response result in the acquisition of enhanced bronchial responsiveness (Empey *et al.*,1977; Jennings *et al.*, 1987; Cockroft, 1989). The mechanistic relationships between the functional manifestation of bronchial hyperresponsiveness and histological changes occurring in the airway mucosa are currently unknown. However, the apparent association between the presence of activated inflammatory cells, injury of the airway epithelium and the appearance of bronchial hyperresponsiveness have fostered the belief that airway inflammation is of primary and causal significance in its pathophysiological development. Superficially, this viewpoint is attractive because inflammatory cells certainly do have the potential to liberate chemical mediators, such as free radicals, cytotoxic proteins and proteolytic enzymes that are known to elicit cell injury (Gleich *et al.*, 1988; Gleich, 1990). This site-directed injury might result in the exposure of intraepithelial nerve endings, cause a reduction in the production or release of epithelium-derived inhibitory factors and facilitate the destruction of a cellular diffusion barrier; events which together might account for augmented bronchial responsiveness.

In studies of patients with mild asthma Beasley and colleagues (1989) reported an inverse correlation between the number of exfoliated epithelial cells in bronchoalveolar lavage fluid and the provocation concentration to methacholine. Other workers have reported the existence of an inverse correlation between the proportion of eosinophils present in bronchoalveolar lavage fluid (Lam *et al.*, 1987; Wardlaw *et al.*, 1988) or the airway mucosa (Ohashi *et al.*, 1992) and the degree of bronchial responsiveness to inhaled methacholine. Likewise, in asthmatic patients treated with a topically active corticosteroid, data have been presented which apparently link a reduction in airway eosinophil numbers of a diminution (but not ablation) of bronchial hyperresponsiveness (Djukanović *et al.*, 1992). Similar evidence associating inflammatory cell infiltration with heightened bronchial responsiveness exists in experimental animals (Marsh *et al.*, 1985; Murphy *et al.*, 1986). On the basis of these studies it has been argued that there is likely to be a causal link between eosinophils, epithelial injury and the acquisition of heightened bronchial responsiveness.

However, several investigations in man and experimental animal models have provided contrary evidence which dissociates the presence of increased numbers of eosinophils in the airway from the development of bronchial hyperresponsiveness, or at least casts doubt on the obligatory and dominant role of the eosinophil in this process (Sanjar *et al.*, 1990; Chapman *et al.*, 1991; Djukanović *et al.*, 1990; 1992; Elwood *et al.*, 1992). The implication of these experiments is that airway inflammation is not causally related to bronchial hyperresponsiveness, or that the link between them is more complex than originally believed. Thus, the relationships

[1] Author for correspondence.

between eosinophils, epithelial damage and smooth muscle responsiveness require further appraisal.

In the present paper we report the results of experiments in which we have continued our mechanistic investigations into mucosal injury and its relationship to functional changes in the airway. Specifically we have compared the effects on smooth muscle responsiveness of treatment with the poly-basic polymer polyarginine (a surrogate for the arginine-rich eosinophil granule proteins), treatment with eosinophils or mechanical denudation of the epithelium. A preliminary account of this work was presented to the British Pharmacological Society (Omari *et al.*, 1991a).

Methods

Isovolumic bronchial segment preparation

Fresh bovine lungs were obtained from a local abattoir and used not more than 1 h *post mortem*. On arrival at the laboratory, bronchial segments, approximately 2 cm in length and with a distal internal diameter of 0.3 cm, were dissected from the upper lobes and cannulated at both ends. The segments were placed in a modified organ bath (Omari & Sparrow, 1992) and bathed at 37°C in Krebs solution (composition, mM: NaCl 121, KCl 5.4, $MgSO_4$ 1.2, NaH_2PO_4 1.2, $NaHCO_3$ 25, glucose 11.5 and $CaCl_2$ 2.5) and gassed with 5% CO_2 in O_2. Krebs solution was also perfused through the lumen of the segment from an external reservoir. The Krebs solution bathing both the luminal and adventitial surfaces was exchanged for fresh solution at regular intervals throughout the experiment. Changes in muscle tone were recorded by closing off proximal and distal taps leaving the segment in series with a differential pressure transducer (type MPX10DP, Motorola Semiconductors, Phoenix, USA). Responses were recorded on a Rikadenki R-50 chart recorder.

Agonists were introduced either on to the adventitial surface of the segments or into the lumen, by use of a syringe and 3-way tap situated at the distal end of the preparation. The segments were also prepared to permit electrical field stimulation (EFS) with platinum ring electrodes and a Grass S44 stimulator. The tissues were maintained at a resting intraluminal pressure of 6 cmH_2O, this being determined as optimal by studying the relationship between EFS stimulation and response at different resting pressures (Figure 1). Cumulative responses were recorded to acetylcholine (ACh) added to the adventitial surface, while responses to ACh introduced into the lumen were recorded non-cumulatively. In some cases the tissues were also challenged with a KCl depolarizing solution that contained 121 mM KCl in place of NaCl.

In all experiments control responses to agonists and EFS were first determined before undertaking a variety of manipulations when the tissues had resumed their resting tone and showed consistent responses to EFS.

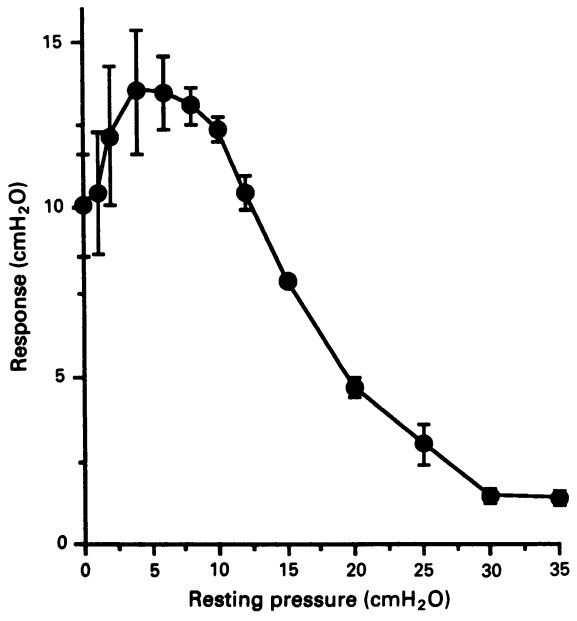

Figure 1 Responses of the bovine isovolumic bronchial segment preparation to electrical field stimulation (60 V, 0.5 ms, 20 Hz) via platinum ring electrodes after being maintained at a range of resting intraluminal pressures. Data are mean ± s.e.mean of 4 separate experiments.

Mechanical injury of bronchial epithelium

As a control for other manipulations, we examined the responsiveness of bronchial segments that had been subjected to mechanical injury of their epithelium. The epithelium was damaged by inserting into the lumen a cotton applicator tip soaked in Krebs solution and rubbing it along the length of the segment.

Treatment with polyarginine

Polyarginine was dissolved in Krebs solution each day and diluted to appropriate concentrations for use. To determine the effect of polyarginine when added to the lumen, exposures of 1 mg ml^{-1} for 1 h as well as 10 and 100 $\mu g\ ml^{-1}$ for 2 h were tested. In experiments comparing the adventitial and luminal administration of polyarginine, an exposure of 100 $\mu g\ ml^{-1}$ was used. In this set of experiments, after obtaining control responses to EFS and ACh, the segments were exposed to polyarginine via the adventitial surface and the effects on the responses of the tissue observed. After complete recovery, the lumen was then exposed to polyarginine and the responses to ACh studied once again. Thus, in contrast to tissues in which the epithelium had been injured mechanically, these studies incorporated within segment rather than between segment control responses.

Experiments with inflammatory cells

For each experiment, paired segments from the same lung were used. After control responses had been obtained, each segment was exposed to either stimulated or unstimulated cells that had been obtained as described below.

Stimulation of eosinophils and neutrophils was achieved with 5 μM ionophore A23187, a concentration that we have previously shown to activate these cell types (Herbert *et al.*, 1991). The ionophore (or its dimethylsulphoxide (DMSO) vehicle at a final concentration of 1.6%) was added to the cells 1 min before they were introduced into the lumen of the segments. After an exposure period of 1 h the segments were then flushed with fresh Krebs solution and the perfusate collected for the measurement of leukotriene B_4 by radioimmunoassay.

Preparation of inflammatory cells

A peritoneal eosinophilia was established in guinea-pigs by injecting male Dunkin-Hartley strain animals i.p. with 1 mg ml^{-1} polymyxin B in saline twice weekly for 4 weeks. At 24 h after the last injection, the animals were anaesthetized with metofane and a 16G cannula (Critikon Ltd, Ascot, Berks.) inserted into the peritoneal cavity. The cavity was lavaged with 50 ml sterile saline and the lavage return collected into a polypropylene tube. The lavage fluid was centrifuged at 150 *g* for 10 min at room temperature and resuspended in 2 ml of Dulbecco's phosphate buffered saline (DPBS, Ca^{2+}- and Mg^{2+}-free). Erythrocytes were lysed by use of hypotonic saline and an initial differential cell count then performed by

use of eosin/pontamine sky blue. In some experiments the cells were resuspended in an appropriate volume of Krebs solution and used without further purification. In those experiments which used purified eosinophils, further enrichment was obtained by resuspending the cells in Tyrode solution containing gelatin and deoxyribonuclease (DNase) and subjecting the cells to density centrifugation on Metrizamide gradients.

The washed lavage cells were overlaid onto density gradients which consisted of a cushion of 2 ml Maxidens upon which a discontinuous gradient of 16, 18, 20, 22, 24, 26 and 30% Metrizamide in Tyrode solution (supplemented with gelatin and DNase) had been prepared. Each step in the gradient had a volume of 2 ml and a maximum of 10^8 cells was loaded onto each gradient. Centrifugation was performed at 1200 *g* for 45 min at room temperature. The eosinophil-rich band at the 24–26% Metrizamide interface was carefully aspirated., washed in DPBS and the number and purity of cells determined by use of eosin/pontamine sky blue. Viability was determined by exclusion of trypan blue and was generally >90%.

Human neutrophils were obtained from the blood of volunteers who had taken no medication within at least one week prior to donation. Eight volumes of citrate-anticoagulated blood were treated with 1 volume of 6% dextran (M_r 500,000) and 1 volume of normal saline. Erythrocytes were sedimented at 1 *g* for 30 min, after which the plasma layer was carefully aspirated, mixed with an equal volume of phosphate-buffered saline and layered as 5 ml aliquots onto 5 ml of Mono-Poly resolving medium. After centrifugation at 400 *g* for 30 min the polymorphonuclear cell layer was aspirated, the cells washed in Krebs solution and an aliquot taken for a differential cell count by use of Wright's stain and an assessment of cell viability with trypan blue.

Histology

At the end of the experiment segments were fixed for 48 h in 4% formaldehyde solution. Small pieces were then dissected and embedded in Cryo-M-Bed prior to the preparation of 10 μm cryostat sections. Sections were stained with haematoxylin and eosin and the appearance of the airway mucosa assessed by light microscopy (Zeiss Axiovert 10 or Leitz Laborlux 12).

Data presentation

Data are shown as either the increase in intraluminal pressure above the resting value of 6 cmH_2O or as a percentage of the maximal response to 10 mM ACh. The sensitivities of the segments to adventitially added ACh were compared by determining the EC_{50} values. The responses to intraluminal ACh rarely exceeded 30% of maximum and consequently the sensitivities were compared by calculating concentrations corresponding to EC_{20} of the maximum adventitial response. Results are expressed as the mean ± s.e.mean of *n* preparations. The significance of any difference between means was evaluated with Student's *t* test, with $P \leqslant 0.05$ being considered statistically significant. Tests for paired samples were used to compare data obtained within individual segments (i.e. control versus subsequent manipulation), whereas unpaired tests were used to evaluate data between experiments.

Materials

The following were purchased from Sigma (Poole, Dorset): acetylcholine, ionophore A23187, polyarginine (M_r 11,600), polymyxin B sulphate, dimethysulphoxide, gelatin (from bovine skin) and DNase. DPBS and Mono-Poly resolving medium were obtained from Flow Laboratories (Rickmansworth, Herts). Metrizamide and Maxidens were purchased from Nycomed (Birmingham). Metofane (methoxyfluorane) was obtained from C-Vet Ltd (Bury St Edmunds, Suffolk). Reagents for the radioimmunoassay of leukotriene B_4 were purchased from NEN-Du Pont Research Products (Stevenage, Herts). Stains for microscopy and all other laboratory reagents were purchased from BDH (Poole, Dorset).

Results

Responses of the preparation

The responses of a bovine bronchial segment maintained at a resting transmural pressure of 6 cmH_2O are shown in Figure 2. Electrical field stimulation (EFS) at 60 V with a duration of 0.5 ms and frequency of 20 Hz produced an increase in intraluminal pressure which relaxed readily upon cessation of the stimulus (Figure 2a). Also illustrated in Figure 2a is a typical cumulative response to ACh that had been applied to the adventitial surface, whereas Figure 2b displays the significantly smaller and non-cumulative dose-response characteristics for ACh injected intraluminally. For example, 10 mM ACh applied adventitially elicited a contraction that produced a mean increase in pressure of 33.0 ± 1.8 cmH_2O ($n = 45$), whereas introduction of ACh into the lumen produced a pressure change of only 12.1 ± 1.2 cmH_2O ($n = 45$, $P \leqslant 0.01$).

Effect of polyarginine

In these experiments, luminal or adventitial surfaces of bovine bronchial segments were exposed to several concentrations of polyarginine. By itself, polyarginine altered neither the resting tone of the bronchi, nor the responses to EFS. However, the responses of bronchial segments to ACh added intraluminally were significantly enhanced by prior exposure of the lumen to 100 μg ml^{-1} polyarginine for 2 h (Figure 3a). For example, the response to 10 mM ACh added into the lumen was increased from 7.3 ± 1.6 to 28.9 ± 3.9 cmH_2O ($n = 4$, $P \leqslant 0.01$). This effect was not seen if the polyarginine was added to the adventitial bathing medium (Figure 3a). In contrast, the responses to ACh added adventitially were unchanged by exposure of either the luminal or adventitial surfaces to polyarginine when using the same treatment regime (Figure 3b, $n = 4$ for each type of exposure). In the case of EFS, the responses of bronchial segments were unchanged by polyarginine, even after 1 h exposure to 1 mg ml^{-1} (21.7 ± 6.2 versus 22.2 ± 7.4 cmH_2O in control and treated tissues respectively, $n = 4$). However, it was of interest that the responses to depolarization by KCl

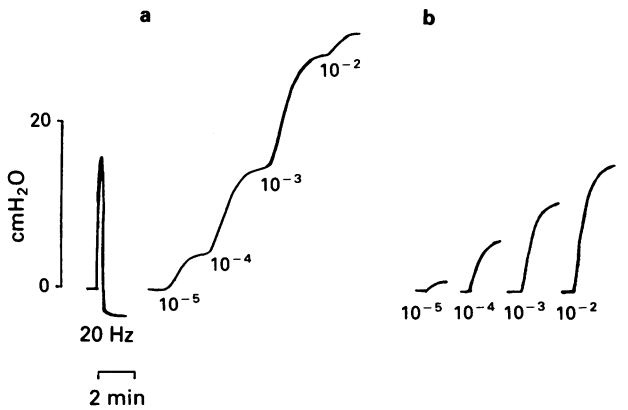

Figure 2 Increases in the intraluminal pressure of a bronchial segment contracting isovolumically to electrical field stimulation (EFS) and acetylcholine (ACh) from a resting pressure of 6 cmH_2O: (a) illustrates the response to EFS and cumulative responses to ACh added to the adventitial surface; (b) illustrates single responses to ACh administered intraluminally.

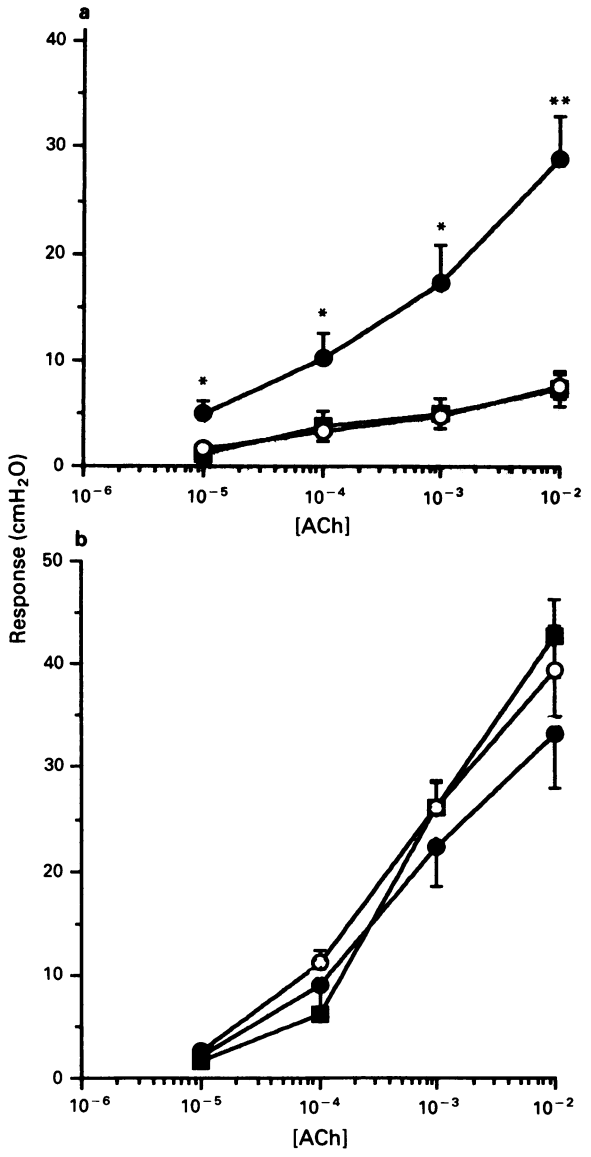

Figure 3 Effect of polyarginine on the responsiveness to acetylcholine (ACh). In (a), ACh was added into the lumen. In (b), ACh was added to the adventitial surface. Each tissue served as its own control (■) before exposure of the lumen (●) or the adventitial surface (○) to 100 μg ml^{-1} polyarginine for 2 h. Data are mean ± s.e.mean of 4 separate experiments. *$P \leqslant 0.05$; **$P \leqslant 0.01$ with respect to appropriate control.

were enhanced in a similar way to those of ACh (Figure 4).

Table 1 summarizes the effect of different treatments with polyarginine, as well as mechanical injury, on the EC_{20} and EC_{50} values which indicate the sensitivity to luminally and adventitially applied ACh respectively. Exposure to 10 μg ml^{-1} polyarginine for 120 min did not alter the sensitivity to ACh at all, whereas higher concentrations in the lumen (100 μg ml^{-1} and 1 mg ml^{-1}) enhanced the sensitivity to luminally-applied ACh by 110 and 135 fold respectively. The EC_{50} values for ACh applied to the outside of the tissue were unchanged by these treatments. Similarly, tissues that had been subjected to mechanical trauma of the epithelium were on average 32 fold more sensitive to ACh added into the lumen when compared with epithelium-intact segments for the same lung. However, there was no change in sensitivity to ACh added to the adventitial side of mechanically injured preparations (Table 1). Overall, there was no significant difference in the changes in tissue sensitivity evoked by polyarginine or mechanical trauma. That mechanical injury appeared to be less effective than polyarginine treatment is probably a reflection of the limitations of the different experimental protocols used and the way in which control re-

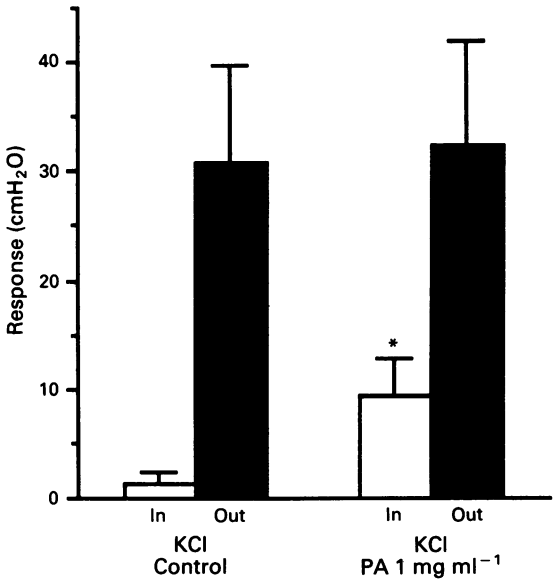

Figure 4 Effect of polyarginine (PA, 1 mg ml^{-1}, 1 h in the lumen) on the response to electrical field stimulation (EFS) and depolarization evoked by K^+. Data are mean ± s.e.mean from 4 separate experiments. *$P \leqslant 0.01$ with respect to appropriate control.

Table 1 Calculated EC_{20} and EC_{50} values for acetylcholine (ACh) added to either the luminal or adventitial sides of bovine bronchial segments before and after exposure to polyarginine: also included are values obtained from tissues where the epithelium had been injured mechanically and their corresponding epithelium-intact controls from the same lungs

Treatment	*log_{10} EC_{20} ACh* (luminal)	*log_{10} EC_{50} ACh* (adventitial)
Polyarginine (10 μg ml^{-1}, 2 h)		
pre-exposure	− 2.66 ± 0.17	− 3.55 ± 0.11
post-exposure	− 2.93 ± 0.32	− 3.30 ± 0.22
Polyarginine (100 μg ml^{-1}, 2 h)		
pre-exposure	− 2.12 ± 0.11	− 3.22 ± 0.12
post-exposure	− 4.18 ± 0.26**	− 3.29 ± 0.08
Polyarginine (1 mg ml^{-1}, 1 h)		
pre-exposure	− 2.05 ± 0.36	− 3.55 ± 0.12
post-exposure	− 4.18 ± 0.33*	− 3.48 ± 0.08
Epithelium-intact segments	− 2.48 ± 0.26	− 3.36 ± 0.09
Mechanically injured segments	− 3.99 ± 0.12†	− 3.34 ± 0.20

Asterisks indicate significant differences between pre- and post-exposure values, *$P \leqslant 0.05$; **$P \leqslant 0.01$. †Significantly different from intact segments, $P \leqslant 0.01$. All data are mean ± s.e.mean values from four experiments in each case.

sponses were determined (see Methods). It is also possible that mechanical injury failed to remove significant amounts of the epithelium.

Effect of inflammatory cells

Bronchial segments were exposed to ionophore A23187 (5 μM, intraluminally) to establish whether A23187 could be used as a means of activating inflammatory cells without interfering with the responsiveness of bronchial smooth muscle. The ionophore produced a slow increase in bronchial tone that reached 50% of the maximal response after approximately 3 h (Figure 5). Despite the change in tone, the smooth muscle responsiveness to ACh applied either intraluminally or adventitially was unaltered by a 60 min exposure to 5 μM A23187 in the lumen (Figure 6).

When bronchial segments were exposed to either stimulated or unstimulated guinea-pig peritoneal eosinophils ($15.9 \pm 0.1 \times 10^6$ ml^{-1} for 60 min) there were no significant effects on the responsiveness to ACh administered intraluminally when this was compared with the corresponding control responses made prior to the addition of cells (Figure 7). This was true irrespective of whether the eosinophils were used as unfractionated peritoneal lavage cells or whether they had been purified by density gradient centrifugation. However, when ACh was applied adventitially after exposure to eosinophils it was noted that there was a small reduction in the magnitude of response compared with the pre-eosinophil control values. In segments exposed to stimulated eosinophils this tendency was statistically significant at all but the highest dose of ACh (Figure 7). Pre- and post-exposure EC_{20} and EC_{50} values derived from these dose-response curves are illustrated in Table 2. In one series of studies we incubated bronchial segments with eosinophil populations at 91.6×10^6 ml^{-1} and purity of 92.6% (with and without ionophore stimulation) and even under these conditions there was no increase in muscle responsiveness (data not shown). As judged by the release of immunoreactive leukotriene B_4, the eosinophils were activated for mediator release by A23187, with a net release of 1.39 ± 0.29 ng LTB_4 per 10^6 eosinophils being detected in the fluid returned from the bronchial lumen.

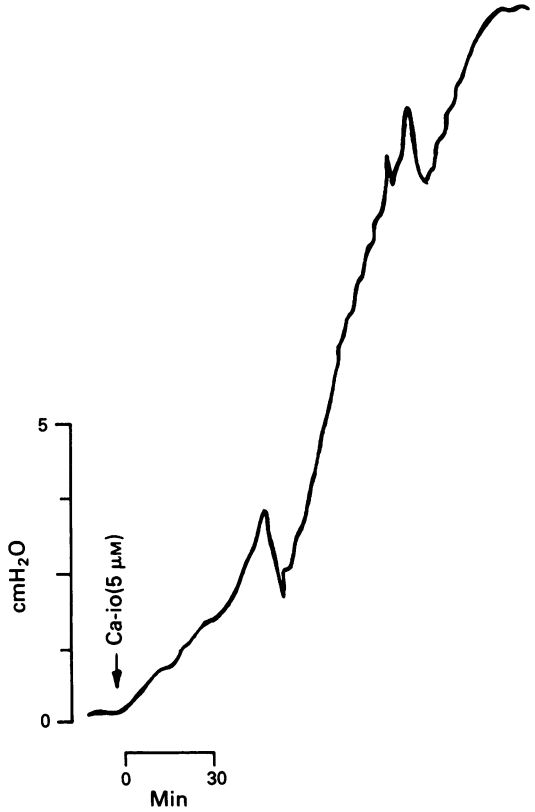

Figure 5 A tracing of changes in intraluminal pressure in a bovine bronchial segment that had been exposed to 5 μM A23187 (Ca-io) on the luminal side.

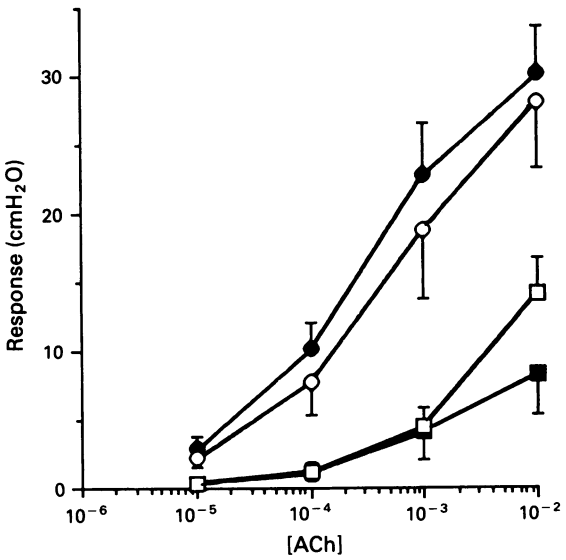

Figure 6 Concentration-response curve to acetylcholine (ACh) added either luminally (●) or adventitially (○) under control conditions. Tissues were then exposed to 5 μM A23187 added into the lumen (□) or into the adventitial bathing medium (■) for 60 min before retesting tissue responsiveness. Data are mean ± s.e.mean of six experiments.

Similar experiments were performed with human neutrophils with 60 min exposures of bronchial segments to cell numbers ranging from $6-330 \times 10^6$ neutrophils ml^{-1} at an average purity of 88.6 ± 4.2%. In no case was the responsiveness of the tissues materially altered by these treatments (data not shown). These cells exhibited a net release of leukotriene B_4, (LTB_4), confirming their stimulation by A23187, with a net 2.81 ± 2.27 ng LTB_4 per 10^6 neutrophils being detected in the fluid recovered from the bronchial lumen.

Histological effects

Cryostat sections prepared from control bronchial segments or tissues that had been exposed to 10 μg ml^{-1} polyarginine for 60 min showed preservation of a relatively intact, healthy epithelium. At high magnification, abundant cilia were evident on cells, and focal intercellular contact was a notable feature between suprabasal epithelial cells. In contrast, those segments exposed to higher concentrations of polyarginine exhibited cytoplasmic shrinkage, loss of interepithelial adhesion and evidence of exfoliation (Figure 8). Interestingly, the areas where exfoliation was noted showed retention of basal cells and cellular debris on the matrix substratum.

Bronchial segments that had been exposed to either unstimulated or ionophore-stimulated eosinophils and neutrophils were also examined. In contrast to the effects of polyarginine, the exposure to inflammatory cells was characterized by little effect on the gross morphology of the airway mucosa.

Discussion

In this series of experiments we have demonstrated that exposure of the bronchial lumen to the basic amino acid

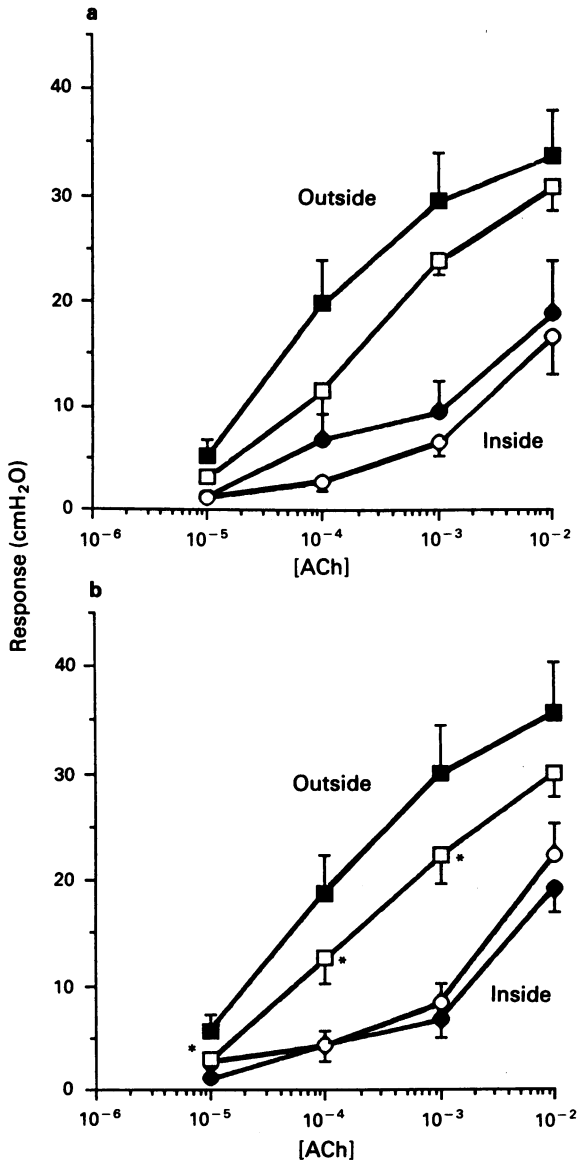

Figure 7 The effect of exposure of bronchial segments to either unstimulated (a) or ionophore stimulated (b) eosinophils. Control concentration-response curves to acetylcholine (ACh) (solid symbols) were initially undertaken before addition of the unfractionated peritoneal eosinophils to the bronchial lumen ($15.9 \pm 0.1 \times 10^6$ ml at an average purity of $68.6 \pm 0.1\%$, $n = 5$). Responses after exposure to eosinophils are denoted by open symbols. In each experiment one tube of each pair dissected from the lung received unstimulated eosinophils, the other received cells which had been activated by the ionophore. Data are mean ± s.e.mean of 5 experiments and asterisks denote significant differences from the appropriate control values.

Table 2 Calculated EC_{20} and EC_{50} values for acetylcholine (ACh) added luminally or adventitially before and after exposure of bronchial segments to guinea-pig peritoneal eosinophils (15.9×10^6 ml^{-1})

Treatment	*log_{10} EC_{20} ACh* (luminal)	*log_{10} EC_{50} ACh* (adventitial)
Unstimulated eosinophils		
pre-exposure	-3.38 ± 0.47	-4.06 ± 0.22
post-exposure	-3.00 ± 0.16	-3.72 ± 0.12
Stimulated eosinophils		
pre-exposure	-3.21 ± 0.41	-4.01 ± 0.23
post-exposure	-3.52 ± 0.38	-3.52 ± 0.27

Data are from five experiments in each case.

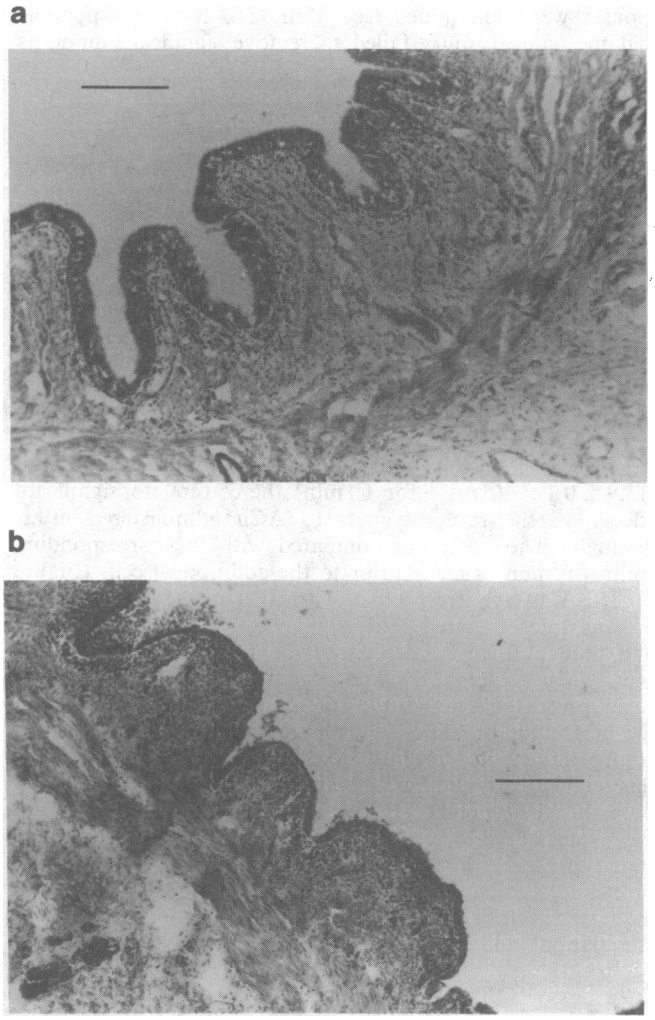

Figure 8 Sections of bronchial segments following (a) control treatment, or (b) exposure for 2 h to 100 μg ml^{-1} polyarginine. The scale bars represent 200 μm in each case.

polymer, polyarginine, results in a relatively rapid augmentation of the responsiveness of the underlying smooth muscle to ACh and KCl-induced depolarizations, but not to EFS. This enhancement was not observed if the adventitial surface of the preparation was similarly treated. A further feature of the 'sidedness' of this phenomenon was that only the responses to agonists introduced into the bronchial lumen were enhanced. Responses to agonists applied adventitially were unchanged, even in those bronchial segments which had been treated with polyarginine in the bronchial lumen.

This pattern of alteration in the responsiveness of the bronchial smooth muscle was similar to that seen in segments in which the bronchial mucosa had been injured mechanically (this study; Munakata *et al.*, 1989; Sparrow & Mitchell, 1991; Omari & Sparrow, 1991) and is consistent with the effects seen after exposure of the mucosa to proteinases (Omari *et al.*, 1991b; Omari & Sparrow, 1992). Collectively, these similarities suggest that polyarginine may be causing disruption of the airway muscosa, a view that was verified experimentally by undertaking a histological evaluation before and after treatment with various concentrations of polyarginine. Tissues that had not been exposed to polyarginine, or those which had experienced only low concentrations, exhibited a normal appearance with an essentially intact epithelium. In contrast, tissues incubated with concentrations of polyarginine that significantly augmented the smooth muscle responsiveness were characterized by evidence of cytolytic damage, cytoplasmic shrinkage and frank exfoliation. It was

of interest that areas of mucosa that had been denuded of epithelial cells in this way still retained a significant number of basal cells. This pattern of tissue injury is thus in many ways similar to that produced by stimulated eosinophils in an *in vitro* model of mucosal injury (Herbert *et al.*, 1991) which has been suggested to represent a convenient model of the mucosal lesion which characterizes lung diseases such as bronchial asthma (Herbert *et al.*, 1991; Montefort *et al.*, 1992). The retention of basal cells in injury of the airway mucosa may arise because the desmosomal attachment of columnar epithelial cells to basal cells is more susceptible to cleavage than is the adhesion of basal cells to the biomatrix (Montefort *et al.*, 1992).

As the airway epithelium functions, in part, as a protective barrier it seems plausible that one effect of polyarginine is to render the mucosa more permeable to solutes as a consequence of the cellular injury and loss of interepithelial tight junctions. In support of this view Herbert *et al.* (1991) demonstrated that polyarginine ($1\ mg\ ml^{-1}$) significantly increased the permeability of the bovine bronchial mucosa to serum albumin. The failure of a lower concentration of polyarginine to produce a significant effect on the net unidirectional flux of albumin, compared to the present results in smooth muscle, probably relates to the fact that Herbert and colleagues focused their attention on macromolecular solute permeability rather than highly diffusible low molecular mass drugs.

The airway epithelium has also been suggested as a source of poorly-characterized factors which inhibit the responsiveness of the underlying smooth muscle (Barnes *et al.*, 1985; Vanhoutte, 1988; Spina *et al.*, 1992). It is therefore possible that removal of such inhibitory factors may contribute to the heightened responsiveness seen in the present experiments. Whilst the bovine bronchial epithelium does release substances, such as prostaglandin E_2 (PGE_2), which have relaxant effects on airway smooth muscle (Herbert & Robinson, unpublished), we discount this as an explanation for our observations in this study. Moreover, we also argue against the possibility that polyarginine enhances responsiveness by releasing bronchoconstrictor agents (e.g. histamine from mast cells). The principal evidence against these hypotheses is that addition of polyarginine to the bronchial lumen does not change the responses of the tissue to agonists added adventitially, even though the responses to intraluminal ACh are enhanced. Furthermore, in a study of mast cell heterogeneity in bovine lung Hunt *et al.* (1991) demonstrated the refractoriness of bovine mast cells to polybasic secretagogues. Thus, we favour the view that the principal effect of polyarginine is to disrupt the epithelial diffusion barrier. The behaviour of the airway epithelium as a diffusion barrier capable of modulating the actions of pharmacological agonists has been suggested on the basis of other studies with bronchial segments (Small *et al.*, 1990; Sparrow & Mitchell, 1991; Omari & Sparrow, 1992; Omari *et al.*, 1993).

One of our reasons for studying polyarginine in the present experiments is that it may be a useful model of the arginine-rich cytotoxic proteins of the eosinophil (Butterworth *et al.*, 1979; Uchida *et al.*, 1990). Attention has been focussed on the role of eosinophil-derived proteins, in particular the major basic protein (MBP), in the pathogenesis of mucosal injury (Gleich *et al.*, 1988). Deposits of MBP have been found adjacent to areas of epithelial exfoliation in the asthmatic lung (Filley *et al.*, 1982) and at relatively high concentrations *in vitro* it is known to cause disruption of nasal and bronchial epithelium (Frigas *et al.*, 1980; Hastie *et al.*, 1987; Ayars *et al.*, 1989; Motojima *et al.*, 1989) and a modest increase in the responsiveness of airway smooth muscle (Flavahan *et al.*, 1988). Other studies have demonstrated that MBP causes an epithelium-dependent increase in bronchial tone in the guinea-pig and monkey (White *et al.*, 1990; Gundel *et al.*, 1990) and an augmentation of responses to agonists administered intravenously (Brofman *et al.*, 1989; White *et al.*, 1990). However, the mechanism(s) of these changes are not understood. In our studies polyarginine had no effect on the resting tone of the bronchial segments, nor did we observe any change in the response of the tissue to ACh added adventitially. These data suggest that there may be important differences between the action of MBP and basic amino acid polymers, implying that the interaction between MBP and target cells is more subtle than that defined by cationic nature alone. Clearly, further work is necessary to establish exactly how polyarginine, MBP and other eosinophil proteins cause such an apparently targeted injury of epithelial cells.

In view of the established toxicity of eosinophil granule proteins and other eosinophil-derived mediators towards airway epithelium it was surprising to find that guinea-pig peritoneal eosinophils that had been stimulated by A23187 produced only a small decrease in the responsiveness to ACh added to the adventitial surface of the preparation. The basis of this effect remains unknown. Relatively small numbers of eosinophils were used in the present studies and it is conceivable that the quantities of eosinophil-derived mediators released were inadequate to affect airway function over the time course of the experiment. Interestingly, Jongejan (1991) did not observe any change in the sensitivity of human bronchial rings to methacholine after exposure to granulocytes ($1-5 \times 10^6$ of which $>90\%$ were neutrophils) that had been activated by zymosan. However, bronchial rings incubated with larger numbers of granulocytes ($10-20 \times 10^6$) exhibited a decreased responsiveness. Similarly, McAlpine and colleagues (1988) found that zymosan-activated neutrophils did not affect the responsiveness of rabbit bronchi. The stimulation of the eosinophils and neutrophils was confirmed in our own experiments by demonstrating a net release of leukotriene B_4 in the fluid recovered from the segments after incubation with the cells. The most likely sources of this leukotriene are the eosinophils and neutrophils because, in contrast to the leukocytes bovine bronchial mucosa is only a poor source of this eicosanoid (Sun *et al.*, 1989; Herbert, 1992).

In contrast to the unexpected effect on bronchial responsiveness in this study, relatively small numbers of guinea-pig eosinophils and human neutrophils ($3-10 \times 10^6\ ml^{-1}$) have been shown to increase the net unidirectional flux of albumin across the bovine bronchial mucosa by causing the exfoliation of epithelial cells (Herbert *et al.*, 1991; Herbert, 1992). In the present work, histological examination of the bronchial segments that had been exposed to stimulated leukocytes showed considerably less disruption than those exposed to polyarginine. These findings are in marked contrast to the tissue morphology reported previously after exposure to eosinophils obtained and stimulated by methods identical to those used in the present study (Herbert *et al.*, 1991). However, there are several important differences which may account for the absence of eosinophil-induced tissue injury. Firstly, in the current study the eosinophils were added to the bronchial lumen and not the adventitial side of the isolated epithelium as reported by Herbert *et al.* (1991). Secondly, no special measures were taken to promote eosinophil adhesion to the target tissue within the bronchial lumen. This is in contrast to the experiments performed by Herbert *et al.* (1991) in which eosinophils were incubated in a small volume under conditions which promoted settling onto a limited and defined area of bronchial mucosa. Moreover, these authors presented specific evidence which indicated that the eosinophil-dependent injury to the mucosa was a contact-dependent phenomenon (Herbert *et al.*, 1991).

In summary, these studies have shown that polyarginine is able to augment the responsiveness of bronchial smooth muscle to ACh in an effect which is dependent on the removal of the diffusion barrier presented by the airway epithelium. Eosinophils stimulated by the ionophore A23187 were unable to reproduce this phenomenon, suggesting that if eosinophils are responsible for the bronchial hyperreactivity seen in asthma then their ability to injure the airway mucosa

is a more chronic process than that produced in this *in vitro* system. Alternatively, certain aspects of the interaction between eosinophils and the airway epithelium may be different in certain types of clinical asthma. In view of the findings reported by Herbert *et al.* (1991) one such difference may involve the nature of the physical contact between eosinophils and the mucosal microenvironment.

We thank the British Council, The Medical Research Council and The British Lung Foundation for financial support. Thanks are also due to Dr Carolyn Herbert for helpful discussion.

References

AYARS, G.H., ALTMAN, L.C., MCMANUS, M.M., AGOSTI, J.M., BAKER, C., LUCHTEL, D.L., LOEGERING, D.A. & GLEICH, G.J. (1989). Injurious effect of the eosinophil peroxide-hydrogen peroxide-halide system and major basic protein on human nasal epithelium *in vitro*. *Am. Rev. Respir. Dis.*, **140**, 125–131.

BARNES, P.J., CUSS, F.M. & PALMER, J.B. (1985). The effect of airway epithelium on smooth muscle contractility in bovine trachea. *Br. J. Pharmacol.*, **86**, 685–691.

BEASLEY, R., ROCHE, W.R., ROBERTS, A.J. & HOLGATE, S.T. (1989). Cellular events in the bronchi in mild asthma and after bronchial provocation. *Am. Rev. Respir. Dis.*, **139**, 806–817.

BROFMAN, J.D., WHITE, S.R., BLAKE, J.S., MUNOZ, N.M., GLEICH, C.J. & LEFF, A.R. (1989). Epithelial augmentation of trachealis contraction caused by major basic protein of eosinophils. *J. Appl. Physiol.*, **66**, 1867–1873.

BUTTERWORTH, A.E., WASSOM, D.L., GLEICH, G.J., LOEGERING, D.A. & DAVID, J.R. (1979). Damage to shistosomula of schistosoma mansoni induced directly by eosinophil major basic protein. *J. Immunol.*, **122**, 221–229.

CHAPMAN, I.D., BOUBEKEUR, K. & MORLEY, J. (1991). Airway eosinophilia and airway hyperresponsiveness parallel other sequential events in the guinea pig. In *New Drugs For Asthma*. ed. Morley, J. & Anderson, G. Basle: Birkhauser-Verlag.

COCKROFT, D.W. (1989). Airway hyperresponsiveness: therapeutic implications. *Ann. Allergy*, **59**, 405–414.

DJUKANOVIĆ, R., WILSON, J.W., BRITTEN, K.M., WILSON, S.J., WALLS, A.F., ROCHE, W.R., HOWARTH, P.H. & HOLGATE, S.T. (1990). Quantitation of mast cells and eosinophils in the bronchial mucosa of symptomatic atopic asthmatics and healthy control subjects using immunohistochemistry. *Am. Rev. Respir. Dis.*, **142**, 863–871.

DJUKANOVIĆ, R., WILSON, J.W., BRITTEN, K.M., WILSON, S.J., WALLS, A.F., ROCHE, W.R., HOWARTH, P.H. & HOLGATE, S.T. (1992). Effect of an inhaled corticosteroid on airway inflammation symptoms in asthma. *Am. Rev. Respir. Dis.*, **145**, 669–674.

ELWOOD, W., LÖTVALL, J.O., BARNES, P.J. & CHUNG, K.F. (1992). Effect of dexamethasone and cyclosporin A on allergen-induced airway hyperresponsiveness and inflammatory cell responses in sensitized brown norway rats. *Am. Rev. Respir. Dis.*, **145**, 1289–1294.

EMPEY, D.W., LAITINEN, L.A., JACOBS, L., GOLD, W.M. & NADEL, J.A. (1977). Mechanisms of bronchial hyperreactivity in normal subjects after upper respiratory tract infections. *Am. Rev. Respir. Dis.*, **113**, 131–139.

FILLEY, W.V., HOLLEY, K.E., KEPHART, G.M. & GLEICH, G.J. (1982). Identification by immunofluorescence of eosinophil granule major basic protein in lung tissue of patients with bronchial asthma. *Lancet*, **ii**, 11–16.

FLAVAHAN, N.A., SLIFMAN, N.R., GLEICH, G.J. & VANHOUTTE, P.M. (1988). Human eosinophil major basic protein causes hyperreactivity of respiratory smooth muscle. Role of the epithelium. *Am. Rev. Respir. Dis.*, **138**, 685–688.

FRIGAS, E., LOEGERING, D.A. & GLEICH, G.J. (1980). Cytotoxic effects of the guinea pig eosinophil major basic protein on tracheal epithelium. *Lab Invest.*, **42**, 35–42.

GLEICH, G.J. (1990). The eosinophil and bronchial asthma: current understanding. *J. Allergy Clin. Immunol.*, **85**, 422–436.

GLEICH, G.J., FLAVAHAN, N.A., FUJISAWA, T. & VANHOUTTE, P.M. (1988). The eosinophil as a mediator of damage to respiratory epithelium: a model for bronchial hyperreactivity. *J. Allergy Clin. Immunol.*, **81**, 776–781.

GUNDEL, R.H., LETTS, L.G. & GLEICH, G.J. (1991). Human eosinophil major basic protein induces airway constriction and airway hyperresponsiveness in primates. *J. Clin. Invest.*, **87**, 1470–1473.

HASTIE, A.T., LOEGERING, D.A., GLEICH, G.J. & KUEPPERS, G. (1987). The effect of purified eosinophilic major basic protein on mammalian ciliary activity. *Am. Rev. Respir. Dis.*, **135**, 848–853.

HERBERT, C.A. (1992). The effects of leukocytes, local hormones and selected peptides on the permeability of the bronchial mucosa to albumin *in vitro*. *Ph.D. Thesis. University of Southampton.*

HERBERT, C.A., EDWARDS, D., BOOT, J.R. & ROBINSON, C. (1991). *In vitro* modulation of the eosinophil-dependent enhancement of the permeability of the bronchial mucosa. *Br. J. Pharmacol.*, **104**, 391–398.

JENNINGS, L.C., BARNS, G. & DAWSON, K.P. (1987). The association of viruses with acute asthma. *N.Z. Med. J.*, **100**, 488–490.

JONGEJAN, R.C. (1991). Responsiveness of isolated human airways. Modulation by inflammatory cells, mediators and physical stimuli. *Ph.D. Thesis. Erasmus University, Rotterdam, The Netherlands.*

LAM, S., LERICHE, J., PHILLIPS, D. & CHAN-YEUNG, M. (1987). Cellular and protein changes in bronchial lavage fluid after late asthmatic reaction in patients with red cedar asthma. *J. Allergy Clin. Immunol.*, **80**, 44–50.

MARSH, W.R., IRVIN, C.G., MURPHY, K.R., BEHRENS, B.L. & LARSEN, G.L. (1985). Increases in airway reactivity to histamine and inflammatory cells in bronchoalveolar lavage after the late asthmatic response in an animal model. *Am. Rev. Respir. Dis.*, **131**, 875–879.

MCALPINE, L.G., MCGRATH, J.C., THOMSON, N.C. & WILSON, E.P. (1988). Effect of activated human neutrophils on histamine response of rabbit secondary bronchi smooth muscle *in vitro*. *Br. J. Pharmacol.*, **95**, 526P.

MONTEFORT, S., HERBERT, C.A., ROBINSON, C. & HOLGATE, S.T. (1992). The bronchial epithelium as a target for inflammatory attack in asthma. *Clin. Exp. Allergy*, **22**, 511–520.

MOTOJIMA, S., FRIGAS, E., LOEGERING, D.A. & GLEICH, G.J. (1989). Toxicity of eosinophil cationic proteins for guinea pig tracheal epithelium *in vitro*. *Am. Rev. Respir. Dis.*, **139**, 801–805.

MUNAKATA, M., HUANG, I., MITZNER, W. & MENKES, H. (1989). The protective role of the epithelium in the guinea pig. *J. Appl. Physiol.*, **66**, 1547–1552.

MURPHY, K.R., WILSON, M.C., IRVIN, C.G., GLEZEN, G.S., MARSH, W.R., HASLETT, C., HENSON, P.M. & LARSEN, G.L. (1986). The requirement for polymorphonuclear leukocytes in the late asthmatic response and heightened airways reactivity in an animal model. *Am. Rev. Respir. Dis.*, **134**, 62–68.

OHASHI, Y., MOTOJIMA, S., FUKUDA, T. & MAKINO, S. (1992). Airway hyperresponsiveness, increased intracellular spaces of bronchial epithelium, and increased infiltration of eosinophils and lymphocytes in bronchial mucosa in asthma. *Am. Rev. Respir. Dis.*, **145**, 1469–1476.

OMARI, T.I., HERBERT, C.A., SPARROW, M.P., CHURCH, M.K., HOLGATE, S.T. & ROBINSON, C. (1991a). Effects of polyarginine on bronchial mucosal permeability and its relationship to smooth muscle contraction in isovolumic bronchial segments. *Br. J. Pharmacol.*, **102**, 179P.

OMARI, T.I., MITCHELL, H.W. & SPARROW, M.P. (1991b). Epithelial damage and responsiveness of bronchial segments. *Clin. Exp. Pharmacol. Physiol.*, **18** (Suppl.) 47.

OMARI, T.I. & SPARROW, M.P. (1992). Epithelial disruption by proteases augments the responsiveness of porcine bronchial segments. *Clin. Exp. Pharmacol. Physiol.*, **19**, 785–794.

OMARI, T.I., SPARROW, M.P. & MITCHELL, H.M. (1993). Responsiveness of human isolated bronchial segments and its relationship to epithelial loss. *Br. J. Clin. Pharmacol.*, **35**, (in press).

SANJAR, S., AOKI, S., KRISTERSSON, A., SMITH, D. & MORLEY, J. (1990). Antigen challenge induces pulmonary airway eosinophil accumulation and airway hyperreactivity in sensitized guinea pigs: the effect of antiasthma drugs. *Br. J. Pharmacol.*, **99**, 679–686.

SMALL, R.C., GOOD, D.M., DIXON, J.S. & KENNEDY, I. (1990). The effects of epithelium removal on the actions of cholinomimetic drugs in opened segments and perfused tubular preparations of guinea pig trachea. *Br. J. Pharmacol.*, **100**, 516–522.

SPARROW, M.P. & MITCHELL, H.W. (1991). Modulation by the epithelium of the extent of bronchial narrowing produced by substances perfused through the lumen. *Br. J. Pharmacol.*, **103,** 1160–1164.

SPINA, D., FERNANDES, L.B., PREUSS, J.M.H., HAY, D.W.P., MUCCITELLI, R.M., PAGE, C.P. & GOLDIE, R.G. (1992). Evidence that epithelium-dependent relaxation of vascular smooth muscle detected by co-axial bioassays is not attributable to hypoxia. *Br. J. Pharmacol.*, **105,** 799–804.

SUN, F.F., CZUK, C.I. & TAYLOR, B.M. (1989). Arachidonic acid metabolism in guinea pig eosinophils: synthesis of thromboxane B_2 and leukotriene B_4 in response to soluble or particulate activation. *J. Leukocyt. Biol.*, **46,** 152–160.

UCHIDA, D.A., LARSEN, G.L. & IRVIN, C.G. (1990). Cationic charge may be responsible for the increase in airways responsiveness associated with major basic protein. *Am. Rev. Respir. Dis.*, **141,** A174.

VANHOUTTE, P.M. (1988). Epithelium-derived relaxing factor: myth or reality? *Thorax*, **43,** 665–668.

WARDLAW, A.J., DUNETTE, S., GLEICH, G.J., COLLINS, J.V. & KAY, A.B. (1988). Eosinophils and mast cells in bronchoalveolar lavage in subjects with mild asthma. *Am. Rev. Respir. Dis.*, **137,** 62–69.

WHITE, S.R., OHNO, S., MUNOZ, N.M., GLEICH, G.J., ABRAHAMS, C., SOLWAY, J. & LEFF, A.R. (1990). Epithelium-dependent contraction of airway smooth muscle caused by eosinophil MBP. *Am. J. Physiol.*, **259,** L294–L303.

(Received November 18, 1992
Revised January 28, 1993
Accepted February 18, 1993)

Br. J. Pharmacol. (1993), **109**, 562–568 © Macmillan Press Ltd, 1993

Hoe 694, a new Na^+/H^+ exchange inhibitor and its effects in cardiac ischaemia

[1]W. Scholz, U. Albus, H.J. Lang, W. Linz, P.A. Martorana, H.C. Englert & B.A. Schölkens

Hoechst AG, Postfach 800 320, 6230 Frankfurt/M. 80, Germany

1 The benzoylguanidine derivative Hoe 694 ((3-methylsulphonyl-4-piperidino-benzoyl) guanidine methanesulphonate) was characterized as an inhibitor of Na^+/H^+ exchange in rabbit erythrocytes, rat platelets and bovine endothelial cells. The potency of the compound was slightly lower or comparable to ethylisopropyl amiloride (EIPA).

2 To investigate a possible cardioprotective role of the Na^+/H^+ exchange inhibitor Hoe 694, rat isolated working hearts were subjected to ischaemia and reperfusion. In these experiments all untreated hearts suffered ventricular fibrillation on reperfusion. Addition of 10^{-7} M Hoe 694 to the perfusate almost abolished reperfusion arrhythmias in the rat isolated working hearts.

3 Hoe 694 reduced the release of lactate dehydrogenase (LDH) and creatine kinase (CK), which are indicators of cellular damage during ischaemia, into the venous effluent of the hearts by 60% and 54%, respectively.

4 The tissue content of glycogen at the end of the experiments was increased by 60% and the high energy phosphates ATP and creatine phosphate were increased by 240% and 270% respectively in the treated hearts as compared to control hearts.

5 Antiischaemic effects of the Na^+/H^+ exchange inhibitor, Hoe 694, were investigated in a second experiment in anaesthetized rats undergoing coronary artery ligation. In these animals, pretreatment with Hoe 694 caused a dose-dependent reduction of ventricular premature beats and ventricular tachycardia as well as a complete suppression of ventricular fibrillation down to doses of 0.1 mg kg^{-1}, i.v. Blood pressure and heart rate remained unchanged.

6 We conclude that the new Na^+/H^+ exchange inhibitor, Hoe 694, shows cardioprotective and antiarrhythmic effects in ischaemia and reperfusion in rat isolated hearts and in anaesthetized rats. In view of the role which Na^+/H^+ exchange seems to play in the pathophysiology of cardiac ischaemia these effects could probably be attributed to Na^+/H^+ exchange inhibition.

Keywords: Hoe 694; Na^+/H^+ exchange, ischaemia; arrhythmia, cardiac protection

Introduction

The plasma membrane Na^+/H^+ exchanger is an ubiquitous pH regulating cellular ion transport system. It is driven by the Na^+ gradient and extrudes protons from the cytosol in exchange for extracellular Na^+ ions (Aronson 1985; Frelin *et al.*, 1988). In cardiac tissue the exchanger seems to have a major role in the control of intracellular pH. At the onset of cardiac ischaemia and in reperfusion, Na^+/H^+ exchange is excessively activated by low intracellular pH (Lazdunski *et al.*, 1985; Frelin *et al.*, 1985). Since the deleterious Na^+ influx in this condition was found to originate mainly from Na^+/H^+ exchange (Frelin *et al.*, 1984; Schömig *et al.*, 1988), the exchanger seems responsible for an increase in cytosolic sodium in ischaemic cells. The accumulation of intracellular Na^+ causes an activation of Na^+/K^+ ATPase (Frelin *et al.*, 1984; Rassmussen *et al.*, 1989) which in turn increases ATP consumption. During ischaemia the anaerobic metabolism of glucose terminates in lactic acid. A vicious circle leads to a further decrease of intracellular pH and to a further activation of Na^+/H^+ exchange, resulting in energy depletion, cellular Na^+ overload and finally due to the coupling of Na^+ and Ca^{2+} transport via Na^+/Ca^{2+} exchange, cellular Ca^{2+} overload (Frelin *et al.*, 1984; Lazdunski *et al.*, 1985; Tani & Neely, 1990). Especially in ischaemic cardiac tissue where Na^+/H^+ exchange is the dominant pH regulating ion transport system (Frelin *et al.*, 1985; Weissenberg *et al.*, 1989) these pathophysiological events could lead to increased excitability and precipitation of cellular death.

Therefore it seemed desirable to find potent and well tolerated inhibitors of Na^+/H^+ exchange which should be able to interrupt this vicious cycle, to conserve cellular energy stores and to diminish excitability and necrosis in cardiac ischaemia. In previous experiments we have demonstrated such effects with the relatively weak or toxic standard inhibitors of Na^+/H^+ exchange, amiloride and ethylisopropyl amiloride (Scholz *et al.*, 1991; 1992).

In the present study a new compound, the benzoyl guanidine derivative, Hoe 694 (Figure 1) was characterized as a Na^+/H^+ exchange inhibitor in erythrocytes, platelets, and endothelial cells. Possible anti-ischaemic effects of Hoe 694 were investigated in rat isolated working hearts with ischaemia-reperfusion injuries. Furthermore, the *in vivo* activity

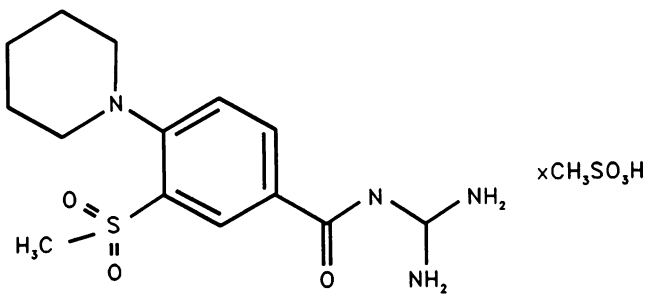

Figure 1 Hoe 694 (3-methylsulphonyl-4-piperidinobenzoyl) guanidine methanesulphonate.

[1] Author for correspondence.

of Hoe 694 in myocardial ischaemia was examined in anaesthetized rats with ligation of a coronary artery.

Methods

Sodium influx into erythrocytes

New Zealand white rabbits (Ivanovas) were fed a rabbit standard chow with 2% cholesterol for 6 weeks to increase the Na^+/H^+ exchange (Scholz *et al.*, 1990) and to make the erythrocytes suitable for measurement of sodium influx via Na^+/H^+ exchange by flame photometry. Blood was drawn from the ear artery of the rabbits and coagulation prevented with 25 i.u. ml^{-1} potassium heparin. The haematocrit of the sample was determined in duplicate by centrifugation. Aliquots of 100 µl were taken to measure the initial sodium content of the erythrocytes.

To determine the amiloride sensitive sodium influx into erythrocytes, 100 µl of each blood sample was added to 5 ml of buffer made hyperosmolar by sucrose (in mM: NaCl 140, KCl 3, sucrose 150, ouabain 0.1, tris-hydroxy-methylaminomethane 20, pH 7.4) and incubated for 60 min at 37°C. Subsequently, the erythrocytes were washed three times in ice-cold $MgCl_2$-ouabain-solution (in mM: $MgCl_2$ 112, ouabain 0.1) with centrifugation.

For determination of intracellular Na^+ content, the cells were haemolysed in distilled water, the cell membranes were centrifuged and the sodium concentration of the haemolysate was measured by flame-photometry.

Net influx of sodium into the erythrocytes was calculated from the difference between the initial sodium content and the sodium content after the incubation. Amiloride-sensitive Na^+ influx was calculated from the difference between Na^+ content of erythrocytes incubated with and without amiloride 3×10^{-4} M. Each experiment was done with the erythrocytes of 6 different animals. In each case the comparison of Na^+ content was made between erythrocytes from the same animal.

Statistical analysis of the data obtained was performed with Student's *t* test for paired groups. Differences were considered significant if $P < 0.05$. Results are given as mean values ± s.e.mean.

Inhibition of Na^+/H^+ exchange in platelets

Wistar rats (Möllegard, 250 g–350 g) were used for the experiments. Blood (approx. 5 ml) was withdrawn from the abdominal aorta under ethylether anaesthesia. Coagulation was inhibited by 0.8 ml acid citrate dextrose (in mM: citric acid 65, glucose 11, and trisodium citrate 85). The blood was immediately centrifuged at 90 *g* for 10 min and a platelet count was done from the platelet rich plasma (PRP) with a Casey 1 multichannelyser (Schärfe System, D7410 Reutlingen). Each of the experiments was performed with 10–50 µl PRP containing 20×10^6 platelets which was made up to a volume of 100 µl with saline. To activate Na^+/H^+ exchange in the platelets by intracellular acidification, 500 µl propionate buffer (mM: Na-propionate 135, HCl 1, $CaCl_2$ 1, $MgCl_2$ 1, glucose 10, HEPES 20, pH 6.7, 22°C) was added to the PRP/NaCl solution. Decrease of the optical density of the PRP solution as a result of the platelet swelling was measured with a Turbitimer (Behringwerke, Marburg, Germany). The device was activated photometrically by the addition of propionate buffer to the cuvette. To identify Na^+/H^+ exchange-induced change of extinction the experiments were performed with and without the Na^+/H^+ exchange inhibitor 5-(N-ethyl-N-isopropyl)amiloride (EIPA). During the experiments all solutions were kept at 22°C in a temperature controlled water bath.

Results are given as means ± s.d. Student's *t* test was employed for statistical evaluation. A *P*-value of < 0.05 was considered significant.

Inhibition of Na^+/H^+ exchange in bovine aortic endothelial cells

Bovine aortic endothelial cells (BAEC) were isolated by dispase digestion from bovine aorta obtained from animals killed at the local slaughter house. The cells were cultured on 35 mm dishes and grown to confluency in Dulbecco's Minimum Essential Medium (DMEM, Gibco) under an atmosphere containing 10% CO_2. Three days after confluency the cells were used for measurement of $^{22}Na^+$ influx.

The cells were washed twice with Krebs-Ringer-solution buffered with Hepes/Tris (KRB) in which sodium chloride had been replaced by choline chloride (in mM: choline chloride 130, $CaCl_2$ 1.5, KCl 5, $MgCl_2$ 1, HEPES 20, pH 7.0 with Tris) and then incubated for 20 min at 37°C in the same buffer which also contained 0.1% bovine serum albumin (BSA) and glucose 10 mM. To stimulate Na^+/H^+ exchange the culture dishes were incubated for another 10 min with 500 µl/dish KRB in which all sodium chloride had been replaced by 65 mM each of choline chloride and Na^+-propionate or with KRB in which 50% of the sodium chloride had been replaced by choline chloride for unstimulated controls. In addition the buffer contained 2 µCi ml^{-1} $^{22}Na^+$ and the test compounds EIPA or Hoe 694. After the stimulation period, sodium influx was terminated by washing the cells twice with ice-cold stop solution (in mM: $MgCl_2$ 0.1, Tris 10, pH 7.0). Subsequently, the cells were lysed with 250 µl trichloric acid and scraped from the dishes. Radioactivity was determined in a Packard gamma counter.

Results are given as mean ± s.d. Statistical analysis of the data obtained was performed with Student's *t* test for independent groups. Differences were considered significant if $P < 0.05$.

Rat isolated working heart preparation

Isolated working hearts prepared from Wistar rats of either sex weighing 280–300 g were used in all experiments as described before (Linz *et al.*, 1986). Animals were injected intraperitoneally with sodium heparin (500 u kg^{-1}) 1 h before they were killed.

The hearts were excised and placed in ice-cold perfusion medium until contraction had ceased (after approximately 5 s). Isolated hearts were then perfused via the aorta at a constant perfusion pressure equivalent to 65 mmHg (Neely *et al.*, 1967) with a modified Krebs-Henseleit buffer (mM: NaCl 113.8, $NaHCO_3$ 22, KCl 4.7, KH_2PO_4 1.2, $MgSO_4$ 1.1, $CaCl_2$ 2.5, glucose 11.0, Na pyruvate 2.0). The medium was gassed with 95% O_2 plus 5% CO_2 at 37°C and pH 7.4. The perfusate was not recirculated. Thereafter, a silicone balloon was introduced into the left ventricle through the mitral valve. Preload was held at 7.4 mmHg and afterload as well as coronary perfusion was kept constant at 65 mmHg. Hoe 694 10^{-7} M was present in the respective experiments throughout the perfusion period. This concentration was chosen because the IC_{50} of Hoe 694 on Na^+/H^+ exchange was close to 10^{-7} M in several tissues (see results). The compound was dissolved in the perfusion medium without the use of any solvent.

After the perfusion had started the hearts immediately began to pump into the artificial systemic circulation and to perform pressure volume work (for detailed description see Linz *et al.*, 1986). Hearts were perfused for an initial 20 min period (control perfusion period). Acute regional myocardial ischaemia was then produced by clamping the left coronary artery close to its origin for 15 min (ischaemic period). Thereafter, the clip was reopened and changes during reperfusion were monitored for 30 min (reperfusion period).

The following parameters were measured: left ventricular pressure (LVP) via a Statham pressure transducer P23 Db, which on differentiation yielded $LV\ dP/dt_{max}$ and heart rate (HR). Coronary flow (CF) was determined by an electromagnetic flow probe in the aortic cannula. An epicardial

electrocardiogram recording was obtained via two silver electrodes attached to the heart. All parameters were recorded on a Brush 2600 recorder.

For the determination of lactate release, lactate dehydrogenase (LDH) and creatine kinase (CK) activities in the perfusate, samples were taken from the coronary effluent for spectrophotometrical measurements (Linz *et al.*, 1986). All heart weights are given in g of wet tissue. Wet weight of the hearts (approximately 1.2 g) was determined immediately after excision from the rats and before they were mounted in the perfusion chamber. Dry tissue weight (approximately 240 mg) was measured after drying the hearts for 12 h at 110°C.

After the experiments, hearts were rapidly frozen in liquid nitrogen and stored at minus 80°C. For tissue analysis of lactate, glycogen and high energy phosphates 500 mg of the left ventricle were taken, put into 5 ml ice-cold $HClO_4$ (0.6 M), and homogenized with an Ultra-Turrax (Junke & Kunkel, Ika-Werk, Model TP).

Glycogen was hydrolized to glucose with amyloglycosidase (pH 4.8) (Linz *et al.*, 1986). Lactate was assayed spectrophotometrically according to Noll (1984). ATP and creatine phosphate (CP) were measured according to Trautschold *et al.* (1985) and Heinz & Weisser (1985).

Results are given as mean values ± s.e.mean. Statistical analysis of the data obtained was performed with Student's *t* test for independent groups. Differences were considered significant if $P < 0.05$.

Anaesthetized rats

Male Sprague-Dawley rats (280–440 g) were anaesthetized with sodium pentobarbitone (60 mg kg^{-1}, i.p.). A tube was tied into the trachea and the animals were ventilated with room air 10–13 ml kg^{-1} at 54 breaths min^{-1} by a Rhema respirator (Frankfurt, Germany).

A catheter was inserted into the left carotid artery and connected to a pressure transducer (Type P23 Dd, Statham, Hato Ray, Puerto Rico) to record blood pressure with a Brush Mark 220 polygraph.

The ECG was recorded from lead II and arrhythmias were evaluated according to the guidelines of the Lambeth conventions (Walker *et al.*, 1988) where: VPB's (ventricular premature beats) were defined as discrete and identifiable premature QRS complexes (premature in relation to the P wave). All the VPB's occurring in the ischaemic period (15 min) were counted except runs of VPB's which had to be defined as VT. VT (ventricular tachycardia) was defined as a run of four or more consecutive ventricular premature beats. The duration of VT, in seconds, was measured. VF (ventricular fibrillation) was defined as a signal for which individual QRS deflections could no longer be distinguished from one another. The duration of VF, in seconds, was measured. The heart rate was counted from the ECG.

Thoracotomy for coronary artery ligation was performed at the fifth intercostal space. During an equilibration period of 5 min rats with spontaneous arrhythmias or a systolic blood pressure below 70 mmHg were rejected. The left coronary artery was then ligated for 15 min. For intravenous applications a catheter was placed into the right jugular vein.

Hoe 694 (0.001 to 3 mg kg^{-1} body weight) was given intravenously as a bolus 5 min before coronary artery occlusion.

The results are presented as mean ± s.e.mean. Differences between mean values were analysed with Mann-Whitneys U-test for independent groups. Differences were considered significant if $P < 0.05$. Differences of the incidences of arrhythmias between treated groups and controls were analysed with the Chi-square test and were considered significant at a level of 95%.

Results

Sodium influx into rabbit erythrocytes

As shown in Figure 2, Hoe 694 caused a concentration-dependent inhibition of Na^+ influx into the rabbit erythrocytes. This effect was limited to amiloride-inhibitable Na^+ influx. There was no additional effect of Hoe 694 on Na^+ influx when the erythrocytes were pretreated with 3×10^{-4} M amiloride. The IC_{50} for the inhibition of amiloride inhibitable Na^+ influx by Hoe 694 was 0.8×10^{-6} M.

Na^+/H^+ exchange in rat platelets

Intracellular acidification with Na propionate caused a decrease of the optical density of the platelet solution. The time course of the rate of this decrease of extinction is shown in Figure 3 as well as its inhibition by the Na^+/H^+ exchange inhibitor EIPA at 10^{-5} M or by Hoe 694 at 10^{-5} M. Figure 4 demonstrates the concentration-dependency of the inhibition of platelet swelling by EIPA or by Hoe 694 20 s after the beginning of the reaction. The IC_{50} values were close to 1×10^{-7} M for both compounds.

Inhibition of Na^+/H^+ exchange in bovine aortic endothelial cells

In bovine aortic endothelial cells, acidification with propionate caused a marked increase of $^{22}Na^+$ influx which was totally inhibited by 10^{-5} M EIPA. The Na^+/H^+ exchange

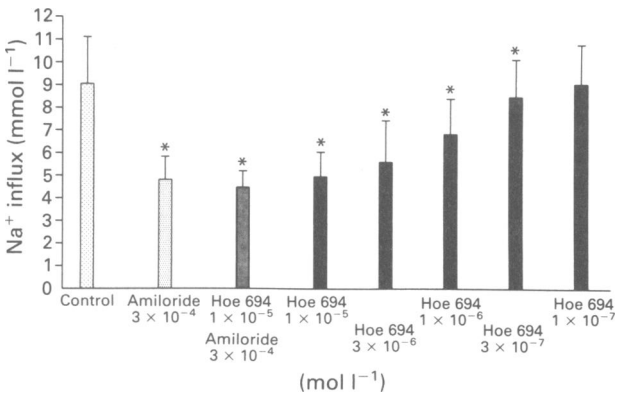

Figure 2 Concentration-dependent inhibition of amiloride-sensitive Na^+ influx in rabbit erythrocytes by Hoe 694. Mean with s.e.mean, $n = 6$ for each data point. $^*P < 0.05$ vs control.

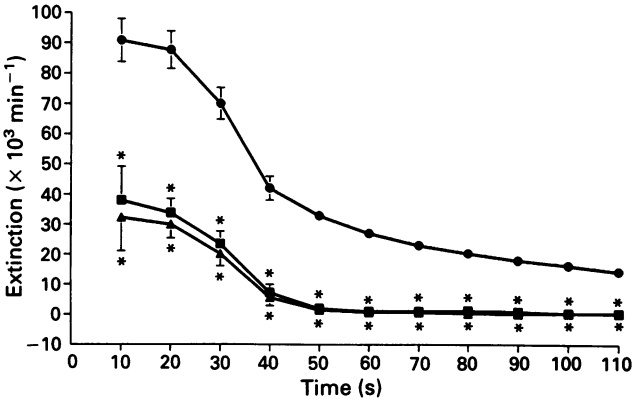

Figure 3 Rates of decrease of extinction of rat platelet solutions after intracellular acidification by propionate. Control (●), inhibition by 5-(N-ethyl-*N*-isopropyl) amiloride (▲) and by Hoe 694 (■) at 10^{-5} mol l^{-1}. Mean with s.d., $n = 6$ for each data point. $^*P < 0.05$ vs control.

inhibitor had no effect in non-acidified controls (Figure 5). Hoe 694 caused a concentration-dependent inhibition of EIPA-sensitive $^{22}Na^+$ influx induced by propionate (Figure 6). When given together with EIPA into the incubation medium, Hoe 694 had no additional effect on $^{22}Na^+$ influx. The IC_{50} of Hoe 694 was estimated to be in the range of 10^{-7} M which is comparable to the IC_{50} of EIPA in the same experimental setup (Figures 5,6).

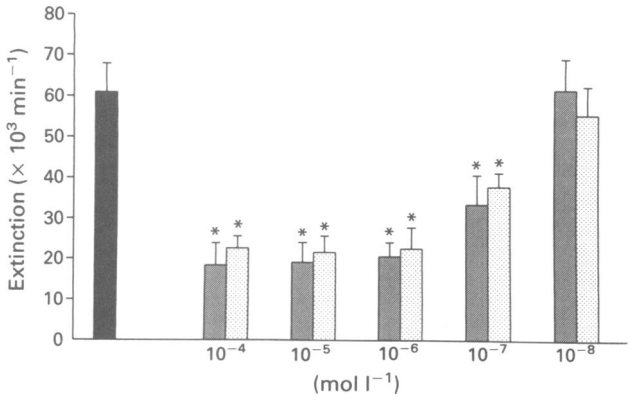

Figure 4 Rate of decrease of extinction of acidified rat platelet solutions 20 s after the beginning of the reaction. Concentration-dependent inhibition by 5-(N-ethyl-*N*-isopropyl) amiloride (hatched columns) and Hoe 694 (stippled columns). Means, s.d., $n = 4$ for each data point. $^*P < 0.05$ vs control.

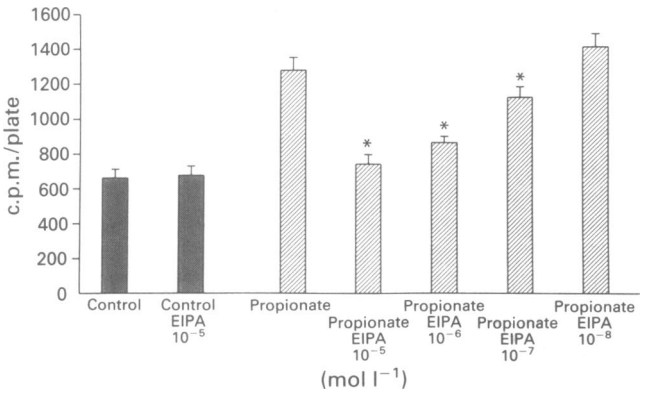

Figure 5 $^{22}Na^+$ influx measured as counts per min per plate (c.p.m./plate) into bovine aortic endothelial cells with and without intracellular acidification by propionate. Concentration-dependent inhibition by 5-(N-ethyl-*N*-isopropyl) amiloride (EIPA). Mean, with s.d., $n = 6$ for each data point. $^*P < 0.05$ vs control.

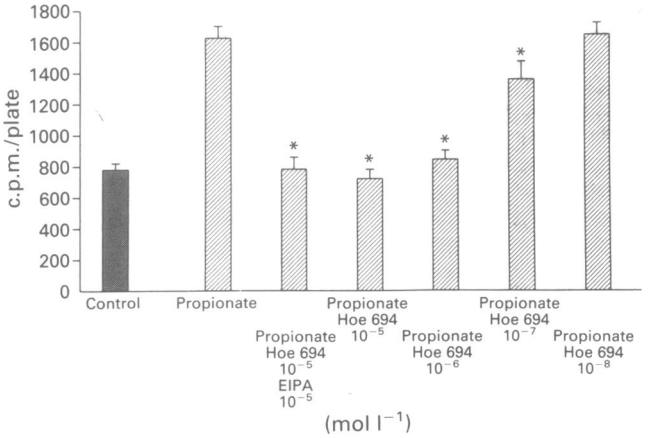

Figure 6 $^{22}Na^+$ influx measured as counts per min per plate (c.p.m./plate) into bovine aortic endothelial cells with and without intracellular acidification by propionate. Concentration-dependent inhibition by Hoe 694. Mean, with s.d., $n = 6$ for each data point. $^*P < 0.05$ vs control.

Rat isolated working heart preparation

To investigate a possible protective role of Hoe 694 under ischaemic conditions rat isolated hearts were subjected to ischaemia and reperfusion. In these experiments all untreated hearts suffered ventricular fibrillation with a mean duration of 15.4 ± 3.2 min (mean ± s.e.mean) during the reperfusion period of 30 min. However, when 10^{-7} M Hoe 694 was added to the perfusion solution, ventricular fibrillation during reperfusion was reduced to 1.3 ± 0.6 min in the working rat hearts (Figure 7).

During ischaemia LV *dP/dt* significantly increased in hearts treated with 10^{-7} M Hoe 694 as compared to control hearts while coronary flow (CF) and heart rate were not affected by the compound (Figure 7).

In addition, the release of LDH, CK and lactate into the venous effluent from the hearts treated with Hoe 694 was markedly reduced during ischaemia (Figure 7).

Analysis of the energy stores of the treated hearts at the end of the experiments showed marked differences in the levels of glycogen, ATP and CP as compared to control hearts. Tissue contents of glycogen, ATP and CP (μM g^{-1} dry wt ± s.d.) were increased from 73.5 ± 3.7, 5.5 ± 0.4 and 4.9 ± 0.3 to 119.3 ± 2.5, 18.4 ± 1.0, and 18.3 ± 0.9, respectively, while lactate (μM g^{-1} dry wt ± s.d.) was decreased from 15.3 ± 1.8 to 10.4 ± 1.2 in Hoe 694-treated hearts as compared to control hearts (Figure 7).

Anaesthetized rats

The effects of Hoe 694 in cardiac ischaemia were investigated under *in vivo* conditions, in which the compound was given intravenously at doses (mg kg^{-1} body wt) of 0.001, 0.01, 0.3, 1.0 or 3.0 to anaesthetized rats 5 min before they underwent coronary artery ligation.

Approximately 5 min after the occlusion of the coronary artery, control animals which received the vehicle only, showed marked ventricular ectopic activity which lasted for about 10 min. All control rats exhibited VPB and 9 out of 10 controls showed VT. In addition 5 out of 10 animals showed VF. However, pretreatment of the animals with Hoe 694 caused a dose-dependent reduction of VPB, VT and VF (Figures 8–10). In particular, VPB were significantly reduced at doses of Hoe 694 ranging from 0.1–3 mg kg^{-1} (Figure 8).

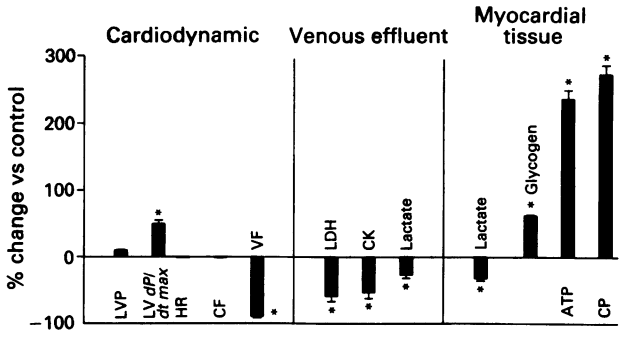

Figure 7 Changes in cardiodynamics, enzyme release and high energy phosphates tissue content in rat isolated working hearts caused by Hoe 694 10^{-7} M. Cardiodynamics: LVP, LV *dP/dt max.*, heart rate (HR) and coronary flow (CF) during ischaemia, ventricular fibrillation (VF) during reperfusion. Venous effluent: release of lactate dehydrogenase (LDH), creatine kinase (CK) and lactate during ischaemia. Myocardial tissue: glycogen, high energy phosphates and lactate after ischaemia and reperfusion. Mean, with s.e.mean, $n = 6$. $^*P < 0.05$ vs control.

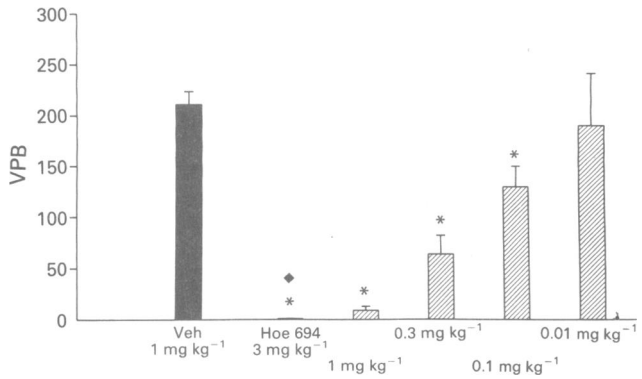

Figure 8 Dose-dependent effect of intravenous Hoe 694 on ventricular premature beats (VPB) in anaesthetized rats during cardiac ischaemia, $n = 10$ for each data point, mean, with s.e.mean. Veh = vehicle. $^*P < 0.05$ vs control for number or duration of arrhythmias; ◆Chi-Square >95% vs control for incidence of arrhythmias.

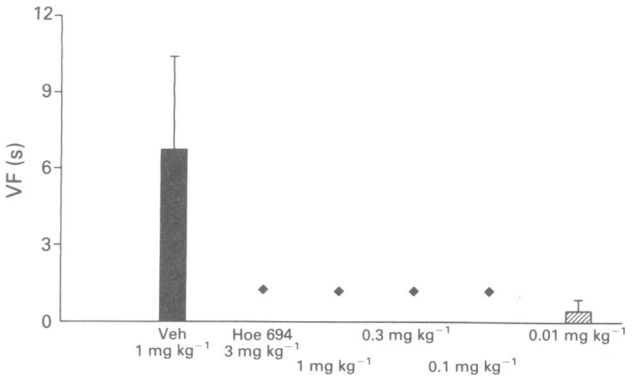

Figure 10 Dose-dependent effect of Hoe 694 on ventricular fibrillation (VF) in anaesthetized rats during cardiac ischaemia, $n = 10$ for each data point, mean, with s.e.mean. Veh = vehicle. $^*P < 0.05$ vs control for number or duration of arrhythmias; ◆ Chi-square >95% vs control for incidence of arrhythmias.

VT was abolished at doses of 1 and 3 mg kg^{-1} (Figure 9) and significantly reduced at 0.1 and 0.3 mg kg^{-1}. VF was completely prevented at doses ranging from 0.1 to 3 mg kg^{-1} Hoe 694 (Figure 10). Incidences (out of 10) of VPB were 10, 10, 8, 6, 3, incidences of VT were 9, 2, 1, 0, 0 and of VF were 1, 0, 0, 0, 0 at doses of Hoe 694 of 0.01, 0.1, 0.3, 1 and 3 mg kg^{-1}. As compared to controls the incidence of VPB was significantly reduced at 3 mg kg^{-1} (Figure 8) and for VT and VF at doses ranging from 0.1 mg kg^{-1} to 3 mg kg^{-1} (Figures 9, 10). The compound was well tolerated by the rats and had no effect on blood pressure or heart rate.

Discussion

In previous experiments using amiloride and EIPA, well characterized inhibitors of Na^+/H^+ exchange (Aickin & Thomas, 1977; Rindler *et al.*, 1979; Vigne *et al.*, 1983), it has been shown that erythrocytes from rabbits fed a high cholesterol diet exhibit enhanced Na^+/H^+ exchange activity (Scholz *et al.*, 1990). In the present study this erythrocyte model was used to investigate possible effects of the benzoyl guanidine compound, Hoe 694, on Na^+/H^+ exchange. Hoe 694 was found to inhibit amiloride-sensitive Na^+ influx into rabbit erythrocytes with an IC_{50} of 0.8×10^{-6} M. When the erythrocytes were exposed to amiloride and Hoe 694 at the same time no additional effect of Hoe 694 on Na^+ influx could be observed. Since particularly the amiloride-sensitive fraction of Na^+ influx was affected by the compound it is likely that Hoe 694 selectively inhibited Na^+ influx via Na^+/H^+ exchange in the erythrocytes.

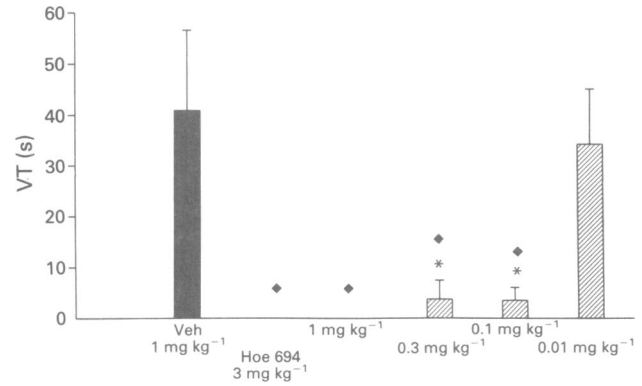

Figure 9 Dose-dependent effect of Hoe 694 on ventricular tachyarrhythmias (VT) in anaesthetized rats during cardiac ischaemia, $n = 10$ for each data point, mean, with s.e.mean. Veh = vehicle. $^*P < 0.05$ vs control for number or duration of arrhythmias; ◆ Chi-square >95% vs control for incidence of arrhythmias.

Some years ago it was found by Livne *et al.* (1987a) that intracellular acidification of platelets led to a pronounced swelling of these blood cells. This effect was caused by an activation of Na^+/H^+ exchange and could be prevented by Na^+/H^+ exchange inhibitors (Livne *et al.*, 1987a). Other investigators had shown that the volume regulatory properties of platelets can be measured photometrically (Fantl, 1968). In recent experiments it was demonstrated that the light transmission of a platelet solution was increased when the acidified platelets were swelling and that the rate of the increase was correlated to Na^+/H^+ exchange activity (Rosskopf *et al.*, 1991). In the present study both EIPA and Hoe 694 inhibited the decrease of extinction which occurs in rat platelet solutions after intracellular acidification with propionate. The IC_{50} was about 10^{-7} M. Although the data do not prove that the effects of Hoe 694 on platelet swelling are definitely due to Na^+/H^+ exchange inhibition, it can be stated that the compound showed the same actions and the same potency as the Na^+/H^+ exchange inhibitor, EIPA, in this experiment.

Furthermore, the effect of Hoe 694 on EIPA-sensitive $^{22}Na^+$ influx was investigated in bovine endothelial cells. While EIPA had no effect under normal conditions, the increase of Na^+ influx caused by acidification was almost totally inhibited by EIPA and by Hoe 694 in concentrations of 10^{-6} M. For both compounds the IC_{50} of this effect was close to 10^{-7} M. These observations suggest a marked activation of Na^+/H^+ exchange in acidified bovine endothelial cells which could be blocked by EIPA or Hoe 694. Since Hoe 694 had no additional effect on $^{22}Na^+$ influx in the presence of EIPA it seems that, as in the erythrocyte experiment, the compound is a specific inhibitor of Na^+ influx by inhibiting Na^+/H^+ exchange.

Altogether these results indicate that Hoe 694 is a potent and specific inhibitor of Na^+/H^+ exchange in different tissues. In addition, the compound has been evaluated in porcine cerebral endothelial cells using the ammonium chloride prepulse technique (Schmid *et al.*, 1991; 1992). In these studies Hoe 694 qualified as Na^+/H^+ exchange inhibitor by preventing pH recovery after intracellular acidification with the same profile and the same potency as EIPA.

In our experiments with rat isolated working hearts Hoe 694 ameliorated cardiac performance and reduced the release of intracellular enzymes during ischaemia indicating a reduction of cell injury and cell death. It also prevented reperfusion arrhythmias and caused a very marked preservation of

cellular energy stores during ischaemia and reperfusion. The tissue levels of high energy phosphates and glycogen in Hoe 694-treated hearts were comparable to those found in non-ischaemic working control hearts of a previous study which was also performed in our lab (Linz *et al.*, 1986; glycogen 114.3 ± 4.3, ATP 16.4 ± 1.6, CP 17.3 ± 2.1 $\mu M\ g^{-1}$ dry weight).

Furthermore, Hoe 694 showed marked antiarrhythmic activity in an animal model of cardiac ischaemia. In a large range of dosages the compound effectively reduced arrhythmias and prevented ventricular fibrillation during ischaemia in coronary artery ligated rats.

We have observed cardioprotective effects of a similar character in previous experiments with amiloride and EIPA (Scholz *et al.*, 1991; 1992) which are considered to be standard inhibitors of Na^+/H^+ exchange. Another investigator (Maron, 1989) has found cardioprotective effects in ischaemic hearts by using the Na^+/H^+ exchange inhibitor methylisobutyl amiloride (MIBA). Altogether these studies seem to indicate that cardioprotection in ischaemia and reperfusion could be a common effect of Na^+/H^+ exchange inhibitors which would suggest that the exchanger plays a crucial role under these conditions.

Several investigators have already proposed that Na^+/H^+ exchange might be important in the pathophysiology of cardic ischaemia (Frelin *et al.*, 1984; 1985; Lazdunski *et al.*, 1985). This assumption was based on the observation of intracellular Na^+ overload that occurs during ischaemia as the consequence of an over-activated Na^+/H^+ exchange. Due to the decreased energy stores in this condition, the Na^+ ions cannot be extruded sufficiently by the ATP-dependent Na^+/K^+ pump. The resulting high concentration of intracellular Na^+ impairs in turn the outward Ca^{2+} transport by Na^+/Ca^{2+} exchange which might even switch to operate in the reversed mode and could cause an additional Ca^{2+} influx (Frelin *et al.*, 1985; Lazdunski *et al.*, 1985; Rabkia, 1989; Lederer *et al.*, 1990; Pierce *et al.*, 1990; Tani & Neely, 1990). Thus, a vicious cycle of intracellular Na^+ and Ca^{2+} overload and a decrease of high energy phosphates could continue during the onset of ischaemia to a point where Na^+/H^+ exchange would be inhibited by extracellular acidification. This inhibition of Na^+/H^+ exchange is to be expected when the decrease of extracellular pH has reached about 6.0 (Frelin *et al.*, 1984; Lazdunski *et al.*, 1985; Wallert & Fröhlich, 1989; Weissenberg *et al.*, 1989), which is supposed to take several minutes (Cobbe & Poole-Wilson, 1980). In the case of reperfusion the extracellular acid would be washed out, which would reactivate Na^+/H^+ exchange and the vicious cycle could start again leading to arrhythmias and cardiac necrosis. From this consideration, an intervention at the step of the Na^+/H^+ exchanger with an inhibitor would retard necrosis of the tissue during ischaemia and reperfusion.

In the present experiments the benzoyl guanidine, Hoe 694, has been characterized as a potent and specific inhibitor of Na^+/H^+ exchange in different tissues. The cardioprotective and antiarrhythmic effects of the substance are probably due to the interference with the exchange system during cardiac ischaemia and reperfusion. It is suggested that the inhibition of Na^+/H^+ exchange might become a new approach in the therapy of cardiac ischaemia.

For technical assistance in the *in vitro* studies we thank Mr Gerald Fischer, Mrs Patricia Petry and Mrs Antje Schlüter. For assistance in the *in vivo* experiments we thank Mr Ottmar Speth.

References

AICKIN, M.G. & THOMAS, R. (1977). An investigation of the ionic mechanism of intracellular pH regulation in mouse soleus muscle fibres. *J. Physiol.*, **273**, 295–311.

ARONSON, P.S. (1985). Kinetic properties of the plasma membrane Na^+/H^+ -exchanger. *Annu. Rev. Phsyiol.*, **47**, 545–560.

COBBE, S.M. & POOLE-WILSON, P.A. (1980). The time of onset and severity of acidosis in myocardial ischaemia. *J. Mol. Cell. Cardiol.*, **12**, 745–760.

FANTL, P. (1968). Osmotic stability of blood platelets. *J. Physiol.*, **198**, 1–16.

FRELIN, C., VIGNE, P. & LAZDUNSKI, M. (1984). The role of Na^+/H^+ exchange system in cardiac cells in relation to the control of the internal Na^+ concentration. *J. Biol. Chem.*, **259**, 8880–8885.

FRELIN, C., VIGNE, P. & LAZDUNSKI, M. (1985). The role of the Na^+/H^+ exchange system in the regulation of the internal pH in cultured cardiac cells. *Eur. J. Biochem*, **149**, 1–4.

FRELIN, C., VIGNE, P. & LAZDUNSKI, M. (1988). The regulation of the intracellular pH in cells from vertebrates. *Eur. J. Biochem.*, **174**, 3–14.

HEINZ, F. & WEISSER, H. (1985). Creatine phosphate. In *Methods of Enzymatic Analysis. Metabolites 3: Lipids, Amino Acids and Related Compounds.* Vol. 8. ed. Bergemeyer, H.U., Bergemeyer, J. & Grassl, M. pp. 507–514. Weinheim, Deerfield Beach, Florida, Basel: Verlag Chemie.

LAZDUNSKI, M., FRELIN, C. & VIGNE, P. (1985). The sodium/hydrogen exchange system in cardiac cells: its biochemical and pharmacological properties and its role in regulating internal concentrations of sodium and internal pH. *J. Mol. Cell. Cardiol.*, **17**, 1029–1042.

LEDERER, W.J., NIGGLI, E. & HADLEY, R.W. (1990). Sodium-calcium exchange in excitable cells. fuzzy space. *Science*, **248**, 283.

LINZ, W., SCHÖLKENS, B.A. & HAN, Y.-F. (1986). Beneficial effects of the converting enzyme inhibitor ramipril in ischaemic rat hearts. *J. Cardiovasc. Pharmacol*, **8** (Suppl. 10), S91–S99.

LIVNE, A., GRINSTEIN, S. & ROTHSTEIN, A. (1987a). Characterization of Na^+/H^+ exchange in platelets. *Thromb. Haemost.*, **58**, 971–977.

LIVNE, A., GRINSTEIN, S. & ROTHSTEIN, A. (1987b). Volume regulating behavior of human platelets. *J. Cell. Physiol.*, **131**, 354–363.

MARON, R. (1989). Functional and metabolic protection by Na^+/H^+ exchange inhibition in global ischaemia (Abstract). *J. Mol. Cell. Cardiol.*, **21**, 1226.

NEELY, J.R., LIEBERMEISTER, H., BATTERSBY, E.J. & MORGAN, H.E. (1967). Effect of pressure development on oxygen consumption by isolated rat heart. *Am. J. Physiol*, **212**, 804–814.

NOLL, F. (1984). (+)-lactate. In *Methods of Enzymatic Analysis. Metabolities 1: Carbohydrates.* Vol. 6 ed. Bergemeyer, H.U., Bergemeyer, J. & Grassl, M. pp. 582–588. Weinheim, Deerfield Beach, Florida, Basel: Verlag Chemie.

PIERCE, G.N., MADDAFORD, T.G., KROEGER, E.A. & CRAGOE, E.J. (1990). Protection by benzamil against dysfunction and damage in rat myocardium after calcium depletion and repletion. *Am. J. Physiol.*, **258**, H17–H23.

RABKIN, S.W. (1989). Comparison of the effect of amiloride and its analogue dichlorobenzamil on cardiac chronotropic responses to ouabain in myocardial cell aggregates in culture. *Pharmacology*, **39**, 230–239.

RASMUSSEN, H.H., CRAGOE, E.J. & TEN EICK, R.E. (1989). Na^+-dependent activation of Na^+-K^+ pump in human myocardium during recovery from acidosis. *Am. J. Physiol.*, **256**, H256–H264.

RINDLER, M.J., TAUB, M. & SAIER, M.H. (1979). Uptake of ^{22}Na by cultured dog kidney cells (MDCK). *J. Biol. Chem.*, **254**, 11431–11439.

ROSSKOPF, D., MORGENSTERN, E., SCHOLZ, W., OSSWALD, U. & SIFFERT, W. (1991). Rapid determination of the elevated Na^+/H^+ exchange in platelets of patients with essential hypertension using an optical swelling assay. *J. Hypertension*, **9**, 231–238.

SCHMID, A., POPP, R., ENGLERT, H.C., LANG, H.J., SCHOLZ, W. & SCHÖLKENS, B.A. (1991). Inhibition of Na^+/H^+ exchange in porcine brain capillary endothelial cells. *Eur. J. Physiol.*, **419** (Suppl. 1), R115 (Abstr.).

SCHMID, A., SCHOLZ, W., LANG, H.J. & POPP, R. (1992). Na^+/H^+ exchange in porcine brain capillary endothelial cells is inhibited by benzoylguanidine derivative. *Biochem. Biophys. Res. Commun.*, **184**, 112–117.

SCHOLZ, W., ALBUS, U., HROPOT, M., KLAUS, E., LINZ, W., SCHÖLKENS, B.A. (1990). Zunahme des Na^+/H^+-Austausches an Kaninchenerythrozyten unter atherogener Diät. In *Arteriosklerose – Neue Aspekte aus Zellbiologie und Molekulargenetik, Epidemiologie und Klinik*. ed. Assmann, G., Betz, E., Heinle, H. & Schulte, H. pp. 296–302. Braunschweig; Wiesbaden: Vieweg.

SCHOLZ, W., ALBUS, U., LINZ, W., MARTORANA, P., LANG, H.J. & SCHÖLKENS, B.A. (1992). Effects of Na^+/H^+ exchange inhibitors in cardiac ischaemia. *J. Mol. Cell. Cardiol.*, **24**, 731–740.

SCHOLZ, W., ALBUS, U., LINZ, W. & SCHÖLKENS, B.A. (1991). Effect of Na^+/H^+ exchange inhibition in cardiac ischaemia. *Eur. Heart J.*, **12** (Suppl.), 124 (Abstr.).

SCHÖMIG, A., KURZ, T., RICHARDT, G. & SCHÖMIG, E. (1988). Neuronal sodium homoeostasis and axoplasmic amine concentration determine calcium-independent noradrenaline release in normoxic and ischaemic rat heart. *Circ. Res.*, **63**, 214–226.

TANI, M. & NEELY, J.R. (1990). Na^+ accumulation increases Ca^+ overload and impairs function in anoxic rat heart. *J. Mol. Cell. Cardiol.*, **22**, 57–72.

TRAUTSCHOLD, I., LAMPRECHT, W. & SCHWEITZER, G. (1985). Adenosine-5'-triphosphate. UV method with hexokinase and glycose-6-phosphate dehydrogenase. In *Methods of Enzymatic Analysis. Metabolites 2: Tri- and Dicarboxylic Acids, Purines Pyrimidines and Derivatives, Coenzymes, Inorganic Compounds*. Vol. 7. ed. Bergemeyer, H.U., Bergemyer, J., Grassl, M. pp. 346–357. Weinheim, Deerfield Beach, Florida, Basel: Verlag Chemie.

VIGNE, P., FRELIN, C., CRAGOE, E.J. & LAZDUNSKI, M. (1983). Ethyliospropylamiloride: a new and highly potent derivative of amiloride for the inhibition of the Na^+/H^+ exchange system in various cells types. *Biochem. Biophys. Res. Commun*, **116**, 86–90.

WALKER, M.J.A., CURTIS, M.J., HEARSE, D.J., CAMPBELL, R.W.F., JANSE, M.J., YELLON, D.M., COBBE, S.M., COKERS, S.J., HARNESS, J.B., HARRON, D.W.G., HIGGINS, S.J., JULIAN, D.G., LAB, M.J., MANNING, A.S., NORTHOVER, B.J., PARRATT, J.R., RIEMERSMA, R.A., RIVA, E., RUSSELL, D.G., SHERIDAN, D.J., WINSLOW, E. & WOODWARD, B. (1988). The Lambeth convention: Guidelines for the study of arrhythmias in ischaemia, infarction and reperfusion. *Cardiovasc. Res.*, **22**, 447–455.

WALLERT, M.A. & FRÖHLICH, O. (1989). Na^+/H^+ exchange in isolated myocytes from adult rat heart. *Am. J. Physiol.*, **257**, C207–C213.

WEISSENBERG, P.L., LITTLE, P.J., CRAGOE, E.J. & BOBIK, A. (1989). The pH of spontaneously beating cultured rat heart cells is regulated by an ATP-calmodulin-dependent Na^+/H^+ antiport. *Circ. Res.*, **64**, 676–685.

(Received January 26, 1993
Accepted February 18, 1993)

Br. J. Pharmacol. (1993), **109**, 569–576 © Macmillan Press Ltd, 1993

Renal tubular dopamine outward transfer during Na^+-H^+ exchange activation by α_1- and α_2-adrenoceptor agonists

P. Soares-da-Silva

Department of Pharmacology and Therapeutics, Faculty of Medicine, 4200 Porto, Portugal

1 The present work describes the effects of inhibitors (amiloride and ethylisopropylamiloride) and activators (quinoxaline and phenylephrine) of the Na^+-H^+ exchanger on the outflow of dopamine in rat kidney slices loaded with L-dihydroxyphenylalanine (L-DOPA).

2 Incubation of kidney slices loaded with 50 μM L-DOPA in the presence of increasing concentrations of amiloride or ethylisopropylamiloride (EIPA) resulted in a concentration-dependent decrease in the outflow of newly-formed dopamine; the IC_{50} value for EIPA was 5.6 ± 0.3 μM. Phenylephrine and quinoxaline were found to produce a concentration-dependent increase in the outflow of newly-formed dopamine; the EC_{50} values for the phenylephrine and quinoxaline were, respectively, 0.9 ± 0.1 and 0.08 ± 0.01 μM.

3 The facilitatory effect of phenylephrine on the outflow of dopamine was found not to be affected by yohimbine (100 nM), but was abolished by prazosin (1 μM), whereas that of quinoxaline was found to be selectively antagonized by yohimbine (100 nM), but not by prazosin (1 μM); EIPA (10 μM) was also found to abolish the effect of both phenylephrine and quinoxaline. The facilitatory effect of quinoxaline was also found to be reduced by 42–48% and 56–78% by, dibutyryl adenosine cyclic 3',5'-monophosphate (dibutyryl cyclic AMP; 250 μM) and forskolin (10 μM), respectively, but not by the protein kinase C (PKC) inhibitor, (+)-sphingosine (10 μM). In contrast, (+)-sphingosine (10 μM) was found to antagonize markedly (43– 69% reduction) the facilitatory effect of phenylephrine; dibutyryl cyclic AMP (250 μM) and forskolin (10 μM) were also found to reduce significantly the facilitatory effect of phenylephrine, by 42–53% and 44–59% respectively.

4 A synergistic effect between α_1- and α_2-adrenoceptors was observed for submaximal concentrations of quinoxaline (50 nM) and phenylephrine or submaximal concentrations of phenylephrine (0.5 μM) and quinoxaline, but not for maximal effective concentrations of either agonist. Dibutyryl cyclic AMP (250 μM) or forskolin (10 μM) produced a marked decrease (35–85% reduction) of the synergistic effect between phenylephrine and quinoxaline. The addition of phorbol 12,13-dibutyrate (PDBu; 500 nM) was found not to alter the outflow of newly-formed dopamine, but did potentiate (18–42% increase) the facilitatory effect of quinoxaline on the amine outflow. This effect was found to occur for submaximal concentrations of quinoxaline (10, 50 and 100 nM) and found to be antagonized by (+)-sphingosine (10 μM). In contrast, PDBu (500 nM) was found not to potentiate the facilitatory effect of phenylephrine on dopamine outflow.

5 In conclusion, inhibition of the Na^+-H^+ antiport by amiloride and EIPA results in considerable reduction in the outflow of newly-formed dopamine, whereas the activation of this mechanism by both phenylephrine and quinoxaline results in facilitation of the outflow of dopamine; this effect is selectively reversed by α_1- and α_2-adrenoceptor antagonists and EIPA. The synergistic effect between quinoxaline and phenylephrine may be related to an amplification of a reaction at a given point in the post-receptor transducing pathway.

Keywords: Dopamine; kidney, α-adrenoceptors; ethylisopropylamiloride; phorbol 12,13-dibutyrate; (+)-sphingosine; dibutyryl cyclic AMP; forskolin

Introduction

In kidney, the activation of type D_1 dopamine receptors located in tubular epithelial cells produces an increased natriuresis, mainly as a result of a decreased tubular reabsorption of Na^+ (Hedge *et al.*, 1989; Jose *et al.*, 1992). There is evidence to suggest that the dopamine responsible for this natriuretic effect is of renal origin (Jose *et al.*, 1986; Siragy *et al.*, 1989). In fact, tubular epithelial cells, namely those of proximal convoluted tubules, are endowed with a high aromatic L-amino acid decarboxylase (AAAD) activity and circulating dihydroxyphenylalanine (DOPA) is converted to dopamine after being taken up into this cellular compartment (Hayashi *et al.*, 1990; Seri *et al.*, 1990; Soares-da-Silva & Fernandes, 1990a). The fact that in the kidney dopamine is produced in close proximity to renal cells which contain D_1 receptors introduces the possibility that the amine may act in a cell-to-cell manner, as a paracrine or autocrine substance (Carey *et al.*, 1990). On the other hand, the vectorial transport of Na^+ has been demonstrated to play a determining role in the renal formation of dopamine by tubular epithelial cells (Soares-de-Silva & Fernandes, 1990b). Recently, we have reported in human and rat kidney slices that the production of dopamine is not only closely dependent on the extracellular sodium, but also related to the transtubular reabsorption of sodium (Soares-da-Silva & Fernandes, 1992a; Soares-de-Silva *et al.*, 1992) and on the integrity of the tubular cytoskeleton and the functional integrity of the Na^+-K^+-ATPase (Soares-da-Silva, 1992a). In good agreement with these results is also the finding that the α-human atrial natriuretic peptide and the guanosine cyclic 3',5'-monophosphate (cyclic GMP), effective inhibitors of the tubular transport of sodium (Harris *et al.*, 1987; Garvin, 1989), were also found to decrease the intracellular availability of L-DOPA in rat kidney slices and reduce the renal formation of dopamine (Soares-da-Silva & Fernandes, 1991; 1992b).

More recently, while studying the role of the Na^+-H^+ exchanger in the renal formation of dopamine we have found the inhibition of this system by 5-(N-ethyl-*N*-isopropyl)-amiloride (EIPA) results in an increased accumulation of newly-formed dopamine in rat kidney slices; however, this effect was not related to an increased formation of dopamine from L-DOPA, but dependent on a reduced ability of the dopamine to leave the cell (Soares-da-Silva *et al.*, 1993). The flux of Na^+ across tubular epithelial cells is largely dependent on Na^+-K^+ ATPase activity (Katz, 1987), whereas the Na^+-H^+ exchanger has a major role in the transport of Na^+ into these cells (Aronson, 1983; Pouyssegur *et al.*, 1987). Several studies have clearly demonstrated the presence of a Na^+-H^+ exchanger on the luminal membrane of proximal tubular cells (Kinsella & Aronson, 1980; Nord *et al.*, 1986; Preisig & Rector, 1988). This luminal Na^+-H^+ exchanger is thought to be responsible for the bulk of active Na^+ reabsorption in the proximal nephron, as well as functioning in the reabsorption of HCO^-_3 and secretion of H^+ (Mahnensmith & Aronson, 1985). Recent studies performed in the proximal nephron indicate that the Na^+-H^+ exchanger has also a crucial role in the regulation of cell volume and intracellular pH; changes in intracellular pH may, on the other hand, serve as a signal for generating a biological response (Mahnensmith & Aronson, 1985; Gesek & Schoolwerth, 1989).

The aim of the present work was to evaluate the role of the Na^+-H^+ exchanger on the renal outward transport of dopamine; the results described here are on the effects of inhibitors (amiloride and EIPA; Vigne *et al.*, 1984) and activators (quinoxaline and phenylephrine; Nord *et al.*, 1987; Gesek & Schoolwerth, 1989; Gesek *et al.*, 1989) of the Na^+-H^+ exchanger on the outflow of dopamine in rat kidney slices loaded with L-DOPA. A preliminary account of some these findings has been presented previously (Soares-da-Silva, 1992b).

Methods

The experimental protocol used was similar to that reported in the accompanying study (Soares-da-Silva, 1993). In brief, after preincubation, renal slices were incubated for 15 min in Krebs solution with added L-DOPA; both the preincubation and incubation were carried out in glass test tubes, continuously shaken throughout the experiment. After the incubation, renal slices were collected with fine forceps and immediately placed in 2 ml of 0.2 M perchloric acid at 4°C for the next 24 h. In order to allow the determination of the amount of dopamine which has leaked into the incubation medium, 250 µl of 2.0 M perchloric acid was added to the incubation medium after renal tissues had been collected; the samples of the incubation medium were also kept at 4°C for the next 24 h, until quantification of dopamine.

In experiments in which the importance of the Na^+-H^+ exchanger in the control of dopamine outflow was studied, kidney slices were incubated with 50 µM L-DOPA for 15 min; the compounds to be tested were present both during the preincubation and incubation periods. To test the effects of phorbol 12,13-dibutyrate (PDBu) and (+)-sphingosine, the activator and inhibitor of protein kinase C (PKC) respectively, on the outflow of dopamine, kidney slices were loaded with L-DOPA (50 µM) in the presence of these compounds or their respective vehicles [PDBu was dissolved in dimethylsulphoxide (final concentration $<0.01\%$) and (+)-sphingosine in ethanol (final concentration $<0.1\%$)]. In this set of experiments, the amount of newly-formed dopamine accumulated in the tissue and that present in the incubation medium was determined as described above.

The assay of dopamine in kidney slices and the incubation medium was performed by means of high performance liquid chromatography (h.p.l.c.) with electrochemical detection, as described in the accompaining work (Soares-da-Silva, 1993).

Statistics

Mean values ± s.e.mean of n experiments are given. Significance of differences between one control and several experimental groups was evaluated by Tukey-Kramer methods (Sokal & Rolhf, 1981). A P value less than 0.05 was assumed to denote a significant difference.

Drugs

Amiloride, L-dihydroxyphenylalanine (L-DOPA), dibutyryl adenosine 3',5'-cyclic monophosphate, dimethylsulphoxide, dopamine hydrochloride, HEPES (4-(2-hydroxyethyl)-1-piperazenethanesulphonic acid), (−)-α-methyl-*P*-tyrosine, pargyline hydrochloride, phenylephrine hydrochloride, phorbol 12,13-dibutyrate, (+)-sphingosine, tropolone hydrochloride and yohimbine hydrochloride were purchased from Sigma Chemical Company (St. Louise, Mo, U.S.A.). 5-(N-ethyl-*N*-isopropyl)amiloride was kindly donated by Dr E. Schömig (Department of Pharmacology, University of Wurzburg, Germany). Quinoxaline (U.K. 14,304; 5-bromo-6 [2-imidazoline-2-yl amino]) and prazosin were kindly donated by the producer (Pfizer, Sandwich, Kent, England).

Results

Incubation of kidney slices loaded with 50 µM L-DOPA in the presence of increasing concentrations of amiloride or EIPA (0.1 to 100 µM), two well known Na^+-H^+ exchanger inhibitors, resulted in a concentration-dependent decrease in the outflow of newly-formed dopamine. As shown in Figure 1, this effect was significantly more marked for EIPA than for amiloride; the IC_{50} value for EIPA was 5.6 ± 0.3 µM. By contrast, phenylephrine and quinoxaline, selective α_1- and α_2-adrenoceptor agonists, respectively, and both known to activate the renal Na^+-H^+ exchanger, were found to produce

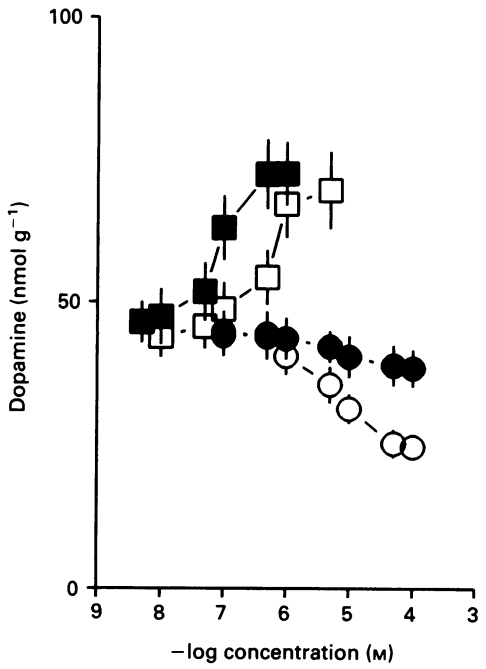

Figure 1 Effect of increasing concentrations of quinoxaline (■), phenylephrine (□), amiloride (●) and ethylisopropylamiloride (○) on the outflow of newly-formed dopamine in rat renal cortical slices previously loaded with 50 µM L-DOPA. The levels of dopamine accumulated in the tissue slice and the total amount formed are given in Table 1. Each point represents the mean with s.e.mean of four to five experiments per group.

a concentration-dependent increase in the outflow of newly-formed dopamine; the EC_{50} values for phenylephrine and quinoxaline were, respectively, 0.9 ± 0.1 and 0.08 ± 0.01 μM.

The increasing effect of phenylephrine on the outflow or dopamine was found not to be affected by yohimbine (100 nM), but abolished by prazosin (1 μM) and EIPA (10 μM) (Figure 2). The facilitatory effect of quinoxaline on the outflow of newly-formed dopamine was found to be selectively antagonized by yohimbine (100 nM), but not by prazosin (1 μM); EIPA (10 μM) was also found to abolish the effect of quinoxaline (Figure 3).

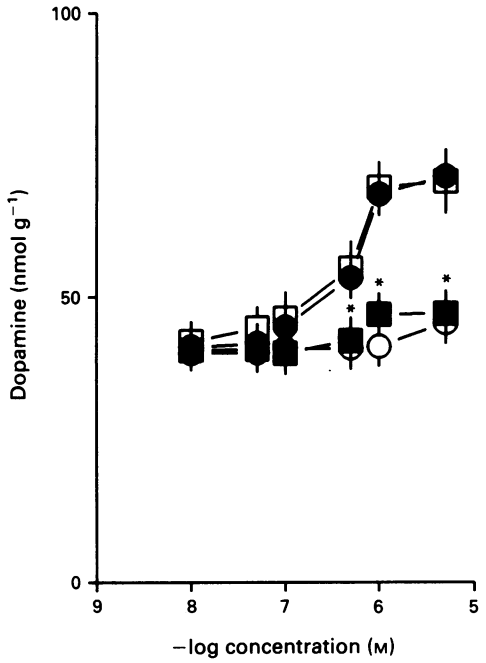

Figure 2 Effect of yohimbine (100 nM; ●), ethylisopropylamiloride (10 μM; ○) and prazosin (1 μM; ■) on the facilitatory effect of phenylephrine (□) on the outflow of newly-formed dopamine in rat renal cortical slices previously loaded with 50 μM L-DOPA. Each point represents the mean with s.e.mean of four to give experiments per group. *Significantly different from corresponding values for phenylephrine alone ($P<0.01$).

The activation of α_1-adrenoceptors in tubular epithelial cells results in stimulation of the enzyme phospholipase C with the subsequent increase in the formation of inositol trisphosphate (IP_3) and diacylglycerol (DAG); synthetic DAGs and phorbol esters, through stimulation of PKC, have been demonstrated to increase Na^+-H^+ exchanger activity (Burns & Rozengurt, 1983; Moolenaar *et al.*, 1984). The stimulation of renal tubular α_2-adrenoceptors, on the other hand, has been found to decrease intracellular levels of adenosine 3',5'-cyclic monophosphate (cyclic AMP) as a result of inhibition of adenylate cyclase (Pettinger *et al.*, 1987). As shown in Figure 4, the facilitatory effect of quinoxaline on the outflow of newly-formed dopamine was found to be reduced by 42–48% and 56–78%, respectively, by dibutyryl cyclic AMP (250 μM) and forskolin (10 μM); the PKC inhibitor, (+)-sphingosine (10 μM), did not affect the facilitatory effect of quinoxaline (Figure 4). In contrast, (+)-sphingosine (10 μM) was found to antagonise markedly (43–69% reduction) the facilitatory effect of phenylephrine on the outflow of newly-formed dopamine (Figure 5); however, quite unexpectedly dibutyryl cyclic AMP (250 μM) and forskolin (10 μM) were also found to reduce significantly the effect of phenylephrine, by 42–53% and 44–59% respectively (Figure 5).

Submaximal concentrations of quinoxaline (50 nM) were found to potentiate the facilitatory effect of phenylephrine on the outflow of dopamine; this potentiation was found to occur for submaximal concentrations of phenylephrine (0.05, 0.1 and 0.5) and found to be antagonized by 100 nM yohimbine (Figure 6). The addition of dibutyryl cyclic AMP (250 μM) or forskolin (10 μM) markedly decreased (35–85% reduction) the facilitatory effect of phenylephrine plus submaximal concentrations of quinoxaline (50 nM) on the

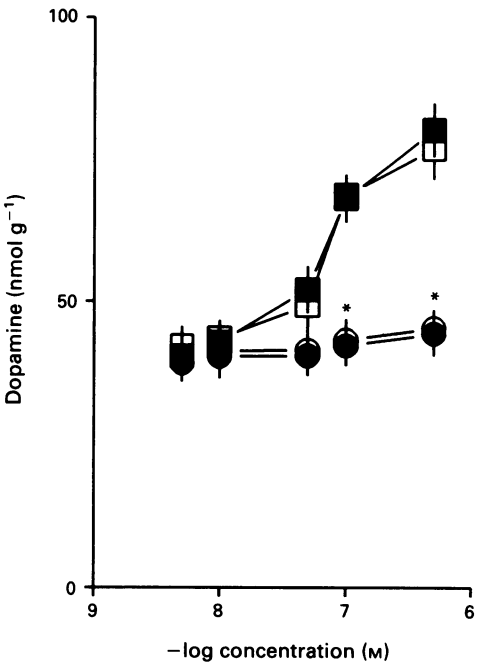

Figure 3 Effect of yohimbine (100 nM; ●), ethylisopropylamiloride (10 μM; ○) and prazosin (1 μM; □) on the facilitatory effect of quinoxaline (■) on the outflow of newly-formed dopamine in rat renal cortical slices previously loaded with 50 μM L-DOPA. Each point represents the mean with s.e.mean of four to five experiments per group. *Significantly different from correponding values for quinoxaline alone ($P<0.01$).

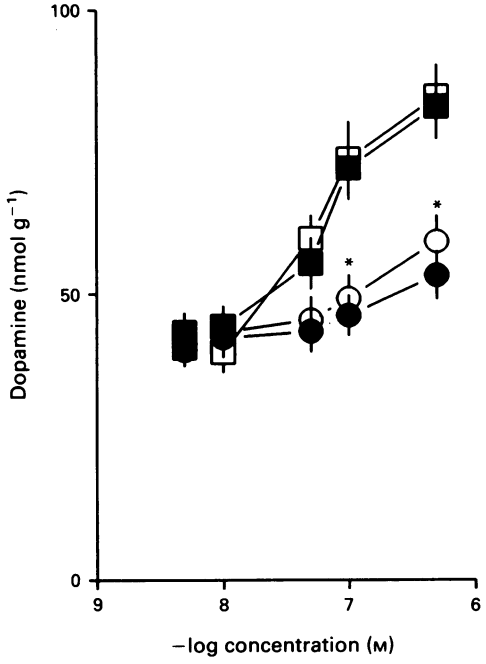

Figure 4 Effect of dibutyryl adenosine 3',5'-cyclic monophosphate (250 μM; ○), forskolin (10 μM; ●) and (+)-sphingosine (10 μM; □) on the facilitatory effect of quinoxaline (■) on the outflow of newly-formed dopamine in rat renal cortical slices previously loaded with 50 μM L-DOPA. Each point represents the mean with s.e.mean of four to five experiments per group. *Significantly different from corresponding values for quinoxaline along ($P<0.01$).

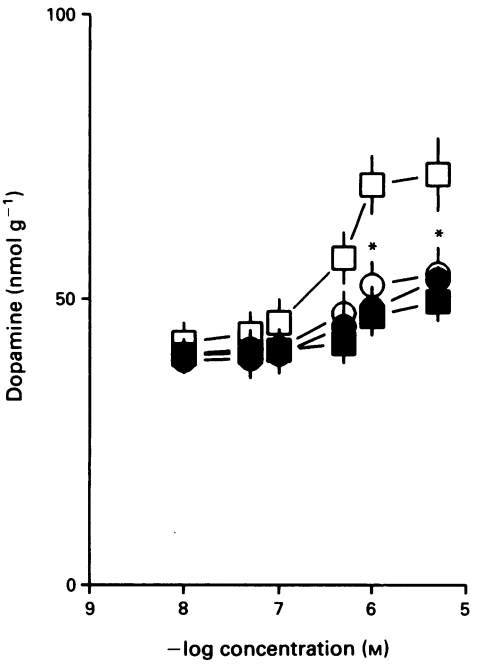

Figure 5 Effect of dibutyryl adenosine 3',5'-cyclic monophosphate (250 μM; ○), forskolin (10 μM; ●) and (+)-sphingosine (10 μM, ■) on the facilitatory effect of phenylephrine (□) on the outflow of newly-formed dopamine in rat renal cortical slices previously loaded with 50 μM L-DOPA. Each point represents the mean with s.e.mean of four to five experiments per group. *Significantly different from corresponding values for phenylephrine alone ($P<0.01$).

outflow of dopamine (Figure 6). Similarly, submaximal concentrations of phenylephrine (0.5 μM) were found to potentiate the facilitatory effect of quinoxaline on the outflow of dopamine (Figure 7). Again, this potentiation was only found to occur for submaximal concentrations of quinoxaline (10, 50 and 100 nM) and found to be antagonized by 1.0 μM prazosin (Figure 7). As described for phenylephrine, dibutyryl cyclic AMP (250 μM) or forskolin (10 μM) were also found to antagonize the facilitatory effect of quinoxaline plus submaximal concentrations of phenylephrine (0.5 μM) on the outflow of dopamine (Figure 7).

The addition of PDBu (500 nM), a PKC activator, was found not to alter the outflow of newly-formed dopamine in kidney slices loaded with 50 μM L-DOPA (data not shown); however, PDBu (500 nM) did potentiate the facilitatory effect of quinoxaline on the amine outflow. This effect was found to occur for submaximal concentrations of quinoxaline (10, 50 and 100 nM) and found to be antagonized by (+)-sphingosine (10 μM) (Figure 8). In contrast, PDBu (500 nM) was found not to potentiate the facilitatory effect of phenylephrine on the outflow of dopamine (Figure 9).

The total amount of L-DOPA decarboxylated into dopamine was found to be neither affected by amiloride and EIPA nor by the α_1- and α_2-adrenoceptor agonists and antagonists, PDBu and (+)-sphingosine (Table 1).

Discussion

The outward transfer of dopamine in renal tissues has been demonstrated to involve the activation of a carrier-mediated process and follow a Michaelis-Menten kinetics (Soares-de-Silva, 1993). This appears to be an important mechanism for the outward transfer of dopamine in tubular epithelial cells and the results reported here suggest that the

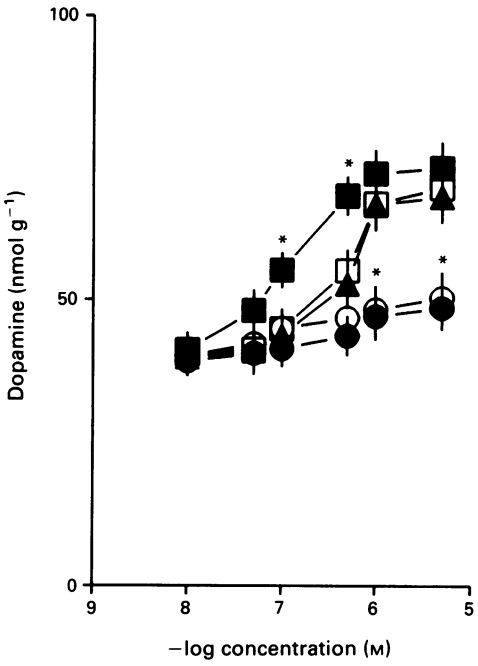

Figure 6 Potentiation of the facilitatory effect of phenylephrine (□) on the outflow of newly-formed dopamine in rat renal cortical slices previously loaded with 50 μM L-DOPA by submaximal concentrations of quinoxaline (50 nM; ■) and its reversability by yohimbine (100 nM; ▲). The potentiation of the facilitatory effect of phenylephrine by submaximal concentrations of quinoxaline (50 nM) was also abolished by dibutyryl adenosine 3',5'-cyclic monophosphate (250 μM; ○), forskolin (10 μM; ●). Each point represents the mean with s.e.mean of four to five experiments per group. *Significantly different from corresponding values for phenylephrine alone ($P<0.01$).

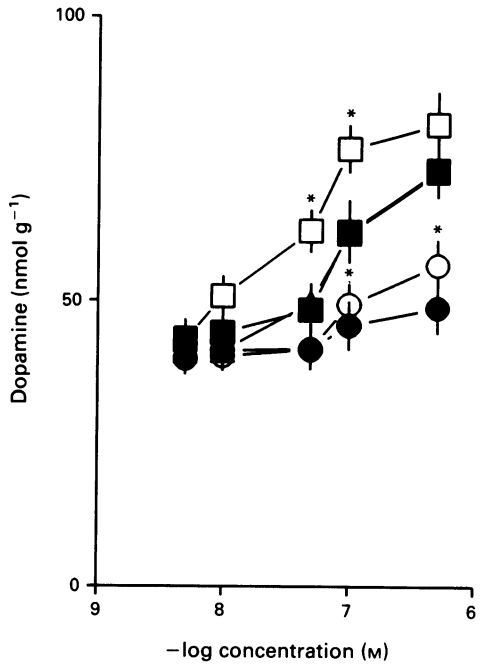

Figure 7 Potentiation of the facilitatory effect of quinoxaline (■) on the outflow of newly-formed dopamine in rat renal cortical slices previously loaded with 50 μM L-DOPA by submaximal concentrations of phenylephrine (0.5 μM; □) and its reversability by prazosin (1 μM; △). The potentiation of the facilitatory effect of quinoxaline by submaximal concentrations of phenylephrine (0.5 μM) was also abolished by dibutyryl adenosine 3',5'-cyclic monophosphate (250 μM; ○), forskolin (10 μM; ●). Each point represents the mean with s.e.mean of four to five experiments per group. *Significantly different from corresponding values for quinoxaline alone ($P<0.01$).

outward transport of the amine in kidney slices loaded with L-DOPA is sensitive to α_1- and α_2-adrenoceptor activation and probably involves changes in the activity of the Na^+-H^+ exchanger.

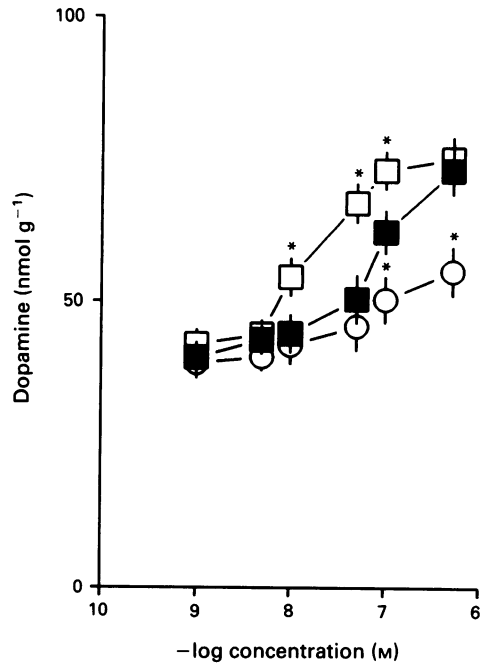

Figure 8 Potentiation of the facilitatory effect of quinoxaline (■) on the outflow of newly-formed dopamine in rat renal cortical slices previously loaded with 50 μM L-DOPA by ineffective concentrations of phorbol 12,13-dibutyrate (500 nM; □) and its reversability by (+)-sphingosine (10 μM; ○). Each point represents the mean with s.e.mean of four to five experiments per group. *Significantly different from corresponding values for quinoxaline alone ($P<0.01$).

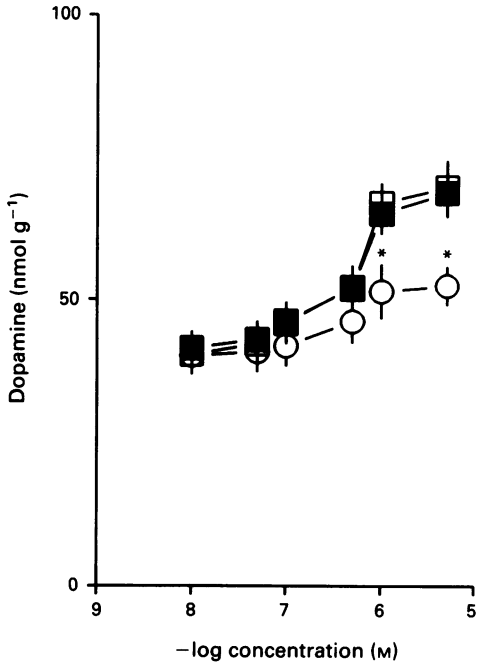

Figure 9 Effect of phenylephrine (□), phenylephrine plus 500 nM phorbol 12,13-dibutyrate (■) and phenylephrine plus 500 nM phorbol 12,13-dibutyrate plus 10 μM (+)-sphingosine (○) on the outflow of newly-formed dopamine in rat renal cortical slices previously loaded with 50 μM L-DOPA. Each point represents the mean with s.e.mean of four to five experiments per group. *Significantly different from corresponding values for phenylephrine alone ($P<0.01$).

Table 1 Levels (in nmol g^{-1}) of dopamine (DA) accumulated in slices of renal cortex and the total amount of amine formed during incubation with 50 μM L-dihydroxyphenylalanine (L-DOPA)

Treatment	*Accumulated DA*	*Total DA*	n
Control	37.9 ± 1.2	88.2 ± 5.6	26
Quinoxaline (500 nM)	17.5 ± 2.1	91.4 ± 7.9	22
Phenylephrine (5 μM)	19.2 ± 1.5	85.3 ± 9.5	24
Amiloride (100 μM)	48.7 ± 5.1	86.4 ± 7.5	5
EIPA (100 μM)	63.7 ± 5.4	87.9 ± 9.4	5
PDBu (500 nM)	36.9 ± 4.2	88.6 ± 9.4	5
(+)-Sphingosine (10 μM)	38.6 ± 4.1	90.4 ± 7.3	5

Values are means ± s.e.mean of *n* experiments.

Evidence for the involvement of the Na^+-H^+ antiport in the regulation of the outward transport of newly-formed dopamine is, however, circumstantial and stands mainly on the fact that amiloride and EIPA are well-known inhibitors of the Na^+-H^+ antiport, EIPA being far more potent than amiloride (Vigne *et al.*, 1984). This and the finding that EIPA was more potent than amiloride in reducing the outflow of dopamine strongly suggests that inhibition of the Na^+-H^+ antiport affects the cell outward transport of dopamine. Another result which supports this suggestion is that the activation of Na^+-H^+ antiport by the by α_1- and α_2-adrenoceptor agonists facilitates the cell outward transfer of dopamine and this effect is antagonized by EIPA. This compares favourably with the evidence that 10 μM EIPA was found to abolish the alkalinization of the cytoplasm observed by activation of α_1- and α_2-adrenoceptors in rat proximal tubular segments (Gesek & Schoolwerth, 1989). It should be mentioned that EIPA has been chosen because it has been demonstrated to be relatively specific for the inhibition of the proximal luminal Na^+-H^+ exchanger without significantly interfering with the binding of α-adrenoceptors (Nord *et al.*, 1987). An argument which favours the view that the effects of both phenylephrine and quinoxaline are mediated through the activation of, α_1- and α_2-adrenoceptors respectively, is that on the selective antagonism of their effects. In fact, the facilitatory effect of quinoxaline was reversed by yohimbine (100 nM), but not by prazosin (1 μM), whereas the effect of phenylephrine was found to be reversed by prazosin (1 μM), but not by yohimbine (100 nM).

Other results which favour the view that the regulation of the cell outward transfer of dopamine by α_1- and α_2-adrenoceptors are independent receptor-mediated events are those obtained by dibutyryl cyclic AMP, forskolin and (+)-sphingosine. The antinatriuretic action resulting from the stimulation of renal tubular α_2-adrenoceptors is believed to be dependent on the activation of the Na^+-H^+ exchanger (Insel *et al.*, 1985; Nord *et al.*, 1987; Gesek *et al.*, 1989) and would involve inhibition of the enzyme adenylate cyclase (Pettinger *et al.*, 1987); on the other hand, dibutyryl cyclic AMP has been demonstrated to inhibit Na^+-H^+ exchanger activity (Kahn *et al.*, 1985; Weinman *et al.*, 1987). The results presented here show that the facilitatory effect of quinoxaline can, in fact, be reversed by dibutyryl cyclic AMP and forskolin, an activator of the enzyme adenylate cyclase, but not by (+)-sphingosine, the PKC inhibitor. The activation of α_1-adrenoceptors in tubular epithelial cells has been demonstrated to increase Na^+-H^+ exchanger activity (Gesek & Schoolwerth, 1989); there are reasons to believe this effect is related to the stimulation of phospholipase C with the subsequent increase in the formation of DAG (Burns & Rozengurt, 1983; Moolenaar *et al.*, 1984). The results presented here are in line with this evidence; in fact, the facilitatory effect of phenylephrine was found to be antagonized by (+)-spingosine, the PKC inhibitor. However, dibutyryl cyclic AMP and forskolin were also found to inhibit partially the

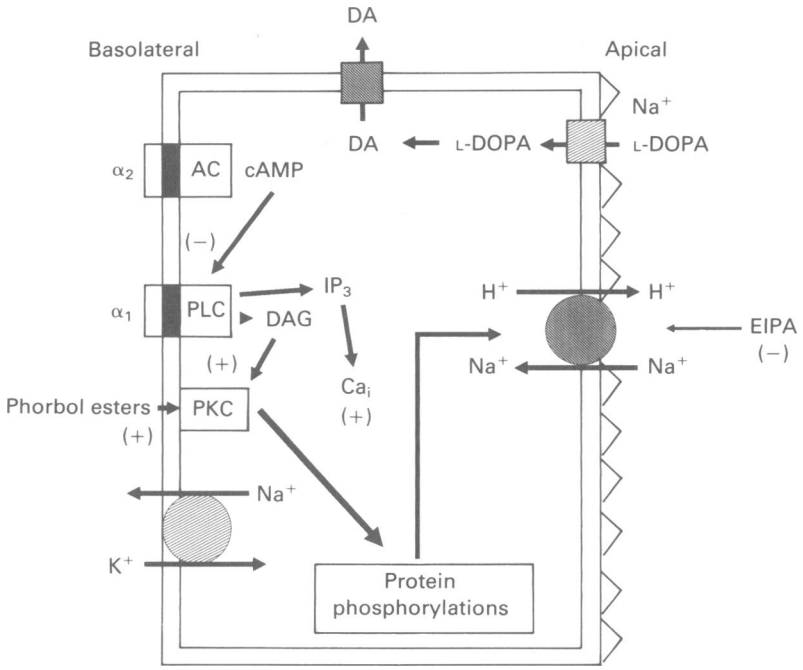

Figure 10 Schematic representation of the proposed mechanisms involved in the modulation of the dopamine outward transport in tubular epithelial cells during activation of the Na^+-H^+ exhanger by α_1 and α_2-adrenoceptor agonists. Stimulation of α_1-adrenoceptors increases phospholipase C (PLC) activity resulting in enhanced formation of inositol 1,4,5-trisphosphate (IP_3) and diacylglycerol (DAG), leading to intracellular calcium (Ca_i) mobilization and activation of protein kinase C (PKC). Stimulation of α_2-adrenoceptors through activation of inhibitory guanine nucleotide protein results in inhibition of adenylate cyclase (AC) and decreased cellular formation of adenosine 3'5'-cyclic monophosphate (cAMP); this would lead to an increased breakdown of phosphoinositides and production of DAG as a result of the removal of the inhibitory influence of cyclic AMP upon PLC and ultimately would explain the synergistic effect between α_1- and α_2-adrenoceptor agonists. Increases in PKC activity lead to protein phosphorylations, that together with mobilized calcium, can influence Na^+-H^+ exchange. The tubular uptake of L-DOPA is a sodium-dependent mechanism; once inside the cell, L-DOPA is decarboxylated into dopamine (DA) which is then transported into the extracellular medium. Activation of the Na^+-H^+ exchanger enhances the outward transport of DA, whereas inhibition of this system by ethylisopropylamiloride (EIPA) has the opposite effect; this would suggest that changes in intracellular pH may be important in the regulation of the outward transport system of renal DA. Inhibitory effects, (−); stimulatory effects, (+).

facilitatory effect of phenylephrine. This result might suggest the presence of a cooperative mechanism between the transducing pathways activated during stimulation of α_1- and α_2-adrenoceptors. A synergistic action between α_1- and α_2-adrenoceptors has been reported before, namely on the activation of the rat proximal nephron Na^+-H^+ exchanger (Gesek *et al.*, 1989; Gesek & Schoolwerth, 1990). The present study also reports on a synergistic facilitatory effect between phenylephrine and quinoxaline on the outflow of newly-formed dopamine.

The synergistic effect between α_1- and α_2-adrenoceptors was observed for submaximal concentrations of both agonists, but not for maximal effective concentrations of either agonist. This might suggest the involvement of an amplification effect in the post-receptor transducing pathway. Two sets of arguments support this suggestion. Firstly, the synergistic effects observed for submaximal concentrations of both quinoxaline and phenylephrine were antagonized by selective antagonists. Secondly, dibutyryl cyclic AMP and forskolin were found to produce a marked decrease in the potentiation of the facilitatory effect of quinoxaline by submaximal concentrations of phenylephrine or the potentiation of the facilitatory effect of phenylephrine by submaximal concentrations of quinoxaline. Thirdly, the potentiation of the facilitatory effect of quinoxaline, but not that of phenylephrine, by PDBu (500 nM) and its reversal by the PKC inhibitor, (+)-sphingosine (10 μM), further suggests that the synergistic effect between quinoxaline and phenylephrine may involve an amplification of a reaction at a given point in the post-receptor transducing pathway. The site of interaction cannot be deduced from the data obtained in this study, however, there is evidence in the literature suggesting that the synergistic action between α_1- and α_2-adrenoceptors might be related to a facilitation by α_2-adrenoceptors in the activation of the transducing pathway activated by α_1 adrenoceptors. Baines & Ho (1988) have reported that the simultaneous activation of both types of adrenoceptors results in an increased accumulation of DAG in tubular cells of the proximal nephron. In line with this evidence are the results by Neylon & Summers (1988) on the inhibition by cyclic AMP of phosphoinositide production in response to α_1-adrenoceptor activation in the rat kidney slices. This also agrees with the view that an increase in the intracellular levels of cyclic AMP decrease phospholipase C activity leading to a reduction in phosphoinositide breakdown (Nishizuka, 1984; 1989). This might constitute a possible explanation for the inhibitory effect of dibutyryl cyclic AMP and forskolin on the phenylephrine induced response. On the other hand, activation of α_2-adrenoceptors, with its subsequent decrease in cyclic AMP cellular levels, would remove the inhibitory influence upon phospholipase C, leading to an increased breakdown of phosphoinositides and increased production of DAG (Gesek & Schoolwerth, 1990). One result favouring this suggestion is that of the potentiation of the quinoxaline-mediated event by ineffective concentrations of PDBu. Cyclic AMP has been demonstrated to inhibit Na^+-H^+ exchanger activity directly by phosphorylating apical proteins associated with the antiporter by cyclic AMP-dependent protein kinases (Weinman *et al.*, 1987), whereas activation of PKC by phorbol esters results in increase of Na^+-H^+ exchange in rat proximal tubules and brush border membranes (Weinman & Shenolkar, 1986; Gesek *et al.*, 1989). Figure 10 is a schematic representation of the renal tubular dopamine outward transport, the hypothetical

mechanisms which may interfere with this system and of the interactions between the signal transducing pathways used by α_1- and α_2-adrenoceptors.

In conclusion, inhibition of the Na^+-H^+ antiport by amiloride and EIPA results in considerable reduction in the outflow of newly-formed dopamine, whereas the activation of this mechanism by both phenylephrine and quinoxaline results in facilitation of the outflow of dopamine; this effect is selectively reversed by α_1- and α_2-adrenoceptor antagonists and EIPA. It is suggested that the synergistic effect between quinoxaline and phenylephrine may be related to an amplification of a reaction at a given point in the post-receptor transducing pathway.

This work was supported grant number PBIC/C/CEN/ 1139/92 from Junta Nacional de Investigação Cientifica e Tecnológica.

References

ARONSON, P.S. (1983). Mechanisms of active H^+ secretion in the proximal tubule. *Am. J. Physiol.*, **245,** F647–F659.

BAINES, A.D. & HO, P. (1988). High salt reduces alpha-1 and alpha-2 adrenergic stimulation of diacylglycerol (DAG) production in rat renal proximal tubules. *Kidney Int.*, **33,** 338.

BURNS, C.P. & ROZENGURT, E. (1983). Serum, platelet derived growth factor and phorbol esthers increase intracellular pH in Swiss 3T3 cell. *Biochem. Biophys. Res. Commun.*, **116,** 931–938.

CAREY, R.M., SIRAGY, H.M. & FELDER, R.A. (1990). Physiological modulation of renal function by the renal dopaminergic system. *J. Auton. Pharmacol.*, **10** (Suppl. 1), s47–s51.

GARVIN, J.L. (1989). Inhibition of Jv by ANF in the rat proximal straight tubules requires angiotensin. *Am. J. Physiol.*, **257,** F907–F911.

GESEK, F.A., CRAGOE, Jr. E.J. & STRANDHOY, J.W. (1989). Synergistic alpha-1 and alpha-2 adrenergic stimulation of rat proximal nephron Na^+/H^+ exchange. *J. Pharmacol. Exp. Ther.*, **249,** 694–700.

GESEK, F.A. & SCHOOLWERTH, A.C. (1989). Effects of alpha-adrenergic agonists on intracellular and intramitochondrial pH in rat proximal nephrons. *Am. J. Physiol.*, **257,** F623–F630.

GESEK, F.A. & SCHOOLWERTH, A.C. (1990). Hormonal interactions with the proximal Na^+-H^+ exchanger. *Am. J. Physiol.*, **258,** F514–F521.

HARRIS, P.J., THOMAS, D. & MORGAN, T.O. (1987). Atrial natriuretic peptide inhibits angiotension-stimulated proximal tubular sodium and water reabsorption. *Nature*, **326,** 697–698.

HAYASHI, M., YAMAJI, Y., KITAJIMA, W. & SARUTA, T. (1990). Aromatic L-amino acid decarboxylase activity along the rat nephron. *Am. J. Physiol.*, **258,** F28–F33.

HEDGE, S.S., RICCI, A., AMENTA, F. & LOKHANDWALA, M.F. (1989). Evidence from functional and autoradiographic studies for the presence of tubular dopamine-1 receptors and their involvement in the renal effects of fenoldopam. *J. Pharmacol. Exp. Ther.*, **251,** 1237–1245.

INSEL, P.A., SNAVELY, M.D., HEALY, D.P., MUNZEL, P.A., POTENZA, C.L. & NORD, E.P. (1985). Radioligand binding and functional assays demonstrate postsynaptic alpha2-receptors on proximal tubules of rat and rabbit kidney. *J. Cardiovasc. Pharmacol.*, **7,** (Suppl. 8), S9–S17.

JOSE, P.A., FELDER, R.A., HOLLOWAY, R.R. & EISNER, G.M. (1986). Dopamine receptors modulate sodium excretion in denervated kidney. *Am. J. Physiol.*, **250,** F1033–F1038.

JOSE, P.A., RAYMOND, J.R., BATES, M.D., APERIA, A., FELDER, R.A. & CAREY, R.M. (1992). The renal dopamine receptors. *J. Am. Soc. Nephrol.*, **2,** 1265–1278.

KAHN, A.M., DOLSON, G.M.. HISE, M.K., BENNETT, S.C. & WEINMAN, E.J. (1985). Parathyroid hormone and dibutyryl cAMP inhibit Na^+/H^+ exchanger in renal brush border vesicles. *Am. J. Physiol.*, **248,** F212–F218.

KATZ, A.I. (1987). Renal Na-K-ATPase: its role in tubular sodium and potassium transport. *Am. J. Physiol.*, **242,** F207–F219.

KINSELLA, J.L. & ARONSON, P.S. (1980). Properties of the Na^+-H^+ exchanger in renal microvillus membrane vesicles. *Am. J. Physiol.*, **241,** C220–C226.

MAHNENSMITH, R.L. & ARONSON, P.S. (1985). The plasma membrane sodium-hydrogen exchanger and its role in physiological and pathophysiological processes. *Circ. Res.*, **57,** 773–778.

MOOLENAAR, W.H., TERTOOLEN, G.J. & DELAAT, S.W. (1984). Phorbol esthers and diacylglycerol mimic growth factors raising cytoplasmic pH. *Nature*, **312,** 371–374.

NEYLON, C.B. & SUMMERS, R.J. (1988). Inhibition by cAMP of the phosphoinositide response to alpha1-adrenoceptor stimulation in rat kidney. *Eur. J. Pharmacol.*, **148,** 441–444.

NISHIZUKA, Y. (1984). The role of protein kinase C in cell surface signal transduction and tumour promotion. *Nature*, **308,** 693–698.

NISHIZUKA, Y. (1989). The family of protein kinase C for signal transduction. *J. Am. Med. Ass.*, **262,** 1826–1833.

NORD, E.P., GOLDFARB, D., MIKHAIL, N., MORADESHAGI, P., HAFEZI, A., VAYSTUB, S., CRAGOE Jr. E.J. & FINE, L. (1986). Characteristics of the Na^+-H^+ antiporter in the intact renal proximal tubular cell. *Am. J. Physiol.*, **250,** F539–F550.

NORD, E.P., GOLDFARB, D., MIKHAIL, N., MORADESHAGI, P., HAFEZI, A., VAYSTUB, S. & INSEL, P. (1987). Alpha2-adrenergic agonists stimulate Na^+-H^+ antiport activity in the rabbit proximal tubule. *J. Clin. Invest.*, **80,** 1755–1762.

PETTINGER, W.A., UMEMURA, S., SMITH, D.D. & JEFFRIES, W.B. (1987). Renal alpha2-adrenoceptors and the adenylate cyclase cAMP system: biochemical and physiological interactions. *Am. J. Physiol.*, **252,** F199–F208.

POUYSSEGUR, J. & FRANCHI, C. (1987). Genetic approach to structure, function and regulation of the Na^+-H^+ antiporter. *Kidney Int.*, **32,** 5144–5149.

PREISIG, P.A. & RECTOR, Jr. F.C. (1988). Role of the Na^+-H^+ antiport in rat proximal tubule NaCl absorption. *Am. J. Physiol.*, **255,** F461–F465.

SERI, I., KONE, B.C., GULLANS, S.R., APERIA, A., BRENNER, B.A. & BALLERMANN, B.J. (1990). Influence of Na^+ intake on dopamine-induced inhibition of renal cortical Na^+-K^+-ATPase. *Am. J. Physiol.*, **258,** F52–F60.

SIRAGY, H.M., FELDER, R.A., HOWELL, N.L., CHEVALIER, R.L., PEACH, M.J. & CAREY, R.M. (1989). Evidence that intrarenal dopamine acts as a paracrine substance at the renal tubule. *Am. J. Physiol.*, **257,** F469–F477.

SOARES-DA-SILVA, P. (1992a). Actin cytoskeleton, tubular sodium and the renal synthesis of dopamine. *Biochem. Pharmacol.*, **44,** 1883–1886.

SOARES-DA-SILVA, P. (1992b). Renal Na^+-H^+ exchanger activity, alpha-adrenoceptors and the control of dopamine outflow. *Br. J. Pharmacol.*, **106,** 20P.

SOARES-DA-SILVA, P. (1993). Kinetic study of the tubular dopamine outward transporter in the rat and dog kidney. *Br. J. Pharmacol.*, **109,** 577– 580.

SOARES-DA-SILVA, P. & FERNANDES, M.H. (1990a). Synthesis and metabolism of dopamine in the kidney. Effects of sodium chloride, monoamine oxidase inhibitors and atrial natruiretic peptide. *Am. J. Hypertens.*, **3,** 7S–10S.

SOARES-DA-SILVA, P. & FERNANDES, M.H. (1990b). Regulation of dopamine synthesis in the rat. *J. Auton. Pharmacol.*, **10** (Suppl 1), s25–s30.

SOARES-DA-SILVA, P. & FERNANDEZ, M.H. (1991). Inhibitory effects of guanosine 3':5'-cyclic monophosphate on the synthesis of dopamine in the rat kidney. *Br. J. Pharmacol.*, **103,** 1923–1927.

SOARES-DA-SILVA, P. & FERNANDES, M.H. (1992a). Sodium-dependence and ouabain-sensitivity of the synthesis of dopamine in renal tissues of the rat. *Br. J. Pharmacol.*, **105,** 811–816.

SOARES-DA-SILVA, P. & FERNANDES, M.H. (1992b). Effect of α-human atrial natriuretic peptide on the synthesis of dopamine in the rat kidney. *Br. J. Pharmacol.*, **105,** 869–874.

SOARES-DA-SILVA, P., FERNANDES, M.H., ALBINO-TEIXEIRA, A., AZEVEDO, I. & PESTANA, M. (1992). Brief transient ischemia induces long-term depletion of norepinephrine without affecting the aromatic amino acid decarboxylase and monoamine oxidase activities in the rat kidney. *J. Pharmacol. Exp. Ther.*, **260,** 902–908.

SOARES-DA-SILVA, P., FERNANDES, M.H. & PESTANA, M. (1993). Studies on the role of sodium on the synthesis of dopamine in the rat kidney. *J. Pharmacol. Exp. Ther.*, (in press).

SOKAL, R.R. & ROHLF, F.J. (1981). *Biometry. The Principles and Practice of Statistics in Biological Research.* New York: Freeman and Company.

VIGNE, P., FRELIN, C., CRAGOE, Jr. E.J. & LUDZINSKI, M. (1984). Structure-activity relationships of amiloride and certain of its analogues in relation to the blockade of the Na^+-H^+ exchange system. *Mol. Pharmacol.*, **25,** 131–136.

WEINMAN, E.J. & SHENOLIKAR, S. (1986). Protein kinase C activates the renal apical membrane Na/H exchanger. *J. Memb. Biol.*, **93,** 133–139.

WEINMAN, E.J., SHENOLIKAR, S. & KAHN, A.M. (1987). cAMP associated inhibition of the Na^+-H^+ exchanger in rabbit kidney bruach border membranes. *Am. J. Physiol.*, **252,** F19–F25.

(Received September 22, 1992
Revised February 11, 1993
Accepted February 19, 1993)

Br. J. Pharmacol. (1993), **109**, 577–580 © Macmillan Press Ltd, 1993

Kinetic study of the tubular dopamine outward transporter in the rat and dog kidney

P. Soares-da-Silva

Department of Pharmacology and Therapeutics, Faculty of Medicine, 4200 Porto, Portugal

1 The present study has determined the kinetic characteristics of the outflow of dopamine of renal origin in slices of rat and dog renal cortex loaded with exogenous L-dihydroxyphenylalanine (L-DOPA 5 to 5000 μM).

2 In both dog and rat renal tissues the production of dopamine was found to be dependent on the concentration of L-DOPA used and reached its maximum at 2500 μM L-DOPA. The decarboxylation of L-DOPA in rat cortical slices (16.4 ± 2.6 to 1479.2 ± 85.2 nmol g^{-1}) was 6 fold that in the dog (2.2 ± 0.4 to 252.1 ± 21.2 nmol g^{-1}). In the rat kidney a large amount (approximately 50%) of the dopamine (5.2 ± 0.6 to 743.4 ± 58.3 nmol g^{-1}) was found to escape into the incubation medium, whereas in dog renal slices the amount of newly-formed dopamine escaping into the incubation medium (0.7 ± 0.2 to 46.5 ± 9.3 nmol g^{-1}) was less than 25% of the total amount of the amine formed.

3 The application of the Michaelis-Menten equation to the net transport of newly-formed dopamine has allowed the identification of a saturable (carrier-mediated transfer) and a non-saturable component (diffusion). The V_{max} (nmol g^{-1} 15 min^{-1}) and K_m (nM) values for the saturable component were, respectively, 340 ± 41 and 396 ± 45 in the rat kidney and 112 ± 16 and 319 ± 35 in the dog kidney. In both rat and dog renal tissues, the magnitude of the non-saturable component was found to be of minor importance up to a concentration of 250 nmol g^{-1} of dopamine to be transported. At high concentrations of the amine (greater then 250 nmol g^{-1}), only attainable in rat kidney slices, most of the dopamine was found to leave the compartment where the synthesis did occur through a non-saturable transport system.

4 In conclusion, the results presented here show that the outflow of newly-formed dopamine in both dog and rat kidney slices loaded with exogenous L-DOPA follows Michaelis-Menten kinetics with a saturable component and a non-saturable one, the latter assuming particular importance only at higher concentrations of the amine.

Keywords: Dopamine; kidney; cell outward transport

Introduction

The proximal nephron is endowed with a high aromatic L-amino acid decarboxylase (AAAD) activity and epithelial cells of proximal tubules have been demonstrated to synthetize dopamine from 3,4-dihydroxyphenylalanine (DOPA) present in the tubular filtrate (Hayashi *et al.*, 1990; Seri *et al.*, 1990; Soares-da-Silva & Fernandes, 1990a,b). The dopamine formed in tubular epithelial cells has been shown to be of particular importance in the renal handling of water and electrolytes (Jose *et al.*, 1986; Hedge *et al.*, 1989; Siragy *et al.*, 1989); the natriuretic effects of the amine appear to result from the activation of specific receptors located in renal tubules (Jose *et al.*, 1992) and would involve inhibition of both the Na^+-H^+ exchanger (Felder *et al.*, 1990) and Na^+-K^+ ATPase (Aperia *et al.*, 1987).

The cellular uptake of DOPA in renal proximal tubules has been shown to occur through an energy-dependent and stereoselective carrier-mediated process (Chan, 1974) and evidence produced subsequently favours the view that sodium may play a part in this process. In fact, sodium loading has been reported to be accompanied by an increased urinary excretion of dopamine in both man and laboratory animals (Alexander *et al.*, 1974; Ball *et al.*, 1978; Bains, 1982; Goldstein *et al.*, 1989; Hayashi *et al.*, 1990) and a low sodium diet results in a decrease in the urinary excretion of dopamine (Baines, 1982; Goldstein *et al.*, 1989; Hayashi *et al.*, 1990). In line with this evidence, it has been reported in both human and rat kidney preparations that the production of dopamine is not only closely dependent on the extracellular sodium, but also appears to be related to the transtubular reabsorption of sodium (Soares-da-Silva & Fernandes, 1991; 1992a,b; Soares-da-Silva *et al.*, 1992; 1993a,c) and on the integrity of the tubular cytoskeleton and the functional integrity of the Na^+-K^+-ATPase (Soares-da-Silva, 1992a). More recently, inhibition or stimulation of the Na^+-H^+ exchanger has been found to affect the outward transport of newly-formed dopamine in rat kidney slices (Soares-da-Silva, 1992b), thus suggesting that both the cellular uptake of L-DOPA and the outflow of dopamine may directly depend on sodium or may be under the influence of mechanisms which are responsible for the tubular transport of sodium. On the other hand, this may suggest that the tubular cell outward transfer of dopamine would involve the stimulation of an active transport system for the amine. The outflow of newly-formed dopamine in rat kidney slices has been shown to follow a monoexponential pattern of decay with a half-life of about 20 min (Pestana & Soares-da-Silva, 1992).

The aim of the present work was to evaluate the presence of an active transport system for dopamine in slices of rat and dog renal cortex loaded with L-DOPA and to determine the kinetic characteristics of the outflow of dopamine of renal origin.

Methods

The rat and dog renal tissues were obtained from, respectively, male Wistar rats (biotério do Instituto Gulbenkian de Ciência, Oeiras, Portugal) aged 45–60 days and weighing 200 to 280 g and male mongrel dogs of undetermined age and weighing 18 to 25 kg. Rats were kept two per cage under controlled environmental conditions (12 h light/dark cycle room temperature 24°C). Food and tap water were allowed *ad libitum*. The rats were killed by decapitation under ether anaesthesia and both kidneys removed and rinsed free from

blood with saline (0.9% w/v saline solution). Dogs were anaesthetized with sodium pentobarbitone (30 mg kg^{-1}) given i.v. and both kidneys quickly removed through a midline incision of the abdominal wall. The kidneys were then placed on an ice cold glass plate, the kidney poles removed and slices of the renal cortex approximately 0.5 mm thick and weighing about 25 mg wet weight were prepared with a scalpel. Thereafter, renal slices were preincubated for 30 min in 2 ml gassed (95% O_2 and 5% CO_2) and warm (37°C) Krebs solution. The Krebs solution had the following composition (mM): NaCl 120, KCl 4.7, $CaCl_2$ 2.4, $MgSO_4$ 1.2, KH_2PO_4 1.2, $NaHCO_3$ 25, EDTA 0.4, ascorbic acid 0.57 and glucose 11; 1-α-methyl-*p*-tyrosine (50 μM), pargyline (0.1 mM), tropolone (50 μM) and copper sulphate (10 μM) were also added to the Krebs solution in order to inhibit the enzymes, tyrosine hydroxylase, monoamine oxidase and catechol-*O*-methyltransferase and inhibit the endogenous inhibitors of dopamine β-hydroxylase, respectively. After preincubation, renal slices were incubated for 15 min in Krebs solution with added L-DOPA. The preincubation and incubation were carried out in glass test tubes, continuously shaken throughout the experiment. After the incubation, renal slices were collected with fine forceps and immediately placed in 2 ml of 0.2 M perchloric acid at 4°C for the next 24 h. In order to allow the determination of the amount of dopamine which had leaked into the incubation medium, 250 μl of 2.0 M perchloric acid was added to the incubation medium after renal tissues had been collected; the samples of the incubation medium were also kept at 4°C for the next 24 h, until quantification of dopamine.

In the experiments performed with the aim of determining the presence and characterize the kinetic parameters of an outward transport mechanism for dopamine in renal slices, tissues were loaded with increasing concentrations (5 to 5000 μM) of L-DOPA for 15 min and the amount of newly-formed dopamine accumulated in the tissue and that which has escaped into the incubation medium determined; up to a concentration of 5000 μM L-DOPA, the pH of the incubation medium remained stable at 7.4. K_m and V_{max} values for the outward transport of newly-formed dopamine were calculated from linear regression analysis; the substrate transported (nmol of dopamine present in the incubation medium) was plotted against the product of the division between the substrate transported by the amount of the total dopamine formed (obtained from the algebraic sum of the amount accumulated in the tissue plus that present in the incubation medium). In these experimental conditions, the movement of newly-formed dopamine is expected to be mainly from the intracellular to the extracellular medium; though it may be hypothetized that the net transfer of dopamine would involve a carrier-mediated transport, diffiusion may also contribute to total amine transfer. The determination of carrier transport and diffusion in this experimental model was performed as defined by Neame & Richards (1972) by use of the expression

$$(V_{max}\ [S]/[S] + K_m) + (K_d.[S])$$
$$\text{(carrier transport)} + \text{(diffusion)}$$

where [S] is the concentration of the substrate to be transported and K_d the diffusion constant. Values for K_m and V_{max} were obtained by the method described above.

The assay of dopamine in kidney slices and the incubation medium was performed by means of high performance liquid chromatography (h.p.l.c.) with electrochemical detection, as previously described (Soares-da-Silva *et al.*, 1992). In brief, aliquots of 1.5 ml of perchloric acid in which tissues have been kept or 0.5 ml of acidified incubation medium were placed in 5 ml conical-based glass vials with 50 mg alumina and the pH of the samples adjusted to pH 8.6 by the addition of Tris buffer. The adsorbed catecholamines were then eluted from the alumina with 200 μl of 0.2 M perchloric acid on Millipore microfilters (MF1); 50 μl of the eluate was injected into a high pressure liquid chromatograph (Gilson Medical Electronics, Villiers le Bel, France). The lower limit for detection of dopamine was 10 fmol μl^{-1}.

Statistics

Mean values ± s.e.mean of *n* experiments are given. Significance of differences between one control and several experimental groups was evaluated by Tukey-Kramer method (Sokal & Rohlf, 1981). A *P* value less than 0.05 was assumed to denote a significant difference.

Drugs

L-Dihydroxyphenylalanine (L-DOPA), dopamine hydrochloride, 1-α-methyl-*p*-tyrosine pargyline hydrochloride and tropolone hydrochloride were purchased from Sigma Chemical Company (St. Louis, Mo, U.S.A.).

Results

In Figure 1 are shown the levels of total dopamine formed, obtained by the algebraic sum of their respective levels in the tissue and the incubation medium, and the amount of that dopamine which has remained in the tissue, in rat and dog kidney slices incubated with increasing concentrations (5 to 5000 μM) of L-DOPA. In both dog and rat renal tissues the production of dopamine was found to be dependent on the concentration of L-DOPA used and reached its maximum at 2500 μM L-DOPA. The decarboxylation of L-DOPA in rat cortical slices (16.4 ± 2.6 to 1479.2 ± 85.2 nmol g^{-1}) was 6 fold that in the dog (2.2 ± 0.4 to 252.1 ± 21.2 nmol g^{-1}); also, in the rat kidney a high proportion (approximately 50%) of dopamine (5.2 ± 0.6 to 743.4 ± 58.3 nmol g^{-1}) was

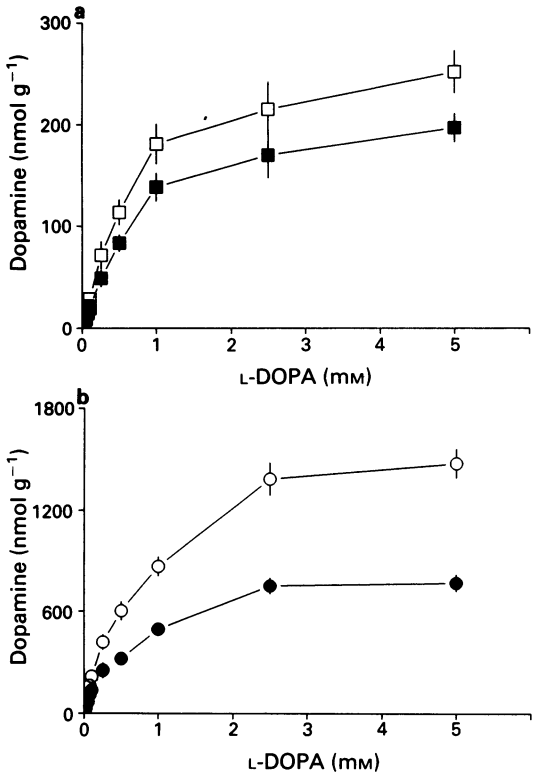

Figure 1 Levels of total dopamine formed (open symbols), obtained by the sum of their amounts in the tissue and the incubation medium, and the amount of that dopamine which has remained in the tissue (closed symbols), in (a) dog and (b) rat slices of renal cortex incubated with increasing concentrations (5 to 5000 μM) of L-DOPA for 15 min. Each point represents the mean with s.e.mean of five to six experiments per group.

found to escape into the incubation medium, whereas in dog renal slices the amount of newly-formed escaping into the incubation medium (0.7 ± 0.2 to 46.5 ± 9.3 nmol g^{-1}) was less than 25% of the total amine formed. The tissue levels of noradrenaline in kidney slices did not change significantly in the course of these experiments even when 5000 μM L-DOPA was used (data not shown, but see Fernandes & Soares-da-Silva, 1990).

A considerable amount of the total dopamine formed from added L-DOPA in kidney slices, depending on the species used, was found to escape into the incubation medium. The application of the Michaelis-Menten equation to the net transport of newly-formed dopamine has allowed the identification of a saturable (carrier-mediated transfer) and a non-saturable component (diffusion). In Figure 2 are shown the two components of dopamine transport and the total rate of amine transfer, as a plot of the amount of dopamine which has escaped into the incubation medium (rate of transport) against the total amount of dopamine formed (substrate concentration) in both the rat and dog kidney slices. The corresponding Eadie-Hofstee plot of the saturable component is shown in Figure 3. The V_{max} (nmol g^{-1} 15 min^{-1}) and K_m (nM) values for the saturable component were, respectively, 340 ± 41 and 396 ± 45 in the rat kidney and 112 ± 16 and 319 ± 35 in the dog kidney. In both rat and dog renal tissues, the magnitude of the non-saturable component was found of minor importance up to a concentration of 250 nmol g^{-1} of dopamine to be transported (Figure 2). At high concentrations of the amine (greater than 250 nmol g^{-1}), only attainable in rat kidney slices, most of the dopamine was found to leave the compartment where the synthesis did occur through a non-saturable transport system (Figure 2).

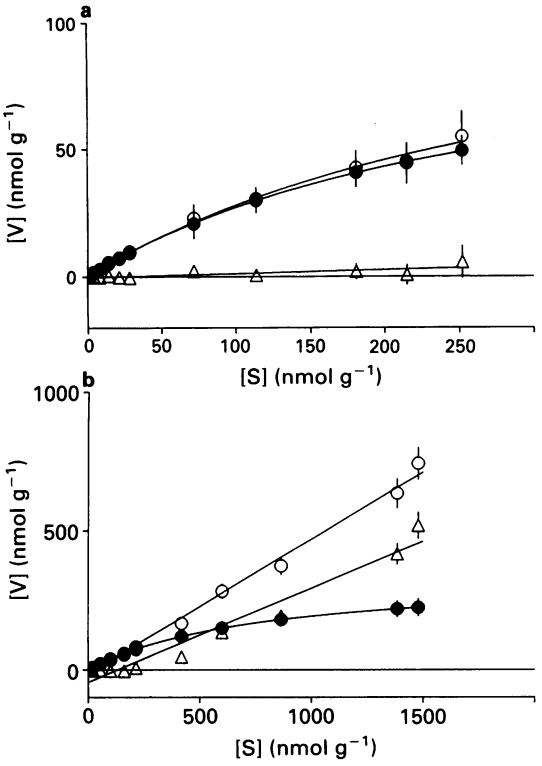

Figure 2 Outward transfer of newly-formed dopamine in slices of (a) dog and (b) rat renal cortex incubated with increasing concentrations of L-DOPA (5 to 5000 μM) for 15 min. The results are on the two components of dopamine transfer, saturable (●) and non-saturable (△), and the total rate of amine transfer (○), as a plot of the amount of dopamine which has escaped into the incubation medium (rate of amine transport; [V], in nmol g^{-1} 15 min^{-1}) against the total amount of dopamine formed (amine concentration; [S], in nmol g^{-1}) in both the rat and dog kidney slices.

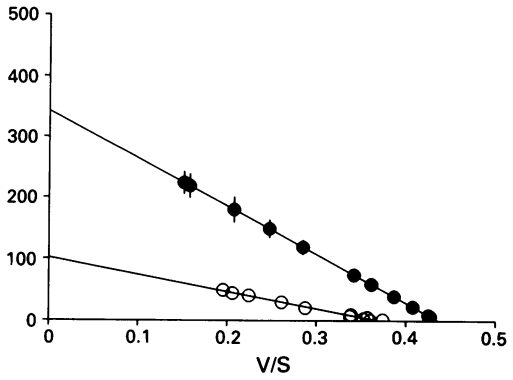

Figure 3 Eadie-Hofstee plot of the saturable component of newly-formed outward transfer in slices of dog (○) and rat (●) renal cortex incubated with increasing concentrations of L-DOPA (5 to 5000 μM) for 15 min. The V_{max} (nmol g^{-1} 15 min^{-1}) and K_m (nM) values for the saturable component were, respectively, 340 ± 41 and 396 ± 45 in the rat kidney and 112 ± 16 and 319 ± 35 in the dog kidney.

Discussion

In order to be active, the dopamine formed in tubular epithelial cells has to leave the compartment where the synthesis has occurred, since the receptors activated by the amine are believed to be located in the external surface of the cell membrane (Jose *et al.*, 1992). The identification and kinetic characterization of an outward transport system for dopamine in renal tissues is, therefore, of particular relevance, considering that the dopamine synthesized in tubular epithelial cells may have important physiological actions in the control of tubular reabsorption of sodium. The results presented here show that the cell outward transfer of dopamine through a carrier-mediated system appears to be an important mechanism for the transport of the amine in tubular epithelial cells, though diffusion may play a role at high concentrations of dopamine.

The data reported here show that the outflow of newly-formed dopamine in kidney slices loaded with exogenous L-DOPA follow Michaelis-Menten kinetics with a saturable component and a non-saturable one, the latter assuming particular importance only at higher concentrations of the amine. Similar K_m values for the saturable component of dopamine outflow in the rat and dog kidney suggests that the renal outward transporter of dopamine in the two species may share some functional properties. In contrast, higher V_{max} values in the rat may suggest the presence of a high number of outward transporter units in the rat kidney. Another difference between dog and rat renal tissues concerns the greater ability of rat cortical slices to convert L-DOPA into dopamine. This, however, appears to be related to a higher AAAD activity in the rat in comparison with that in the dog, as determined in kidney homogenates (Soares-da-Silva *et al.*, 1993b). Until now, it has not been clarified whether there is a preferential cell outward transport of dopamine at the basolateral or the apical cell borders. Because the apical cell border may not be in operation due to collapse of tubular lumen while using kidney slices (Wedeen & Weiner, 1973), the results reported here on the outflow of dopamine would mainly reflect the outward transfer of dopamine at the basolateral cell border.

The intrinsic mechanisms involved in the modulatory process of the renal outward dopamine transfer have not yet been fully elucidated, but evidence has been presented favouring the involvement of both the organic cation transporter (Rennick & Pryor, 1965; Hakim *et al.*, 1970) and the Na^+-H^+ exchanger. The accompanying work (Soares-da-

Silva, 1993) presents evidence suggesting that the outward transport of the amine in kidney slices can be influenced by activators and inhibitors of the Na^+-H^+ exchanger. Recent studies performed in the proximal nephron indicate that changes in cell volume and intracellular pH observed during the activation of the Na^+-H^+ exchanger may serve as a signal for generating a biological response (Mahnensmith & Aronson, 1985; Gesek & Schoolwerth, 1989). Thus, it may be possible that modulation of cell outward transport of tubular dopamine by the Na^+-H^+ exchanger depends upon changes in intracellular pH, Na^+ flux or even changes in the activity of the organic cation transporter (Ross & Holohan, 1983).

In conclusion, the results presented here show that the outflow of newly-formed dopamine in both dog and rat kidney slices loaded with exogenous L-DOPA follows Michaelis-Menten kinetics with a saturable component and a non-saturable one, the latter assuming particular importance only at higher concentrations of the amine.

This work was supported by grant number PBIC/C/CEN/1139/92 from Junta Nacional de Investigação Científica e Technológica.

References

ALEXANDER, R.W., GILL, J.R. JR, YAMABE, H., LOVENBERG, W. & KEISER, H.R. (1974). Effects of dietary sodium and acute saline infusion on the interelationship between dopamine excretion and adrenergic activity in man. *J. Clin. Invest.*, **54**, 194–200.

APERIA, A., BERTORELLO, A.M. & SERI, I. (1987). Dopamine causes inhibition of Na^+-K^+-ATPase activity in rat proximal convoluted tubule segments. *Am. J. Physiol.*, **252**, F39–F45.

BAINES, A.D. (1982). Effects of salt intake and renal denervation on catecholamine catabolism and excretion. *Kidney Int.*, **21**, 316–322.

BALL, S.G., OATES, N.S. & LEE, M.R. (1978). Urinary dopamine in man and rat: effects of inorganic salts on dopamine excretion. *Clin. Sci. Mol. Med.*, **55**, 167–173.

CHAN, Y.L. (1974). Cellular mechanisms of renal tubular transport of L-DOPA and its derivatives in the rat: microperfusions studies. *J. Pharmacol. Exp. Ther.*, **199**, 17–24.

FELDER, C.C., CAMPBELL, T., ALBRECHT, F. & JOSE, P.A. (1990). Dopamine inhibits Na^+-H^+ exchanger activity in renal BBMV by stimulation of adenylate cyclase. *Am. J. Physiol.*, **259**, F297–F303.

FERNANDES, M.H. & SOARES-DA-SILVA, P. (1990). Effects of MAO-A and MAO-B selective inhibitors Ro 41-1049 and Ro19-6327 on the deamination of newly-formed dopamine in the rat kidney. *J. Pharmacol. Exp. Ther.*, **255**, 1309–1313.

GESEK, F.A. & SCHOOLWERTH, A.C. (1989). Effects of alpha-adrenergic agonists on intracellular and intramitochondrial pH in rat proximal nephrons. *Am. J. Physiol.*, **257**, F623–F630.

GOLDSTEIN, D.S., STULL, R., EISENHOFER, G. & GILL, J.R. JR (1989). Urinary excretion of dihydroxyphenylalanine and dopamine during alterations of dietary salt intake in humans. *Clin. Sci.*, **76**, 517–522.

HAKIM, R., WATROUS, W.M. & FUJIMOTO, J.M. (1970). The renal tubular transport and metabolism of serotonin (5-HT) and 5-hydroindolacetic acid (5-HIAA) in the chicken. *J. Pharmacol. Exp. Ther.*, **175**, 749–762.

HAYASHI, M., YAMAJI, Y., KITAJIMA, W. & SARUTA, T. (1990). Aromatic L-amino acid decarboxylase activity along the rat nephron. *Am. J. Physiol.*, **258**, F28–F33.

HEDGE, S.S., RICCI, A., AMENTA, F. & LOKHANDWALA, M.F. (1989). Evidence from functional and autoradiographic studies for the presence of tubular dopamine-1 receptors and their involvement in the renal effects of fenoldopam. *J. Pharmacol. Exp. Ther.*, **251**, 1237–1245.

JOSE, P.A., FELDER, R.A., HOLLOWAY, R.R. & EISNER, G.M. (1986). Dopamine receptors modulate sodium excretion in denervated kidney. *Am. J. Physiol.*, **250**, F1033–F1038.

JOSE, P.A., RAYMOND, J.R., BATES, M.D., APERIA, A., FELDER, R.A. & CAREY, R.M. (1992). The renal dopamine receptors. *J. Am. Soc. Nephrol.*, **2**, 1265–1278.

MAHNENSMITH, R.L. & ARONSON, P.S. (1985). The plasma membrane sodium-hydrogen exchanger and its role in physiological and pathophysiological processes. *Circ. Res.*, **57**, 773–778.

NEAME, K.D. & RICHARDS, T.G. (1972). *Elementary Kinetics of Membrane Carrier Transport*. Oxford: Blackwell Scientific Publications.

PESTANA, M. & SOARES-DA-SILVA, P. (1992). Renal outflow of dopamine: a comparative study with L-DOPA and γ-glutamyl-L-DOPA. *Br. J. Pharmacol.*, **106**, 82P.

RENNICK, B.R. & PRYOR, M.Z. (1965). Effects of autonomic drugs on renal tubular transport of catecholamines in the chicken. *J. Pharmacol. Exp. Ther.*, **148**, 262–269.

ROSS, C.R. & HOLOHAN, P.D. (1983). Transport of organic anions and cations in isolated renal plasma membranes. *Annu. Rev. Pharmacol. Toxicol.*, **23**, 65–85.

SERI, I., KONE, B.C., GULLANS, S.R., APERIA, A., BRENNER, B.A. & BALLERMANN, B.J. (1990). Influence of Na^+ intake on dopamine-induced inhibition of renal cortical Na^+-K^+-ATPase. *Am. J. Physiol.*, **258**, F52–F60.

SIRAGY, H.M., FELDER, R.A., HOWELL, N.L., CHEVALIER, R.L., PEACH, M.J. & CAREY, R.M. (1989). Evidence that intrarenal dopamine acts as a paracrine substance at the renal tubule. *Am. J. Physiol.*, **257**, F469–F477.

SOARES-DA-SILVA, P. (1992a). Actin cytoskeleton, tubular sodium and the renal synthesis of dopamine. *Biochem. Pharmacol.*, **44**, 1883–1886.

SOARES-DA-SILVA, P. (1992b). Renal Na^+-H^+ exchanger activity, alpha-adrenoceptors and the control of dopamine outflow. *Br. J. Pharmacol.*, **106**, 20P.

SOARES-DA-SILVA, P. (1993). Renal tubular dopamine outward transfer during Na^+-H^+ exchange activation of α_1- and α_2-adrenoceptor agonists. *Br. J. Pharmacol.*, **109**, 569–576.

SOARES-DA-SILVA, P. & FERNANDES, M.H. (1990a). Synthesis and metabolism of dopamine in the kidney. Effects of sodium chloride, monoamine oxidase inhibitors and atrial natriuretic peptide. *Am. J. Hypertens.*, **3**, 7S–10S.

SOARES-DA-SILVA, P. & FERNANDES, M.H. (1990b). Regulation of dopamine synthesis in the rat. *J. Auton. Pharmacol.*, **10** (Suppl 1), s25–s30.

SOARES-DA-SILVA, P. & FERNANDES, M.H. (1991). Inhibitory effects of guanosine 3':5'-cyclic monophosphate on the synthesis of dopamine in the rat kidney. *Br. J. Pharmacol.*, **103**, 1923–1927.

SOARES-DA-SILVA, P. & FERNANDES, M.H. (1992a). Sodium-dependence and ouabain-sensitivity of the synthesis of dopamine in renal tissues of the rat. *Br. J. Pharmacol.*, **105**, 811–816.

SOARES-DA-SILVA, P. & FERNANDES, M.H. (1992b). Effect of α-human atrial natriuretic peptide on the synthesis of dopamine in the rat kidney. *Br. J. Pharmacol.*, **105**, 869–874.

SOARES-DA-SILVA, P., FERNANDES, M.H., ALBINO-TEIXEIRA, A., AZEVEDO, I. & PESTANA, M. (1992). Brief transient ischemia includes long-term depletion of norepinephrine without affecting the aromatic amino acid decarboxylase and monoamine oxidase activities in the rat kidney. *J. Pharmacol. Exp. Ther.*, **260**, 902–908.

SOARES-DA-SILVA, P., FERNANDES, M.H. & PESTANA, M. (1993a). Studies on the role of sodium on the synthesis of dopamine in the rat kidney. *J. Pharmacol. Exp. Ther.*, **264**, 406–414.

SOARES-DA-SILVA, P., PESTANA, M.H. & FERNANDES, M.H. (1993c). Involvement of tubular sodium in the formation of dopamine in the human renal cortex. *J. Am. Soc. Soc. Nephrol.* in press.

SOKAL, R.R. & ROHLF, F.J. (1981). *Biometry. The Principles and Practice of Statistics in Biological Research*. New York: Freeman & Company.

WEDEEN, R.P. & WEINER, B. (1973). The distribution of p-aminohippuric acid in rat kidney slices. I. Tubular localization. *Kidney Int.*, **3**, 205–213.

(Received September 22, 1992
Revised February 11, 1993
Accepted February 19, 1993)

Br. J. Pharmacol. (1993), **109**, 581–586 © Macmillan Press Ltd, 1993

Comparison between carvedilol and captopril in rats with partial ablation-induced chronic renal failure

[1]David P. Brooks, Brian G. Short, Matthew J. Cyronak, Lisa C. Contino, Martin DiCristo, Yi-Xin Wang & Robert R. Ruffolo, Jr.

Departments of Renal Pharmacology, Toxicology-U.S. and Drug Metabolism, and Division of Pharmacological Sciences, SmithKline Beecham Pharmaceuticals, King of Prussia, PA 19406-0939, U.S.A.

1 The effect of the novel β-adrenoceptor antagonist and vasodilator, carvedilol (SK&F 105517, ~70 mg kg^{-1} daily in the food), and captopril (~38 mg kg^{-1} daily in the drinking fluid) on the progression of chronic renal failure in rats was studied.

2 Six weeks following partial renal ablation, the urinary protein excretion of the carvediol- (60 ± 21 mg day^{-1}) and captopril-treated (35 ± 9 mg day^{-1}) animals was less than 50% that of control rats (133 ± 27 mg d^{-1}).

3 Serum creatinine (Scr) and urea nitrogen (SUN) concentrations of the carvedilol-(Scr, 0.63 ± 0.09 mg dl^{-1}; SUN, 11.3 ± 1.2 mg dl^{-1}) and captopril-treated (Scr, 0.82 ± 0.05 mg dl^{-1}; SUN, 14.1 ± 1.5 mg dl^{-1}) animals were also significantly ($P<0.05$) lower than that observed in control animals (Scr, 1.4 ± 0.3 mg dl^{-1}; SUN, 19.2 ± 3.9 mg dl^{-1}), indicating that glomerular filtration rate was improved by both drugs. Plasma renin activity was significantly ($P<0.05$) higher in captopril-treated rats (24.7 ± 4.6 ng angiotensin I ml^{-1} h^{-1}) than in either carvedilol-treated (7.9 ± 1.4 ng angiotensin I ml^{-1} h^{-1}) or control animals (7.4 ± 1.0 ng angiotensin I ml^{-1} h^{-1}).

4 Histological examination of the kidneys demonstrated a significantly reduced glomerular hypertrophy and glomerulosclerosis in those animals receiving carvedilol or captopril compared to controls.

5 Serum carvedilol concentration measured every 6 h for 24 h was variable and ranged on average from 57 ± 13 ng ml^{-1} at 16 h 00 min to 121 ± 31 ng ml^{-1} at 03 h 00 min. These data indicate that the rats probably had 24 h systemic exposure to carvedilol.

6 The present study indicates that carvedilol is effective in attenuating the progression of chronic renal failure in rats.

Keywords: Chronic renal failure; carvedilol; α-adrenoceptor antagonist; β-adrenoceptor antagonist; vasodilator; angiotensin converting enzyme inhibitor; captopril

Introduction

Partial renal ablation in rats leads to progressive renal failure and is characterized by proteinuria, hypertension and glomerulosclerosis (Shimamura & Morrison, 1975). Control of hypertension both in experimental models of renal failure and patients with chronic renal disease can attenuate the progressive decline in renal function (Klahr, 1991). Reduction in blood pressure alone, however, may not be the sole reason why antihypertensive drugs are beneficial since some classes of antihypertensives have advantages over others. For example, angiotensin converting enzyme (ACE) inhibition appears to have a greater benefit than α_1-adrenoceptor antagonists in human subjects with chronic renal disease (Rosenberg & Hostetter, 1991). It is possible that better control of glomerular hypertension and/or inhibition of the proliferative effects of angiotensin II by ACE inhibitors may be important factors in the possible advantage of this class of drugs over other antihypertensive agents. Carvedilol (SK&F 105517) is a novel multiple action drug that has recently been introduced to the market for the treatment of mild to moderate hypertension (see Ruffolo *et al.*, 1991 for review). Carvedilol is both a competitive β-adrenoceptor antagonist and an arterial vasodilator. At higher concentrations, carvedilol is also a calcium channel antagonist (Ruffolo *et al.*, 1991) and has antiproliferative effects on both vascular smooth muscle (Sung *et al.*, 1993) and mesangial (Albrightson *et al.*, 1992) cells. In the present study, therefore, we have compared the effects of carvedilol and the angiotensin converting enzyme inhibitor, captopril, on the hypertension, proteinuria and glomerulosclerosis associated with partial renal ablation in rats.

Methods

Male Sprague-Dawley rats with initial body weights between 250 and 300 g were used. All rats were fed a powdered rodent chow (23.5% protein by weight; Ziegler Brothers, Inc., open formula, NIH-07). One week before and 1, 2, 4, and 6 weeks after partial renal ablation, rats were housed individually in metabolic cages for 48 h and urine collected for the second 24 h period. Food and fluid intakes and urine volume were measured over the second 24 h period and urinary protein excretion determined by the sulphosalicyclic method (Davidsohn & Henry, 1969). Twenty-four hours before renal ablation, 14 rats were given powdered rodent chow containing 600 p.p.m. carvedilol (SK&F 105517) and 14 rats were given captopril in their drinking water (250 mg l^{-1}). A further 14 rats served as controls. Following baseline measurements (week 0) animals underwent 5/6 renal ablation. Under sodium pentobarbitone anaesthesia a midline incision was made, the right kidney was removed; and approximately 2/3 of the left kidney was infarcted by ligating 2 or 3 branches of the left renal artery. A small number of animals did not survive beyond the first week following surgery (control group, 2; carvedilol group, 3; captopril group, 1) and the data for these animals were not included in

[1]Author for correspondence at: SmithKline Beecham Pharmaceuticals, Department of Renal Pharmacology, UW2521, P.O. Box 1539, King of Prussia, PA 19406-0939, U.S.A.

the study. All available data from animals who died subsequently (i.e., after week 1) were included. Ten control, 10 carvedilol-treated and 13 captopril-treated rats completed the study.

During the final week of study, blood samples from the tail vein of the carvedilol-treated rats were taken every 6 h for 24 h (09 h 00 min, 15 h 00 min, 21 h 00 min, 03 h 00 min) to determine serum carvedilol concentrations. Serum carvedilol concentration was determined by high performance liquid chromatographic methods as described in detail previously (Reiff, 1987). The lower limit of detection was 3 ng ml^{-1} based on 0.1 ml of serum. The average between day coefficient of variation for this assay was 3.9%.

At the conclusion of the experiment, the animals were anaesthetized with Inactin (100 mg kg^{-1}, i.p.; Andrew Lockwood Associates, Sturdevant, WI, U.S.A.) and the femoral artery catheterized with Tygon tubing in order to measure mean arterial blood pressure and heart rate with a Statham transducer and Gilson recorder. This was performed during the morning (i.e., within approximately 6–12 h after feeding). A blood sample was taken for measurement of serum creatinine, serum urea nitrogen concentrations (Synchon AS8 clinical analyzer), plasma renin activity, and the kidneys removed for histological examination.

Plasma samples for the assay of renin activity were treated with EDTA and stored at −30°C. Plasma renin activity was determined with an angiotensin I (AI) radioimmunoassay kit (New England Nuclear, Boston, MA, U.S.A.): 0.5 ml plasma was used and angiotensin I generated for 2 h in pH 6 maleate buffer. Data are expressed as ng AI ml^{-1} h^{-1}.

Kidneys were fixed in 10% buffered formalin. Transverse kidney slices were embedded in paraffin, sectioned at 5 μm, and stained with hematoxylin-eosin. Kidneys were examined by light microscopy using coded slides and scored by a pathologist. A total of 75 to 100 glomeruli from each rat were scored from 0 to 4 based on the severity of glomerulosclerosis as follows (Nahas *et al.*, 1991); grade 0, normal glomerulus; grade 1, presence of mesangial expansion/thickening of the basement membrane; grade 2, mild/moderate segmental hyalinosis/sclerosis involving less than 50% of the glomerular tuft; grade 3, diffuse glomerular hyalinosis/sclerosis involving more than 50% of the tuft; grade 4, diffuse glomerulosclerosis with total tuft obliteration and collapse. Mean glomerular score was calculated for each rat. Glomerular scarring was also quantified by the assessment of the percentage of glomeruli displaying significant sclerosis (grade ≥ 2). A computer-assisted morphometric unit (Magiscan Image Analysis System, Vickers Plc., Dukesway, England) was used to measure the mean glomerular cross-sectional areas for 50 glomerular profiles contained in one kidney section in each rat. The mean volume (V_G) of glomeruli was then calculated from the mean glomerular area (A_G) as:

$$V_G = \beta/K \times A_G^{3/2}$$

where $\beta = 1.38$ is the size-distribution coefficient and $K = 1.1$ is the shape coefficient for glomeruli idealized as a sphere (Weibel, 1979; Hirose *et al.*, 1982).

The tubulointerstitium was examined for tubular dilatation, intratubular hyaline casts, tubular atrophy and regeneration, and interstitial infiltration with mononuclear cells and interstitial fibrosis. Tubulointerstitial change was graded on a scale of from 0 to 4 as follows: grade 0, a normal kidney; grade 1, minimal abnormalities affecting <10% of the renal parenchyma; grade 2, mild (10–25%); grade 3, moderate (25–50%); and grade 4, severe (>50% of the kidney manifested tubulointerstitial abnormalities) (Trachtman *et al.*, 1992).

Data were expressed as mean ± s.e.mean and were compared statistically by analysis of variance for repeated measures and subsequently a Scheffe *F* test.

Carvedilol (SK&F 105517) was synthesized by Boehringer Mannheim, and captopril was purchased from Sigma.

Results

Partial renal ablation resulted in a progressive proteinuria in control rats with urinary protein excretion increasing from a baseline of approximately 9 mg day^{-1} to 133 mg day^{-1} at week 6 (Figure 1). Treatment with either carvedilol or captopril resulted in a significant blunting of proteinuria throughout the period of study such that by week 6, urinary protein excretion in the carvedilol- and captopril-treated groups was less than 50% of the control value (Figure 1).

Control animals grew at a slightly slower rate than animals receiving either carvedilol or captopril, but by week 6 there was little difference in body weight between that 3 groups. The slower growth of control animals during the first few weeks of the study may have been due to a smaller food intake in the control rats compared to the carvedilol- and captopril-treated rats during the first week following surgery. The food intake in the captopril- and carvedilol-treated animals tended to be higher than control animals during week 1. Fluid intake was variable throughout the study, increasing slightly over time in the control group. Measurement of food and fluid intakes permitted calculation of the carvedilol and captopril doses, respectively (Table 1). Thus, average doses of carvedilol and captopril over the time course of the experiment averaged approximately 70 and 38 mg kg^{-1} day^{-1} respectively. During the last week of study, the carvedilol dose (55 mg kg^{-1} day^{-1}) was associated with mean serum carvedilol concentrations ranging between

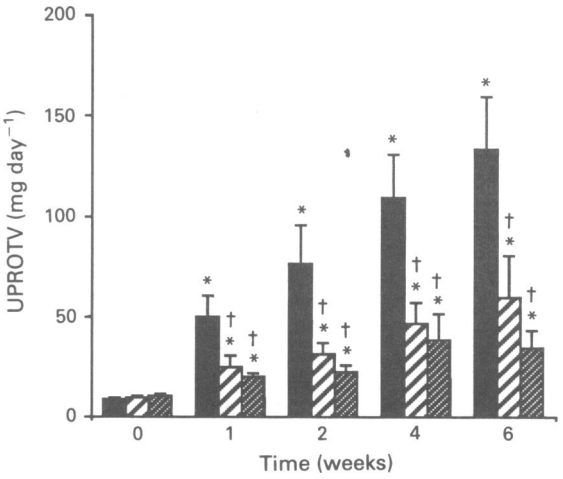

Figure 1 Effect of vehicle (solid columns), carvedilol (600 p.p.m. in the food; hatched columns) or captopril (250 mg l^{-1} in the drinking water; stippled columns) on the urinary protein excretion (UPROTV) of rats with partial renal ablation ($n = 10–13$ rats/group). Data are mean ± s.e.mean. *$P<0.05$ vs week 0; †$P<0.05$ vs control.

Table 1 Calculated doses of carvedilol and captopril based on food (carvedilol concentration 600 p.p.m.) and fluid (captopril concentration 250 mg l^{-1}) intakes respectively

	Time (weeks)			
	1	*2*	*4*	*6*
Carvedilol (mg kg^{-1} day^{-1})	109 ± 31	62 ± 11	55 ± 8	55 ± 13
Captopril (mg kg^{-1} day^{-1})	43 ± 15	43 ± 3	39 ± 3	28 ± 15

Data are mean ± s.e.mean

57 ± 13 ng ml^{-1} and 121 ± 31 ng ml^{-1} over a 24 h period. Although the serum concentrations of carvedilol were highly variable at each sampling time, all rats studied had measurable concentrations over the sampling period. This suggests that the rats had 24 h systemic exposure to carvedilol.

Renal function as assessed by serum creatinine and serum urinary nitrogen concentrations and measured during the final week of study was significantly improved in both carvedilol- and captopril-treated animals. Thus, the serum creatinine and serum urea nitrogen concentrations in carvedilol-treated animals were approximately half those observed in the control animals (Figure 2). Serum creatinine and urea nitrogen concentrations in captopril-treated animals were similar to those observed in the carvedilol-treated animals (Figure 2). Plasma renin activity in carvedilol-treated animals was not significantly different from that observed in control animals, however, plasma renin activity was approximately 3 times higher in rats receiving captopril (Figure 2).

Mean arterial blood pressure was significantly lower in both the carvedilol- and captopril-treated animals when compared to control animals, as determined by direct measurement from an arterial catheter in inactin-anaesthetized rats. Heart rate in the captopril-treated animals was similar to that observed in control animals. Rats receiving carvedilol had a lower heart rate than those animals receiving captopril (Figure 3). However, the difference in heart rate between carvedilol-treated and control animals did not reach statistical significance. The small effect of carvedilol on heart rate was presumably due to its β-adrenoceptor blocking activity.

Histological examination of kidneys demonstrated lesions consisting of segmental to global glomerulosclerosis, with tubular regeneration, tubular dilatation with proteinaceous casts, and a lymphocytic interstitial infiltrate. The severity of glomerulosclerosis was considerably reduced in carvedilol- and captopril-treated rats (score 1.15 ± 0.14 and 0.93 ± 0.14, respectively) compared to control rats (score 1.95 ± 0.30). Furthermore, a smaller percentage of glomeruli were sclerotic in carvedilol- and captopril-treated rats ($23\% \pm 8\%$ and $18\% \pm 7\%$, respectively) than in control rats ($55\% \pm 10\%$; Figure 4). Tubulointerstitial changes were characterized by tubular dilatation with hyaline casts, tubular atrophy and regeneration, and interstitial infiltration with mononuclear

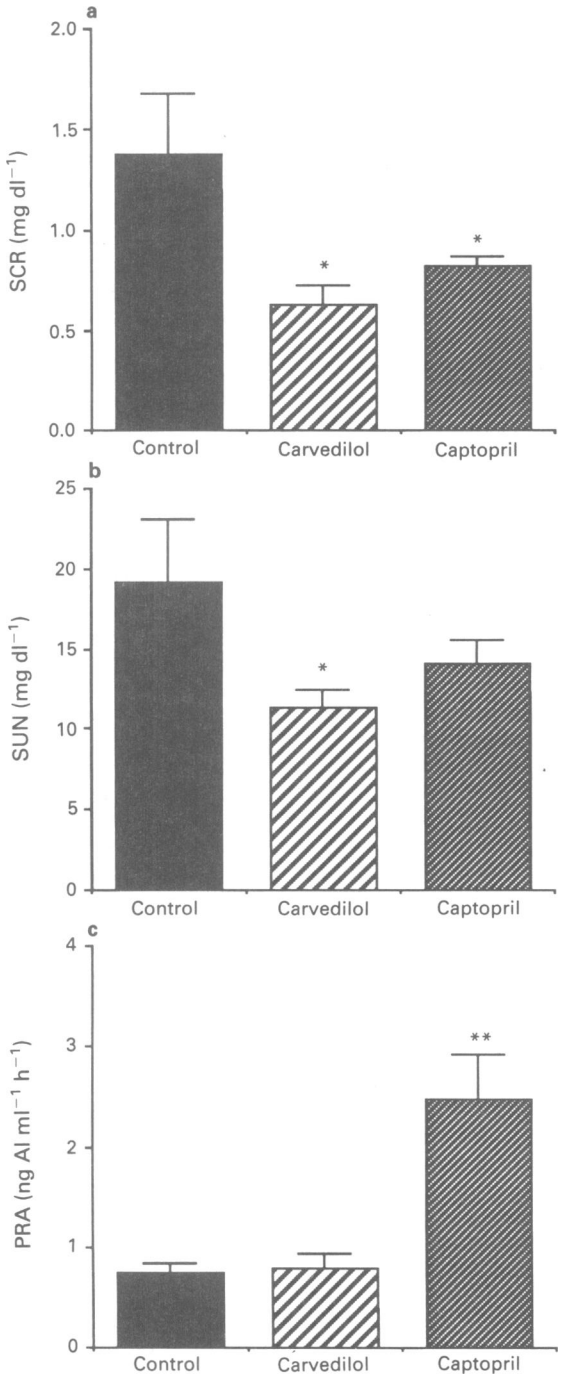

Figure 2 Effect of vehicle (solid columns), carvedilol (hatched columns) or captopril (stippled columns) on the serum creatinine concentration (SCR; a), serum urea nitrogen concentration (SUN; b) and plasma renin activity (PRA; c) of rats 6 weeks following partial renal ablation ($n = 10-13$ rats/group). Data are mean ± s.e.mean. *$P < 0.05$ vs control.

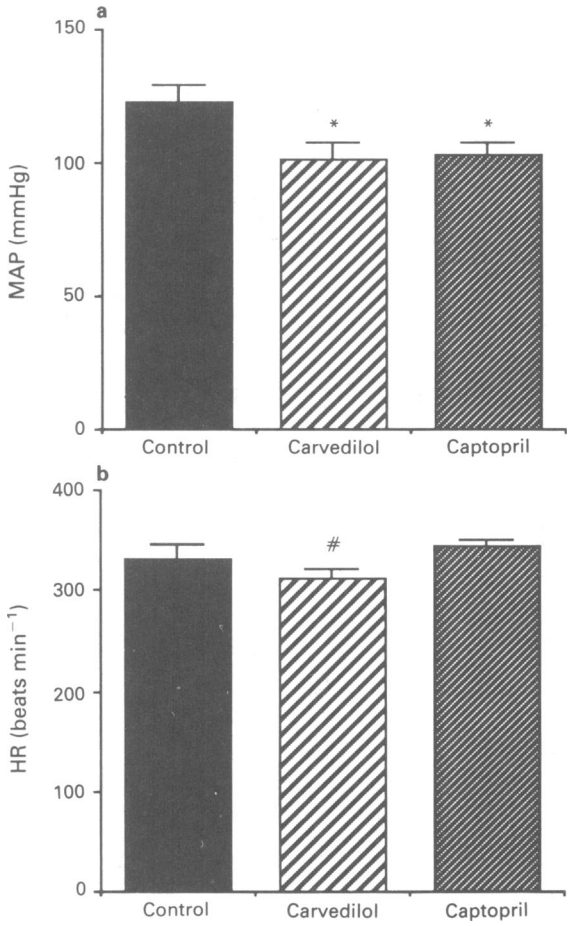

Figure 3 Effect of vehicle (solid columns), carvedilol (hatched columns) or captopril (stippled columns) on mean arterial pressure (MAP; a) and heart rate (HR; b) of rats 6 weeks following partial renal ablation ($n = 10-13$ rats/group). Data are mean ± s.e.mean. *$P < 0.05$ vs control; #$P < 0.05$ vs captopril.

cells and interstitial fibrosis. The severity to tubulointerstitial changes was less in carvedilol- and captopril-treated rats (score 1.20 ± 0.36 and 0.77 ± 0.20, respectively) than in control rats (score 2.6 ± 0.45). Morphometric studies showed that glomerular volume was decreased 33–35% in carvedilol- or captopril-treated rats, compared to control rats. Glomerular volume averaged $1.62 \pm 0.13 \times 10^6 \mu m^3$ in carvedilol-treated rats and $1.55 \pm 0.10 \times 10^6 \mu m^3$ in captopril-treated rats; these values were significantly less ($P < 0.05$, t test) than mean glomerular volume of $2.4 \pm 0.28 \times 10^6 \mu m^3$ in control rats.

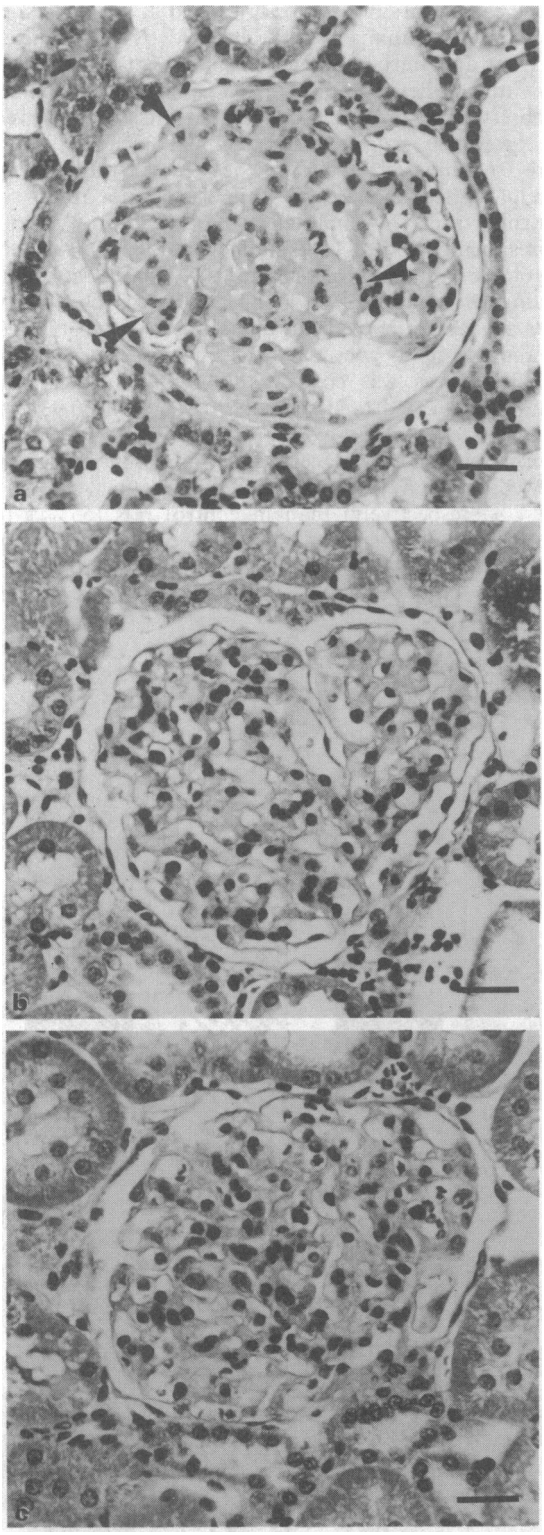

Figure 4 Glomerular lesions. (a) Characteristic glomerular lesion from an ablation control rat, exhibiting diffuse glomerular hyalinosis/sclerosis (arrowheads) involving more than 50% of the tuft (grade 3). (b) In comparison, the majority of glomeruli from carvedilol-treated rats had only mesangial expansion and thickening of the basement membrane (grade 1). Glomeruli from captopril-treated rats (c) were similar to carvedilol-treated rats (H&E; calibration bar = 26 μm).

Discussion

In the present study we have demonstrated that carvedilol attenuated the hypertension, proteinuria and glomerulosclerosis associated with 5/6 renal ablation in rats. Furthermore, 6 weeks following partial renal ablation, rats receiving carvedilol had a significantly better renal function that control rats as demonstrated by lower concentrations of serum creatinine and urea nitrogen. These data are consistent with the 'renal sparing' activity of antihypertensive doses of carvedilol in spontaneously hypertensive rats (Gellai *et al.*, 1990) and the antiproteinuric effects observed in carvedilol-treated spontaneously hypertensive rats that had undergone 3/5 nephrectomy and had a high salt diet (Nakamoto *et al.*, 1988).

The protective effects of carvedilol in partially nephrectomized rats appear to be greater than those reported for propranolol (Radin *et al.*, 1987) and are noteworthy since pure β-adrenoceptor antagonists may exacerbate renal dysfunction in hypertensive patients (Ibsen & Sederberg-Olsen, 1973; Warren, 1976; Weber & Drayer, 1980). Thus, improved renal function and reduced proteinuria observed in the present study suggests that multiple actions of carvedilol are responsible for the reno-protective effects of this drug. Carvedilol did not appear to provide any protection by inhibition of renin production since the plasma renin activity of carvedilol-treated and control animals was similar. The increased plasma renin activity observed in the captopril-treated animals was expected and was presumably due to removal of the negative feedback effects of angiotensin II on renin secretion.

The beneficial effects of carvedilol were comparable to those observed with the ACE inhibitor, captopril, which has been reported to delay the progression of renal failure in rats (Hall *et al.*, 1985). Furthermore, ACE inhibitors have been shown to provide a greater benefit than α-adrenoceptor antagonists in human patients with chronic renal disease (Rosenberg & Hostetter, 1991), suggesting that additional effects of carvedilol beyond β-adrenoceptor and α_1-adrenoceptor blockade contribute to the protective effects observed in the present study.

There is some debate as to the mechanisms involved in the progression of chronic renal failure. Some investigators (e.g. Brenner, 1985) suggest that following 5/6 renal ablation, adaptive processes that lead to increased glomerular capillary pressure, single nephron glomerular filtration rate and single nephron blood flow lead to further nephron damage, thus setting up an inexorable vicious cycle, culminating eventually in end-stage renal failure. Lowering glomerular capillary pressure should reduce glomerular injury and slow the progression of the disease. Angiotensin II is thought to mediate the glomerular hypertension associated with partial nephrectomy. Thus, converting enzyme inhibition may reduce glomerular hypertension and hyperfiltration by preventing the intraglomerular vascular actions of angiotensin II (Anderson *et al.*, 1985; Brenner, 1985). Other investigators have suggested that factors other than glomerular hypertension are important for the progression of chronic renal failure. Thus, glomerular hypertrophy rather than glomerular hypertension has been suggested to be important in the disease process (Yoshida *et al.*, 1988a,b). The protective effect of converting enzyme inhibition might therefore be due to inhibition of angiotensin II-induced mitogenic activity. It is interesting, therefore, that carvedilol, in addition to its antihypertensive activities, also possesses anti-proliferative

properties. Thus, in mesangial cells, carvedilol (10^{-7}–10^{-5} M) caused a concentration-dependent inhibition of both EGF and thrombin-induced [^{3}H]-thymidine incorporation, and carvedilol was more potent than either propranolol or celiprolol (Albrightson *et al.*, 1992). Carvedilol has also been shown to produce a dose-dependent (0.1–10 μM) decrease in basal or stimulated tritiated thymidine incorporation into rat aortic smooth muscle cells in culture (Sung *et al.*, 1993). These antiproliferative actions of carvedilol were not shared by other β-blockers such as propranolol, labetalol or sotalol, while celiprolol augmented thymidine incorporation into vascular smooth muscle cells. The IC_{50} of carvedilol for inhibition of endothelin-1-stimulated vascular smooth muscle cell proliferation was 1 μM which is not markedly greater than the serum concentration generated in the present study (120 ng ml^{-1} ~0.3 μM). This does not, however, take into account any protein binding, which in the rat is >95%, tissue accumulation or the presence of an active metabolite. It is interesting to note, however, that there is growing evidence that renal endothelin production is increased in rats with partial renal ablation-induced chronic renal failure (Brooks *et al.*, 1991; Benigni *et al.*, 1991).

In this study, the protective effects of carvedilol on glomerulosclerosis and glomerular hypertrophy were comparable to those observed with captopril. Several studies have demonstrated that ACE inhibitors afford protection from glomerulosclerosis in the ablation model in association with a decrease in glomerular volume (Yoshida *et al.*, 1988a,b). Glomerular enlargement is considered to be a crucial factor in the pathogenesis of progressive glomerulosclerosis following renal ablation or initial loss of functioning nephrons from other causes in animals and man (Fries *et al.*, 1989; Fogo & Ichikawa, 1991). However, it is unknown whether this enlargement is independent from glomerular hypertension (Lafferty & Brenner, 1990).

Carvedilol also possesses other properties including calcium channel blockade (>1 μM; Ruffolo *et al.*, 1991) and antioxidant activity leading to inhibition of lipid peroxidation (IC_{50}>5 μM; Yue & Feuerstein, 1992). Any speculation as to the contribution of these actions to the renal protection observed in the present study would be premature. Certainly, data in normotensive animals would indicate that the primary pharmacological effects of carvedilol reside in its β-blocking and vasodilator properties (Ruffolo *et al.*, 1991). Whether it is merely adequate control of hypertension by carvedilol that provides the beneficial effects in chronic renal failure is not clear. Given the complexity of the mechanisms involved in the development of chronic renal failure (see above) this question remains to be answered. Certainly, the data of Anderson *et al.* (1985) indicate that it is control of glomerular rather than systemic hypertension that is of prime importance, and studies on the effects of carvedilol on glomerular haemodynamics might provide some more insight.

In summary, carvedilol, a novel multiple action drug that is currently being used for the treatment of mild to moderate hypertension and is in clinical trials for utility in angina and congestive heart failure, may also demonstrate utility in chronic renal failure. Our observation that carvedilol has similar effectiveness as the converting enzyme, captopril, in reducing the hypertension, proteinuria and glomerulosclerosis associated with 5/6 nephrectomy in rats portends chronic renal disease as a therapeutic target for this drug.

The authors are grateful to Sue Tirri for expert secretarial assistance.

References

ALBRIGHTSON, C.R., ZABKO-POTAPOVICH, B. & BROOKS, D.P. (1992). Effect of carvedilol in mitogen-stimulated mesangial cell proliferation. *Pharmacol. Commun.*, **1**, 267–272.

ANDERSON, S., MEYER, T.W., RENNKE, H.G. & BRENNER, B.M. (1985). Control of glomerular hypertension limits glomerular injury in rats with reduced renal mass. *J. Clin. Invest.*, **76**, 612–619.

BENIGNI, A., PERICO, N., GASPARI, F., ZOJA, C., BELLIZZI, L., GABANELLI, M. & REMUZZI, G. (1991). Increased renal endothelin production in rats with renal mass reduction. *Am. J. Physiol.*, **260**, F331–F339.

BRENNER, B.M. (1985). Nephron adaptation to renal injury or ablation. *Am. J. Physiol.*, **249**, F324–F337.

BROOKS, D.P., CONTINO, L.C., STORER, B. & OHLSTEIN, E.H. (1991). Increased endothelin excretion in rats with renal failure induced by partial nephrectomy. *Br. J. Pharmacol.*, **104**, 987–989.

DAVIDSOHN, L. & HENRY, J.B. (1969). *Clinical Diagnosis by Laboratory Methods*, 14th ed., p. 48. Philadelphia: W.B. Saunders.

FOGO, A. & ICHIKAWA, I. (1991). Evidence for a pathologic linkage between glomerular hypertrophy and sclerosis. *Am. J. Kid. Dis.*, **17**, 666–669.

FRIES, J.W.U., SANDSTROM, D.J., MEYER, T.W. & RENNKE, H.G. (1989). Glomerular hypertrophy and epithelial cell injury modulate progressive glomerulosclerosis in the rat. *Lab. Invest.*, **60**, 205–218.

GELLAI, M., DEWOLF, R.A & RUFFOLO, R.R. Jr. (1990). Effect of carvedilol and renal hemodynamics and renal excretory function in spontaneously hypertensive rat. *Pharmacology*, **41**, 200–206.

HALL, R.L., WILKE, W.L. & FETTMAN, M.J. (1985). Captopril slows the progression of chronic renal disease in partially nephrectomized rats. *Toxicol. Appl. Pharmacol.*, **80**, 517–526.

HIROSE, D.R., OSTERBY, M.N. & GUNDERSON, H.J.G. (1982). Development of glomerular lesions experimental long-term diabetes in the rat. *Kidney Int.*, **21**, 689–695.

IBSEN, K. & SEDERBERG-OLSEN, P. (1973). Changes in glomerular filtration rate during long-term treatment with propranolol in patients with arterial hypertension. *Clin. Sci.*, **44**, 129–134.

KLAHR, S. (1991). Chronic renal failure: management. *The Lancet*, **338**, 423–427.

LAFFERTY, H.M. & BRENNER, B.M. (1990). Are glomerular hypertension and 'hypertrophy' independent risk factors for progression of renal disease? *Semin. Nephol.*, **10**, 294–304.

NAHAS, A.M., BASSETT, A.H., COPE, G.H. & LECARPENTIER, J.E. (1991). Role of growth hormone in the development of renal scarring. *Kidney Int.*, **40**, 29–34.

NAKAMOTO, H., SUZUKI, H., KATSUMATA, H., OHISHI, A., SARUTA, T. & SAKAGUCHI, H. (1988). Effects of carvedilol on renal function and blood pressure in three-fifths nephrectomized spontaneously hypertensive rats loaded with high salt. *Drugs*, **36** (Suppl. 6), 160–164.

RADIN, M.J., WILKE, W.L. & FETTMAN, M.J. (1987). Effect of propranolol on progression of chronic renal failure. *Res. Commun. Chem. Pathol. Pharmacol.*, **57**, 3–13.

REIFF, K. (1987). High-performance liquid chromatographic method for the determination of carvedilol and its desmethyl metabolite in body fluids. *J. Chromatogr.*, **413**, 355–362.

ROSENBERG, M.E. & HOSTETTER, T.H. (1991). Comparative effects of antihypertensives on proteinuria: angiotensin-converting enzyme inhibitor versus alpha-1 antagonist. *Am. J. Kidney Dis.*, **18**, 472–482.

RUFFOLO, R.R. Jr., BOYLE, D.A., VENUTI, R.P. & LUKAS, M.A. (1991). Carvedilol (Kredex®): a novel multiple action cardiovascular agent. *Drugs Today*, **27**, 465–492.

SHIMAMURA, T. & MORRISON, A.B. (1975). A progressive glomerulosclerosis occurring in partial five-sixths nephrectomy. *Am. J. Pathol.*, **79**, 407–417.

SUNG, C.-P., ARLETH, A.J. & OHLSTEIN, E.H. (1993). Carvedilol inhibits vascular smooth muscle cell proliferation. *J. Cardiovasc. Pharmacol.*, **21**, 221–227.

TRACHTMAN, H., DEL PIZZO, R., FUTTERWEIT, S., LEVINE, D., RAO, P.S., VALDERRAMA, E. & STURMAN, J.A. (1992). Taurine attenuates renal disease in chronic puromycin aminonucleoside nephropathy. *Am. J. Physiol.*, **31**, F117–F123.

WARREN, D.J. (1976). β-Adrenergic receptor blockade and renal function. *Am. Heart J.*, **91**, 255–266.

WEBER, M.A. & DRAYER, J.I.M. (1980). Renal effects of β-adrenoceptor blockade. *Kidney Int.*, **18**, 686–699.

WEIBEL, E.R. (1979). *Stereological Methods: Practical Methods for Biological Morphometry*. Vol. 1. pp. 51–57. London: Academic.

YOSHIDA, Y., FOGO, A. & SHIRAGA, H. (1988a). Serial micropuncture analysis of a single nephron function in the rat model of subtotal renal ablation. *Kidney Int.*, **33**, 855–867.

YOSHIDA, Y., FOGO, A., SHIRAGA, H., GLICK, A.D. & ICHIKAWA, I. (1988b). Serial micropuncture analysis of single nephron function in arresting progressive renal ablation. *Kidney Int.*, **33**, 855–867.

YUE, T.-L., LIU, T. & FEUERSTEIN, G.Z. (1992). Carvedilol, a new vasodilator and β-adrenoceptor, inhibits oxygen-radical-mediated lipid peroxidation in swine ventricular membranes. *Pharmacol. Commun.*, **1**, 27.

(Received December 14, 1992
Revised February 17, 1993
Accepted February 22, 1993)

Br. J. Pharmacol. (1993), **109**, 587–591 © Macmillan Press Ltd, 1993

Impairment of pulmonary-artery endothelium-dependent relaxation in chronic obstructive lung disease is not due to dysfunction of endothelial cell membrane receptors nor to L-arginine deficiency

[1]A.T. Dinh-Xuan, J. Pepke-Zaba, A.Y. Butt, G. Cremona & [2]T.W. Higenbottam

Department of Respiratory Physiology, Papworth Hospital, Cambridge CB3 8RE

1 Endothelium-dependent relaxation mediated by endothelium-derived relaxing factor (EDRF) or nitric oxide (NO), is impaired in pulmonary arteries (PA) of hypoxic patients with chronic obstructive lung disease (COLD). To determine the mechanisms responsible for this impairment, we compared the response of rings of isolated PA from 12 COLD patients and 8 controls to the endothelium-dependent vasodilators acetylcholine (ACh), adenosine diphosphate (ADP), and the calcium ionophore, A23187. The response of PA rings to the endothelium-independent nitro-vasodilator sodium nitroprusside (SNP) was also studied in both groups. The PA rings had been pre-contracted by the α-adrenoceptor agonist phenylephrine (PE).

2 Endothelium-dependent relaxation was significantly reduced in PA rings from COLD patients as compared with controls when tested with ACh (37.8 ± 8.8% vs 73.4 ± 7.9%), ADP (38.4 ± 6.7% vs 80 ± 5.6%), and the calcium ionophore, A23187 (35.8 ± 6.1% vs 87 ± 6.6%). Relaxation with SNP was, however, significantly greater in PA rings from COLD patients (99.4 ± 0.6% vs 90.3 ± 3.1%), as was the contractile response to PE (1.91 ± 0.21 g vs 1.33 ± 0.15 g). Pretreatment with the specific inhibitor of NO formation, N^G-monomethyl-L-arginine (L-NMMA; 10^{-4} M) significantly reduced the relaxation to ACh in all PA rings. This inhibition could be reversed by L-arginine (10^{-3} M), the substrate for NO synthesis. Pretreatment with L-arginine alone, however, did not restore the impaired endothelium-dependent relaxation of PA rings from COLD patients.

3 We conclude that EDRF (NO) production is impaired in PA rings from COLD patients and that this impairment is neither due to endothelial receptors dysfunction nor a defect of L-arginine availability and/or transport. Our hypothesis is that the abnormality must lie within the biosynthesis pathway of NO from L-arginine, possibly involving the endothelial enzyme cell, NO synthase, the normal function of which might be altered by chronic hypoxia.

Keywords: Nitric oxide; L-arginine; pulmonary hypertension; endothelial cell membrane receptors; nitrovasodilators

Introduction

Pulmonary hypertension often develops in patients with end-stage chronic obstructive lung disease (COLD) as a result of structural alterations of lung vessels and increased pulmonary vascular reactivity (Reeves & Voelkel, 1989). Remodelling of the intima is among the early markers of pulmonary vascular disease in COLD patients (Magee *et al.*, 1988). The endothelial cells, one of the main cell types of the intima, normally synthesize and release the powerful endothelium-derived relaxing factor (EDRF) (Furchgott & Zawadzki, 1980), now identified as nitric oxide (NO) (Palmer *et al.*, 1987). NO is formed from L-arginine (Palmer *et al.*, 1988), by a cytosolic enzyme, called NO synthase (NOS) (Palmer & Moncada, 1989). This enzyme exists in different isoforms including an inducible and a constitutive one (Moncada *et al.*, 1991). The latter is the predominant form in endothelial cells. The formation of NO can be stereospecifically inhibited by the L-arginine analogue, N^G-monomethyl-L-arginine (L-NMMA) (Rees *et al.*, 1989), which has been used to study the physiological roles of NO (Moncada *et al.*, 1991; Vane *et al.*, 1990).

NO modulates pulmonary vascular tone in man in both disease (Dinh-Xuan *et al.*, 1989; 1990a; 1991) and health (Dinh-Xuan *et al.*, 1990b). We found that relaxation of pulmonary arteries in response to the endothelium-dependent vasodilators, acetylcholine (ACh) and adenosine diphosphate (ADP), is impaired in patients with pulmonary hypertension in Eisenmenger's syndrome and COLD, including cystic fibrosis. This impairment could be due to altered function of muscarinic receptors and purinoceptors, or to endothelial cell dysfunction which is beyond the receptor-agonist coupling mechanism. Alternatively, it could result from a deficiency of L-arginine, a substrate for NO synthesis. To assess which mechanism is responsible, we report studies of the relaxation of isolated pulmonary arteries from COLD patients in response to various endothelium-dependent vasodilators, including the calcium ionophore, A23187. The latter is known to induce the release of NO non-specifically, without involving endothelial cell membrane receptors stimulation. We also report the effect of pretreatment *in vitro* with L-arginine on the impaired pulmonary endothelium-dependent relaxation in these patients. The aim of this study was to determine whether dysfunction of endothelial cell membrane receptors, substrate deficiency, or abnormal NOS activity, causes the impaired pulmonary endothelium-dependent relaxation in COLD patients.

Methods

Subjects

Isolated pulmonary arterial (PA) rings were studied from the explanted lungs of 12 patients undergoing lung transplantation for end-stage COLD (Higenbottam *et al.*, 1990). Control pulmonary arterial rings were obtained from 8 patients undergoing lobectomy or pneumonectomy for lung car-

[1] Present address: Laboratoire d'Explorations Fonctionnelles, Hôpital Cochin, 75014 Paris, France.
[2] Author for correspondence.

Table 1 Clinical characteristics and preoperative lung function and arterial blood gas values of the study groups

Diagnosis	*Age*	*Sex*	FEV_1*	*FVC** litres (% of predicted)	*RV**	Pa_{O_2}	Pa_{CO_2} kPa†
COLD patients							
Emphysema	47	F	0.5 (17)	2.8 (76)	5.3 (279)	8.7	7.1
Emphysema	56	F	0.2 (09)	0.8 (27)	8.5 (472)	NA*	NA
Cystic fibrosis	27	F	0.5 (18)	1.2 (37)	3.8 (345)	8.6	5.6
Cystic fibrosis	33	M	1.3 (33)	1.7 (35)	3.6 (212)	9.0	5.1
Cystic fibrosis	24	F	0.7 (21)	1.5 (41)	2.3 (209)	7.7	4.5
Cystic fibrosis	29	F	0.5 (16)	1.2 (33)	4.3 (307)	8.0	5.5
Bronchiectasis	48	M	0.3 (08)	1.3 (27)	7.2 (351)	6.1	6.6
Emphysema	56	M	0.2 (07)	1.3 (27)	7.8 (380)	3.5	6.6
Cystic fibrosis	30	F	0.6 (24)	1.6 (52)	2.6 (236)	9.6	5.7
Cystic fibrosis	28	M	0.6 (16)	1.3 (29)	4.3 (287)	6.8	7.5
Cystic fibrosis	41	M	0.5 (13)	2.4 (48)	6.1 (313)	6.6	5.2
Emphysema	54	M	0.4 (10)	4.0 (79)	7.4 (315)	7.8	6.1
Control patients							
§Lung carcinoma	62	M	2.7 (83)	3.3 (80)	2.7 (115)	11.7	5.2
§Lung carcinoma	53	F	2.2 (92)	2.9 (98)	2.0 (118)	NA	NA
§Lung carcinoma	55	M	2.3 (74)	3.9 (98)	3.0 (102)	11.4	5.1
§Lung carcinoma	50	M	2.9 (78)	3.7 (79)	2.2 (102)	10.9	5.6
Lung carcinoma	56	F	2.4 (98)	3.6 (118)	2.1 (117)	11.8	5.3
§Lung carcinoma	67	M	3.1 (102)	4.5 (115)	3.4 (136)	11.2	5.2
§Lung carcinoma	74	M	2.2 (81)	2.8 (80)	3.0 (115)	12.8	5.0
Lung carcinoma	63	F	2.2 (116)	3.1 (132)	2.2 (133)	12.3	5.3

*FEV_1 denotes forced expiratory volume in one second, FVC, forced vital capacity; RV, residual volume; NA, data not available.
†To convert values for Pa_{O_2} and Pa_{CO_2} to mmHg multiply by 7.5.
§Smoker ($\geq$10 pack years).

cinoma who did not have evidence of other chronic lung disease. Their individual diagnoses, anthropometric data, and pre-operative lung function tests together with blood gas measurements are listed in Table 1.

In vitro *study*

Tissue preparation Details of the preparation of PA rings have been described (Dinh-Xuan *et al.*, 1990b; 1991). In brief, the excised lung was immediately placed in Krebs-Ringer bicarbonate solution at 4°C which had been pregassed with 95% O_2 and 5% CO_2. Pairs of rings were obtained from lobar, segmental and subsegmental pulmonary arteries which had been carefully dissected and cleaned of excess connective tissue. The endothelium was carefully removed from some rings with a pipe cleaner. All pulmonary arterial rings obtained from the same patient were similar in size (range of external diameter, 1.3 to 2.2 mm), and were cut from adjacent parts of the middle of pulmonary arterial branches.

Cumulative dose-relaxation studies The PA rings were studied in 20 ml organ baths filled with Krebs-Ringer bicarbonate buffer, bubbled continuously with 95% O_2 and 5% CO_2, and kept at 37°C by an outer water bath warmed by a recirculating heater (Circulator C-400, Techne Ltd., Cambridge, U.K.). Changes in isometric tension were recorded in each ring preset at its optimal length for tension development by a force transducer (Category No. 52-9529, Harvard Bioscience, Massachussets, U.S.A.) connected to a chart drive recorder (PM 8252A, Philips, Eindhoven, The Netherlands). The rings were then allowed to equilibrate in the bath for at least 90 min during which time the fluid in the bath was changed every 15 min. After equilibration, all rings were preincubated for 30 min with indomethacin (10^{-5} M) which remained in the bath throughout the studies. All rings were submaximally precontracted with phenylephrine dichloride (PE) (10^{-6} M) to obtain a stable plateau of increased tension. Cumulative concentrations of the endothelium-dependent vasodilators, acetylcholine (ACh; 10^{-10} to 10^{-5} M), adenosine diphosphate (ADP; 10^{-10} to 10^{-5} M), and the calcium ionophore A23187 (10^{-8} to 10^{-3} M) were then added to the rings which were studied either with or without endothelium. Relaxation to cumulative doses of the endothelium-independent vasodilator, sodium nitroprusside (SNP; 10^{-8} to 10^{-4} M), was also studied in intact PA rings from both patient groups.

Inhibition of NO synthesis and pretreatment with L-arginine The optimal time of incubation (10 min), and the optimal dose of L-NMMA (10^{-4} M) were determined in preliminary studies on PA rings from 3 control and 3 COLD patients. Also, the endothelium-dependent rise in tension after adding L-NMMA was found to be maximal after submaximal contraction of the rings with PE. This led to a fixed protocol for the studies. To both rings with and without endothelium, L-NMMA (10^{-4} M) was added after PE, then after a delay of 10 min, the cumulative dose-response studies to ACh (10^{-10} to 10^{-5} M) were performed. To see whether L-arginine could reverse the inhibitory effects of L-NMMA, some rings were incubated for 10 min with both L-NMMA (10^{-4} M) and L-arginine. In addition, some rings were studied over 30 min (range, 30 to 45 min) incubation with L-arginine (10^{-3} M) alone to see whether *in vitro* supplementation of L-arginine could alter the endothelium-dependent relaxation to ACh in both diseased and control PA rings.

Drugs

All the drugs were purchased from Sigma Chemical (Poole, Dorset), except for L-NMMA which was donated by Wellcome Research Laboratories (Beckenham, Kent). The drugs were diluted in distilled water, except for indomethacin and the calcium ionophore, A23187, which were dissolved in 50% ethanol and dimethylsulphoxide, respectively. The final concentration of dimethylsulphoxide in the organ bath did not exceed 0.2% which, in itself, did not have any effect on the tissue, nor did 50% ethanol have any effect. All solutions were freshly prepared before use.

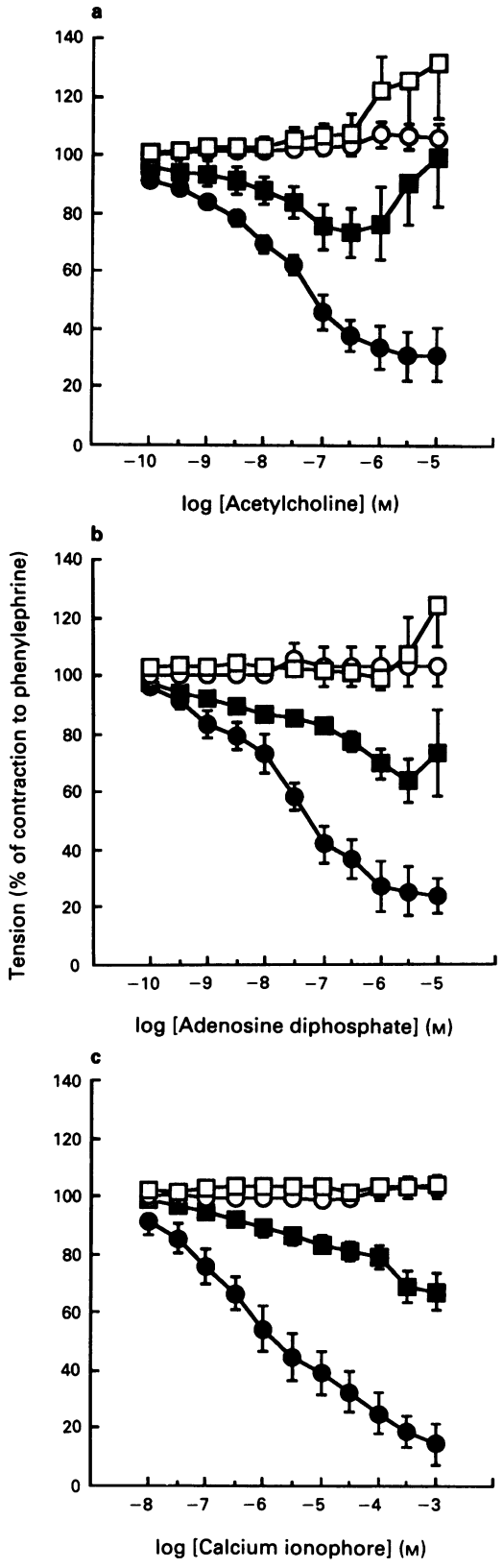

Figure 1 Endothelium-dependent relaxation in rings with (closed symbols) and without (open symbols) endothelium in response to cumulative doses of acetylcholine (a), adenosine diphosphate (b) and the calcium ionophore A23187 (c) in control (circles) and COLD (squares) patients. Results are expressed as means ± s.e.mean of 4 to 12 observations.

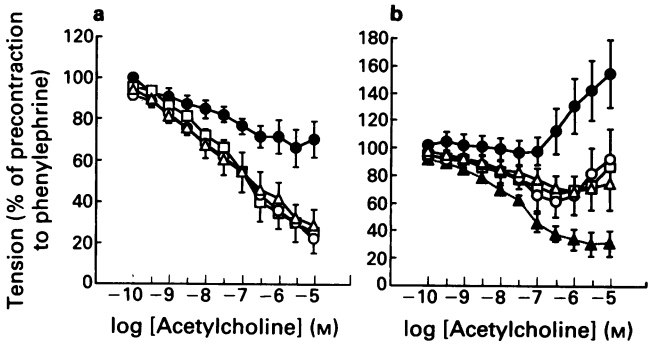

Figure 2 Dose-response curves in response to acetylcholine in rings from control (a) and COLD (b) patients. The rings are divided into 4 groups as follows; untreated (○), treated with N^G-monomethyl-L-arginine (L-NMMA, 10^{-4} M) (●), treated with L-NMMA (10^{-4} M) + L-arginine (10^{-3} M) (□), and treated with L-arginine (10^{-3} M) (△). In (b) results from untreated rings from controls (▲) are shown for comparison with L-arginine-treated rings from COLD patients (△). The results are expressed as means ± s.e.mean of 5–7 observations.

Statistical analysis

Student's *t* test for paired and unpaired values were used. When more than two groups of observations were compared, an analysis of variance was performed. This was followed by multiple comparisons using Scheffé's method to assess significant differences among group means. All data are expressed as mean ± s.e.mean. A *P* value of less than 0.05 was considered significant.

Results

All COLD patients had severe airflow obstruction FEV_1 = 16 ± 2% of predicted; range, 7–33%) and had arterial hypoxaemia (PaO_2 = 7.5 ± 0.5 kPa, range, 3.5–9.6 kPa) (Table 1). By contrast, none of the control patients had impaired lung function (FEV_1 = 90.5 ± 5% of predicted; range, 74–116%) and none had values of PaO_2 below 10.9 kPa (range, 10.9–12.8 kPa) (Table 1).

In both patient groups, ACh, ADP and the calcium ionophore, A23187, caused a concentration-dependent relaxation in PA rings where the endothelium was left intact, but not in those where the endothelium had been removed (Figure 1). Compared with controls there was a significant impairment of endothelium-dependent relaxation to ACh, ADP and the calcium ionophore A23187, in PA rings from COLD patients (Figure 1).

Pretreatment with L-NMMA (10^{-4} M) significantly inhibited endothelium-dependent relaxation to ACh in PA rings from both patient groups (Figure 2). However, this inhibition could be reversed by an excess of L-arginine (10^{-3} M) in all PA rings (Figure 2). Incubation of the rings with L-arginine (10^{-3} M) for over 30 min (range, 30 to 45 min) did not increase the endothelium-dependent relaxation to ACh of pulmonary arterial rings from either the control or the COLD patients (Figure 2). Impaired endothelium-dependent relaxation to ACh remained in the L-arginine-treated rings from COLD patients (maximal relaxation = 41.4 ± 9%) as compared with rings from control patients (maximal relaxation = 77.8 ± 7.2%) ($P < 0.05$) (Figure 2).

Rings of COLD patients developed a greater tension (1.91 ± 0.21 g) in response to phenylephrine (10^{-6} M) than rings from control patients (1.33 ± 0.15 g) ($P < 0.05$). However, this difference was eliminated by either mechanical removal of the endothelium or pretreatment with L-NMMA (10^{-4} M) (Figure 3). Both procedures resulted in a significantly greater contraction in response to phenylephrine (10^{-6} M) in control PA rings, but not in rings from COLD patients (Figure 3).

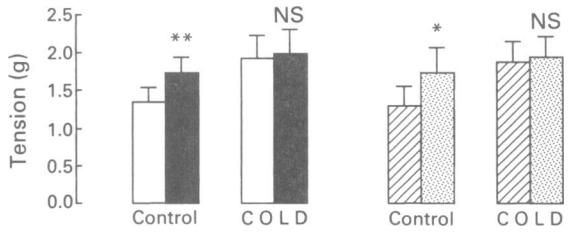

Figure 3 Absolute tension developed in response to phenylephrine (10^{-6} M) in rings with (open columns) and without (solid columns) endothelium, and rings treated (stippled columns) and untreated (hatched columns) with N^G-monomethyl-L-arginine (L-NMMA). Both removal of endothelium and L-NMMA pretreatment cause a significant rise in tension in rings from controls but not in COLD rings. $*P<0.05$; $**P<0.01$; NS (not significant). The results are expressed as means ± s.e.mean of 5–12 observations.

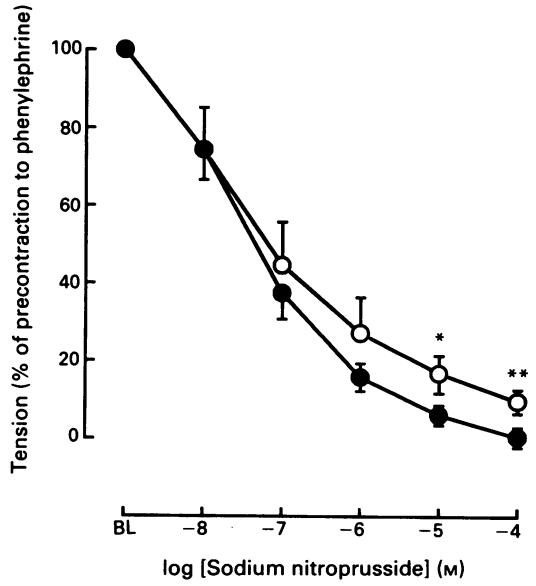

Figure 4 Endothelium-independent relaxation to sodium nitroprusside in rings with endothelium from control (○) and COLD (●) patients. Results are expressed as means ± s.e.mean of 6–8 observations. BL is baseline tension after precontraction to phenylephrine and before addition of sodium nitroprusside. $*P<0.05$; $**P<0.01$.

There was no significant difference between the concentration of SNP needed to achieve a 50% relaxation (EC_{50}) in PA rings from control patients ($-\log EC_{50} = 7.7 \pm 1.1$) and COLD rings ($-\log EC_{50} = 7.8 \pm 0.7$). However, there was a significantly greater degree of maximum relaxation in COLD rings compared with controls when tested with 10^{-5} M SNP ($94 \pm 1.5\%$ vs $83.3 \pm 4.9\%$; $P<0.05$) and with 10^{-4} M SNP ($99.4 \pm 0.6\%$ vs $90.3 \pm 3.1\%$; $P<0.01$) (Figure 4).

Discussion

These results confirm that endothelium-dependent relaxation in the PA of COLD patients is impaired (Dinh-Xuan *et al.*, 1991). They are consistent with the experimental observation that chronic hypoxia impairs pulmonary endothelium-dependent relaxation (Adnot *et al.*, 1991). The reduced EDRF (NO) release also accounts for the greater tension with PE in the PA rings from COLD patients. This effect is endothelium-dependent as mechanical removal or inhibition of NOS resulted in a similar rise in tension with PE in control rings but not those from COLD patients (Figure 3). Conversely, greater relaxation of PA rings from COLD patients occurred in response to SNP compared with controls (Figure 4). This is consistent with the view that a chronic reduction of endothelial NO production has occurred in COLD patients' pulmonary arteries.

A defective receptor-agonist coupling mechanism of the endothelial cell could account for the reduced EDRF (NO) release in the PA of COLD patients. Such a selective receptor dysfunction has been described in systemic arteries with atherosclerosis (Bossaller *et al.*, 1987) or after oxygen-derived free radical injury (Pieper & Gross, 1989). This was inferred from the impaired endothelium-dependent relaxation with both ACh and ADP, whilst normal relaxation occurred with the calcium ionophore, A23187. The calcium ionophore activates the endothelium NOS without requiring a specific membrane receptor, unlike ACh and ADP. By contrast, we observed comparable impaired endothelium-dependent relaxation not only with ACh and ADP but also calcium ionophore. This suggests an abnormality in the PA of COLD patients lies beyond the membrane receptor-agonist coupling mechanism.

The enzyme NOS has a recognition site for its substrate L-arginine and requires the dioxygen (O_2) molecule for the other substrate (Kwon *et al.*, 1990; Moncada *et al.*, 1991). A deficiency of L-arginine is unlikely to account for our results. Incubation with L-arginine can restore impaired endothelium-dependent relaxation in foetal pulmonary arteries (Abman *et al.*, 1991) and in cerebral vessels of hypercholesterolaemic rabbits (Rossitch *et al.*, 1991). Incubation with L-arginine however failed to improve the reduced endothelium-dependent relaxation in the PA of COLD patients or in normals.

The failure of incubation of the PA with excess L-arginine to restore relaxation is not due to defective transmembrane uptake of L-arginine into the endothelium. The inhibitory effects of L-NMMA, which utilizes a common transport system with L-arginine (Mann *et al.*, 1990), were readily reversed by an excess of L-arginine (10^{-3} M) in both normals and COLD patients PA (Figure 2).

Acute hypoxia can reduce EDRF release (Johns *et al.*, 1989; Warren *et al.*, 1989). This is putatively causing a substrate deficiency for the enzyme NOS. A similar explanation cannot account for our results from patients with chronic hypoxaemia. The PA rings were studied after 90 min equilibration under hyperoxic conditions in the organ baths, which resulted in values of PaO_2 in excess of 75 kPa (Pepke-Zaba *et al.*, 1992). Experimental chronic alveolar hypoxia causes a reversible impairment of pulmonary endothelium-dependent relaxation (Adnot *et al.*, 1991). In this study the COLD patients were all hypoxaemic. We have previously shown a significant correlation between the impaired endothelium-dependent relaxation in COLD patients with their degree of pre-operative chronic hypoxaemia (Dinh-Xuan *et al.*, 1991). It is possible that chronic hypoxia reduces the activity of pulmonary endothelial NOS although the mechanism requires elucidation.

In summary the pulmonary arteries, studied *in vitro*, from patients with COLD have evidence of impaired endothelium-dependent relaxation. This is not the result of substrate deficiency nor membrane receptor-agonist coupling dysfunction. It appears to reside within the cell as a reduction of activity of the pulmonary endothelium NOS activity.

We thank Mr J. Wallwork, Mr F.C. Wells and Mr S.R. Large (Department of Cardiothoracic Surgery, Papworth Hospital), and Drs S. Stewart and N. Cary (Department of Histopathology, Papworth Hospital) for their support and for allowing us to study pulmonary vascular tissue. We also thank Mr Ben Milstein for his patient editorial comments and criticisms, and Mrs Carolyn Williams for her assistance with the preparation of this manuscript.

This study was supported by grants No. 90/36 from the British Heart Foundation and No. 326 from the Cystic Fibrosis Research Trust, and by a travel grant from the Foundation Simone and Cino del Duca.

References

ABMAN, S.H., CHATFIELD, B.A., RODMAN, D.M., HALL, S.L. & MCMURTRY, I.F. (1991). Maturational changes in endothelium-derived relaxing factor activity of ovine pulmonary arteries in vitro. *Am. J. Physiol.*, **260**, L280–L285.

ADNOT, S., RAFFESTIN, B., EDDAHIBI, S., BRAQUET, P. & CHABRIER, P.-E. (1991). Loss of endothelium-dependent relaxant activity in the pulmonary circulation of rats exposed to chronic hypoxia. *J. Clin. Invest.*, **87**, 155–162.

BOSSALLER, C., HABIB, C.B., YAMAMOTO, H., WILLIAMS, C., WELLS, S. & HENRY, P.D. (1987). Impaired muscarinic endothelium-dependent relaxation and cyclic guanosine 5'-monophosphate production in atherosclerotic human coronary artery and rabbit aorta. *J. Clin. Invest.*, **79**, 170–174.

DINH-XUAN, A.T., HIGENBOTTAM, T.W., CLELLAND, C.A., PEPKE-ZABA, J., CREMONA, G., BUTT, A.Y., LARGE, S.R., WELLS, F.C. & WALLWORK, J. (1991). Impairment of endothelium-dependent pulmonary-artery relaxation in chronic obstructive lung disease. *N. Engl. J. Med.*, **324**, 1539–1547.

DINH-XUAN, A.T., HIGENBOTTAM, T.W., CLELLAND, C.A., PEPKE-ZABA, J., CREMONA, G. & WALLWORK, J. (1990a). Impairment of pulmonary endothelium-dependent relaxation in patients with Eisenmenger's syndrome. *Br. J. Pharmacol.*, **99**, 9–10.

DINH-XUAN, A.T., HIGENBOTTAM, T.W., CLELLAND, C.A., PEPKE-ZABA, J., WELLS, F.C. & WALLWORK, J. (1990b). Acetylcholine and adenosine diphosphate cause endothelium-dependent relaxation of isolated human pulmonary arteries. *Eur. Respir. J.*, **3**, 633–638.

DINH-XUAN, A.T., HIGENBOTTAM, T.W., PEPKE-ZABA, J., CLELLAND, C.A. & WALLWORK, J. (1989). Reduced endothelium-dependent relaxation of cystic fibrosis pulmonary arteries. *Eur. J. Pharmacol.*, **163**, 401–403.

FURCHGOTT, R.F. & ZAWADZKI, J.V. (1980). The obligatory role of endothelial cells in the relaxation of arterial smooth muscle by acetylcholine. *Nature*, **288**, 373–376.

HIGENBOTTAM, T.W., OTULANA, B.A. & WALLWORK, J. (1990). Transplantation of the lung. *Eur. Respir. J.*, **3**, 594–605.

JOHNS, R.A., LINDEN, J.M. & PEACH, M.J. (1989). Endothelium-dependent relaxation and cyclic GMP accumulation in rabbit pulmonary artery are selectively impaired by moderate hypoxia. *Circ. Res.*, **65**, 1508–1515.

KWON, N.S., NATHAN, C.F., GILKER, C., GRIFFITH, O.W., MATTHEWS, D.E. & STUEHR, D.J. (1990). L-citrulline production from L-arginine by macrophage nitric oxide synthase: the ureido oxygen derives from dioxygen. *J. Biol. Chem.*, **265**, 13442–13445.

MAGEE, F., WRIGHT, J.L., WIGGS, B.R. & HOGG, J.C. (1988). Pulmonary vascular structure and function in chronic obstructive pulmonary disease. *Thorax*, **43**, 183–189.

MONCADA, S., PALMER, R.M.J. & HIGGS, E.A. (1991). Nitric oxide: physiology, pathophysiology, and pharmacology. *Pharmacol. Rev.*, **43**, 109–142.

MANN, G.E., SHERIFF, C.-J. & PEARSON, J.D. (1990). In *Nitric Oxide from L-Arginine: A Bioregulatory System*. ed. Moncada, S. & Higgs, E.A. pp. 331–339. Amsterdam: Elsevier.

PALMER, R.M.J., ASHTON, D.S. & MONCADA, S. (1988). Vascular endothelial cells synthesize nitric oxide from L-arginine. *Nature*, **333**, 664–666.

PALMER, R.M.J., FERRIGE, A.G. & MONCADA, S. (1987). Nitric oxide release accounts for the biological activity of endothelium-derived relaxing factor. *Nature*, **327**, 524–526.

PALMER, R.M.J. & MONCADA, S. (1989). A novel citrulline-forming enzyme implicated in the formation of nitric oxide by vascular endothelial cells. *Biochem. Biophys. Res. Commun.*, **158**, 348–352.

PEPKE-ZABA, J., HIGENBOTTAM, T.W., CREMONA, G., BUTT, A.Y. & DINH-XUAN, A.T. (1992). Ouabain inhibits hypoxia-induced relaxation of human conduit pulmonary arteries. *Am. Rev. Respir. Dis.*, **145**, A226.

PIEPER, G.M. & GROSS, G.J. (1989). Selective impairment of endothelium-dependent relaxation by oxygen-derived free radicals: distinction between receptor versus nonreceptor mediators. *Blood Vessels*, **26**, 44–47.

REES, D.D., PALMER, R.M.J., HODSON, H.F. & MONCADA, S. (1989). A specific inhibitor of nitric oxide formation from L-arginine attenuates endothelium-dependent relaxation. *Br. J. Pharmacol.*, **96**, 418–424.

REEVES, J.T. & VOELKEL, N.F. (1989). Mechanisms of chronic pulmonary hypertension: basic considerations. In *Pulmonary Circulation: Advances and Controversies*. ed. Wagenvoort, C.A. & Denolin, H. pp. 27–39. Amsterdam: Elsevier.

ROSSITCH, E. Jr., ALEXANDER III, E., BLACK, P.McL. & COOKE, J.P. (1991). L-arginine normalizes endothelial function in cerebral vessels from hypercholesterolemic rabbits. *J. Clin. Invest.*, **87**, 1295–1299.

VANE, J.R., ÄNGGÅRD, E.E. & BOTTING, R.M. (1990). Mechanisms of disease: regulatory functions of the vascular endothelium. *N. Engl. J. Med.*, **323**, 27–36.

WARREN, J.B., MALTBY, N.H., MACCORMACK, D. & BARNES, P.J. (1989). Pulmonary endothelium-derived relaxing factor is impaired in hypoxia. *Clin. Sci.*, **77**, 671–676.

(Received June 5, 1992
Revised February 19, 1993
Accepted February 22, 1993)

Br. J. Pharmacol. (1993), **109**, 592–599 © Macmillan Press Ltd, 1993

The antiarrhythmic effects of the nucleoside transporter inhibitor, R75231, in anaesthetized pigs

[1]C.L. Wainwright, J.R. Parratt & *H. Van Belle

Department of Physiology & Pharmacology, University of Strathclyde, Glasgow, and *Department of Biochemistry, Janssen Research Foundation, Beerse, Belgium

1 The effect of R75231, an inhibitor of purine nucleoside transport, were examined on ischaemic arrhythmias in anaesthetized pigs.

2 In closed chest pigs ($n = 4$), R75231 exerted a moderate dose-dependent decrease in mean arterial blood pressure (from 97 ± 4 mmHg to 95 ± 4, 90 ± 1 and 83 ± 2 mmHg at 25, 50 and 100 $\mu g\,kg^{-1}$ respectively) and produced a dose-related shift to the left of the blood pressure dose-response curve to intravenous bolus doses of adenosine. The degree of inhibition of adenosine uptake by R75231, assessed *ex vivo* in erythrocyte suspensions, was $43 \pm 5\%$, 64 ± 13 and $114 \pm 15\%$ at doses of 25, 50 and 100 $\mu g\,kg^{-1}$ respectively.

3 In open chest pigs, intravenous injection of R75231 (50 $\mu g\,kg^{-1}$; $n = 6$ and 100 $\mu g\,kg^{-1}$; $n = 10$) induced a dose-related decrease in both systolic and diastolic arterial blood pressure which was more marked than in closed-chest pigs (mean pressure 86 ± 4 to 70 ± 2 mmHg and 88 ± 6 to 60 ± 6 mmHg with 50 and 100 $\mu g\,kg^{-1}$ respectively), without affecting heart rate or myocardial contractility. Coronary artery occlusion in these pigs caused a secondary decrease in blood pressure. This was not observed in controls ($n = 10$). The lower dose of R75231 did not exert any antifibrillatory effects, whereas the higher dose significantly reduced the incidence of ventricular fibrillation, from 80% in control pigs to 30%. Neither dose modified the incidence of ventricular tachycardia (33% and 40% with 50 and 100 $\mu g\,kg^{-1}$ respectively, compared to 30% in controls) or had any effect on the total number of ventricular ectopic beats (85 ± 47 and 130 ± 31 vs 110 ± 19 in controls). R75231, at a dose of 100 $\mu g\,kg^{-1}$, also attenuated the ischaemia-induced shortening of QRS-interval, but neither dose modified the ST-segment depression seen following occlusion.

4 These results show that the nucleoside transport inhibitor, R75231, exerts an antifibrillatory effect in a model of severe myocardial ischaemia in a dose which completely inhibits adenosine uptake *ex vivo*. However, while this agent has minimal haemodynamic effects in closed chest animals, the reduction in blood pressure induced by R75231 in open-chest pigs cannot be excluded as a possible contributory mechanism of the antiarrhythmic effects of this drug.

Keywords: Myocardial ischaemia; coronary artery occlusion; pigs; nucleoside transport inhibition; adenosine; R75231; arrhythmias

Introduction

Since the demonstration in 1970 by Olsson that the accumulation and subsequent release of adenosine is an early consequence of myocardial ischaemia there has been increasing interest in its potential action as a cardioprotective substance. There is a substantial literature (for a recent excellent review see Forman *et al.*, 1993) on the cardioprotective effects of adenosine against myocardial injury induced by reperfusion, involving a variety of mechanisms such as modulation of neutrophil infiltration (Olafsson *et al.*, 1987), preservation of vascular function (Babbitt *et al.*, 1989) and reduction of neutrophil free radical generation (Cronstein *et al.*, 1990). In addition to injury resulting from myocardial ischaemia and reperfusion, adenosine has been shown to protect against coronary occlusion-induced ventricular arrhythmias in rats (Fagbemi & Parratt, 1984) and dogs (Wainwright & Parratt, 1988). Adenosine has long been known to be protective in treating supraventricular arrhythmias in man (Belhassen & Pelleg, 1984) and its clinical use is largely limited to treatment of these arrhythmias (Barber, 1992) because of the frequency of side effects (such as chest pain and dyspnoea; Rankin *et al.*, 1989) associated with its action at A_2-adenosine receptors which are universally distributed throughout the body. As a result, little is known about its ability to reduce ischaemia-induced ventricular arrhythmias in the clinical setting. This therefore restricts not only the use of adenosine but also of stable A_2-adenosine analogues as potential antiarrhythmic therapy. Since adenosine production occurs as an early response to ischaemia, an alternative approach to antiarrhythmic therapy could be to utilize the protective effects of endogenous adenosine by enhancing its concentration at the site(s) where it is required.

Adenosine exerts a role as a 'retaliatory metabolite' (Newby, 1984; Fredholm *et al.*, 1983); that is, its production is increased or 'switched on' by harmful stimuli (such as myocardial ischaemia) as a compensatory mechanism to try to override the underlying problem (e.g. by vasodilatation). This endogenous production of adenosine is, in general, temporary and very localized. The adenosine produced is generally prevented from spreading further than the site of injury by, firstly, rapid uptake by the endothelial cells and, secondly and more slowly, by the erythrocytes, both of which catabolise adenosine to inactive metabolites. If the uptake transport process into endothelial cells were to be inhibited then this would prolong the time adenosine is present in the local area. Thus nucleoside transport inhibition should effectively raise the endogenous levels of adenosine at the site where it is needed and, if the hypothesis that adenosine acts as an 'endogenous cardioprotective substance' is correct (Fagbemi & Parratt, 1984), this kind of intervention could be expected

[1] Author for correspondence at Department of Physiology & Pharmacology, University of Strathclyde, Royal College, 204 George Street, Glasgow G1 1XW

to modify the consequences of acute myocardial ischaemia.

Previous studies with the few existing nucleoside transport inhibitors such as dipyridamole (Wainwright & Parratt, 1988) and lidoflazine (Coker *et al.*, 1982) have indeed shown protection against ventricular arrhythmias during coronary occlusion in dogs. Furthermore, dipyridamole (Blumenthal *et al.*, 1981), lidoflazine (Flameng *et al.*, 1981), mioflazine (Wood *et al.*, 1985) and dilazep (Gupta *et al.*, 1989) have all been shown to reduce infarct size and/or improve functional recovery after myocardial ischaemia in canine hearts. Most of these agents, however, are not 'pure' nucleoside transport inhibitors. Dipyridamole is well documented as possessing the ability to inhibit vascular phosphodiesterase isoenzymes (Ahn *et al.*, 1989) and enhance prostacyclin synthesis (Blass *et al.*, 1980), whereas dilazep possesses calcium antagonist activity. These are effects which are seen at micromolar concentrations and could therefore contribute to their observed cardioprotective effects. R75231 (2-(aminocarbonyl)-*N*-(4-amino-2,6-dichlorophenyl)-4-[5,5-*bis*-(4-fluorphenyl)pentyl]-1-piperazine acetamide (free base); Ijzerman *et al.*, 1989) is a lidoflazine analogue which has been described as a specific inhibitor of nucleoside transport (Van Belle & Jansen, 1991). The term specific is applied in so far as it has been shown to be devoid of activity in a wide range of *in vitro* and *in vivo* systems designed to test activity at specified receptors and it is also ineffective against adenosine deaminase, nucleoside phosphorylase, adenosine kinase and phosphodiesterase (Van Belle *et al.*, 1992) in micromolar concentrations. In addition to this apparent specificity for nucleoside transport inhibition, R75231 has an added advantage over existing transport inhibitors in that it has a longer duration of action (hours compared to minutes in the cases of dilazep and dipyridamole; Van Belle & Janssen, 1991) and is orally active, compared to the variable oral bioavailability with dipyridamole (Stringer *et al.*, 1992). Its potency *in vitro* is comparable with other transport inhibitors (IC_{50} for inhibition of adenosine uptake by packed erythrocytes: 1.1×10^{-8} M for R75231 vs 1.9×10^{-8} M and 1.75×10^{-8} M for dipyridamole and myoflazine respectively; Van Belle & Janssen, 1991). Thus R75231 possesses properties which would improve its potential for therapeutic use over existing nucleoside transport inhibitors. The aim of the present study therefore was to assess the ability of R75231 to suppress ventricular arrhythmias in a model of severe ischaemia in open-chest anaesthetized pigs.

Methods

Animal preparation

Large White/Welsh Landrace cross breed pigs (25–40 kg) were used in the study. Sedation prior to anaesthesia was achieved by intramuscular injection of azaperone (Stresnil; Janssen), and anaesthesia induced by halothane (4% in oxygen). The animals were then intubated and maintained on halothane anaesthesia (1% in air) until an intravenous line had been introduced. The pigs were ventilated with a Palmer respiration pump (16 strokes min^{-1}) and the stroke volume and oxygen content of inspired air were adjusted to maintain arterial CO_2 and O_2 tensions of 45–50 mmHg and 100 mmHg respectively (giving a pH of approximately 7.4). Catheters were placed in the aorta and vena cava via the femoral vessels for measurement of arterial blood pressure and administration of drugs respectively. At this point the halothane was discontinued and chloralose (100 mg kg^{-1}, i.v.) was administered. Intracardiac catheters were placed under fluoroscopic control (Siemens image intensifier) in the pulmonary artery (via the left external jugular vein; Swan Ganz 7Fr) and the left ventricular cavity (via the left carotid artery; Angiomedics pigtail catheter 7Fr) for measurement of pulmonary artery pressure (PAP) and left ventricular pressure (LVP).

Studies in closed-chest pigs

A preliminary study to assess an adequate dosage of R75231 was performed in 4 pigs which were prepared for haemodynamic measurement as described above. In each pig dose-response curves to adenosine were obtained before and after administration of each of three cumulative doses of R75231 (25, 50 and 100 $\mu g\ kg^{-1}$). Adenosine was administered as a bolus intravenous injection (maximum injection volume 0.5 ml) over a 2–3 s period. Twenty minutes were allowed between completion of each dose-response curve and administration of R75231, and a further 20 min before starting the next dose-response curve, to allow assessment of the effects of R75231 on baseline haemodynamics.

Venous blood samples were withdrawn prior to administration of R75231 and 20 min after each dose of the drug for *ex vivo* assessment of the extent of adenosine uptake inhibition as described below.

Studies in open-chest pigs subjected to coronary artery occlusion

Following preparation as described above a thoracotomy was performed midsternally, from the xyphoid cartilage to the clavicle, and the pericardium opened to gain access to the coronary vessels. The left anterior descending coronary artery (LAD) was dissected free below the second major diagnonal branch, approximately two thirds of the distance from the origin to the apex of the heart, and a silk ligature placed around it. The ends of the ligature were threaded through a small piece of polythene tubing to produce a snare, such that when the tubing was clamped in place the coronary artery was occluded. All surgical procedures were carried out to conform with the guidelines of the UK Home Office (Project Licence PPL60/00307).

A total of 26 pigs were entered into this part of the study and were allocated to either control (solvent vehicle; 10 pigs), R75231 50 $\mu g\ kg^{-1}$, i.v. (6 pigs) or R75231 100 $\mu g\ kg^{-1}$, i.v. (10 pigs) groups prior to surgery. The pigs were allowed to stabilize for approximately 1 h after surgery before any intervention. Blood samples were taken for arterial blood gas and pH analysis immediately prior to and 15 min after drug administration. Twenty minutes after drugs were given the coronary artery was occluded by tightening the snare.

Arrhythmia analysis

Arrhythmia analysis was performed under the guidelines of the Lambeth Convention (Walker *et al.*, 1988). The arrhythmias following coronary artery occlusion were analysed over 1 min intervals for the 30 min occlusion time to obtain a profile of distribution and a total count of ventricular arrhythmias. The percentage incidence of ventricular tachycardia (VT) and ventricular fibrillation (VF) was noted. The time to VF was recorded in all animals which developed this arrhythmia and was calculated as a mean for those animals. When ventricular fibrillation did occur, the hearts were defibrillated (within 40–60 s) by direct cardioversion to allow the experiment to continue until 30 min post-occlusion.

Data acquisition

In all experiments blood pressures were recorded with Gould capacitance transducers and the signals passed through a Buxco haemodynamnics analyser (Buxco Electronics, U.S.A.) for calculation of systolic, diastolic and mean pressures, heart rate (from the electrocardiogram; ECG), left ventricular end-diastolic pressure (LVEDP), $LVdP/dt_{max}$ and $LVdP/dt/P$ (as indices of myocardial contractility). $LVdP/dt/P$ was taken as the preferable index of LV contractility, since it is independent of afterload, and was calculated by the analyser as $LVdP/dt$ divided by (LVP-LVEDP) at the point on the dP/dt wave where LVP-LVEDP equalled 30 mmHg. All parameters

were measured by the analyser on a beat to beat basis and the values for a 1 min period automatically meaned by a personal computer (Vanilla Computers, England). The 1 min recordings were then stored on the hard disk for subsequent analysis. Numerical values were constantly updated on the visual display unit and wave pressure traces were continuously displayed on a six channel chart recorder (Gould). Calculation of rapid and transient responses, e.g. after an intravenous bolus dose of adenosine, was confirmed by measurement of the peak of the response from the chart recording. The ECG was recorded from lead II of standard limb leads, and the signal processed by an ECG analyser (Buxco Electronics, U.S.A.) to measure R-wave amplitude, R–R, QT and QRS intervals and positive and negative fluctuations in ST-segment. As with the haemodynamic data, the numerical data were continuously displayed and stored on computer and the ECG trace constantly monitored on the chart paper.

Ex vivo *estimation of adenosine uptake inhibition by R75231*

Estimation of the extent of nucleoside transport inhibition by R75231 was made by determining adenosine uptake into erythrocytes isolated from blood samples taken before and after the cumulative administration of 25, 50 and 100 $\mu g\ kg^{-1}$ R75231 in closed chest pigs. Five 4 ml venous blood samples were withdrawn at different times (see below) from each pig ($n = 4$) into syringes containing 1 ml acid/citrate/dextrose (sodium citrate 62 mM, citric acid 25 mM, glucose 86 mM) and centrifuged for 5 min at 3000 *g*. An erythrocyte suspension was made by suspending 100 μl of the packed erythrocytes in 500 μl of MOPS-NaCl buffer (10 mM 4-morpholinopropanesulphonic acid in isotonic saline, pH = 7.4). The erythrocyte samples were then taken through the assay protocol as summarized in Figure 1. The final supernatant was stored frozen until analysis of adenosine, inosine and hypoxanthine content was performed by high performance liquid chromatography (h.p.l.c.) using the method described by Wynants & Van Belle (1985).

Calculation of the extent of inhibition of adenosine uptake into the erythrocyte and inosine and hypoxanthine release from the erythrocyte were calculated by the following formulae:

$$\%\ \text{inhibition adenosine uptake in } ex\ vivo \text{ sample} = \frac{(A_x - A_o) \times 100}{(A_c - A_o)}$$

$$\%\ \text{inhibition inosine/hypoxanthine efflux in } ex\ vivo \text{ sample} = \frac{(I_c - I_x) \times 100}{(I_o - I_c)}$$

Where: A_o, I_o = % of [total nucleoside] in time zero sample with no R75231 present (0% inhibition).

A_c, I_c = % of [total nucleoside] in time zero sample with 1 μM R75231 present (100% inhibition).

A_x, I_x = % of [total nucleoside] in sample taken after *in vivo* administration of 25, 50 or 100 $\mu g\ kg^{-1}$ R75231.

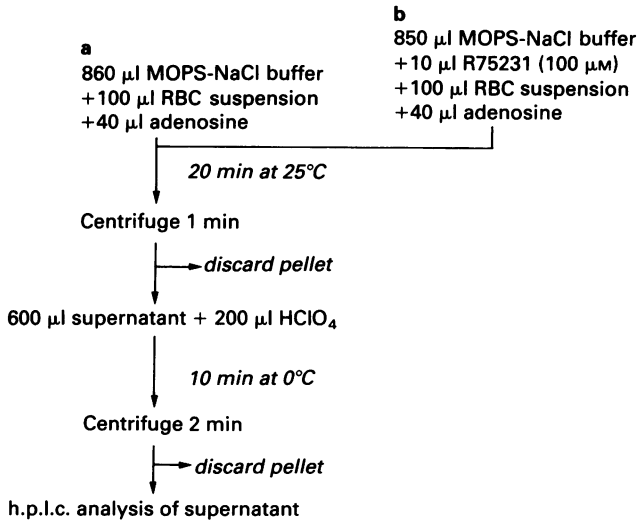

Figure 1 Flow diagram to illustrate the assay protocol for the determination of adenosine uptake by suspended erythrocytes.

Statistics

All values are expressed as mean ± s.e.mean of n experiments. Changes within each group were compared by a paired t test, whereas differences between groups were assessed by an independent t test or Mann Whitney U-test. Changes in the incidences of events were analysed by Fishers Irwin (Chi^2 with Yates correction) test. Results were considered to be statistically significant at $P < 0.05$.

Results

Studies in closed-chest pigs

Table 1 summarizes the changes in blood pressure, heart rate and LV$dP/dt/P$ following intravenous administration of cumulative doses of R75231. There was a moderate, dose-related fall in mean blood pressure (which was significant at the highest dose) within 15 min of drug administration. There were no significant effects on either heart rate or LV$dP/dt/P$. R75231 caused a dose-related shift to the left of the dose-response curve for the diastolic blood pressure response to intravenous bolus injections of adenosine (Figure 2). With the doses used there was no observed bradycardia or decrease in LV$dP/dt/P$ following adenosine injection. The blood pressure responses to adenosine prior to administration of R75231 persisted for 1.5 to 2 min. Following R75231 the responses were progressively prolonged to 4–5 min at the highest dose.

Haemodynamic effects of R75231 in open-chest pigs prior to coronary artery occlusion

The intravenous administration of R75231 produced a dose-related decrease in mean arterial pressure which started

Table 1 Haemodynamic changes in response to cumulative doses of R75231 in closed-chest pigs

		Dose R75231 ($\mu g\ kg^{-1}$)		
	Control	25	50	100
Mean arterial pressure (mmHg)	97 ± 4	95 ± 4	90 ± 1	83 ± 2*
Heart rate (beats min^{-1})	121 ± 10	123 ± 10	122 ± 17	115 ± 14
LV$dP/dt/P$ (s^{-1})	24.0 ± 0.9	21.7 ± 1.1	21.5 ± 1.0	20.9 ± 1.6
n	4	4	4	4

*$P < 0.05$ (paired t test) compared to control value prior to any drug administration. Post-drugs values were measured 10 min after drug administration.

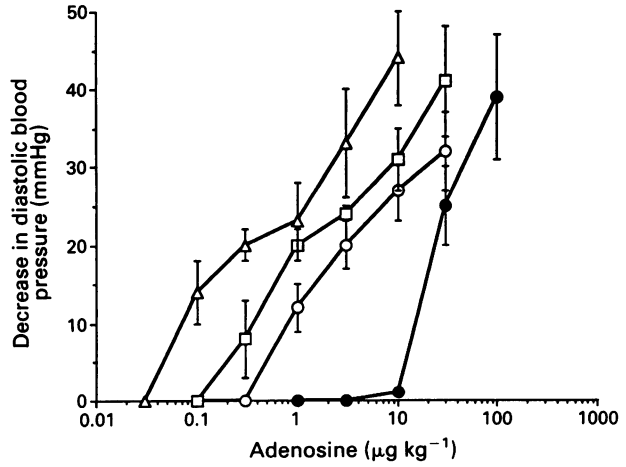

Figure 2 Decrease in diastolic pressure in response to intravenous bolus doses of adenosine prior to (●) and following cumulative administration of 25 (○), 50 (□) and 100 μg kg^{-1} (△) R75231 in closed-chest pigs ($n = 4$ pigs).

immediately following injection and reached a maximum within 5 min. Arterial pressure remained depressed for the duration of the experiment and thus by the time the coronary artery was occluded mean blood pressure was reduced by 16 ± 3 mmHg and 28 ± 6 mmHg by 50 μg kg^{-1} and 100 μg kg^{-1} R75231 respectively. This blood pressure response to R75231 was greater than that seen in closed-chest pigs. Neither dose of R75231 had any effect on any other haemodynamic parameters (Table 2).

Haemodynamic effects of coronary artery occlusion in controls and pigs treated with R75231

A 30 min period of coronary artery occlusion in control pigs resulted in no change in heart rate or arterial blood pressure compared to pre-occlusion values (Table 2). There was, however, a significant reduction in myocardial contractility assessed by both LV$dP/dt_{max}$ and LV$dP/dt/P$. In both groups of pigs given R75231, coronary artery occlusion resulted in decreases in LV$dP/dt_{max}$ and, in the case of the lower dose, LV$dP/dt/P$ which were similar to those seen in control pigs. Furthermore, in both groups given R75231, coronary artery occlusion resulted in a secondary fall in blood pressure, despite the fact that blood pressure had already decreased following drug administration.

The effects of R75231 on electrocardiographic changes seen during coronary artery occlusion

In control pigs, coronary artery occlusion had no effect on the QT interval (238.6 ± 23.7 ms preocclusion vs 214.9 ± 23.6 ms post-occlusion), but there was a significant depression of the ST-segment (from 32 ± 2 to −14 ± 6 μV: $P <$ 0.05), which became evident within 2 min post-occlusion and was maintained for the 30 min occlusion period. Coronary occlusion also resulted in a significant shortening of the QRS interval, from 27.1 ± 1.9 ms immediately prior to occlusion to 23.9 ± 1.2 ms 30 min post-occlusion ($P < 0.05$). Neither dose of R75231 exerted any effects on the ECG prior to occlusion, nor did it modify the ischaemia-induced ST-segment depression. However, the shortening of the QRS-interval was prevented by both doses of R75231 (24.2 ± 0.3 and 26.3 ± 2.0 ms 30 min post-occlusion vs 23.9 ± 0.3 and 24.1 ± 1.8 ms preocclusion with 50 and 100 μg kg^{-1} respectively).

The effects of R75231 on arrhythmias following coronary artery occlusion

Coronary artery occlusion in control pigs resulted, within 2 min, in the development of spontaneous ventricular arrhythmias which occurred over two phases. The first phase (phase 1a) appeared during the 2–10 min post-occlusion period and consisted mostly of single ventricular premature beats with some salvos (couplets and triplets). The second phase, commencing 18–20 min post-occlusion, was usually abrupt in onset and generally consisted of one or two 'warning beats' followed by ventricular fibrillation. The average time to the onset of VF in the 8 pigs which fibrillated was 25.5 ± 2.1 min post-occlusion. The incidence of ventricular tachycardia (identified as a run of 4 or more consecutive ectopic beats) was low in this model (30%), whereas the incidence of ventricular fibrillation was high (80%).

Ventricular ectopic activity following coronary artery occlusion in pigs given either dose of R75231 was similar to that seen in controls and showed a similar pattern of distribution. The total number of premature ventricular beats was also similar to controls in both groups (Figure 3). The higher (100 μg kg^{-1}) dose of R75231, however, significantly reduced the incidence of ventricular fibrillation, from 80% in controls to 30% ($P < 0.05$; Figure 4). Neither dose influenced the incidence of ventricular tachycardia and the time to onset of ventricular fibrillation was similar to that seen in controls (22.9 ± 3.9 min; $n = 5$ and 19.7 ± 2.8 min; $n = 3$ for 50 and 100 μg kg^{-1} R75231).

Table 2 The effects of R75231 (50 and 100 μg kg^{-1}; given at −20 min) and coronary occlusion (at 0 min) on haemodynamics in anaesthetized open-chest pigs

	Control			*R75231* (50 μg kg^{-1})			*R75231* (100 μg kg^{-1})		
	−21 min	−1 min	+30 min	−21 min	−1 min	+30 min	−21 min	−1 min	+30 min
n	10	10	10	6	6	6	10	10	10
Heart rate (beats min^{-1})	84 ± 5	89 ± 12	85 ± 7	108 ± 7	107 ± 7	96 ± 5	103 ± 8	96 ± 1	95 ± 8
Arterial pressure (mmHg)									
Systolic	109 ± 8	100 ± 13	97 ± 7	109 ± 3	91 ± 3*	84 ± 5[a]	112 ± 6	82 ± 8**	60 ± 8[a]
Diastolic	72 ± 7	64 ± 8	64 ± 3	75 ± 4	60 ± 2*	50 ± 2[a]	76 ± 6	48 ± 5**	35 ± 5[b]
Mean	84 ± 7	75 ± 10	75 ± 4	86 ± 4	70 ± 2*	61 ± 2[b]	88 ± 6	60 ± 6**	49 ± 4[a]
LVEDP (mmHg)	4.6 ± 0.4	3.9 ± 0.1	5.0 ± 0.8	3.9 ± 0.7	3.6 ± 0.4	4.9 ± 0.1	5.9 ± 0.6	4.2 ± 0.2	4.3 ± 0.2
LV$dP/dt_{max}$ (mmHg s^{-1})	1603 ± 139	1716 ± 258	1211 ± 171[b]	2176 ± 260	2446 ± 128	1113 ± 408[a]	2219 ± 249	2090 ± 376	1463 ± 294[a]
LV$dP/dt/P$ (s^{-1})	18.4 ± 1.0	20.1 ± 2.0	15.9 ± 0.7[a]	20.5 ± 1.8	22.1 ± 1.5	18.2 ± 0.9[b]	20.4 ± 1.1	21.2 ± 1.6	20.2 ± 1.4

*$P < 0.05$; **$P < 0.01$ compared to −21 min (pre-drug) value. [a]$P < 0.05$; [b]$P < 0.01$ compared to −1 min (preocclusion) value. (Paired *t* test).

Nucleoside uptake inhibition by R75231

Table 3 gives adenosine, inosine, hypoxanthine and total nucleoside concentrations in the assay samples generated from blood withdrawn before and after *in vivo* administration of R75231. The inhibition of adenosine uptake into the erythrocytes, calculated from the % contribution of adenosine to total nucleoside content, increased with increasing dose of R75231. The contributions of both inosine and hypoxanthine to total nucleoside count were decreased with increasing doses of R75231, demonstrating a reduced efflux of these nucleosides from the erythrocytes, since this is achieved by the same transport protein as adenosine uptake. This, in tandem with the reduced uptake of adenosine, reflects a slowed rate of conversion of adenosine to these two metabolites by the erythrocytes. The total nucleoside concentration in samples obtained from blood withdrawn after *in vivo* administration of R75231 tended to increase with the two lower doses. Although nucleoside concentrations were not measured in samples which had not had adenosine added, the same concentration of adenosine (40 μM) was added to all assay samples. This may reflect an increase in circulating nucleoside levels following administration of R75231.

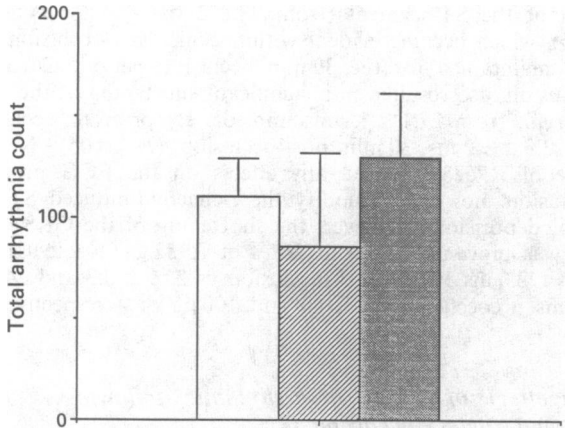

Figure 3 Total number of ventricular arrhythmias (seen as single ectopic beats, salvos and ventricular tachycardia) during 30 min of coronary occlusion in control pigs (open column) and pigs given either 50 (hatched column) or 100 μg kg^{-1} (shaded column) R75231.

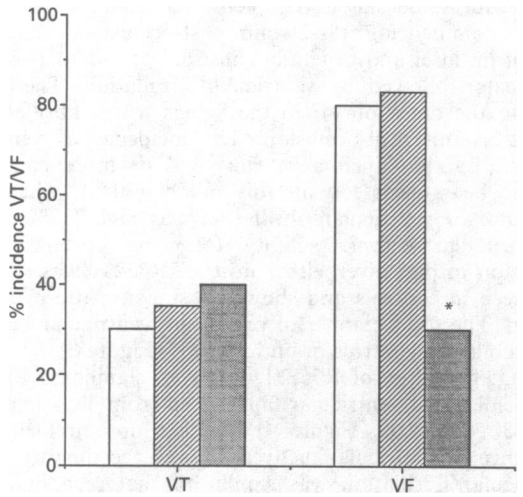

Figure 4 Percentage incidence of ventricular tachycardia (VT) and ventricular fibrillation (VF) following coronary artery occlusion in control pigs (open columns) and pigs given 50 (hatched columns) or 100 μg kg^{-1} (shaded columns) R75231. *$P<0.05$ compared to control group (Fischer Irwin test).

Discussion

The protective effects of adenosine against ventricular arrhythmias have been demonstrated previously in a number of different experimental models (reviewed in Boachie-Ansah *et al.*, 1993). In our own laboratory we have shown that exogenous administration of adenosine markedly reduces the incidence and severity of ischaemic arrhythmias in both rats (Fagbemi & Parratt, 1984) and greyhound dogs (Wainwright & Parratt, 1988). More recently, a study in beagle dogs demonstrated that intracoronary adenosine was able to terminate noradrenaline-induced ventricular tachycardia (Friedrichs & Merrill, 1991). Although adenosine is a useful agent in reducing arrhythmias (usually of supraventricular origin) in patients (Barber, 1992), the major problem with the clinical use of adenosine as an antiarrhythmic agent is that it is often poorly tolerated in patients due to intense chest pain (Rankin *et al.*, 1989) and occasionally dyspnoea and AV-block. Although these side effects are often transient and seldom require treatment there has been an increasing interest in exploiting the adenosine produced by the heart during a period of myocardial ischaemia by developing drugs which either enhance adenosine release, or prolong its biological lifetime, to act as a locally produced antiarrhythmic agent. A number of strategies for enhancing local adenosine concentration have already been employed. For example, inhibitors of adenosine deaminase, which converts adenosine to inosine, have been tested against both reperfusion injury and arrhythmias in rat isolated hearts (Zhu *et al.*, 1990), where treatment with erythro-9-(2-hydroxy-3-nonyl)adenine was found to reduce the incidence of reperfusion-induced

Table 3 Inhibition of uptake of adenosine into erythrocytes by R75231

	Time zero − *R75231*	*Time zero* + *R75231* (1 μM)	*R75231* in vivo 25 μg kg^{-1}	50 μg kg^{-1}	100 μg kg^{-1}
Adenosine					
[μM]	0.9 ± 0.2	3.1 ± 0.1	1.6 ± 0.2	2.4 ± 0.5	3.9 ± 0.8
% [total nucleoside]	0.5 ± 0.1	1.9 ± 0.3	1.1 ± 0.2	1.4 ± 0.4	2.1 ± 0.8
% inhibition	0	100	42 ± 5	64 ± 13	114 ± 14
Inosine					
[μM]	175 ± 11	166 ± 25	137 ± 35	184 ± 23	192 ± 24
% [total nucleoside]	96 ± 0.5	93.6 ± 0.6	95.2 ± 1.8	93.9 ± 2.5	93.1 ± 1.4
% inhibition	0	100	33 ± 12	87 ± 16	121 ± 22
Hypoxanthine					
[μM]	6.2 ± 1.8	4.4 ± 1.5	4.4 ± 0.7	5.8 ± 0.7	5.5 ± 1.4
% [total nucleoside]	3.4 ± 0.4	2.5 ± 0.7	3.1 ± 0.5	2.9 ± 0.6	2.7 ± 0.8
% inhibition	0	100	33 ± 5	55 ± 3	75 ± 9
[Total nucleoside]	182 ± 14	173 ± 21	144 ± 15	199 ± 15	202 ± 18

See text for details of calculations.

ventricular fibrillation, an effect which was attributed to both adenosine accumulation and inhibition of the production of superoxide radicals during the final step of adenosine metabolism. In another study an improvement in myocardial functional recovery following reperfusion was observed with 2-deoxyformycin, an effect which was attributed to an accelerated repletion of adenine nucleotide stores (Bolling *et al.*, 1990). Finally, acadesine (AICA riboside; 5-amino-1-β-D-ribofuranosyl-imidazole-4-carboaxmide) which increases intracellular adenosine concentrations only during periods of increased ATP metabolism (by an unclarified mechanism) has been shown to suppress arrhythmias and reduce ischaemic myocardial injury in dogs (Gruber *et al.*, 1989). Most of these interventions, however, do not raise adenosine concentration in the interstitium, unlike nucleoside transport inhibitors, which would allow adenosine better access to its receptors. A few studies with existing nucleoside transport inhibitors, such as lidoflazine and dipyridamole have demonstrated antiarrhythmic effects (Coker *et al.*, 1982; Wainwright & Parratt, 1988). In the present study we have shown a marked antifibrillatory effect of a new nucleoside transport inhibitor derived from lidoflazine, R75231, in a model of severe myocardial ischaemia in pigs.

R75231 has been described as a highly selective and potent inhibitor of the transport process which removes adenosine from the vicinity of its receptors (Ijzerman *et al.*, 1989). Under conditions of an increased oxygen demand in the myocardium the breakdown of purine nucleotides within the myocardial cell to adenosine monophosphate (AMP) is accelerated (Van Belle *et al.*, 1987). Until fairly recently the classical concept of adenosine release from cardiac myocytes was that AMP is converted to adenosine inside the myocyte by cytosolic 5'-nucleotidase, after which the adenosine was transported out of the cell by a transport protein. With such a mechanism a nucleoside transport inhibitor would be expected to retain adenosine within the cell, where clearly it would not reach its receptors. Recent evidence, however, has led to the growing belief that dephosphorylation to adenosine takes place outside the cell by an ecto 5'-nucleotidease on the endothelial cell membrane, since it is now known that a number of species possess low AMP conversion activity in the cytosol of the myocyte (Nees, 1989a; Borst & Schrader, 1991). Thus adenosine is most likely to be produced in the interstitium. Furthermore, even if AMP were to be converted to adenosine within the myocyte, it is now considered probable that simple diffusion accounts for the efflux of adenosine, rather than a transport process, which would therefore be unaffected by nucleoside transport inhibition (Van Belle, 1993). Once adenosine is in the interstitium it is transferred into the endothelial cell by a transporter protein, which has been localized on coronary microvessels (Parkinson & Clanachan, 1991) and cultured endothelial cells (Nees, 1989b). Degradation to inosine and hypoxanthine then takes place in the cytosol of the endothelial cell. The consequence of inhibition of this transport protein would therefore be an accumulation of adenosine in the interstitial spaces where it can gain better and more prolonged access to its receptors on the myocyte and vascular smooth muscle. In addition, efflux of inosine from the endothelial cells will be reduced since this is achieved by the same transport protein. Nucleoside transport inhibition, therefore, does not affect the production of adenosine but alters the ratio between adenosine and its metabolites in the interstitium. Leakage of adenosine through the clefts between endothelial cells may also occur, providing an access route to the lumen.

Although we did not measure tissue levels of adenosine in the present studies, indirect evidence of *in vivo* nucleoside transport inhibition by R75231 was obtained from the assays in packed erythrocytes which demonstrated an *ex vivo* dose-related inhibition of adenosine uptake, and of inosine efflux. Although this is not a direct measure of endothelial cell uptake *in vivo*, this method is regarded as an efficient tool to assess uptake inhibition *ex vivo* since it is representative for other cells with similar uptake mechanisms (Van Belle & Janssen, 1991). Other evidence to show that R75231 was inhibiting adenosine uptake *in vivo* in the doses used in the present study is the enhanced response to intravenous bolus doses of adenosine in closed-chest animals. The dose-response curves show a dose-related shift to the left of the depressor response to adenosine. Following administration of the higher dose of R75231, baseline blood pressure was approximately 10 mmHg lower than before administration of any dose of R75231 (Table 1). This could conceivably have reduced vasodilator reserve for observing maximal depressor responses. However injections of adenosine were not associated with any bradycardia or LV$dP/dt/P$ which could have contributed to the fall in arterial pressure, which suggests that the depressor responses seen in response to adenosine after the highest dose of R75231 were due to peripheral vasodilatation.

The main question pertaining to this study is what is the mechanism underlying the antifibrillatory effect of R75231? Is it due to elevation of adenosine levels within the heart or due to the reduction in afterload seen on administration of R75231? The hypotensive response to R75231 may play a part in the antiarrhythmic effects, since a reduction in afterload would decrease cardiac work and myocardial oxygen consumption, which would ultimately decrease the severity of ischaemia. While this is an appealing explanation, we have shown in this same model that other agents which decrease afterload to a similar degree, either by an action at A_2-adenosine receptors (e.g. CV1808; Wainwright & Parratt, 1991) or independent of adenosine receptors (e.g. pirsidomine; Wainwright & Martorana, 1993), display a different antiarrhythmic profile from that seen with R75231 in that they reduce total arrhythmia count, but have no effects on the incidence of ventricular fibrillation. Furthermore, R75231 did not modify the ST-segment changes which are indicative of the severity of ischaemia, suggesting a lack of anti-ischaemic effect. The role of the reduction in afterload in the antifibrillatory action of R75231 is therefore open to question but could be assessed more clearly by determining its antiarrythmic activity in closed-chest animals where a much smaller reduction in afterload by R75231 was seen.

The blood pressure response to R75231 is of interest however, since a primary aim in the development of these agents is to minimize systemic effects. In both closed-chest and open-chest pigs the response was probably due to an increase in circulating adenosine levels rather than a direct vasodilator effect of the drug since firstly, responses of a similar magnitude would be expected in both preparations (with the same starting pressure) on administration of a directly-acting vasodilator and, second, there is no evidence to suggest that R75231 possesses vasodilator properties, either direct or indirect (Van Belle *et al.*, 1992). The enhanced depressor response to R75231 in open-chest pigs may be related to a stimulation of adenosine production by the thoracotomy, since this was the only difference between the two preparations. Similarly, the secondary hypotensive response to coronary occlusion seen in treated pigs probably reflects the R75231-assisted leakage of adenosine, released by the heart in response to ischaemia, into the systemic circulation. This would not occur in control pigs since any adenosine produced by the heart would be rapidly taken up by the endothelial cells.

If R75231 exerts its antiarrhythmic effects by increasing local cardiac adenosine concentrations, rather than by the systemic responses described above, another question which arises relates to which of the actions of adenosine on the heart could be responsible. At the vascular level, A_2-receptors mediate a direct vasodilatation (King *et al.*, 1990), while a similar receptor type on the endothelium causes the release of endothelium-derived nitric oxide (Rose'Meyer & Hope, 1990). R75231 has been shown to reduce basal coronary resistance in rabbit isolated blood-perfused hearts (Galinanes *et al.*, 1993), but it would be difficult to envisage how a

coronary vasodilator effect could improve the situation within the ischaemic myocardium of a heart with the low collateral flow present in this model (<6%). Adenosine also acts via A_2-receptors to release prostacyclin from endothelial cells (Karwatowska-Prokopczuk *et al.*, 1988) and inhibit platelet function (Paul *et al.*, 1990). Prostacyclin has known antiarrhythmic properties and has been shown to be released into coronary venous blood in the early stages of ischaemia (Coker & Parratt, 1983). Similarly, substances released from platelets in response to ischaemia, such as thromboxane A_2, could contribute to the ischaemic arrhythmias (Coker *et al.*, 1981) and inhibition of platelet activation by adenosine could therefore be of importance. As mentioned above, however, the antiarrhythmic profile of R75231 is quite different from those seen with selective A_2-adenosine agonists in this model (Wainwright & Parratt, 1991; Wainwright *et al.*, 1992) which suggests an alternative mechanism.

The reduction in ventricular fibrillation by R75231 bears a closer similarity to the antiarrhythmic profile seen in this model with an A_1-adenosine agonist (**R**-PIA; Wainwright & Parratt, 1993). A_1-adenosine receptors are predominant on the sino-atrial node, where they mediate a bradycardia (Belardinelli *et al.*, 1983; Collis *et al.*, 1983), the atrioventricular node, where they slow conduction (Clemo & Belardinelli, 1986) and on the ventricular myocyte, where they modify the responses to sympathetic nerve stimulation (Schrader *et al.*, 1979). Any one of these effects could mediate an antiarrhythmic effect (reviewed by Boachie-Ansah *et al.*, 1993). While the antiarrhythmic effect of **R**-PIA was associated with a reduced heart rate, R75231 did not produce a bradycardia *per se*. However, there is evidence from this study that A_1-adenosine receptors were activated. The profound fall in blood pressure in response to R75231 would be expected to elicit a reflex tachycardia, which it did not. While it could be argued that anaesthesia depressed reflex activity (which is less likely in the chloralose anaesthetized animal than with barbiturate anaesthesia), we have observed a reflex tachycardia following administration of a selective A_2 agonist in this pig model, but not with an infusion of adenosine (which acts at both A_1- and A_2-receptors) producing the same degree of hypotension (Wainwright *et al.*, 1992). Since A_1-adenosine receptors on the sino-atrial node mediate a direct bradycardia and those at sympathetic nerve endings modulate catecholamine release it is reasonable to assume that the lack of reflex tachycardia seen with both adenosine and R75231 is due to A_1-receptor activation which overrides the reflex.

The cardioprotective effects of R75231 have also been demonstrated in other studies. In a model of rabbit isolated hearts subjected to global ischaemia, R75231 improved functional recovery and cardiac output on restoration of flow (Masuda *et al.*, 1991). R75231 has also been shown to decrease mortality and infarct size in a model of catecholamine-induced myocardial toxicity in rabbits (Van Belle *et al.*, 1992). In this respect it demonstrates a similar cardioprotective profile to other nucleoside transport inhibitors. However, as outlined in the introduction, R75231 has a number of advantages over the existing agents, such as an improved bioavailability and longer duration of action, which may make it more suitable for clinical use (Van Belle & Janssen, 1991). The speculation over whether or not the antiarrhythmic effect of R75231 is mediated by one or other (or both) of the subtypes of adenosine receptor can only be answered by concomitant administration of selective antagonists at the A_1- and A_2-receptors with R75231.

The authors would like to thank Professor S.M. Cobbe for allowing use of the Facilities in the Department of Medical Cardiology, Glasgow Royal Infirmary. C.L.W. is a Janssen Foundation Research Lecturer.

References

AHN, H.S., CRIM, W., ROMANO, M., SYBERTZ, E. & PITTS, E. (1989). Effects of selective inhibitors on cyclic nucleotide phosphodiesterases of rabbit aorta. *Biochem. Pharmacol.*, **38**, 3331–3339.

BABBITT, D.G., VIRMANI, R. & FORMAN, M.B. (1989). Intracoronary adenosine administered after reperfusion limits vascular injury after prolonged ischaemia in the canine model. *Circulation*, **80**, 1388–1399.

BARBER, M.J. (1992). Clinical use of adenosine for arrhythmias. *Coronary Art. Dis.*, **3**, 1127–1134.

BELARDINELLI, L., WEST, A., CRAMPTON, R. & BERNE, R.M. (1983). Choronotropic and dromotropic effects of adenosine. In *Regulatory Function of Adenosine*. ed. Berne, R.M. & Rubio, P. pp. 377–398. The Hague: Martinus Nijhoff.

BELHASSEN, B. & PELLEG, A. (1984). Acute management of paroxysmal supraventricular tachycardia: verapamil, adenosine triphosphate or adenosine? *Am. J. Cardiol.*, **54**, 225–227.

BLASS, K.-E., BLOCK, H.-U., FORSTER, W. & PONICKE, K. (1980). Dipyridamole: a potent stimulator of prostacyclin (PGI_2) biosynthesis. *Br. J. Pharmacol.*, **68**, 71–73.

BLUMENTHAL, D.S., HUTCHINS, G.M., JUGDUTT, B.I. & BECKER, L.C. (1981). Salvage of ischaemic myocardium by dipyridamole in the conscious dog. *Circulation*, **64**, 915–923.

BOACHIE-ANSAH, G., KANE, K.A. & PARRATT, J.R. (1993). Is adenosine an endogenous myocardial protective (antiarrhythmic) substance under conditions of ischaemia? *Cardiovasc. Res.*, **27**, 77–83.

BOLLING, S.F., BIES, L.E., BOVE, E.L. & GALLAGHER, K.P. (1990). Augmenting intracellular adenosine improves myocardial recovery. *J. Thorac. Cardiovasc. Surg.*, **99**, 469–474.

BORST, M.M. & SCHRADER, J. (1991). Adenine nucleotide release from isolated perfused guinea pig hearts and extracellular formation of adenosine. *Circ. Res.*, **68**, 797–806.

CLEMO, H.F. & BELARDINELLI, L. (1986). Effect of adenosine on atrioventricular conduction. 2. Modulation of atrioventricular node transmission by adenosine in hypoxic isolated guinea pig hearts. *Circ. Res.*, **59**, 437–446.

COKER, S.J., FAGBEMI, O. & PARRATT, J.R. (1982). Lidoflazine in the early stages of acute myocardial ischaemia. *Br. J. Pharmacol.*, **72**, 347–354.

COKER, S.J. & PARRATT, J.R. (1983). Prostacyclin – antiarrhythmic or arrhythmogenic? Comparison of the effects of intravenous and intracoronary prostacyclin and ZK36374 during coronary artery occlusion and reperfusion in anaesthetised greyhounds. *J. Cardiovasc. Pharmacol.*, **5**, 557–567.

COKER, S.J., PARRATT, J.R., LEDINGHAM, I.McA & ZEITLIN, I.J. (1981). Thromboxane and prostacyclin release from ischaemic myocardium in relation to arrhythmias. *Nature*, **291**, 323–324.

COLLIS, M.G. (1983). Evidence for an A_1 adenosine receptor in the guinea-pig atrium. *Br. J. Pharmacol.*, **78**, 207–212.

CRONSTEIN, B.N., DAGUMA, L., NICHOLS, D., HUTCHINSON, A.J. & WILLIAMS, M. (1990). The adenosine/neutrophil paradox resolved: human neutrophils possess both A_1 and A_2 receptors that promote chemotaxis and inhibit $O_2^{\cdot-}$ generation respectively. *J. Clin. Invest.*, **85**, 1150–1157.

FAGBEMI, O. & PARRATT, J.R. (1984). Antiarrhythmic actions of adenosine in the early stages of experimental myocardial ischaemia. *Eur. J. Pharmacol.*, **100**, 243–244.

FLAMENG, W., DAENEN, W., BORGERS, M., THONE, F., XHONNEUX, R., VAN DE WATER, A. & VAN BELLE, H. (1981). Cardioprotective effects of lidoflazine during 1 hour normothermic global ischaemia. *Circulation*, **64**, 796–807.

FORMAN, M.B., VELASCO, C.E. & JACKSON, E.K. (1993). Adenosine attenuates reperfusion injury following regional myocardial ischaemia. *Cardiovasc. Res.*, **27**, 9–17.

FREDHOLM, B.B., GUSTAFSSON, L.E., HEDQVIST, P. & SOLLEVI, A. (1983). Adenosine in the regulation of transmitter release in the peripheral nervous system. In *Regulatory Function of Adenosine*. ed. Berne, R.M., Rall, T.W. & Rubio, R. pp. 479–495. The Hague-Boston-London: Matrinus Nijhoff.

FRIEDRICHS, G.S. & MERRILL, G.F. (1991). Adenosine deaminase and adenosine attenuate ventricular arrhythmias caused by norepinephrine. *Am. J. Physiol.*, **260**, H979–H984.

GALINANES, M., QIU, Y., VAN BELLE, H. & HEARSE, D.J. (1993). Metabolic and functional effects of the nucleoside transport inhibitor R75231 in the ischaemic and blood-reperfused rabbit heart. *Cardiovasc. Res.*, **27**, 90–95.

GRUBER, H.E., HOFFER, M.E., MCALLISTER, D.R., LAIKIND, P.K., LANE, T.A., SCHMIDSCHOENBEIN, G.W. & ENGLER, R.L. (1989). Increased adenosine concentration in blood from ischaemic myocardium by Aica Riboside – effects on flow, granulocytes and injury. *Circulation*, **80**, 1400–1411.

GUPTA, J.B., SETH, S.D., SINGH, U. & VYAS, D.S. (1989). Effect of dilazep in evolving myocardial infarction in dogs: a biochemical study. *Int. J. Cardiol.*, **23**, 165–171.

IJZERMAN, A.P., THEDINGA, K.H., CUSTERS, A.F.C.M., HOOS, B. & VAN BELLE, H. (1989). Inhibition of nucleoside transport by a series of compounds related to lidoflazine and mioflazine. *Eur. J. Pharmacol. Mol. Pharmacol.*, **172**, 273–281.

KARWATOWSKA-PROKOPCZUK, E., CIABATTONI, G. & WENNMALM, A. (1988). Effect of adenosine on the formation of prostacyclin in the rabbit isolated heart. *Br. J. Pharmacol.*, **94**, 721–728.

KING, A.D., MILAVEC-KRIZMAN, M. & MULLER-SCHWEINITZER, E. (1990). Characterisation of the adenosine receptor in porcine coronary arteries. *Br. J. Pharmacol.*, **100**, 483–486.

MASUDA, M., DEMEULEMEESTER, A., CHANG-CHUNN, C. & FLAMENG, W. (1991). Cardioprotective effects of nucleoside transport inhibition in ischaemia-reperfused rabbit hearts – a role of endogenous adenosine. *J. Mol. Cell Cardiol.*, **23** (Suppl V), S127.

NEES, S. (1989a). The adenosine hypothesis of metabolic regulation of coronary flow in light of the newly recognised properties of the coronary endothelium. *Z. Kardiol.*, **78** (Suppl 6), 42–49.

NEES, S. (1989b). Coronary flow increases induced by adenosine and adenine nucleotides are mediated by the coronary endothelium: a new principle of the regulation of coronary flow. *Eur. Heart J.*, **10**, 28–35.

NEWBY, A.C. (1984). Adenosine and the concept of 'retaliatory metabolites'. *Trends. Biol. Sci.*, **9**, 42–44.

OLAFSSON, B., FORMAN, M.B. & PUET, D.W. (1987). Reduction of reperfusion injury in the canine preparation by intracoronary adenosine: importance of the endothelium and the 'no-reflow' phenomenon. *Circulation*, **76**, 1135–1145.

OLSSON, R.A. (1970). Changes in content of purine nucleoside in canine myocardium during coronary occlusion. *Circ. Res.*, **26**, 310–316.

PARKINSON, F.E. & CLANACHAN, A.S. (1991). Adenosine receptors and nucleoside transport sites in cardiac cells. *Br. J. Pharmacol.*, **104**, 399–405.

PAUL, S., FEOKTISTOV, I., HOLLISTER, A.S., ROBERTSON, D. & BIAGGIONI, I. (1990). Adenosine inhibits the rise in intracellular calcium and platelet aggregation produced by thrombin – evidence that both effects are coupled to adenylate cyclase. *Mol. Pharmacol.*, **37**, 870–875.

RANKIN, A.C., OLDROYD, K.G., CHONG, E., RAE, A.P. & COBBE, S.M. (1989). Value and limitations of adenosine in the diagnosis and treatment of narrow and broad complex tachycardias. *Br. Heart J.*, **62**, 195–203.

ROSE'MEYER, R.B. & HOPE, W. (1990). Evidence that A_2 purinoceptors are involved in endothelium-dependent relaxation of the rat thoracic aorta. *Br. J. Pharmacol.*, **100**, 576–580

SCHRADER, J., GERLACH, E. & BAUMANN, G. (1979). Sites and mode of action of adenosine in the heart. In *Physiological and Regulatory Functions of Adenosine and Adenine Nucleotides*. ed. Baer, B.P. & Drummond, G.I. pp. 137–144. New York: Raven Press.

STRINGER, K.A., BRANCONI, J.M., ABADIER, R., WILTON, J.H. & ROYAL, S.H. (1992). Disposition of oral dipyridamole in patients undergoing Thallium-201 myocardial imaging. *Pharmacotherapy*, **12**, 83–87.

VAN BELLE, H. (1993). Nucleoside transport inhibition: a therapeutic approach to cardioprotection via adenosine? *Cardiovasc. Res.*, **27**, 68–76.

VAN BELLE, H. & JANSSEN, P.A.J. (1991). Comparative pharmacology of nucleoside transport inhibitors. *Nucleosides and Nucleotides*, **10**, 975–982.

VAN BELLE, H., GOOSSENS F. & WYNANTS, J. (1987). Formation and release of purine catabolites during hypoperfusion, anoxia and ischaemia. *Am. J. Physiol.*, **252**, H886–H893.

VAN BELLE, H., VERHEYEN, W., VER DONCK, C., JANSSEN, P.A.J. & ROBERTSON, J.R.S. (1992). Prevention of catecholamine-induced cardiac damage and death with a nucleoside transport inhibitor. *J. Cardiovasc. Pharmacol.*, **20**, 173–178.

WAINWRIGHT, C.L. & MARTORANA, P.A. (1993). Pirsidomine, a novel nitric oxide donor, suppresses ischaemic arrhythmias in anaesthetised pigs. *J. Cardiovasc. Pharmacol.* (in press).

WAINWRIGHT, C.L. & PARRATT, J.R. (1988). An antiarrhythmic effect of adenosine during myocardial ischaemia and reperfusion. *Eur. J. Pharmacol.*, **146**, 183–194.

WAINWRIGHT, C.L. & PARRATT, J.R. (1991). The effects of CV1808, an A_2-adenosine receptor agonist, on ischaemic arrhythmias in anaesthetised pigs. *Br. J. Pharmacol.*, **104**, 20P.

WAINWRIGHT, C.L. & PARRATT, J.R. (1993). The effects of R-PIA, a selective A_1-adenosine agonist, on haemodynamics and ischaemic arrhythmias in pigs. *Cardiovasc. Res.*, **27**, 84–89.

WAINWRIGHT, C.L., PARRATT, J.R., TWEDDEL, A.C., MARTIN, W. & COBBE, S.M. (1992). Adenosine and an A_2-agonist, CGS21680, reduce arrhythmias and suppress white cell accumulation in the porcine ischaemic myocardium. *Br. J. Pharmacol.*, **107**, 97P.

WALKER, M.J.A., CURTIS, M.J., HEARSE, D.J. ET AL. (1988). The Lambeth Conventions: guidelines for the study of arrhythmias in ischaemia, reperfusion and infarction. *Cardiovasc. Res.*, **22**, 447–455.

WOOD, A.J., ISTED, K., HYND, J., MAIN, M.J., NOBLE, M.I., PARKER, J. & DRAKE-HOLLAND, A.J. (1985). Mioflazine, a potentially protective drug against ischaemic damage: a study in dogs. *Eur. Heart J.*, **6**, 695–701.

WYNANTS, J. & VAN BELLE, H. (1985). Single-run high performance liquid chromatography of nucleotides, nucleosides and major purine bases and its application to different tissue extracts. *Annal. Biochem.*, **144**, 258–264.

ZHU, Q.Y., CHEN, S.G. & ZOU, C.M. (1990). Protective effects of an adenosine deaminase inhibitor on ischaemia-reperfusion injury in isolated perfused rat heart. *Am. J. Physiol.*, **259**, H835–H838.

(Received October 28, 1992
Revised February 5, 1993
Accepted February 22, 1993)

British Journal of Pharmacology

VOLUME 109 (2) JUNE 1993

SPECIAL REPORTS

A.D. Michel, R.K. Phul, T.L. Stewart & P.P.A. Humphrey. Characterization of the binding of [^{3}H]-L-N^G-nitro-arginine in rat brain 287

E.W. Hillhouse & K. Mosley. Peripheral endotoxin induces hypothalamic immunoreactive interleukin-1β in the rat 289

A. Zhang, T.P.-O. Cheng, B.T. Altura & B.M. Altura. Mg^{2+} and caffeine-induced intracellular Ca^{2+} release in human vascular endothelial cells 291

PAPERS

Z. Qiu & J.P. Morgan. Differential effects of cocaine and cocaethylene on intracellular Ca^{2+} and myocardial contraction in cardiac myocytes 293

S. Al-Damluji, L.Z. Krsmanovic & K.J. Catt. High-affinity uptake of noradrenaline in postsynaptic neurones 299

E.P. Finta, L. Harms, J. Sevcik, H.-D. Fischer & P. Illes. Effects of potassium channel openers and their antagonists on rat locus coeruleus neurones 308

D.G. MacGregor & T.W. Stone. Inhibition by the adenosine analogue, (R)-N^6-phenylisopropyladenosine, of kainic acid neurotoxicity in rat hippocampus after systemic administration 316

Z.M. Chu & L.J. Beilin. Mechanisms of vasodilatation in pregnancy: studies of the role of prostaglandins and nitric-oxide in changes of vascular reactivity in the *in situ* blood perfused mesentery of pregnant rats 322

S. Hishinuma, Y. Matsumoto, M.K. Uchida & M. Kurokawa. Novel regulation of muscarinic receptors and their coupling with G proteins in smooth muscle: transient resensitization during desensitizing process 330

Q. Chen & C. van Breemen. The superficial buffer barrier in venous smooth muscle: sarcoplasmic reticulum refilling and unloading 336

S.J. Roberts, P. Molenaar & R.J. Summers. Characterization of propranolol-resistant (−)-[^{125}I]-cyanopindolol binding sites in rat soleus muscle 344

D.R. Bristow & M.R. Zamani. Desensitization of histamine H_1 receptor-mediated inositol phosphate production in HeLa cells 353

M. Waelbroeck, J. Camus, M. Tastenoy, G. Lambrecht, E. Mutschler, M. Kropfgans, J. Sperlich, F. Wiesenberger, R. Tacke & J. Christophe. Thermodynamics of antagonist binding to rat muscarinic M_2 receptors: antimuscarinics of the pridinol, sila-pridinol, diphenidol and sila-diphenidol type 360

A.C. MacKinnon, M. Spedding & C.M. Brown. Sodium modulation of ^{3}H-agonist and ^{3}H-antagonist binding to α_2-adrenoceptor subtypes 371

G.J. Birrell & F.W. Marcoux. Excitatory amino acid receptor-stimulated phosphoinositide turnover in primary cerebrocortical cultures 379

M.D. Randall & T.M. Griffith. Modulation of vasodilatation to levcromakalim by hypoxia and EDRF in the rabbit isolated ear: a comparison with pinacidil, sodium nitroprusside and verapamil 386

H.L. Wiener, G.P. Thalody & S. Maayani. Interactions between responses mediated by activation of adenosine A_2 receptors and α_1-adrenoceptors in the rabbit isolated aorta 394

S.J.G. McAuliffe, H.M. Snow, B. Cox, C.C.T. Smith & M.I.M. Noble. Interaction between the effects of 5-hydroxytryptamine and adrenaline on the growth of platelet thrombi in the coronary artery of the anaesthetized dog 405

M. Del Zompo, M.P. Piccardi, S., Ruiu, M. Quartu, G.L. Gessa & A. Vaccari. Selective MPP^+ uptake into synaptic dopamine vesicles: possible involvement in MPTP neurotoxicity 411

K. Kitamura, Q. Lian, A. Carl & H. Kuriyama. S-nitrosocysteine, but not sodium nitroprusside, produces apamin-sensitive hyperpolarization in rat gastric fundus 415

A. Vials & G. Burnstock. A_2-purinoceptor-mediated relaxation in the guinea-pig coronary vasculature: a role for nitric oxide 424

D. Salvemini, A. Pistelli, & V. Mollace. Release of nitric oxide from glyceryl trinitrate by captopril but not enalaprilat: *in vitro* and *in vivo* studies 430

B.A. Kenny, A.C. MacKinnon, M. Spedding & C.M. Brown. Changes in [^{3}H]-PK 11195 and [^{3}H]-8-OH-DPAT binding following forebrain ischaemia in the gerbil 437

H. Nishimura, T. Matsubara, Y. Ikoma, S. Nakayama & N. Sakamoto. Effects of prolonged application of isoprenaline on intracellular free magnesium concentration in isolated heart of rat 443

J.P. Turner. Anion transport blockers inhibit DL-2-amino-4-phosphonobutyrate responses induced by quisqualate in the rat cerebral cortex 449

H. Uneyama, N. Harata & N. Akaike. Caffeine and related compounds block inhibitory amino acid-gated Cl^- currents in freshly dissociated rat hippocampal neurones 459

H. Hasséssian, P. Bodin & G. Burnstock. Blockade by glibenclamide of the flow-evoked endothelial release of ATP that contributes to vasodilatation in the pulmonary vascular bed of the rat 466

Y. Igawa, A. Mattiasson & K.-E. Andersson. Functional importance of cholinergic and purinergic neuro-transmission for micturition contraction in the normal, unanaesthetized rat 473

G. Khurana & M.R. Bennett. Nitric oxide and arachidonic acid modulation of calcium currents in postganglionic neurones of avian cultured ciliary ganglia 480

H. Karaki, S.A. Sudjarwo, M. Hori, M. Takai, Y. Urade & T. Okada. Induction of endothelium-dependent relaxation in the rat aorta by IRL 1620, a novel and selective agonist at the endothelin ET_B receptor 486

G. Grignaschi, B. Mantelli, C. Fracasso, M. Anelli, S. Caccia & R. Samanin. Reciprocal interaction of 5-hydroxytryptamine and cholecystokinin in the control of feeding patterns in rats 491

A.S.O. Adeagbo & C.R. Triggle. Interactions of nitric oxide synthase inhibitors and dexamethasone with α-adrenoceptor-mediated responses in rat aorta 495

M.D. Ivorra, C. Lugnier, M. Catret, E. Anselmi, D. Cortes & P. D'Ocon. Investigations of the dual contractile/relaxant properties showed by antioquine in rat aorta **502**

U. Kachintorn, M. Vajanaphanich, A.E. Traynor-Kaplan, K. Dharmsathaphorn & K.E. Barrett. Activation by calcium alone of chloride secretion in T_{84} epithelial cells **510**

J.C. Oliveira, A.M. Sebastião & J.A. Ribeiro. On the high affinity binding site for [^{3}H]-1,3-dipropyl-8-cyclopentylxanthine in frog brain membranes **518**

M. Hirafuji & H. Shinoda. Roles of prostacyclin, EDRF and active oxygens in leukocyte-dependent platelet adhesion to endothelial cells induced by platelet-activating factor *in vitro* **524**

L. McMurdo, P.S. Lidbury, C. Thiemermann & J.R. Vane. Mediation of endothelin-1-induced inhibition of platelet aggregation via the ET_B receptor **530**

J. McGivern, C.N. Scholfield & J.O. Dolly. Action of α-dendrotoxin on K^+ currents in nerve terminal regions of axons in rat olfactory cortex **535**

R.A. Marangoni, E. Antunes, S.D. Brain & G. de Nucci. Activation by *Phoneutria nigriventer* (armed spider) venom of tissue kallikrein-kininogen-kinin system in rabbit skin *in vivo* **539**

R.A.D. Rutherford, J. Wharton, A. McCarthy, L. Gordon, M.H.F. Sullivan, M.G. Elder & J.M. Polak. Differential localization of endothelin ET_A and ET_B binding sites in human placenta **544**

T. Omari, M.P. Sparrow, M.K. Church, S.T. Holgate & C. Robinson. A comparison of the effects of polyarginine and stimulated eosinophils on the responsiveness of the bovine isovolumic bronchial segment preparation **553**

W. Scholz, U. Albus, H.J. Lang, W. Linz, P.A. Martorana, H.C. Englert & B.A. Schölkens. Hoe 694, a new Na^+/H^+ exchange inhibitor and its effects in cardiac ischaemia **562**

P. Soares-da-Silva. Renal tubular dopamine outward transfer during Na^+-H^+ exchange activation by α_1- and α_2-adrenoceptor agonists **569**

P. Soares-da-Silva. Kinetic study of the tubular dopamine outward transporter in the rat and dog kidney **577**

D.P. Brooks, B.G. Short, M.J. Cyronak, L.C. Contino, M. DiCristo, Y-X. Wang & R.R. Ruffolo, Jr. Comparison between carvedilol and captopril in rats with partial ablation-induced chronic renal failure **581**

A.T. Dinh-Xuan, J. Pepke-Zaba, A.Y. Butt, G. Cremona & T.W. Higenbottam. Impairment of pulmonary-artery endothelium-dependent relaxation in chronic obstructive lung disease is not due to dysfunction of endothelial cell membrane receptors nor to L-arginine deficiency **587**

C.L. Wainwright, J.R. Parratt & H. Van Belle. The antiarrhythmic effects of the nucleoside transporter inhibitor, R75231, in anaesthetized pigs **592**

SPECIAL REPORTS

The purpose of *Special Reports* is to provide rapid publication for **new** and **important** results which the Editorial Board considers are likely to be of special pharmacological significance. *Special Reports* will have publication priority over all other material and so authors are asked to consider carefully the status of their work before submission.

In order to speed publication there is normally no revision allowed beyond very minor typographical or grammatical corrections. If significant revision is required, the Board may either invite rapid re-submission or, more probably, propose that it be re-written as a Full Paper and be re-submitted for consideration. In order to reduce delays, proofs of *Special Reports* will be sent to authors but **essential corrections must reach the Production Office within 48 hours of receipt.** Authors should ensure that their submitted material conforms exactly to the following requirements.

Special Reports should normally occupy no more than two printed pages of the Journal; two illustrations (Figures or Tables, with legends) are permitted. As a guideline, with type face of 12 pitch and double-line spacing, a page of A4 paper could contain about 400 words. The absolute maximum length of the *Special Report* is 1700 words. For each Figure or Table, please deduct 200 words. The manuscript should comprise a Title page with key words (maximum of 10), a Summary consisting of a single short paragraph, followed by Introduction, Methods, Results, Discussion and References (maximum of 10). In all other respects, the requirements are the same as for Full Papers (see current 'Instructions to Authors').

Edited for the British Pharmacological Society by

A.T. Birmingham *(Chairman)*
R.W. Horton *(Secretary)*
W.A. Large *(Secretary)*

EDITORIAL BOARD

J.A. Angus Victoria, Australia
M.L.J. Ashford Cambridge
G.W. Bennett Nottingham
W.C. Bowman Glasgow
N.G. Bowery London
Alison F. Brading Oxford
S.D. Brain London
K.T. Bunce Ware
K.D. Butler Horsham
M. Caulfield London
M.K. Church Southampton
S.J. Coker Liverpool
R.A. Coleman Ware
A.J. Cross London
V. Crunelli Cardiff
T.C. Cunnane Oxford
F. Cunningham London
A. Dray London
J.R. Docherty Dublin
J.M. Edwardson Cambridge
W. Feniuk Cambridge
J.R. Fozard Basle, Switzerland
Allison D. Fryer Baltimore, USA
Sheila M. Gardiner Nottingham
C.J. Garland Southampton
L.G. Garland Beckenham
A. Gibson London
R. Gristwood Barcelona, Spain
T. Hedner Gothenburg, Sweden
P.E. Hicks Leuville-sur-Orge, France
S.J. Hill Nottingham
J.C. Hunter Cambridge
C.C. Jordan Ware
K.A. Kane Glasgow
D.A. Kendall Nottingham
P. Leff Loughborough
H.D. Lux Planegg, Germany
R. McMillan Macclesfield
J. Maclagan London
G. Martin Beckenham
W. Martin Glasgow
A. Mathie London
D.N. Middlemiss Harlow
R.C. Miller Strasbourg, France
P.K. Moore London
R.J. Naylor Bradford
C.D. Nicholson Oss, The Netherlands
C.P. Page London
B.K. Park Liverpool
A.N. Payne Beckenham
F.L. Pearce London
J.D. Pearson London
M.H.T. Roberts Cardiff
P.J. Roberts Bristol
C. Robinson London
G.J. Sanger Harlow
M.A. Simmonds London
J.M. Sneddon Sunderland
P. Sneddon Glasgow
K. Starke Freiburg, Germany
P.V. Taberner Bristol
C. Thiemermann London
M.D. Tricklebank Harlow
M.B. Tyers Ware
S.P. Watson Oxford
K.J. Watling Cambridge
A.H. Weston Manchester
B.J.R. Whittle Beckenham
Eileen Winslow Riom, France

CORRESPONDING EDITORS

P.R. Adams Stony Brook, U.S.A.
C. Bell Melbourne, Australia
F.E. Bloom La Jolla, U.S.A.
A.L.A. Boura Clayton, Australia
N.J. Dun Toledo, U.S.A.
R.F. Furchgott New York, U.S.A.
T. Godfraind Brussels, Belgium
S.Z. Langer Paris, France
R.J. Miller Chicago, U.S.A.
R.C. Murphy Denver, U.S.A.
E. Muscholl Mainz, Germany
R.A. North Portland, U.S.A.
M. Otsuka Tokyo, Japan
M.J. Rand Melbourne, Australia
S. Rosell Södertalje, Sweden
P. Seeman Toronto, Canada
L. Szekeres Szeged, Hungary
B. Uvnas Stockholm, Sweden
P.A. Van Zwieten Amsterdam, Netherlands
V.M. Varagič Belgrade, Yugoslavia
G. Velo Verona, Italy
Wang Zhen Gang Beijing, China
M.B.H. Youdim Haifa, Israel

Papers will be considered for publication on all aspects of pharmacology, including chemotherapy.

Manuscripts (two copies) should be sent to Editorial Office, British Journal of Pharmacology, St. George's Hospital Medical School, Cranmer Terrace, London SW17 0RE. Authors should consult the Instructions to Authors and the Nomenclature Guidelines for Authors in Vol. 108, 275–284. These Instructions and Guidelines also appear with the journal Index for volumes 105–107, 1992.

The *British Journal of Pharmacology* is published monthly by the Scientific & Medical Division, Macmillan Press Ltd. The journal is covered by *Current Contents*, *Excerpta Medica* and *Index Medicus*.

All business correspondence and reprint requests should be addressed to the Scientific & Medical Division, Macmillan Press Ltd., Houndmills, Basingstoke, Hampshire RG21 2XS, UK. Telephone: (0256) 29242; Fax: (0256) 810526.

Enquiries concerning advertising space or rates should be addressed to: Michael Rowley, Advertisement Manager, Macmillan Press Ltd., 4 Little Essex Street, London WC2R 3LF. Telephone: 071 836 6633; Fax: 071 379 0820.

Annual subscription prices for 1993 EC £455, elsewhere £499/US$923 (sterling rate is definitive). Orders must be accompanied by remittance. Cheques should be made payable to Macmillan Press, and sent to: Macmillan Press Ltd., Subscription Department, Brunel Road, Houndmills, Basingstoke, Hampshire RG21 2XS, UK.
Overseas subscribers may make payments into UK Post Office Giro Account No. 5192455. Full details must accompany the payment.

British Journal of Pharmacology (ISSN 0007–1188) is published monthly by Macmillan Publishers Ltd, c/o Mercury Airfreight International Ltd, 2323 Randolph Avenue, Avenel, NJ 07001, USA. Subscription price is $923.00 per annum. 2nd class postage is paid at Rahway NJ. *Postmaster*: send address corrections to Macmillan Publishers, c/o Mercury Airfreight International Ltd, 2323 Randolph Avenue, Avenel NJ 07001.

All rights of reproduction are reserved in respect of all papers, articles, illustrations, etc., published in this journal in all countries of the world.

All material published in this journal is protected by copyright, which covers exclusive rights to reproduce and distribute the material. No material published in this journal may be reproduced or stored on microfilm or in electronic, optical or magnetic form without the written authorisation of the Publisher.

Authorization to photocopy items for internal or personal use, or the internal or personal use of specific clients, is granted by Macmillan Press Ltd for libraries and other users registered with the Copyright Clearance Center (CCC) Transactional Reporting Service, provided that the base fee of $9.00 per copy is paid directly to CCC, 21 Congress St. Salem, MA 01970, USA.

Apart from any fair dealing for the purposes of research or private study, or criticism or review, as permitted under the Copyright, Designs and Patent Act 1988, this publication may be reproduced, stored or transmitted, in any form or by any means, only with the prior permission in writing of the publishers, or in the case of reprographic reproduction, in accordance with the terms of licences issued by the Copyright Licensing Agency.

© The British Pharmacological Society & Macmillan Press Ltd, 1993.
ISSN 0007–1188

0007–1188/93 $9.00 + $0.00

M.D. Ivorra, C. Lugnier, M. Catret, E. Anselmi, D. Cortes & P. D'Ocon. Investigations of the dual contractile/relaxant properties showed by antioquine in rat aorta **502**

U. Kachintorn, M. Vajanaphanich, A.E. Traynor-Kaplan, K. Dharmsathaphorn & K.E. Barrett. Activation by calcium alone of chloride secretion in T_{84} epithelial cells **510**

J.C. Oliveira, A.M. Sebastião & J.A. Ribeiro. On the high affinity binding site for [^{3}H]-1,3-dipropyl-8-cyclopentylxanthine in frog brain membranes **518**

M. Hirafuji & H. Shinoda. Roles of prostacyclin, EDRF and active oxygens in leukocyte-dependent platelet adhesion to endothelial cells induced by platelet-activating factor *in vitro* **524**

L. McMurdo, P.S. Lidbury, C. Thiemermann & J.R. Vane. Mediation of endothelin-1-induced inhibition of platelet aggregation via the ET_B receptor **530**

J. McGivern, C.N. Scholfield & J.O. Dolly. Action of α-dendrotoxin on K^+ currents in nerve terminal regions of axons in rat olfactory cortex **535**

R.A. Marangoni, E. Antunes, S.D. Brain & G. de Nucci. Activation by *Phoneutria nigriventer* (armed spider) venom of tissue kallikrein-kininogen-kinin system in rabbit skin *in vivo* **539**

R.A.D. Rutherford, J. Wharton, A. McCarthy, L. Gordon, M.H.F. Sullivan, M.G. Elder & J.M. Polak. Differential localization of endothelin ET_A and ET_B binding sites in human placenta **544**

T. Omari, M.P. Sparrow, M.K. Church, S.T. Holgate & C. Robinson. A comparison of the effects of polyarginine and stimulated eosinophils on the responsiveness of the bovine isovolumic bronchial segment preparation **553**

W. Scholz, U. Albus, H.J. Lang, W. Linz, P.A. Martorana, H.C. Englert & B.A. Schölkens. Hoe 694, a new Na^+/H^+ exchange inhibitor and its effects in cardiac ischaemia **562**

P. Soares-da-Silva. Renal tubular dopamine outward transfer during Na^+-H^+ exchange activation by α_1- and α_2-adrenoceptor agonists **569**

P. Soares-da-Silva. Kinetic study of the tubular dopamine outward transporter in the rat and dog kidney **577**

D.P. Brooks, B.G. Short, M.J. Cyronak, L.C. Contino, M. DiCristo, Y-X. Wang & R.R. Ruffolo, Jr. Comparison between carvedilol and captopril in rats with partial ablation-induced chronic renal failure **581**

A.T. Dinh-Xuan, J. Pepke-Zaba, A.Y. Butt, G. Cremona & T.W. Higenbottam. Impairment of pulmonary-artery endothelium-dependent relaxation in chronic obstructive lung disease is not due to dysfunction of endothelial cell membrane receptors nor to L-arginine deficiency **587**

C.L. Wainwright, J.R. Parratt & H. Van Belle. The antiarrhythmic effects of the nucleoside transporter inhibitor, R75231, in anaesthetized pigs **592**

SPECIAL REPORTS

The purpose of *Special Reports* is to provide rapid publication for **new** and **important** results which the Editorial Board considers are likely to be of special pharmacological significance. *Special Reports* will have publication priority over all other material and so authors are asked to consider carefully the status of their work before submission.

In order to speed publication there is normally no revision allowed beyond very minor typographical or grammatical corrections. If significant revision is required, the Board may either invite rapid re-submission or, more probably, propose that it be re-written as a Full Paper and be re-submitted for consideration. In order to reduce delays, proofs of *Special Reports* will be sent to authors but **essential corrections must reach the Production Office within 48 hours of receipt.** Authors should ensure that their submitted material conforms exactly to the following requirements.

Special Reports should normally occupy no more than two printed pages of the Journal; two illustrations (Figures or Tables, with legends) are permitted. As a guideline, with type face of 12 pitch and double-line spacing, a page of A4 paper could contain about 400 words. The absolute maximum length of the *Special Report* is 1700 words. For each Figure or Table, please deduct 200 words. The manuscript should comprise a Title page with key words (maximum of 10), a Summary consisting of a single short paragraph, followed by Introduction, Methods, Results, Discussion and References (maximum of 10). In all other respects, the requirements are the same as for Full Papers (see current 'Instructions to Authors').

PREPARATION OF MANUSCRIPTS

Authors are strongly recommended to read the full *Instructions to Authors* and *Nomenclature Guidelines for Authors* (*Br. J. Pharmacol.* 1993, **108,** 275–284) before submitting a manuscript for publication in the *British Journal of Pharmacology*. The manuscript and cover letter should be checked against the following list before mailing.

The original and one copy of the manuscript must be supplied. Manuscripts must be typed in double-line spacing on one side of A4 paper, in type not smaller than 12 characters per inch or 10 point. Both copies to include Tables and a set of labelled Figures. One set of Figures without numbers or letters is also to be included. The text to be arranged in the following subsections:

1. **Title**—To have no more than 150 characters on a separate page, which should also include a Short Title (50 characters maximum) and the name and address of the author for correspondence.

2. **Summary**—To be arranged in numbered paragraphs (Full Papers) or a single paragraph (Special Reports).
   —to include aims, principal results and conclusions.
   —to include Key words (10 maximum) at end of summary.

3. **Introduction**—To contain concise statements of the problem and the aims of the investigation.

4. **Methods**—To have brief but adequate account of the procedures; *full names of drugs* (*including those referred to by manufacturer's code*), sources of drugs and statistical tests to be stated.

5. **Results**—To have no repetition of data in Figures, Tables and text.

6. **Discussion**—Findings and conclusions to be placed in context of other relevant work.
   NB Simple repetition of results and unwarranted speculation are not acceptable.

7. **Acknowledgments**—Sources of support. Sources of drugs not widely available commercially.

8. **References**—All references in the text to be included in the Reference List and *vice versa*. References in alphabetical order with complete citations; Journals publishing 'in press' papers identified.
   References to manuscripts submitted to other journals but not yet accepted are not allowed.

9. **Tables**—Each on a separate page and prepared in accordance with current requirements of the Journal.

10. **Figures**—Both labelled and non-labelled Figures to be prepared in accordance with current requirements of the Journal (see *Instructions to Authors*, 1993, **108,** 275–281) and provided with Figure Number and Authors' names on back (*in pencil*).
    —each legend to be typed on a separate page and carrying keys to symbols.
    —keys to symbols and histograms must not appear on the figures themselves, but in the respective legends.
    —'box style' figures are not in keeping with the Journal style; line drawings etc must have only left-hand and bottom axes.

11. **Manuscripts**—To be accompanied by a declaration signed by each author that
    (a) results are original
    (b) approval of all persons concerned has been given to submit manuscripts for consideration (see also 12b)
    (c) the same material is neither 'in press' (i.e. is in proof or has definitely been accepted for publication) nor under consideration elsewhere. Furthermore it will not be submitted or published elsewhere before a decision has been reached by the Editorial Board of the *British Journal of Pharmacology* and will not be submitted elsewhere if accepted by the *British Journal of Pharmacology*.
    (d) Copyright assignment is included.

12. **Cover letter**—To state clearly
    (a) Corresponding author's full postal address, telephone, telex or Fax number
    (b) where appropriate, that *either* ethical approval has been given for investigation *or* Company or Institutional permission to publish work has been received.

13. **Reminder**—Packaging to be sufficiently robust to protect Figures and to withstand mailing.

Failure to comply with *Instructions to Authors* may lead to substantial delays in processing, review and publication and may even jeopardize acceptance of the manuscript.

NOMENCLATURE

Authors are reminded that accepted receptor and associated terminology is laid out in *Nomenclature Guidelines for Authors,* as published in the *British Journal of Pharmacology, Br. J. Pharmacol.*, 1993, **108,** 282–284.

BRITISH JOURNAL OF PHARMACOLOGY VOLUME 109 (2) 1993

SPECIAL REPORTS

A.D. Michel, R.K. Phul, T.L. Stewart & P.P.A. Humphrey. Characterization of the binding of [^{3}H]-L-N^G-nitro-arginine in rat brain 287

E.W. Hillhouse & K. Mosley. Peripheral endotoxin induces hypothalamic immunoreactive interleukin-1β in the rat 289

A. Zhang, T.P.-O. Cheng, B.T. Altura & B.M. Altura. Mg^{2+} and caffeine-induced intracellular Ca^{2+} release in human vascular endothelial cells 291

PAPERS

Z. Qiu & J.P. Morgan. Differential effects of cocaine and cocaethylene on intracellular Ca^{2+} and myocardial contraction in cardiac myocytes 293

S. Al-Damluji, L.Z. Krsmanovic & K.J. Catt. High-affinity uptake of noradrenaline in postsynaptic neurones 299

E.P. Finta, L. Harms, J. Sevcik, H.-D. Fischer & P. Illes. Effects of potassium channel openers and their antagonists on rat locus coeruleus neurones 308

D.G. MacGregor & T.W. Stone. Inhibition by the adenosine analogue, (R)-N^6-phenylisopropyladenosine, of kainic acid neurotoxicity in rat hippocampus after systemic administration 316

Z.M. Chu & L.J. Beilin. Mechanisms of vasodilatation in pregnancy: studies of the role of prostaglandins and nitric-oxide in changes of vascular reactivity in the *in situ* blood perfused mesentery of pregnant rats 322

S. Hishinuma, Y. Matsumoto, M.K. Uchida & M. Kurokawa. Novel regulation of muscarinic receptors and their coupling with G proteins in smooth muscle: transient resensitization during desensitizing process 330

Q. Chen & C. van Breemen. The superficial buffer barrier in venous smooth muscle: sarcoplasmic reticulum refilling and unloading 336

S.J. Roberts, P. Molenaar & R.J. Summers. Characterization of propranolol-resistant (−)-[^{125}I]-cyanopindolol binding sites in rat soleus muscle 344

D.R. Bristow & M.R. Zamani. Desensitization of histamine H_1 receptor-mediated inositol phosphate production in HeLa cells 353

M. Waelbroeck, J. Camus, M. Tastenoy, G. Lambrecht, E. Mutschler, M. Kropfgans, J. Sperlich, F. Wiesenberger, R. Tacke & J. Christophe. Thermodynamics of antagonist binding to rat muscarinic M_2 receptors: antimuscarinics of the pridinol, sila-pridinol, diphenidol and sila-diphenidol type 360

A.C. MacKinnon, M. Spedding & C.M. Brown. Sodium modulation of ^{3}H-agonist and ^{3}H-antagonist binding to α_2-adrenoceptor subtypes 371

G.J. Birrell & F.W. Marcoux. Excitatory amino acid receptor-stimulated phosphoinositide turnover in primary cerebrocortical cultures 379

M.D. Randall & T.M. Griffith. Modulation of vasodilatation to levcromakalim by hypoxia and EDRF in the rabbit isolated ear: a comparison with pinacidil, sodium nitroprusside and verapamil 386

H.L. Wiener, G.P. Thalody & S. Maayani. Interactions between responses mediated by activation of adenosine A_2 receptors and α_1-adrenoceptors in the rabbit isolated aorta 394

S.J.G. McAuliffe, H.M. Snow, B. Cox, C.C.T. Smith & M.I.M. Noble. Interaction between the effects of 5-hydroxytryptamine and adrenaline on the growth of platelet thrombi in the coronary artery of the anaesthetized dog 405

M. Del Zompo, M.P. Piccardi, S., Ruiu, M. Quartu, G.L. Gessa & A. Vaccari. Selective MPP^+ uptake into synaptic dopamine vesicles: possible involvement in MPTP neurotoxicity 411

K. Kitamura, Q. Lian, A. Carl & H. Kuriyama. S-nitrosocysteine, but not sodium nitroprusside, produces apamin-sensitive hyperpolarization in rat gastric fundus 415

A. Vials & G. Burnstock. A_2-purinoceptor-mediated relaxation in the guinea-pig coronary vasculature: a role for nitric oxide 424

D. Salvemini, A. Pistelli, & V. Mollace. Release of nitric oxide from glyceryl trinitrate by captopril but not enalaprilat: *in vitro* and *in vivo* studies 430

B.A. Kenny, A.C. MacKinnon, M. Spedding & C.M. Brown. Changes in [^{3}H]-PK 11195 and [^{3}H]-8-OH-DPAT binding following forebrain ischaemia in the gerbil 437

H. Nishimura, T. Matsubara, Y. Ikoma, S. Nakayama & N. Sakamoto. Effects of prolonged application of isoprenaline on intracellular free magnesium concentration in isolated heart of rat 443

J.P. Turner. Anion transport blockers inhibit DL-2-amino-4-phosphonobutyrate responses induced by quisqualate in the rat cerebral cortex 449

H. Uneyama, N. Harata & N. Akaike. Caffeine and related compounds block inhibitory amino acid-gated Cl^- currents in freshly dissociated rat hippocampal neurones 459

H. Hassessian, P. Bodin & G. Burnstock. Blockade by glibenclamide of the flow-evoked endothelial release of ATP that contributes to vasodilatation in the pulmonary vascular bed of the rat 466

Y. Igawa, A. Mattiasson & K.-E. Andersson. Functional importance of cholinergic and purinergic neuro-transmission for micturition contraction in the normal, unanaesthetized rat 473

G. Khurana & M.R. Bennett. Nitric oxide and arachidonic acid modulation of calcium currents in postganglionic neurones of avian cultured ciliary ganglia 480

H. Karaki, S.A. Sudjarwo, M. Hori, M. Takai, Y. Urade & T. Okada. Induction of endothelium-dependent relaxation in the rat aorta by IRL 1620, a novel and selective agonist at the endothelin ET_B receptor 486

G. Grignaschi, B. Mantelli, C. Fracasso, M. Anelli, S. Caccia & R. Samanin. Reciprocal interaction of 5-hydroxytryptamine and cholecystokinin in the control of feeding patterns in rats 491

A.S.O. Adeagbo & C.R. Triggle. Interactions of nitric oxide synthase inhibitors and dexamethasone with α-adrenoceptor-mediated responses in rat aorta 495

M.D. Ivorra, C. Lugnier, M. Catret, E. Anselmi, D. Cortes & P. D'Ocon. Investigations of the dual contractile/relaxant properties showed by antioquine in rat aorta 502

U. Kachintorn, M. Vajanaphanich, A.E. Traynor-Kaplan, K. Dharmsathaphorn & K.E. Barrett. Activation by calcium alone of chloride secretion in T_{84} epithelial cells 510

J.C. Oliveira, A.M. Sebastião & J.A. Ribeiro. On the high affinity binding site for [^{3}H]-1,3-dipropyl-8-cyclopentylxanthine in frog brain membranes 518

M. Hirafuji & H. Shinoda. Roles of prostacyclin, EDRF and active oxygens in leukocyte-dependent platelet adhesion to endothelial cells induced by platelet-activating factor *in vitro* 524

L. McMurdo, P.S. Lidbury, C. Thiemermann & J.R. Vane. Mediation of endothelin-1-induced inhibition of platelet aggregation via the ET_B receptor 530

J. McGivern, C.N. Scholfield & J.O. Dolly. Action of α-dendrotoxin on K^+ currents in nerve terminal regions of axons in rat olfactory cortex 535

R.A. Marangoni, E. Antunes, S.D. Brain & G. de Nucci. Activation by *Phoneutria nigriventer* (armed spider) venom of tissue kallikrein-kininogen-kinin system in rabbit skin *in vivo* 539

R.A.D. Rutherford, J. Wharton, A. McCarthy, L. Gordon, M.H.F. Sullivan, M.G. Elder & J.M. Polak. Differential localization of endothelin ET_A and ET_B binding sites in human placenta 544

T. Omari, M.P. Sparrow, M.K. Church, S.T. Holgate & C. Robinson. A comparison of the effects of polyarginine and stimulated eosinophils on the responsiveness of the bovine isovolumic bronchial segment preparation 553

W. Scholz, U. Albus, H.J. Lang, W. Linz, P.A. Martorana, H.C. Englert & B.A. Schölkens. Hoe 694, a new Na^+/H^+ exchange inhibitor and its effects in cardiac ischaemia 562

P. Soares-da-Silva. Renal tubular dopamine outward transfer during Na^+-H^+ exchange activation by α_1- and α_2-adrenoceptor agonists 569

P. Soares-da-Silva. Kinetic study of the tubular dopamine outward transporter in the rat and dog kidney 577

D.P. Brooks, B.G. Short, M.J. Cyronak, L.C. Contino, M. DiCristo, Y-X. Wang & R.R. Ruffolo, Jr. Comparison between carvedilol and captopril in rats with partial ablation-induced chronic renal failure 581

A.T. Dinh-Xuan, J. Pepke-Zaba, A.Y. Butt, G. Cremona & T.W. Higenbottam. Impairment of pulmonary-artery endothelium-dependent relaxation in chronic obstructive lung disease is not due to dysfunction of endothelial cell membrane receptors nor to L-arginine deficiency 587

C.L. Wainwright, J.R. Parratt & H. Van Belle. The antiarrhythmic effects of the nucleoside transporter inhibitor, R75231, in anaesthetized pigs 592

Typeset by Elite Typesetting Techniques, Southampton, Hampshire
and printed in Great Britain by Unwin Brothers Ltd., The Gresham Press, Old Woking, Surrey